EVALUATION OF MULTIPLE CORROSION PROTECTION SYSTEMS AND STAINLESS STEEL CLAD REINFORCEMENT FOR REINFORCED CONCRETE

By

Lien Gong

David Darwin

JoAnn P. Browning

Carl E. Locke, Jr.

A Report on Research Sponsored by

UNITED STATES DEPARTMENT OF TRANSPORTATION
FEDERAL HIGHWAY ADMINISTRATION
Contract No. DTFH61-03-C-00131

KANSAS DEPARTMENT OF TRANSPORTATION
Contract Nos. C1131 and C1281

SOUTH DAKOTA DEPARTMENT OF TRANSPORTATION
Project No. SD 2002-16

THE NATIONAL SCIENCE FOUNDATION
Research Grant No. CMS - 9812716

Structural Engineering and Engineering Materials

SM Report No. 82

THE UNIVERSITY OF KANSAS CENTER FOR RESEARCH, INC.

LAWRENCE, KANSAS

January 2006

ABSTRACT

The corrosion performance of multiple corrosion protection systems and stainless steel clad reinforcement is compared and evaluated in this study. Conventional steel and conventional epoxy-coated steel coated with 3M™ Scotchkote™ 413 Fusion Bonded Epoxy are used as "control" systems. The corrosion protection systems, which are compared to the control systems based on macrocell and bench-scale tests, include stainless steel clad reinforcement, conventional epoxy-coated reinforcement cast in concrete containing one of three corrosion inhibitors (DCI-S, Rheocrete 222^{+}, or Hycrete), epoxy-coated steel with the epoxy applied over a primer coat that contains microencapsulated calcium nitrite, epoxy-coated steel with the epoxy applied after pretreatment of the steel with zinc chromate to improve adhesion between the epoxy and the steel, epoxy-coated steel using improved adhesion epoxies developed by DuPont and Valspar, and multiple coated steel with a zinc layer underlying the DuPont 8-2739 Flex West Blue epoxy layer. Macrocell tests are conducted on bare bars and bars symmetrically embedded in a mortar cylinder. Bench-scale tests include the Southern Exposure, cracked beam, and ASTM G 109 tests.

The results indicate stainless steel clad reinforcement exhibits very good corrosion performance when the cladding is intact. In uncracked mortar or concrete containing corrosion inhibitors, corrosion rates and losses are lower than observed using the same mortar and concrete with no inhibitor. For concrete with cracks above and parallel to the reinforcing steel, the presence of corrosion inhibitors does not provide an advantage in protecting the reinforcing steel. In uncracked concrete, a lower water-cement ratio results in corrosion rates and losses that are lower than observed at the higher water-cement ratio. In cracked concrete, a lower-water cement ratio provides only limited additional corrosion protection when cracks provide a direct path for the chlorides to the steel.

When adhesion loss between epoxy and steel is not considered, a 230-mm (9 in.) deck reinforced with conventional epoxy-coated steel or one of the three high adhesion epoxy-coated steels is the most cost-effective. When the potential effects of adhesion loss are considered, at a discount rate of 2%, the most cost-effective option is a 216-mm deck containing stainless steel clad reinforcement.

Key Words: chlorides; concrete; corrosion; corrosion testing; multiple corrosion protection systems; stainless steel clad reinforcement;

ACKNOWLEDGEMENTS

This report is based on a thesis submitted by Lien Gong in partial fulfillment of the requirements of the Ph.D. degree. Major funding and material support for this research was provided by the United States Department of Transportation Federal Highway Administration under Contract No. DTFH61-03-C-00131, with technical oversight by Yash Paul Virmani, the Kansas Department of Transportation under Contract Nos. C1131 and C1281, with technical oversight by Dan Scherschligt and Don Whisler, the South Dakota Department of Transportation under project SD 2002-16, with supervision by Technical Panel Chair, Dan Johnston, and the National Science Foundation under NSF Grant No. CMS – 9812716. Additional support for this project was provided by the Concrete Steel Reinforcing Institute, DuPont Powder Coatings, 3M Corporation, Valspar Corporation, Degussa Construction Chemicals, W. R. Grace & Co., Broadview Technologies, Inc., Western Coating, Inc., and LRM Industries.

TABLE OF CONTENTS

LIST OF TABLES

LIST OF FIGURES

CHAPTER 1
INTRODUCTION

1.1 GENERAL

The corrosion of reinforcing steel in highway structures costs billions of dollars in maintenance and replacement in the United States. Deicing salts used during winter may result in the deterioration of bridges as the deicers diffuse through bridge decks and cause corrosion of the reinforcing steel. Chlorides in the seawater can similarly attack the substructures of bridges in marine environments. In 1992, it was estimated that in the United States the cost of bridge repairs in the federal-aid system due to corrosion damage was 51 billion dollars (Fliz el al. 1992). The average annual direct cost of corrosion of highway bridges is estimated at 8.3 billion dollars, with indirect costs to users to be more than 10 times that value due to traffic delays and lost productivity (Yunovich el at. 2002). Thus, cost-effective methods to prevent the corrosion of reinforcing steel are aggressively being pursued.

Current methods to reduce corrosion of reinforcing steel can be divided into two categories. The first category includes methods that slow the initiation of corrosion, that is, the time it takes the chlorides to reach a threshold value at the reinforcing steel in the concrete. This category involves methods such as the use of some corrosion inhibitors, low permeability concrete, and increased concrete cover over the reinforcing steel. The second category includes methods that lengthen the corrosion period, that is, the time from the initiation of corrosion to the end of the service life. Methods such as the use of corrosion-resistant steel, epoxy-coated steel, corrosion inhibitors, and cathodic protection belong to the second category.

The combination of using epoxy-coated reinforcement (ECR) and increased concrete cover over the reinforcing bars is the principal corrosion protection technique now in use to lengthen the life of bridge decks. However, there are still

some concerns about this combination. The increased concrete cover increases the bridge self weight and the cost of construction. And, if poorly adhering epoxy coatings are used on the reinforcement, corrosion problems may be increased. These problems include imperfections in the coating that cause disbondment between the coatings and the steel. Even if the coating has no local defects, the permeation of water, and, to a lesser extent oxygen and chloride ions, through the film may result in corrosion (Manning 1996). This happened for poorly applied coatings in substructures in Florida (Sagues el al. 1994). Based on research, even properly applied coatings will lose adhesion over a period of time (Manning 1996, Smith and Virmani 1996), which means the coatings could deteriorate to the extent that epoxy cannot protect the reinforcement once the chlorides reach the reinforcing steel.

To help solve these problems, other combinations of corrosion protection procedures have been pursued. These combinations incorporate epoxy-coated reinforcement with corrosion inhibitors added to concrete, an epoxy coating that encapsulates the corrosion inhibitors into the epoxy powder, and reinforcing bars with dual-phase coatings of zinc and epoxy. Chemical treatments and coating formulations are also used to increase the adhesion between the reinforcing steel and the coating with the goal of improving the durability of the coating. Moreover, some forms of corrosion-resistant reinforcement, such as stainless steel clad and solid stainless steel, have been developed to limit corrosion problems.

This report describes work to evaluate the performance of stainless steel clad reinforcement and multiple corrosion protection systems that include epoxy-coated reinforcement. The goal of this research is to determine the ability of these systems to slow the initiation of corrosion and lengthen the corrosion period.

1.2 BACKGROUND

Reinforcing steel embedded in concrete is usually protected from corrosion due to the high pH of the concrete pore solution. This high level of alkalinity protects steel by causing the formation of a γ-ferric oxyhydroxide coating on the steel surface that is self-maintaining and prevents corrosion.

$$2Fe(OH)_2 + 1/2O_2 \rightarrow 2\gamma\text{- } FeOOH + H_2O \quad (1.1)$$

As long as the passive film on the reinforcing steel remains intact, corrosion will not occur. The pH of the concrete pore solution is required to be between 11.5 and 13.8 to sustain the passivity of the steel. If the pH is decreased, the film becomes unstable and oxygen is able to react with the steel, causing corrosion.

The passive film can be disrupted by carbonation, due to the penetration of CO_2 into the concrete, which lowers the pH of the pore solution, or by the presence of aggressive ions, principally Cl^-, found in deicing salts and seawater, which react with the passive layer.

1.2.1 Carbonation

Carbonation is related to thin concrete cover, poor concrete quality, poor consolidation, and age. If atmospheric carbon dioxide diffuses into concrete continuously, the pH of the pore solution will be decreased because dissolution of CO_2 in water produces a weak acid that will reach with hydroxyl ions in concrete pore solution. Carbonation can reduce the pH of the pore solution to as low as 8.0, causing the protective film to break down and the steel to corrode. The reactions involved in the carbonation of calcium hydroxide are

$$CO_2 + H_2O \rightarrow H_2CO_3 \quad (1.2)$$

$$H_2CO_3 + Ca(OH)_2 \rightarrow CaCO_3 + 2H_2O \quad (1.3)$$

1.2.2 Chlorides

The presence of chloride ions is a serious problem in concrete. Chloride ions can react with available iron ions from the passive film on the bar surface to form an

ion-chloride complex. The complex is then converted to iron oxide and chloride ions, which are again available to react with the iron in the reinforcement.

$$Fe^{2+} + 4Cl^- \rightarrow (FeCl_4)^{2-} \quad (1.4)$$

$$(FeCl_4)^{2-} + 2H_2O \rightarrow Fe(OH)_2 + 2H^+ + 4Cl^- \quad (1.5)$$

To initiate corrosion, a "threshold" level of chloride ions is needed. According to ACI 318, the ratio of chloride ions to the weight of cement needs to be larger than 0.15%, which means that the concentration of chloride ions in concrete needs to exceed 0.6 kg/m^3 (1 lb/yd^3) for corrosion to initiate in a typical bridge deck with a cement content of 390 kg/m^3 (657 lb/yd^3). Due to the importance of hydroxyl ions in protecting steel from corrosion, the threshold can also be expressed as a ratio of chloride to hydroxyl ions, $[Cl^-]/[OH^-]$. Passivity is lost when $[Cl^-]/[OH^-]$ exceeds 0.6 (Hausmann 1967).

1.2.3 Electrochemistry

The corrosion of reinforcing steel in concrete is an electrochemical process that includes the flow of electric current and several chemical reactions. An electrochemical cell is necessary for corrosion to occur. There are four components in the electrochemical cell: an anode, a cathode, an electron path, and an electrolyte. The anode is the region where oxidation occurs, where iron releases electrons. The cathode is the region where reduction occurs, where electrons combine with other molecules. The electrons released at the anode move to the cathode along an electronic path. The electrolyte is an ionic solution, such as the pore solution in concrete.

In a corrosion cell, iron is oxidized at the anode, releasing electrons and ferrous ions.

$$Fe \rightarrow Fe^{2+} + 2e^- \quad (1.6)$$

Electrons released at the anode flow to the cathode and combine with water and oxygen to form hydroxyl ions.

$$\tfrac{1}{2}O_2 + H_2O + 2e^- \rightarrow 2OH^- \quad (1.7)$$

The ferrous ions, which dissolve in the solution surrounding the steel, combine with the hydroxyl ions to form ferrous hydroxide.

$$Fe^{2+} + 2OH^- \rightarrow Fe(OH)_2 \quad (1.8)$$

This compound is unstable in oxygenated solutions and is further oxidized to the ferric hydroxide.

$$2Fe(OH)_2 + H_2O + \tfrac{1}{2}O_2 \rightarrow 2Fe(OH)_3 \quad (1.9)$$

$$2Fe(OH)_3 \rightarrow Fe_2O_3 \bullet 3H_2O \quad (1.10)$$

The final product is rust, which has a greater volume than that of the original steel. This increase in volume produces tensile stresses in the concrete and may induce concrete to crack.

Two types of corrosion can occur on reinforcing steel in concrete structures. One is called microcell corrosion, where the anode and the cathode are located on the same bar. The other is called macrocell corrosion, where entire layers or regions of reinforcing steel act as anodes and cathodes. To protect steel from corrosion, one or more of the four components in the electrochemical cell must be eliminated.

1.2.4 Corrosion Potential and Corrosion Rate

From a thermodynamics point of view, the electrochemical reactions of corrosion are driven by the potential difference between the anode and the cathode. The potential of the anode and cathode can be used to determine the tendency for corrosion to occur. These potentials are used in the Gibbs and Nernst equations (Uhlig and Revie 1985) to determine if the coupled reactions are spontaneous.

If the Gibbs and Nernst equations show that energy is released, corrosion will occur. However, a spontaneous reaction does not necessarily mean a rapid reaction. Thermodynamic analysis of corrosion only provides information concerning tendencies of reactions and does not tell anything about rates at which the reaction will occur.

Chemical kinetics can be used to determine the rates of electrochemical reactions. According to chemical kinetics, there is a rate corresponding to the potential of a reaction at which that reaction will occur. The relationship between the potential and the rate of a reaction is logarithmic and given by the Tafel Equation:

$$\eta = \pm \beta \log_{10}(i/i_0) \tag{1.11}$$

where: $\eta = \phi_{meas.} - \phi_{equil.}$ = polarization or overvoltage

$\phi_{meas.}$ = the measured potential when a reaction is not at equilibrium

$\phi_{equil.}$ = the potential at equilibrium

β = Tafel slope

i = current density

i_0 = exchange current density = current density at equilibrium

When a reaction is at equilibrium, it means the reaction occurring in the forward direction is equal in rate to the reaction occurring in the reverse direction.

Chemical kinetics also describes the behavior of an electrochemical cell. The potentials and rates of the anodic and cathodic reactions in an electrochemical cell will shift to common intermediate values, so both the cathodic and anodic reactions will have the same potential and rate as required by the equilibrium condition. This reaction rate is known as the corrosion rate.

The open circuit corrosion potentials of the anode and cathode, along with the corrosion rate, are the basic corrosion monitoring methods used in this study. Potential is measured with respect to a reference electrode. Although the absolute amount of energy in a metal cannot be measured, the difference in energy between two reactions can be quantified. Therefore, a standard reaction has been chosen to have zero potential and all other reaction potentials are defined as the difference in potential from the standard (Jones 1992). The standard reaction is:

$$2H^+ + 2e^- \leftrightarrows H_2 \tag{1.12}$$

The electrode used to produce the standard reaction is called the standard hydrogen electrode (SHE). By setting up an electrochemical cell between a metal and the electrode, the potential difference can be measured using a voltmeter. Other electrodes that have more stable reactions are often used instead of SHE. The copper-copper sulfate electrode (CSE) is frequently used for bridge decks and has a potential difference of 0.318 V with respect to the SHE.

The corrosion rate of a macrocell may be determined by measuring the voltage drop across a resistor placed in series with the electron path between the anode and the cathode.

1.3 PREVIOUS WORK

1.3.1 Epoxy-coated Reinforcement

Epoxy-coated reinforcement has been used to protect reinforced concrete bridge decks from corrosion since mid 1970s. The epoxy powder is applied at a required temperature (typically 230°C) over the freshly blasted steel surface. The epoxy melts, flows and cures on the bars, which then are quenched, usually with a water spray bath (Manning 1996). The epoxy coating works in two ways to prevent corrosion: (1) it acts as a physical barrier to keep oxygen and moisture from reaching the steel surface; (2) it acts as an electrical barrier between adjacent steel locations (Kepler et al. 2000). ASTM A 775 and A 934 provide specifications to control the quality of epoxy coatings during coating, handling, shipping, and storage.

In 1973, epoxy-coated reinforcement was installed in a four-span bridge over the Schuylkill River near Philadelphia for the first time. By the fall of 1977, 17 states had adopted the use of epoxy-coated bars as a standard construction procedure and nine others had installed coated bars on an experimental basis (Manning 1996). Epoxy-coated bars in combination of a greater concrete cover have been used to protect bridges in US and Canada for more than a decade. However, the effectiveness

of epoxy-coated steel has been seriously questioned in the last few years. Cases of damage to structures resulting from corrosion of epoxy-coated steel have been reported from Florida, New York, and Ontario.

In the Florida Keys, severe corrosion of epoxy-coated rebar was found in the substructures of five major bridges after six to thirteen years of service. The damage tended to affect portions of the substructure in the splash and evaporation zone. Upon examination, it was revealed that disbondment of the coating had occurred in many cases, with liquid of pH 5 found beneath the coating (Manning 1996). The Florida Department of Transportation, along with the University of South Florida, started a series of laboratory and field studies to find possible reasons for the failures (Sagues et al. 1994). The research suggested that electrochemical disbondment of epoxy coatings could be initiated due to exposure to salt water and subsequent macrocell action during service in bridge substructures. It was assumed that handling and storage in a salty environment caused additional surface damage of the coatings. It was also assumed that some of the bars were disbonded, even before they were installed in the structure.

In March 1993, a research study titled “Study of Adhesion Loss Mechanism on Epoxy-Coated Rebar” was funded by the Ontario Ministry of Transportation and initiated at the University of Western Ontario. The purpose of the study was to determine the mechanisms involved in the loss of adhesion in epoxy-coated reinforcement and the effect of adhesion loss on the corrosion performance of coated bars containing defects. It was concluded that adhesion is improved by an increase in surface roughness and decreased by the presence of contaminants. The main mechanism of adhesion loss is due to the permeation of water through the epoxy coating, which then displaces the epoxy from the steel surface. The test results also suggested that simple adhesion loss in a “defect-free” coating did not change the short-term corrosion performance. If defects were present, however, corrosion

performance deteriorated and was related directly to the adhesion of the coating (*Adhesion* 1995). In 1996, the epoxy-coated reinforcement samples extracted from 18 bridge decks in Virginia were evaluated (Pyc et al. 2000). The results indicated that epoxy would not remain bonded to reinforcing steel in humid concrete environments. If the coating had already disbonded when chloride ions arrived at the surface of the reinforcement, corrosion would occur under the coating. Other studies have also found that reinforcement in highly moist concrete usually showed reduced adhesion of coating (Shiessl 1992, Smith and Virmani 1996, Weyer et al. 1997).

KCC Inc. studied the effectiveness of epoxy-coated reinforcement beginning in 1982, under programs sponsored by the Concrete Reinforcing Steel Institute (CRSI) and Eltech Research Corporation, in a Canadian SHRP study, and under NCHRP 10-37(Clear et al. 1992). The apparent failure mechanisms of epoxy-coated reinforcement during the studies included cathodic disbondment, loss of epoxy's insulative properties under macrocell action, and the evolution of hydrogen at secondary cathodes developed on the macroanode after the pH decreased due to macrocell action (Clear et al. 1992, Schiessl 1992). Based on these results, it was concluded that epoxy-coated reinforcing steel technology could not be relied on to provide long-term corrosion protection for highway structures exposed to corrosive environments (Clear et al. 1995). The following procedures were suggested by KCC to assure a corrosion free life for structures: (1) electrical interconnection of all reinforcing steel in new structures built with epoxy-coated reinforcement so that cathodic protection or other electrochemical procedures could be implemented when necessary, (2) high quality concrete and deep cover, (3) additional protective systems in severe environments, (4) a maximum of two months outdoor storage of epoxy-coated reinforcing steel, (5) quality control based on in-place coating impedance and in-place defect density of bars, rather than on the defect density that exists at the production plant (Clear et al. 1992, 1995).

In May 1992, FHWA started a five-year research project on the corrosion resistance of reinforcement for concrete (McDonald et al. 1998). The aim of the study was to develop new cost-effective organic, inorganic, ceramic, and metallic coatings, as well as metallic alloys, which should have superior characteristics and provide a corrosion-free design life between 75 to 100 years. Thirty-three organic-coated reinforcing bar types were selected for prescreening tests. The two best bendable and two best nobendable epoxies from the screening tests, along with Scotchkote 213(the major epoxy-coating material used at the time), were chosen for the in-concrete test. Based on the test results, the presence of cracks in the concrete and the amount of damage to the bars had significant effects on the performance of the reinforcement. The type of epoxy also affected the performance of the epoxy-coated bars. However, these effects were extensively reduced if epoxy-coated cathodes were used. The improved adhesion coating, as measured by the cathodic disbondment test, was not directly related to improved corrosion resistance, while the mat-to-mat resistance was clearly correlated with the corrosion resistance of epoxy-coated reinforcement. This research supported the use of epoxy-coated reinforcement as an effective corrosion protection system for bridge decks. To get the best performance, McDonald et al. (1998) made the following recommendations: (1) epoxy-coated bars should be used throughout the structure, not just top mat in the bridge deck, and (2) damage sites on epoxy-coated bars and the cracks in the concrete should be repaired to maximize the life of the epoxy-coated bars.

In 1996, FHWA published a report that summarized the results of investigations performed by highway agencies in the United States and Canada to evaluate the performance of epoxy-coated reinforcement (Smith and Virmani 1996). The evaluation included a total of 92 bridge decks, two bridge barrier walls, and one noise barrier wall located in 11 states and 3 provinces. Overall, the structures were generally in good condition. The deterioration of concrete was usually in isolated

areas and often not correlated with corrosion of the epoxy-coated reinforcement. Delaminations were detected in only 10 of the bridge decks and half of them were small. The total chloride concentration was determined in 40 bridge decks, and in most cases, the chloride concentrations at the steel level were at or above the corrosion initiation threshold of 0.6 kg/m^3 (1 lb/yd^3) for conventional reinforcing steel. The water-soluble chloride concentration was determined in 16 other bridge decks and one third of them were equal to or greater than 0.6 kg/m^3 (1 lb/yd^3). One hundred sixty two out of 202 epoxy-coated bars that were extracted from the bridge decks for examination did not show any sign of corrosion. The corrosion exhibited by some of the remaining bars might have been present prior to construction since chloride concentrations at the time of evaluation were less than the initiation threshold. Only four epoxy-coated bars had experienced noticeable corrosion during service. The corrosion was more significant at locations with relatively thin concrete cover, high chloride concentrations, and cracking. It was also found that the number of defects in the coating and the extent of coating disbondment affected the performance of epoxy-coated reinforcement.

Cramer et al. (2002) addressed five technologies to reduce the cost of chloride-induced corrosion to bridge infrastructure: (1) using conductive coating anodes for cathodic protection (CP) on existing reinforced concrete (RC) bridges; (2) using epoxy-coated reinforcement to lengthen RC bridge service life; (3) using stainless steel reinforcing bars and (4) high quality concrete to produce economical 120^+ year bridges; and (5) using economical, long-service metal coatings for steel bridges. Based on literature research, the authors concluded that epoxy-coated reinforcement has continually improved as an economical and effective means to prevent corrosion and provide added service life to reinforced concrete structures, particularly bridge decks. But its use required adherence to standards of production, quality control and job-site handling.

1.3.2 Stainless Steel

The term “stainless steel” refers to iron-based alloys that contain at least 12% chromium. The high chromium content results in the formation of a passive layer on the surface of the steel that resists oxidation. Some stainless steel can provide corrosion resistance in severely corrosive environments without the use of other protective measures. The most common types of stainless steel used as reinforcement are Types 304, 316 and 316 LN. Two relatively new types of duplex stainless steel, 2101 (containing approximately 21% chromium and 1% nickel) and 2205 (containing approximately 22% chromium and 5% nickel), are also being used on a smaller scale.

The FHWA five-year study (McDonald et al. 1998) included 304 and 316 stainless steel. The concrete test specimens in this study contained either stainless steel in both the top and bottom mat or stainless steel in the top mat and conventional steel in the bottom mat. Type 304 stainless steel showed the lowest corrosion rate, 0.2 percent of that for the conventional steel control specimens, even when tested in precracked concrete, when the Type 304 stainless bars were used at both top and bottom mat. However, when conventional reinforcing bars were used as the cathode, significant corrosion was found on a few stainless steel anodes. This observation suggested that Type 304 stainless steel should not be combined with conventional steel in concrete structures. With a corrosion rate equal to 0.5 percent of that for the control specimens, even in precracked concrete, the Type 316 stainless steel bars did not show any significant corrosion, with or without a conventional bar cathode. This indicated that the Type 316 stainless steel might be more effective as a corrosion protection system than the Type 304 stainless steel.

In 2002, Clemena and Virmani published the results of a study that compared the behavior of 304, 316 LN and 2205 solid stainless steel bars, stainless steel clad bars, and conventional ASTM A 615 bars. After two years of salt exposure, the specimens containing solid stainless steel showed no sign of corrosion. The chloride

concentration in the concrete adjacent to the stainless steel bars was 15 times higher than the corrosion initiation threshold of conventional steel at end of the test period.

During ongoing research at the University of Kansas, duplex stainless steels, 2101 and 2205, were evaluated in both a pickled and a non-pickled condition. Based on the results, 2205 steel generally performed better than 2101 steel when tested in either the pickled or non-pickled condition. For the same type of steel, pickled bars showed a lower corrosion tendency than non-pickled bars. Of the bars under test, 2205 pickled and 2101 pickled steel performed best.

The Oregon Department of Transportation has completed two bridge projects using stainless steel reinforcing bars at a total cost of $21 million. In these two bridges, stainless steel was used in the deck, beams, and precast girders. Conventional steel was used in compression members such as columns and arches. Although the in-place cost of stainless steel is three times more than conventional steel, the use of stainless steel in the projects raised the total project costs by only 10% compared to the equivalent bridge using conventional steel. Use of stainless steel is expected to provide a 120^{+} year bridge life and substantially reduce inspection costs, reduce maintenance and repair costs, and eliminate the need to replace bridge decks during the service life (Cramer et al. 2002)

1.3.3 Stainless Steel Clad Reinforcement

Studies have demonstrated that solid stainless steel bars can provide significantly improved corrosion resistance in severely corrosive environments. However, due to the significant cost of using solid stainless steel, its use has been limited to very few structures. To lower the material cost, stainless clad steel reinforcement is considered to be a viable alternative. Compared to solid stainless steel, a disadvantage of stainless clad steel is the fact that the cladding may be damaged during shipping, handling or bending. Exposed ends must also be protected.

Rasheeduzzafar et al. (1992) compared the corrosion resistance of Type 304 stainless clad bars and conventional bars over a seven-year period. After seven years of embedment in a concrete, the conventional steel exhibited severe corrosion damage and significant cracking occurred in all specimens. In contrast, the stainless clad bars exhibited good corrosion resistance. At a chloride concentration of 19.2 kg/m^3 (32.4 lb/yd^3), no corrosion or cracking of concrete was observed in any of the stainless clad steel bar specimens tested. Therefore, the chloride threshold of stainless clad steel was believed to be at least 32 times the corrosion threshold for conventional steel in concrete.

In 1983-1984, a bridge deck containing 304 stainless-clad reinforcing bars was constructed by the New Jersey Department of Transportation (McDonald et al 1995). Four cores, which contained nine stainless clad bars, were taken from the bridge deck and examined. These nine bars were in excellent condition, showing no sign of corrosion on the surface. Corrosion, however, was found on the conventional steel under the plastic end cap on one bar.

A study by Darwin et al. (1999) and Kahrs et al. (2001) at the University of Kansas indicated that the 304 stainless steel clad reinforcement exhibited superior corrosion resistance compared to conventional reinforcing steel. In the study, epoxy applied to the cut ends of stainless steel clad bars, where the conventional steel core was not protected with cladding, did not protect against corrosion. To provide adequate protection, plastic caps filled with epoxy were used to seal the ends of bars. Although a crack in the cladding was observed using a scanning electron microscope, the crack did not penetrate the stainless steel. At the observed corrosion rates, it was concluded that the cladding was thick enough to protect the conventional steel core.

1.3.4 MMFX Reinforcement

An iron-alloy containing 9% chromium, known as MMFX microcomposite steel, was developed by the MMFX Steel Corporation. The steel was designed to

minimize the formation of microgalvanic cells in the steel structure and to be corrosion resistant.

Trejo (2002) presented the results of a study to determine the chloride thresholds and corrosion rates for ASTM A615 conventional steel, ASTM A 706 low-alloy steel, 304 stainless steel, MMFX microcomposite steel, and 316LN stainless steel. Based on the results, the chloride corrosion threshold of MMFX was observed to be approximately nine times that of conventional steel and very close to that of 304 stainless steel.

Darwin et al. (2002) and Gong et al. (2002) compared the corrosion properties of MMFX microcomposite steel to ASTM A 615 conventional steel and epoxy-coated reinforcement. It was concluded that MMFX had a higher corrosion threshold and a lower corrosion rate than conventional steel. However, the study concluded that MMFX steel was less cost-effective than epoxy-coated reinforcement. Also, it was recommended that MMFX steel not be combined with conventional steel in reinforced concrete structures because the combination showed higher corrosion rates than that exhibited by MMFX steel alone.

1.3.5 Galvanized Reinforcement

Evidence started to appear in the early 1960s that zinc-coated, or galvanized, steel might provide better corrosion performance in concrete than uncoated steel (McCrum and Arnold 1993). Zinc-coated steel is produced by a hot-dip process. The steel is first cleaned by pickling and then immersed in molten zinc. Similar to steel, the corrosion products from zinc occupy more volume than the original metal, therefore, causing concrete to crack. When zinc corrodes sacrificially, $Zn(OH)_2$ forms on the surface of steel, which provides a barrier layer at active corrosion sites that prevents further corrosion from occurring (McCrum and Arnold 1993).

In 1968, the Michigan Department of Transportation started a study to compare galvanized to uncoated reinforcing steel and also to look at the effects of concrete

cover and water/cement ratio on corrosion performance (McCrum and Arnold 1993). In 1973, the study was expanded to compare epoxy-coated reinforcement to galvanized and uncoated reinforcement. Specimens were constructed using galvanized, epoxy-coated, and conventional steel. Based the results, it was concluded that the benefits of using galvanized steel in bridge decks in Michigan would prevail over the cost increase, assuming that the cost of galvanized reinforcement to be no more than 1.65 times that of conventional steel, but that epoxy-coated steel was a better option for long-term corrosion protection. In 1972, Michigan began a study to compare the performance of galvanized and uncoated steel in bridges (McCrum et al. 1995). This study concluded that, when chloride ions were diffusing through the concrete cover, galvanized reinforcement could provide a few more years of protection before the chloride concentration reached the corrosion threshold of the galvanized reinforcement. Nevertheless, there was no advantage of using galvanized reinforcement once the chloride concentrations reached levels above the threshold of either black or galvanized steel. Therefore, the extra cost of using galvanized steel in bridge decks was questionable due to uncertainty as to the extension in service life that it could provide.

In 1992, Rasheeduzzafar et al. presented test results on the performance of galvanized reinforcing steel compared to other corrosion resisting steels. The authors concluded that when galvanized reinforcing bars were used in equivalent chloride-bearing concrete, there was a delay in the beginning of cracking, a reduction in metal loss, and an amelioration in the incidence and severity of concrete spalling compared to uncoated steel. But in higher chloride concentrations, severe corrosion, along with concrete cracking, was observed in specimens with galvanized steel. These results indicated that using galvanized steel in concrete with high concentrations of chloride only delayed concrete failure a limited period of time and did not provide a permanent solution. Concrete failure in the tests was characterized by the onset and

propagation of cracking, which resulted in concrete spalling. For example, at a chloride concentration in concrete of 19 kg/m^3 (32 lb/yd^3), the first crack occurred within 65 and 172 days of casting due to corrosion for conventional and galvanized steel, respectively. The performance of galvanized bars at the low chloride level showed significantly better corrosion resistance than that of uncoated bars and suggested that the major benefit provided by the use of galvanized bars would be obtained in low chloride-bearing concrete, with chlorides contents up to 1.2 kg/m^3 (2 lb/yd^3) (Rasheeduzzafar et al. 1992).

Yeomans, S. R. (1994) investigated the corrosion performance of conventional steel, galvanized steel, and epoxy-coated steel in concrete. It was found that the chloride threshold level for galvanized steel in concrete was approximately 2.5 times that of conventional steel. Zinc provided sacrificial protection for a period of 4 to 5 times that for the initiation of corrosion for conventional steel in equivalent conditions. At the cut ends of galvanized bars, the Zn locally protected the exposed steel to a distance of approximately 8 mm.

In 1999, the Virginia Transportation Research Council published a report of a study of the effectiveness of corrosion inhibiting admixtures. Galvanized steel was tested as part of the study. Three types of corrosion inhibitors and one type of galvanized steel were evaluated in concrete specimens. It was found that galvanized steel provided good protection in the higher quality concrete. The specimens using galvanized steel showed no sign of corrosion in concrete with a water-cement ratio of 0.45. However, with a water-cement ratio of 0.71, the galvanized steel specimens exhibited excessive cracking due to corrosion (Zemajtis et al. 1999).

1.3.6 Corrosion Inhibitors

Corrosion inhibitors can be added to the concrete to elevate the chloride corrosion initiation threshold, delay the beginning of corrosion, and slow the corrosion rate of reinforcing steel. A corrosion inhibitor is, by the definition favored

by National Association of Corrosion Engineers (NACE), a substance that retards corrosion when added to an environment in small concentrations. If chloride-induced corrosion of steel reinforcement in concrete is considered, a corrosion inhibitor can function by (1) blocking the ingress of chlorides from the environment; (2) increasing the degree to which these chlorides are chemically bound or physically trapped in the concrete cover; (3) increasing the resistance of the passive film on the steel to breakdown by chlorides; (4) creating a barrier film on the steel; (5) scavenging the oxygen dissolved in the pore solution; or (6) blocking the ingress of oxygen (Hansson et al. 1998). The advantages of using corrosion inhibitors are that the inhibitor is distributed throughout the concrete, protecting all of the steel, while the low permeability of the concrete prevents the inhibitor from being lost. A disadvantage is that the inhibitor must not have adverse effects on the concrete properties in either the plastic or hardened state (Berke 1991).

Corrosion inhibitors can be divided into three groups: inorganic, organic, or vapor-phase inhibitors. However, they are typically classified as anodic, cathodic, or mixed corrosion inhibitors for reinforced concrete. Calcium nitrite is the most common anodic inhibitor used in concrete. It was commercially available as Darex Corrision Inhibitor (DCI and DCI-S) for many years, but is also available under other trade names. Both DCI and DCI-S contain 30 percent calcium nitrite and 70 percent water. Calcium nitrite has been used successfully because (1) it provides corrosion inhibition in the presence of chlorides; (2) it is not damaging to concrete properties; and (3) it is available in sufficient quantities for commercial use in concrete (Berke 1991). It functions by reacting with ferrous ions to form a film of γ-ferric oxide around the anode according to the following:

$$Fe^{2+} + OH^- + NO_2^- \rightarrow NO\uparrow + \gamma - FeOOH \qquad (1.13)$$

It is believed that nitrite and chloride ions engage in competing reactions [Eq. (1-4) or (1-13)], both of which influence the corrosion process. In contrast to the

inhibiting action of the nitrite ion, the chloride ion promotes corrosion. The recommended dosage for DCI is 10-30 L/m^3 (2-6 gal/yd^3), depending on the expected chloride level (Virmani and Clemena 1998)

An organic-based corrosion inhibiting admixture Rheocrete 222$^+$, a combination of amines and esters in a water medium, was developed as an alternative approach for protecting steel reinforcement. According to manufacturer, this mixture forms a protective film on reinforcing steel, which serves as a physical barrier to both the anodic and cathodic corrosion reactions. This mixture also reduces the ingress of chloride ions in the concrete by lining the concrete pores with hydrophobic chemical compounds. The recommended dosage for Rheocrete 222$^+$ is 5 L/m^3 (Nmai 1992).

Some other corrosion inhibitors, such as Armatec 2000 and Hycrete, are also available.

In 1983, FHWA released the results of the first large-scale study using calcium nitrite (Virmani et al.1983). They concluded that calcium nitrite could provide more than an order of magnitude reduction in the corrosion rate. Their final conclusions were that calcium nitrite was effective at chloride-to-nitrite ratios of 1.79 or less. A more recent review of calcium nitrite showed that a more realistic maximum chloride-to-nitrite ratio is 0.9 (Virmani 1990).

Berke et al. (1991) compared the corrosion performance of conventional steel and galvanized steel in control concrete, and the same metals in concrete containing calcium nitrite. They observed that calcium nitrite not only protected conventional steel in concrete, but also effectively delayed and reduced the corrosion of galvanized steel.

Senecal et al. (1995) evaluated calcium nitrite and Rheocrete 222 (a predecessor to Rheocrete 222$^+$) using Southern Exposure and cracked beam specimens. To increase the permeability of the concrete to accelerate the tests, a water-cement ratio of 0.5 was used. The results showed that specimens with either inhibitor had better

corrosion performance than regular concrete specimens, but overall, specimens with Rheocrete 222 performed better than those with calcium nitrite.

Pyc et al. (1999) published a study of the effectiveness of corrosion-inhibiting admixtures. Three commercial corrosion-inhibiting admixtures, Rheocrete 222, Armatec 2000, and DCI, were evaluated by testing their performance in a simulated concrete pore water solution (immersion test) and in concrete (ponding test). The results showed that DCI was the only corrosion inhibitor that performed well under the experiment conditions. The other two corrosion inhibitors, Rheocrete 222 and Armatec 2000 showed little to no corrosion inhibition in any of the experiment stages (Pyc et al. 1999).

In 2001, calcium nitrite (DCI-S) and Rheocrete 222^{+} were tested as part of a study by Ge et al. (2004). The corrosion inhibitors were used in uncracked and cracked concrete. Based on the results for uncracked concrete specimens, both inhibitors used in this study, Rheocrete 222^{+} and DCI-S, significantly decreased the corrosion rate of the steel in a salt environment. However, Rheocrete and DCI-S provided no advantage compared to concrete without an inhibitor in protecting against corrosion in cracked concrete.

1.3.7 Water-Cement Ratio

A low water-cement ratio can be used to reduce the permeability and increase the strength of concrete. Due to the decreased permeability, the quantity of water, oxygen and chloride ions that can penetrate the concrete is limited, and the time required for the stresses caused by corrosion of the steel reinforcement to cause the concrete to crack is extended (Virmani and Clemena 1998).

Sherman et al. (1996) reported that impermeable concrete could be manufactured using conventional mixes with water-cement ratios between 0.3 and 0.32. To protect reinforced concrete structures exposed to deicers from corrosion, ACI 318 limits the water-cement ratio to a maximum of 0.40.

When a 35 year-old bridge in Windsor, Connecticut was demolished in 1992, it was found that the slab reinforcement exhibited no sign of corrosion in the demolition debris or in cores extracted from the concrete. The reasons of this good performance were a low water-cement ratio, high cement content, well graded fine aggregate, a high dosage of water reducer/retarder, good consolidation, minimum cracking, and a bituminous wearing course that, together, protected the concrete from chloride ions. The concrete mix used on the bridge had a water-cement ratio of 0.35 (Schupack and Stark 1998).

Based on their research results, Ge et al. (2004) concluded that for an uncracked concrete structure in a high salt environment, a low water-cement ratio is advantageous for protecting steel from corrosion. For a cracked concrete structure, however, a lower water-cement ratio provides no advantage in protecting the reinforcing steel.

The Kansas DOT uses a water-cement ratio of 0.4 to 0.44 on monolithic decks and subdecks and a water-cement ratio of 0.36 to 0.4 in bridge deck overlays (Miller and Darwin 2000).

1.3.8 Concrete Cracking due to Uniform or Localized Steel Corrosion

As mentioned in Section 1.2.3, the corrosion product (rust) has a larger volume than that of the original steel, which produces tensile stresses in the concrete and may induce concrete to crack.

Pfeifer (2002) reviewed related literature, as well as analytical studies from some corrosion studies at Wiss, Janney, and Elstner Associates, Inc. (WJE), to determine the amount of uniform metal loss for conventional reinforcing bars that will cause concrete to crack as follows:

- From four FHWA and Concrete Reinforcing Steel Institute (CRSI) studies [McDonald, D. B., Sherman, M. R., and Pfeifer, D. W. (1995), McDonald, D. B., Sherman, M. R., and Pfeifer, D. W. (1996), McDonald, D. B.,

Pfeifer, D. W., and Blake, G. T. (1996), McDonald et al. (1998)], the metal loss ranged from 0.0013 to 0.038 mm (0.000051 to 0.0015 in.), with an average of 0.014 mm (0.00055 in.).

- From a study of Rodriguez et al. (1994), the reduction of bar radius (metal loss due to corrosion) ranged from 0.015 to 0.038 mm (0.00059 to 0.0015 in.) at the time that cracks appeared.
- Several analytical studies showed that concrete will crack at a concrete tensile stress of 6.89 MPa (1000 psi) which corresponds to corrosion by-products produced by a metal loss of 0.015 mm (0.00059 in.) with no creep and 0.005 (0.00020 in.) with a creep factor of 3 for concrete creep in tension. It is also believed that crack initiation at the bar perimeter is independent of clear cover, although the propagation of that crack to the concrete surface due to internal pressure increases when the rust is dependent on the depth of the clear cover.

Based on the above reviews, the author concluded that minimal skin thickness loss of about 0.025 mm or 25 μm (0.00098 in.) of a reinforcing bar would result in a volume of corrosion by-product that can crack concrete.

Torres-Acosta and Sagues (2005) estimated the critical value of metal loss needed for concrete cover cracking of a reinforced concrete element if only a portion of a steel bar is corroding. In this study, 16 cylindrical concrete specimens with various dimensions and 22 prismatic beam concrete specimens with dimensions of 140 × 140 × 406 mm (5.5 × 5.5 × 16 in.) were tested. Pipes cast in the center of the cylindrical specimens were mechanically continuous but had a center segment (anodic region) made of carbon steel pipe with a machined surface and two polyvinyl chloride (PVC) pipe sections for the remainder. The carbon steel pipe segment had 21mm (0.83 in.) external diameter, 3 mm (0.12 in.) wall thickness, and length ranging from 19.1 to 95 mm (0.75 to 3.74 in.). The concrete covers varied from 27.5 to 65.7

mm (1.08 to 2.59 in.), with water-cement ratios of 0.47, 0.49, and 0.51. The concrete cylinders were used to measure the critical amount of steel corrosion penetration (x_{CRIT}) upon autopsy, as well as pressure at the steel/concrete interface and dimensional changes during corrosion of the embedded steel pipe segment using strain gauges. The prismatic beam contained one dual-material reinforcing bar placed lengthwise centered on one of the cross section sides, with a carbon steel segment at the center and two Type 316 LN stainless steel segments at both ends. No.2 and No.4 (6 and 13 mm diameter, respectively) reinforcing bars were used in these specimens, with length ranging from 18.7 to 408.4 mm (0.74 to 16 in.) for carbon steel segments. The concrete covers varied from 13 to 45 mm (0.51 to 1.77 in.), with water-cement ratios of 0.47, 0.49, and 0.51. The beam specimens were used to estimate the value of x_{CRIT} only.

After the tests were completed, x_{CRIT} and the length of anodic region (L) were obtained experimentally for the specimen. An empirical relationship between x_{CRIT} and L was obtained.

$$x_{CRIT} = 0.011(c/\phi)(C/L+1)^2 \qquad (1.13)$$

where x_{CRIT} = critical amount of steel corrosion penetration, in mm

c = concrete cover

ϕ = reinforcing bar diameter

L = length of a local corrosion region (anodic ring region) on the bar

1.4 TESTING TECHNIQUES

Two testing techniques are used to evaluate the corrosion properties of different corrosion protection systems in this study: rapid tests and bench-scale tests. Rapid tests usually give results in 15 weeks, whereas, bench-scale tests have a testing period of 2 years. These tests are briefly described in this section and in greater detail in Chapter 2.

1.4.1 Rapid Macrocell Tests

The rapid macrocell test measures the macrocell corrosion rate and corrosion potentials of reinforcing bars. One specimen is placed in simulated concrete pore solution with a specific concentration of salt, acting as the anode. Two specimens are placed in simulated concrete pore solution, acting as the cathode. Air is supplied to the pore solution at the cathode. Steel specimens may be bare or wrapped in mortar. Crushed mortar fill is added to the containers with mortar-wrapped specimens to simulate the concrete environment. The specimens are immersed to a depth of 75 mm (3 in.) in the liquid. The solutions in the containers are connected by a salt bridge. The specimens at the anode and cathode are electrically connected across a 10-ohm resistor. The corrosion current is determined by measuring the voltage drop across the resistor. The corrosion rate is determined by using Faraday's law.

$$r = ia/(nFD) \tag{1.14}$$

where: r = macrocell corrosion rate (thickness loss per unit time)

a = atomic weight (55.84 g for iron)

i = current density (amperes/cm^2 or coulombs/cm^2.sec)

n = number of ion equivalents exchanged (For Fe^{2+} = 2)

F = Faraday's constant (96500 amp-sec/equivalent)

D = density of metal (7.87g/cm^3 for steel)

For current density (i) in μA/cm^2,

$$r = 11.59i \text{ (μm/yr)} \tag{1.15}$$

The corrosion potentials of the anode and the cathode are measured with respect to a saturated calomel electrode after the macrocell circuit has been disconnected for at least two hours.

The macrocell tests used in this study were first developed by Martinez, Darwin, McCabe, and Locke (1990) under the SHRP program. The research goal was to develop and evaluate the test specimen and the results obtained with three deicing

chemicals (calcium chloride, sodium chloride, and calcium magnesium acetate) at different concentrations. Corrosion potential and corrosion macrocell tests were performed.

The specimen configuration used in the early research was partly based on the work done by Yonezewa et al. (1988) in their study of pore solution composition and the effects of chlorides on the corrosion of steel in concrete. To get uniform cover and easier fabrication, Martinez et al. (1990) made several modifications to the "lollipop" specimen used by Yonezewa et al. (1988). The test specimen used by Martinez et al. consisted of a 127 mm (5 in.) long, No. 13 (No. 4) reinforcing bar, embedded 76 mm (3 in.) in a 30 mm (1.2 in.) diameter cylinder. An epoxy band was applied to the steel at the interface between the steel and the mortar to prevent crevice corrosion. To measure corrosion potential, a single specimen was placed in a container with either simulated pore solution or pore solution containing a deicer. A standard calomel reference electrode (SCE) was put in another container that contained a saturated potassium chloride solution. These two containers were connected with a salt bridge, and the potential difference between the specimen and the SCE was obtained. In the macrocell tests, one specimen was exposed to simulated pore with a deicer in a container, and the second specimen was exposed to simulated pore solution in another container. These two specimens were electrically connected across a 100,000-ohm resistor and ionically connected by a salt bridge. The specimen in pore solution with deicers functioned as the anode, and the specimen in pore solution functioned as the cathode. Martinez et al. recommended using a much lower resistance, modifying the salt bridge, and using multiple specimens at both the anode and cathode.

The test was modified by Smith et al. (1995) under the NCHRP-IDEA program. A No. 16 (No.5) bar was used to replace the original No. 13 (No. 4) bar to reduce the mortar cover with the goal of minimizing the initiation time of corrosion process. A 10-ohm resistor was used in place of the 100,000-ohm resistor to increase the

corrosion current. Three specimens each were placed at the anode and the cathode. To provide adequate oxygen for corrosion to occur, compressed air that was scrubbed to remove carbon dioxide was bubbled into the cathode. Since corrosion was found underneath the epoxy at steel-mortar interface, a different epoxy was recommended to use in the future.

Schwensen et al. (1995) made additional modifications to the test, also under the NCHRP-IDEA program. A key change was to increase the number of specimens used at the cathode relative to the number at the anode so that the corrosion would not be cathode limited. Two specimens were placed at the anode and four specimens were placed at cathode for the evaluation of steel in NaCl solution. One specimen was placed at anode and two specimens were placed at cathode for the evaluation of steel in $CaCl_2$ and CMA solution. The latter configuration was recommended for future study.

During early research reported by Ge et al. (2004), corrosion products were observed on the exposed portion of "lollipop" specimens or on the portion of the bare bars above solution. They assumed that this was due to the high humidity between the solution surface and the lid on the container. They recommended that the test configuration to be modified. In 2001, Darwin et al. (2002) and Gong et al. (2002) modified the test based on this observation. The reinforcing bar was completely, instead of partially, embedded in the mortar cylinder, converting the "lollipop" specimen into mortar-wrapped specimen. The lid was lowered to a position just above the level of the solution in the container for both bare and mortar-wrapped specimens.

1.4.2 Bench Scale Tests

Bench-scale tests include Southern Exposure tests (SE), cracked beam tests (CB), and ASTM G 109 tests. The difference between SE and CB tests is that the SE test simulates an uncracked bridge deck, whereas the CB test simulates a bridge deck with cracks parallel to and above the reinforcing steel. Bench-scale tests provide a

very severe corrosion environment and are generally believed to simulate 15 to 20 years of exposure for marine structures and 30 to 40 years of exposure for bridges within a 48-week period (Perenchio 1992).

In the SE and CB tests, rapid chloride ion transport is achieved by using a thin concrete cover over the reinforcing bars, a water-cement ratio of 0.35, 0.45 or 0.5, and an unusual "weathering" scheme. The weathering scheme involves ponding salt water on the SE and CB specimens for a period of time and then drying the specimen. The ponding and drying cycles are repeated, creating high concentrations of chloride ions in the concrete over a short period of time.

ASTM G 109, the "Standard Test Method for Determining the Effects of Chemical Admixtures on the Corrosion of Embedded Steel Reinforcement in Concrete Exposed to Chloride Environment," uses a cycle that includes ponding the specimens for two weeks and then drying the specimens for another two weeks. The cycle is repeated until a corrosion current of 10 μA is measured on at least one-half the specimens.

SE, CB and ASTM G 109 specimens have two mats of steel cast in the concrete. The top layer of steel acts as the anode, and the bottom layer of steel acts as the cathode. The cathode contains twice as many bars as the anode so that corrosion is not limited by the cathodic reaction. The top and bottom layers of steel are connected across an external resistor. Measurements are taken every week to determine the macrocell corrosion rate and corrosion potential.

SE tests were developed by Pfeifer and Scali (1981) in a study to evaluate concrete sealers for protection of bridges. This accelerated weathering test was developed to simulate the long-term exposure conditions in southern climates. The specimens include unreinforced concrete slabs that simulated uncracked concrete. The specimens were tested using weekly cycles. The seven-day cycle started with ponding the specimens for 100 hours with a 15 percent NaCl solution at lab

temperature. Then specimens were dried and put in a heat chamber at 100°F for 68 hours. The cycles were repeated for a total testing period of 24 weeks.

Tourney et al. (1993) presented their test results in a paper titled "A Call for Standardized Tests for Corrosion Inhibiting Admixtures." Cracked beam specimens were used in their study. The beams were cracked perpendicular to the direction of the reinforcing steel using flexural load bearing techniques, and the cracks were shimmed to a width of 0.01 in. to maintain a consistent crack size throughout the test. The specimens were cyclically ponded for two weeks with 3 percent NaCl solution and dried for two weeks. Macrocell current was measured on the eighth wet day of the ponding cycle.

Nmai et al. (1994) presented the results of a study to determine if sodium thiocyanate-based admixtures are safe to use in reinforced concrete structures Southern Exposure test were used in this research. A weekly cycle consisted of ponding specimens for 96 hours, followed by drying specimens for 72 hours. The specimens were air dried at 70°F instead of 100°F. This modification was due to a lack of laboratory space for the heat boxes. Macrocell corrosion current between the top and bottom mats of steel and half-cell potentials of the top mat were measured every week. The specimens were tested for 52 weeks and were then broken to evaluate the nature of the corrosion products on the reinforcing steel.

Senecal et al. (1995) used SE and CB tests to evaluate the corrosion performance of microalloyed reinforcing steel. Epoxy-coated wooden dams, attached to the concrete with silicone caulk, were placed around the top of the specimens to hold salt water. Transverse cracks, created by cutting a notch across the top center of the specimen and then applying a three point bending load, were used for the cracked beam specimens. The weekly cycle used by Pfeifer et al. (1981) was adopted. The test period was 48 weeks. Senecal et al. recommended that test period be extended to two years to observe how corrosion products cause concrete to crack. A longer testing

cycle was also recommended to increase the chloride concentration for the SE and CB tests. Since the wooden dams of the CB specimens started to leak after 9 months, a concrete dam cast monolithically with the specimen was recommended for the future study. Plastic wedges were suggested to use to maintain the crack widths in CB specimens. The authors also stated that 15% salt water used in this research should be reduced to 3 or 4 percent to provide more realistic conditions.

McDonald et al. (1998) used SE and CB tests to evaluate the corrosion performance of epoxy-coated, metal-clad, and solid metal reinforcing bars in concrete. In the study, the testing cycle was modified. It started with 12 weeks of ponding (4 days) and drying (3 days), followed by continuous ponding for 12 weeks. This 24-week cycle was repeated three more times for a total test period of 96 weeks. A good correlation was found between the mat-to-mat resistance and the corrosion performance of the bars.

1.4.3 Correlation between Rapid Macrocell Testing and Bench-Scale Testing.

The results from rapid macrocell tests with lollipop specimens and bench-scale tests were compared by Ge et al. (2004). It was stated in the report that, considering the relatively short test period, the rapid macrocell test appeared to provide an effective method to evaluate steel performance in uncracked concrete exposed to a salty environment. The rapid macrocell tests within each group, however, were less consistent than the bench-scale tests due to the effect of corrosion on the exposed portion of the bars in the lollipop specimens. Changes in the test, such as completely enclosing the bars in mortar, should improve the consistency of the rapid macrocell tests.

1.5 OBJECTIVE AND SCOPE

The objectives of this research are to (1) evaluate the corrosion resistance of stainless steel clad SMI-316 SC^{TM} reinforcing bars, (2) study techniques to make

epoxy-coated reinforcement (ECR) more corrosion resistant by using multiple corrosion protection strategies in bridge decks, as well as for bridge members in a marine environment that is hot, wet, and has abundant salt, and (3) compare the cost effectiveness of bridge decks with different corrosion protection systems.

These objectives will be achieved by evaluating the following corrosion protection systems:

1) 316 LN stainless steel clad reinforcement
2) Epoxy-coated reinforcement cast in concrete containing one of three corrosion inhibitors, calcium nitrite (DCI-S), Rheocrete 222^{+}, or Hycrete, cast with water/cement ratios of 0.45 and 0.35.
3) Epoxy-coated reinforcement with the epoxy applied over a primer coat that contains microencapsulated calcium nitrite [$Ca(NO_2)_2$] at the two water/cement ratios described in item 2.
4) Epoxy-coated reinforcement with the epoxy applied after pretreatment of the steel with zinc chromate to improve adhesion between the epoxy and the steel and epoxy-coated reinforcement using improved adhesion epoxies developed by DuPont and Valspar.
5) The three epoxy-coated reinforcements, described in item 4, cast in concrete containing the corrosion inhibitor calcium nitrite (DCI-S).
6) Multiple coated reinforcement with a zinc layer underlying the epoxy.

Conventional reinforcement and conventional epoxy-coated reinforcement are evaluated as controls.

The rapid macrocell tests, including specimens with or without mortar-cladding, and bench-scale tests, including the Southern Exposure, cracked beam, and ASTM G 109 tests, are used to evaluate the corrosion protection systems.

CHAPTER 2
EXPERIMENTAL WORK

This chapter describes the experimental work performed in this study. Both stainless steel clad reinforcement and multiple corrosion protection systems are evaluated. The corrosion test methods include the rapid macrocell and bench-scale tests. A description of the test specimens, specimen fabrication, and test procedures is presented for each of the test methods. The methods used for the polarization resistance, cathodic disbondment, and mechanical tests, and the analyses of stainless cladding thickness and corrosion product microstructure using the scanning electron microscope are also presented.

2.1 CORROSION PROTECTION SYSTEMS

The reinforcing steel, corrosion inhibitors, and water-cement ratios used in corrosion protection systems in this study are listed below.

Reinforcing steels:

Tests are performed on ASTM A 615 No. 16 [No. 5] deformed reinforcing bars.

- Conventional reinforcing bars
- Conventional epoxy-coated reinforcing bars coated with 3M™ Scotchkote™ 413 Fusion Bonded Epoxy
- 316 LN stainless steel clad reinforcing bars
- Epoxy-coated reinforcing bars with a primer coat that contains microencapsulated calcium nitrite [$Ca(NO_2)_2$]
- Epoxy-coated reinforcing bars with increased adhesion epoxy produced by DuPont

- Epoxy-coated reinforcing bars with increased adhesion epoxy produced by Valspar
- Epoxy-coated reinforcing bars pretreated with zinc chromate to improve adhesion between the epoxy and the steel
- Multiple coated reinforcing bars with a metallic layer containing 98% zinc and 2% aluminum underlying the DuPont 8-2739 Flex West Blue epoxy

Corrosion Inhibitors:

- Darex corrosion inhibitor (DCI-S), which contains 30% calcium nitrite, 70% water, and a set retarder, from W. R. Grace (specific gravity = 1.2-1.3, solids content = 33%)
- Rheocrete 222^{+}, which is aqueous mixture of amines and esters, from Degussa Admixtures, Inc. (specific gravity = 0.98-0.99, solids content = 10-16%)
- Hycrete DSS, which consists of water (70-85%) and a mixture of organic alkenyl dicarboxylic acid salts and additives (15-30%), from Broadview Technologies (specific gravity = 1.04-1.07, solids content = 19.5-20.5%)

Water-cement ratios used in concrete:

- 0.35
- 0.45

The following corrosion protection systems are evaluated:

- Conventional steel cast in concrete with water-cement ratios of 0.35 or 0.45 and in mortar with a water-cement ratio of 0.5

- 316 LN stainless clad reinforcement cast in concrete with a water-cement ratio of 0.45 and in mortar with a water-cement ratio of 0.5
- Conventional epoxy-coated reinforcement cast in concrete with water-cement ratios of 0.35 or 0.45 and in mortar with a water-cement ratio of 0.5, with one of three corrosion inhibitors, DCI-S, Rheocrete 222+, or Hycrete
- Epoxy-coated reinforcement with a primer coat that contains microencapsulated calcium nitrite [$Ca(NO_2)_2$] cast in concrete with water-cement ratios of 0.35 and 0.45 and in mortar with a water-cement ratio of 0.5
- Epoxy-coated reinforcement with zinc chromate pretreatment of the steel to improve adhesion between the epoxy and the steel and epoxy-coated reinforcement using improved adhesion epoxies developed by DuPont and Valspar cast in concrete with a water-cement ratio of 0.45 and in mortar with a water-cement ratio of 0.5, with and without the corrosion inhibitor DCI-S.
- Multiple coated reinforcement cast in concrete with a water-cement ratio of 0.45 and in mortar with a water-cement ratio of 0.5

2.2 RAPID MACROCELL TESTS

The rapid macrocell tests are used to measure the macrocell corrosion rates and corrosion potentials of both bare and mortar-wrapped specimens. The test specimens are designed so that chloride ions can rapidly reach the steel surface, resulting in the early initiation of corrosion.

2.2.1 Materials

a) Mortar – The mortar is made with Type I/II portland cement, ASTM C 778 graded Ottawa sand, and distilled water. The water-cement ratio is 0.5, and the sand-cement ratio is 2.0 by weight.

b) Epoxies for use in specimen fabrication – Herberts O′Brien™ 7-1870 Nap-Guard Rebar Patch Kit, and Sewer Guard HBS 100 Epoxy Liner, from Degussa Admixtures, Inc.

2.2.2 Test Specimens

In the rapid macrocell test, corrosion resistance is evaluated using bare and mortar-wrapped specimens. For conventional and epoxy-coated reinforcement, the bare bar specimens are straight. For stainless steel clad reinforcement, both straight and bent bars are used. All mortar-wrapped bars are straight. Bare bar specimens are prepared as following:

a) Straight bar - The reinforcing bar is cut to a length of 127 mm (5 in.), and the sharp edges on the bar ends are smoothed with a grinder. One end of the bar is drilled and tapped for a No. 10-24 machine screw to a depth of 13 mm (½ in.). The threaded hole is used for an electrical connection. To remove oil, grease and dust, conventional and stainless steel clad bars are cleaned with acetone, while the epoxy-coated bars are cleaned with soap and warm water. On some epoxy-coated, multiple coated, and stainless steel clad bars, the coating or cladding is breeched by four 3.2-mm ($^1/_8$-in.) diameter holes to a depth of 0.4 mm (15 mils) or 1 mm (40 mils), respectively, using a 3.2-mm ($^1/_8$-in) diameter drill bit mounted on a drill press, to simulate damage. On some multiple coated bars, the holes are created to penetrate the epoxy without

damaging the zinc layer underlying the epoxy. This is done using a soldering gun set to a temperature of 400°F, which is above the melting temperature of the epoxy but below the melting temperature of the zinc so that the zinc layer will not be damaged. Two holes are placed on one side, respectively 25 mm (1 in.) and 51 mm (2 in.) from the unthreaded end of the bar. The other two holes are placed in the same pattern on the other side. The unthreaded ends of the epoxy-coated and stainless steel clad bars, which will be submerged during the tests, are protected using a 16-mm ($^5/_8$-in.) diameter, 13-mm ($^1/_2$-in.) high plastic cap half-filled with Herberts O'Brien Rebar Patch Kit epoxy. End protection is not provided to some of the stainless clad bars to evaluate the corrosion performance of the bars with exposed ends.

b) Bent bare bar – The reinforcing bar is cut to a length of 305 mm (12 in.), and the sharp edges on the ends of the bar are smoothed with a grinder. One end of the bar is drilled and tapped for a 10-24 threaded bolt to a depth of 13 mm (½ in.). The bar is then bent cold through 180° around a cylindrical steel mandrel with a diameter of 50 mm (2 in.). Bending causes some small indentations to the bar surface where it contacts with a pin that confines the bar from moving during bending. The bar is then cleaned with acetone. The end and edges around the end of the bar that is not drilled and tapped are covered with Herberts O'Brien Rebar Patch Kit epoxy.

c) Mortar-wrapped specimens consist of a 127 mm (5 in.) long No. 16 [No. 5] reinforcing bar, symmetrically embedded in a 30 mm (1.18 in.) diameter mortar cylinder. The cylinder is 154 mm (6 in.) long and provides a mortar cover of 7 mm around the reinforcing bar. The specimen is shown in Figure 2.1.

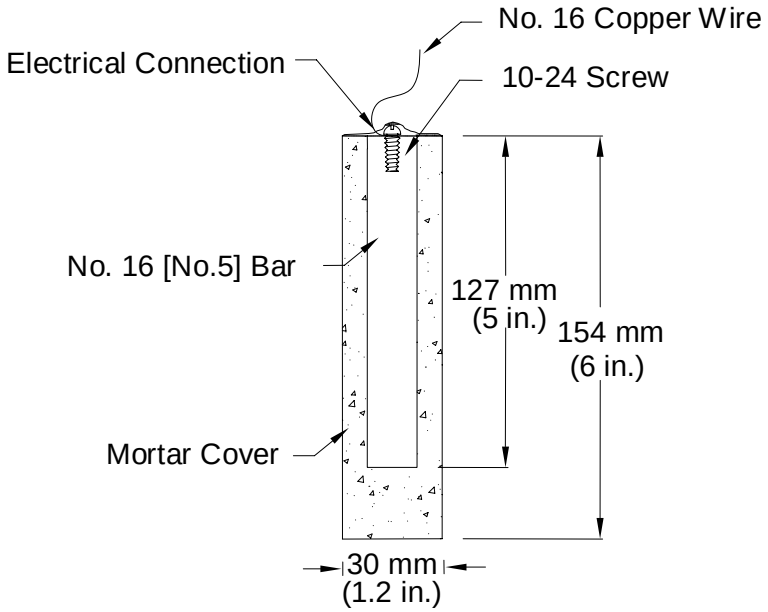

Figure 2.1 - Cross-Section of Mortar-Wrapped Test Specimen Used for Rapid Macrocell Test

The specimen is fabricated in the following order:

a) Reinforcing Bar Preparation – The bars are prepared in the same manner as the straight bare bars, as described earlier.

b) Mold Assembly – The mold used to cast the specimen is made of PVC pipe and fittings that are available at the local hardware store. The specimen mold and mold holder, shown in Figure 2.2, require the following materials:

- One laboratory grade No. 6½ rubber stopper with a centered 4 mm ($^1/_6$ in.) diameter hole (A).
- One ASTM D 2466 32 mm (1¼ in.) to 32 mm (1¼ in.) PVC fitting, 42 mm (1.65 in.) internal diameter, shortened by 14 mm (0.55 in.) on one end (B).

- One ASTM D 2241 SDR 21 25.4 mm (1 in.) PVC pipe, 30 mm (1.18 in.) internal diameter and 154 mm (6 in.) long. The pipe is sliced longitudinally to facilitate the removal of specimen (C).
- Two pieces of 2×8 pressure treated lumber. Holes and recesses are bored into the flat surfaces to hold up to eight specimen molds during casting (D).
- Six threaded rods and wing nuts (E).

Assembly is explained in the following steps:

1) The rubber stopper, A, is inserted in the machined end of the PVC fitting, B. The wider end of the rubber stopper is placed in contact with the internal surface of the PVC fitting.
2) A No. 10-24 bolt is inserted from the hole centered in the rubber stopper. The tapped end of the reinforcing bar is then attached to the bolt.
3) The longitudinal slice along the side of the PVC pipe, C, is covered with masking tape. The pipe is then inserted in the free end of the PVC fitting.
4) The assembled mold is placed through the wooden boards, D, in the holes and recesses provided. The threaded rods, E, are then inserted through the wooden boards. The rods are used to hold the molds together and center the reinforcing bar within the mold by tightening or loosening the wing nuts on the rods.

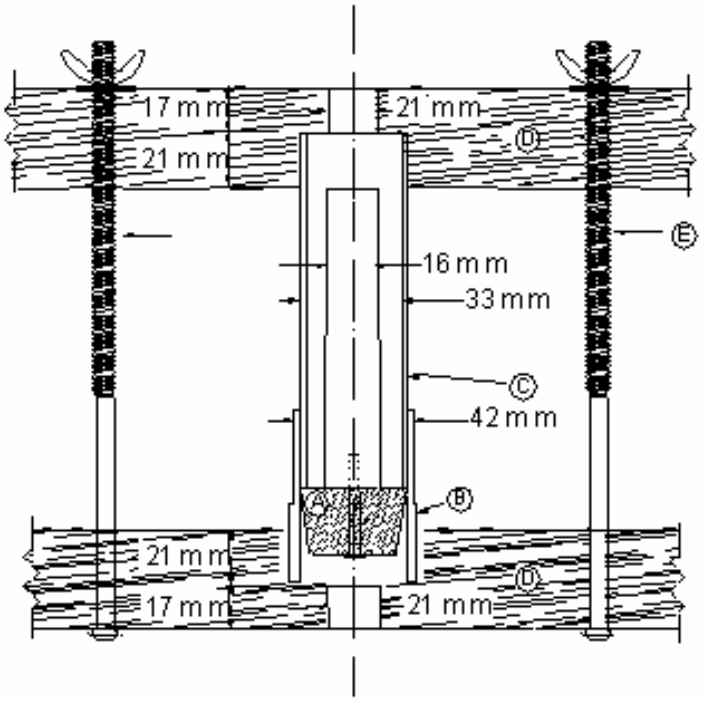

Figure 2.2 - Cross Section of the Mold for Mortar-Wrapped Specimen

c) Mortar – The mortar mixture proportions are given in Table 2.1. The corrosion inhibitor dosage rates are based on the recommended dosage rates for concrete. For 1 m^3 (1.31 yd^3) of concrete, if the recommended dosage rate of a corrosion inhibitor is 1.2 L/m^3 (0.24 gal/yd^3) and the mortar volume is 0.6 m^3 (0.78 yd^3), the dosage rate for mortar should be 1.2/0.6 = 2 L/m^3 (0.4 gal/yd^3). A Hobart mixer, Model N-50, is used for mixing the mortar. Mixing is accomplished in accordance with ASTM C 305: The water and cement are placed in the dry mixer and mixed at a slow speed (140 ± 5 r/min) for 30 seconds. The entire quantity of sand is added slowly over the 30 second period, while mixing at slow speed. Mixing is continued at medium speed (285 ± 10 r/min) for 30 seconds. The mixer is then stopped, and the mortar is

allowed to stand for 1½ minutes. Finally, the mortar is mixed for 1 minute at medium speed (285 ± 10 r/min).

Table 2.1 Mortar Mix Proportions

cement g (oz)	water g (oz)	sand g (oz)	Rheocrete mL (fl. oz)	DCI-S mL (fl. oz)	Hycrete g (oz)
800 (28.2)	400 (14.1)	1600 (56.4)	-	-	-
800 (28.2)	391 (13.8)	1600 (56.4)	10.3 (0.35)	-	-
800 (28.2)	374 (13.2)	1600 (56.4)	-	31 (1.05)	-
800 (28.2)	386.5 (13.6)	1600 (56.4)	-	-	18 (0.63)
Inhibitor dosage rate: Rheocrete 222+: 7.96 L/m^3 (1.61 gal/yd^3) in mortar DCI-S: 23.87 L/m^3 (4.82 gal/yd^3) in mortar Hycrete: 2.25% of cement					

d) Casting – The specimens are cast in four layers of equal height. Each layer is rodded 25 times with a 2 mm (0.08 in.) diameter rod that is 305 mm (12 in.) long. The rod is allowed to penetrate the previous layer. Each layer is then consolidated on a vibrating table with amplitude of 0.15 mm (0.006 in.) and a frequency of 60 Hz for 30 seconds.

e) Curing – After casting, the specimens are cured in the molds for 24 hours at room temperature. They are then removed from the molds and placed in lime-saturated water for 13 days.

After 14 days of curing, the mortar-wrapped specimens are dried with compressed air. The specimens to be used as anodes are hand picked based on minimum visible cracks on the surface. All specimens are then vacuum dried for one day. For both bare bar and mortar-wrapped specimens, a 16-gauge copper wire is attached to the tapped end of each specimen with a 10-24 13-mm (½-in.) long steel screw. The top of the screw, wire, and bar are then coated with two layers of Herberts O'Brien epoxy for bare bars and two layers of Degussa epoxy for mortar-

wrapped bars to prevent crevice corrosion. Each layer is dried for at least 4 hours at room temperature after application prior to the next step.

2.2.3 Test Procedure

The rapid macrocell test (Figures 2.3 and 2.4) measures the macrocell corrosion rates and corrosion potentials of reinforcing steels when they are exposed to specific concentrations of NaCl.

Two specimens are placed in simulated concrete pore solution and act as the cathode, while a third specimen is placed in pore solution with a specific concentration of sodium chloride (1.6 m or 6.04 m) and acts as the anode. The anode and cathode are ionically connected by a salt bridge between the two solutions and are electrically connected by a wire across a 10-ohm resistor. Air, scrubbed to remove CO_2, is supplied to the cathode solution.

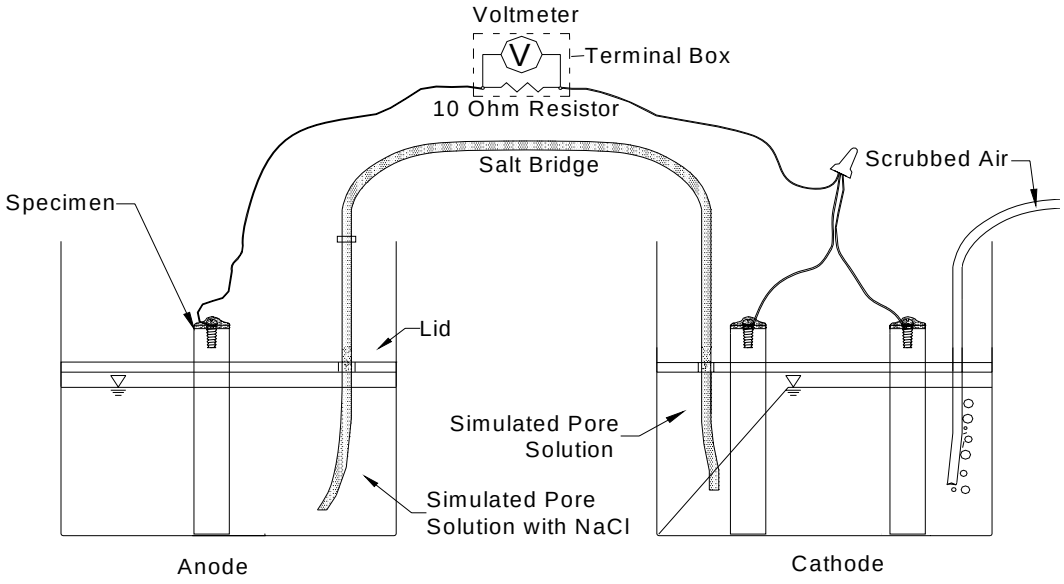

Figure 2.3 - Schematic of the Rapid Macrocell Test (Bare Bar)

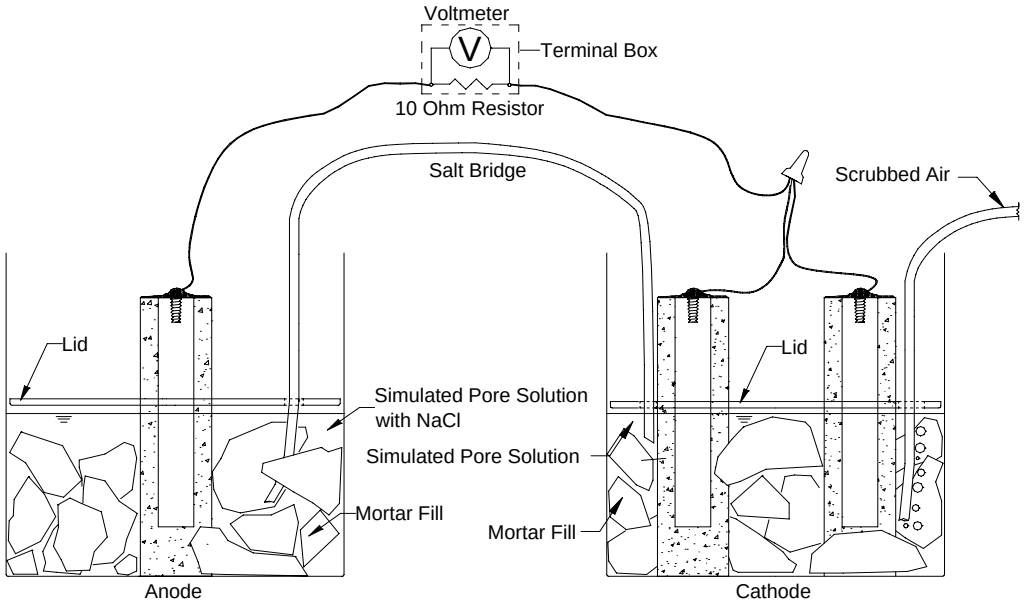

Figure 2.4 - Schematic of the Rapid Macrocell Test (Mortar-Wrapped Specimen)

Details of the test with bare bar specimens follow:

a) Specimen – The bar is prepared according to the procedures described in Section 2.2.2.

b) Concrete Pore Solution – Based on an analysis by Fazammehr (1985), one liter of simulated pore solution contains 974.8 g of distilled water, 18.81 g of KOH, and 17.87 g of NaOH.

c) NaCl Solution – Two molal ion concentrations of NaCl are used in this study: 1.6 m (4.47%) and 6.04 m (15%). To obtain these concentrations, 45.6 g and 172.1 g, respectively, of NaCl are used per liter of pore solution.

d) Container – The specimen and solution are held in a 4.5-liter (1.2-gallon) container with a lid. The container is 178 mm (7 in.) in diameter and 191 mm (7½ in.) in height.

e) Salt Bridge – The salt bridge consists of a conductive gel in a flexible tube. It is prepared following procedures described by Steinbach and King (1950): 4.5 grams of agar, 30 grams of potassium chloride (KCl), and 100 grams of distilled water are mixed and heated over a burner or hotplate until the ingredients start to congeal; the mixture is poured into four flexible Tygon tubes, each 0.6 m (2 feet) long. The salt bridges are then placed in boiling water for about one hour and, after that, are allowed to cool until solid. The gel in the salt bridge should be continuous to provide an ionic path.

f) Resistor – A 10-ohm resistor with 5% tolerance based on manufacturer's specifications (3% actual tolerance was measured for all resistors used in this study) is used to electronically connect the specimens at the anode and cathode.

g) Terminal Box – A terminal box is used to take electrical measurements of the test specimens. The box is 178 × 102 × 51 mm (7 × 4 × 2 in.). Six pairs of binding posts (one red and one black) are attached to the top of the box. A 10-ohm resistor is connected across each pair of binding posts.

h) Wire – An insulated 16 gauge copper wire is used to connect the test specimen to the terminal box.

i) Air Scrubber – Compressed air is used to supply oxygen to the cathode solution. An air scrubber is used to remove the carbon dioxide in the compressed air, because CO_2 lowers the pH of the pore solution. The air scrubber is a 19-liter (5-gallon) plastic container filled with 1M NaOH solution. Compressed air is directed into the scrubber and out to the specimens through latex tubing. The procedure for preparing the air scrubber is explained in the following steps [This procedure is taken from Balma et al. (2005)]:

   1) Two barbed fittings are inserted on the top of the container.
   2) A 1.5 m (5 ft) piece of plastic tubing is cut. On one end of the tubing, 1.2 m (4 ft) is perforated with a knife, making hundreds of holes to allow the air to produce small bubbles. The end of the tubing closest to the holes is sealed with a clamp.
   3) The end with the holes is coiled at the bottom of the container and trap rock is used to hold down the tubing. The other end of the tubing is connected to the inside part of one of the barbed fittings.
   4) The other side of the barbed fitting is connected to a plastic tube, which is connected to the compressed air outlet.
   5) Another piece of plastic tubing is connected to the outside of the other barbed fitting. The air is distributed to the solution surrounding the

cathodes using 0.3 m (1 ft) lengths of latex tubing and polypropylene T-shaped connectors.

6) Screw clamps are placed on the tubing to regulate the amount of air bubbled into each container.

Distilled water is regularly added to the container to replace water that is evaporated. NaOH is also added as needed to maintain the pH of the solution at 12.5.

j) Saturated Calomel Electrode (SCE) – The potential of the specimens is measured with respect to a SCE.

k) Voltmeter – A digital voltmeter with an accuracy of 0.5 μV is used to measure the voltage drop and corrosion potential.

The voltage drop across the resistor and the potentials of anode and cathode with respect to a SCE are measured once a day for the first week and once a week after that. The voltage drop is measured by connecting the voltmeter to the binding posts on the terminal box to which the resistor is connected. The potentials are obtained by immersing an SCE in the solution after disconnecting the wires from the binding posts for at least 2 hours. The SCE and the disconnected wire from the anode or cathode are connected to the voltmeter to measure the potential.

Tests with wrapped specimens (Figure 2.4) are similar to those for the bare bar specimens except that mortar fill is added to the container. The fill is the same as the mortar mix used for the specimens without a corrosion inhibitor (Table 2.1). The fill is cast in metal baking sheets, 25 mm (1 in.) deep, at the same time as the test specimens are fabricated. The mortar is cured for one day and then crushed into pieces no larger than 75 × 75 mm (3 × 3 in.).

2.2.4 Tests Performed

A total of thirty-eight material combinations were tested using the rapid macrocell tests. These include eighteen groups with bare bar specimens in 1.6 m ion concentration NaCl solution, three groups with bare bar specimens in 6.04 m ion concentration NaCl solution, and seventeen groups with mortar-wrapped specimens in 1.6 m ion concentration NaCl solution. The test program is summarized in Table 2.2.

Table 2.2 – Rapid Tests Performed

Bare Bar Specimens			
Steel	**NaCl**	**Number**	
Designation[a]	**Concentration**	**of Specimens**	**Notes**
Conv.	1.6 m	6	
ECR	1.6 m	6	w/ 4 drilled holes
ECR-no holes	1.6 m	3	w/o holes
SMI	1.6 m	6	w/ end cap, w/o holes
SMI-d	1.6 m	6	w/ end cap and holes
SMI-nc	1.6 m	6	w/o end cap, w/o holes
SMIh	6.04 m	6	w/ end cap, w/o holes
SMIh-d	6.04 m	6	w/ end cap and holes
SMIh-nc	6.04 m	6	w/o end cap, w/o holes
SMI-b	1.6 m	6	SMI bent 180 degree as anode
SMI/Conv.	1.6 m	3	SMI w/o holes as anode, Conv. as cathode
Conv./SMI	1.6 m	3	Conv. as anode, SMI w/o holes as cathode
MC(only epoxy penetrated)	1.6 m	6	w/ 4 burned holes
MC(both layers penetrated)	1.6 m	6	w/ 4 drilled holes
ECR(DuPont)	1.6 m	6	w/ 4 drilled holes
ECR(Chromate)	1.6 m	6	w/ 4 drilled holes
ECR(Valspar)	1.6 m	6	w/ 4 drilled holes
MC-no holes	1.6 m	3	w/o holes
ECR(DuPont)-no holes	1.6 m	3	w/o holes
ECR(Chromate)-no holes	1.6 m	3	w/o holes
ECR(Valspar)-no holes	1.6 m	3	w/o holes
Mortar-Wrapped Specimens			
Conv.	1.6 m	6	
ECR	1.6 m	6	w/ 4 drilled holes
ECR-no holes	1.6 m	3	w/o holes
SMI	1.6 m	6	w/ end cap, w/o holes
SMI-d	1.6 m	6	w/ end cap and holes
SMI-nc	1.6 m	6	w/o end cap, w/o holes
ECR(Rheocrete)	1.6 m	6	w/ 4 drilled holes
ECR(DCI)	1.6 m	6	w/ 4 drilled holes
ECR(Hycrete)	1.6 m	6	w/ 4 drilled holes
ECR(primer/$Ca(NO_2)_2$)	1.6 m	6	w/ 4 drilled holes
MC(only epoxy penetrated)	1.6 m	6	w/ 4 burned holes
MC(both layers penetrated)	1.6 m	6	w/ 4 drilled holes
ECR(DuPont)	1.6 m	6	w/ 4 drilled holes
ECR(Chromate)	1.6 m	6	w/ 4 drilled holes
ECR(Valspar)	1.6 m	6	w/ 4 drilled holes
ECR(DuPont)-DCI	1.6 m	6	w/ 4 drilled holes
ECR(Chromate)-DCI	1.6 m	6	w/ 4 drilled holes
ECR(Valspar)-DCI	1.6 m	6	w/ 4 drilled holes
ECR(Rheocrete)-no holes	1.6 m	3	w/o holes
ECR(DCI)-no holes	1.6 m	3	w/o holes
ECR(Hycrete)-no holes	1.6 m	3	w/o holes
ECR(primer/$Ca(NO_2)_2$)-no holes	1.6 m	3	w/o holes
MC-no holes	1.6 m	3	w/o holes
ECR(DuPont)-no holes	1.6 m	3	w/o holes
ECR(Chromate)-no holes	1.6 m	3	w/o holes
ECR(Valspar)-no holes	1.6 m	3	w/o holes

Table 2.2 continued:

[a] Conv. = conventional steel. ECR= normal epoxy-coated steel.
SMI = Stainless steel clad reinforcement SMI-316 SC™ reinforcing bars.
ECR(Rheocrete) = normal ECR in concrete with corrosion inhibitor Rheocrete
ECR(DCI) = normal ECR in concrete with corrosion inhibitor DCI
ECR(Hycrete) = normal ECR in concrete with corrosion inhibitor Hycrete
ECR(primer/$Ca(NO_2)_2$)= ECR with calcium nitrite primer
MC(both layers penetrated)=multiple coated bars with both layers penetrated.
MC(only epoxy penetrated) = multiple coated bars with only epoxy penetrated
ECR(DuPont) = high adhesion Dupont bars.
ECR(Chromate) = ECR with chromate pretrement
ECR(Valspar) = high adhesion Valspar bars.
ECR(DuPont)-DCI = ECR(Dupont) in mortar with corrosion inhibitor DCI
ECR(Chromate)-DCI = ECR(Chromate) in mortar with corrosion inhibitor DCI
ECR(Valspar)-DCI = ECR(Valspar) in mortar with corrosion inhibitor DCI

2.3 BENCH-SCALE TESTS

The Southern Exposure (SE), cracked beam (CB), and ASTM G 109 tests are accelerated tests used to study macrocell corrosion of reinforcing bars in concrete when exposed to NaCl solution. Measurements include macrocell corrosion rate, corrosion potential, and mat-to-mat resistance. At this writing, the tests have reached between 14 and 52 weeks and will last a total of 96 weeks.

2.3.1 Materials

a) Concrete – The concrete is air entrained, with 6% air (±1%), and a 76 mm (3 in.) slump [±13 mm (±0.5 in.)]. Two water-cement ratios, 0.45 or 0.35, are used. The concrete materials are:
   1) Cement - Type I/II portland cement.
   2) Coarse aggregate - 19 mm (¾ in.) Crushed limestone, from Fogle Quarry, KS [bulk specific gravity (ssd) = 2.58, absorption (dry) = 2.33%].
   3) Fine aggregate – Kansas River sand, KS [bulk specific gravity (ssd) = 2.62, absorption (dry) = 0.52%].
   4) Air Entraining Agent – Daravair 1400, from W. R. Grace, Inc.

b) Epoxy coating for specimen fabrication – Sewer Guard HBS 100 Epoxy Liner, from Degussa Admixtures, Inc.

c) Silicone Caulk –100 percent silicone caulk manufactured by Macklenburg-Duncan.

2.3.2 Test Specimens

The Southern Exposure test specimen is shown in Figure 2.5. It consists of six reinforcing bars embedded in a concrete block with a length of 305 mm (12 in.), a width of 305 mm (12 in.), and a height of 178 mm (7 in.). Two reinforcing bars are placed with a clear cover of 25 mm (1 in.) from the top of the specimen and four reinforcing bars are placed with a clear cover of 25 mm (1 in.) from the bottom. Each bar is 305 mm (12 in.) long. The bars are drilled and tapped at both ends to provide connections for bolts so that they can be fixed in molds and to provide an electrical connection to the bars during tests. A dam is cast around the top surface of the specimen to facilitate ponding during the test.

The cracked beam test specimen is shown in Figure 2.6. The specimen is similar to the SE specimen, except it is one-half the width, with one bar on the top and two bars on the bottom. A 0.3-mm (0.012-in.) wide, 152-mm (6-in.) long simulated crack is placed in the concrete parallel to the top bars, as will be described in Section 2.3.3.

The ASTM G 109 test specimen is shown in Figure 2.7. The specimen is 279 mm (11 in.) long, 114 mm (4.5 in.) wide, and 152 mm (6 in.) high. Similar to the cracked beam specimen, the ASTM G 109 specimen contains one bar in the top layer and two bars in the bottom layer. A Plexiglas dam is attached to the top of the specimen for ponding the salt solution. The dam has dimensions of 150 mm (6 in.) × 75 mm (3 in.).

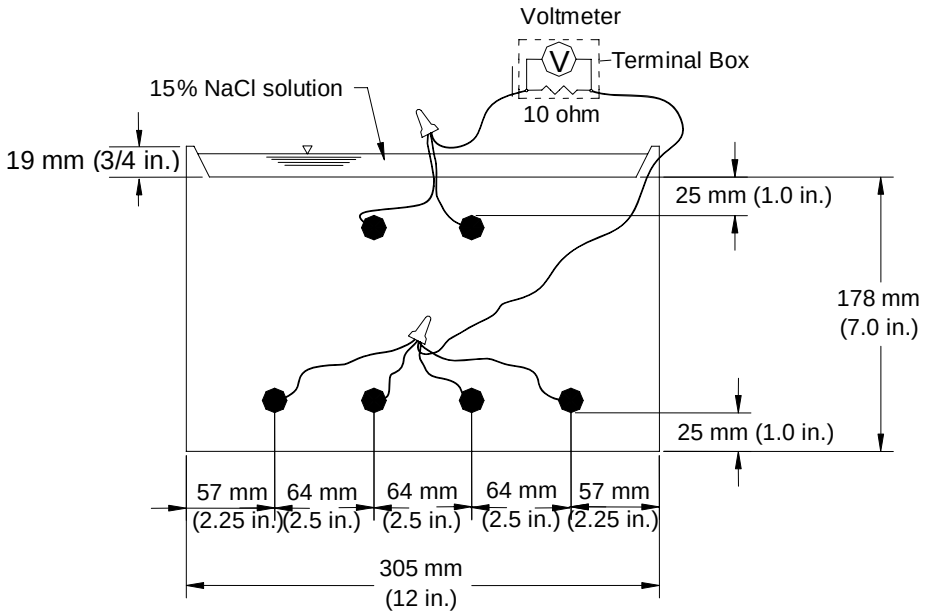

Figure 2.5 - Test Specimen for Southern Exposure Test

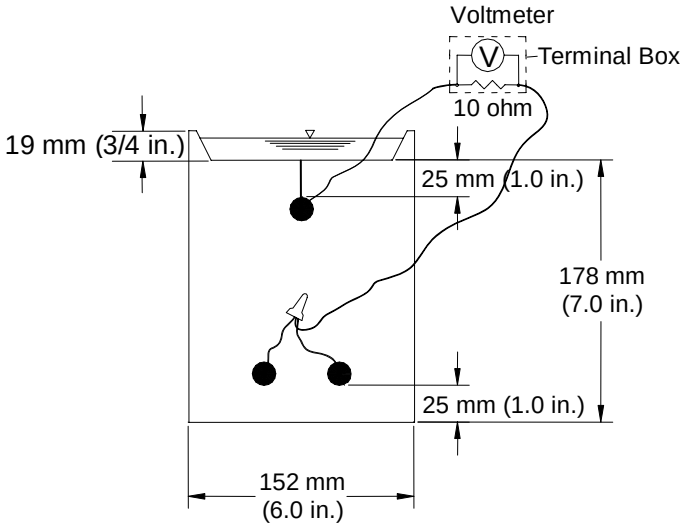

Figure 2.6 - Test Specimen for Cracked Beam Test

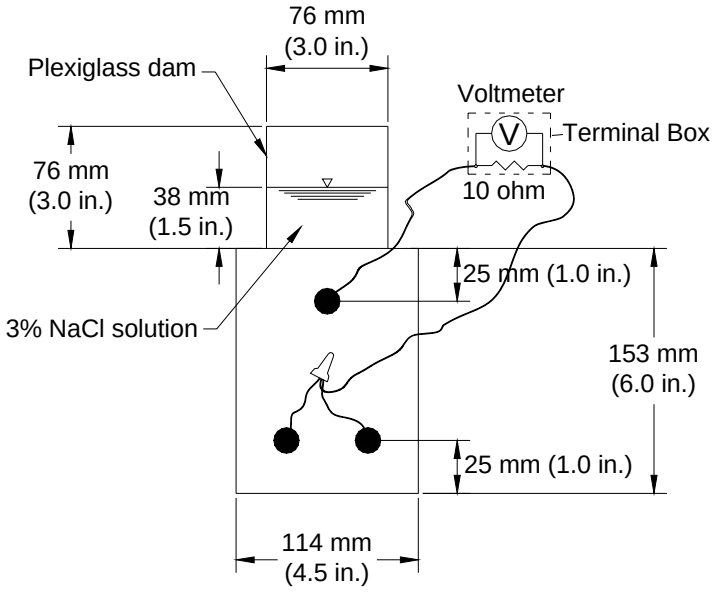

Figure 2.7 – Test Specimen for ASTM G 109 Test

2.3.3 Test Specimen Fabrication

The SE, CB, and ASTM G 109 specimens are fabricated as follows:

a) Reinforcing Bar Preparation – For conventional and epoxy-coated reinforcement, all of the bars used in the bench-scale specimens are straight. For stainless steel clad reinforcement, most bars are straight, while a few are bent for use in SE specimens.

   a. Straight bars - each reinforcing bar is cut to a length of 305 mm (12 in.) for the SE and CB specimens and 279 mm (11 in.) for the ASTM G 109 specimens. Both ends of the bar are drilled and tapped for a 10-24 threaded bolt to a depth of 13 mm (½ in.). Conventional and stainless steel clad bars are then cleaned with acetone, while epoxy-coated bars are cleaned with soap and warm water. For all epoxy-coated, some multiple coated, and some stainless steel clad bars, the coating or cladding is drilled with four or ten 3.2-mm (⅛-in.) diameter holes, using a 3.2-mm (⅛-in.)

diameter drill bit mounted on a drill press, to simulate defects in the coating. The holes are drilled to a depth of 0.4 mm (15 mils) from the surface of the epoxy and 1 mm (40 mils) from the surface of the cladding. On some multiple coated bars, the holes are made to penetrate the epoxy without damaging the zinc layer. This is done using a soldering gun set to a temperature of 205°C (400°F), which is above the melting temperature of the epoxy but below the melting temperature of zinc so that the zinc layer will not be damaged.

b. Bent bars - each reinforcing bar is cut to a length of 686 mm (27 in.). Both ends of the bar are drilled and tapped for a 10-24 threaded bolt to a depth of 13 mm (0.5 in.). The bar is then bent cold through 180° around a cylindrical mandrel with a diameter of 50 mm (2 in.). Bending causes some small indentations on the bar surface where it contacts with a pin that confines the bar from moving during bending. The bar is then cleaned with acetone.

b) Form Assembly – The forms are made of 19-mm (¾-in.) thick plywood and consist of four sides and a bottom. For the SE and CB specimens, a rectangular piece of wood with beveled edge that is slightly smaller than the bottom is bolted to the bottom piece to create a dam in the edge of the specimen when the specimen is cast upside down. The five pieces are fastened with metal clamps, and the inside corners are sealed with caulk. Small holes are drilled in two sides of the assembled mold to support the reinforcing bars using bolts. For the cracked beam specimens, a slot is cut in the bottom of the form and a 0.3-mm (0.012-in.) wide, 152-mm (6-in.) long stainless steel shim is inserted to produce a simulated crack to the steel surface.

c) Concrete Mixing – Concrete is mixed following the requirements of ASTM C 192. The mix proportions are given in Table 2.3.

Table 2.3 Concrete Mix Proportions

w/c	cement	water	Fine Aggregate	Coarse Aggregate	Air-entraining Agent	Rheocrete	DCI-S	Hycrete	S.P.*
	kg/m^3 (lb/yd^3)	kg/m^3 (lb/yd^3)	kg/m^3 (lb/yd^3)	kg/m^3 (lb/yd^3)	mL/m^3 (gal/yd^3)	mL/m^3 (gal/yd^3)	mL/m^3 (gal/yd^3)	kg/m^3 (lb/yd^3)	mL/m^3 (gal/yd^3)
0.45	355 (598)	160 (270)	852 (1436)	874 (1473)	90 (0.02)	-	-	-	-
	355 (598)	155.7 (262)	852 (1436)	874 (1473)	320 (0.06)	5000 (1.01)	-	-	-
	355 (598)	147.4 (248)	852 (1436)	874 (1473)	140 (0.03)	-	15000 (3.03)	-	-
	355 (598)	154 (260)	852 (1436)	874 (1473)	35 (0.01)	-	-	8 (13.5)	-
0.35	438 (738)	153 (258)	764 (1288)	862 (1453)	355 (0.07)	-	-	-	1765 (0.36)
	438 (738)	146.7 (247)	764 (1288)	862 (1453)	2648 (0.53)	5000 (1.01)	-	-	1765 (0.36)
	438 (738)	140.4 (237)	764 (1288)	862 (1453)	740 (0.15)	-	15000 (3.03)	-	2120 (0.43)
	438 (738)	145.6 (245)	764 (1288)	862 (1453)	330 (0.07)	-	-	9.9 (16.7)	2120 (0.43)
Inhibitor dosage rate: Rheocrete 222+: 5 L/m^3 (1.01 gal/yd^3); DCI-S: 15 L/m^3 (3.03 gal/yd^3); Hycrete: 2.25% of cement									

*S.P.= superplasticizer, Rheobuild 1000

d) Specimen Casting – The specimens are cast in two layers. In accordance to ASTM C 192, each layer is consolidated on a vibrating table with amplitude of 0.15 mm (0.006 in.) and a frequency of 60 Hz for 30 seconds. The upper surface is finished with a wooden float. Southern Exposure and cracked beam specimens are cast in an inverted position.

e) Specimen Curing – After the specimens are cast, the molds are covered with plastic, and the SE specimens are cured for 24 hours while CB specimens are cured between 8 to 12 hours at room temperature. The SE and CB specimens are then removed from the molds and cured in a plastic bag containing water at room temperature until 72 hours after casting. The specimens are then removed from the bag and cured in air for 25 days at a relative humidity of 50%. After the first 24 hours, the G 109 specimens are removed from the molds and placed in a curing room, with a temperature of 23 ± 2°C (73.4 ± 3.6°F) and a relative humidity above 95%, for 28 days. The G 109 specimens

are then allowed to dry for 2 weeks at a relative humidity of 50%. Before the test begins, the upper surface of the SE and CB specimens are lightly sanded with 150 grit sandpaper.

f) Cracked Beam Specimen – Between 8 and 12 hours after casting, the stainless steel shim is removed.

g) Concrete Epoxy – Before testing begins, two coats of the Degussa epoxy are applied to the vertical sides of the specimen. The epoxy is mixed and applied according to the recommendations of the manufacturer.

h) Plexiglas dams – The dams are attached to top of the G 109 specimens using superglue 42 days after casing. The joints are sealed with silicone to avoid leaking.

i) Wiring – One day before testing begins; 16-gauge copper wires are used to connect the top and bottom steel to the exterior binding post on a terminal box. The exposed connections are also coated with two layers of the Degussa epoxy.

2.3.4 Bench-Scale Test Procedures

The test procedures are the same for the Southern Exposure and cracked beam tests. Ponding-drying cycles and ponding cycles are designed to accelerate the diffusion of chloride ions into the concrete.

a) Ponding-drying cycle — A 15% (6.04 m ion) NaCl solution is ponded on the top of the specimen for four days at room temperature [21 ± 1.5°C (70 ± 3°F)]. The specimens are covered with a plastic sheet to reduce evaporation. After four days, the voltage drop and the mat-to-mat resistance of the specimen are measured. The salt solution is removed using a shop vacuum cleaner and the corrosion potentials of the anode and the cathode are

measured. The specimens are then heated to 38 ± 1.5°C (100 ± 3°F) for three days under a portable heating tent to complete one cycle of testing. The specimens undergo 12 cycles (weeks) of testing.

b) Ponding Cycle — the 15% NaCl solution is ponded continuously on the top of the specimen for 12 weeks at room temperature. The specimens are covered with a plastic sheet to reduce evaporation. On the fourth day of each week, the voltage drop, mat-to-mat resistance, and corrosion potential of the specimens are measured.

The two 12-week cycles are alternated for a total test period of 96 weeks.

The ponding and drying cycles in the G 109 test are different from those used in the SE and CB tests. For the G 109 test, a 3% NaCl solution is ponded on the top of the specimens for two weeks. The solution is then removed with a vacuum cleaner and the specimens are kept dry at room temperature for two weeks. The ponding and drying cycles are repeated during the full test period.

Details of the test with SE, CB and G 109 specimens follow:

a) Specimen – The specimen is prepared according to the procedures described in Section 2.3.3.

b) Ponding Solution – For the SE and CB specimens, 1 kg of ponding solution contains 850 g of distilled water and 150 g of NaCl. For the ASTM G 109 specimens, 1 kg of ponding solution consists of 970 g of distilled water and 30 g of NaCl.

c) Heating Tent – The heating tent used for the ponding-drying cycles for the SE and CB specimens is movable and can hold up to 12 SE and 12 CB specimens. The tent is 1.2 m (3.5 ft) high, 1.33 m (4 ft) wide, and 2.67 m (8 ft) long. The roof and ends are made of 19 mm (3/4 in.) thick plywood and are connected by

six 2.67 m (8 ft) 2 × 4 studs. The sides of the tent are covered with two layers of plastic sheeting, separated by 25 mm (1 in.). Three 250-watt heating lamps are evenly spaced along the roof of the tent. When the tent is placed over the specimens, the lamps are 450 mm (18 in.) above the specimens. A thermostat is used to maintain the required temperature.

d) Resistor – For the SE and CB specimens, a 10-ohm resistor is used to connect the top and bottom mats. For the ASTM G 109 specimens, a 100-ohm resistor is used. The tolerance of these resistors is 5% based on manufacturer's specifications; a lower tolerance, 3%, was measured for the resistors used in this study.

e) Terminal Box and Wire – The terminal box and wire are the same as described in Section 2.2.3.

f) Saturated Calomel Electrode (SCE) – The potentials of specimens are measured with respect to a SCE during ponding cycles.

g) Copper-Copper Sulfate Electrode (CSE) – The potentials of specimens are measured with respect to a CSE during ponding-drying cycles.

h) Ohmmeter – An AC milliohmmeter with accuracy of 0.1 ohm is used to measure the resistance between top and bottom mats.

i) Voltmeter – The voltmeter is the same as described in Section 2.2.3.

The voltage drop, mat-to-mat resistance, and corrosion potentials of both top and bottom mats of steel are measure once a week. The voltage drop is measured across the resistor when the circuit is closed. The circuit is then disconnected and the mat-to-mat resistance is measured. Two hours after disconnecting the circuit, the corrosion potentials of both mats of steel are measured. For specimens in the ponding cycle, the corrosion potential is measured by immersing a saturated calomel electrode

(SCE) in the solution. For specimens in the ponding-drying cycle, the corrosion potential is obtained using a copper-copper sulfate electrode (CSE) in contact with the surface at the beginning of each drying period. The CSE gives corrosion potentials that are approximately 75 mV more negative than those measured with a SCE.

2.3.5 Tests Performed

The Southern Exposure, cracked beam and ASTM G 109 tests are currently underway. The Southern Exposure and cracked beam tests are used for all corrosion protection systems evaluated in this study, while the ASTM G 109 tests are only used for specimens containing multiple coated steel and the control (conventional and epoxy-coated steel) specimens. ASTM G 109 tests provide a lower gradient with respect to chloride content than do the SE tests and involve relatively slow wet-dry cycling that is more conductive and perhaps more realistic for the evaluation of zinc systems. The test specimens were fabricated between January and December 2004.

The tests are summarized in Tables 2.4-2.6. The results as of March 15, 2005 are summarized in Chapter 3.

Table 2.4 Southern Exposure Test

Steel Designation[a]	Number of Specimens	Notes
Conv.	6	
ECR	6	w/ 4 drilled holes
Conv.-35	3	w/c=0.35
ECR-10h	3	w/ 10 drilled holes
ECR-10h-35	3	w/ 10 drilled holes, w/c=0.35
SMI-d	6	w/4 drilled holes
SMI	6	w/o drilled holes
SMI/Conv.	3	SMI w/o holes at top, Conv. at bottom
Conv./SMI	3	Conv. at top, SMI w/o holes at bottom
SMIb	3	SMI bent 180 degree at top
ECR(Rheocrete)	3	w/ 4 drilled holes
ECR(Rheocrete)-10h	3	w/ 10 drilled holes
ECR(Rheocrete)-10h-35	3	w/ 10 drilled holes, w/c=0.35
ECR(DCI)	3	w/ 4 drilled holes
ECR(DCI)-10h	3	w/ 10 drilled holes
ECR(DCI)-10h-35	3	w/ 10 drilled holes, w/c=0.35
ECR(Hycrete)	3	w/ 4 drilled holes
ECR(Hycrete)-10h	3	w/ 10 drilled holes
ECR(Hycrete)-10h-35	3	w/ 10 drilled holes, w/c=0.35
ECR(primer/$Ca(NO_2)_2$)	3	w/ 4 drilled holes
ECR(primer/$Ca(NO_2)_2$)-10h	3	w/ 10 drilled holes
ECR(primer/$Ca(NO_2)_2$)-10h-35	3	w/ 10 drilled holes, w/c=0.35
MC(only epoxy penetrated)	3	w/ 4 burned holes
MC(only epoxy penetrated)-10h	3	w/ 10 burned holes
MC(both layers penetrated)	3	w/ 4 drilled holes
MC(both layers penetrated)-10h	3	w/ 10 drilled holes
ECR(Chromate)	3	w/ 4 drilled holes
ECR(Chromate)-10h	3	w/ 10 drilled holes
ECR(Chromate)-DCI	3	w/ 4 drilled holes, cast with DCI
ECR(DuPont)	3	w/ 4 drilled holes
ECR(DuPont)-10h	3	w/ 10 drilled holes
ECR(DuPont)-DCI	3	w/ 4 drilled holes, cast with DCI
ECR(Valspar)	3	w/ 4 drilled holes
ECR(Valspar)-10h	3	w/ 10 drilled holes
ECR(Valspar)-DCI	3	w/ 4 drilled holes, cast with DCI

[a] Conv. = conventional steel. ECR= normal epoxy-coated steel.

SMI = Stainless steel clad reinforcement SMI-316 SC™ reinforcing bars.

ECR(Rheocrete) = normal ECR in concrete with corrosion inhibitor Rheocrete

ECR(DCI) = normal ECR in concrete with corrosion inhibitor DCI

ECR(Hycrete) = normal ECR in concrete with corrosion inhibitor Hycrete

ECR(primer/$Ca(NO_2)_2$)= ECR with calcium nitrite primer

MC(both layers penetrated)=multiple coated bars with both layers penetrated.

MC(only epoxy penetrated) = multiple coated bars with only epoxy penetrated

ECR(Chromate) = ECR with chromate pretrement

ECR(DuPont) = high adhesion Dupont bars.

ECR(Valspar) = high adhesion Valspar bars.

ECR(Chromate)-DCI = ECR(Chromate) in concrete with corrosion inhibitor DCI

ECR(DuPont)-DCI = ECR(Dupont) in concrete with corrosion inhibitor DCI

ECR(Valspar)-DCI = ECR(Valspar) in concrete with corrosion inhibitor DCI

10h = epoxy coated bar penetrated with 10 holes, otherwise 4 holes

35 = concrete w/c=0.35, otherwise w/c=0.45

Table 2.5 Cracked Beam Test

Steel Designation[a]	Number of Specimens	Notes
Conv.	6	
ECR	6	w/ 4 drilled holes
Conv.-35	3	w/c=0.35
ECR-10h	3	w/ 10 drilled holes
ECR-10h-35	3	w/ 10 drilled holes, w/c=0.35
SMI-d	6	w/4 drilled holes
SMI	6	w/o drilled holes
ECR(Rheocrete)	3	w/ 4 drilled holes
ECR(Rheocrete)-10h	3	w/ 10 drilled holes
ECR(Rheocrete)-10h-35	3	w/ 10 drilled holes, w/c=0.35
ECR(DCI)	3	w/ 4 drilled holes
ECR(DCI)-10h	3	w/ 10 drilled holes
ECR(DCI)-10h-35	3	w/ 10 drilled holes, w/c=0.35
ECR(Hycrete)	3	w/ 4 drilled holes
ECR(Hycrete)-10h	3	w/ 10 drilled holes
ECR(Hycrete)-10h-35	3	w/ 10 drilled holes, w/c=0.35
ECR(primer/$Ca(NO_2)_2$)	3	w/ 4 drilled holes
ECR(primer/$Ca(NO_2)_2$)-10h	3	w/ 10 drilled holes
ECR(primer/$Ca(NO_2)_2$)-10h-35	3	w/ 10 drilled holes, w/c=0.35
MC(only epoxy penetrated)	3	w/ 4 burned holes
MC(only epoxy penetrated)-10h	3	w/ 10 burned holes
MC(both layers penetrated)	3	w/ 4 drilled holes
MC(both layers penetrated)-10h	3	w/ 10 drilled holes
ECR(Chromate)	3	w/ 4 drilled holes
ECR(Chromate)-10h	3	w/ 10 drilled holes
ECR(DuPont)	3	w/ 4 drilled holes
ECR(DuPont)-10h	3	w/ 10 drilled holes
ECR(Valspar)	3	w/ 4 drilled holes
ECR(Valspar)-10h	3	w/ 10 drilled holes

[a] Conv. = conventional steel. ECR= normal epoxy-coated steel.

SMI = Stainless steel clad reinforcement SMI-316 SC™ reinforcing bars.

ECR(Rheocrete) = normal ECR in concrete with corrosion inhibitor Rheocrete

ECR(DCI) = normal ECR in concrete with corrosion inhibitor DCI

ECR(Hycrete) = normal ECR in concrete with corrosion inhibitor Hycrete

ECR(primer/$Ca(NO_2)_2$)= ECR with calcium nitrite primer

MC(both layers penetrated)=multiple coated bars with both layers penetrated.

MC(only epoxy penetrated) = multiple coated bars with only epoxy penetrated

ECR(Chromate) = ECR with chromate pretrement

ECR(DuPont) = high adhesion Dupont bars.

ECR(Valspar) = high adhesion Valspar bars.

10h = epoxy coated bar penetrated with 10 holes, otherwise 4 holes

35 = concrete w/c=0.35, otherwise w/c=0.45

Table 2.6 ASTM G 109 Test

Steel Designation[a]	Number of Specimens	Notes
Conv.	6	
ECR	3	w/ 4 drilled holes
ECR-10h	6	w/ 10 drilled holes
MC(only epoxy penetrated)	3	w/ 4 burned holes
MC(only epoxy penetrated)-10h	3	w/ 10 burned holes
MC(both layers penetrated)	3	w/ 4 drilled holes
MC(both layers penetrated)-10h	3	w/10 drilled holes

[a] Conv. = conventional steel. ECR= normal epoxy-coated steel.
MC(both layers penetrated)=multiple coated bars with both layers penetrated.
MC(only epoxy penetrated) = multiple coated bars with only epoxy penetrated
10h = epoxy coated bar penetrated with 10 holes, otherwise 4 holes

2.4 POLARIZATION RESISTANCE TESTS

Polarization resistance tests are used to obtain the microcell corrosion rates for bench-scale specimens. In the tests, cell current readings are taken during a short, slow sweep of the potential. The sweep typically is from -20 to +20 mV relative to open circuit potential E_{oc}. In this range, the current versus voltage curve is roughly linear. A linear fit of the data to a standard model gives an estimate of the polarization resistance R_u, which can be used to calculate corrosion density I_{corr} and corrosion rate. The tests are performed using a PC4/750 Potentiostat and DC105 corrosion measurement system from Gamry Instruments.

Figure 2.8 shows a sample input screen from the DC105 software. In Figure 2.8, *Initial E* and *Final E* define the starting and ending points for the potential sweep during data acquisition, respectively. *Scan rate* defines the speed of the potential sweep in mV/sec. *Sample period* determines the spacing between data points. *Sample area* is the surface area of the sample (in cm^2) exposed to the solution. *Density and Equiv. Wt*. are the density (in g/cm2) and equivalent weight (atomic weight of an

element divided by its valence) of iron, respectively. *Beta An.* and *Beta Cat.* are the anodic and cathodic Tafel slopes, respectively?

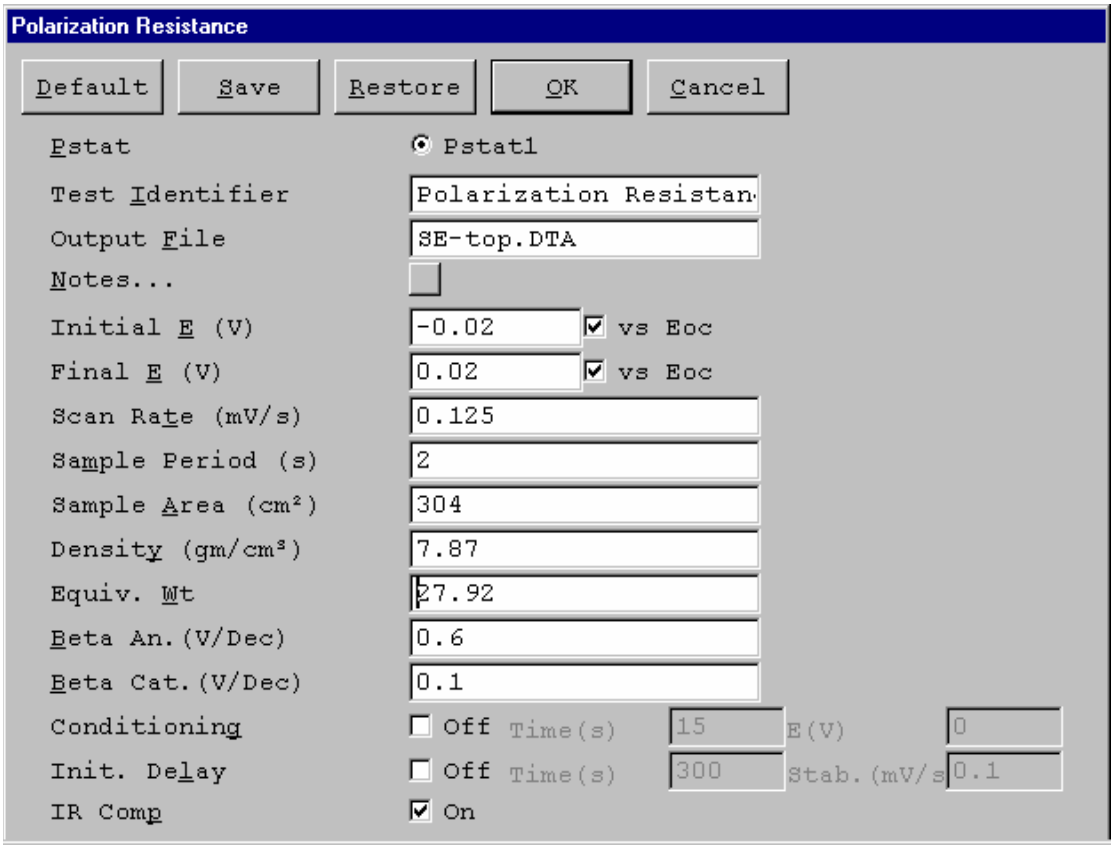

Figure 2.8 – Input screen for polarization resistance tests

The tests are carried out every four weeks for bench-scale specimens to obtain the microcell corrosion rates for top and bottom mats, separately, when the circuits are disconnected; and every eight weeks for the same specimens to determine the microcell corrosion rates when the circuits are connected. In the tests, the top or bottom mats are used as the working electrode, a saturated calomel electrode immersed in salt solution on the top of the specimen is used as the reference electrode, and a platinum strip immersed in salt solution on the top of the specimen is used as the counter electrode.

The data file from a polarization resistance test is analyzed by the Polres data analysis package provided with the DCI 105. This analysis software can read the data file and plot a graph based on the data in the file. When a new graph is created in this package, the user picks a range of region in the graph and the software automatically uses a linear fit of the data in the selected range to calculate the polarization resistance. Then, the corrosion current density and corrosion rate can be determined using the polarization resistance.

In this study, the tests performed are summarized in Table 2.7. For specimens containing conventional, epoxy-coated, and multiple coated steel, one each of Southern Exposure, cracked beam, and ASTM G 109 specimen is chosen for linear polarization resistance testing. For the other corrosion protection systems listed in Table 2.7, one each of Southern Exposure and cracked beam specimen is selected.

Table 2.7 – Polarization Resistance Tests

Steel Designation[a]	**Type of Specimen**
Conv.	SE, CB, G109
ECR	SE, CB, G109
Conv.-35	SE, CB
ECR-10h	SE, CB, G109
ECR-10h-35	SE, CB
ECR(Rheocrete)	SE, CB
ECR(Rheocrete)-10h	SE, CB
ECR(Rheocrete)-10h-35	SE, CB
ECR(DCI)	SE, CB
ECR(DCI)-10h	SE, CB
ECR(DCI)-10h-35	SE, CB
ECR(Hycrete)	SE, CB
ECR(Hycrete)-10h	SE, CB
ECR(Hycrete)-10h-35	SE, CB
ECR(primer/$Ca(NO_2)_2$)	SE, CB
ECR(primer/$Ca(NO_2)_2$)-10h	SE, CB
ECR(primer/$Ca(NO_2)_2$)-10h-35	SE, CB
MC(only epoxy penetrated)	SE, CB, G109
MC(only epoxy penetrated)-10h	SE, CB, G109
MC(both layers penetrated)	SE, CB, G109
MC(both layers penetrated)-10h	SE, CB, G109
ECR(Chromate)	SE, CB
ECR(Chromate)-10h	SE, CB
ECR(Chromate)-DCI	SE, CB
ECR(DuPont)	SE, CB
ECR(DuPont)-10h	SE, CB
ECR(DuPont)-DCI	SE, CB
ECR(Valspar)	SE, CB
ECR(Valspar)-10h	SE, CB
ECR(Valspar)-DCI	SE, CB

[a] Conv. = conventional steel. ECR= normal epoxy-coated steel.
ECR(Rheocrete) = normal ECR in concrete with corrosion inhibitor Rheocrete
ECR(DCI) = normal ECR in concrete with corrosion inhibitor DCI
ECR(Hycrete) = normal ECR in concrete with corrosion inhibitor Hycrete
ECR(primer/$Ca(NO_2)_2$)= ECR with calcium nitrite primer
MC(both layers penetrated)=multiple coated bars with both layers penetrated.
MC(only epoxy penetrated) = multiple coated bars with only epoxy penetrated
ECR(Chromate) = ECR with chromate pretrement
ECR(DuPont) = high adhesion Dupont bars.
ECR(Valspar) = high adhesion Valspar bars.
ECR(Chromate)-DCI = ECR(Chromate) in concrete with corrosion inhibitor DCI
ECR(DuPont)-DCI = ECR(Dupont) in concrete with corrosion inhibitor DCI
ECR(Valspar)-DCI = ECR(Valspar) in concrete with corrosion inhibitor DCI
10h = epoxy coated bar penetrated with 10 holes, otherwise 4 holes
35 = concrete w/c=0.35, otherwise w/c=0.45

2.5 CATHODIC DISBONDMENT TESTS

Cathodic disbondment tests are performed on conventional epoxy-coated steel, epoxy-coated reinforcement with chromate pretreatment, and epoxy-coated reinforcement using improved adhesion epoxies developed by DuPont and Valspar.

Details of the test follow:

a) Test Vessel – A 4.5-liter plastic container with lid is used as test vessel. The container is 178 mm (7 in.) in diameter and 191 mm (7.5 in.) in height.

b) Test Specimen – The test specimens is a 250-mm (10-in.) long epoxy-coated reinforcing bar.

c) Anode – The anode is a 150-mm (6-in.) long solid platinum electrode [1.6 mm (0.06 in.) nominal diameter] or platinized wire [3.2 mm (0.125 in.) nominal diameter].

d) Connectors – A 14-gage, insulated copper wire connects the anode to test specimen. The wire is bolted to the nonimmersed end of the test specimen, and the top of screw, wire, and bar are coated with two layer of Herberts O'Brien epoxy.

e) Reference Electrode – A saturated calomel electrode is used.

f) Electrolyte – The electrolyte solution is 3% NaCl by mass dissolved in distilled water.

The tests are accomplished according to ASTM A 775 and G 8: The coating of test specimen is damaged using a 3.2-mm (1/8-in) diameter drill bit mounted on a drill press. The specimen is then immersed in the electrolyte and connected to the anode as shown in Figure 2.9. The holiday is positioned so that it faces away from the anode. The test specimen is marked at the correct immersion level with a grease pencil and the level is maintained by the daily addition of distilled water. The

electrolyte temperature is kept at 24 ± 2° C (75 ± 3.6° F). To ascertain whether the test cell is functioning, the potential between test specimen and the reference electrode is measured immediately after starting the test and immediately before terminating it. The test lasts 168 hours.

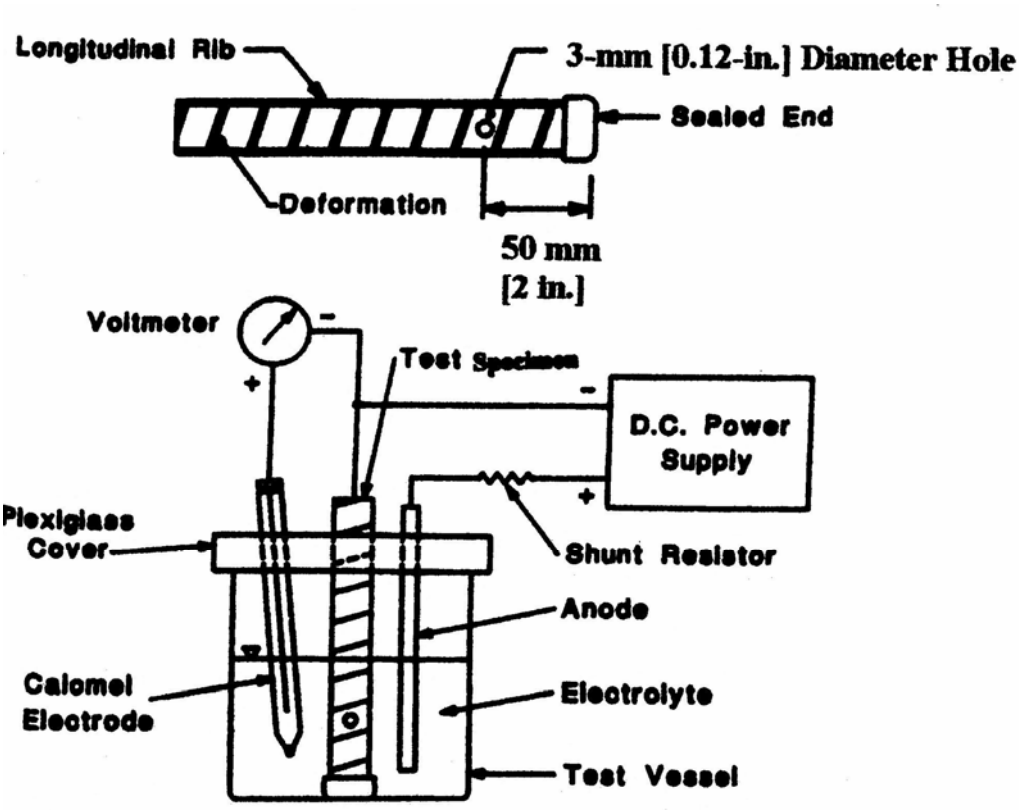

Figure 2.9 - Cathodic Disbondment Test Equipment Configuration (from ASTM A 775)

An examination is performed immediately upon termination of the test as follows: At the end of the test period, the cell is disassembled and the test area is rinsed with warm tap water. The sample is immediately wiped dry and the entire test area coating is visually examined at the edge of the holiday. A new holiday, to serve as a reference, is then drilled in the coating in an area that was not immersed. A radial 45° cut is made through the coating intersecting at the center of both intentional

holidays with a sharp, thin-bladed knife. An attempt is then made to lift the coating at both the reference holiday and the submerged holiday with the point of the knife. The bond at the reference holiday is used to judge the quality of the bond at the submerged holiday. Finally, the total area of disbonded coating at the submerged holiday is measured and recorded.

2.6 MECHANICAL TESTS

The stainless steel clad SMI-316 SC^{TM} bars are tested in tension to determine the yield strength, tensile strength, and elongation, using an Instron servo-hydraulic testing machine under stroke control. A four-inch gage extensometer from Epsilon Technology Corp. is used to obtain strain. Dual loading speeds are used to meet requirements in ASTM E 8. A stress rate between 10,000 psi/min and 100,000 psi/min is used before the steel yields, and a strain rate between 5%/min and 50%/min is used after the steel yields.

The steel is also tested in bending to determine compliance with the requirements of ASTM A 615.

2.7 SMI-316 CLADDING THICKNESS ANALYSIS

The stainless steel clad reinforcement is evaluated for cladding uniformity and thickness variability using a Philips 515 scanning electron microscope (SEM). Three longitudinal specimens and three transverse specimens are evaluated for each of three No. 16 (No. 5) and three No. 19 (No. 6) bars.

The methods used for the evaluation are described next: Following the procedures used by Darwin et al. (1999) and Kahrs et al. (2001), the bars are cut using a band saw and cleaned with acetone to remove grease, dust, and oils. The

specimens are then polished by hand using progressively finer grades of silicon carbide (SiC) paper, starting with 150 grade SiC paper and proceeding to 300, 600, 1000 and 2000 grades. The specimens are cleaned using soap and water before moving to the next polishing step. Finally, the specimens are mounted on aluminum stubs using conductive double-sided carbon-coated tape.

The specimens are observed using backscatter electron imaging. Images are recorded using an ELMDAS digital image acquisition system at an accelerating voltage of 20 kV with a spot size of 100 nm at a pixel density of 512 in both the vertical and horizontal directions. Four micrographs are taken for each longitudinal specimen, six micrographs are taken for No. 16 (No. 5) bar transverse specimens, and seven micrographs are taken for No. 19 (No. 6) bar transverse specimens. On each micrograph, the maximum and minimum cladding thicknesses, along with the thicknesses at three other representative points, are measured in millimeters.

2.8 MICROSTRUCTURE ANALYSIS FOR CORROSION PRODUCTS

Corrosion products that form on the conventional steel and exposed portion of the stainless steel clad bars (regions penetrated by drilled holes or ends not covered with plastic caps) are observed using a Philips 515 scanning electron microscope (SEM) after completion of the rapid macrocell tests. The technique used follows that developed by Axelsson et al (1999) and reported by Darwin et al. (2002) and Gong et al. (2002).

When the macrocell tests are completed, the specimens are visually inspected. For wrapped specimens, the mortar is removed to allow an evaluation of the bar surface. The surface damage and corrosion products are evaluated. The bar surface is examined with a light microscope to select areas on the specimen to be observed

using the SEM. The reinforcing bar is then sliced into pieces using a hacksaw to obtain specimens that are small enough for SEM imaging.

The pieces of steel are mounted on aluminum stubs with conductive double-sided sticky carbon tabs. Conductive carbon paint is used to provide a good conductive path from the top of the specimen to the stub. An Anatech Hummer X sputter coater is used to coat the specimens with a 20 nm thick layer of gold-palladium to prevent charging.

Specimens are observed using secondary electron imaging to record surface morphology. Images are recorded using an ELMDAS digital image acquisition system at an accelerating voltage of 20 kV with a spot size of 100 nm at a pixel density of 1024×768, respectively, in the horizontal and vertical directions.

CHAPTER 3
RESULTS AND EVALUATION

This chapter presents the results of the rapid macrocell, bench-scale, linear polarization resistance, cathodic disbondment, and mechanical tests, along with the results of the cladding thickness and corrosion product microstructure analyses. The chapter is divided into ten sections, covering the corrosion test results for (1) conventional and epoxy-coated steel, (2) stainless steel clad reinforcement, (3) epoxy-coated reinforcement with improved adhesion epoxies, (4) epoxy-coated reinforcement cast with corrosion inhibitors, and (5) multiple coating steel, and the results from (6) the polarization resistance, (7) the cathodic disbondment, and (8) the mechanical property tests, plus (9) the cladding thickness analysis for stainless steel clad reinforcement, and (10) the microstructure analysis of corrosion products for conventional and stainless steel clad reinforcement.

The results of the rapid macrocell tests include the corrosion rate, total corrosion loss, and corrosion potentials of the anode and cathode. The results of the bench-scale tests include the corrosion rate, total corrosion loss, mat-to-mat resistance, and corrosion potential of the top and bottom mats of steel. The linear polarization resistance tests present the microcell corrosion current densities and corrosion rates of the top and bottom mats for selected bench-scale specimens for each corrosion protection system. The cathodic disbondment test measures the total area of disbonded coating at an intentional holiday on epoxy-coated steel. The mechanical property tests are used to determine the yield strength, tensile strength, elongation, and bending properties of steel. The cladding thickness analysis evaluates the cladding thickness for uniformity and variability. The microstructure analysis of

corrosion products compares the structure of corrosion products from conventional steel and stainless steel clad reinforcement.

The test results presented in this chapter are discussed further in Chapter 4 and combined with an economic analysis to establish both the relative performance and the cost effectiveness of the corrosion protection systems evaluated in this study.

3.1 CONVENTIONAL AND EPOXY-COATED REINFORCEMENT

This section presents the results of the rapid macrocell and bench-scale tests for conventional and epoxy-coated steel. The average corrosion rates and corrosion losses for the specimens are summarized in Tables 3.1 and 3.2 for the rapid macrocell and bench-scale tests, respectively. Results for individual specimens are presented in Appendix A.

3.1.1 Rapid Macrocell Tests

Both bare and mortar-wrapped specimens were used to evaluate conventional and epoxy-coated steel in the rapid macrocell test. The mortar used for casting the mortar-wrapped specimens had a water-cement ratio of 0.50. Six bare and six mortar-wrapped tests were performed for both forms of steel. On the epoxy-coated bars, the coating was penetrated with four 3.2-mm (⅛-in.) diameter holes, as described in Section 2.2.2, to simulate the surface damage. In addition, three bare and three mortar-wrapped tests were performed on epoxy-coated bars in the "as delivered" condition.

3.1.1.1 Macrocell Tests for Bare Bar Specimens

The average corrosion rates and total corrosion losses over the 15-week test period are shown in Figures 3.1 and 3.2, respectively. Figures 3.1 (b) and 3.2 (b)

expand the vertical axes in Figures 3.1 (a) and 3.2 (a). The corrosion rates and corrosion losses for the epoxy-coated bars (ECR) are calculated based on both the total area of the bars exposed to solution and the exposed area of the four 3.2-mm (⅛-in.) diameter holes drilled in the epoxy. To distinguish the values based the total area and the exposed area, an asterisk (*) is added to the steel designation in the tables and figures in this report where the corrosion rates and corrosion losses are based on the exposed area of the holes drilled through the coating for all types of epoxy-coated reinforcement. For example, ECR* identifies results based on the exposed area of conventional epoxy-coated reinforcement. Due to the precision of the voltmeter and the 10-ohm resister used, the minimum corrosion rate that can be obtained is 0.029 μm/yr based on the total bar area exposed to solution.

Based on the total bar area exposed to the solution, the average corrosion rate of ECR was far below that of conventional steel. At 15 weeks, the epoxy-coated bars had an average corrosion rate of 1.2 μm/year based on the total area exposed to solution, equal to 4% of the corrosion rate of conventional steel, 28 μm/year. Based on the exposed steel area for the bare epoxy-coated bars, the average corrosion rate reached a value as high as 150 μm/year during the tests and a value of 118 μm/yr at week 15, as shown in Figure 3.1 (a) and Table 3.1. The results demonstrate that very high corrosion rates can occur in localized areas. The three epoxy-coated bars without drilled holes (ECR-nh) had an average corrosion rate of 0.02 μm/year at 15 weeks (based on corrosion in one specimen – see Table 3.1), demonstrating the high corrosion resistance provided by an undamaged epoxy coating for short periods of exposure.

Based on the total area, the corrosion loss for ECR was 0.4 μm after 15 weeks, equal to 5% of the total loss for the conventional bars (8 μm), as shown in Figure 3.2.

The total corrosion loss for the epoxy-coated bars, based on the exposed area of the four holes, was 40 μm at week 15. For ECR bars without drilled holes, the corrosion loss was less than 0.01 μm, as indicated by the symbol β in Table 3.1.

The average corrosion potentials of the anodes and cathodes are shown in Figures 3.3 and 3.4, respectively. The corrosion potentials are measured with respect to a saturated calomel electrode (SCE), and values more negative than –0.275 V indicate active corrosion. At 15 weeks, all anode bars were undergoing active corrosion, with an average value of –0.515 V for conventional bars and –0.521 V for epoxy-coated (ECR) specimens. The average corrosion potentials for the cathodes were –0.205 V and –0.250 V for conventional and epoxy-coated specimens, respectively, indicating that the bars remained passive. Due to the insulative properties of epoxy, epoxy-coated bars without holes did not exhibit stable corrosion potentials for either the anodes or the cathodes.

Table 3.1 – Average corrosion rates and corrosion losses for conventional and epoxy-coated steel as measured in the macrocell tests

CORROSION RATE AT WEEK 15 (μm/year)

Steel Designation	Specimen						Average	Std. Deviation
	1	2	3	4	5	6		
Bare bar specimens								
Conv.	31.23	22.16	16.68	40.66	26.74	31.12	28.10	8.30
ECR	0.73	1.76	1.43	1.76	1.35	0.04	1.18	0.67
ECR*	73.20	175.68	142.74	175.68	135.42	3.66	117.73	67.30
ECR-nh	0	0.07	0	-	-	-	0.02	0.04
Mortar-wrapped specimens								
Conv.	21.37	25.81	21.84	14.41	14.5	31.58	21.59	6.63
ECR	0.07	0.07	0	0	0	0	0.02	0.04
ECR*	7.32	7.32	0	0	0	0	2.44	3.78
ECR-nh	0	0	0	-	-	-	0	-

TOTAL CORROSION LOSS AFTER WEEK 15 (μm)

Steel Designation	Specimen						Average	Std. Deviation
	1	2	3	4	5	6		
Bare bar specimens								
Conv.	8.76	7.18	6.34	9.84	8.83	6.78	7.95	1.38
ECR	0.29	0.74	0.24	0.43	0.59	0.07	0.4	0.24
ECR*	29.28	74.33	24.42	42.86	59.19	7.11	39.53	24.47
ECR-nh	β	0.01	β	-	-	-	β	-
Mortar-wrapped specimens								
Conv.	5.83	7.95	3.47	3.8	3.76	5.41	5.04	1.72
ECR	β	β	β	0	β	β	β	-
ECR*	0.77	0.56	0.63	0.07	0.21	0.21	0.41	0.28
ECR-nh	β	β	β	-	-	-	β	-

[1] Conv.: Conventional, normalized A 615 reinforcing steel

[2] ECR: Epoxy-coated steel with four 3.2-mm (1/8-in.) diameter holes in epoxy based on total area of bar exposed to solution

[3] ECR*: Epoxy-coated steel based on exposed area of four 3.2-mm (1/8-in.) diameter holes in epoxy

[4] ECR-nh: Epoxy-coated steel without any drilled holes based on total area of bar exposed to solution

[5] β: corrosion loss less than 0.01 μm

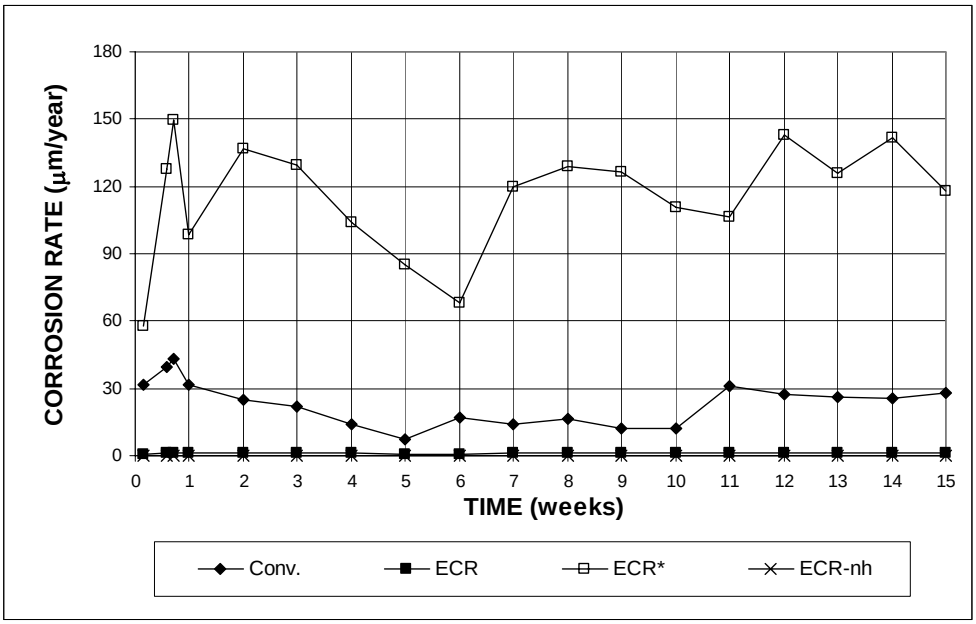

Figure 3.1 (a) - Macrocell Tests. Average Corrosion Rate. Bare bar specimens of conventional and epoxy-coated reinforcement in simulated concrete pore solution with 1.6 m ion NaCl. Refer to footnote of Table 3.1 for specimen identification.

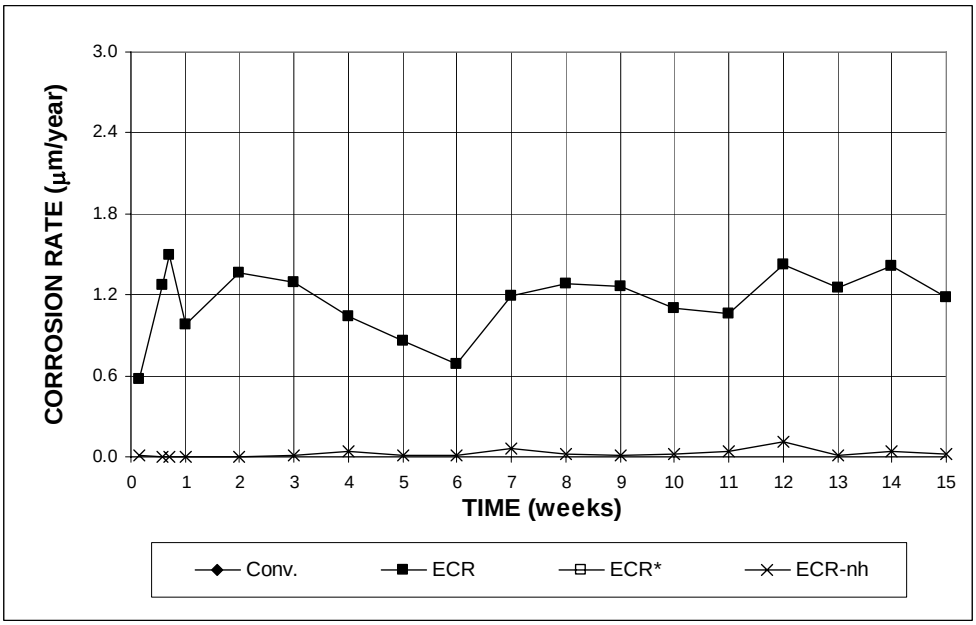

Figure 3.1 (b) - Macrocell Tests. Average Corrosion Rate. Bare bar specimens of conventional and epoxy-coated reinforcement in simulated concrete pore solution with 1.6 m ion NaCl. Refer to footnote of Table 3.1 for specimen identification.

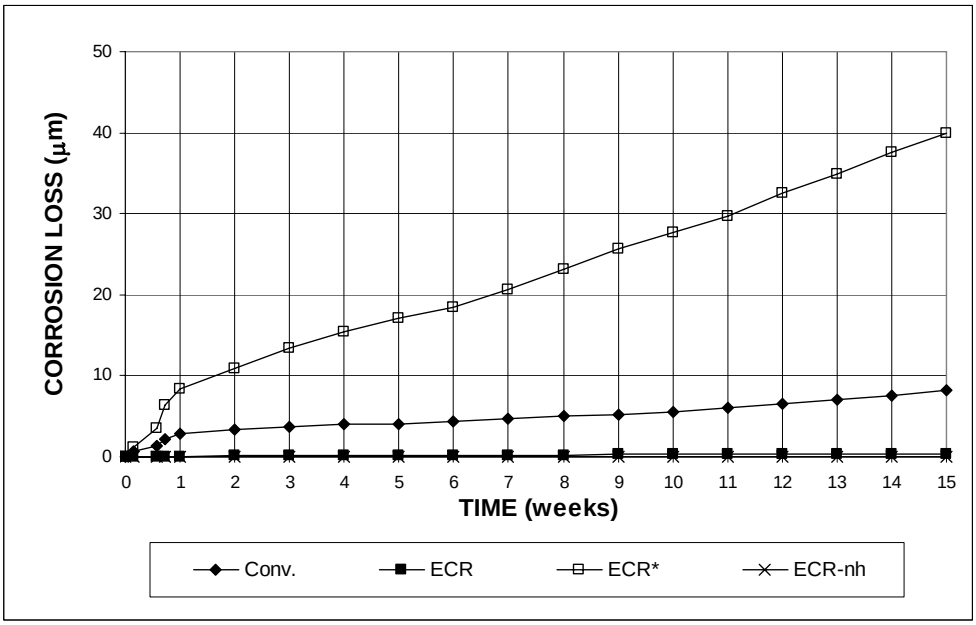

Figure 3.2 (a) - Macrocell Tests. Total Corrosion Loss. Bare bar specimens of conventional and epoxy-coated reinforcement in simulated concrete pore solution with 1.6 m ion NaCl. Refer to footnote of Table 3.1 for specimen identification.

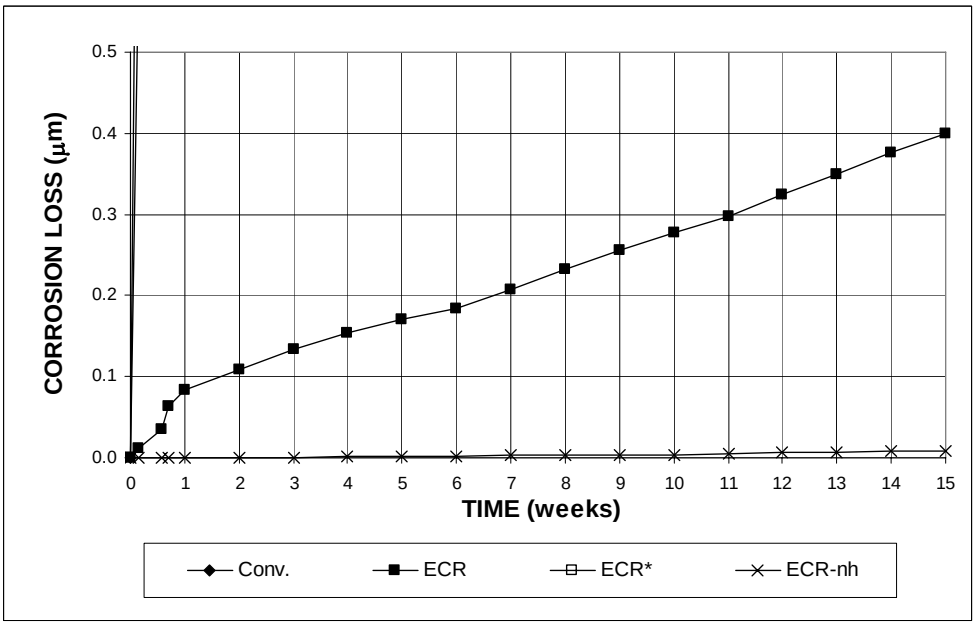

Figure 3.2 (b) - Macrocell Tests. Total Corrosion Loss. Bare bar specimens of conventional and epoxy-coated reinforcement in simulated concrete pore solution with 1.6 m ion NaCl. Refer to footnote of Table 3.1 for specimen identification.

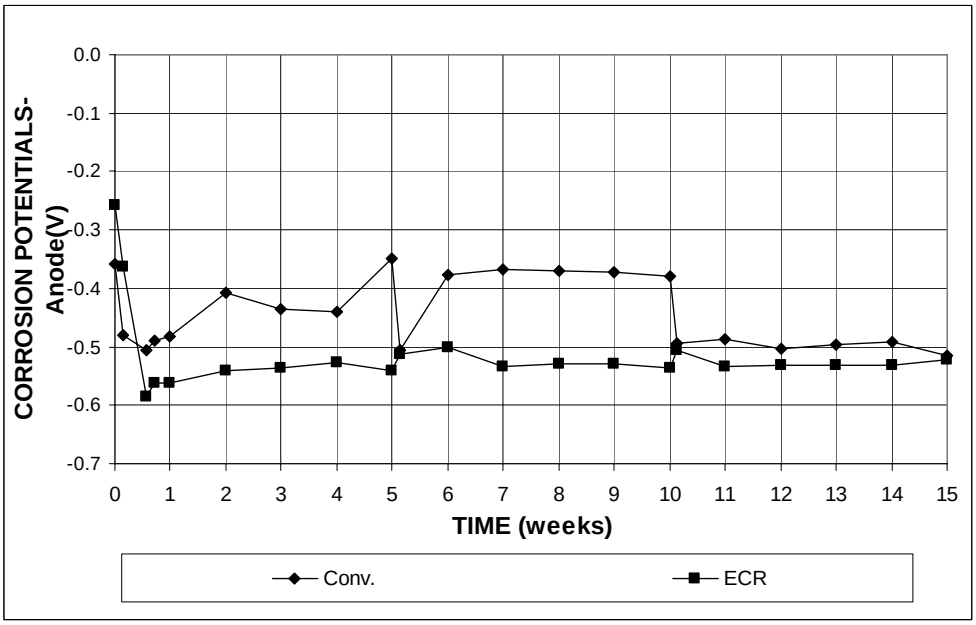

Figure 3.3 - Macrocell Tests. Average Corrosion Potential with respect to SCE at Anode. Bare bar specimens of conventional and epoxy-coated reinforcement in simulated concrete pore solution with 1.6 m ion NaCl. Refer to footnote of Table 3.1 for specimen identification.

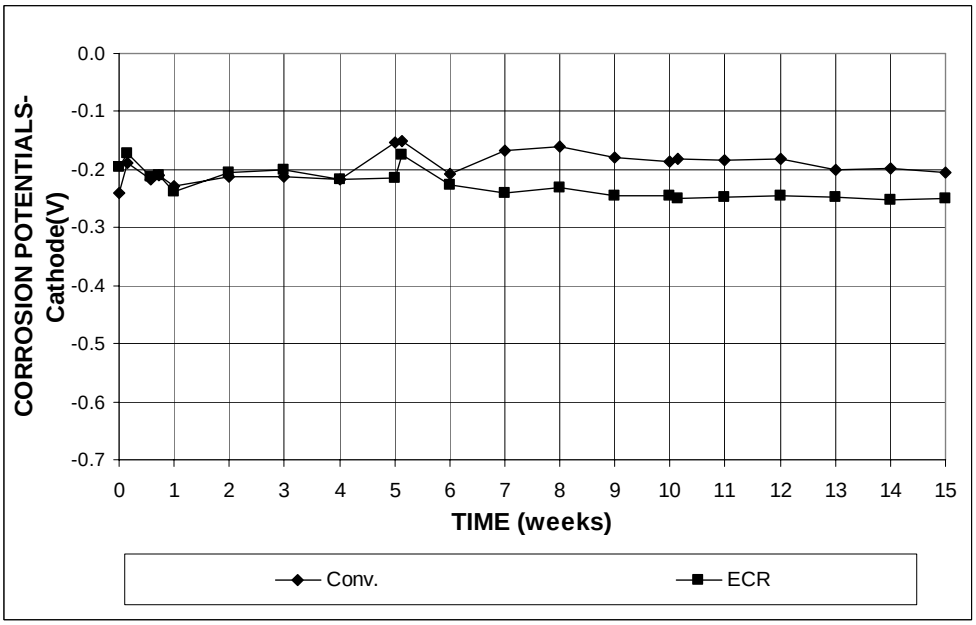

Figure 3.4 - Macrocell Tests. Average Corrosion Potential with respect to SCE at Cathode. Bare bar specimens of conventional and epoxy-coated reinforcement in simulated concrete pore solution with 1.6 m ion NaCl. Refer to footnote of Table 3.1 for specimen identification.

3.1.1.2 Macrocell Tests for Mortar-Wrapped Specimens

Figure 3.5 shows the average corrosion rates for the mortar-wrapped specimens. Figure 3.5 (b) expands the vertical axis in Figure 3.5 (a).

At 15 weeks, the epoxy-coated steel exhibited a corrosion rate of 0.02 μm/yr based on the total bar area, equal to 0.1% of that for conventional steel (22 μm/yr). The corrosion rate for these epoxy-coated specimens was 2.4 μm/yr based on the exposed area. The average corrosion rate of the mortar-wrapped ECR specimens is much lower than that exhibited by bare ECR specimens (1.2 μm/yr based on the total area and 120 μm/yr based on the exposed area) for several reasons. These reasons include additional passive protection provided to steel in contact with hydrated cement {principally the effect of calcium hydroxide [Yonezewa, Ashworth, and Procter (1988)]}, a lower rate of diffusion of oxygen and moisture to the cathode, and a lower rate of diffusion of chlorides to the anode. In addition, the non-homogeneous nature of chloride diffusion in mortar may result in a variation in chloride content at the bar surface that could result in a locally low chloride content at the exposed areas on epoxy-coated bars. For ECR bars without damage (ECR-nh), small corrosion currents were detected during the test, as shown in Figure 3.5 (b), although the corrosion loss was less than 0.01 μm at week 15, as indicated (β) in Table 3.1. It is worth noting that the average corrosion currents were similar for the ECR and ECR-nh bars [Figure 3.5(b)], suggesting that the corrosion ascribed to the exposed area (ECR*) may not be realistic. Rather, the measured corrosion currents may be the result of corrosion at holidays that is driven by the different environments at the cathodes and anodes.

The average total corrosion losses versus time are shown in Figure 3.6. Figure 3.6(b) expands the vertical axis of Figure 3.6 (a). Table 3.1 summarizes the average

total corrosion losses at week 15. Based on the total area exposed to the solution, the epoxy-coated bars with or without drilled holes showed corrosion losses below 0.01 μm after 15 weeks, less than 0.1% of that for the conventional steel (5.04 μm). Based on the exposed area, the epoxy-coated specimens with drilled holes showed corrosion losses of 0.4 μm at week 15.

The average corrosion potentials of the anodes and the cathodes with respect to a saturated calomel electrode are shown in Figures 3.7 and 3.8. The conventional steel had an average corrosion potential of as low as –0.581 V (at week 14) and ended with a value of –0.574 V at week 15. The corrosion potential of the epoxy-coated bars remained near –0.250 V for most of the test period and ended at –0.240 V at week 15. The corrosion potential of the conventional steel cathodes stayed close to –0.250 V. For the epoxy-coated bars, the cathode potential remained near –0.180 V, indicating a more passive condition.

After the 15-week test period, the mortar was removed, and the bars were inspected. None of the six epoxy-coated anodes exhibited corrosion products at the holes in the epoxy, an observation that is in concert with the corrosion potentials of the anodes.

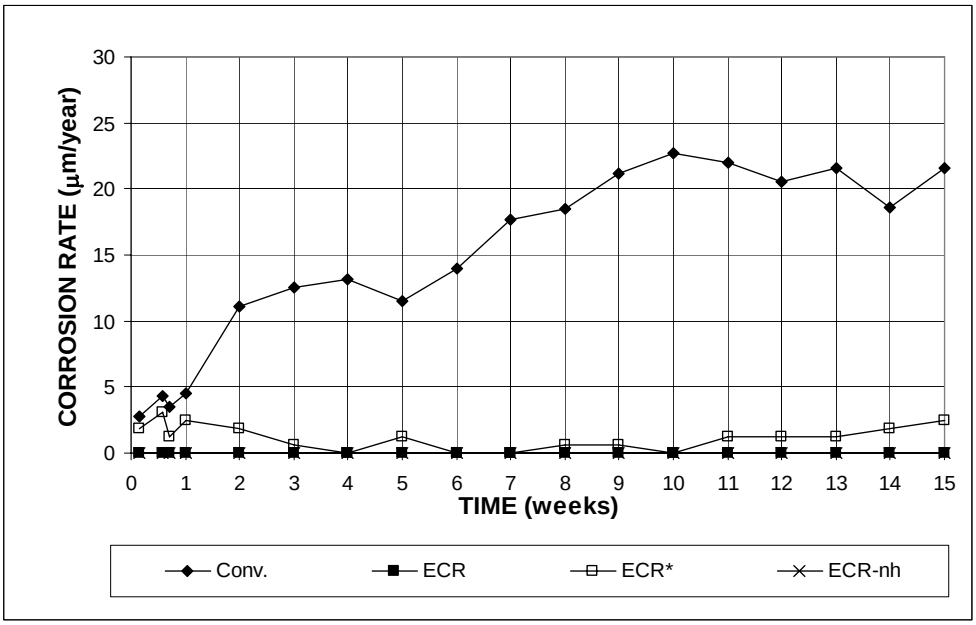

Figure 3.5 (a) - Macrocell Tests. Average Corrosion Rate. Mortar-wrapped specimens of conventional and epoxy-coated reinforcement in simulated concrete pore solution with 1.6 m ion NaCl. Refer to footnote of Table 3.1 for specimen identification.

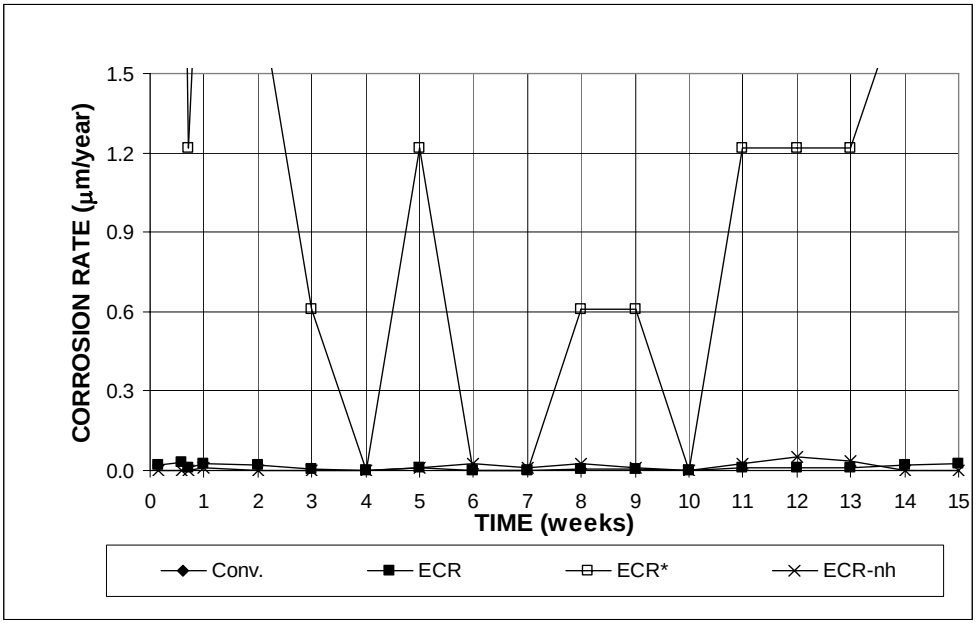

Figure 3.5 (b) - Macrocell Tests. Average Corrosion Rate. Mortar-wrapped specimens of conventional and epoxy-coated reinforcement in simulated concrete pore solution with 1.6 m ion NaCl. Refer to footnote of Table 3.1 for specimen identification.

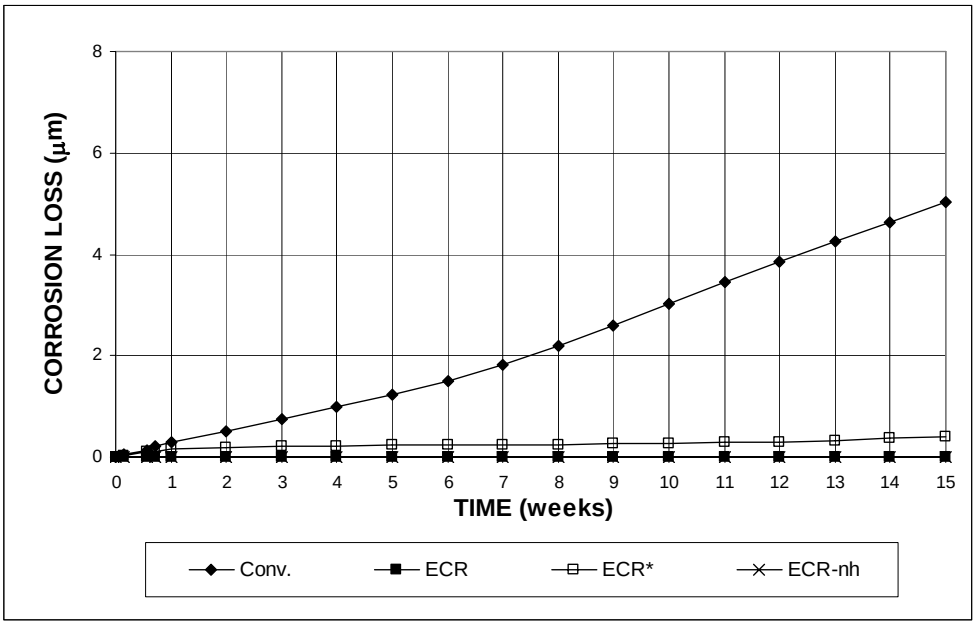

Figure 3.6 (a) - Macrocell Tests. Total Corrosion Loss. Mortar-wrapped specimens of conventional and epoxy-coated reinforcement in simulated concrete pore solution with 1.6 m ion NaCl. Refer to footnote of Table 3.1 for specimen identification.

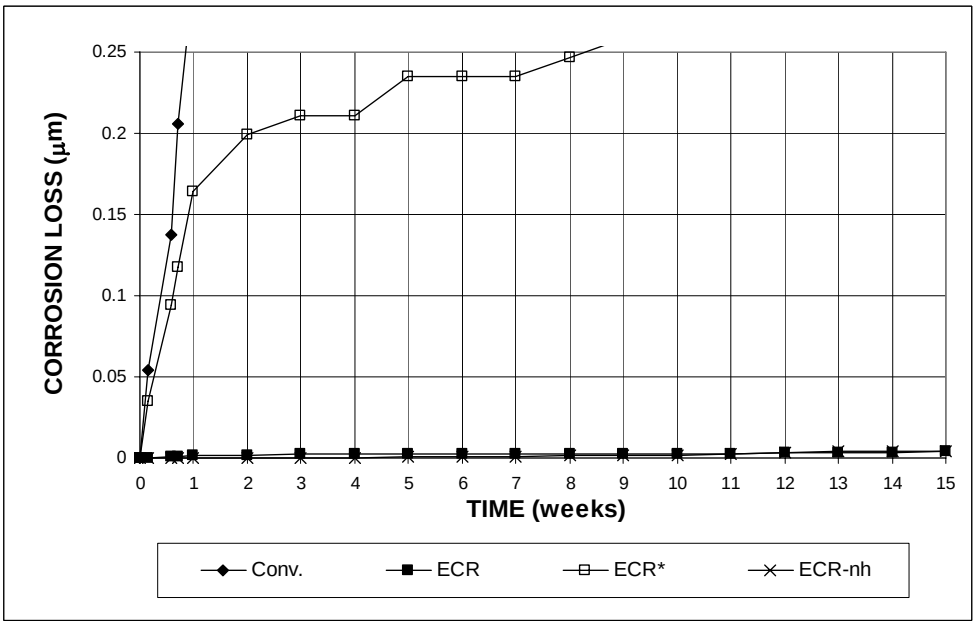

Figure 3.6 (b) - Macrocell Tests. Total Corrosion Loss. Mortar-wrapped specimens of conventional and epoxy-coated reinforcement in simulated concrete pore solution with 1.6 m ion NaCl. Refer to footnote of Table 3.1 for specimen identification.

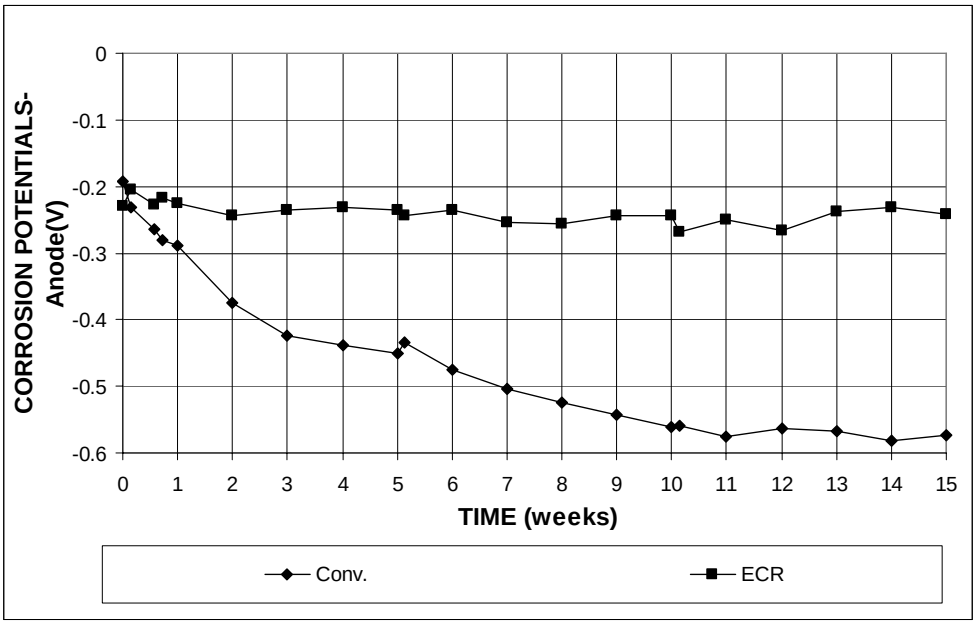

Figure 3.7 - Macrocell Tests. Corrosion Potential with respect to SCE at Anode. Mortar-wrapped specimens of conventional and epoxy-coated reinforcement in simulated concrete pore solution with 1.6 m ion NaCl. Refer to footnote of Table 3.1 for specimen identification.

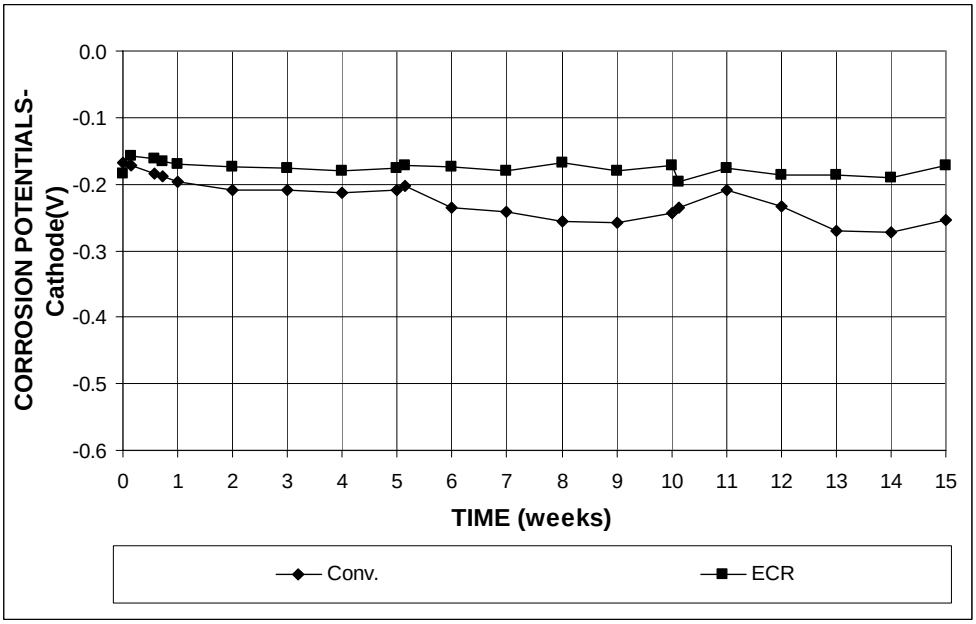

Figure 3.8 - Macrocell Tests. Corrosion Potential with respect to SCE at Cathode. Mortar-wrapped specimens of conventional and epoxy-coated reinforcement in simulated concrete pore solution with 1.6 m ion NaCl. Refer to footnote of Table 3.1 for specimen identification.

3.1.1.3 Visual Inspection

As the tests were discontinued, the specimens were visually inspected. For conventional steel, corrosion products were observed on the bar surface within the solution. In some cases, corrosion products appeared on the bar at contact points with the plastic lid, presumably due to crevice corrosion. Figure 3.9 shows a conventional steel bare anode bar at 15 weeks with corrosion products that formed on the bar below the surface of the solution, while Figure 3.10 shows corrosion products at the contact points between the conventional steel anode and plastic lid. Figure 3.11 shows a bare epoxy-coated bar with the corrosion products that formed on the drilled holes.

For the mortar-wrapped specimens, the specimens were broken and some corrosion product was found under the mortar. Figure 3.12 shows a conventional bar with corrosion products that formed on the bar surface. For mortar-wrapped epoxy-coated bars, no corrosion products were found on the specimens.

Figure 3.9 – Bare conventional anode bar, at 15 weeks, showing corrosion products that formed below the surface of the solution.

Figure 3.10 – Bare conventional anode bar, at 15 weeks, showing corrosion products that formed at contact points between the bar and plastic lid.

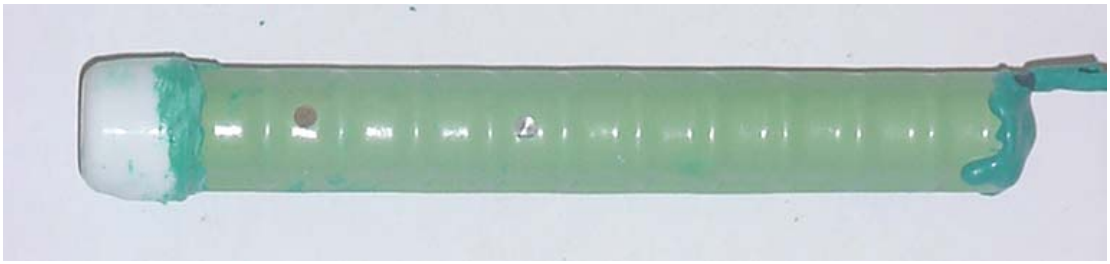

Figure 3.11 – Bare ECR anode bar, at 15 weeks, showing corrosion products that formed at drilled holes.

Figure 3.12 - Conventional anode bar after removal of mortar, at 15 weeks.

3.1.2 Bench-Scale Tests

The average corrosion rates and total corrosion losses as of March 15, 2005 for ongoing Southern Exposure, cracked beam, and ASTM G 109 tests are summarized in Table 3.2. Results for individual specimens are presented in Appendix A.

3.1.2.1 Southern Exposure Tests

The Southern Exposure tests include six specimens each for conventional steel and epoxy-coated reinforcement (ECR) with four drilled holes in concrete with a water-cement (*w/c*) ratio of 0.45 and three specimens each for conventional steel in concrete with a *w/c* ratio of 0.35 and epoxy-coated steel with 10 drilled holes in concrete with *w/c* ratios of 0.35 and 0.45. Average corrosion rates and total corrosion losses are shown in Figures 3.13 and 3.14, respectively. Figures 3.13 (b) and 3.14 (b) expand the vertical axes in Figures 3.13 (a) and 3.14 (a). The corrosion rates and

losses for the epoxy-coated steel are based on both the total area of the bars and the exposed area of the holes drilled in the epoxy.

The results based on the total area (summarized in Table 3.2) show that the ECR specimens with four drilled holes had a corrosion rate of zero at week 49, while the ECR specimens with 10 drilled holes were corroding at an average rate of less than 0.01 μm/yr, as indicated by the symbol α in Table 3.2. At 49 weeks, the specimens with conventional steel were corroding at an average rate of 0.42 μm/yr, after reaching values above 0.7 μm/yr on a number of occasions. For specimens with a (lower) *w/c* ratio of 0.35, the corrosion rates were 0.05 μm/yr for conventional steel and less than 0.01 μm/yr for ECR based on the total area of the steel at week 37.

Based on the exposed area, the ECR specimens with four drilled holes had a corrosion rate of zero at week 49, although the rate reached as high as 7.63 μm/yr a few times before week 49. The corrosion rate for the ECR specimens with 10 drilled holes was 1.22 μm/yr at week 40, with values as high as 3.42 μm/yr before 40 weeks. For the ECR specimens with a *w/c* ratio of 0.35, the corrosion rate was 0.24 μm/yr at week 37, with a maximum rate of 4.15 μm/yr at week 7.

For ECR specimens with four drilled holes, the average total corrosion loss based on total bar surface (less than 0.01 μm) was 3% that of conventional steel (0.34 μm) at 49 weeks, while the ECR specimens with 10 drilled holes exhibited a corrosion loss of less than 0.01 μm at 40 weeks. For specimens with a *w/c* ratio of 0.35, the corrosion losses based on the total area were both less than 0.01 μm for the conventional and ECR specimens at week 37. Based on the exposed area, the corrosion losses were 0.88 μm for ECR with four drilled holes at week 49 and 1.09 μm for ECR with 10 drilled holes. The corrosion loss at 37 weeks for the ECR specimens with a *w/c* ratio of 0.35 was 0.76 μm.

The relatively high corrosion rate and total corrosion loss of the ECR specimens based on the exposed area, as shown in Figures 3.13 and 3.14, respectively, demonstrate again that very high corrosion rates are possible in localized areas. These values, however, may also represent a calculated value that, in fact, may overestimate the actual corrosion rate and loss on the exposed area, due to the inverse relationship in the calculation between the corrosion rate and the exposed area. As shown in Figure 3.14 (b), the total corrosion losses are nearly identical for all ECR specimens when based on total bar area.

The average resistances between the top and bottom mats are shown in Figure 3.15. For all specimens, the mat-to-mat resistances increase with time due to the formation of corrosion products on the surface of the bars as well as a reduction in the concrete pore volume. The ECR specimens with four drilled holes had an average mat-to-mat resistance of over 10,000 ohms at week 49, while the ECR with 10 drilled holes exhibited lower resistances, around 4,000 ohms and 3,000 ohms for concrete with *w/c* ratios of 0.45 and 0.35 at weeks 40 and 37, respectively. Since epoxy coating acts as insulation, the greater the damage to the epoxy, the lower the resistance measured between the top and bottom mats, explaining why the ECR specimens with 10 drilled holes exhibit lower resistance than the ECR specimens with four drilled holes. Conventional steel, with values of *w/c* of 0.35 or 0.45, showed the lowest resistance, at about 400 ohms.

The average corrosion potentials of the top and bottom mats with respect to a copper copper-sulfate electrode (CSE) are shown in Figures 3.16 and 3.17, respectively. For the top mats, conventional steel had the most negative corrosion potential, dropping below −0.350 V (values more negative than −0.350 V with respect to a CSE indicate active corrosion) at week 40 but jumping up to −0.320 V at

week 49, followed by the epoxy-coated bars with 10 drilled holes with a value of −0.310 V at week 40. The corrosion potentials for the ECR with four drilled holes and the conventional and ECR specimens with a *w/c* ratio of 0.35 have remained close to −0.200 V, indicating a low probability of corrosion. For the bottom mats, all specimens, except those with conventional steel with a *w/c* of 0.45, which dropped to near −0.300 V at week 43, (indicating a slight tendency to corrode), exhibited corrosion potentials more positive than −0.200 V.

Table 3.2 – Average corrosion rates for conventional and epoxy-coated steel as measured in the bench-scale tests

CORROSION RATE (μm/year)

Steel Designation	Exposure Time (weeks)	Specimen 1	2	3	4	5	6	Average	Std. Deviation
Southern Exposure specimens									
Conv.	49	0.09	1.65	0.78	0	0	0	0.42	0.68
Conv.-35	37	0	0	0.16	-	-	-	0.05	0.09
ECR	49	0	0	0	0	0	0	0	-
ECR*	49	0	0	0	0	0	0	0	-
ECR-10h	40	0.01	α	0	-	-	-	α	0.01
ECR*-10h	40	2.20	1.46	0	-	-	-	1.22	1.12
ECR-10h-35	37	0	0	α	-	-	-	α	0
ECR*-10h-35	37	0	0	0.73	-	-	-	0.24	0.42
Cracked Beam specimens									
Conv.	49	8.95	2.18	4.4	11.48	5.15	9.42	6.93	3.55
Conv.-35	37	5.94	1.52	1.91	-	-	-	3.12	2.45
ECR	49	α	0.03	α	0.02	α	0.02	0.02	0.01
ECR*	49	3.66	14.64	3.66	10.98	3.66	7.32	7.32	4.63
ECR-10h	40	α	0.02	α	-	-	-	0.01	0.01
ECR*-10h	40	1.46	4.39	1.46	-	-	-	2.44	1.69
ECR-10h-35	37	0.19	0.09	0.14	-	-	-	0.14	0.05
ECR*-10h-35	37	36.6	17.57	27.82	-	-	-	27.33	5.53
ASTM G 109 specimens									
Conv.	51	α	0	0	0	α	α	α	-
ECR	52	0	0	0	-	-	-	0	-
ECR*	52	0	0.37	0.37	-	-	-	0.24	0.21
ECR-10h	42	0	0	0	0	0	0	0	-
ECR*-10h	42	0	0	0	0	0	0	0	-

CORROSION LOSS (μm)

Steel Designation	Exposure Time (weeks)	Specimen 1	2	3	4	5	6	Average	Std. Deviation
Southern Exposure specimens									
Conv.	49	0.02	1.40	0.07	0.31	0	0.23	0.34	0.54
Conv.-35	37	β	β	β	-	-	-	β	-
ECR	49	β	β	β	β	β	β	β	-
ECR*	49	2.50	2.50	3.24	2.18	3.48	3.38	2.88	0.55
ECR-10h	40	β	β	β	-	-	-	β	-
ECR*-10h	40	1.21	1.03	1.04	-	-	-	1.09	0.10
ECR-10h-35	37	β	β	β	-	-	-	β	-
ECR*-10h-35	37	0.76	0.80	0.70	-	-	-	0.76	0.05
Cracked Beam specimens									
Conv.	49	9.83	4.61	5.30	8.09	6.09	4.77	6.45	2.09
Conv.-35	37	3.96	2.02	2.80	-	-	-	2.92	0.97
ECR	49	0.03	0.03	0.02	0.05	0.03	0.02	0.03	0.01
ECR*	49	15.20	15.77	10.63	23.09	16.19	9.78	15.11	4.77
ECR-10h	40	0.03	0.05	0.03	-	-	-	0.04	0.01
ECR*-10h	40	4.93	10.36	6.25	-	-	-	7.18	2.83
ECR-10h-35	37	0.07	0.07	0.08	-	-	-	0.08	0.01
ECR*-10h-35	37	13.49	14.39	15.94	-	-	-	14.60	1.24
ASTM G 109 specimens									
Conv.	51	β	β	β	β	β	β	β	-
ECR	52	β	β	β	-	-	-	β	-
ECR*	52	0.52	0.44	0.48	-	-	-	0.48	0.04
ECR-10h	42	β	β	β	β	β	β	β	-
ECR*-10h	42	0.25	0.24	0.22	0.11	0.19	0.15	0.19	0.05

[1] Conv.: Conventional, normalized A 615 reinforcing steel

[2] Conv.-35: Conventional, normalized A 615 reinforcing steel with a water/cement ratio of 0.35

[3] ECR: Epoxy-coated steel with four drilled holes based on total area of bar exposed to solution

[4] ECR*: Epoxy-coated steel based on exposed area of four 3.2-mm (1/8-in.) diameter holes in epoxy

[5] ECR-10h: Epoxy-coated steel with 10 drilled holes based on total area of bar exposed to solution

[6] ECR*-10h:: Epoxy-coated steel based on exposed area of ten 3.2-mm (1/8-in.) diameter holes in epoxy

[5] ECR-10h-35: Epoxy-coated steel with 10 drilled holes and a water/cement ratio of 0.35 based on total area of bar exposed to solution

[6] ECR*-10h-35:: Epoxy-coated steel with a water/cement ratio of 0.35 based on exposed area of ten 3.2-mm (1/8-in.) diameter holes in epoxy

[7] α: corrosion rate less than 0.01 μm/yr

[8] β: corrosion loss less than 0.01μm

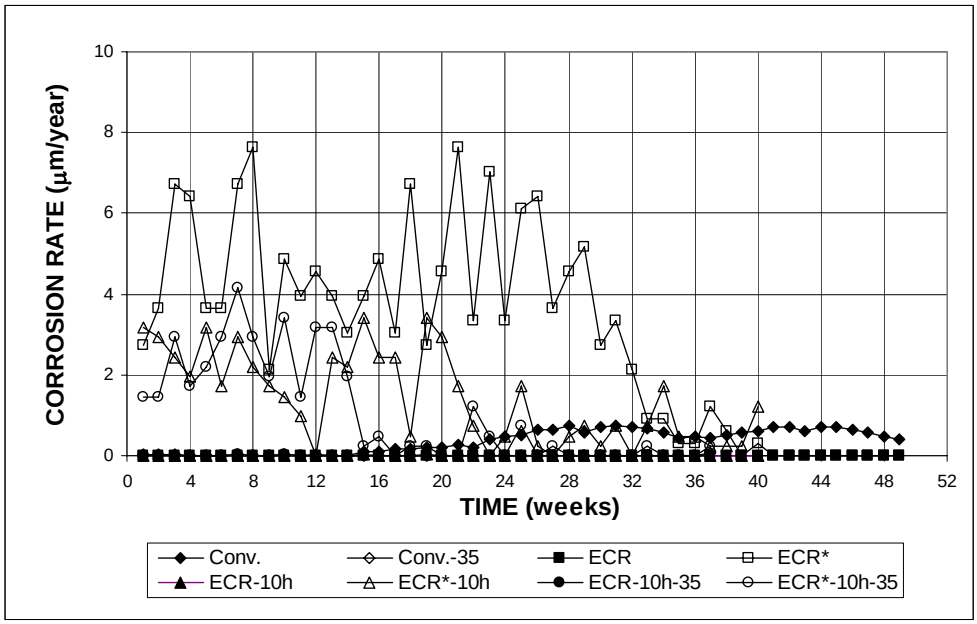

Figure 3.13 (a) – Southern Exposure Tests. Average Corrosion Rate. Specimens of conventional and epoxy-coated reinforcement ponded with 15% NaCl solution. Refer to footnote of Table 3.2 for specimen identification.

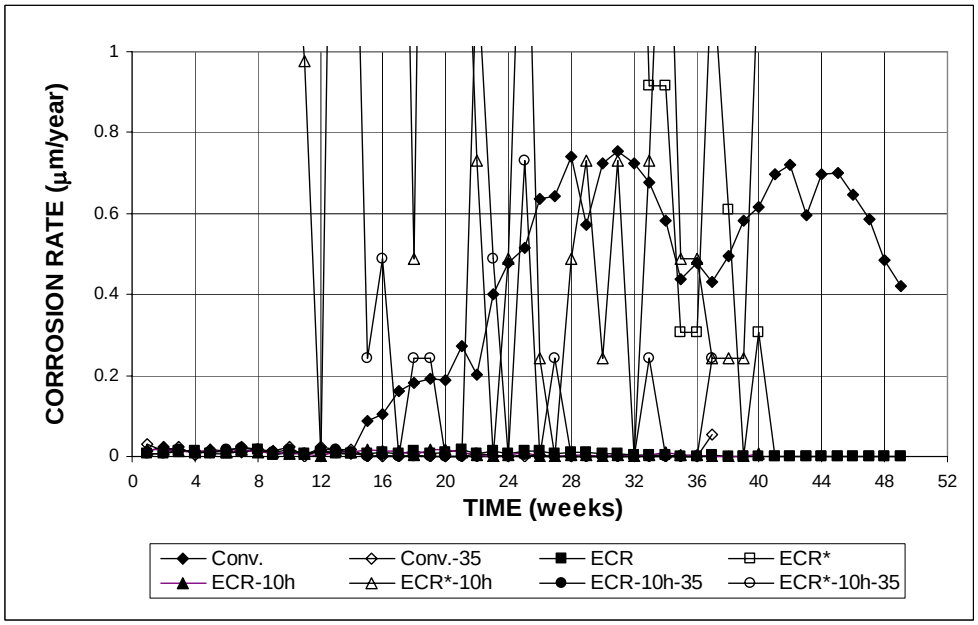

Figure 3.13 (b) – Southern Exposure Tests. Average Corrosion Rate. Specimens of conventional and epoxy-coated reinforcement ponded with 15% NaCl solution. Refer to footnote of Table 3.2 for specimen identification.

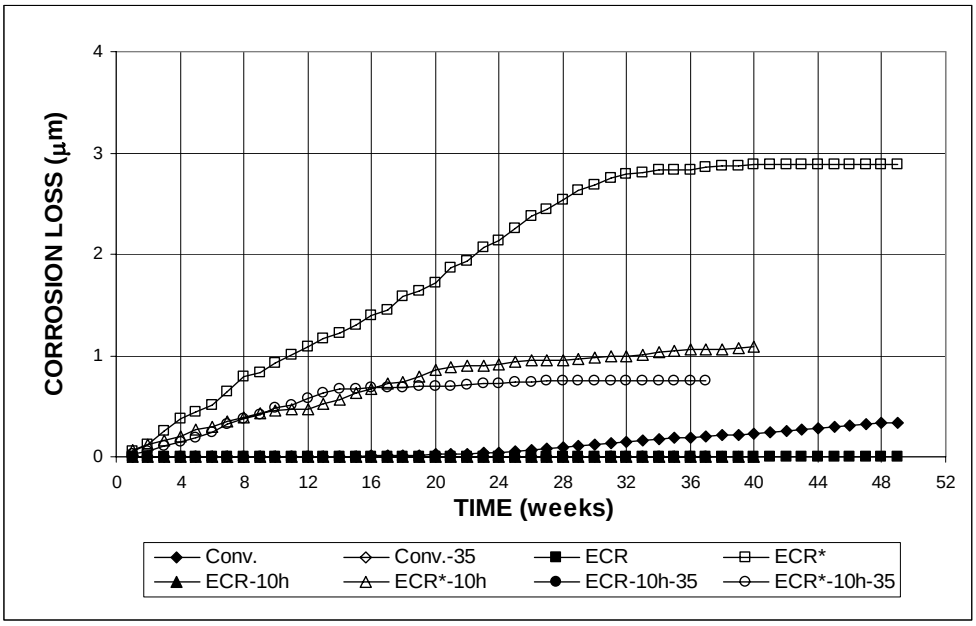

Figure 3.14 (a) – Southern Exposure Tests. Total Corrosion Loss. Specimens of conventional and epoxy-coated reinforcement ponded with 15% NaCl solution. Refer to footnote of Table 3.2 for specimen identification.

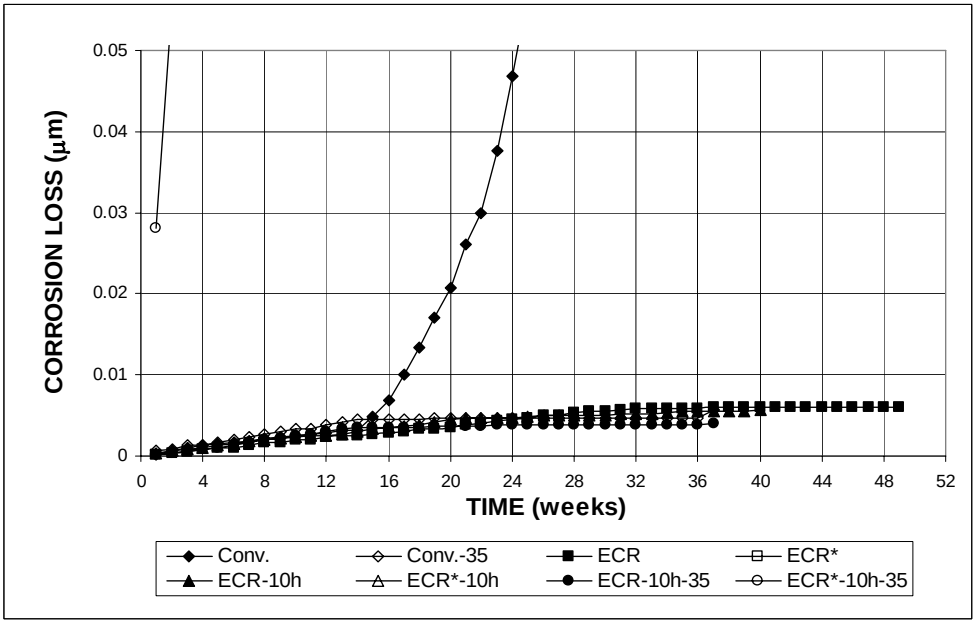

Figure 3.14 (b) – Southern Exposure Tests. Total Corrosion Loss. Specimens of conventional and epoxy-coated reinforcement ponded with 15% NaCl solution. Refer to footnote of Table 3.2 for specimen identification.

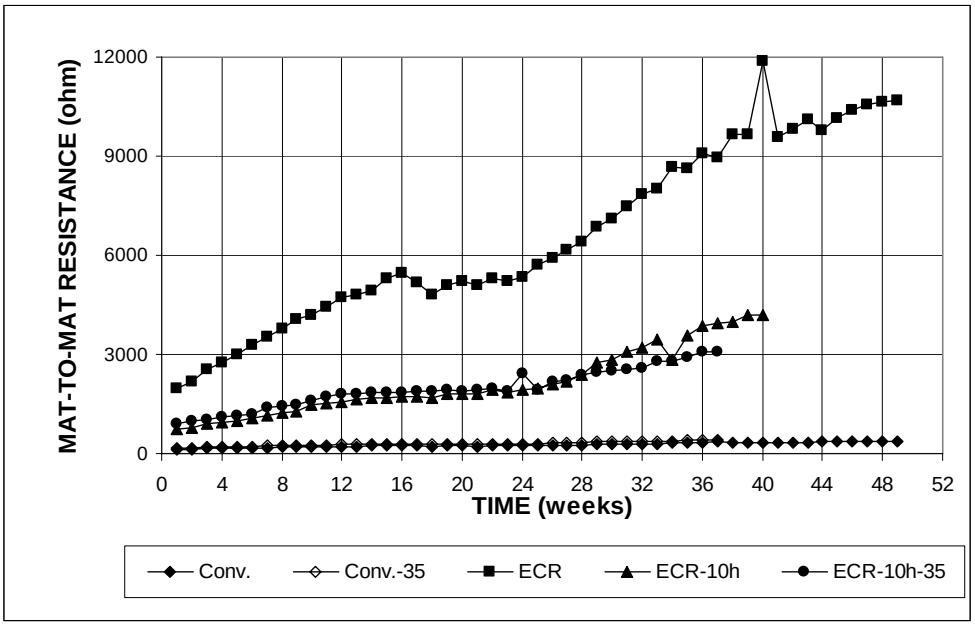

Figure 3.15 – Southern Exposure Tests. Mat-to-mat resistance. Specimens of conventional and epoxy-coated reinforcement ponded with 15% NaCl solution. Refer to footnote of Table 3.2 for specimen identification.

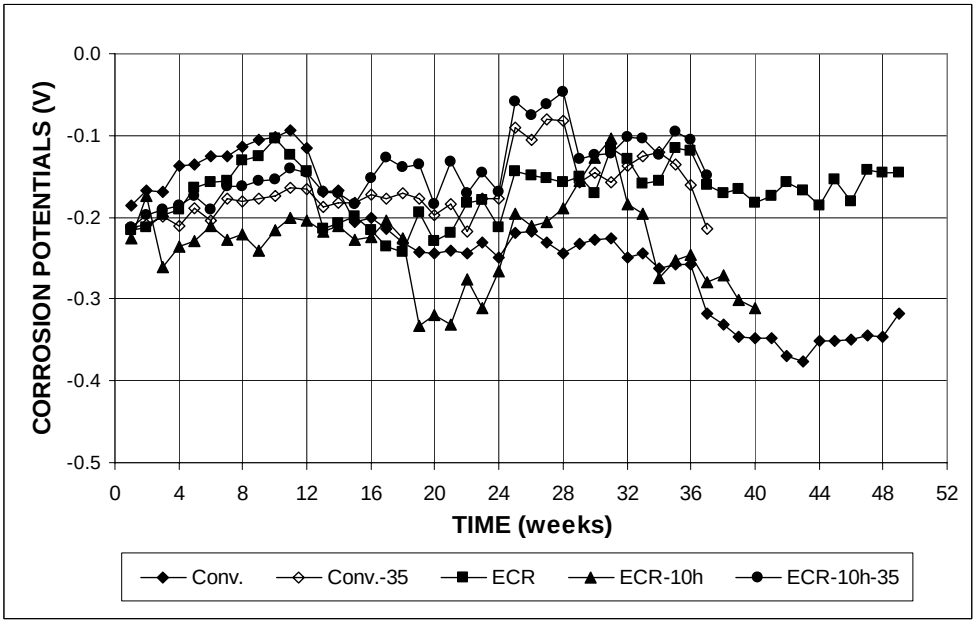

Figure 3.16 – Southern Exposure Tests. Corrosion Potential with respect to CSE at Top Mat. Specimens of conventional and epoxy-coated reinforcement ponded with 15% NaCl solution. Refer to footnote of Table 3.2 for specimen identification.

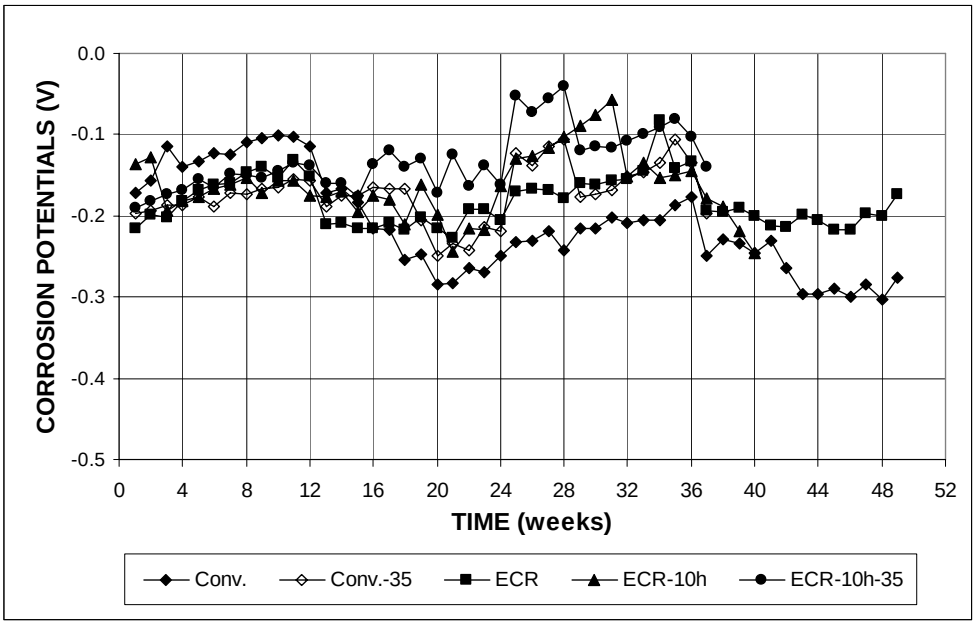

Figure 3.17 – Southern Exposure Tests. Corrosion Potential with respect to CSE at Bottom Mat. The specimens of conventional and epoxy-coated reinforcement ponded with 15% NaCl solution. Refer to footnote of Table 3.2 for specimen identification.

3.1.2.2 Cracked Beam Tests

The cracked beam tests include six specimens each for conventional steel and epoxy-coated reinforcement (ECR) with four drilled holes using concrete with a *w/c* ratio of 0.45, and three specimens each for conventional steel using concrete with a *w/c* ratio of 0.35 and ECR with 10 drilled holes using concrete with *w/c* ratios of 0.35 and 0.45. Average corrosion rates and total corrosion losses are shown in Figures 3.18 and 3.19. Figure 3.18 (b) and 3.19 (b) expand the vertical axes in Figure 3.18 (a) and 3.19 (a). The results (summarized in Table 3.2) show that the specimens containing conventional steel with *w/c* ratios of 0.45 and 0.35 started at average corrosion rates higher than 10 μm/yr, which decreased with time and stabilized after the first few weeks. Larger values were observed during the first few weeks since the cracks in the specimens provide a direct path for chlorides to reach the steel. The decrease in the corrosion rates with time is due to the formation of corrosion products that can seal

the cracks and reduce the penetration of chlorides, oxygen, and moisture. Specimens with conventional steel in concrete with a *w/c* of 0.45 had the highest corrosion rate, 6.93 μm/yr at week 49, followed by the specimens with conventional steel in concrete with a *w/c* ratio of 0.35, at a rate of 3.12 μm/yr at week 37. Based on the total bar area, the ECR specimens with 10 drilled holes in concrete with a *w/c* ratio of 0.35 showed a higher corrosion rate (0.14 μm/yr) than the ECR specimens with a *w/c* of 0.45 (0.02 μm/yr for ECR with four drill holes and 0.01 μm/yr for ECR with 10 drilled holes).

Based on the exposed area [four or 10 3.2-mm ($^1/_8$-in.) diameter holes in the coating], the specimens containing epoxy-coated steel showed much higher corrosion rates. For the ECR specimens with four drilled holes, the corrosion rate was 7.32 μm/yr at week 49, with a maximum value of 35.4 μm/yr at a number of occasions at the first few weeks. The ECR specimens with 10 drilled holes reached an average corrosion rate as high as 28.9 μm/yr at week 6, which decreased to 2.44 μm/yr at 40 weeks. For the ECR specimens with a *w/c* ratio of 0.35, the corrosion rate was 27.33 μm/yr at week 37, while the highest value was 52.7 mm/yr at week 5.

For conventional steel, the average total corrosion losses were 6.45 μm for specimens with a *w/c* ratio of 0.45 at week 49 and 2.92 μm for specimens with a *w/c* ratio of 0.35 at week 37. The ECR specimens showed much lower corrosion losses when based on the total bar surface, with values of 0.03 μm for ECR with four drilled holes and 0.04 μm for ECR with 10 drilled holes for a *w/c* of 0.45 and 0.08 μm for a *w/c* ratio of 0.35 at week 37. If based on the exposed area, the total corrosion were 15.11 μm for ECR with four drilled holes, 7.18 μm for ECR with 10 drilled holes, and 14.6 μm for ECR with a *w/c* ratio of 0.35, as shown in Figures 3.18 and 3.19, respectively.

The mat-to-mat resistances are shown in Figure 3.20. The ECR specimens with four drilled holes showed an average mat-to-mat resistance over 15,000 ohms at week 49, with the highest value (19,000 ohms) at week 35. The ECR specimens with 10 drilled holes exhibited lower resistances, around 13,000 ohms and 10,000 ohms with *w/c* ratios of 0.45 at week 40 and 0.35 at week 37, respectively. The values are higher than those obtained in SE tests because the CB specimens have only one-half of the cross-sectional area of the SE specimens. The conventional steel specimens had the lowest resistance, about 1,000 ohms for specimens with a *w/c* ratio of 0.45 and 1,300 ohms for specimens with a *w/c* ratio of 0.35.

The average corrosion potentials for the top and bottom mats with respect to a copper copper-sulfate electrode are shown in Figure 3.21 and 3.22. The top mats of all specimens showed corrosion potentials more negative than −0.500 V after the first few weeks, indicating a high probability of corrosion. The bottom mats of all specimens, except those with epoxy-coated steel with 10 drilled holes in concrete with *w/c* ratios of 0.35 and 0.45, exhibited corrosion potentials more negative than −0.350 V at some point during the test period. For the specimens with epoxy-coated steel with 10 drilled holes in concrete with a *w/c* ratio of 0.45, the average cathodic potential was more positive than −0.315V. For the specimens with epoxy-coated steel in concrete with a *w/c* ratio of 0.35, the average cathodic potential was always more positive than −0.250V.

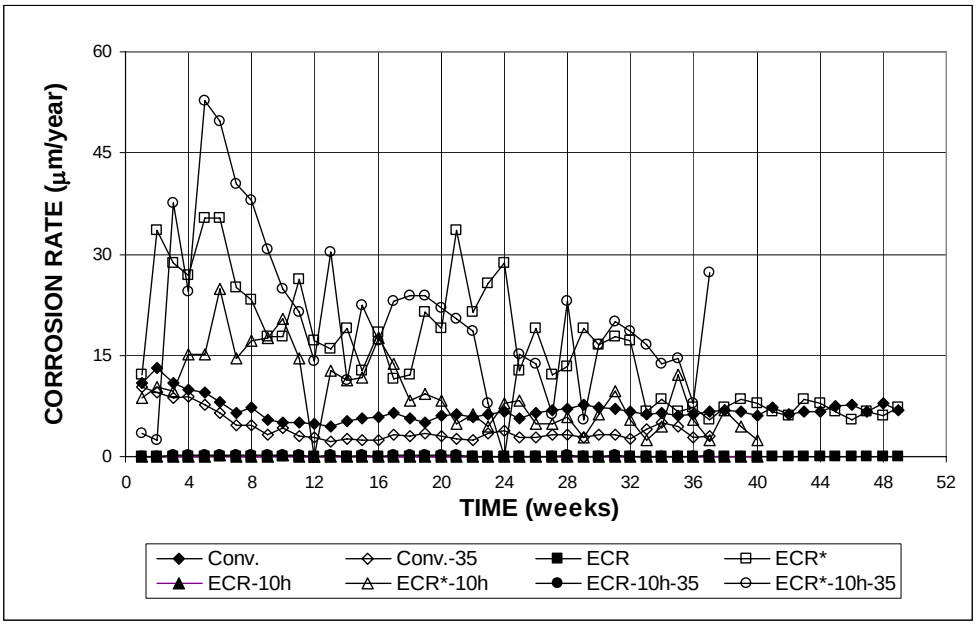

Figure 3.18 (a) – Cracked Beam Tests. Average Corrosion Rate. Specimens of conventional and epoxy-coated reinforcement ponded with 15% NaCl solution. Refer to footnote of Table 3.2 for specimen identification.

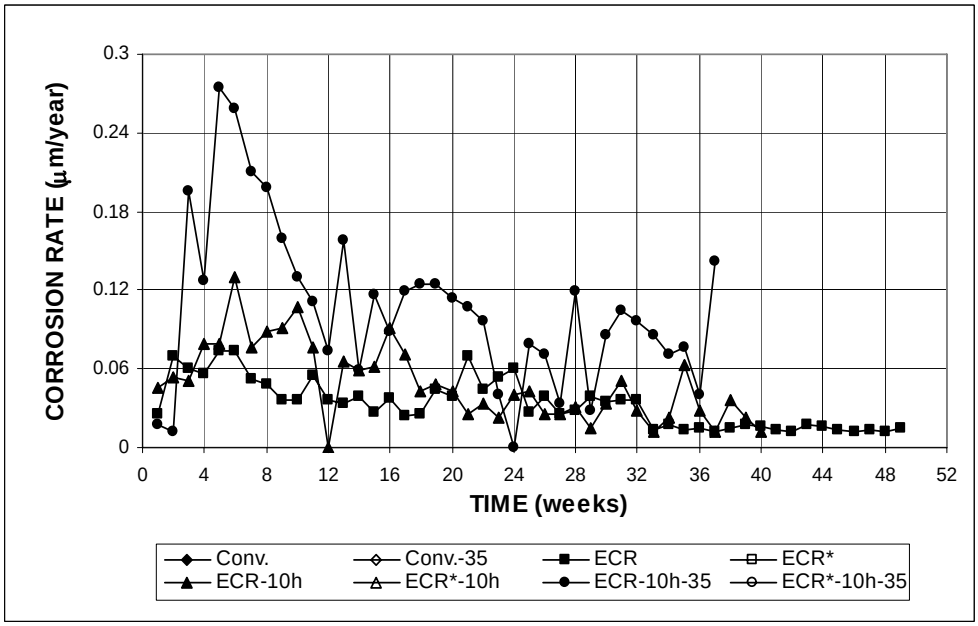

Figure 3.18 (b) – Cracked Beam Tests. Average Corrosion Rate. Specimens of conventional and epoxy-coated reinforcement ponded with 15% NaCl solution. Refer to footnote of Table 3.2 for specimen identification.

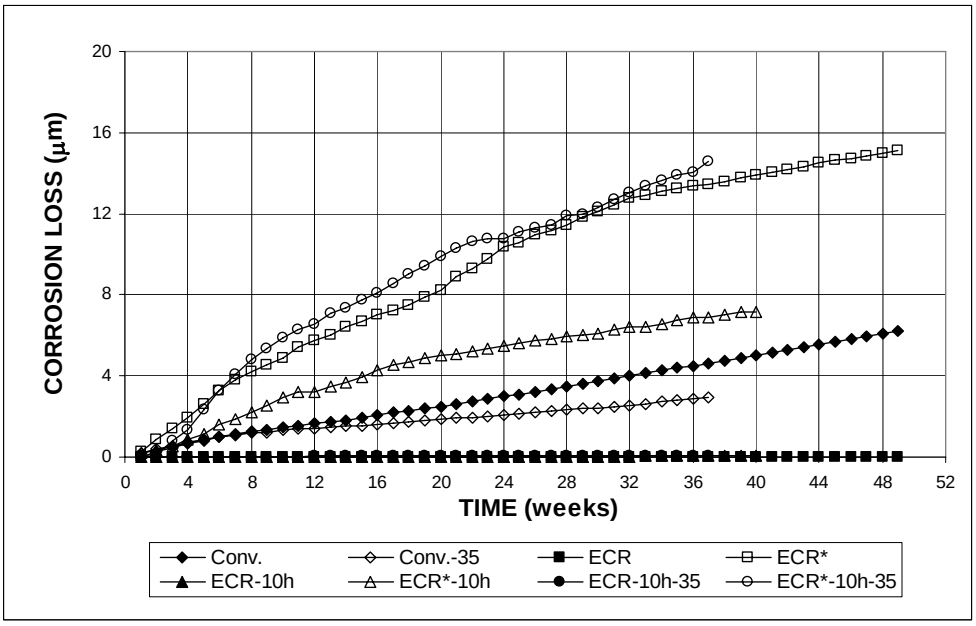

Figure 3.19 (a) – Cracked Beam Tests. Total Corrosion Loss. Specimens of conventional and epoxy-coated reinforcement ponded with 15% NaCl solution. Refer to footnote of Table 3.2 for specimen identification.

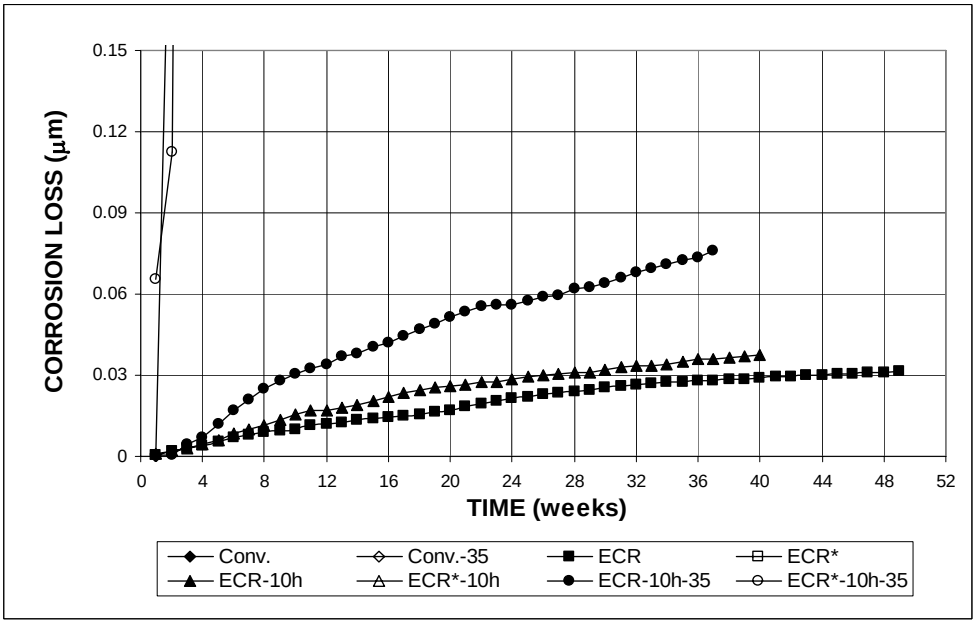

Figure 3.19 (b) – Cracked Beam Tests. Total Corrosion Loss. Specimens of conventional and epoxy-coated reinforcement ponded with 15% NaCl solution. Refer to footnote of Table 3.2 for specimen identification.

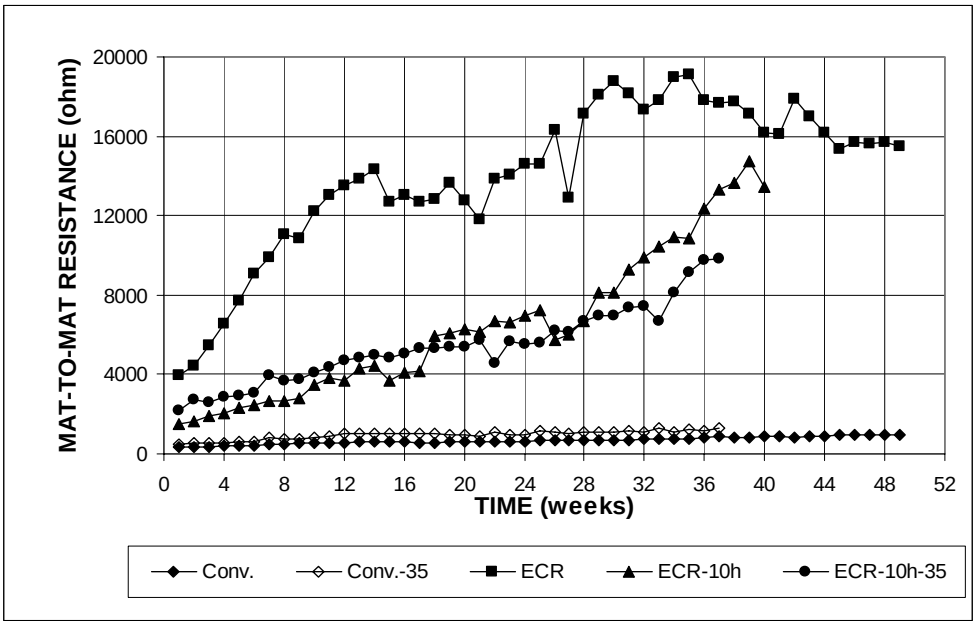

Figure 3.20 – Cracked Beam Tests. Mat-to-mat resistance. Specimens of conventional and epoxy-coated reinforcement ponded with 15% NaCl solution. Refer to footnote of Table 3.2 for specimen identification.

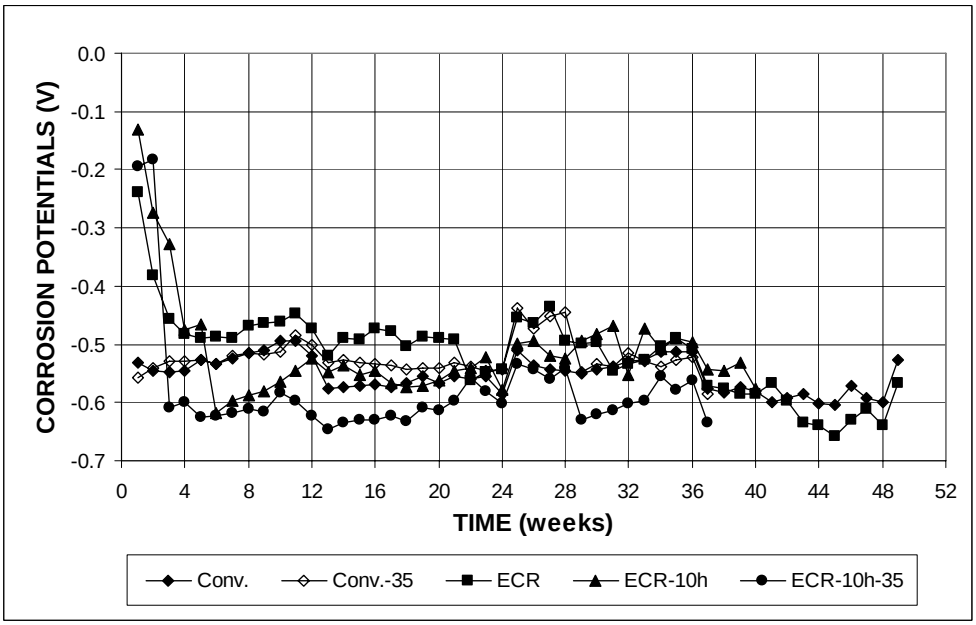

Figure 3.21 – Cracked Beam Tests. Corrosion Potential with respect to CSE at Top Mat. Specimens of conventional and epoxy-coated reinforcement ponded with 15% NaCl solution. Refer to footnote of Table 3.2 for specimen identification.

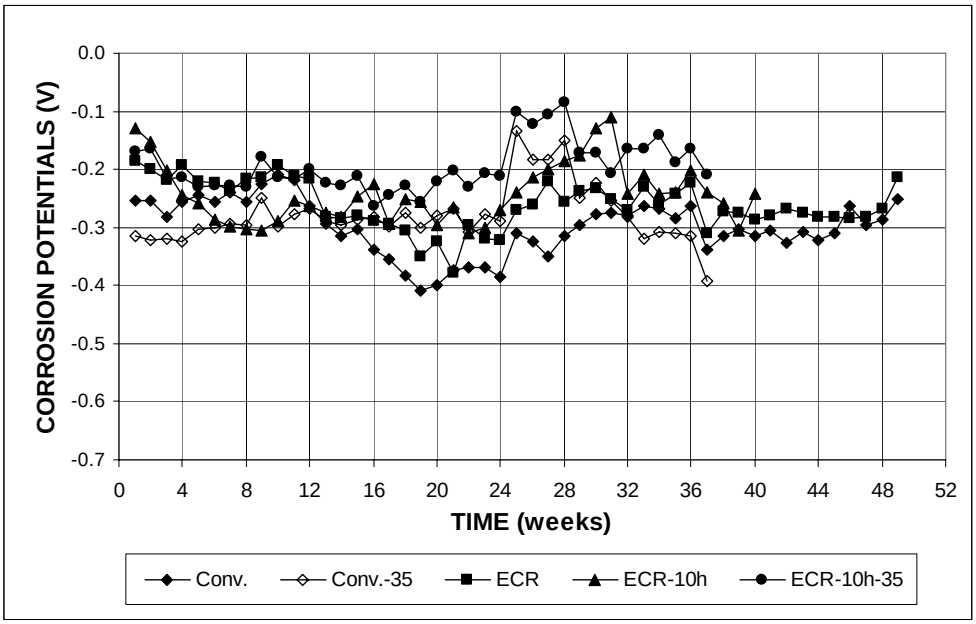

Figure 3.22 – Cracked Beam Tests. Corrosion Potential with respect to CSE at Bottom Mat. Specimens of conventional and epoxy-coated reinforcement ponded with 15% NaCl solution. Refer to footnote of Table 3.2 for specimen identification.

3.1.2.3 ASTM G 109 Tests

The average corrosion rates and total corrosion losses versus time in the ASTM G 109 tests are presented in Table 3.2 and Figures 3.23 and 3.24, respectively, for specimens with conventional and epoxy-coated steel. Based on the total area of the bars, corrosion remains very low for all G 109 specimens containing conventional and epoxy-coated steel. Based on the exposed area, the average corrosion rate observed for ECR bars with four drilled holes was as high as 1.8 μm/yr at week 20, but dropped down after week 27. The ECR bars with 10 drilled holes exhibit similar behavior but at a lower average corrosion rate, starting at 0.5 μm/yr at the beginning and dropping down to 0 at week 26. In all likelihood, the ECR specimens are not, in fact, undergoing significant corrosion since the total corrosion current is about the same as that of the conventional steel specimens. Due to the lower salt concentration

of the ponding solution and the less aggressive ponding and drying cycle, the penetration of chlorides is slower for the G 109 specimens than for the Southern Exposure and cracked beam specimens.

Based on the total area, no significant corrosion losses have been observed on any specimens. Based on the exposed area, the corrosion losses are measured at 0.48 μm for ECR bars with four drilled holes at week 52 and 0.19 μm for ECR bars with 10 drilled holes at week 42.

The average mat-to-mat resistances are shown in Figure 3.25. Similar to the observations for the SE and CB specimens, the ECR specimens with four drilled holes show the highest average mat-to-mat resistance, over 17,000 ohms at week 52 (Figure 3.25), while the ECR bars with 10 drilled holes exhibit a much lower resistance, 5,200 ohms. Conventional steel has the lowest mat-to-mat resistance, 880 ohms at week 51.

The corrosion potentials are shown in Figures 3.26 and 3.27. For both top and bottom mats, all specimens show potentials that are progressively more positive than −0.250 V, indicating a low probability of corrosion. Since the copper copper-sulfate electrode (CSE) used here was out of calibration, only the data obtained using standard calomel electrode is included for analysis, although the results are reported in terms of the CSE.

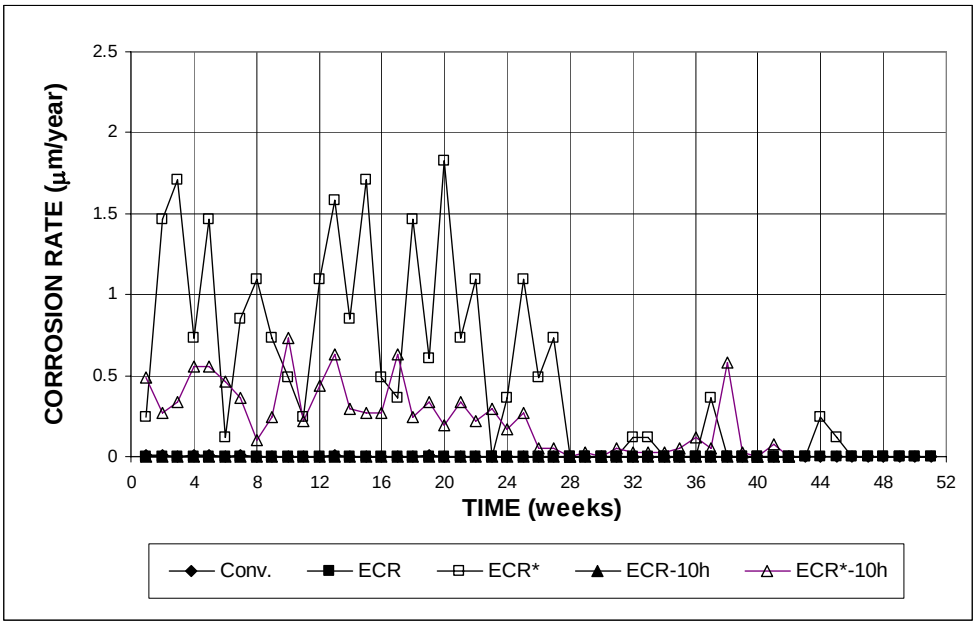

Figure 3.23 (a) – ASTM G 109 Tests. Average Corrosion Rate. Specimens of conventional and epoxy-coated reinforcement. Refer to footnote of Table 3.2 for specimen identification.

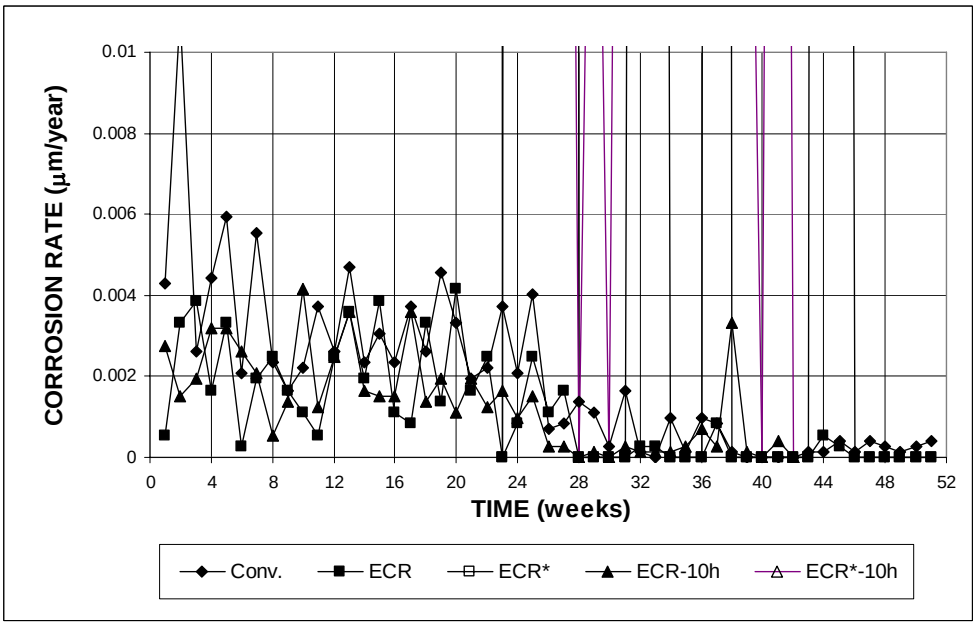

Figure 3.23 (b) – ASTM G 109 Tests. Average Corrosion Rate. Specimens of conventional and epoxy-coated reinforcement. Refer to footnote of Table 3.2 for specimen identification.

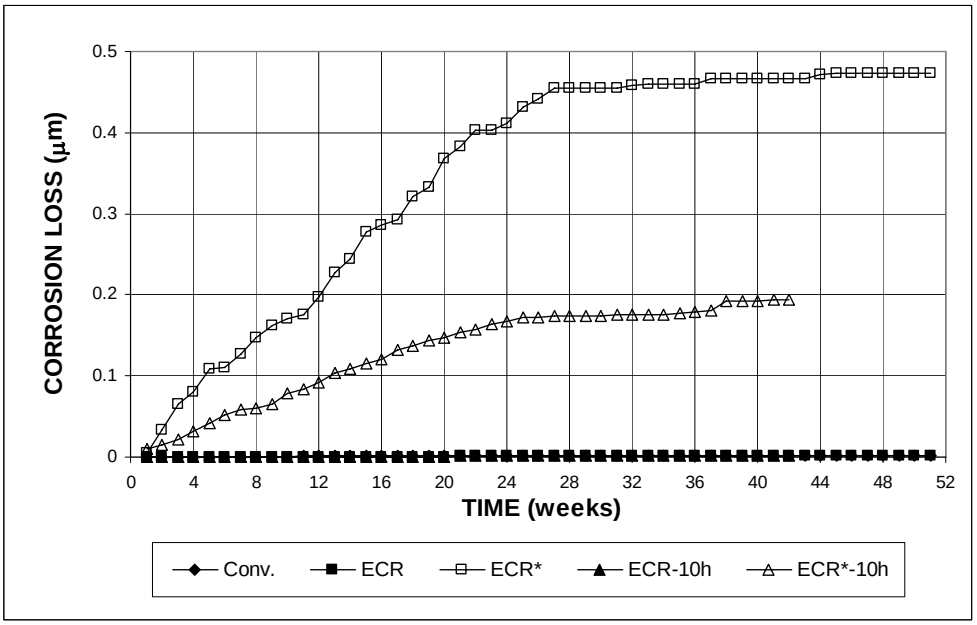

Figure 3.24 (a) – ASTM G 109 Tests. Total Corrosion Loss. Specimens of conventional and epoxy-coated reinforcement. Refer to footnote of Table 3.2 for specimen identification.

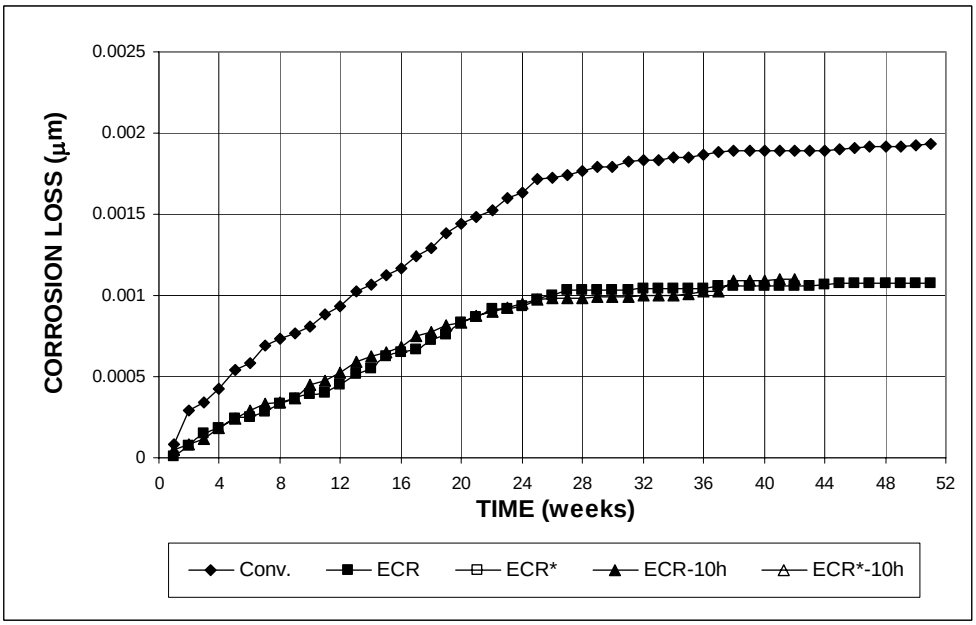

Figure 3.24 (b) – ASTM G 109 Tests. Total Corrosion Loss. Specimens of conventional and epoxy-coated reinforcement. Refer to footnote of Table 3.2 for specimen identification.

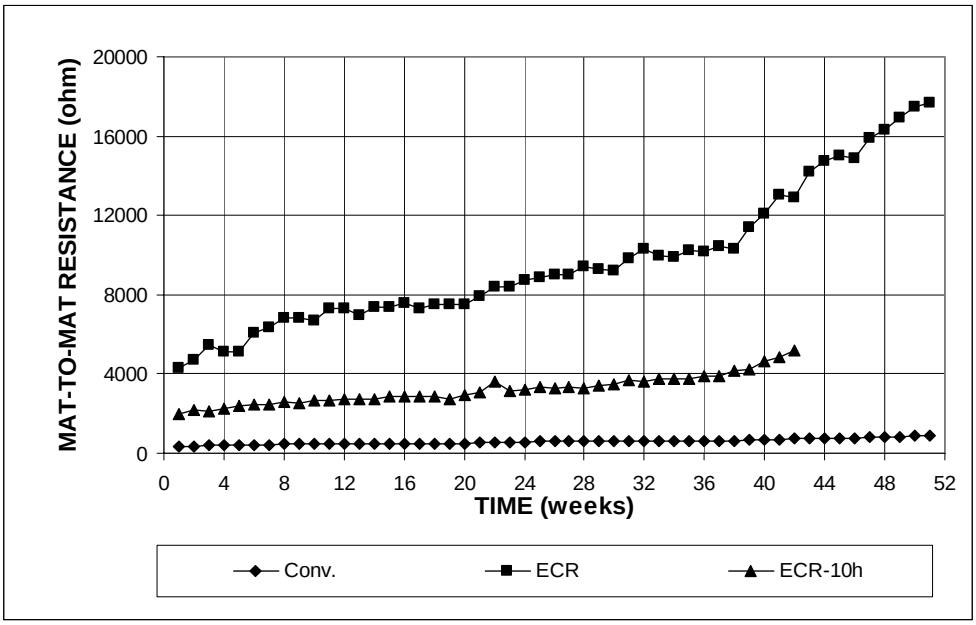

Figure 3.25 – ASTM G 109 Tests. Mat-to-mat resistance. Specimens of conventional and epoxy-coated reinforcement ponded. Refer to footnote of Table 3.2 for specimen identification.

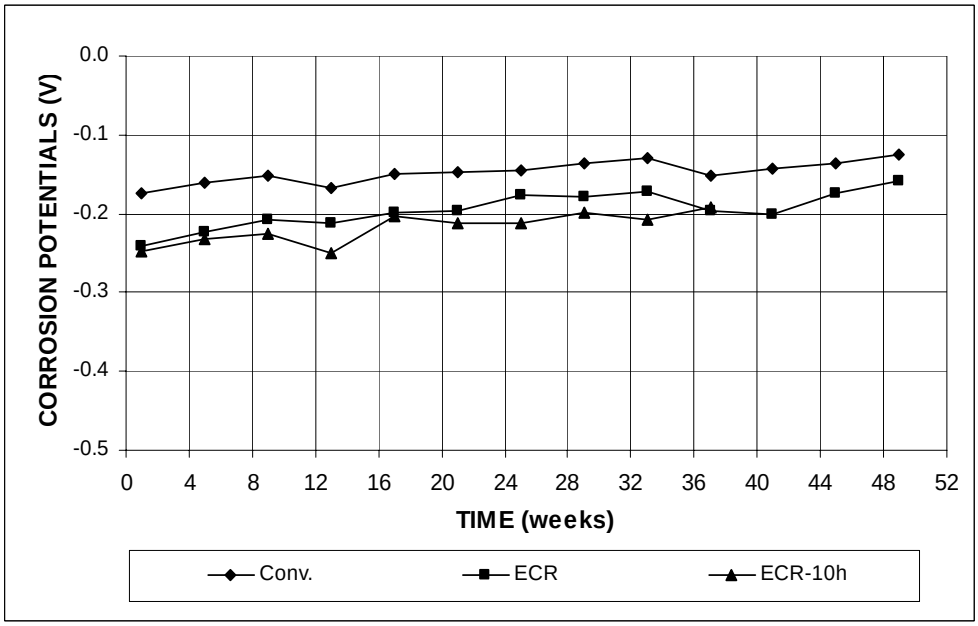

Figure 3.26 – ASTM G 109 Tests. Corrosion Potential with respect to CSE at Top Mat. Specimens of conventional and epoxy-coated reinforcement. Refer to footnote of Table 3.2 for specimen identification.

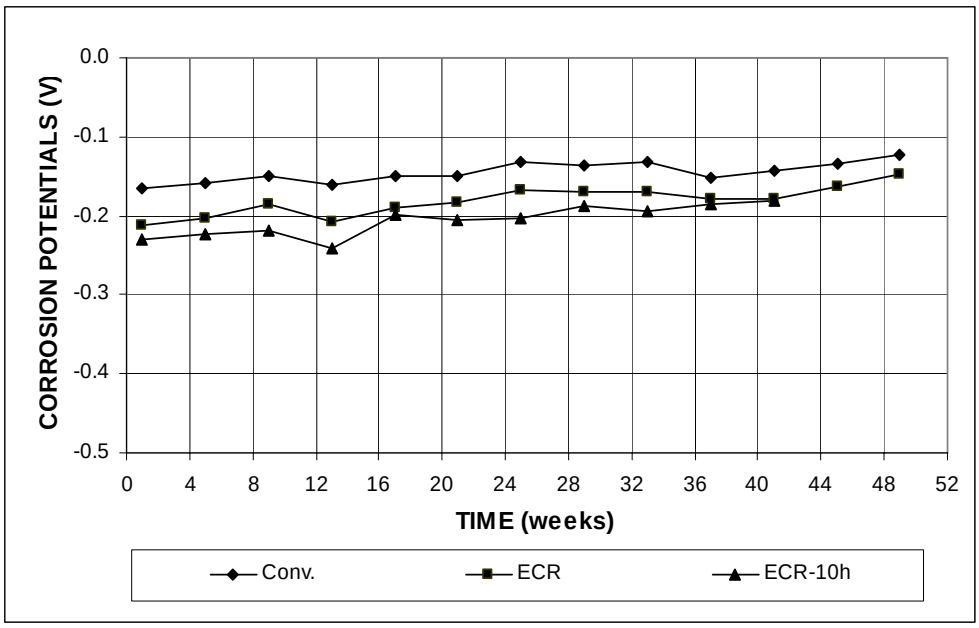

Figure 3.27 – ASTM G 109 Tests. Corrosion Potential with respect to CSE at Bottom Mat. Specimens of conventional and epoxy-coated reinforcement. Refer to footnote of Table 3.2 for specimen identification.

3.2 STAINLESS STEEL CLAD REINFORCEMENT

This section presents the results of the rapid macrocell and bench-scale tests for stainless steel clad reinforcement (SMI-316 SC^{TM}). The average corrosion rates and corrosion losses for the macrocell and bench-scale specimens are summarized in Tables 3.3, 3.4 and 3.5. The results for conventional and epoxy-coated steel are included in the figures in this section, as well as in Sections 3.3 through 3.5, for comparison. Results for individual specimens are presented in Appendix A.

3.2.1 Rapid Macrocell Tests

Both bare and mortar-wrapped specimens were used to evaluate the stainless steel clad reinforcement in the rapid macrocell test. The simulated pore solution with either 1.6 m or 6.04 m ion NaCl was used for bare bar specimens, while the solution with 1.6 m ion NaCl was used for mortar-wrapped specimens. Six bare and six mortar-wrapped specimens were tested in these configurations: (1) without any

protection at ends, (2) with the ends protected by caps, and (3) with cladding penetrated with four 3.2-mm (⅛-in.) diameter drilled holes through the coating and the ends protected by caps. Three tests using bent SMI bars as the anode, three tests using SMI bars with protected ends as the anode and conventional bars as the cathode, and three tests using conventional bars as the anode and SMI bars with protected ends as the cathode were also included.

3.2.1.1 Macrocell Tests for Bare Bar Specimens

The average corrosion rates and total corrosion losses over the 15-week test period for specimens in simulated pore solution with 1.6 m ion NaCl are shown in Figures 3.28 and 3.29, respectively. Figures 3.28 (b), 3.28 (c), and 3.29 (b) expand the vertical axes in Figures 3.28 (a) and 3.29 (a). The corrosion rates for the SMI bars with drilled holes (SMI-d) were calculated based on both the total area of the bars exposed to the solution and the exposed area of the four 3.2-mm (⅛-in.) diameter holes. As mentioned in Section 3.1.1.1, an asterisk (*) is added to the specimen designation in the tables and figures where the corrosion rates and losses are based on the exposed area of the holes drilled through the cladding (SMI-d*). The corrosion rates for the SMI bars with unprotected ends (SMI-nc) were also calculated based on both the total area exposed to solution and the exposed area of the conventional steel core at the bare end. An asterisk (*) is added to the specimen designation, as well, in tables and figures where the corrosion rates and losses are based on the exposed area of the unprotected ends (SMI-nc*). The corrosion rates of intact SMI bars with capped ends (SMI) were only calculated based on the total area exposed to solution since the bars were fully protected. Table 3.3 summarizes the average corrosion rates and total corrosion losses at week 15.

The SMI bars corroded at rates below 0.06 μm/yr during the test period, with an average rate of 0.04 μm/yr at week 15 based on the total area exposed to solution, equal to 0.14% of the rate for conventional steel and 0.85% of the rate for epoxy-coated steel. The SMI-nc specimens started at an average corrosion rate of 0.23 μm/yr, but dropped below 0.1 μm/yr on the second day, and ended at 0.04 μm/yr at week 15. The SMI-d bars reached a corrosion rate as high as 1.9 μm/yr at week 4 and ended at 0.22 μm/yr, that is, lower than the corrosion rates for both conventional (28.1 μm/yr) and epoxy-coated steel (1.18 μm/yr) at week 15. Based on the exposed area, the SMI-nc and SMI-d specimens exhibited significant corrosion rates, as high as 3.12 and 190.3 μm/yr during the testing period, respectively, although the corrosion rates dropped to 0.88 and 22 μm/yr at week 15, below the value for epoxy-coated steel (117.8 μm/yr).

For the mixed SMI and conventional bar tests, when conventional steel was used as the anode and SMI steel was used as the cathode (Conv./SMI), the average corrosion rate reached a value as high as 15.1 μm/year, at week 13, and ended at 13.3 μm/yr at week 15; when SMI steel was used as the anode and conventional steel was used as the cathode (SMI/Conv.), the average corrosion rate started at 0.2 μm/yr at the first day but dropped below 0.1 μm/yr after day 1. At week 10, the corrosion rate increased above 0.1 μm/yr, and ended with a value of 0.4 μm/yr at week 15. In comparison to the tests of conventional steel alone, the average corrosion rate of Conv./SMI is 47% of that of conventional steel at week 15. In comparison to the tests of SMI steel alone, the average corrosion rate of SMI/Conv. is almost nine times of that for SMI at week 15. These comparisons show that SMI steel seems to limit the activity of the cathode.

The average corrosion rate for the tests with bent SMI bars as the anodes (SMI-b) was below 0.05 μm/yr during the test period, ending at 0.01 μm/yr at 15 weeks.

After 15 weeks, the corrosion losses of SMI-nc, SMI, SMI-d, SMI/Conv. and SMI-b (Figure 3.29) were all less than 0.1 μm based on total area. The SMI and SMI-b bars had the lowest average losses, with values below 0.01 μm. The Conv./SMI combination exhibited a significant corrosion loss, 2.19 μm, although this value is lower than that of specimens with conventional steel as both the anode and the cathode (8.16 μm). Based on exposed area, SMI-nc exhibited an observable corrosion loss at 0.4 μm, and SMI-d showed a corrosion loss of 8 μm, which is similar to that of convention steel based on total area.

The average corrosion potentials of the anodes and cathodes are shown in Figures 3.30 and 3.31, respectively. All SMI anode potentials started at values more negative than –0.300 V with respect to a SCE, but achieved values more positive than –0.250 V by the end of week 1, with the exception of SMI-d at week 5 due to a very negative potential of one specimen, as shown in Figures 3.30 and A.14 in Appendix. At week 15, one SMI-d anode (Specimen SMI-d-4, Figure A.14) and all three conventional anodes in the Conv./SMI combination had a corrosion potential more negative than –0.275 V, demonstrating that the bars were undergoing active corrosion, similar to the corrosion potentials of conventional and ECR steel. The average corrosion potentials for all of the cathodes were more positive than –0.200 V for SMI steel, indicating that the bars were passive.

Table 3.3 – Average corrosion rates and corrosion losses for SMI steel in 1.6 m and 6.04 m NaCl solution, as measured in the macrocell tests

CORROSION RATE AT WEEK 15 (μm/year)

Steel Designation	Specimen						Average	Std. Deviation
	1	2	3	4	5	6		
Bare bar specimens in 1.6 m NaCl solution								
SMI-nc	0	0	0.06	0.06	0.06	0.09	0.04	0.04
SMI-nc*	0	0	1.17	1.17	1.17	1.76	0.88	0.72
SMI	0	0	0.04	0.18	0	0	0.04	0.07
SMI-d	0	0	0.07	1.17	0	0.07	0.22	0.47
SMI-d*	0	0	7.32	117.12	0	7.32	21.96	46.76
SMI-b	0.01	0	0.01	0	0.01	0	0.01	0.01
SMI/Conv.	0.26	0.44	0.37	-	-	-	0.35	0.09
Conv./SMI	15.32	16.30	8.21	-	-	-	13.27	4.42
Bare bar specimens in 6.04 m NaCl solution								
SMIh-nc	2.46	7.63	0.23	0	0.46	3.47	2.37	2.93
SMIh-nc*	49.77	154.59	4.68	0	9.37	70.27	48.11	59.21
SMIh	0	0.04	0	0.04	0	0	0.01	0.01
SMIh-d	0	0	0.04	1.02	0.11	0.07	0.21	0.40
SMIh-d*	0	0	3.66	102.48	10.98	7.32	20.74	40.27

TOTAL CORROSION LOSS AFTER WEEK 15 (μm)

Steel Designation	Specimen						Average	Std. Deviation
	1	2	3	4	5	6		
Bare bar specimens in 1.6 m NaCl solution								
SMI-nc	β	β	0.01	β	β	0.09	0.02	0.03
SMI-nc*	0.1	0.06	0.21	0.06	0.09	1.76	0.38	0.68
SMI	β	β	β	0.03	β	β	β	0.01
SMI-d	0.24	β	0.02	0.20	β	β	0.08	0.11
SMI-d*	24.42	0.56	1.55	20.41	0.28	0.49	7.95	11.28
SMI-b	β	β	β	β	β	β	β	-
SMI/Conv.	0.05	0.03	0.02	-	-	-	0.03	0.01
Conv./SMI	2.20	2.20	2.15	-	-	-	2.18	0.03
Bare bar specimens in 6.04 m NaCl solution								
SMI-nc	0.54	0.49	0.17	0.21	0.98	0.83	0.54	0.33
SMI-nc*	10.93	9.84	3.39	4.19	19.83	16.73	10.82	6.58
SMI	β	0.04	β	β	0.01	β	0.01	0.01
SMI-d	β	0.28	0.01	0.05	0.04	0.02	0.07	0.10
SMI-d*	0.28	27.73	1.06	4.58	4.29	1.97	6.65	10.47

[1] SMI-nc: Stainless steel clad reinforcement without end protection, based on total area of bar exposed to solution

[2] SMI-nc: Stainless steel clad reinforcement without end protection, based on exposed area of the ends

[3] SMI: Stainless steel clad reinforcement with end protection, based on total area of bar exposed to solution

[4] SMI-d: Stainless steel clad reinforcement with end protection and drilled holes, based on total area of bar exposed to solution

[5] SMI-d*: Stainless steel clad reinforcement with end protection, based on exposed area of four 3.2-mm (1/8-in.) diameter holes in cladding

[6] SMI-b: Stainless steel clad reinforcement with bent anode, based on total area exposed to solution

[7] SMI/Conv.: Stainless steel clad reinforcement with end protection as anode and conventional steel as cathode, based on total area exposed to solution

[8] Conv./SMI: Conventional steel as anode and stainless steel clad reinforcement with end protection as cathode, based on total area exposed to solution

[9] SMIh-nc: Stainless steel clad reinforcement without end protection in solution with high NaCl concentration, based on total area of bar exposed to solution

[10] SMIh-nc: Stainless steel clad reinforcement without end protection in solution with high NaCl concentration, based on exposed area of the ends

[11] SMIh: Stainless steel clad reinforcement with end protection in solution with high NaCl concentration, based on total area of bar exposed to solution

[12] SMIh-d: Stainless steel clad reinforcement with end protection and drilled holes in solution with high NaCl concentration, based on total area of bar exposed to solution

[13] SMIh-d*: Stainless steel clad reinforcement with end protection in solution with high NaCl concentration, based on exposed area, four 3.2-mm (1/8-in.) diameter holes in cladding

[14] β: corrosion loss less than 0.01μm

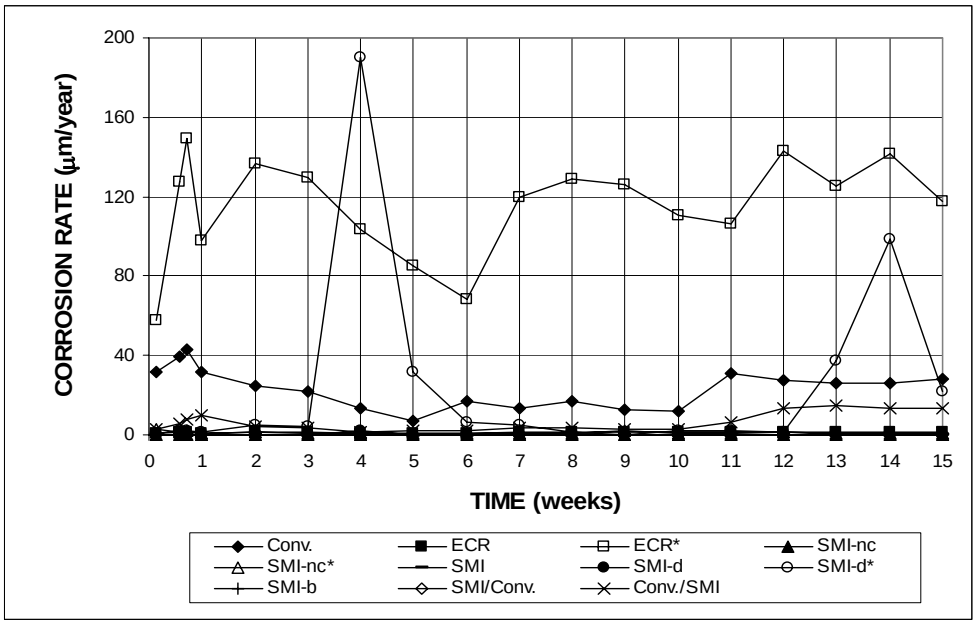

Figure 3.28 (a) - Macrocell Tests. Average Corrosion Rate. Bare bar specimens of conventional, epoxy-coated, and SMI steel in simulated concrete pore solution with 1.6 m ion NaCl. Refer to Table 3.3 for specimen identification.

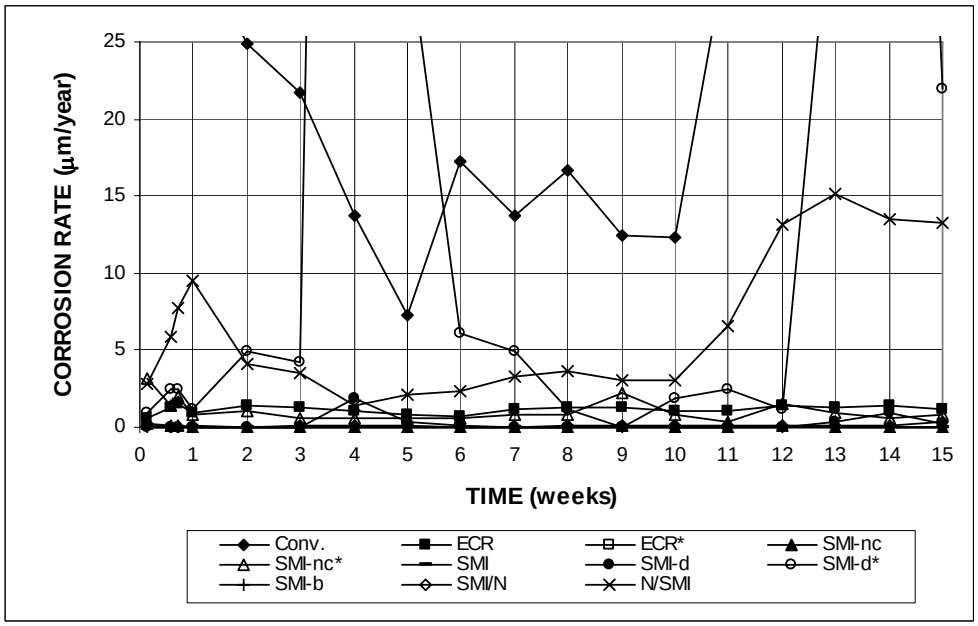

Figure 3.28 (b) - Macrocell Tests. Average Corrosion Rate. Bare bar specimens of conventional, epoxy-coated, and SMI steel in simulated concrete pore solution with 1.6 m ion NaCl. Refer to Table 3.3 for specimen identification.

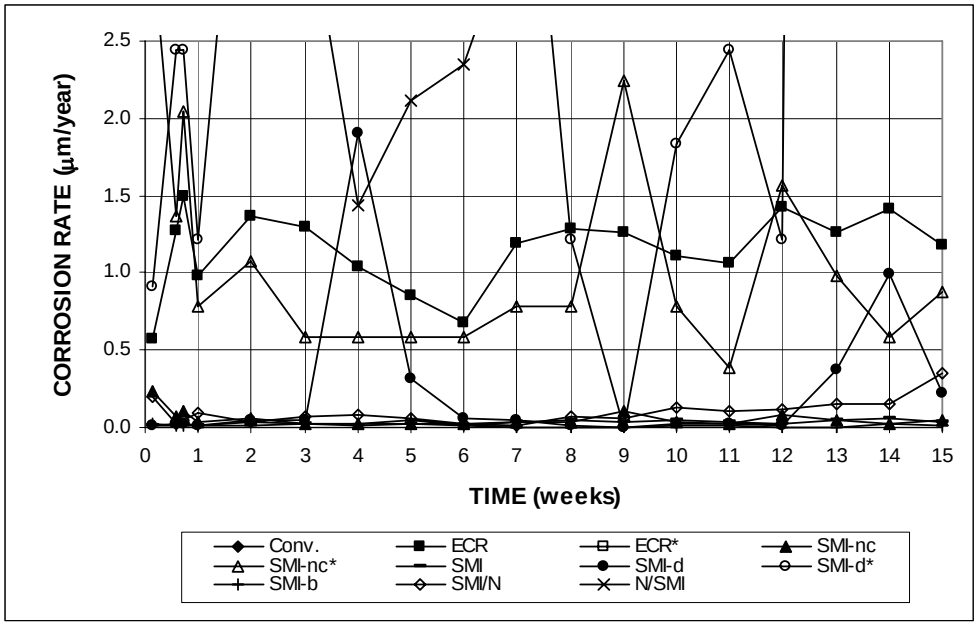

Figure 3.28 (c) - Macrocell Tests. Average Corrosion Rate. Bare bar specimens of conventional, epoxy-coated, and SMI steel in simulated concrete pore solution with 1.6 m ion NaCl. Refer to Table 3.3 for specimen identification.

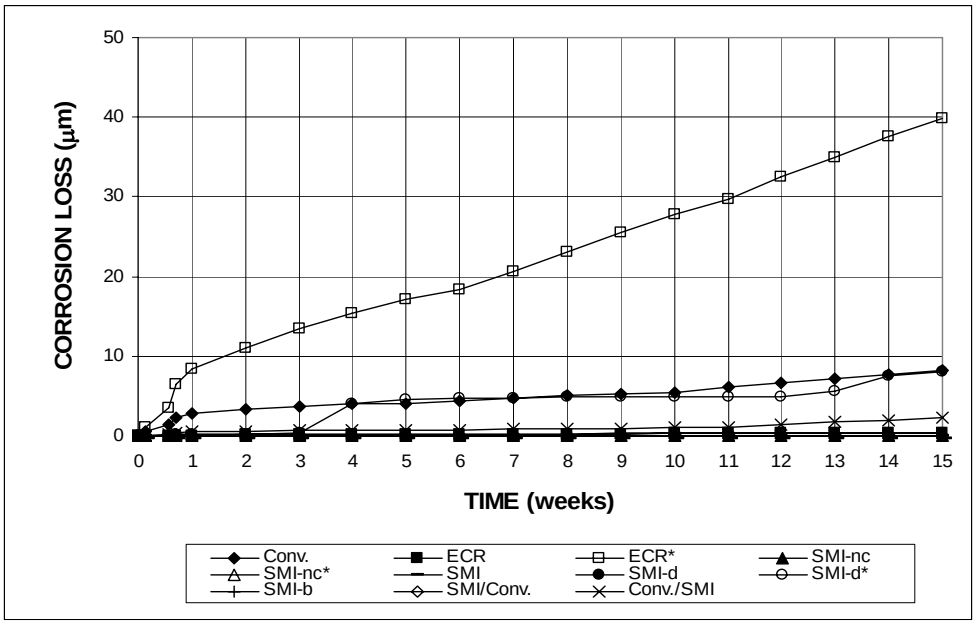

Figure 3.29 (a) - Macrocell Tests. Total Corrosion Loss. Bare bar specimens of conventional, epoxy-coated, and SMI steel in simulated concrete pore solution with 1.6 m ion NaCl. Refer to Table 3.3 for specimen identification.

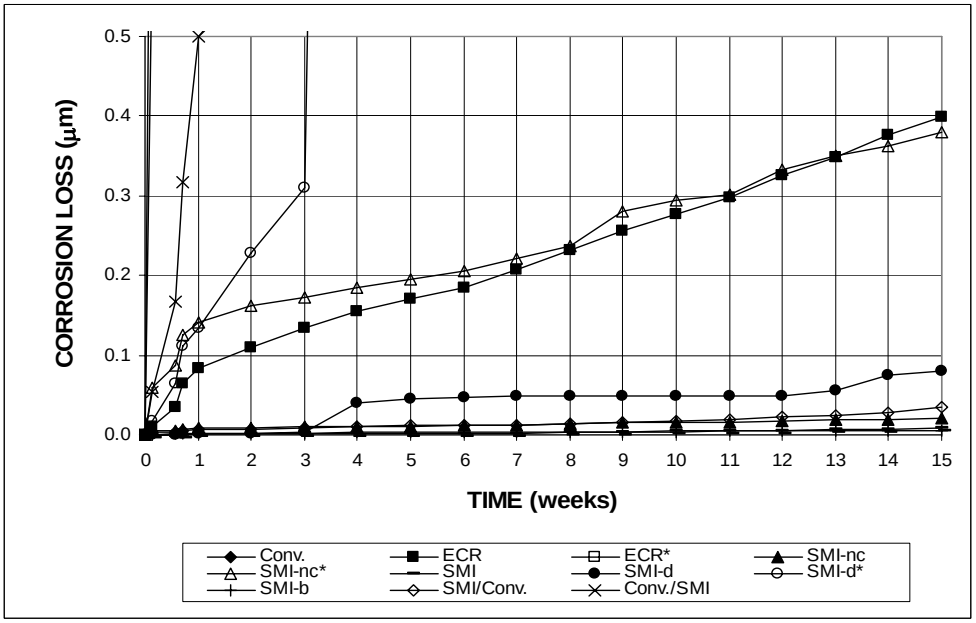

Figure 3.29 (b) - Macrocell Tests. Total Corrosion Loss. Bare bar specimens of conventional, epoxy-coated, and SMI steel in simulated concrete pore solution with 1.6 m ion NaCl. Refer to Table 3.3 for specimen identification.

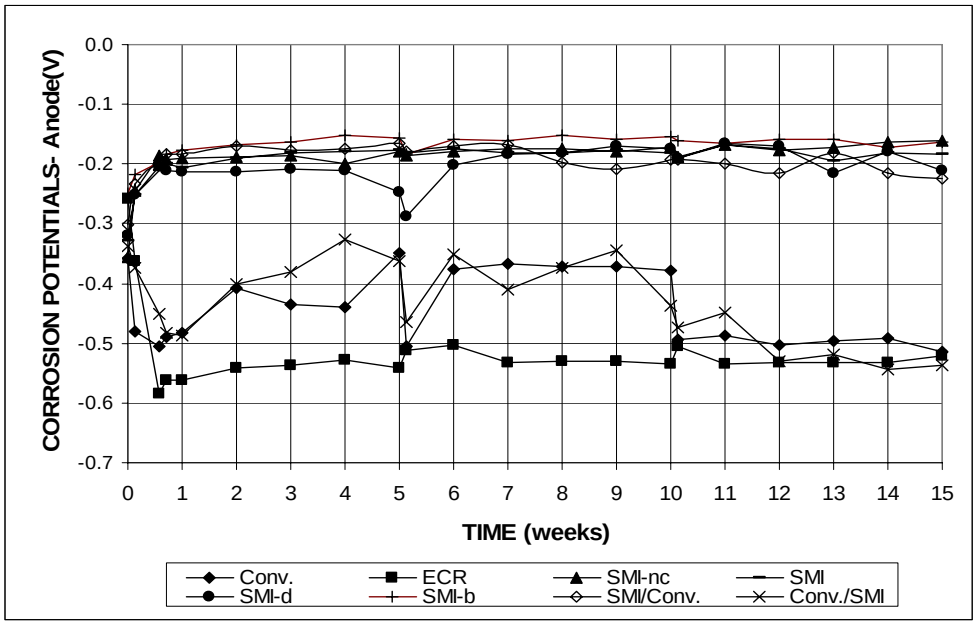

Figure 3.30 - Macrocell Tests. Corrosion Potential with respect to SCE at Anode. Bare bar specimens of conventional, epoxy-coated, and SMI steel in simulated concrete pore solution with 1.6 m ion NaCl. Refer to Table 3.3 for specimen identification.

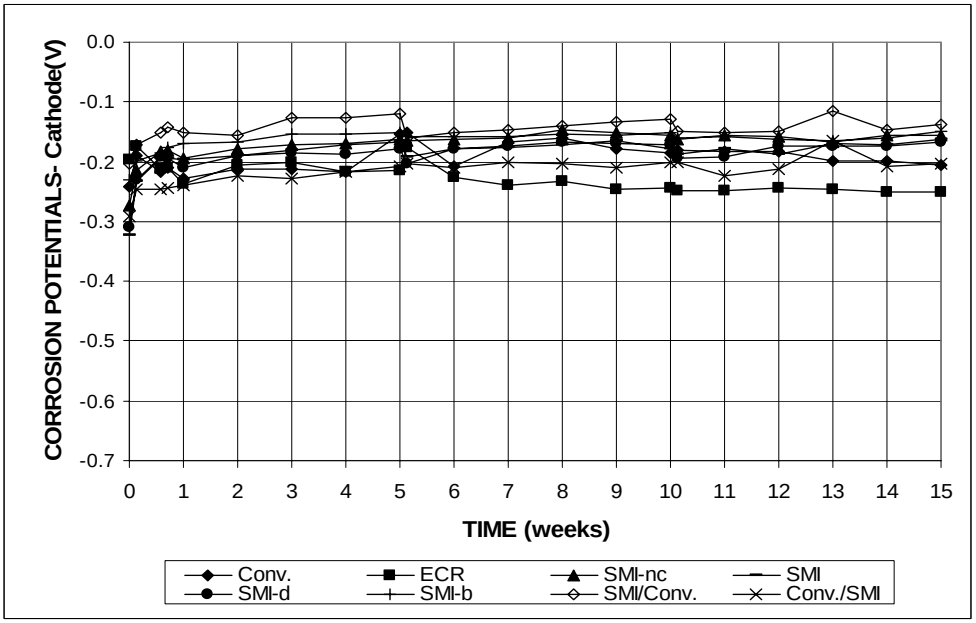

Figure 3.31 - Macrocell Tests. Corrosion Potential with respect to SCE at Cathode. Bare bar specimens of conventional, epoxy-coated, and SMI steel in simulated concrete pore solution with 1.6 m ion NaCl. Refer to Table 3.3 for specimen identification.

As shown in Table 3.3 and Figure 3.32, in pore solution with the 6.04 m ion concentration (NaCl), the SMI bare bar specimens without caps (SMIh-nc) showed obvious corrosion, as high as 6 μm/yr at week 11, and ending at 2.4 μm/yr at week 15, all based on the total area. The SMI bare bar specimens with four 3.2-mm (1/8-in.) diameter drilled holes and with the ends capped (SMIh-d) underwent insignificant corrosion with a rate less than 0.2 μm/yr until week 11. The average corrosion rate of the SMIh-d specimens jumped up at week 12 and reached a value as high as 1.3 μm/yr at week 13, although the rate dropped down at the end of 15 weeks to a value of 0.21 μm/yr, based on the total area. The SMI bare bar tests with cap but without drilled holes (SMIh) exhibited a corrosion rate less than 0.05 μm/yr throughout the testing period, with the exception of week 3 when the corrosion rate jumped to 0.24 μm/yr.

The total corrosion losses as a function of time are shown in Figure 3.33. Based on the total area in contact with the solution, SMIh and SMIh-d both had corrosion losses less than 0.1 μm after 15 weeks, while SMIh-nc showed a more significant corrosion loss at 0.54 μm. Based on exposed area, SMIh-nc and SMIh-d exhibited local corrosion losses of 10.82 and 6.65 μm, respectively.

The average corrosion potentials of the anodes and cathodes are shown in Figures 3.34 and 3.35, respectively. SMIh-nc and SMIh-d started to undergo active corrosion at week 8 and 15, respectively, with average values more negative than –0.275 V with respect to a SCE. The average corrosion potentials for the cathodes were more positive than –0.275 V for all groups, demonstrating the passive condition of the bars.

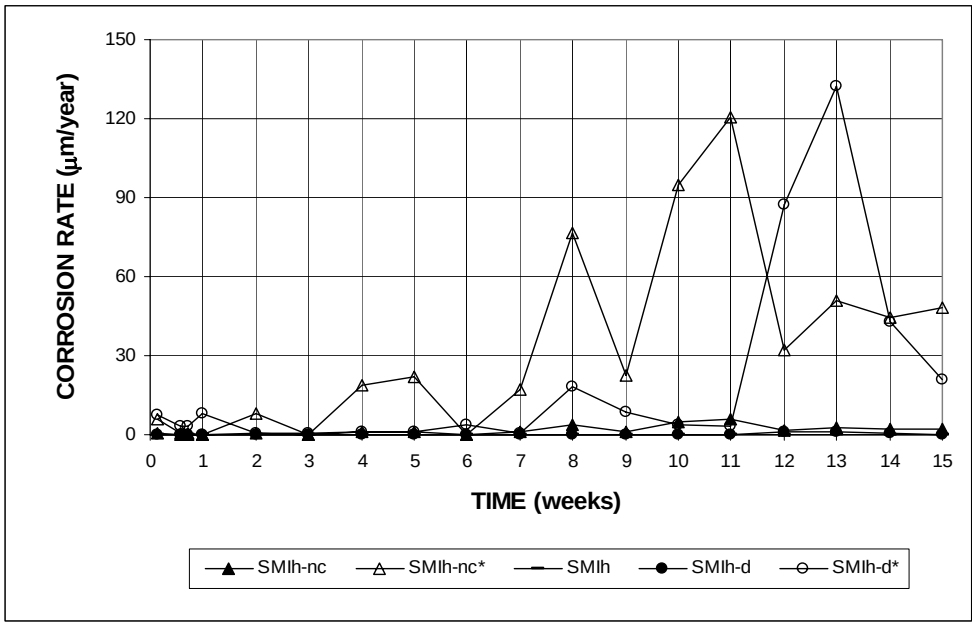

Figure 3.32 (a) - Macrocell Tests. Average Corrosion Rate. Bare bar specimens of SMI steel in simulated concrete pore solution with 6.04 m ion NaCl. Refer to Table 3.4 for specimen identification.

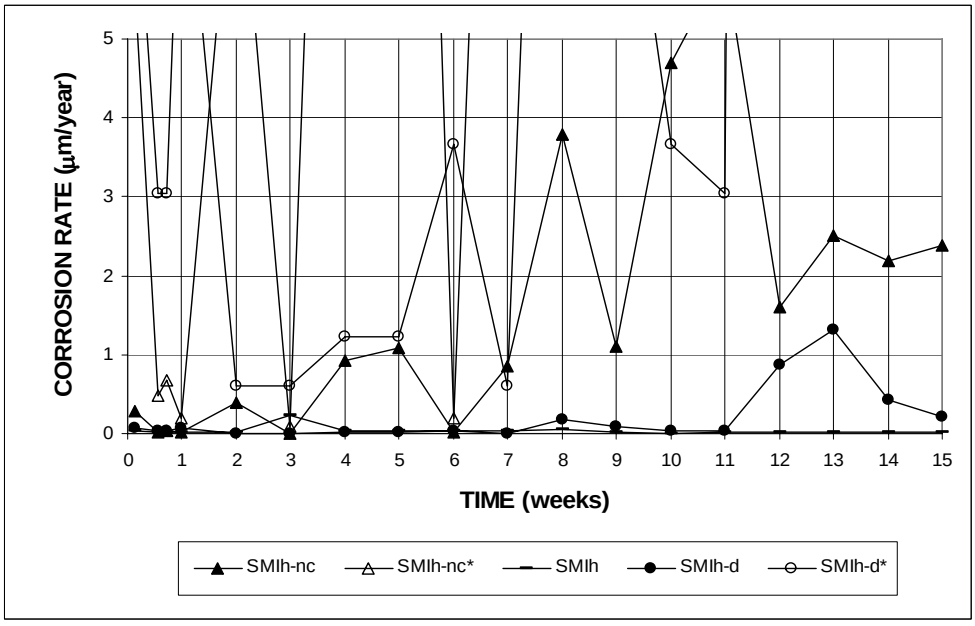

Figure 3.32 (b) - Macrocell Tests. Average Corrosion Rate. Bare bar specimens of SMI steel in simulated concrete pore solution with 6.04 m ion NaCl. Refer to Table 3.4 for specimen identification.

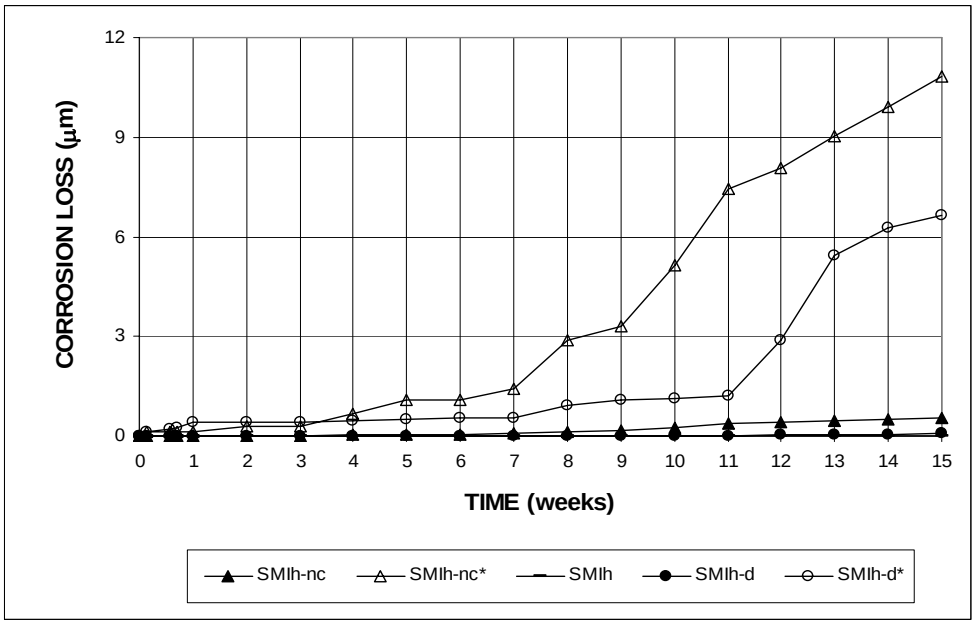

Figure 3.33 (a) - Macrocell Tests. Total Corrosion Loss. Bare bar specimens of SMI steel in simulated concrete pore solution with 6.04 m ion NaCl. Refer to Table 3.4 for specimen identification.

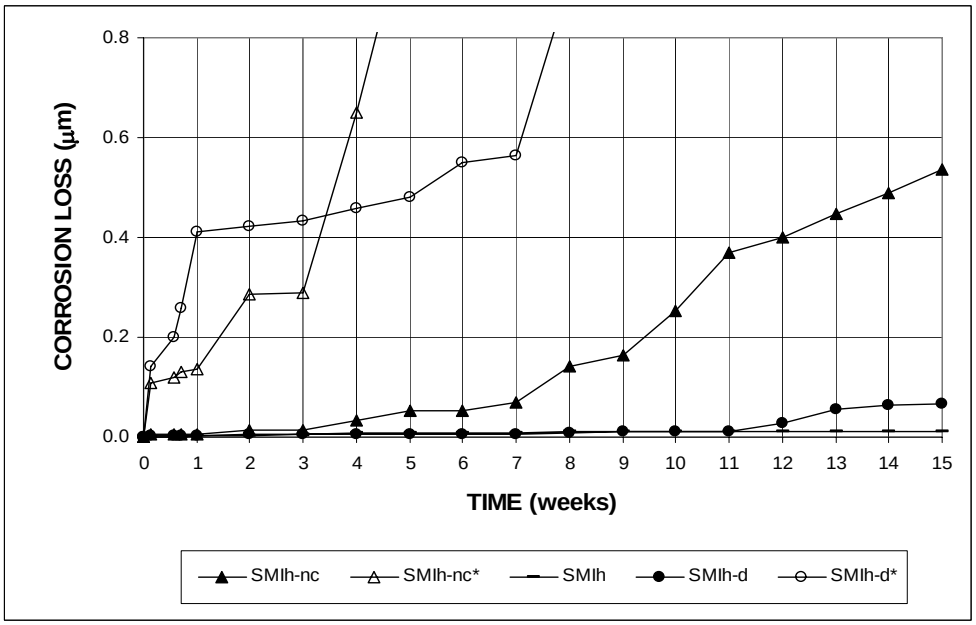

Figure 3.33 (b) - Macrocell Tests. Total Corrosion Loss. Bare bar specimens of SMI steel in simulated concrete pore solution with 6.04 m ion NaCl. Refer to Table 3.4 for specimen identification.

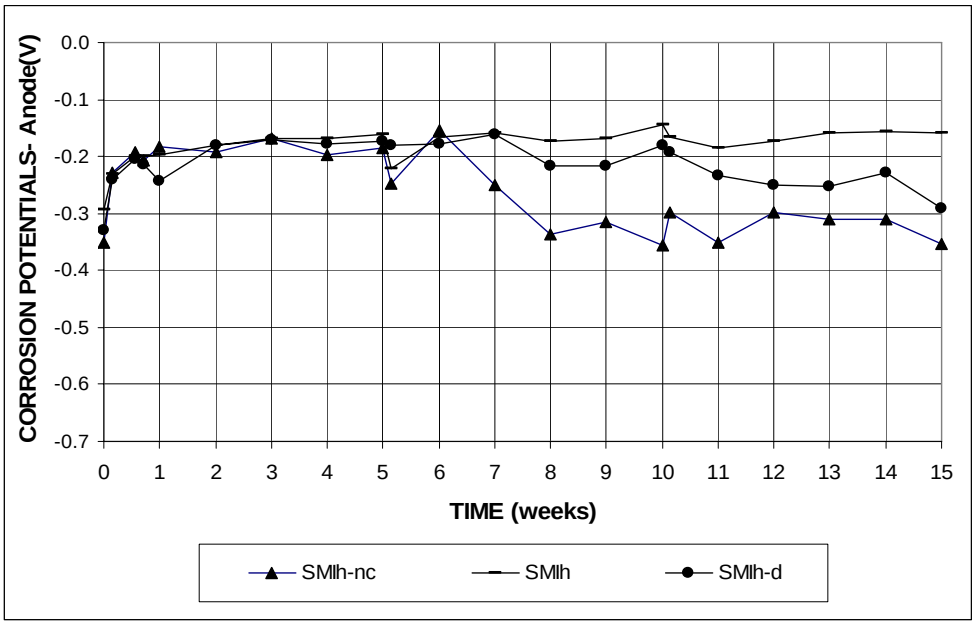

Figure 3.34 - Macrocell Tests. Average Corrosion Potential with respect to SCE at Anode. Bare bar specimens of SMI steel in simulated concrete pore solution with 6.04 m ion NaCl. Refer to Table 3.4 for specimen identification.

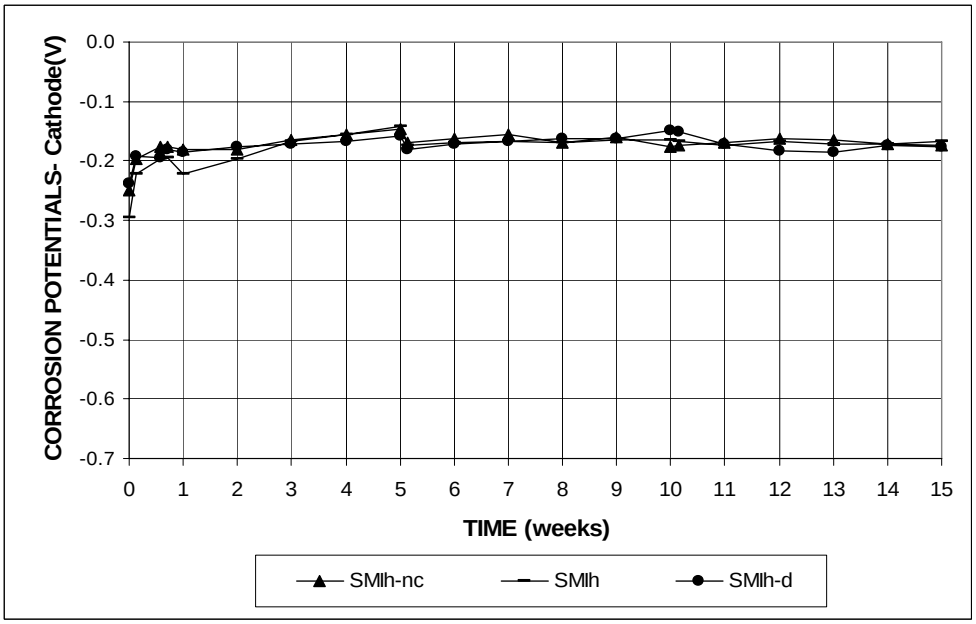

Figure 3.35 - Macrocell Tests. Average Corrosion Potential with respect to SCE at Cathode. Bare bar specimens of SMI steel in simulated concrete pore solution with 6.04 m ion NaCl. Refer to Table 3.4 for specimen identification

3.2.1.2 Macrocell Tests for Mortar-Wrapped Specimens

Figures 3.36 and 3.37 show the average corrosion rates and total corrosion losses for mortar-wrapped specimens. Figures 3.36 (b) and 3.37 (b) expand the vertical axis in Figures 3.36 (a) and 3.37 (a), respectively. The corrosion rates for the SMI bars with drilled holes (SMI-d) were calculated based on both the total area of the bars exposed to the solution and the exposed area of the four 3.2-mm (1/8-in.) diameter holes drilled through the cladding. The corrosion rates for SMI bars with unprotected ends (SMI-nc) were also calculated based on both the total area exposed to solution and the exposed area of the bare ends. Table 3.4 summarizes the average corrosion rates at week 15.

Based on the exposed area, the average corrosion rates for SMI-nc and SMI-d specimens reached values as high as 5.4 and 30.5 μm/year at some points during the test period, and ended at 1.1 and 11.6 μm/yr at week 15, respectively, as shown in Figure 3.36 (a) and Table 3.4. The corrosion rate at week 15 of SMI-nc is 44% of that for ECR (2.44 μm/yr), while the corrosion rate of SMI-d is almost 5 times of that for ECR due to the much larger cathodic area of the SMI specimens compared to that for the epoxy-coated steel specimens. Based on the total bar area exposed to the solution, the SMI bars without drilled holes and with protected ends (SMI) had an average corrosion rate of 0.018 μm/year, 75% of that for the ECR bars (0.024 μm/yr), 40% of that for the SMI-nc bars (0.05 μm/yr), 17% of that for the SMI-d bars (0.12 μm/year), and only 0.1% of that for conventional steel (21.6 μm/yr), demonstrating the good corrosion resistance of undamaged SMI bars.

As shown in Figure 3.37, based on the total area exposed to the solution, the SMI-nc, SMI-d, and SMI bars had average corrosion losses at 15 weeks of 0.02, 0.03, and less than 0.01 μm, respectively. These corrosion losses are similar to losses

exhibited by the ECR specimens (less than 0.1 μm) and much lower than the value for conventional bars (5 μm). Based on the area not protected by cladding, SMI-nc and SMI-d exhibited corrosion losses of 0.33 and 2.93 μm, respectively, 75% and almost seven times of the value for the ECR specimens (0.44 μm).

The average corrosion potentials of the anodes and the cathodes with respect to a saturated calomel electrode are shown in Figures 3.38 and 3.39. The corrosion potentials of all three groups of SMI specimens (SMI-nc, SMI, SMI-d) were more positive than −0.275 V with respect to a SCE for both the anodes and the cathodes. The values are similar to the potentials exhibited by epoxy-coated steel but are more positive than those for conventional steel, indicating a low probability of corrosion.

The lower corrosion rates and more positive corrosion potentials exhibited by damaged SMI bars in mortar-wrapped specimens when compared to bare specimens are due to, as mentioned in Section 3.1.1.2, additional passive protection provided to steel in contact with hydrated cement, a lower rate of diffusion of oxygen and moisture to the cathode, and a lower rate of diffusion of chlorides to the anode. Also, as mentioned in Section 3.1.1.2, the non-homogeneous nature of chloride diffusion through mortar could result in a locally low chloride content at the areas on SMI bars that are not protected by cladding.

Table 3.4 – Average corrosion rates and corrosion losses for SMI steel in 1.6 m NaCl solution, as measured in the macrocell tests

CORROSION RATE AT WEEK 15 (μm/year)

Steel Designation	Specimen						Average	Std. Deviation
	1	2	3	4	5	6		
Mortar-wrapped specimens								
SMI-nc.	0	0.09	0.15	0.06	0	0.03	0.05	0.06
SMI-nc*	0	1.76	2.93	1.17	0	0.59	1.07	1.14
SMI	0.04	0	0	0	0	0.07	0.02	0.03
SMI-d	0	0	0.66	0	0	0.04	0.12	0.27
SMI-d*	0	0	65.88	0	0	3.66	11.59	26.64

TOTAL CORROSION LOSS AFTER WEEK 15 (μm)

Steel Designation	Specimen						Average	Std. Deviation
	1	2	3	4	5	6		
Mortar-wrapped specimens								
SMI-nc.	β	β	0.03	0.04	β	β	0.02	0.02
SMI-nc*	0.07	0.17	0.62	0.87	0.12	0.14	0.33	0.33
SMI	β	β	β	β	β	β	β	-
SMI-d	β	β	0.1	0.05	0.01	β	0.03	0.04
SMI-d*	0.35	0.56	9.78	4.79	1.20	0.92	2.93	3.73

[1] SMI-nc: Stainless steel clad reinforcement without end protection, based on total area of bar exposed to solution

[2] SMI-nc: Stainless steel clad reinforcement without end protection, based on exposed area of the ends

[3] SMI: Stainless steel clad reinforcement with end protection, based on total area of bar exposed to solution

[4] SMI-d: Stainless steel clad reinforcement with end protection and drilled holes, based on total area of bar exposed to solution

[5] SMI-d*: Stainless steel clad reinforcement with end protection, based on exposed area of four 3.2-mm (1/8-in.) diameter holes in cladding

[6] β: corrosion loss less than 0.01μm

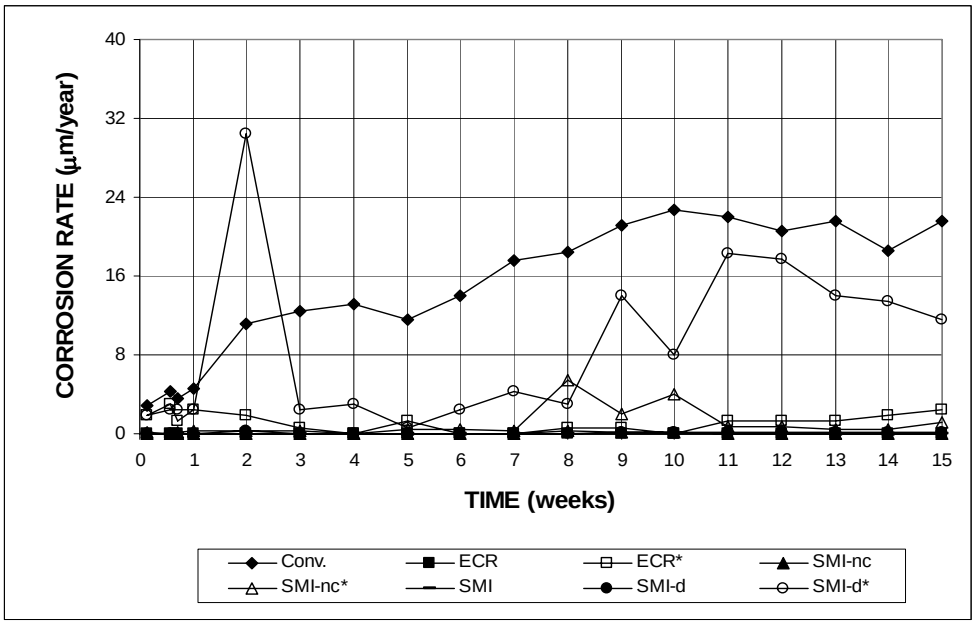

Figure 3.36 (a) - Macrocell Tests. Average Corrosion Rate. Mortar-wrapped specimens of conventional, epoxy-coated, and SMI steel in simulated concrete pore solution with 1.6 m ion NaCl. Refer to Table 3.3 for specimen identification.

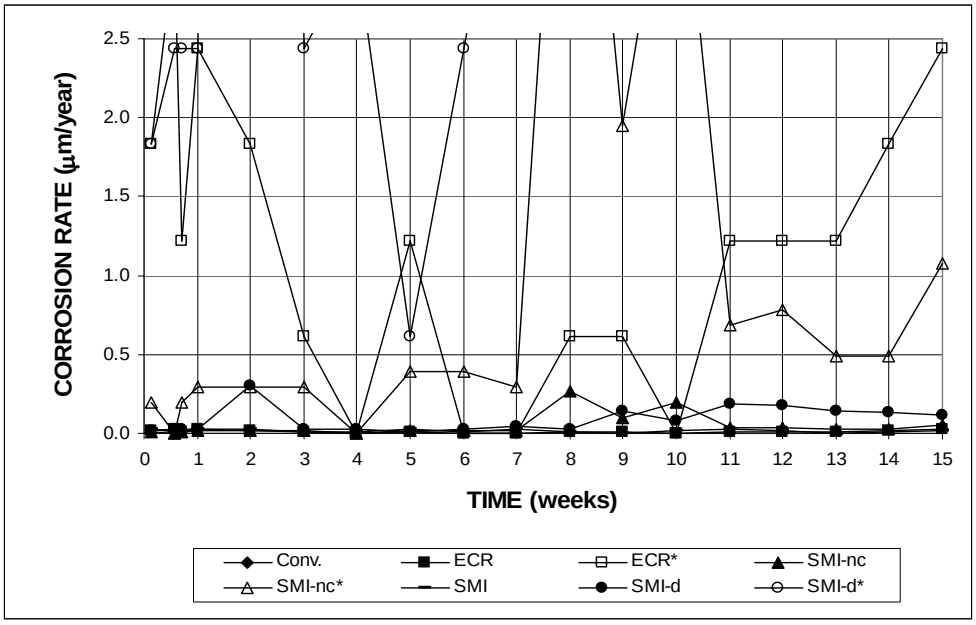

Figure 3.36 (b) - Macrocell Tests. Average Corrosion Rate. Mortar-wrapped specimens of conventional, epoxy-coated, and SMI steel in simulated concrete pore solution with 1.6 m ion NaCl. Refer to Table 3.3 for specimen identification.

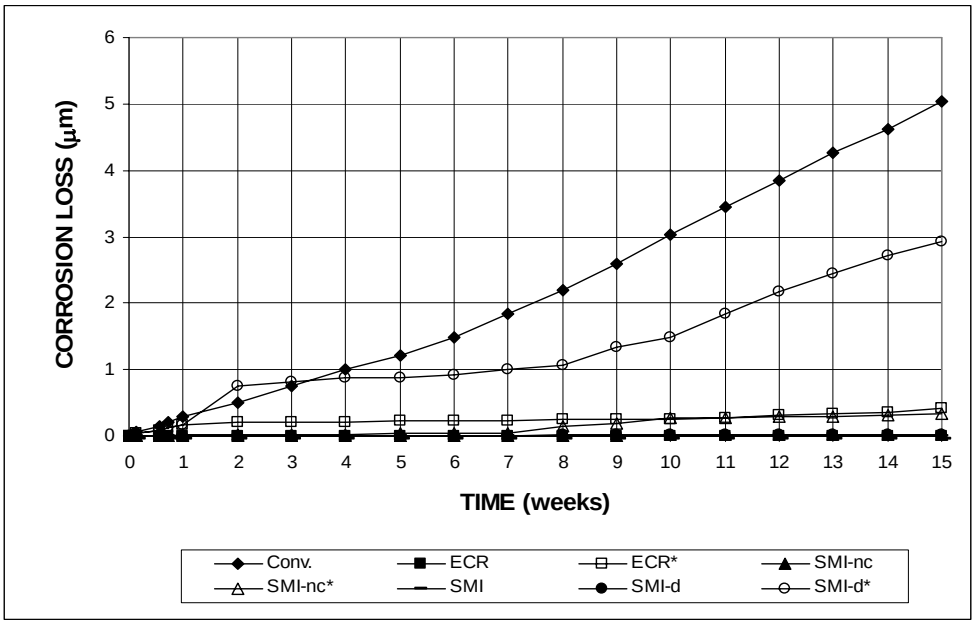

Figure 3.37 (a) - Macrocell Tests. Total Corrosion Loss. Mortar-wrapped specimens of conventional, epoxy-coated, and SMI steel in simulated concrete pore solution with 1.6 m ion NaCl. Refer to Table 3.3 for specimen identification.

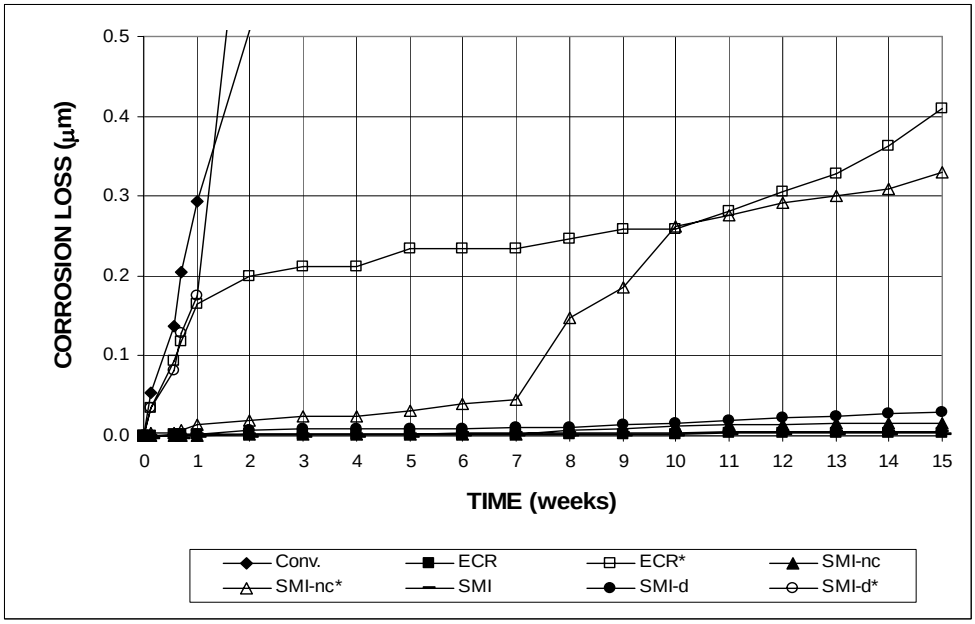

Figure 3.37 (b) - Macrocell Tests. Total Corrosion Loss. Mortar-wrapped specimens of conventional, epoxy-coated, and SMI steel in simulated concrete pore solution with 1.6 m ion NaCl. Refer to Table 3.3 for specimen identification.

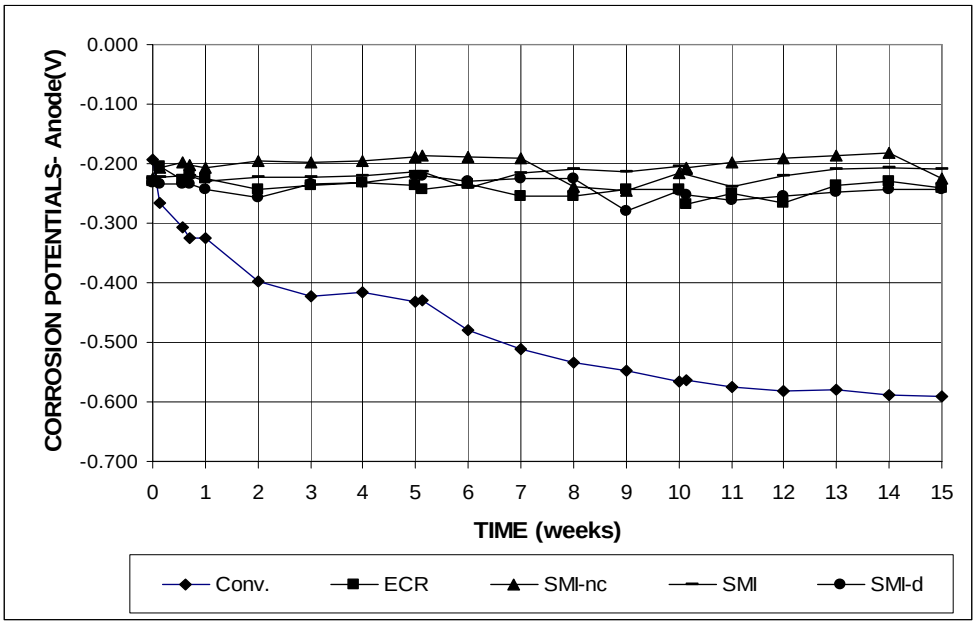

Figure 3.38 - Macrocell Tests. Corrosion Potential with respect to SCE at Anode. Mortar-wrapped specimens of conventional, epoxy-coated, and SMI steel in simulated concrete pore solution with 1.6 m ion NaCl. Refer to Table 3.3 for specimen identification.

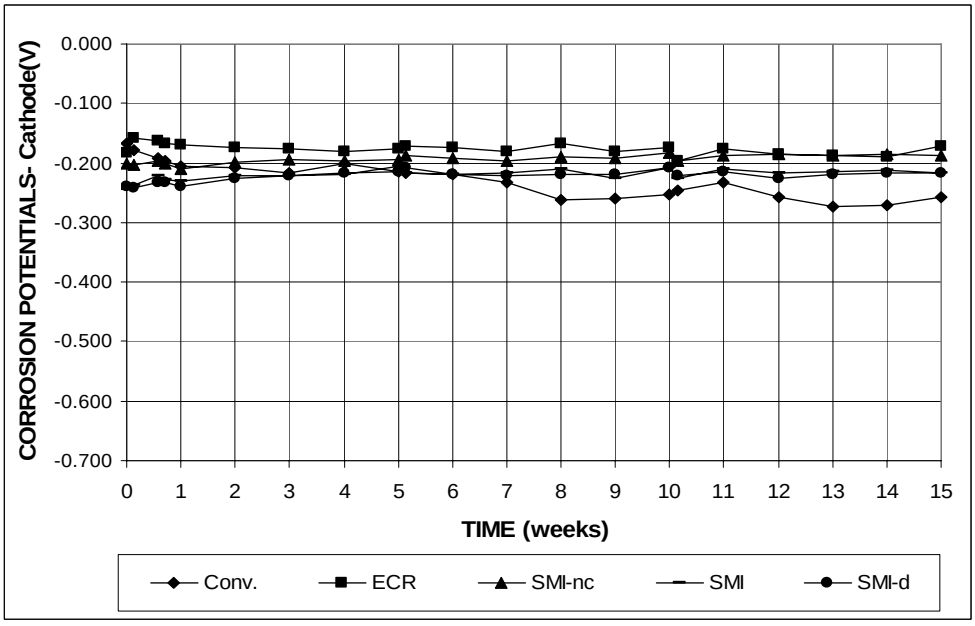

Figure 3.39 - Macrocell Tests. Corrosion Potential with respect to SCE at Cathode. Mortar-wrapped specimens of conventional, epoxy-coated, and SMI steel in simulated concrete pore solution with 1.6 m ion NaCl. Refer to Table 3.3 for specimen identification.

3.2.1.3 Visual Inspection

As the tests were discontinued, the specimens were visually inspected. For bare bar SMI-nc and SMIh-nc specimens, corrosion products were found on the unprotected ends; for bare bar SMI-d and SMIh-d specimens, corrosion products were observed within the drilled holes. No corrosion products appeared on the bare SMI bars with protected ends and without drilled holes. Figure 3.40 shows the end of an SMI-nc anode bar at 15 weeks, with the corrosion products that formed on the uncapped end. Figure 3.41 shows an SMI-d bar, with the corrosion products that formed at the drilled holes.

After the mortar was removed from the mortar-wrapped specimens, some corrosion products were found under the mortar on SMI-nc and SMI-d bars, as shown in Figures 3.42 and 3.43, while no corrosion products were found on the SMI bars.

Figure 3.40 – Bare SMI-nc anode bar from 1.6 m ion salt solution, at 15 weeks, showing corrosion products that formed at the unprotected end.

Figure 3.41 – Bare SMI-d anode bar from 1.6 m ion salt solution, at 15 weeks, showing corrosion products that formed at penetrations through the cladding.

Figure 3.42 – SMI-nc anode bar after removal of mortar, at 15 weeks, showing corrosion products that formed at the unprotected end.

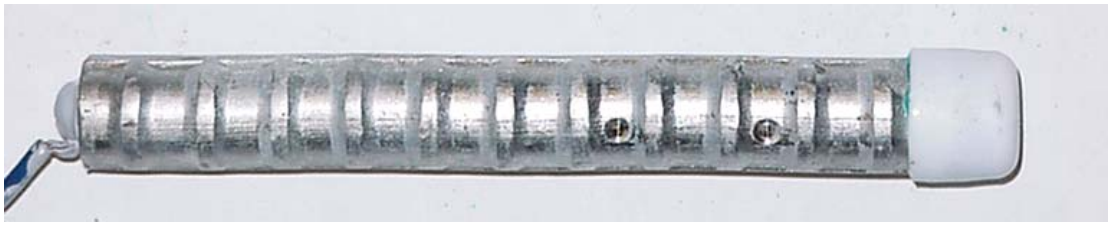

Figure 3.43 – SMI-d anode bar after removal of mortar, at 15 weeks, showing corrosion products that formed at penetrations through the cladding.

3.2.2 Bench-Scale Tests

The average corrosion rates and total corrosion losses as of March 15, 2005 for the Southern Exposure and cracked beam tests are summarized in Table 3.5. Results for individual specimens are presented in Appendix A.

3.2.2.1 Southern Exposure Tests

The Southern Exposure tests include six specimens each for conventional steel, epoxy-coated reinforcement, and SMI stainless steel clad bars. Three specimens using bent SMI bars as the top mat and three tests each for two combinations of SMI and conventional bars are also included. Average corrosion rates, total corrosion losses, mat-to-mat resistances, and corrosion potentials are shown in Figures 3.44-3.48.

The results (summarized in Table 3.5 and Figure 3.44) show that, based on the total area, the average corrosion rate of the SMI specimens with four drilled holes (SMI-d) increased at week 46, reaching a value of 0.08 μm/yr at week 49, equal to

19% of the value for conventional steel (0.42 μm/yr) (see Section 3.1.2.1 and Table 3.2). In contrast, the corrosion rate of the same specimens based on the exposed area of four 3.2-mm ($^1/_8$-in.) diameter holes in the cladding reached 38.5 μm/yr at week 49. The corrosion rate of SMI-d is higher than that of epoxy-coated steel (0 μm based on either total or exposed area), due to the much larger cathodic area provided by the SMI bars.

For the specimens with conventional steel in the top mat and SMI steel in the bottom mat (Conv./SMI), the average corrosion rate is expected to be similar to or less than that obtained from specimens containing conventional steel in both the top and bottom mats. However, the corrosion rate (1.27 μm/yr) was two times higher for Conv./SMI specimens than obtained for conventional steel (0.6 μm/yr) at week 43. At this point in the test, the reason for this difference is not clear. For specimens containing SMI steel without drilled holes (SMI), a bent SMI bar as top mat (SMI-b), and SMI as the top mat and conventional steel as the bottom mat (SMI/Conv.), no significant corrosion was observed.

For SMI bars with drilled holes, the average total corrosion loss at week 49 was only 0.01 μm based on the total bar surface (6.63 μm based on the exposed area), 3% of that for conventional steel (0.34 μm), while the corrosion loss for the Conv./SMI specimens at week 43, 0.46 μm, exceeded that for conventional steel. The corrosion losses were 0.01 μm or less for SMI, SMI/Conv., and SMI-b specimens.

The resistances between top and bottom mats are shown in Figures 3.46 (a) and (b). The ECR specimens with four drilled holes started at an average mat-to-mat resistance around 2,000 ohms and ended at over 10,700 ohms at week 49, while much lower resistances were exhibited by both conventional and SMI specimens, which started at about 100 ohms and ended at below 400 ohms. The ECR specimens exhibit

much higher average mat-to-mat resistances because, as discussed in Section 3.1.2.1, the epoxy coating serves as insulation.

The average corrosion potentials of the top and bottom mats with respect to a copper copper-sulfate electrode (CSE) are shown in Figures 3.47 and 3.48. For the top mat, the specimens with conventional steel in the top mat and SMI steel in the bottom mat (Conv./SMI) exhibited the most negative corrosion potential, with a value below −0.500 V at week 37, and a value of about −0.550 V at week 43. Specimens with all conventional steel showed the second most negative corrosion potential, −0.377 V at week 43 and −0.320 V at week 49, followed by the SMI bars with drilled holes (SMI-d), −0.231 V at week 43 and −0.245 V at week 49, showing that the SMI-d specimens are in a more passive condition than the Conv./SMI or conventional steel specimens. The corrosion potential for the ECR, SMI, SMI/Conv., and SMI-b anodes remained more positive than −0.300 V, indicating a low probability of corrosion. For the bottom mats, all specimens, except conventional steel and Conv./SMI, exhibited corrosion potentials less negative than −0.200 V. For the conventional and Conv./SMI specimens, the cathode potential dropped to around −0.300 V at week 37 and week 20, respectively, indicating a slight tendency to corrode.

Table 3.5 – Average corrosion rates and corrosion losses for SMI stainless steel clad bars as measured in the bench-scale tests

CORROSION RATE (μm/year)

Steel Designation	Exposure Time (weeks)	Specimen 1	2	3	4	5	6	Average	Std. Deviation
Southern Exposure Specimens									
SMI-d	49	0	0	0.18	α	0	0.30	0.08	0.13
SMI*-d	49	0	0	84.18	3.66	0	144.57	38.47	61.64
SMI	43	0	0	0	0	0	0	0	-
SMI/Conv.	46	0	0	0	-	-	-	0	-
Conv./SMI	43	1.32	1.50	1.00	-	-	-	1.27	0.25
SMI-b	40	0	0	α	-	-	-	α	-
Cracked Beam Specimens									
SMI-d	49	1.23	0.96	0	0.30	0.42	0.14	0.51	0.49
SMI*-d	49	592.92	461.16	0	146.40	201.30	65.88	244.61	233.03
SMI	43	0	0	0	0	0	0	0	-

CORROSION LOSS (μm)

Steel Designation	Exposure Time (weeks)	Specimen 1	2	3	4	5	6	Average	Std. Deviation
Southern Exposure Specimens									
SMI-d	49	β	β	0.03	0.01	β	0.02	0.01	0.01
SMI*-d	49	2.96	2.99	12.40	5.96	3.91	11.54	6.63	4.29
SMI	43	β	β	β	β	β	β	β	-
SMI/Conv.	46	β	β	β	-	-	-	β	-
Conv./SMI	43	0.29	0.67	0.42	-	-	-	0.46	0.19
SMI-b	40	β	β	0.02	-	-	-	0.01	0.01
Cracked Beam Specimens									
SMI-d	49	0.83	0.47	0.01	0.26	0.24	0.22	0.34	0.28
SMI*-d	49	400.84	224.32	6.69	126.62	113.39	103.96	162.64	135.67
SMI	43	0.01	0.03	0.01	0.01	0.01	0.01	0.01	0.01

[1] SMI-d: Stainless steel clad reinforcement with end protection and drilled holes, based on total area of bar exposed to solution

[2] SMI-d*: Stainless steel clad reinforcement with end protection, based on exposed area of four 3.2-mm (1/8-in.) diameter holes in cladding

[3] SMI: Stainless steel clad reinforcement with end protection, based on total area of bar exposed to solution

[4] SMI/Conv.: Stainless steel clad reinforcement with end protection as anode and conventional steel as cathode, based on total area exposed to solution

[5] Conv./SMI: Conventional steel as anode and stainless steel clad reinforcement with end protection as cathode, based on total area exposed to solution

[6] SMI-b: Stainless steel clad reinforcement with bent anode, based on total area exposed to solution

[7] α: corrosion rate less than 0.01 μm/yr

[8] β: corrosion loss less than 0.01μm

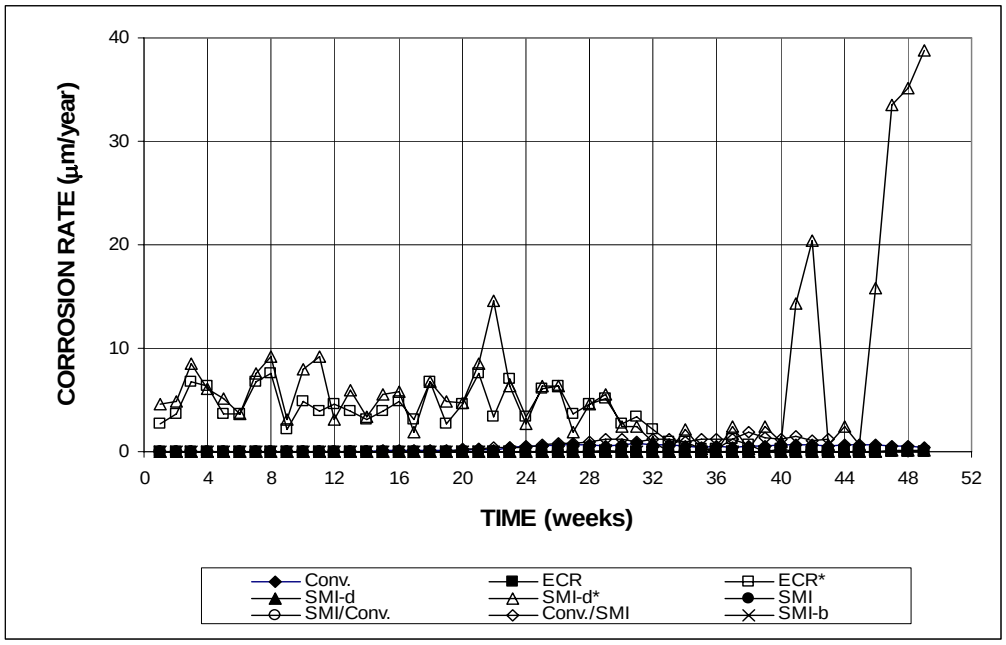

Figure 3.44 (a) – Southern Exposure Tests. Average Corrosion Rate. Specimens of conventional, epoxy-coated, and SMI reinforcement ponded with 15% NaCl solution. Refer to Table 3.5 for specimen identification.

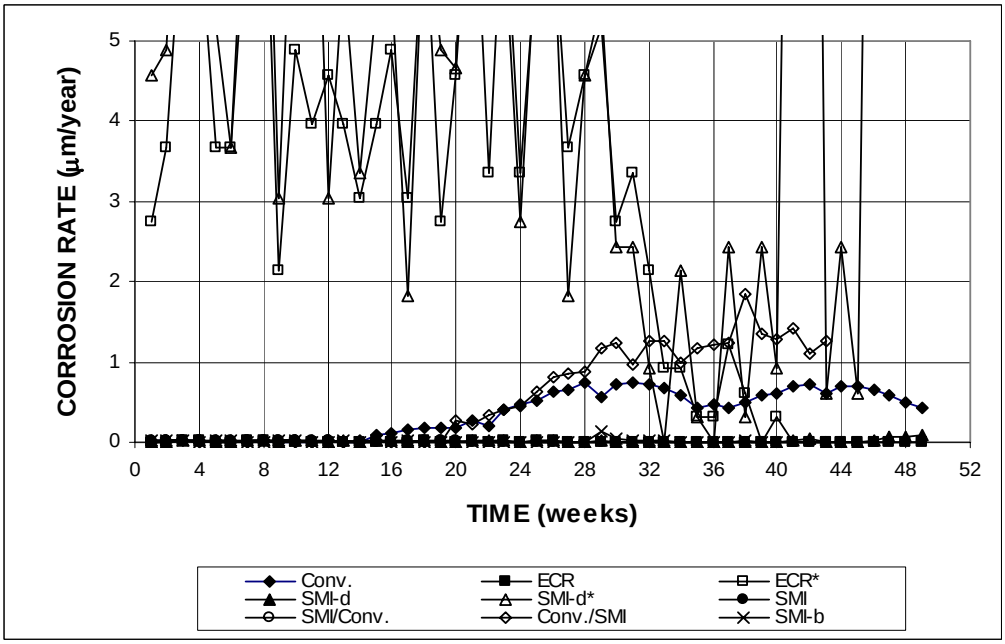

Figure 3.44 (b) – Southern Exposure Tests. Average Corrosion Rate. Specimens of conventional, epoxy-coated, and SMI reinforcement ponded with 15% NaCl solution. Refer to Table 3.5 for specimen identification.

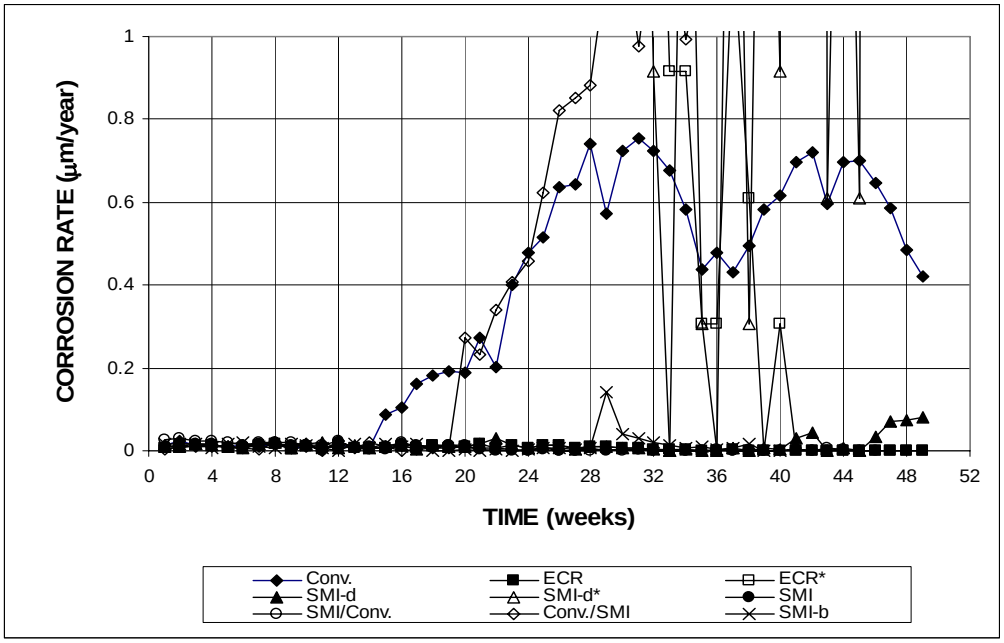

Figure 3.44 (c) – Southern Exposure Tests. Average Corrosion Rate. Specimens of conventional, epoxy-coated, and SMI reinforcement ponded with 15% NaCl solution. Refer to Table 3.5 for specimen identification.

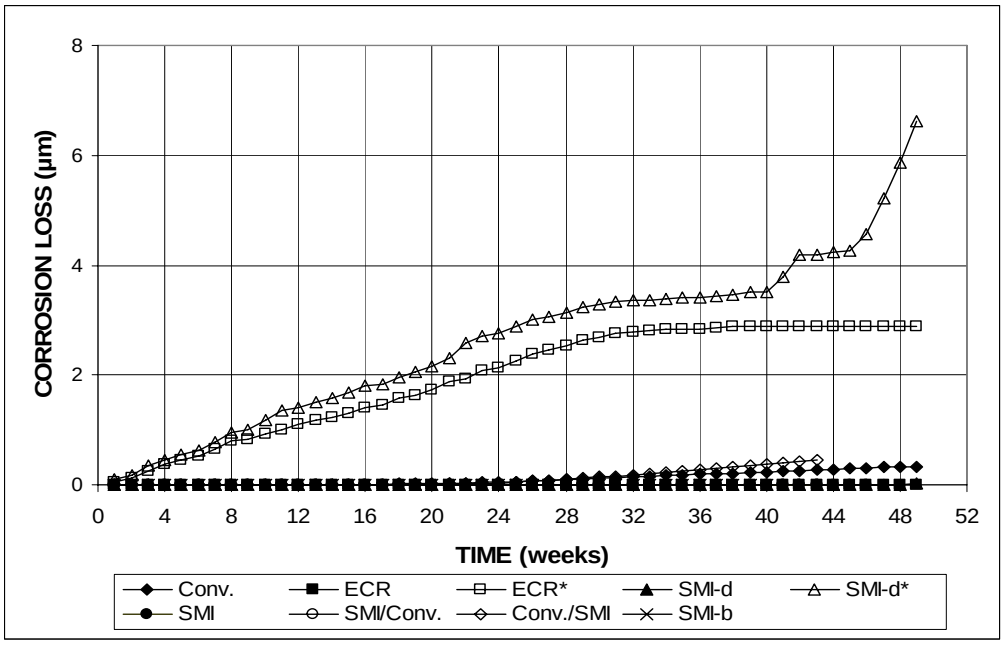

Figure 3.45 (a) – Southern Exposure Tests. Total Corrosion Loss. Specimens of conventional, epoxy-coated, and SMI reinforcement ponded with 15% NaCl solution. Refer to Table 3.5 for specimen identification.

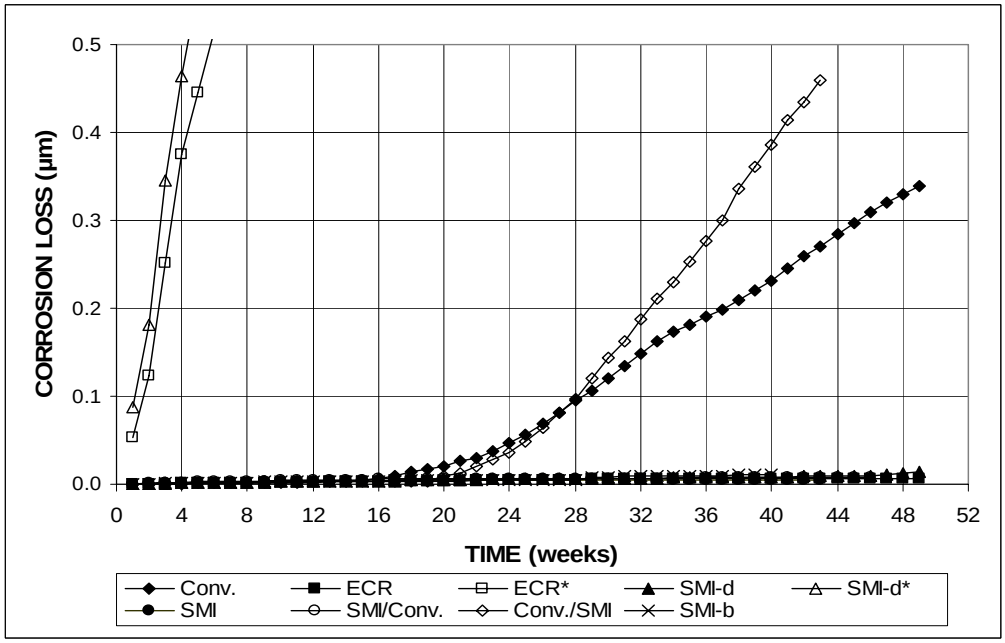

Figure 3.45 (b) – Southern Exposure Tests. Total Corrosion Loss. Specimens of conventional, epoxy-coated, and SMI reinforcement ponded with 15% NaCl solution. Refer to Table 3.5 for specimen identification.

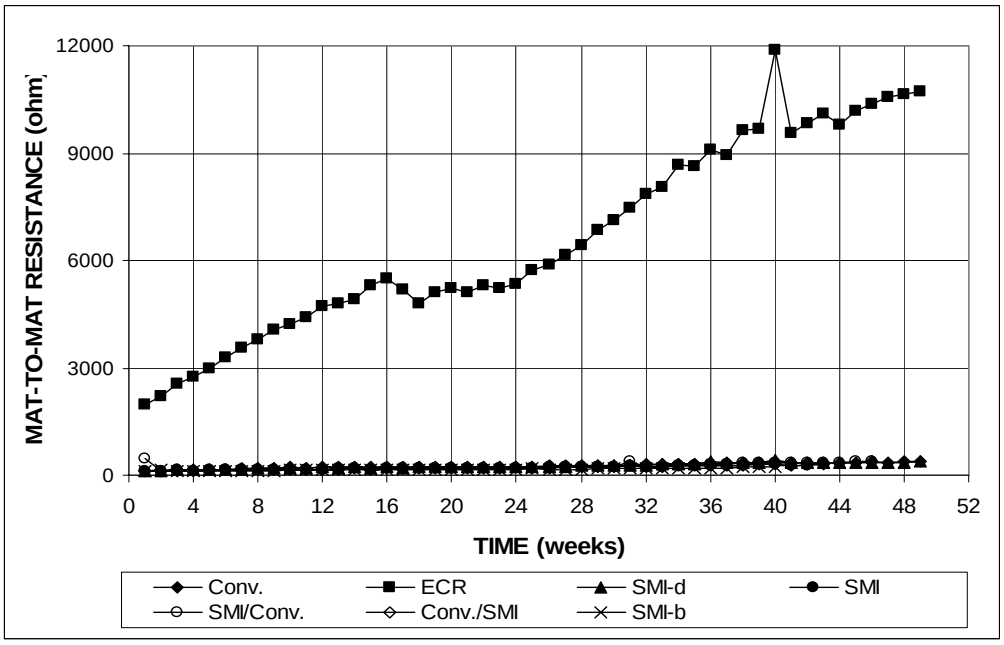

Figure 3.46 (a) – Southern Exposure Tests. Mat-to-mat resistance. Specimens of conventional, epoxy-coated, and SMI reinforcement ponded with 15% NaCl solution. Refer to Table 3.5 for specimen identification.

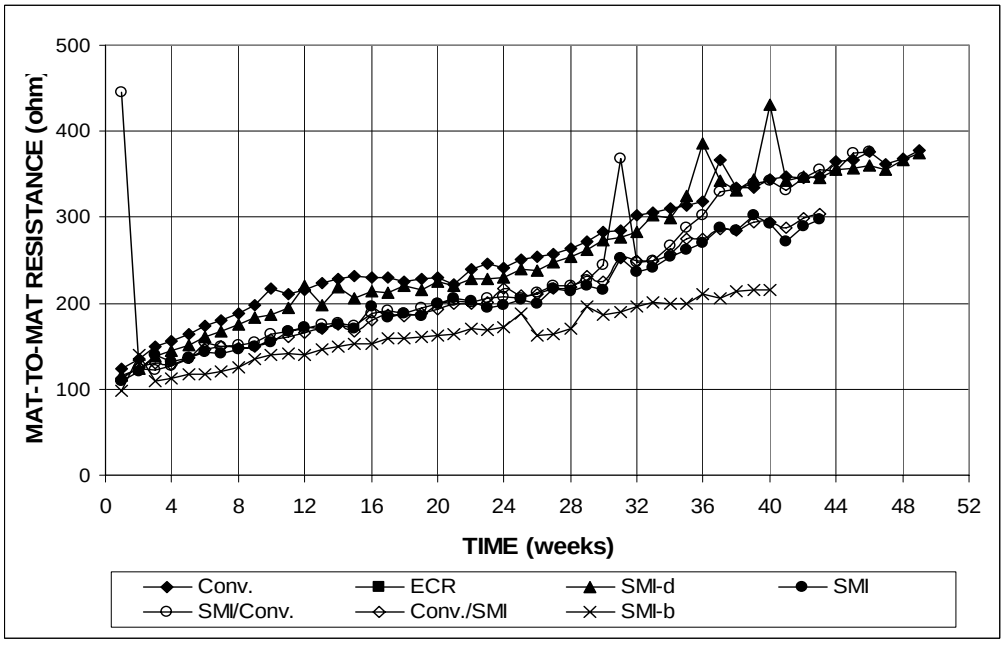

Figure 3.46 (b) – Southern Exposure Tests. Mat-to-mat resistance. Specimens of conventional, epoxy-coated, and SMI reinforcement ponded with 15% NaCl solution. Refer to Table 3.5 for specimen identification.

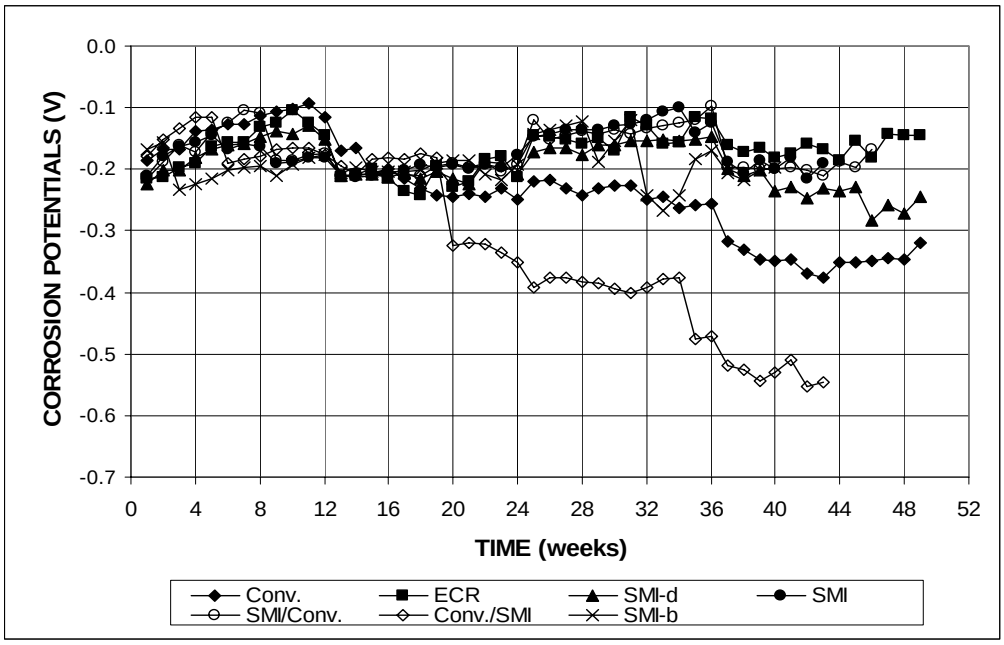

Figure 3.47 – Southern Exposure Tests. Corrosion Potential with respect to CSE at Top Mat. Specimens of conventional, epoxy-coated, and SMI reinforcement ponded with 15% NaCl solution. Refer to Table 3.5 for specimen identification.

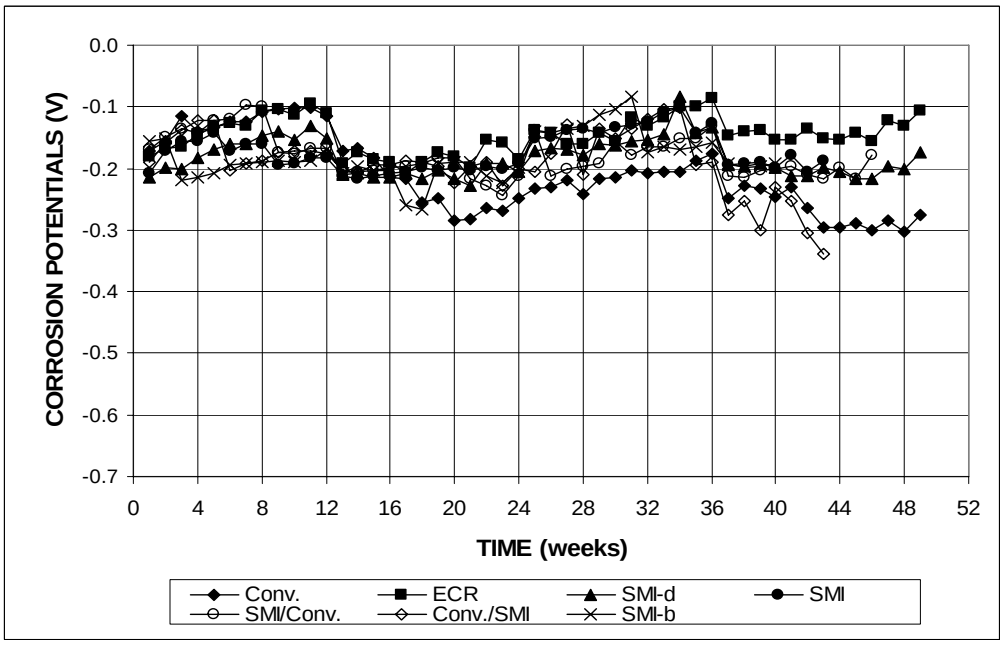

Figure 3.48 – Southern Exposure Tests. Corrosion Potential with respect to CSE at Bottom Mat. Specimens of conventional, epoxy-coated, and SMI reinforcement ponded with 15% NaCl solution. Refer to Table 3.5 for specimen identification.

3.2.2.2 Cracked Beam Tests

The cracked beam tests include six specimens each for conventional steel, epoxy-coated reinforcement with four drilled holes, and SMI stainless steel clad reinforcement without and with four drilled holes. The average corrosion rates, total corrosion losses, mat-to-mat resistances, and corrosion potentials are shown in Figures 3.49-3.53 and summarized in Table 3.5. The results (Figure 3.49) show that, as discussed in Section 3.1.2.2, the specimens containing conventional steel started at an average corrosion rate higher than 10 μm/yr that decreased with time and stabilized after the first few weeks due to the formation of corrosion products on the surface of the steel. Based on the total area, the specimens containing SMI bars with drilled holes (SMI-d) exhibited observable corrosion at an average rate of 0.26 μm/yr from beginning of the test, reaching 0.51 μm/yr by week 49, equal to 7% of the value for conventional steel (6.93 μm/yr). Based on the exposed core area, the corrosion rate of the SMI-d specimens reached 126 μm/yr at week 1 and increased to 245 μm/yr at week 49, equal to 35 times the value for conventional steel.

Compared to the SMI bars with drilled holes, the ECR specimens (same area of holes) had a much lower corrosion rate [Figure 3.49(b) and (c)], equal to 0.02 μm/yr based on the total area and 7.32 μm/yr based on the exposed area. The lower corrosion rate is in all likelihood due to the limited cathodic reaction at the bottom mat for the ECR specimens due to the insulation provided by the epoxy.

The SMI specimens without drilled holes (SMI) reached an average corrosion rate as high as 0.04 μm/yr at a number of occasions, dropping to zero at week 43 [Figure 3.49 (c)]. Only one SMI specimen showed observable corrosion between weeks 20 and 24 (Figure A.72), which may be due to mill scale on the surface of SMI

steel. The SMI-d specimens had a consistently higher average corrosion rate than the intact SMI specimens due to the penetrations in the cladding.

For the conventional steel specimens, the average total corrosion losses equaled 6.45 μm at week 49, 19 times that of the SMI-d specimens (0.34 μm) and 215 times that of ECR specimens (0.03 μm) based on total area [Figure 3.50 (a) and (c)]. Based on the exposed area of the core steel, the SMI-d specimens exhibited a much higher corrosion loss (163 μm) than the ECR specimens (15 μm) due to the much larger cathodic area provide by the SMI cathodes.

Mat-to-mat resistances are shown in Figures 3.51 (a) and (b). The ECR specimens with four drilled holes exhibited an average mat-to-mat resistance close to 4,000 ohms at week 1 that increased to over 15,000 ohms at week 49. The SMI, SMI-d, and conventional steel specimens exhibited much lower resistances, around 300 ohms at the beginning of the test, with the SMI and conventional steel specimens ending at around 1,000 ohms and the SMI-d specimens ending at about 1,700 ohms.

The average corrosion potentials of the top and bottom mats with respect to a copper copper-sulfate electrode are shown in Figures 3.52 and 3.53. For the top mat, the conventional steel specimens exhibited an average corrosion potential more negative than −0.500 V beginning at week 1, while the ECR specimens reached an average potential more negative than −0.500 V at week 13. The SMI-d specimens had a more positive potential compared to the conventional and ECR specimens, representing a somewhat more passive condition. The SMI specimens without drilled holes had a much more positive potential, around −0.200 V, indicating that the bars are still passive. For the bottom mat, the potentials for conventional and epoxy-coated steel dropped to near −0.400 V at week 19 and 21, respectively, but increased to

−0.250 V and −0.214 V at week 49. Other specimens exhibited cathode corrosion potentials more positive than −0.270 V.

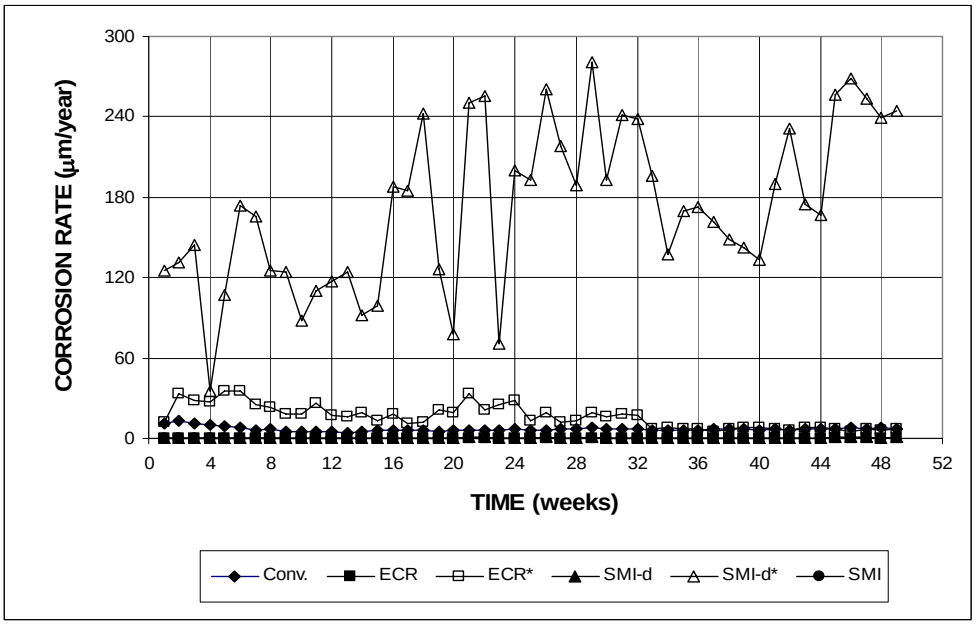

Figure 3.49 (a) – Cracked Beam Tests. Average Corrosion Rate. Specimens of conventional, epoxy-coated, and SMI reinforcement ponded with 15% NaCl solution. Refer to Table 3.5 for specimen identification.

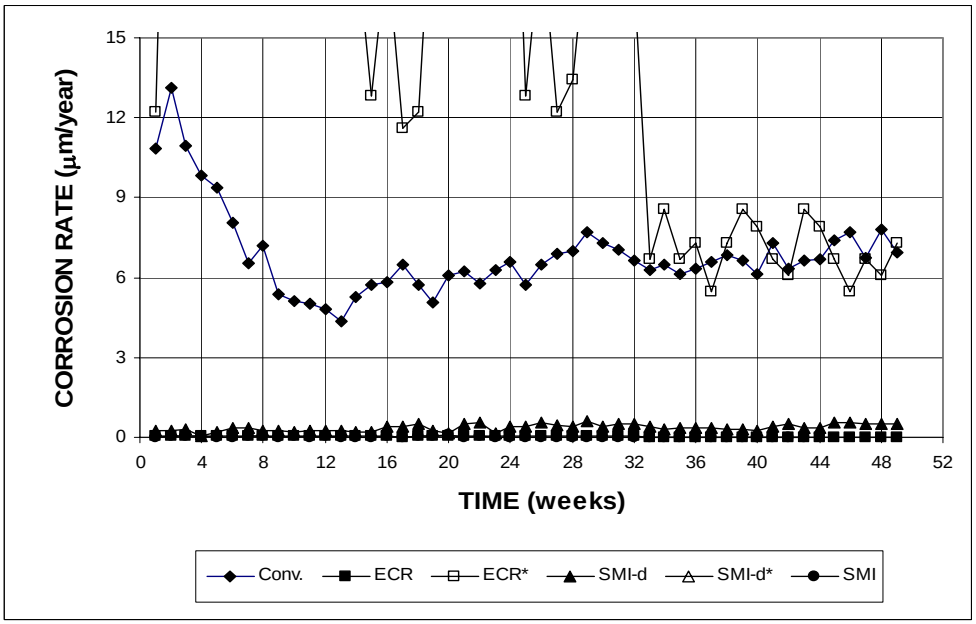

Figure 3.49 (b) – Cracked Beam Tests. Average Corrosion Rate. Specimens of conventional, epoxy-coated, and SMI reinforcement ponded with 15% NaCl solution. Refer to Table 3.5 for specimen identification.

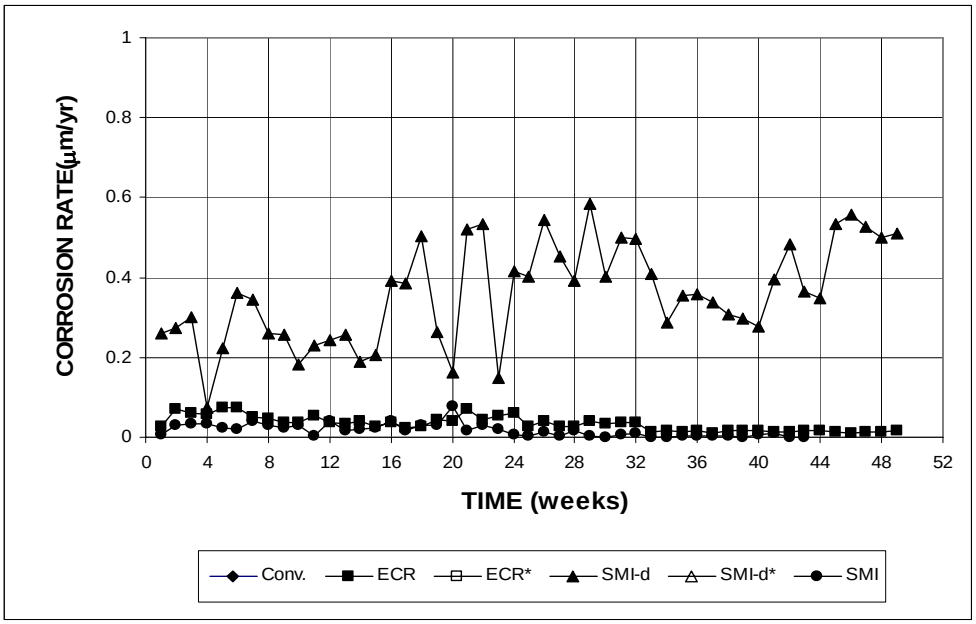

Figure 3.49 (c) – Cracked Beam Tests. Average Corrosion Rate. Specimens of conventional, epoxy-coated, and SMI reinforcement ponded with 15% NaCl solution. Refer to Table 3.5 for specimen identification.

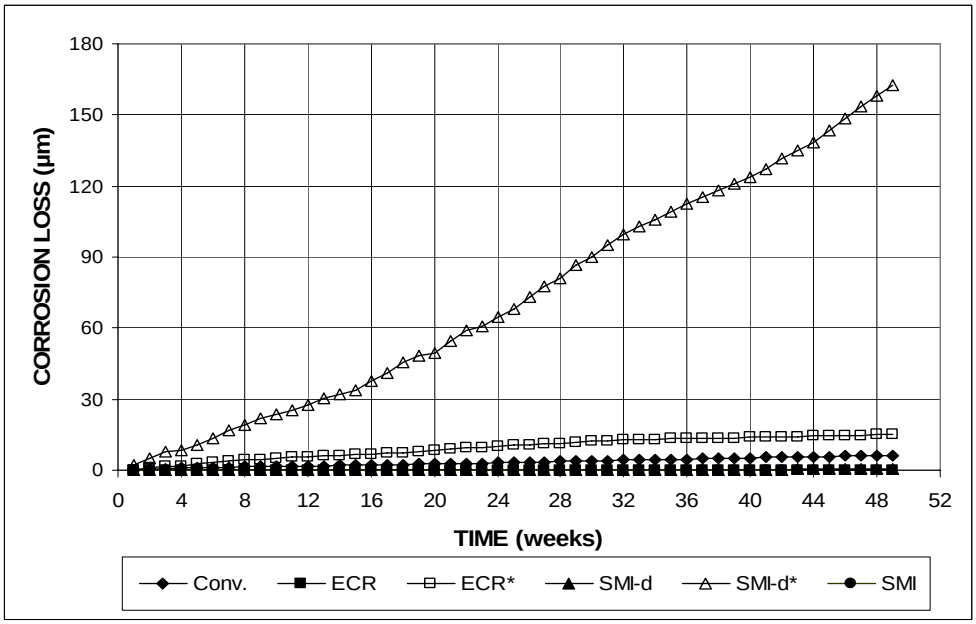

Figure 3.50 (a) – Cracked Beam Tests. Total Corrosion Loss. Specimens of conventional, epoxy-coated, and SMI reinforcement ponded with 15% NaCl solution. Refer to Table 3.5 for specimen identification.

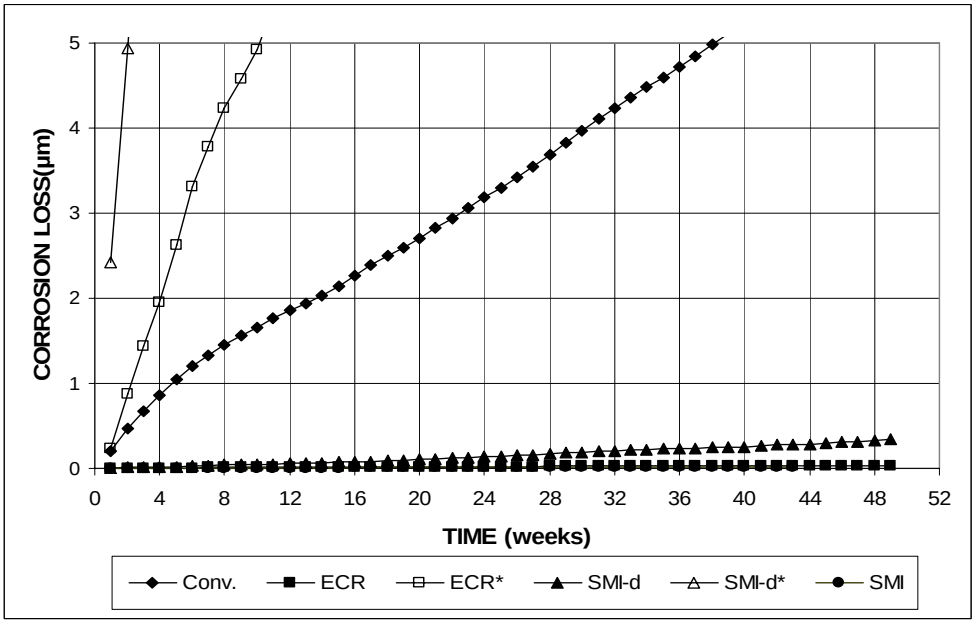

Figure 3.50 (b) – Cracked Beam Tests. Total Corrosion Loss. Specimens of conventional, epoxy-coated, and SMI reinforcement ponded with 15% NaCl solution. Refer to Table 3.5 for specimen identification.

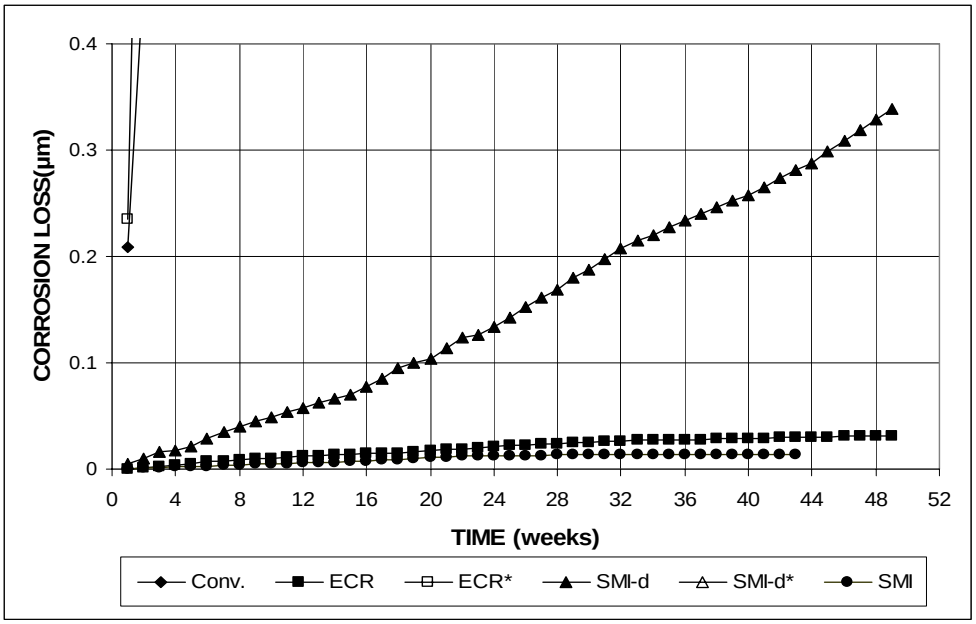

Figure 3.50 (c) – Cracked Beam Tests. Total Corrosion Loss. Specimens of conventional, epoxy-coated, and SMI reinforcement ponded with 15% NaCl solution. Refer to Table 3.5 for specimen identification.

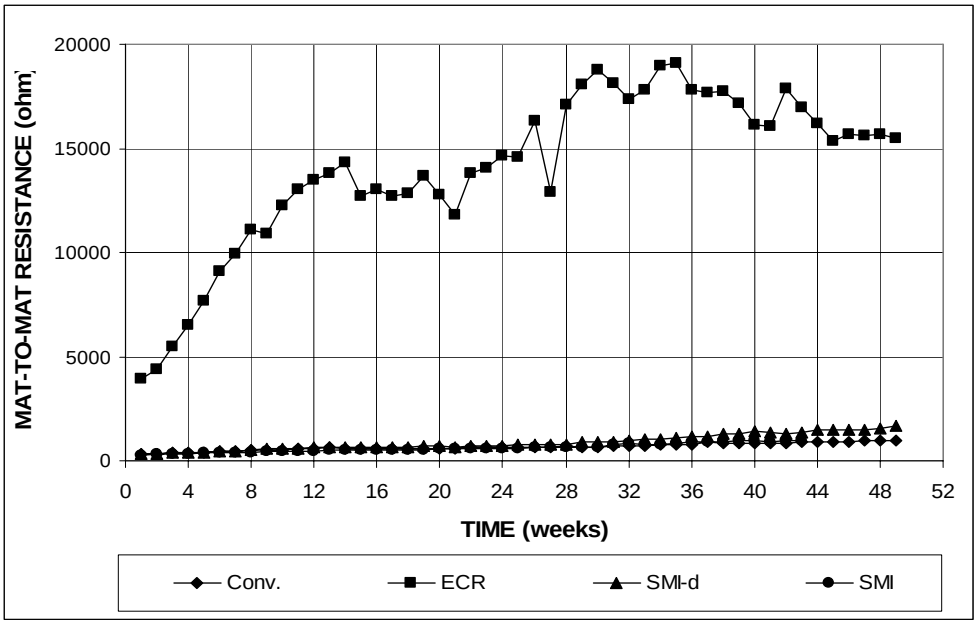

Figure 3.51 (a) – Cracked Beam Tests. Mat-to-mat resistance. Specimens of conventional, epoxy-coated, and SMI reinforcement ponded with 15% NaCl solution. Refer to Table 3.5 for specimen identification.

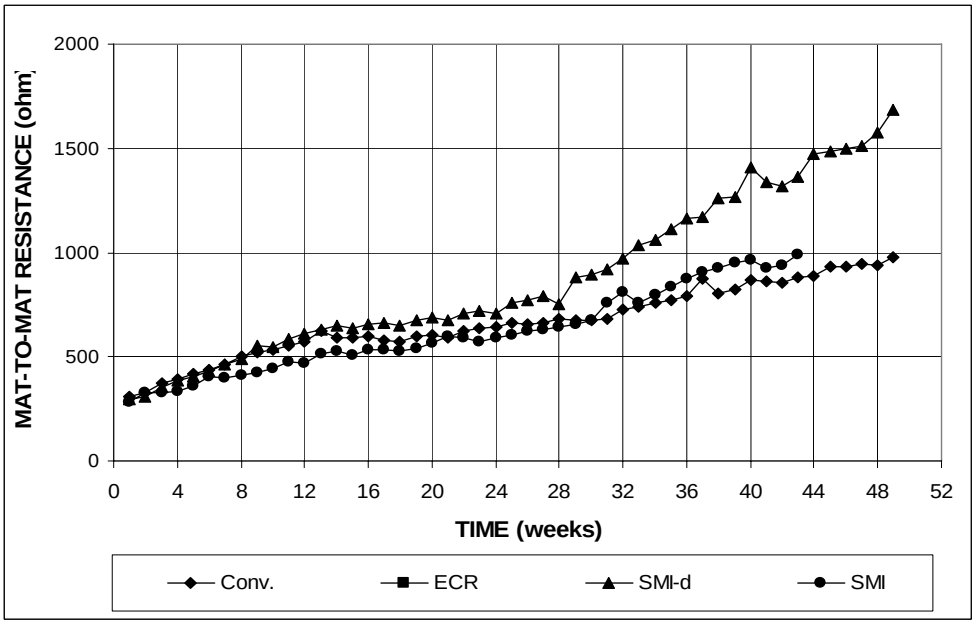

Figure 3.51 (b) – Cracked Beam Tests. Mat-to-mat resistance. Specimens of conventional, epoxy-coated, and SMI reinforcement ponded with 15% NaCl solution. Refer to Table 3.5 for specimen identification.

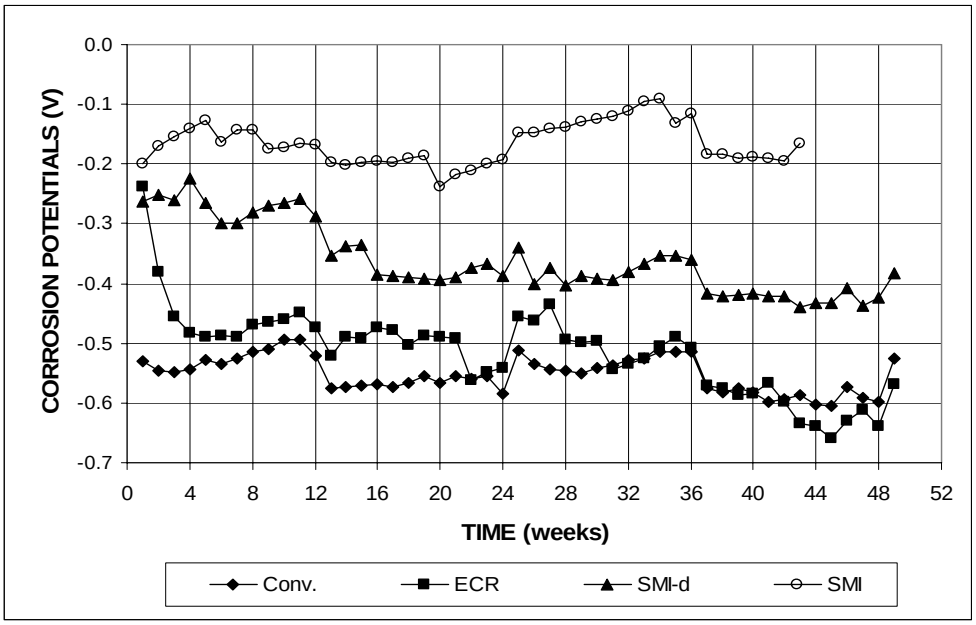

Figure 3.52 – Cracked Beam Tests. Corrosion Potential with respect to CSE at Top Mat. Specimens of conventional, epoxy-coated, and SMI reinforcement ponded with 15% NaCl solution. Refer to Table 3.5 for specimen identification.

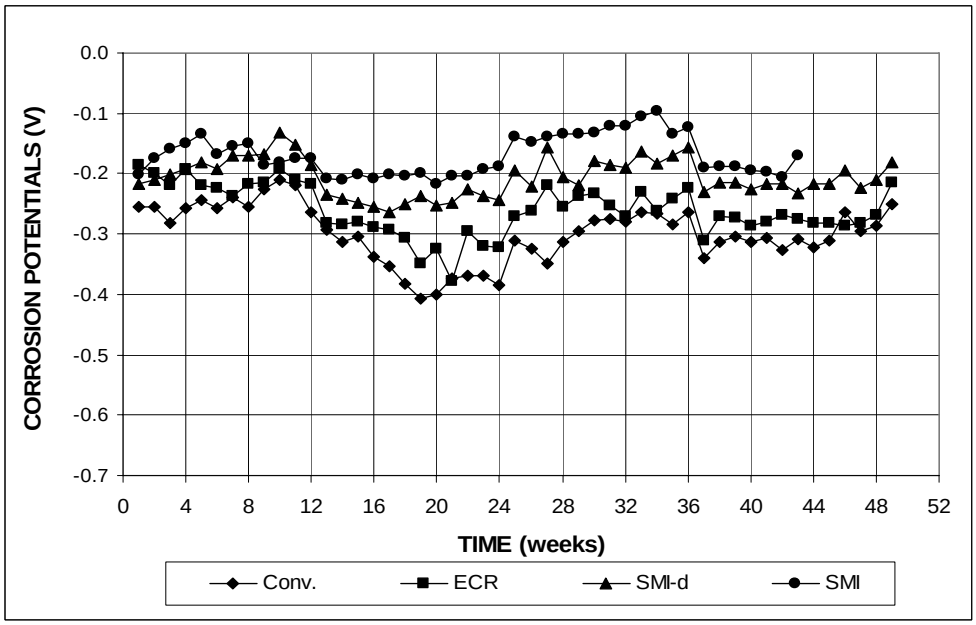

Figure 3.53 – Cracked Beam Tests. Corrosion Potential with respect to CSE at Bottom Mat. Specimens of conventional, epoxy-coated, and SMI reinforcement ponded with 15% NaCl solution. Refer to Table 3.5 for specimen identification.

3.3 EPOXY-COATED REINFORCEMENT WITH IMPROVED ADHESION BETWEEN EPOXY AND STEEL

This section presents the results of rapid macrocell and bench-scale tests for epoxy-coated reinforcement with improved adhesion between the epoxy and the steel. The bars tested include reinforcement to which epoxy was applied after pretreatment of the steel with zinc chromate to improve adhesion of the epoxy and the steel [ECR(Chromate)] and epoxy-coated reinforcement coated with improved adhesion epoxies produced by DuPont [ECR(DuPont)] and Valspar [ECR(Valspar)]. The three types of epoxy-coated reinforcement with improved adhesion are also tested in conjunction with the corrosion inhibitor DCI-S. The average corrosion rates and corrosion losses for the macrocell and bench-scale specimens are summarized in Tables 3.6 and 3.7. Results for individual specimens are presented in Appendix A. The test results of conventional epoxy-coated steel, when used with corrosion inhibitors, are presented in Section 3.4.

3.3.1 Rapid Macrocell Tests

Six bare and six mortar-wrapped specimens were used in the rapid macrocell tests for each bar type with the epoxy penetrated by four 3.2-mm (1/8-in.) diameter holes. Three bare and three mortar-wrapped tests were performed on the bars in the "as delivered" condition.

3.3.1.1 Macrocell Test for Bare Bar Specimens

The average corrosion rates and total corrosion losses over the 15-week test period for specimens in simulated pore solution with 1.6 m ion NaCl are shown in Figures 3.54 to 3.57. The corrosion rates for the bars with drilled holes are calculated based on both the exposed area of the four 3.2-mm (1/8-in.) diameter holes and the

total area of the bars exposed to the solution. Table 3.6 summarizes the average corrosion rates and total corrosion losses at week 15.

As shown in Figures 3.54(a) and (b), the ECR(DuPont) and ECR(Valspar) bars behaved very much like the conventional ECR specimens, while the ECR(Chromate) specimens corroded at much lower rate over the 15 week test period. Based on the total area, the ECR(DuPont) specimens started at an average corrosion rate of 0.6 μm/yr, similar to the rate exhibited by conventional ECR specimens at week 1, and ended at 0.7 μm/yr, equal to about 60% of the corrosion rate for the ECR specimens (1.2 μm/yr) at week 15. Compared to the ECR(DuPont), the ECR(Valspar) specimens corroded at a lower rate (0.3 μm/yr) at the beginning but ended at a higher rate (0.9 μm/yr) at week 15 (75% of the rate for ECR). The lower values at the end of the test for ECR(DuPont) and ECR(Valspar) do not appear to have great significance and likely represent fluctuations in the test results rather than a trend. The corrosion rate of ECR(Chromate) reached as high as 0.3 μm/yr at week 5 and eventually ended at 0.1 μm/yr, equal to just 8% of the value for conventional epoxy-coated steel. Based on the exposed area, the corrosion rates were 71 μm/yr, 90 μm/yr and 13 μm/yr at week 15 for ECR(DuPont), ECR(Valspar) and ECR(Chromate), respectively. For the specimens without drilled holes, no measurable corrosion was observed for any individual bar as shown in Figures 3.56 and 3.57.

After 15 weeks, the total corrosion losses (Figure 3.55) for the ECR(DuPont) and ECR(Valspar) bars were just below 0.4 μm based on the total bar area, essentially equal to the value measured for conventional ECR. The losses for the ECR(Chromate) specimens were much lower, at 0.03 μm. Based on the exposed area, the ECR(DuPont), ECR(Valspar), and conventional ECR specimens exhibited corrosion losses of 38, 36, and 40 μm, respectively. The ECR(Chromate) specimens

showed a corrosion loss of 3 μm, equal to less than 10% of the value for the other three epoxy-coated steels.

The average corrosion potentials of the anodes and cathodes are shown in Figures 3.58 and 3.59, respectively. The conventional steel and ECR anodes showed most negative potentials at the beginning and end of the test period, with some fluctuations during the test. At week 15, the potential for both was about −0.520 V. The ECR(DuPont) and ECR(Valspar) anodes exhibited potentials more negative than −0.400 V beginning in week 1, ending at −0.480 V and −0.400 V, respectively, at week 15. The ECR (Chromate) anodes exhibited a more positive potential, −0.200 V, at the start of the test and ended with a more positive value, −0.230 V, as well, indicating a low probability of corrosion. The results demonstrate that the ECR(DuPont), ECR(Valspar), and ECR specimens were in a more active condition throughout the test period compared to the ECR(Chromate) specimens. The average corrosion potentials for the cathodes were around −0.200 V for all three types increased adhesion bars. The undamaged bars exhibited unstable corrosion potentials for both anodes and cathodes since the epoxy worked as an electrical insulator.

Table 3.6 – Average corrosion rates and corrosion losses for epoxy-coated steel with increased adhesion as measured in the macrocell tests

CORROSION RATE AT WEEK 15 (μm/year)

Steel Designation	Specimen 1	2	3	4	5	6	Average	Std. Deviation
Bare bar specimens								
ECR(DuPont)	0	0.70	0	1.13	1.02	1.39	0.71	0.59
ECR(DuPont)*	0	69.54	0	113.46	102.48	139.08	70.76	59.19
ECR(DuPont)-nh	0	0	0	-	-	-	0	-
ECR(Chromate)	0.77	0	0	0	0	0	0.13	0.31
ECR(Chromate)*	76.86	0	0	0	0	0	12.81	31.38
ECR(Chromate)-nh	0	0	0	-	-	-	0	-
ECR(Valspar)	1.24	0.04	1.76	0	0	2.38	0.90	1.04
ECR(Valspar)*	124.44	3.66	175.68	0	0	237.90	90.28	103.98
ECR(Valspar)-nh	0	0	0	-	-	-	0	-
Mortar-wrapped specimens								
ECR(DuPont)	0	0.04	0	0.04	0	0	0.01	0.02
ECR(DuPont)*	0	3.66	0	3.66	0	0	1.22	1.89
ECR(DuPont)-DCI	0	0	0	0	0	0	0	-
ECR(DuPont)*-DCI	0	0	0	0	0	0	0	-
ECR(DuPont)-nh	0	0	0	-	-	-	0	-
ECR(Chromate)	0	0	0.04	0	0	0	α	0.01
ECR(Chromate)*	0	0	3.66	0	0	0	0.61	1.49
ECR(Chromate)-DCI	0	0	0	0	0	0.04	α	0.01
ECR(Chromate)*-DCI	0	0	0	0	0	3.66	0.61	1.49
ECR(Chromate)-nh	0	0	0	-	-	-	0	-
ECR(Valspar)	0	0	0	0	0.04	0	α	0.01
ECR(Valspar)*	0	0	0	0	3.66	0	0.61	1.49
ECR(Valspar)-DCI	0	0	0	0	0	0	0	-
ECR(Valspar)*-DCI	0	0	0	0	0	0	0	-
Valspar-nh	0	0	0	-	-	-	0	-

TOTAL CORROSION LOSS AFTER WEEK 15 (μm)

Steel Designation	Specimen 1	2	3	4	5	6	Average	Std. Deviation
Bare bar specimens								
ECR(DuPont)	β	0.44	0.42	0.40	0.48	0.50	0.38	0.19
ECR(DuPont)*	0.35	43.99	42.02	40.40	48.21	50.18	37.53	18.58
ECR(Dupont)-nh	β	β	0	-	-	-	β	0
ECR(Chromate)	0.10	β	β	β	β	0.05	0.03	0.04
ECR(Chromate)*	10.35	0.35	0.42	0.14	0.42	5.49	2.86	4.21
ECR(Chromate)-nh	0	0	0	-	-	-	0	-
ECR(Valspar)	0.32	0.43	0.66	0.09	0.06	0.61	0.36	0.26
ECR(Valspar)*	31.81	43.08	66.37	8.59	5.98	61.45	36.21	25.65
ECR(Valspar)-nh	β	β	β	-	-	-	β	-
Mortar-wrapped specimens								
ECR(DuPont)	β	β	β	β	β	β	β	-
ECR(DuPont)*	0.07	0.42	0.07	0.70	0.21	0.92	0.40	0.35
ECR(DuPont)-DCI	β	β	0	0	0	0	β	-
ECR(DuPont)*-DCI	0.07	0.14	0	0	0	0	0.04	0.06
ECR(DuPont)-nh	0	0	0	-	-	-	0	-
ECR(Chromate)	β	0	β	β	β	β	β	-
ECR(Chromate)*	0.07	0	0.14	0.35	0.07	0.07	0.12	0.12
ECR(Chromate)-DCI	0	β	0	0	0	β	β	-
ECR(Chromate)*-DCI	0	0.14	0	0	0	0.07	0.04	0.06
ECR(Chromate)-nh	0	0	0	-	-	-	0	-
ECR(Valspar)	β	β	β	β	β	β	β	-
ECR(Valspar)*	0.28	0.07	0.21	0.07	0.14	0.21	0.16	0.09
ECR(Valspar)-DCI	0	β	0	0	β	0	β	0
ECR(Valspar)*-DCI	0	0.14	0	0	0.07	0	0.04	0.06
Valspar-nh	0	0	0	-	-	-	0	-

Table 3.6 continued:

[1] ECR(DuPont): Epoxy-coated steel with increased adhesion epoxy by DuPont , based on total area of bar exposed to solution

[2] ECR(DuPont)*: Epoxy-coated steel with increased adhesion epoxy by DuPont, based on exposed area of four 3.2-mm (1/8-in.) diameter holes in epoxy

[3] ECR(DuPont)-DCI: Epoxy-coated steel with increased adhesion epoxy by DuPont and cast with corrosion inhibitor DCI, based on total area of bar exposed to solution

[4] ECR(DuPont)*-DCI: Epoxy-coated steel with increased adhesion epoxy by DuPont and cast with corrosion inhibitor DCI, based on exposed area in epoxy

[5] ECR(DuPont)-nh: Epoxy-coated steel with increased adhesion epoxy by DuPont and without any drilled holes

[6] ECR(Chromate): Epoxy-coated steel with chromate pretreatment, based on total area of bar exposed to solution

[7] ECR(Chromate)*:Epoxy-coated steel with chromate pretreatment, based on exposed area of four 3.2-mm (1/8-in.) diameter holes in epoxy

[8] ECR(Chromate)-DCI: Epoxy-coated steel with chromate pretreatment and cast with corrosion ihibitor DCI, based on total area of bar exposed to solution

[9] ECR(Chromate)*-DCI: Epoxy-coated steel with chromate pretreatment and cast with corrosion inhibitor DCI, based on exposed area in epoxy

[10] ECR(Chromate)*-nh: Epoxy-coated steel with chromate pretreatment and without any drilled holes

[11] ECR(Valspar): Epoxy-coated steel with increased adhesion epoxy by Valspar , based on total area of bar exposed to solution

[12] ECR(Valspar)* : Epoxy-coated steel with increased adhesion epoxy by Valspar, based on exposed area of four 3.2-mm (1/8-in.) diameter holes in epoxy

[13] ECR(Valspar)-DCI: Epoxy-coated steel with increased adhesion epoxy by Valspar and cast with corrosion inhibitor DCI, based on total area of bar exposed to solution

[14] ECR(Valspar)*-DCI: Epoxy-coated steel with increased adhesion epoxy by Valspar and cast with corroson ihibitor DCI, based on exposed area in epoxy

[15] ECR(Valspar) - nh: Epoxy-coated steel with increased adhesion epoxy by Valspar and without any drilled holes

[16] α: corrosion rate less than 0.01 μm/yr

[17] β: corrosion loss less than 0.01μm

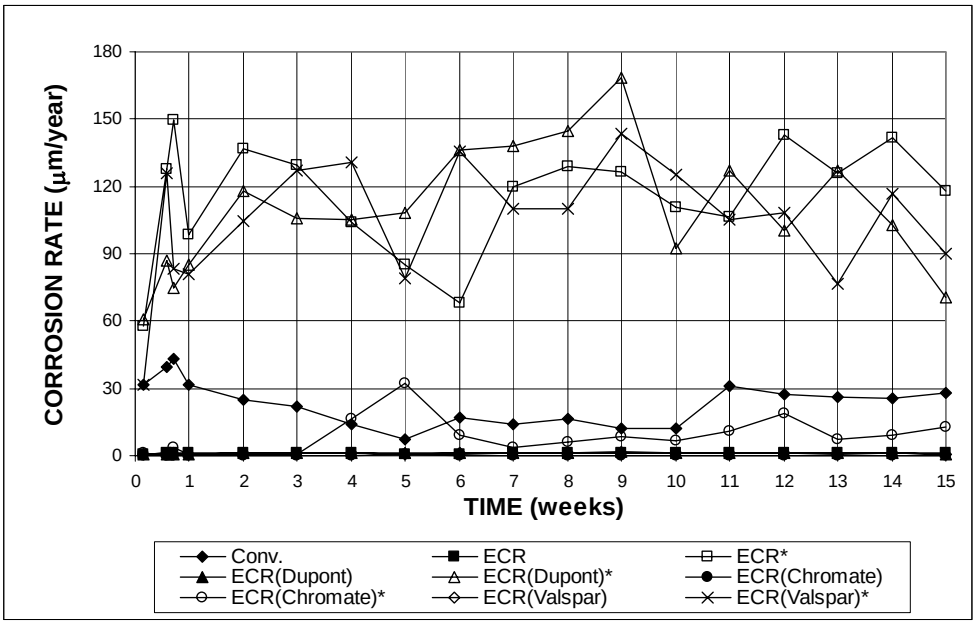

Figure 3.54 (a) - Macrocell Tests. Average Corrosion Rate. Bare bar specimens of conventional, epoxy-coated, and increased adhesion ECR steel in simulated concrete pore solution with 1.6 m ion NaCl. Refer to Table 3.6 for specimen identification.

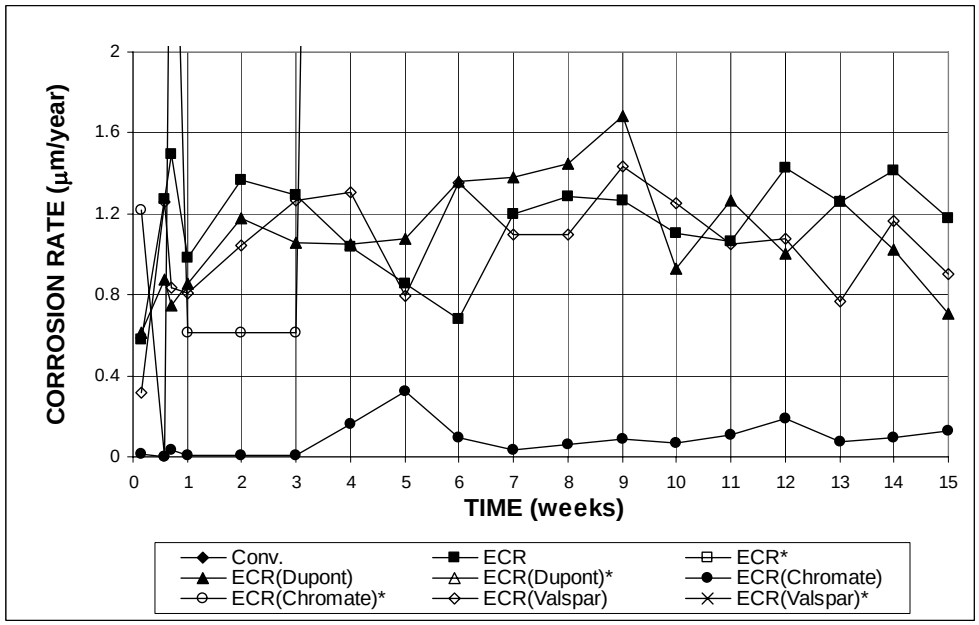

Figure 3.54 (b) - Macrocell Tests. Average Corrosion Rate. Bare bar specimens of conventional, epoxy-coated, and increased adhesion ECR steel in simulated concrete pore solution with 1.6 m ion NaCl. Refer to Table 3.6 for specimen identification.

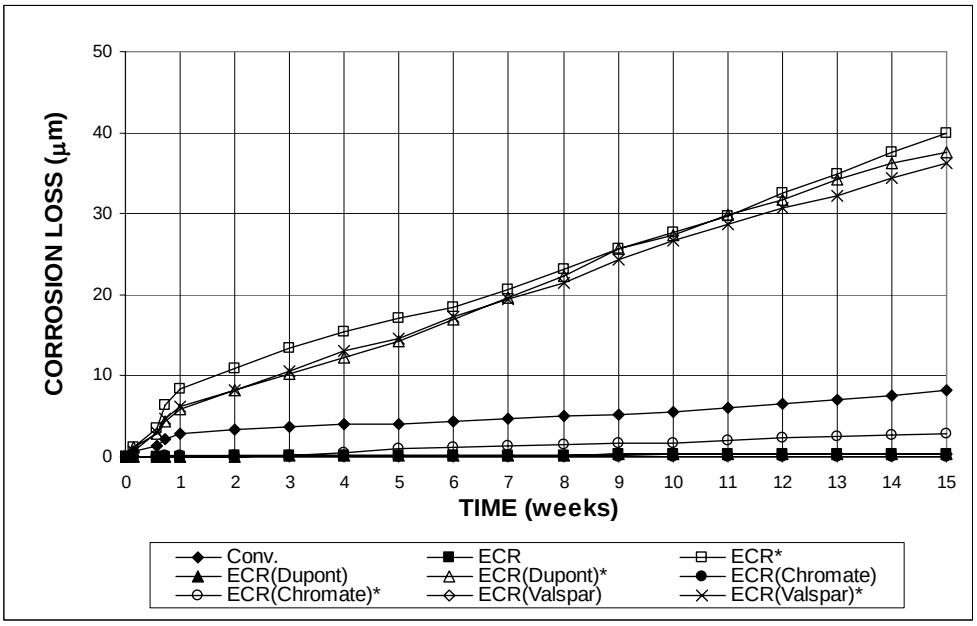

Figure 3.55 (a) - Macrocell Tests. Total Corrosion Loss. Bare bar specimens of conventional, epoxy-coated, and increased adhesion ECR steel in simulated concrete pore solution with 1.6 m ion NaCl. Refer to Table 3.6 for specimen identification.

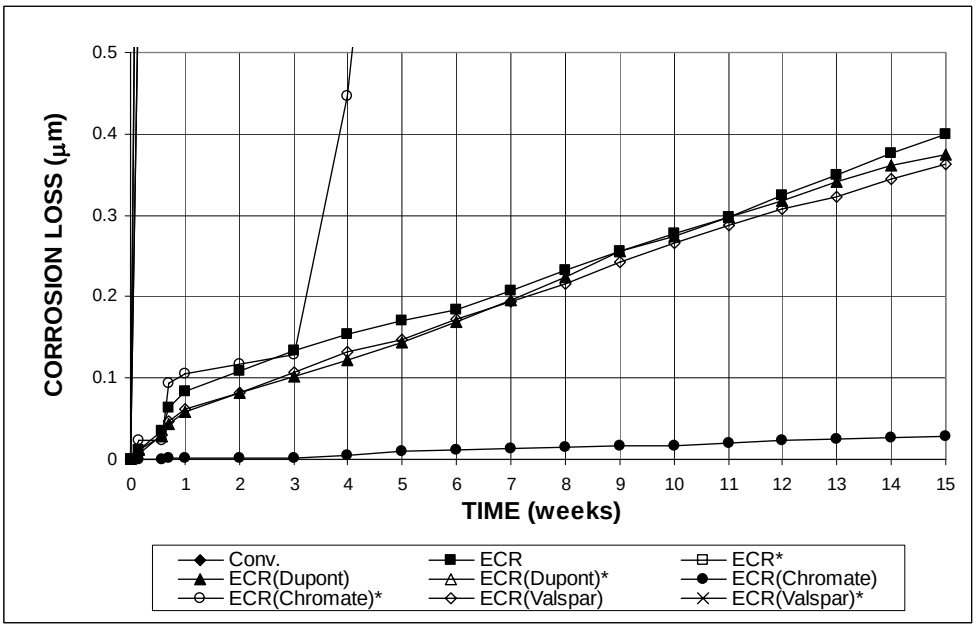

Figure 3.55 (b) - Macrocell Tests. Total Corrosion Loss. Bare bar specimens of conventional, epoxy-coated, and increased adhesion ECR steel in simulated concrete pore solution with 1.6 m ion NaCl. Refer to Table 3.6 for specimen identification.

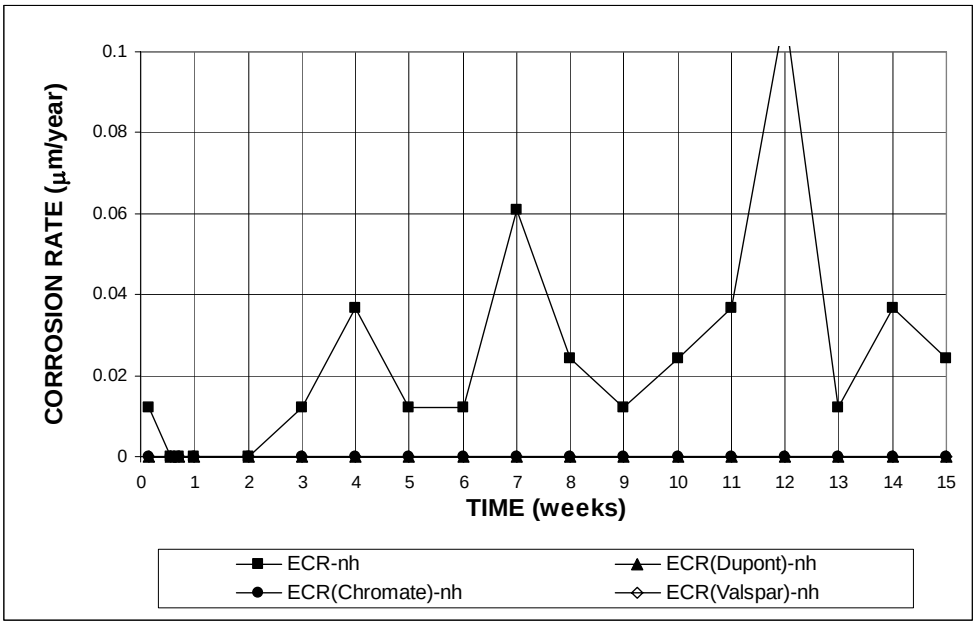

Figure 3.56 - Macrocell Tests. Average Corrosion Rate. Bare bar specimens of epoxy-coated and increased adhesion ECR bars without drilled holes in simulated concrete pore solution with 1.6 m ion NaCl. Refer to Table 3.6 for specimen identification.

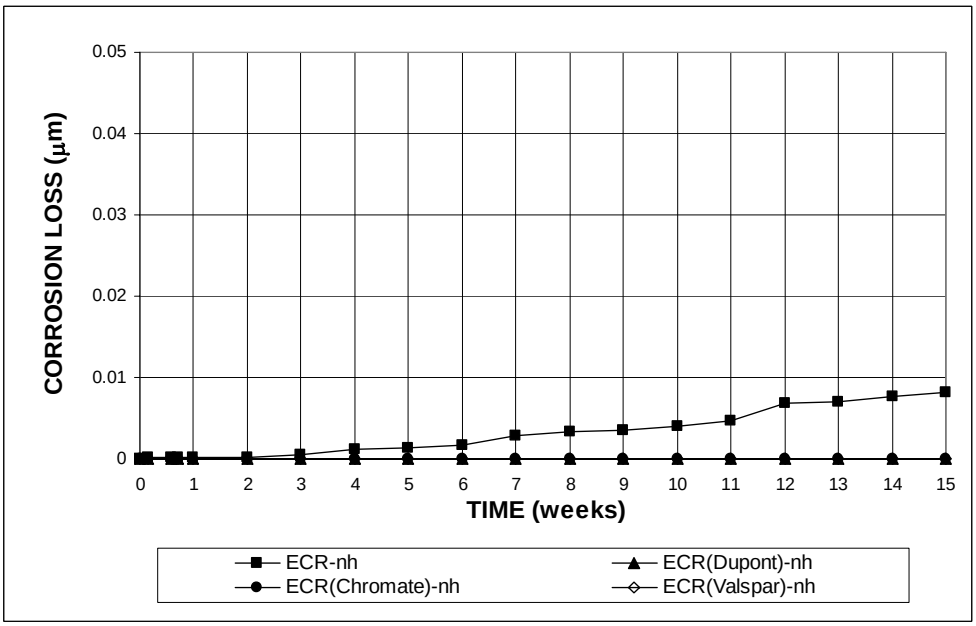

Figure 3.57 - Macrocell Tests. Total Corrosion Loss. Bare bar specimens of epoxy-coated and increased adhesion ECR bars without drilled holes in simulated concrete pore solution with 1.6 m ion NaCl. Refer to Table 3.6 for specimen identification.

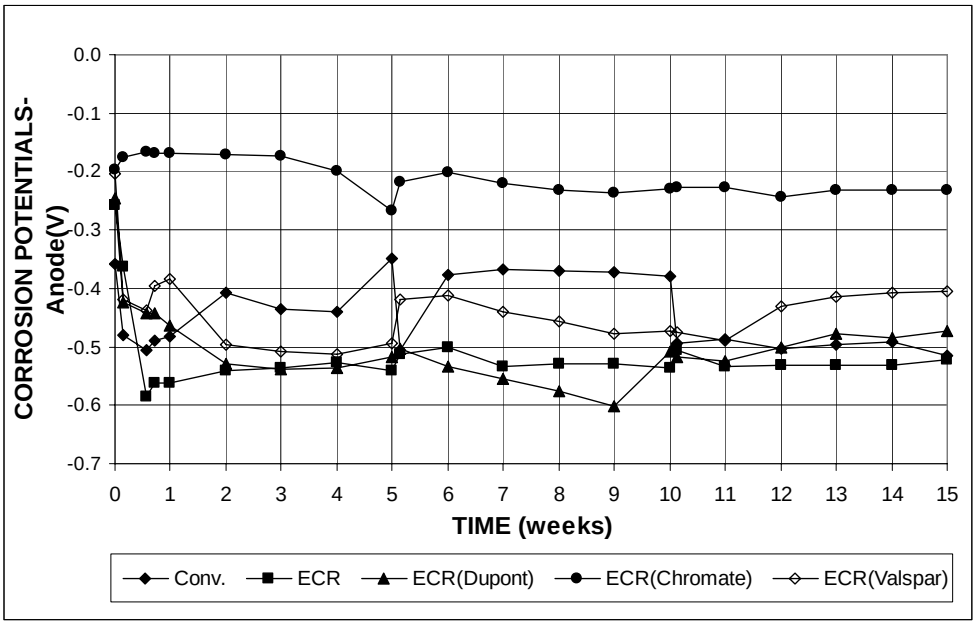

Figure 3.58 - Macrocell Tests. Corrosion Potential with respect to SCE at Anode. Bare bar specimens of conventional, epoxy-coated, and increased adhesion ECR steel in simulated concrete pore solution with 1.6 m ion NaCl. Refer to Table 3.6 for specimen identification.

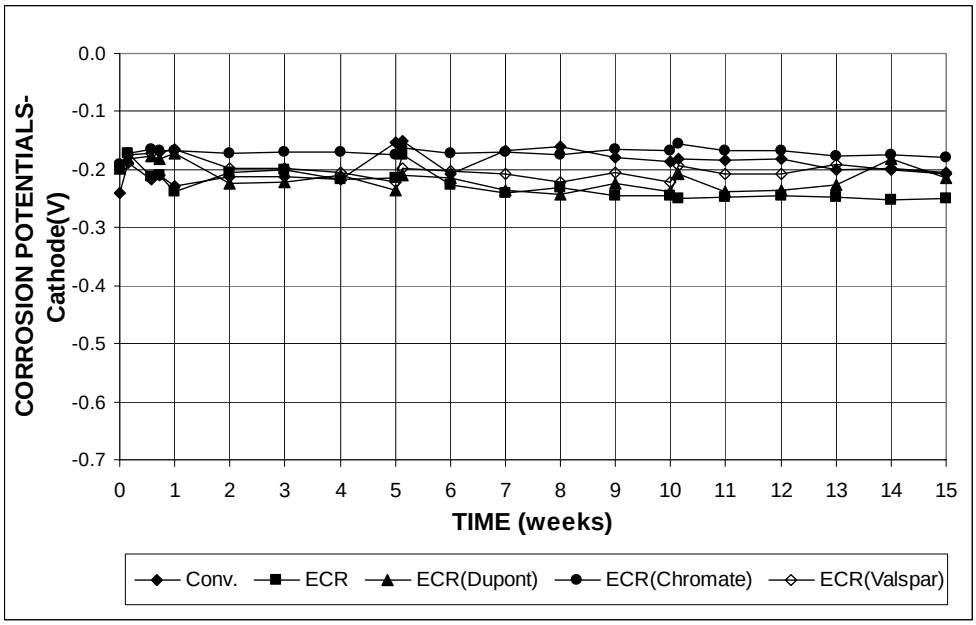

Figure 3.59 - Macrocell Tests. Corrosion Potential with respect to SCE at Cathode. Bare bar specimens of conventional, epoxy-coated, and increased adhesion ECR steel in simulated concrete pore solution with 1.6 m ion NaCl. Refer to Table 3.6 for specimen identification.

3.3.1.2 Macrocell Tests for Mortar-Wrapped Specimens

The average corrosion rates and total corrosion losses for the mortar-wrapped specimens in simulated pore solution with 1.6 m ion NaCl are shown in Figures 3.60-3.65. The corrosion rates for the bars with drilled holes are calculated based on both the exposed area of the four 3.2-mm (1/8-in.) diameter holes drilled through the epoxy and the total area of the bars exposed to solution. Table 3.6 summarizes the average corrosion rates and total corrosion losses at week 15. The results for conventional epoxy-coated steel in combination of the corrosion inhibitor DCI-S, presented and discussed in Section 3.4.1, are cited in this section for comparison.

During the test period, all three types of increased adhesion ECR bar exhibited very low corrosion rates and ended at the similar corrosion rates around 0.01 μm/yr, based on the total area, which is about half of that exhibited by conventional epoxy-coated steel (0.02 μm/yr) (Table 3.1). Based on the exposed area, the corrosion rates were 1.22 μm/yr, 0.61 μm/yr, and 0.61 μm/yr for the ECR(DuPont), ECR(Valspar) and ECR(Chromate) bars, which are lower than the value of 2.44 μm/yr for the conventional ECR specimens, presented in Section 3.1.1.2. For high adhesion epoxy-coated specimens cast in mortar with the corrosion inhibitor DCI, insignificant corrosion (at less than 0.01 μm/yr based on the total area exposed to the solution) was observed, which is similar to the corrosion rate of conventional ECR in conjunction of DCI. No significant corrosion was observed for any of the specimens without drilled holes.

After 15 weeks, the corrosion losses were less than 0.01 μm based on the total area for all three increased adhesion ECR specimens, as well as the conventional ECR specimens, with and without corrosion inhibitor DCI. Based on the exposed area for specimens without DCI, the ECR(DuPont) bars exhibited a corrosion loss at 0.4 μm,

equal to that of conventional ECR (0.4 μm) but higher than the values for ECR(Chromate) (0.12 μm) and ECR(Valspar) (0.16 μm). For specimens with DCI, all three increased adhesion bars showed the same corrosion loss, 0.04 μm, a value below that for specimens without DCI, indicating that the corrosion inhibitor helped the corrosion performance of the high adhesion bars in mortar. A similar conclusion is reached in Section 3.4.1 for conventional ECR bars in mortar-wrapped specimens with DCI, as well as two other corrosion inhibitors.

The average corrosion potentials of the anodes and cathodes are shown in Figures 3.66 and 3.67, respectively (the potentials of conventional ECR cast with the corrosion inhibitor DCI-S are shown in Figures 3.86 and 3.87). All anodic specimens started at around −0.200 V on day 1. Except for the ECR(Chromate) bars with DCI, all other ECR anodes showed potentials more positive than −0.250 V at week 15. The ECR(Chromate) bars with DCI had an average corrosion potential of −0.280 V at week 15, which is still much lower than the corrosion potential of the conventional specimens (−0.574 V). The average corrosion potentials for the cathodes were around −0.200 V for the conventional ECR and three types of increased adhesion bars, except that ECR(Chromate) with DCI had an average value of −0.250 V. The undamaged bars exhibited unstable corrosion potentials for both anodes and cathodes since the epoxy served as an electrical insulation.

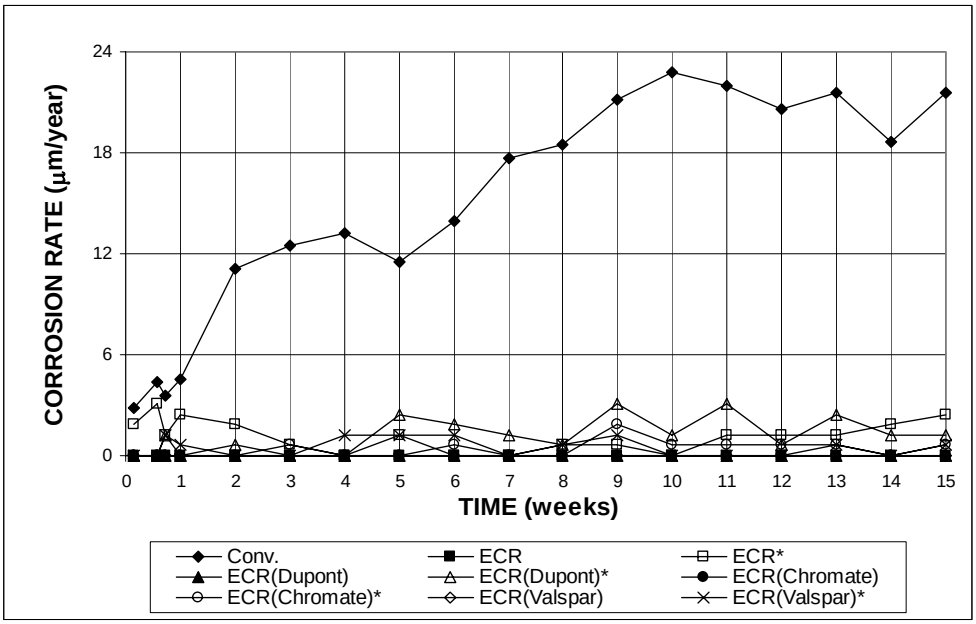

Figure 3.60 (a) - Macrocell Tests. Average Corrosion Rate. Mortar-wrapped specimens of conventional, epoxy-coated, and increased adhesion ECR steel in simulated concrete pore solution with 1.6 m ion NaCl. Refer to Table 3.6 for specimen identification.

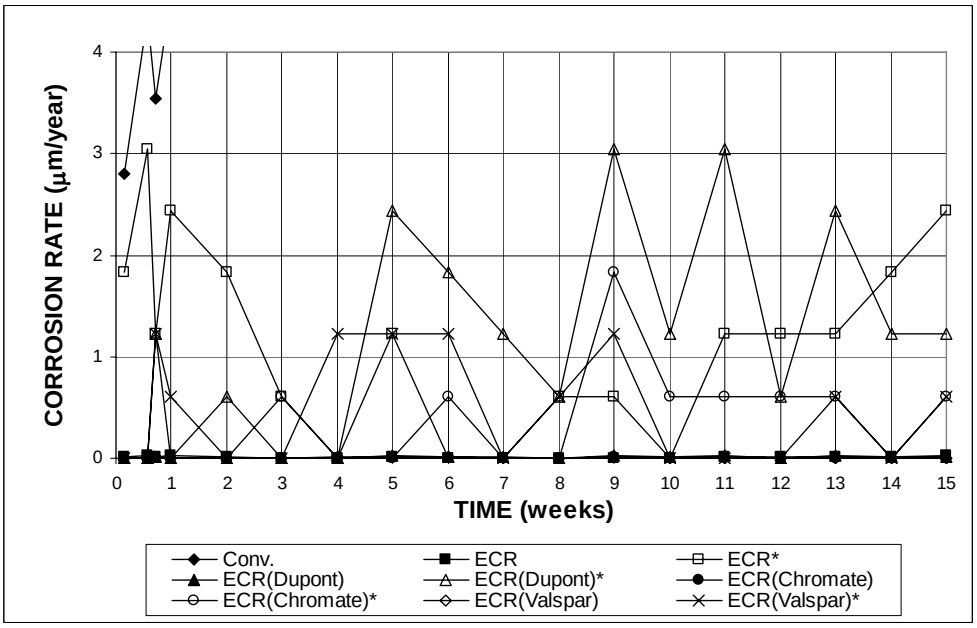

Figure 3.60 (b) - Macrocell Tests. Average Corrosion Rate. Mortar-wrapped specimens of conventional, epoxy-coated, and increased adhesion ECR steel in simulated concrete pore solution with 1.6 m ion NaCl. Refer to Table 3.6 for specimen identification.

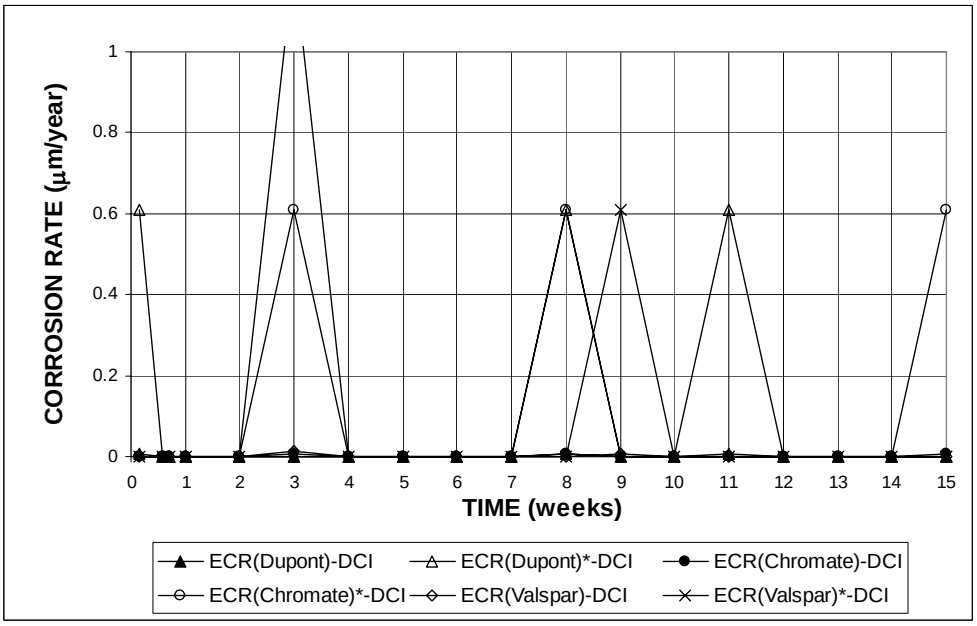

Figure 3.61 (a) - Macrocell Tests. Average Corrosion Rate. Mortar-wrapped specimens with the corrosion inhibitor DCI of conventional, epoxy-coated, and increased adhesion ECR steel in simulated concrete pore solution with 1.6 m ion NaCl. Refer to Table 3.6 for specimen identification.

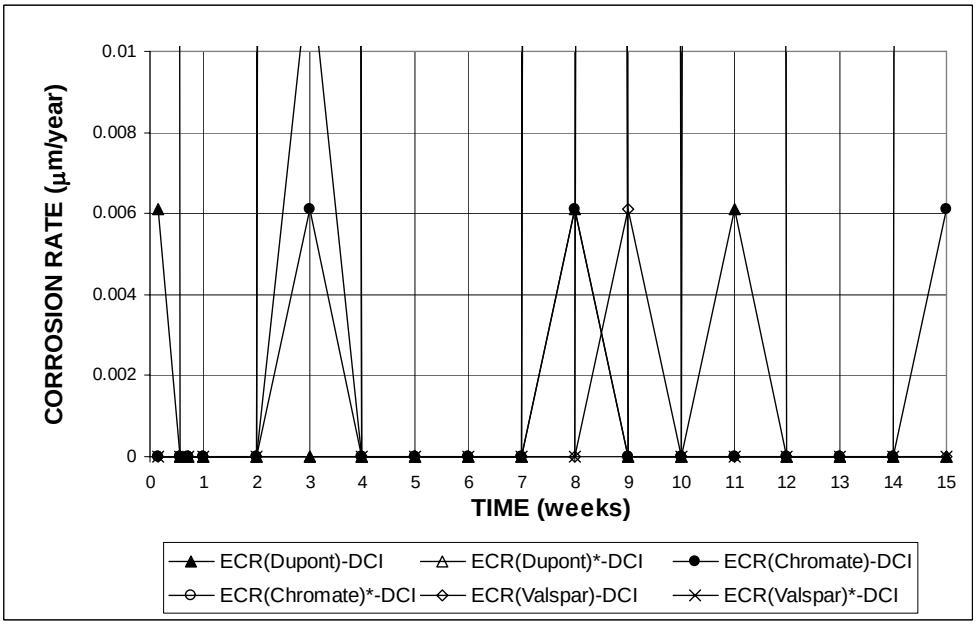

Figure 3.61 (b) - Macrocell Tests. Average Corrosion Rate. Mortar-wrapped specimens with corrosion inhibitor DCI of conventional, epoxy-coated, and increased adhesion ECR steel in simulated concrete pore solution with 1.6 m ion NaCl. Refer to Table 3.6 for specimen identification.

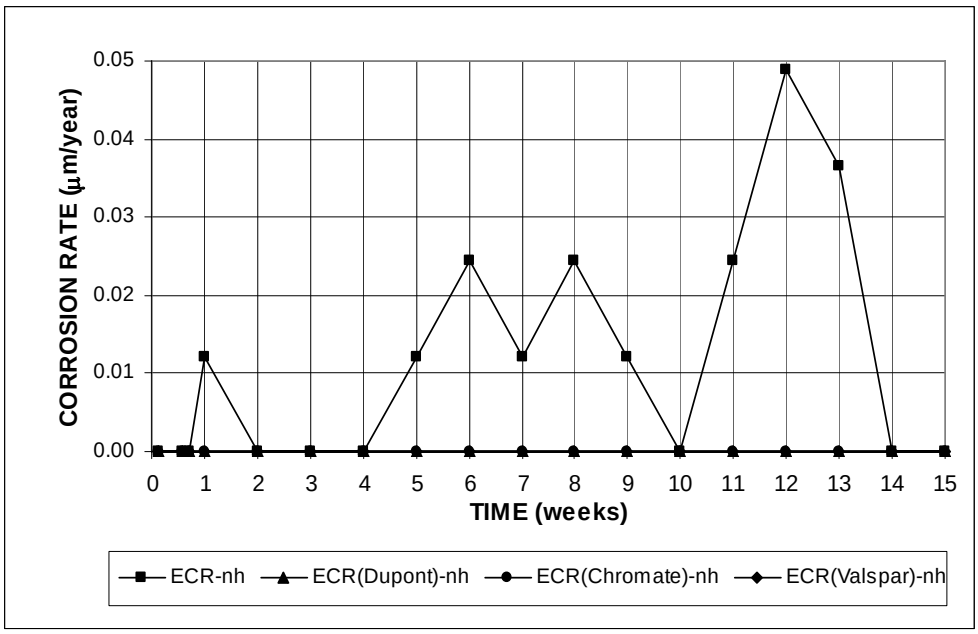

Figure 3.62 - Macrocell Tests. Average Corrosion Rate. Mortar-wrapped specimens of epoxy-coated and increased adhesion ECR steel without drilled holes in simulated concrete pore solution with 1.6 m ion NaCl. Refer to Table 3.6 for specimen identification.

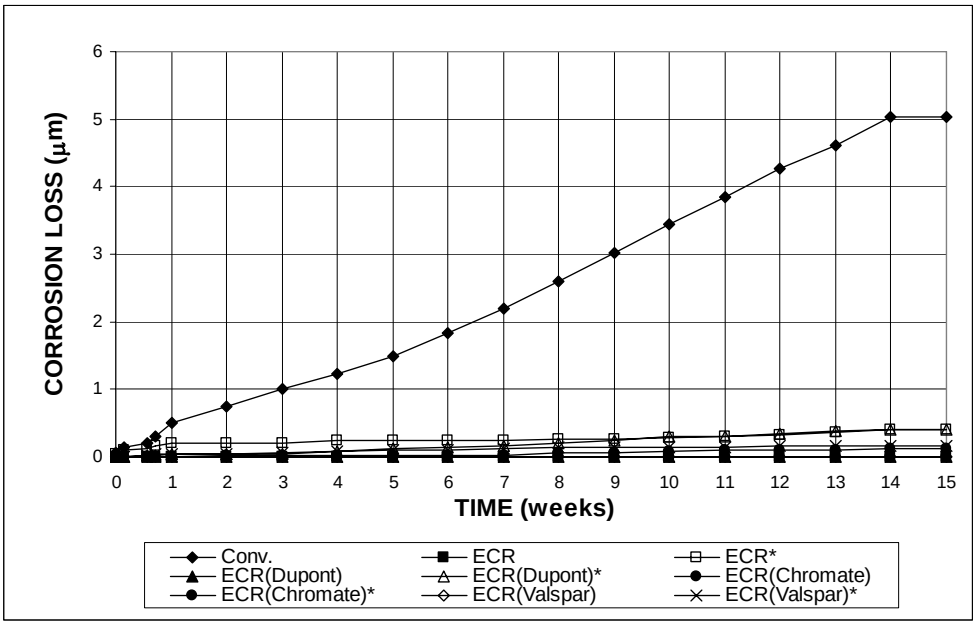

Figure 3.63 (a) - Macrocell Tests. Total Corrosion Loss. Mortar-wrapped specimens of conventional, epoxy-coated, and increased adhesion ECR steel in simulated concrete pore solution with 1.6 m ion NaCl. Refer to Table 3.6 for specimen identification.

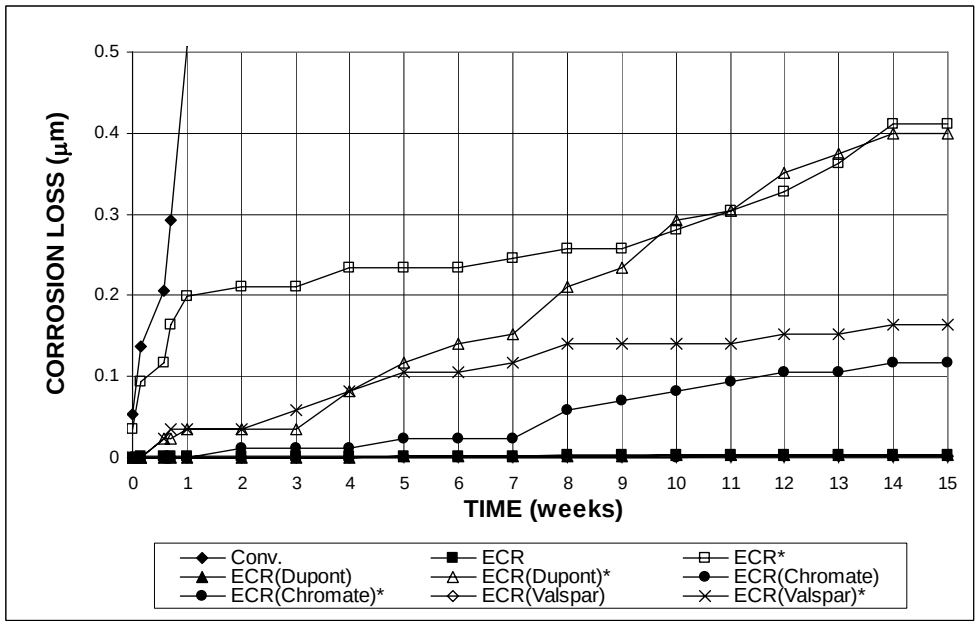

Figure 3.63 (b) - Macrocell Tests. Total Corrosion Loss. Mortar-wrapped specimens of conventional, epoxy-coated, and increased adhesion ECR steel in simulated concrete pore solution with 1.6 m ion NaCl. Refer to Table 3.6 for specimen identification.

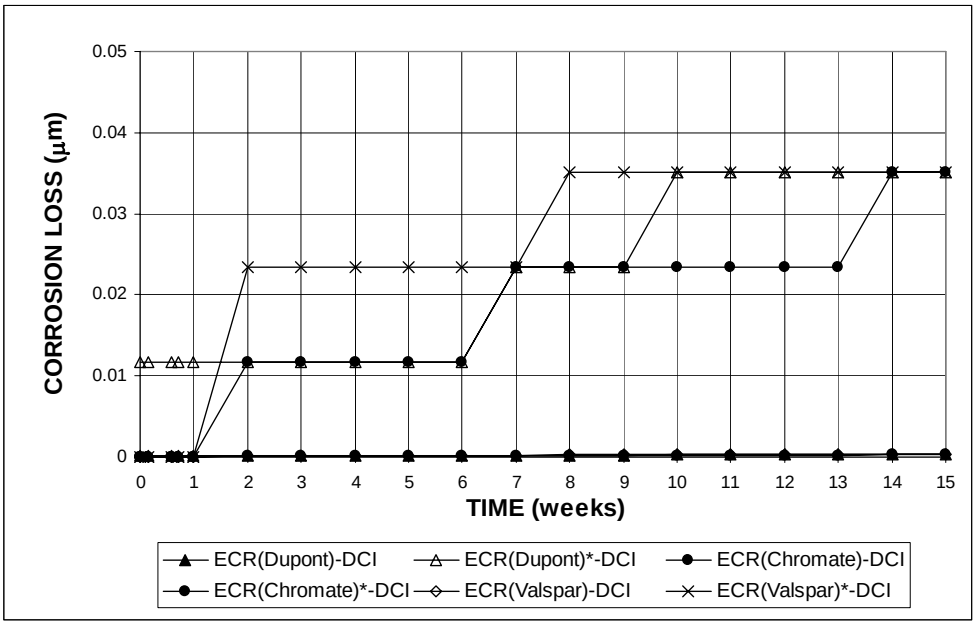

Figure 3.64 - Macrocell Tests. Total Corrosion Loss. Mortar-wrapped specimens with the corrosion inhibitor DCI of conventional, epoxy-coated, and increased adhesion ECR steel in simulated concrete pore solution with 1.6 m ion NaCl. Refer to Table 3.6 for specimen identification.

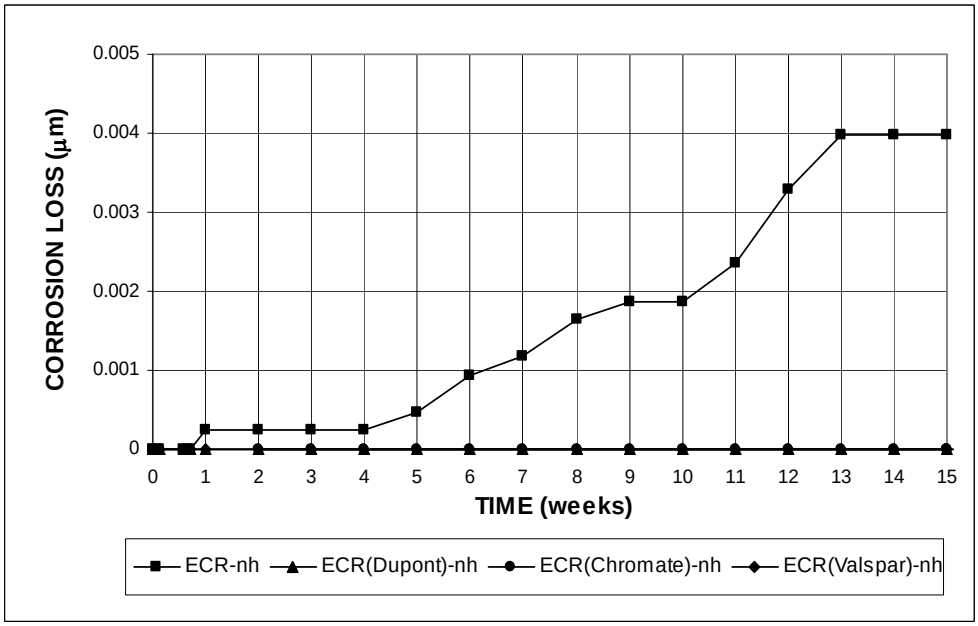

Figure 3.65 - Macrocell Tests. Total Corrosion Loss. Mortar-wrapped specimens of epoxy-coated and increased adhesion ECR steel without drilled holes in simulated concrete pore solution with 1.6 m ion NaCl. Refer to Table 3.6 for specimen identification.

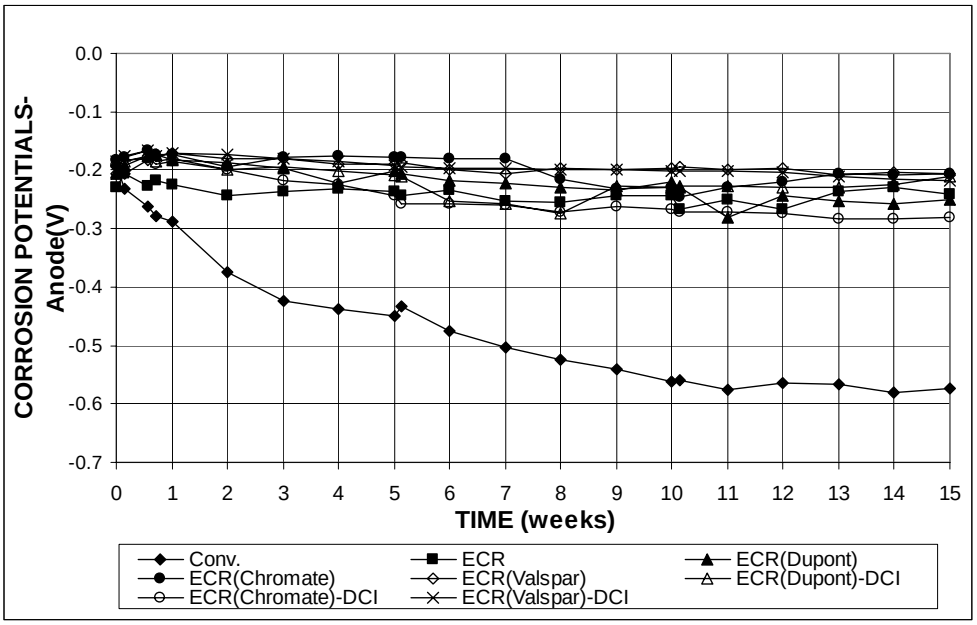

Figure 3.66 - Macrocell Tests. Corrosion Potential with respect to SCE at Anode. Mortar-wrapped specimens of conventional, epoxy-coated, and increased adhesion ECR steel in simulated concrete pore solution with 1.6 m ion NaCl. Refer to Table 3.6 for specimen identification.

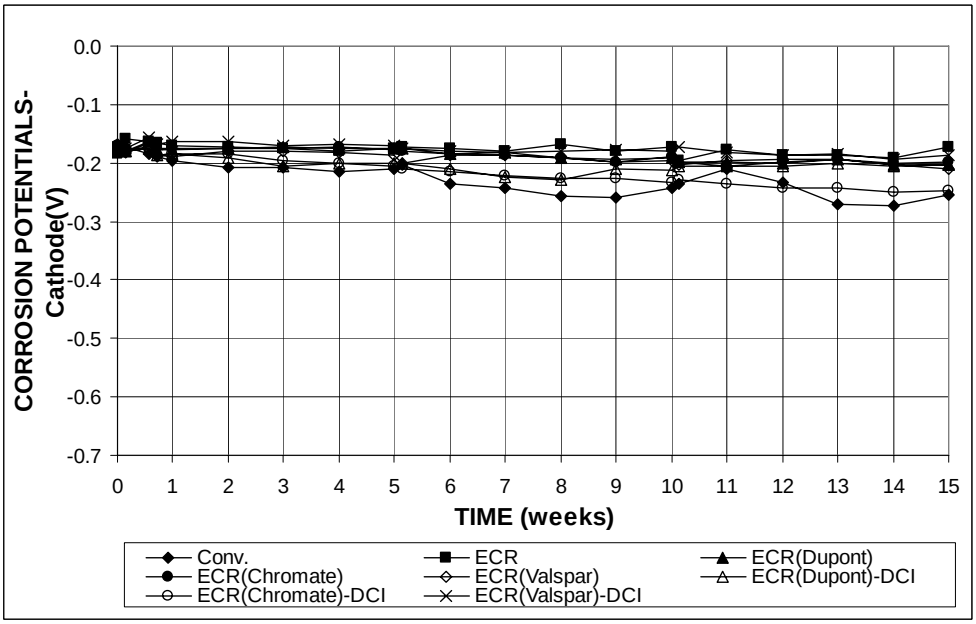

Figure 3.67 - Macrocell Tests. Corrosion Potential at with respect to SCE at Cathode. Mortar-wrapped specimens of conventional, epoxy-coated, and increased adhesion ECR steel in simulated concrete pore solution with 1.6 m ion NaCl. Refer to Table 3.6 for specimen identification.

3.3.1.3 Visual Inspection

As the tests were discontinued, the specimens were visually inspected. For bare bar specimens with ECR(DuPont) and ECR(Valspar) bars, corrosion products were found at the drilled holes. No corrosion products appeared on the bare bar specimens of ECR(Chromate) with drilled holes or any of the epoxy-coated bars without drilled holes. Figures 3.68 and 3.69 show bare anode bars at 15 weeks with the corrosion products that formed at the drilled holes on ECR(DuPont) and ECR(Valspar) specimens.

For mortar-wrapped specimens, the specimens were broken but no obvious corrosion products were found under the mortar.

Figure 3.68 – Bare ECR(DuPont) anode bar, at 15 weeks, showing corrosion products that formed at drilled holes.

Figure 3.69 – Bare ECR(Valspar) anode bar, at 15 weeks, showing corrosion products that formed at drilled holes.

3.3.2 Bench-Scale Tests

The average corrosion rates and total corrosion losses as of March 15, 2005 for the Southern Exposure and cracked beam tests are summarized in Table 3.7. Results for individual specimens are presented in Appendix A.

3.3.2.1 Southern Exposure Test

The Southern Exposure tests include three specimens each with ECR(DuPont), ECR(Chromate), and ECR(Valspar) bars with four and 10 drilled holes. Since one specimen each of ECR(DuPont), ECR(Chromate), and ECR(Valspar) with 10 drilled holes had been under test for less than 10 weeks as of the data cutoff point, the results for these tests in Figures 3.70-3.76 represent the average of two, rather than three specimens. For the same reason, the results of increased adhesion bars in conjunction of the corrosion inhibitor DCI-S are not presented here. Average corrosion rates, total corrosion losses, mat-to-mat resistances, and corrosion potentials are shown in Figures 3.70- 3.76.

For the specimens with four drilled holes (Figure 3.70), the three increased adhesion ECR specimens showed insignificant corrosion, at a rate less than 0.01 μm/yr based on the total area, as of week 33, similar to the rate for conventional ECR. Corrosion at rates of 3.1, 1.8, and 1.8 μm/yr were obtained based on the exposed area for the ECR(DuPont), ECR(Chromate), and ECR(Valspar) specimens, respectively, as compared to 0.92 μm/yr for the conventional ECR specimens.

For specimens with 10 drilled holes (Figure 3.71), all three increased adhesion ECR specimens showed similar corrosion rates, around 0.01 μm/yr at week 31, compared to the conventional ECR specimens, while exhibited a corrosion rate of less than 0.01 μm/yr at the same point in time.

The average corrosion losses are shown in Figures 3.72 and 3.73, for specimens with four and 10 holes, respectively. Based on the total area, the high adhesion ECR specimens with four drilled holes showed no corrosion losses greater than 0.01 μm at week 33, compared to the conventional ECR specimens which showed an average total corrosion loss of 0.01 μm at the same point in time. All increased adhesion ECR specimens with 10 drilled holes exhibited corrosion losses close to 0.01 μm, similar to the value observed for conventional ECR steel.

The results for mat-to-mat resistance are shown in Figure 3.74. The increased adhesion ECR specimens with four drilled holes started at average resistances of around 2,000 ohms, and increasing to between 7,000 and 10,000 ohms. The specimens with 10 drilled holes exhibited lower resistances, around 900 ohms at the beginning and 3,500 ohms at the end of the period for which the data were recorded. As described in Section 3.1.2.1, the ECR specimens with four drilled holes exhibit higher resistance than ECR specimens with 10 drilled holes due to the lower damage to the epoxy.

The average corrosion potentials of the top and bottom mats with respect to a copper copper-sulfate electrode are shown in Figures 3.75 and 3.76. For the top mat, all of the high adhesion ECR specimens with 10 drilled holes exhibited corrosion potentials more negative than −0.350 V, indicating that these specimens are undergoing active corrosion, while the specimens with four drilled holes showed corrosion potentials more positive than −0.220 V. For the bottom mat, the corrosion potential of ECR(Valspar) with 10 drilled holes dropped to a value more negative than −0.250 V at week 28 but rebounded to −0.166 V at week 33. All other specimens, except for conventional steel and conventional ECR, exhibited corrosion potentials more positive than −0.200 V.

Table 3.7 – Average corrosion rates and corrosion losses for epoxy-coated steel with increased adhesion measured in the bench-scale tests

CORROSION RATE (μm/year)

Steel Designation	Exposure Time	Specimen 1	Specimen 2	Specimen 3	Average	Std. Deviation
Southern Exposure Specimens						
ECR(DuPont)	33	0	α	0.01	α	0.01
ECR(DuPont)*	33	0	3.66	5.49	3.05	2.80
ECR(DuPont)-10h	31	α	α	-	α	-
ECR(DuPont)*-10h	31	0.73	1.46	-	1.10	0.52
ECR(Chromate)	33	0	0	0.01	α	0.01
ECR(Chromate)*	33	0	0	5.49	1.83	3.17
ECR(Chromate)-10h	31	0	0.02	-	α	0.01
ECR(Chromate)*-10h	31	0	2.93	-	1.46	2.07
ECR(Valspar)	33	0	0	0.01	α	0.01
ECR(Valspar)*	33	0	0	5.49	1.83	3.17
ECR(Valspar)-10h	31	α	0.02	-	0.01	0.01
ECR(Valspar)*-10h	31	1.46	2.93	-	2.20	1.04
Cracked Beam Specimens						
ECR(DuPont)	33	0.05	0.18	0.03	0.09	0.08
ECR(DuPont)*	33	25.62	87.84	14.64	42.7	39.48
ECR(DuPont)-10h	31	0.08	0.06	-	0.07	0.01
ECR(DuPont)*-10h	31	14.64	11.71	-	13.18	2.07
ECR(Chromate)	33	0.03	0.02	0.10	0.05	0.04
ECR(Chromate)*	33	14.64	10.98	47.58	24.40	20.16
ECR(Chromate)-10h	31	α	0.14	-	0.07	0.09
ECR(Chromate)*-10h	31	1.46	26.35	-	13.91	17.6
ECR(Valspar)	33	0.11	0.04	0.02	0.06	0.05
ECR(Valspar)*	33	54.90	18.30	7.32	26.84	24.91
ECR(Valspar)-10h	31	0.08	0.02	-	0.05	0.04
ECR(Valspar)*-10h	31	14.64	2.93	-	8.78	8.28

CORROSION LOSS (μm)

Steel Designation	Exposure Time	Specimen 1	Specimen 2	Specimen 3	Average	Std. Deviation
Southern Exposure Specimens						
ECR(DuPont)	33	β	β	β	β	-
ECR(DuPont)*	33	1.48	1.27	1.97	1.57	0.36
ECR(DuPont)-10h	31	β	β	-	β	-
ECR(DuPont)*-10h	31	0.86	1.48	-	1.17	0.44
ECR(Chromate)	33	β	β	β	β	-
ECR(Chromate)*	33	1.44	2.22	1.23	1.63	0.52
ECR(Chromate)-10h	31	β	0.01	-	β	0.01
ECR(Chromate)*-10h	31	0.55	1.93	-	1.24	0.98
ECR(Valspar)	33	β	β	β	β	-
ECR(Valspar)*	33	1.37	1.44	1.37	1.40	0.04
ECR(Valspar)-10h	31	β	β	-	β	-
ECR(Valspar)*-10h	31	0.58	1.27	-	0.92	0.49
Cracked Beam Specimens						
ECR(DuPont)	33	0.05	0.02	0.02	0.03	0.02
ECR(DuPont)*	33	24.85	11.97	9.43	15.41	8.27
ECR(DuPont)-10h	31	0.05	0.04	-	0.04	0.01
ECR(DuPont)*-10h	31	9.60	6.87	-	8.24	1.93
ECR(Chromate)	33	0.05	0.04	0.04	0.04	0.01
ECR(Chromate)*	33	23.93	18.02	17.81	19.92	3.48
ECR(Chromate)-10h	31	0.01	0.05	-	0.03	0.02
ECR(Chromate)*-10h	31	2.79	9.07	-	5.93	4.44
ECR(Valspar)	33	0.10	0.05	0.01	0.06	0.05
ECR(Valspar)*	33	50.25	23.02	5.98	26.42	22.33
ECR(Valspar)-10h	31	0.04	0.02	-	0.03	0.02
ECR(Valspar)*-10h	31	8.45	2.96	-	5.70	3.88

Table 3.7 continued

[1] ECR(DuPont): Epoxy-coated steel with increased adhesion epoxy by DuPont , based on total area of bar exposed to solution

[2] ECR(DuPont)*: Epoxy-coated steel with increased adhesion epoxy by DuPont, based on exposed area of four 3.2-mm (1/8-in.) diameter holes in epoxy

[3] ECR(DuPont)-10h: Epoxy-coated steel with increased adhesion epoxy by DuPont and with 10 drilled holes, based on total area of bar exposed to solution

[4] ECR(DuPont)*-10h: Epoxy-coated steel with increased adhesion epoxy by DuPont, based on exposed area of ten 3.2-mm (1/8-in.)diameter holes in epoxy

[5] ECR(Chromate): Epoxy-coated steel with chromate pretreatment, based on total area of bar exposed to solution

[6] ECR(Chromate)*:Epoxy-coated steel with chromate pretreatment, based on exposed area of four 3.2-mm (1/8-in.) diameter holes in epoxy

[7] ECR(Chromate)-10h: Epoxy-coated steel with chromate pretreatment and with 10 drilled holes, based on total area of bar exposed to solution

[8] ECR(Chromate)*-10h: Epoxy-coated steel with chromate pretreatment, based on exposed area of ten 3.2-mm (1/8-in.)diameter holes in epoxy

[9] ECR(Valspar): Epoxy-coated steel with increased adhesion epoxy by Valspar , based on total area of bar exposed to solution

[10] ECR(Valspar)* : Epoxy-coated steel with increased adhesion epoxy by Valspar, based on exposed area of four 3.2-mm (1/8-in.) diameter holes in epoxy

[11] ECR(Valspar)-10h: Epoxy-coated steel with increased adhesion epoxy by Valspar and with 10 drilled holes, based on total area of bar exposed to solution

[12] ECR(Valspar)*-10h: Epoxy-coated steel with increased adhesion epoxy by Valspar, based on exposed area of ten 3.2-mm (1/8-in.)diameter holes in epoxy

[13] α: corrosion rate less than 0.01 μm/yr

[14] β: corrosion loss less than 0.01μm

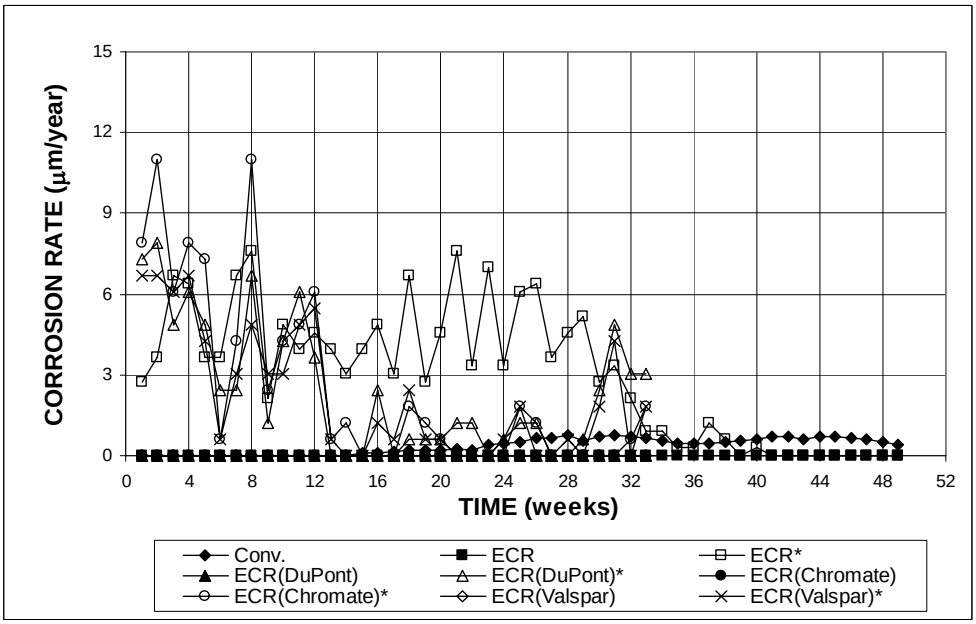

Figure 3.70 (a) – Southern Exposure Tests. Average Corrosion Rate. Specimens of conventional, epoxy-coated, and increased adhesion ECR bars ponded with 15% NaCl solution. All epoxy-coated specimens with four drilled holes. Refer to Table 3.7 for specimen identification.

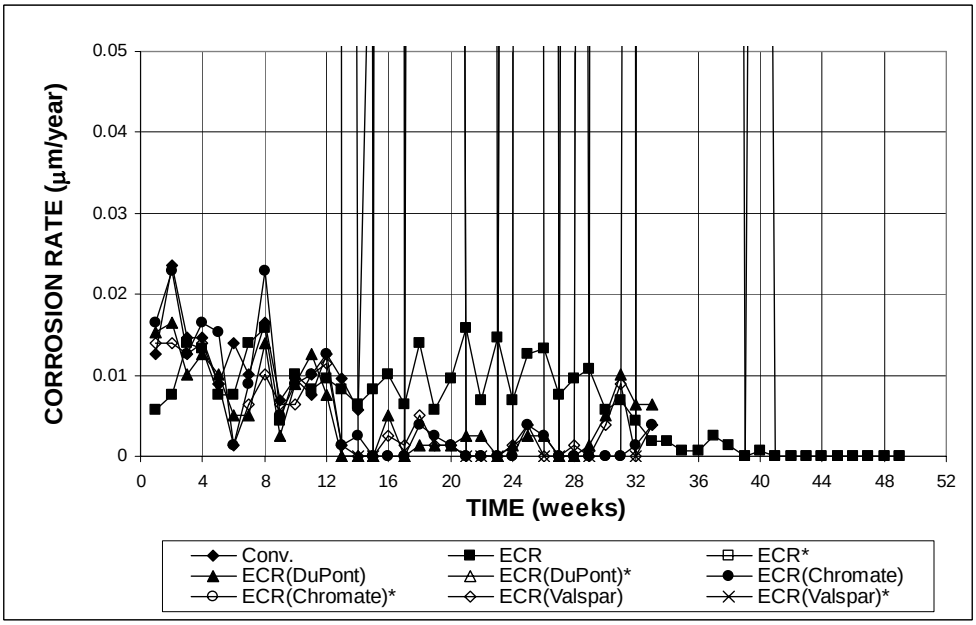

Figure 3.70 (b) – Southern Exposure Tests. Average Corrosion Rate. Specimens of conventional, epoxy-coated, and increased adhesion ECR bars ponded with 15% NaCl solution. All epoxy-coated specimens with four drilled holes. Refer to Table 3.7 for specimen identification.

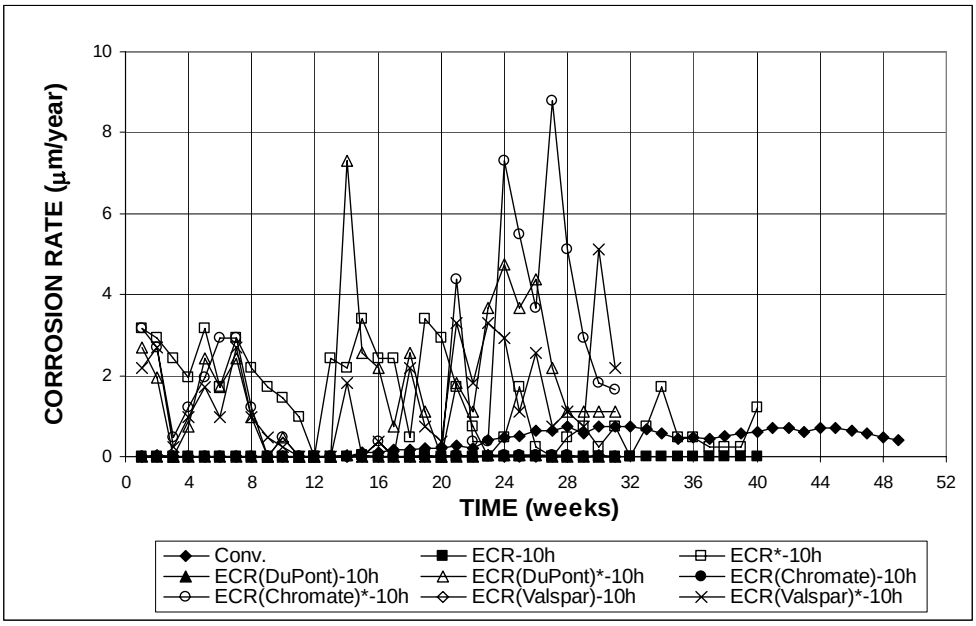

Figure 3.71 (a) – Southern Exposure Tests. Average Corrosion Rate. Specimens of conventional, epoxy-coated, and increased adhesion ECR bars ponded with 15% NaCl solution. All epoxy-coated specimens with 10 drilled holes. Refer to Table 3.7 for specimen identification.

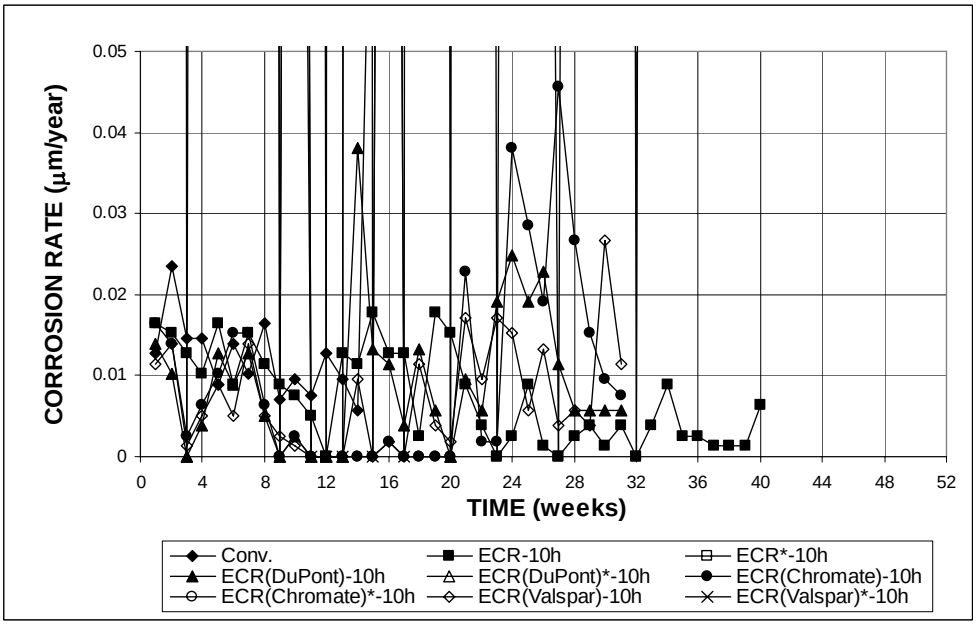

Figure 3.71 (b) – Southern Exposure Tests. Average Corrosion Rate. Specimens of conventional, epoxy-coated, and increased adhesion ECR bars ponded with 15% NaCl solution. All epoxy-coated specimens with 10 drilled holes. Refer to Table 3.7 for specimen identification.

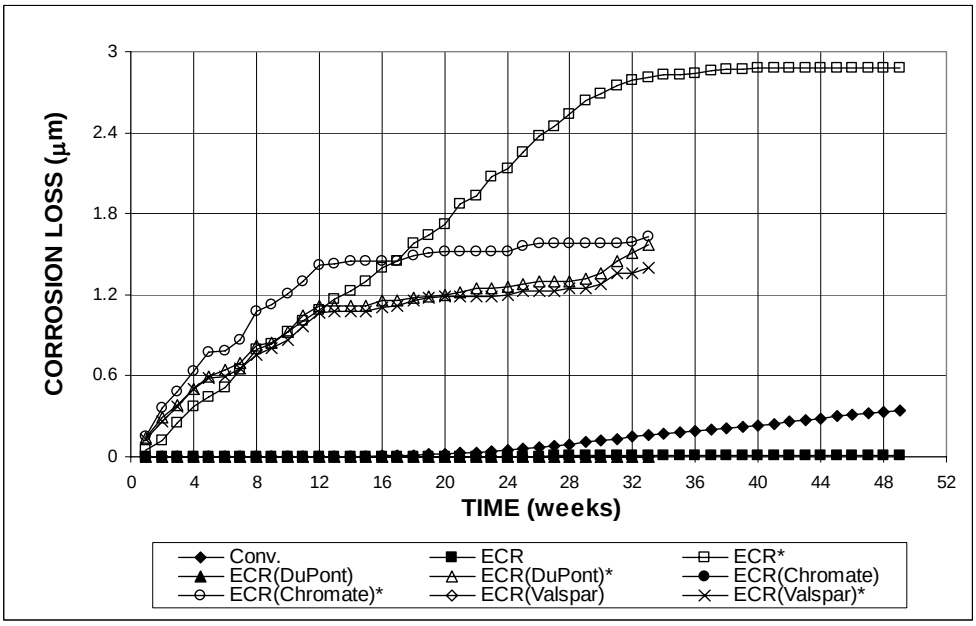

Figure 3.72 (a) – Southern Exposure Tests. Total Corrosion Loss. Specimens of conventional, epoxy-coated, and increased adhesion ECR bars ponded with 15% NaCl solution. All epoxy-coated specimens with four drilled holes. Refer to Table 3.7 for specimen identification.

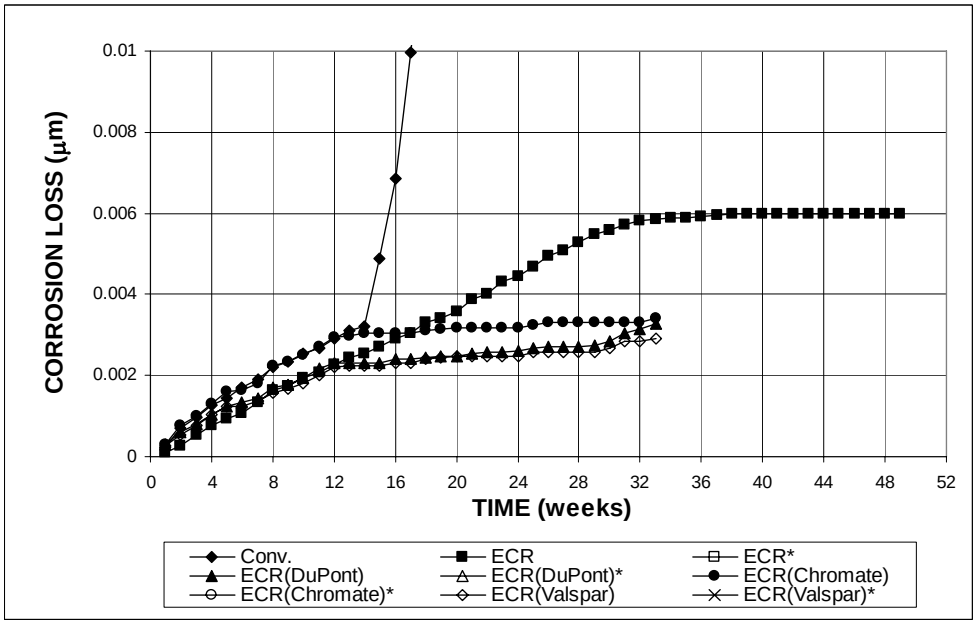

Figure 3.72 (b) – Southern Exposure Tests. Total Corrosion Loss. Specimens of conventional, epoxy-coated, and increased adhesion ECR bars ponded with 15% NaCl solution. All epoxy-coated specimens with four drilled holes. Refer to Table 3.7 for specimen identification.

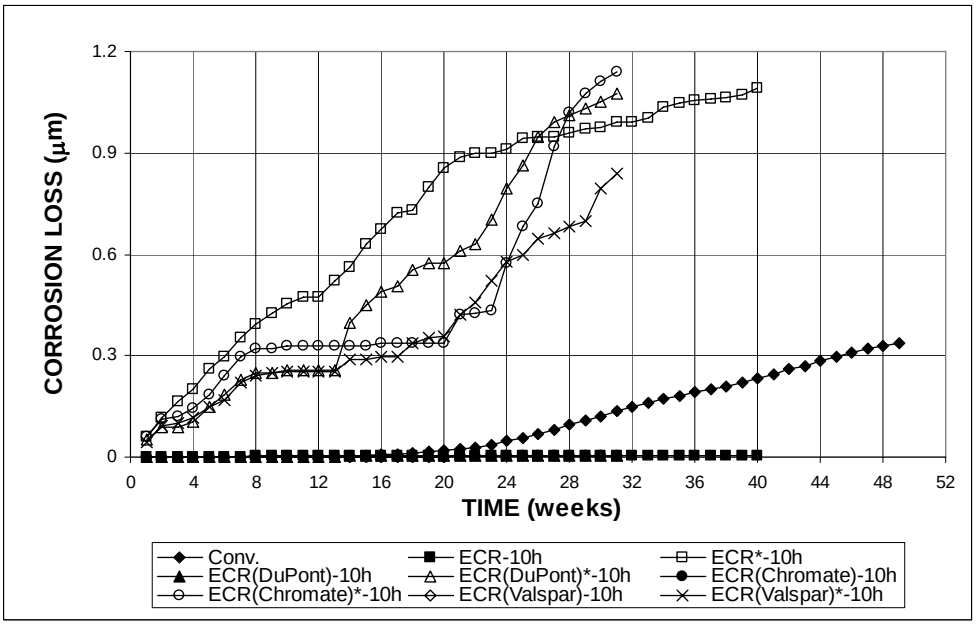

Figure 3.73 (a) – Southern Exposure Tests. Total Corrosion Loss. Specimens of conventional, epoxy-coated, and increased adhesion ECR bars ponded with 15% NaCl solution. All epoxy-coated specimens with 10 drilled holes. Refer to Table 3.7 for specimen identification.

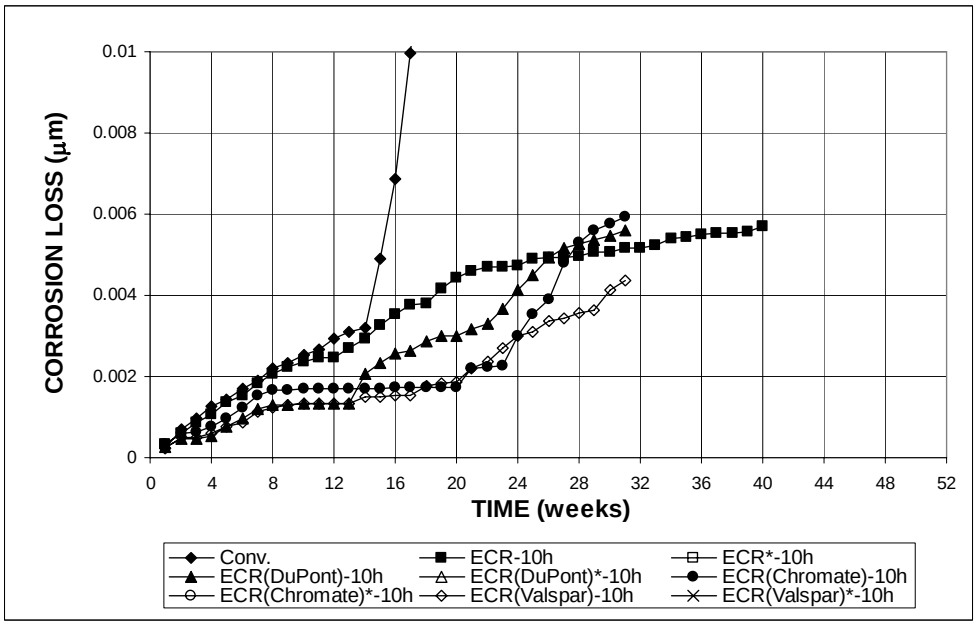

Figure 3.73 (b) – Southern Exposure Tests. Total Corrosion Loss. Specimens of conventional, epoxy-coated, and increased adhesion ECR bars ponded with 15% NaCl solution. All epoxy-coated specimens with 10 drilled holes. Refer to Table 3.7 for specimen identification.

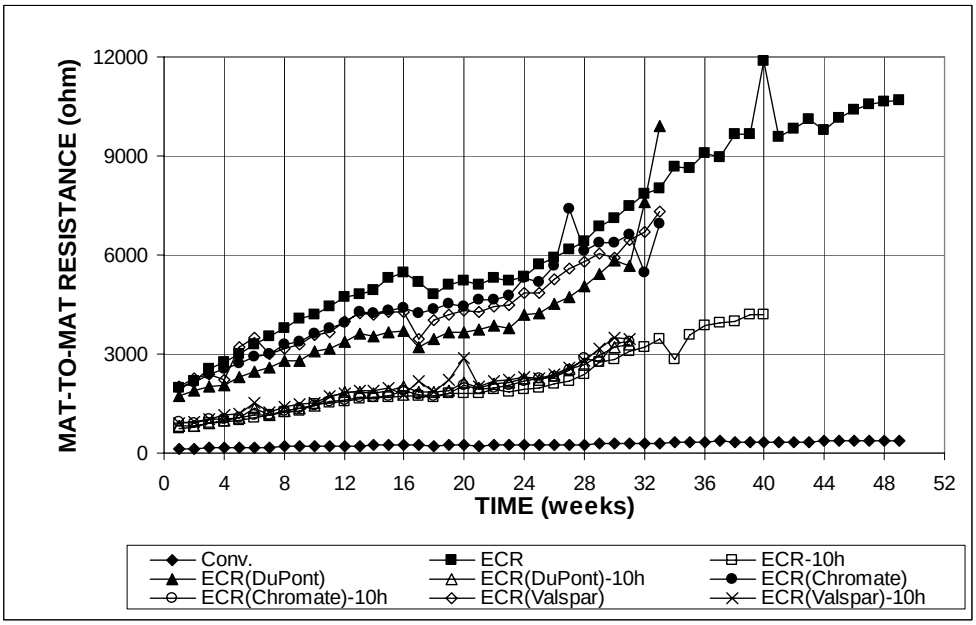

Figure 3.74 – Southern Exposure Tests. Mat-to-mat resistance. Specimens of conventional, epoxy-coated, and increased adhesion ECR bars ponded with 15% NaCl solution. Refer to Table 3.7 for specimen identification.

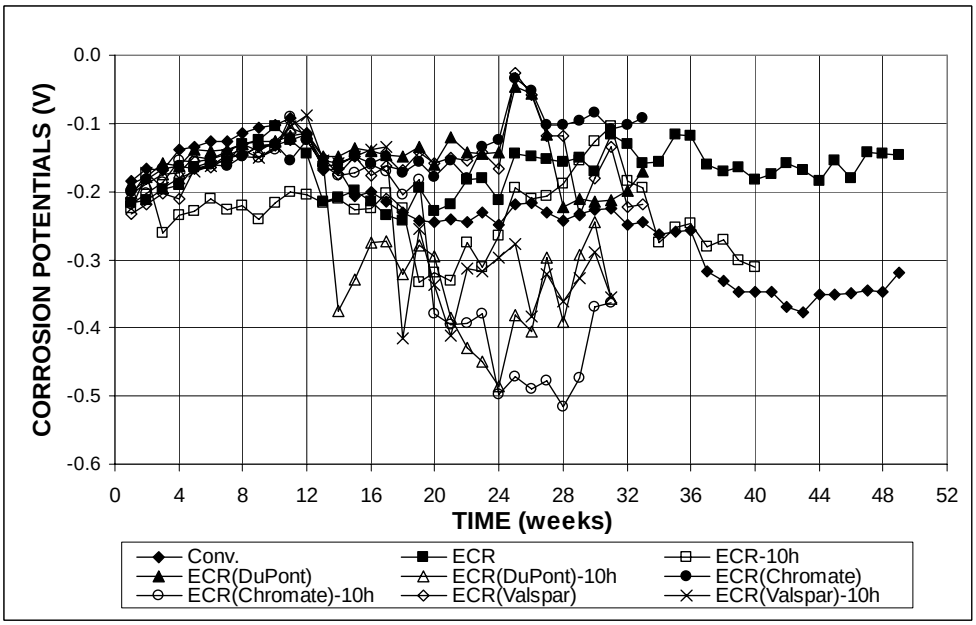

Figure 3.75 – Southern Exposure Tests. Corrosion Potential with respect to CSE at Top Mat. Specimens of conventional, epoxy-coated, and increased adhesion ECR bars ponded with 15% NaCl solution. Refer to Table 3.7 for specimen identification.

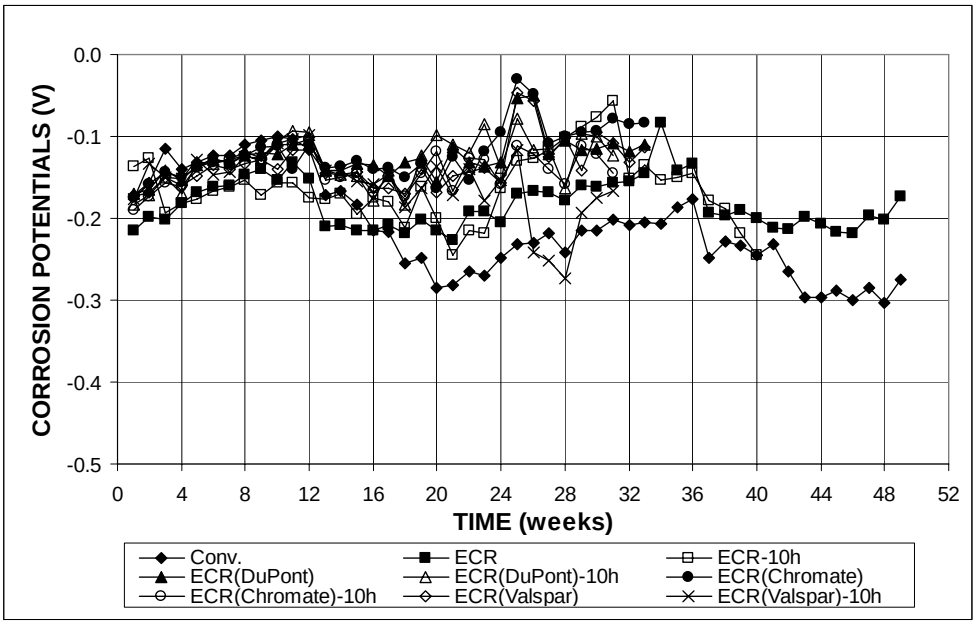

Figure 3.76 – Southern Exposure Tests. Corrosion Potential with respect to CSE at Bottom Mat. Specimens of conventional, epoxy-coated, and increased adhesion ECR bars ponded with 15% NaCl solution. Refer to Table 3.7 for specimen identification.

3.3.2.2 Cracked Beam Tests

The cracked beam tests include three specimens each for ECR(DuPont), ECR(chromate), and ECR(Valspar) with four and 10 drilled holes. As with the Southern Exposure tests, one specimen each for ECR(DuPont), ECR(chromate), and ECR(Valspar) with 10 drilled holes were under test for less than 10 weeks and are not included in the average value presented in this section. Average corrosion rates, total corrosion losses, mat-to-mat resistances, and corrosion potentials are shown in Figures 3.77-3.83.

As shown in Figures 3.77 and 3.78, the high adhesion ECR specimens with four holes showed higher corrosion rates than that of conventional ECR specimens, while the high adhesion ECR specimens with 10 holes exhibited similar corrosion rates to the conventional ECR specimens. For specimens with four drilled holes (Figure 3.77), the ECR(DuPont) specimens reached a corrosion rate as high as 0.11 μm/yr at week

30 and showed the highest value among the increased adhesion ECR specimens at week 33, 0.09 μm/yr based on the total area, equal to six times that of conventional ECR (0.014 μm/yr). Although the ECR(Chromate) and ECR (Valspar) specimens exhibited higher corrosion rates than that of the ECR(DuPont) before week 30, they exhibited lower rates at week 33, with values of 0.06 and 0.05 μm/yr based on the total area, respectively. As with the results based on the total area, the highest corrosion rate at week 33 (42.7 μm/yr) based on the exposed area was observed for the ECR(DuPont) specimens, followed by the ECR(Chromate)and ECR(Valspar) specimens (24.4 and 26.8 μm/yr, respectively), although these specimens showed higher corrosion rates during the first 30 weeks.

For specimens with 10 drilled holes (Figure 3.78), based on the total area, the ECR(DuPont) and ECR(Chromate) specimens reached corrosion rates as high as 0.015 and 0.14 μm/yr, respectively, at week 8, and showed similar corrosion rates, about 0.07 μm/yr, at week 31, a value that is higher than the corrosion rate of the conventional ECR specimens at the some point in time (0.05 μm/yr). The ECR(Valspar) specimens showed a lower corrosion rate during most of the test period compared to the ECR(DuPont) and ECR(Chromate), and exhibited a somewhat lower corrosion rate, 0.05 μm/yr, at week 31. Based on exposed area, the ECR(DuPont), ECR(Chromate), and ECR(Valspar) specimens showed corrosion rates of 13.6, 13.8, and 8.8 μm/yr, respectively, at week 31. Conventional ECR specimens exhibited a rate of 9.76 μm/yr at the same point in time.

For specimens with four drilled holes (Figure 3.79), the ECR(Valspar) specimens showed higher average total corrosion loss (0.06 μm based on total area and 26.4 μm based on exposed area) at week 33 than the conventional ECR specimens (0.03 μm based on total area and 12.9 μm based on exposed area). The

corrosion losses for the ECR(DuPont) (0.03 μm based on total area and 15.4 μm based on exposed area) and ECR(Chromate) specimens (0.04 μm based on total area and 19.9 μm based on exposed area) are similar to those for ECR steel. For specimens with 10 drilled holes (Figure 3.80), the total corrosion losses are 0.04, 0.03, and 0.03 μm based on total area at week 31 (8.2, 5.9, and 5.7 μm based on exposed area) for ECR(DuPont), ECR(Chromate) and ECR(Valspar), respectively, all of which are close to that exhibited by conventional ECR specimens with 10 drilled holes (0.03 μm based on total area and 6.3 μm based on exposed area).

The mat-to-mat resistance results are shown in Figure 3.81. As with the Southern Exposure specimens, the increased adhesion ECR specimens with 10 drilled holes exhibited lower resistances than those with four holes. The specimens with four drilled holes started with values of about 3,500 ohms, reaching values between 12,000 and 19,000 ohms at 31 to 33 weeks, while the specimens with 10 drilled holes started at values of about 1,700 ohms, reaching values between 8,000 ad 11,000 ohms at the same age.

The average corrosion potentials of the top and bottom mats with respect to a copper copper-sulfate electrode are shown in Figures 3.82 and 3.83. For the top mat, all specimens exhibited corrosion potentials more negative than −0.400 V, indicating that the bars are undergoing active corrosion. For the bottom mat, all specimens, except conventional and conventional epoxy-coated steel, exhibited corrosion potentials more positive than −0.250 V through 33 weeks, indicating that chlorides have not yet reached the bottom layers of steel.

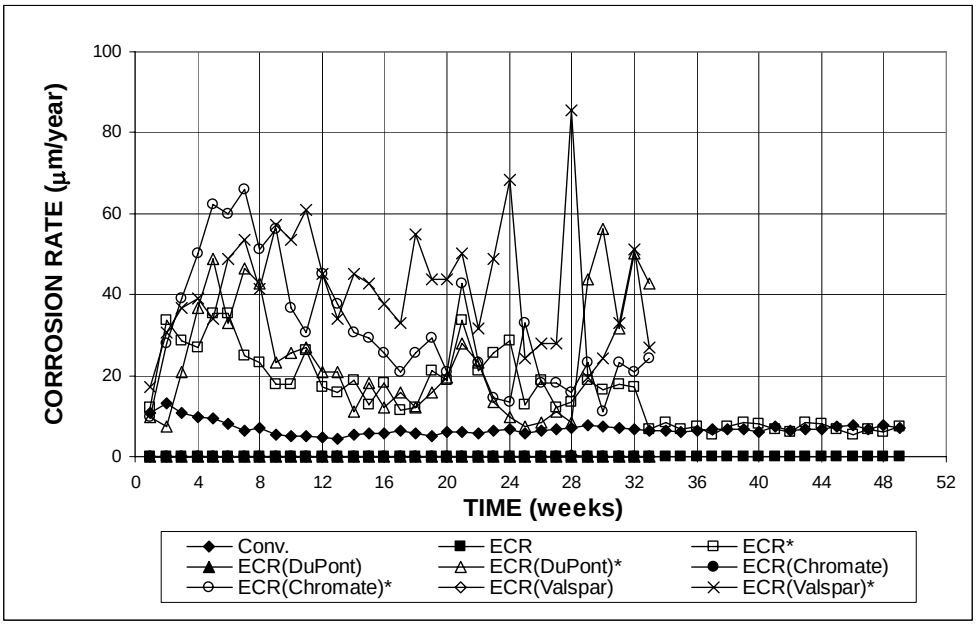

Figure 3.77 (a) – Cracked Beam Tests. Average Corrosion Rate. Specimens of conventional, epoxy-coated, and increased adhesion ECR steel ponded with 15% NaCl solution. All epoxy-coated specimens with four drilled holes. Refer to Table 3.7 for specimen identification.

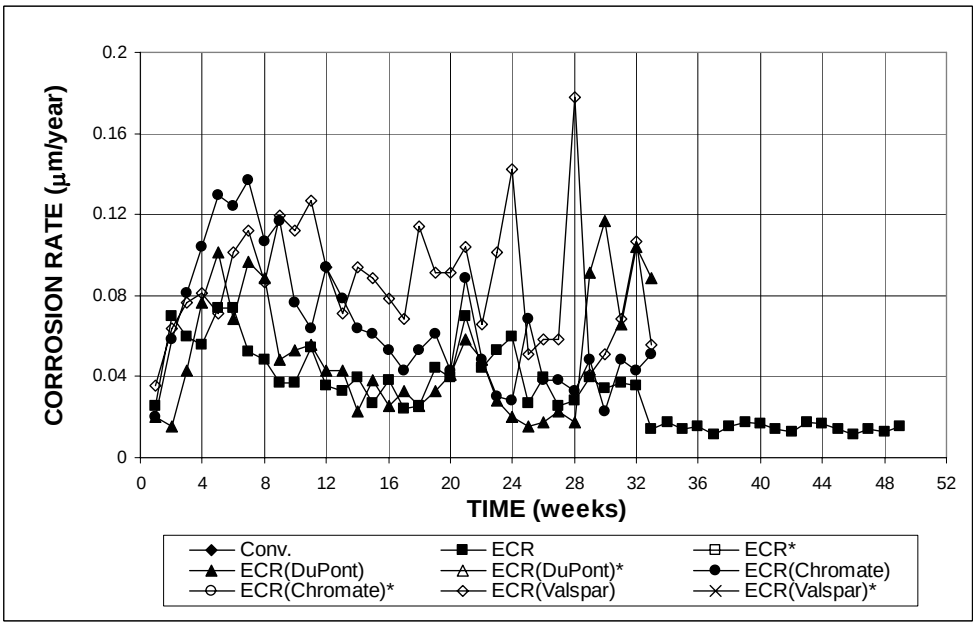

Figure 3.77 (b) – Cracked Beam Tests. Average Corrosion Rate. Specimens of conventional, epoxy-coated, and increased adhesion ECR steel ponded with 15% NaCl solution. All epoxy-coated specimens with four drilled holes. Refer to Table 3.7 for specimen identification.

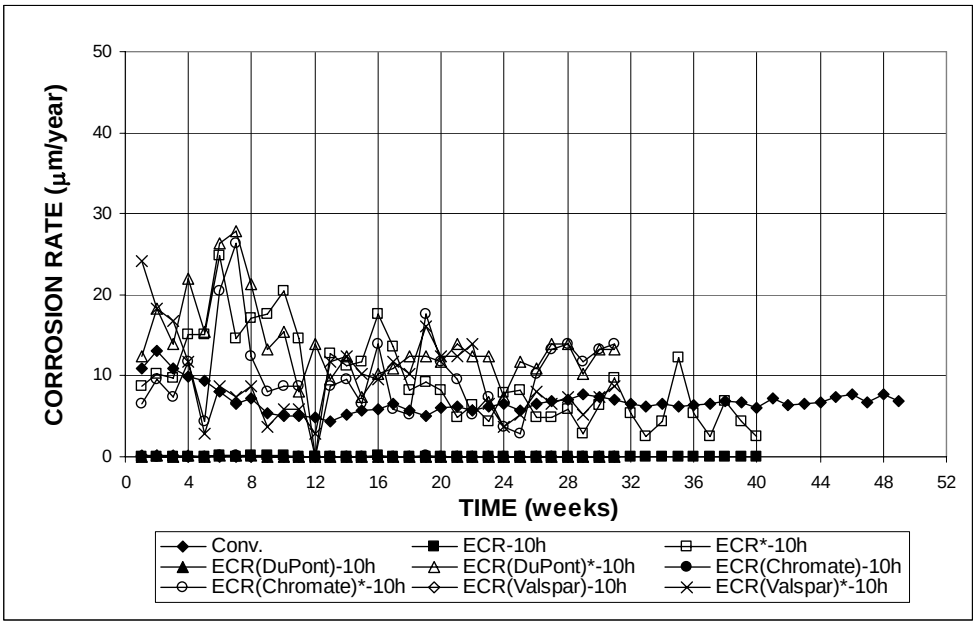

Figure 3.78 (a) – Cracked Beam Tests. Average Corrosion Rate. Specimens of conventional, epoxy-coated, and increased adhesion ECR steel ponded with 15% NaCl solution. All epoxy-coated specimens with 10 drilled holes. Refer to Table 3.7 for specimen identification.

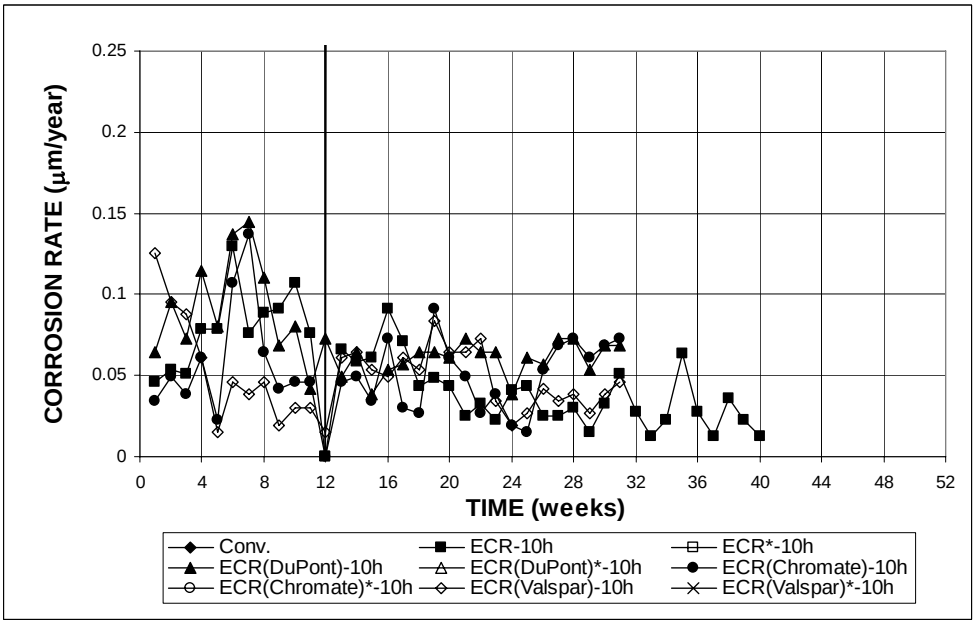

Figure 3.78 (b) – Cracked Beam Tests. Average Corrosion Rate. Specimens of conventional, epoxy-coated, and increased adhesion ECR steel ponded with 15% NaCl solution. All epoxy-coated specimens with 10 drilled holes. Refer to Table 3.7 for specimen identification.

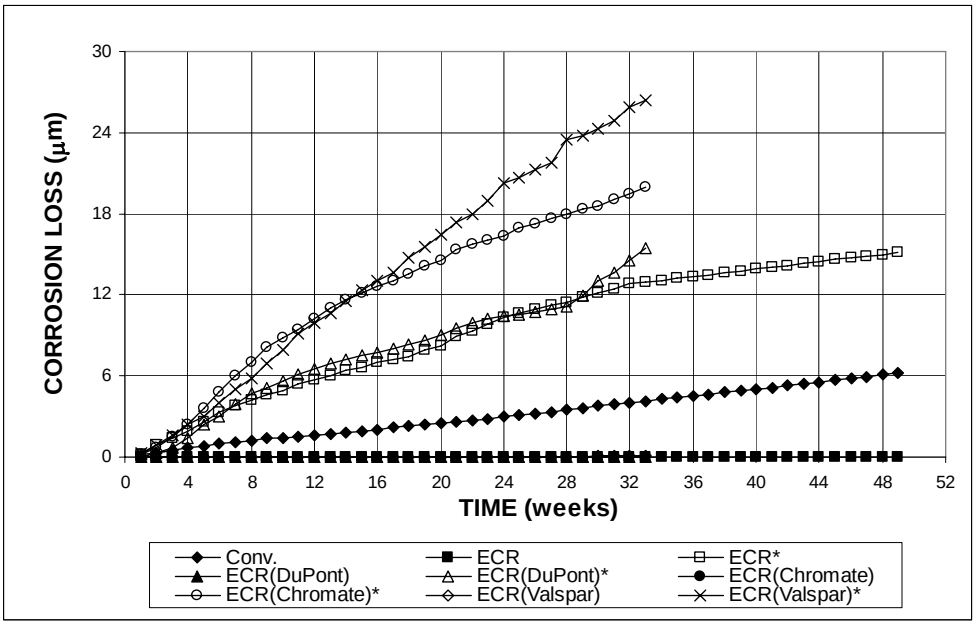

Figure 3.79 (a) – Cracked Beam Tests. Total Corrosion Loss. Specimens of conventional, epoxy-coated, and increased adhesion ECR steel ponded with 15% NaCl solution. All epoxy-coated specimens with four drilled holes. Refer to Table 3.7 for specimen identification.

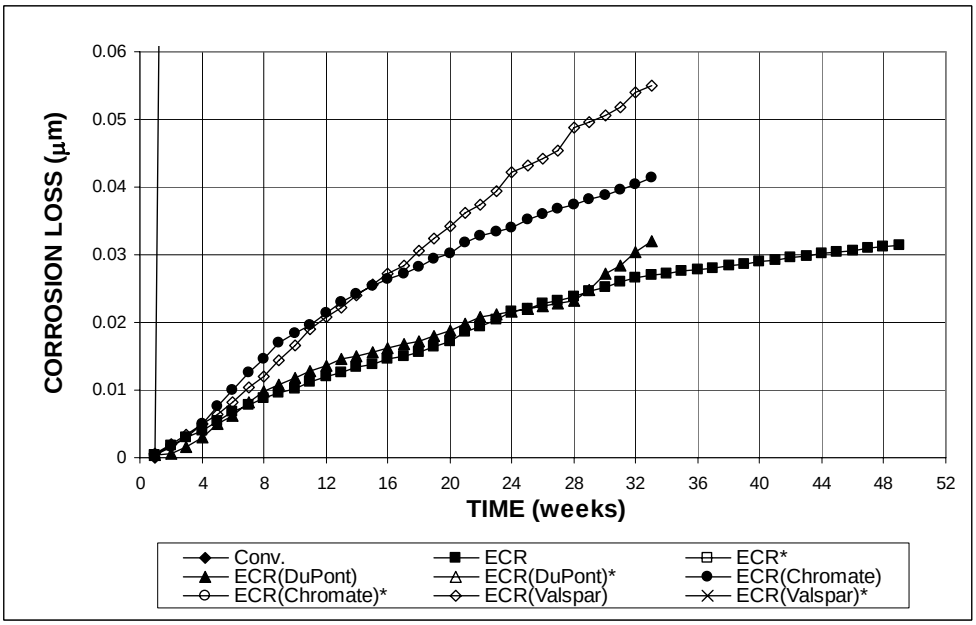

Figure 3.79 (b) – Cracked Beam Tests. Total Corrosion Loss. Specimens of conventional, epoxy-coated, and increased adhesion ECR steel ponded with 15% NaCl solution. All epoxy-coated specimens with four drilled holes. Refer to Table 3.7 for specimen identification.

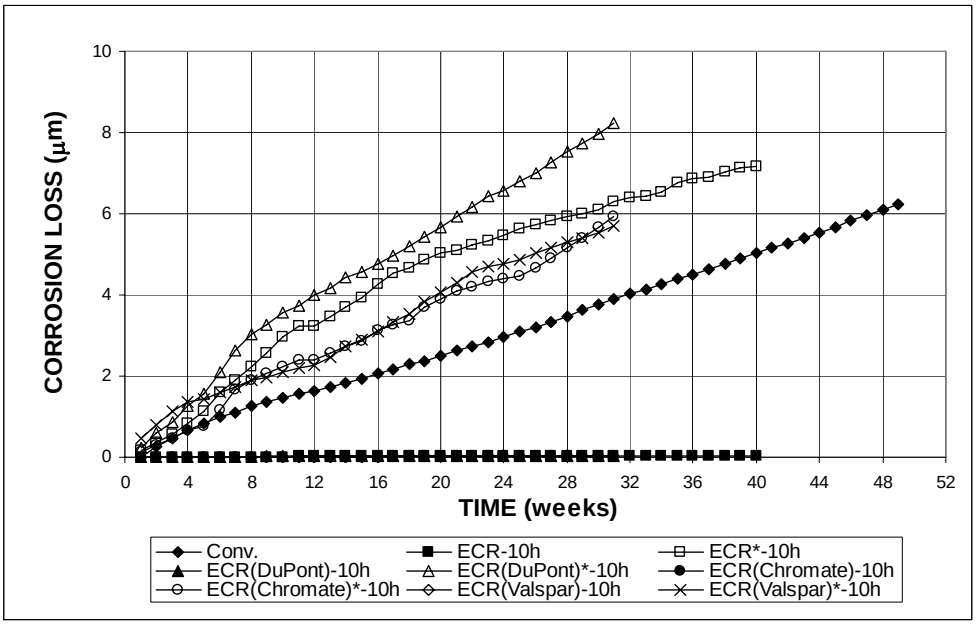

Figure 3.80 (a) – Cracked Beam Tests. Total Corrosion Loss. Specimens of conventional, epoxy-coated, and increased adhesion ECR steel ponded with 15% NaCl solution. All epoxy-coated specimens with 10 drilled holes. Refer to Table 3.7 for specimen identification.

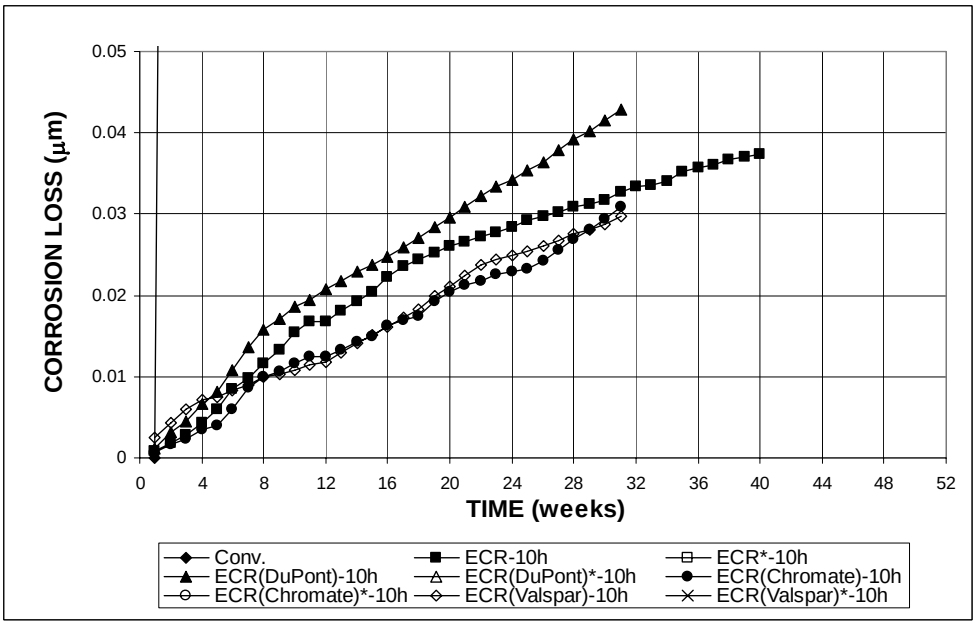

Figure 3.80 (b) – Cracked Beam Tests. Total Corrosion Loss. Specimens of conventional, epoxy-coated, and increased adhesion ECR steel ponded with 15% NaCl solution. All epoxy-coated specimens with 10 drilled holes. Refer to Table 3.7 for specimen identification.

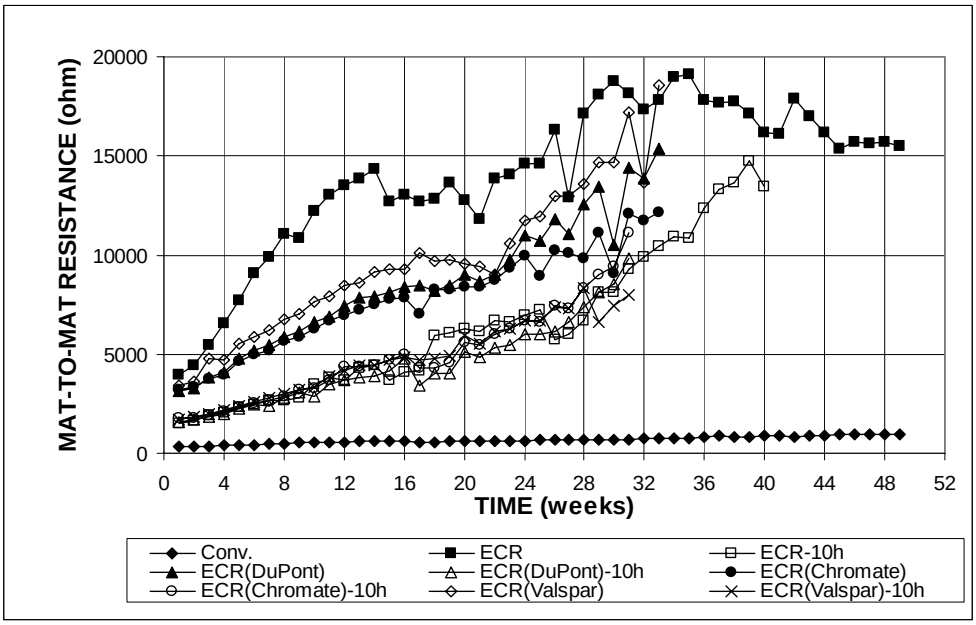

Figure 3.81 – Cracked Beam Tests. Mat-to-mat resistance. Specimens of conventional, epoxy-coated, and increased adhesion ECR steel ponded with 15% NaCl solution. Refer to Table 3.7 for specimen identification.

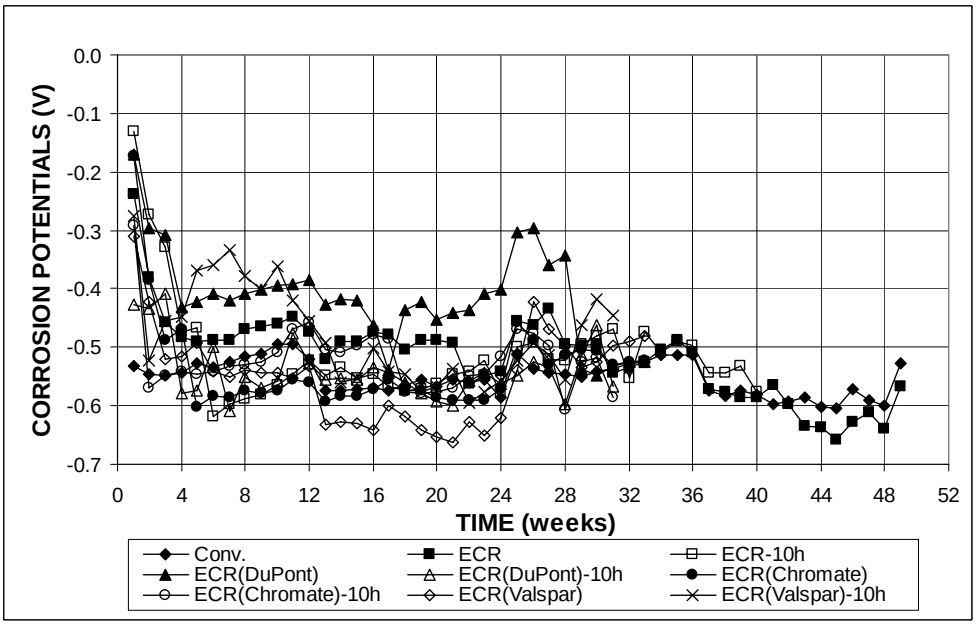

Figure 3.82 – Cracked Beam Tests. Corrosion Potential with respect to CSE at Top Mat. Specimens of conventional, epoxy-coated, and increased adhesion ECR steel ponded with 15% NaCl solution. Refer to Table 3.7 for specimen identification.

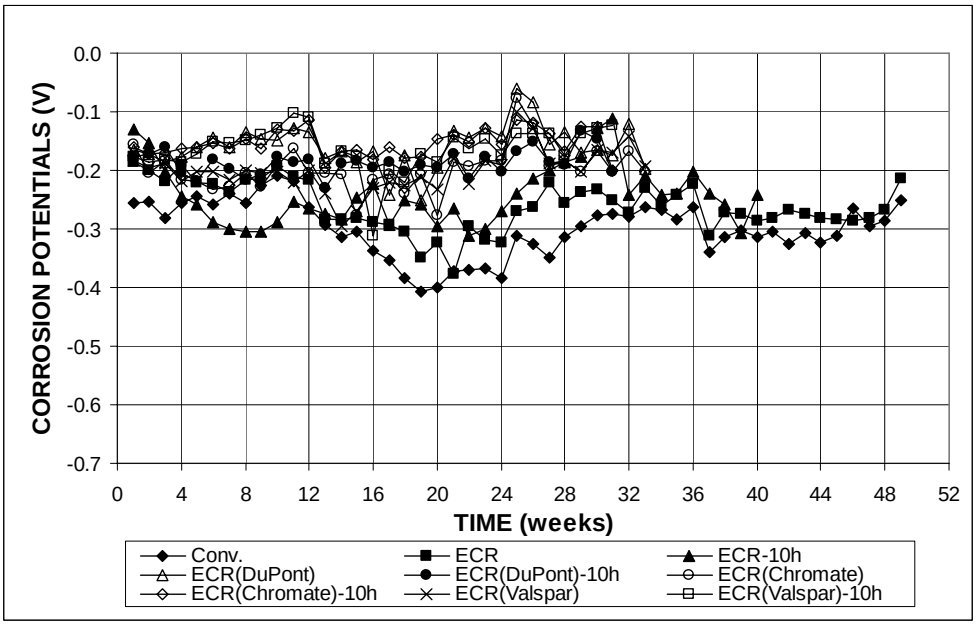

Figure 3.83 – Cracked Beam Tests. Corrosion Potential with respect to CSE at Bottom Mat. Specimens of conventional, epoxy-coated, and increased adhesion ECR steel ponded with 15% NaCl solution. Refer to Table 3.7 for specimen identification.

3.4 CORROSION INHIBITORS

This section describes the results of rapid macrocell and bench-scale tests of epoxy-coated reinforcement cast in mortar or concrete with one of three corrosion inhibitors, Rheocrete 222+, DCI-S, or Hycrete. Tests of epoxy-coated reinforcement with a primer containing calcium nitrite, ECR(primer/$Ca(NO_2)_2$), are also described in this section. In the latter case, the calcium nitrite will, in theory, leach into the concrete or mortar surrounding the bar, if the epoxy is damaged, providing corrosion protection. Obvious damage and delamination were observed on the ECR(primer/$Ca(NO_2)_2$) bars, usually at one end of a 20-foot long bar over a length of 30 to 60 cm (one to two feet). The color of the epoxy varied for different ECR(primer/$Ca(NO_2)_2$) bars. Results for the three types of increased adhesion ECR in combination of the corrosion inhibitor DCI-S, evaluated using the rapid macrocell test, are presented in Section 3.3.1.2.

3.4.1 Rapid Macrocell Tests

Mortar-wrapped specimens were used in the rapid macrocell tests. Six tests were used for ECR cast in mortar with each of the different corrosion inhibitors along with six tests of the ECR(primer/$Ca(NO_2)_2$)bars. As in the other macrocell tests of epoxy-coated reinforcement, the epoxy was penetrated with four 3.2-mm (1/8 in.) diameter drilled holes. Three mortar-wrapped tests were also performed using bars in the "as delivered" condition.

3.4.1.1 Macrocell Tests for Mortar-Wrapped Specimens

The average corrosion rates and total corrosion losses for the mortar-wrapped specimens in 1.6 m ion NaCl and simulated concrete pore solution are shown in Figures 3.84 and 3.85. Table 3.8 summarizes the average corrosion rates and corrosion losses at week 15. The results based on the total area exposed to the solution show that the specimens with a calcium nitrite primer [ECR(primer/($Ca(NO_2)_2$)] and specimens cast in mortar with no inhibitor (ECR) (Table 3.1) corroded at higher rates than the specimens cast in mortar containing a corrosion inhibitor, although the corrosion rates of ECR(primer/$Ca(NO_2)_2$) and ECR were only 0.03 and 0.02 μm/yr, respectively. Specimens cast in mortar with Rheocrete 222+ [ECR(Rheocrete)] had an average corrosion rate of 0.01 μm/year, equal to that for specimens cast in mortar with DCI-S [ECR(DCI)]. Specimens cast in mortar with Hycrete [ECR(Hycrete)] showed no corrosion rate after week 4, with a highest value of 0.01 μm/yr at week 3 and 4. Based on the exposed area, noticeable local corrosion was found on ECR, ECR(primer/$Ca(NO_2)_2$), ECR(Rheocrete), and ECR(DCI) specimens. ECR specimens had an average corrosion rate of 2.44 μm/yr (Table 3.1), which was lower than that of ECR(primer/$Ca(NO_2)_2$) (3.05 μm/yr), but

higher than ECR(Rheocrete) and ECR(DCI) (both at 1.22 μm/yr). As with the results based on the total area, no corrosion rate was detected on ECR(Hycrete) after week 4, although the rate was as high as 1.22 μm/yr at week 3 and 4.

At week 15, ECR(primer/$Ca(NO_2)_2$) showed the highest local corrosion loss, at 1.04 μm, based on the exposed area (254% of the corrosion loss for ECR), followed by ECR(Rheocrete) and ECR(DCI) at 0.23 and 0.21 μm (56% and 51% of the corrosion loss for ECR), respectively, and ECR(Hycrete) at 0.07 μm (17% of the corrosion loss for ECR) (Table 3.8 and Figure 3.85). Based on the total area, corrosion losses of less than 0.01 μm were found on all mortar-wrapped specimens. The results demonstrate that, as observed in Section 3.3.1.2 for the high adhesion bars cast in mortar-wrapped specimens with DCI, the use of the corrosion inhibitors improves the corrosion resistance of conventional epoxy-coated reinforcement. Using the epoxy-coated steel with a primer containing calcium nitrite, however, does not provide any advantage.

The average corrosion potentials of the anodes and cathodes are shown in Figures 3.86 and 3.87, respectively. All of the epoxy-coated bars exhibited anodic potentials equal to or more positive than −0.275 V after week 6, with the exception of the ECR(primer/$Ca(NO_2)_2$) anodes which had an average potential around −0.400 V for the weeks 7 through 15, indicating that the ECR(primer/$Ca(NO_2)_2$) specimens were the only ECR specimens with an inhibitor corroding during the test period. The ECR(primer/$Ca(NO_2)_2$) cathodes were also the only cathodes among the epoxy-coated specimens in this group that showed an average potential (−0.300 V) more negative than −0.275 V, indicating active corrosion.

The corrosion rates and corrosion losses for specimens tested in the “as delivered” condition are shown in Figures 3.88 and 3.89 and Table 3.8. Only

insignificant corrosion was observed on any of these epoxy-coated specimens at week 15.

Table 3.8 – Average corrosion and total corrosion losses for epoxy-coated steel with corrosion inhibitors as measured in the macrocell test

CORROSION RATE AT WEEK 15 (μm/year)

Steel Designation	Specimen						Average	Std. Deviation
	1	2	3	4	5	6		
Mortar-wrapped specimens								
ECR(Rheocrete)	0.04	0	0	0	0	0.04	0.01	0.02
ECR(Rheocrete)*	3.66	0	0	0	0	3.66	1.22	1.89
ECR(Rheocrete)-nh	0	0	0	-	-	-	0	-
ECR(DCI)	0.07	0	0	0	0	0	0.01	0.03
ECR(DCI)*	7.32	0	0	0	0	0	1.22	2.99
ECR(DCI)-nh	0	0	0	-	-	-	0	0
ECR(Hycrete)	0	0	0	0	0	0	0	-
ECR(Hycrete)*	0	0	0	0	0	0	0	-
ECR(Hycrete)-nh	0	0	0	-	-	-	0	-
ECR(primer/$Ca(NO_2)_2$	0.04	0	0	0	0.11	0.04	0.03	0.04
ECR(primer/$Ca(NO_2)_2$*	3.66	0	0	0	10.98	3.66	3.05	4.28
ECR(primer/$Ca(NO_2)_2$-nh	0	0	0	-	-	-	0	-

TOTAL CORROSION LOSS AFTER WEEK 15 (μm)

Steel Designation	Specimen						Average	Std. Deviation
	1	2	3	4	5	6		
Mortar-wrapped specimens								
ECR(Rheocrete)	β	β	β	β	0	β	β	-
ECR(Rheocrete)*	0.49	0.42	0.07	0.14	0	0.28	0.23	0.20
ECR(Rheocrete)-nh	β	0	0	-	-	-	β	0
ECR(DCI)	0.01	0	β	0	0	β	β	-
ECR(DCI)*	1.13	0	0.07	0	0	0.07	0.21	0.45
ECR(DCI)-nh	β	0	0	-	-	-	β	-
ECR(Hycrete)	0	β	0	β	β	0	β	-
ECR(Hycrete)*	0	0.07	0	0.28	0.07	0	0.07	0.11
ECR(Hycrete)-nh	0	β	β	-	-	-	β	-
ECR(primer/$Ca(NO_2)_2$	β	0.01	β	0	0.02	0.03	0.01	0.01
ECR(primer/$Ca(NO_2)_2$*	0.07	1.06	0.14	0	2.18	2.82	1.04	1.21
ECR(primer/$Ca(NO_2)_2$-nh	β	β	0	-	-	-	β	-

[1] ECR(Rheocrete): Epoxy-coated steel cast with Rheocrete , based on total area of bar exposed to solution

[2] ECR(Rheocrete)*: Epoxy-coated steel cast with Rheocrete, based on exposed area of four 3.2-mm (1/8-in.) diameter holes in epoxy

[3] ECR(Rheocre)-nh: Epoxy-coated steel cast with Rheocrete and without any drilled holes

[4] ECR(DCI): Epoxy-coated steel cast with DCI, based on total area of bar exposed to solution

[5] ECR(DCI)*: Epoxy-coated steel with DCI, based on exposed area of four 3.2-mm (1/8-in.) diameter holes in epoxy

[6] ECR(DCI)-nh: Epoxy-coated steel cast with DCI and without any drilled holes

[7] ECR(Hycrete): Epoxy-coated steel cast with Hycrete, based on total area of bar exposed to solution

[8] ECR(Hycrete)*: Epoxy-coated steel with Hycrete, based on exposed area of four 3.2-mm (1/8-in.) diameter holes in epoxy

[9] ECR(Hycrete)-nh: Epoxy-coated steel cast with Hycrete and without any drilled holes

[10] ECR(primer/$Ca(NO_2)_2$: Epoxy-coated steel with a calcium nitrite primer , based on total area of bar exposed to solutio

[11] ECR(primer/$Ca(NO_2)_2$ *: Epoxy-coated steel with a calcium nitrite primer, based on exposed area of four 3.2-mm (1/8-in.) diameter holes in epoxy

[12] ECR(primer/$Ca(NO_2)_2$ -nh: Epoxy-coated steel with a calcium nitrite primer and without any drilled holes

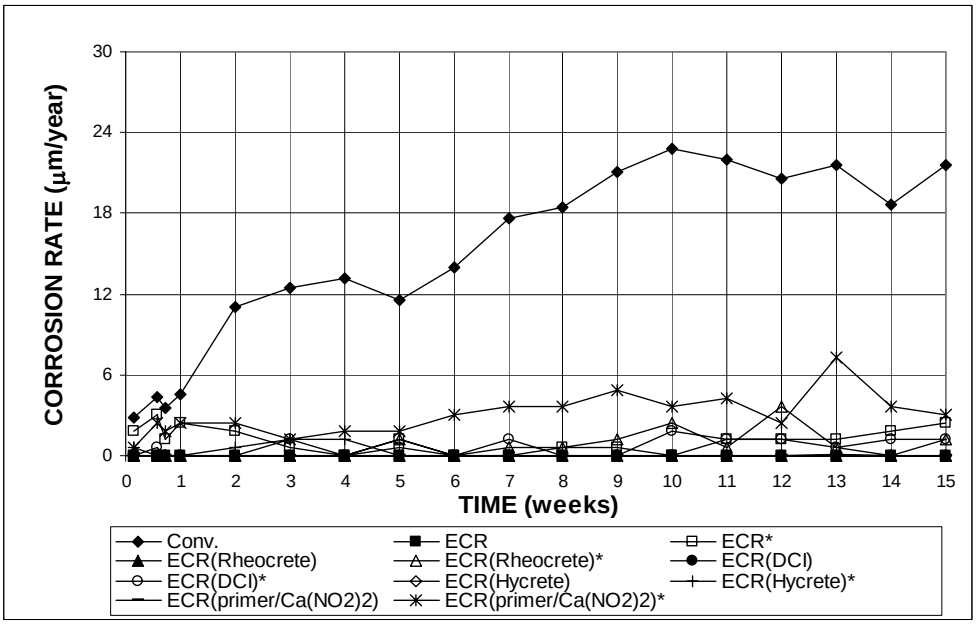

Figure 3.84 (a) – Macrocell Test. Average Corrosion Rate. Mortar-wrapped specimens of conventional and epoxy-coated steel, epoxy-coated steel cast with corrosion inhibitors, and epoxy-coated steel with a calcium nitrite primer in simulated concrete pore solution with 1.6 m ion NaCl. Refer to Table 3.8 for specimen identification.

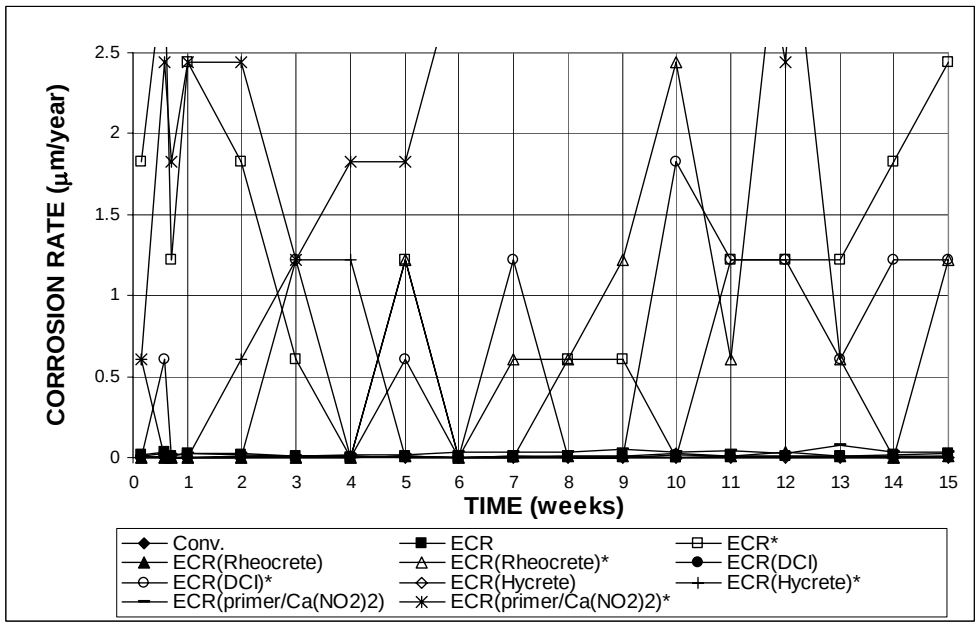

Figure 3.84 (b) – Macrocell Test. Average Corrosion Rate. Mortar-wrapped specimens of conventional and epoxy-coated steel, epoxy-coated steel cast with corrosion inhibitors, and epoxy-coated steel with a calcium nitrite primer in simulated concrete pore solution with 1.6 m ion NaCl. Refer to Table 3.8 for specimen identification.

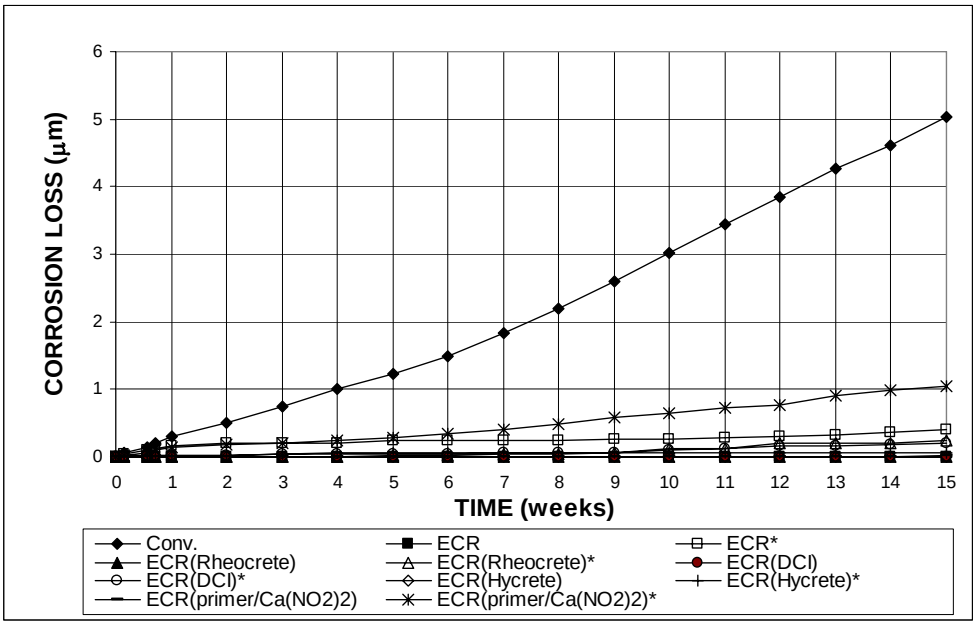

Figure 3.85 (a) – Macrocell Test. Total Corrosion Losses. Mortar-wrapped specimens of conventional and epoxy-coated steel, epoxy-coated steel cast with corrosion inhibitors, and epoxy-coated steel with a calcium nitrite primer in simulated concrete pore solution with 1.6 m ion NaCl. Refer to Table 3.8 for specimen identification.

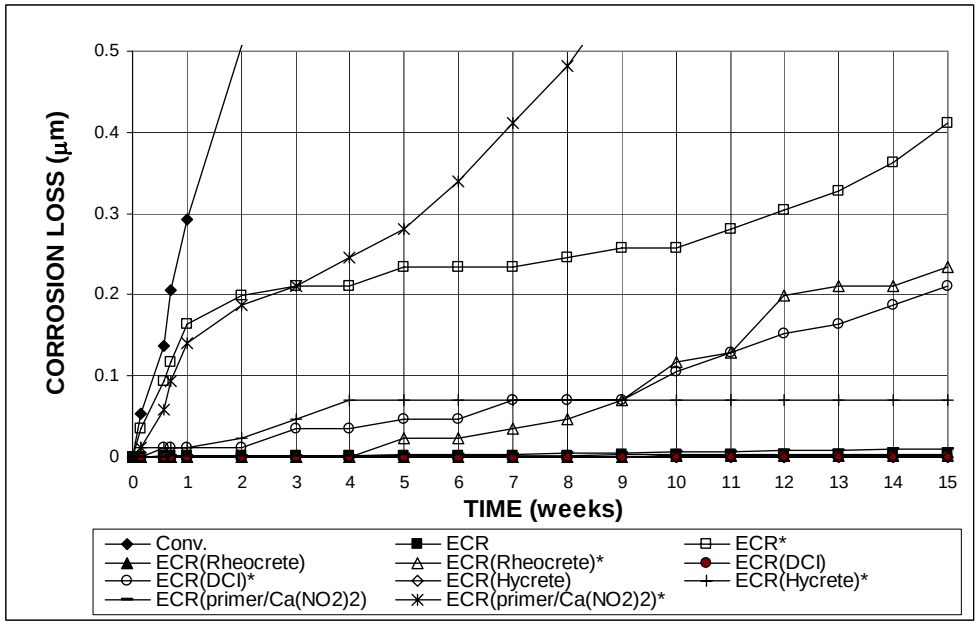

Figure 3.85 (b) – Macrocell Test. Total Corrosion Losses. Mortar-wrapped specimens of conventional and epoxy-coated steel, epoxy-coated steel cast with corrosion inhibitors, and epoxy-coated steel with a calcium nitrite primer in simulated concrete pore solution with 1.6 m ion NaCl. Refer to Table 3.8 for specimen identification.

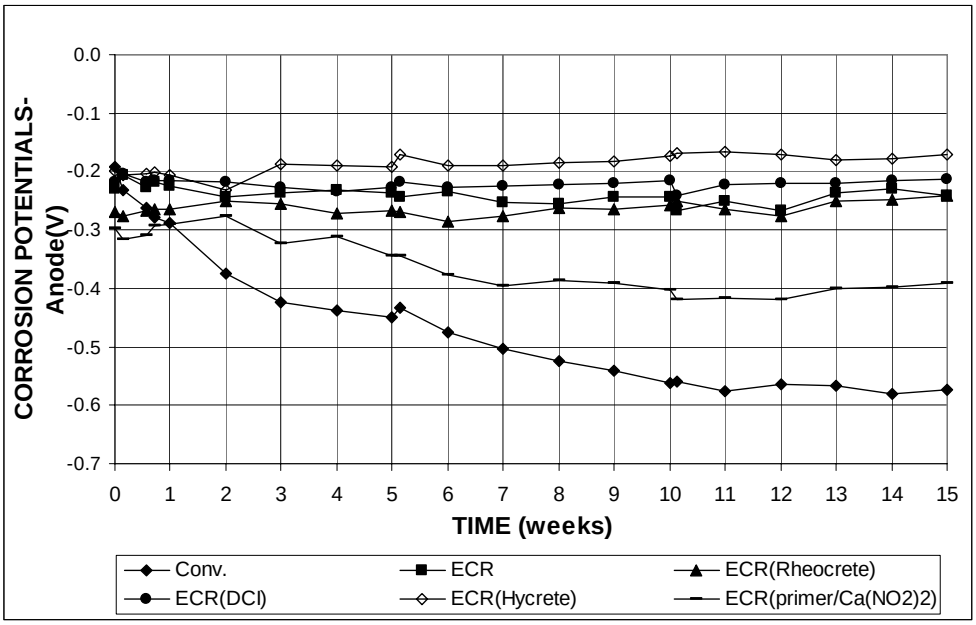

Figure 3.86 - Macrocell Tests. Average Corrosion Potential with respect to SCE at Anode. Mortar-wrapped specimens of conventional and epoxy-coated steel, epoxy-coated steel cast with corrosion inhibitors, and epoxy-coated steel with a calcium nitrite primer in simulated concrete pore solution with 1.6 m ion NaCl. Refer to Table 3.8 for specimen identification.

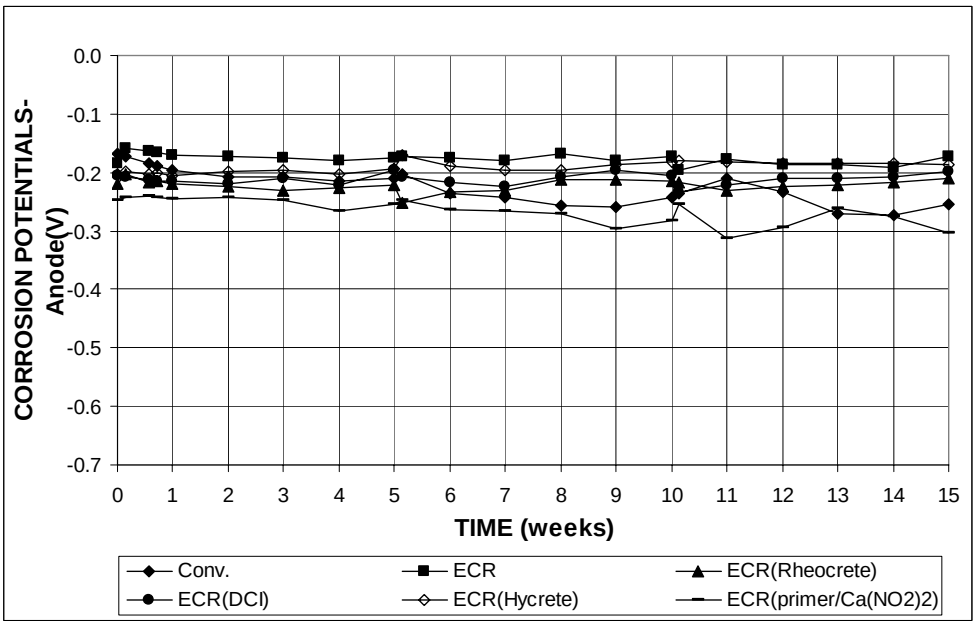

Figure 3.87 - Macrocell Tests. Average Corrosion Potential with respect to SCE at Anode. Mortar-wrapped specimens of conventional and epoxy-coated steel, epoxy-coated steel cast with corrosion inhibitors, and epoxy-coated steel with a calcium nitrite primer in simulated concrete pore solution with 1.6 m ion NaCl. Refer to Table 3.8 for specimen identification.

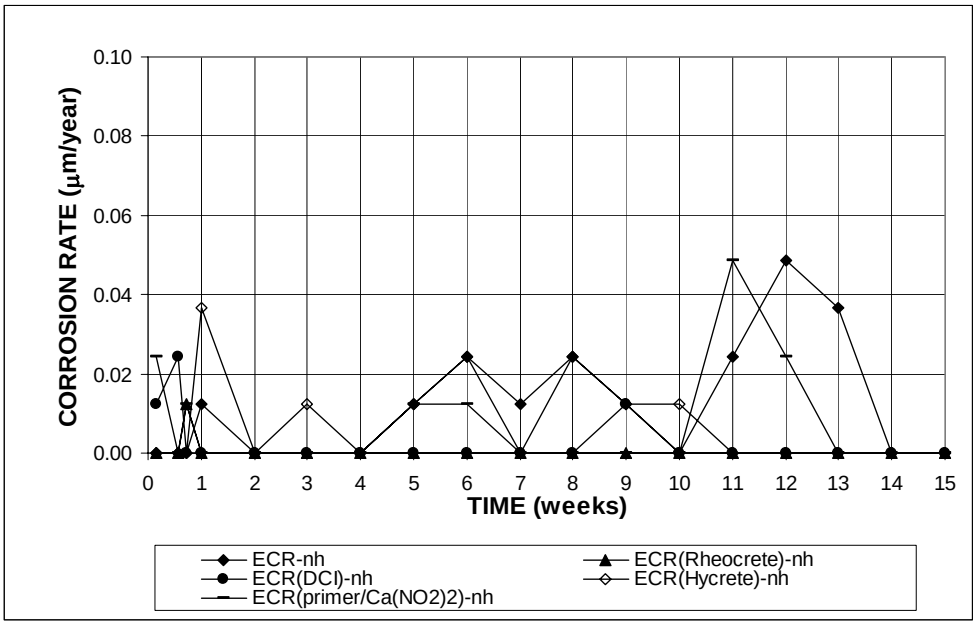

Figure 3.88 – Macrocell Test. Average Corrosion Rate. Mortar-wrapped specimens of conventional and epoxy-coated steel, epoxy-coated steel cast with corrosion inhibitors, and epoxy-coated steel with a calcium nitrite primer in simulated concrete pore solution with 1.6 m ion NaCl. Refer to Table 3.8 for specimen identification.

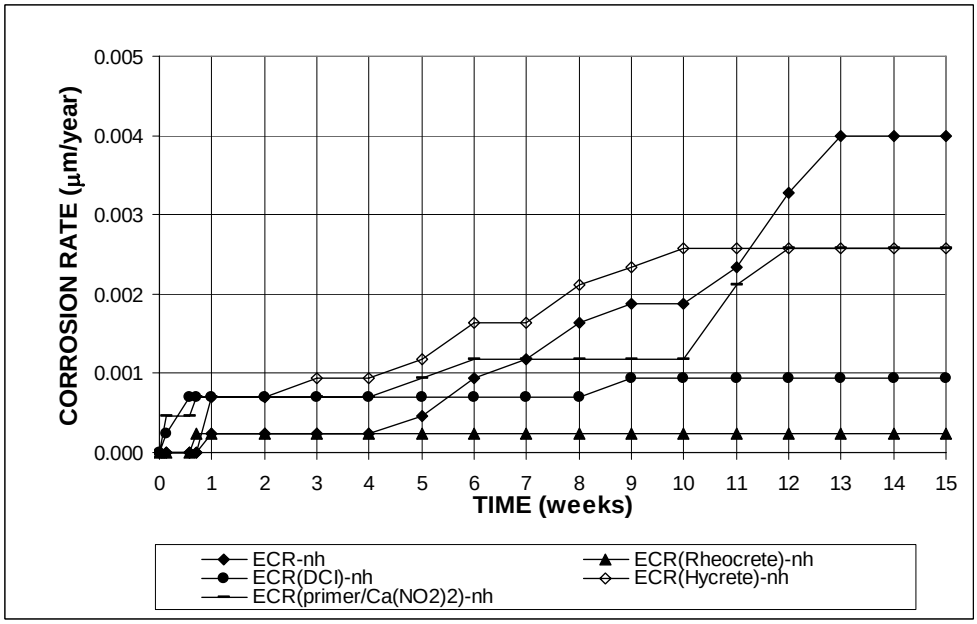

Figure 3.89 – Macrocell Test. Total Corrosion Loss. Mortar-wrapped specimens of conventional and epoxy-coated steel, epoxy-coated steel cast with corrosion inhibitors, and epoxy-coated steel with a calcium nitrite primer in simulated concrete pore solution with 1.6 m ion NaCl. Refer to Table 3.8 for specimen identification.

3.4.1.2 Visual Inspection

As the tests were discontinued, the ECR specimens cast in mortar with one of the three corrosion inhibitors were broken and visually inspected. No corrosion products were found under the mortar for all bars, as with the observation on the conventional ECR specimens without a corrosion inhibitor, as presented in Section 3.1.1.3, and the increased adhesion ECR specimens with the corrosion inhibitor DCI-S, as presented in Section 3.3.1.3.

3.4.2 Bench-Scale Tests

The average corrosion rates and total corrosion losses as of March 15, 2005 for the Southern Exposure and cracked beam tests are summarized in Tables 3.9 and 3.10. Results for individual specimens are presented in Appendix A.

3.4.2.1 Southern Exposure Tests

The Southern Exposure tests include three tests each for ECR(Rheocrete), ECR(DCI), ECR(Hycrete), and ECR(primer/$Ca(NO_2)_2$) with four drilled holes and a *w/c* ratio of 0.45 and with 10 drilled holes and *w/c* ratios of 0.35 and 0.45. Average corrosion rates, total corrosion losses, mat-to-mat resistances, and corrosion potentials are shown in Figures 3.90 to 3.104.

For the specimens with four drilled holes (Figure 3.90), no corrosion with a rate of more than 0.01 μm/yr was observed based on total area during the test period at ages ranging from 23 to 30 weeks. However, noticeable local corrosion rates, as high as 1.22, 8.5, 1.22, and 10.98 μm/yr, based on the exposed area were measured for the ECR(Rheocrete), ECR(DCI), ECR(Hycrete), and ECR(primer/$Ca(NO_2)_2$) specimens, respectively. As of March 15, 2005, corrosion rates of 1.22, 1.22, and 0.06 μm/yr based on the exposed area were obtained for the ECR(Rheocrete), ECR(DCI), and

ECR(primer/$Ca(NO_2)_2$) bars, respectively. No corrosion was observed on the ECR(Hycrete) and conventional ECR specimens at the same point in time.

For specimens with 10 drilled holes at *w/c* ratios of 0.35 and 0.45 (Figures 3.91 and 3.92), insignificant corrosion, with a rate less than 0.01 μm/yr, was found on all specimens based on the total area, while observable corrosion was exhibited by the ECR(DCI), ECR(Hycrete) and ECR(primer/$Ca(NO_2)_2$ specimens based on the exposed area. At a *w/c* ratio of 0.35, the corrosion rates were measured at 0.24 and 0.73 μm/yr for the ECR(DCI) and ECR(Hycrete) specimens at week 21, respectively, and 0.73 μm/yr for ECR(primer/$Ca(NO_2)_2$ bars at week 18. At a *w/c* ratio of 0.45, the same corrosion rates were measured for the ECR(DCI) and ECR(Hycrete) specimens at 0.24 μm/yr at week 27 and 25, respectively. The ECR(primer/$Ca(NO_2)_2$ specimens exhibited a corrosion rate of just 0.02 μm/yr at week 30, although the rate was as high as 3.05 μm/yr at day 1 and 2.17 μm/yr at week 27. For the ECR(Rheocrete) specimens, the corrosion rates were as high as 2.9 and 1.8 μm/yr for *w/c* ratios of 0.35 and 0.45, respectively, but dropped to 0 at week 23. The corrosion rates of all specimens with corrosion inhibitors are lower or equal to that of the conventional ECR specimens at the same points in time.

The average corrosion losses versus time are shown in Figures 3.93 to 3.95. Based on the total area, all specimens with four (Figure 3.93) and 10 drilled holes (Figure 3.94) exhibited corrosion losses below 0.01 μm. Based on the exposed area, noticeable corrosion losses were found on all specimens with corrosion inhibitors. Generally, the same type of specimens with a *w/c* ratio of 0.35 had less corrosion loss than the specimens with a *w/c* ratio of 0.45. For the specimens with four drilled holes, the conventional ECR specimens exhibited the highest corrosion loss, at 2.04 μm, followed by the ECR(DCI) (0.62 μm), ECR(primer/$Ca(NO_2)_2$) (0.55 μm),

ECR(Rheocrete) (0.18 μm), and ECR(Hycrete) (0.15 μm) at the same point in time (21 weeks), as shown in Figure 3.93. For the specimens with 10 drilled holes and a *w/c* ratio of 0.45, the corrosion losses of all ECR specimens with a corrosion inhibitor were less than 0.2 μm, with the exception of the ECR(Rheocrete) specimens with 10 holes and a *w/c* ratio of 0.45, which had a corrosion loss of 0.36 μm at week 23, a value that is still lower than that of the conventional ECR specimens (0.9 μm) (Figure 3.94). For the specimens with 10 drilled holes and a *w/c* ratio of 0.35, the corrosion losses of all ECR specimens with a corrosion inhibitor were less or equal to 0.16 μm (Figure 3.95).

Mat-to-mat resistance results are shown in Figures 3.96-3.98. The ECR specimens with corrosion inhibitors drilled with four drilled holes (Figure 3.96) started with values of approximately 2,000 ohms and increased to average mat-to-mat resistances between 4,000 and 8,000 ohms. The specimens with 10 drilled holes at *w/c* ratios of 0.45 (Figure 3.97) or 0.35 (Figure 3.98) exhibited lower resistances that were about 1,000 ohms at the beginning, increasing with time at a similar rate to values close to 4,000 ohms. No obvious differences in mat-to-mat resistances were observed between the ECR specimens with and without corrosion inhibitors.

The average corrosion potentials of the top and bottom mats with respect to a copper copper-sulfate electrode are shown in Figures 3.99 to 3.104. For the top mat, the ECR specimens cast in concrete with corrosion inhibitors exhibited corrosion potentials more positive than −0.300 V, except for the ECR(Rheocrete) specimens with 10 drilled holes and a *w/c* ratio of 0.45, which exhibited a more negative average potential of −0.328 V at week 23, indicating a slight tendency to corrode (Figure 3.100). The potentials of ECR(Rheocrete) and ECR(primer/$Ca(NO_2)_2$) anodes with ten drilled holes and *w/c* ratios of 0.35 and 0.45, respectively, were as low as −0.280

V and −0.308 V at week 17 and 18, but jumped above −0.250 V after that. For the bottom mat, the corrosion potential of ECR(primer/$Ca(NO_2)_2$) with 10 drilled holes at a *w/c* ratio of 0.45 dropped to a value more negative than −0.250 V at week 17 but increased above −0.200 V after week 24. All other specimens, except for the conventional steel and conventional ECR bars with 10 drilled holes at a *w/c* ratio of 0.45, exhibited stable corrosion potentials more positive than −0.200 V.

Table 3.9 – Average corrosion rates for epoxy-coated steel cast with corrosion inhibitors measured in the bench-scale

CORROSION RATE (μm/year)

Steel Designation	Exposure Time (weeks)	Specimen 1	Specimen 2	Specimen 3	Average	Std. Deviation
Southern Exposure Specimens						
ECR(Rheocrete)	23	α	α	0	α	-
ECR(Rheocrete)*	23	1.83	1.83	0	1.22	1.06
ECR(Rheocrete)-10h	23	0	0	0	0	-
ECR(Rheocrete)*-10h	23	0	0	0	0	-
ECR(Rheocrete)-10h-35	18	0	0	0	0	-
ECR(Rheocrete)*-10h-35	18	0	0	0	0	-
ECR(DCI)	27	0	0	0	0	-
ECR(DCI)*	27	0	0	0	0	-
ECR(DCI)-10h	27	α	0	0	α	-
ECR(DCI)*-10h	27	0.73	0	0	0.24	0.42
ECR(DCI)-10h-35	21	0	0	α	α	-
ECR(DCI)*-10h-35	21	0	0	0.73	0.24	0.42
ECR(Hycrete)	25	0	0	0	0	-
ECR(Hycrete)*	25	0	0	0	0	-
ECR(Hycrete)-10h	25	0	0	α	α	-
ECR(Hycrete)*-10h	25	0	0	0.73	0.24	0.42
ECR(Hycrete)-10h-35	21	0	α	α	α	-
ECR(Hycrete)*-10h-35	21	0	1.46	0.73	0.73	0.73
ECR(primer/$Ca(NO_2)_2$	30	0	α	0	α	-
ECR(primer/$Ca(NO_2)_2$*	30	0	0.18	0	0.06	0.11
ECR(primer/$Ca(NO_2)_2$-10h	30	α	0	0	α	-
ECR(primer/$Ca(NO_2)_2$*-10h	30	0.07	0	0	0.02	0.04
ECR(primer/$Ca(NO_2)_2$-10h-35	18	0.01	0	0	α	0.01
ECR(primer/$Ca(NO_2)_2$*-10h-35	18	2.20	0	0	0.73	1.27
Cracked Beam Specimens						
ECR(Rheocrete)	23	0.08	0.18	0.04	0.10	0.08
ECR(Rheocrete)*	23	36.6	87.84	18.3	47.58	36.05
ECR(Rheocrete)-10h	23	0.20	0.11	0.02	0.11	0.09
ECR(Rheocrete)*-10h	23	38.06	21.96	2.93	20.98	17.59
ECR(Rheocrete)-10h-35	18	0.08	0.29	0.08	0.15	0.12
ECR(Rheocrete)*-10h-35	18	14.64	55.63	14.64	28.30	23.67
ECR(DCI)	27	0.02	0.02	0	0.01	0.01
ECR(DCI)*	27	7.32	7.32	0	4.88	4.23
ECR(DCI)-10h	27	α	0	0.05	0.02	0.02
ECR(DCI)*-10h	27	1.46	0	8.78	3.42	4.71
ECR(DCI)-10h-35	21	0.09	0	0.47	0.19	0.25
ECR(DCI)*-10h-35	21	17.57	0	90.77	36.11	48.14
ECR(Hycrete)	25	α	0.02	0.09	0.04	0.04
ECR(Hycrete)*	25	3.66	10.98	43.92	19.52	21.45
ECR(Hycrete)-10h	25	0	0.05	0.03	0.03	0.03
ECR(Hycrete)*-10h	25	0	10.25	5.86	5.37	5.14
ECR(Hycrete)-10h-35	21	0.18	0.14	0.49	0.27	0.19
ECR(Hycrete)*-10h-35	21	35.14	27.82	93.7	52.22	36.11
ECR(primer/$Ca(NO_2)_2$	30	0.05	α	0.04	0.03	0.02
ECR(primer/$Ca(NO_2)_2$*	30	25.62	3.66	18.3	15.86	11.18
ECR(primer/$Ca(NO_2)_2$-10h	30	0.09	0.05	0.07	0.07	0.02
ECR(primer/$Ca(NO_2)_2$*-10h	30	17.71	9.96	12.88	13.52	3.92
ECR(primer/$Ca(NO_2)_2$-10h-35	18	0.26	0.05	0.25	0.19	0.12
ECR(primer/$Ca(NO_2)_2$*-10h-35	18	49.78	10.25	48.31	36.11	22.41

Table 3.10 – Total corrosion losses for epoxy-coated steel cast with corrosion inhibitors measured in the bench-scale tests

CORROSION LOSS (μm)

Steel Designation	Exposure Time (weeks)	Specimen 1	Specimen 2	Specimen 3	Average	Std. Deviation
Southern Exposure Specimens						
ECR(Rheocrete)	23	β	β	β	β	-
ECR(Rheocrete)*	23	0.11	0.35	0.07	0.18	0.15
ECR(Rheocrete)-10h	23	β	β	β	β	-
ECR(Rheocrete)*-10h	23	0.1	0.34	0.65	0.36	0.28
ECR(Rheocrete)-10h-35	18	β	β	β	β	-
ECR(Rheocrete)*-10h-35	18	0.17	0.13	0.18	0.16	0.03
ECR(DCI)	27	β	β	0	β	-
ECR(DCI)*	27	0.88	0.95	0.21	0.68	0.41
ECR(DCI)-10h	27	β	β	β	β	-
ECR(DCI)*-10h	27	0.18	0.11	0.08	0.13	0.05
ECR(DCI)-10h-35	21	β	0	β	β	-
ECR(DCI)*-10h-35	21	0.01	0	0.07	0.03	0.04
ECR(Hycrete)	25	0	β	β	β	-
ECR(Hycrete)*	25	0	0.39	0.07	0.15	0.21
ECR(Hycrete)-10h	25	β	0	β	β	-
ECR(Hycrete)*-10h	25	0.06	0	0.35	0.14	0.19
ECR(Hycrete)-10h-35	21	β	β	β	β	-
ECR(Hycrete)*-10h-35	21	0.01	0.23	0.13	0.12	0.11
ECR(primer/$Ca(NO_2)_2$	30	β	β	β	β	-
ECR(primer/$Ca(NO_2)_2$*	30	0.92	0.16	0.88	0.65	0.43
ECR(primer/$Ca(NO_2)_2$-10h	30	β	β	β	β	-
ECR(primer/$Ca(NO_2)_2$*-10h	30	0.21	0.06	0.31	0.19	0.13
ECR(primer/$Ca(NO_2)_2$-10h-35	18	β	β	β	β	-
ECR(primer/$Ca(NO_2)_2$*-10h-35	18	0.27	0.08	0.06	0.14	0.11
Cracked Beam Specimens						
ECR(Rheocrete)	23	0.01	0.01	0.01	0.01	-
ECR(Rheocrete)*	23	6.90	6.05	6.26	6.41	0.44
ECR(Rheocrete)-10h	23	0.03	0.05	0.05	0.04	0.01
ECR(Rheocrete)*-10h	23	5.83	9.35	9.74	8.31	2.15
ECR(Rheocrete)-10h-35	18	0.03	0.06	0.02	0.04	0.02
ECR(Rheocrete)*-10h-35	18	5.01	12.16	3.15	6.78	4.76
ECR(DCI)	27	0.01	0.01	β	β	0.01
ECR(DCI)*	27	6.05	5.07	0.99	4.04	2.69
ECR(DCI)-10h	27	0.02	0.01	0.02	0.02	0.01
ECR(DCI)*-10h	27	4.00	2.34	4.42	3.58	1.10
ECR(DCI)-10h-35	21	0.04	0.02	0.20	0.09	0.10
ECR(DCI)*-10h-35	21	7.63	3.21	38.51	16.45	19.23
ECR(Hycrete)	25	β	β	0.02	0.01	0.01
ECR(Hycrete)*	25	2.39	2.96	11.61	5.65	5.17
ECR(Hycrete)-10h	25	β	0.05	0.05	0.03	0.03
ECR(Hycrete)*-10h	25	0.84	9.23	10.08	6.72	5.11
ECR(Hycrete)-10h-35	21	0.09	0.05	0.23	0.12	0.09
ECR(Hycrete)*-10h-35	21	17.29	8.9	43.67	23.28	18.14
ECR(primer/$Ca(NO_2)_2$	30	0.04	0.01	0.03	0.03	0.02
ECR(primer/$Ca(NO_2)_2$*	30	20.69	6.33	14.71	13.91	7.21
ECR(primer/$Ca(NO_2)_2$-10h	30	0.08	0.04	0.04	0.05	0.02
ECR(primer/$Ca(NO_2)_2$*-10h	30	15.52	7.09	7.51	10.04	4.75
ECR(primer/$Ca(NO_2)_2$-10h-35	18	0.09	0.05	0.07	0.07	0.02
ECR(primer/$Ca(NO_2)_2$*-10h-35	18	17.29	9.6	13.37	13.42	3.84

Tables 3.9 and 3.10 continued:

[1] ECR(Rheocrete): Epoxy-coated steel cast with Rheocrete , based on total area of bar exposed to solution

[2] ECR(Rheocrete)*: Epoxy-coated steel cast with Rheocrete, based on exposed area of four 3.2-mm (1/8-in.) diameter holes in epoxy

[3] ECR(Rheocre)-10h: Epoxy-coated steel cast with Rheocrete and with ten drilled holes, based on total area of bar exposed to solution

[4] ECR(Rheocre)*-10h: Epoxy-coated steel cast with Rheocrete and with ten drilled holes, based on exposed area of ten 3.2-mm (1/8- in.) diameter holes in epoxy

[5] ECR(Rheocre)-10h-35: Epoxy-coated steel cast with Rheocrete and with ten drilled holes at w/c ratio of 0.35, based on total area of bar exposed to solution

[6] ECR(Rheocre)*-10h-35: Epoxy-coated steel cast with Rheocrete and with ten drilled holes at w/c ratio of 0.35, based on exposed area in epoxy

[7] ECR(DCI): Epoxy-coated steel cast with DCI, based on total area of bar exposed to solution

[8] ECR(DCI)*: Epoxy-coated steel cast with DCI, based on exposed area of four 3.2-mm (1/8-in.) diameter holes in epoxy

[9] ECR(DCI)-10h: Epoxy-coated steel cast with DCI and with ten drilled holes, based on total area of bar exposed to solution

[10] ECR(DCI)*-10h: Epoxy-coated steel cast with DCI and with ten drilled holes, based on exposed area of ten 3.2-mm (1/8-in.) diameter holes in epoxy

[11] ECR(DCI)-10h-35: Epoxy-coated steel cast with DCI and with ten drilled holes at w/c ratio of 0.35, based on total area of bar exposed to solution

[12] ECR(DCI)*-10h-35: Epoxy-coated steel cast with DCI and with ten drilled holes at w/c ratio of 0.35, based on exposed area in epoxy

[13] ECR(Hycrete): Epoxy-coated steel cast with Hycrete, based on total area of bar exposed to solution

[14] ECR(Hycrete)*: Epoxy-coated steel cast with Hycrete, based on exposed area of four 3.2-mm (1/8-in.) diameter holes in epoxy

[15] ECR(Hycrete)-10h: Epoxy-coated steel cast with Hycrete and with ten drille holes, based on total area of bar exposed to solution

[16] ECR(Hycrete)*-10h: Epoxy-coated steel cast with Hycrete and with ten drilled holes, based on exposed area of ten 3.2-mm (1/8-in.) diameter holes in epoxy

[17] ECR(Hycrete)-10h-35 Epoxy-coated steel cast with Hycrete and with ten drilled holes at w/c ratio of 0.35, based on total area of bar exposed to solution

[18] ECR(Hycrete)*-10h-35: Epoxy-coated steel cast with Hycrete and with ten drilled holes at w/c ratio of 0.35, based on exposed area in epoxy

[19] ECR(primer/$Ca(NO_2)_2$: Epoxy-coated steel cast with a calcium nitrite primer , based on total area of bar exposed to solution

[20] ECR(primer/$Ca(NO_2)_2$ *: Epoxy-coated steel cast with a calcium nitrite primer, based on exposed area of four 3.2-mm (1/8-in.) diameter holes in epoxy

[21] ECR(primer/$Ca(NO_2)_2$ -10h: Epoxy-coated steel cast with a calcium nitrite primer and with 10 drilled holes, based on total are of bar exposed to solution

[22] ECR(primer/$Ca(NO_2)_2$* -10h: Epoxy-coated steel cast with a calcium nitrite primer and with 10 drilled holes, based on exposed area in epoxy

[23] ECR(primer/$Ca(NO_2)_2$ -10h-35: Epoxy-coated steel cast with a calcium nitrite primer and with 10 drilled holes at w/c ratio of 0.35, based on total are of bar exposed to solution

[24] ECR(primer/$Ca(NO_2)_2$* -10h-35: Epoxy-coated steel cast with a calcium nitrite primer and with 10 drilled holes at w/c ratio of 0.35, based on exposed area in epoxy

[25] α: corrosion rate less than 0.01 μm/yr

[26] β: corrosion loss less than 0.01μm

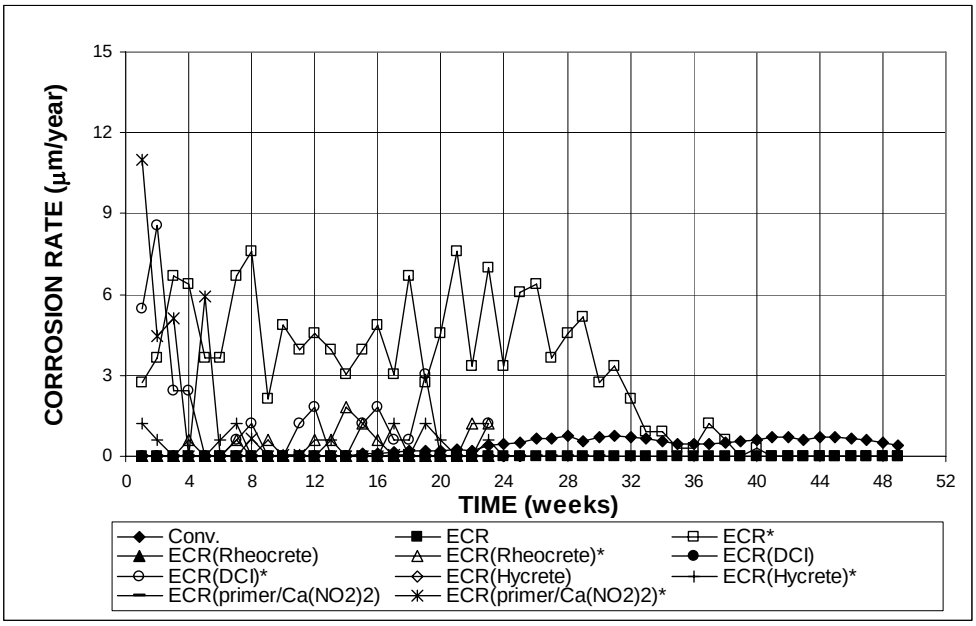

Figure 3.90 (a) – Southern Exposure Tests. Average Corrosion Rate. Specimens of conventional and epoxy-coated steel, epoxy-coated steel cast with corrosion inhibitors, and epoxy-coated steel with a calcium nitrite primer ponded with 15% NaCl solution. All epoxy-coated specimens with four drilled holes and a w/c ratio of 0.45. Refer to Table 3.9 for specimen identification.

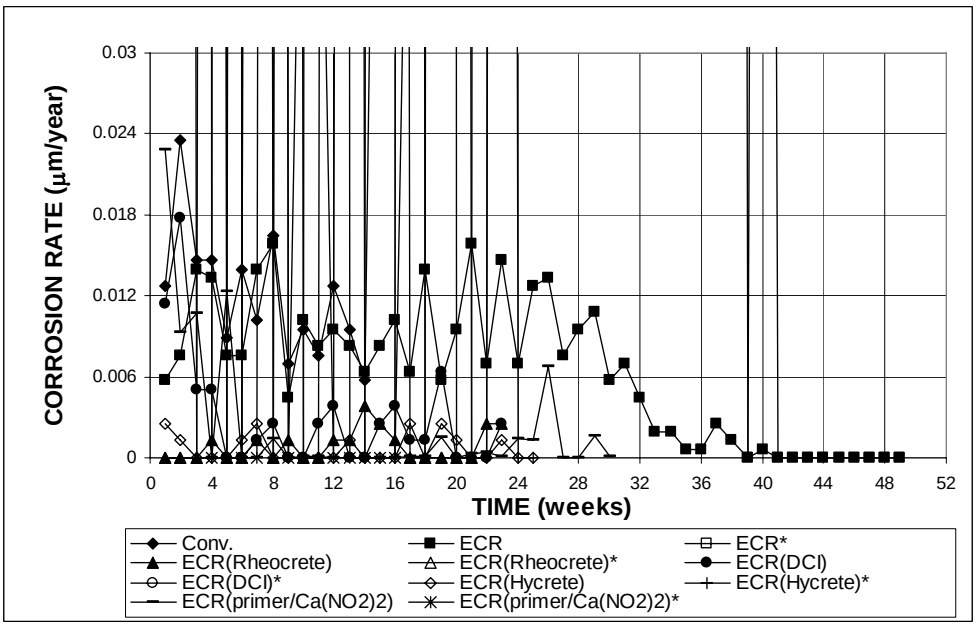

Figure 3.90 (b) – Southern Exposure Tests. Average Corrosion Rate. Specimens of conventional and epoxy-coated steel, epoxy-coated steel cast with corrosion inhibitors, and epoxy-coated steel with a calcium nitrite primer ponded with 15% NaCl solution. All epoxy-coated specimens with four drilled holes and a w/c ratio of 0.45. Refer to Table 3.9 for specimen identification.

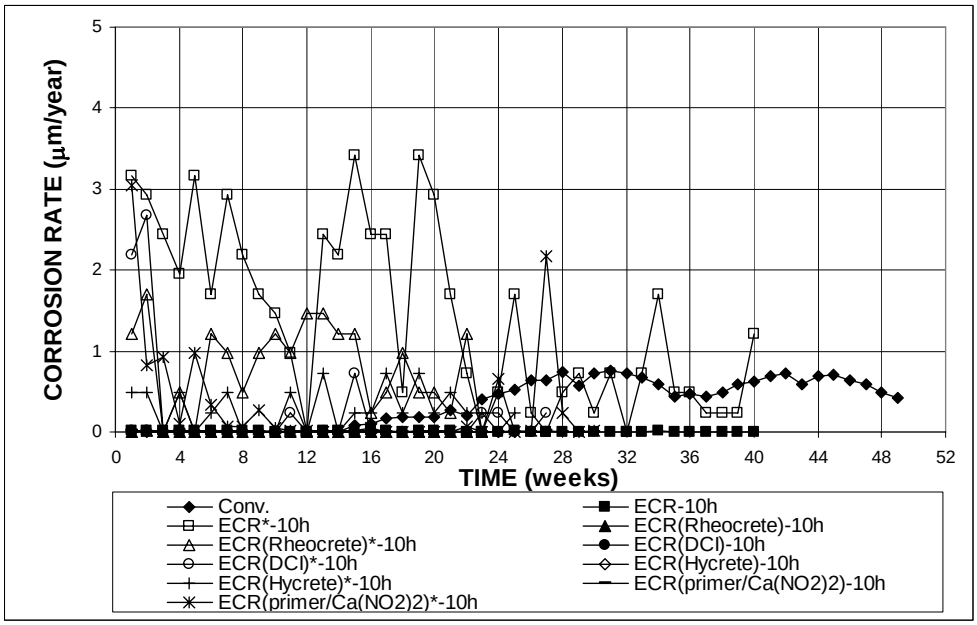

Figure 3.91 (a) – Southern Exposure Tests. Average Corrosion Rate. Specimens of conventional and epoxy-coated steel, epoxy-coated steel cast with corrosion inhibitors, and epoxy-coated steel with a calcium nitrite primer ponded with 15% NaCl solution. All epoxy-coated specimens with 10 drilled holes and a w/c ratio of 0.45. Refer to Table 3.9 for specimen identification.

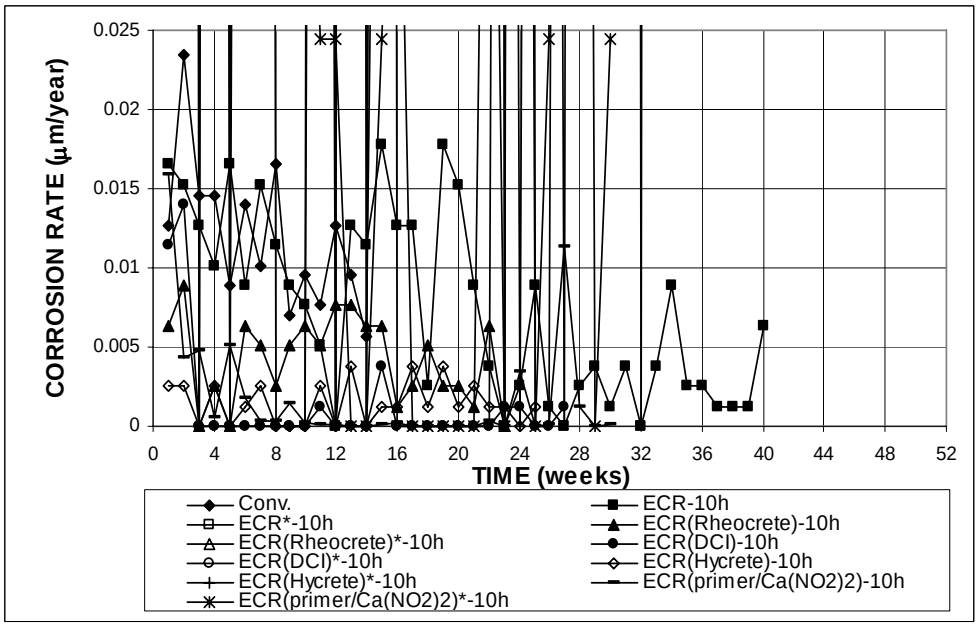

Figure 3.91 (b) – Southern Exposure Tests. Average Corrosion Rate. Specimens of conventional and epoxy-coated steel, epoxy-coated steel cast with corrosion inhibitors, and epoxy-coated steel with a calcium nitrite primer ponded with 15% NaCl solution. All epoxy-coated specimens with 10 drilled holes and a w/c ratio of 0.45. Refer to Table 3.9 for specimen identification.

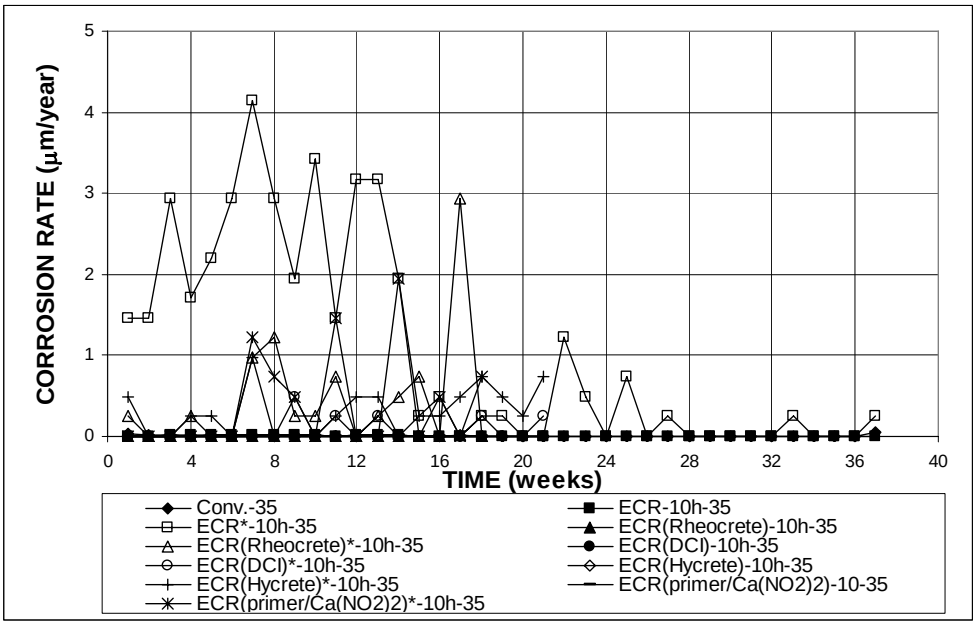

Figure 3.92 (a) – Southern Exposure Tests. Average Corrosion Rate. Specimens of conventional and epoxy-coated steel, epoxy-coated steel cast with corrosion inhibitors, and epoxy-coated steel with a calcium nitrite primer ponded with 15% NaCl solution. All epoxy-coated specimens with 10 drilled holes and a w/c ratio of 0.35. Refer to Table 3.9 for specimen identification.

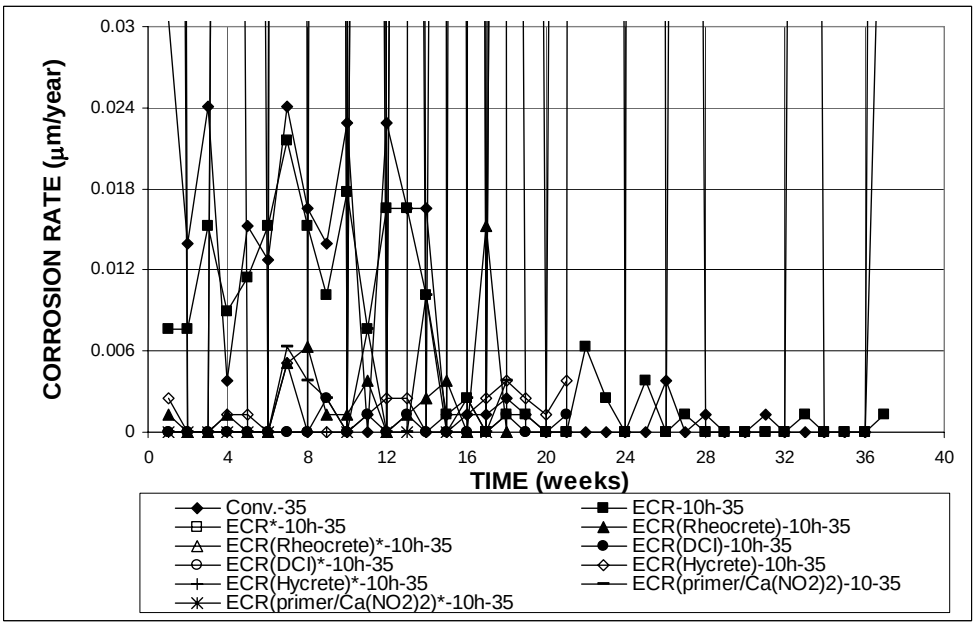

Figure 3.92 (b) – Southern Exposure Tests. Average Corrosion Rate. Specimens of conventional and epoxy-coated steel, epoxy-coated steel cast with corrosion inhibitors, and epoxy-coated steel with a calcium nitrite primer ponded with 15% NaCl solution. All epoxy-coated specimens with 10 drilled holes and a w/c ratio of 0.35. Refer to Table 3.9 for specimen identification.

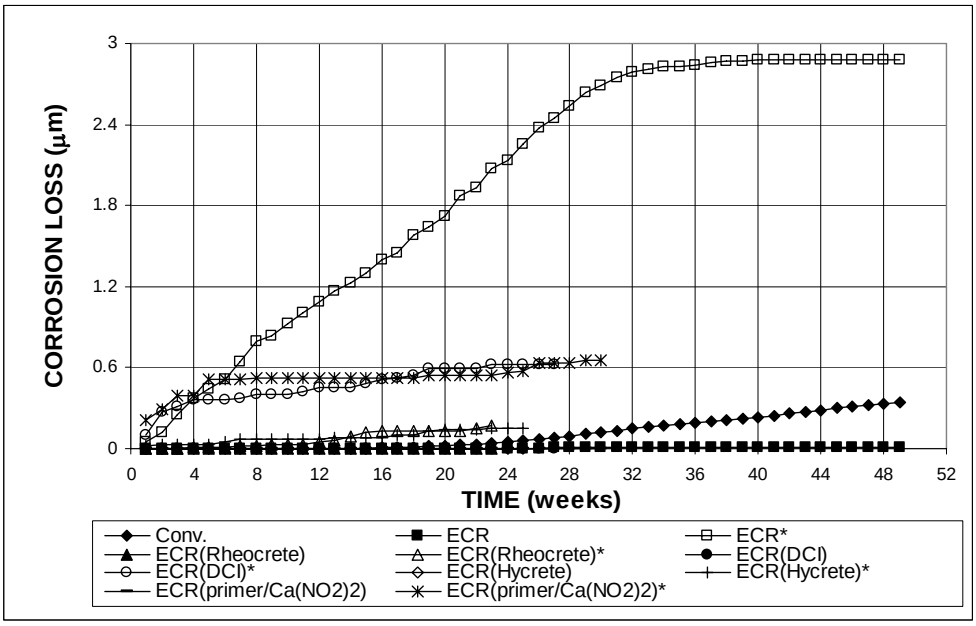

Figure 3.93 (a) – Southern Exposure Tests. Total Corrosion Loss. Specimens of conventional and epoxy-coated steel, epoxy-coated steel cast with corrosion inhibitors, and epoxy-coated steel with a calcium nitrite primer ponded with 15% NaCl solution. All epoxy-coated specimens with four drilled holes and a w/c ratio of 0.45. Refer to Table 3.10 for specimen identification.

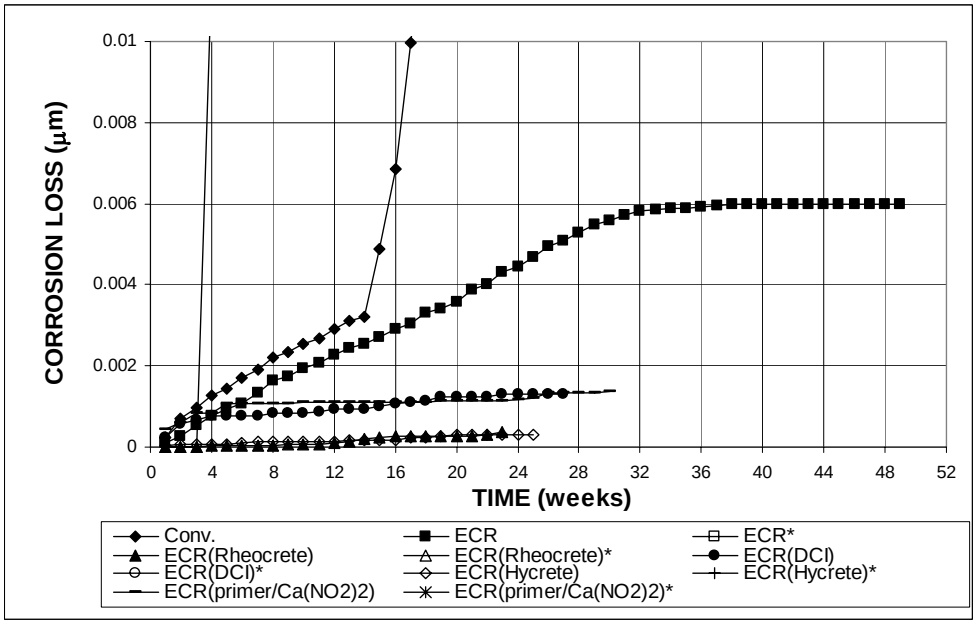

Figure 3.93 (b) – Southern Exposure Tests. Total Corrosion Loss. Specimens of conventional and epoxy-coated steel, epoxy-coated steel cast with corrosion inhibitors, and epoxy-coated steel with a calcium nitrite primer ponded with 15% NaCl solution. All epoxy-coated specimens with four drilled holes and a w/c ratio of 0.45..Refer to Table 3.10 for specimen identification.

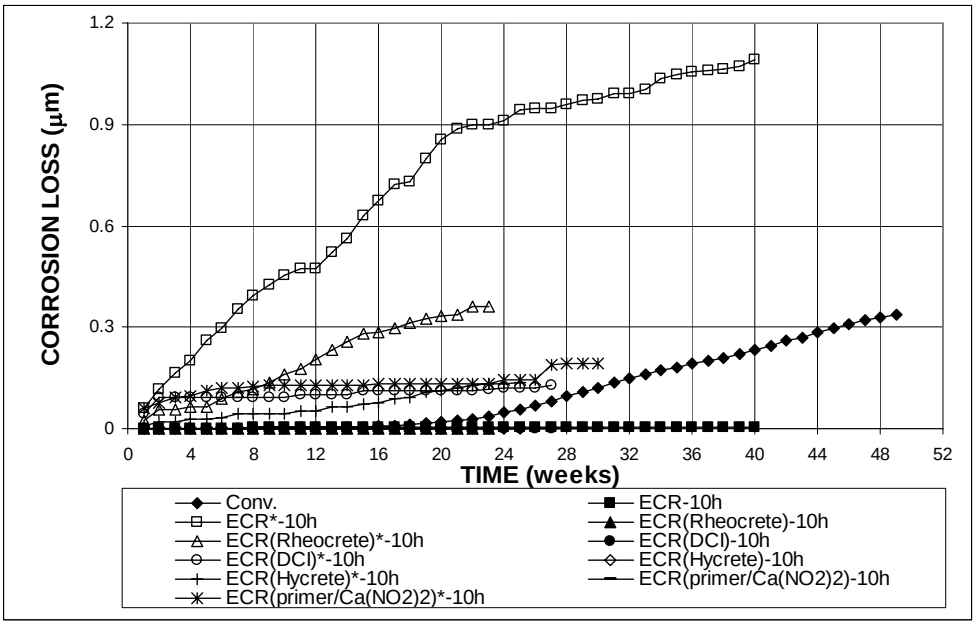

Figure 3.94 (a) – Southern Exposure Tests. Total Corrosion Loss. Specimens of conventional and epoxy-coated steel, epoxy-coated steel cast with corrosion inhibitors, and epoxy-coated steel with a calcium nitrite primer ponded with 15% NaCl solution. All epoxy-coated specimens with 10 drilled holes and a w/c ratio of 0.45. Refer to Table 3.10 for specimen identification.

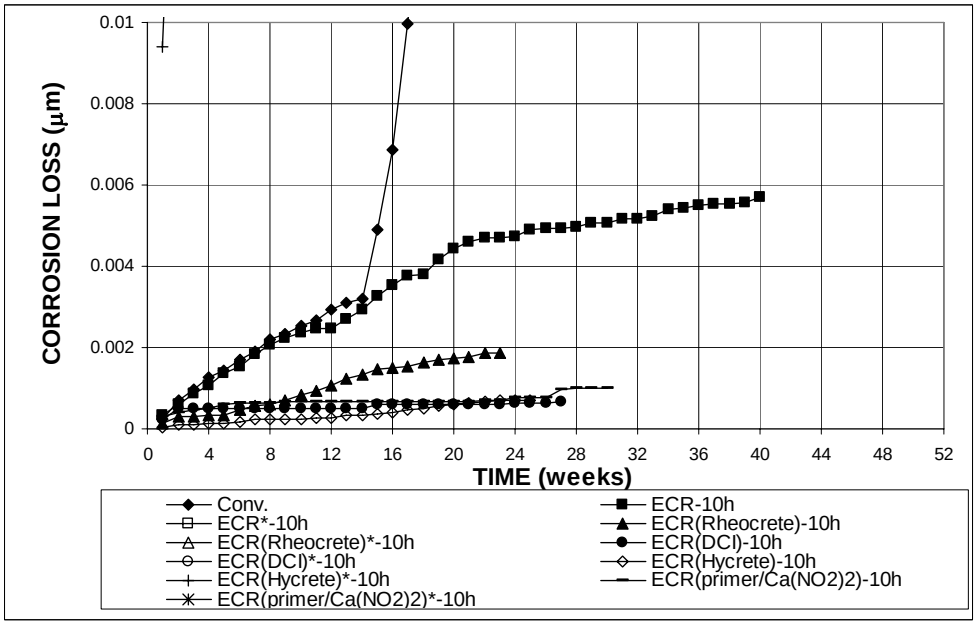

Figure 3.94 (b) – Southern Exposure Tests. Total Corrosion Loss. Specimens of conventional and epoxy-coated steel, epoxy-coated steel cast with corrosion inhibitors, and epoxy-coated steel with a calcium nitrite primer ponded with 15% NaCl solution. All epoxy-coated specimens with 10 drilled holes and a w/c ratio of 0.45. Refer to Table 3.10 for specimen identification.

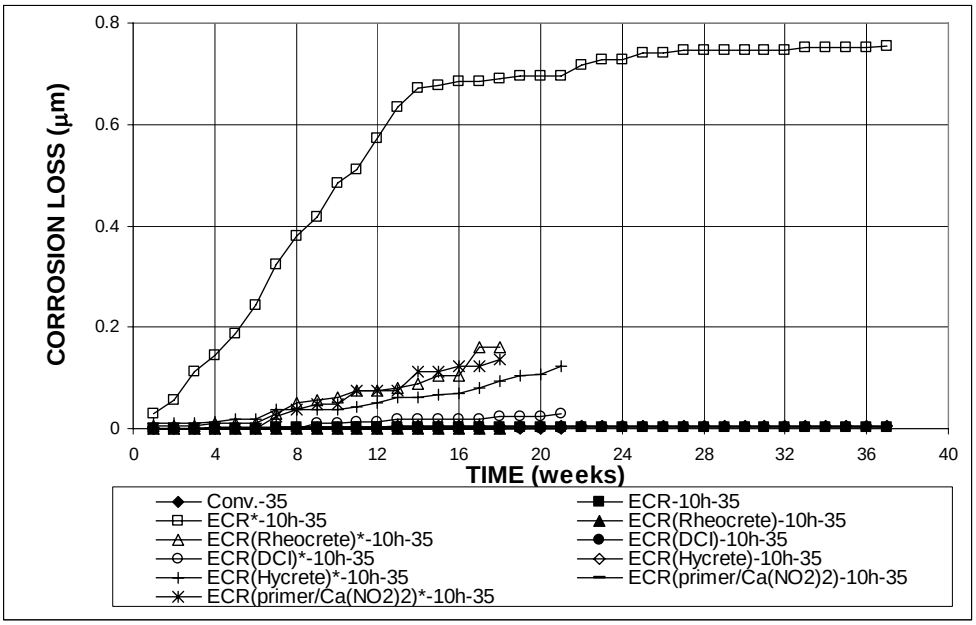

Figure 3.95 (a) – Southern Exposure Tests. Total Corrosion Loss. Specimens of conventional and epoxy-coated steel, epoxy-coated steel cast with corrosion inhibitors, and epoxy-coated steel with a calcium nitrite primer ponded with 15% NaCl solution. All epoxy-coated specimens with 10 drilled holes and a w/c ratio of 0.35. Refer to Table 3.10 for specimen identification.

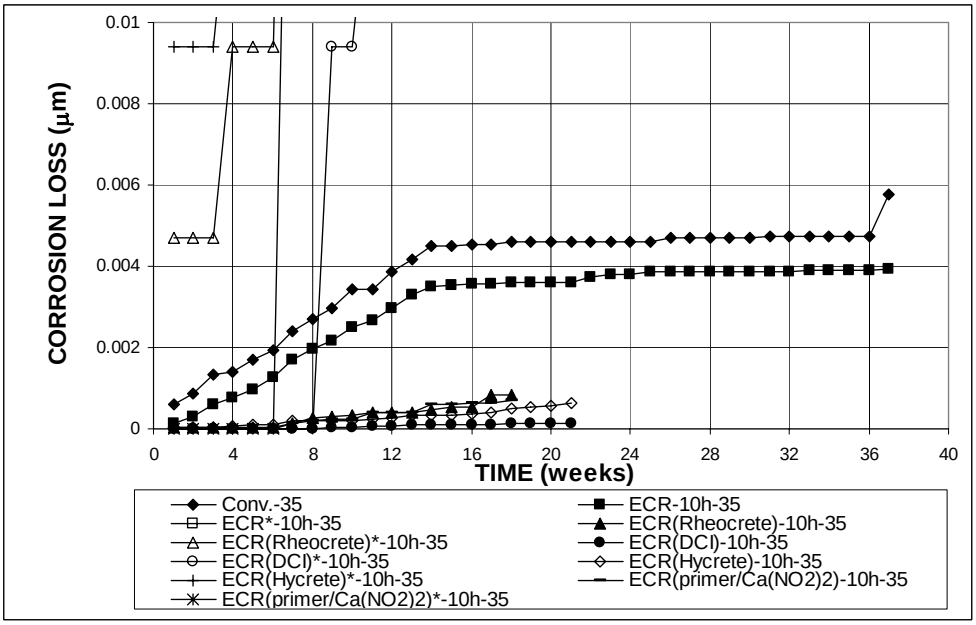

Figure 3.95 (b) – Southern Exposure Tests. Total Corrosion Loss. Specimens of conventional and epoxy-coated steel, epoxy-coated steel cast with corrosion inhibitors, and epoxy-coated steel with a calcium nitrite primer ponded with 15% NaCl solution. All epoxy-coated specimens with 10 drilled holes and a w/c ratio of 0.35. Refer to Table 3.10 for specimen identification.

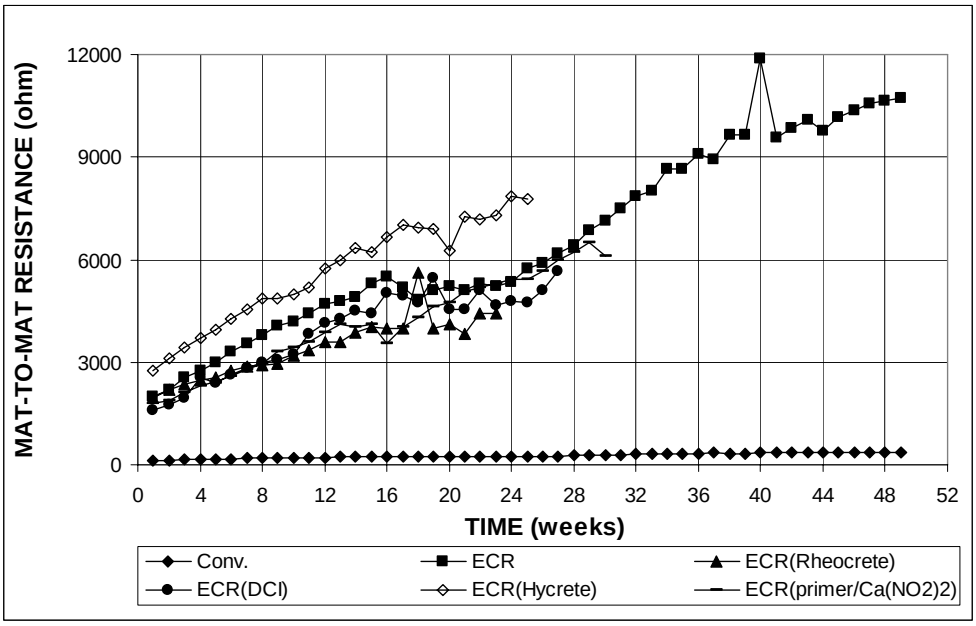

Figure 3.96 – Southern Exposure Tests. Mat-to-mat resistance. Specimens of conventional and epoxy-coated steel, epoxy-coated steel cast with corrosion inhibitors, and epoxy-coated steel with a calcium nitrite primer ponded with 15% NaCl solution. All epoxy-coated specimens with four drilled holes and a w/c ratio of 0.45. Refer to Table 3.9 for specimen identification.

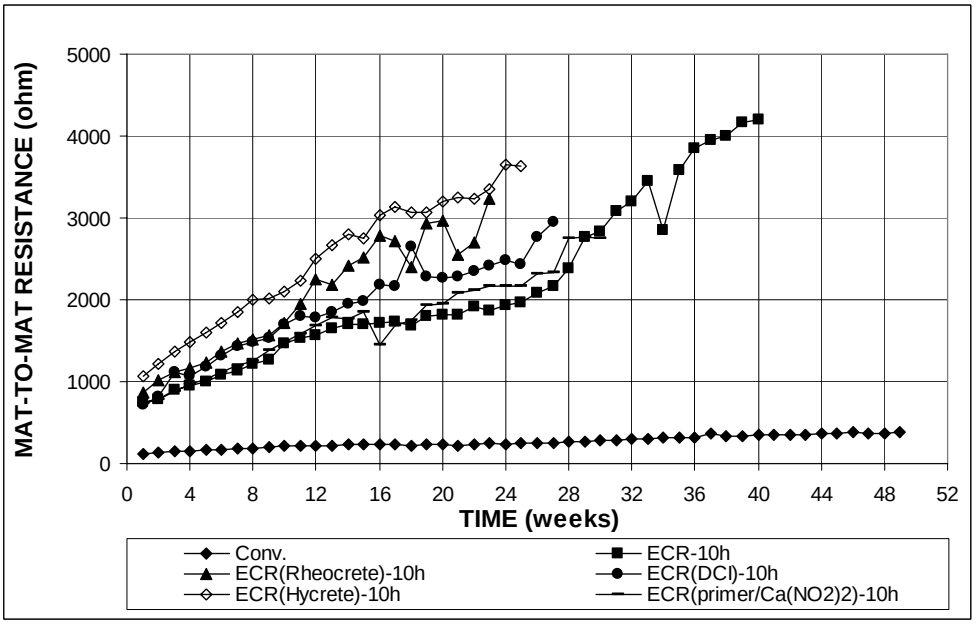

Figure 3.97 – Southern Exposure Tests. Mat-to-mat resistance. Specimens of conventional and epoxy-coated steel, epoxy-coated steel cast with corrosion inhibitors, and epoxy-coated steel with a calcium nitrite primer ponded with 15% NaCl solution. All epoxy-coated specimens with 10 drilled holes and a w/c ratio of 0.45. Refer to Table 3.9 for specimen identification.

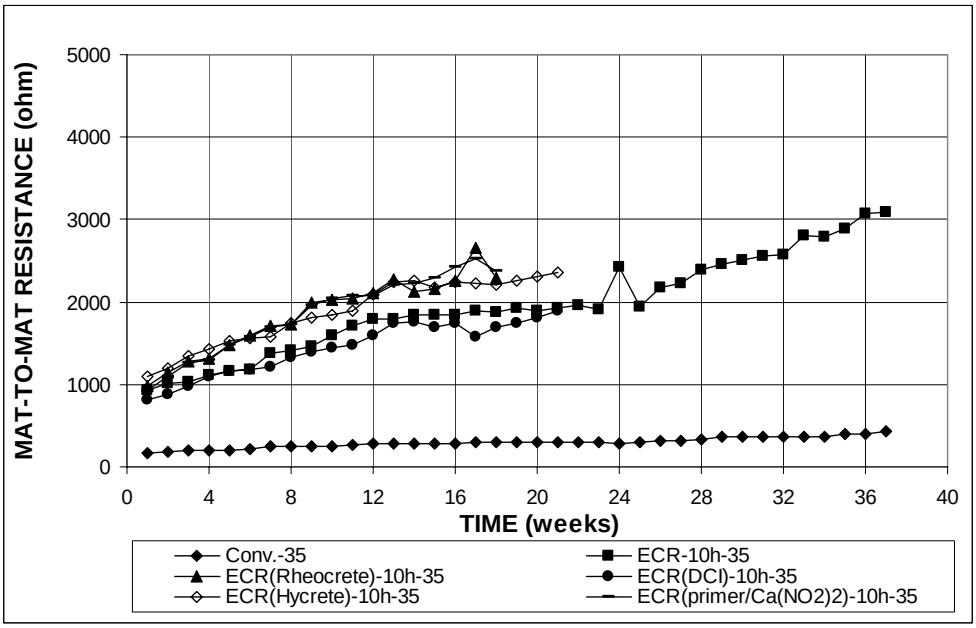

Figure 3.98 – Southern Exposure Tests. Mat-to-mat resistance. Specimens of conventional and epoxy-coated steel, epoxy-coated steel cast with corrosion inhibitors, and epoxy-coated steel with a calcium nitrite primer ponded with 15% NaCl solution. All epoxy-coated specimens with 10 drilled holes and a w/c ratio of 0.35. Refer to Table 3.9 for specimen identification.

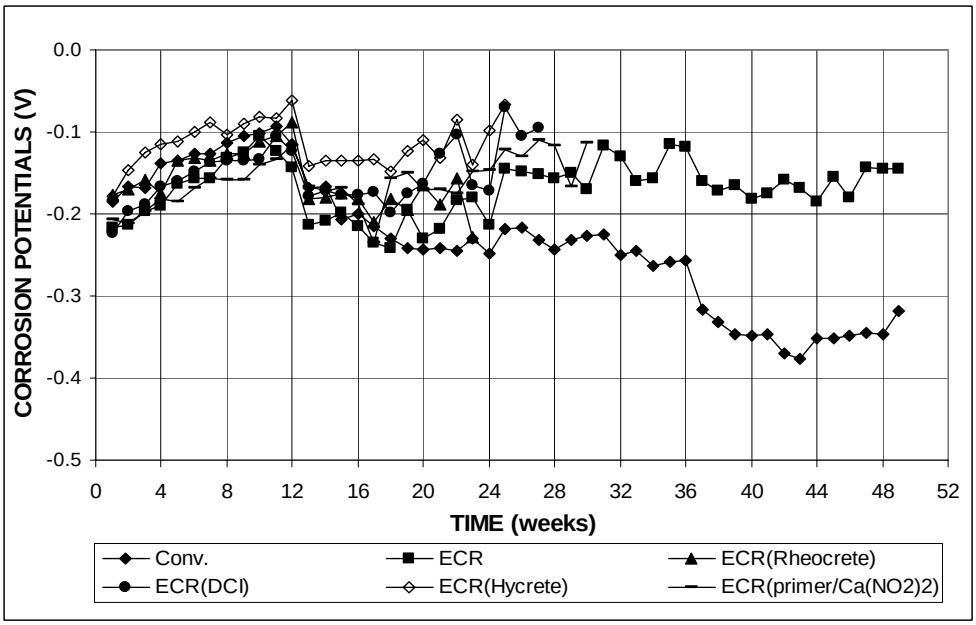

Figure 3.99 – Southern Exposure Tests. Corrosion Potential with respect to CSE at Top Mat. Specimens of conventional and epoxy-coated steel, epoxy-coated steel cast with corrosion inhibitors, and epoxy-coated steel with a calcium nitrite primer ponded with 15% NaCl solution. All epoxy-coated specimens with four drilled holes and a w/c ratio of 0.45. Refer to Table 3.9 for specimen identification.

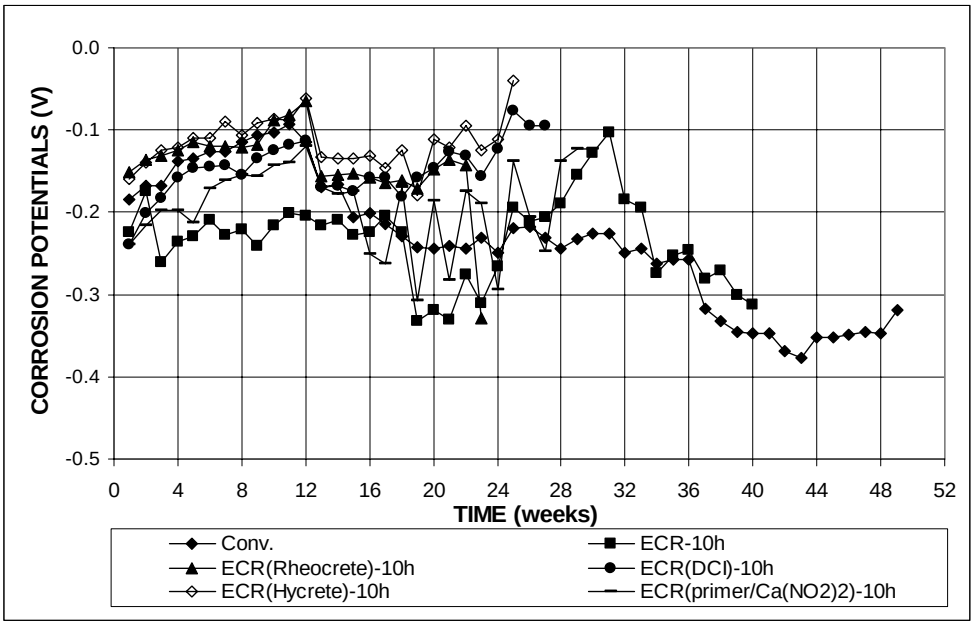

Figure 3.100 – Southern Exposure Tests. Corrosion Potential with respect to CSE at Top Mat. Specimens of conventional and epoxy-coated steel, epoxy-coated steel cast with corrosion inhibitors, and epoxy-coated steel with a calcium nitrite primer ponded with 15% NaCl solution. All epoxy-coated specimens with 10 drilled holes and a w/c ratio of 0.45. Refer to Table 3.9 for specimen identification.

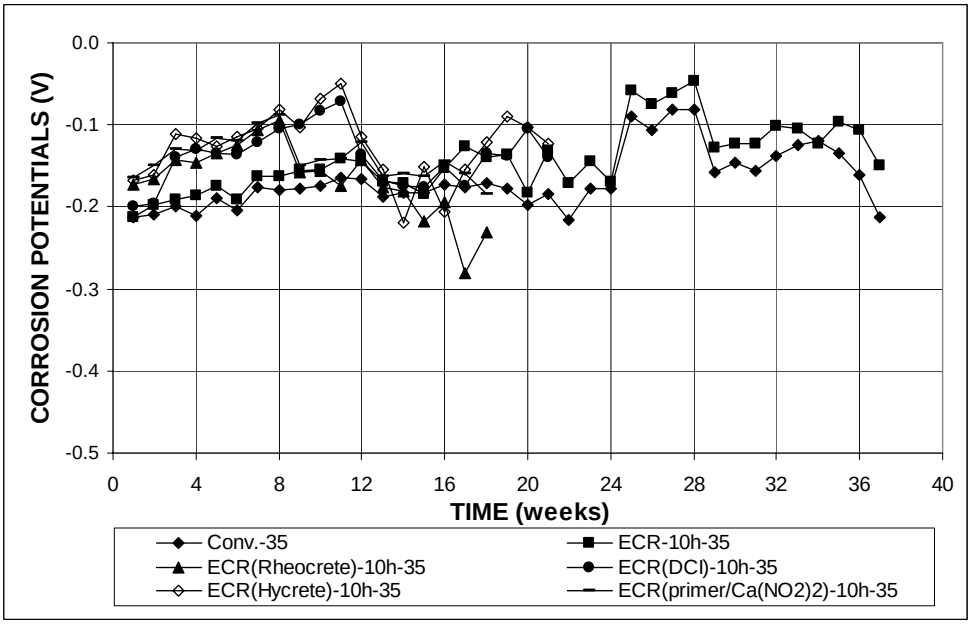

Figure 3.101 – Southern Exposure Tests. Corrosion Potential with respect to CSE at Top Mat. Specimens of conventional and epoxy-coated steel, epoxy-coated steel cast with corrosion inhibitors, and epoxy-coated steel with a calcium nitrite primer ponded with 15% NaCl solution. All epoxy-coated specimens with 10 drilled holes and a w/c ratio of 0.35. Refer to Table 3.9 for specimen identification.

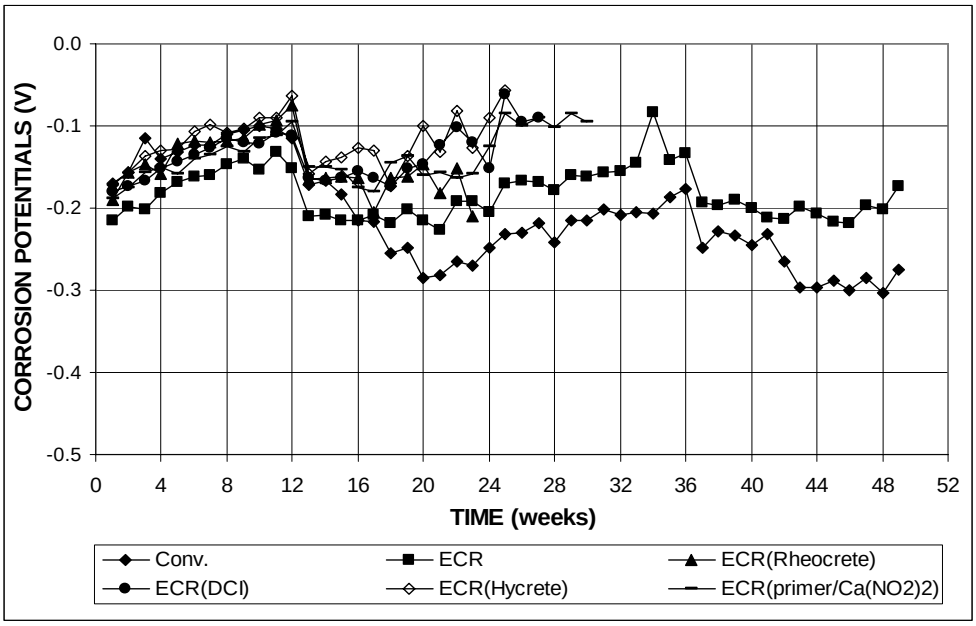

Figure 3.102 – Southern Exposure Tests. Corrosion Potential with respect to CSE at Bottom Mat. Specimens conventional and epoxy-coated steel, epoxy-coated steel cast with corrosion inhibitors, and epoxy-coated steel with a calcium nitrite primer ponded with 15% NaCl solution. All epoxy-coated specimens with four drilled holes and a w/c ratio of 0.45. Refer to Table 3.9 for specimen identification.

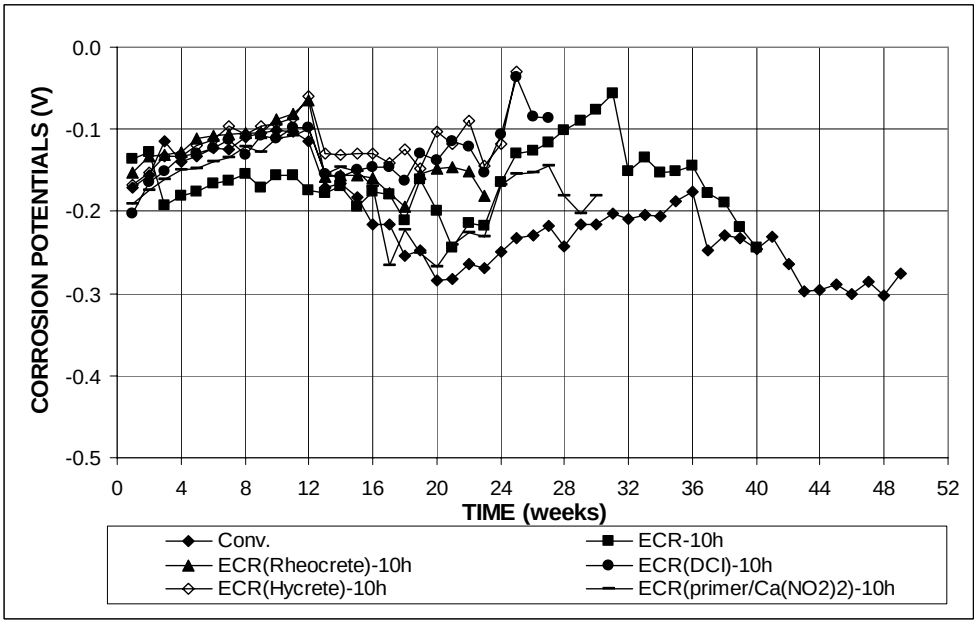

Figure 3.103 – Southern Exposure Tests. Corrosion Potential with respect to CSE at Bottom Mat. Specimens conventional and epoxy-coated steel, epoxy-coated steel cast with corrosion inhibitors, and epoxy-coated steel with a calcium nitrite primer ponded with 15% NaCl solution. All epoxy-coated specimens with 10 drilled holes and a w/c ratio of 0.45. Refer to Table 3.9 for specimen identification.

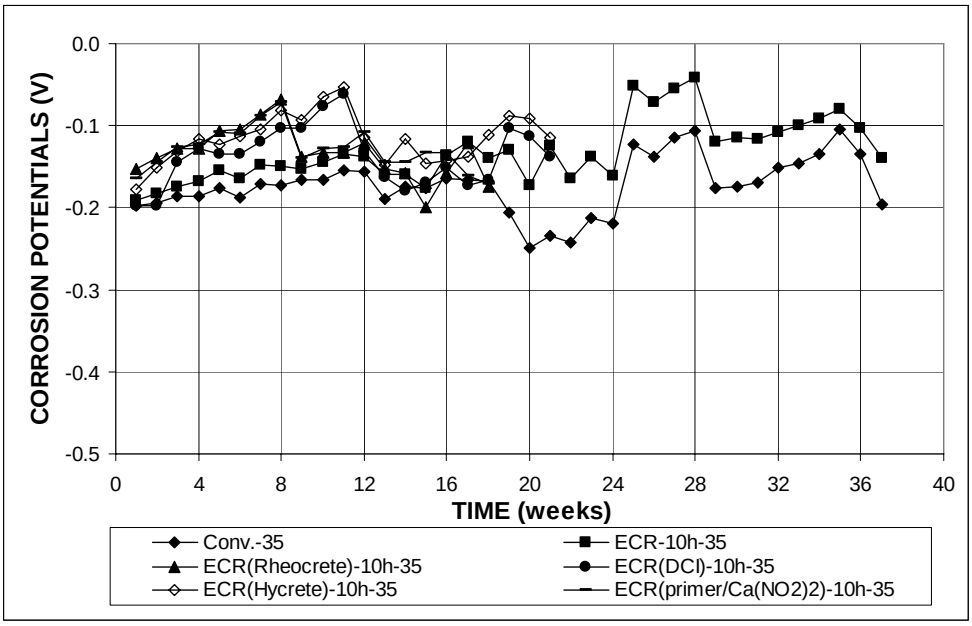

Figure 3.104 – Southern Exposure Tests. Corrosion Potential with respect to CSE at Bottom Mat. Specimens conventional and epoxy-coated steel, epoxy-coated steel cast with corrosion inhibitors, and epoxy-coated steel with a calcium nitrite primer ponded with 15% NaCl solution. All epoxy-coated specimens with 10 drilled holes and a w/c ratio of 0.35. Refer to Table 3.9 for specimen identification.

3.4.2.2 Cracked Beam Tests

As with the Southern Exposure tests, the cracked beam tests include three specimens each for ECR(Rheocrete), ECR(DCI), ECR(Hycrete), and ECR($Ca(NO_2)_2$) with four drilled holes and a *w/c* ratio of 0.45 and with 10 drilled holes and *w/c* ratios of 0.35 and 0.45.

For specimens with four drilled holes (Figure 3.105), the average corrosion rate based on the total area exposed to the solution for the ECR(Rheocrete) specimens increased to 0.1 μm/yr at week 23, twice the rate of the conventional ECR specimens (0.05 μm/year) at the same point in time. With a peak of 0.06 μm/yr at week 11, the ECR(Hycrete) specimens had a rate of 0.04 μm/yr at week 25, similar to that of the conventional ECR specimens (0.03 μm/yr). The ECR(primer/$Ca(NO_2)_2$) specimens exhibited a corrosion rate as high as 0.12 μm/yr at week 5, dropping to 0.03 μm/yr at

week 30, equal to the rate of the conventional ECR specimens. The ECR(DCI) specimens had the lowest corrosion rate, 0.01 μm/yr at week 27, 40% of that of the conventional ECR specimens (0.025 μm/yr), although values as high as 0.03 μm/yr were earlier.

For specimens with 10 drilled holes in concrete with a *w/c* ratio of 0.45 (Figure 3.106), based on total area, the average corrosion rate of the ECR(primer/$Ca(NO_2)_2$ specimens was 0.07 μm/yr at week 30, equal to more than twice the rate of the convention ECR specimens (0.03 μm/yr). The ECR(primer/$Ca(NO_2)_2$) specimens had a maximum corrosion rate of 0.17 μm/yr at weeks 3 and 4. The ECR(Rheocrete) specimens also exhibited obvious corrosion with a rate as high as 0.17 μm/yr at week 8, dropping to 0.11 μm/yr at week 23, a value that is more than five times the rate of the conventional ECR specimens (0.02 μm/yr). Although the peak corrosion rate of the ECR(Hycrete) specimens was twice the maximum rate of the ECR(DCI) specimens, both specimens had similar corrosion rates, 0.02 and 0.03 μm/yr at week 25 and 27, respectively. The rates of the ECR (Hycrete) and ECR(DCI) equaled 50% and 100% of the corrosion rate of the conventional ECR specimens, respectively, at the same point in time. For specimens with a *w/c* ratio of 0.35 (Figure 3.107), no obvious decrease in corrosion rate was observed when compared to specimens with a *w/c* ratio of 0.45. The corrosion rates at the data cutoff point were 0.15, 0.19, 0.27, and 0.19 μm/yr for the ECR(Rheocrete), ECR(DCI), ECR(Hycrete), and ECR(primer/$Ca(NO_2)_2$) specimens, respectively, all higher than the corrosion rate of the conventional ECR specimens at the same point in time. Based on the exposed area, higher corrosion rates were obtained for all cracked beam specimens.

The total corrosion losses are shown in Figures 3.108-3.110. Based on the total area, all specimens with four drilled holes had similar corrosion losses, around 0.01

μm (Figure 3.108), except for the ECR(primer/$Ca(NO_2)_2$) specimens, which exhibited an average corrosion loss of 0.03 μm. For specimens with 10 drilled holes and a *w/c* ratio of 0.45 (Figure 3.109), the ECR(Rheocrete), ECR(DCI), ECR(Hycrete), and ECR(primer/$Ca(NO_2)_2$) specimens had corrosion losses of 0.04, 0.02, 0.03 μm, and 0.05 μm between weeks 23 and 30, respectively, all close to the value for the conventional ECR specimens (0.03 μm at both weeks 23 and 30). For specimens with a *w/c* ratio of 0.35 (Figure 3.110), the corrosion losses were 0.04, 0.09, 0.12, and 0.07 μm for the ECR(Rheocrete), ECR(DCI), ECR(Hycrete), and ECR(primer/$Ca(NO_2)_2$) specimens between weeks 18 and 21, respectively, compared to the losses of about 0.05 μm for the conventional ECR specimens between weeks 18 and 21. Based on the exposed area, the corrosion losses are 500 or 200 times higher (actually 480 and 192 times higher) than the corresponding losses based on the total area for specimens with four or 10 drilled holes, respectively. No obvious improvement in the corrosion resistance of epoxy-coated steel was observed using the lower water-cement ratio concrete or with the corrosion inhibitors. Compared to the specimens with 10 drilled holes, lower total corrosion losses were observed on specimens with four drilled holes since the epoxy was damaged less.

Mat-to-mat resistance results are shown in Figures 3.111-3.113. The ECR specimens, with and without corrosion inhibitors with four drilled holes (Figure 3.111), started with average mat-to-mat resistances between 2,500 and 4,000 ohms. The resistances increased to values between 8,000 and 14,000 ohms for specimens with corrosion inhibitors and around 18,000 ohms for specimens without inhibitors, likely due to the formation of corrosion products on the surface. The specimens with 10 drilled holes at *w/c* ratios of either 0.45 or 0.35 (Figures 3.112 and 3.113)

exhibited lower resistances, with and without corrosion inhibitors, starting around 1,500 ohms and increasing with time to values less than 8,500 ohms.

The average corrosion potentials of the top and bottom mats with respect to a copper copper-sulfate electrode are shown in Figures 3.114-3.119. For the top mat, all ECR specimens exhibited corrosion potentials that started around −0.200 V, except ECR(Hycrete), with started at about −0.300 V, but quickly dropped to values more negative than −0.400 V, indicating a high probability of corrosion. For the bottom mat, all ECR specimens with corrosion inhibitors, except the ECR(primer/$Ca(NO_2)_2$) specimens with 10 drilled holes and a *w/c* ratio of 0.35, exhibited corrosion potentials more positive than −0.300 V, demonstrating the bottom bars were still in a passive condition. For the ECR(primer/$Ca(NO_2)_2$) specimens with 10 drilled holes and a *w/c* ratio of 0.35, the potential dropped to below −0.300 V after week 13, indicating a slight tendency to corrode.

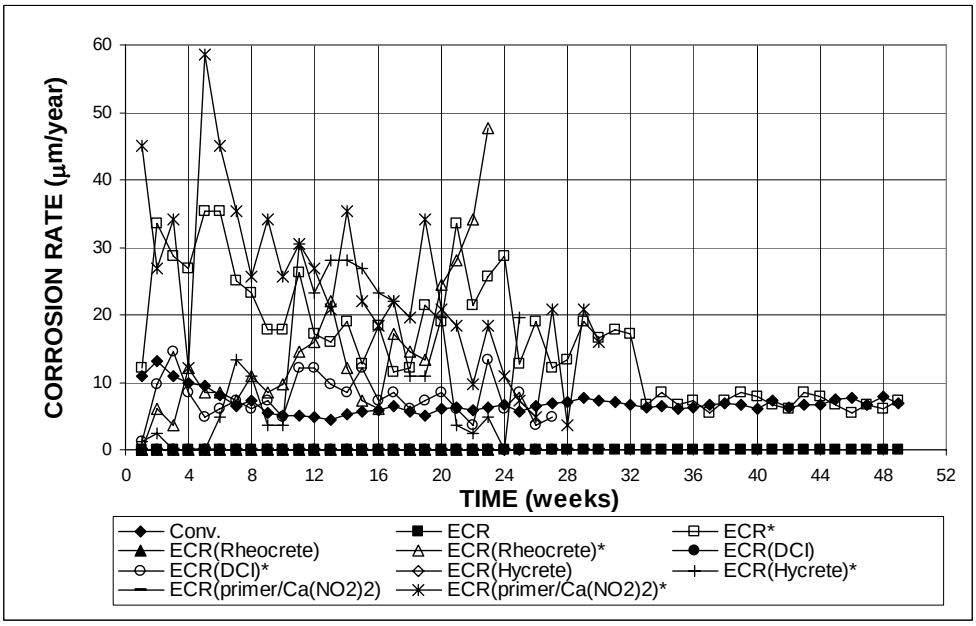

Figure 3.105 (a) – Cracked Beam Tests. Average Corrosion Rate. Specimens of conventional and epoxy-coated steel, epoxy-coated steel cast with corrosion inhibitors, and epoxy-coated steel with a calcium nitrite primer ponded with 15% NaCl solution. All epoxy-coated specimens with four drilled holes and a w/c ratio of 0.45. Refer to Table 3.9 for specimen identification.

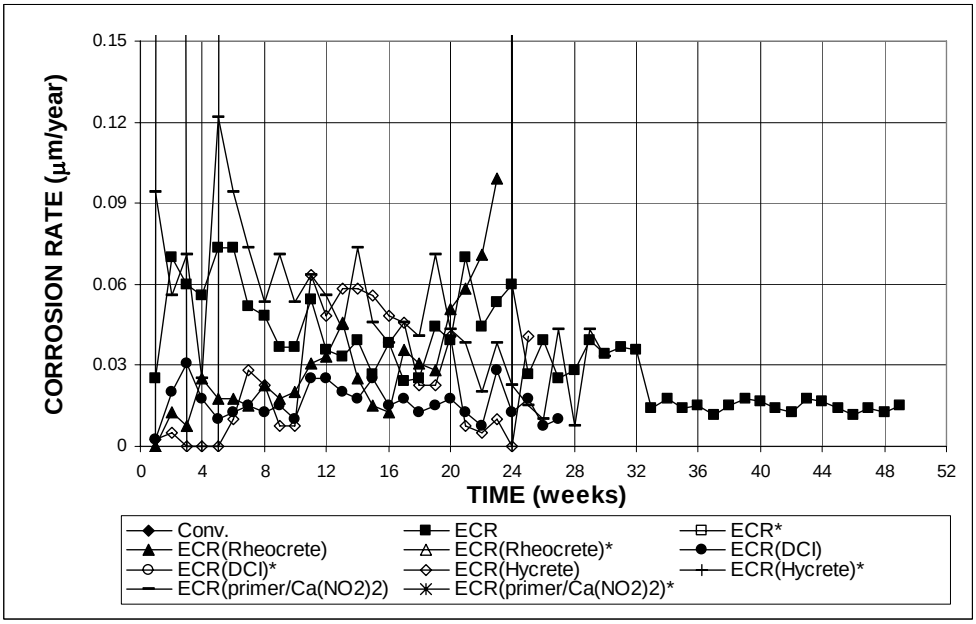

Figure 3.105 (b) – Cracked Beam Tests. Average Corrosion Rate. Specimens of conventional and epoxy-coated steel, epoxy-coated steel cast with corrosion inhibitors, and epoxy-coated steel with a calcium nitrite primer ponded with 15% NaCl solution. All epoxy-coated specimens with four drilled holes and a w/c ratio of 0.45. Refer to Table 3.9 for specimen identification.

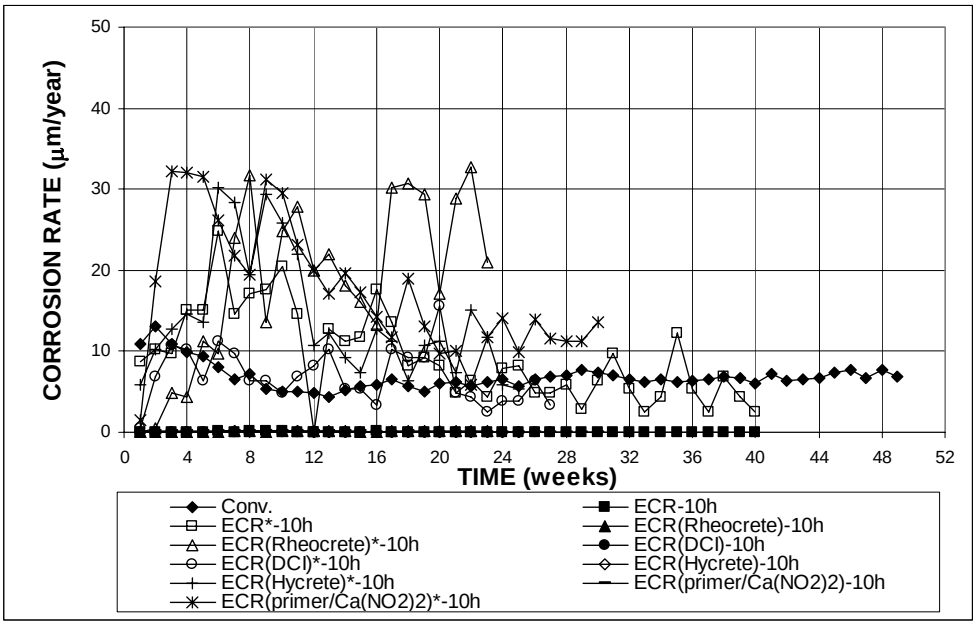

Figure 3.106 (a) – Cracked Beam Tests. Average Corrosion Rate. Specimens of conventional and epoxy-coated steel, epoxy-coated steel cast with corrosion inhibitors, and epoxy-coated steel with a calcium nitrite primer ponded with 15% NaCl solution. All epoxy-coated specimens with 10 drilled holes and a w/c ratio of 0.45. Refer to Table 3.9 for specimen identification.

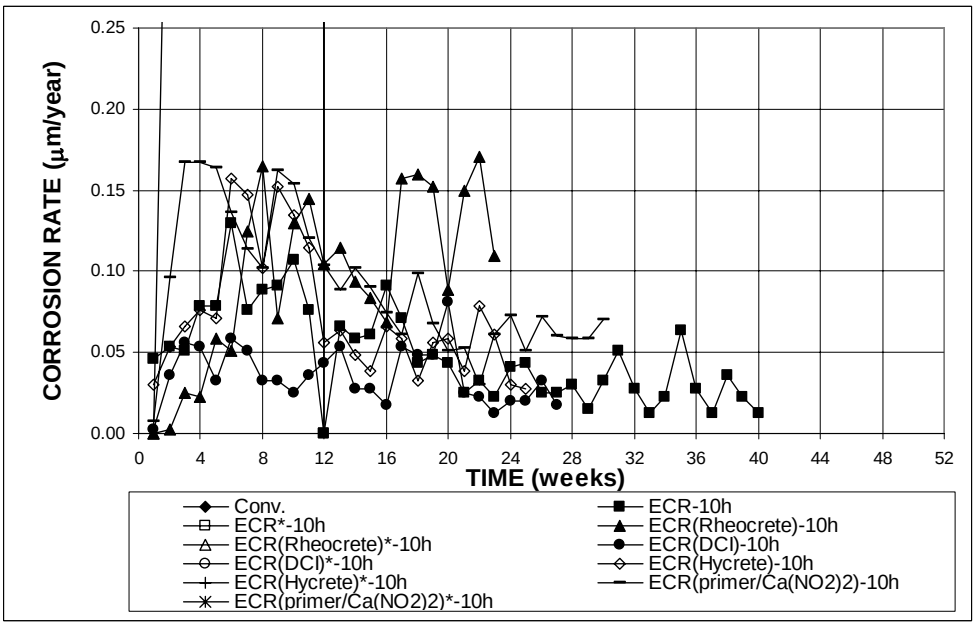

Figure 3.106 (b) – Cracked Beam Tests. Average Corrosion Rate. Specimens of conventional and epoxy-coated steel, epoxy-coated steel cast with corrosion inhibitors, and epoxy-coated steel with a calcium nitrite primer ponded with 15% NaCl solution. All epoxy-coated specimens with 10 drilled holes and a w/c ratio of 0.45. Refer to Table 3.9 for specimen identification.

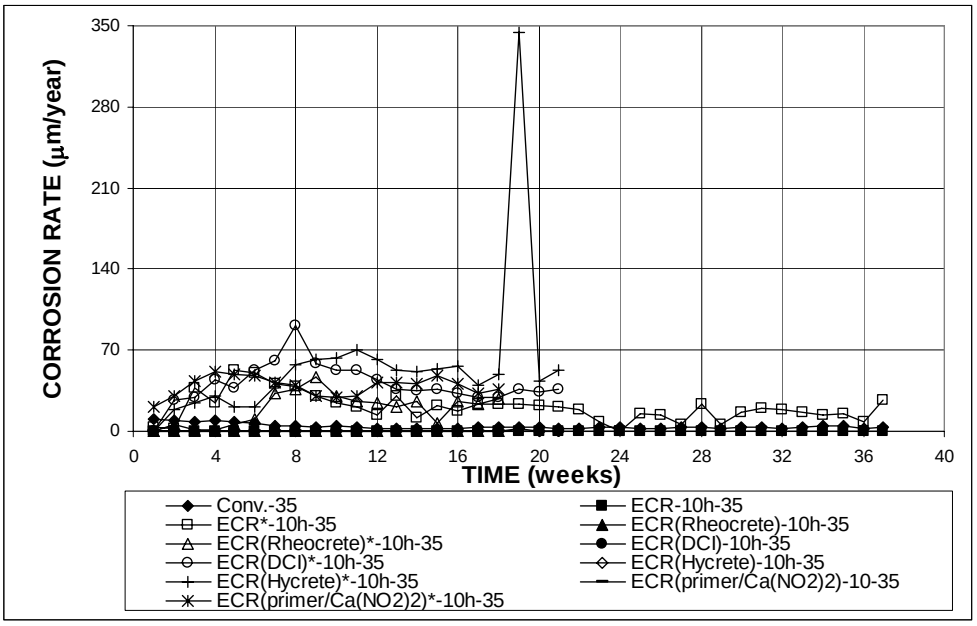

Figure 3.107 (a) – Cracked Beam Tests. Average Corrosion Rate. Specimens of conventional and epoxy-coated steel, epoxy-coated steel cast with corrosion inhibitors, and epoxy-coated steel with a calcium nitrite primer ponded with 15% NaCl solution. All epoxy-coated specimens with 10 drilled holes and a w/c ratio of 0.35. Refer to Table 3.9 for specimen identification.

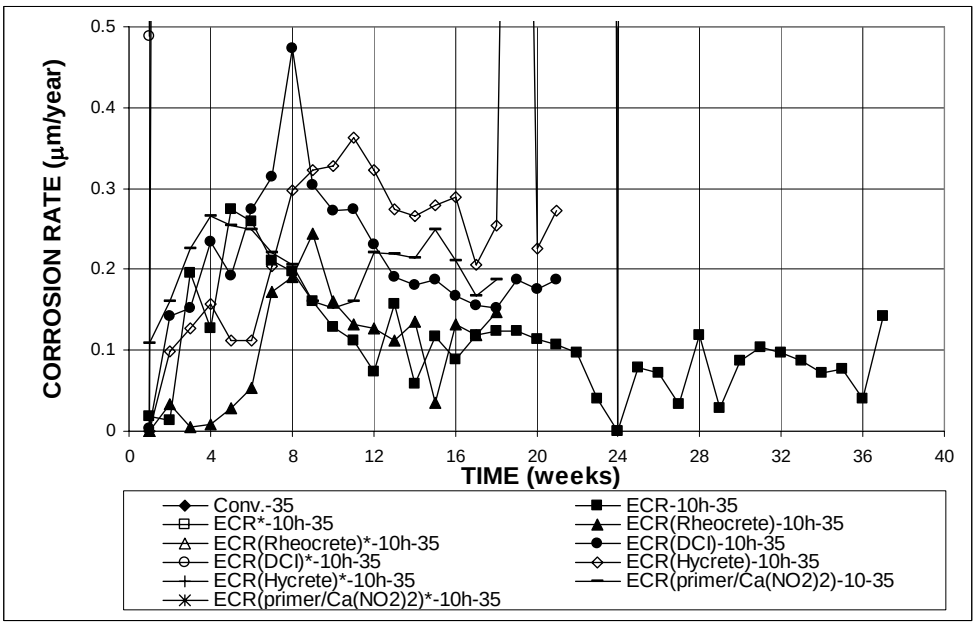

Figure 3.107 (b) – Cracked Beam Tests. Average Corrosion Rate. Specimens of conventional and epoxy-coated steel, epoxy-coated steel cast with corrosion inhibitors, and epoxy-coated steel with a calcium nitrite primer ponded with 15% NaCl solution. All epoxy-coated specimens with 10 drilled holes and a w/c ratio of 0.35. Refer to Table 3.9 for specimen identification.

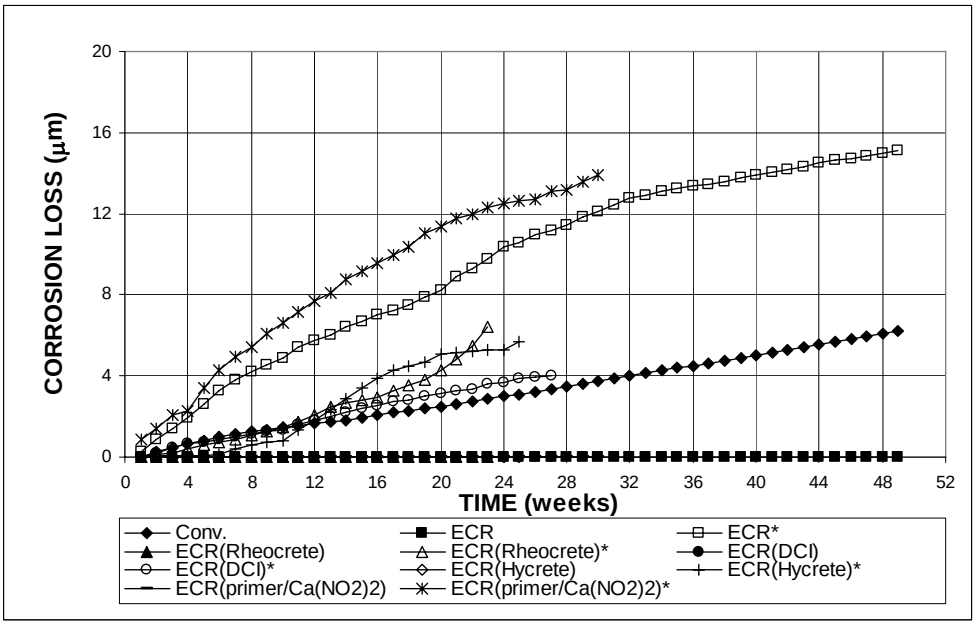

Figure 3.108 (a) – Cracked Beam Tests. Total Corrosion Loss. Specimens of conventional and epoxy-coated steel, epoxy-coated steel cast with corrosion inhibitors, and epoxy-coated steel with a calcium nitrite primer ponded with 15% NaCl solution. All epoxy-coated specimens with four drilled holes and a w/c ratio of 0.45. Refer to Table 3.10 for specimen identification.

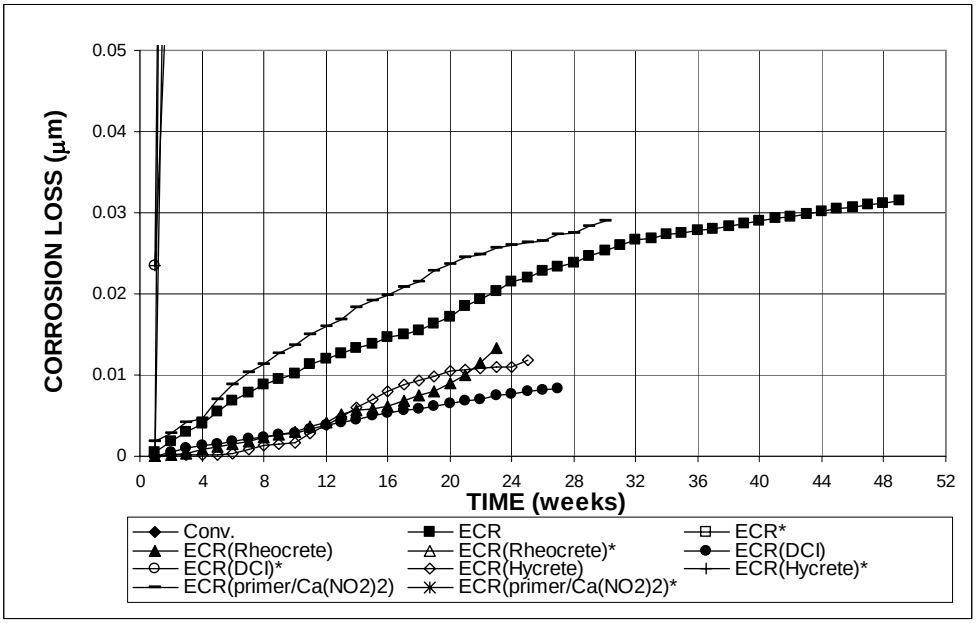

Figure 3.108 (b) – Cracked Beam Tests. Total Corrosion Loss. Specimens of conventional and epoxy-coated steel, epoxy-coated steel cast with corrosion inhibitors, and epoxy-coated steel with a calcium nitrite primer ponded with 15% NaCl solution. All epoxy-coated specimens with four drilled holes and a w/c ratio of 0.45. Refer to Table 3.10 for specimen identification.

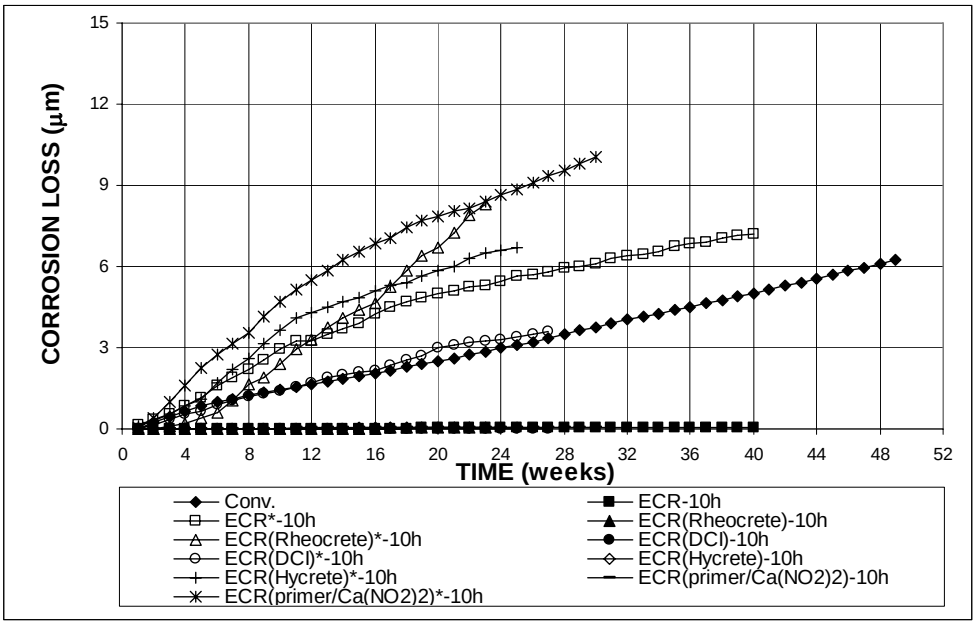

Figure 3.109 (a) – Cracked Beam Tests. Total Corrosion Loss. Specimens of conventional and epoxy-coated steel, epoxy-coated steel cast with corrosion inhibitors, and epoxy-coated steel with a calcium nitrite primer ponded with 15% NaCl solution. All epoxy-coated specimens with 10 drilled holes and a w/c ratio of 0.45. Refer to Table 3.10 for specimen identification.

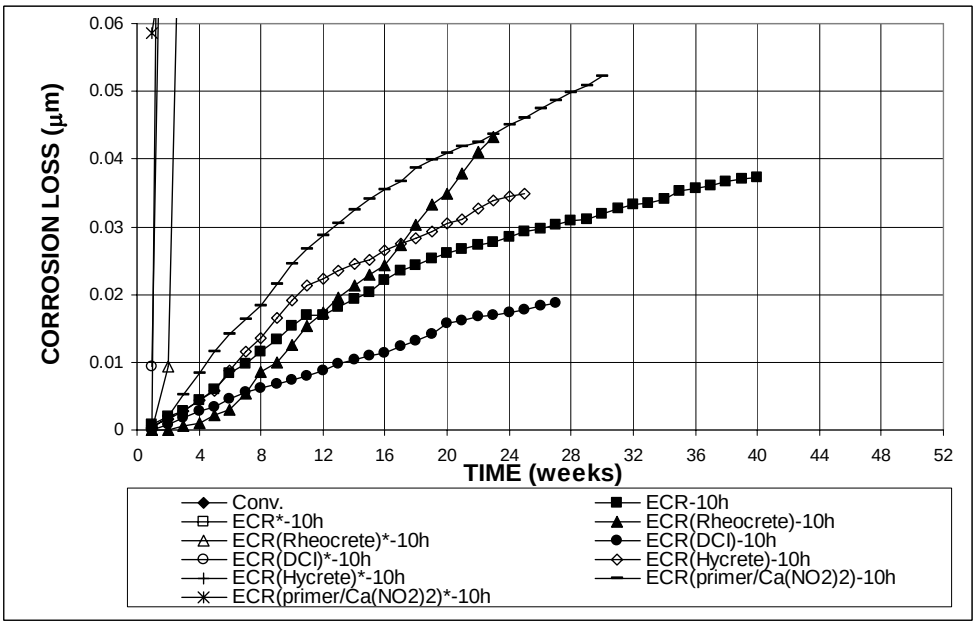

Figure 3.109 (b) – Cracked Beam Tests. Total Corrosion Loss. Specimens of conventional and epoxy-coated steel, epoxy-coated steel cast with corrosion inhibitors, and epoxy-coated steel with a calcium nitrite primer ponded with 15% NaCl solution. All epoxy-coated specimens with 10 drilled holes and a w/c ratio of 0.45. Refer to Table 3.10 for specimen identification.

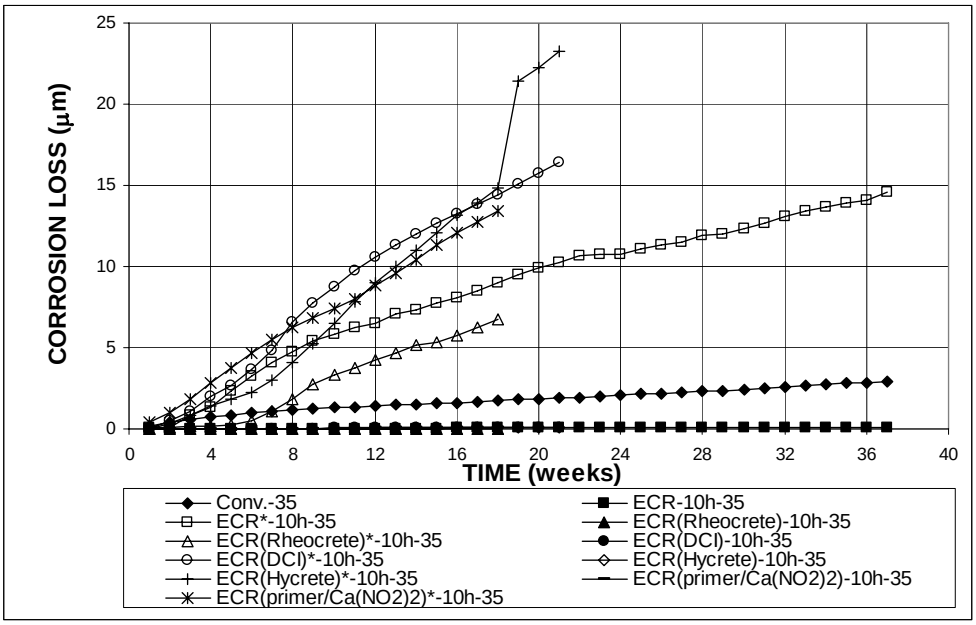

Figure 3.110 (a) – Cracked Beam Tests. Total Corrosion Loss. Specimens of conventional and epoxy-coated steel, epoxy-coated steel cast with corrosion inhibitors, and epoxy-coated steel with a calcium nitrite primer ponded with 15% NaCl solution. All epoxy-coated specimens with 10 drilled holes and a w/c ratio of 0.35. Refer to Table 3.10 for specimen identification.

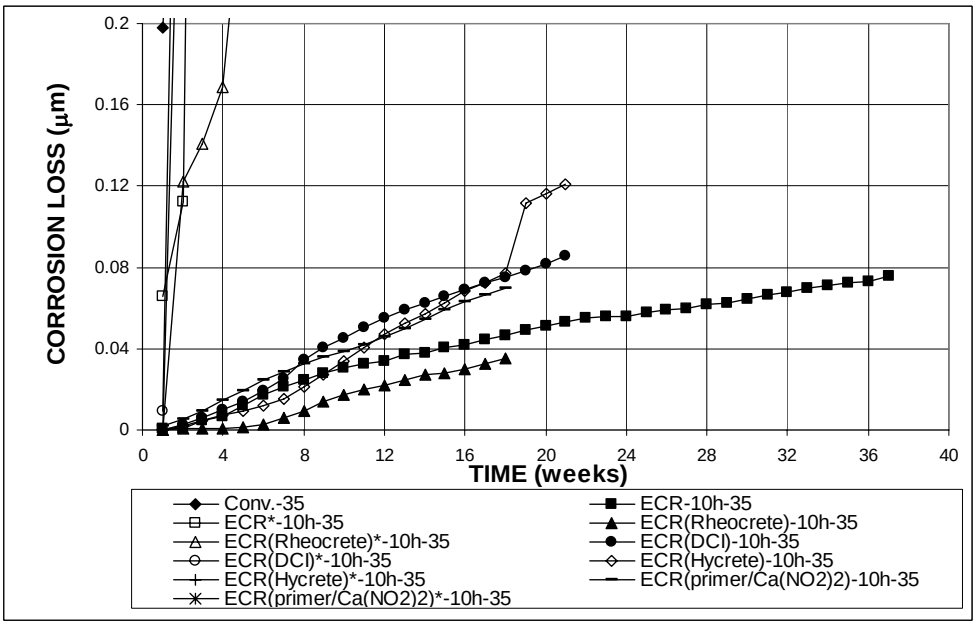

Figure 3.110 (b) – Cracked Beam Tests. Total Corrosion Loss. Specimens of conventional and epoxy-coated steel, epoxy-coated steel cast with corrosion inhibitors, and epoxy-coated steel with a calcium nitrite primer ponded with 15% NaCl solution. All epoxy-coated specimens with 10 drilled holes and a w/c ratio of 0.35. Refer to Table 3.10 for specimen identification.

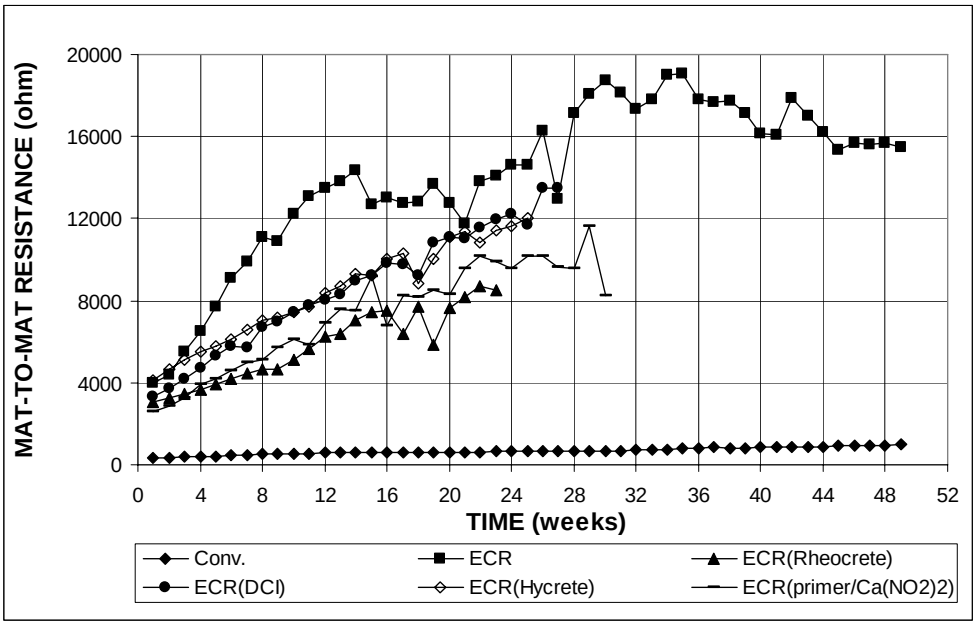

Figure 3.111 – Cracked Beam Tests. Mat-to-mat resistance. Specimens of conventional, conventional and epoxy-coated steel, epoxy-coated steel cast with corrosion inhibitors, and epoxy-coated steel with a calcium nitrite primer ponded with 15% NaCl solution. All epoxy-coated specimens with four drilled holes and a w/c ratio of 0.45. Refer to Table 3.9 for specimen identification.

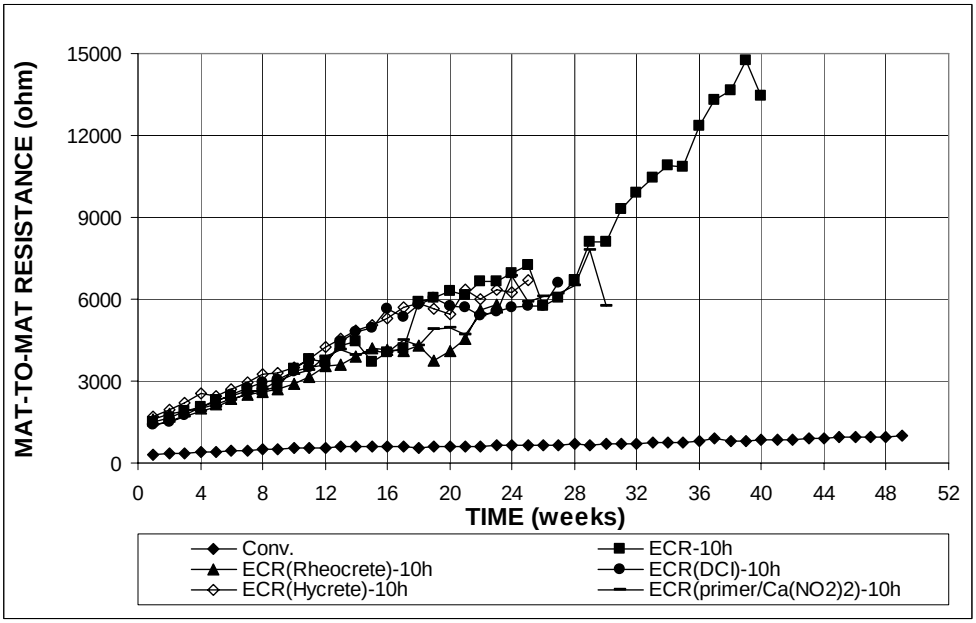

Figure 3.112 – Cracked Beam Tests. Mat-to-mat resistance. Specimens of conventional, conventional and epoxy-coated steel, epoxy-coated steel cast with corrosion inhibitors, and epoxy-coated steel with a calcium nitrite primer ponded with 15% NaCl solution. All epoxy-coated specimens with 10 drilled holes and a w/c ratio of 0.45. Refer to Table 3.9 for specimen identification.

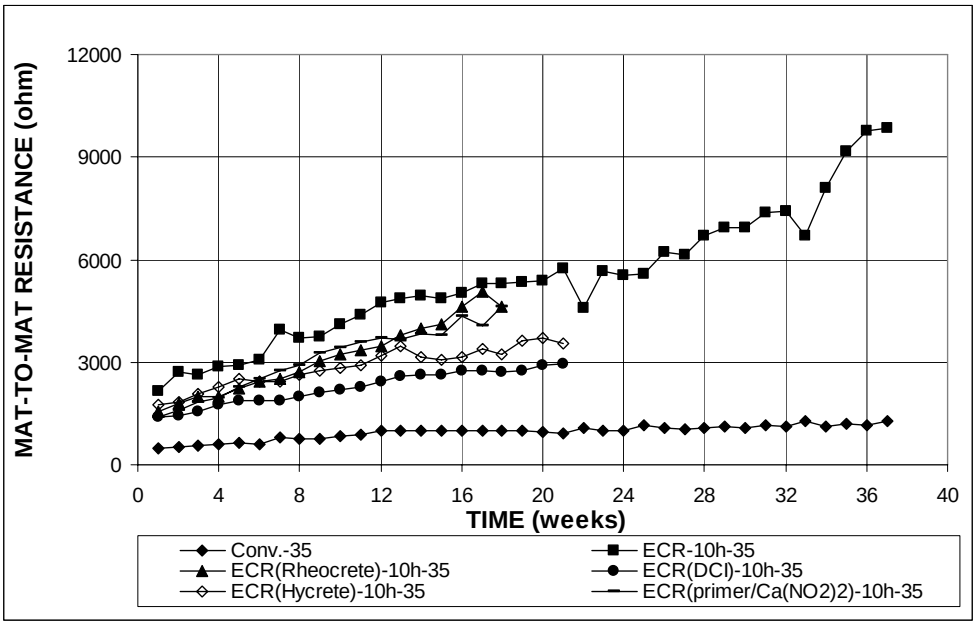

Figure 3.113 – Cracked Beam Tests. Mat-to-mat resistance. Specimens of conventional, conventional and epoxy-coated steel, epoxy-coated steel cast with corrosion inhibitors, and epoxy-coated steel with a calcium nitrite primer ponded with 15% NaCl solution. All epoxy-coated specimens with 10 drilled holes and a w/c ratio of 0.35. Refer to Table 3.9 for specimen identification.

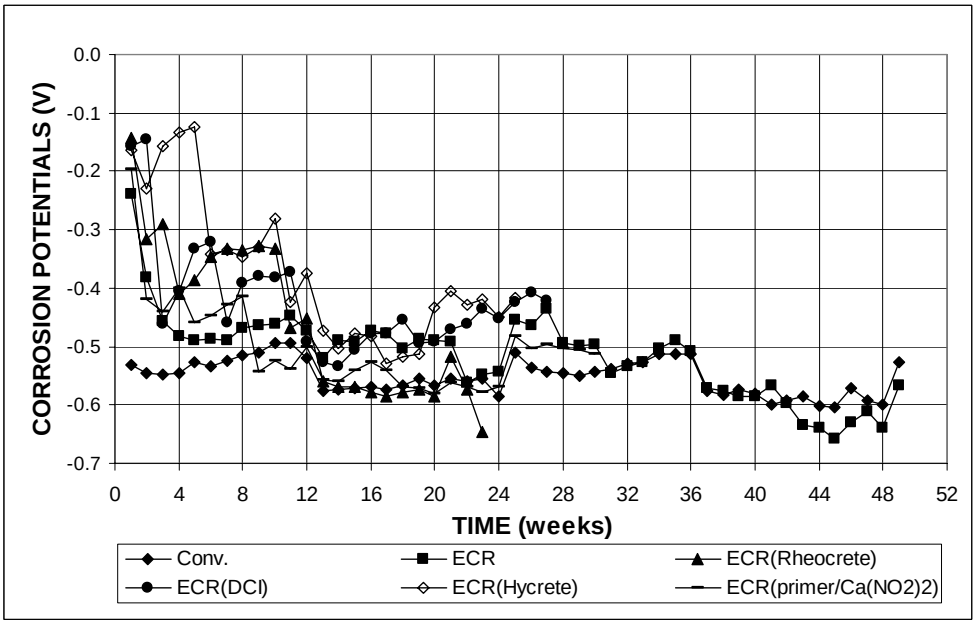

Figure 3.114 – Cracked Beam Tests. Corrosion Potential with respect to CSE at Top Mat. Specimens of conventional and epoxy-coated steel, epoxy-coated steel cast with corrosion inhibitors, and epoxy-coated steel with a calcium nitrite primer ponded with 15% NaCl solution. All epoxy-coated specimens with four drilled holes and a w/c ratio of 0.45. Refer to Table 3.9 for specimen identification.

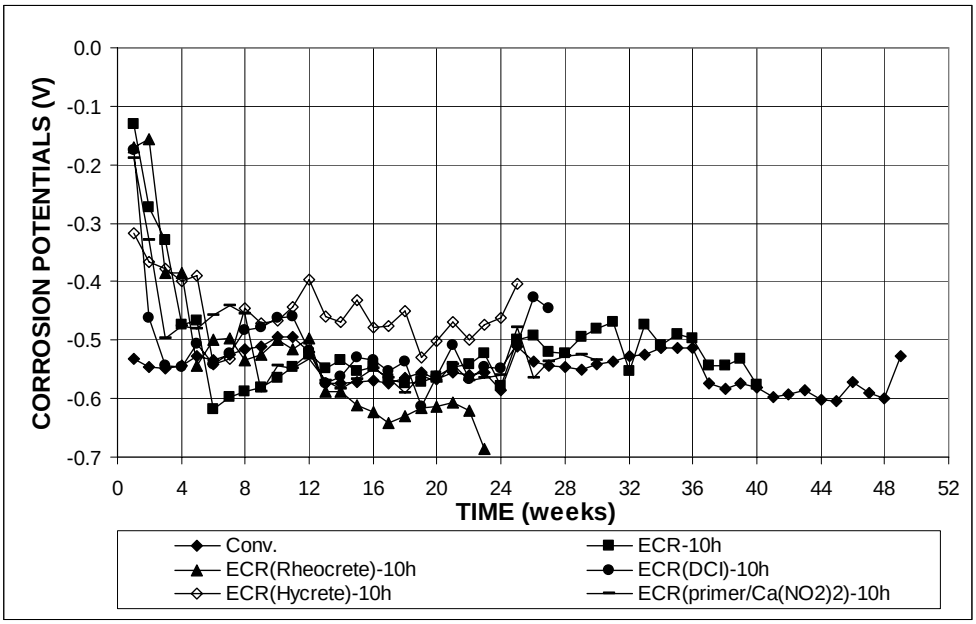

Figure 3.115 – Cracked Beam Tests. Corrosion Potential with respect to CSE at Top Mat. Specimens of conventional and epoxy-coated steel, epoxy-coated steel cast with corrosion inhibitors, and epoxy-coated steel with a calcium nitrite primer ponded with 15% NaCl solution. All epoxy-coated specimens with 10 drilled holes and a w/c ratio of 0.45. Refer to Table 3.9 for specimen identification.

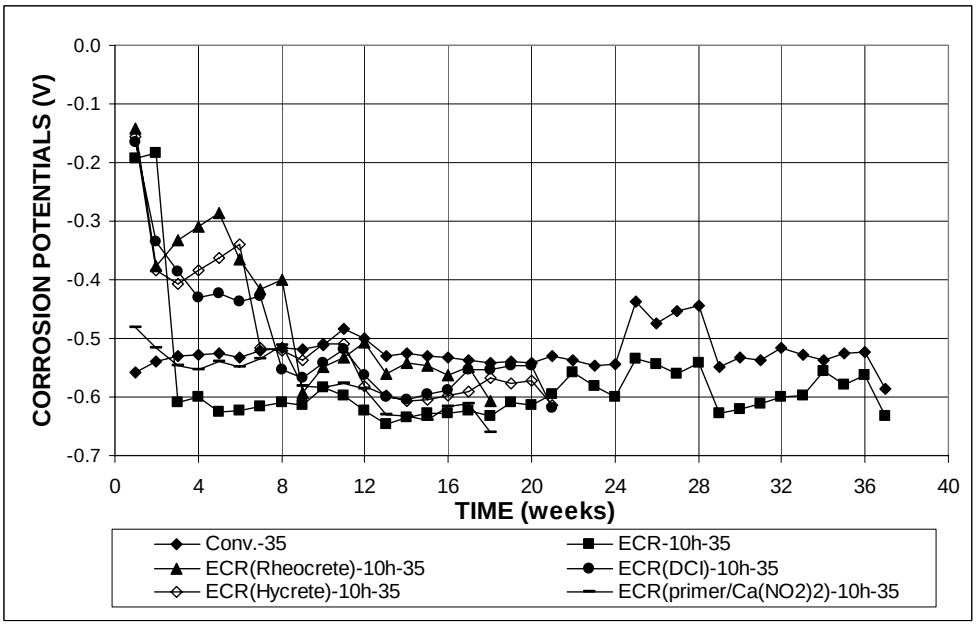

Figure 3.116 – Cracked Beam Tests. Corrosion Potential with respect to CSE at Top Mat. Specimens of conventional and epoxy-coated steel, epoxy-coated steel cast with corrosion inhibitors, and epoxy-coated steel with a calcium nitrite primer ponded with 15% NaCl solution. All epoxy-coated specimens with 10 drilled holes and a w/c ratio of 0.35. Refer to Table 3.9 for specimen identification.

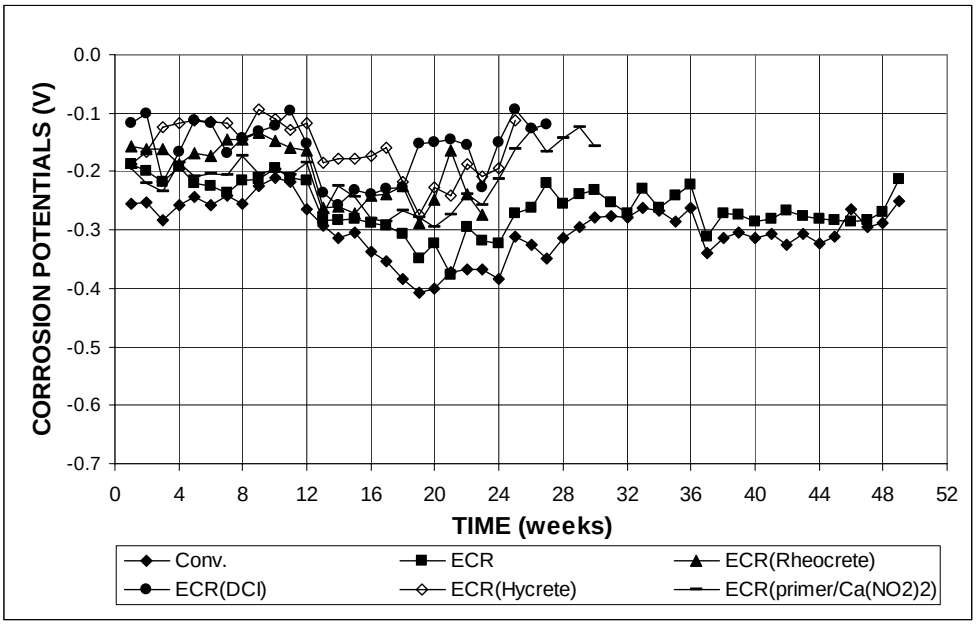

Figure 3.117 – Cracked Beam Tests. Corrosion Potential with respect to CSE at Bottom Mat. Specimens of conventional and epoxy-coated steel, epoxy-coated steel cast with corrosion inhibitors, and epoxy-coated steel with a calcium nitrite primer ponded with 15% NaCl solution. All epoxy-coated specimens with four drilled holes and a w/c ratio of 0.45. Refer to Table 3.9 for specimen identification.

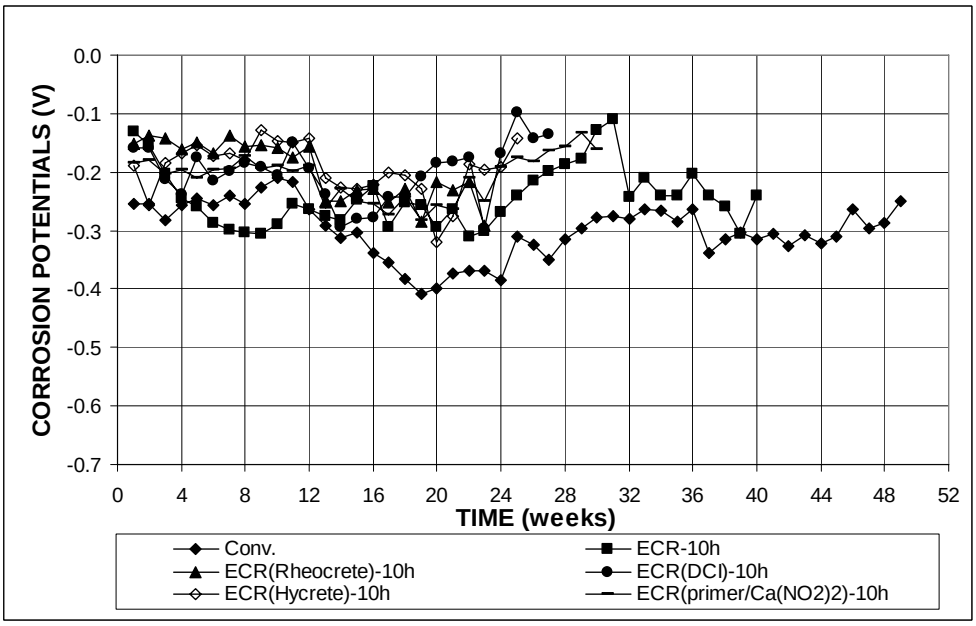

Figure 3.118 – Cracked Beam Tests. Corrosion Potential with respect to CSE at Bottom Mat. Specimens of conventional and epoxy-coated steel, epoxy-coated steel cast with corrosion inhibitors, and epoxy-coated steel with a calcium nitrite primer ponded with 15% NaCl solution. All epoxy-coated specimens with 10 drilled holes and a w/c ratio of 0.45. Refer to Table 3.9 for specimen identification.

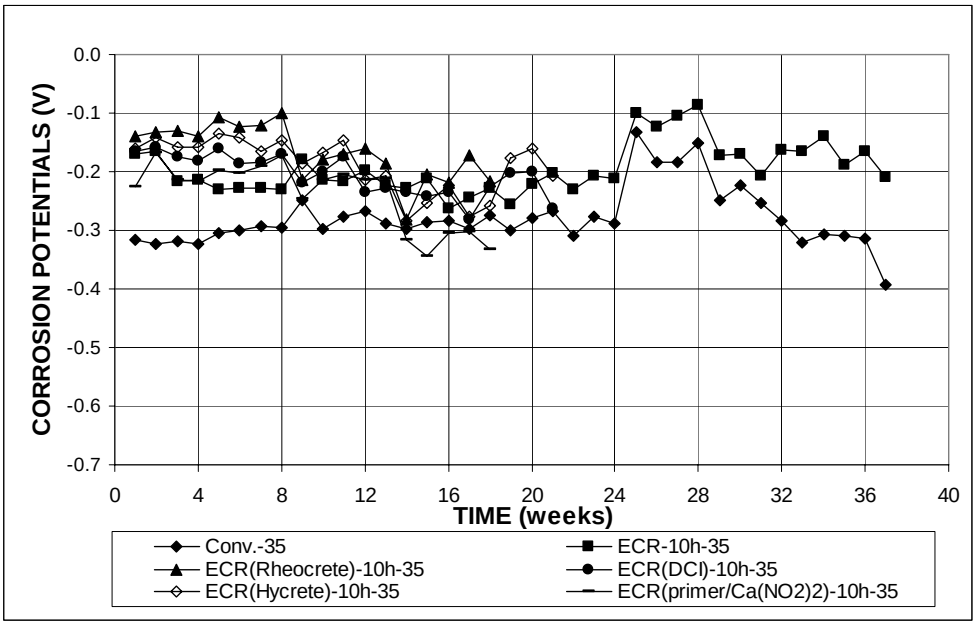

Figure 3.119 – Cracked Beam Tests. Corrosion Potential with respect to CSE at Bottom Mat. Specimens of conventional and epoxy-coated steel, epoxy-coated steel cast with corrosion inhibitors, and epoxy-coated steel with a calcium nitrite primer ponded with 15% NaCl solution. All epoxy-coated specimens with 10 drilled holes and a w/c ratio of 0.35. Refer to Table 3.9 for specimen identification.

3.5 MULTIPLE COATED REINFORCEMENT

In this section, the multiple coated reinforcement, which has a zinc layer underlying the epoxy layer, is evaluated using macrocell and bench scale tests. The corrosion rate and corrosion loss results are summarized in Tables 3.11 and 3.12.

3.5.1 Rapid Macrocell Test

Bare and mortar-wrapped specimens were used in the rapid macrocell tests. The epoxy coating on six bare and six mortar-wrapped specimens was penetrated with four 3.2-mm (1/8 in.) diameter holes without damaging the zinc layer. Both the epoxy and the zinc were penetrated on six other bare and mortar-wrapped specimens. Three

bare and three mortar-wrapped tests were performed on the bars in the “as delivered” condition.

3.5.1.1 Macrocell Tests for Bare Bar Specimens

The average corrosion rates and total corrosion losses for the multiple coated specimens (MC) in 1.6 m ion NaCl and simulated concrete pore solution are shown in Figures 3.120-3.123. Table 3.11 summarizes the average corrosion rates and corrosion losses at week 15. The corrosion rates and losses are calculated based on the characteristics of zinc for the MC specimens with only the epoxy penetrated and based on the characteristics of iron for the MC specimens with both layers penetrated. As used for the other coated specimens, an asterisk (*) is added to the specimen designation in the tables and figures where the corrosion rates and losses are based on the exposed area of holes in the coating. Based on the total area, the MC specimens with only the epoxy penetrated and with both layers penetrated showed corrosion rates that were 19% and 14 % of the corrosion rate of conventional epoxy-coated steel at week 15 (1.2 μm/yr) as shown in Figure 3.120, respectively, with maximum values of 0.58 μm/yr at week 11 and 0.34 μm/yr at day 4. The MC specimens with both layers penetrated exhibited a negative average corrosion rate from week 5 through week 10, indicating that some cathodes were corroding. This is due to the amphoteric nature of zinc, which results in corrosion in an alkaline environment. Based on the exposed area, the corrosion rates were 22 μm/yr and 16 μm/yr at week 15 for the MC specimens with only the epoxy penetrated and with both layers penetrated, respectively, with values as high as 60 μm/yr and 25 μm/yr during the test period. No corrosion rate higher than 0.05 μm/yr was detected on intact specimens (Figure 3.122).

Based on the total area, the average total corrosion losses (Figure 3.121) were 0.09 μm for the MC specimens with only the epoxy penetrated, 23% of the value for the conventional epoxy-coated steel (ECR), and 0.05 μm for the MC specimens with both layers penetrated, 13% of the value for the conventional ECR. Based on the exposed area, the values at 15 weeks were 9 and 5 μm for the MC specimens with only epoxy penetrated and with both layers penetrated, respectively. The MC specimens without drilled holes exhibited average corrosion losses of less than 0.005 μm (Figure 3.123).

The average corrosion potentials of the anodes and cathodes are shown in Figures 3.124 and 3.125, respectively. The corrosion potentials are measured with respect to a saturated calomel electrode. The MC specimens with both layers penetrated started with an anode potential of −1.200 V at the beginning of the test, which increased to −0.500 V at week 3, indicating that zinc around the drilled holes was protecting steel only during first few weeks. The MC specimens with only the epoxy penetrated started at a potential of −1.400 V, which gradually increased to −0.650 V at week 15, showing that the zinc at the drilled holes had largely corroded away during the test period. The cathode potentials were just slightly more positive than the anode potentials for the MC specimens, suggesting that the alkaline environment had a similar effect on the exposed portions of the bars.

Table 3.11 – Average corrosion rates and corrosion losses for multiple coated steel as measured in the macrocell tests

CORROSION RATE AT WEEK 15 (μm/year)

Steel Designation	Specimen						Average	Std. Deviation
	1	2	3	4	5	6		
Bare bar specimens								
MC (only epoxy penetrated)	0.19	0.14	0.34	0.14	0.29	0.24	0.22	0.08
MC (only epoxy penetrated)*	19.16	14.37	33.54	14.37	28.75	23.96	22.36	7.82
MC(both layers penetrated)	0	0.07	0.04	0.22	0.22	0.40	0.16	0.15
MC(both layers penetrated)*	0	7.32	3.66	21.96	21.96	40.26	15.86	15.12
MC-nh	0	0	0.04	-	-	-	0.01	0.02
Mortar-wrapped specimens								
MC (only epoxy penetrated)	0	0	0	0.14	0	0.05	0.03	0.02
MC (only epoxy penetrated)*	0	0	0	14.37	0	4.79	3.19	1.96
MC(both layers penetrated)	-0.04	-0.04	0.07	0.04	-0.11	-0.11	-0.03	0.07
MC(both layers penetrated)*	-3.66	-3.66	7.32	3.66	-10.98	-10.98	-3.05	7.41
MC-nh	0	0	0	-	-	-	0	0

TOTAL CORROSION LOSS AFTER WEEK 15 (μm)

Steel Designation	Specimen						Average	Std. Deviation
	1	2	3	4	5	6		
Bare bar specimens								
MC (only epoxy penetrated)	0.10	0.05	0.13	0.13	0.06	0.09	0.09	0.03
MC (only epoxy penetrated)*	10.13	4.51	12.9	12.99	5.62	8.66	9.14	3.41
MC(both layers penetrated)	0.10	0.10	0.04	0.03	0.01	0.04	0.05	0.04
MC(both layers penetrated)*	10.35	9.50	3.87	2.67	1.06	3.59	5.17	3.82
MC-nh	β	β	β	-	-	-	β	-
Mortar-wrapped specimens								
MC (only epoxy penetrated)	0.03	0.05	0.03	0.05	0.02	0.04	0.04	0.01
MC (only epoxy penetrated)*	3.22	4.61	2.67	4.79	2.21	4.42	3.65	0.83
MC(both layers penetrated)	β	β	0.02	β	0	β	β	0.01
MC(both layers penetrated)*	0.14	0.63	2.11	0.84	0	0.07	0.63	0.80
MC-nh	0	β	0	-	-	-	β	-

[1] MC(only epoxy penetrated): Multiple coated steel with epoxy layer penetrated, based on total area of bar exposed to solution

[2] MC(only epoxy penetrated)*: Multiple coated steel with epoxy layer penetrated, based on exposed area of four 3.2-mm (1/8-in.) diameter holes in epoxy

[3] MC(both layers penetrated): Multiple coated steel with both layers penetrated, based on total area of bar exposed to solution

[4] MC(both layers penetrated)*: Multiple coated steel with both layers penetrated, based on exposed area of four 3.2-mm (1/8-in.) diameter holes in epoxy

[5] MC-nh: Multiple coated steel without any drilled holes

[6] β: corrosion loss less than 0.01μm

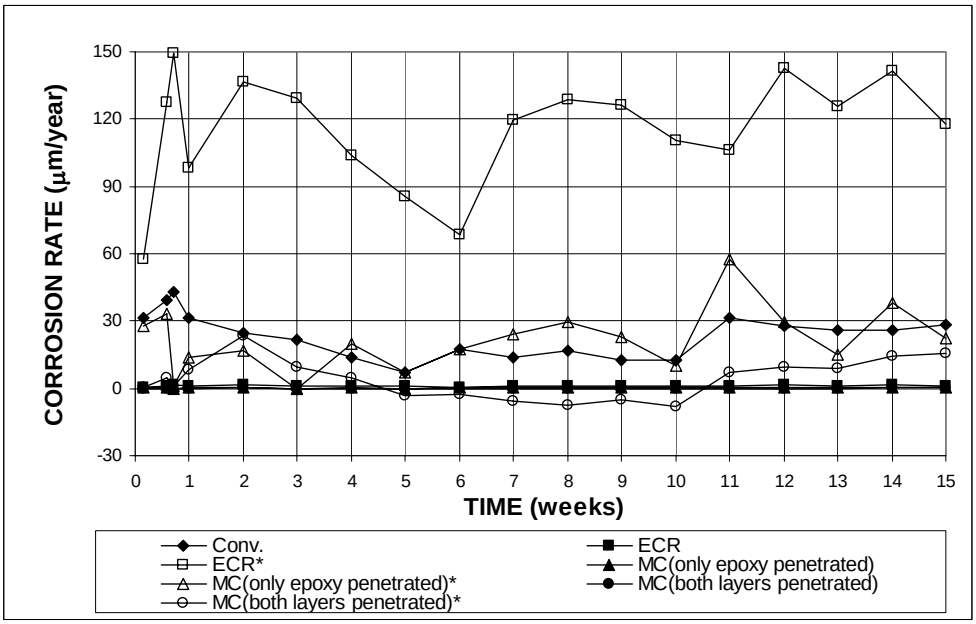

Figure 3.120 (a) – Macrocell Test. Average Corrosion Rate. Bare bar specimens of conventional, epoxy-coated, and multiple coated steel in simulated concrete pore solution with 1.6 m ion NaCl. Refer to Table 3.11 for specimen identification.

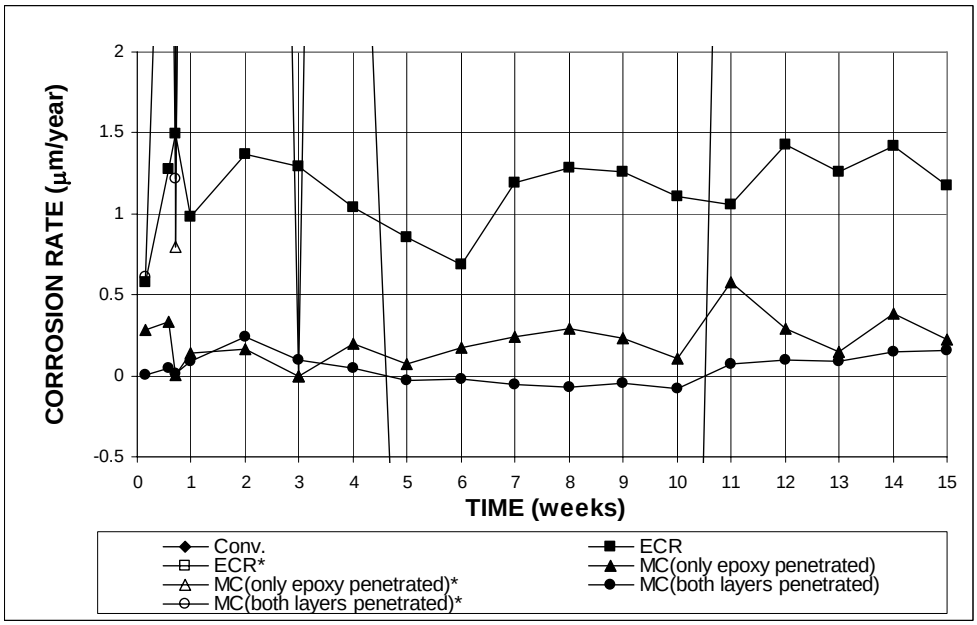

Figure 3.120 (b) – Macrocell Test. Average Corrosion Rate. Bare bar specimens of conventional, epoxy-coated, and multiple coated steel in simulated concrete pore solution with 1.6 m ion NaCl. Refer to Table 3.11 for specimen identification.

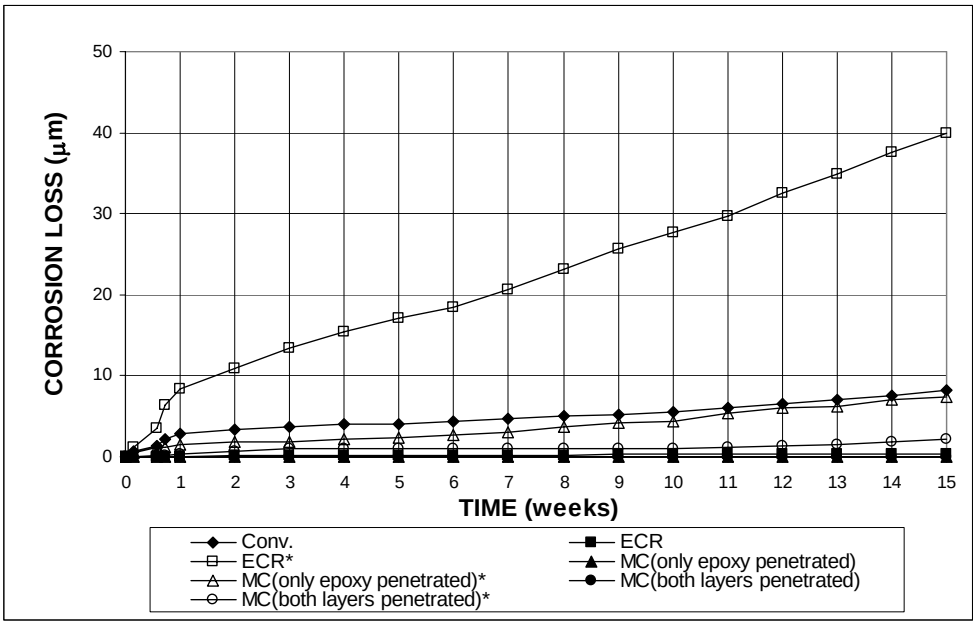

Figure 3.121 (a) – Macrocell Test. Total Corrosion Loss. Bare bar specimens of conventional, epoxy-coated, and multiple coated steel in simulated concrete pore solution with 1.6 m ion NaCl. Refer to Table 3.11 for specimen identification.

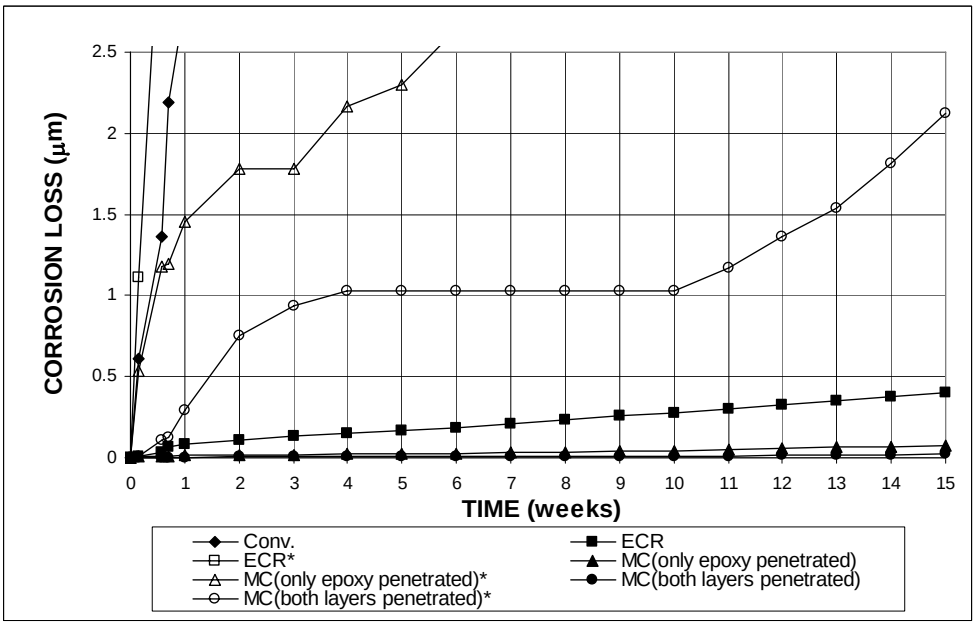

Figure 3.121 (b) – Macrocell Test. Total Corrosion Loss. Bare bar specimens of conventional, epoxy-coated, and multiple coated steel in simulated concrete pore solution with 1.6 m ion NaCl. Refer to Table 3.11 for specimen identification.

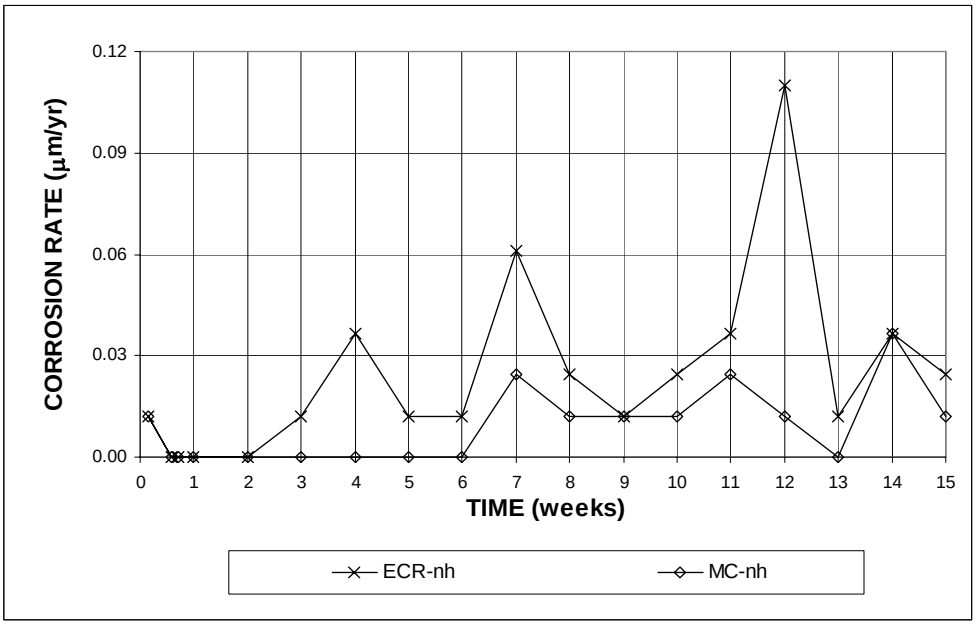

Figure 3.122 – Macrocell Test. Average Corrosion Rate. Bare bar specimens of multiple coated steel without drilled holes in simulated concrete pore solution with 1.6 m ion NaCl. Refer to Table 3.11 for specimen identification.

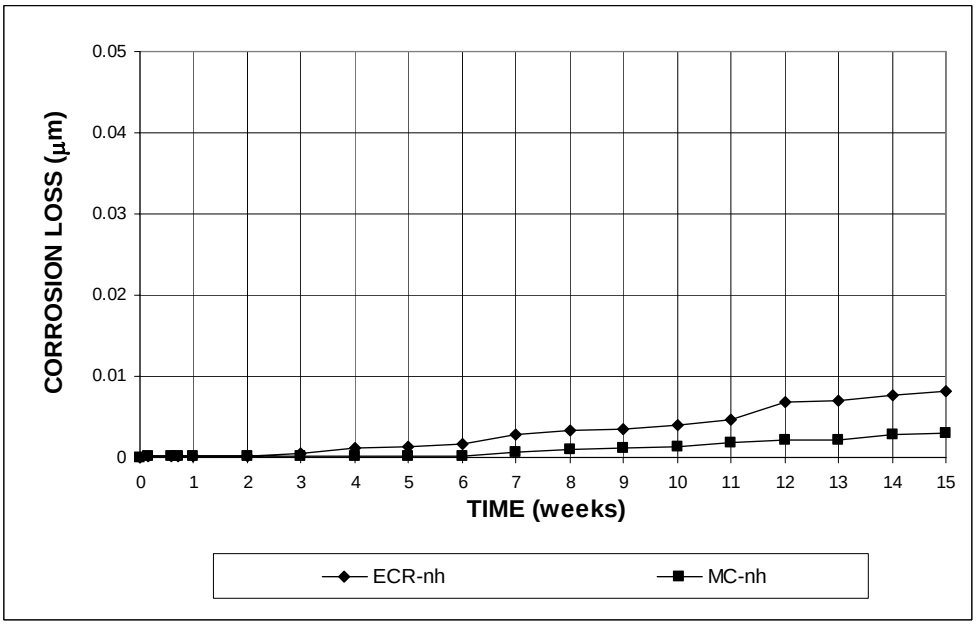

Figure 3.123 – Macrocell Test. Total Corrosion Loss. Bare bar specimens of multiple coated steel without drilled holes in simulated concrete pore solution with 1.6 m ion NaCl. Refer to Table 3.11 for specimen identification.

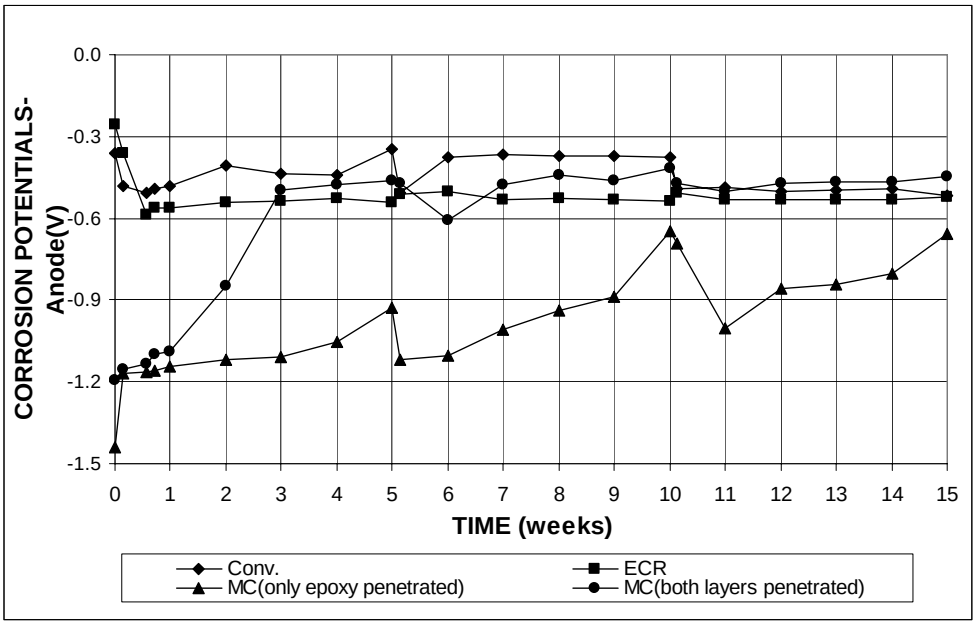

Figure 3.124 – Macrocell Test. Average Corrosion Potential with respect to SCE at anode. Bare bar specimens of conventional, epoxy-coated, and multiple coated steel in simulated concrete pore solution with 1.6 m ion NaCl. Refer to Table 3.11 for specimen identification.

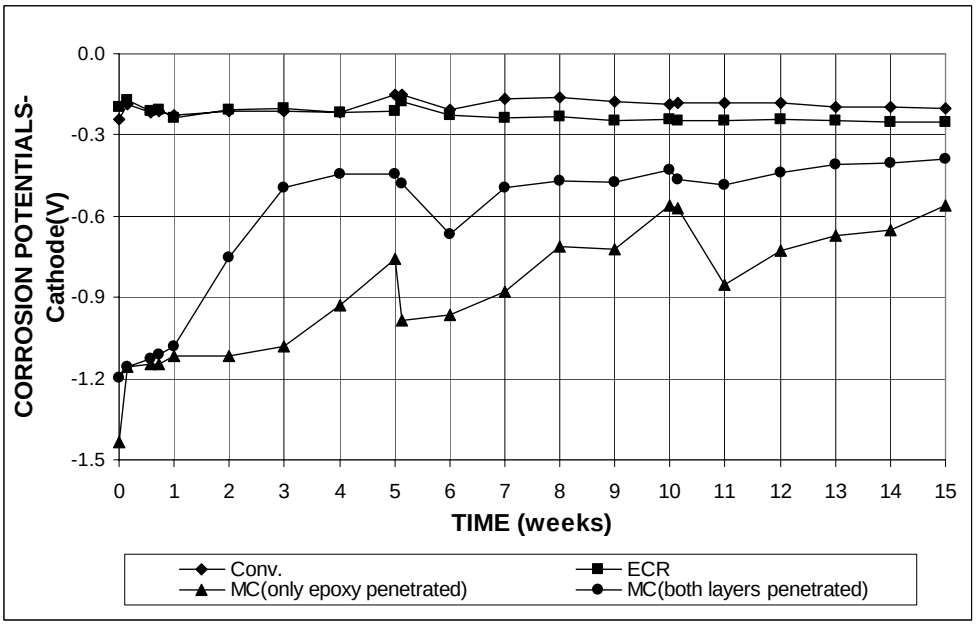

Figure 3.125 – Macrocell Test. Average Corrosion Potential with respect to SCE at cathode. Bare bar specimens of conventional, epoxy-coated, and multiple coated steel in simulated concrete pore solution with 1.6 m ion NaCl. Refer to Table 3.11 for specimen identification.

3.5.1.2 Macrocell Tests for Mortar-Wrapped Specimens

Average corrosion rates and total corrosion losses for mortar-wrapped specimens with multiple coated steel (MC) in simulated concrete pore solution with 1.6 m ion NaCl are shown in Figures 3.126-3.129. Table 3.11 summarizes the average corrosion rates and corrosion losses at week 15. Based on the bar total area exposed to the solution, the MC specimens with only the epoxy penetrated had an average corrosion rate that started higher than 0.1 μm/yr, reaching a maximum value of 0.39 μm/yr at week 5, then dropping below 0.04 μm/yr after week 6, and ending at 0.03 μm/yr at week 15. The MC specimens with both layers penetrated exhibited negative corrosion rates beginning with week 2 and ending at −0.03 μm/yr at week 15. The negative corrosion rates indicate that some of the cathodes of the MC specimens with both layers penetrated were undergoing corrosion, as can be demonstrated by Figure A.230, which shows that two cathodes exhibited active corrosion. These corrosion rates are similar to that exhibited by conventional epoxy-coated steel (0.02 μm/yr). Based on the exposed area, corrosion rates at 15 weeks translate to 3 μm/yr and −3 μm/yr for the MC specimens with only the epoxy penetrated and with both layers penetrated, respectively. Insignificant corrosion with a rate less than 0.005 μm/yr was observed on the undamaged specimens.

Based on the total area, the average total corrosion loss at the anodes is 0.04 μm for the specimens with only the epoxy penetrated, which is higher than the value for conventional epoxy-coated steel (ECR) (less than 0.01 μm), and less than 0.01 μm for the MC specimens with both layers penetrated, when the negative corrosion loss is not included. Based on the exposed area, the values were 3.65 μm for the MC specimens with only the epoxy penetrated and 0.63 μm for the MC specimens with

both layers penetrated. As shown in Figures 3.128 and 3.129, the MC specimens without drilled holes did not exhibit noticeable corrosion loss.

The average corrosion potentials of both anode and cathode are shown in Figures 3.130 and 3.131, respectively. The MC specimens with both layers penetrated started with an anode potential of −0.600 V and stabilized at about −0.700 V after week 5, indicating that salt had penetrated the mortar and the zinc around the drilled holes served as a sacrificial anode, protecting the steel. The MC specimens with only the epoxy penetrated started at a more positive value (−0.400 V), which gradually decreased to −0.700 V at week 15, showing that exposed zinc was corroding. For the cathode potentials, the MC specimens with both layers penetrated began at −0.500 V and slowly dropped to −0.800 V over 15 weeks; the MC specimens with only the epoxy penetrated started at around −0.340 V and dropped to −0.600 V at week 15.

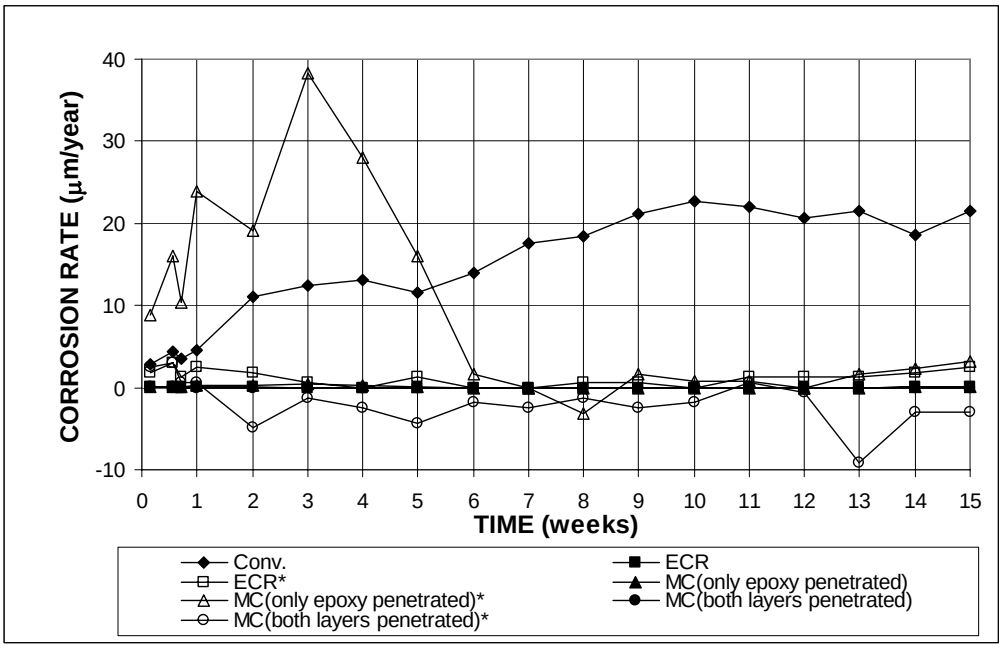

Figure 3.126 (a) – Macrocell Test. Average Corrosion Rate. Mortar-wrapped specimens of conventional, epoxy-coated, and multiple coated steel in simulated concrete pore solution with 1.6 m ion NaCl. Refer to Table 3.11 for specimen identification.

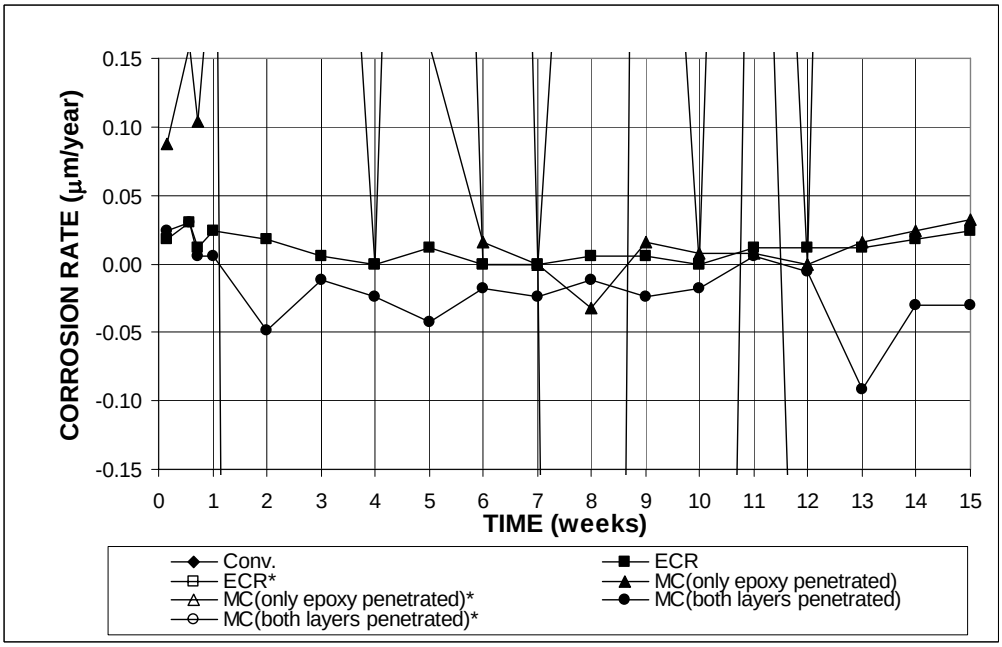

Figure 3.126 (b) – Macrocell Test. Average Corrosion Rate. Mortar-wrapped specimens of conventional, epoxy-coated, and multiple coated steel in simulated concrete pore solution with 1.6 m ion NaCl. Refer to Table 3.11 for specimen identification.

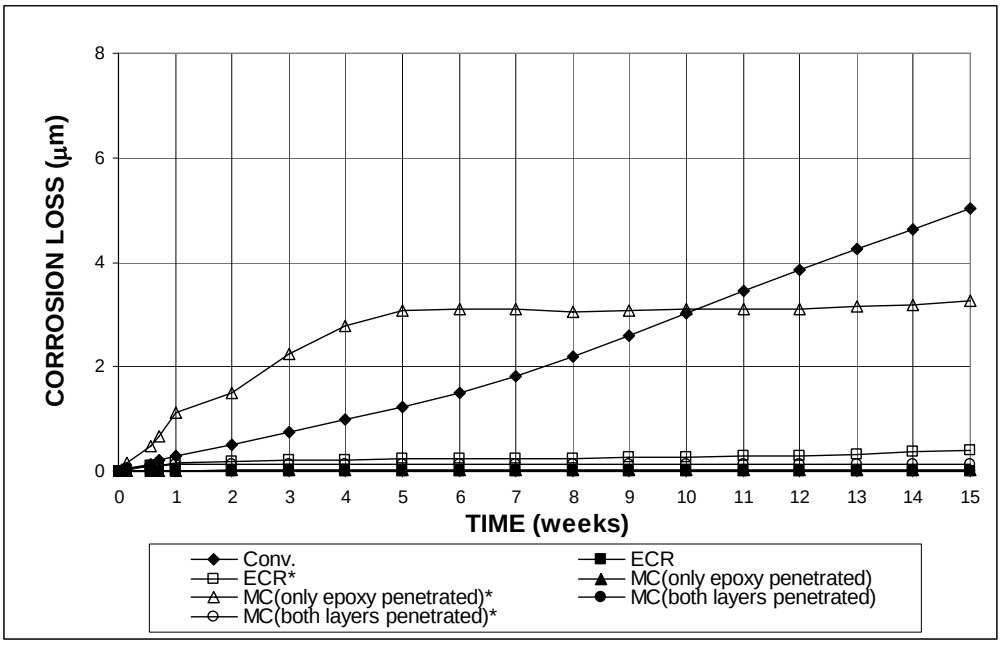

Figure 3.127 (a) – Macrocell Test. Total Corrosion Loss. Mortar-wrapped specimens of conventional, epoxy-coated, and multiple coated steel in simulated concrete pore solution with 1.6 m ion NaCl. Refer to Table 3.11 for specimen identification.

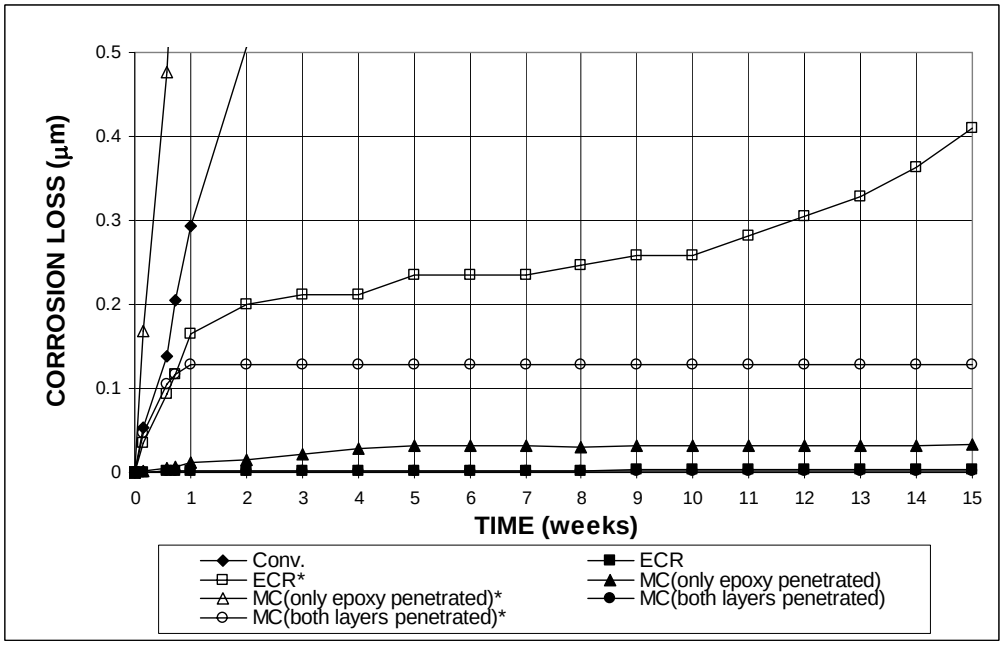

Figure 3.127 (b) – Macrocell Test. Total Corrosion Loss. Mortar-wrapped specimens of conventional, epoxy-coated, and multiple coated steel in simulated concrete pore solution with 1.6 m ion NaCl. Refer to Table 3.11 for specimen identification.

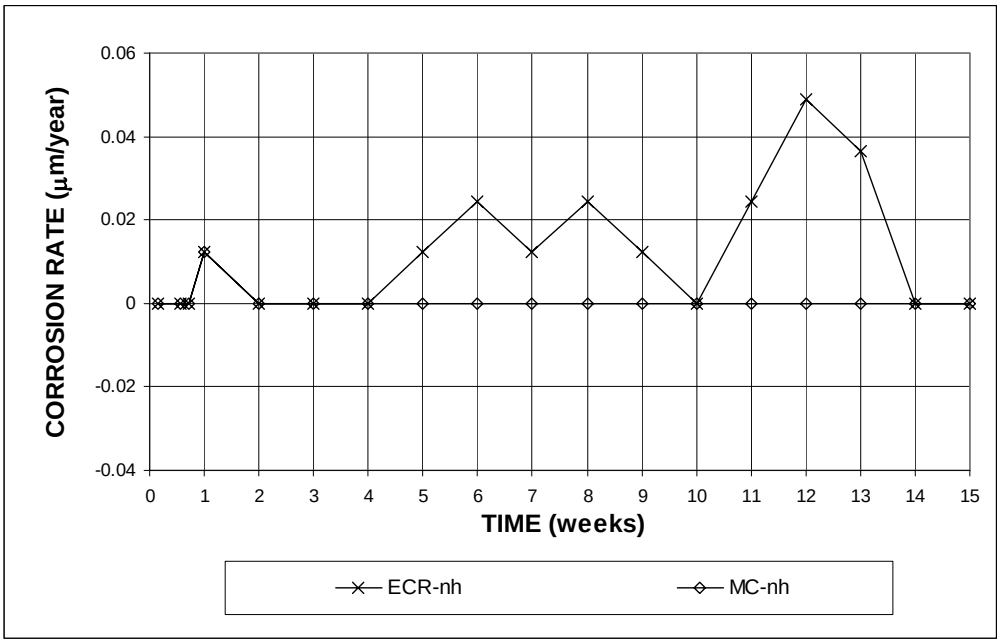

Figure 3.128 – Macrocell Test. Average Corrosion Rate. Mortar-wrapped specimens of multiple coated steel without drilled holes in simulated concrete pore solution with 1.6 m ion NaCl. Refer to Table 3.11 for specimen identification.

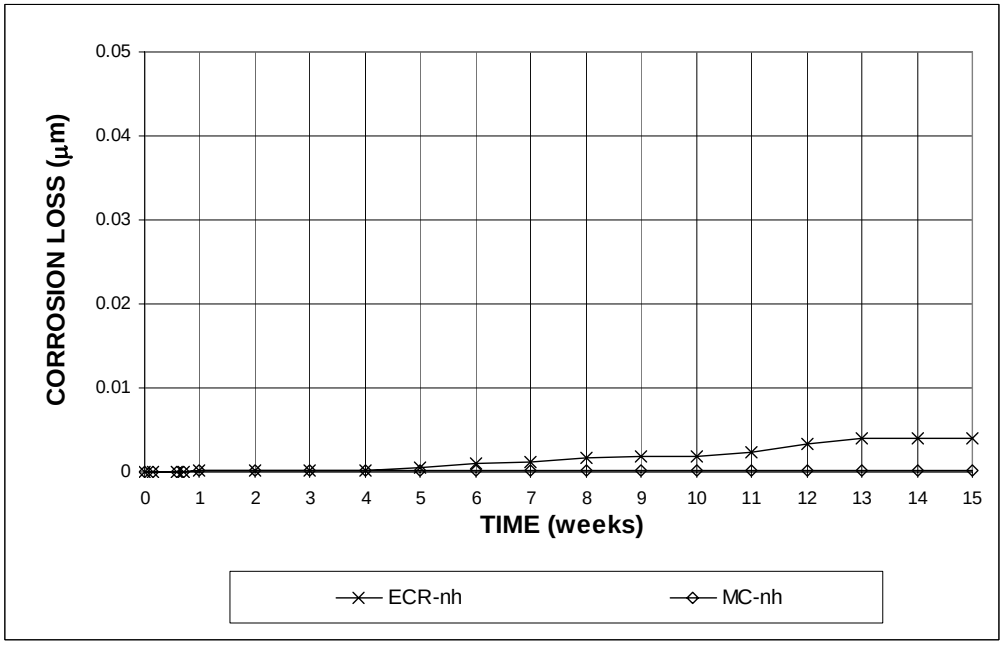

Figure 3.129 – Macrocell Test. Total Corrosion Loss. Mortar-wrapped specimens of multiple coated steel without drilled holes in simulated concrete pore solution with 1.6 m ion NaCl. Refer to Table 3.11 for specimen identification.

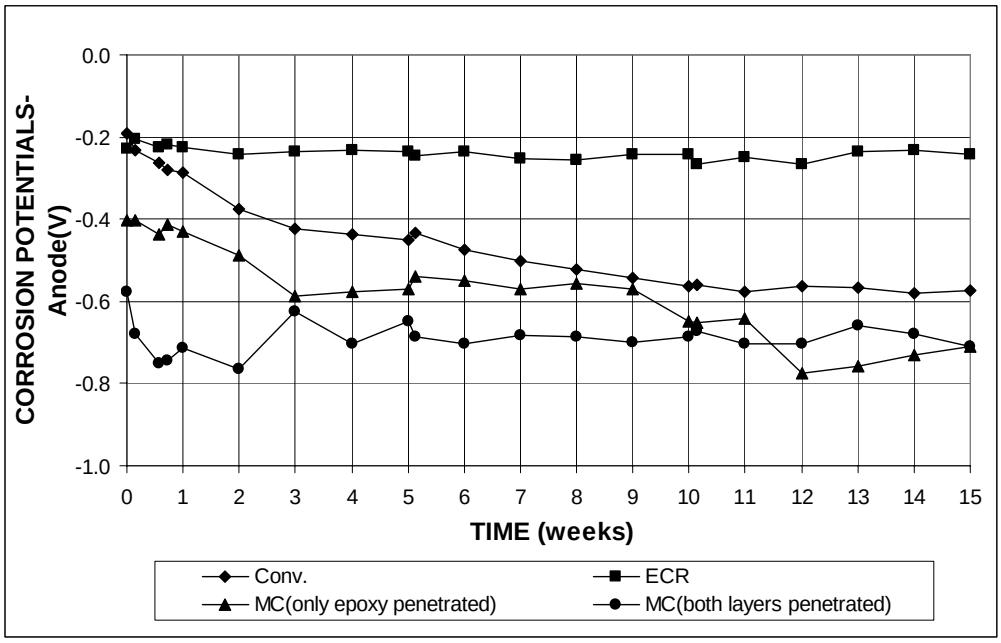

Figure 3.130 – Macrocell Test. Average Corrosion Potential with respect to SCE at Anode. Mortar-wrapped specimens of conventional, epoxy-coated, and multiple coated steel in simulated concrete pore solution with 1.6 m ion NaCl. Refer to Table 3.11 for specimen identification.

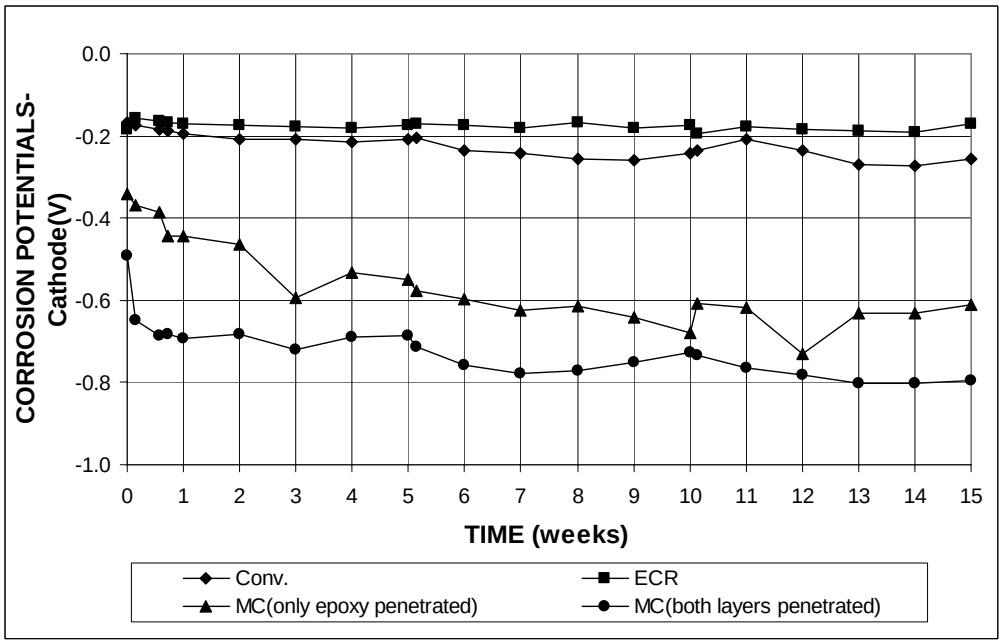

Figure 3.131 – Macrocell Test. Average Corrosion Potential with respect to SCE at Cathode. Mortar-wrapped specimens of conventional, epoxy-coated, and multiple coated steel in simulated concrete pore solution with 1.6 m ion NaCl. Refer to Table 3.11 for specimen identification.

3.5.1.3 Visual Inspection

As the tests were discontinued, the specimens were visually inspected. For the bare multiple coated steel with either the epoxy penetrated or both layers penetrated, corrosion products were observed at holes through the coating. Figure 3.132 shows a multiple coated bar with corrosion products that have formed on the holes with epoxy penetrated. Figure 3.133 shows a multiple coated bar with corrosion products at the holes when both layers penetrated.

For mortar-wrapped specimens, the specimens were broken and no obvious corrosion products were found on the bars.

Figure 3.132 – Bare MC anode bar with only epoxy penetrated, at 15 weeks, showing corrosion products that formed at drilled holes

Figure 3.133 – Bare MC anode bar with both layers penetrated, at 15 weeks, showing corrosion products that formed at drilled holes

3.5.2 Bench-Scale Tests

The average corrosion rates and total corrosion losses as of March 15, 2005 for the Southern Exposure, cracked beam, and ASTM G 109 tests are summarized in Table 3.12. Results for individual specimens are presented in Appendix A.

3.5.2.1 Southern Exposure Tests

The Southern Exposure tests include three specimens each for multiple coated reinforcement (MC) with only the epoxy or with both the epoxy and the zinc layers penetrated by four or 10 holes for a total of twelve specimens. Average corrosion rates, total corrosion losses, mat-to-mat resistances, and corrosion potentials are shown in Figures 3.134 - 3.140. As with the macrocell tests, the corrosion rates and losses are calculated based on the characteristics of zinc for the MC specimens with only the epoxy penetrated and based on the characteristics of iron for the MC specimens with both layers penetrated. The results (summarized in Table 3.12) show that the MC specimens with only the epoxy penetrated by four holes (Figure 3.134) exhibited average corrosion rates below 0.01 μm/yr through 14 weeks based on the total area and below 2.5 μm/yr based on the exposed area, slightly lower than that of the conventional ECR specimens during the first 14 weeks. For the MC bars with both layers penetrated by four holes (Figure 3.134), the average corrosion rate based on the total area increased from below 0.01 μm/yr to above 0.04 μm/yr following week 9, reaching a maximum value of 0.1 μm/yr at week 12, and dropping to 0.08 μm/yr at week 14. The rate is higher than that of the conventional ECR specimens after week 8. Based on the exposed area, the corrosion rate of the MC specimens with both layers penetrated by four holes was 39 μm/yr, equal to 13 times higher than the rate for the conventional ECR specimens at week 14.

The MC specimens with the epoxy penetrated by 10 holes (Figure 3.135) showed noticeable corrosion following week 15, at a rate of 0.06 μm/yr at week 16 based on total area and 11 μm/yr based on the exposed area. The corrosion rate of the MC specimens with both layers penetrated by 10 holes, based on total area, jumped from below 0.01 μm/yr to 0.042 μm/yr at week 8, and reaching a value as high as 0.14 μm/yr at week 16. Both rates were higher than the value of the conventional ECR specimens at the data cutoff date.

For the specimens with four holes (Figures 3.136), the MC specimens with both layers penetrated exhibited the highest corrosion loss based on either the total or the exposed area, followed by the conventional ECR specimens and the MC specimens with only the epoxy penetrated, at week 14. The average losses were all less than 0.01 μm when based on total area, and 3.6, 1.2, and 0.3 μm when based on the exposed area for the MC specimens with both layers penetrated, the conventional ECR specimens, and the MC specimens with only the epoxy penetrated, respectively. For the specimens damaged with 10 holes (Figure 3.137), the MC specimens with both layers penetrated by 10 holes reached a corrosion loss of 0.01 μm based on total area (2.7 μm based on the exposed area) at week 16, while the MC specimens with only the epoxy penetrated and conventional ECR specimens exhibited corrosion losses less than 0.01 μm based on the total area (0.8 and 0.7 μm based on the exposed area, respectively).

The resistances between top and bottom mats are shown in Figure 3.138. The MC specimens with four holes showed average mat-to-mat resistances starting from 2,000 ohms and increasing to over 6,000 ohms, higher than that measured for the conventional ECR specimens at week 14 (4900 ohms). The MC and conventional ECR specimens with 10 holes exhibited lower resistances, initially around 800 ohms

and rising close to 2,600 ohms for the MC specimens with only the epoxy penetrated and 1,700 ohms for both the MC specimens with both layers penetrated and the conventional ECR specimens.

The average corrosion potentials of the top and bottom mats are shown in Figures 3.139 and 3.140, respectively. With respect to a copper copper-sulfate electrode, values more negative than −0.596 V indicate active corrosion of zinc. For the top mat, the MC specimens with both layers penetrated with four holes started with a potential more negative than −0.400 V in the first week, a value that jumped above −0.400 V at week 3 but dropped down again after week 5, reaching –0.568 V at week 14. The MC specimens with only the epoxy penetrated by 10 holes also started at a value more negative than –0.400 V, and increased to above -0.400 V at week 3 but dropped to –0.609 V at week 16. The other MC specimens (both layers penetrated by 10 holes and only the epoxy penetrated by four holes) started at potentials around –0.300 V, which dropped below –0.400 V at the data cutoff date. The conventional ECR specimens had more positive potentials, which were around –0.200 V, than the MC specimens at the same period of time. For the bottom mats, the MC specimens with only the epoxy penetrated by four or 10 holes started at around or below −0.400 V and increased with time to above −0.350 V at the data cutoff date. The MC specimens with both layers penetrated by four holes began at −0.260 V, which increased to around –0.200 V in week 2, dropping to −0.270 V at week 14. The MC specimens with both layers penetrated by 10 holes and the conventional ECR specimens exhibited corrosion potentials around −0.200 V for the first 16 weeks.

Table 3.12 – Average corrosion rates for multiple coated steel as measured in the bench-scale tests

CORROSION RATE (μm/year)

Specimen Designation	Exposure Time (weeks)	Specimen			Average	Std. Deviation
		1	2	3		
Southern Exposure Specimens						
MC (only epoxy penetrated)	14	α	α	0	α	-
MC (only epoxy penetrated)*	14	2.36	2.36	0	1.57	1.36
MC (only epoxy penetrated)-10h	16	0	0.02	0.15	0.06	0.08
MC (only epoxy penetrated)*-10h	16	0	4.73	28.35	11.03	15.19
MC(both layers penetrated)	14	0	0	0.24	0.08	0.14
MC(both layers penetrated)*	14	0	0	117.12	39.04	67.62
MC(both layers penetrated)-10h	16	0.02	0.19	0.19	0.14	0.10
MC(both layers penetrated)*-10h	16	3.66	37.33	37.33	26.11	19.44
Cracked Beam Specimens						
MC (only epoxy penetrated)	14	0	0.05	0.16	0.07	0.08
MC (only epoxy penetrated)*	14	0	23.61	75.54	33.05	38.64
MC (only epoxy penetrated)-10h	16	0.05	0.10	0.30	0.15	0.13
MC (only epoxy penetrated)*-10h	16	9.45	18.9	56.7	28.35	25
MC(both layers penetrated)	14	0.11	0.02	α	0.05	0.06
MC(both layers penetrated)*	14	54.9	10.98	3.66	23.18	27.71
MC(both layers penetrated)-10h	16	0.14	0.79	0.14	0.36	0.38
MC(both layers penetrated)*-10h	16	26.35	152.26	27.82	68.81	72.27
ASTM G 109 Specimens						
MC (only epoxy penetrated)	48	α	α	0	α	-
MC (only epoxy penetrated)*	48	0.47	0.47	0	0.31	0.27
MC (only epoxy penetrated)-10h	45	0	0	α	α	-
MC (only epoxy penetrated)*-10h	45	0	0	0.19	0.06	0.11
MC(both layers penetrated)	48	0	0	α	α	-
MC(both layers penetrated)*	48	0	0	0.47	0.16	0.27
MC(both layers penetrated)-10h	45	0	0	0	0	0
MC(both layers penetrated)*-10h	45	0	0	0	0	0

CORROSION LOSS (μm)

Specimen Designation	Exposure Time (weeks)	Specimen			Average	Std. Deviation
		1	2	3		
Southern Exposure Specimens						
MC (only epoxy penetrated)	14	β	β	β	β	-
MC (only epoxy penetrated)*	14	0.73	0.14	0.09	0.32	0.35
MC (only epoxy penetrated)-10h	16	β	β	0.01	β	-
MC (only epoxy penetrated)*-10h	16	0.02	0.58	1.74	0.78	0.88
MC(both layers penetrated)	14	β	β	0.02	β	0.01
MC(both layers penetrated)*	14	0.39	0.25	10.1	3.58	5.65
MC(both layers penetrated)-10h	16	β	0.03	0.01	0.01	0.01
MC(both layers penetrated)*-10h	16	0.77	5.46	1.96	2.73	2.44
Cracked Beam Specimens						
MC (only epoxy penetrated)	14	0.01	0.01	0.06	0.03	0.03
MC (only epoxy penetrated)*	14	5.45	5.36	30.01	13.6	14.21
MC (only epoxy penetrated)-10h	16	0.04	0.06	0.07	0.05	0.01
MC (only epoxy penetrated)*-10h	16	7.67	11.01	12.5	10.4	2.48
MC(both layers penetrated)	14	0.04	0.03	0.04	0.04	0.01
MC(both layers penetrated)*	14	19.78	14.99	20.13	18.3	2.87
MC(both layers penetrated)-10h	16	0.06	0.17	0.06	0.10	0.07
MC(both layers penetrated)*-10h	16	12.19	33.36	10.92	18.83	12.61
ASTM G 109 Specimens						
MC (only epoxy penetrated)	48	β	β	β	β	-
MC (only epoxy penetrated)*	48	0.83	1.13	1.24	1.07	0.22
MC (only epoxy penetrated)-10h	45	β	β	β	β	-
MC (only epoxy penetrated)*-10h	45	0.32	0.31	0.55	0.39	0.14
MC(both layers penetrated)	48	β	β	β	β	-
MC(both layers penetrated)*	48	0.86	0.90	0.94	0.9	0.04
MC(both layers penetrated)-10h	45	β	β	β	β	-
MC(both layers penetrated)*-10h	45	0.26	0.30	0.19	0.25	0.05

Table 3.12 continued:

[1] MC(only epoxy penetrated): Multiple coated steel with epoxy layer penetrated, based on total area of bar exposed to solution

[2] MC(only epoxy penetrated)*: Multiple coated steel with epoxy layer penetrated, based on exposed area of four 3.2-mm (1/8-in.) diameter holes in epoxy

[3] MC(both layers penetrated): Multiple coated steel with both layers penetrated, based on total area of bar exposed to solution

[4] MC(both layers penetrated)*: Multiple coated steel with both layers penetrated, based on exposed area of four 3.2-mm (1/8-in.) diameter holes in epoxy

[5] MC(only epoxy penetrated)-10h: Multiple coated steel with epoxy layer penetrated by ten holes, based on total area of bar exposed to solution

[6] MC(only epoxy penetrated)*-10h: Multiple coated steel with epoxy layer penetrated by ten holes, based one xposed area of ten holes in epoxy

[7] MC(both layers penetrated)-10h: Multiple coated steel with both layers penetrated by ten holes, based on total area of bar exposed to solution

[8] MC(only epoxy penetrated)*-10h: Multiple coated steel with both layers penetrated by ten holes, based on exposed area of ten holes in epoxy

[9] α: corrosion rate less than 0.01 μm/yr

[10] β: corrosion loss less than 0.01μm

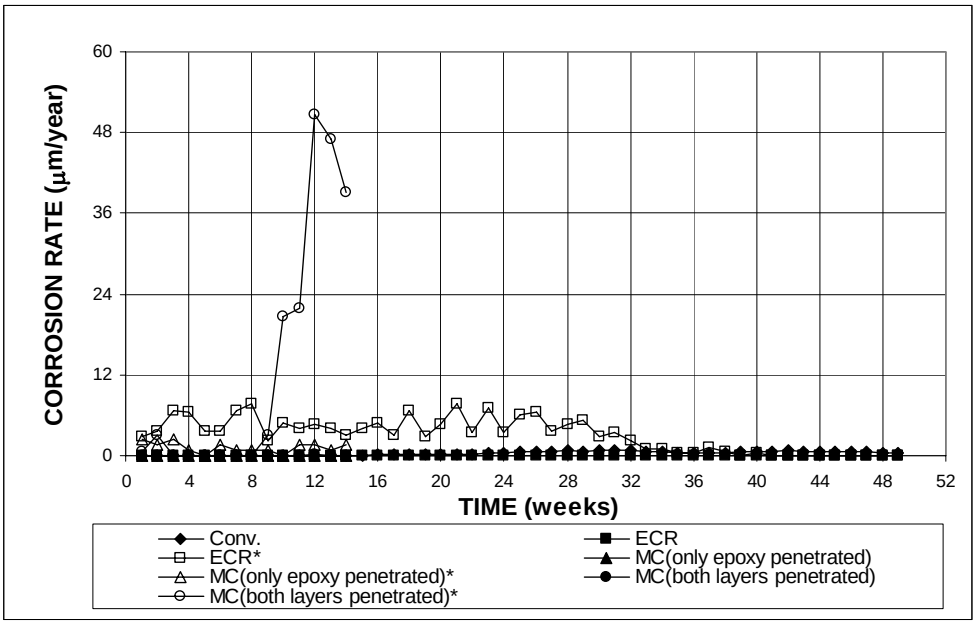

Figure 3.134 (a) – Southern Exposure Tests. Average Corrosion Rate. Specimens of conventional, epoxy-coated, and multiple coated reinforcement ponded with 15% NaCl solution. Epoxy and multiple coating penetrated with four holes. Refer to Table 3.12 for specimen identification.

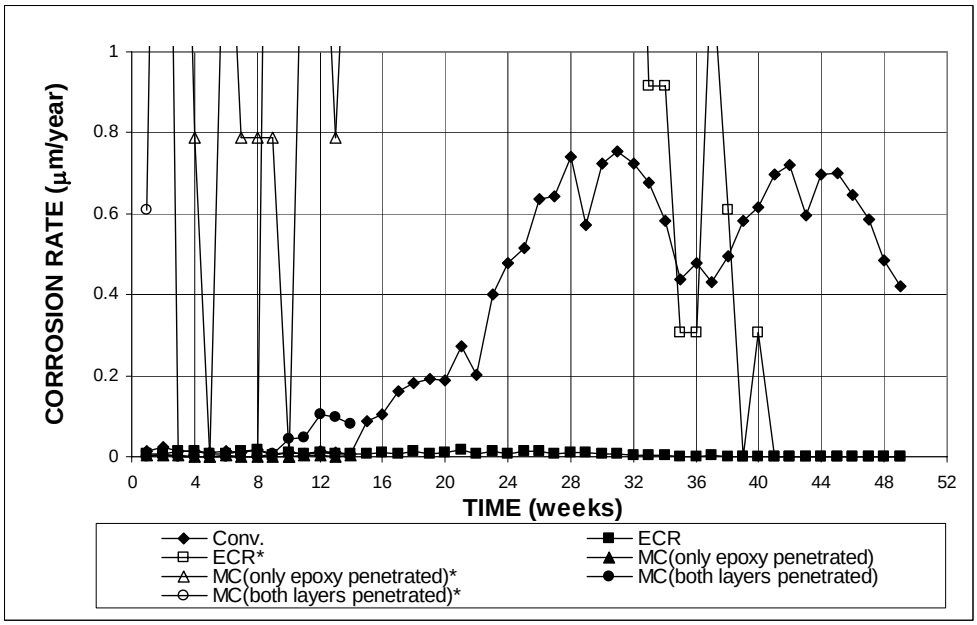

Figure 3.134 (b) – Southern Exposure Tests. Average Corrosion Rate. Specimens of conventional, epoxy-coated, and multiple coated reinforcement ponded with 15% NaCl solution. Epoxy and multiple coating penetrated with four holes. Refer to Table 3.12 for specimen identification.

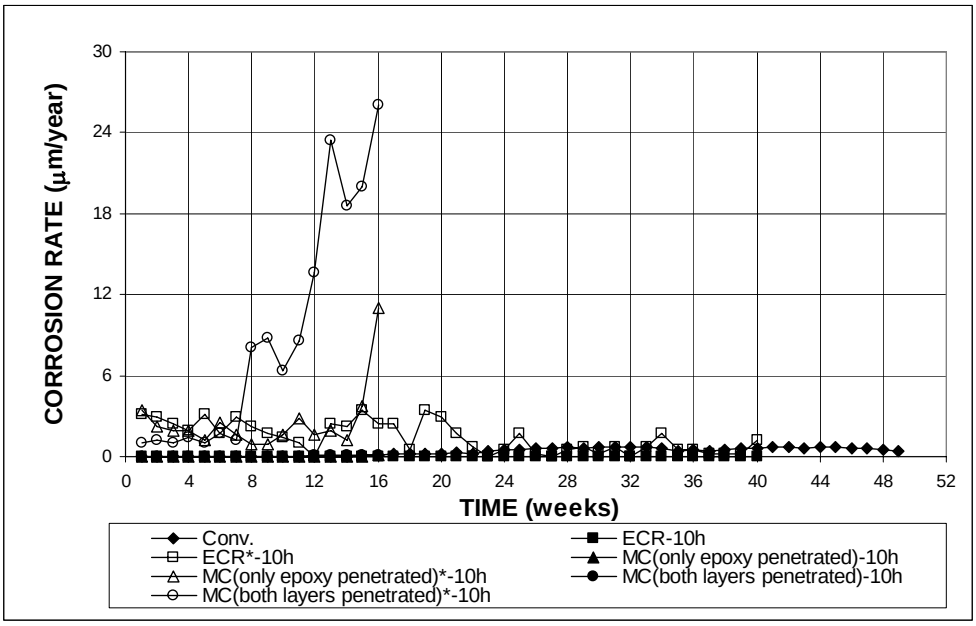

Figure 3.135 (a) – Southern Exposure Tests. Average Corrosion Rate. Specimens of conventional, epoxy-coated, and multiple coated reinforcement ponded with 15% NaCl solution. Epoxy and multiple coating penetrated with 10 holes. Refer to Table 3.12 for specimen identification.

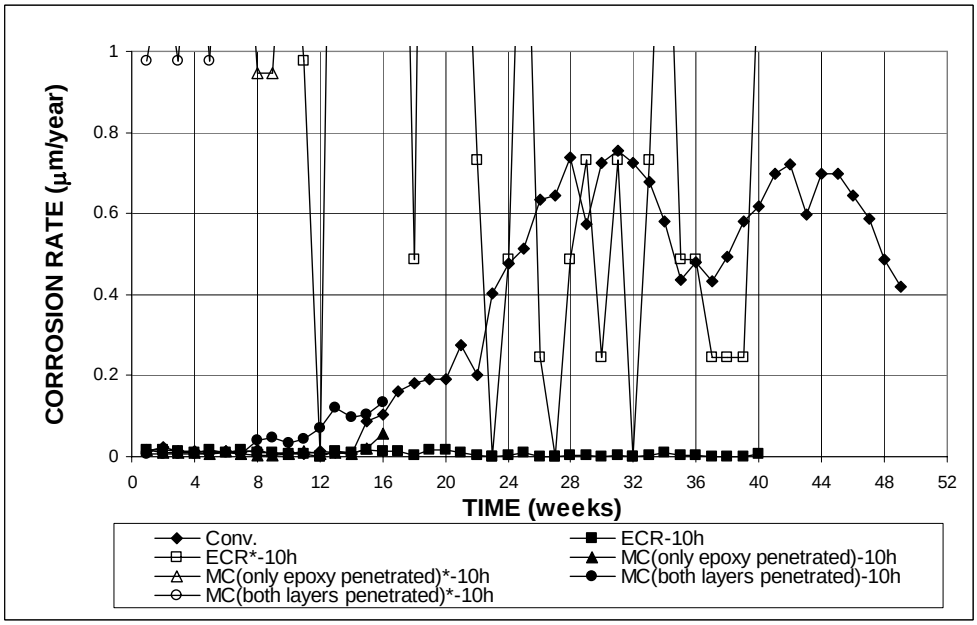

Figure 3.135 (b) – Southern Exposure Tests. Average Corrosion Rate. Specimens of conventional, epoxy-coated, and multiple coated reinforcement ponded with 15% NaCl solution. Epoxy and multiple coating penetrated with 10 holes. Refer to Table 3.12 for specimen identification.

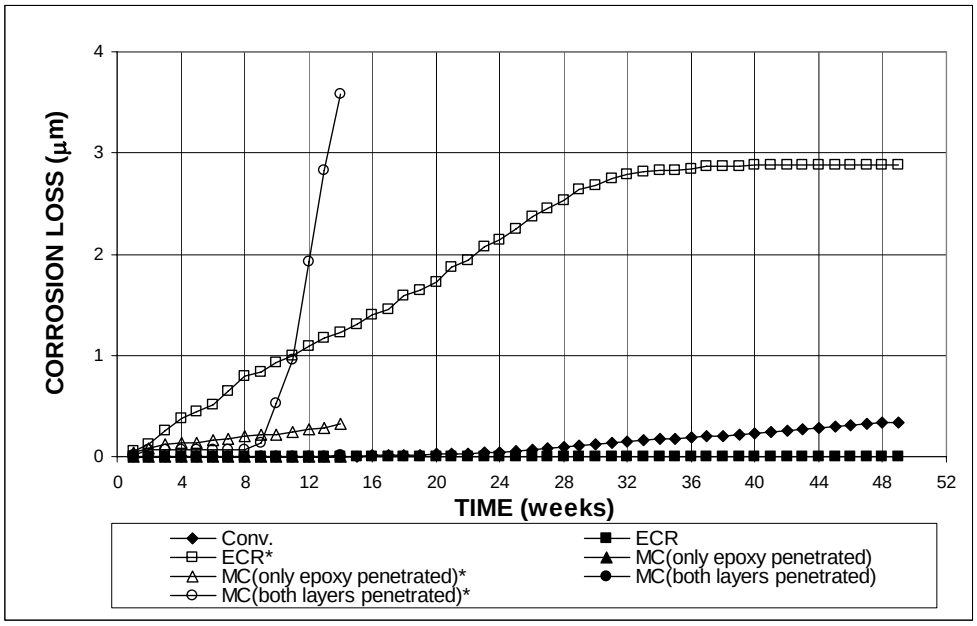

Figure 3.136 (a) – Southern Exposure Tests. Total Corrosion Loss. Specimens of conventional, epoxy-coated, and multiple coated reinforcement ponded with 15% NaCl solution. Epoxy and multiple coating penetrated with four holes. Refer to Table 3.12 for specimen identification.

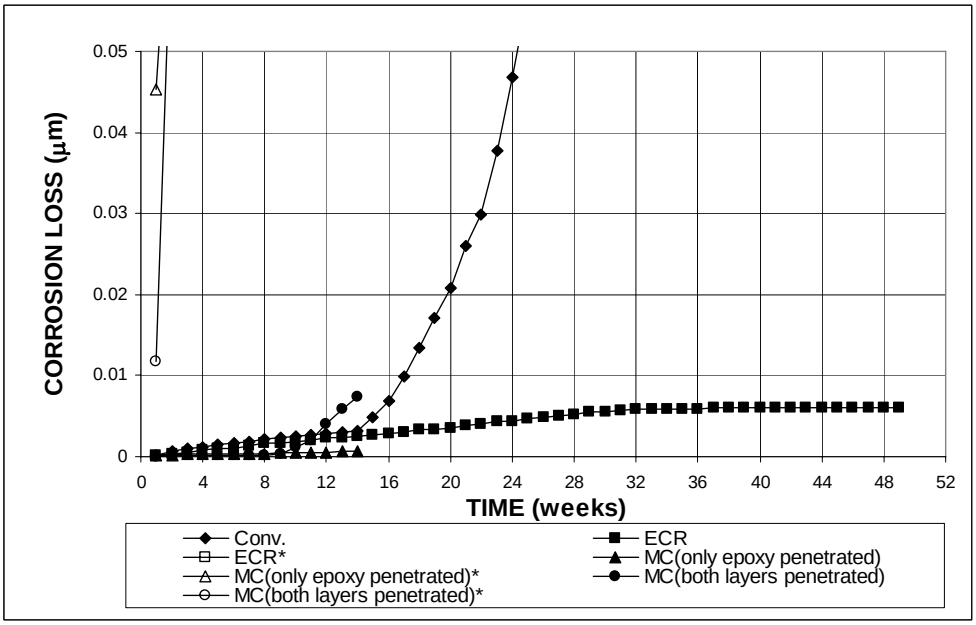

Figure 3.136 (b) – Southern Exposure Tests. Total Corrosion Loss. Specimens of conventional, epoxy-coated, and multiple coated reinforcement ponded with 15% NaCl solution. Epoxy and multiple coating penetrated with four holes. Refer to Table 3.12 for specimen identification.

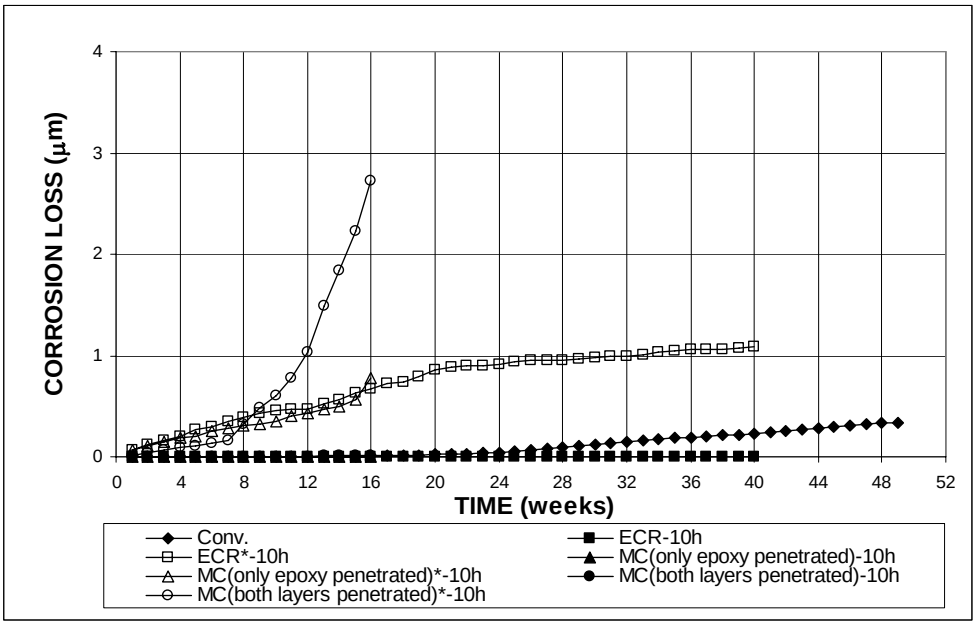

Figure 3.137 (a) – Southern Exposure Tests. Total Corrosion Loss. Specimens of conventional, epoxy-coated, and multiple coated reinforcement ponded with 15% NaCl solution. Epoxy and multiple coating penetrated with 10 holes. Refer to Table 3.12 for specimen identification.

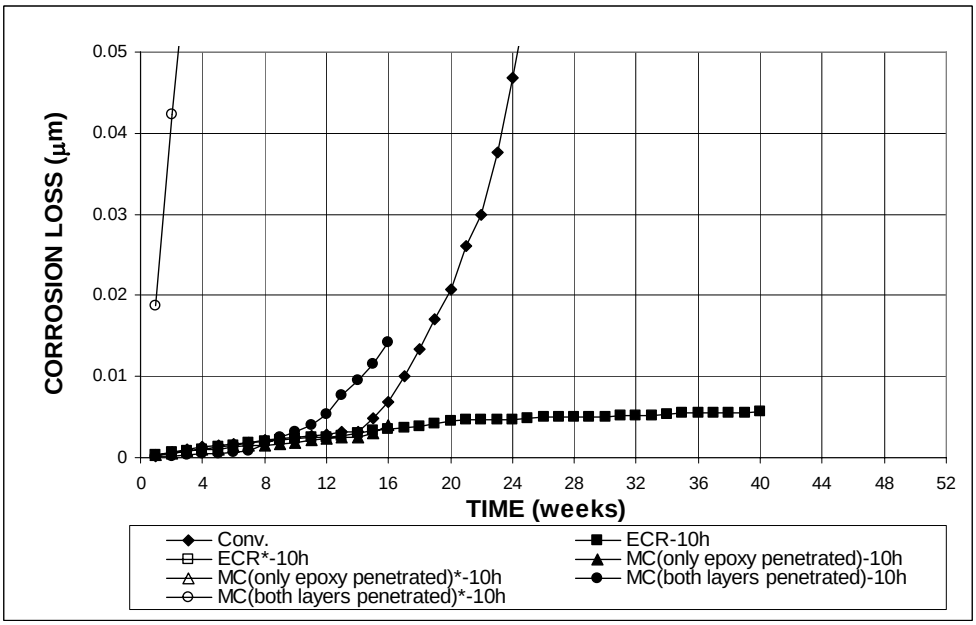

Figure 3.137 (b) – Southern Exposure Tests. Total Corrosion Loss. Specimens of conventional, epoxy-coated, and multiple coated reinforcement ponded with 15% NaCl solution. Epoxy and multiple coating penetrated with 10 holes. Refer to Table 3.12 for specimen identification.

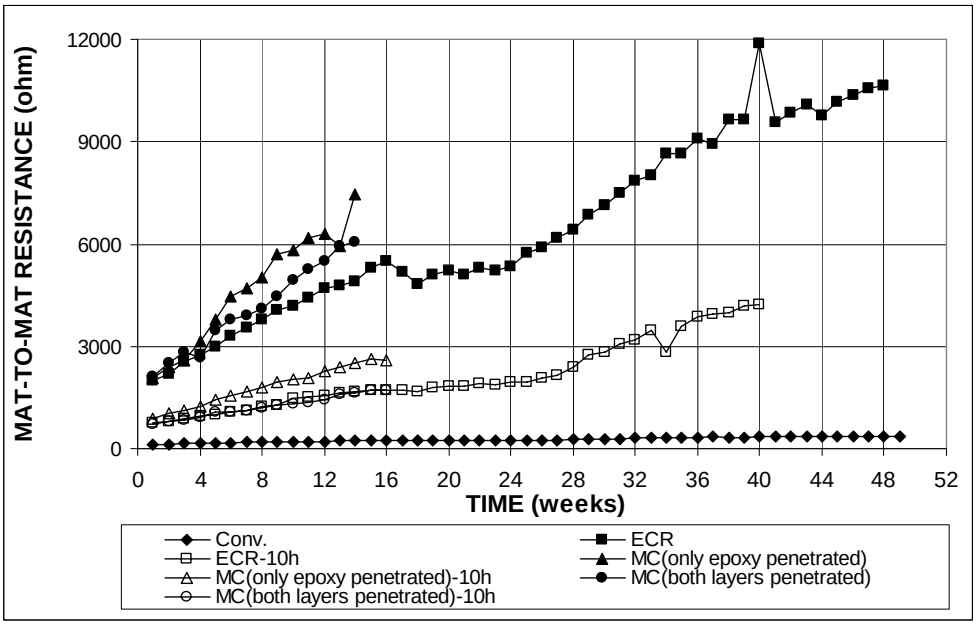

Figure 3.138 – Southern Exposure Tests. Mat-to-mat resistance. Specimens of conventional, epoxy-coated, and multiple coated reinforcement ponded with 15% NaCl solution. Refer to Table 3.12 for specimen identification.

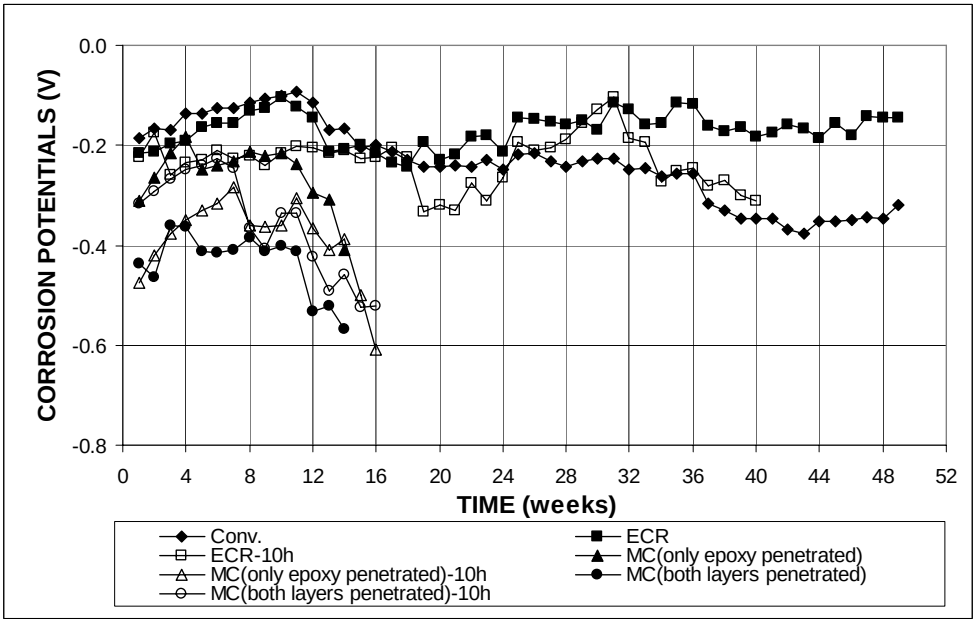

Figure 3.139 – Southern Exposure Tests. Corrosion Potential with respect to CSE at Top Mat. Specimens of conventional, epoxy-coated, and multiple coated reinforcement ponded with 15% NaCl solution. Refer to Table 3.12 for specimen identification.

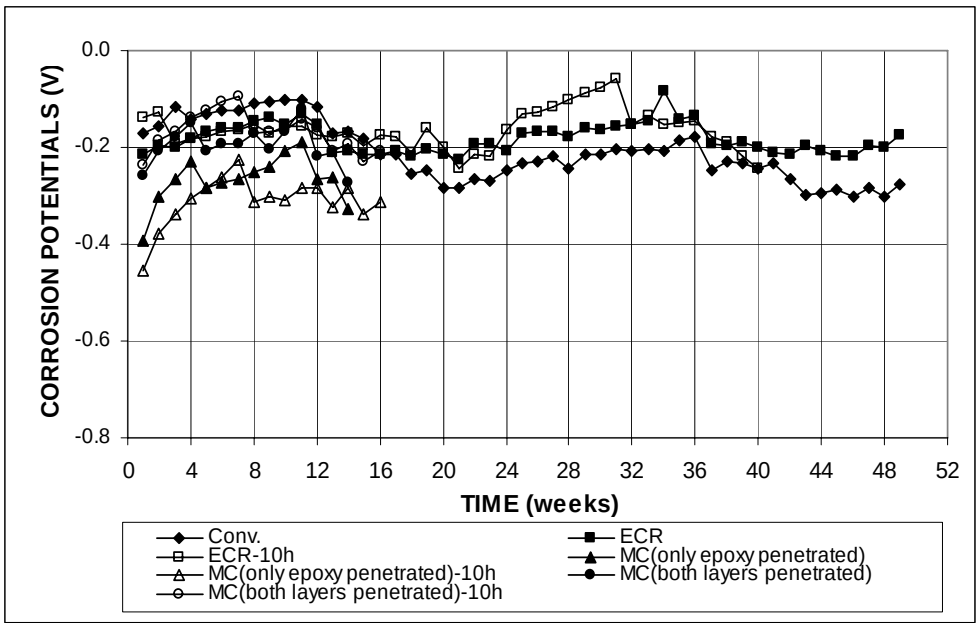

Figure 3.140 – Southern Exposure Tests. Corrosion Potential with respect to CSE at Bottom Mat. Specimens of conventional, epoxy-coated, and multiple coated reinforcement ponded with 15% NaCl solution. Refer to Table 3.12 for specimen identification.

3.5.2.2 Cracked Beam Tests

The cracked beam tests include three specimens each for multiple coated reinforcement (MC) with only the epoxy or both the epoxy and the zinc layers penetrated by four or 10 holes. Average corrosion rates, total corrosion losses, mat-to-mat resistances, and corrosion potentials are shown in Figures 3.141-3.147. The results (summarized in Table 3.12) show that, based on total area, the specimens containing MC steel with both layers penetrated by four holes (Figure 3.141) reach an average corrosion rate as high as 0.2 μm/yr a few times during the test period, which decreases to 0.05 μm/yr at week 14. The MC specimens with only the epoxy penetrated by four holes (Figure 3.141) start at a corrosion rate of 0.14 μm/yr at week 1, dropping to 0.07 μm/yr at week 14. The specimens containing MC steel with both layers penetrated by 10 holes (Figure 3.142) show a corrosion rate as high as 0.5 μm/yr at week 2, dropping to 0.36 μm/yr at week 16. The MC specimens with only

the epoxy penetrated by 10 holes (Figure 3.142) exhibit the maximum value of 0.32 μm/yr at week 6, reaching at a corrosion rate of 0.15 μm/yr at week 16. When based on the exposed area, the specimens containing MC steel with both layers penetrated by four holes have an average corrosion rate of 23 μm/yr at week 14, with a maximum value of 96 μm/yr at week 6. The corrosion rate of the MC specimens with only the epoxy penetrated by four holes start at 68 μm/yr at week 1, dropping to 33 μm/yr at week 14. The corrosion rate of the MC specimens with both layers penetrated by 10 holes is 69 μm/yr at week 16, with a maximum value of 95 μm/yr at week 2. The MC specimens with only the epoxy penetrated by 10 holes exhibit the rate as high as 60 μm/yr at week 6, dropping to 28 μm/yr at week 16. The specimens containing conventional ECR bars, based on either the total or exposed area, exhibit lower corrosion rates than the MC specimens during the same test period.

For the MC steel with both layers penetrated by 10 holes (shown in Figure 3.144), the average total corrosion loss is 0.1 μm based on total area and 18.8 μm based on the exposed area, which was the highest corrosion loss among all MC specimens. The corrosion losses are 0.03, 0.05, and 0.04 μm based on total area and 13.6, 10.4, and 18.3 μm based on the exposed area for the MC bars with only epoxy penetrated by four holes (Figure 3.143), by 10 holes (Figure 3.144), and the MC bars with both layers penetrated by four holes (Figure 3.143), respectively. The corrosion losses of the conventional ECR specimens are lower than the MC specimens, based on either the total or the exposed area, at the corresponding weeks.

The mat-to-mat resistances are shown in Figure 3.145. The MC specimens with either only the epoxy or both layers penetrated by four holes start with average mat-to-mat resistances around 3,000 ohms, which increase to over 8,000 ohms at week 14, while the mat-to-mat resistance of conventional ECR specimens with four holes starts

around 4000 ohms and increases to 14,400 ohms. The MC bars with either only the epoxy or both layers penetrated by 10 holes exhibit lower resistances that begin at below 1,500 ohms and rise to above 3,500 ohms at week 16, similar to that of the conventional ECR specimens with 10 holes.

The average corrosion potentials of the top and bottom mats with respect to a copper copper-sulfate electrode are shown in Figures 3.146 and 3.147, respectively. For the top mat, the MC specimens with only epoxy penetrated by four or 10 holes start with more negative corrosion potentials than the corresponding MC specimens with both layers penetrated. However, all MC specimens reach similar potentials after 14 weeks, with values between −0.560 and −0.625 V, more negative than those of the conventional ECR specimens. For the bottom mat, all conventional ECR and MC specimens exhibited corrosion potentials more positive than −0.350 V after week 2, indicating that the bars are still in a passive condition.

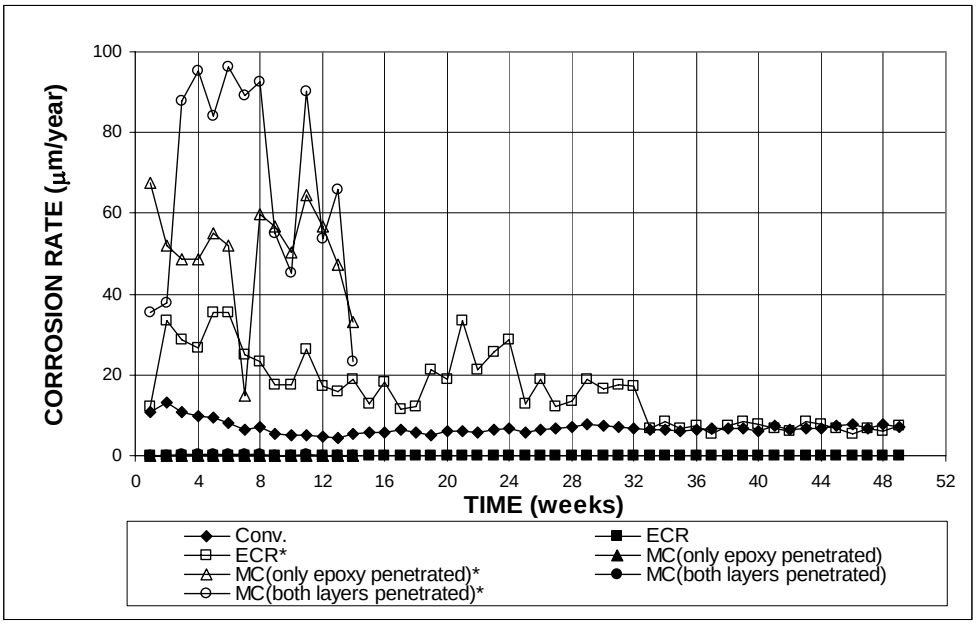

Figure 3.141 (a) – Cracked Beam Tests. Average Corrosion Rate. Specimens of conventional and epoxy-coated reinforcement ponded with 15% NaCl solution. Epoxy and multiple coating penetrated with four holes. Refer to Table 3.12 for specimen identification.

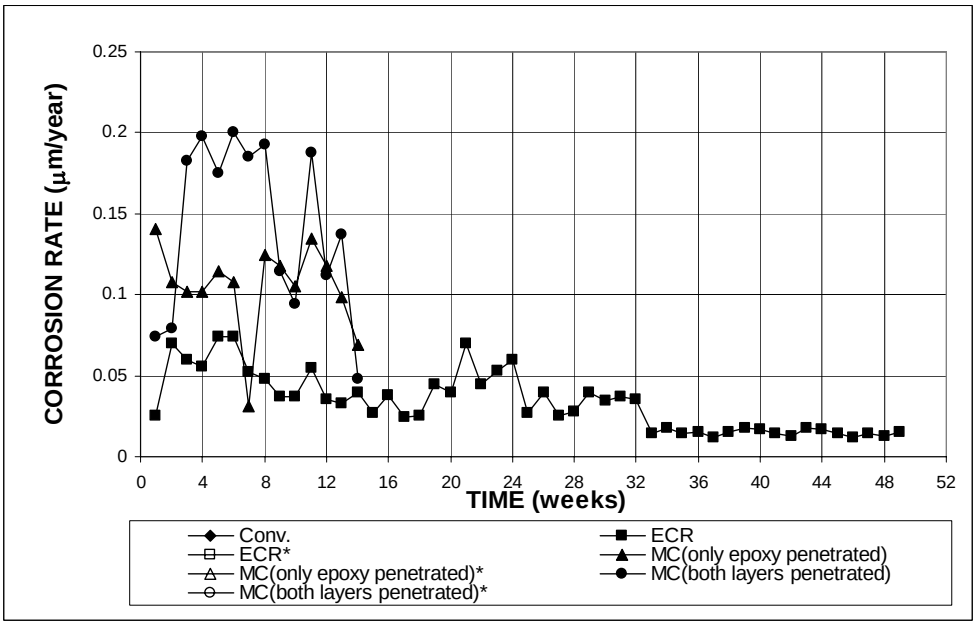

Figure 3.141 (b) – Cracked Beam Tests. Average Corrosion Rate. Specimens of conventional and epoxy-coated reinforcement ponded with 15% NaCl solution. Epoxy and multiple coating penetrated with four holes. Refer to Table 3.12 for specimen identification.

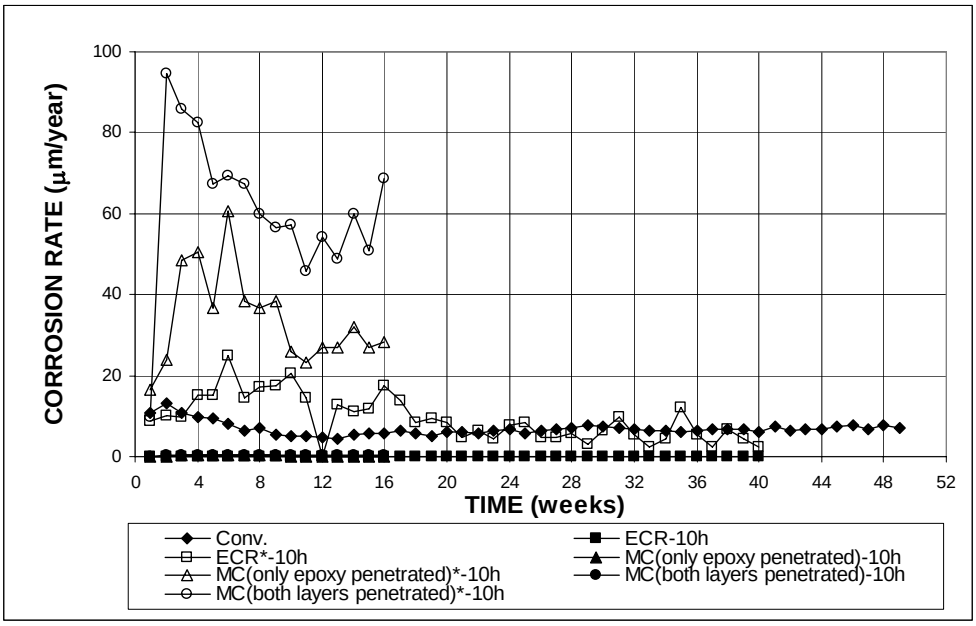

Figure 3.142 (a) – Cracked Beam Tests. Average Corrosion Rate. Specimens of conventional and epoxy-coated reinforcement ponded with 15% NaCl solution. Epoxy and multiple coating penetrated with 10 holes. Refer to Table 3.12 for specimen identification.

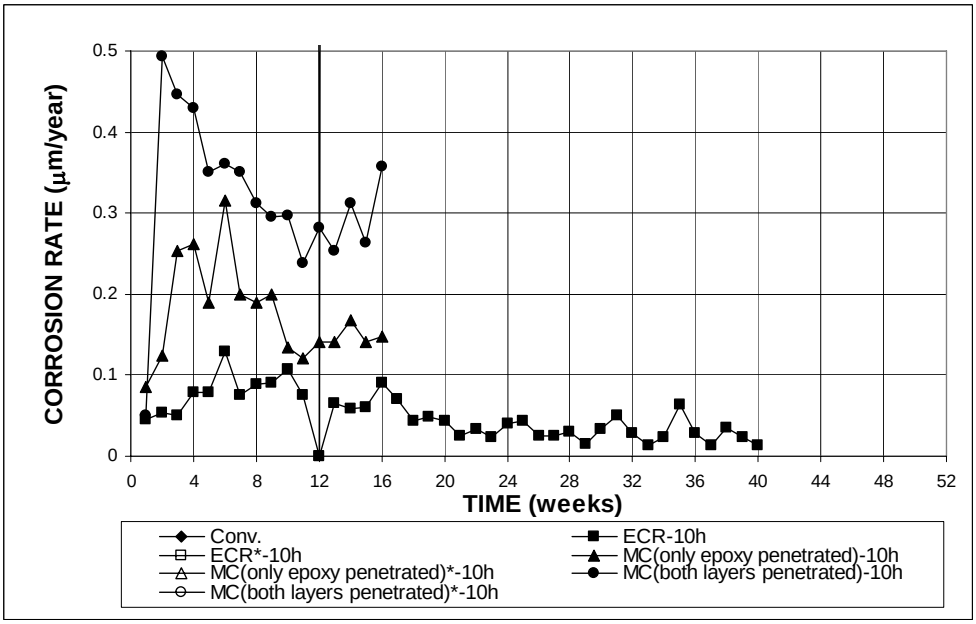

Figure 3.142 (b) – Cracked Beam Tests. Average Corrosion Rate. Specimens of conventional and epoxy-coated reinforcement ponded with 15% NaCl solution. Epoxy and multiple coating penetrated with 10 holes. Refer to Table 3.12 for specimen identification.

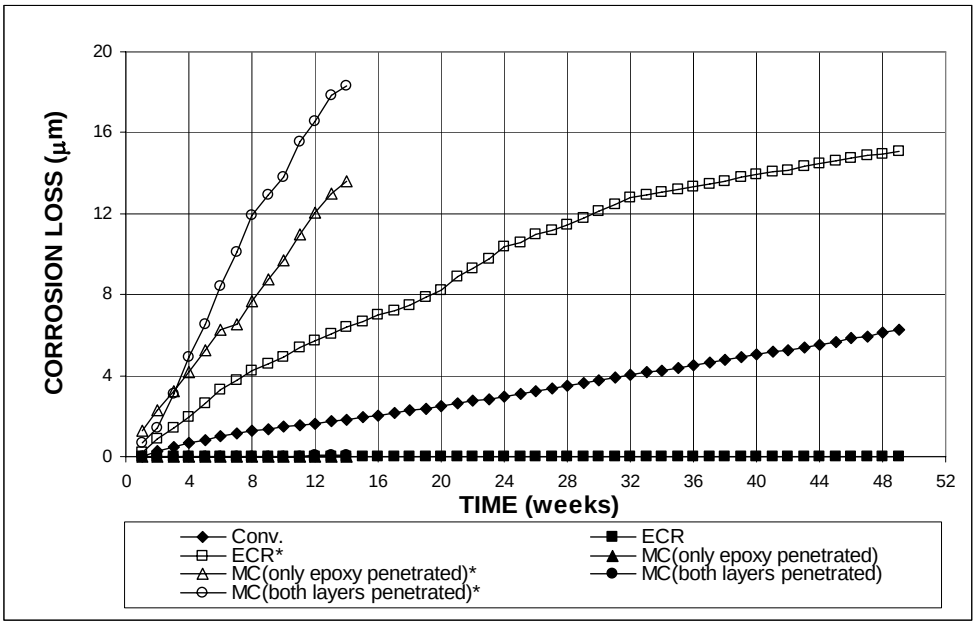

Figure 3.143 (a) – Cracked Beam Tests. Total Corrosion Loss. Specimens of conventional and epoxy-coated reinforcement ponded with 15% NaCl solution. Epoxy and multiple coating penetrated with four holes. Refer to Table 3.12 for specimen identification.

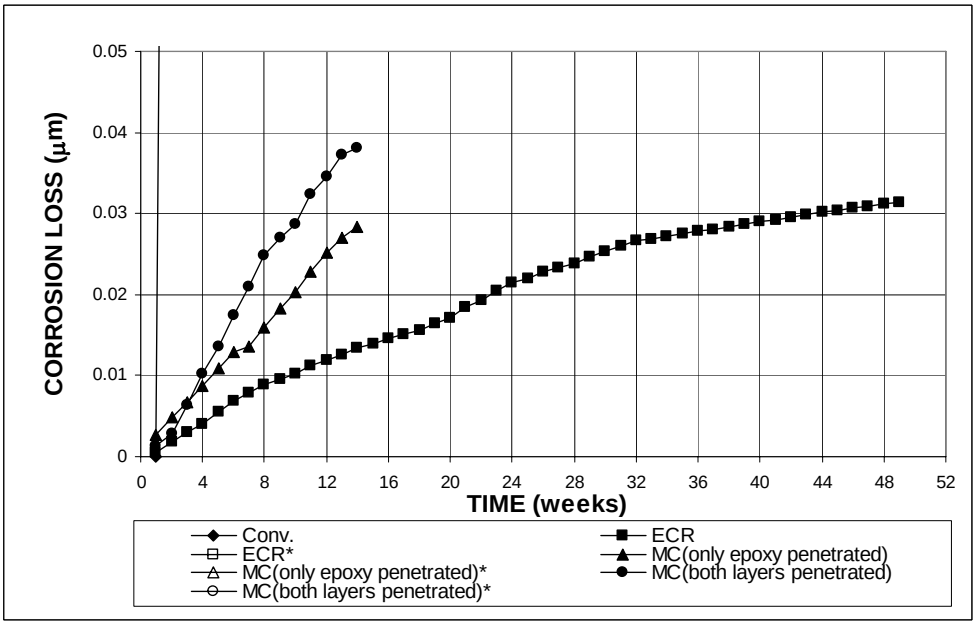

Figure 3.143 (b) – Cracked Beam Tests. Total Corrosion Loss. Specimens of conventional and epoxy-coated reinforcement ponded with 15% NaCl solution. Epoxy and multiple coating penetrated with four holes. Refer to Table 3.12 for specimen identification.

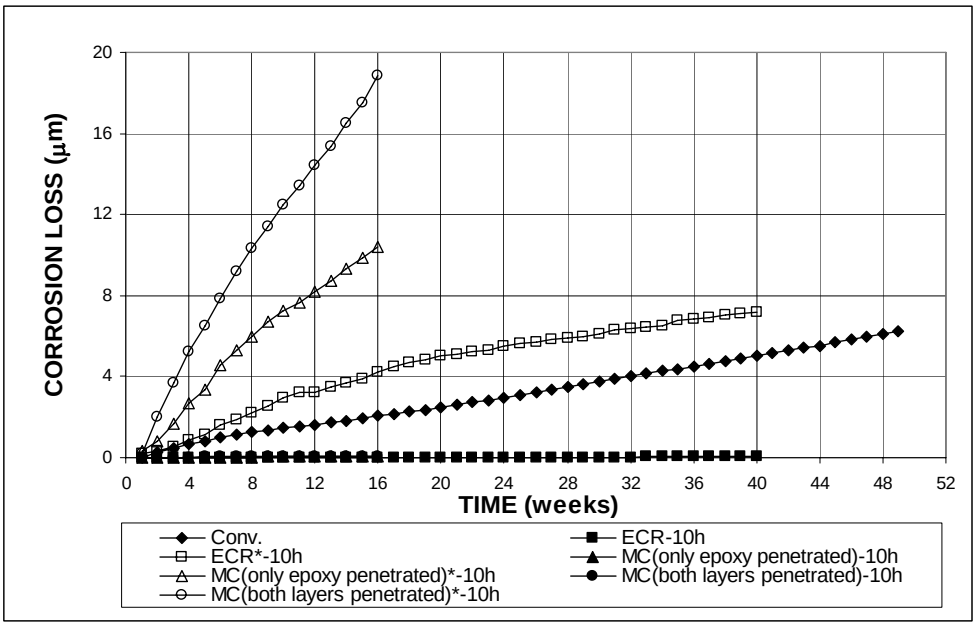

Figure 3.144 (a) – Cracked Beam Tests. Total Corrosion Loss. Specimens of conventional and epoxy-coated reinforcement ponded with 15% NaCl solution. Epoxy and multiple coating penetrated with 10 holes. Refer to Table 3.12 for specimen identification.

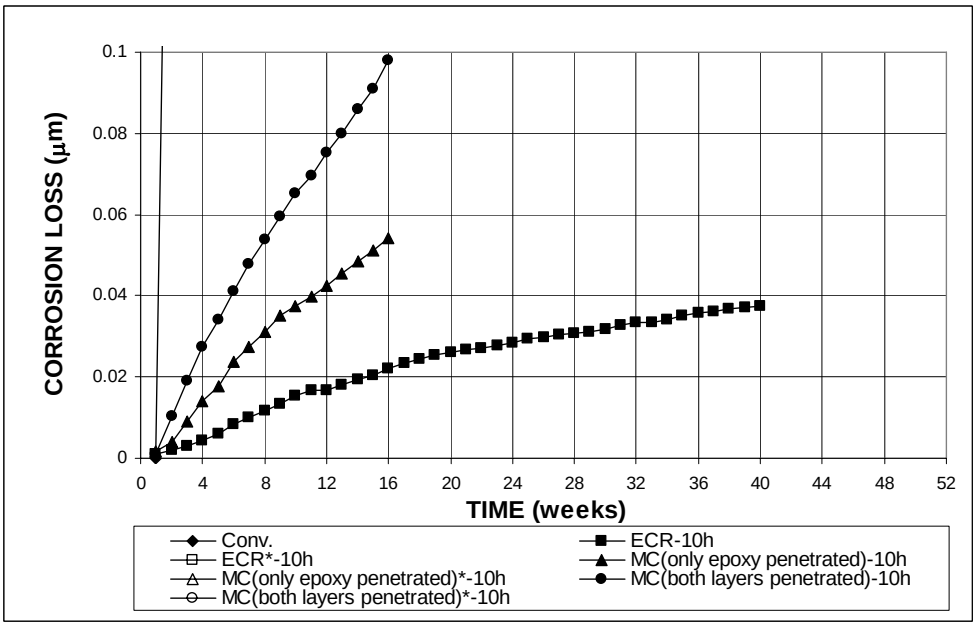

Figure 3.144 (b) – Cracked Beam Tests. Total Corrosion Loss. Specimens of conventional and epoxy-coated reinforcement ponded with 15% NaCl solution. Epoxy and multiple coating penetrated with 10 holes. Refer to Table 3.12 for specimen identification.

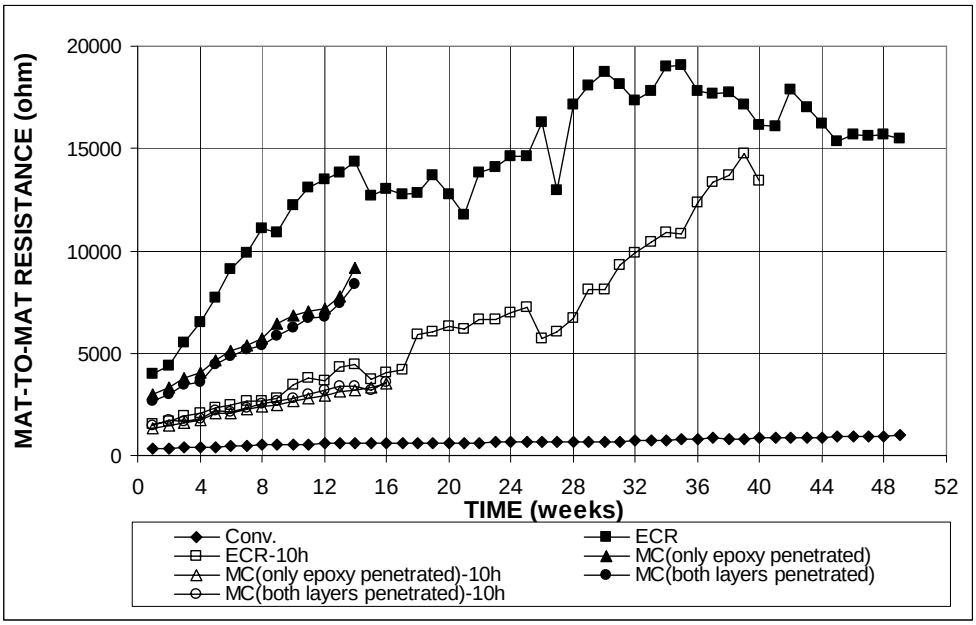

Figure 3.145 – Cracked Beam Tests. Mat-to-mat resistance. Specimens of conventional and epoxy-coated reinforcement ponded with 15% NaCl solution. Refer to Table 3.12 for specimen identification.

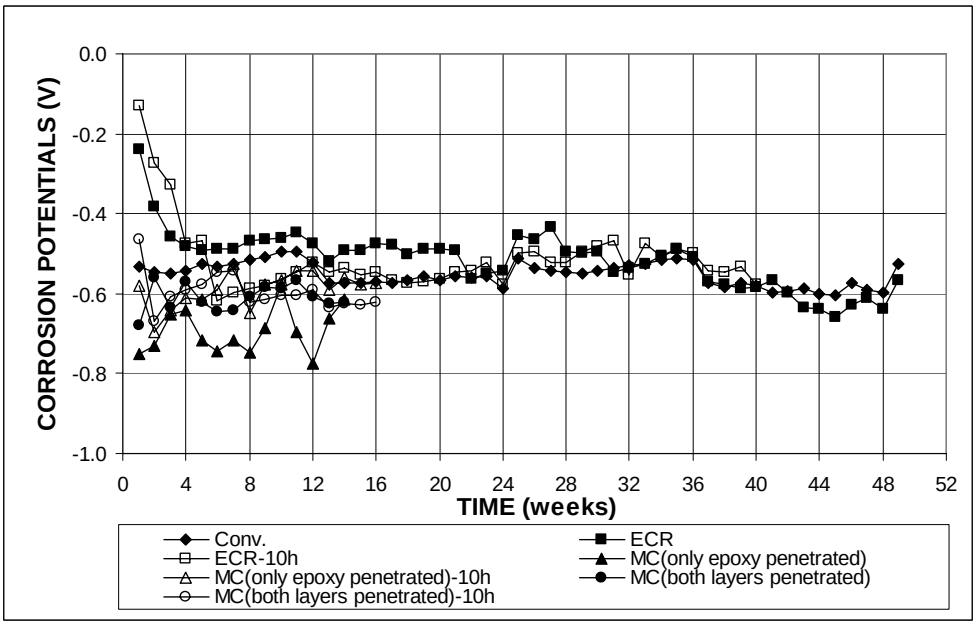

Figure 3.146 – Cracked Beam Tests. Corrosion Potential with respect to CSE at Top Mat. Specimens of conventional and epoxy-coated reinforcement ponded with 15% NaCl solution. Refer to Table 3.12 for specimen identification.

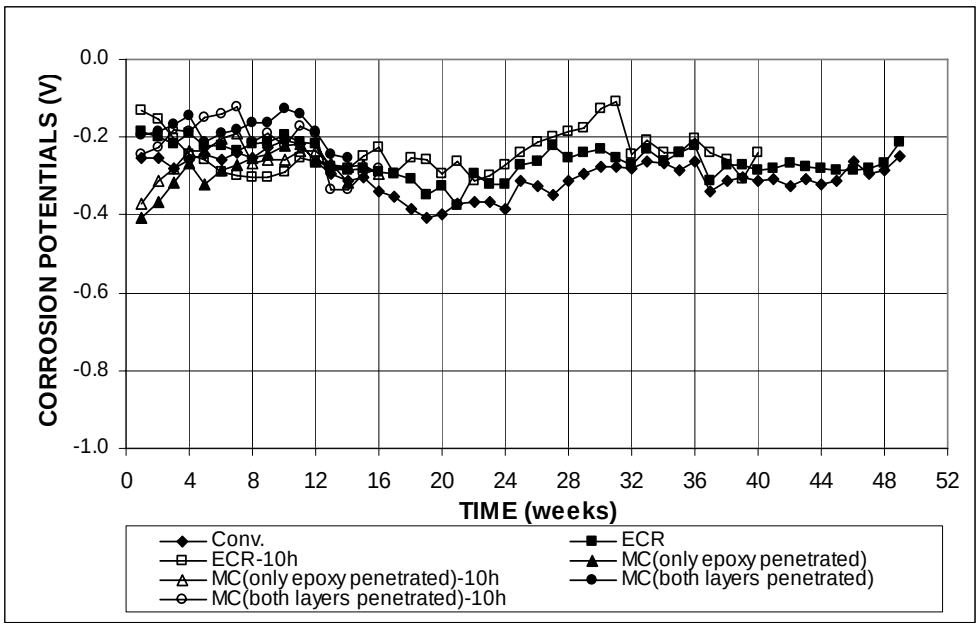

Figure 3.147 – Cracked Beam Tests. Corrosion Potential with respect to CSE at Bottom Mat. Specimens of conventional and epoxy-coated reinforcement ponded with 15% NaCl solution. Refer to Table 3.12 for specimen identification.

3.5.2.3 ASTM G 109 Tests

The average corrosion rates versus time in the ASTM G 109 tests are presented in Figures 3.148 and 3.149 for specimens with multiple coated bars with four and 10 drilled holes, respectively. Insignificant corrosion rates (less than 0.01 μm/yr) are obtained for all G 109 specimens containing multiple coated steel based on the total area. Based on either the total or the exposed area, the average corrosion rates started at relatively high values and dropped to lower numbers after a period (Figure 3.148). When based on total area, insignificant corrosion (with a rate less than 0.01 μm/yr) was observed on all G 109 specimens at the data cutoff date. Based on the exposed area, the corrosion rates were 0.31 μm/yr for the MC specimens with only epoxy penetrated by four holes at week 48, 0.06 μm/yr for the MC specimens with only epoxy penetrated by 10 holes at week 45, and 0.16 μm/yr for the MC specimens with

both layers penetrated by four holes at week 48. No significant corrosion was found on the MC specimens with both layers penetrated by 10 holes and the conventional ECR specimens at the corresponding points in time.

The average total corrosion losses are shown in Figures 3.150 and 3.151 for the MC specimens with four and 10 holes, respectively. Based on the total area, the MC specimens had higher corrosion losses than the conventional ECR specimens, although no corrosion losses larger than 0.01 μm were observed. The MC specimens with only the epoxy penetrated had a slightly higher average corrosion loss than the MC specimens with both layers penetrated. The average corrosion loss of the specimens containing conventional steel was lower than that of the MC specimens with only the epoxy penetrated by four or 10 holes and the MC specimens with both layers penetrated by four holes, but higher than the loss of the MC specimens with both layers penetrated by 10 holes. Based on the exposed area, the corrosion losses were 1.07 and 0.9 μm for the MC specimens with only epoxy and both layers penetrated by four holes at week 48, respectively, higher than the value for the conventional ECR specimens at the same point in time (0.47 μm). Corrosion losses of 0.39 and 0.25 μm were measured for the MC specimens with only epoxy and both layers penetrated by 10 holes at week 45, respectively, which are higher than the value for the conventional ECR specimens at week 42 (0.19 μm).

As shown in Figure 3.152, the MC specimens with four holes started with the average mat-to-mat resistance of approximately 4,000 ohms, which increased to above 14,000 ohms for specimens with both layers penetrated and 18,000 ohms for specimens with only the epoxy penetrated, similar to that of the conventional ECR specimens (around 16,000 ohms at week 48). The MC bars with 10 drilled holes exhibit much lower resistances that start below 2,800 ohms and increase to close to

7,200 ohms for specimens with both layers penetrated and 7,900 ohms for specimens with only epoxy penetrated at week 45, both higher than that of the conventional steel at week 42 (5,200 ohms).

The corrosion potentials are shown in Figures 3.153 and 3.154. For both the top and bottom mats, the MC specimens with only the epoxy penetrated show more negative corrosion potentials than the MC specimens with both layers penetrated, indicating that the zinc is functioning. Since the copper copper-sulfate electrode used here was out of calibration, the data obtained using the saturated calomel electrode is used, but is expressed on the basis of a copper copper-sulfate electrode.

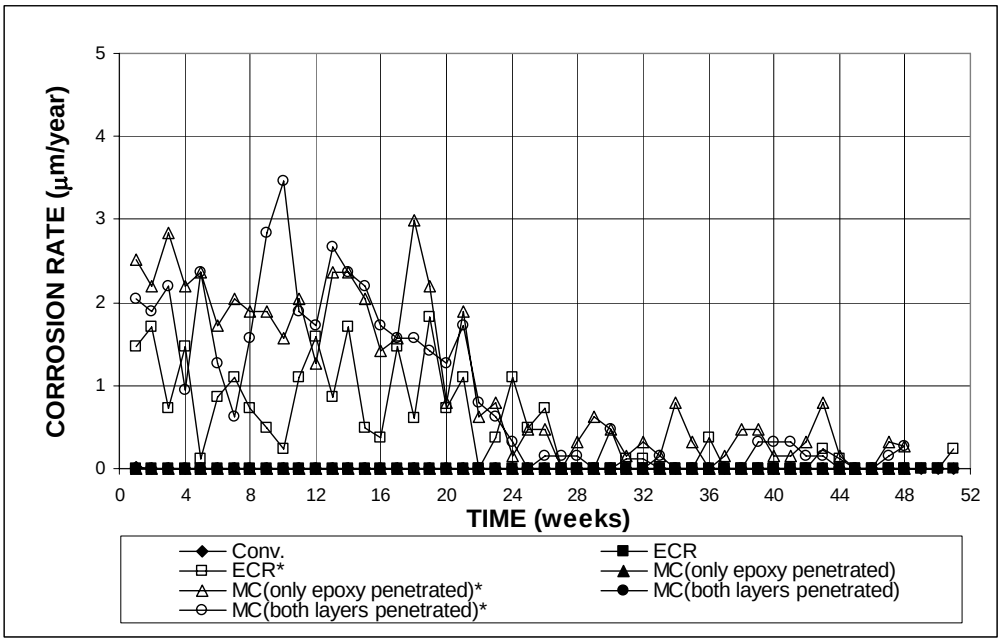

Figure 3.148 (a) – ASTM G 109 Tests. Average Corrosion Rate. Specimens of conventional, epoxy-coated, and multiple coated reinforcement. Epoxy and multiple coating penetrated with four holes. Refer to Table 3.12 for specimen identification.

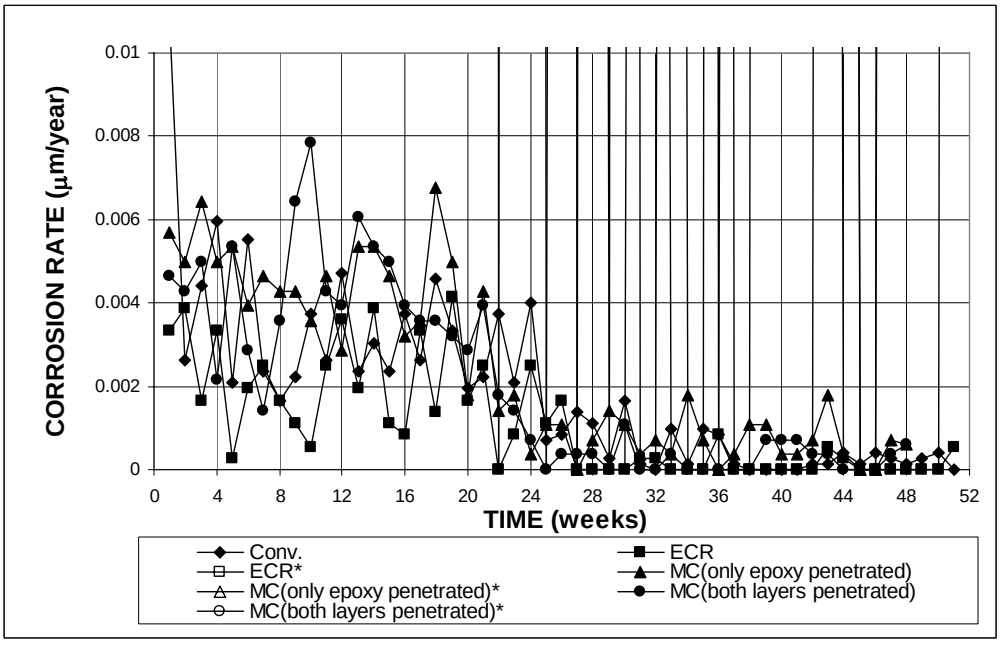

Figure 3.148 (b) – ASTM G 109 Tests. Average Corrosion Rate. Specimens of conventional, epoxy-coated, and multiple coated reinforcement. Epoxy and multiple coating penetrated with four holes. Refer to Table 3.12 for specimen identification.

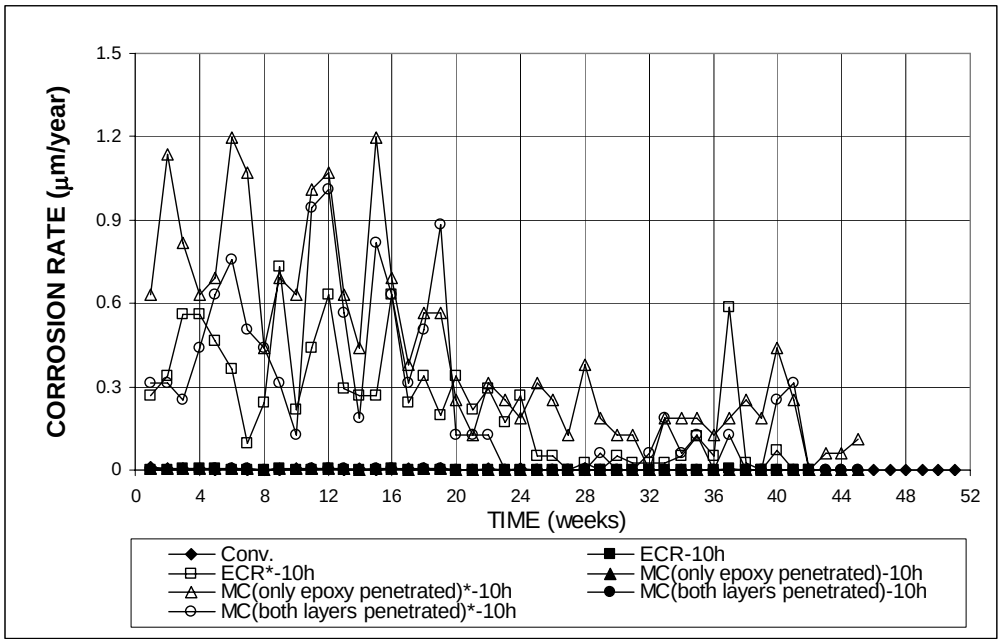

Figure 3.149 (a) – ASTM G 109 Tests. Average Corrosion Rate. Specimens of conventional, epoxy-coated, and multiple coated reinforcement. Epoxy and multiple coating penetrated with 10 holes. Refer to Table 3.12 for specimen identification.

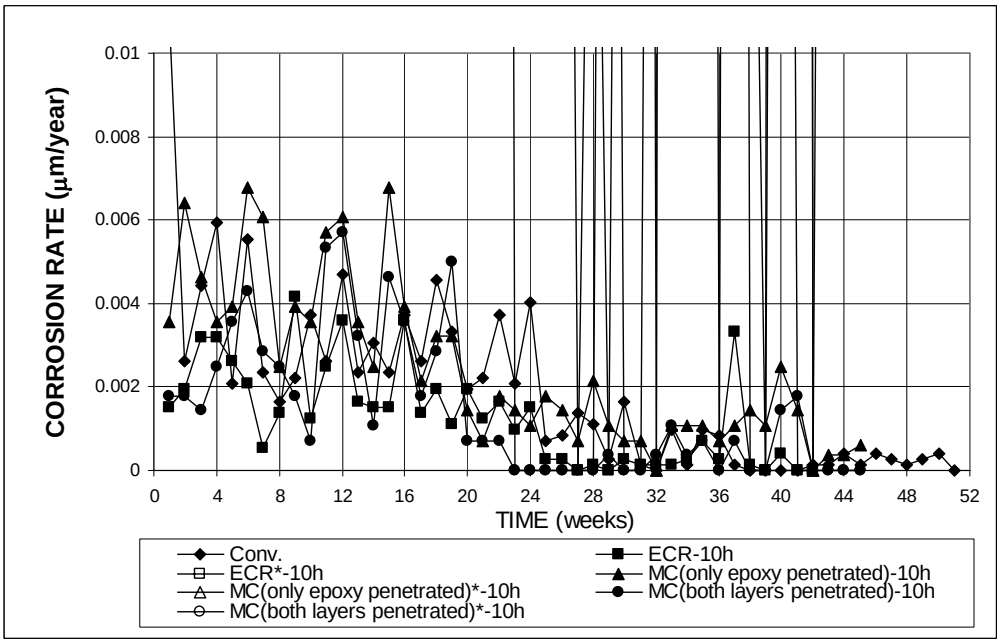

Figure 3.149 (b) – ASTM G 109 Tests. Average Corrosion Rate. Specimens of conventional, epoxy-coated, and multiple coated reinforcement. Epoxy and multiple coating penetrated with 10 holes. Refer to Table 3.12 for specimen identification.

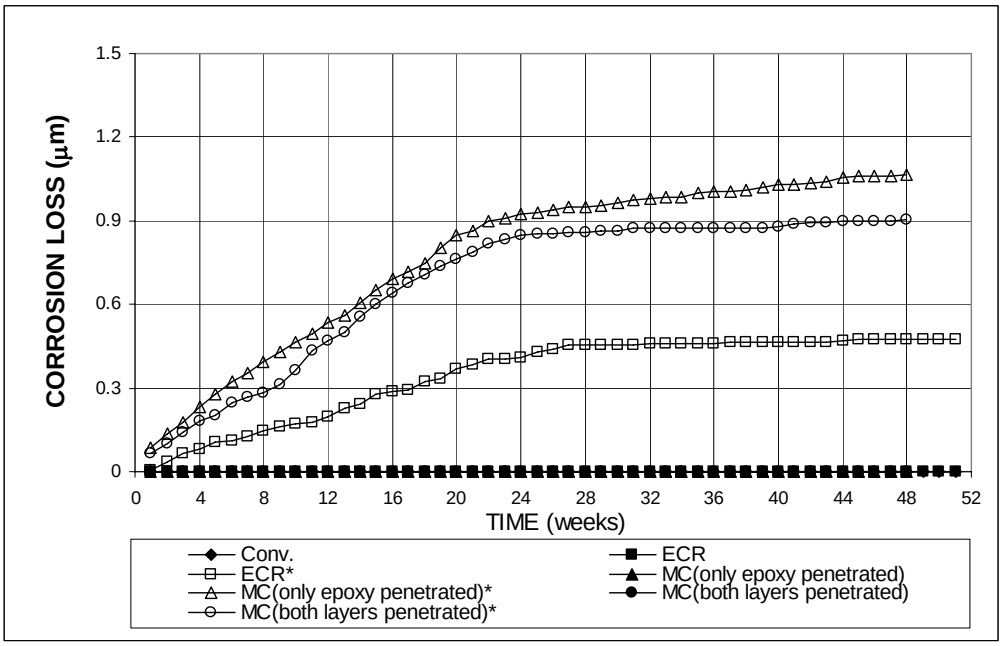

Figure 3.150 (a) – ASTM G 109 Tests. Total Corrosion Loss. Specimens of conventional, epoxy-coated, and multiple coated reinforcement. Epoxy and multiple coating penetrated with four holes. Refer to Table 3.12 for specimen identification.

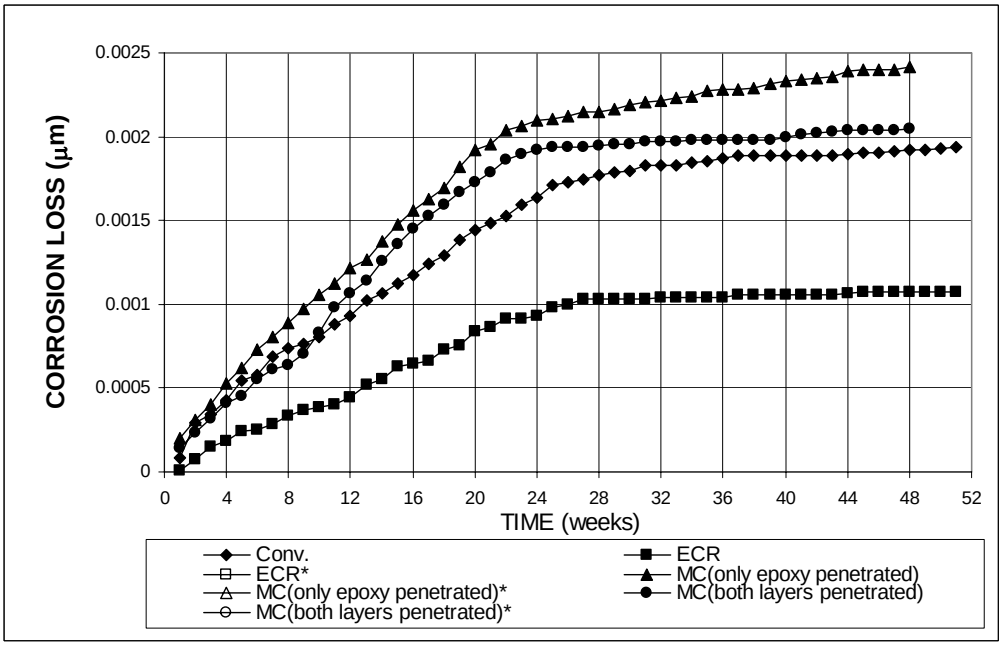

Figure 3.150 (b) – ASTM G 109 Tests. Total Corrosion Loss. Specimens of conventional, epoxy-coated, and multiple coated reinforcement. Epoxy and multiple coating penetrated with four holes. Refer to Table 3.12 for specimen identification.

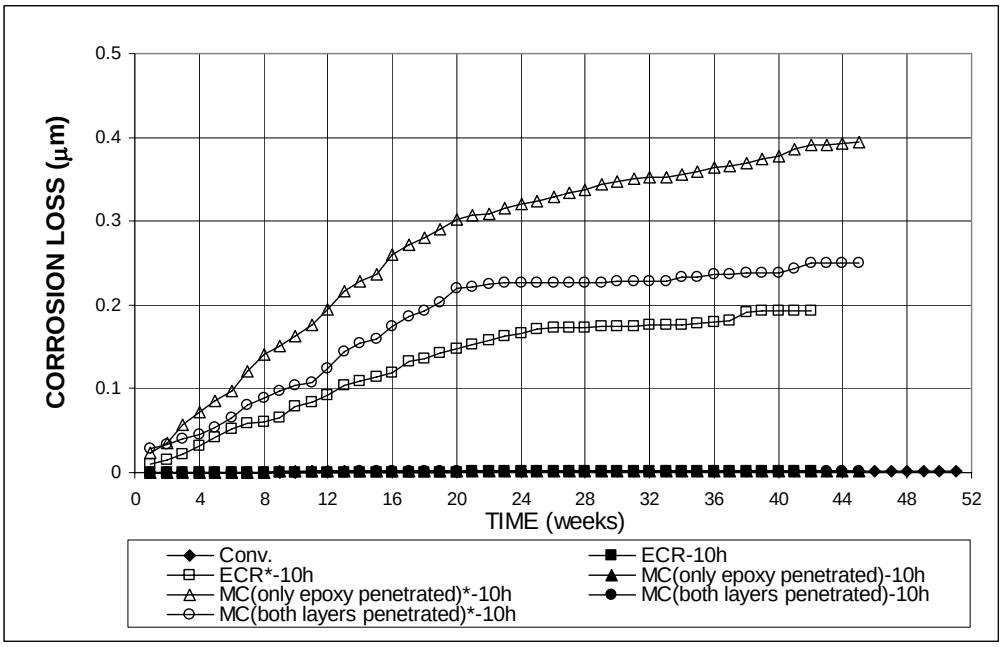

Figure 3.151 (a) – ASTM G 109 Tests. Total Corrosion Loss. Specimens of conventional, epoxy-coated, and multiple coated reinforcement. Epoxy and multiple coating penetrated with 10 holes. Refer to Table 3.12 for specimen identification.

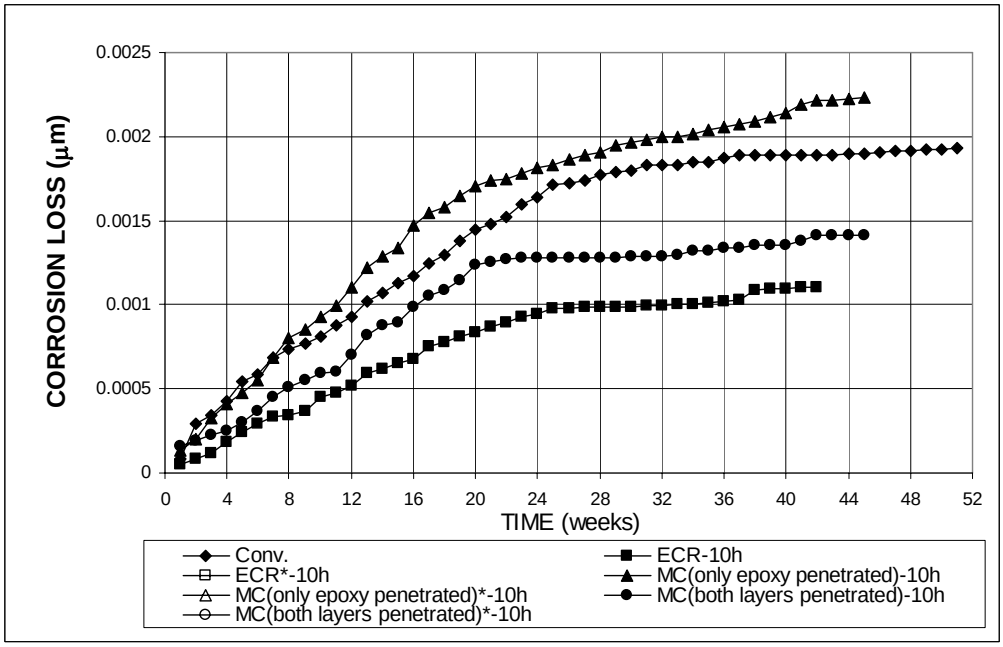

Figure 3.151 (b) – ASTM G 109 Tests. Total Corrosion Loss. Specimens of conventional, epoxy-coated, and multiple coated reinforcement. Epoxy and multiple coating penetrated with 10 holes. Refer to Table 3.12 for specimen identification.

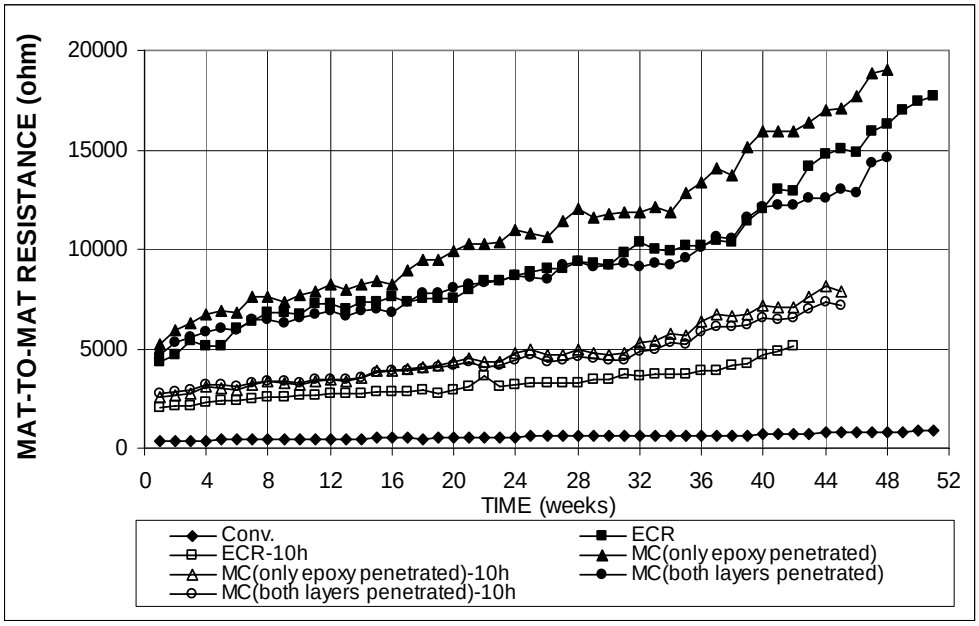

Figure 3.152 – ASTM G 109 Tests. Mat-to-mat resistance. Specimens of conventional, epoxy-coated, and multiple coated reinforcement. Refer to Table 3.12 for specimen identification.

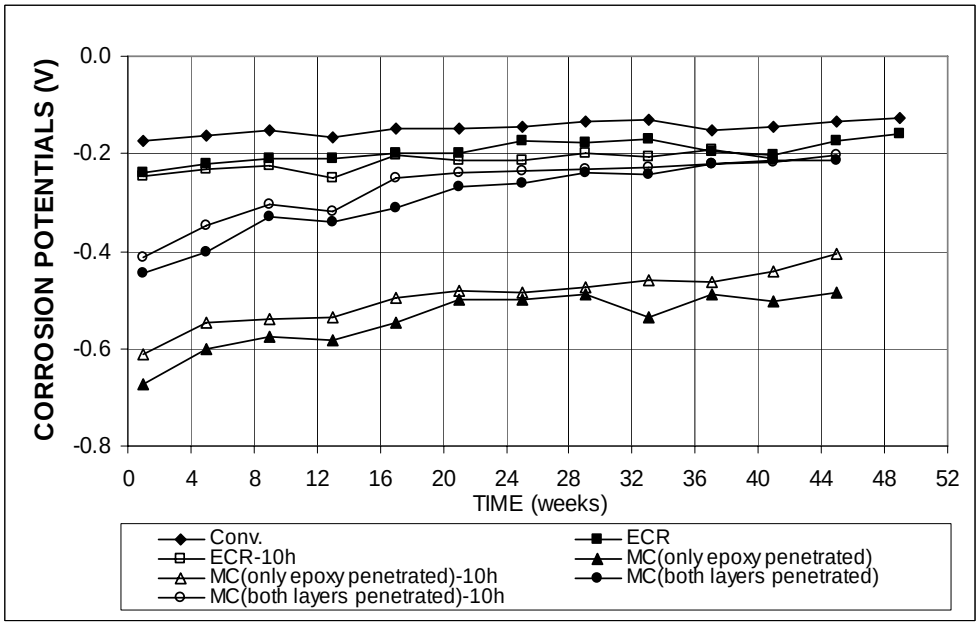

Figure 3.153 – ASTM G 109 Tests. Corrosion Potential with respect to CSE at Top Mat. Specimens of conventional, epoxy-coated, and multiple coated reinforcement. Refer to Table 3.12 for specimen identification.

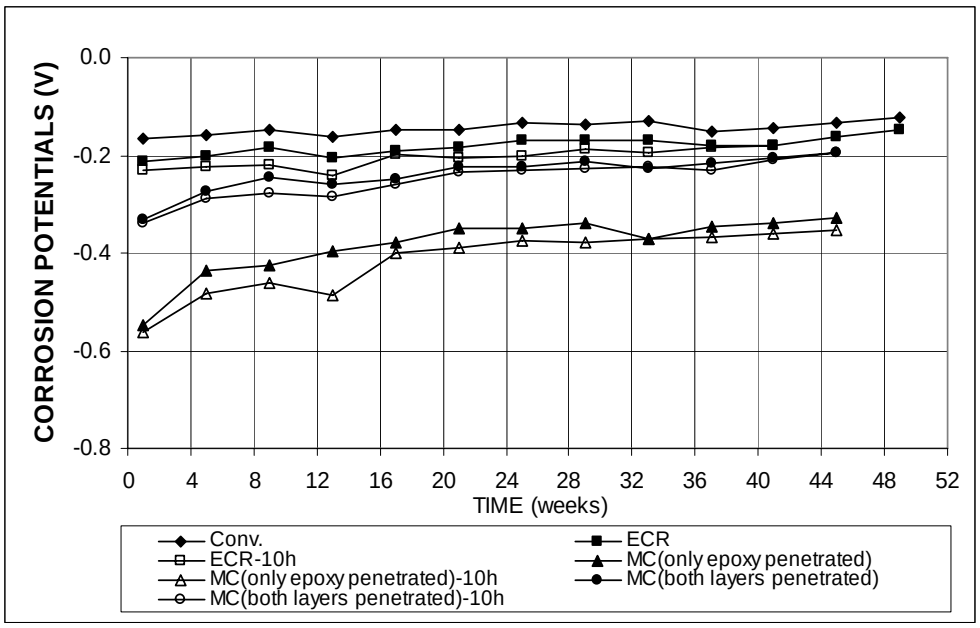

Figure 3.154 – ASTM G 109 Tests. Corrosion Potential at with respect to CSE at Bottom Mat. Specimens of conventional, epoxy-coated, and multiple coated reinforcement. Refer to Table 3.12 for specimen identification.

3.6 LINEAR POLARIZATION RESISTANCE TESTS

Microcell corrosion current densities and corrosion rates for selected bench-scale specimens are measured using the linear polarization resistance (LPR) test. As described in Chapter 2, readings are taken every four weeks for disconnected top and bottom mats and every eight weeks for the connected circuit. Due to human error, some initial tests started at week 16, instead of week 4. The tests include one specimen for each corrosion protection system, as presented in Table 2.7. The current densities and corrosion rates obtained from the tests are summarized in Tables 3.13-3.15 as of March 15, 2005. The corrosion rates of the top mats are shown as a function of time in Figures 3.155-3.166, while the corrosion rates for bottom mats and connected circuits are presented in Appendix B. The specimens containing conventional steel and conventional epoxy-coated steel will be used as control specimens to compare with the specimens containing increased adhesion ECR, one of

the three corrosion inhibitors, ECR with calcium nitrite primer, and the multiple coated bars.

From Tables 3.13 and 3.14, it can be observed that all of the cracked beam specimens have much higher corrosion rates than the corresponding Southern Exposure specimens in the top mats, in both mats when connected, and in all but a few cases in the bottom mats. It also can be concluded that the microcell corrosion rates of the bottom mats are usually one to two orders of magnitude lower than those of top mats, and the results when the two mat are connected are somewhere between the values for the top and bottom mats for the CB specimens, but not necessarily for the SE specimens.

Table 3.13 – Microcell corrosion current densities from linear polarization resistance test for Southern Exposure specimens

Steel Designation[a]	Exposure time (weeks)	Corrosion current densities (μA/cm^2) from PR[b]			Corrosion rates (μm/yr) from PR[b]		
		top mat	bottom mat	connected	top mat	bottom mat	connected
Conv.	48	1.03E-02	3.37E-03	-	1.19E-01	3.91E-02	-
Conv.-35	36	4.02E-02	7.50E-03	-	4.66E-01	8.70E-02	-
ECR	48	2.25E-05	2.62E-05	-	2.61E-04	3.04E-04	-
ECR-10h	40	9.75E-03	5.24E-04	3.19E-04	1.13E-01	6.08E-03	3.70E-03
ECR-10h-35	36	1.50E-03	1.26E-03	-	1.74E-02	1.46E-02	-
ECR(Rheocrete)	20	1.54E-04	1.24E-04	9.75E-05	1.79E-03	1.44E-03	1.13E-03
ECR(Rheocrete)-10h	20	1.69E-03	8.51E-04	3.20E-04	1.96E-02	9.87E-03	3.71E-03
ECR(Rheocrete)-10h-35	16	8.52E-04	8.62E-04	-	9.88E-03	1.00E-02	-
ECR(DCI)	20	4.40E-05	5.29E-05	2.82E-05	5.10E-04	6.14E-04	3.27E-04
ECR(DCI)-10h	20	5.94E-04	6.36E-04	5.58E-05	6.89E-03	7.38E-03	6.47E-04
ECR(DCI)-10h-35	20	1.41E-04	1.81E-04	9.31E-05	1.64E-03	2.10E-03	1.08E-03
ECR(Hycrete)	24	2.18E-04	1.99E-04	9.16E-05	2.53E-03	2.31E-03	1.06E-03
ECR(Hycrete)-10h	24	4.86E-04	2.86E-04	1.40E-04	5.64E-03	3.32E-03	1.62E-03
ECR(Hycrete)-10h-35	20	2.49E-04	2.53E-04	-	2.89E-03	2.93E-03	-
ECR(primer/$Ca(NO_2)_2$)	28	2.42E-04	3.78E-04	-	2.81E-03	4.38E-03	-
ECR(primer/$Ca(NO_2)_2$)-10h	28	4.85E-04	5.21E-04	-	5.63E-03	6.04E-03	-
ECR(primer/$Ca(NO_2)_2$)-10h-35	16	1.34E-03	8.78E-04	-	1.55E-02	1.02E-02	-
MC(only epoxy penetrated)	12	1.91E-03	1.13E-04	-	2.22E-02	1.31E-03	-
MC(only epoxy penetrated)-10h	20	8.50E-03	1.47E-04	1.55E-03	9.86E-02	1.71E-03	1.80E-02
MC(both layers penetrated)	12	9.84E-03	1.20E-04	-	1.14E-01	1.39E-03	-
MC(both layers penetrated)-10h	16	1.32E-02	1.10E-03	6.46E-03	1.53E-01	1.28E-02	7.49E-02
ECR(DuPont)	32	3.88E-04	1.41E-04	-	4.50E-03	1.64E-03	-
ECR(DuPont)-10h	28	3.55E-03	1.18E-04	-	4.12E-02	1.37E-03	-
ECR(Chromate)	32	6.09E-04	2.81E-04	-	7.06E-03	3.26E-03	-
ECR(Chromate)-10h	28	1.71E-03	1.23E-04	-	1.98E-02	1.43E-03	-
ECR(Valspar)	32	9.36E-05	1.17E-04	-	1.09E-03	1.36E-03	-
ECR(Valspar)-10h	28	7.23E-04	1.25E-03	-	8.39E-03	1.45E-02	-

Table 3.14 – Microcell corrosion current densities from linear polarization resistance test for Cracked Beam specimens

Steel Designation[a]	Exposure time (weeks)	Corrosion current densities (μA/cm^2) from PR[b]			Corrosion rates (μm/yr) from PR[b]		
		top mat	bottom mat	connected	top mat	bottom mat	connected
Conv.	48	6.64E+00	3.55E-02	-	7.70E+01	4.12E-01	-
Conv.-35	36	7.85E+00	3.85E-02	-	9.10E+01	4.47E-01	-
ECR	48	6.49E-02	1.24E-04	-	7.53E-01	1.44E-03	-
ECR-10h	40	2.31E-02	2.80E-04	1.24E-02	2.68E-01	3.24E-03	1.44E-01
ECR-10h-35	36	5.70E-02	9.59E-04	-	6.61E-01	1.11E-02	-
ECR(Rheocrete)	20	5.35E-02	2.37E-04	1.87E-02	6.21E-01	2.75E-03	2.17E-01
ECR(Rheocrete)-10h	20	4.46E-02	7.12E-04	1.42E-02	5.17E-01	8.26E-03	1.65E-01
ECR(Rheocrete)-10h-35	16	2.96E-02	7.71E-04	-	3.43E-01	8.94E-03	-
ECR(DCI)	20	1.64E-02	6.39E-05	9.13E-03	1.90E-01	7.41E-04	1.06E-01
ECR(DCI)-10h	20	2.23E-02	3.61E-04	2.15E-02	2.59E-01	4.19E-03	2.49E-01
ECR(DCI)-10h-35	20	1.07E-01	1.66E-03	3.84E-02	1.24E+00	1.93E-02	4.45E-01
ECR(Hycrete)	24	8.01E-03	3.80E-04	1.29E-03	9.29E-02	4.41E-03	1.50E-02
ECR(Hycrete)-10h	24	5.56E-02	3.21E-04	1.72E-02	6.45E-01	3.72E-03	2.00E-01
ECR(Hycrete)-10h-35	20	1.76E-02	2.06E-03	8.82E-03	2.04E-01	2.39E-02	1.02E-01
ECR(primer/$Ca(NO_2)_2$)	28	2.91E-02	3.43E-04	-	3.38E-01	3.98E-03	-
ECR(primer/$Ca(NO_2)_2$)-10h	28	2.56E-02	7.20E-04	-	2.97E-01	8.35E-03	-
ECR(primer/$Ca(NO_2)_2$)-10h-35	16	9.00E-02	1.31E-03	-	1.04E+00	1.52E-02	-
MC(only epoxy penetrated)	12	1.16E-01	3.63E-04	-	1.35E+00	4.21E-03	-
MC(only epoxy penetrated)-10h	20	1.93E-02	1.59E-03	-	2.24E-01	1.84E-02	-
MC(both layers penetrated)	12	1.72E-01	3.48E-04	-	2.00E+00	4.04E-03	-
MC(both layers penetrated)-10h	16	1.50E-01	1.07E-03	4.87E-02	1.74E+00	1.24E-02	5.65E-01
ECR(DuPont)	32	2.38E-02	4.96E-04	-	2.76E-01	5.75E-03	-
ECR(DuPont)-10h	28	3.71E-02	3.49E-04	-	4.30E-01	4.05E-03	-
ECR(Chromate)	32	1.16E-01	4.17E-04	-	1.35E+00	4.84E-03	-
ECR(Chromate)-10h	28	5.79E-03	7.67E-05	-	6.72E-02	8.90E-04	-
ECR(Valspar)	32	1.69E-01	2.31E-04	-	1.96E+00	2.68E-03	-
ECR(Valspar)-10h	28	9.09E-02	2.04E-04	-	1.05E+00	2.37E-03	-

Table 3.15 – Microcell corrosion current densities from linear polarization resistance test for ASTM G 109 specimens

Steel Designation[a]	Exposure time (weeks)	Corrosion current densities (μA/cm^2) from PR[b]			Corrosion rates (μm/yr) from PR[b]		
		top mat	bottom mat	connected	top mat	bottom mat	connected
Conv.	53	6.07E-03	3.75E-03	8.29E-03	7.04E-02	4.35E-02	9.62E-02
ECR	53	5.45E-05	2.83E-05	-	6.32E-04	3.28E-04	-
ECR-10h	41	3.17E-03	1.11E-02	1.56E-03	3.68E-02	-	1.81E-02
MC(both layers penetrated)	45	4.99E-05	5.05E-05	5.16E-05	5.79E-04	5.86E-04	5.99E-04
MC(both layers penetrated)-10h	45	3.29E-04	1.52E-04	-	3.82E-03	1.76E-03	-
MC(only epoxy penetrated)	45	8.48E-05	6.07E-05	5.91E-05	9.84E-04	7.04E-04	6.86E-04
MC(only epoxy penetrated)-10h	45	2.54E-04	1.47E-04	-	2.95E-03	1.71E-03	-

Tables 3.13, 3.14, and 3.15 continued:

[a] Conv. = conventional steel. ECR = normal epoxy-coated steel.
ECR(DuPont) = high adhesion DuPont bars.
ECR(Chromate) = ECR with the chromate pretreatment.
ECR(Valspar) = high adhesion Valspar bars.
ECR(Rheocrete) = normal ECR in concrete with corrosion inhibitor Rheocrete.
ECR(DCI) = normal ECR in concrete with corrosion inhibitor DCI.
ECR (Hycrete) = normal ECR in concrete with corroson inhibitor Hycrete.
MC(only epoxy penetrated) = mutiple coated bars with only epoxy penetrated.
MC(both layers penetrated) = multiple coated bars with both layers penetrated.
10h = epoxy-coated rebar with 10 holes, otherwise 4 holes.
35 = concrete w/c=0.35, otherwise w/c=0.45.

[b] The scan range: + and - 20 mV of corrosion potentials. The scan rate is 0.125 mV/s. Tafel constant β is 0.0373
Corrosion current densities are based on total area of bars.

3.6.1 Southern Exposure Tests

The microcell corrosion rates of top mats of Southern Exposure specimens are shown in Figures 3.155-3.159. Figures 3.155 (b) to 3.159 (b) expand the vertical axes in Figures 3.155 (a) to 3.159 (a). The results of some specimens started from week 16, instead of week 4, since the dates for testing were missed for weeks 4 and 8. The corrosion rate of the specimen containing conventional steel with a *w/c* ratio of 0.45 (Figure 3.155) increases rapidly at week 32 and reaches a value as high as 3.4 μm/yr at week 44, but drops to 0.11 μm/yr at week 48. For any of the epoxy-coated specimens in concrete with a *w/c* ratio of 0.45 and four drilled holes, no obvious corrosion (rate of more than 0.01 μm/yr) is observed based on the total area. For the epoxy-coated specimens with a *w/c* ratio of 0.45 and 10 drilled holes (Figure 3.156), the conventional ECR specimen approaches a value as high as 0.12 μm/yr, followed by ECR(DuPont) at 0.04 μm/yr, and ECR(Chromate) and ECR(Rheocrete) both at 0.02 μm/yr. To convert to a value based on the exposed area, the value based on the total area should be multiplied by 480.

For specimens cast in concrete with a *w/c* ratio of 0.35 (Figure 3.157), conventional steel shows the highest corrosion rate, 0.5 μm/yr at week 36. The conventional ECR, ECR(Rheocrete) and ECR(primer/$Ca(NO_2)_2$) specimens with 10 holes also exhibit measurable corrosion rates (above 0.01 μm/yr) based on the total area, while the ECR(DCI) and ECR(Hycrete) with 10 holes have corrosion rates of less than 0.005 μm/yr.

The multiple coated specimens penetrated with four holes (Figure 3.158) exhibit measurable corrosion rates after only eight weeks, with MC with both layers penetrated showing a corrosion rate close to 0.12 μm/yr and MC with only the epoxy layer penetrated showing a value as high as 0.02 μm/yr at week 12. Both of the corrosion rates exhibited by multiple coated specimens are higher than for the conventional ECR specimen (0 μm/yr at week 16). For specimens with 10 holes (Figure 3.159), the corrosion rates of the multiple coated specimens with either both layers or only the epoxy penetrated increase rapidly at weeks 12 and 16, respectively, and reach 0.15 and 0.1 μm/yr later. The values are higher than for the conventional ECR specimen with 10 holes at the same point in time (0 μm/yr), but close to that exhibited by ECR specimen at week 40 (0.11 μm/yr).

Compared to the macrocell corrosion rates of the corresponding Southern Exposure specimens, the microcell corrosion rates from linear polarization tests are of the same magnitude for all specimens, except for the specimens containing conventional steel, for which the microcell corrosion rate is one order of magnitude higher than the macrocell corrosion rate between weeks 36 and 44.

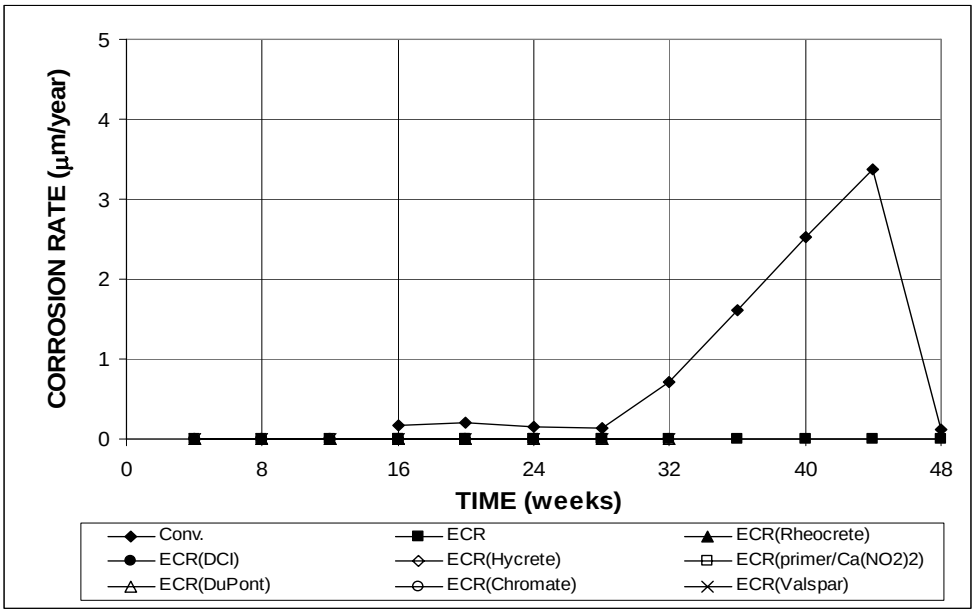

Figure 3.155 (a) – Southern Exposure Tests. Microcell Corrosion Rate. Specimens of conventional and epoxy-coated steel, epoxy-coated steel cast with corrosion inhibitors, epoxy-coated steel with a calcium nitrite primer, and high adhesion ECR steel ponded with 15% NaCl solution. All epoxy-coated specimens penetrated with four holes. Refer to Table 3.13 for specimen identification.

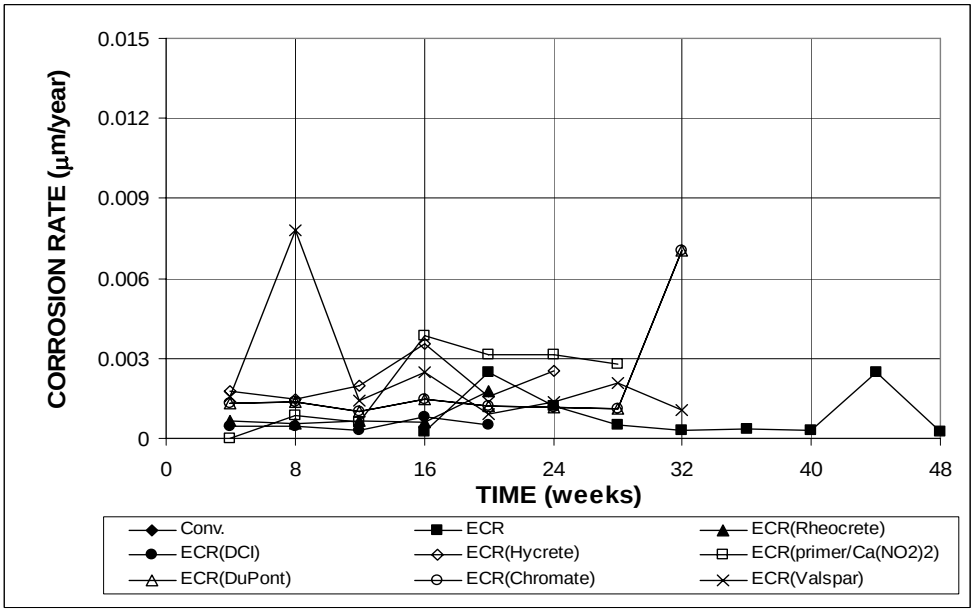

Figure 3.155 (b) – Southern Exposure Tests. Microcell Corrosion Rate. Specimens of conventional and epoxy-coated steel, epoxy-coated steel cast with corrosion inhibitors, epoxy-coated steel with a calcium nitrite primer, and high adhesion ECR steel ponded with 15% NaCl solution. All epoxy-coated specimens penetrated with four holes. Refer to Table 3.13 for specimen identification.

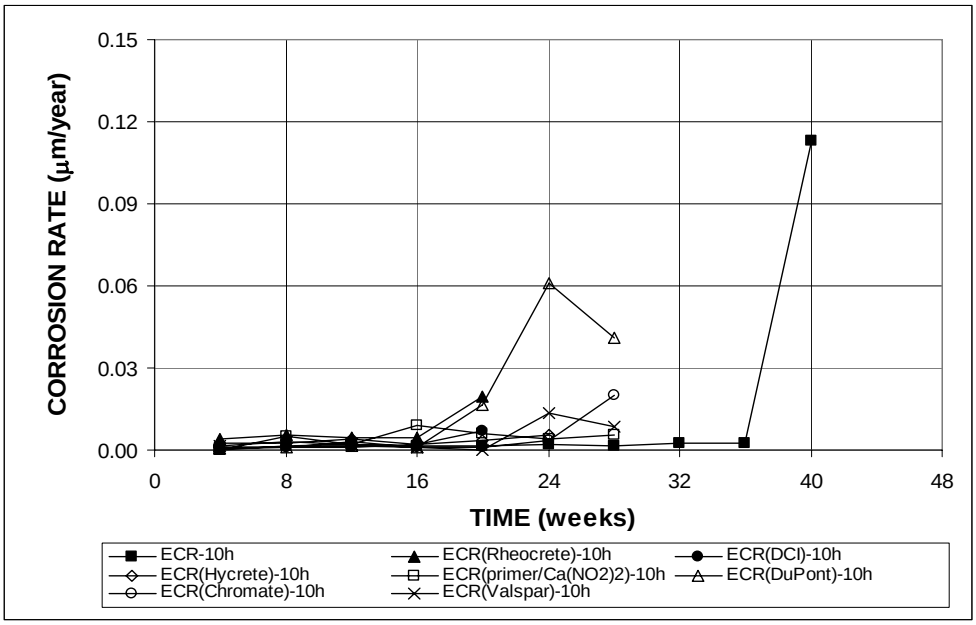

Figure 3.156 (a) – Southern Exposure Tests. Microcell Corrosion Rate. Specimens of epoxy-coated steel, epoxy-coated steel cast with corrosion inhibitors, epoxy-coated steel with a calcium nitrite primer, and high adhesion ECR steel ponded with 15% NaCl solution. All epoxy-coated specimens penetrated with 10 holes. Refer to Table 3.13 for specimen identification.

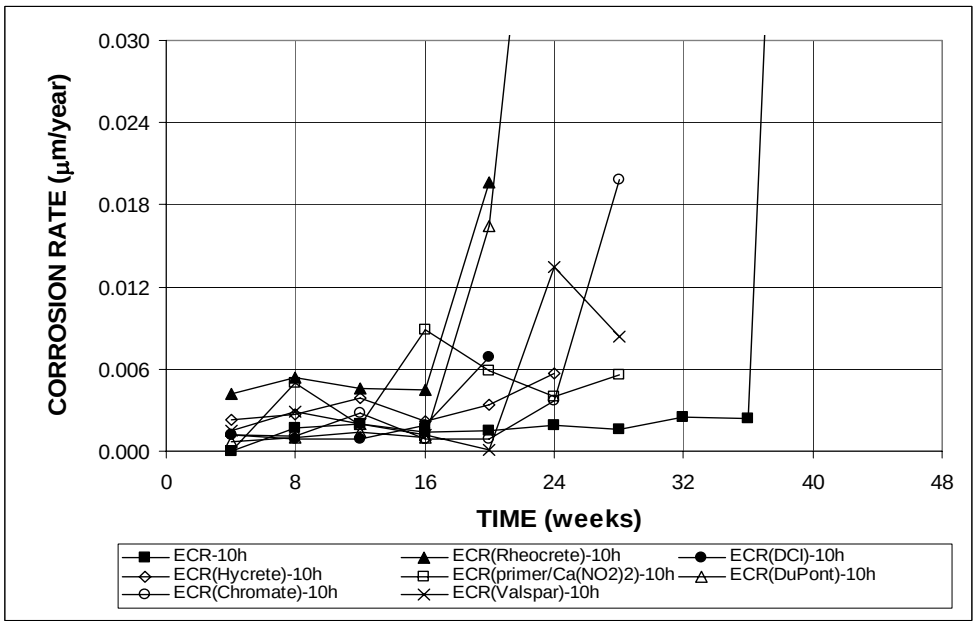

Figure 3.156 (b) – Southern Exposure Tests. Microcell Corrosion Rate. Specimens of epoxy-coated steel, epoxy-coated steel cast with corrosion inhibitors, epoxy-coated steel with a calcium nitrite primer, and high adhesion ECR steel ponded with 15% NaCl solution. All epoxy-coated specimens penetrated with 10 holes. Refer to Table 3.13 for specimen identification.

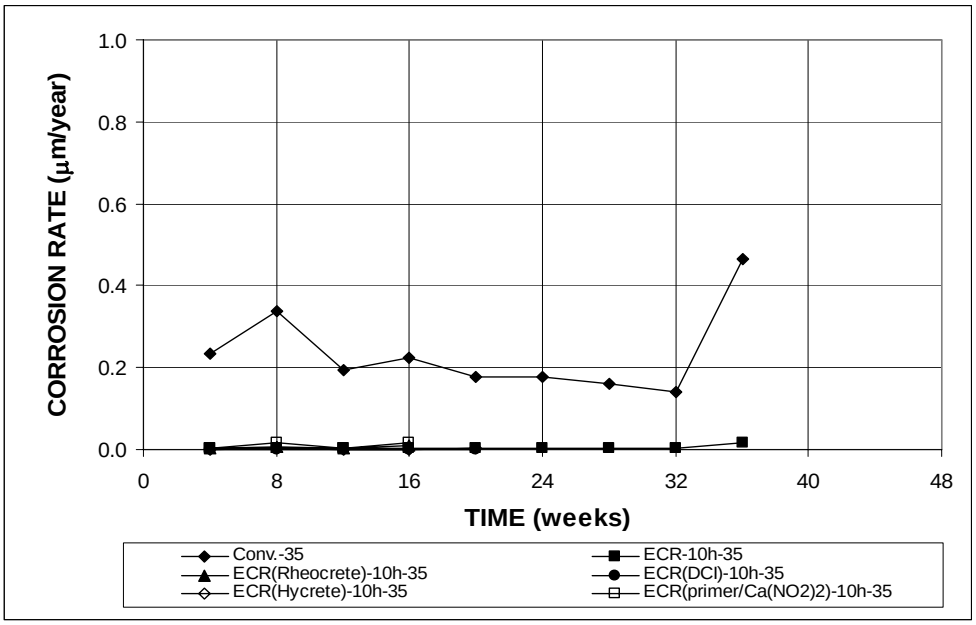

Figure 3.157 (a) – Southern Exposure Tests. Microcell Corrosion Rate. Specimens of conventional and epoxy-coated steel, epoxy-coated steel cast with corrosion inhibitors, and epoxy-coated steel with a calcium nitrite primer ponded with 15% NaCl solution. All epoxy-coated specimens penetrated with 10 holes. Refer to Table 3.13 for specimen identification.

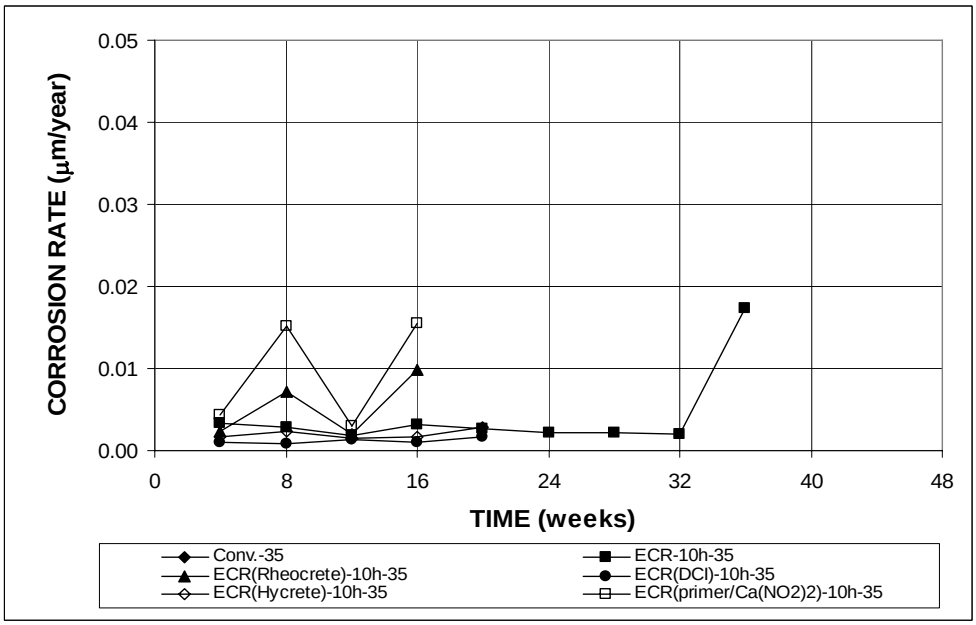

Figure 3.157 (b) – Southern Exposure Tests. Microcell Corrosion Rate. Specimens of conventional and epoxy-coated steel, epoxy-coated steel cast with corrosion inhibitors, and epoxy-coated steel with a calcium nitrite primer ponded with 15% NaCl solution. All epoxy-coated specimens penetrated with 10 holes. Refer to Table 3.13 for specimen identification.

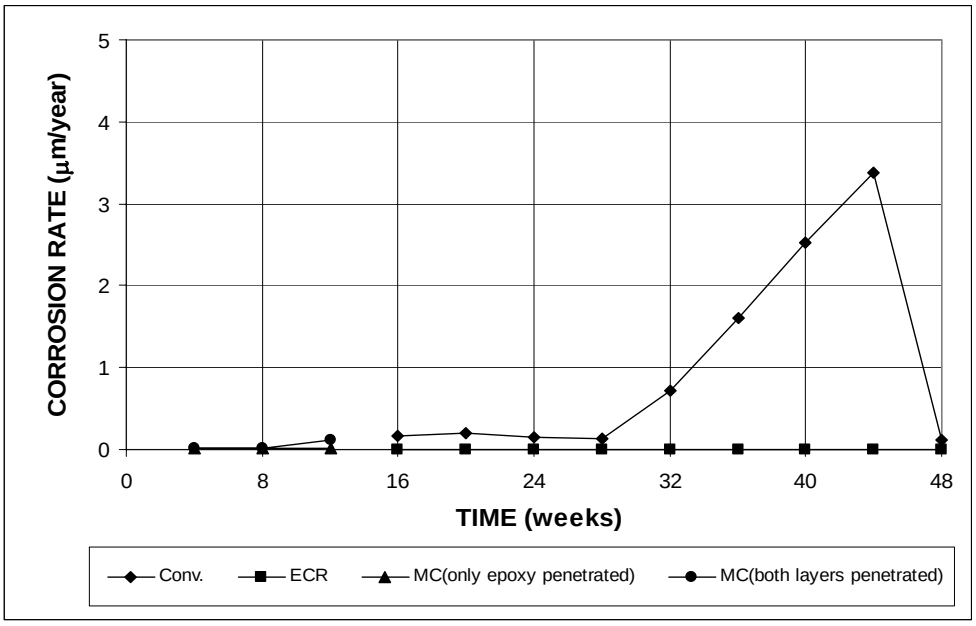

Figure 3.158 (a) – Southern Exposure Tests. Microcell Corrosion Rate. Specimens of conventional, epoxy-coated, and multiple coated steel ponded with 15% NaCl solution. All epoxy-coated and multiple coated specimens penetrated with four holes. Refer to Table 3.13 for specimen identification.

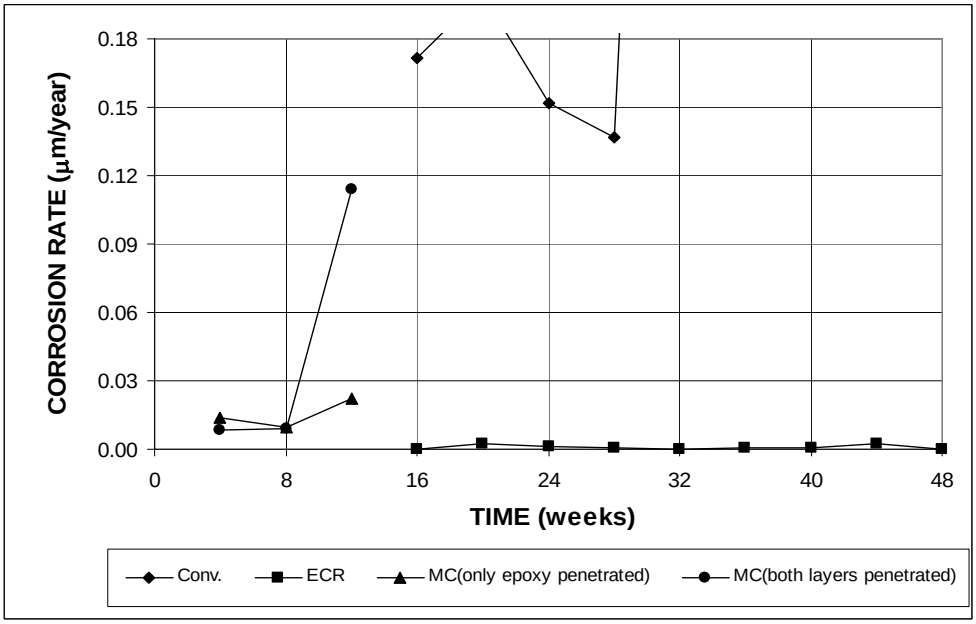

Figure 3.158 (b) – Southern Exposure Tests. Microcell Corrosion Rate. Specimens of conventional, epoxy-coated, and multiple coated steel ponded with 15% NaCl solution. All epoxy-coated and multiple coated specimens penetrated with four holes. Refer to Table 3.13 for specimen identification.

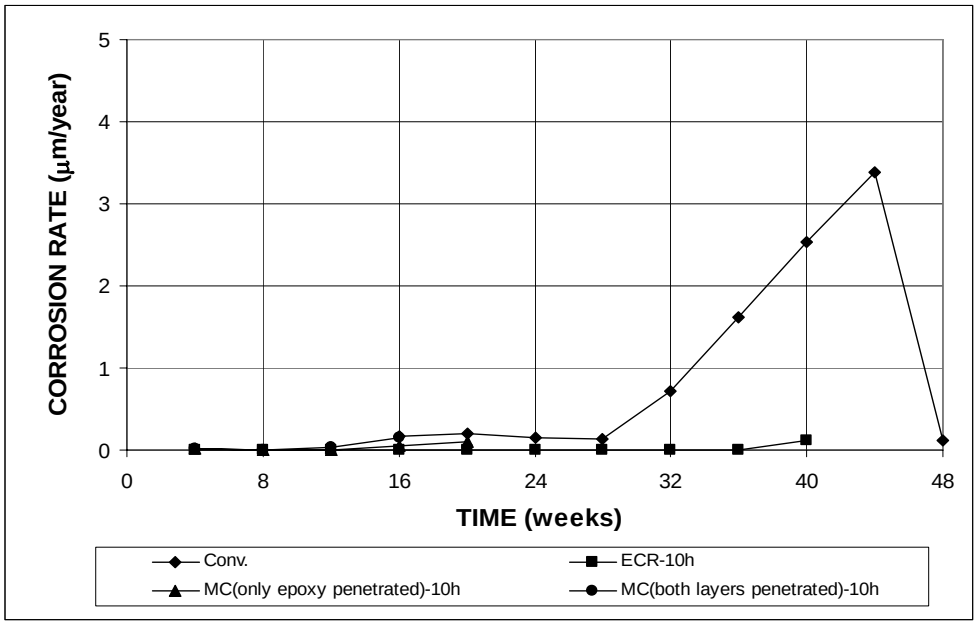

Figure 3.159 (a) – Southern Exposure Tests. Microcell Corrosion Rate. Specimens of conventional, epoxy-coated, and multiple coated steel ponded with 15% NaCl solution. All epoxy-coated and multiple coated specimens penetrated with 10 holes. Refer to Table 3.13 for specimen identification.

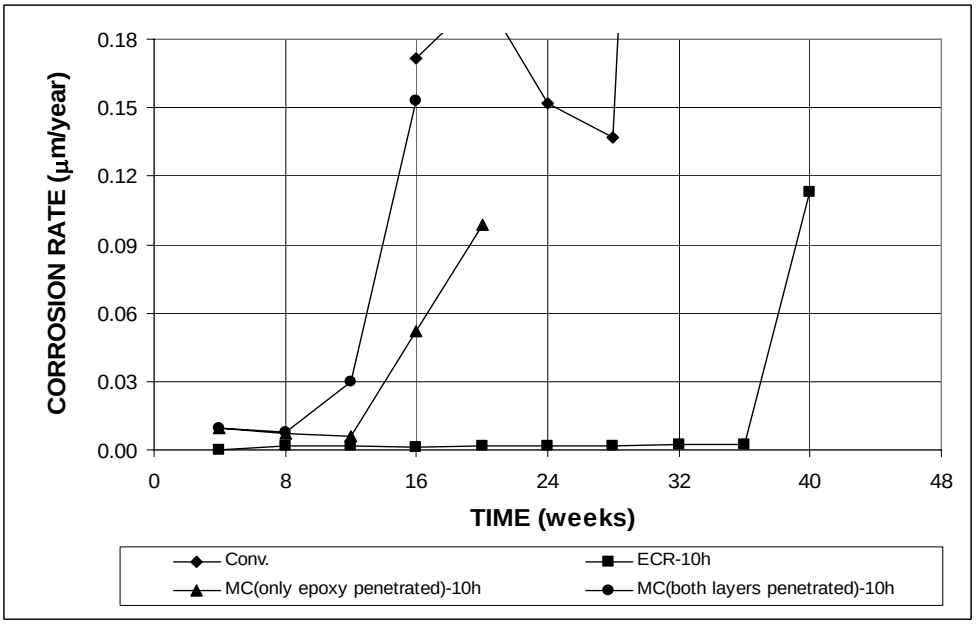

Figure 3.159 (b) – Southern Exposure Tests. Microcell Corrosion Rate. Specimens of conventional, epoxy-coated, and multiple coated steel ponded with 15% NaCl solution. All epoxy-coated and multiple coated specimens penetrated with 10 holes. Refer to Table 3.13 for specimen identification.

3.6.2 Cracked Beam Tests

The microcell corrosion rates of top mats of cracked beam specimens are presented in Figures 3.160-3.164. The corrosion rate of the specimens containing conventional steel with a *w/c* ratio of 0.45 (Figure 3.160) started at 32 μm/yr at week 16, reaching a maximum value of 85 μm/yr at week 40 and slightly dropping to 77 μm/yr at week 48. For the epoxy-coated specimens with four drilled holes, the ECR(Valspar) specimen exhibited a corrosion rate of zero at the beginning of test period, increasing to 2 μm/yr at week 32. The corrosion rate of the ECR(Chromate) specimen started at 0.5 μm/yr at week 4, rising to 1.3 μm/yr at week 32. The conventional ECR specimen exhibited no corrosion until week 36, but reached a rate of 0.8 μm/yr at week 48. The ECR specimens cast in concrete with corrosion inhibitors and the ECR(DuPont) specimen also exhibited observable corrosion rates, between 0.09 and 0.62 μm/yr, with no specimens reaching a rate above 1 μm/yr during the test period, except the ECR (DCI) specimen, which jumped to 1.15 μm/yr at week 12. The results indicate that corrosion inhibitors do not improve the corrosion resistance of steel in cracked concrete.

For the epoxy-coated specimens with 10 drilled holes (Figure 3.161), the corrosion rate of the ECR(Chromate) specimen started below 0.5 μm/yr, increasing to a value as high as 1.3 μm/yr at week 32. The next highest value was exhibited by the ECR(Valspar) specimen, with a rate of 1.1 μm/yr at week 28. Other specimens have also undergone active corrosion at top mats, with corrosion rates between 0.3 to 0.6 μm/yr. The conventional ECR specimen exhibits lower corrosion rates than all other specimens during most of the test period, except at weeks 8 and 28.

For specimens cast in concrete with a *w/c* ratio of 0.35 and 10 drilled holes (Figure 3.162), the conventional steel specimen, starting at a rate of 0 and jumping

above 30 μm/yr beginning in week 8, has the highest corrosion rate at week 36, 91 μm/yr. The ECR(DCI) specimen reached a rate as high as 2 μm/yr at week 12, dropping to 1.3 μm/yr at week 20. The corrosion rate of ECR(primer/$Ca(NO_2)_2$) specimen has been around 1 μm/yr since the initiate of the test. The ECR(Rheocrete) and ECR(Hycrete) specimens exhibited corrosion rates below 0.5 μm/yr during the test period, with the exception of the ECR(Hycrete) specimen at week 16 (0.7 μm/yr). The conventional ECR specimen exhibited a corrosion rate lower than 0.5 μm/yr until week 28, increasing to 0.7 μm/yr at week 36. The results demonstrate that a lower water-cement ratio does not protect steel from corrosion in cracked concrete.

The multiple coated specimens penetrated with four holes (Figure 3.163) exhibit significant corrosion rates (above 0.5 μm/yr) at week 8, with the MC(both layers penetrated) showing a corrosion rate of 2 μm/yr and MC(only epoxy layer penetrated) showing a value of 1.3 μm/yr at week 12. Both of the corrosion rates exhibited by the multiple coated specimens are higher than for the conventional ECR specimen (0 μm/yr at 16 weeks). For specimens with 10 holes (Figure 3.164), the corrosion rate of the multiple coated specimens with both layers penetrated increased rapidly after the test started, reaching 1.7 μm/yr by week 16. The corrosion rate of the specimen containing multiple coated steel with only the epoxy penetrated by 10 holes increased up at week 8 and has been stable at around 0.2 μm/yr.

The microcell corrosion rates from the linear polarization tests are about one order higher in magnitude than the macrocell corrosion rates of the corresponding cracked beam specimens.

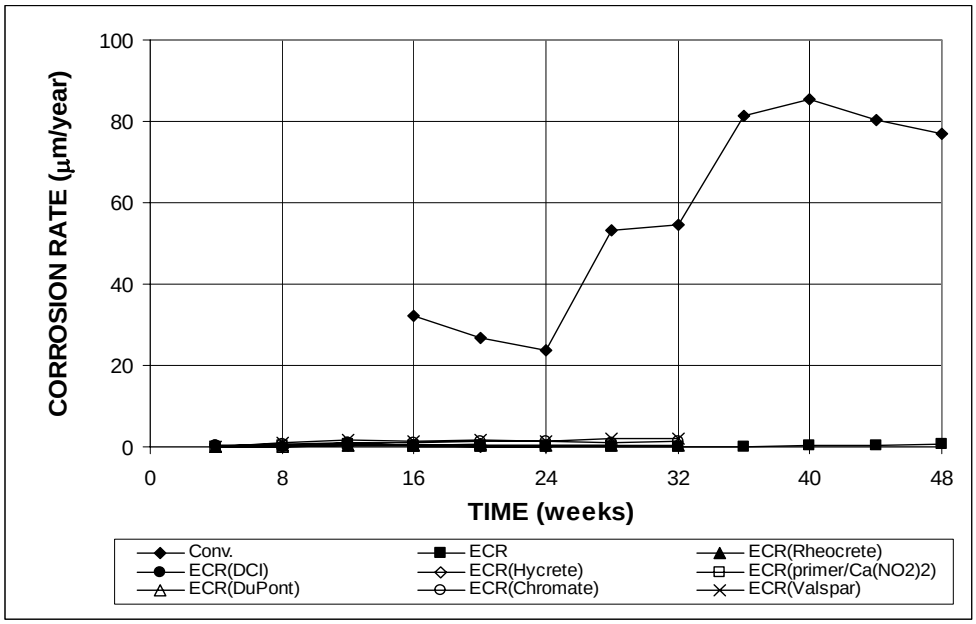

Figure 3.160 (a) – Cracked Beam Tests. Microcell Corrosion Rate. Specimens of conventional and epoxy-coated steel, epoxy-coated steel cast with corrosion inhibitors, epoxy-coated steel with a calcium nitrite primer, and high adhesion ECR steel ponded with 15% NaCl solution. All epoxy-coated specimens penetrated with four holes. Refer to Table 3.14 for specimen identification.

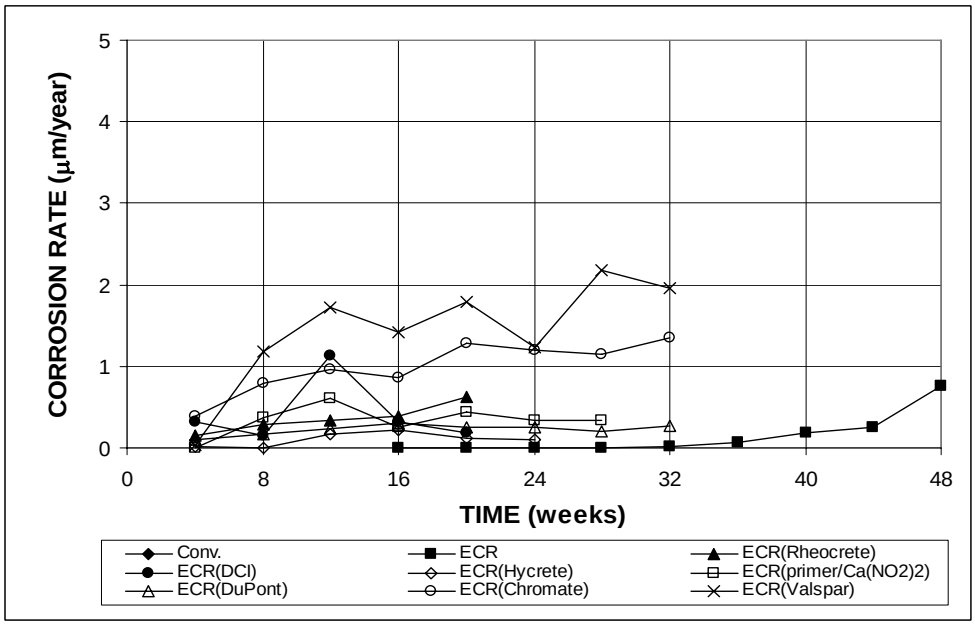

Figure 3.160 (b) – Cracked Beam Tests. Microcell Corrosion Rate. Specimens of conventional and epoxy-coated steel, epoxy-coated steel cast with corrosion inhibitors, epoxy-coated steel with a calcium nitrite primer, and high adhesion ECR steel ponded with 15% NaCl solution. All epoxy-coated penetrated with four holes. Refer to Table 3.14 for specimen identification.

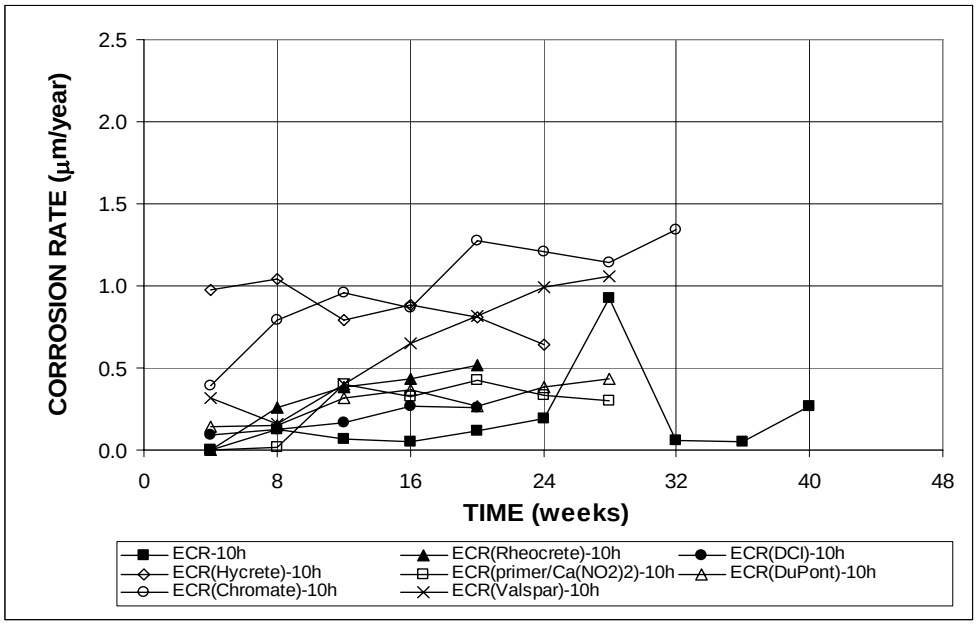

Figure 3.161 – Cracked Beam Tests. Microcell Corrosion Rate. Specimens of epoxy-coated steel, epoxy-coated steel cast with corrosion inhibitors, epoxy-coated steel with a calcium nitrite primer, and high adhesion ECR steel ponded with 15% NaCl solution. All epoxy-coated specimens penetrated with 10 holes. Refer to Table 3.14 for specimen identification.

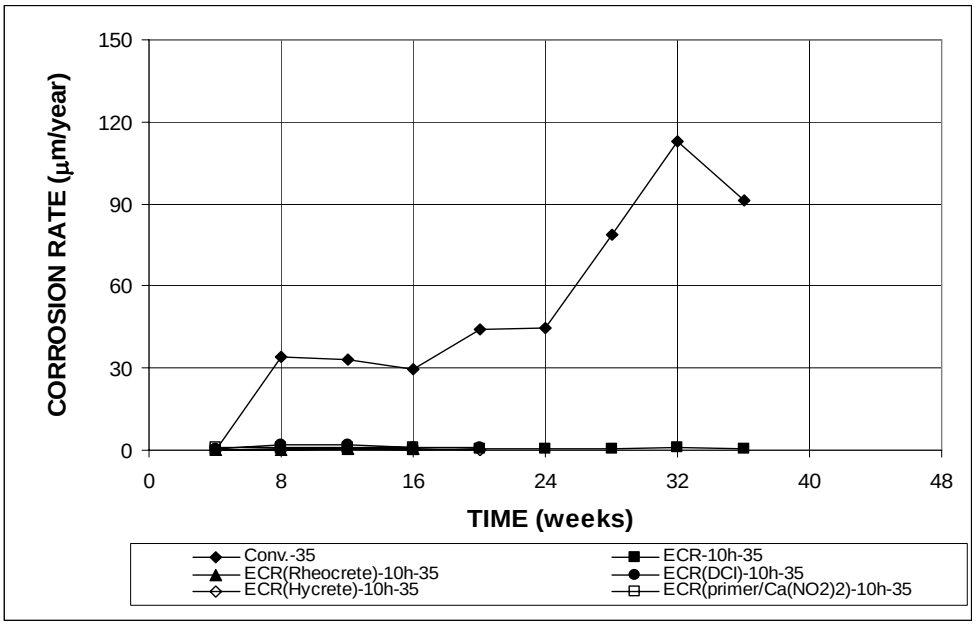

Figure 3.162 (a) – Cracked Beam Tests. Microcell Corrosion Rate. Specimens of conventional and epoxy-coated steel, epoxy-coated steel cast with corrosion inhibitors, and epoxy-coated steel with a calcium nitrite primer ponded with 15% NaCl solution. All epoxy-coated specimens penetrated with 10 holes. Refer to Table 3.14 for specimen identification.

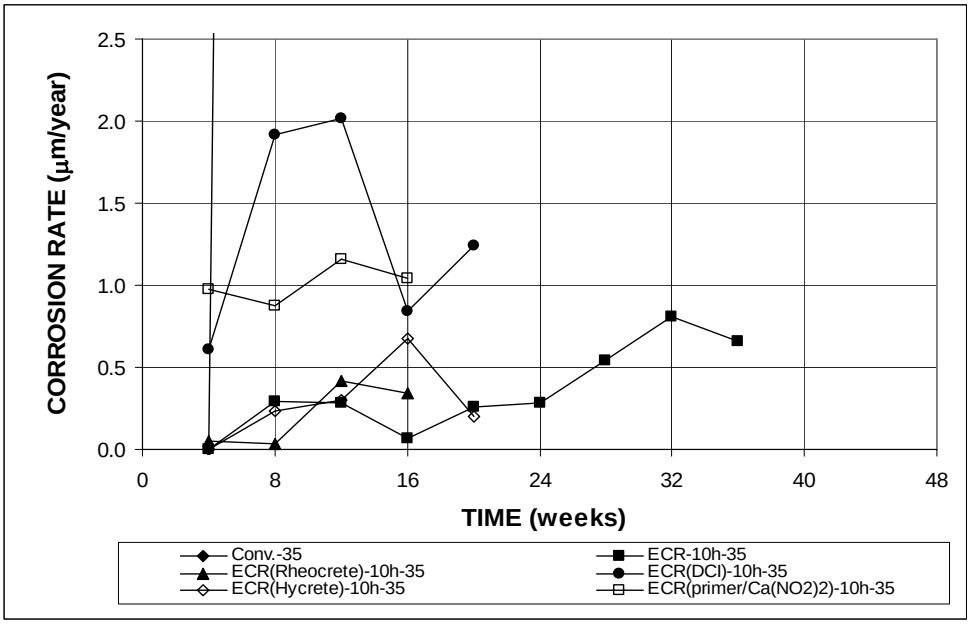

Figure 3.162 (b) – Cracked Beam Tests. Microcell Corrosion Rate. Specimens of conventional and epoxy-coated steel, epoxy-coated steel cast with corrosion inhibitors, and epoxy-coated steel with a calcium nitrite primer ponded with 15% NaCl solution. All epoxy-coated specimens penetrated with 10 holes. Refer to Table 3.14 for specimen identification.

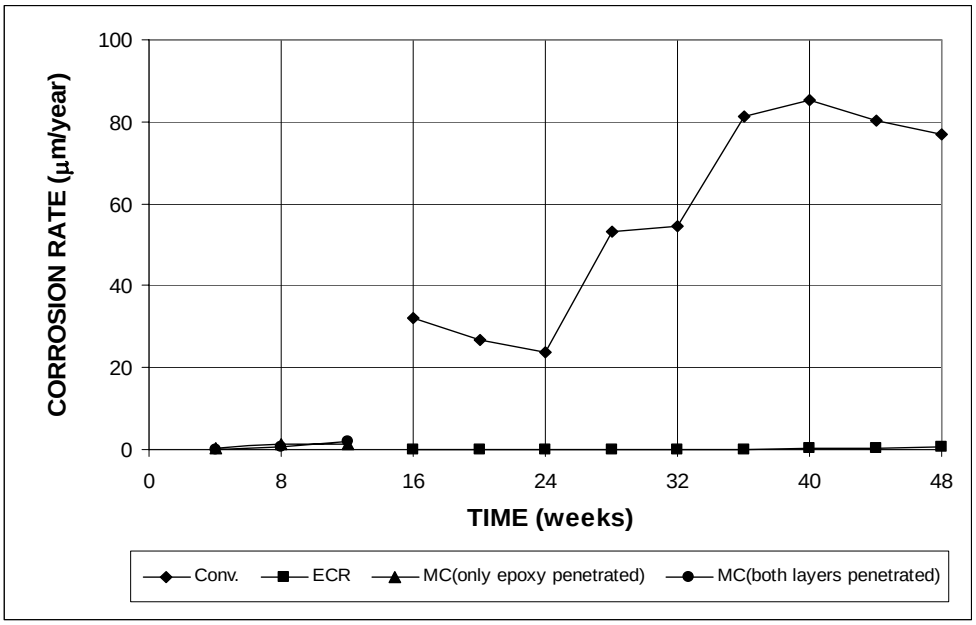

Figure 3.163 (a) – Cracked Beam Tests. Microcell Corrosion Rate. Specimens of conventional, epoxy-coated, and multiple coated steel ponded with 15% NaCl solution. All epoxy-coated and multiple coated specimens penetrated with four holes. Refer to Table 3.14 for specimen identification.

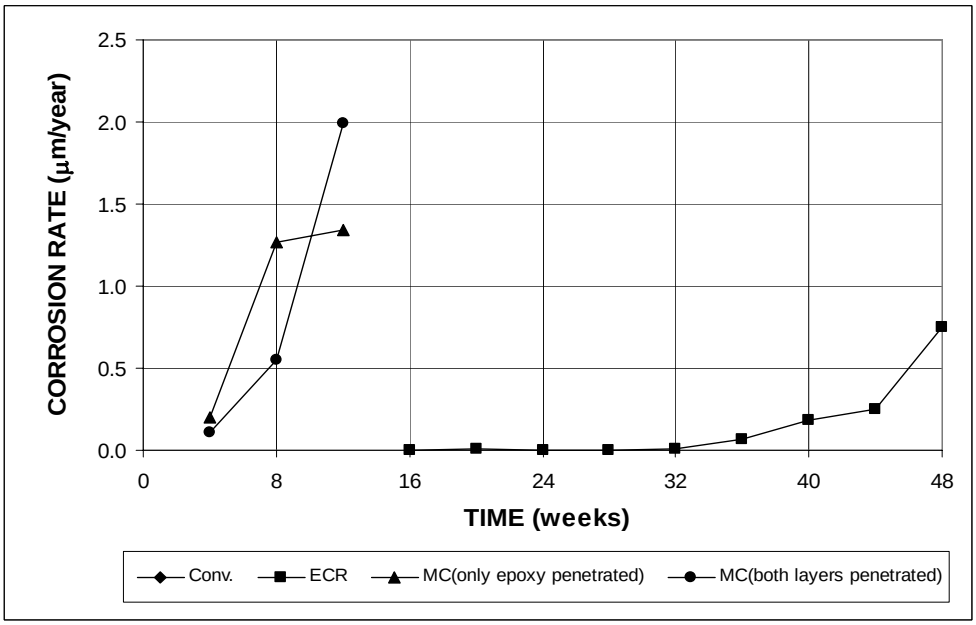

Figure 3.163 (b) – Cracked Beam Tests. Microcell Corrosion Rate. Specimens of conventional, epoxy-coated, and multiple coated steel ponded with 15% NaCl solution. All epoxy-coated and multiple coated specimens penetrated with four holes. Refer to Table 3.14 for specimen identification.

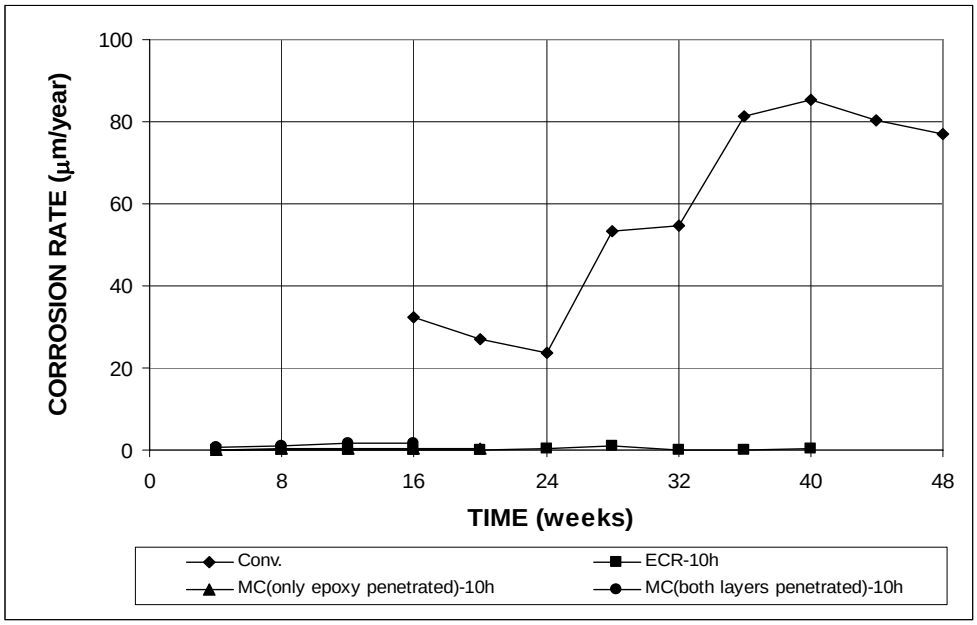

Figure 3.164 (a) – Cracked Beam Tests. Microcell Corrosion Rate. Specimens of conventional, epoxy-coated, and multiple coated steel ponded with 15% NaCl solution. All epoxy-coated and multiple coated specimens penetrated with 10 holes. Refer to Table 3.14 for specimen identification.

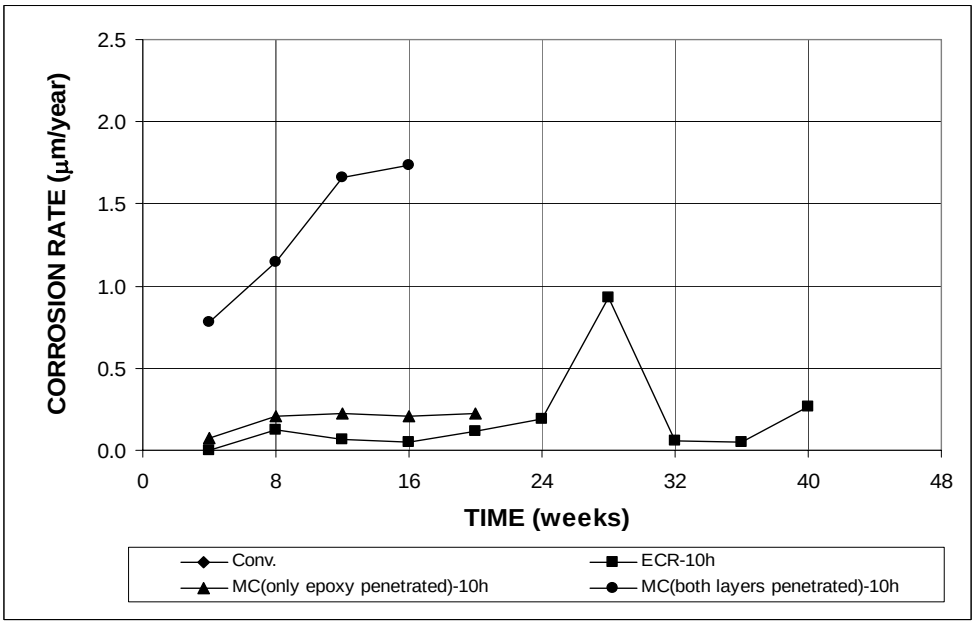

Figure 3.164 (b) – Cracked Beam Tests. Microcell Corrosion Rate. Specimens of conventional, epoxy-coated, and multiple coated steel ponded with 15% NaCl solution. All epoxy-coated and multiple coated specimens penetrated with 10 holes. Refer to Table 3.14 for specimen identification.

3.6.3 ASTM G 109 Tests

The results for the ASTM G 109 specimens are shown in Figures 3.165 and 3.166. The specimen containing conventional steel (Figure 3.165) exhibits a corrosion rate as high as 0.15 μm/yr at some points during the test period, with a rate of 0.07 μm/yr at week 53. The conventional ECR specimen with 10 drilled holes (Figure 3.166) shows a corrosion rate as high as 0.05 μm/yr at week 37, with a value of 0.04 μm/yr at week 41. The corrosion rate of the multiple coated steel with both layers penetrated by 10 holes jumps to 0.13 μm/yr at week 41 but drops below 0.01 μm/yr after that. Corrosion at a rate more than 0.005 μm/yr is not detected on any other specimens.

Compared to the macrocell corrosion rates of the corresponding ASTM G 109 specimens, the microcell corrosion rates from linear polarization tests are similar in magnitude for all specimens, except for conventional steel, for which the microcell corrosion rate is one order higher in magnitude than the macrocell corrosion rate.

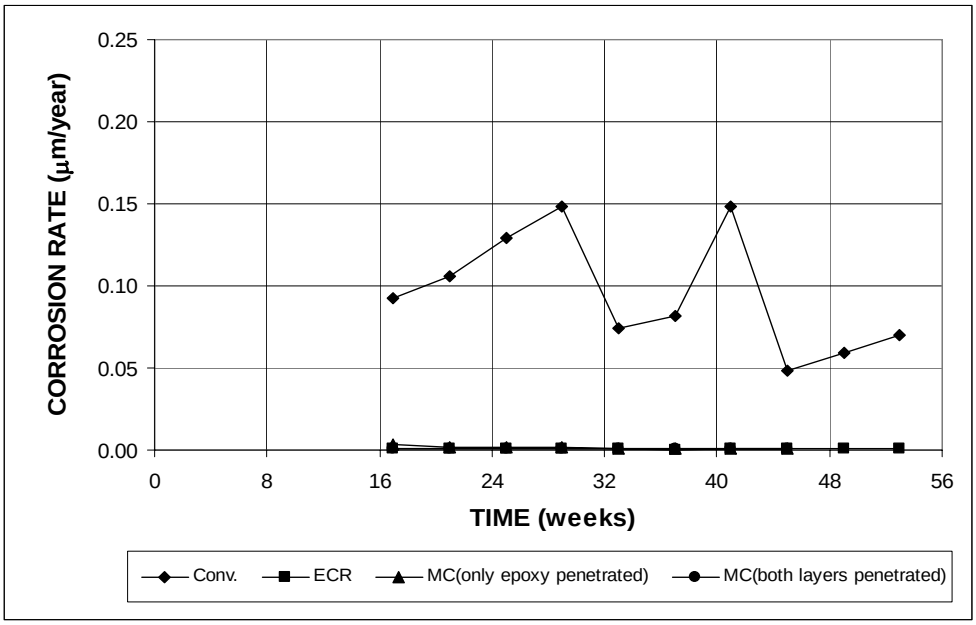

Figure 3.165 (a) – ASTM G 109 Tests. Microcell Corrosion Rate. Specimens of conventional, epoxy-coated, and multiple coated steel ponded with 15% NaCl solution. All epoxy-coated and multiple coated specimens penetrated with four holes. Refer to Table 3.14 for specimen identification.

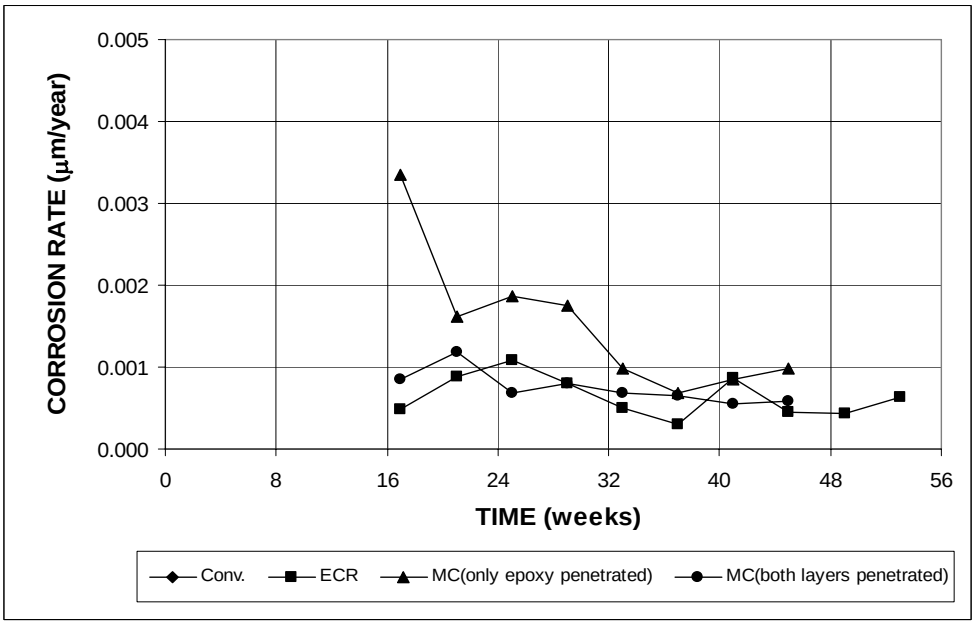

Figure 3.165 (b) – ASTM G 109 Tests. Microcell Corrosion Rate. Specimens of conventional, epoxy-coated, and multiple coated steel ponded with 15% NaCl solution. All epoxy-coated and multiple coated specimens penetrated with four holes. Refer to Table 3.14 for specimen identification.

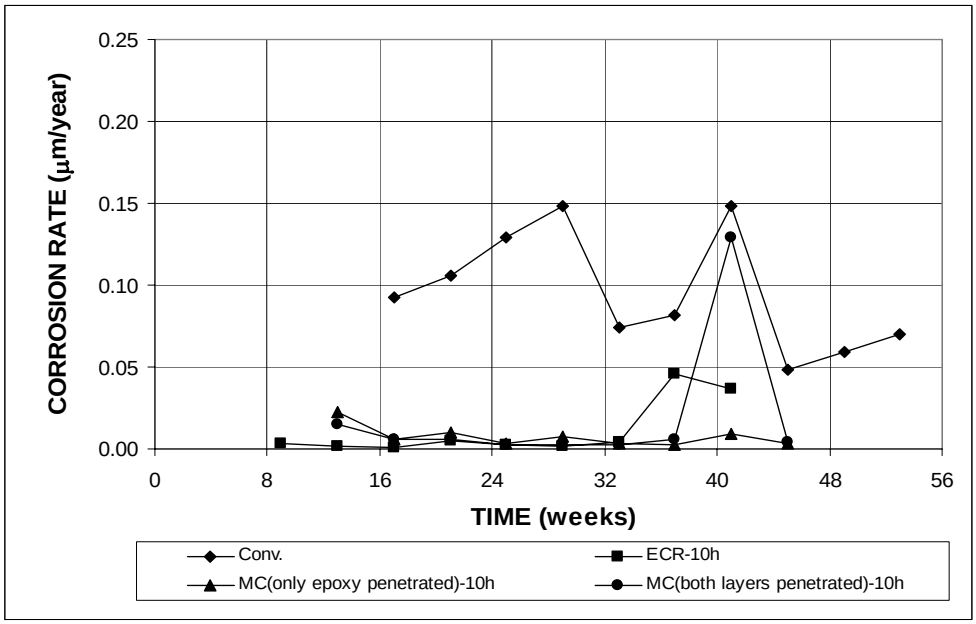

Figure 3.166 (a) – ASTM G 109 Tests. Microcell Corrosion Rate. Specimens of conventional, epoxy-coated, and multiple coated steel ponded with 15% NaCl solution. All epoxy-coated and multiple coated specimens penetrated with 10 holes. Refer to Table 3.14 for specimen identification.

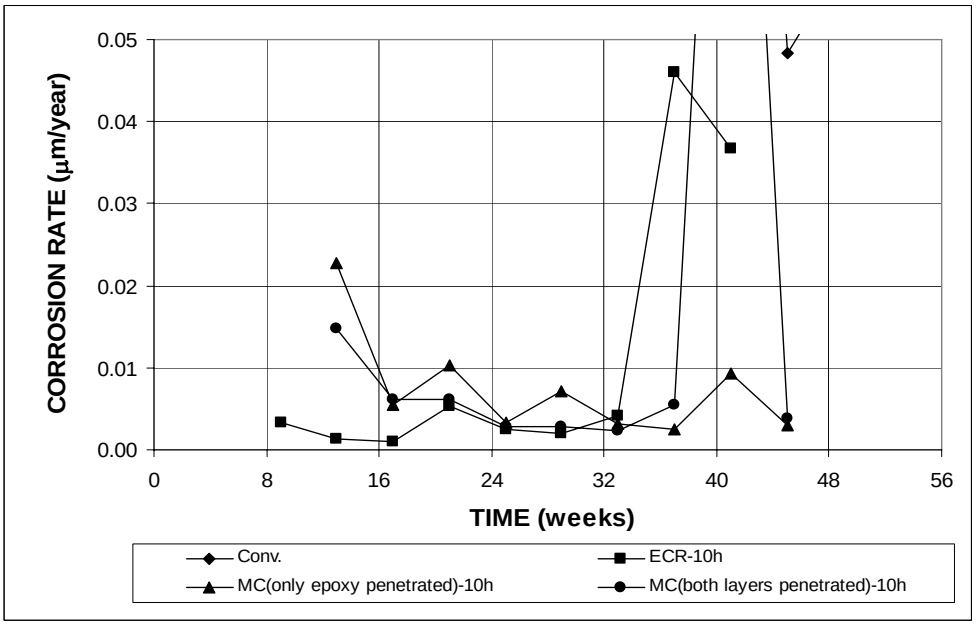

Figure 3.166 (b) – ASTM G 109 Tests. Microcell Corrosion Rate. Specimens of conventional, epoxy-coated, and multiple coated steel ponded with 15% NaCl solution. All epoxy-coated and multiple coated specimens penetrated with 10 holes. Refer to Table 3.14 for specimen identification.

3.7 CATHODIC DISBONDMENT TESTS

Three rounds of cathodic disbondment testing, with one specimen each, were carried out for the conventional ECR, ECR with improve adhesion between steel and epoxy as described in Section 3.3, ECR with a primer containing calcium nitrite, and multiple coated bars. In accordance with ASTM A 775, four measurements were taken at 0°, 90°, 180°, and 270° and the values were averaged. The cathodic disbondment test results were recorded in terms of both the area of the disbonded coating and the average coating disbondment radius (four measurements), respectively. The results are summarized in Table 3.16. The area of the disbonded coating listed in Table 3.16 is the area that is peeled off using a knife at the intentional holiday.

As shown in Table 3.16, the average coating disbondment radius of three tests is above 4 mm (the maximum allowed in Annex A1 of ASTM A 775) for conventional ECR (5.9 mm) and high adhesion Valspar bars (4.9 mm), indicating that these bars failed the coating disbondment requirements. Multiple coated reinforcement (0.27 mm), high adhesion DuPont bars (2.8 mm), ECR with the chromate pretreatment (1.0 mm), and ECR with a calcium nitrite primer (2.6 mm) meet the coating disbondment requirements.

Table 3.16 shows that the conventional ECR exhibited the highest area of disbonded coating, with an average value of 1.78 cm^2. The high adhesion Valspar bars had an area of disbonded coating of 1.51 cm^2, followed by ECR with a calcium nitrite primer at 0.67 cm^2 and high adhesion DuPont bars at 0.65 cm^2, respectively. Multiple coated reinforcement and ECR with the chromate pretreatment showed the lowest areas of disbonded coating, with average values of 0.27 and 0.20 cm^2, respectively.

The requirements in Annex A1 of A 775 are qualification requirements for the epoxy coating itself and are not meant to be applied to production bars. Because the conventional epoxy-coated bars tested in this study do not meet the cathodic disbondment criterion in Annex A1 of ASTM A 775, it is recommended that cathodic disbondment should be added to the quality control checks applied to production bars, rather than serve only as a tool for process control, as currently specified.

Table 3.16 – Disbonded area for convention ECR, ECR with high adhesion between epoxy and steel, and multiple coated steel from cathodic disbondment test

Type of coating[a]	No. of test	Thickness (mils)	Coating disbondment radius (mm)[b]					Area of disbonded coating (cm^2)[c]	Visual examination
			0^o	90^o	180^o	270^o	Average		
ECR	1st		6.5	6.5	6	5.5	6.1	1.83	rust on exposured area, black color at surrounding area
	2nd		6.5	5	3.5	4	4.8	1.33	no rust
	3rd	9.8	6.5	6.5	7.5	6.5	6.8	2.19	little rust
	Average						**5.9**	**1.78**	
ECR^+	1st	11.8	5.5	6.5	5.5	5	5.6	1.70	no rust
	2nd	10.8	5.5	4.5	4.5	5.5	5.0	1.61	no rust
	3rd	9.5	6.5	5.5	5.5	5.5	5.8	1.74	no rust
							5.5	**1.68**	
MC	1st		2.5	1.5	1	1	1.5	0.22	rust on exposured area
	2nd		2	1.5	1.5	3	2.0	0.35	rust on exposured area
	3rd	11.2	0.5	2.5	1.5	1.5	1.5	0.25	rust on exposured area
	Average						**1.7**	**0.27**	
ECR(DuPont)	1st		4	3	3.5	3.5	3.5	0.93	no rust
	2nd		1.5	1	1.5	1	1.3	0.19	no rust
	3rd	8.8	3.5	4	3.5	4	3.8	0.83	no rust
	Average						**2.8**	**0.65**	
ECR(Valspar)	1st		4.5	4	4.5	4	4.3	1.33	rust on exposured area
	2nd		6	4.5	5.5	4.5	5.1	1.67	no rust
	3rd	10.6	6.5	4.5	5.5	4.5	5.3	1.54	no rust
	Average						**4.9**	**1.51**	
ECR(Chromate)	1st		0.5	1	0	0	0.4	0.06	rust on exposured area
	2nd		1	0.5	2	2.5	1.5	0.35	rust on exposured area
	3rd	11	1.5	0.5	0.5	1.5	1.0	0.19	no rust
	Average						**1.0**	**0.20**	
ECR(primer/ $Ca(NO_2)_2$)	1st		1.5	2	2	2	1.9	0.58	no rust
	2nd		3.5	2.5	4.5	2.5	3.3	0.77	no rust
	3rd	8	3	2.5	2.5	2.5	2.6	0.67	no rust
	Average						**2.6**	**0.67**	

[a] ECR = normal epoxy-coated reinforcement. ECR^+ = previous batch of normal epoxy-coated reinforcment.
MC = multiple coated reinforcement. ECR(DuPont) = high adhesion DuPont bars.
ECR(Valspar) = high adhesion Valspar bars. ECR(Chromate) = ECR with the zinc and chromate pretreatment.
ECR(primer/$Ca(NO_2)_2$) = ECR with a primer containing calcium nitrite.

[b] Coating disbonement radius is measured from the edge of a 3-mm diameter hole..

[c] Area of disbonded coating is the total area after disbondment minus the original area of a 3-mm diameter hole.

3.8 MECHANICAL TESTING OF THE REINFORCING BARS

Both stainless steel clad reinforcement and conventional steel were tested for mechanical properties. The yield strength, tensile strength, elongation, and bending results are summarized in Table 3.17.

The yield strengths for conventional steel were obtained based on a well-defined yield point. The average yield strengths ranged from a low of 459.9 MPa (66.7 ksi) for a heat of No. 13 [No. 4] bars to a high of 510.9 MPa (74.1 ksi) for a heat of No. 19 [No. 6] bars. Average tensile strengths were between 749.5 MPa (108.7 ksi) and 816.3 MPa (118.4 ksi). Average elongations ranged from 13.6 to 16.8%, with a low of 10.9% for an individual test.

The No. 16 [No. 5] stainless steel clad reinforcement does not have an obvious yield plateau, while the No. 19 [No. 6] stainless steel clad reinforcement does. Based on 0.35% total strain, the yield strengths for the No. 16 [No. 5] bars ranged from 77.1 to 80.0 ksi, with an average of 78.9 ksi. For the No. 19 [No. 6] bars, the yield strengths ranged from 75.1 to 77.7 ksi, with an average of 76.4 ksi. The tensile strengths averaged 112.2 ksi for the No. 16 [No. 5] bars and 104.4 ksi for the No. 19 [No. 6] bars. Average elongations for an 8 in. gage length were 13.7% and 19.1%, respectively. All conventional and stainless steel clad bars passed the bend test.

The tests demonstrate that the No. 5 and No. 6 SMI bars satisfy the physical and mechanical properties required by ASTM A 615 and can be used as replacements for conventional No. 5 and No. 6 bars.

Table 3.17 – Mechanical test results

Steel	Heat No.	Size	Sample Number	Yield Strength MPa (ksi)	Tensile Strength MPa (ksi)	Elongation % in 8 in.	Bending
Conv.	S46753	No. 13 (No. 4)	1	451.6 (65.5)	733.6 (106.4)	14.1	Pass
			2	455.1 (66.0)	747.4 (108.4)	12.5	
			3	473.7 (68.7)	768.1 (111.4)	12.5	
			Average	459.9 (66.7)	749.5 (108.7)	13	
Conv.	S46757	No. 13 (No. 4)	1	501.2 (72.7)	790.8 (114.7)	12.5	Pass
			2	476.4 (69.1)	767.4 (111.3)	12.9	
			3	475.7 (69.0)	768.8 (111.5)	15.6	
			Average	484.7 (70.3)	775.7 (112.5)	13.7	
Conv.	S46760	No. 13 (No. 4)	1	495.7 (71.9)	768.8 (111.5)	12.5	Pass
			2	482.6 (70.0)	764.6 (110.9)	10.9	
			3	477.8 (69.3)	760.5 (110.3)	13.3	
			Average	485.4 (70.4)	764.6 (110.9)	12.2	
Conv.	S44407	No. 16 (No. 5)	1	470.2 (68.2)	761.9 (110.5)	16.4	Pass
			2	461.9 (67.0)	748.1 (108.5)	15.6	
			3	460.6 (66.8)	746.7 (108.3)	14.8	
			Average	464.0 (67.3)	752.2 (109.1)	15.6	
Conv.	S44420	No. 16 (No. 5)	1	469.5 (68.1)	779.8 (113.1)	12.5	Pass
			2	470.2 (68.2)	764.6 (110.9)	15.6	
			3	481.3 (69.8)	790.8 (114.7)	14.1	
			Average	473.7 (68.7)	778.4 (112.9)	14.1	
Conv.	S47695	No. 19 (No. 6)	1	511.6 (74.2)	819.1 (118.8)	14.1	Pass
			2	515.0 (74.7)	821.9 (119.2)	12.5	
			3	504.7 (73.2)	808.1 (117.2)	14.1	
			Average	510.2 (74.0)	816.3 (118.4)	13.6	
Conv.	S47790	No. 19 (No. 6)	1	508.1 (73.7)	797.0 (115.6)	12.9	Pass
			2	516.4 (74.9)	810.8 (117.6)	14.1	
			3	509.5 (73.9)	798.4 (115.8)	18.8	
			Average	510.9 (74.1)	801.9 (116.3)	15.3	
Conv.	S47814	No. 19 (No. 6)	1	473.0 (68.6)	759.1 (110.1)	18.4	Pass
			2	479.2 (69.5)	766.0 (111.1)	16.4	
			3	475.0 (68.9)	759.8 (110.2)	15.6	
			Average	475.7 (69.0)	761.9 (110.5)	16.8	
				0.35% total strain*			
SMI 316		No. 16 (No. 5)	1	546.1 (79.2)	775.7 (112.5)	12.5	Pass
			2	539.2 (78.2)	782.6 (113.5)	13.8	
			3	550.2 (79.8)	757.1 (109.8)	14.3	
			4	531.6 (77.1)	772.9 (112.1)	13.8	
			5	551.6 (80.0)	779.1 (113.0)	14.3	
			Average	544.0 (78.9)	773.6 (112.2)	13.7	
SMI 316		No. 19 (No. 6)	1	519.2 (75.3)	712.2 (103.3)	18.8	Pass
			2	517.8 (75.1)	714.3 (103.6)	23.4	
			3	530.2 (76.9)	724.7 (105.1)	17.2	
			4	530.9 (77.0)	725.3 (105.2)	18.8	
			5	535.7 (77.7)	721.2 (104.6)	17.2	
			Average	526.8 (76.4)	719.8 (104.4)	19.1	

* The yield strength for No.16 (No.5) bars are based on the stress corresponding to a strain of 0.35% from the stress-strain diagram.

3.9 CLADDING THICKNESS ANALYSIS

Three longitudinal specimens and three transverse specimens for each of three No. 16 (No. 5) and three No. 19 (No. 6) stainless steel clad bars were evaluated for cladding uniformity and thickness variation. The micrographs obtained using the scanning electron microscope demonstrated that a metallurgical bond had been obtained between the 316 LN stainless steel cladding and the mild steel core of the bars (Figure 3.167). No unclad regions or cracks through the cladding were observed. The measured thickness values are presented in Tables 3.18a to 3.18f.

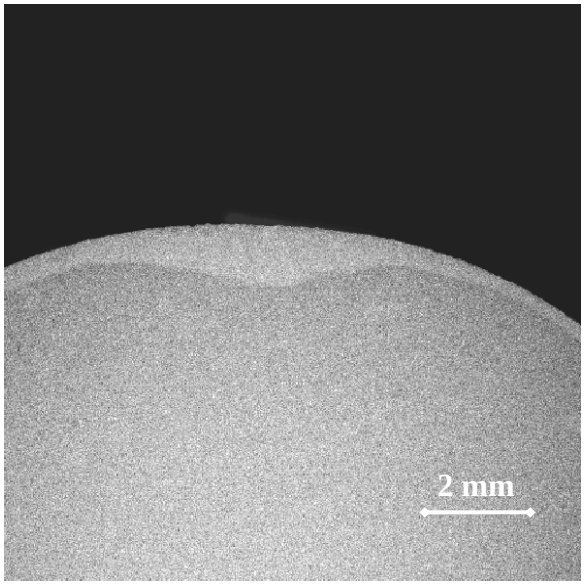

Figure 3.167 – Scanning electron image of cladding (transverse surface)

For the three different No. 16 (No. 5) bars, the average cladding thicknesses varied between 0.65 and 0.75 mm (26 and 30 mils), with standard deviations between 0.20 and 0.34 mm (8 and 13 mils). For the three No. 19 (No. 6) bars, the average cladding thicknesses ranged from 0.62 to 1.13 mm (24 to 45 mils), with standard deviation between 0.15 and 0.34 mm (6 and 13 mils).

Table 3.18a - Cladding thickness of SMI stainless steel clad bars (Bar 1) No. 16 (No. 5) bar

Sample and Number		Measured Thickness(mm)					Max. Thickness (mm)		Min. Thickness (mm)		Average Thickness (mm)		Standard Deviation	
Longitudinal	1	0.75	0.52	0.65	0.65	0.41	0.91	1.05	0.41	0.23	0.72	0.66	0.13	0.20
		0.8	0.77	0.78	0.66	0.61								
		0.91	0.84	0.86	0.79	0.79								
		0.88	0.81	0.63	0.76	0.58								
	2	0.84	0.71	0.77	0.76	0.73	0.97		0.44		0.68		0.14	
		0.97	0.81	0.83	0.84	0.78								
		0.65	0.61	0.58	0.54	0.5								
		0.67	0.6	0.46	0.52	0.44								
	3	1.05	0.95	0.69	0.81	0.54	1.05		0.23		0.56		0.26	
		0.83	0.76	0.82	0.81	0.77								
		0.38	0.38	0.32	0.35	0.31								
		0.47	0.31	0.24	0.24	0.23								
Transverse	1	1.23	1.21	0.88	1.08	0.81	1.23	1.31	0.18	0.18	0.71	0.71	0.29	0.30
		0.94	0.26	0.44	0.68	0.18								
		0.82	0.79	0.5	0.66	0.4								
		1.16	1.05	0.91	0.84	0.81								
		0.96	0.47	0.26	0.4	0.25								
		0.84	0.78	0.66	0.5	0.49								
	2	1.15	0.94	0.86	0.95	0.74	1.31		0.22		0.68		0.32	
		0.91	0.63	0.29	0.35	0.26								
		0.65	0.39	0.26	0.4	0.22								
		1.31	1.04	0.94	1.15	0.89								
		0.9	0.55	0.8	0.52	0.47								
		1.24	0.44	0.5	0.32	0.32								
	3	1.11	0.92	0.76	0.94	0.69	1.19		0.21		0.74		0.27	
		0.92	0.41	0.5	0.82	0.86								
		0.9	0.57	0.77	0.8	0.54								
		1.19	1.13	0.86	0.99	0.86								
		0.97	0.76	0.41	0.34	0.21								
		1.02	0.95	0.49	0.36	0.26								

Table 3.18b - Cladding thickness of SMI stainless steel clad bars (Bar 2) No. 16 (No. 5) bar

Sample and Number		Measured Thickness(mm)					Max. Thickness (mm)		Min. Thickness (mm)		Average Thickness (mm)		Standard Deviation	
Longitudinal	1	1.12	0.78	1.07	1	0.73	1.12	1.15	0.56	0.16	0.83	0.75	0.16	0.25
		1.09	1.06	0.91	0.68	0.67								
		0.96	0.73	0.8	0.73	0.71								
		0.82	0.73	0.67	0.75	0.56								
	2	1.07	0.9	0.94	0.81	0.72	1.07		0.16		0.54		0.27	
		0.83	0.75	0.54	0.71	0.53								
		0.39	0.39	0.29	0.27	0.27								
		0.41	0.39	0.2	0.27	0.16								
	3	1.15	0.91	0.82	1.06	0.69	1.15		0.61		0.87		0.14	
		1.1	1.02	0.88	0.83	0.81								
		0.98	0.86	0.91	0.86	0.83								
		0.92	0.68	0.67	0.86	0.61								
Transverse	1	1.12	1.04	0.86	0.81	0.76	1.23	1.36	0.26	0.25	0.72	0.71	0.26	0.29
		0.93	0.86	0.5	0.61	0.43								
		0.64	0.37	0.43	0.59	0.34								
		1.05	0.33	0.69	0.44	0.26								
		1.23	1.13	1.05	0.9	0.76								
		0.8	0.71	0.69	0.8	0.52								
	2	1.13	1.05	0.85	0.9	0.74	1.21		0.28		0.67		0.27	
		0.69	0.63	0.55	0.64	0.43								
		0.84	0.43	0.54	0.81	0.42								
		1.21	1.02	0.93	0.83	0.73								
		0.58	0.37	0.34	0.29	0.28								
		1.09	0.46	0.55	0.35	0.31								
	3	1.27	1.17	1.22	0.95	0.92	1.36		0.25		0.74		0.34	
		0.94	0.83	0.47	0.34	0.33								
		1.36	0.64	0.51	0.83	0.49								
		1.27	0.88	0.86	1.07	0.75								
		0.79	0.43	0.39	0.26	0.25								
		1.02	0.95	0.49	0.36	0.26								

Table 3.18c - Cladding thickness of SMI stainless steel clad bars (Bar 3) No. 16 (No. 5) bar

Sample and Number		Measured Thickness(mm)					Max. Thickness (mm)		Min. Thickness (mm)		Average Thickness (mm)		Standard Deviation	
Longitudinal	1	0.58	0.56	0.52	0.35	0.33	1.42	1.42	0.33	0.15	0.82	0.65	0.37	0.34
		0.58	0.52	0.53	0.43	0.37								
		1.42	1.13	1.28	1.11	0.95								
		1.37	1.21	1.18	1.05	0.93								
	2	0.65	0.57	0.49	0.6	0.39	1.22		0.38		0.76		0.28	
		0.66	0.53	0.6	0.51	0.38								
		1.22	0.98	1.21	1.13	0.78								
		1.2	1.05	0.96	0.71	0.62								
	3	0.31	0.3	0.29	0.29	0.24	0.6		0.15		0.38		0.14	
		0.28	0.23	0.2	0.2	0.15								
		0.57	0.53	0.48	0.56	0.37								
		0.6	0.53	0.55	0.49	0.47								
Transverse	1	0.75	0.52	0.43	0.47	0.33	1.6	1.6	0.21	0.21	0.66	0.67	0.34	0.31
		0.75	0.58	0.72	0.49	0.34								
		1.6	1.07	1.14	0.81	0.55								
		1.6	0.73	0.83	0.49	0.21								
		0.59	0.4	0.34	0.44	0.25								
		1	0.56	0.77	0.61	0.44								
	2	1.04	0.8	0.82	0.68	0.57	1.52		0.24		0.71		0.32	
		1.17	0.62	0.82	0.88	0.46								
		0.61	0.5	0.43	0.43	0.41								
		1.44	0.96	1.02	0.86	0.47								
		1.52	0.65	1.03	0.61	0.24								
		0.66	0.61	0.33	0.37	0.29								
	3	1.36	0.76	0.61	0.73	0.24	1.36		0.24		0.65		0.26	
		0.78	0.52	0.33	0.43	0.26								
		0.89	0.47	0.88	0.47	0.34								
		1.23	0.63	1.17	0.75	0.53								
		0.85	0.74	0.58	0.57	0.5								
		0.72	0.62	0.48	0.63	0.42								

Table 3.18d - Cladding thickness of SMI Stainless steel clad bars (Bar 1) No. 19 (No. 6) bar

Sample and Number		Measured Thickness(mm)					Max. Thickness (mm)		Min Thickness (mm)		Average Thickness (mm)		Standard Deviation	
Longitudinal	1	1.45	1.21	1.25	1.20	1.18	1.71	1.71	0.75	0.69	1.30	1.13	0.20	0.23
		1.24	1.13	1.15	1.03	0.75								
		1.71	1.33	1.59	1.46	1.29								
		1.47	1.44	1.34	1.41	1.31								
	2	1.13	1.10	0.88	0.81	0.73	1.63		0.73		1.08		0.21	
		0.88	0.93	0.91	0.97	0.91								
		1.34	1.18	1.25	1.19	0.96								
		1.63	1.24	1.09	1.29	1.09								
	3	1.13	0.96	1.07	0.91	0.79	1.36		0.69		1.02		0.19	
		0.94	0.93	0.91	0.81	0.77								
		1.36	1.22	1.17	1.22	1.17								
		1.26	0.82	1.17	1.03	0.69								
Transverse	1	1.04	0.71	0.76	0.81	0.42	1.80	1.80	0.36	0.22	0.80	0.82	0.30	0.34
		1.30	1.04	0.96	1.04	0.81								
		0.96	0.53	0.60	0.62	0.41								
		1.03	0.50	0.54	0.78	0.46								
		0.88	0.80	0.80	0.78	0.67								
		1.80	0.90	1.47	1.05	0.73								
		0.90	0.48	0.55	0.64	0.36								
	2	1.21	0.77	0.80	0.57	0.51	1.60		0.22		0.74		0.33	
		1.06	0.81	0.54	0.40	0.40								
		0.81	0.59	0.81	0.74	0.58								
		1.60	1.40	1.18	1.09	0.92								
		1.29	0.58	0.68	0.74	0.57								
		0.78	0.57	0.40	0.30	0.22								
		1.05	0.74	0.43	0.37	0.29								
	3	1.36	0.73	0.87	0.69	0.61	1.73		0.30		0.91		0.37	
		0.79	0.31	0.72	0.78	0.30								
		1.02	0.94	0.81	0.95	0.62								
		0.90	0.64	0.64	0.51	0.38								
		0.97	0.86	0.64	0.75	0.59								
		1.73	1.44	1.71	1.17	1.15								
		1.57	1.57	1.08	1.19	0.84								

Table 3.18e - Cladding thickness of SMI stainless steel clad bars (Bar 2) No. 19 (No. 6) bar

Sample and Number		Measured Thickness(mm)					Max. Thickness (mm)		Min Thickness (mm)		Average Thickness (mm)		Standard Deviation	
Longitudinal	1	1.48	1.23	1.29	1.44	1.21	1.48	1.78	0.60	0.44	1.18	1.08	0.24	0.34
		1.45	1.34	1.40	0.86	0.64								
		1.43	1.11	1.15	1.38	1.04								
		1.20	1.14	1.18	1.11	0.60								
	2	1.15	1.07	1.15	1.10	0.58	1.42		0.50		0.99		0.24	
		1.42	1.18	1.29	1.21	0.75								
		1.05	0.99	0.71	1.05	0.50								
		1.11	1.08	0.84	0.76	0.71								
	3	1.78	1.66	1.59	1.55	1.44	1.78		0.44		1.08		0.45	
		1.70	1.66	1.52	1.01	0.81								
		0.83	0.77	0.64	0.64	0.64								
		0.83	0.71	0.70	0.73	0.44								
Transverse	1	0.80	0.77	0.54	0.39	0.38	1.34	1.57	0.38	0.33	0.82	0.79	0.26	0.27
		1.15	1.01	0.73	0.81	0.73								
		1.34	1.34	1.19	0.93	0.71								
		1.06	0.57	0.65	0.80	0.53								
		0.68	0.65	0.67	0.65	0.63								
		1.22	1.07	1.03	0.74	0.68								
		1.30	0.61	1.03	0.79	0.49								
	2	0.76	0.61	0.56	0.59	0.54	1.57		0.37		0.79		0.26	
		1.01	0.92	0.77	0.83	0.67								
		0.94	0.90	0.70	0.73	0.69								
		1.07	0.55	0.63	0.85	0.39								
		0.96	0.81	0.77	0.37	0.37								
		1.57	1.25	1.07	0.86	0.73								
		1.34	0.58	0.80	1.03	0.47								
	3	0.66	0.48	0.57	0.44	0.36	1.36		0.33		0.75		0.27	
		1.36	1.05	0.67	0.68	0.57								
		1.26	1.03	1.01	1.06	1.00								
		1.22	0.78	0.84	0.96	0.74								
		0.75	0.63	0.61	0.65	0.56								
		0.81	0.48	0.49	0.65	0.33								
		1.11	0.80	0.85	0.56	0.34								

Table 3.18f - Cladding thickness of SMI stainless steel clad bars (Bar 3) No. 19 (No. 6) bar

Sample and Number		Measured Thickness(mm)					Max. Thickness (mm)		Min Thickness (mm)		Average Thickness (mm)		Standard Deviation	
Longitudinal	1	0.97	0.84	0.80	0.77	0.67	1.19	1.19	0.57	0.53	0.87	0.81	0.18	0.15
		1.06	0.89	0.75	1.05	0.57								
		1.00	0.90	0.92	0.97	0.61								
		1.19	0.69	1.17	0.94	0.64								
	2	0.84	0.64	0.81	0.63	0.60	1.00		0.60		0.79		0.13	
		0.75	0.71	0.70	0.67	0.63								
		1.00	0.78	0.97	0.84	0.75								
		0.99	0.86	0.98	0.92	0.78								
	3	0.84	0.68	0.80	0.68	0.65	1.00		0.53		0.75		0.12	
		0.70	0.59	0.69	0.69	0.59								
		1.00	0.85	0.94	0.85	0.78								
		0.90	0.73	0.86	0.70	0.53								
Transverse	1	0.80	0.76	0.71	0.63	0.50	1.15	1.15	0.25	0.25	0.61	0.62	0.21	0.20
		0.78	0.59	0.59	0.56	0.51								
		0.71	0.39	0.52	0.58	0.39								
		0.55	0.50	0.45	0.47	0.43								
		1.14	1.06	0.86	0.81	0.79								
		1.15	0.47	0.55	0.52	0.44								
		0.58	0.50	0.43	0.44	0.25								
	2	0.68	0.44	0.50	0.56	0.41	1.10		0.39		0.65		0.20	
		0.60	0.58	0.49	0.49	0.46								
		1.03	0.58	0.73	0.79	0.56								
		1.10	0.72	0.71	0.93	0.48								
		0.59	0.48	0.45	0.47	0.39								
		1.02	0.54	0.83	0.56	0.52								
		1.09	0.76	0.72	0.86	0.60								
	3	0.54	0.37	0.45	0.50	0.36	1.09		0.34		0.60		0.21	
		0.57	0.56	0.47	0.50	0.42								
		1.07	0.84	1.07	0.91	0.66								
		1.09	0.75	0.88	0.82	0.58								
		0.64	0.37	0.51	0.56	0.34								
		0.72	0.50	0.50	0.49	0.46								
		0.71	0.45	0.43	0.65	0.42								

3.10 SEM ANALYSIS OF CORROSION PRODUCTS

The scanning electron microscope was used to obtain images of corrosion products from both conventional and stainless steel clad bars. The selected images are shown in Figures 3.168-3.177. The images of corrosion products from conventional steel are shown on the left (a) and the images of corrosion products from the mild steel cores of the stainless steel clad bars are shown on the right (b). The figures show corrosion products on the anode bars from bare steel macrocell tests.

Figure 3.168 shows corrosion products with nodular structures for both conventional and SMI clad steel. The corrosion products are similar but the product from the SMI steel shown in Figure 3.168(b) is not covered with short fibers as those shown in Figure 3.168 (a). Figures 3.169 and 3.170 show corrosion products consisting of amorphous structures with angular crystal-like elements. Figure 3.171 shows a smoother amorphous structure, with fewer crystal-like elements compared to Figures 3.169 and 3.170. Figure 3.172 shows nodular structures similar to those seen in Figure 3.168, but the corrosion products from both steels are not covered with fibers. Figures 3.173 and 3.174 show an amorphous structure that is very similar for both materials. Figure 3.175 shows corrosion products with fibrous structure, while Figure 3.176 shows corrosion products with shorter fiber structure, for both convention and SMI steel. The corrosion products shown in Figure 3.177 are dissimilar, with the conventional steel [Figure 3.177(a)] showing obviously crystal-like particles.

The images shown here only cover a portion of the corrosion product structures. However, it can be concluded that 1) the structure of the corrosion products can vary widely and 2) products with similar morphology are observed on both metals, indicating that the presence of the stainless steel cladding does not alter

the nature of the corrosion products formed in an exposed region of the mild steel core.

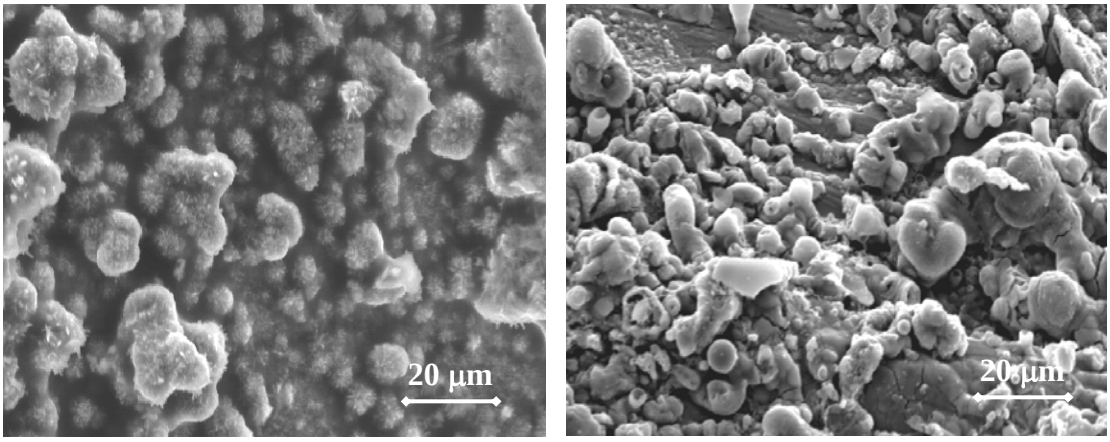

(a) **(b)**

Figure 3.168 - Nodular corrosion products with fibers on bare bar anodes for (a) Conventional and (b) SMI steel at unprotected ends. 680X

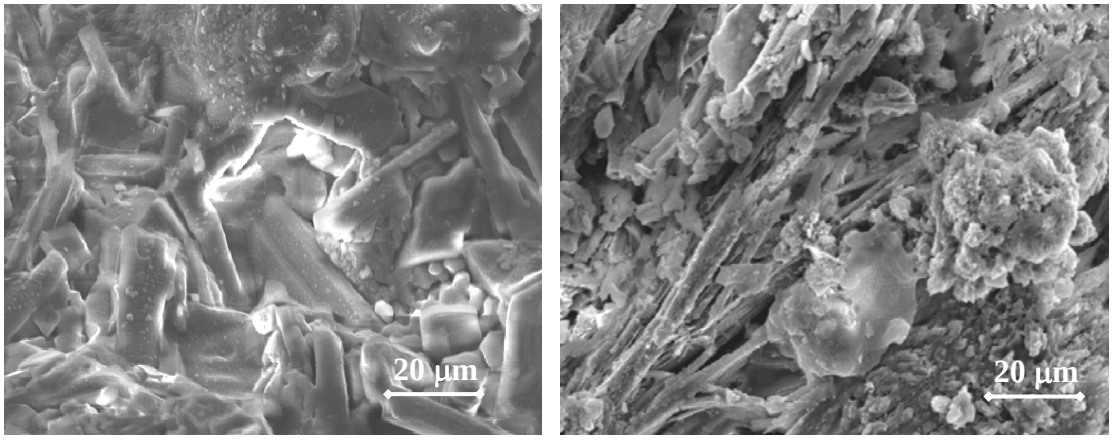

(a) **(b)**

Figure 3.169 - Amorphous corrosion products with crystal-like elements on bare bar anodes for (a) conventional and (b) SMI steel at penetrations through the cladding**.** 680X

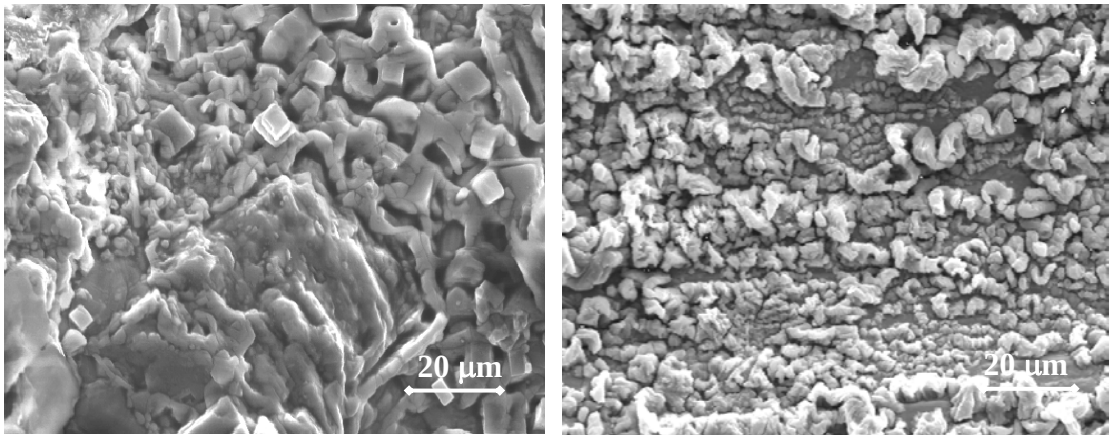

(a) **(b)**

Figure 3.170 - Amorphous corrosion products on bare bar anodes for (a) conventional and (b) SMI steel at unprotected ends**.** 680X

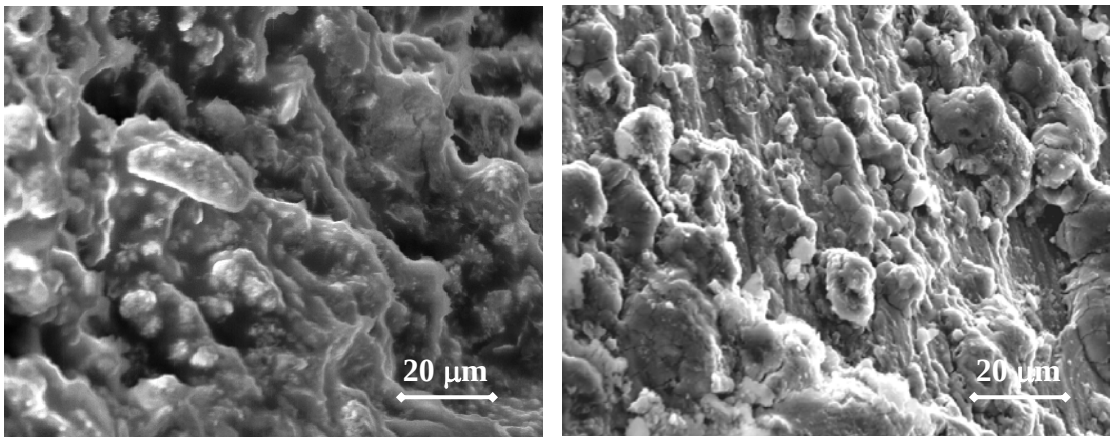

(a) **(b)**

Figure 3.171 - Amorphous corrosion products with small crystal-like elements on bare bar anodes for (a) MMFX and (b) conventional steel at unprotected ends**.** 680X

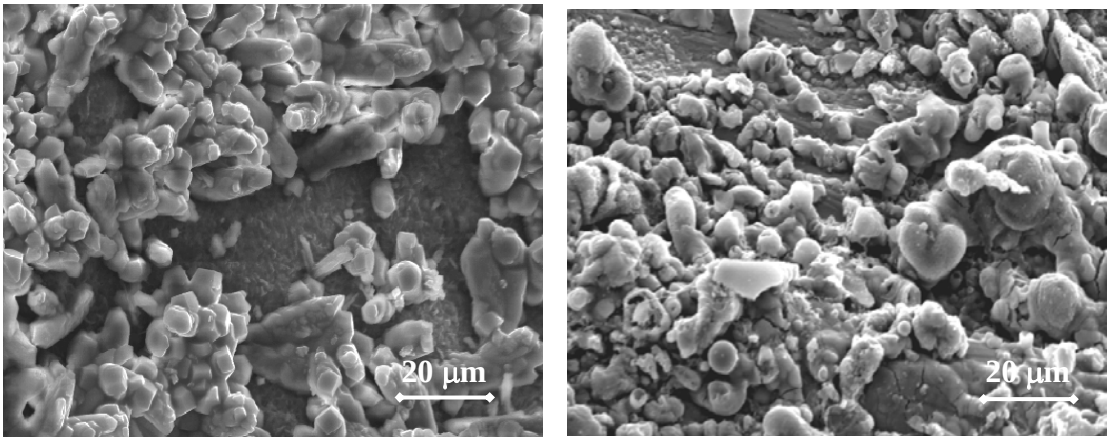

(a) **(b)**

Figure 3.172 - Nodular corrosion products on anode bars for (a) conventional and (b) SMI steel at unprotected ends**.** 680X

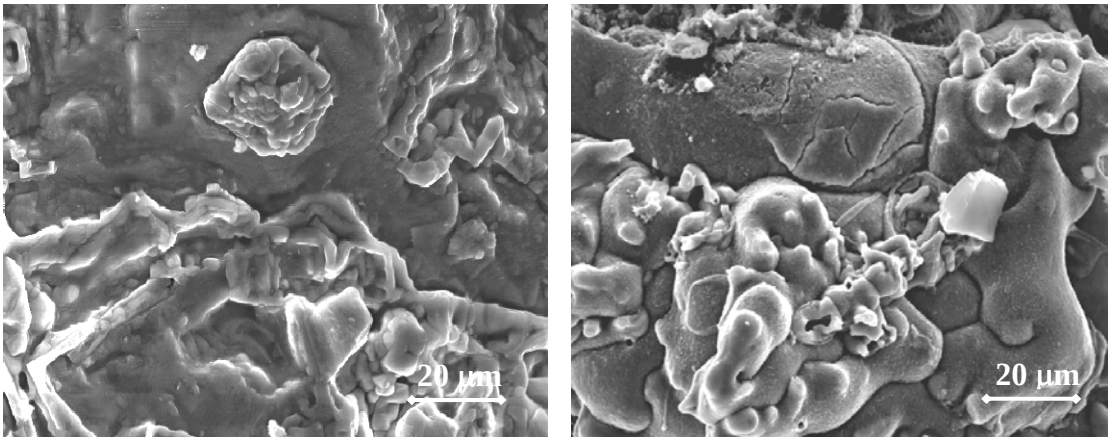

(a) **(b)**

Figure 3.173 – Smooth, amorphous corrosion products on anode bars for (a) conventional and (b) SMI steel at unprotected ends**.** 680X

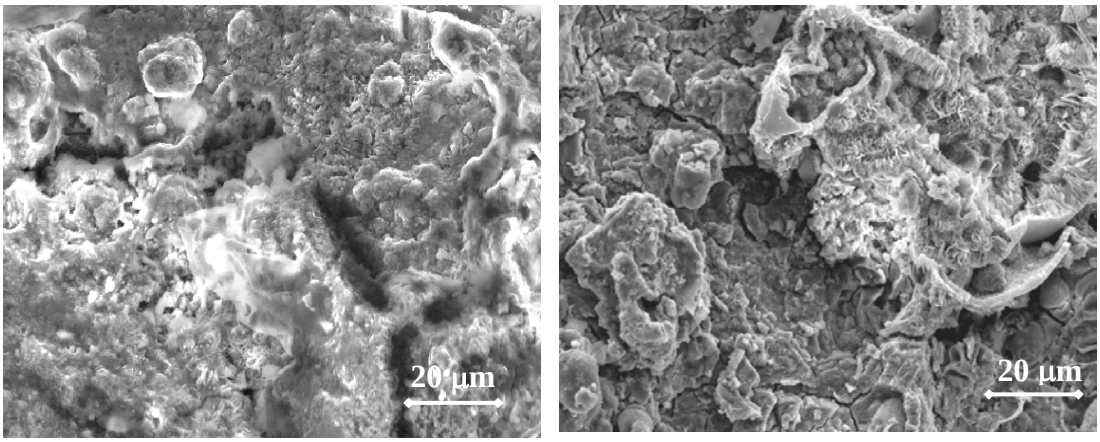

(a) **(b)**

Figure 3.174 - Amorphous corrosion products for anode bars for (a) conventional and (b) SMI steel at penetrations through the cladding**.** 680X

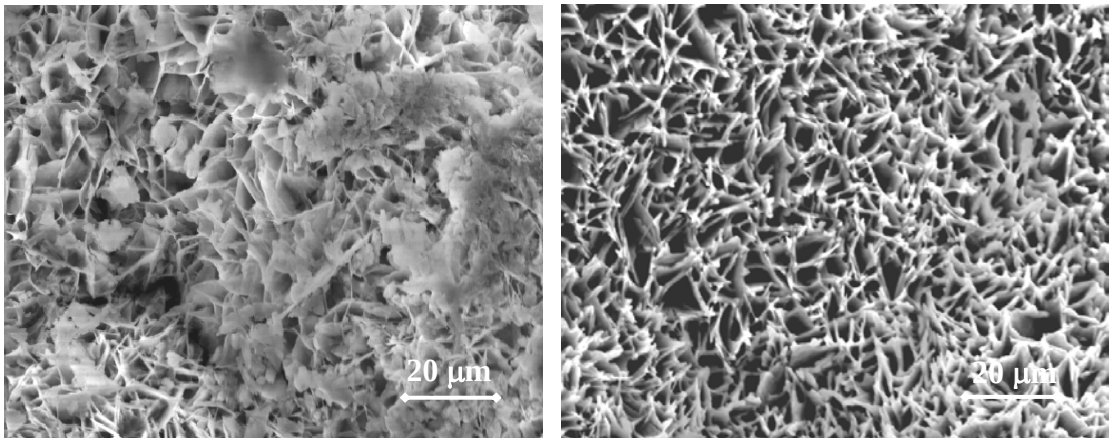

(a) **(b)**

Figure 3.175 - Corrosion products with long fiber structure for anode bars for (a) conventional and (b) SMI steel at unprotected ends**.** 680X

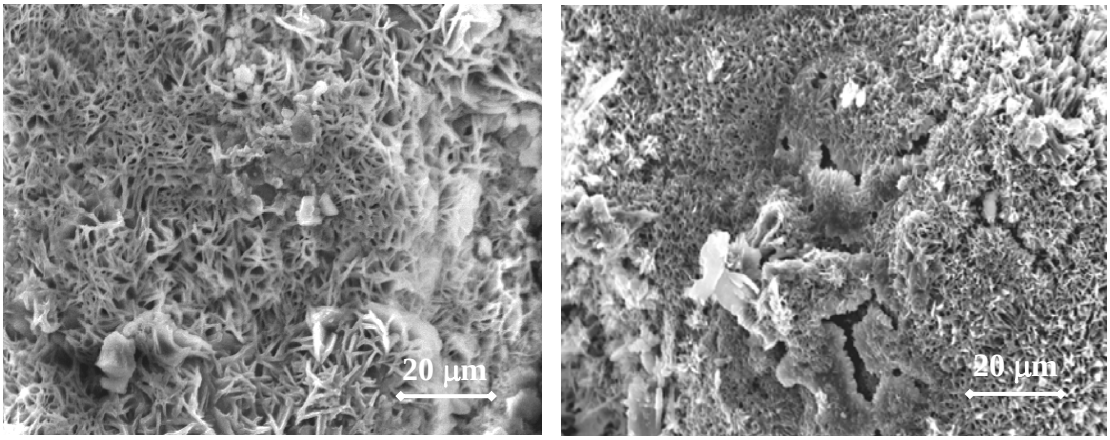

(a) **(b)**

Figure 3.176 - Corrosion products with short fiber structure for anode bars for (a) conventional and (b) SMI steel at penetrations through the cladding**.** 680X

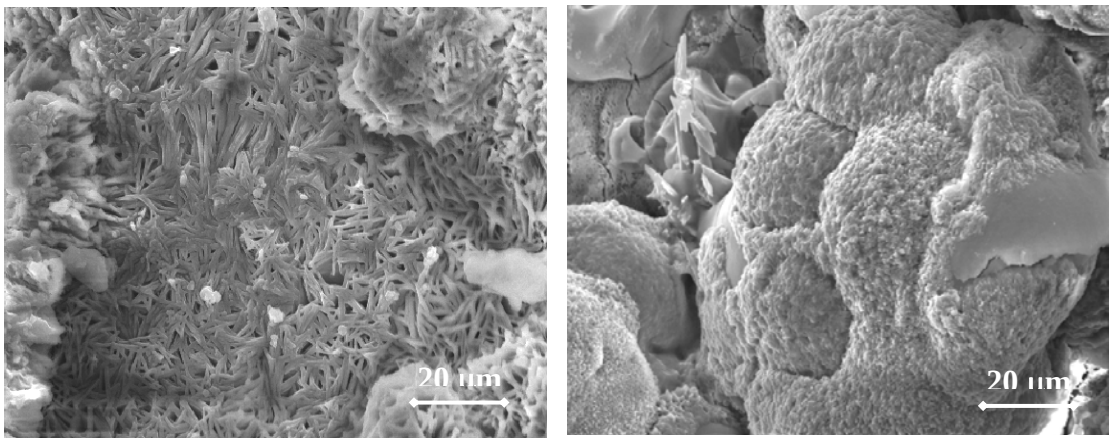

(a) **(b)**

Figure 3.177 - Corrosion products dissimilar structure for anode bars for (a) conventional and (b) SMI steel at penetrations through the cladding**.** 680X

CHAPTER 4
DISCUSSION OF RESULTS FOR CORROSION PROTECTION SYSTEMS AND ECONOMIC ANALYSIS

This chapter includes a discussion of the corrosion test results and an economic analysis of bridge decks built with different corrosion protection systems. The discussion summarizes, compares, and analyzes all corrosion test results. The economic analysis compares the present costs for bridge decks with several corrosion protection options and indicates the most cost-effective option based on a 75-year service life.

4.1 DISCUSSION OF CORROSION TEST RESULTS

This section presents a discussion of the corrosion test results covered in Chapter 3. At this writing, the rapid macrocell tests are complete, while the bench-scale tests are still underway.

4.1.1 Summary of Results

Based on total area, epoxy-coated steel shows low corrosion losses, with values between 0 to 5% of that for conventional steel.

SMI stainless steel clad reinforcement exhibits an improvement in corrosion performance compared to conventional reinforcing steel and epoxy-coated steel when the cladding is intact, but corrodes at similar or even higher rates than epoxy-coated steel when the cladding is damaged. Due to the thickness of the cladding and the nature of the metallurgical bond, however, the cladding is not likely to be damaged.

ECR bars with improved adhesion have corrosion losses that range from 0 to 5% of the corrosion loss of conventional steel, exhibiting similar corrosion

performance to conventional epoxy-coated steel. Based on the results of cathodic disbondment tests, all three types of ECR with improved adhesion exhibit increased adhesion between the epoxy and the steel when compared to conventional epoxy-coated steel, although the adhesion properties of ECR(Valspar) appear to be similar to those of the conventional epoxy coatings.

Corrosion inhibitors and low water-cement ratios are effective in improving the corrosion protection of the steel in uncracked concrete, but are not as helpful in cracked concrete.

Multiple coated steel exhibits average corrosion losses that range from 23 to 231% of the corrosion losses for conventional epoxy-coated steel when only the epoxy layer is penetrated, and between 13 to 455% of the corrosion losses for conventional epoxy-coated steel when both layers are penetrated. The performance of multiple coated steel differs from that of the other steels evaluated in this study in that corrosion is observed at cathodes for some of the macrocell specimens due to the amphoteric nature of the zinc layer.

For cracked beam specimens, the microcell corrosion rates of the bottom mats based on linear polarization resistance tests are usually one to two orders of magnitude lower than those of the top mats, and the results from connected circuits are somewhere between those for the top and bottom mats. For Southern Exposure or ASTM G 109 specimens, however, the microcell corrosion rates of bottom mats are basically the same magnitude as those of top mats, and the results from connected circuits can be higher, lower, or somewhat between those for the top and bottom mats. Compared to the macrocell corrosion rates of the corresponding bench-scale specimens, the microcell corrosion rates are about the same magnitude for most

Southern Exposure and ASTM G 109 specimens, while they are about one order higher in magnitude for cracked beam specimens.

The comparison of corrosion products from conventional and stainless steel clad reinforcement, using scanning electron microscope, demonstrates that the structure of the corrosion products can vary widely and the presence of the stainless steel cladding does not alter the nature of the corrosion products formed in an exposed region of the mild steel core.

4.1.2 Conventional Epoxy-Coated Steel

Conventional epoxy-coated steel was evaluated using rapid macrocell and bench-scale tests. The bars were evaluated in both the bare and mortar-wrapped condition in the macrocell test. Balma et al. (2005) evaluated epoxy-coated steel with four holes drilled through the epoxy, with epoxy-coated steel as the anode and uncoated conventional steel as the cathode, in rapid macrocell tests with mortar-wrapped specimens and bench-scale tests. Average corrosion losses, based on the total bar area exposed to the solution, were 0.39 μm for mortar-wrapped specimens from rapid macrocell tests over a 15-week test period and 1.41 μm from Southern Exposure tests and 2.92 μm from cracked beam tests over a 96-week test period.

The macrocell test results in this study, summarized in Table 3.1 and Figures 3.1 through 3.8, show that the total corrosion losses of the specimens containing epoxy-coated steel with four drilled holes range from 0% to 5% of those for specimens containing conventional steel. Compared to the corrosion loss of 0.39 μm from Balma's study (2005) in mortar-wrapped specimens, the corrosion loss exhibited by specimens using epoxy-coated steel as both the anode and the cathode in this study is much lower (less than 0.01 μm), indicating that the use of epoxy-coated

steel throughout a bridge deck will significantly increase the corrosion resistance of epoxy-coated steel.

In the Southern Exposure and cracked beam tests, the corrosion losses of specimens containing epoxy-coated steel at both top and bottom mats, based on the total area of the bars, are between 0.5% and 3% of those for specimens containing conventional steel tested in this study, 0.25% of those for specimens containing conventional steel tested in Balma's study, and 0.4% of those for specimens with epoxy-coated steel at top mat and conventional steel at bottom mat tested in Balma's study (Balma et al. 2005) at the same point of time.

In the ASTM G 109 tests, no detectable corrosion was measured for specimens reinforced with conventional epoxy-coated steel at the data cutoff point for this report, March 15 2005.

4.1.3 Stainless Steel Clad Reinforcement

Stainless steel clad reinforcement was evaluated in the rapid macrocell test, using bare bar specimens in simulated concrete pore solution in 1.6 and 6.04 m ion salt concentrations, and mortar-wrapped specimens in a 1.6 m ion salt concentration. The bars were tested without protection at the ends, with caps at the ends, and with four 3.2-mm (⅛-in.) diameter drilled holes through the coating and caps at the ends. Bent SMI bars were used as the anode to evaluate the effect of the resulting residual stresses. Two combinations of bare SMI and conventional bars were tested to evaluate the effect of mixing SMI and conventional steel. The results of macrocell tests, summarized in Tables 3.3 and 3.4 and Figures 3.28 through 3.39, demonstrate the superior corrosion resistance of undamaged stainless steel clad bars with protected ends, in both the 1.6 and 6.04 m ion salt solutions. For mortar-wrapped specimens with exposed ends or drilled holes, higher corrosion losses were observed compared

to conventional epoxy-coated steel, which in all likelihood is due to the much larger cathodic area of the stainless steel clad test specimens compared to that of the epoxy-coated steel test specimens. The results also show that, if conventional steel and stainless steel clad reinforcement are combined, the corrosion rate is not increased for either material.

In the Southern Exposure tests, after 43 weeks, the SMI steel with intact cladding does not show any sign of corrosion. Two SMI specimens with damaged cladding show observable corrosion at week 49. In the cracked beam tests, SMI specimens with intact cladding exhibit no sign of corrosion during the test period, except that one specimen had a measurable corrosion rate between weeks 20 and 24, possibly due to mill scale on the bar surface, which dropped to zero after week 24. The SMI specimens with drilled holes had an average corrosion loss equal to 5% of that for conventional steel and 11 times that of epoxy-coated steel with the same exposed area. As with the macrocell test specimens, the much higher corrosion loss exhibited by the stainless steel clad bars is likely due to the much larger cathodic area of the bottom mats of the stainless steel clad specimens compared to the epoxy-coated steel specimens. As with the results from the macrocell tests, the data from bench-scale specimens shows that the combination of conventional steel and stainless steel clad reinforcement does not increase the corrosion rate for either material.

Based on the cladding thickness analysis, the average cladding thicknesses ranged from 0.65 to 0.75 mm (26 to 30 mils) for No. 16 (No. 5) bars and from 0.62 to 1.13 mm (24 to 45 mils) for No. 19 (No. 6) bars. Due to the thickness of the cladding, as well as the nature of the metallurgical bond between the stainless steel cladding and the mild steel core, it is unlikely that the cladding will be penetrated in practice.

4.1.4 Epoxy-Coated Reinforcement with Improved Adhesion between Epoxy and Steel

Two epoxy-coated steels with increased adhesion epoxy were evaluated along with one epoxy-coated steel with the epoxy applied after zinc chromate pretreatment of the steel to improve adhesion between the epoxy and the steel. The bars were evaluated in both bare and mortar-wrapped condition in the macrocell test. The macrocell test results, summarized in Tables 3.6 and 3.7 and Figures 3.54 through 3.67, indicate no obvious improvement in corrosion resistance for the high adhesion steels compared to conventional epoxy-coated steel.

To date in the Southern Exposure tests, neither the epoxy-coat steels with improved adhesion nor the conventional epoxy-coated steel has exhibited any corrosion at a rate of greater than 0.01 μm/yr. In the cracked beam tests, the three types of ECR bars with improved adhesion with four drilled holes show average corrosion losses from 119% to 204% of that for the conventional epoxy-coated steel at the same point of time. For specimens with ten drilled holes, ECR(DuPont) shows a higher corrosion loss (131%) than conventional epoxy-coated steel, while ECR(Chromate) and ECR(Valspar) exhibit slightly lower corrosion losses (94% and 91%, respectively) than conventional epoxy-coated steel at week 31.

Cathodic disbondment testing was performed to evaluate and compare the adhesion between epoxy and steel for conventional ECR and ECR with improved adhesion. The results indicate that ECR(Chromate) and ECR(DuPont) exhibit clearly improved adhesion compared to conventional ECR, while ECR(Valspar) shows just somewhat better adhesion than the conventional ECR. Both the conventional ECR and ECR(Valspar) failed the coating disbondment requirements of Annex A1 ASTM A 775, while ECR(Chromate) and ECR(DuPont) met those requirements. These

results indicate that cathodic disbondment tests should be added to the quality control checks applied to production bars.

A comparison between ECR with improved adhesion and conventional ECR indicates that the improved adhesion coating does not directly correspond to better corrosion performance. However, due to the relatively short testing period at this writing and the fact that the adhesion properties for epoxy-coated bars with improved adhesion have not been evaluated over the long term, no conclusions are appropriate at this time.

4.1.5 Corrosion Inhibitors and Low Water-Cement Ratio

Corrosion inhibitors and a lower water-cement ratio in concrete were evaluated using the macrocell and bench-scale tests, along with steel with an epoxy-coating that contains a calcium nitrite primer. Obvious damage and delamination were observed on the as delivered epoxy-coated steel with calcium nitrite primer, usually over a length of about two feet near the ends of the 20-foot long bars. The epoxy color was not consistent from one bar to the next.

Specimens containing epoxy-coated steel were cast in mortar with a water-cement ratio of 0.5, with and without corrosion inhibitors, in the rapid macrocell tests, and with water-cement ratios of 0.35 and 0.45, with and without corrosion inhibitors, in the bench-scale tests. The corrosion inhibitors evaluated were Rheocrete 222+, DCI-S, and Hycrete.

For the macrocell tests, the specimens with corrosion inhibitors were compared to control specimens, which were cast in mortar with conventional epoxy-coated steel and no inhibitor. The specimens with corrosion inhibitors had corrosion losses between 0 and 33% of the average corrosion loss for the control specimens (Table 3.8 and Figures 3.85), while the epoxy-coated steel with the calcium nitrite primer had an

average corrosion loss equal to two times that of the control specimens. The corrosion potentials of the anode (Figure 3.86) demonstrate that, of the specimens with epoxy-coated steel in this portion of the study only the epoxy-coated steel with calcium nitrite primer exhibited active corrosion (corrosion potential with respect to SCE below −0.275 V).

For the Southern Exposure tests, the control specimens were fabricated with conventional steel and conventional epoxy-coated steel in concrete with water-cement ratios of 0.35 and 0.45 and no corrosion inhibitors. At week 37, the control specimens containing conventional steel with a water-cement ratio of 0.35 exhibited an average total corrosion loss equal to 3% of that for the control specimens containing conventional steel with a water-cement ratio of 0.45. For the control specimens containing the epoxy-coated steel in concrete with a water-cement ratio of 0.35 and with ten drilled holes in the epoxy, the corrosion loss was 67% of that for the control specimens with epoxy-coated steel and a water-cement ratio of 0.45, although both corrosion losses were much lower than exhibited by specimens containing conventional steel. ECR specimens with ten drilled holes and cast in concrete with one of the three corrosion inhibitors and a water-cement ratio of either 0.35 or 0.45 show no measurable corrosion at this writing. The specimens containing the epoxy-coated steel with the calcium nitrite primer in concrete with a water-cement ratio of 0.45 and drilled with ten holes exhibit an average corrosion loss equal to that of the control specimens containing epoxy-coated steel with a water-cement ratio of 0.45.

For the cracked beam tests, the control specimens were also fabricated with conventional steel and conventional epoxy-coated steel in concrete with water-cement ratios of 0.35 and 0.45 and no corrosion inhibitors. The average corrosion loss, shown

in Table 3.2, for control specimens with conventional steel made with a water-cement ratio of 0.35 is 63% of the corrosion loss of control specimens with a water-cement ratio of 0.45. Hence, the lower-water cement ratio provided limited additional corrosion protection since the lower permeability of the concrete reduces the diffusion rate of oxygen and moisture to the bottom bars. For specimens containing epoxy-coated steel with four drilled holes in the epoxy in concrete with a water-cement ratio of 0.45 and with the corrosion inhibitors Rheocrete 222+, DCI-S, and Hycrete, the corrosion losses were 65%, 35%, and 55%, respectively, of the corrosion loss of control specimens containing epoxy-coated steel with four drilled holes and no inhibitors. For specimens containing epoxy-coated steel with 10 drilled holes in concrete with a water-cement ratio of 0.45 and with the corrosion inhibitors Rheocrete 222+, DCI-S, and Hycrete, the corrosion losses were 154%, 63%, and 120%, respectively, of the corrosion loss of control specimens containing epoxy-coated steel with ten drilled holes and no inhibitors. For specimens with a water-cement ratio of 0.35 (also with 10 holes), the corrosion losses were 74%, 162%, and 228% for specimens with Rheocrete 222+, DCI-S, and Hycrete, respectively, of the corrosion loss of specimens containing epoxy-coated steel with no inhibitors. For cracked concrete, the use of corrosion inhibitors does not appear to improve the corrosion protection of the steel significantly.

4.1.6 Multiple Coated Steel

Multiple coated steel with a metallic layer underlying the epoxy layer was evaluated in both the bare and mortar-wrapped condition in the rapid macrocell test. In the tests with bare bars, the average corrosion loss was 23% of the corrosion loss of conventional epoxy-coated steel when only the epoxy was penetrated and 13% of that for conventional epoxy-coated steel when both layers penetrated. For the tests

with mortar-wrapped specimens, the multiple coated steel with only the epoxy penetrated had an average corrosion loss of 0.04 μm based on the total area and 3.65 μm based on the exposed area, twice as much as that for conventional epoxy-coated steel, indicating the higher activity of the zinc layer. The multiple coated steel with both layers penetrated had an average corrosion loss of less than 0.01 μm based on the total area and 0.63 μm based on the exposed area, equaling that for conventional epoxy-coated steel, probably indicating that iron rather than zinc was undergoing active corrosion.

In the Southern Exposure tests, specimens containing multiple coated steel with either the epoxy layer penetrated or both layers penetrated exhibited small but detectable corrosion losses that were not observed for the specimens containing epoxy-coated steel at the same point of time.

In the cracked beam tests, the average corrosion losses of the multiple coated steel with only the epoxy penetrated by four and ten holes equal 231% and 227% of the corrosion losses of conventional epoxy-coated steel with four and ten holes at the same point of time, respectively. For the multiple coated specimens with both layers penetrated with four and ten holes, higher corrosion losses are also obtained, equal to 308% and 455%, respectively, of the losses for conventional epoxy-coated steel at the same point of time.

In the ASTM G 109 tests, neither multiple coated nor conventional epoxy-coated steel exhibited any corrosion after 45 to 51 weeks of testing.

4.2 ECONOMIC ANALYSIS

An economic analysis is performed to compare bridge decks reinforced with conventional steel, epoxy-coated steel, stainless steel clad reinforcement, ECR with

improved adhesion, and ECR cast in concrete with corrosion inhibitors, following the procedures used by Kepler et al. (2000), Darwin et al. (2002), and Balma et al. (2005). A prototype bridge deck with 76.2 mm (3 in.) concrete cover and cracks parallel to and on top of the reinforcing steel is used in the analysis. The cost of a new bridge deck and repair costs over the 75-year economic life are compared on a present-worth basis. To determine the repair costs, the time needed to initiate corrosion once a bridge deck is placed in service and the time needed for corrosion products to cause the concrete to crack once corrosion has been initiated need to be determined. The sum of the two is considered to be the time to first repair. After the first repair, further repairs are assumed to be needed every 25 years (Kepler et al. 2000). This section presents the methods to determine the time to first repair for the corrosion protection systems evaluated in this study and an economic analysis based on the time to first repair.

4.2.1 Time to First Repair

The time to first repair for a bridge deck consists of the time for corrosion to initiate plus the time it takes for the corrosion products to produce cracking and spalling of the concrete cover.

4.2.1.1 Time to Corrosion Initiation

The time to corrosion initiation for bridges containing the different corrosion protection systems is determined based on (1) the test results obtained at the University of Kansas, (2) data reported in other studies [Berke (1991)], (3) recommendations made by state maintenance engineers in Kansas and South Dakota Departments of Transportation, and (4) bridge deck surveys completed by Miller and Darwin (2000) and Lindquist, Darwin, and Browning (2005).

For any corrosion protection system, the time to corrosion initiation depends on (1) the range of chloride contents in concrete corresponding to corrosion initiation, referred to as the critical chloride corrosion threshold and (2) the time required to reach that chloride content in the structure.

The chloride corrosion thresholds for bridge decks containing conventional and epoxy-coated steel are obtained based on chloride threshold tests at the University of Kansas. Because these chloride threshold tests are still underway, the chloride corrosion thresholds for some corrosion protection systems are obtained from other studies. The chloride threshold for concrete cast with the corrosion inhibitor DCI-S is based on results presented by Berke (1991). The chloride threshold for bridge decks with stainless clad steel reinforcement is based on the values for stainless steel from previous study in the University of Kansas (Balma et al. 2005).

Once the chloride threshold is determined, the time to reach that specific chloride content in a prototype bridge deck, which has 76.2 mm (3 in.) concrete cover and cracks parallel to and on top of the top layer of reinforcement, can be determined using results from bridge surveys reported by Miller and Darwin (2000) and Lindquist et al. (2005). Cracked decks are selected for this model because the surveys demonstrate that reinforced concrete bridge decks exhibit significant cracking parallel to and immediately above the reinforcing bars. Based on the chloride data presented by Lindquist et al. (2005), which includes the results from both studies, the correlation between average chloride concentration (C, in kg/m^3) and time (T, in months) at a depth of 76.2 mm (3 in.) at crack locations in bridges with an AADT greater than 7500 can be obtained using a linear trend line:

$$C = 0.0187T + 0.4414 \tag{4.1}$$

[Note: Eq. (4.1) was developed after the publication of the SM report No.78 by Lindquist et al. (2005) and does not appear in the report.]

The average time to reach a chloride corrosion threshold value of C_C is:

$$T_c = (C_c - 0.4414)/0.0187 \qquad (4.2)$$

Where, C_c = chloride threshold, kg/m^3

T_c = time to reach chloride threshold, months

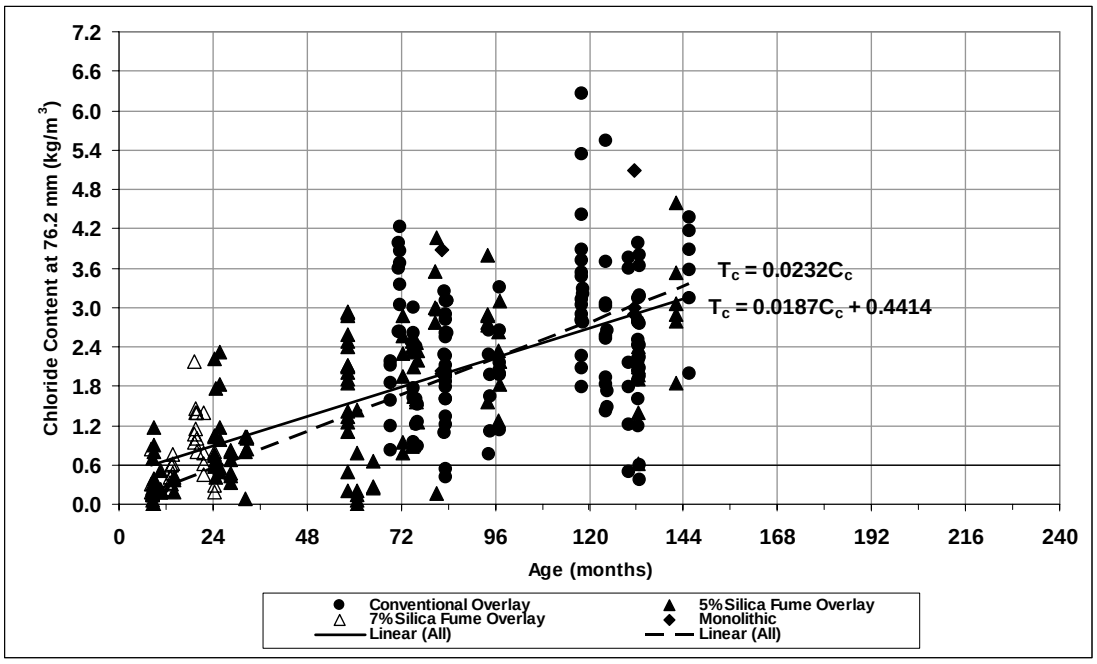

Figure 4.1 - Chloride content taken on cracks interpolated at a depth of 76.2 mm (3.0 in.) versus placement age for bridges with an AADT greater than 7500.

For example, if the chloride content x required for corrosion to initiate is 1.2 kg/m^3 (2 lb/yd^3) for a bridge deck, the average time T_c to reach that chloride concentration is (1.2–0.4414)/0.0187 = 40.6 months (3.4 years), which is the time to corrosion initiation at cracks. In practice, it is more appropriate to represent chloride thresholds as ranges. When they are, the time to corrosion initiation will also be represented as a range. For conventional steel and epoxy-coated steel with a damaged

coating, the chloride threshold range is between 0.6 and 1.2 kg/m^3 (1 and 2 lb/yd^3), which gives a range of corrosion initiation times between 8.5 and 40.6 months (0.7 and 3.4 years) at crack locations. For concrete mixed with the corrosion inhibitor DCI-S, the chloride threshold is dependent of the dosage rate. Recommended dosage rates for DCI-S range between 10 and 30 L/m^3 (2 to 6 gal/yd^3), which yield chloride thresholds between 3.6 to 9.5 kg/m^3 (6 to 16 lb/yd^3) (Berke 1987), giving a range of corrosion initiation times from 169 to 484 months (14 to 40 years) at crack locations. For concrete mixed with the corrosion inhibitors Rheocrete and Hycrete, the chloride threshold is assumed to be the same as that of concrete without a corrosion inhibitor. This is because Rheocrete and Hycrete offer protection mainly by forming a protective film at the steel surface and reducing the ingress of chloride ions, oxygen, and water into the concrete, which do not appreciably increase the corrosion initiation time for the fully cracked concrete that is analyzed in this report.

Table 4.1 - Corrosion initiation time for bridge decks containing different corrosion protection systems

Steel designation	Chloride corrosion threshold	Time to corrosion initiation*
	kg/m^3 (lb/yd^3)	years
Conv.	0.6 (1) 1.2 (2)	0.7 3.4
ECR	0.6 (1) 1.2 (2)	0.7 3.4
SMI	15$^+$ (25$^+$)	75$^+$
ECR(Rheocrete)	0.6 (1) 1.2 (2)	0.7 3.4
ECR(DCI)	3.6(6) 9.5 (16)	14 40
ECR(Hycrete)	0.6 (1) 1.2 (2)	0.7 3.4
ECR(DuPont)	0.6 (1) 1.2(2)	0.7 3.4
ECR(Chromate)	0.6 (1) 1.2(2)	0.7 3.4
ECR(Valspar)	0.6 (1) 1.2(2)	0.7 3.4

* Assume reinforcement located under a crack

4.2.1.2 Time to Cracking

To calculate the time to cracking for a bridge deck after corrosion initiates, the corrosion loss that corresponds to the quantity of corrosion product that causes the cracking and spalling of the concrete cover, along with the average corrosion rate of each corrosion protection system, is used to determine when a repair is needed.

A total corrosion loss of about 25 μm will cause concrete to crack when the loss is relatively uniform along the length of a reinforcing bar (Pfeifer 2000). For cases where only a fraction of the reinforcing bar is subject to corrosion, such as epoxy-coated bars with limited damage on the coating, the total corrosion loss needed to crack the concrete cover can be calculated using an empirical equation developed by Torres-Acosta and Sagues (2004), as presented in Chapter 1.

$$x_{CRIT} = 0.011(c/\phi)(c/L+1)^2 \qquad (1.13)$$

where x_{CRIT} = critical amount of steel corrosion penetration, mm

c = concrete cover, mm

ϕ = reinforcing bar diameter, mm

L = length of a local corrosion region (anodic ring region) on the bar, mm

Thus, the damaged region is represented by a ring of length L on the bar.

To evaluate the accuracy of Eq. (1.13), the corrosion losses of bench-scale specimens containing damaged epoxy-coated steel as the anode and conventional steel as cathode, which are presented in Balma et al. (2005) and McDonald et al. (1998), are used as follows:

1. The SE specimens used by Balma et al. (2005) were fabricated using damaged epoxy-coated steel as the anodes and conventional steel as the cathodes. The macrocell corrosion rates based on the exposed area on the anodes ranged from 500 to 2700 μm/yr at week 96 (Balma et al. Figure A.141). At week 49,

an average total corrosion loss of about 100 μm was obtained (Balma et al. Figure 3.87), which is two orders of magnitude higher than the corrosion loss measured on specimens with epoxy-coated bars as both the anodes and cathodes in this study at the same point of time. The higher corrosion loss observed in Balma's study is due to the use of conventional steel cathodes, which provide a much larger cathodic area compared to epoxy-coated steel with limited damage. At week 96, the average total corrosion loss was 700 μm for six specimens (Balma et al. Figure 3.87), with one specimen reaching a corrosion loss of 1500 μm (Balma et al. Figure A.141). Using Eq. (1.13) and the parameters for a Southern Exposure specimen in Balma's study [concrete cover c = 25.4 mm (1 in.), bar diameter ϕ = 15.875 mm (⅝ in.), and the diameter of the drilled holes 3.175-mm (⅛-in.) in the epoxy = L], a total corrosion loss of 1426 μm will cause the concrete to crack [$0.011 \times (25.4/15.875) \times (25.4/3.175+1)^2 = 1.426$ mm]. However, the tensile stress produced by the increased volume of the corrosion products from isolated damage on one side of the epoxy-coated steel should be at most one-half of that caused by the rust over a ring shaped region with length L. This reasoning leads to the conclusion that twice the corrosion loss given by Eq. (1.13), 2852 μm, will be needed to crack the concrete cover of a Southern Exposure specimen. The highest corrosion loss exhibited by an individual specimen in this study, 1500 μm, is smaller than the value of 2852 μm required to crack concrete, so it can be concluded that the corrosion products would not be sufficient to crack concrete at end of week 96. Visual inspection for these specimens at week 96 showed that no cracks were observed (Balma et al.

2005), which means that Eq. (1.13) (as interpreted here) is in agreement with the observed behavior.

2. McDonald et al. (1998) tested conventional bars coated with six different epoxies, identified as epoxies A through F. The uncracked Southern Exposure specimens, using epoxy-coated steel with 0.5% surface damage [two 6.35 mm (¼-in.) diameter holes] as anodes and conventional steel as cathodes, had a concrete cover of 25.4 mm (1 in.), a bar diameter of 15.875 mm (⅝ in.), and a length of anodic zone of 6.35 mm (¼ in.). According to Eq. (1.13), the corrosion loss for these parameters to crack concrete is 440 μm. Using the reasoning presented in previous paragraph, twice the calculated corrosion loss, 880 μm, would cause a crack in concrete cover of a Southern Exposure specimen. Two types of epoxy, Epoxy-C and Epoxy-F, exhibited average corrosion losses of 1818 and 6443 μm, respectively, which are higher than the value of 880 μm required to crack concrete. The specimens containing Epoxy-C and Epoxy-F steel were found cracked. For specimens with epoxies A, B, and D, the average corrosion losses on the exposed regions were 84, 830, and 16 μm, respectively, lower than 880 μm. No cracks were found in these specimens. For the Epoxy-E steel specimens, however, the average corrosion loss was 3130 μm, and these specimens exhibited no cracks, although the corrosion loss is higher than the corrosion loss required to crack concrete.

In spite of the observations on the Epoxy-E steel tests by McDonald et al. (1998), the test results indicate that, in most cases, Eq. (1.13) provides a reasonable tool to predict the corrosion loss on damaged ECR required to crack concrete.

As mentioned in the beginning of this section, the corrosion rates for different corrosion protection systems are needed in addition to the corrosion losses to cause

cracking in order to calculate the time to cracking after corrosion initiation. Half of the average value of corrosion rates from the Southern Exposure and cracked beam tests in this study is used as the corrosion rate for a bridge deck with the corresponding corrosion protection system, because the Southern Exposure and cracked beam specimens are subjected to higher salt concentration of the ponding solutions and more aggressive exposure cycles than actual structures. The corrosion results obtained between weeks 50 to 70 in bench-scale tests are recommended for use in economical analysis since the corrosion behavior for specimens at this period is more stable than before or after (Balma et al. 2005). For bridge decks reinforced with conventional steel or conventional epoxy-coated steel, the average corrosion rates between weeks 40 to 49 are used for the reason that the cutoff date of the data is week 49. For bridge decks containing stainless steel clad reinforcement, the corrosion rate used to determine the time to first repair after corrosion initiates is not of interest because, from a practical point of view, that reinforcement will not corrode during the 75-year service life, as discussed in Section 4.2.1.1. Therefore, the highest corrosion rate observed during the first 49 week in bench-scale specimens is used as the corrosion rate of bridge decks reinforced with stainless steel clad bars. For bridge decks containing one of the three types of epoxy-coated steel with improve adhesion, the corrosion rates are assumed to be the same as for conventional epoxy-coated steel because the corrosion behavior of these steels is not significantly different. For bridge decks containing epoxy-coated steel cast in concrete with one of the three corrosion inhibitors, the corrosion rates obtained from bench-scale tests in this study are not used due to the relatively short testing period (between weeks 18 to 27) at the data cutoff date and the considerable scatter in the individual results. To obtain the corrosion rates of bridge decks with corrosion inhibitors, an approach used in this

analysis is to find a ratio of average corrosion rates for conventional steel cast in concrete with corrosion inhibitor Rheocrete or DCI-S vs. conventional steel cast in concrete with no corrosion inhibitor, based on the results from Balma et al. (2005). After that, the corrosion rate of bridge decks with epoxy-coated steel and no corrosion inhibitor is multiplied by the ratio to obtain the corrosion rate for a bridge deck with either corrosion inhibitor. Because Hycrete works in a similar way to Rheocrete, the corrosion rate in concrete with Hycrete is assumed to be the same as that in concrete with Rheocrete.

Based on the methods presented above, the corrosion rates can be calculated for bridge decks with different corrosion protection systems. For bridges containing conventional steel, the corrosion rate is [(0.6 + 7.0)/2]/2 = 1.9 μm/yr (0.6 μm/yr from SE tests and 7.0 μm/yr from CB tests in this study). This corrosion rate is somewhat lower than used by Darwin et al. (2002). Based on a total corrosion loss of 25 μm to cause concrete cracking, the time to first repair after corrosion initiates is 25/1.9 = 13.2 years. For bridges containing conventional epoxy-coated steel or epoxy-coated steel with increased adhesion, the corrosion rate is [(0 + 7)/2]/2 = 1.7 μm/yr (0 μm/yr from SE tests and 7 μm/yr from CB tests based on the exposed area). Using a total corrosion loss of 2852 μm for concrete to crack, based on Eq. (1.13), the time to first repair after corrosion initiates is clearly more than 75 years (2852/1.7 = 1678 years). Therefore based on this model, no repair will be needed for bridge decks containing epoxy-coated steel. For bridge decks containing epoxy-coated steel with the corrosion inhibitor Rheocrete or DCI-S, the corrosion rates are obtained, using the approach described in the previous paragraph, as follows.

(1) From Balma et al. (2005), the corrosion losses over 96 weeks are 6, 7.5, and 10 μm for specimens with the corrosion inhibitors Rheocrete and DCI-S and

without any corrosion inhibitor, respectively. Therefore, the average corrosion rates over 96 weeks are 6/96 = 0.06, 7.5/96 = 0.075, and 10/96 = 0.1 μm/yr for specimens with the corrosion inhibitors Rheocrete and DCI and without any corrosion inhibitor, respectively.

(2) The ratios of average corrosion are 0.06/0.1 = 0.6 for specimens with the corrosion inhibitor Rheocrete and 0.075/0.1 = 0.75 for specimens with the corrosion inhibitor DCI-S.

(3) Since the corrosion rate of epoxy-coated steel without corrosion inhibitors is estimated to be 1.7 μm/yr, the corrosion rates for a bridge deck containing epoxy-coated steel and corrosion inhibitors Rheocrete and DCI-S are 0.6×1.7 =1.0 and 0.75×1.7 =1.3 μm/yr, respectively.

Using the corrosion rates obtained above and a total corrosion loss of 2852 μm based on Eq. (1.13), the time to first repair after corrosion initiates is beyond 75 years (2852/1.0 = 2852 years, 2852/1.3 = 2194 years). Because the corrosion rate of epoxy-coated steel cast in concrete with Hycrete is assumed to be the same as that with Rheocrete, the time to cracking after corrosion initiation is also more than 75 years for bridge decks containing epoxy-coated steel and Hycrete. Compared to the results of bridge decks containing epoxy-coated steel and no corrosion inhibitor, corrosion inhibitors are not needed to obtain a repair-free bridge deck in a 75-year service life.

The time to first repair for a prototype bridge deck can be estimated by adding the time to corrosion initiation (Section 4.2.1.1) and the time to cracking after corrosion initiates (Section 4.2.1.2) together. For a bridge deck containing conventional steel, the corrosion initiation time is between 0.7 and 3.4 years, and the time to cracking after corrosion initiates is 13.2 years. Therefore, the time to first repair is between 0.7 + 13.2 = 13.9 and 3.4 + 13.2 = 16.6 years. For bridge decks

containing stainless steel clad reinforcement or epoxy-coated steel, the time to first repair is beyond 75-year service life. The calculations for epoxy-coated steel do not, however, consider the potential effects of loss of adhesion between the epoxy and the steel.

For a bridge deck containing conventional epoxy-coated steel, adhesion loss between the epoxy and the steel may reduce the time to first repair (Sagues et al. 1994, *Adhesion* 1995). To consider the effects of adhesion loss, times to first repair for bridges containing epoxy-coated steel of 30 and 35 years (recommended by the bridge management engineer for KDOT) and 40 years (recommended by the bridge management engineer for SDDOT) (Darwin et al. 2002, Gong et al. 2002, Balma et al. 2005) are included in the economic analyses that follow. For bridge decks containing any type of ECR with improved adhesion, the 30, 35, and 40 year times to first repair recommended by state engineers are also used, along with the repair-free option based on corrosion rates, as they are for bridge decks containing epoxy-coated steel and the corrosion inhibitors Rheocrete and Hycrete. For bridge decks containing epoxy-coated steel and corrosion inhibitor DCI-S, the corrosion initiation time is between 14 and 40 years. When considering the 30, 35 and 40 year times to first repair for epoxy-coated steel, the time to cracking after corrosion initiation is between 30 – 3.4 = 27 and 40 – 0.7 = 39 years. Therefore, for bridge decks with ECR and corrosion inhibitor DCI-S, the time to first repair ranges from 14 + 27 = 41 to 14 + 39 = 53 years when corrosion initiates after 14 years and from 40 + 27 = 67 to 40 + 39 = 79 years when corrosion initiates after 40 years. Since the time to first repair is, in fact, a range, 41 and 53 years are used for corrosion initiating at 14 years and 67 years is used for corrosion initiating at 40 years in this analysis. A time of 79 years is automatically included in this case with a time to first repair beyond 75 years.

The time to first repair for bridge decks with different corrosion protection systems tested in this study, based on the corrosion initiation time and the time to cracking after corrosion initiates, are listed in Table 4.2. The recommended time to first repair for bridge reinforced with epoxy-coated steel, obtained from state maintenance engineers, is also incorporated in Table 4.2.

Table 4.2 – Time to first repair for bridge decks containing different corrosion protection systems

Steel designation	Average corrosion rate (μm/yr)	Total corrosion loss to crack concrete (μm)	Corrosion initiation time (years)	Time to cracking after corrosion initiation based on corrosion rate (years)	Time to first repair, based on corrosion rate or adhesion loss (years)
Conv.	1.9	25	0.7 3.4	13.2	14* 17*
ECR	1.7	2852	0.7 3.4	1678	30* 35* 40* >75**
SMI	0.02	25	75^{+}	1250	75^{+}
ECR(Rheocrete)	1.0	2852	0.7 3.4	2852	30* 35* 40* $>75^{+}$
ECR(DCI)	1.3	2852	14	2194	41* 53* >75**
			40	2194	67* >75**
ECR(Hycrete)	1.0	2852	0.7 3.4	2852	30* 35* 40* >75**
ECR(DuPont)	1.7	2852	0.7 3.4	1678	30* 35* 40* >75**
ECR(Chromate)	1.7	2852	0.7 3.4	1678	30* 35* 40* >75**
ECR(Valspar)	1.7	2852	0.7 3.4	1678	30* 35* 40* >75**

* Time to first repair based on an analysis of lab results

**Time to first repair based on estimation by bridge management engineers

4.2.2 Cost Effectiveness

The cost effectiveness of different corrosion protection systems is compared using a prototype bridge deck. The prototype deck is 230 mm (9 in) thick, either monolithic or consisting of a 191-mm (7½-in.) concrete subdeck with a 38-mm (1½-in.) silica fume concrete overlay (SFO). Since stainless steel is assumed to have superior corrosion resistance, the concrete cover for a bridge deck containing stainless steel clad reinforcement can be reduced from 78 mm (3 in.) to 64 mm (2.5 in.). Therefore, a 216-mm monolithic bridge deck containing stainless steel clad bars is also included. The analysis considers the cost of constructing a new bridge along with the cost of repairs over a 75-year service life. The time to first repair is obtained in Section 4.2.1. After the first repair, supplementary repairs are based on 25-year cycles in all cases.

For new construction, the cost of concrete is \$475.30/m^3 (\$363.40/yd^3), based on average bids on KDOT projects for the years 2000 through 2003 (Balma et al. 2005). The average density of reinforcing steel used in a typical bridge deck is 143 kg/m^3 (241 lb/yd^3) (Kepler et al. 2000). The costs of materials, fabrication, delivery, and placement were obtained from manufacturers and fabricators in 2004 and 2005. For conventional and epoxy-coated steel, the cost is \$0.55/kg (\$0.25/lb) and \$0.68/kg (\$0.31/lb) at the mill, respectively. The combined costs of fabrication, delivery, and placement are \$1.30/kg (\$0.59/lb) for conventional steel and \$1.41/kg (\$0.64/lb) for epoxy-coated steel, giving total in-place costs of \$1.85/kg (\$0.84/lb) and \$2.09/kg (\$0.95/lb) for conventional and epoxy-coated steel, respectively. The cost of SMI stainless steel clad reinforcement is \$2.75/kg (\$1.25/lb) at the mill according to the manufacturer. The cost for fabrication, delivery, and placement is \$1.43/kg (\$0.65/lb) based on the fabrication cost for conventional steel and the shipping and placement

cost for epoxy-coated steel, plus an assumed cost of \$0.04/kg (\$0.02/lb) for end protection, giving an in-place cost of \$4.18/kg (\$1.90/lb) for stainless steel clad reinforcement. For the three different high adhesion ECR bars, the cost at mill and the cost of fabrication, shipping, and placement are the same as those for the conventional ECR steel, giving a total cost of \$2.09/kg (\$0.95/lb) for all three types of high adhesion ECR steel. The costs of corrosion inhibitors, Rheocrete 222+, DCI-S, and Hycrete, were provided by the manufacturers as \$4.21/L (\$16/gal), \$1.84/L (\$7/gal), and \$3.94/L (\$15/gal), respectively. The dosage rates recommended for Rheocrete 222+, DCI-S, and Hycrete are 5 L/m^3 (1 gal/yd^3), 10-30 L/m^3 (2-6 gal/yd^3), and 5-10 L/m^3 (1-2 gal/yd^3), respectively. All costs are expressed in dollars per square meter as shown below:

230-mm concrete deck

$$\frac{\$475.30}{\mathrm{m}^3} \times \frac{0.230\,\mathrm{m}^3}{\mathrm{m}^2} = \$109.32/\mathrm{m}^2$$

191-mm concrete subdeck + 38-mm silica fume overlay

$$\frac{\$475.30}{\mathrm{m}^3} \times \frac{0.191\,\mathrm{m}^3}{\mathrm{m}^2} + \$43.61/\mathrm{m}^2 = \$134.39/\mathrm{m}^2$$

216-mm concrete deck

$$\frac{\$475.30}{\mathrm{m}^3} \times \frac{0.216\,\mathrm{m}^3}{\mathrm{m}^2} = \$102.66/\mathrm{m}^2$$

Conventional steel

$$\frac{\$1.85}{\mathrm{kg}} \times \frac{143\,\mathrm{kg}}{\mathrm{m}^3} \times \frac{0.230\,\mathrm{m}^3}{\mathrm{m}^2} = \$60.85/\mathrm{m}^2$$

Epoxy-coated steel

$$\frac{\$2.09}{\mathrm{kg}} \times \frac{143\,\mathrm{kg}}{\mathrm{m}^3} \times \frac{0.230\,\mathrm{m}^3}{\mathrm{m}^2} = \$68.74/\mathrm{m}^2$$

Stainless steel clad reinforcement

$$\frac{\$4.18}{\mathrm{kg}} \times \frac{143\,\mathrm{kg}}{\mathrm{m}^3} \times \frac{0.230\,\mathrm{m}^3}{\mathrm{m}^2} = \$137.48/\mathrm{m}^2$$

High adhesion ECR (DuPont)

$$\frac{\$2.09}{\text{kg}} \times \frac{143\,\text{kg}}{\text{m}^3} \times \frac{0.230\,\text{m}^3}{\text{m}^2} = \$68.74/\text{m}^2$$

High adhesion ECR (Chromate)

$$\frac{\$2.09}{\text{kg}} \times \frac{143\,\text{kg}}{\text{m}^3} \times \frac{0.230\,\text{m}^3}{\text{m}^2} = \$68.74/\text{m}^2$$

High adhesion ECR (Valspar)

$$\frac{\$2.09}{\text{kg}} \times \frac{143\,\text{kg}}{\text{m}^3} \times \frac{0.230\,\text{m}^3}{\text{m}^2} = \$68.74/\text{m}^2$$

Rheocrete 222+

$$\frac{\$4.21}{\text{L}} \times \frac{5\,\text{L}}{\text{m}^3} \times \frac{0.230\,\text{m}^3}{\text{m}^2} = \$4.84/\text{m}^2$$

DCI-S

$$\frac{\$1.84}{\text{L}} \times \frac{10\,\text{L}}{\text{m}^3} \times \frac{0.230\,\text{m}^3}{\text{m}^2} = \$4.23/\text{m}^2$$

$$\frac{\$1.84}{\text{L}} \times \frac{30\text{L}}{\text{m}^3} \times \frac{0.230\,\text{m}^3}{\text{m}^2} = \$12.70/\text{m}^2$$

Hycrete

$$\frac{\$3.94}{\text{L}} \times \frac{5\,\text{L}}{\text{m}^3} \times \frac{0.230\,\text{m}^3}{\text{m}^2} = \$4.53/\text{m}^2$$

$$\frac{\$3.94}{\text{L}} \times \frac{10\,\text{L}}{\text{m}^3} \times \frac{0.230\,\text{m}^3}{\text{m}^2} = \$9.06/\text{m}^2$$

Based on information obtained from KDOT on bridges that were repaired in 1999, Kepler et al. (2000) reported that, on the average, 6% of a deck received a full depth repair and 22% of a deck received a partial depth repair. The costs for full and partial deck repairs are $\$380.30/\text{m}^2$ and $\$125.77/\text{m}^2$, respectively, based on the average low-bid costs reported by KDOT from 2000 through 2003 (Balma et al. 2005). Other costs for bridges undergoing repair include machine preparation at $\$13.13/\text{m}^2$, a 38-mm silica fume overlay at $\$43.61/\text{m}^2$, and incidental costs at $\$154.89/\text{m}^2$ (Balma et al. 2005). Based on the cost information given above, the average cost of repair can be calculated as shown below.

$$0.22 \times \frac{\$126.77}{\text{m}^2} + 0.06 \times \frac{\$380.30}{\text{m}^2} + \frac{\$13.13}{\text{m}^2} + \frac{\$43.61}{\text{m}^2} + \frac{\$154.89}{\text{m}^2} = \$262.34/\text{m}^2$$

The total cost is calculated and compared based on the cost of a new bridge deck and the present value of the cost of repairs over the 75-year service life of the bridge. The present value of the cost of a repair is expressed as:

$$P = F \times (1+i)^{-n} \tag{4.4}$$

where

P = present value

F = cost of repair

i = discount rate (%/100), 2, 4 and 6% are used here.

n = time to repair (in years)

Table 4.3 shows the results of the economic analysis for the different corrosion protection systems. The cost for a new 230-mm bridge deck containing conventional steel is \$170.17/m^2, while the cost for the same deck with conventional ECR or one of the three ECRs with improved adhesion is \$178.06/m^2. The cost for a new 230-mm bridge deck containing stainless steel clad reinforcement is \$246.80/m^2. The costs for new 230-mm bridge decks with epoxy-coated steel cast in concrete with corrosion inhibitors are \$182.90/m^2 (Rheocrete), \$182.29/m^2 (lower bound for DCI-S), \$190.76/m^2 (upper bound for DCI-S), \$182.59/m^2 (lower bound for Hycrete), and \$187.12/m^2 (upper bound for Hycrete). The use of a 216-mm bridge deck, instead of a 230-mm bridge deck, decreases the cost by \$6.66/m^2.

Based on the present costs for all of the options listed in Table 4.3, when the effect of adhesion loss is not considered, the lowest cost option is a 230-mm monolithic deck reinforced with conventional ECR or one of the three types of ECR with improved adhesion, with a cost of \$178.06/m^2. When corrosion inhibitors are

used, the lowest cost deck is a 230-mm deck containing epoxy-coated steel with corrosion inhibitor DCI-S if the lower bound of the dosage rate is used, at a cost of $\$182.29/m^2$. The cost increases to $\$190.76/m^2$ when the upper bound of the DCI-S dosage is used, which is higher than that of bridge decks cast with the other corrosion inhibitors, Rheocrete ($182.90), Hycrete at lower bound of dosage rate ($182.59), and Hycrete at upper bound of dosage rate ($187.12). When a 230-mm deck consisting of 191-mm concrete subdeck and a 38-mm silica fume overlay is used, the additional cost is $\$25.07/m^2$.

When the effect of potential adhesion loss is considered, at a discount rate of 2%, the lowest cost option is a 216-mm deck containing stainless steel clad reinforcement, with a present cost of $\$240.14/m^3$. The second lowest cost choice is a 230-mm monolithic deck containing stainless steel clad reinforcement, with a present cost of $\$246.80/m^2$. A bridge deck reinforced with epoxy-coated bars costs $\$411.17/m^2$, $\$389.19/m^2$, or $\$369.29/m^2$ when the first repair occurs at 30, 35, or 40 years, respectively. When corrosion inhibitors are used, the costs range from $\$260.37/m^2$ (DCI-S) to $\$420.23/m^2$ (Hycrete) as the time to first repair varies between 30 to 70 years. At a discount rate of 4%, the lowest cost option is a 230-mm monolithic bridge deck containing epoxy-coated steel and corrosion inhibitor DCI-S, with a present cost of $\$209.71/m^2$, when the time to first repair occurs at 67 years. For the other options using a 230-mm monolithic bridge deck and corrosion inhibitors, the prices are between $\$215.11/m^2$ to $\$298.35/m^2$, depending on the type of corrosion inhibitor and the time to first repair. When corrosion inhibitors are not used, a bridge deck using epoxy-coated bars as reinforcement costs $\$289.29/m^2$, $\$269.48/m^2$, or $\$253.20/m^2$ when first repair is assumed at 30, 35, or 40 years, respectively. Bridges built with stainless steel clad bars cost the same as those at a discount rate of 2%,

because no repairs are needed during the 75-year economic life of the bridge. At a discount rate of 6%, the lowest cost option is a 230-mm monolithic bridge deck containing epoxy-coated steel with corrosion inhibitor DCI-S, with a present cost of $\$194.25/m^2$, when first repair is needed at 53 years. For the other options using 230-mm monolithic bridge deck and corrosion inhibitors, the costs range from $\$196.05/m^2$ to $\$243.44/m^2$. A bridge deck reinforced with epoxy-coated bars costs $\$234.38/m^2$, $\$220.14/m^2$, or $\$209.51/m^2$ when first repair is assumed at 30, 35, or 40 years, respectively, and no corrosion inhibitors are used.

For each discount rate (2, 4, and 6%), the corrosion protection systems with the lowest costs for a 191 mm concrete bridge deck with a 38-mm silica fume overlay and for a 216 or a 230 mm monolithic concrete bridge deck are the same. For any of the systems, however, a concrete bridge deck with a silica fume overlay yields a higher cost due to the higher cost of the bridge deck itself.

Table 4.3 - Summary of economic analysis for bridge decks reinforced with conventional, epoxy-coated, and stainless steel clad reinforcement

Option	Type of deck	Type of steel	Type of corroison inhibitor	Cost of deck ($/m^2)	Cost of steel ($/m^2)	Cost of corrosion inhibitor ($/m^2)	Initial cost ($/m^2)	Time to repair 1 (years)	Cost of repair 1 ($/m^2)	Time to repair 2 (years)	Cost of repair 2 ($/m^2)	Time to repair 3 (years)	Cost of repair 3 ($/m^2)	Present cost i = 2% ($/m^2)	Present cost i = 4% ($/m^2)	Present cost i = 6% ($/m^2)
1	230-mm	Conventional	—	109.32	60.85	—	170.17	14	262.34	39	262.34	64	262.34	564.05	399.81	319.54
2								17		42		67		541.33	374.32	295.58
3	230-mm	ECR	—	109.32	68.74	—	178.06	30	262.34	55	262.34			411.17	289.29	234.38
4								35		60				389.19	269.48	220.14
5								40		65				369.29	253.20	209.51
6								75^+						178.06	178.06	178.06
7	230-mm	ECR	Rheocrete	109.32	68.74	4.84	182.90	30	262.34	55	262.34			416.01	294.13	239.22
8								35		60				394.03	274.32	224.98
9								40		65				374.13	258.04	214.35
10								75^+						182.9	182.9	182.9
11	230-mm	ECR	DCI-S	109.32	68.74	4.23	182.29	41	262.34	66	262.34			369.77	254.54	211.96
12								53						274.13	215.11	194.25
13								75^+						182.29	182.29	182.29
14						12.7	190.76	67	262.34					260.37	209.71	196.05
15								75^+						190.76	190.76	190.76
16	230-mm	ECR	Hycrete	109.32	68.74	4.53	182.59	30	262.34	55	262.34			415.70	293.82	238.91
17								35		60				393.72	274.01	224.67
18								40		65				373.82	257.73	214.04
19								75^+						182.59	182.59	182.59
20						9.06	187.12	30	262.34	55	262.34			420.23	298.35	243.44
21								35		60				398.25	278.54	229.20
22								40		65				378.35	262.26	218.57
23								75^+						187.12	187.12	187.12
24	230-mm	ECR(DuPont)	—	109.32	68.74	—	178.06	30	262.34	55	262.34			411.17	289.29	234.38
25								35		60				389.19	269.48	220.14
26								40		65				369.29	253.20	209.51
27								75^+						178.06	178.06	178.06
28	230-mm	ECR(Chromate)	—	109.32	68.74	—	178.06	30	262.34	55	262.34			411.17	289.29	234.38
29								35		60				389.19	269.48	220.14
30								40		65				369.29	253.20	209.51
31								75^+						178.06	178.06	178.06
32	230-mm	ECR(Valspar)	—	109.32	68.74	—	178.06	30	262.34	55	262.34			411.17	289.29	234.38
33								35		60				389.19	269.48	220.14
34								40		65				369.29	253.20	209.51
35								75^+						178.06	178.06	178.06

Table 4.3 - Summary of economic analysis for bridge decks reinforced with conventional, epoxy-coated, and stainless steel clad reinforcement (continued)

Option	Type of deck	Type of steel	Type of corroison inhibitor	Cost of deck ($/m^2)	Cost of steel ($/m^2)	Cost of corrosion inhibitor ($/m^2)	Initial cost ($/m^2)	Time to repair 1 (years)	Cost of repair 1 ($/m^2)	Time to repair 2 (years)	Cost of repair 2 ($/m^2)	Time to repair 3 (years)	Cost of repair 3 ($/m^2)	Present cost i = 2% ($/m^2)	Present cost i = 4% ($/m^2)	Present cost i = 6% ($/m^2)
36	191-mm + 38mm SFO	ECR	—	134.39	68.74	—	203.13	30	262.34	55	262.34			436.24	314.36	259.45
37								35		60				414.26	294.55	245.21
38								40		65				394.36	278.27	234.58
39								75$^+$						203.13	203.13	203.13
40	191-mm + 38mm SFO	ECR	Rheocrete	134.39	68.74	4.84	207.97	30	262.34	55	262.34			441.08	319.20	264.29
41								35		60				419.10	299.39	250.05
42								40		65				399.20	283.11	239.42
43								75$^+$						207.97	207.97	207.97
44	191-mm + 38mm SFO	ECR	DCI-S	134.39	68.74	4.23	207.36	41	262.34	66	262.34			394.84	279.61	231.42
45								53						299.20	240.18	219.32
46								75$^+$						207.36	207.36	207.36
47						12.7	215.83	67	262.34		262.34			285.44	234.78	221.12
48								75$^+$						215.83	215.83	215.83
49	191-mm + 38mm SFO	ECR	Hycrete	134.39	68.74	4.53	207.66	30	262.34	55	262.34			440.77	318.89	263.98
50								35		60				418.79	299.08	249.74
51								40		65				398.89	282.80	239.11
52								75$^+$						207.66	207.66	207.66
53						9.06	212.19	30	262.34	55	262.34			445.30	323.42	268.51
54								35		60				423.32	303.61	254.27
55								40		65				403.42	287.33	243.64
56								75$^+$						212.19	212.19	212.19
57	191-mm + 38mm SFO	ECR(DuPont)	—	134.39	68.74	—	203.13	30	262.34	55	262.34			436.24	314.36	259.45
58								35		60				414.26	294.55	245.21
59								40		65				394.36	278.27	234.58
60								75$^+$						203.13	203.13	203.13
61	191-mm + 38mm SFO	ECR(Chromate)	—	134.39	68.74	—	203.13	30	262.34	55	262.34			436.24	314.36	259.45
62								35		60				414.26	294.55	245.21
63								40		65				394.36	278.27	234.58
64								75$^+$						203.13	203.13	203.13
65	191-mm + 38mm SFO	ECR(Valspar)	—	134.39	68.74	—	203.13	30	262.34	55	262.34			436.24	314.36	259.45
66								35		60				414.26	294.55	245.21
67								40		65				394.36	278.27	234.58
68								75$^+$						203.13	203.13	203.13
69	230-mm	SMI	—	109.32	137.48	—	246.80	75$^+$						246.80	246.80	246.80
70	216-mm	SMI	—	102.66	137.48	—	240.14	75$^+$						240.14	240.14	240.14

4.2.3 Summary of Economic Analysis

Based on the analysis presented in the previous section, when adhesion loss between epoxy and steel is not considered, the lowest cost option is a 230-mm deck reinforced with conventional or one of the three high adhesion epoxy-coated steels, with a cost of $\$178.06/m^2$. When the potential effects of adhesion loss are considered, at a discount rate of 2%, the lowest cost option is a 216-mm deck containing stainless steel clad reinforcement, with a present cost of $\$240.14/m^3$. At discount rates of 4% and 6%, the lowest cost option is a 230-mm bridge deck containing epoxy-coated steel with corrosion inhibitor DCI-S, with present costs of $\$209.71/m^2$ (first repair at year 67) and $\$194.25/m^2$ (first repair at year 53). The other options are summarized in Table 4.3.

The use of epoxy-coated steel is definitely the most cost-effective choice if long-term adhesion between epoxy and steel is adequate to attain a repair-free service life. Otherwise, the use of stainless steel clad reinforcement or corrosion inhibitor DCI-S will be a better option. Corrosion inhibitors Rheocrete and Hycrete do not exhibit cost effectiveness in this analysis. The estimates for epoxy-coated bars in concrete containing DCI-S are based on limited data from other studies. More information of the corrosion initiation time and corrosion rates for steel in concrete containing corrosion inhibitors is needed to improve the accuracy of this analysis.

CHAPTER 5
CONCLUSIONS AND RECOMMENDATIONS

5.1 SUMMARY

This report presents the results of the evaluation of corrosion protection systems for reinforcing steel in concrete. The corrosion protection systems evaluated include:

- Conventional reinforcing bars
- Conventional epoxy-coated reinforcing bars coated with 3M™ Scotchkote™ 413 Fusion Bonded Epoxy
- 316 LN stainless steel clad reinforcing bars
- Epoxy-coated bars with conventional epoxy cast in concrete containing one of three corrosion inhibitors, calcium nitrite (DCI-S), Rheocrete 222+, or Hycrete, cast in concrete with water-cement ratios of 0.45 and 0.35
- Epoxy-coated bars with conventional epoxy applied over a primer coat that contains microencapsulated calcium nitrite [$Ca(NO_2)_2$] cast in concrete with water-cement ratios of 0.45 and 0.35
- Three epoxy-coated reinforcing steels with increased adhesion epoxy
  - Epoxy-coated reinforcing bars with increased adhesion epoxy produced by DuPont
  - Epoxy-coated reinforcing bars with increased adhesion epoxy produced by Valspar
  - Epoxy-coated reinforcing bars with conventional epoxy applied after chromate pretreatment

- The three epoxy-coated bars, described as above, cast in concrete containing the corrosion inhibitor calcium nitrite (DCI-S)
- Multiple coated reinforcing bars with a metallic layer containing 98% zinc and 2% aluminum underlying the DuPont 8-2739 Flex West Blue epoxy

Rapid macrocell tests with bare and mortar-wrapped specimens and three bench-scale tests, the Southern Exposure (SE), cracked beam (CB), and ASTM G 109 tests, are used to evaluate the corrosion protection systems. The cost effectiveness of different corrosion protection systems are compared when used in concrete bridge decks.

Linear polarization resistance tests are used to measure the microcell corrosion current densities and corrosion rates of the top and bottom mats of the bench-scale specimens. Cathodic disbondment tests are performed to evaluate the quality of the bond between the epoxy and the steel for the different types of epoxy-coated reinforcing bars. Mechanical property tests are used to determine the yield strength, tensile strength, elongation, and bending properties of conventional steel and stainless steel clad reinforcement. The thickness of the stainless steel cladding is analyzed for the uniformity and variability. The microstructure of corrosion products are observed and compared for conventional steel and stainless steel clad reinforcement.

5.2 CONCLUSIONS

The following conclusions are based on the results and observations presented in this report.

1. Stainless steel clad reinforcement exhibits very good corrosion performance when the cladding is intact. The average corrosion losses for the clad bars ranged from

0.1% to 3% of that for conventional steel and 2.5% to 100% of that for conventional epoxy-coated steel. The higher relative corrosion rates were obtained in SE tests, where all specimens exhibit relatively low corrosion losses at this writing. In most cases, corrosion potentials indicate that stainless steel clad reinforcement has a very low tendency to corrode, even when exposed to high salt concentrations.

2. When cladding is intentionally damaged, the stainless steel clad reinforcement shows average corrosion losses that range from 0.6% to 5% of the corrosion losses of conventional steel. However, the corrosion losses of stainless steel clad reinforcement range from 20% to 1100% of the losses for conventional epoxy-coated steel with the same level of damage, since the cathodic reaction is limited for ECR specimens due to the insulation provided by epoxy, but not for the stainless steel clad reinforcement. Nevertheless, the level of damage used in this study for stainless steel clad bars is not likely to be found in practice due to the thickness of the cladding and the nature of the metallurgic bond.
3. The combination of conventional and stainless steel clad reinforcement does not increase the corrosion rate of either material.
4. Epoxy-coated steels with improved adhesion between the epoxy and the steel show no significant improvement in corrosion resistance compared to conventional epoxy-coated steel at this writing. Therefore, no direct relation is observed between coatings with improved adhesion and corrosion performance during the relatively short testing periods reported.
5. In uncracked mortar or concrete (rapid macrocell and Southern Exposure test) containing corrosion inhibitors, corrosion rates and corrosion losses are lower than observed using the same mortar and concrete with no inhibitor.

6. For concrete with cracks above and parallel to the reinforcing steel (cracked beam test), the presence of corrosion inhibitors does not provide an advantage in protecting the reinforcing steel.
7. In uncracked concrete, a lower water-cement ratio results in corrosion rates and losses that are lower than observed at the higher water-cement ratio. In cracked concrete, a lower-water-cement ratio provides only limited additional corrosion protection when cracks provide a direct path for the chlorides to the steel.
8. Epoxy-coated steel with a primer containing encapsulated calcium nitrite does not exhibit an improvement in corrosion resistance compared to conventional epoxy-coated steel in uncracked or cracked concrete.
9. For multiple coated bars with only the epoxy penetrated, the average corrosion losses range from 0.8 to 57% of the corrosion losses for conventional steel and 23 to 231% of the losses for conventional epoxy-coated steel. For specimens containing multiple coated steel with both layers penetrated, the corrosion losses range from 0.2 to 233% of the corrosion losses for conventional steel and 13 to 455% of those for conventional epoxy-coated steel. The corrosion protection provided by the zinc coating can be observed based on the more negative corrosion potentials exhibited by zinc in comparison to steel. The protection, however, gradually disappears with time as the zinc corrodes.
10. When adhesion loss between epoxy and steel is not considered, a 230-mm (9 in.) deck reinforced with conventional epoxy-coated steel or one of the three high adhesion epoxy-coated steels is the most cost-effective. When the potential effects of adhesion loss are considered, at a discount rate of 2%, the most cost-effective option is a 216-mm deck containing stainless steel clad reinforcement. At

discount rates of 4% and 6%, the most cost-effective option is a 230-mm bridge deck containing epoxy-coated steel with corrosion inhibitor DCI-S.

11. The microcell corrosion current densities and corrosion rates of bottom mats obtained from linear polarization resistance tests are usually one to two orders of magnitude lower than those of top mats, and the results when the two mats are connected are somewhere between the values for the top and bottom mats for CB specimens. This characteristic, however, is not necessarily observed for SE and ASTM G 109 specimens, where some microcell corrosion current densities and corrosion rates of bottom mats are higher than those of top mats, and some results when the two mats are connected are higher than the values for the top mats or lower than the bottom mats.
12. The microcell corrosion rates from linear polarization tests are of the same magnitude to the macrocell corrosion rates for SE and ASTM G 109 specimens, except for specimens containing conventional steel, where the microcell corrosion rates are one order of magnitude higher than the corresponding macrocell corrosion rates. For all CB specimens, the microcell corrosion rates are about one order of magnitude higher than the macrocell corrosion rates.
13. Based on three cathodic disbondment tests for each epoxy type, the epoxy-coated steel with chromate pretreatment exhibits the best bonding between epoxy and steel, overall, followed by the multiple coated steel, the increased adhesion bars with epoxy produced by DuPont, and the epoxy-coated steel with a primer containing calcium nitrite. The conventional epoxy-coated steel and increased adhesion bars with epoxy produced by Valspar show the worst bond quality and fail the cathodic disbondment criterion in Annex A1 of ASTM A 775.

14. The stainless steel clad reinforcement satisfies the physical and mechanical properties required by ASTM A 615.
15. A metallurgical bond is observed between the 316LN stainless steel cladding and the mild steel core of the bars, with no unclad regions or cracks through the cladding.
16. Corrosion products with similar morphology are observed on conventional reinforcement and regions of stainless steel clad reinforcement where the cladding has been penetrated, suggesting that the presence of the stainless steel cladding does not alter the nature of the corrosion products formed in an exposed region of the mild steel core.

5.3 RECOMMENDATIONS

1. Conventional epoxy-coated steel is recommended for use in both the top and bottom mats in reinforced concrete bridge decks. The average total corrosion losses of specimens containing conventional epoxy-coated steel range from 0 % to 5% of the corrosion losses of specimens containing conventional steel, and from 0% to 0.4% of the corrosion losses for specimens containing epoxy-coated steel at top and conventional steel at bottom.
2. SMI steel clad reinforcement also shows good corrosion resistance when the cladding is intact, with average total corrosion losses that range from 0.1% to 3% of that of uncoated conventional steel. SMI steel exhibits corrosion potentials that indicate that the steel has a low probability of corroding, even when exposed to high salt concentrations.
3. Concrete with a lower water-cement ratio or corrosion inhibitors should not be used as the sole corrosion protection system for concrete subjected to chlorides.

The reason is that, while concrete with a low water-cement ratio or a corrosion inhibitor provides good protection in uncracked concrete, it provides no significant corrosion protection in cracked concrete. The total corrosion losses for cracked beam specimens with corrosion inhibitors ranged between 51 and 179% of the corrosion losses of specimens with the same water-cement ratio and no inhibitor.

4. Cathodic disbondment tests should be added to the quality control checks applied to production bars, based on the observation that the conventional ECR and the improved adhesion steel with epoxy provided by Valspar failed in the coating disbondment requirements of Annex A1 ASTM A 775.
5. Based on the economic analysis, decks containing conventional epoxy-coated steel are less expensive than any other corrosion protection systems when the effects of adhesion loss are not considered. Decks containing stainless steel clad reinforcement or corrosion inhibitor DCI-S are the better choices when the effects adhesion loss between epoxy and steel is considered. Additional research is recommended to further evaluate the long-term implications of adhesion loss on the corrosion performance of epoxy-coated reinforcement.
6. For specimens cast in mortar with corrosion inhibitors in macrocell tests, a test period of 30 weeks instead of 15 weeks is recommended due to the slower corrosion initiation for specimens with corrosion inhibitors.

5.4 FUTURE WORK

The following work is necessary in the future to fully understand the findings presented in this report.

1. Test the long-term adhesion between epoxy and steel for different epoxy-coated steels, perhaps in a high temperature, high moisture environment. Adhesion is the key for epoxy-coated steel since adhesion loss may result in a deterioration in the corrosion performance of bridge decks containing epoxy-coated steel.
2. Obtain the area of epoxy damage for epoxy-coated steel in actual bridge decks. These data can be used to better apply the equation developed by Torres-Acosta and Sagues (2005).
3. Obtain the chloride thresholds for different corrosion protection systems so that the time to corrosion initiation can be determined when using chloride concentration profiles from bridge surveys.
4. Use the corrosion rates between weeks 50 and 70 for different corrosion protection systems, which are not available at this writing, to help provide more accurate predictions of the time to first repair.

REFERENCES

Adhesion Loss Mechanisms of Epoxy Coatings on Rebar Surfaces, (1995). Surface Science Western, Concrete Reinforcing Steel Institute, Schaumberg, IL

ASTM A 775/A 775M-01 (2003). "Standard Specification for Epoxy-Coated Steel Reinforcing Bars," *Annual Book of ASTM Standards*, *2002,* American Society for Testing and Materials, West Conshohocken, PA, Vol. 01.04

ASTM A 934/A 934M-01 (2003). "Standard Specification for Epoxy-Coated Reinforcing Steel Bars," *Annual Book of ASTM Standards, 2002*, American Society for Testing and Materials, West Conshohocken, PA, Vol. 01.04

ASTM G109-99ael (2003). "Standard Test Method for Determining the Effects of Chemical Admixtures on the Corrosion of Embedded Steel Reinforcement in Concrete Exposed to Chloride Environments," *2002 ASTM Annual Book of ASTM Standards*, American Society for Testing and Materials, West Conshohocken, PA, Vol. 03.02.

Balma, J., Darwin, D., Browning, J. P., and Locke, C. E. (2005). "Evaluation of corrosion protection systems and corrosion testing methods for reinforcing steel in concrete," *SM Report* No.76, The University of Kansas Center for Research, Inc., Lawrence, KS, 142 pp.

Berke, N. S. (1991). "Corrosion Inhibitors in Concrete," *Concrete International*, vol. 13, no. 7, pp. 24-27

Clear, K. C., and Virmani, Y. P. (1983). *Corrosion of Non-Specification Epoxy-Coated Rebars in Salty Concrete*, Paper No. 114, CORROSION/83, Apr., Anaheim, CA

Clear, K. C. (1992b). "Effectiveness of Epoxy-Coated Reinforcing Steel," *Concrete International*, Vol. 14, No.5, May, pp. 58-64

Clear, K. C., Hartt, W. H., McIntyre, J., and Lee, S. K. (1995). *Performance of Epoxy-Coated Reinforcing Steel in Highway Bridges*, NCHRP Report No. 370, Transportation Research Board, Washington, D. C.

Clemeña, G. G. and Virmani, Y. P. (2002). "Testing of Selected Metallic Reinforcing Bars for Extending the Service Life of Future Concrete Bridges: Testing in Outdoor Concrete Block," Virginia Transportation Research Council, *VTRC 03-R6*, December 2002, 24 pp.

Cramer, S. D., Covino, B. S., Bullard, S. J., Holcomb, G. R., Russell, J. H., Ziomek-Moroz, M., Virmani, Y. P., Butler, J. T., Nelson, F. J., Thompson, N. G. (2002). "Prevention of Chloride-induced Corrosion Damage to Bridges," *ISIJ International*, v 42, n 12 SPEC., 2002, pp. 1376-1385

Darwin, D., and Hadje-Ghaffari, H. (1990). "Effects of PE-217 on Steel-Concrete Bond Strength," *Report*, University of Kansas, Lawrence, Kansas, 10pp

Darwin, D., Locke, C. E., Balma, J., and Kahrs, J. T. (1999). "Evaluation of Stainless Steel Clad Reinforcing Bars," *SL Report* No. 99-3, The University of Kansas Center for Research, Inc., Lawrence, KS, 17 pp.

Darwin, D., Browning, J. P., Nguyen, T. V., and Locke, C. E. (2002). "Mechanical and Corrosion Properties of a High-Strength, High Chromium Reinforcing Steel for Concrete," *SM Report* No. 66, The University of Kansas Center for Research, Inc., Lawrence, KS, 142 pp.

Elsener, B., Buchler, M., and Bohni, H. (1997). " Corrosion Inhibitors for Steel in Concrete," *Corrosion of Reinforcement in Concrete-Monitoring, Prevention and Rehabilitation,* European Federation of Corrosion Publications No.25, Eds. J. Meitz, B. Elsener, and R. Polder

Fliz, J., Akshey, S., Li, D., Kyo, Y., Sabol, S., Pickering, H., and Osseo-Asare, K. (1992). "Condition Evaluation of Concrete Bridges Relative to Reinforcement Corrosion – Volume 2 – Method for Measuring the Corrosion Rate of Steel in Concrete," Strategic Highway Research Program.

Ge, B., Darwin, D., Locke, C. E., and Browning, J. P. (2004). "Evaluation of Corrosion Protection Systems and Testing Methods for Conventional Reinforcing Steel," *SM Report* No. 73, University of Kansas Center for Research, Inc., Lawrence, Kansas, April, 213 pp.

Gong, L., Darwin, D., Browning, J. P., and Locke, C. E. (2002). " Evaluation of Mechanical and Corrosion Properties of MMFX Reinforcing Steel in Concrete," *SM Report* No. 70, The University of Kansas Center for Research, Inc., Lawrence, KS, 112 pp.

Hausmann, D. A. (1967). "Steel Corrosion in Concrete – How Does It Occur?" *Material Protection*, Nov., pp. 19-23

Hansson, C. M., Mammoliti, L., and Hope, B. B. (1998). "Corrosion Inhibitors in Concrete – Part I: The Principles," *Cement and Concrete Research*, v 28, n 12, Dec, 1998, pp. 1775-1781

Jones, D. A. (1992). *Principles and Prevention of Corrosion.*, Macmillan Publishing Company, New York, 568 pp.

Kahrs, J. T., Darwin, D., and Locke, C. E. (2001). "Evaluation of Corrosion Resistance of Type 304 Stainless Steel Clad Reinforcing Bars," *SM Report* No.65, University of Kansas Center for Research, Inc., Lawrence, KS, 76pp

Kaiser, L. (2000). W.R. Grace, personal communication

Kepler, J. L., Darwin, D., and Locke, C. E. (2000). "Evaluation of Corrosion Protection Methods for Reinforced Concrete Highway Structures," *SM Report* No.58, University of Kansas Center for Research, Inc., Lawrence, KS, 221pp

Lindquist, W. D., Darwin, D., and Browning, J. P. (2005). "Cracking and Chloride Contents in Reinforced Concrete Bridge Decks," *SM Report* No. 78, University of Kansas Center for Research, Inc., Lawrence, KS, 453pp

Manning, D. G., Escalante, E., and Whiting, D. (1982). *Panel Report-Galvanized Rebars as Long –Term Protective System*, Washington, D. C.

Manning, D. G. (1996). "Corrosion Performance of Epoxy-Coated Reinforcing Steel: North American Experience," *Construction and Building Materials*, Vol. 10, No.5, Jul. pp.349-365

Martinez, S. L., Darwin, D., McCabe, S. L., and Locke C. E. (1990). "Rapid Test for Corrosion Effects of Deicing Chemicals in Reinforced Concrete," *SL Report* 90-4, The University of Kansas Center for Research, Inc., Lawrence, KS, 61 pp.

McCrum, L., and Arnold, C. J. (1993). "Evaluation of Simulated Bridge Deck Slabs Using Uncoated, Galvanized, and Epoxy Coated Reinforcing Steel," *Research Report* No.R-1320, Michigan Department of Transportation, Lansing, MI.

McCrum, L., Lower, B. R., and Arnold, C. J. (1995). "A Comparison of the Corrosion Performance of Uncoated, Galvanized, and Epoxy Coated Reinforcing Steel in Concrete Bridge Decks," *Research Report* No. R-1321 (FHWA/MI-95 (02)), Michigan Department of Transportation, Lansing, MI.

McDonald, D. B., Sherman, M. R., Pfeifer, D. W., and Virmani, Y. P. (1995). "Stainless Steel Reinforcing as Corrosion Protection," *Concrete International*, Vol. 17, No.5, May, pp.65-70

McDonald, D. B., Sherman, M. R., Pfeifer, D. W. (1995). "The Performance of Bendable and Nonbendable Organic Coatings for Reinforcing Bars in Solution and

Cathodic Debonding Tests," *Report* No. FHWA-RD-94-103, Federal Highway Administration, Research and Development, McLean, VA, 148pp.

McDonald, D. B., Sherman, M. R., Pfeifer, D. W. (1996). "The Performance of Bendable and Nonbendable Organic Coatings for Reinforcing Bars in Solution and Cathodic Debonding Tests: Phase II Screening Tests," *Report* No. FHWA-RD-96-021, Federal Highway Administration, Research and Development, McLean, VA, 121pp.

McDonald, D. B., Pfeifer, D. W., and Blake G. T. (1996). " The Corrosion Performance of Inorganic-, Ceramic-, and Metallic-Clad Reinforcing Bars and Solid Metallic Reinforcing Bars in Accelerated Screening Tests," *Report* No. FHWA-RD-96-085, Federal Highway Administration, Office of Engineering and Highway Operations R&D, McLean, VA, 112 pp.

McDonald, D. B., Pfeifer, D. W., and Sherman, M. R. (1998). "Corrosion Evaluation of Epoxy-Coated, Metallic Clad and Solid Metallic Reinforcing Bars in Concrete," *Publication* No. FHWA-RD-98-153, Federal Highway Administration, Office of Engineering R&D, McLean, VA, 127 pp.

Miller, G. and Darwin, D. (2000). " Performance and Constructability of Silica Fume Bridge Deck Overlays," *SM Report* No. 57, The University of Kansas Center for Research, Inc., Lawrence, KS, 423 pp.

Nmai, C. K., Farrington, S. A., and Bobrowski, G. S. (1992). "Organic-Based Corrosion-Inhibiting Admixture for Reinforced Concrete," *Concrete International*, Vol. 14, No.4, Apr., pp. 45-51

Nmai, C. K., Bury, M. A., and Farzam, H. (1994). "Corrosion Evaluation of a Sodium Thiocyanate-Based Admixture," *Concrete International*, Vol. 24, No. 4, April, pp. 22-24

Perenchio, W. F. (1992). "Corrosion of Reinforcing Bars in Concrete," *Annual Seminar*, Master Builders Technology, Cleveland, OH, Dec.

Pfeifer, D. W. (2000). "High Performance Concrete and Reinforcing Steel with a 100-Year Service Life," *PCI Journal*, Vol. 45, No. 3, pp. 46-54

Pfeifer, D. W. and Scali, M. J. (1981). "Concrete Sealers for Protection of Bridge Structures," National Cooperative Highway Research Board Program *Report* 244, Transportation Research Board, national research Council, Washington, D. C., 138 pp.

Pfeifer, D. W., Landgren, R., and Krauss, P. (1992). *CRSI Performance Research: Epoxy Coated Reinforcing Steel,* Final Report, Concrete Reinforcing Steel Institute, Schaumburg, IL.

Pfeifer, D. W., Landgren, R., and Krauss, P. (1993). "Performance of Epoxy-Coated Rebars: A Review of CRSI Research Studies," *Circular* No. 403, Transportation Research Board, Washington, D. C.

Pyc, W., Zemajtis, J., Weyers, R., and Sprinkel, M. M. (1999). "Evaluation Corrosion-Inhibiting Admixtures," *Concrete International*, Vol. 21, No.4, Apr., pp 39-44.

Pyc, W., Weyers, R. E., Sprinkel M. M., Weyers, R. M., Mokarem, D. W., and Dillard, J. G. (2000). "Performance of Epoxy-Coated Reinforcing Steel," *Concrete International*, Vol. 22, No. 2, Feb., pp. 57-62

Rasheeduzzafar A., Dakhil F. H., Bader, M. A., and Khan, M. M. (1992). "Performance of Corrosion Resisting Steel in Chloride Bearing Concrete," *ACI Materials Journal*, Vol. 89, Sep.-Oct., pp. 439-448

Rodriguez, J., Ortega, L. M., and Garcia, A. M. (1994). "Assessment of Structural Elements with Corroded Reinforcement," *Corrosion and Corrosion Protection of Steel in Concrete*, R. M. Swamy, Sheffield Academic Press, United Kingdom

Sagues, A. A., Powers, R. G., and Kessler, R. (1994). "Corrosion Processes and Field Performance of Epoxy-Coated Reinforcing Steel in Marine Structures," *Corrosion 94*, Paper No. 299, National Association of Corrosion Engineers, Houston, TX

Schiessl, P. (1992). *Review of the KC, Inc. Reports on Effectiveness of Epoxy-Coated Reinforcing Steel*, Canadian Strategic Highway Research Program, Ottawa, ON, 15pp.

Schupack, M. and Stark, D. C. (1998). "Excellent After all These Years," *Concrete International,* Vol. 20, No. 5, May, pp. 29-35

Schwensen, S. M., Darwin, D., and Locke, C. E. (1995). "Rapid Evaluation of Corrosion-Resistant Concrete Reinforcing steel in the Presence of Deicers," *SL Report* 95-6, The University of Kansas Center for Research, Inc., Lawrence, KS, 90 pp.

Senecal, M. R., Darwin, D., and Locke, C. E. (1995). "Evaluation of Corrosion-Resistant Steel Reinforcing Bars," *SM Report* No. 40, The University of Kansas Center for Research, Inc., Lawrence, KS, 142 pp.

Sherman, M. R., McDonald, D. B., and Pfeifer, D. W. (1996). "Durability Aspects of Precast Prestressed Concrete Part 2: Chloride Permeability Study," *PCI Journal*, Vol. 41, No. 4, pp. 76-95

Smith, J. L., and Virmani, Y. P. (1996). "Performance of Epoxy-Coated Rebars in Bridge Decks," *Report* No. FHWA-RD-96-092, Federal Highway Administration, Washington, D. C.

Smith, J. L., Darwin, D., and Locke, C. E. (1995). "Corrosion-Resistant Steel Reinforcing Bars Initial Tests," *SL Report* 95-1, The University of Kansas Center for Research, Inc., Lawrence, KS, 43 pp.

Torres-Acosta, A. A. and Sagues, A. A. (2004). "Concrete Cracking by Localized Steel Corrosion – Geometric effects," *ACI Material Journal*, Vol. 101, No. 6, pp 501-507

Tourney, P. and Berke, N. S. (1993). "A Call for Standardized Tests for Corrosion-Inhibiting Admixtures," *Concrete International*, Vol. 22, No. 4, April, pp 57-62.

Trejo, D. (2002). "Evaluation of The Critical Chloride Threshold and Corrosion Rate for Different Steel Reinforcement Types," Texas Engineering Experimental Station *Interim Report*, July 2002, 38 pp.

Weyers, R. E., Pyc, W., Zemajtis, J., Liu, Y., Mokarem, D., and Sprinkel, M. M. (1997). "Field Investigation of Corrosion-Protection Performance of Bridge Decks Constructed with Epoxy-Coated Reinforcing Steel in Virginia," *Transportation Research Record*, No. 1597, pp. 82-90.

Virmani, Y. P., Clear, K. C., and Pasko, T. J. (1983). " Time to Corrosion of Reinforcing Steel in Concrete Slabs Vol. 5- Calcium Nitrite Admixtures or Epoxy Coated Reinforcing Bars as Corrosion Protection Systems," *Report* No. FHWA-RD-83-012, Federal Highway Administration, Washington, D. C.

Virmani, Y. P. (1990). "Effectiveness of Calcium Nitrite Admixture as Corrosion Inhibitor," *Public Roads*, Vol. 54, No.1, pp. 171-182.

Virmani, Y. P., and Clemeña, G. G. (1998). "Corrosion Protection Concrete Bridges," *Report* No. FHWA-RD-98-099, Federal Highway Administration, Washington, D. C.

Yeomans, S.R. (1994) "Performance of black, galvanized, and epoxy-coated reinforcing steels in chloride-contaminated concrete," *Corrosion 94*, Vol. 50, No. 1, Jan., p 72-81

Yonezawa, T., Ashworth, V., and Procter, R. P. M. (1988). "Study of the Pore Solution Composition and Chloride Effects in the Corrosion of Steel in Concrete," *Corrosion*, Vol. 44, No. 7, pp. 489-499

Yunovich , M., Thompson, N. G., Balvanyos, T., and Lave, L. (2002). "Highway Bridges," Appendix D, *Corrosion Cost and Preventive Strategies in the United States*, By G. H. Koch, M. PO. H. Broongers, N. G. Thompson, Y. P. Virmani, and J. H. Payer, *Report* No. FHWA-RD-01-156, Federal Highway Administration, McLean, VA, Mar., 773pp.

Zemajatis, J., Weyers, R. E., and Sprinkel, M. (1999). "Contract Report: Performance of Corrosion Inhibitors and Galvanized Steel in Concrete Exposure Specimens," *Report* No. VTRC 99-CR4, Virginia Transportation Research Council, Charlottesville, VA.

APPENDIX A

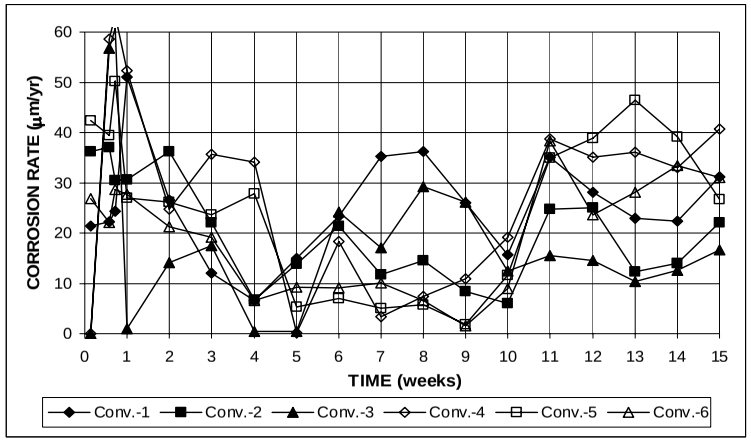

(a)

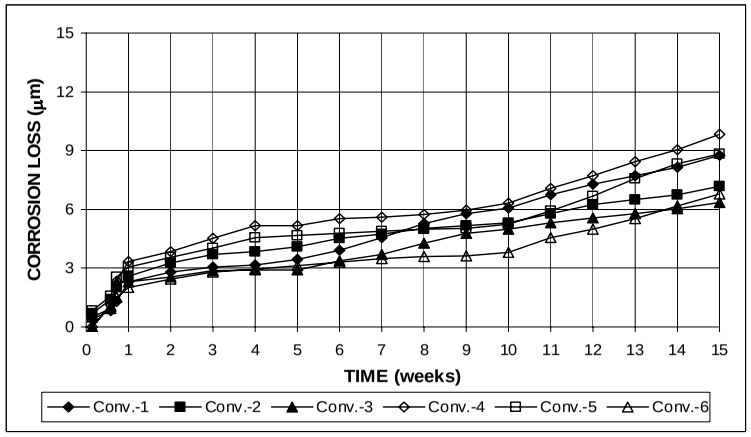

(b)

Figure A.1 - (a) Corrosion rates and (b) total corrosion Losses as measured in the rapid macrocell test for bare conventional steel in 1.6 m ion NaCl and simulated concrete pore solution

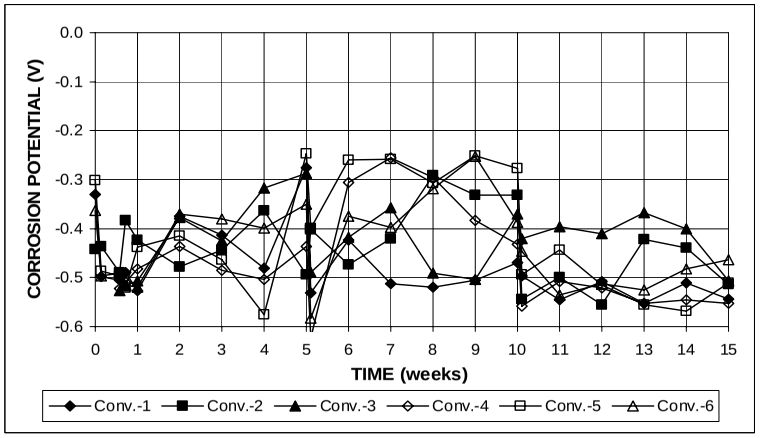

(a)

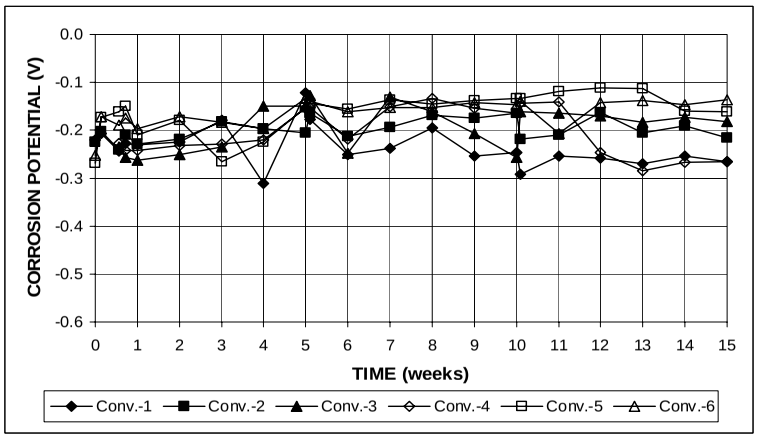

(b)

Figure A.2 - (a) Anode corrosion potentials and (b) cathode corrosion potentials with respect to saturated calomel electrode as measured in the rapid macrocell test for bare conventional steel in 1.6 m ion NaCl and simulated concrete pore solution.

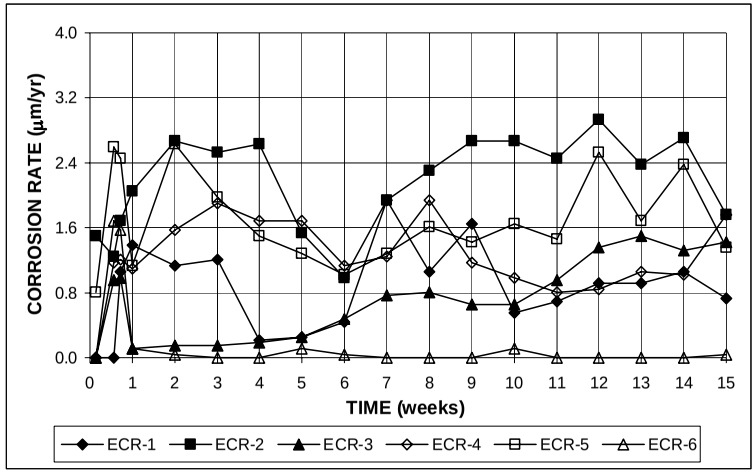

(a)

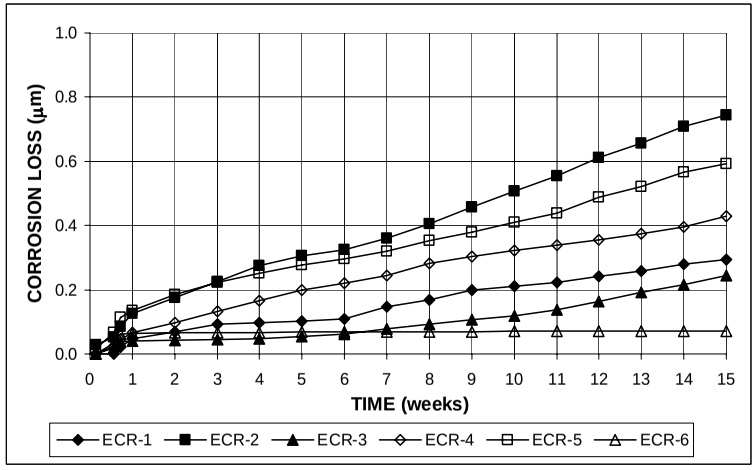

(b)

Figure A.3 - (a) Corrosion rates and (b) total corrosion Losses based on total bar area as measured in the rapid macrocell test for bare epoxy-coated steel in 1.6 m ion NaCl and simulated concrete pore solution

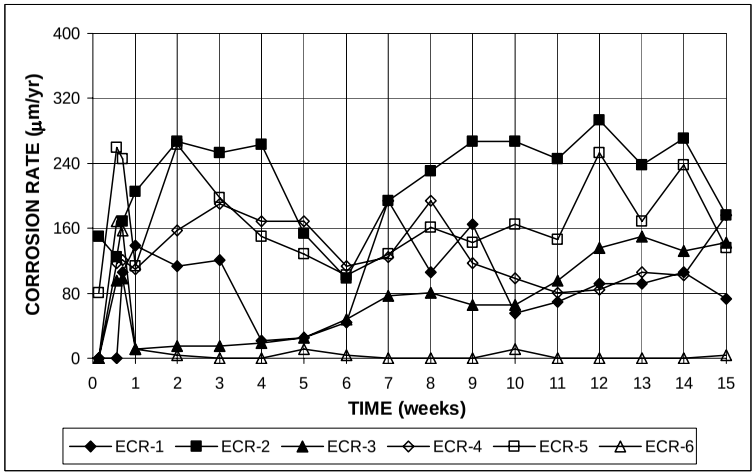

(a)

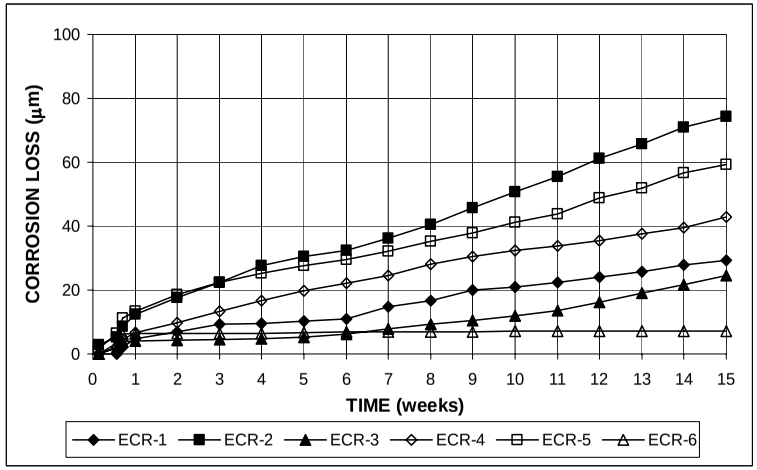

(b)

Figure A.4 - (a) Corrosion rates and (b) total corrosion Losses based on exposed area as measured in the rapid macrocell test for bare epoxy-coated steel in 1.6 m ion NaCl and simulated concrete pore solution

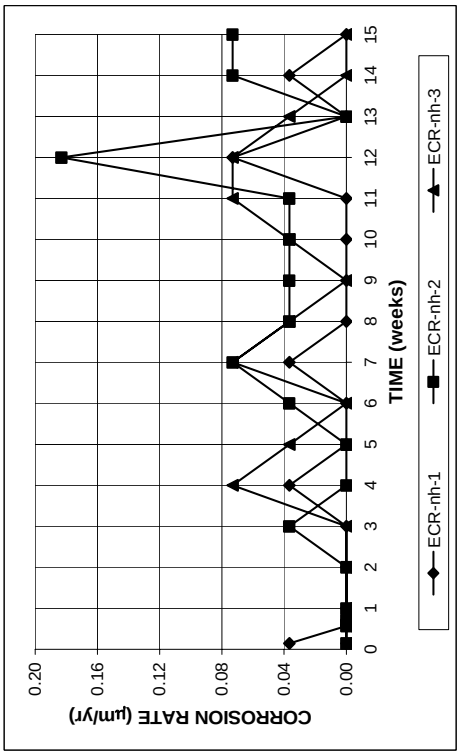

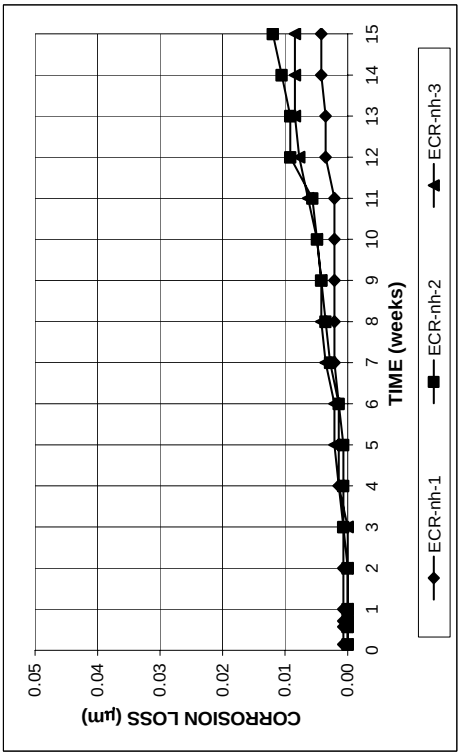

Figure A.6 - (a) Corrosion rates and (b) total corrosion Losses based on total bar area as measured in the rapid macrocell test for bare epoxy-coated steel without drilled holes in 1.6 m ion NaCl and simulated concrete pore solution

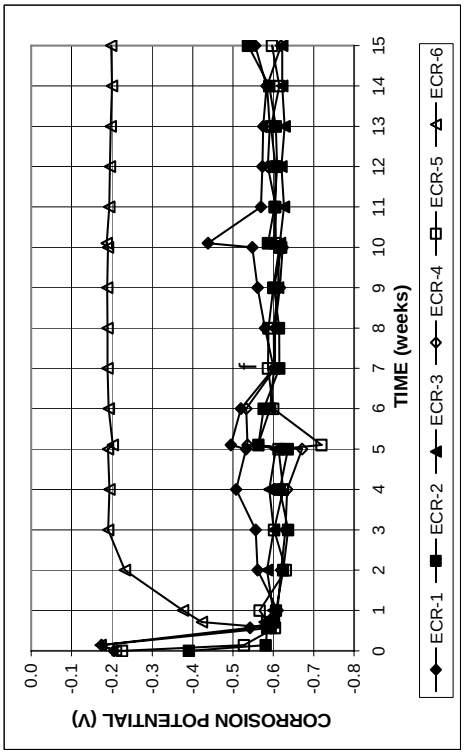

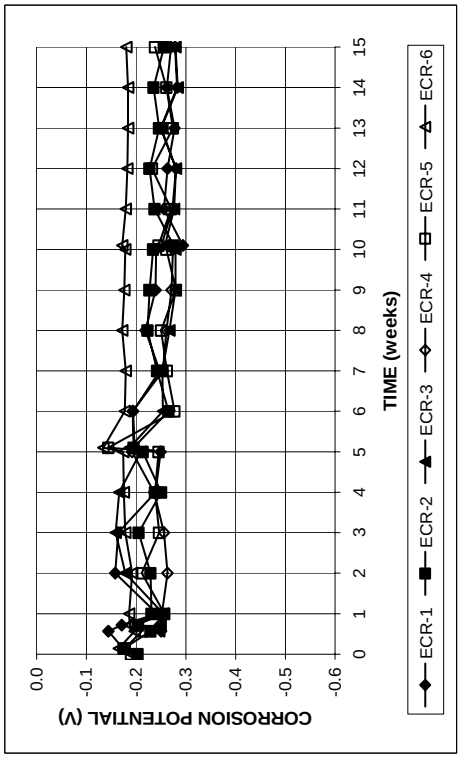

Figure A.5 - (a) Anode corrosion potentials and (b) cathode corrosion potentials with respect to saturated calomel electrode as measured in the rapid macrocell test for bare epoxy-coated steel in 1.6 m ion NaCl and simulated concrete pore solution.

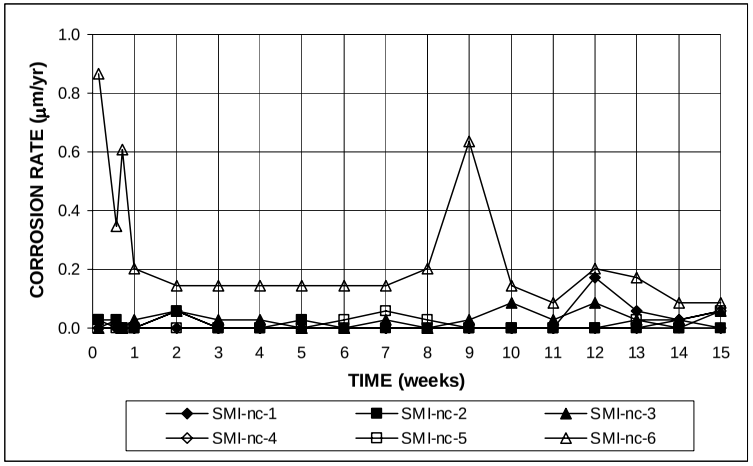

(a)

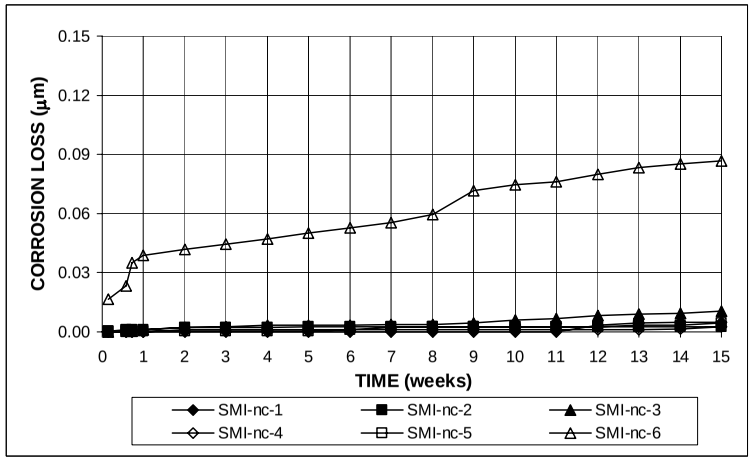

(b)

Figure A.7 - (a) Corrosion rates and (b) total corrosion Losses based on total bar area as measured in the rapid macrocell test for bare stainless steel clad bars without end protection in 1.6 m ion NaCl and simulated concrete pore solution

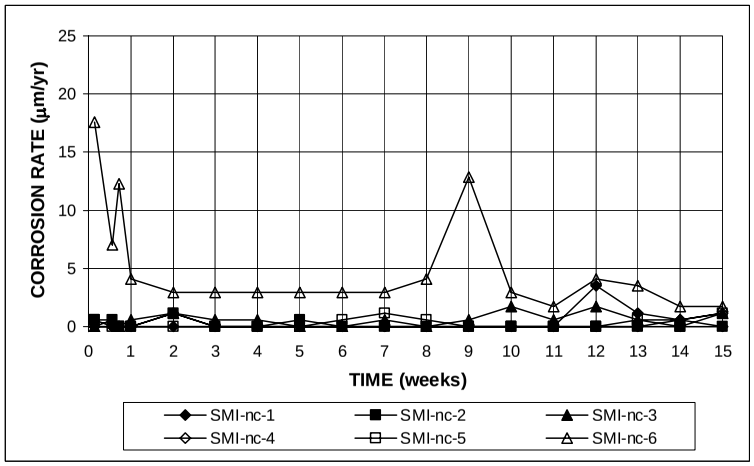

(a)

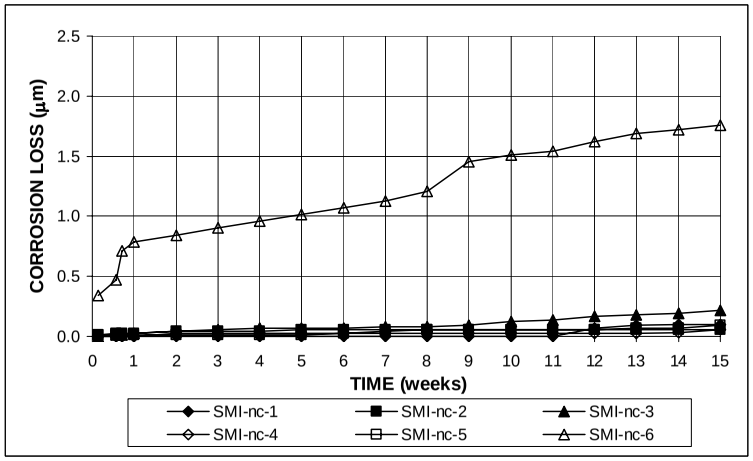

(b)

Figure A.8 - (a) Corrosion rates and (b) total corrosion Losses based on exposed area as measured in the rapid macrocell test for bare stainless steel clad bars without end protection in 1.6 m ion NaCl and simulated concrete pore solution

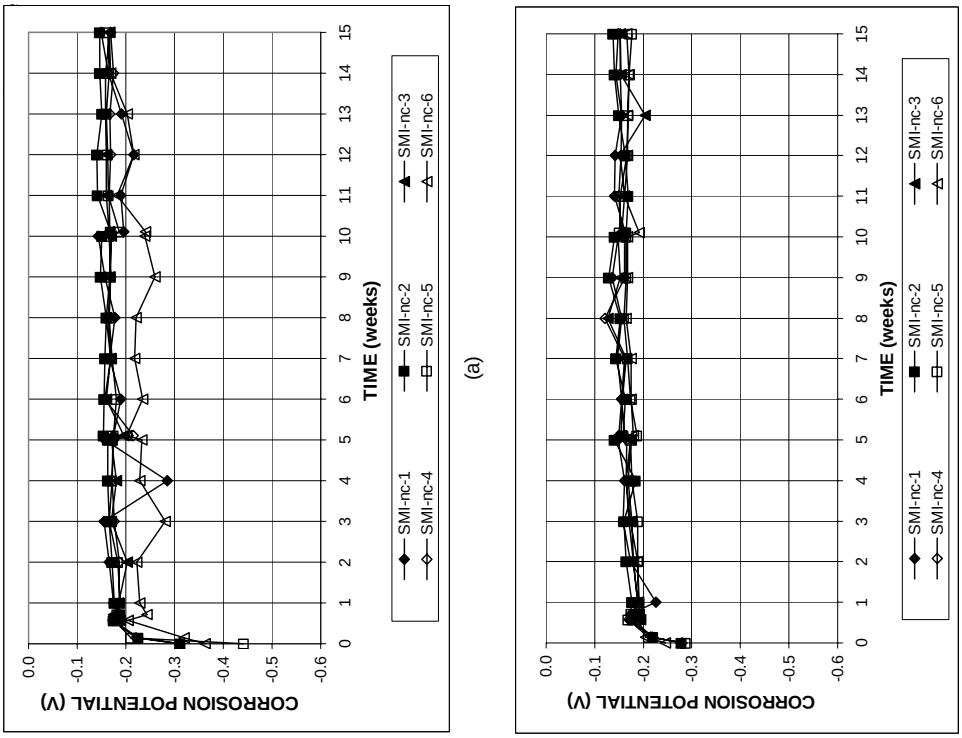

Figure A.9 - (a) Anode corrosion potentials and (b) cathode corrosion potentials with respect to saturated calomel electrode as measured in the rapid macrocell test for bare stainless steel clad bars without end protection in 1.6 m ion NaCl and simulated concrete pore solution.

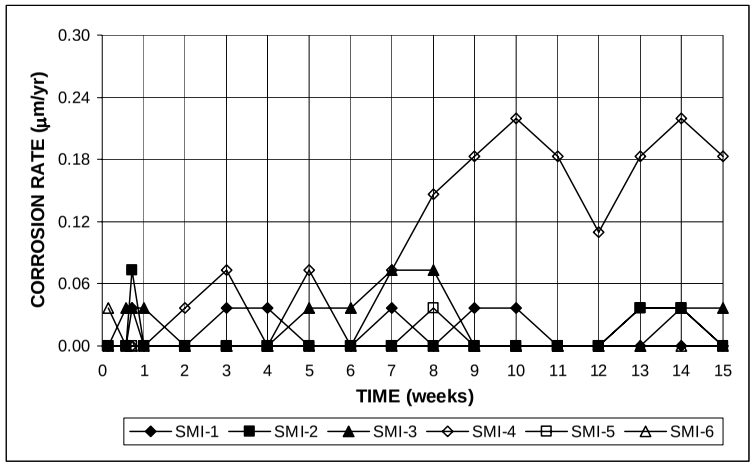

(a)

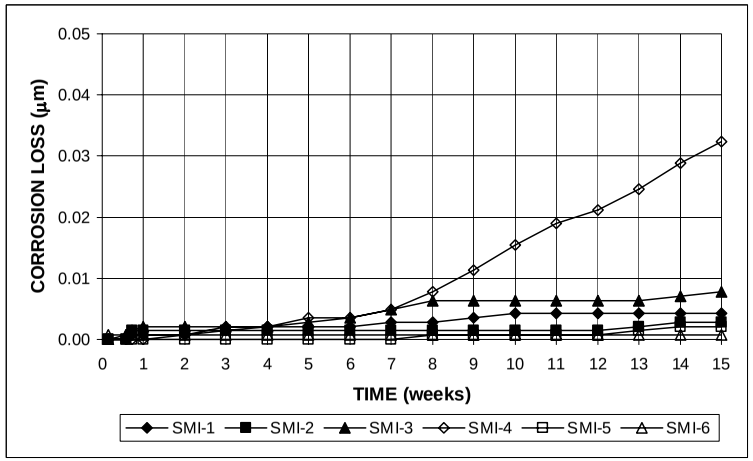

(b)

Figure A.10 - (a) Corrosion rates and (b) total corrosion Losses as measured in the rapid macrocell test for bare stainless steel clad bars in 1.6 m ion NaCl and simulated concrete pore solution

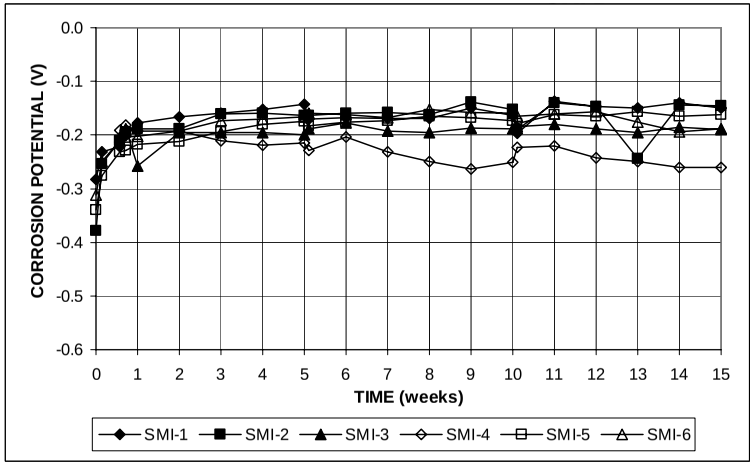

(a)

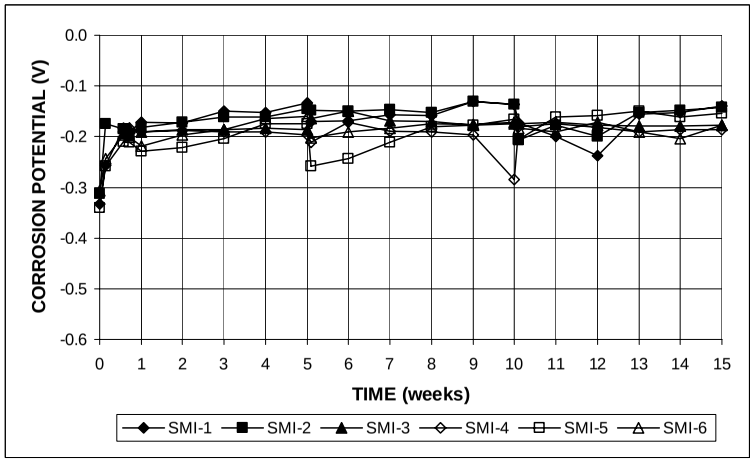

(b)

Figure A.11 - (a) Anode corrosion potentials and (b) cathode corrosion potentials with respect to saturated calomel electrode as measured in the rapid macrocell test for bare stainless steel clad bars in 1.6 m ion NaCl and simulated concrete pore solution.

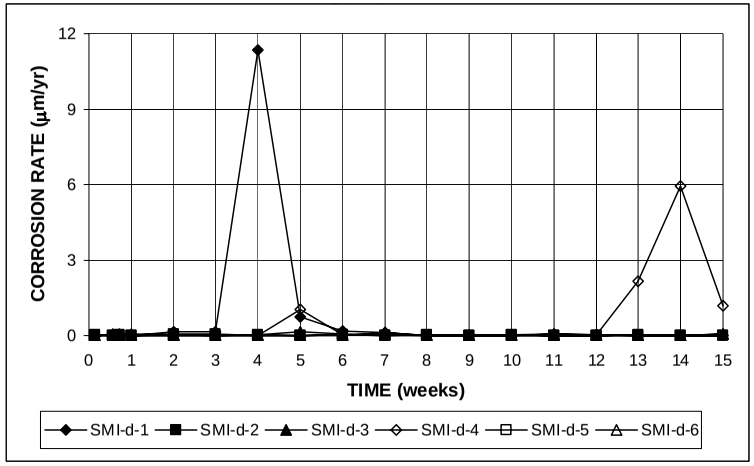

(a)

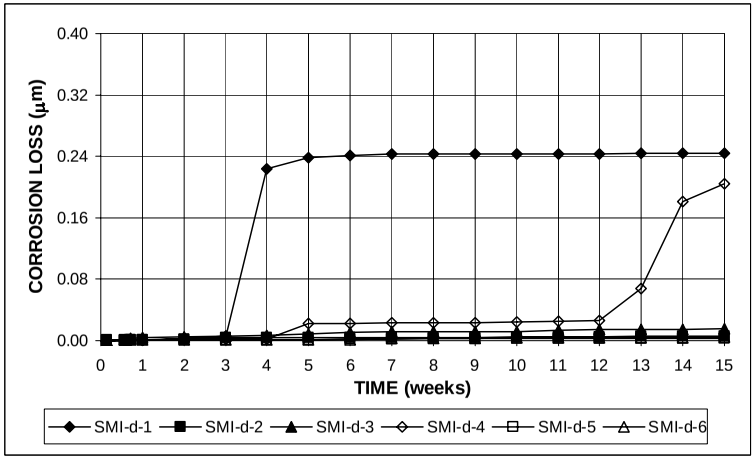

(b)

Figure A.12 - (a) Corrosion rates and (b) total corrosion Losses based on total bar area as measured in the rapid macrocell test for bare stainless steel clad bars with drilled holes in 1.6 m ion NaCl and simulated concrete pore solution

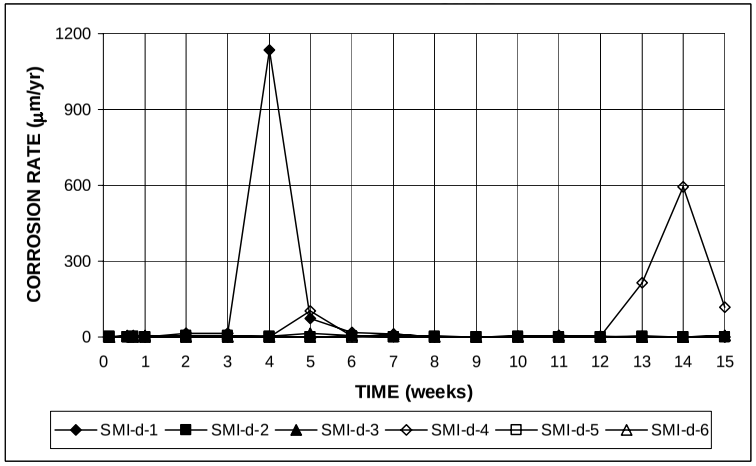

(a)

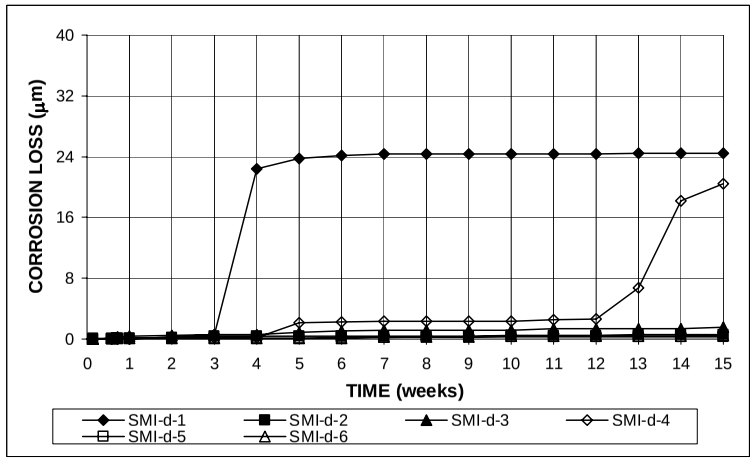

(b)

Figure A.13 - (a) Corrosion rates and (b) total corrosion Losses based on exposed area as measured in the rapid macrocell test for bare stainless steel clad bars with drilled holes in 1.6 m ion NaCl and simulated concrete pore solution

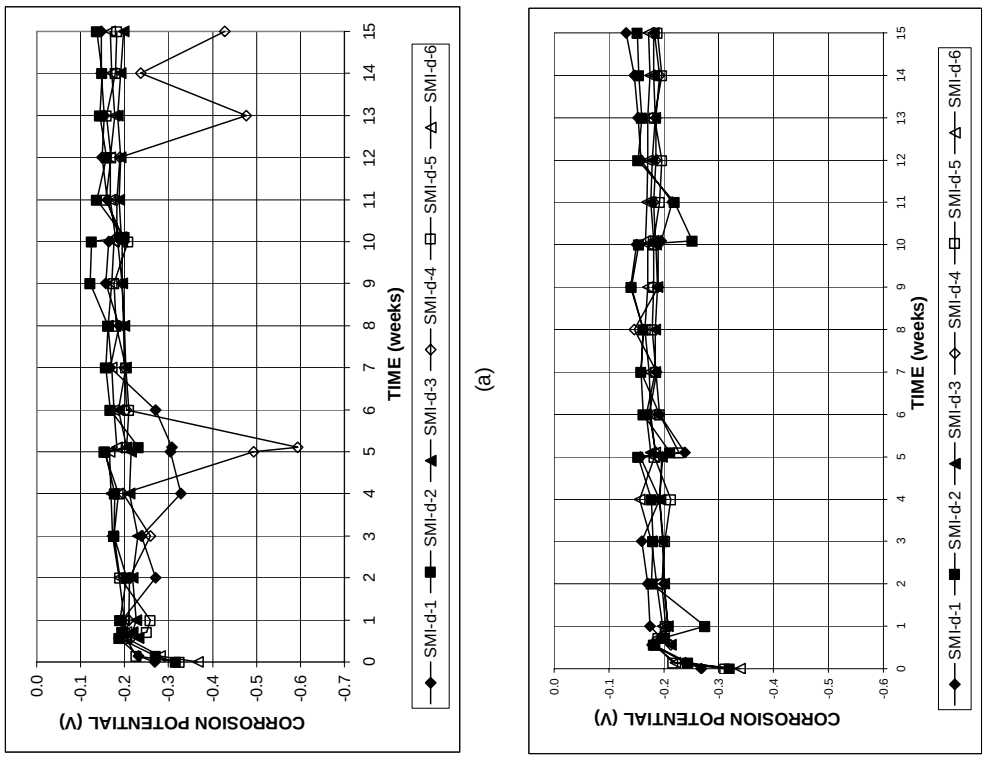

Figure A.14 - (a) Anode corrosion potentials and (b) cathode corrosion potentials with respect to saturated calomel electrode as measured in the rapid macrocell test for bare stainless steel clad bars with drilled holes in 1.6 m ion NaCl and simulated concrete pore solution.

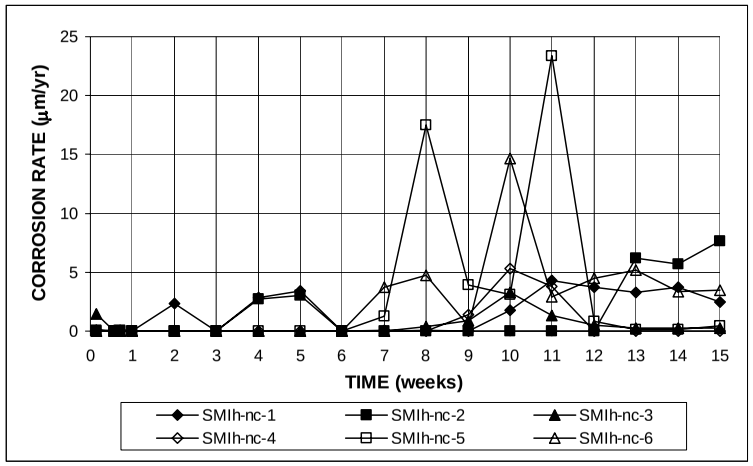

(a)

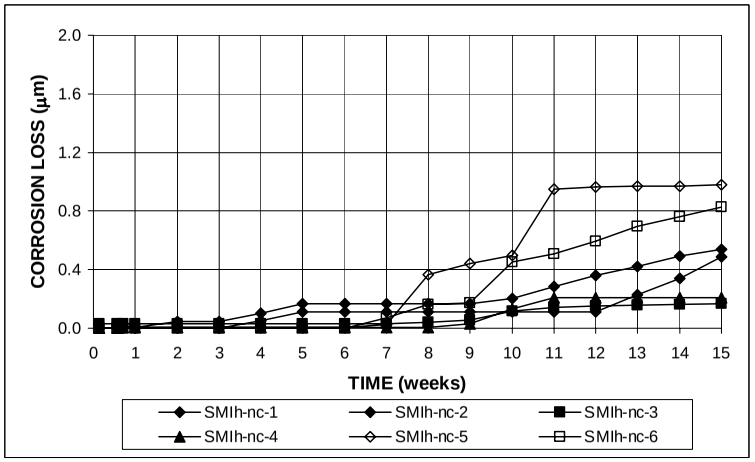

(b)

Figure A.15 - (a) Corrosion rates and (b) total corrosion Losses based on total bar area as measured in the rapid macrocell test for bare stainless steel clad bars without end protection in 6.04 m ion NaCl and simulated concrete pore solution

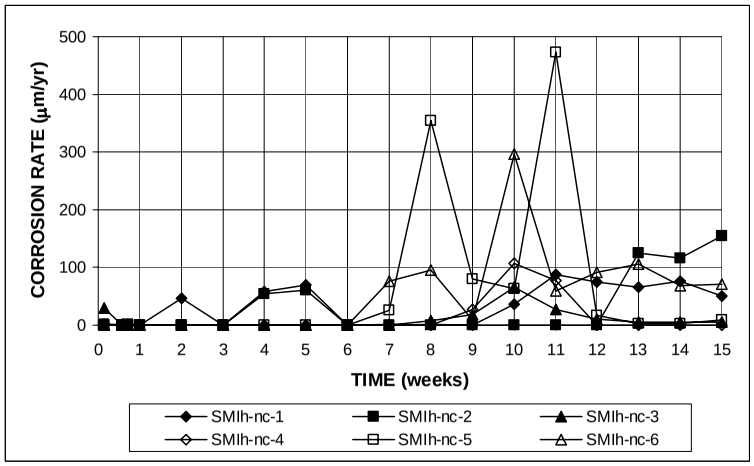

(a)

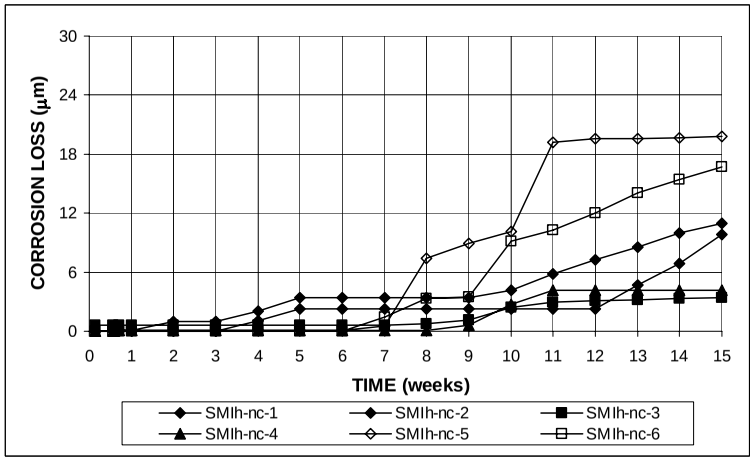

(b)

Figure A.16 - (a) Corrosion rates and (b) total corrosion Losses based on exposed area as measured in the rapid macrocell test for bare stainless steel clad bars without end protection in 6.04 m ion NaCl and simulated concrete pore solution

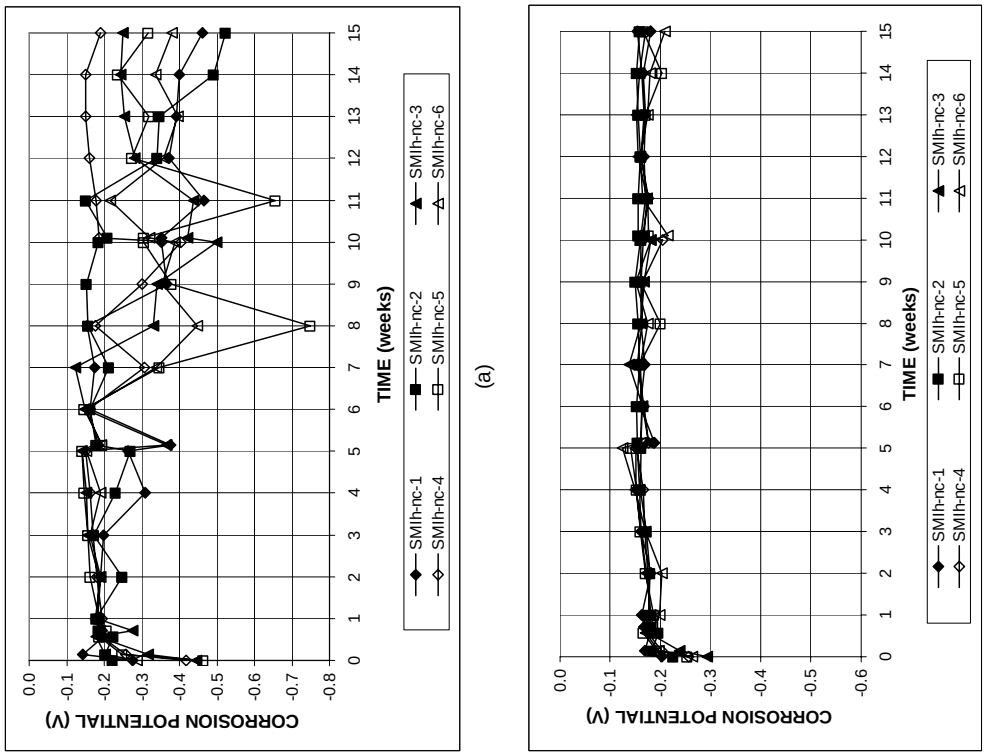

Figure A.17 - (a) Anode corrosion potentials and (b) cathode corrosion potentials with respect to saturated calomel electrode as measured in the rapid macrocell test for bare stainless steel clad bars without end protection in 6.04 m ion NaCl and simulated concrete pore solution.

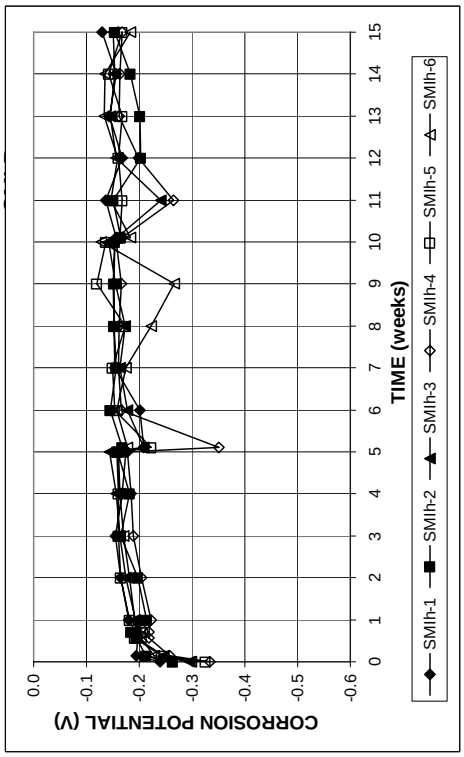

Figure A.19 - (a) Anode corrosion potentials and (b) cathode corrosion potentials with respect to saturated calomel electrode as measured in the rapid macrocell test for bare stainless steel clad bars in 6.04 m ion NaCl and simulated concrete pore solution.

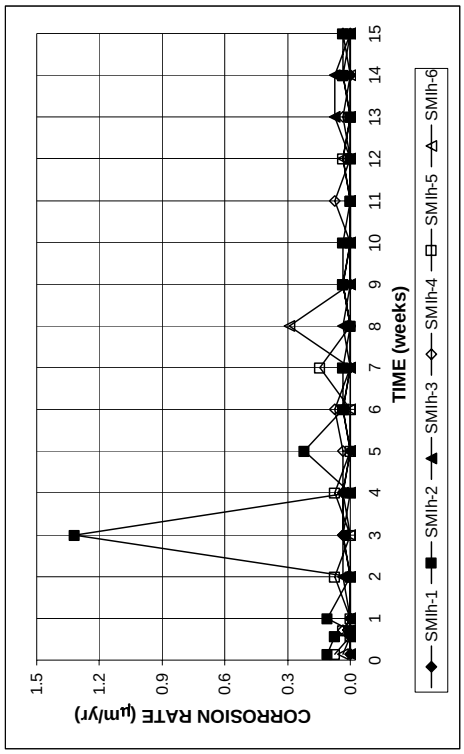

Figure A.18 - (a) Corrosion rates and (b) total corrosion Losses as measured in the rapid macrocell test for bare stainless steel clad bars in 6.04 m ion NaCl and simulated concrete pore solution

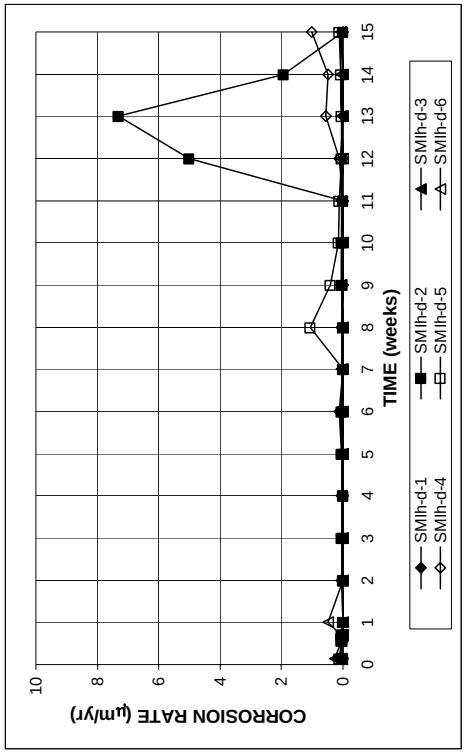

Figure A.20 - (a) Corrosion rates and (b) total corrosion Losses based on total bar area as measured in the rapid macrocell test for bare stainless steel clad bars with drilled holes in 6.04 m ion NaCl and simulated concrete pore solution

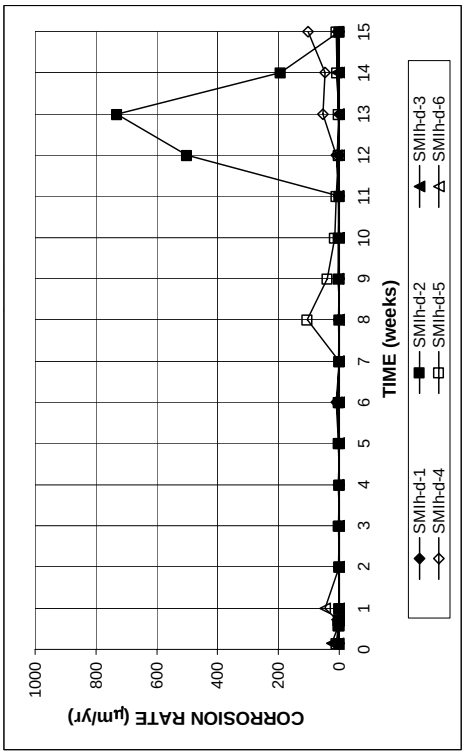

Figure A.21 - (a) Corrosion rates and (b) total corrosion Losses based on exposed area as measured in the rapid macrocell test for bare stainless steel clad bars with drilled holes in 6.04 m ion NaCl and simulated concrete pore solution

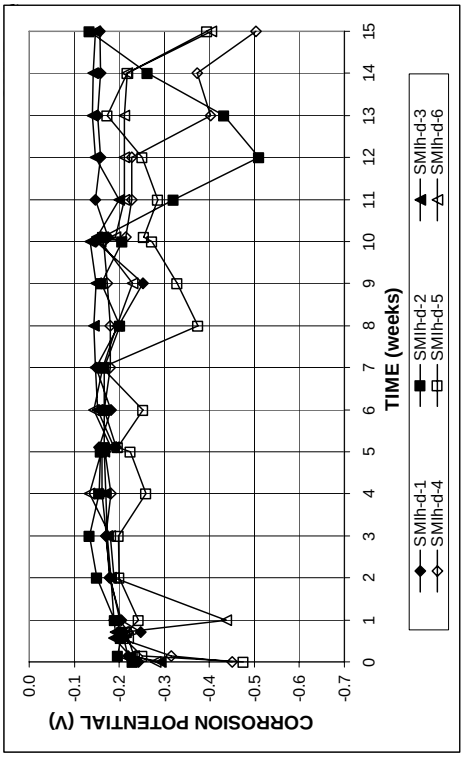

Figure A.22 - (a) Anode corrosion potentials and (b) cathode corrosion potentials with respect to saturated calomel electrode as measured in the rapid macrocell test for bare stainless steel clad bars with drilled holes in 6.04 m ion NaCl and simulated concrete pore solution.

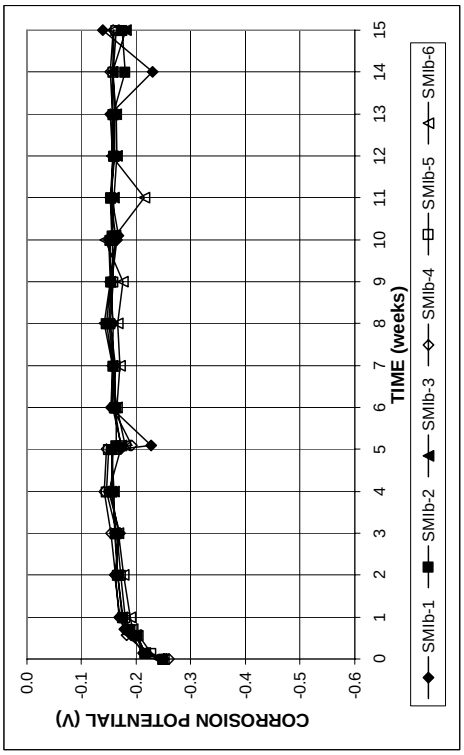

Figure A.24 - (a) Anode corrosion potentials and (b) cathode corrosion potentials with respect to saturated calomel electrode as measured in the rapid macrocell test for bare bent stainless steel clad bars in 1.6 m ion NaCl and simulated concrete pore solution.

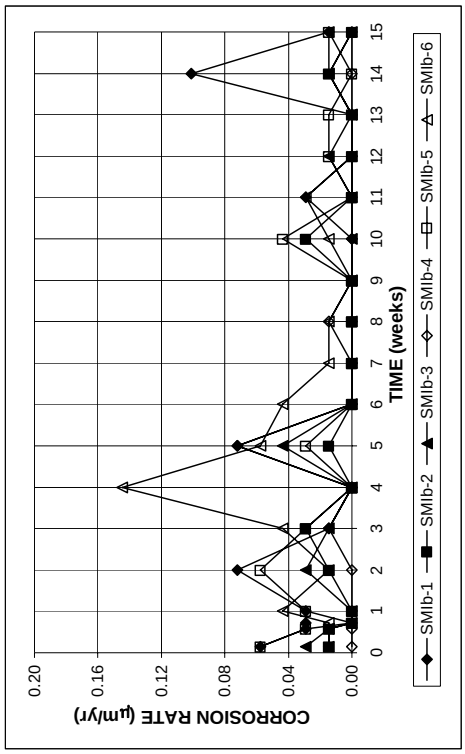

Figure A.23 - (a) Corrosion rates and (b) total corrosion Losses as measured in the rapid macrocell test for bare bent stainless steel clad bars in 1.6 m ion NaCl and simulated concrete pore solution

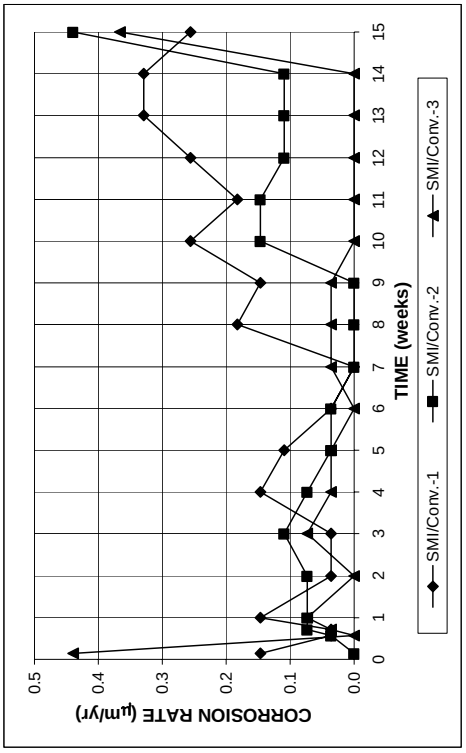

Figure A.25 - (a) Corrosion rates and (b) total corrosion Losses as measured in the rapid macrocell test for stainless steel clad bars as anode and conventional steel as cathode in 1.6 m ion NaCl and simulated concrete pore solution

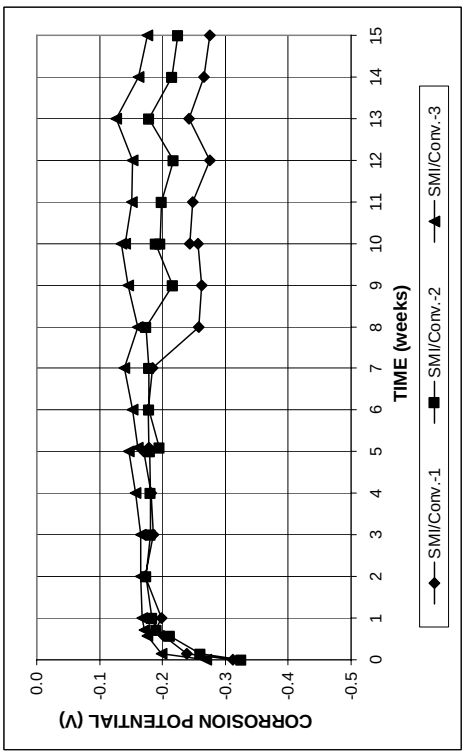

Figure A.26 - (a) Anode corrosion potentials and (b) cathode corrosion potentials with respect to saturated calomel electrode as measured in the rapid macrocell test for stainless steel clad bars as anode and conventional steel as cathode in 1.6 m ion NaCl andsimulated concrete pore solution

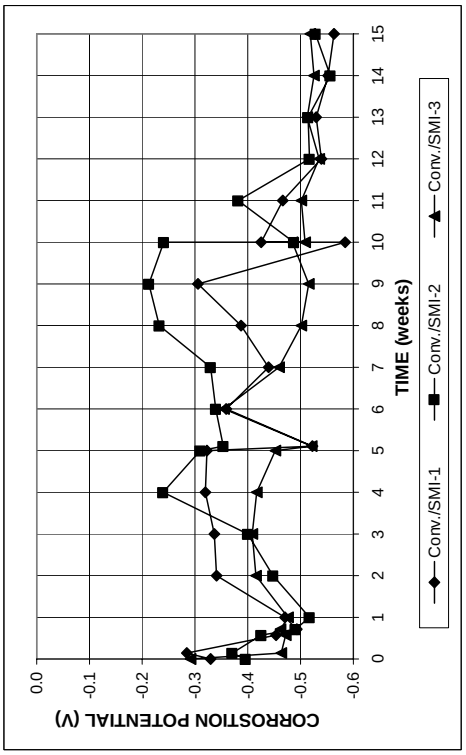

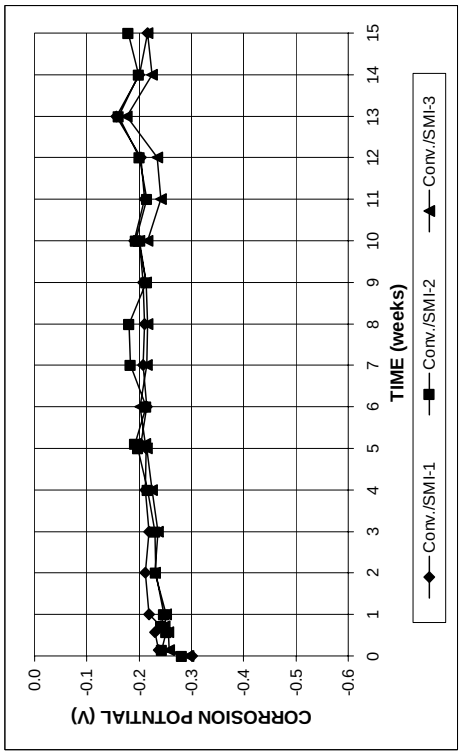

Figure A.28 - (a) Anode corrosion potentials and (b) cathode corrosion potentials with respect to saturated calomel electrode as measured in the rapid macrocell test for conventional steel as anode and stainless steel clad bars as cathode in 1.6 m ion NaCl and simulated concrete pore solution

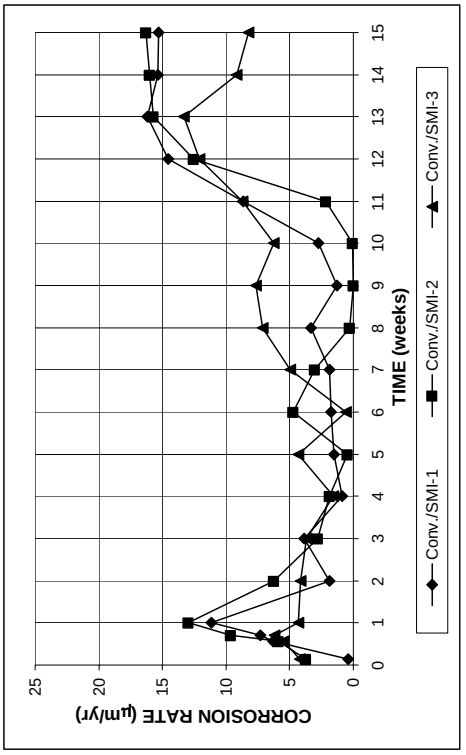

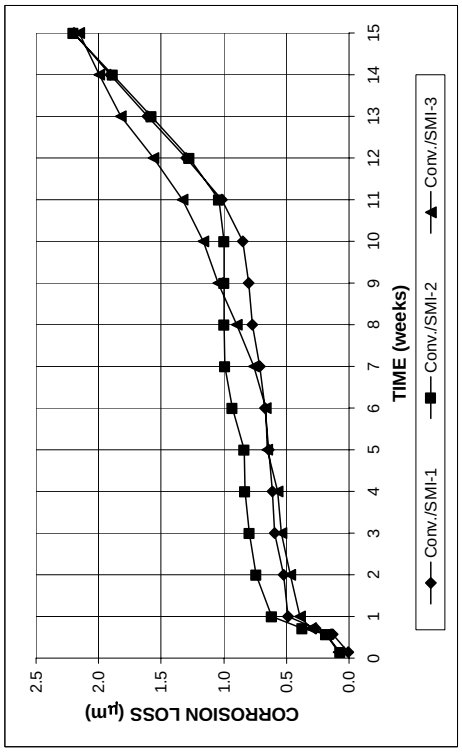

Figure A.27 - (a) Corrosion rates and (b) total corrosion Losses as measured in the rapid macrocell test for conventional steel as anode and stainless steel clad bars as cathode in 1.6 m ion NaCl and simulated concrete pore solution

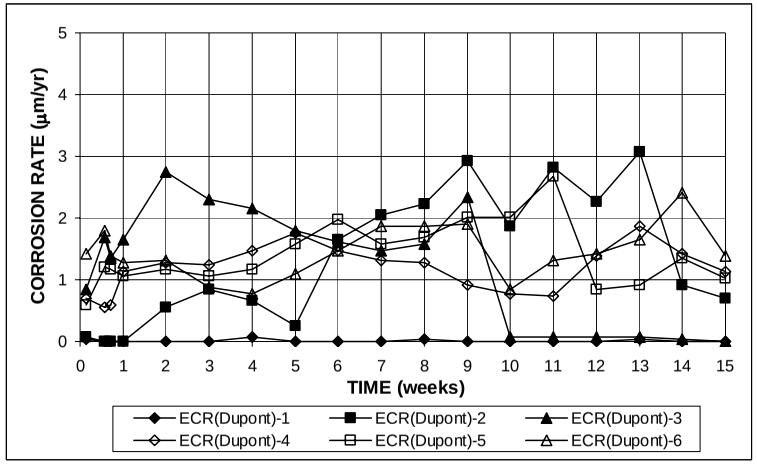

(a)

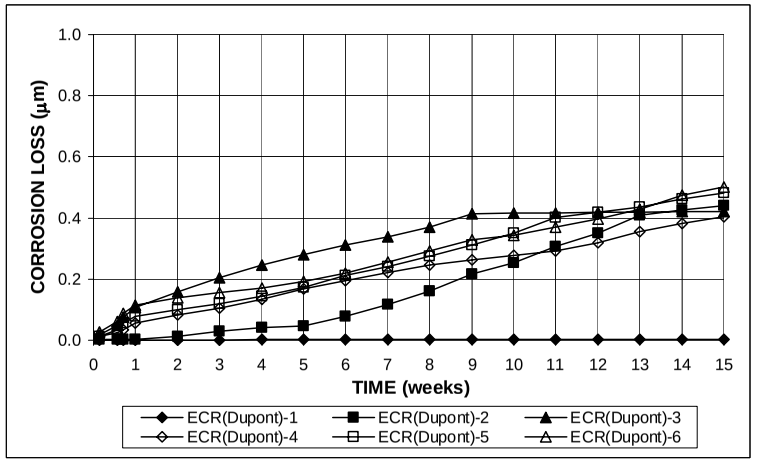

(b)

Figure A.29 - (a) Corrosion rates and (b) total corrosion Losses based on total bar area as measured in the rapid macrocell test for bare ECR(Dupont) bars in 1.6 m ion NaCl and simulated concrete pore solution

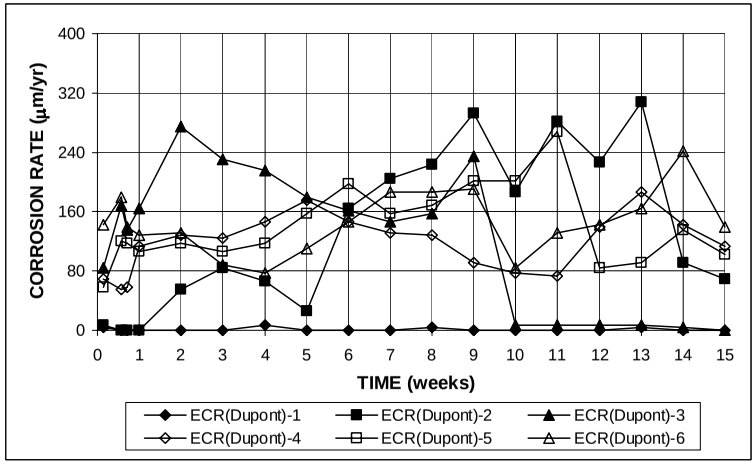

(a)

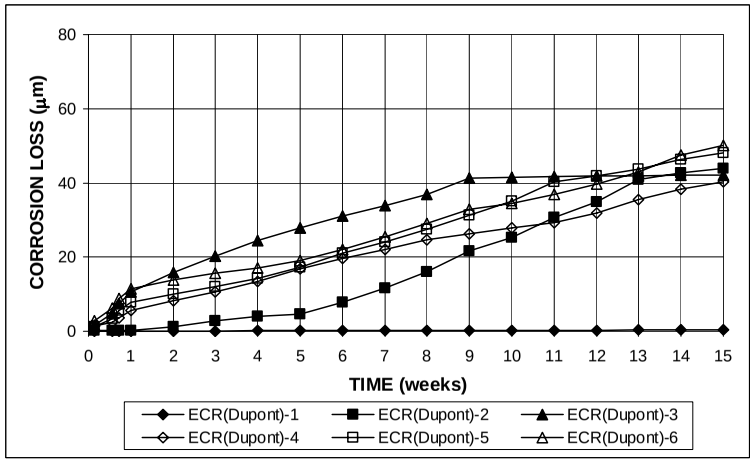

(b)

Figure A.30 - (a) Corrosion rates and (b) total corrosion Losses based on exposed area as measured in the rapid macrocell test for bare ECR(Dupont) bars in 1.6 m ion NaCl and simulated concrete pore solution

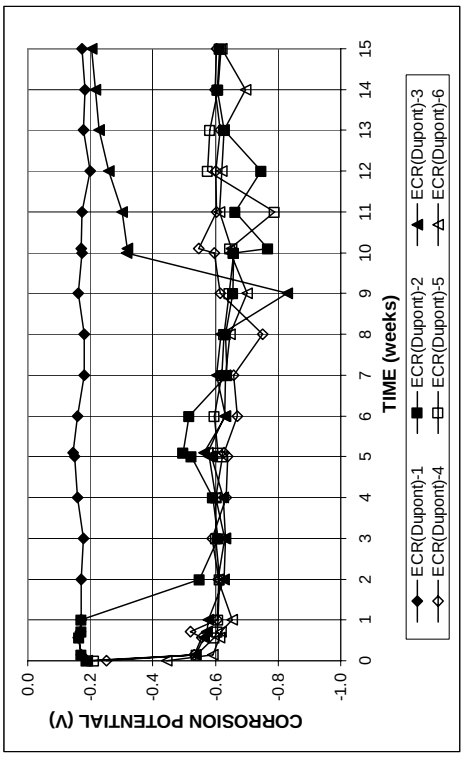

Figure A.31 - (a) Anode corrosion potentials and (b) cathode corrosion potentials with respect to saturated calomel electrode as measured in the rapid macrocell test for bare ECR(Dupont) bars in 1.6 m ion NaCl and simulated concrete pore solution.

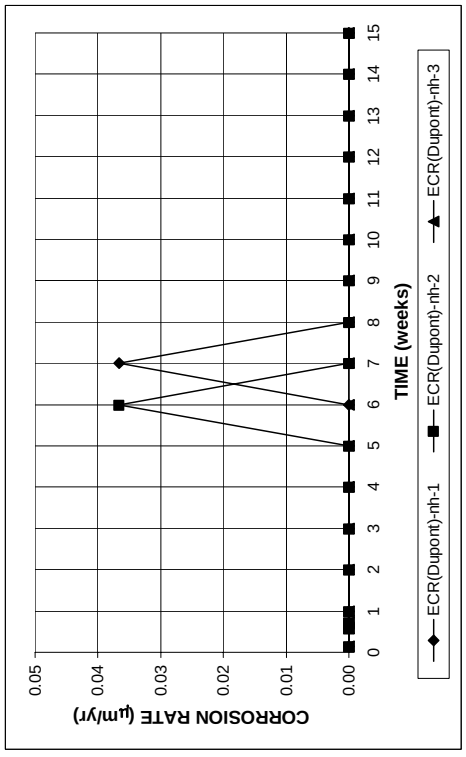

Figure A.32 - (a) Corrosion rates and (b) total corrosion Losses as measured in the rapid macrocell test for bare ECR(Dupont) bars without drilled holes in 1.6 m ion NaCl and simulated concrete pore solution

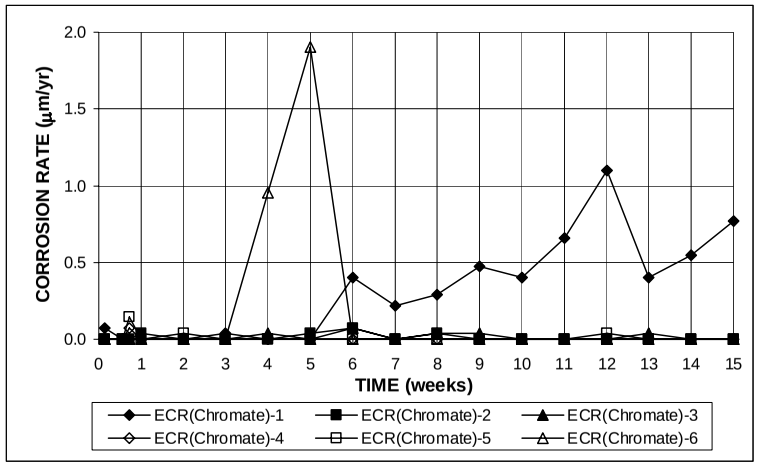

(a)

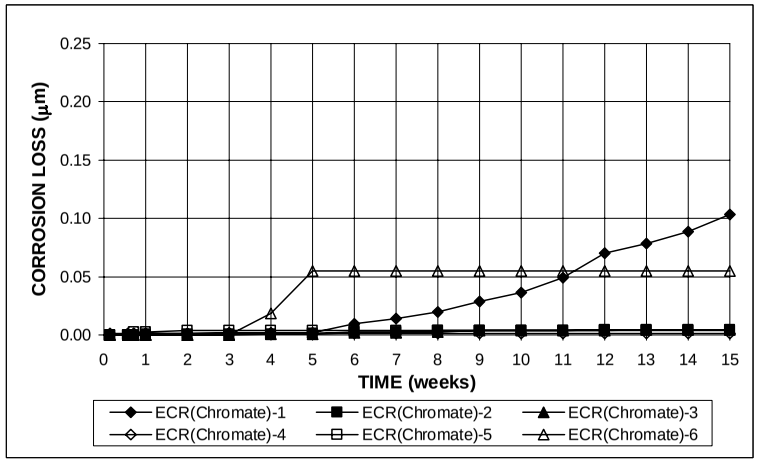

(b)

Figure A.33 - (a) Corrosion rates and (b) total corrosion Losses based on total bar area as measured in the rapid macrocell test for bare ECR(Chromate) bars in 1.6 m ion NaCl and simulated concrete pore solution

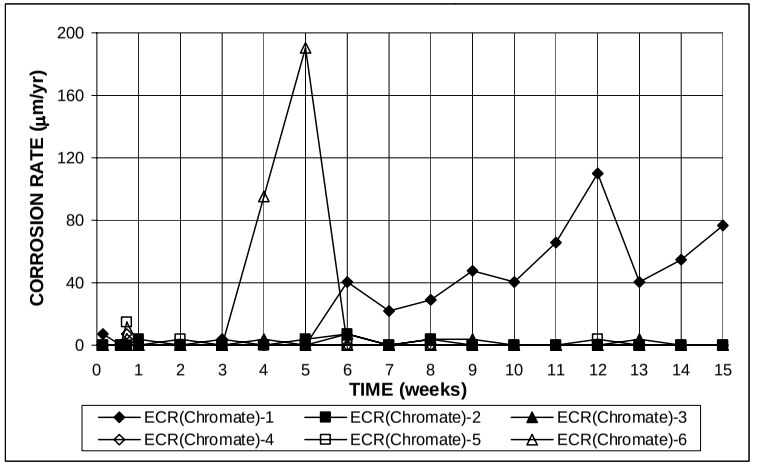

(a)

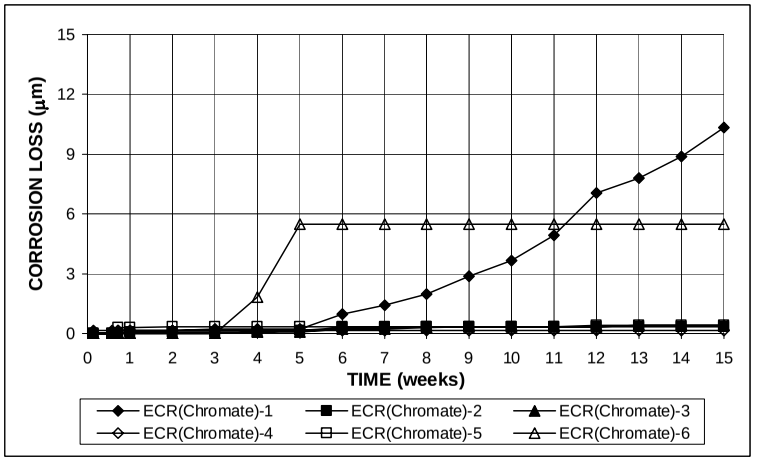

(b)

Figure A.34 - (a) Corrosion rates and (b) total corrosion Losses based on exposed area as measured in the rapid macrocell test for bare ECR(Chromate) bars in 1.6 m ion NaCl and simulated concrete pore solution

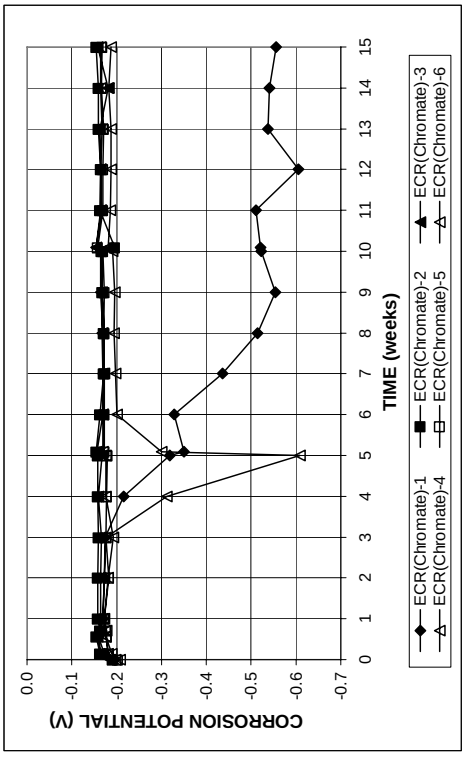

Figure A.35 - (a) Anode corrosion potentials and (b) cathode corrosion potentials with respect to saturated calomel electrode as measured in the rapid macrocell test for bare ECR(Chromate) bars in 1.6 m ion NaCl and simulated concrete pore solution.

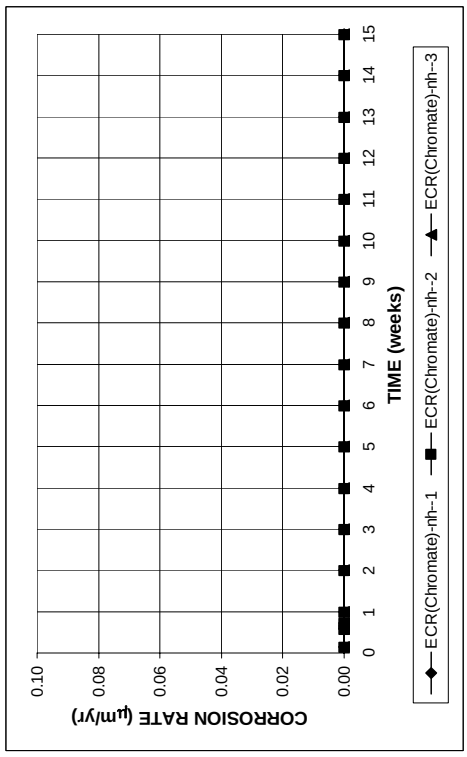

Figure A.36 - (a) Corrosion rates and (b) total corrosion Losses as measured in the rapid macrocell test for bare ECR(Dupont) bars without drilled holes in 1.6 m ion NaCl and simulated concrete pore solution

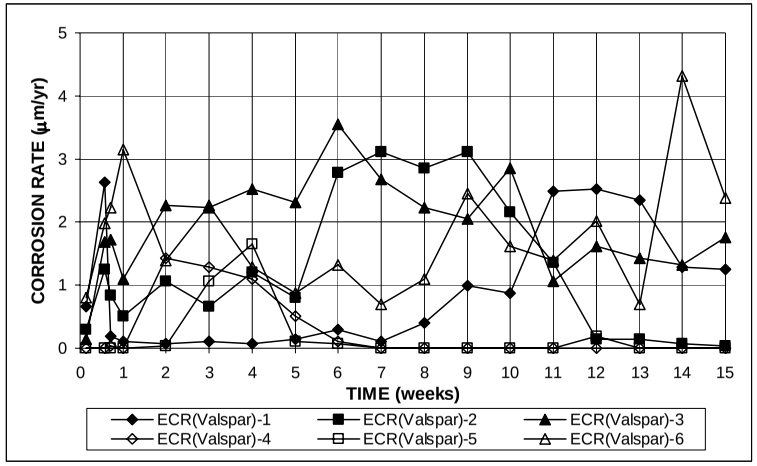

(a)

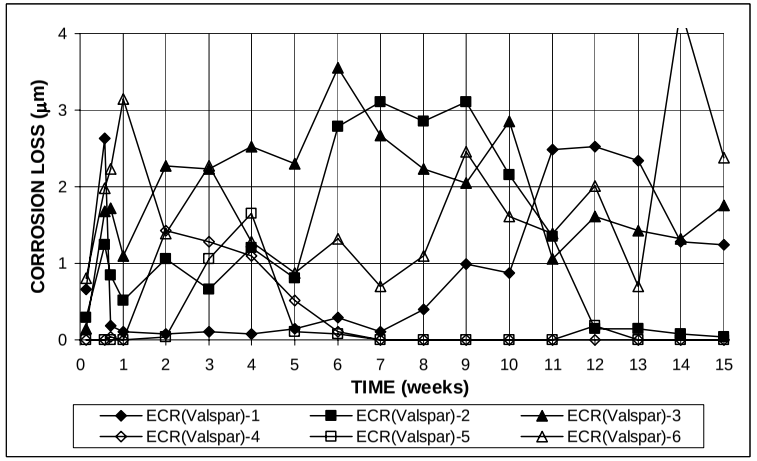

(b)

Figure A.37 - (a) Corrosion rates and (b) total corrosion Losses based on total bar area as measured in the rapid macrocell test for bare ECR(Valspar) bars in 1.6 m ion NaCl and simulated concrete pore solution

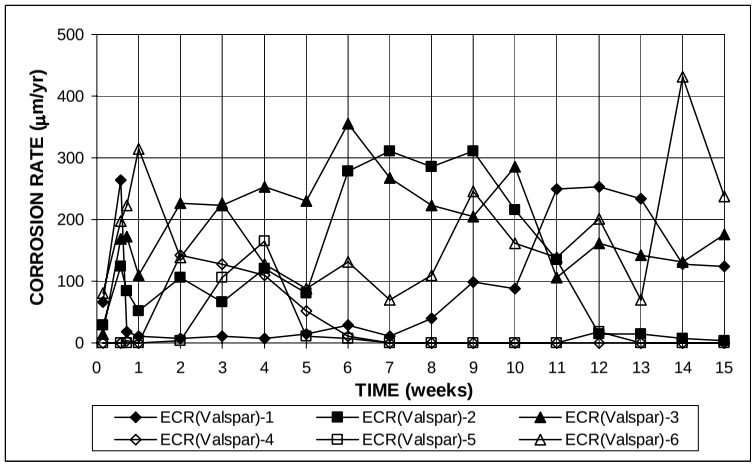

(a)

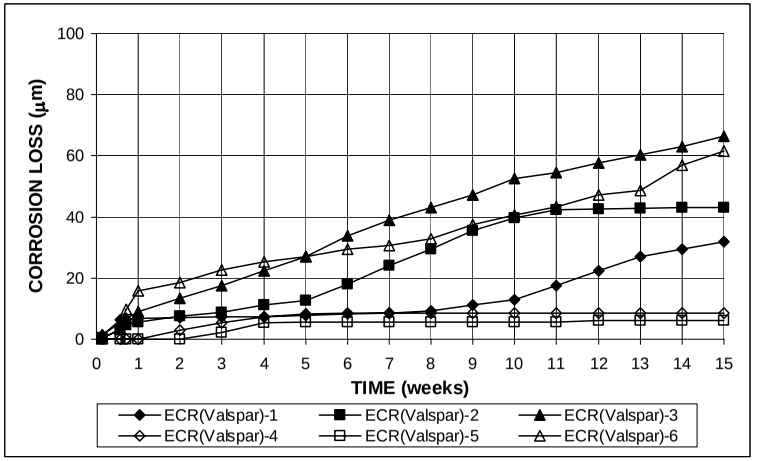

(b)

Figure A.38 - (a) Corrosion rates and (b) total corrosion Losses based on exposed area as measured in the rapid macrocell test for bare ECR(Valspar) bars in 1.6 m ion NaCl and simulated concrete pore solution

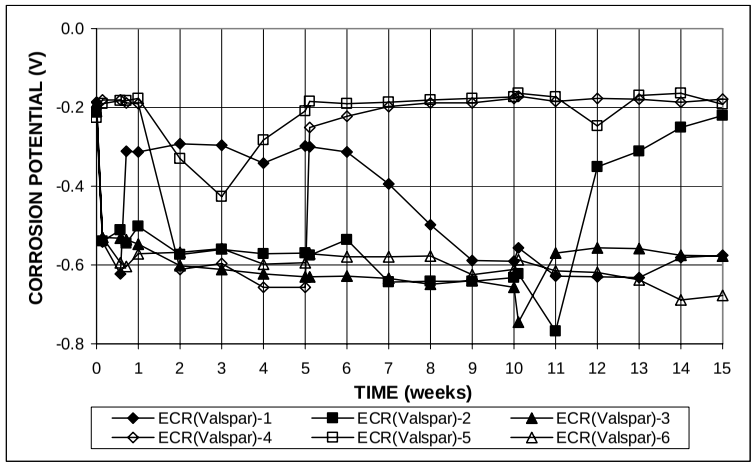

(a)

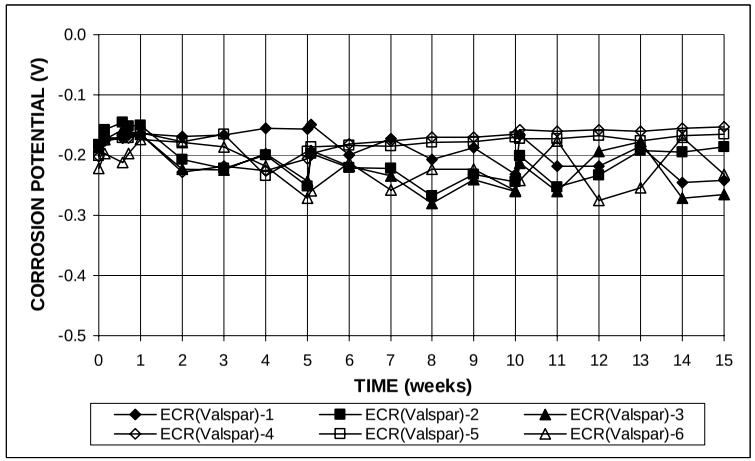

(b)

Figure A.39 - (a) Anode corrosion potentials and (b) cathode corrosion potentials with respect to saturated calomel electrode as measured in the rapid macrocell test for bare ECR(Valspar) bars in 1.6 m ion NaCl and simulated concrete pore solution.

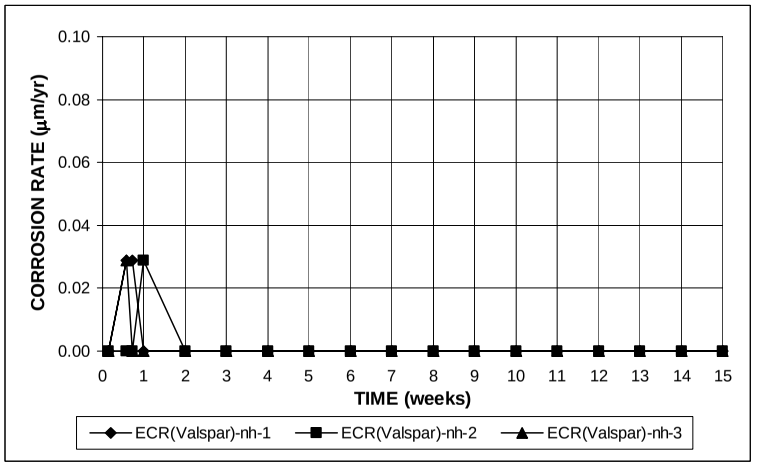

(a)

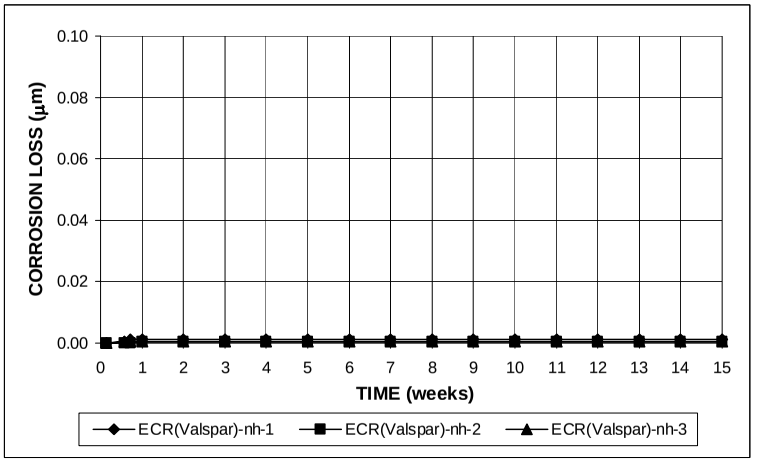

(b)

Figure A.40 - (a) Corrosion rates and (b) total corrosion Losses as measured in the rapid macrocell test for bare ECR(Valspar) bars without drilled holes in 1.6 m ion NaCl and simulated concrete pore solution

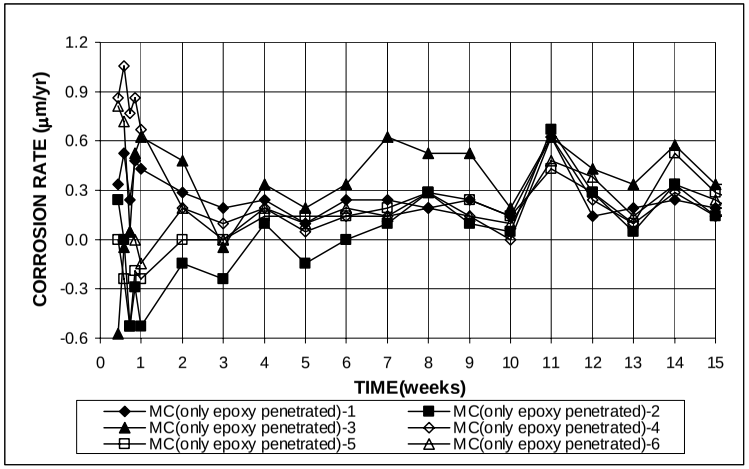

(a)

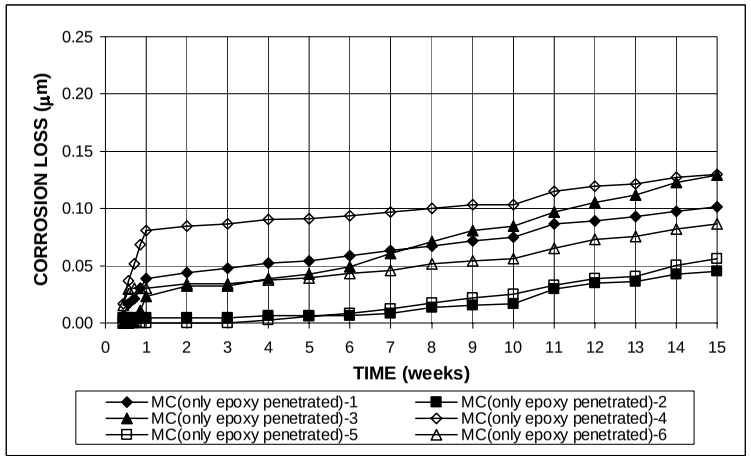

(b)

Figure A.41 - (a) Corrosion rates and (b) total corrosion Losses based on total bar area as measured in the rapid macrocell test for bare multiple coated bars with only epoxy penetrated in 1.6 m ion NaCl and simulated concrete pore solution

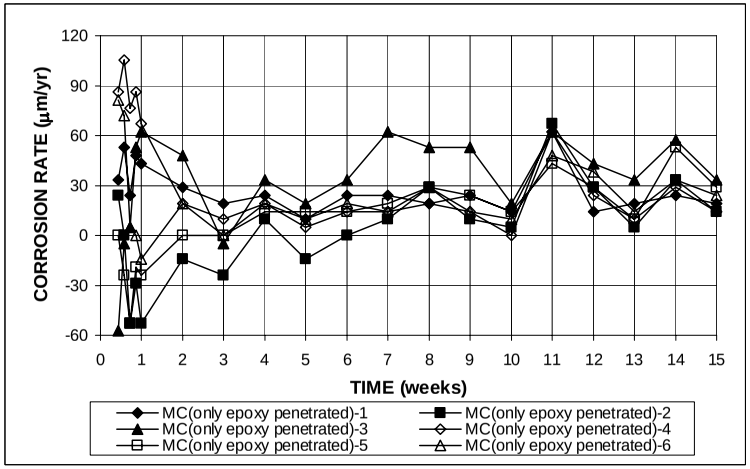

(a)

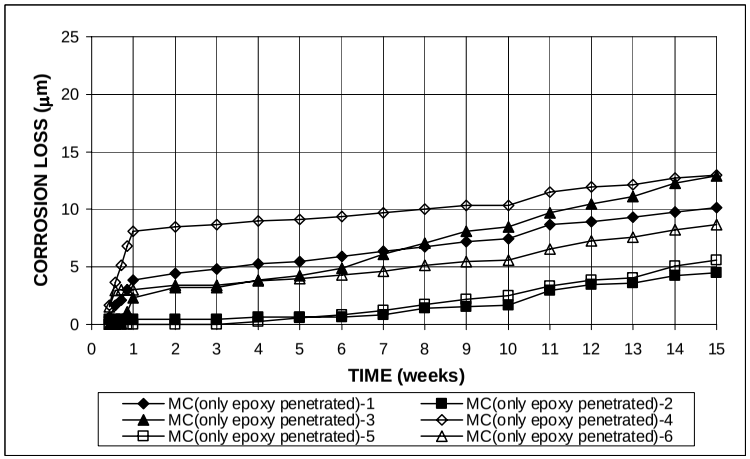

(b)

Figure A.42 - (a) Corrosion rates and (b) total corrosion Losses based on exposed area as measured in the rapid macrocell test for bare multiple coated bars with only epoxy penetrated in 1.6 m ion NaCl and simulated concrete pore solution

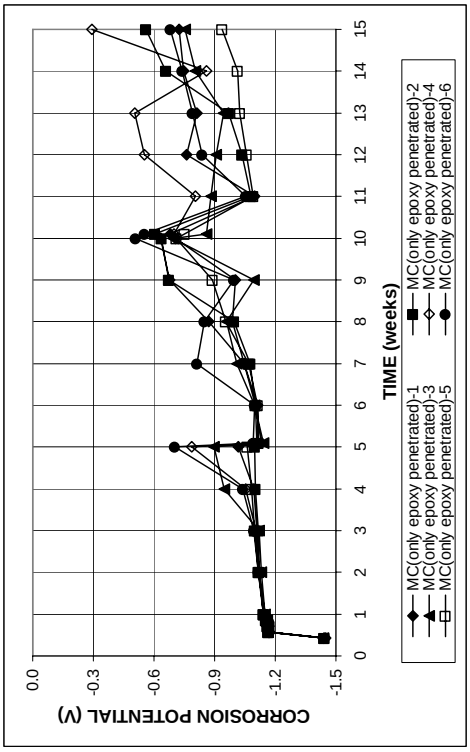

(a)

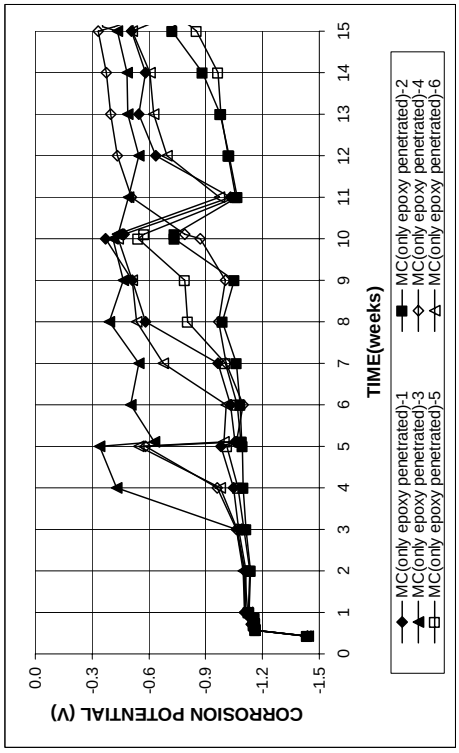

(b)

Figure A.43 - (a) Anode corrosion potentials and (b) cathode corrosion potentials with respect to saturated calomel electrode as measured in the rapid macrocell test for bare multiple coated bars with only epoxy penetrated in 1.6 m ion NaCl and simulated concrete pore solution.

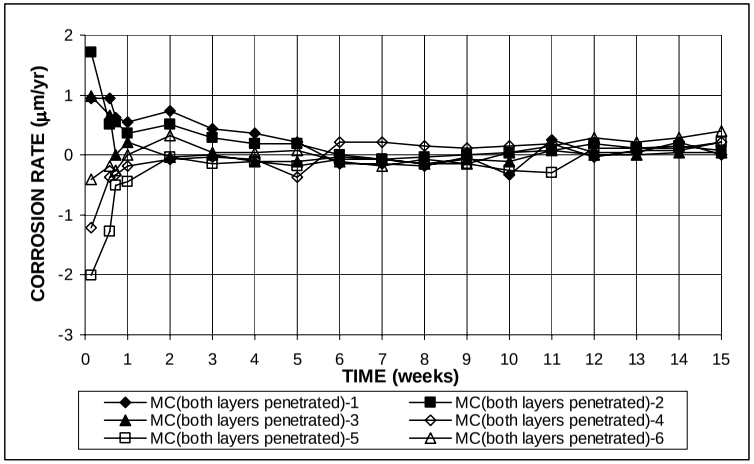

(a)

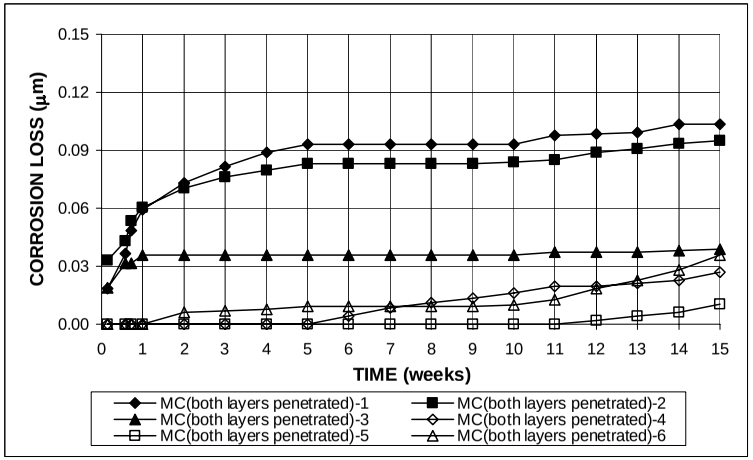

(b)

Figure A.44 - (a) Corrosion rates and (b) total corrosion Losses based on total bar area as measured in the rapid macrocell test for bare multiple coated bars with both layers penetrated in 1.6 m ion NaCl and simulated concrete pore solution

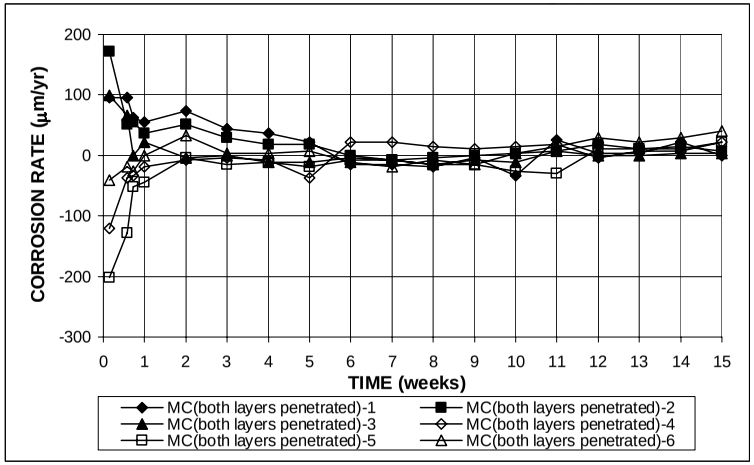

(a)

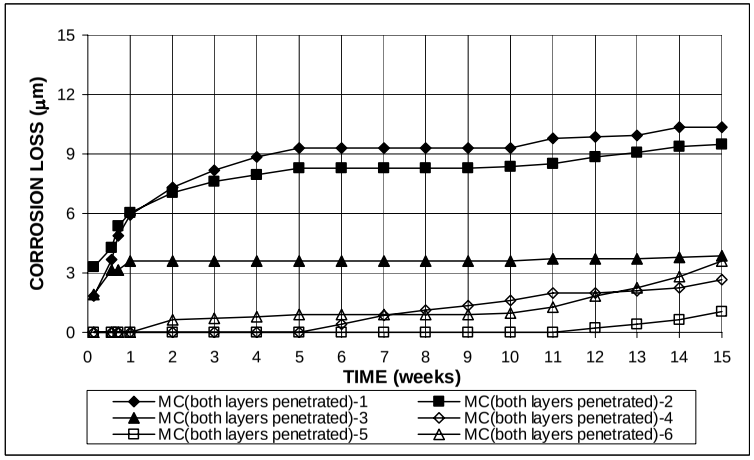

(b)

Figure A.45 - (a) Corrosion rates and (b) total corrosion Losses based on exposed area as measured in the rapid macrocell test for bare multiple coated bars with both layers penetrated in 1.6 m ion NaCl and simulated concrete pore solution

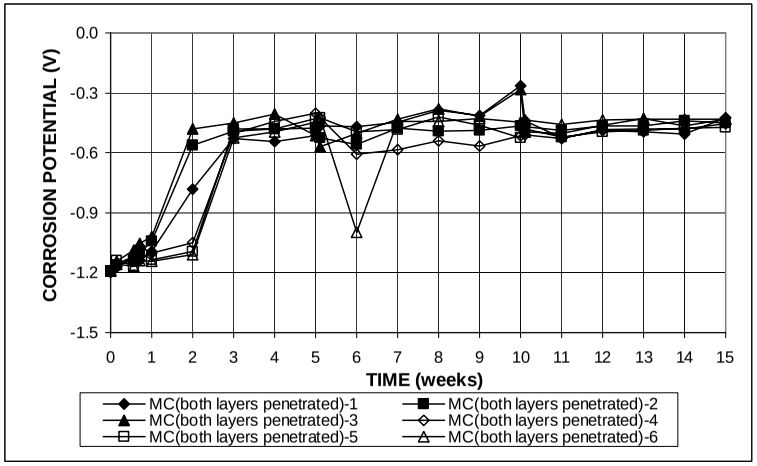

(a)

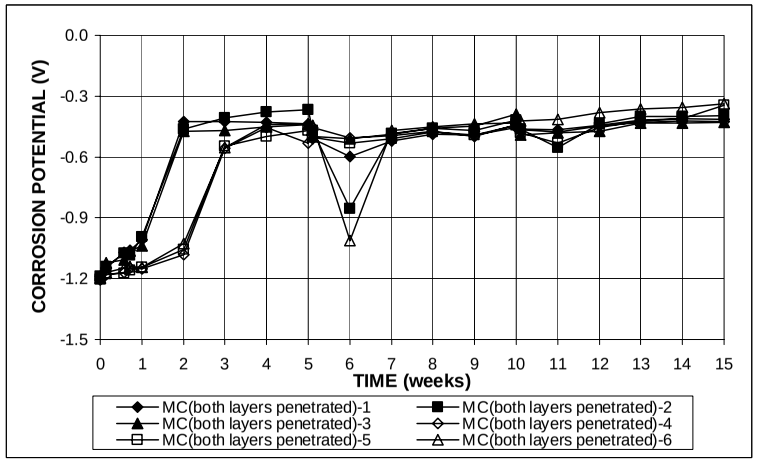

(b)

Figure A.46 - (a) Anode corrosion potentials and (b) cathode corrosion potentials with respect to saturated calomel electrode as measured in the rapid macrocell test for bare multiple coated bars with both layers penetrated in 1.6 m ion NaCl and simulated concrete pore solution.

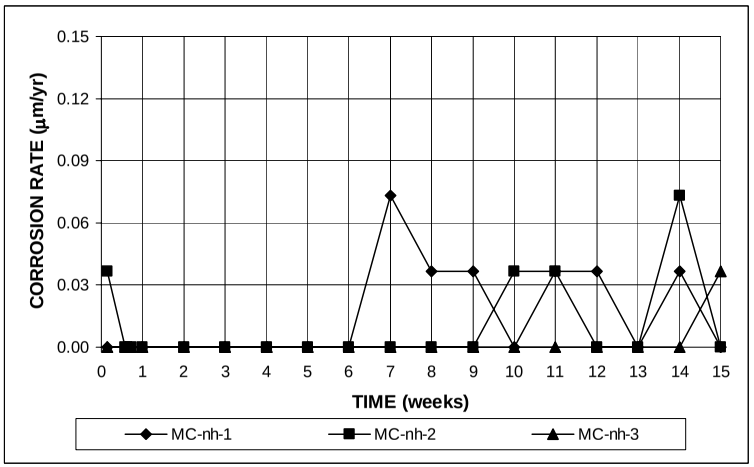

(a)

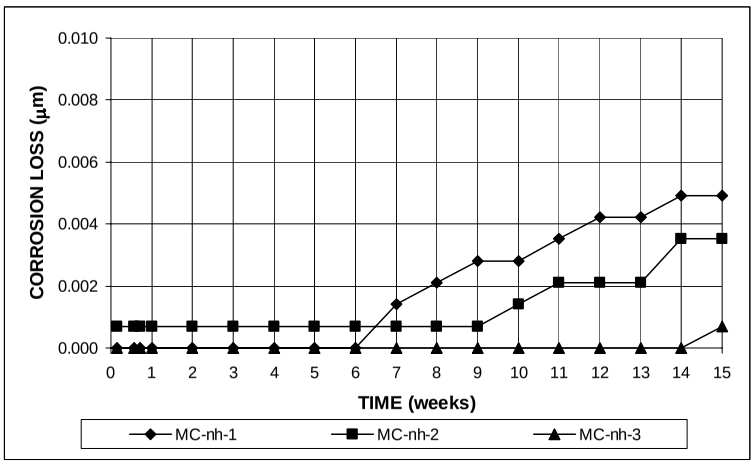

(b)

Figure A.47 - (a) Corrosion rates and (b) total corrosion Losses as measured in the rapid macrocell test for multiple coated without drilled holes in 1.6 m ion NaCl and simulated concrete pore solution

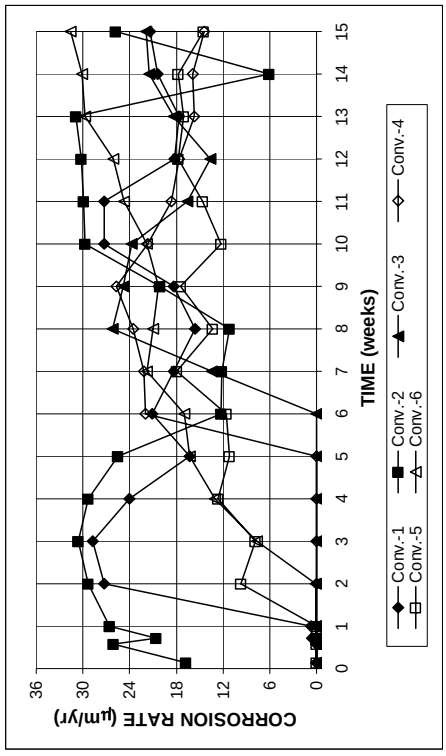

Figure A.48 - (a) Corrosion rates and (b) total corrosion Losses as measured in the rapid macrocell test for mortar-wrapped conventional steel in 1.6 m ion rapid macrocell test for mortar-wrapped conventional steel in 1.6 m ion

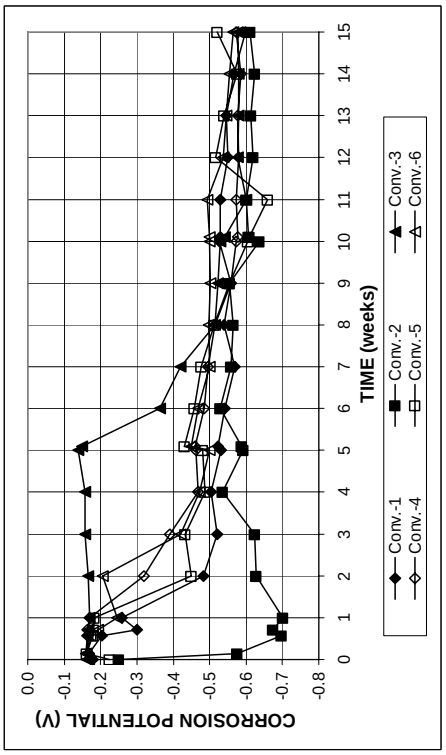

Figure A.49 - (a) Anode corrosion potentials and (b) cathode corrosion potentials with respect to saturated calomel electrode as measured in the rapid macrocell test for mortar-wrapped conventional steel in 1.6 m ion NaCl and simulated concrete pore solution.

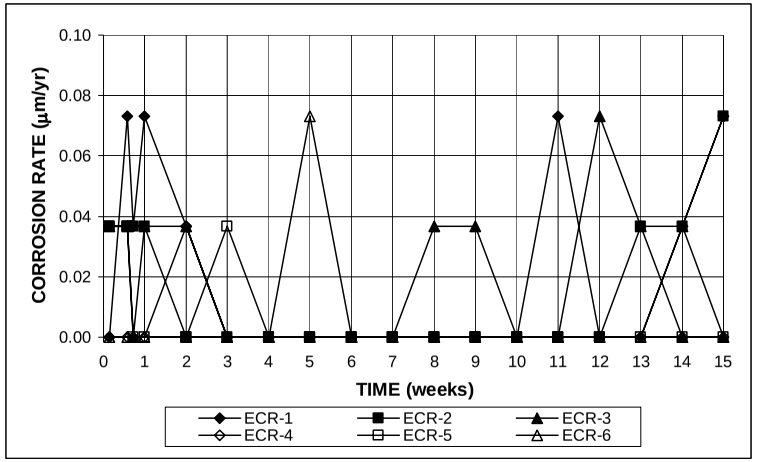

(a)

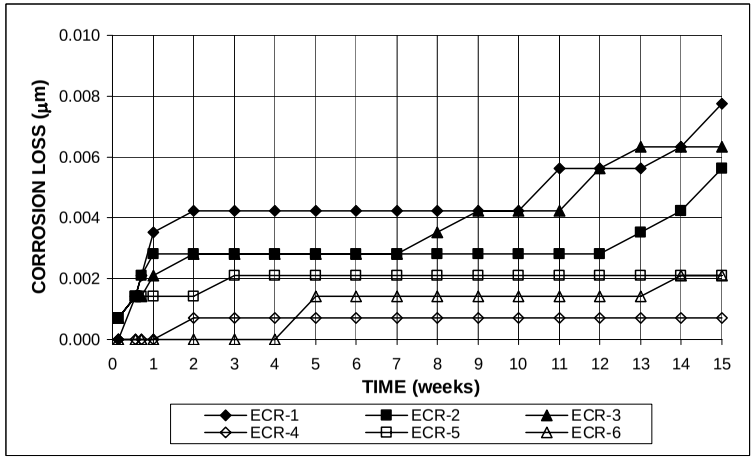

(b)

Figure A.50 - (a) Corrosion rates and (b) total corrosion Losses based on total bar area as measured in the rapid macrocell test for mortar-wrapped epoxy-coated steel in 1.6 m ion NaCl and simulated concrete pore solution

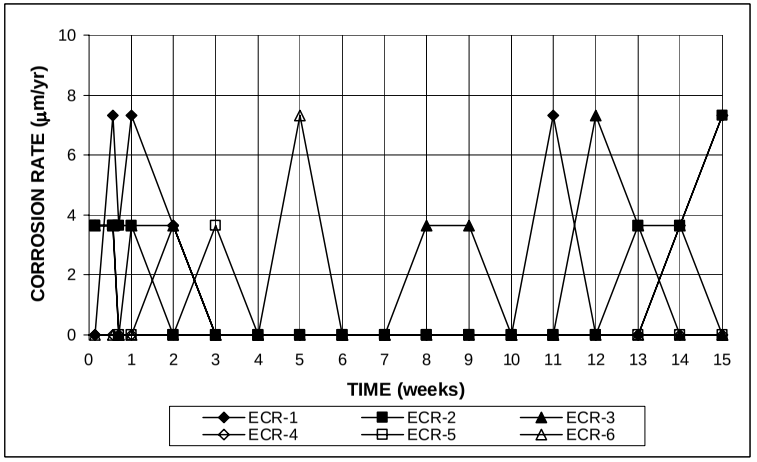

(a)

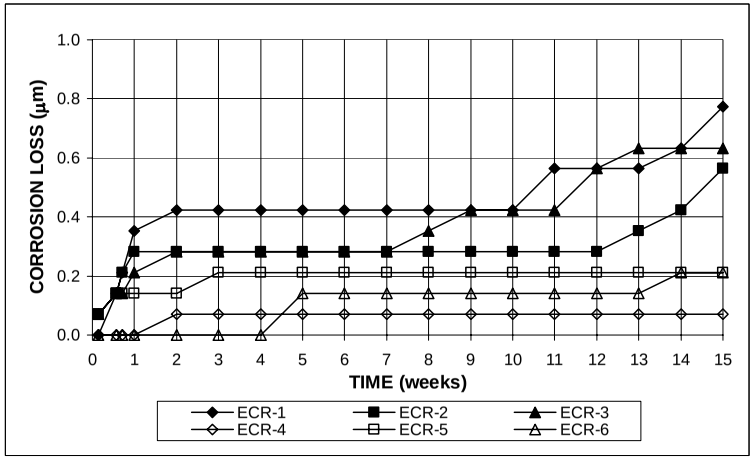

(b)

Figure A.51 - (a) Corrosion rates and (b) total corrosion Losses based on exposed area as measured in the rapid macrocell test for mortar-wrapped epoxy-coated steel in 1.6 m ion NaCl and simulated concrete pore solution

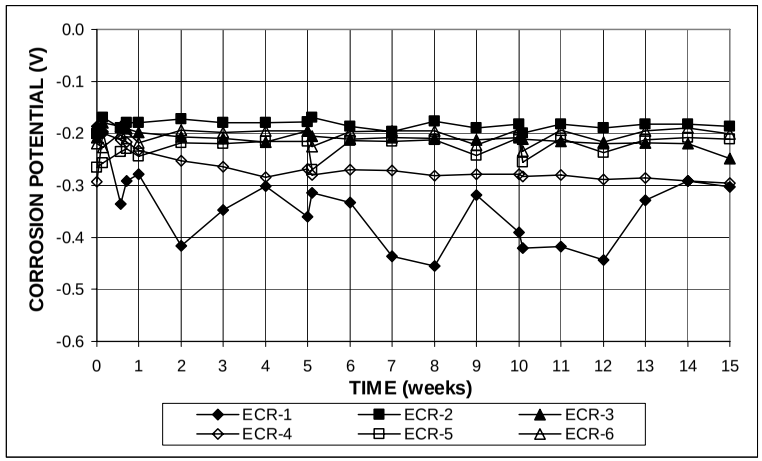

(a)

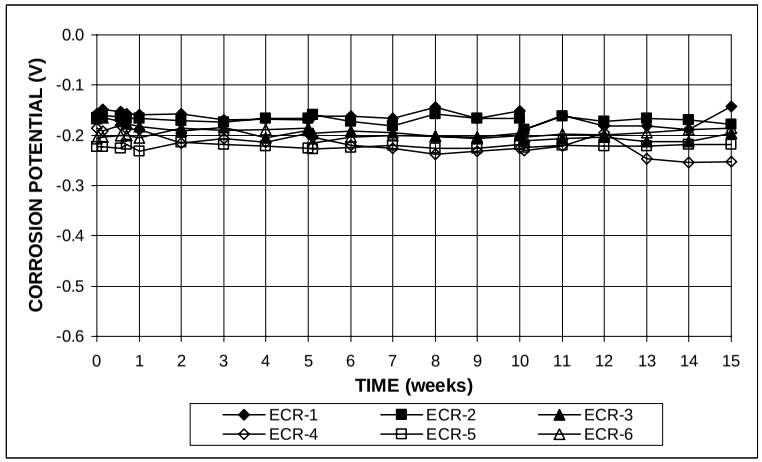

(b)

Figure A.52 - (a) Anode corrosion potentials and (b) cathode corrosion potentials with respect to saturated calomel electrode as measured in the rapid macrocell test for mortar-wrapped epoxy-coated steel in 1.6 m ion NaCl and simulated concrete pore solution.

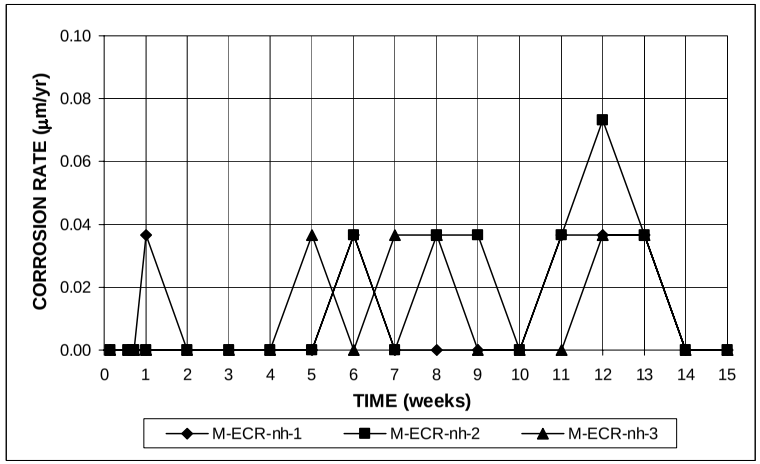

(a)

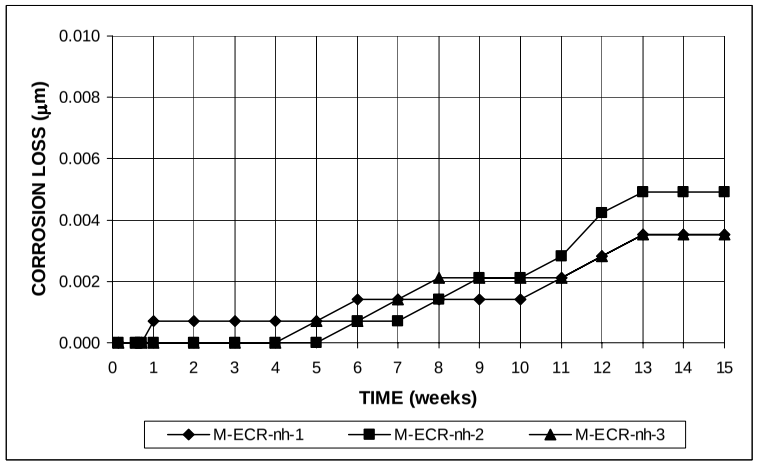

(b)

Figure A.53 - (a) Corrosion rates and (b) total corrosion Losses based on total bar area as measured in the rapid macrocell test for mortar-wrapped epoxy-coated steel without drilled holes in 1.6 m ion NaCl and simulated concrete pore solution

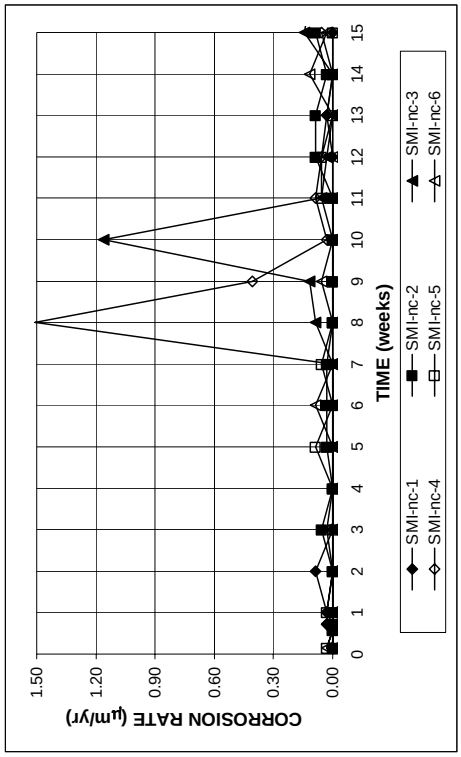

Figure A.54 - (a) Corrosion rates and (b) total corrosion Losses based on total bar area as measured in the rapid macrocell test for mortar-wrapped stainless steel clad bars without end protection in 1.6 m ion NaCl and simulated concrete pore solution

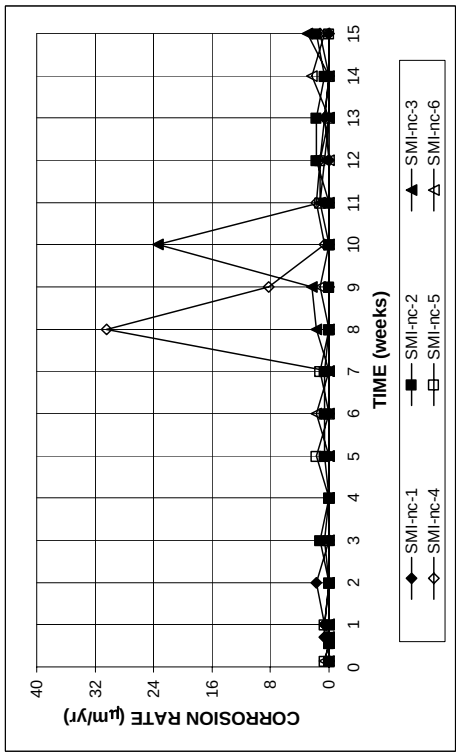

Figure A.55 - (a) Corrosion rates and (b) total corrosion Losses based on exposed area as measured in the rapid macrocell test for mortar-wrapped stainless steel clad bars without end protection in 1.6 m ion NaCl and simulated concrete pore solution

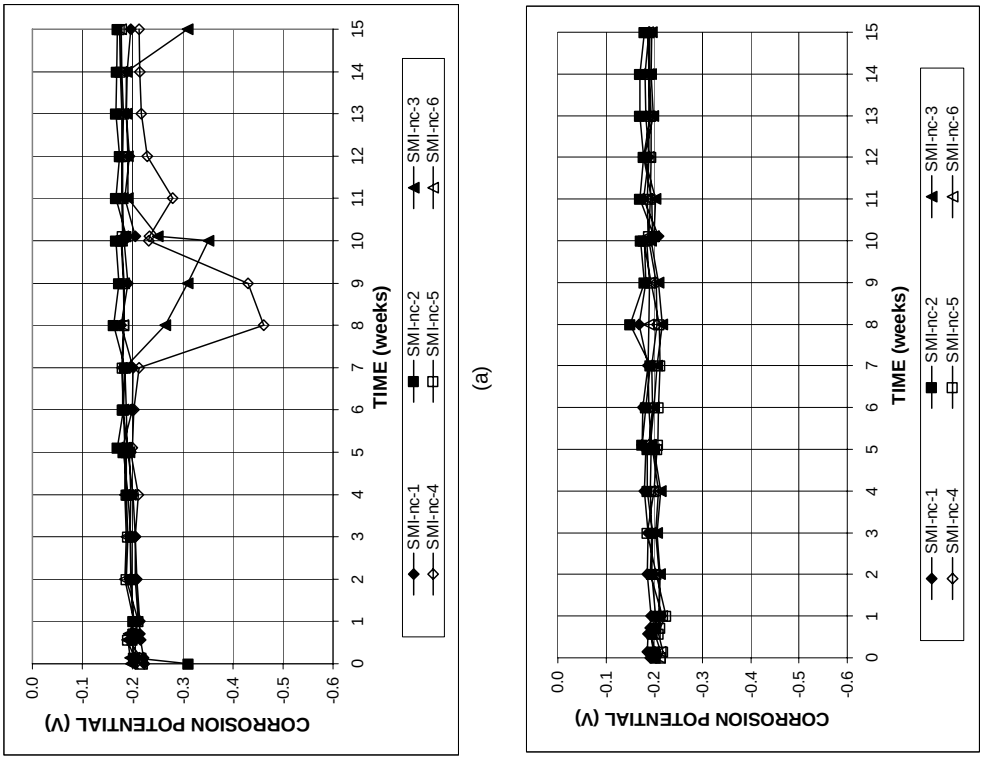

Figure A.56 - (a) Anode corrosion potentials and (b) cathode corrosion potentials with respect to saturated calomel electrode as measured in the rapid macrocell test for mortar-wrapped stainless steel clad bars without end protection in 1.6 m ion NaCl and simulated concrete pore solution.

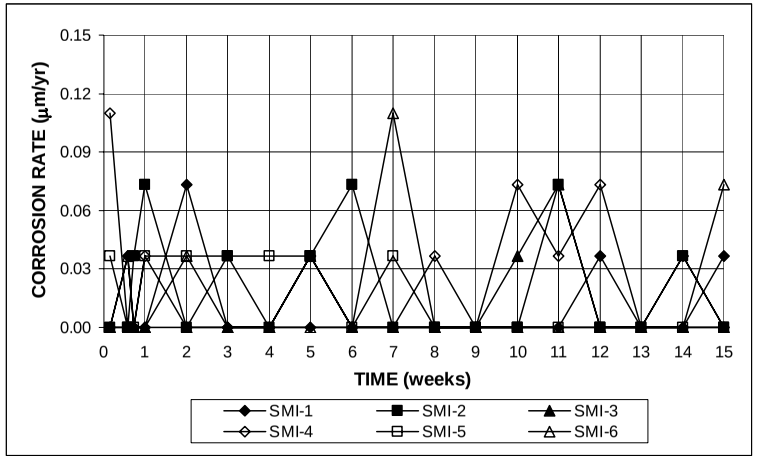

(a)

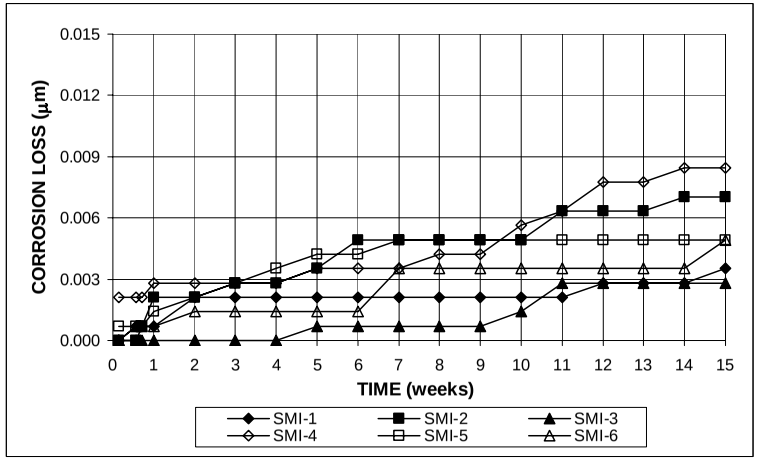

(b)

Figure A.57 - (a) Corrosion rates and (b) total corrosion Losses as measured in the rapid macrocell test for mortar-wrapped stainless steel clad bars in 1.6 m ion NaCl and simulated concrete pore solution

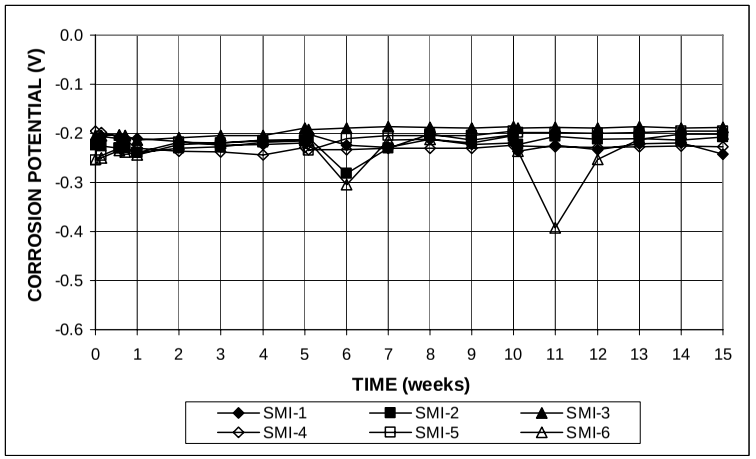

(a)

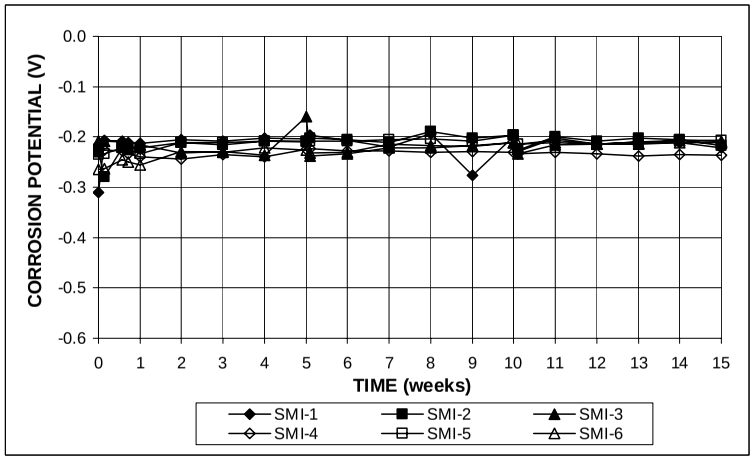

(b)

Figure A.58 - (a) Anode corrosion potentials and (b) cathode corrosion potentials with respect to saturated calomel electrode as measured in the rapid macrocell test for mortar-wrappd stainless steel clad bars in 1.6 m ion NaCl and simulated concrete pore solution.

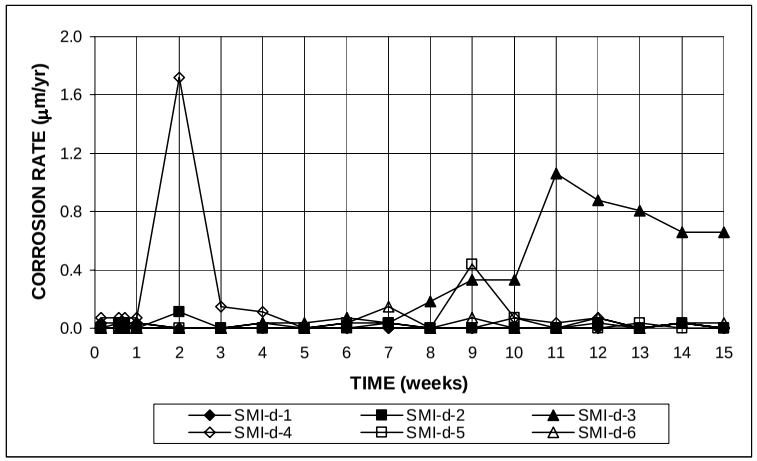

(a)

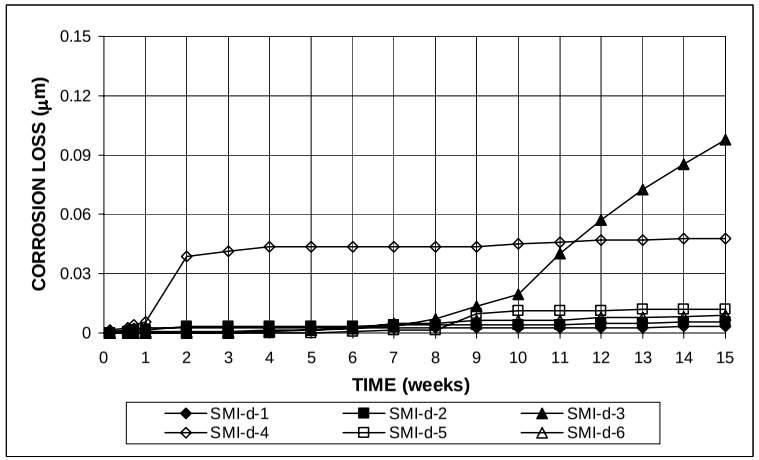

(b)

Figure A.59 - (a) Corrosion rates and (b) total corrosion Losses based on total bar area as measured in the rapid macrocell test for mortar-wrapped stainless steel clad bars with drilled holes in 1.6 m ion NaCl and simulated concrete pore solution

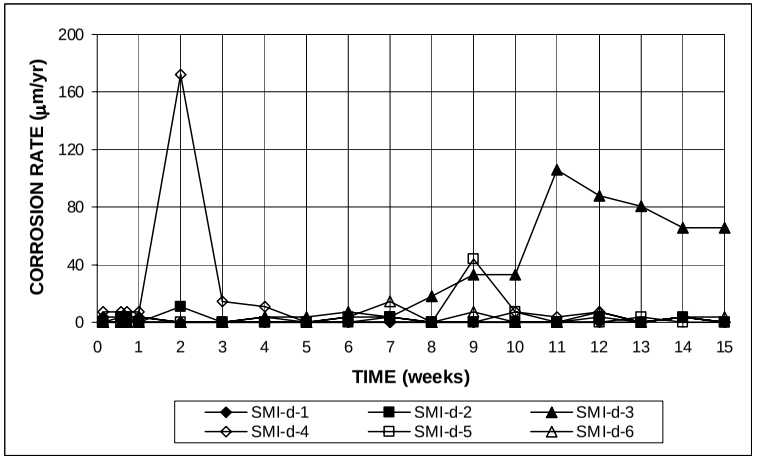

(a)

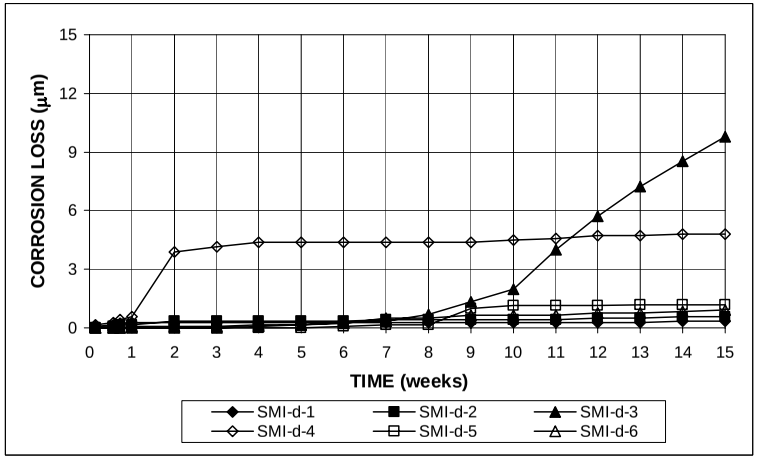

(b)

Figure A.60 - (a) Corrosion rates and (b) total corrosion Losses based on exposed area as measured in the rapid macrocell test for mortar-wrapped stainless steel clad bars with drilled holes in 1.6 m ion NaCl and simulated concrete pore solution

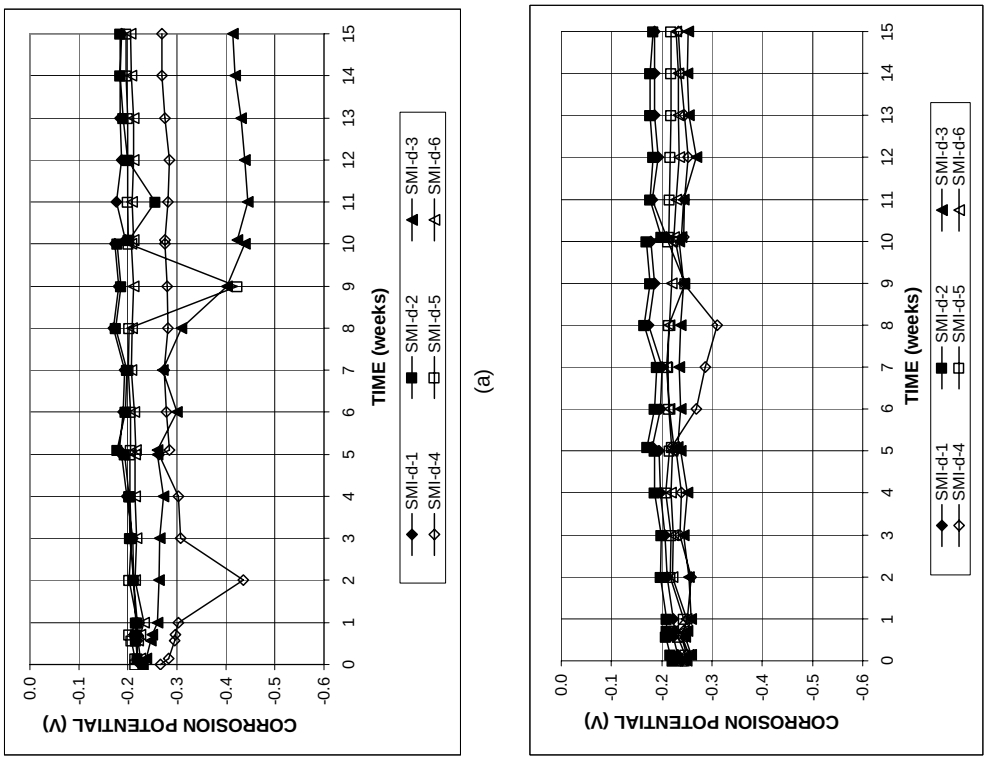

Figure A.61 - (a) Anode corrosion potentials and (b) cathode corrosion potentials with respect to saturated calomel electrode as measured in the rapid macrocell test for mortar-wrapped stainless steel clad bars with drilled holes in 1.6 m ion NaCl and simulated concrete pore solution.

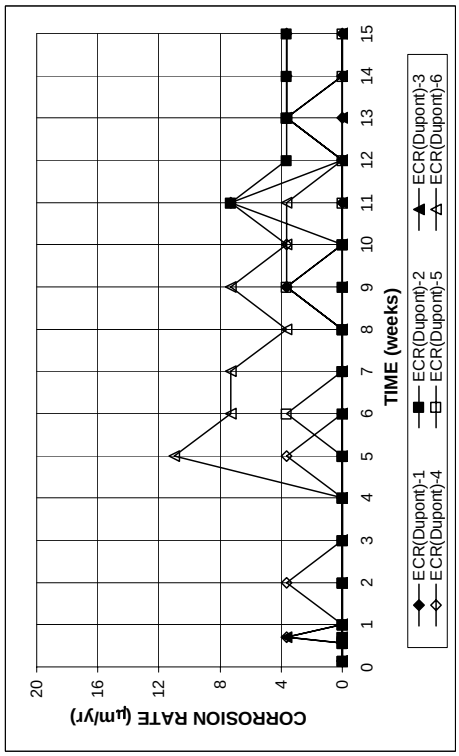

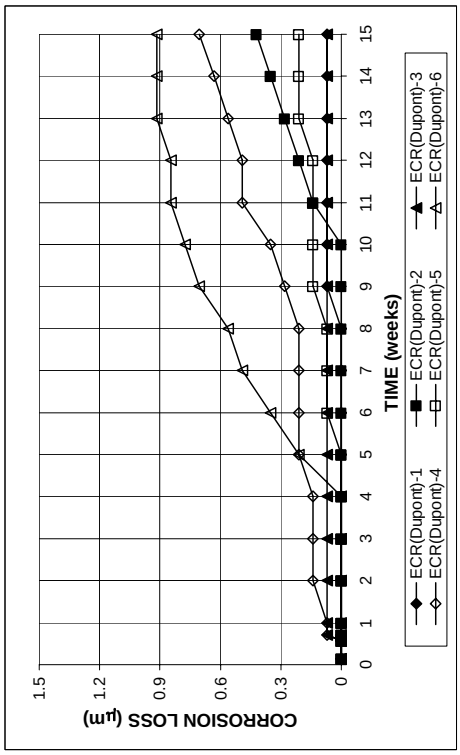

Figure A.63 - (a) Corrosion rates and (b) total corrosion Losses based on exposed area as measured in the rapid macrocell test for mortar-wrapped ECR(Dupont) bars in 1.6 m ion NaCl and simulated concrete pore solution

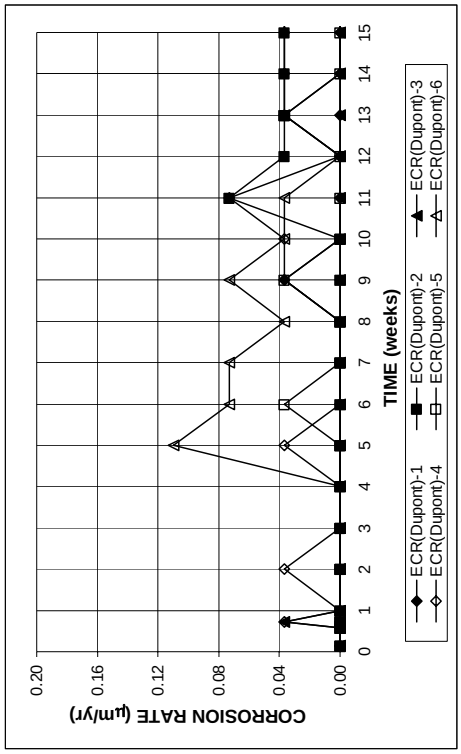

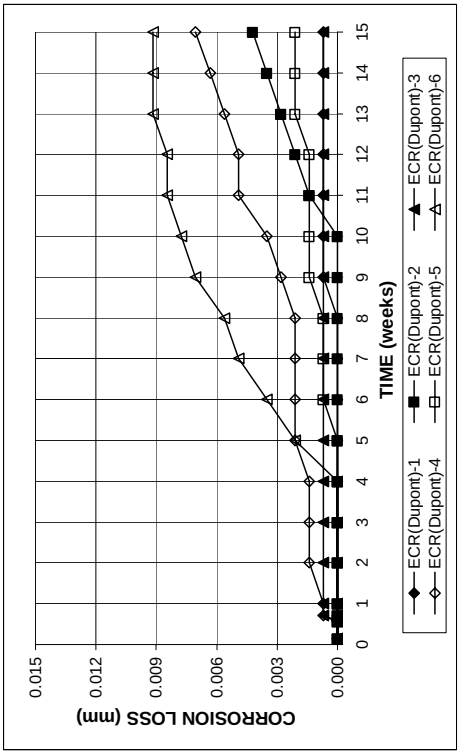

Figure A.62 - (a) Corrosion rates and (b) total corrosion Losses based on total bar area as measured in the rapid macrocell test for mortar-wrapped ECR(Dupont) bars in 1.6 m ion NaCl and simulated concrete pore solution

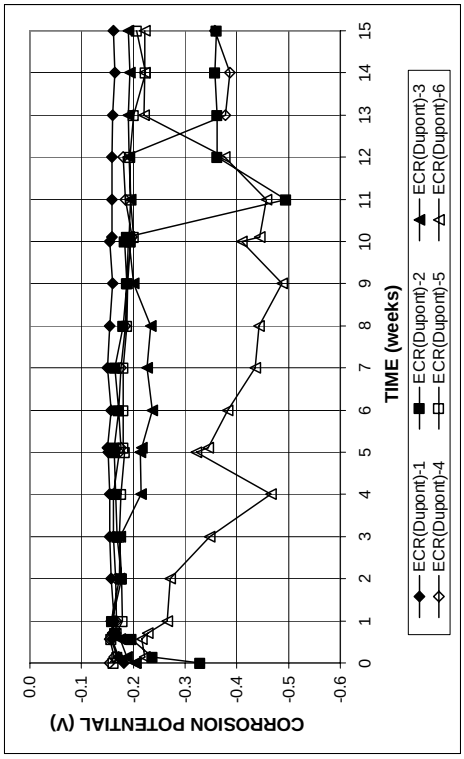

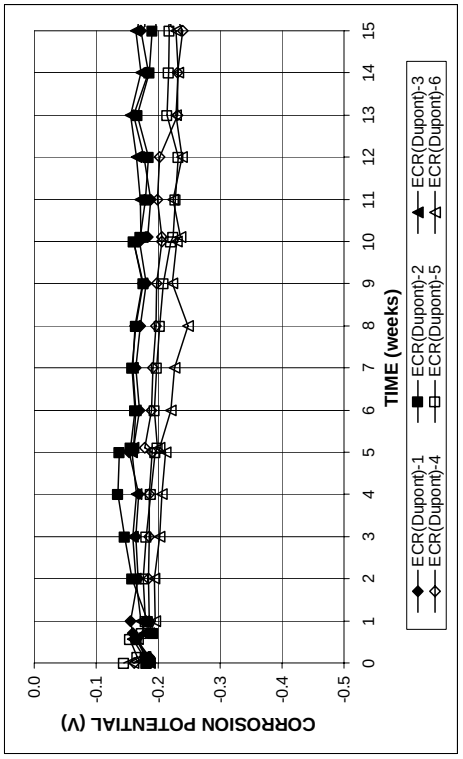

Figure A.64 - (a) Anode corrosion potentials and (b) cathode corrosion potentials with respect to saturated calomel electrode as measured in the rapid macrocell test for mortar-wrapped ECR(Dupont) bars in 1.6 m ion NaCl and simulated concrete pore solution.

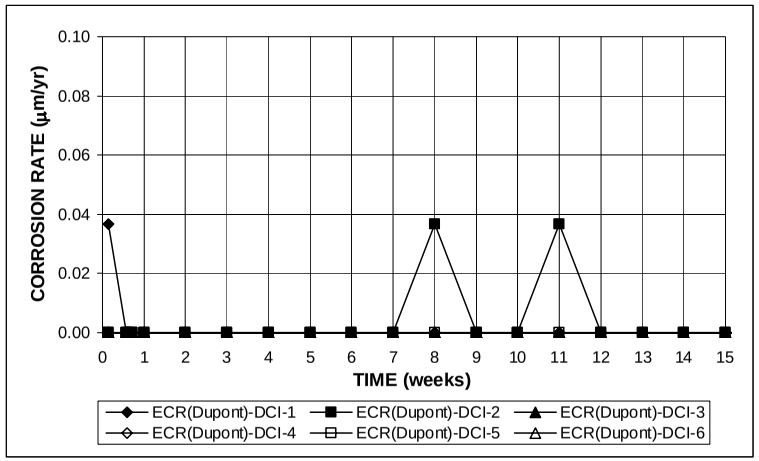

(a)

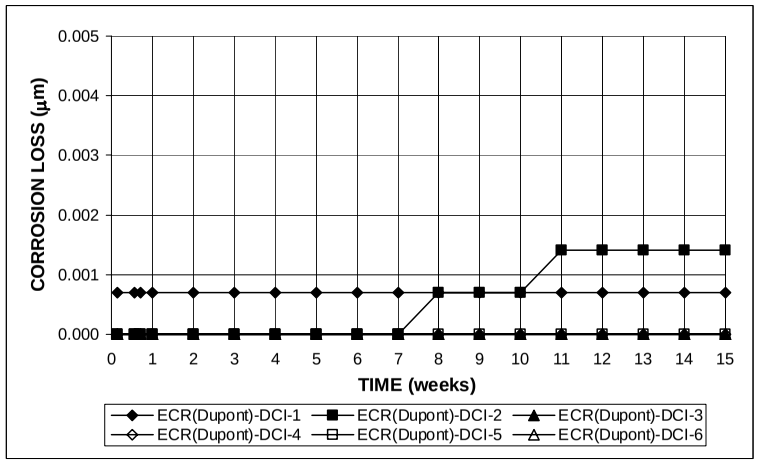

(b)

Figure A.65 - (a) Corrosion rates and (b) total corrosion Losses based on total bar area as measured in the rapid macrocell test for mortar-wrapped ECR(Dupont) bars with corrosion inhibitor DCI in 1.6 m ion NaCl and simulated concrete pore solution

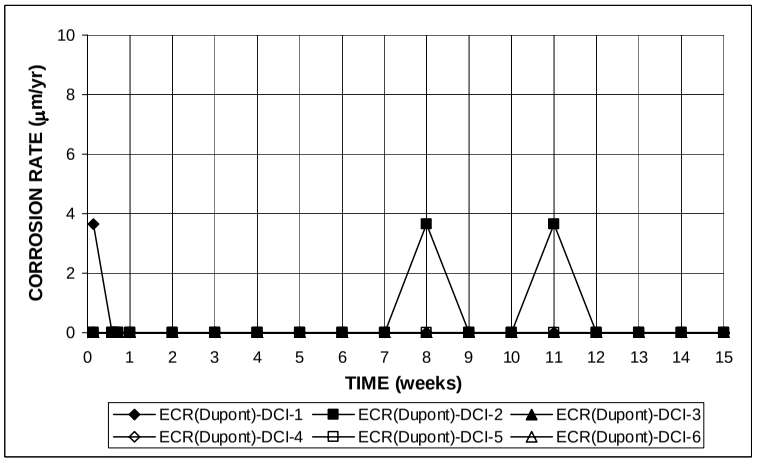

(a)

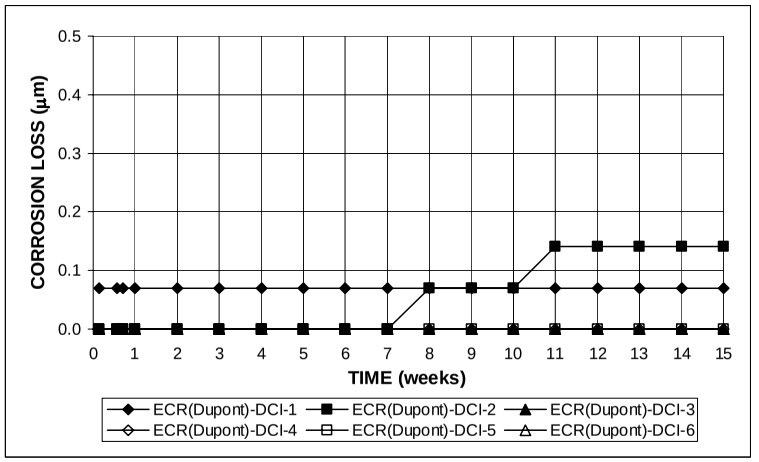

(b)

Figure A.66 - (a) Corrosion rates and (b) total corrosion Losses based on exposed area as measured in the rapid macrocell test for mortar-wrapped ECR(Dupont) bars with corrosion inhibitor DCI in 1.6 m ion NaCl and simulated concrete pore solution

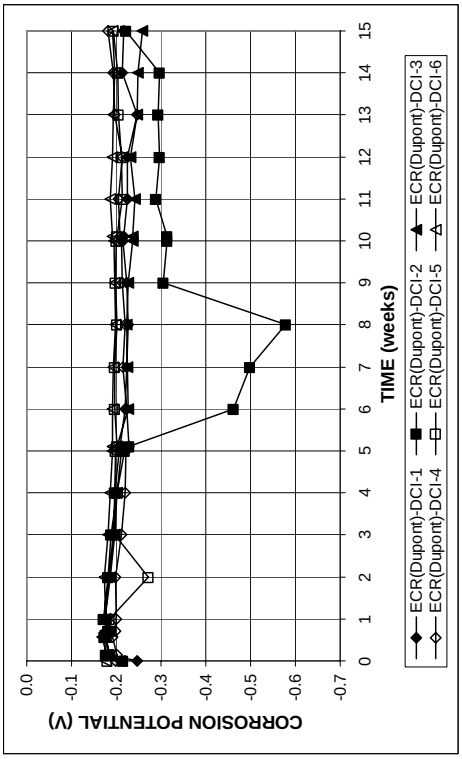

Figure A.67 - (a) Anode corrosion potentials and (b) cathode corrosion potentials with respect to saturated calomel electrode as measured in the rapid macrocell test for mortar-wrapped ECR(Dupont) bars with corrosion inhibitor DCI in 1.6 m ion NaCl and simulated concrete pore solution.

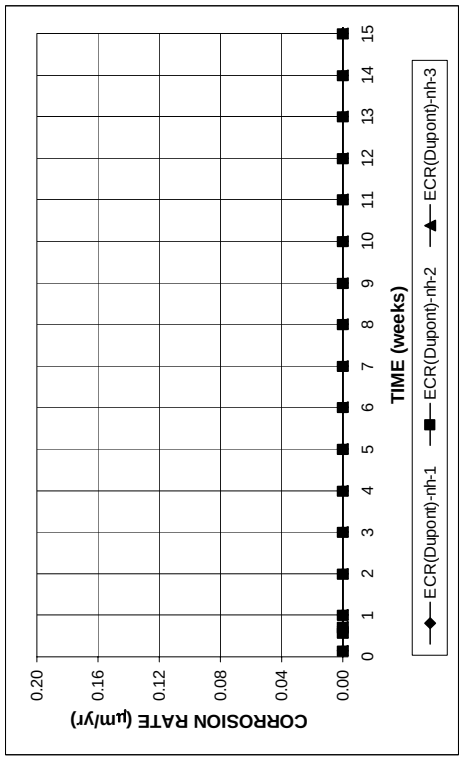

Figure A.68 - (a) Corrosion rates and (b) total corrosion Losses based on total bar area as measured in the rapid macrocell test for mortar-wrapped ECR(Dupont) bars without drilled holes in 1.6 m ion NaCl and simulated concrete pore solution

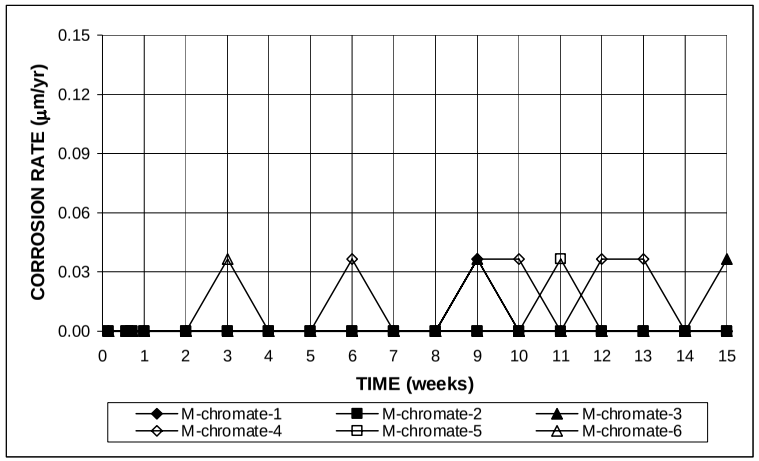

(a)

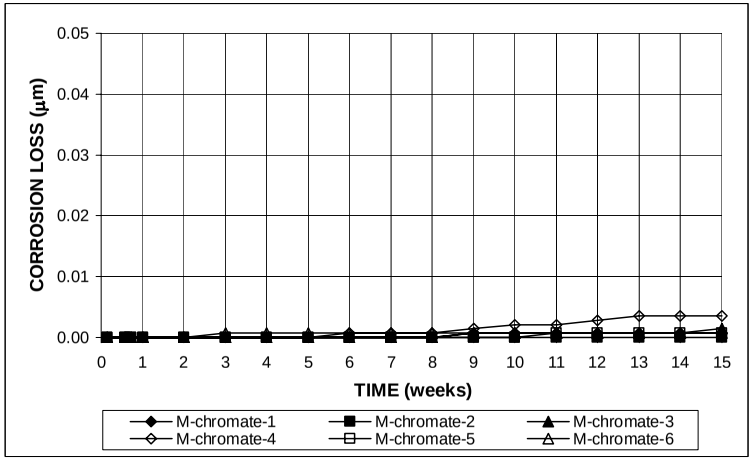

(b)

Figure A.69 - (a) Corrosion rates and (b) total corrosion Losses based on total bar area as measured in the rapid macrocell test for mortar-wrapped ECR(Chromate) bars in 1.6 m ion NaCl and simulated concrete pore solution

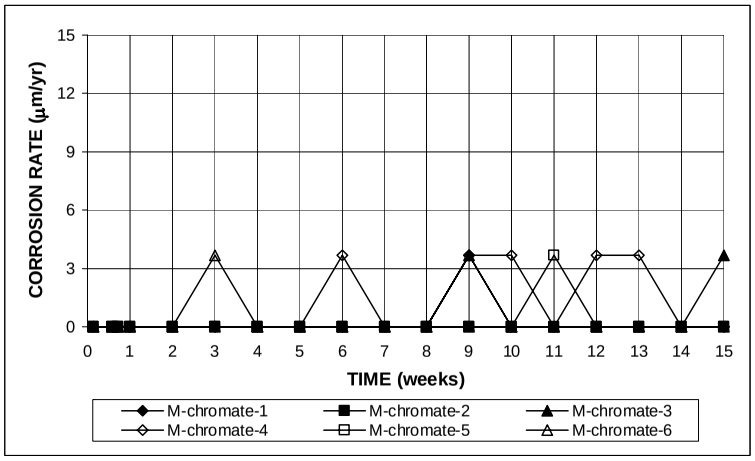

(a)

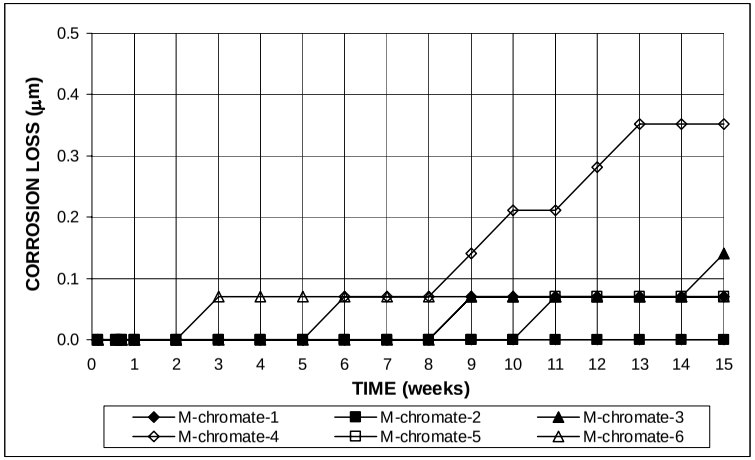

(b)

Figure A.70 - (a) Corrosion rates and (b) total corrosion Losses based on exposed area as measured in the rapid macrocell test for mortar-wrapped ECR(Chromate) bars in 1.6 m ion NaCl and simulated concrete pore solution

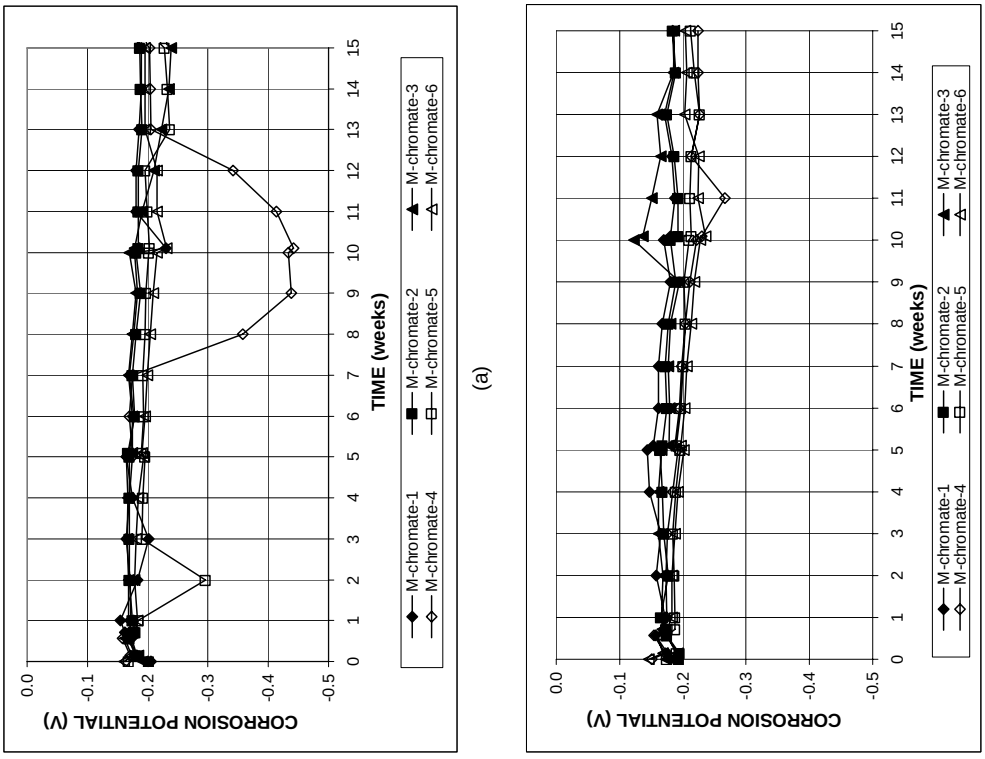

Figure A.71 - (a) Anode corrosion potentials and (b) cathode corrosion potentials with respect to saturated calomel electrode as measured in the rapid macrocell test for mortar-wrapped ECR(Chromate) bars in 1.6 m ion NaCl and simulated concrete pore solution.

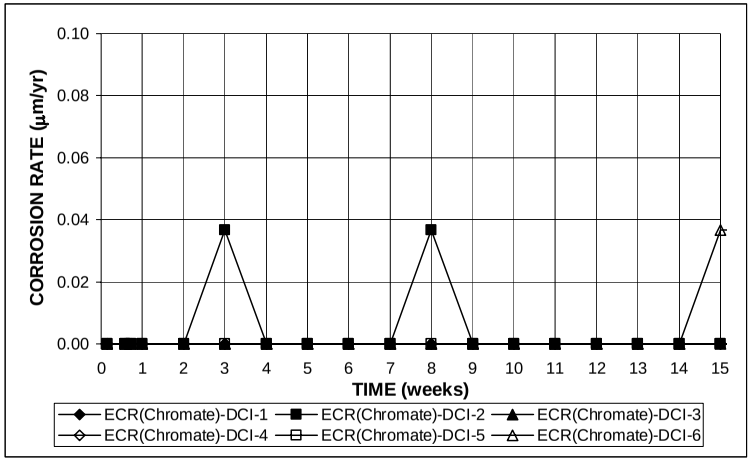

(a)

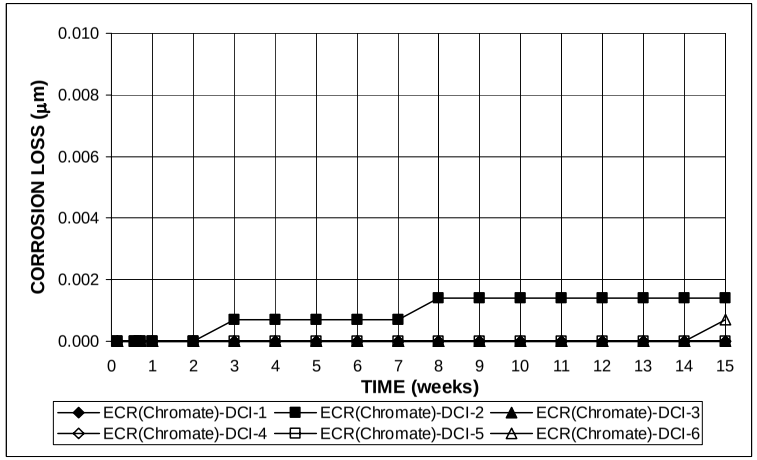

(b)

Figure A.72 - (a) Corrosion rates and (b) total corrosion Losses based on total bar area as measured in the rapid macrocell test for mortar-wrapped ECR(Chromate) bars with corrosion inhibitor DCI in 1.6 m ion NaCl and simulated concrete pore solution

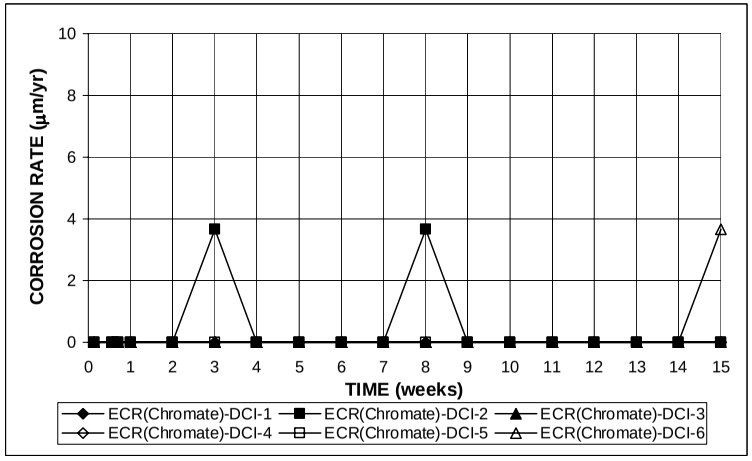

(a)

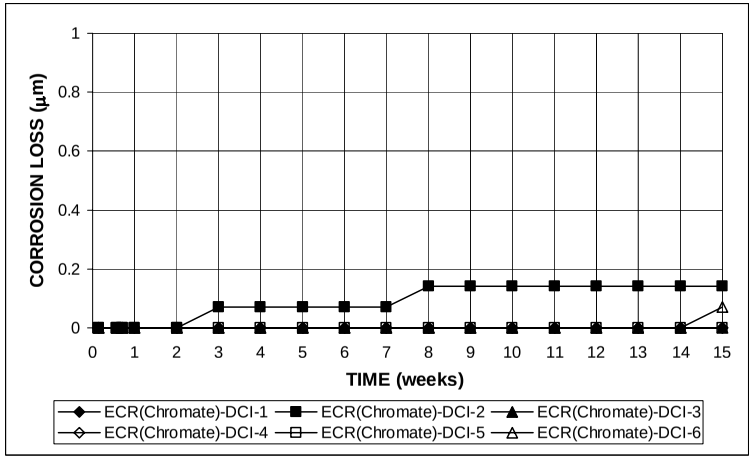

(b)

Figure A.73 - (a) Corrosion rates and (b) total corrosion Losses based on exposed area as measured in the rapid macrocell test for mortar-wrapped ECR(Chromate) bars with corrosion inhibitor DCI in 1.6 m ion NaCl and simulated concrete pore solution

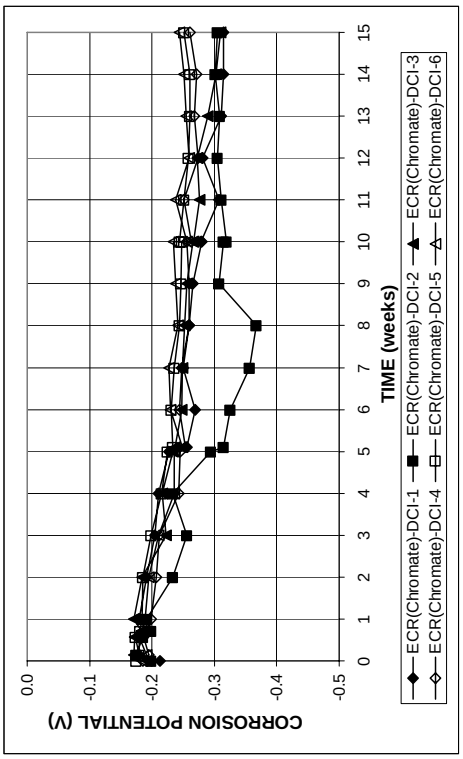

Figure A.74 - (a) Anode corrosion potentials and (b) cathode corrosion potentials with respect to saturated calomel electrode as measured in the rapid macrocell test for mortar-wrapped ECR(Chromate) bars with corrosion inhibitor DCI in 1.6 m ion NaCl and simulated concrete pore solution.

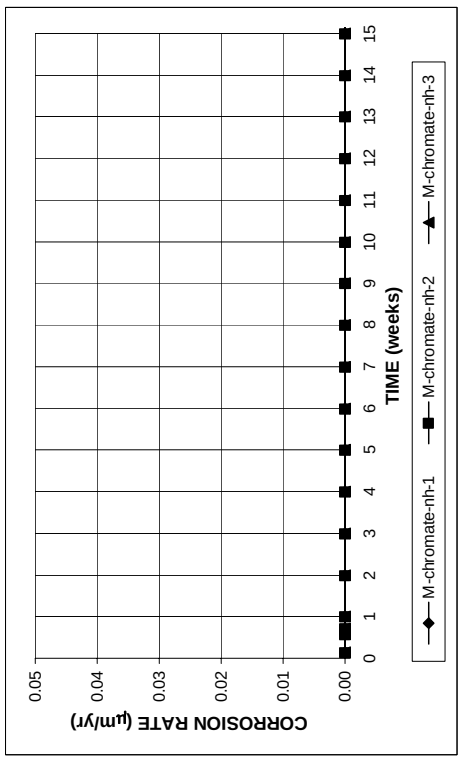

Figure A.75 - (a) Corrosion rates and (b) total corrosion Losses based on total bar area as measured in the rapid macrocell test for mortar-wrapped ECR(Chromate) bars without drilled holes in 1.6 m ion NaCl and simulated concrete pore solution

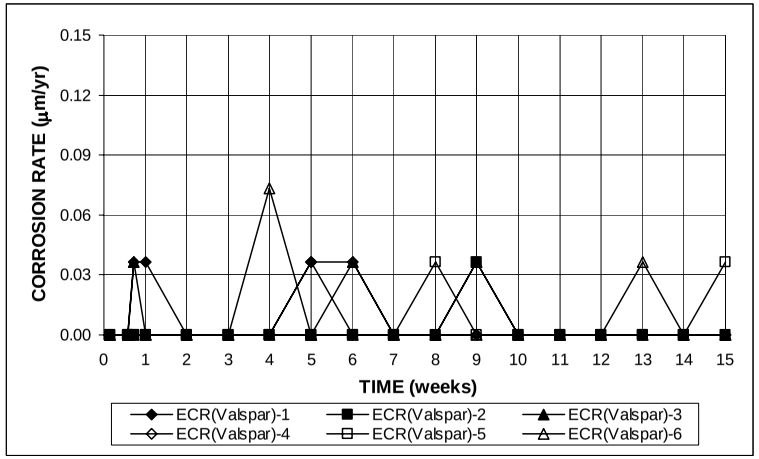

(a)

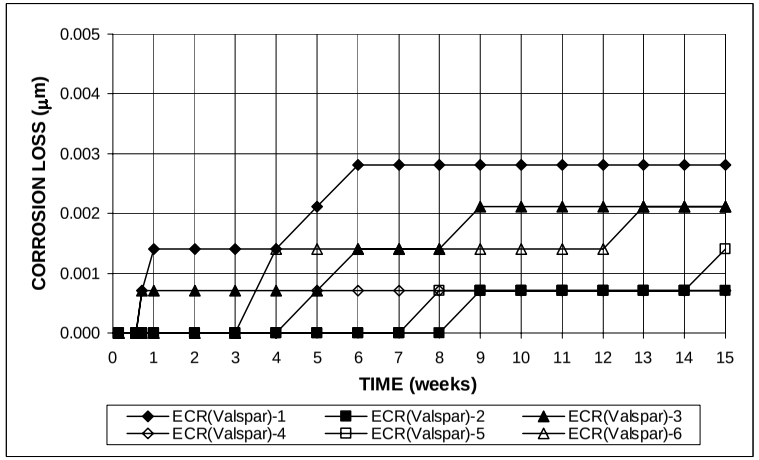

(b)

Figure A.76 - (a) Corrosion rates and (b) total corrosion Losses based on total bar area as measured in the rapid macrocell test for mortar-wrapped ECR(Valsppar) bars in 1.6 m ion NaCl and simulated concrete pore solution

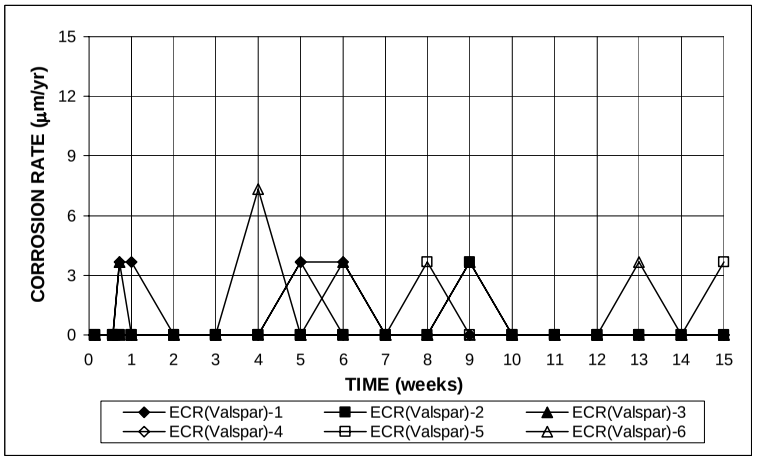

(a)

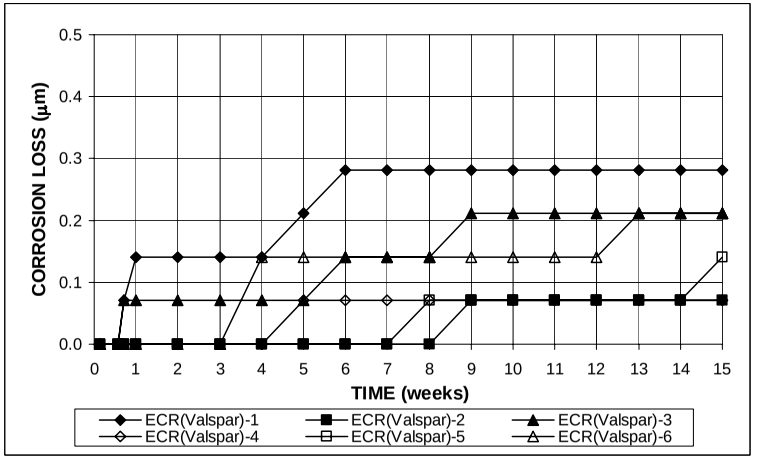

(b)

Figure A.77 - (a) Corrosion rates and (b) total corrosion Losses based on exposed area as measured in the rapid macrocell test for mortar-wrapped ECR(Valspar) bars in 1.6 m ion NaCl and simulated concrete pore solution

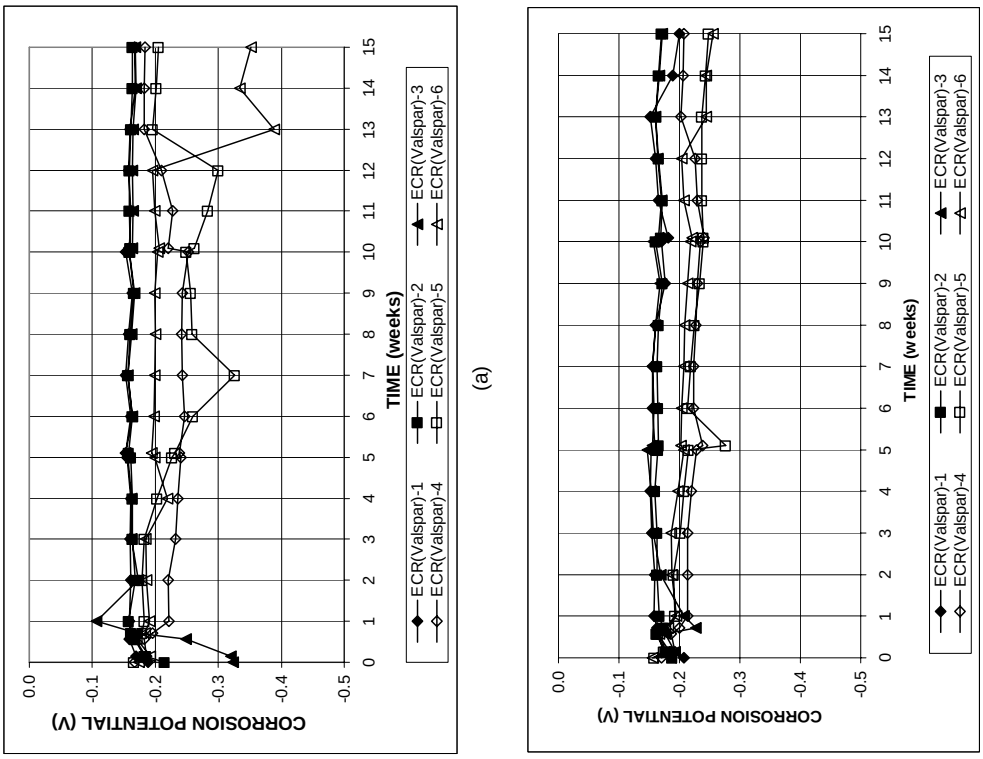

Figure A.78 - (a) Anode corrosion potentials and (b) cathode corrosion potentials with respect to saturated calomel electrode as measured in the rapid macrocell test for mortar-wrapped ECR(Valspar) bars in 1.6 m ion NaCl and simulated concrete pore solution.

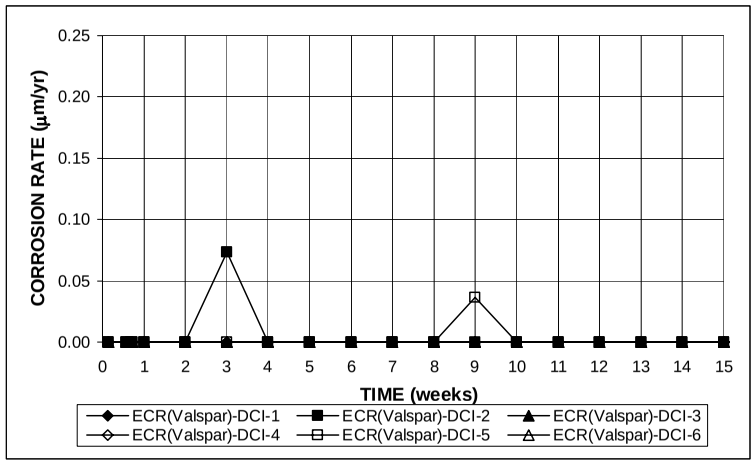

(a)

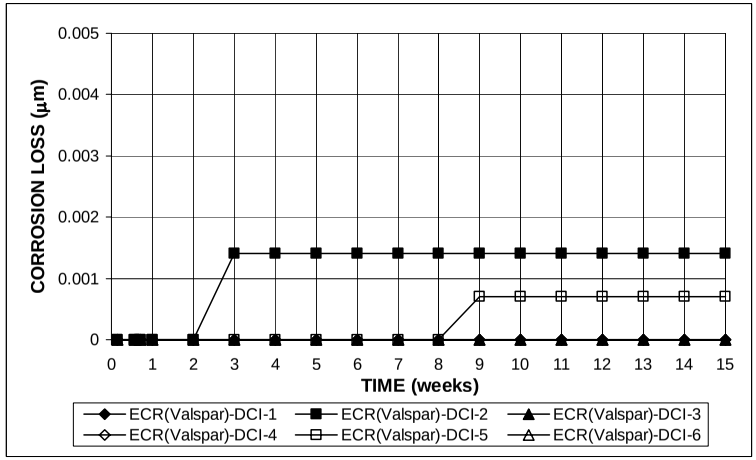

(b)

Figure A.79 - (a) Corrosion rates and (b) total corrosion Losses based on total bar area as measured in the rapid macrocell test for mortar-wrapped ECR(Valspar) bars with corrosion inhibitor DCI in 1.6 m ion NaCl and simulated concrete pore solution

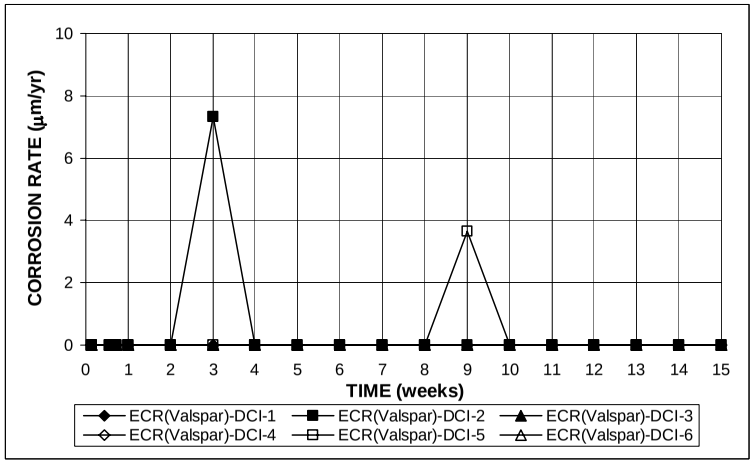

(a)

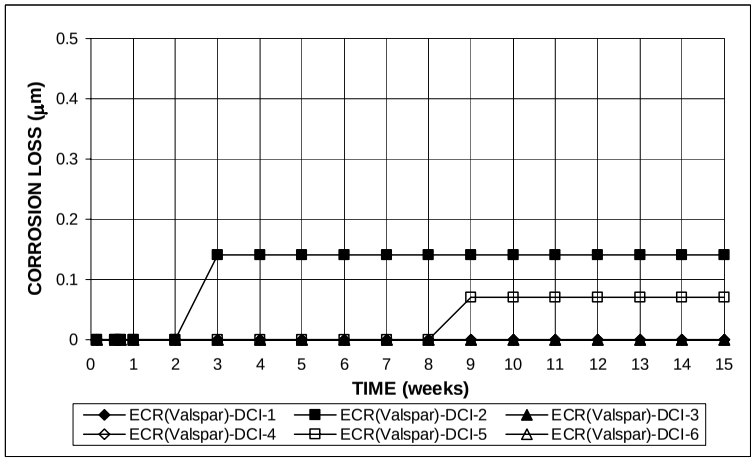

(b)

Figure A.80 - (a) Corrosion rates and (b) total corrosion Losses based on exposed area as measured in the rapid macrocell test for mortar-wrapped ECR(Valspar) bars with corrosion inhibitor DCI in 1.6 m ion NaCl and simulated concrete pore solution

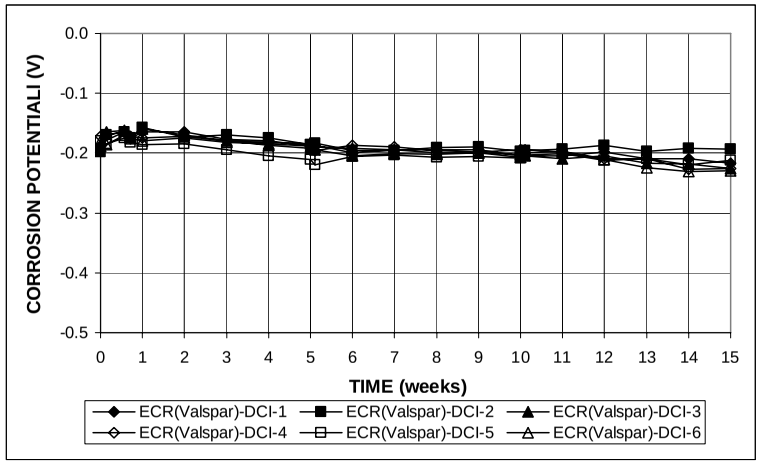

(a)

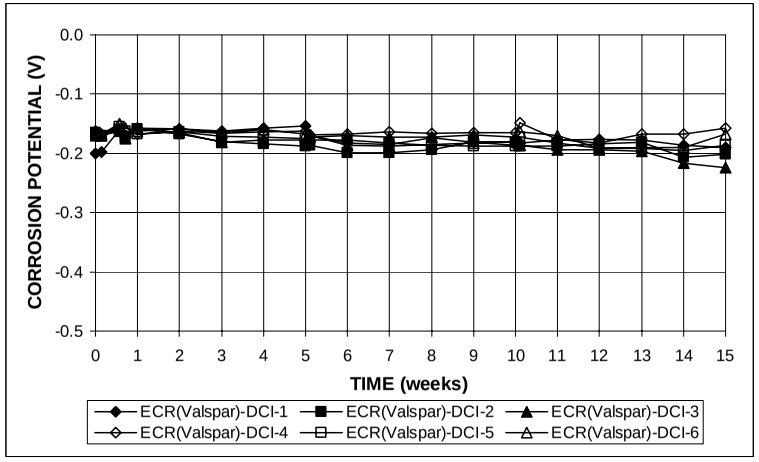

(b)

Figure A.81 - (a) Anode corrosion potentials and (b) cathode corrosion potentials with respect to saturated calomel electrode as measured in the rapid macrocell test for mortar-wrapped ECR(Valspar) bars with corrosion inhibitor DCI in 1.6 m ion NaCl and simulated concrete pore solution.

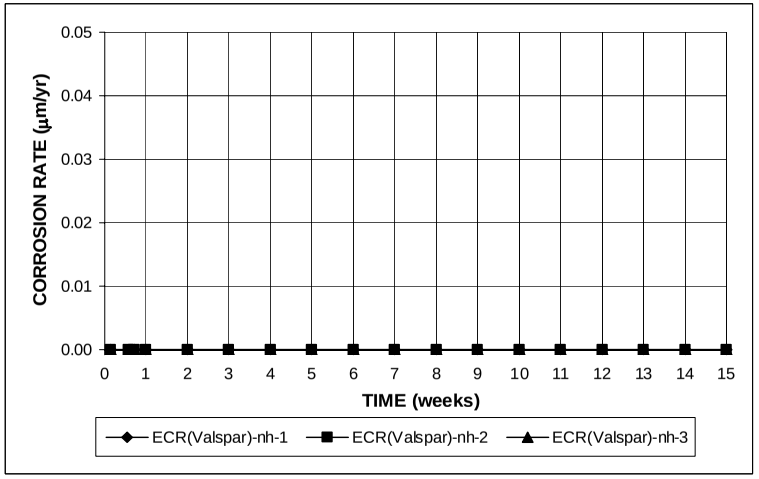

(a)

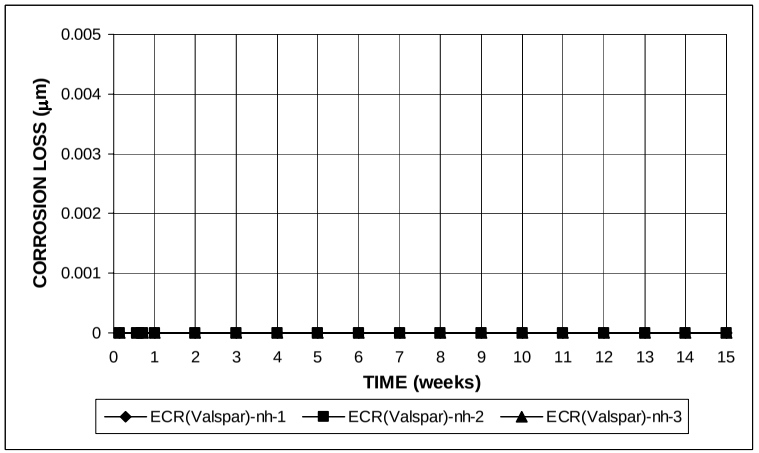

(b)

Figure A.82 - (a) Corrosion rates and (b) total corrosion Losses based on total bar area as measured in the rapid macrocell test for mortar-wrapped ECR(Valspar) bars without drilled holes in 1.6 m ion NaCl and simulated concrete pore solution

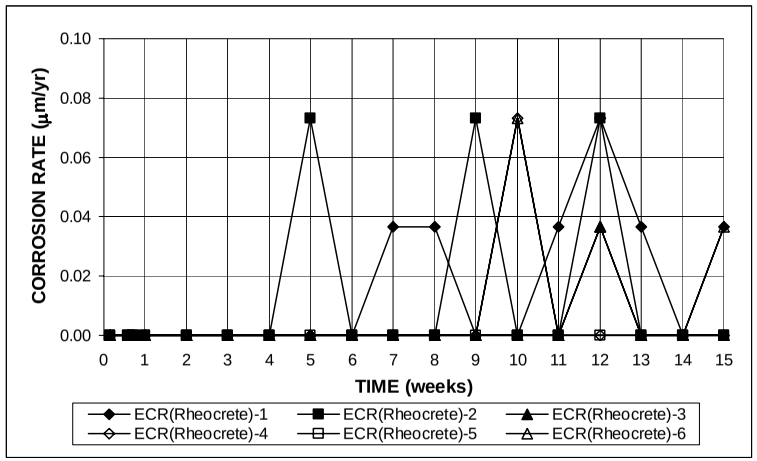

(a)

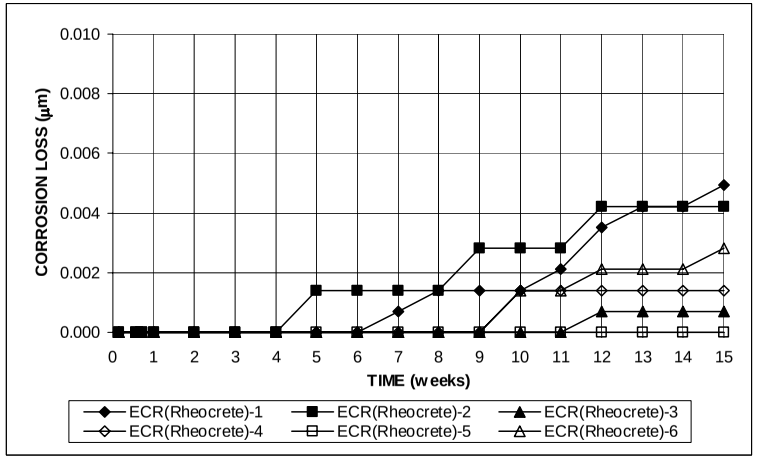

(b)

Figure A.83 - (a) Corrosion rates and (b) total corrosion Losses based on total bar area as measured in the rapid macrocell test for mortar-wrapped ECR bars with corrosion inhibitor Rheocrete in 1.6 m ion NaCl and simulated concrete pore solution

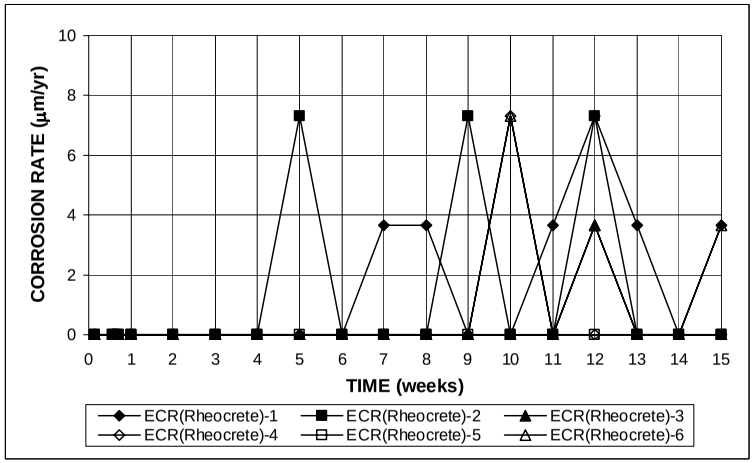

(a)

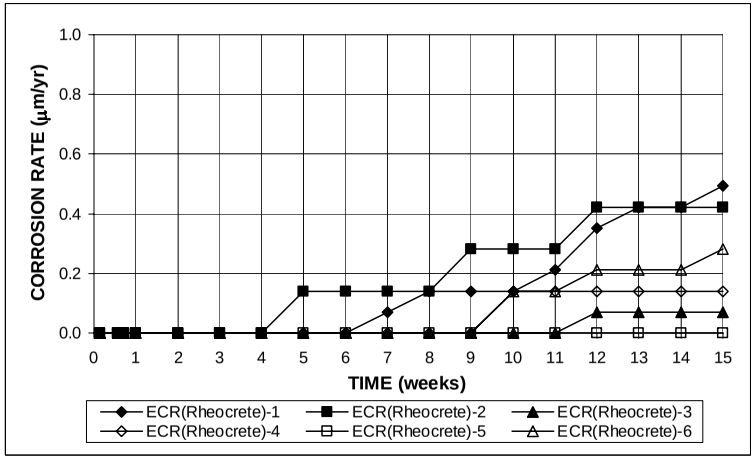

(b)

Figure A.84 - (a) Corrosion rates and (b) total corrosion Losses based on exposed area as measured in the rapid macrocell test for mortar-wrapped ECR bars with corrosion inhibitor Rheocrete in 1.6 m ion NaCl and simulated concrete pore solution

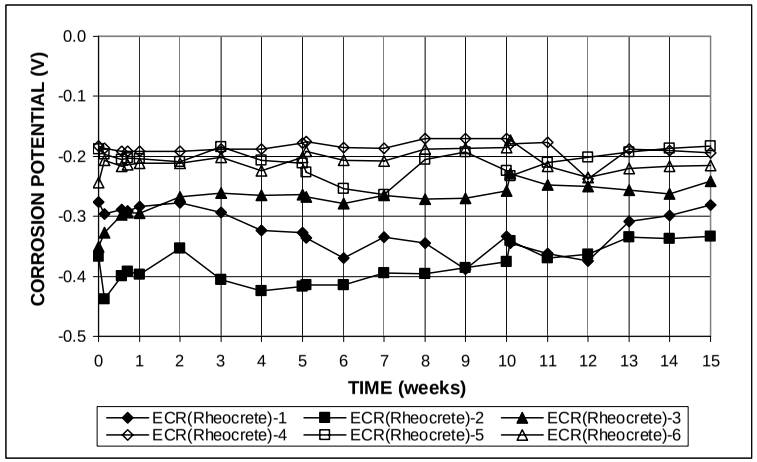

(a)

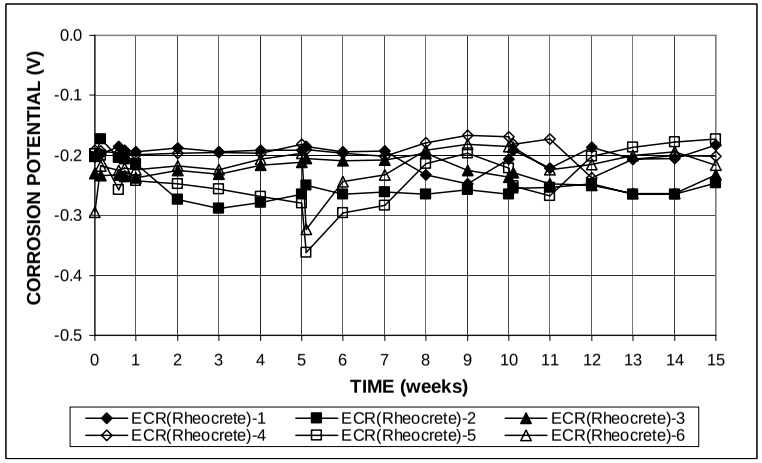

(b)

Figure A.85 - (a) Anode corrosion potentials and (b) cathode corrosion potentials with respect to saturated calomel electrode as measured in the rapid macrocell test for mortar-wrapped ECR bars with corrosion inhibitor Rheocrete in 1.6 m ion NaCl and simulated concrete pore solution.

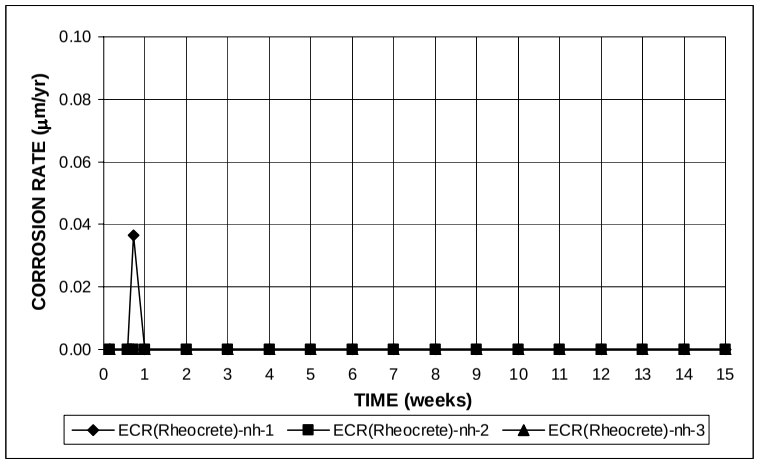

(a)

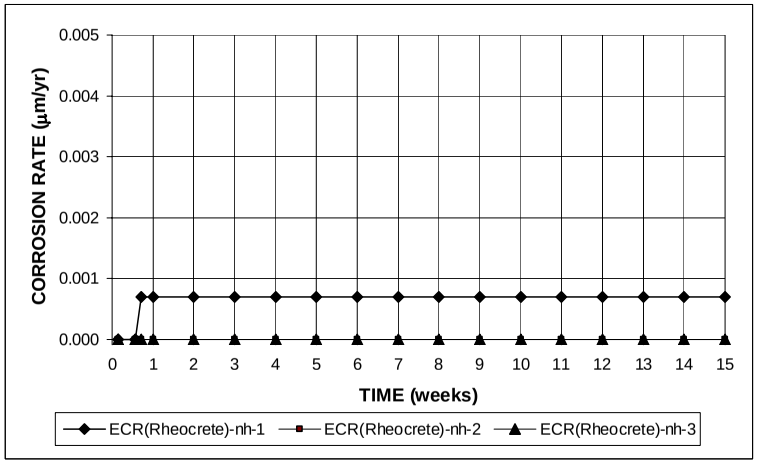

(b)

Figure A.86 - (a) Corrosion rates and (b) total corrosion Losses based on total bar area as measured in the rapid macrocell test for mortar-wrapped ECR bars without drilled holes and with corrosion inhibitor Rheocrete in 1.6 m ion NaCl and simulated concrete pore solution

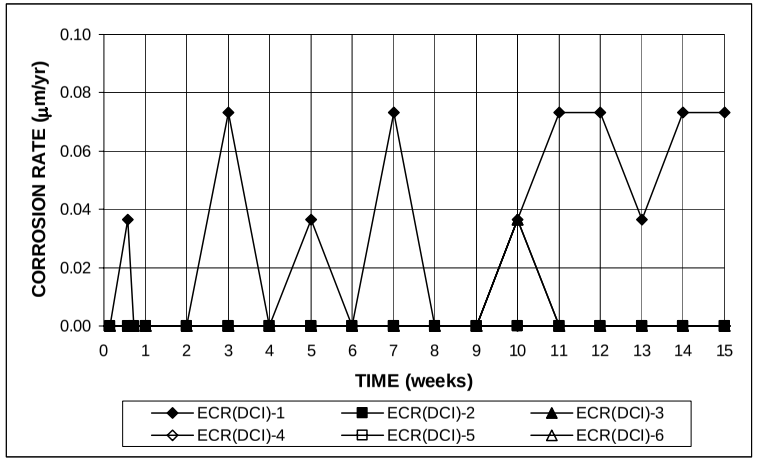

(a)

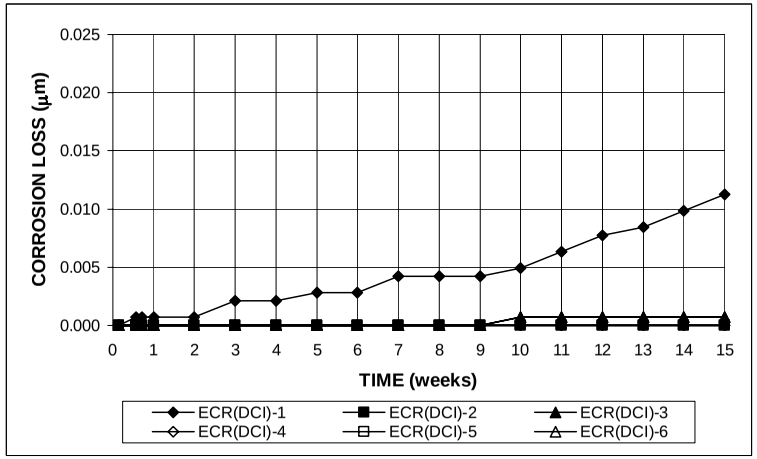

(b)

Figure A.87 - (a) Corrosion rates and (b) total corrosion Losses based on total bar area as measured in the rapid macrocell test for mortar-wrapped ECR bars with corrosion inhibitor DCI in 1.6 m ion NaCl and simulated concrete pore solution

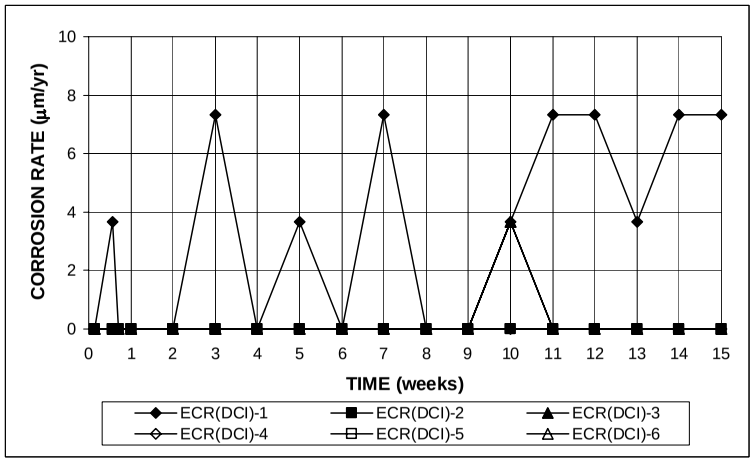

(a)

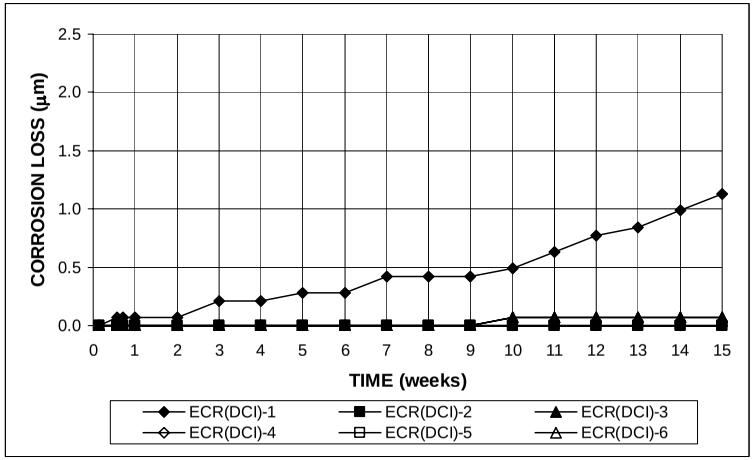

(b)

Figure A.88 - (a) Corrosion rates and (b) total corrosion Losses based on exposed area as measured in the rapid macrocell test for mortar-wrapped ECR bars with corrosion inhibitor DCI in 1.6 m ion NaCl and simulated concrete pore solution

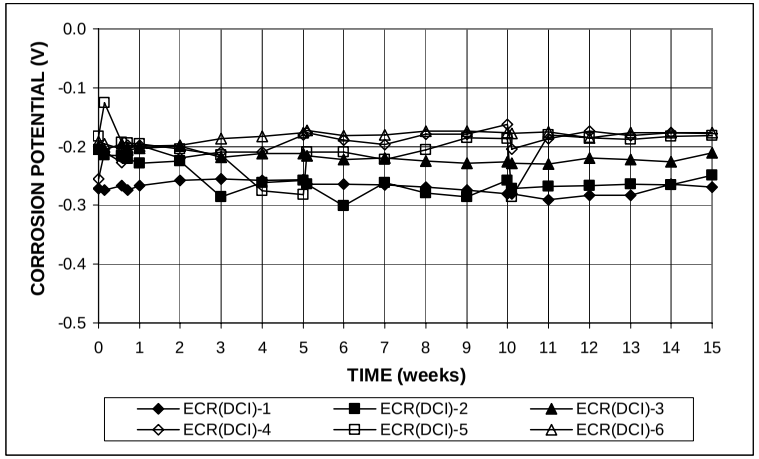

(a)

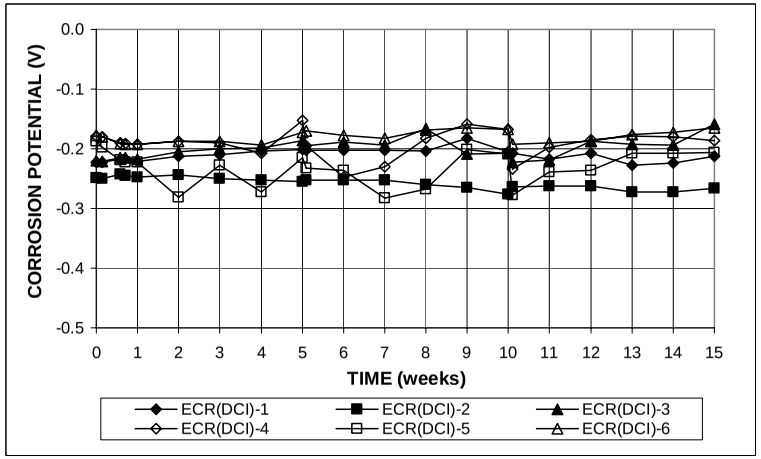

(b)

Figure A.89 - (a) Anode corrosion potentials and (b) cathode corrosion potentials with respect to saturated calomel electrode as measured in the rapid macrocell test for mortar-wrapped ECR bars with corrosion inhibitor DCI in 1.6 m ion NaCl and simulated concrete pore solution.

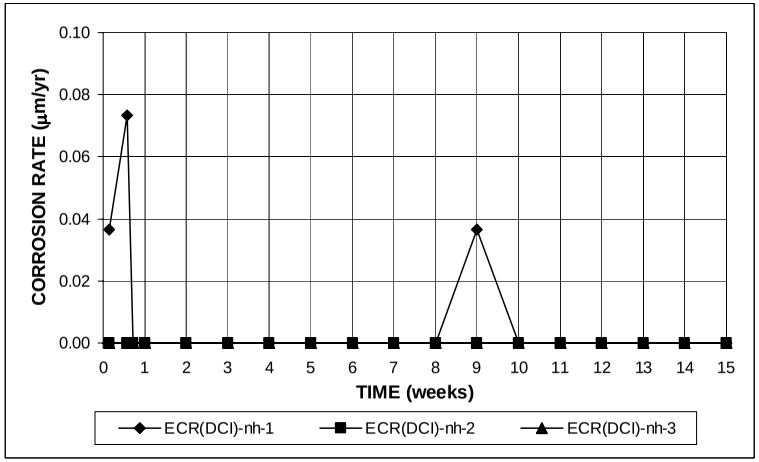

(a)

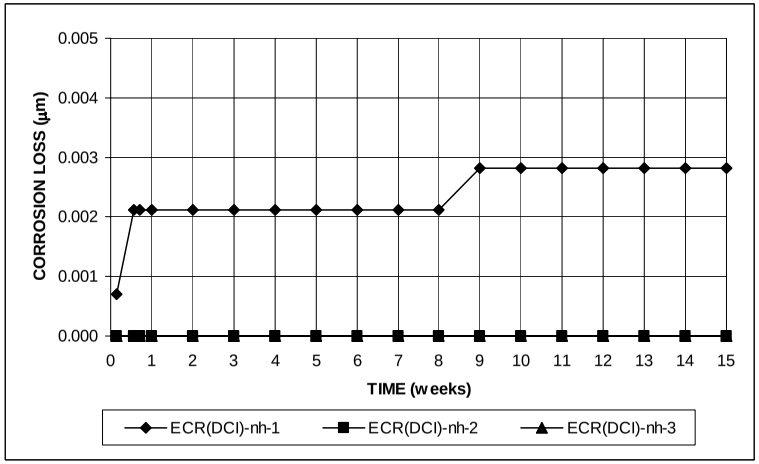

(b)

Figure A.90 - (a) Corrosion rates and (b) total corrosion Losses based on total bar area as measured in the rapid macrocell test for mortar-wrapped ECR bars without drilled holes and with corrosion inhibitor DCI in 1.6 m ion NaCl and simulated concrete pore solution

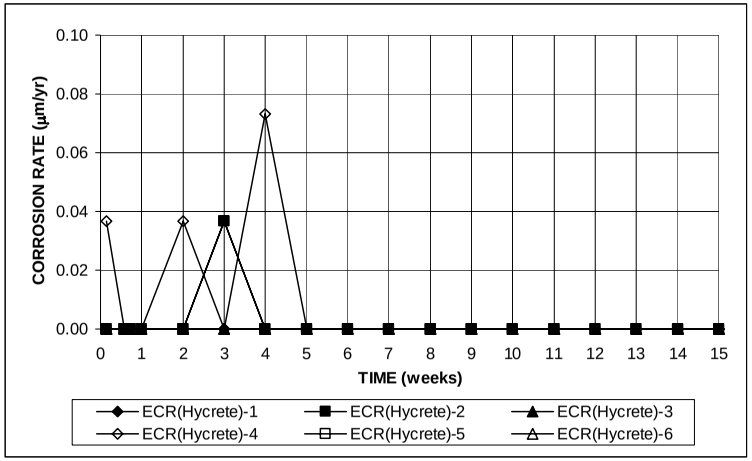

(a)

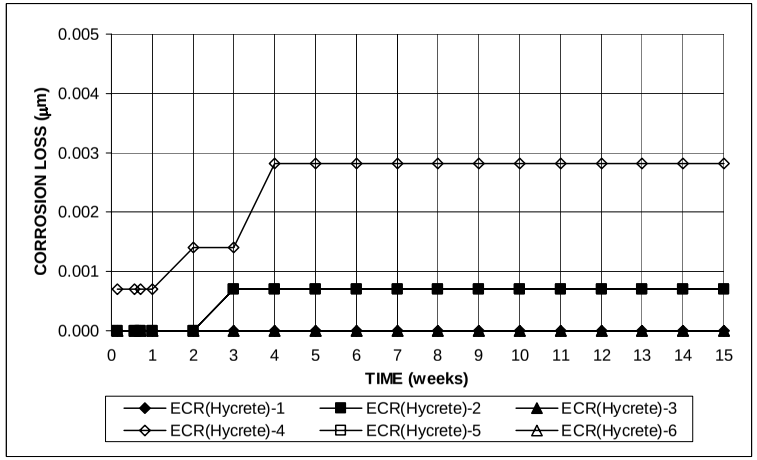

(b)

Figure A.91 - (a) Corrosion rates and (b) total corrosion Losses based on total bar area as measured in the rapid macrocell test for mortar-wrapped ECR bars with corrosion inhibitor Hycrete in 1.6 m ion NaCl and simulated concrete pore solution

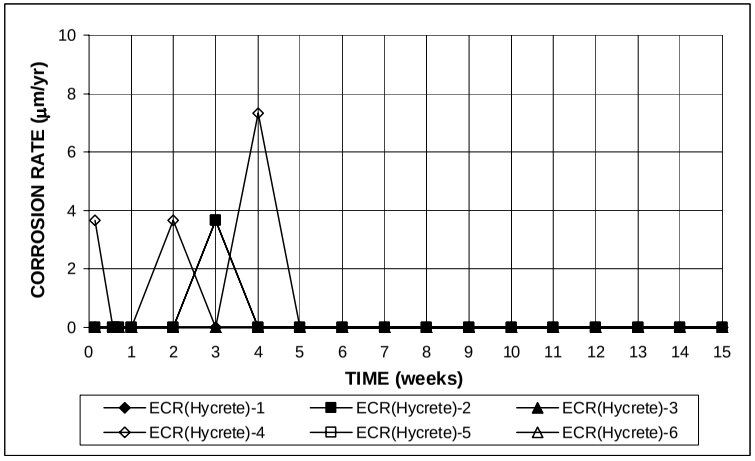

(a)

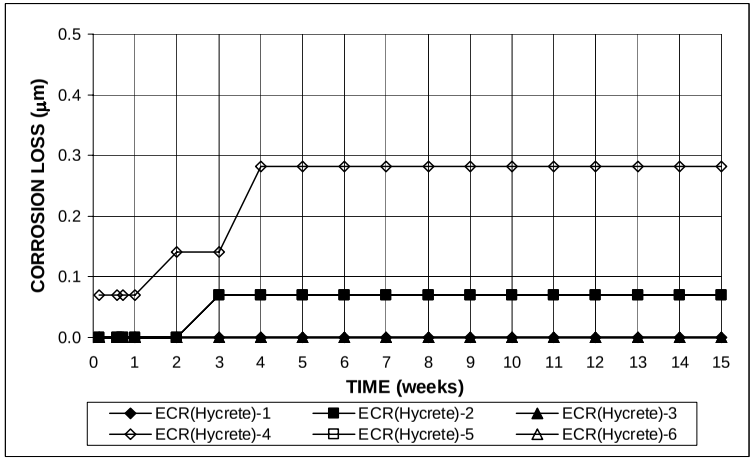

(b)

Figure A.92 - (a) Corrosion rates and (b) total corrosion Losses based on exposed area as measured in the rapid macrocell test for mortar-wrapped ECR bars with corrosion inhibitor Hycrete in 1.6 m ion NaCl and simulated concrete pore solution

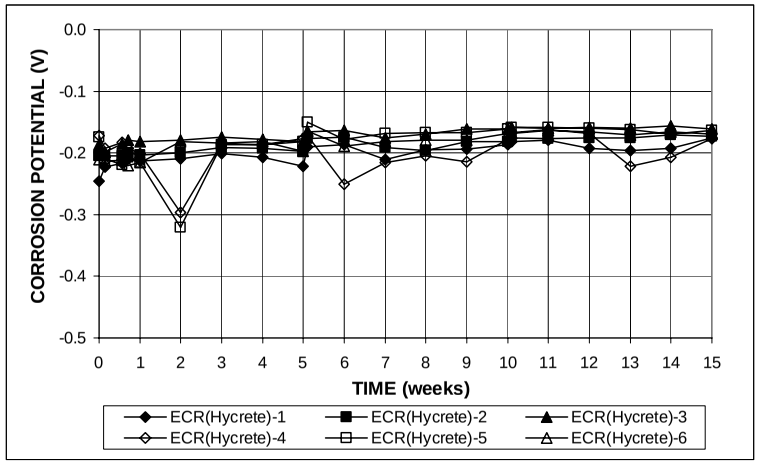

(a)

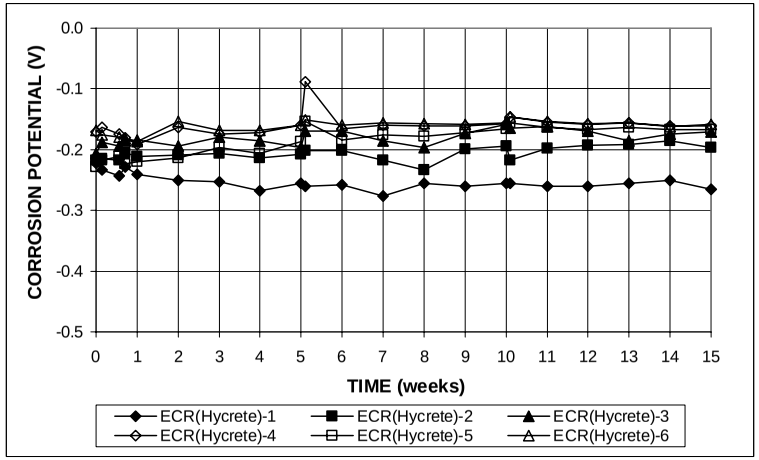

(b)

Figure A.93 - (a) Anode corrosion potentials and (b) cathode corrosion potentials with respect to saturated calomel electrode as measured in the rapid macrocell test for mortar-wrapped ECR bars with corrosion inhibitor Hycrete in 1.6 m ion NaCl and simulated concrete pore solution.

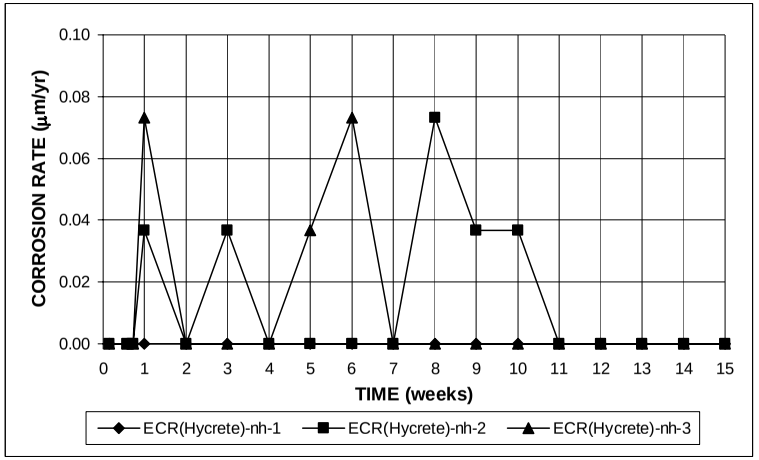

(a)

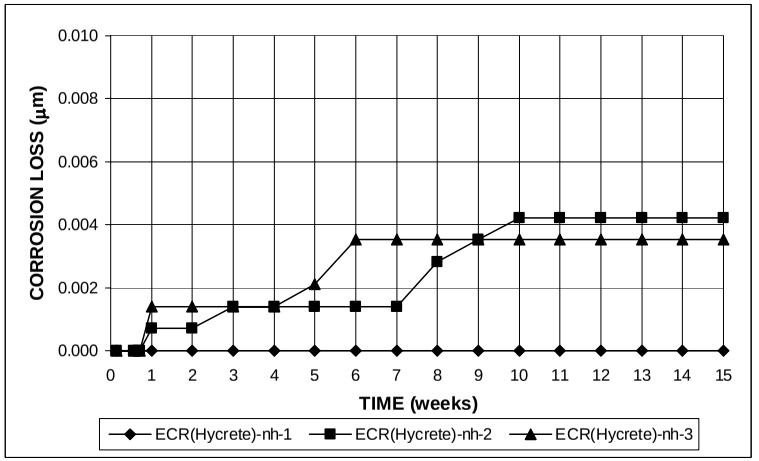

(b)

Figure A.94 - (a) Corrosion rates and (b) total corrosion Losses based on total bar area as measured in the rapid macrocell test for mortar-wrapped ECR bars without drilled holes and with corrosion inhibitor Hycrete in 1.6 m ion NaCl and simulated concrete pore solution

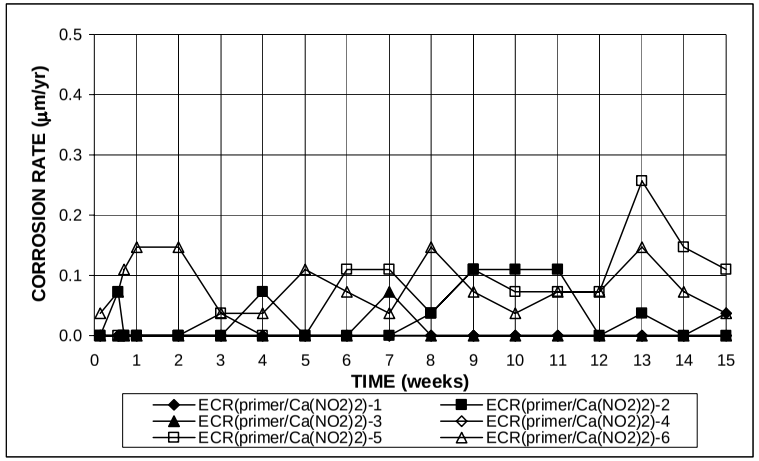

(a)

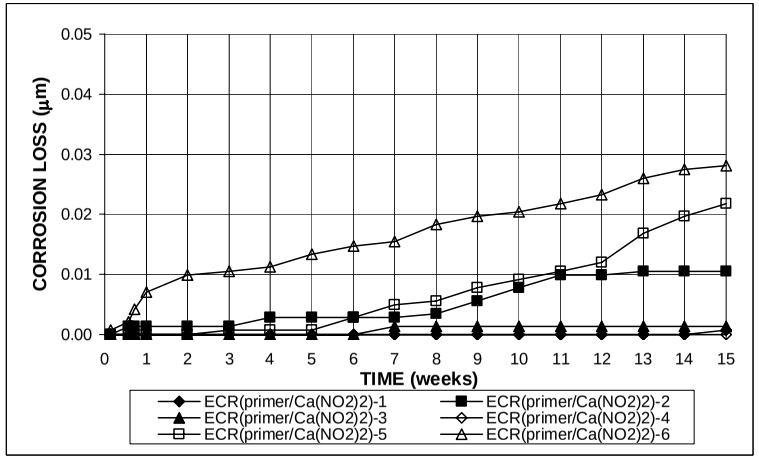

(b)

Figure A.95 - (a) Corrosion rates and (b) total corrosion Losses based on total bar area as measured in the rapid macrocell test for mortar-wrapped ECR(primer/Ca(NO2)2) bars in 1.6 m ion NaCl and simulated concrete and simulated concrete pore solution

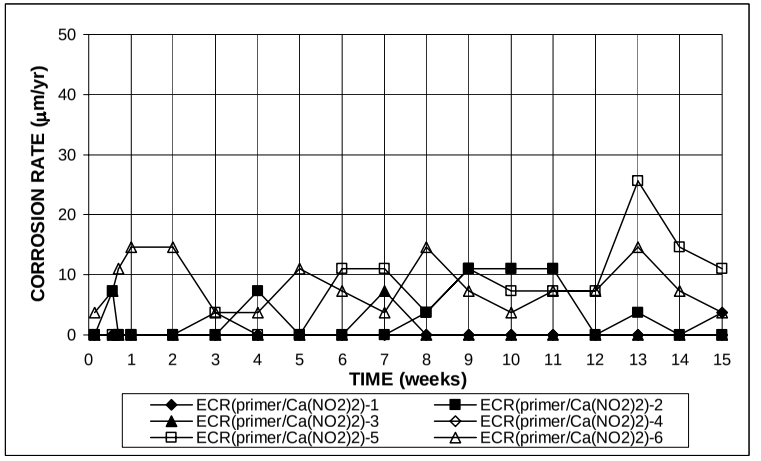

(a)

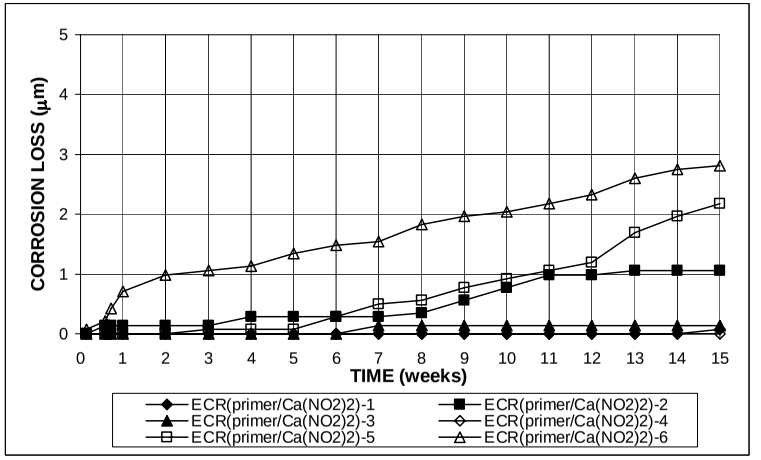

(b)

Figure A.96 - (a) Corrosion rates and (b) total corrosion Losses based on exposed area as measured in the rapid macrocell test for mortar-wrapped ECR(primer/Ca(NO2)2) bars in 1.6 m ion NaCl and simulated concrete and simulated concrete pore solution

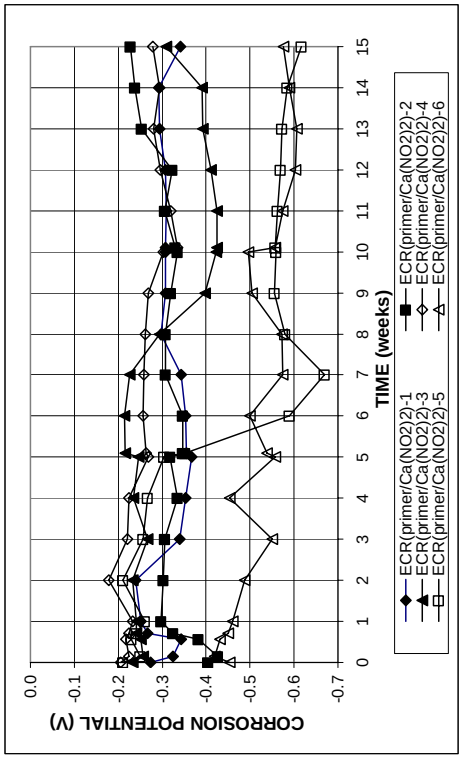

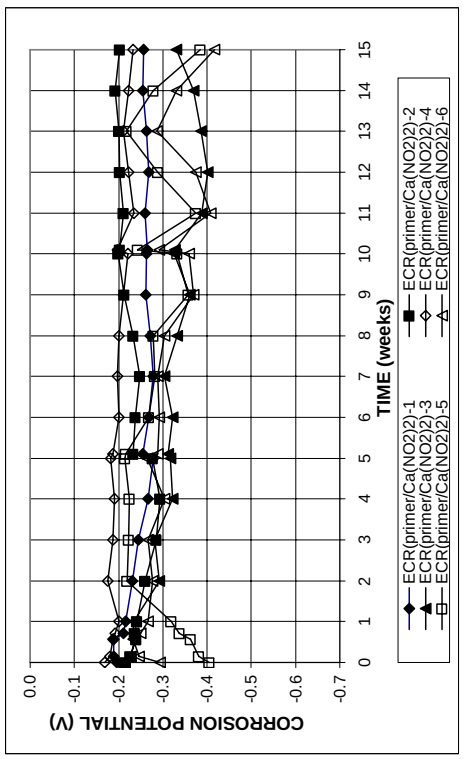

Figure A.97 - (a) Anode corrosion potentials and (b) cathode corrosion potentials with respect to saturated calomel electrode as measured in the rapid macrocell test for mortar-wrapped ECR(primer/Ca(NO2)2) bars in 1.6 m ion NaCl and simulated concrete pore solution.

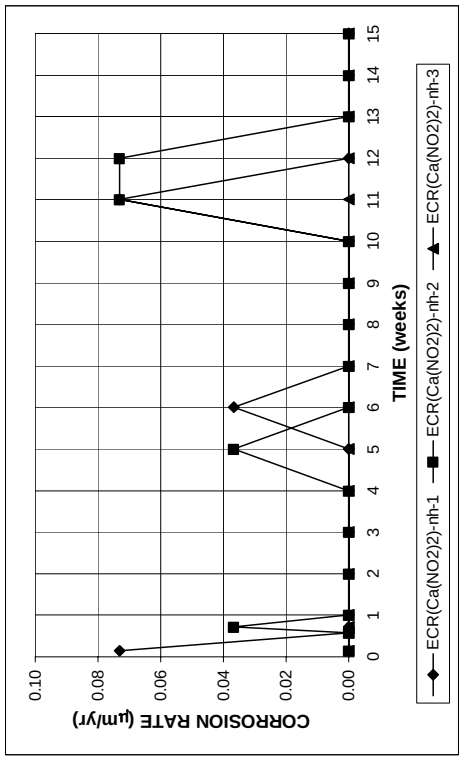

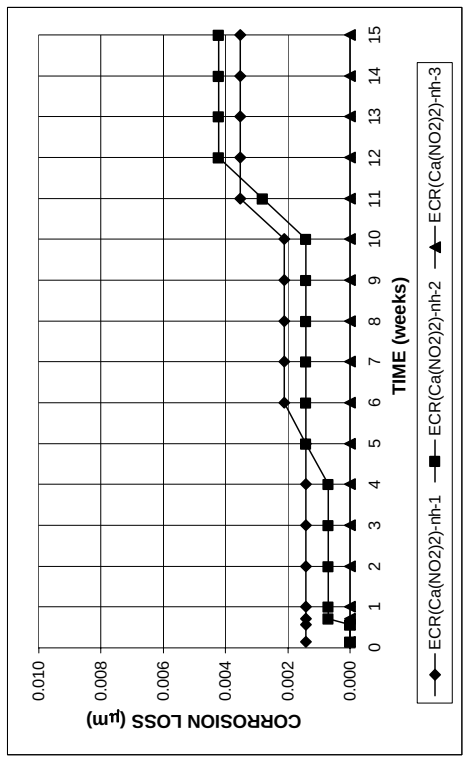

Figure A.98 - (a) Corrosion rates and (b) total corrosion Losses based on total bar area as measured in the rapid macrocell test for mortar-wrapped ECR(primer/Ca(NO2)2) bars without drilled holes in 1.6 m ion NaCl and simulated concrete pore solution

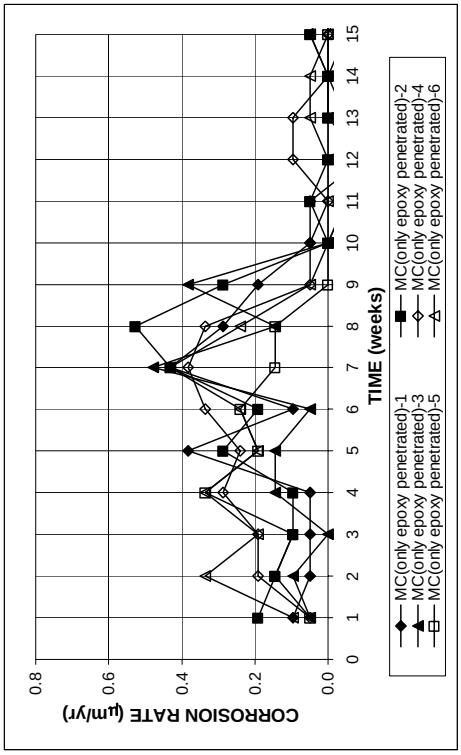

Figure A.99- (a) Corrosion rates and (b) total corrosion Losses based on total bar area as measured in the rapid macrocell test for mortar-wrapped multiple coated bars with only epoxy penetrated in 1.6 m ion NaCl and simulated concrete pore solution

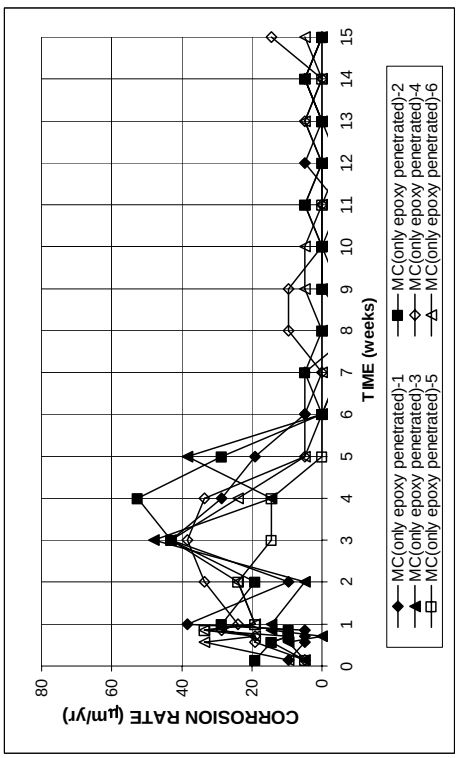

Figure A.100 - (a) Corrosion rates and (b) total corrosion Losses based on exposed area as measured in the rapid macrocell test for mortar-wrapped multiple coated bars with only epoxy penetrated in 1.6 m ion NaCl and simulated concrete pore solution

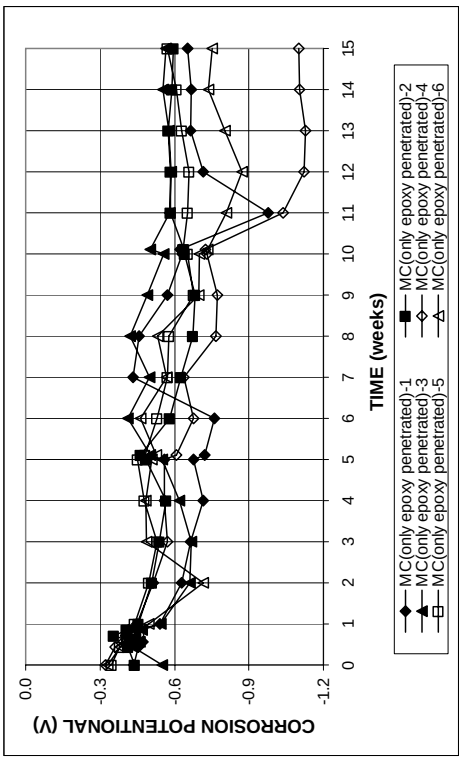

(a)

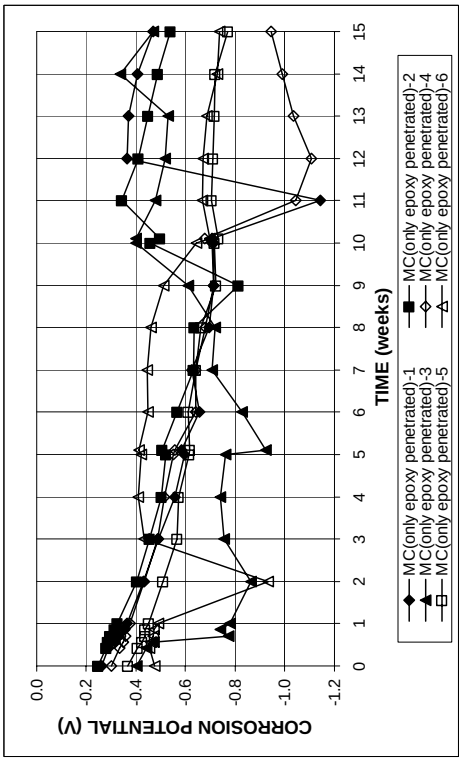

(b)

Figure A.101 - (a) Anode corrosion potentials and (b) cathode corrosion potentials with respect to saturated calomel electrode as measured in the rapid macrocell test for mortar-wrapped multiple coated bars with only epoxy penetrated in 1.6 m ion NaCl and simulated concrete pore solution.

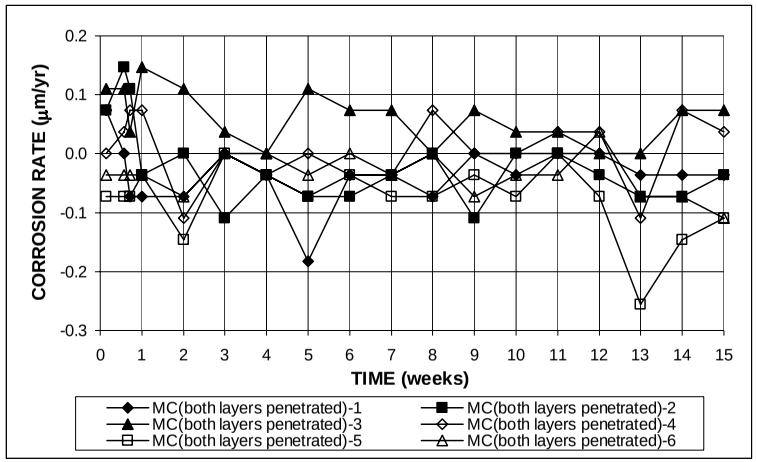

(a)

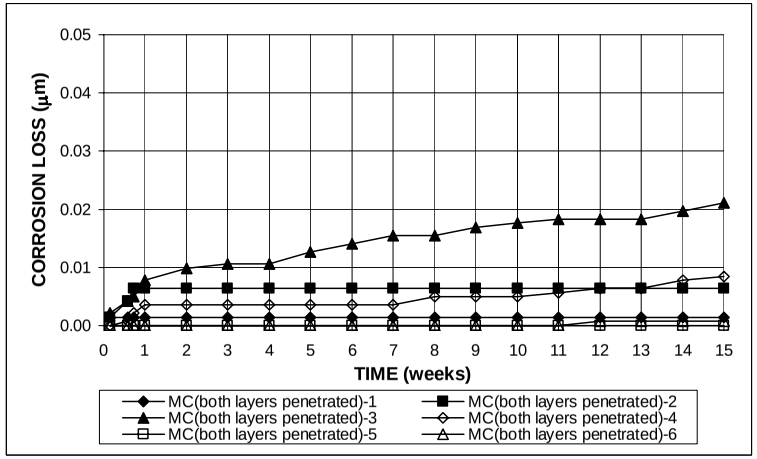

(b)

Figure A.102- (a) Corrosion rates and (b) total corrosion Losses based on total bar area as measured in the rapid macrocell test for mortar-wrapped multiple coated bars with both layers penetrated in 1.6 m ion NaCl and simulated concrete pore solution

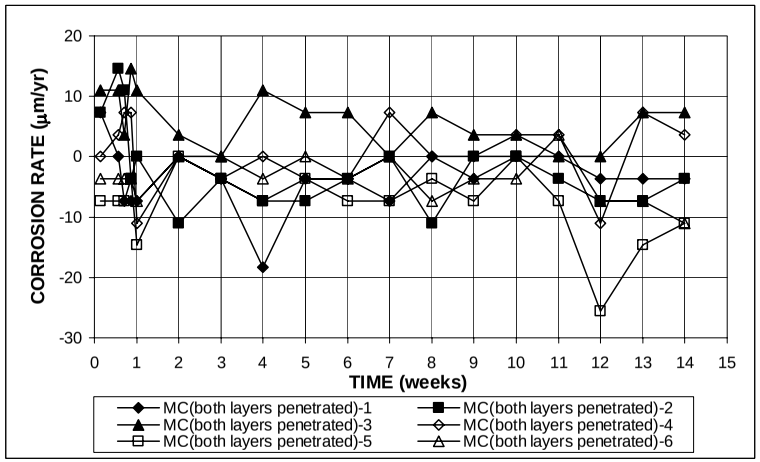

(a)

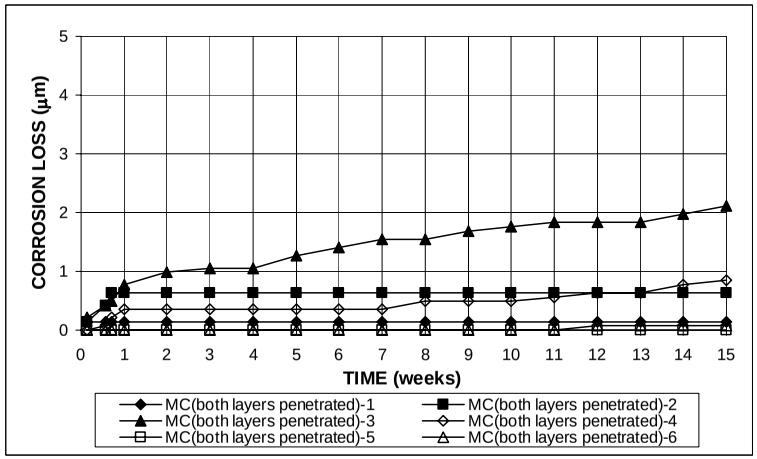

(b)

Figure A.103 - (a) Corrosion rates and (b) total corrosion Losses based on exposed area as measured in the rapid macrocell test for mortar-wrapped multiple coated bars with both layers penetrated in 1.6 m ion NaCl and simulated concrete pore solution

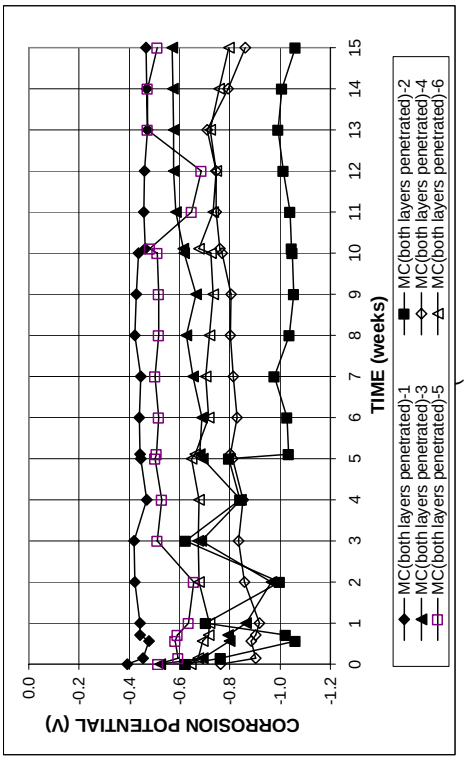

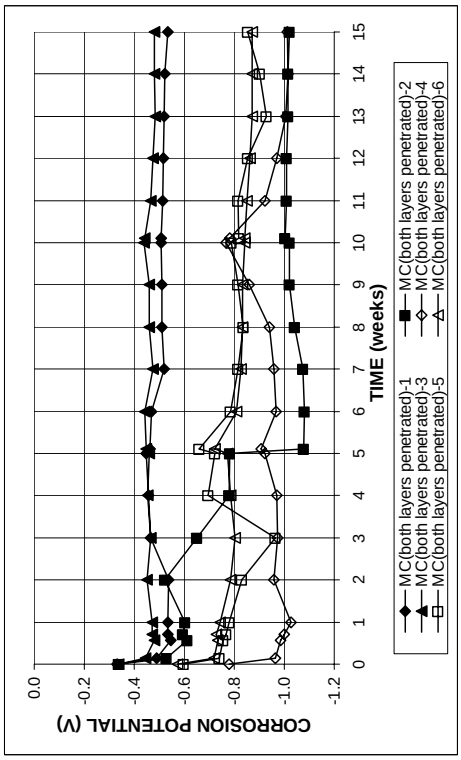

Figure A.104 - (a) Anode corrosion potentials and (b) cathode corrosion potentials with respect to saturated calomel electrode as measured in the rapid macrocell test for mortar-wrapped multiple coated bars with both layers penetrated in 1.6 m ion NaCl and simulated concrete pore solution.

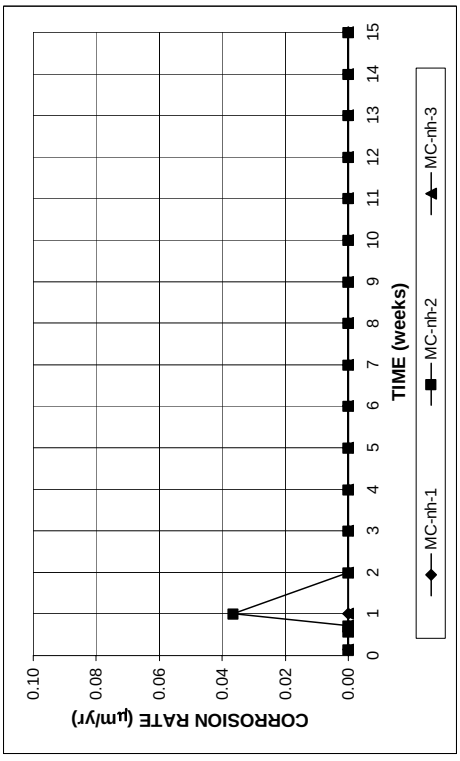

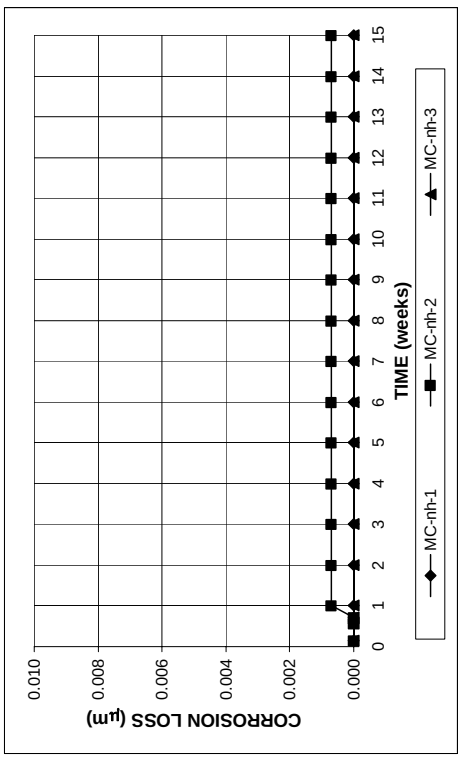

Figure A.105 - (a) Corrosion rates and (b) total corrosion Losses based on total bar area as measured in the rapid macrocell test for mortar-wrapped multiple coated bars without drilled holes in 1.6 m ion NaCl and simulated concrete pore solution

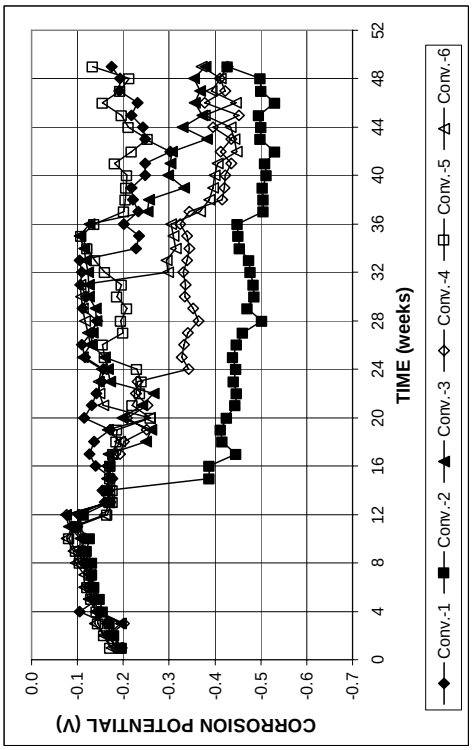

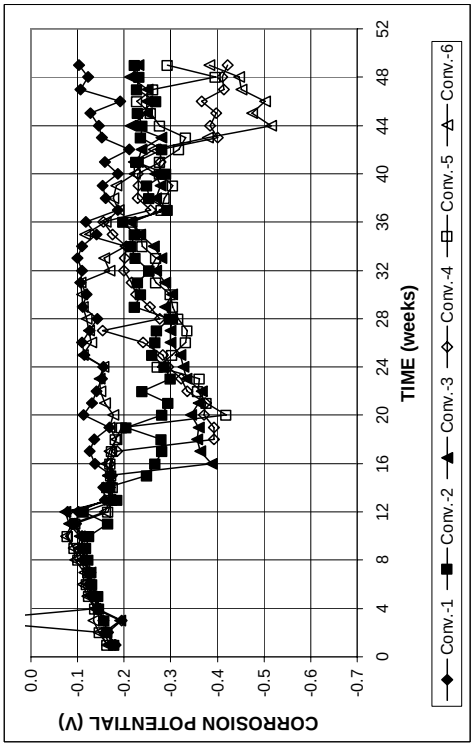

Figure A. 107 - (a) Top mat corrosion potentials and (b) bottom mat corrosion potentials as measured in the Southern Exposure test for specimens containing conventiional steel

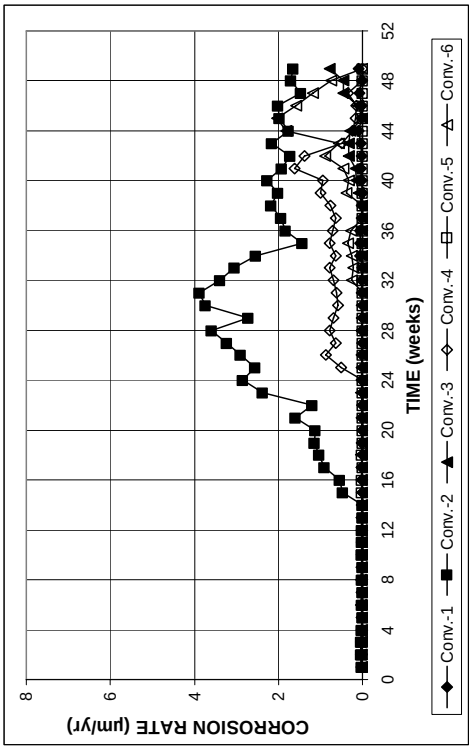

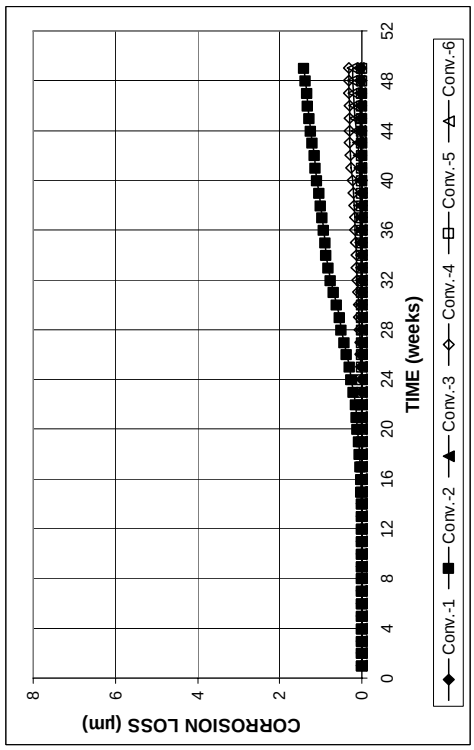

Figure A. 106 - (a) Corrosion rates and (b) total corrosion losses based on total bar area as measured in the Southern Exposure test for specimens containing conventional steel

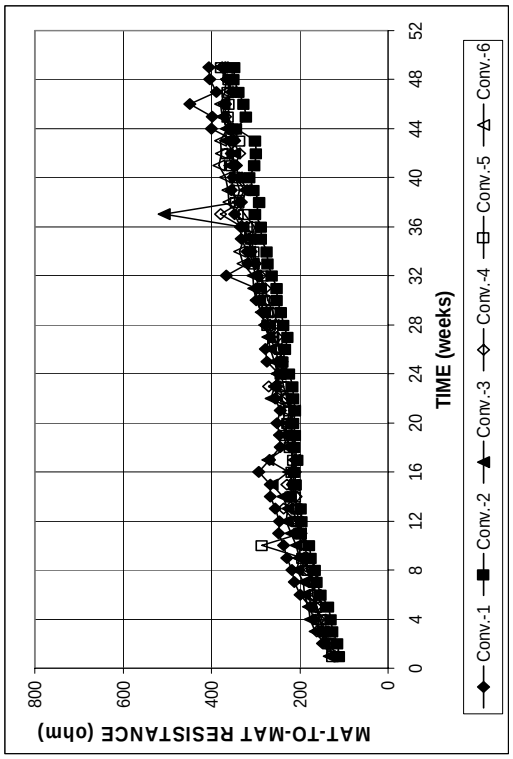

Figure A. 108 - Mat-to-mat resistances as measured in the Southern Exposure test for specimens containing conventional steel

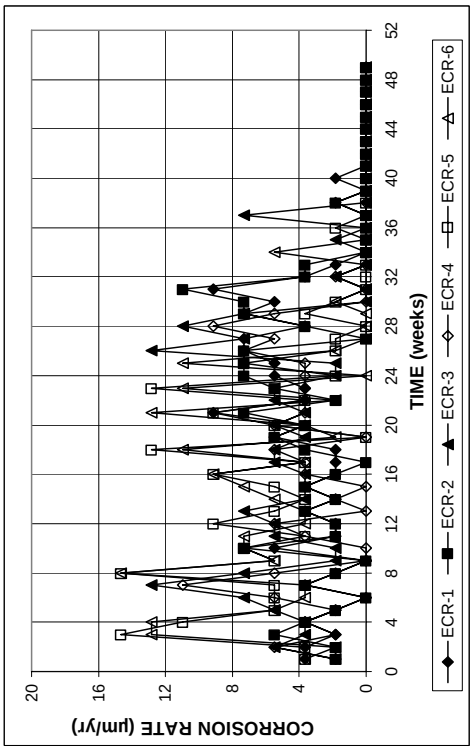

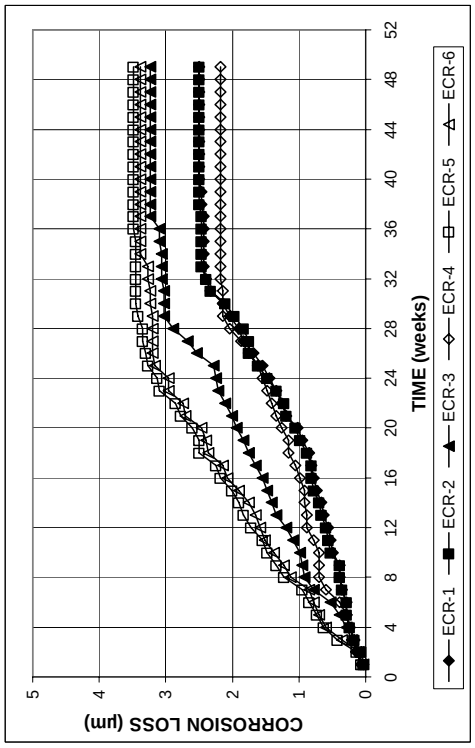

Figure A. 110 - (a) Corrosion rates and (b) total corrosion losses based on exposed area as measured in the Southern Exposure test for specimens containing epoxy-coated bars

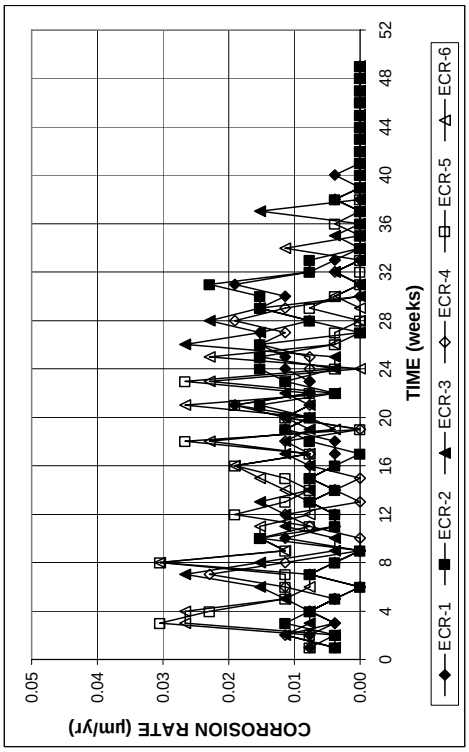

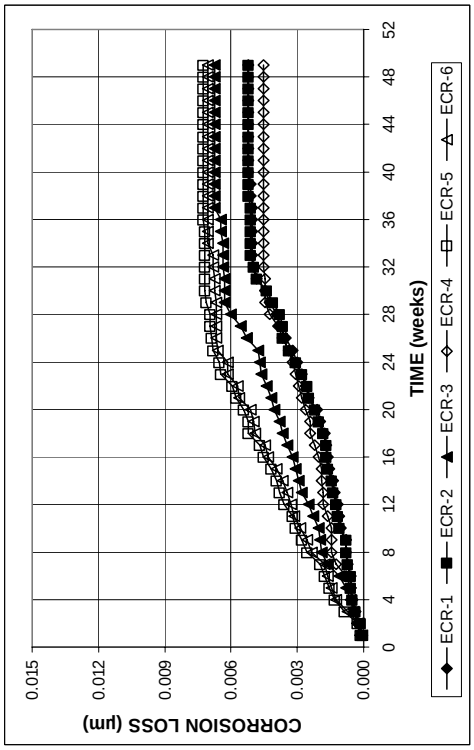

Figure A. 109 - (a) Corrosion rates and (b) total corrosion losses based on total bar area as measured in the Southern Exposure test for specimens containing epoxy-coated bars

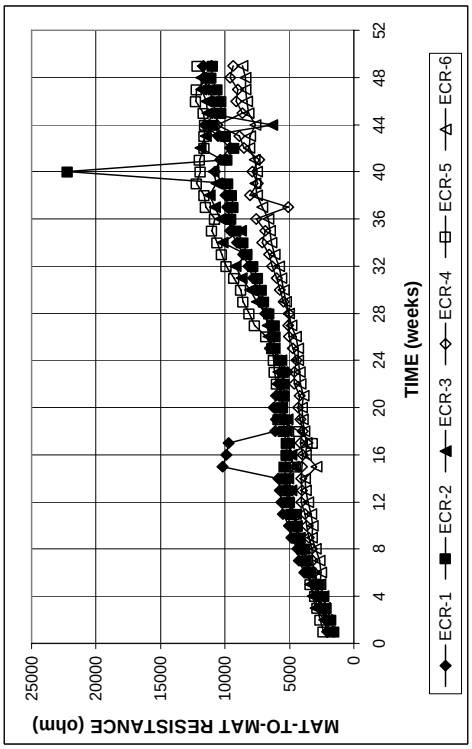

Figure A. 112 - Mat-to-mat resistances as measured in the Southern Exposure test for for specimens containing epoxy-coated bars

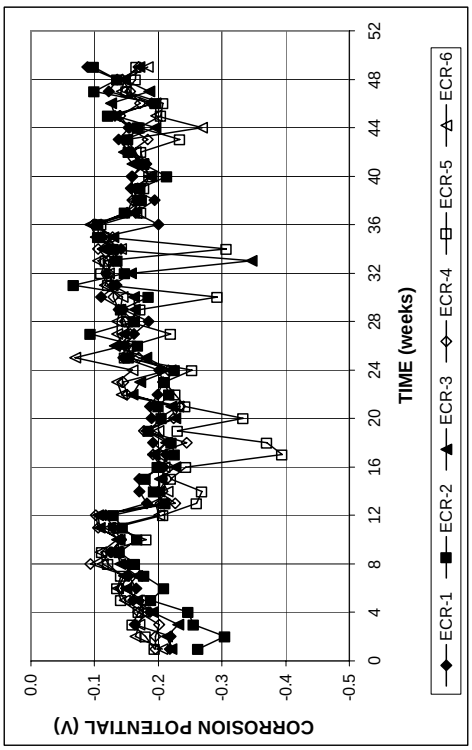

Figure A. 111 - (a) Top mat corrosion potentials and (b) bottom mat corrosion potentials as measured in the Southern Exposure test for specimens containing epoxy-coated bars

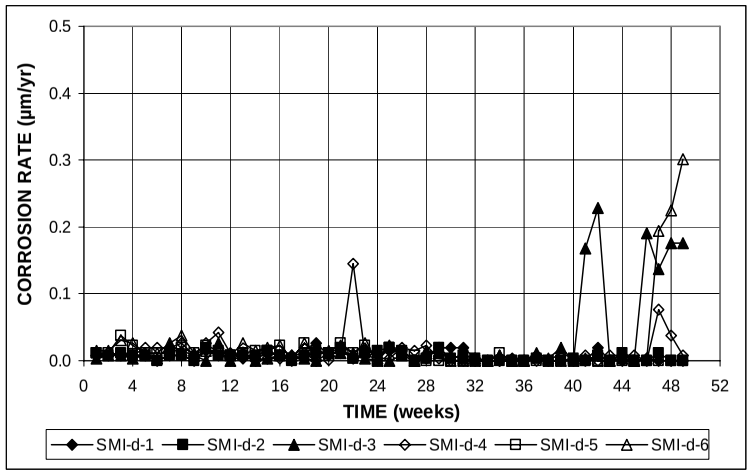

(a)

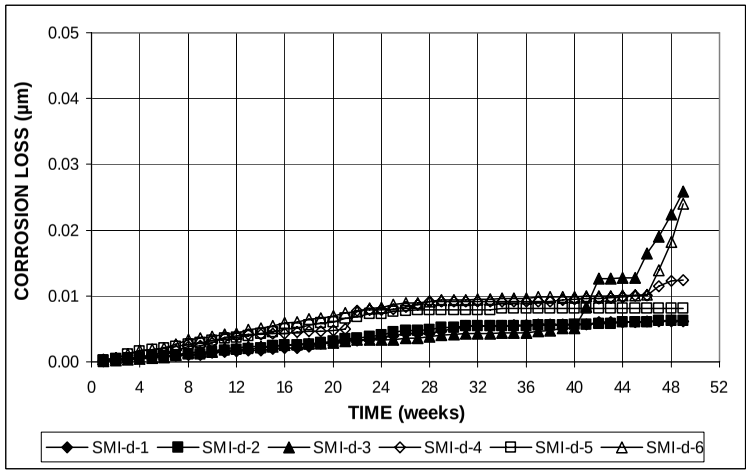

(b)

Figure A. 113 - (a) Corrosion rates and (b) total corrosion losses based on total bar area as measured in the Southern Exposure test for specimens containing stainless steel clad bars with drilled holes

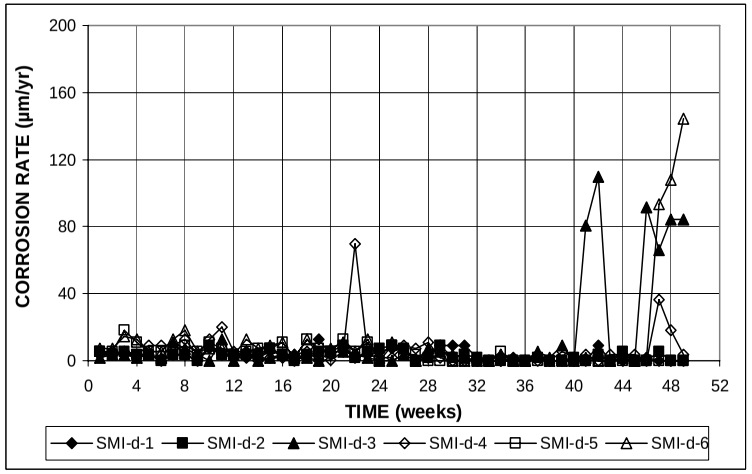

(a)

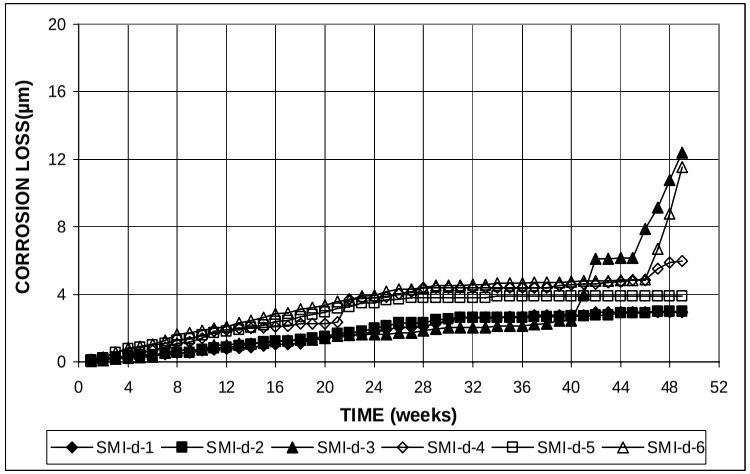

(b)

Figure A. 114 - (a) Corrosion rates and (b) total corrosion losses based on exposed area as measured in the Southern Exposure test for specimens containing stainless steel clad bars with drilled holes

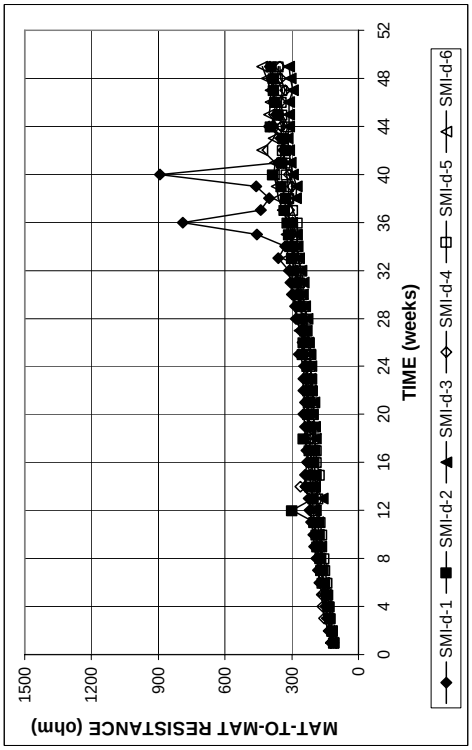

Figure A. 116 - Mat-to-mat resistances as measured in the Southern Exposure test for specimens containing stainless steel clad bars with drilled holes

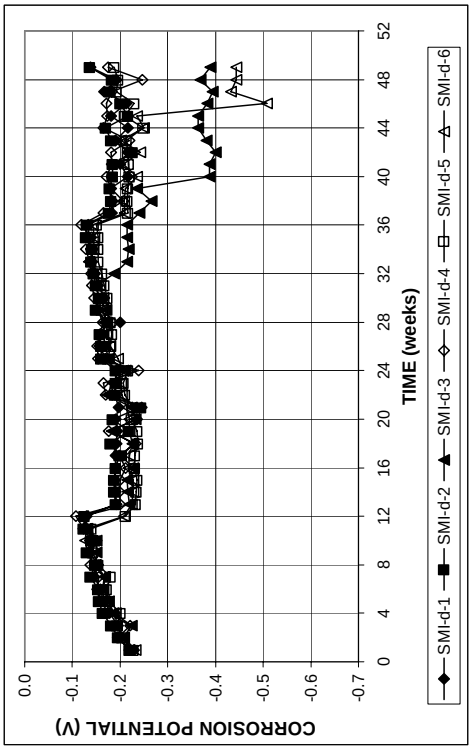

Figure A. 115 - (a) Top mat corrosion potentials and (b) bottom mat corrosion potentials as measured in the Southern Exposure test for specimens containing stainless steel clad bars with drilled holes

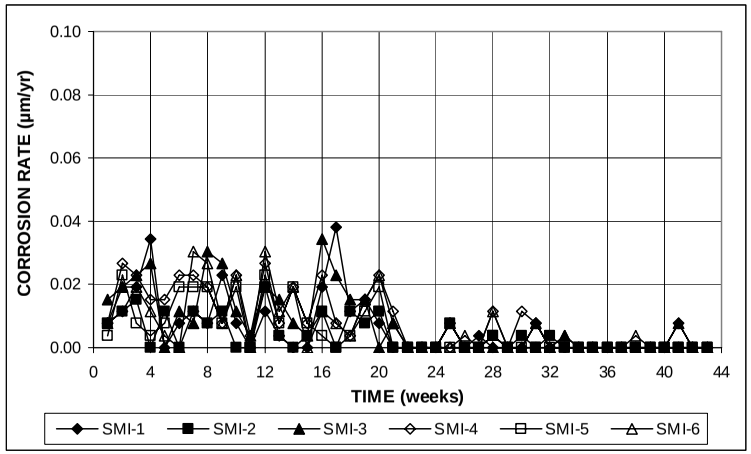

(a)

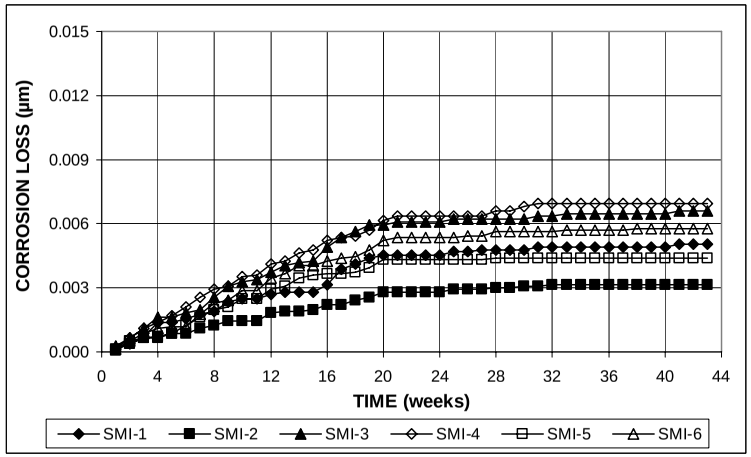

(b)

Figure A. 117 - (a) Corrosion rates and (b) total corrosion losses based on total bar area as measured in the Southern Exposure test for specimens containing stainless steel clad bars with drilled holes

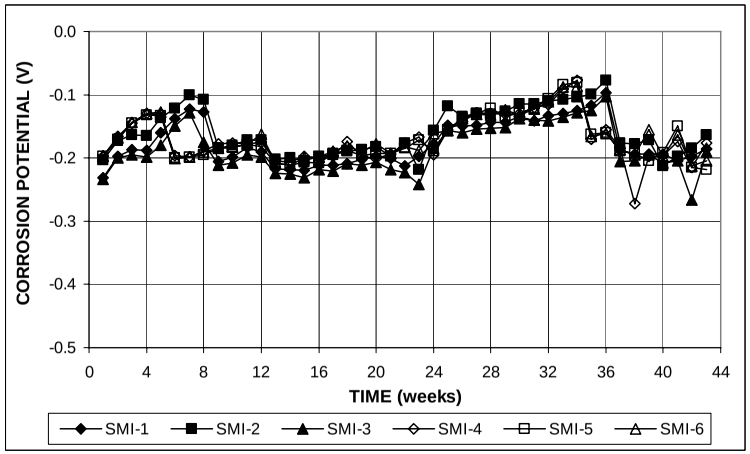

(a)

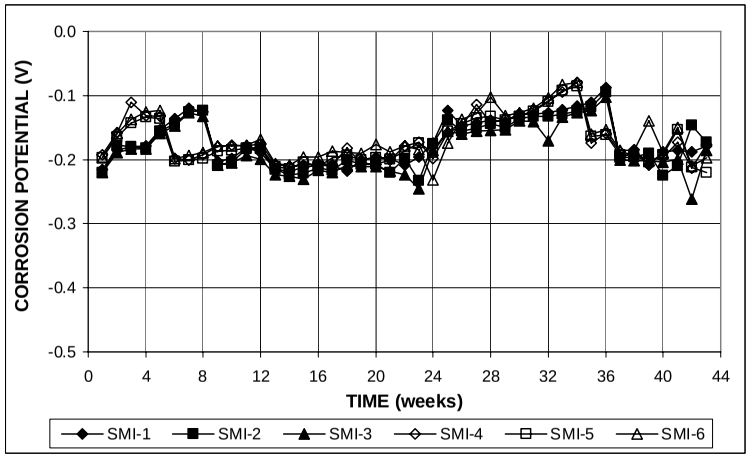

(b)

Figure A. 118 - (a) Top mat corrosion potentials and (b) bottom mat corrosion potentials as measured in the Southern Exposure test for specimens containing stainless steel clad bars with drilled holes

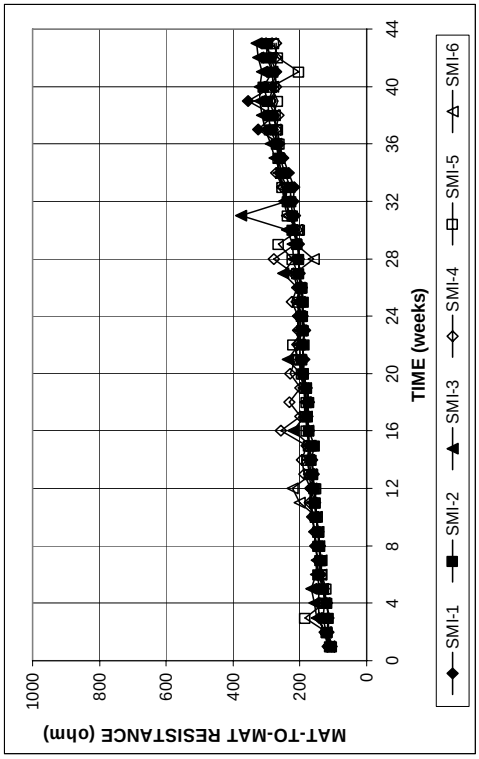

Figure A. 119 - Mat-to-mat resistances as measured in the Southern Exposure test for specimens containing stainless steel clad bars with drilled holes

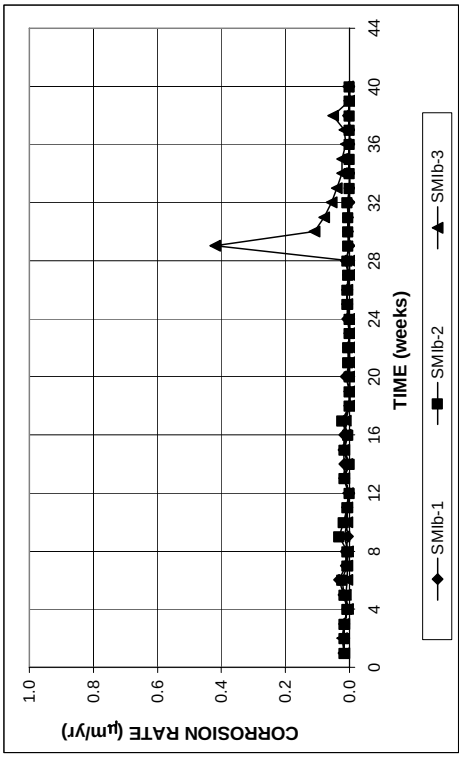

Figure A. 120 - (a) Corrosion rates and (b) total corrosion losses based on total bar area as measured in the Southern Exposure test for specimens containing bent stainless steel clad bars as anode and straight stainless steel clad bars as cathode

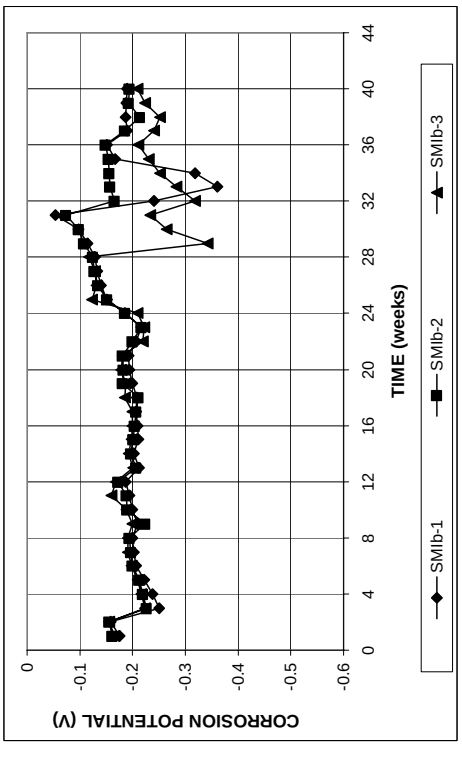

Figure A. 121 - (a) Top mat corrosion potentials and (b) bottom mat corrosion potentials as measured in the Southern Exposure test for specimens containing bent stainless steel clad bars as anode and straight stainless steel clad bars as cathode

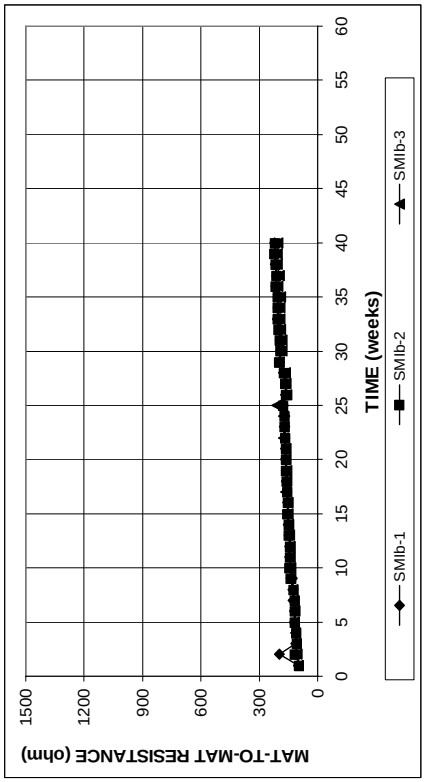

Figure A. 122 - Mat-to-mat resistances as measured in the Southern Exposure test for specimens containing bent stainless steel clad bars as anode and straight stainless steel clad bars as cathode

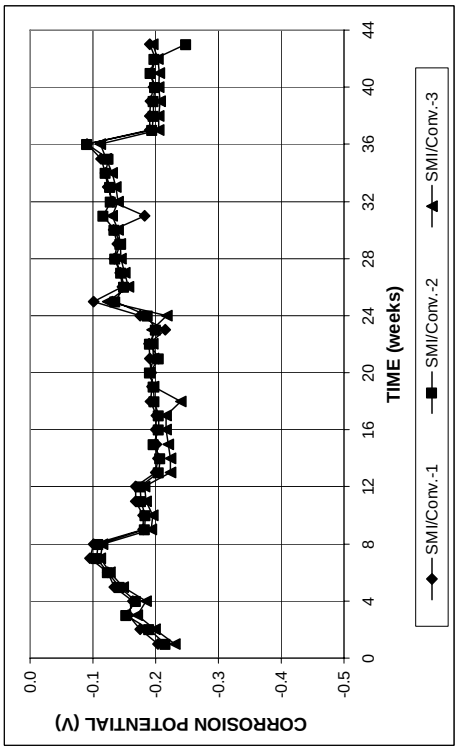

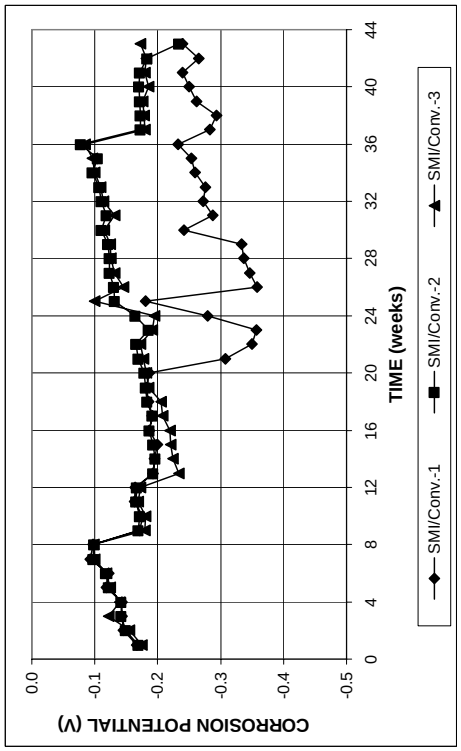

Figure A. 124 - (a) Top mat corrosion potentials and (b) bottom mat corrosion potentials as measured in the Southern Exposure test for specimens containing stainless steel clad bars as anode and conventional steel as cathode

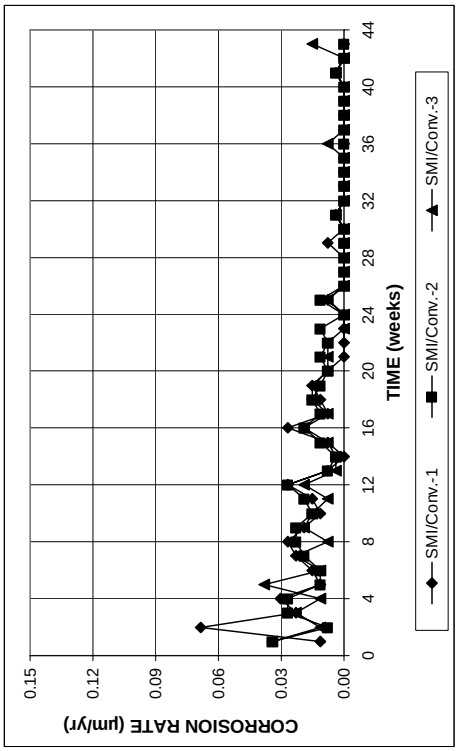

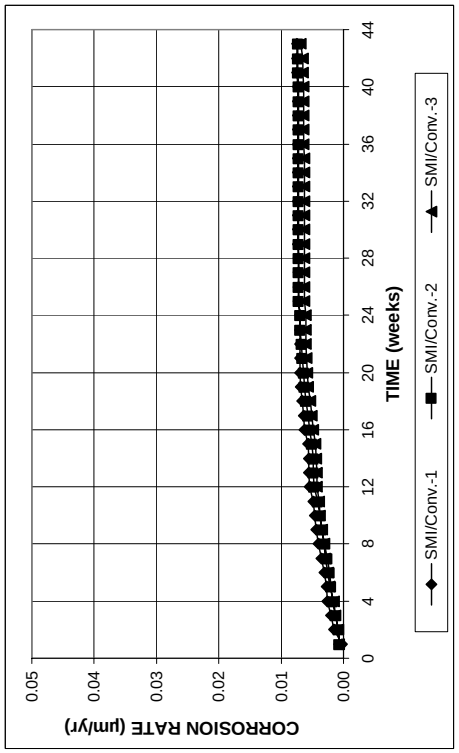

Figure A. 123 - (a) Corrosion rates and (b) total corrosion losses based on total bar area as measured in the Southern Exposure test for specimens containing stainless steel clad bars as anode and conventional steel as cathode

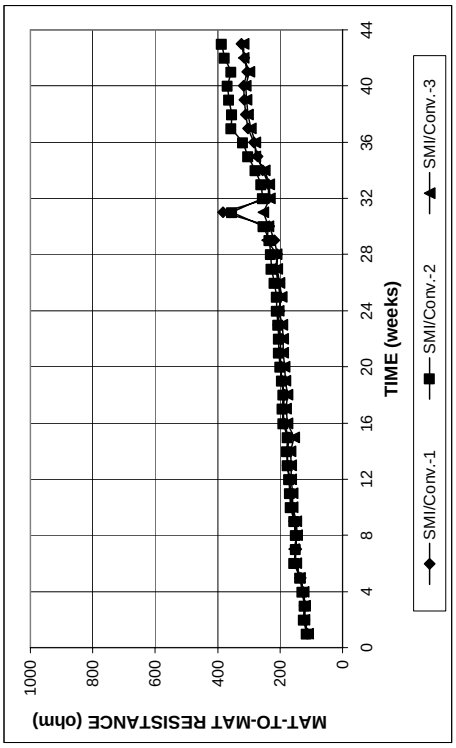

Figure A. 125 - Mat-to-mat resistances as measured in the Southern Exposure test for specimens containing stainless steel clad bars as anode and conventional steel as cathode

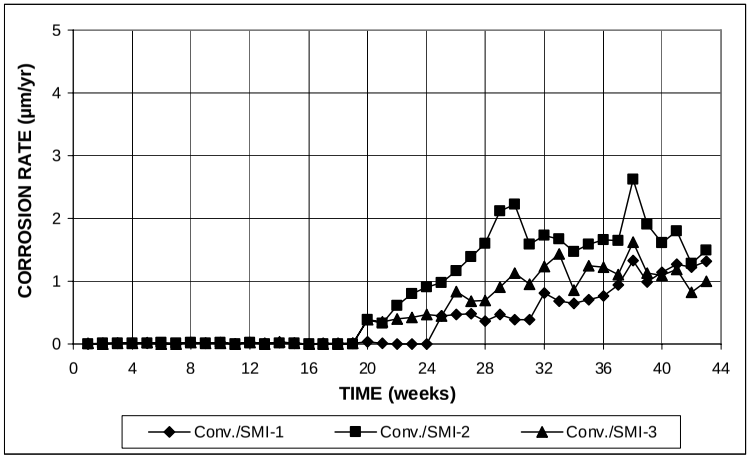

(a)

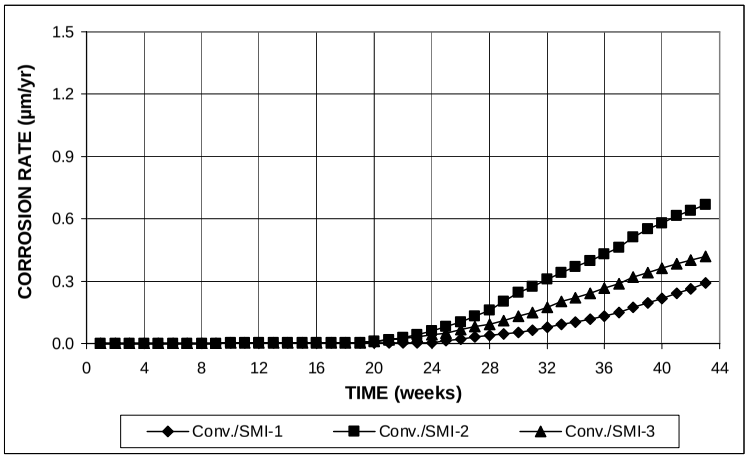

(b)

Figure A. 126 - (a) Corrosion rates and (b) total corrosion losses based on total bar area as measured in the cracked beam test for specimens containing conventional steel as anode and stainless steel clad bars as cathode

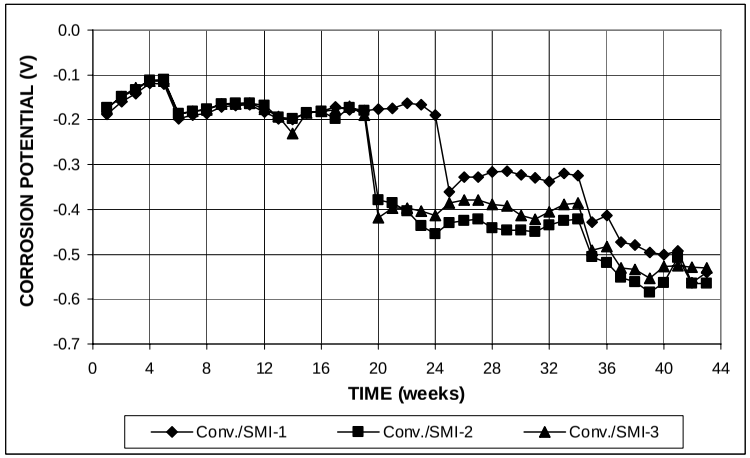

(a)

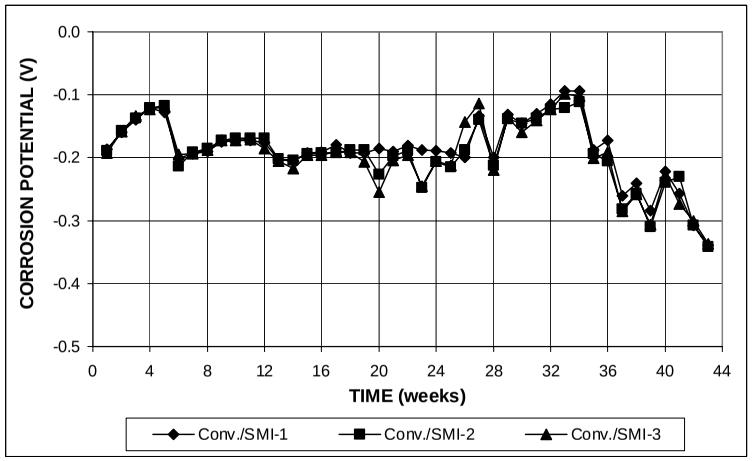

(b)

Figure A. 127 - (a) Top mat corrosion potentials and (b) bottom mat corrosion potentials as measured in the cracked beam test for specimens containing conventional steel as anode and stainless steel clad bars as cathode

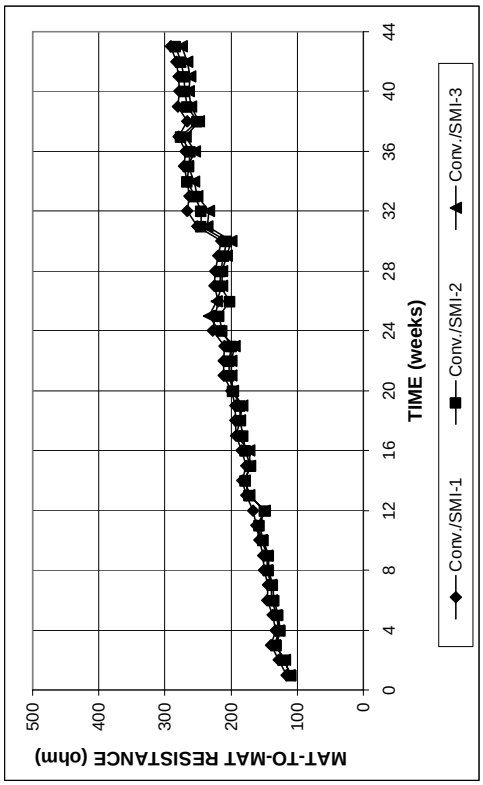

Figure A. 128 - Mat-to-mat resistances as measured in the Southern Exposure test for specimens containing conventional steel as anode and stainless steel clad bars as cathode

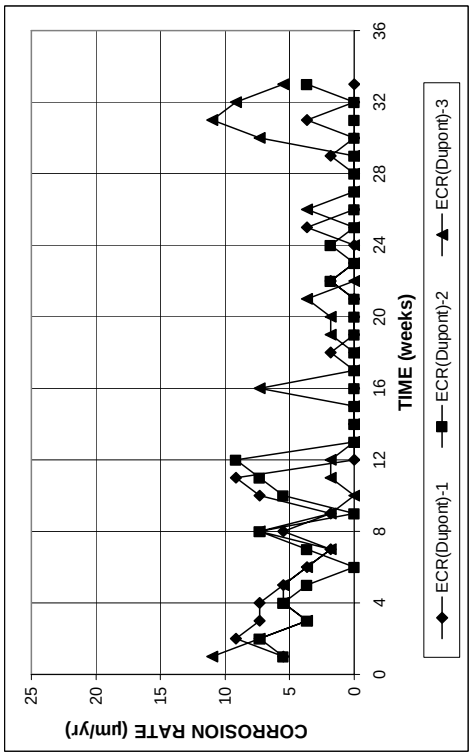

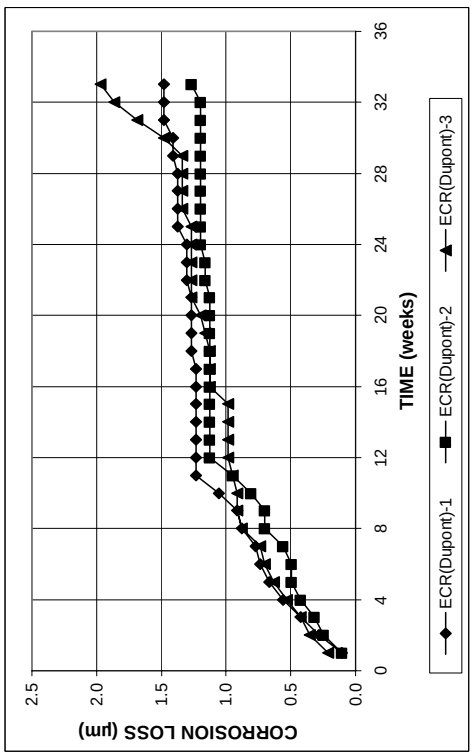

Figure A. 130 - (a) Corrosion rates and (b) total corrosion losses based on total bar area as measured in the Southern Exposure test for specimens containing ECR(Dupont) bars

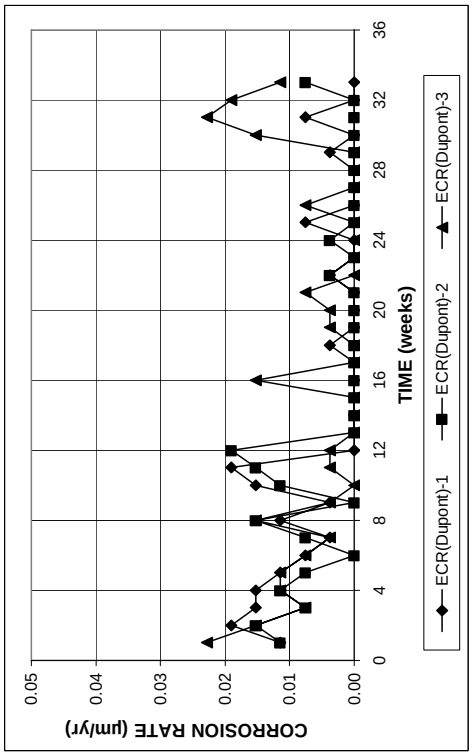

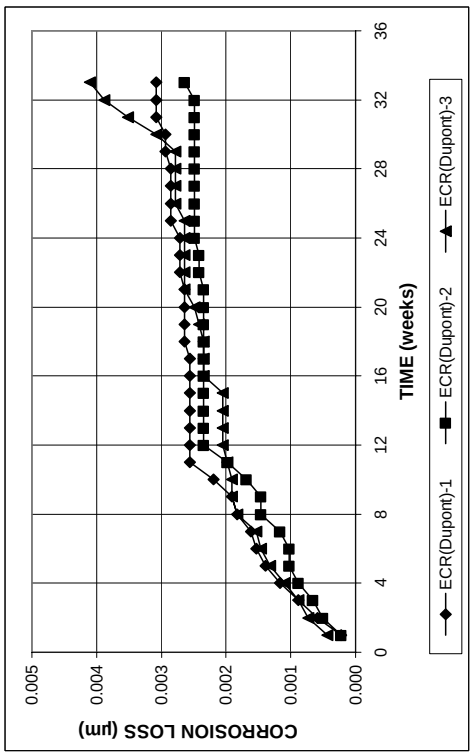

Figure A. 129 - (a) Corrosion rates and (b) total corrosion losses based on total bar area as measured in the Southern Exposure test for specimens containing ECR(Dupont) bars

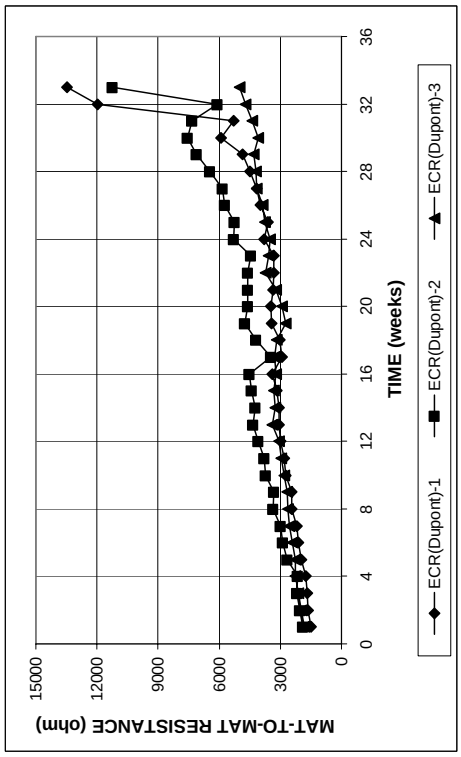

Figure A. 132 - Mat-to-mat resistances as measured in the Southern Exposure test for specimens containing ECR(Dupont) bars

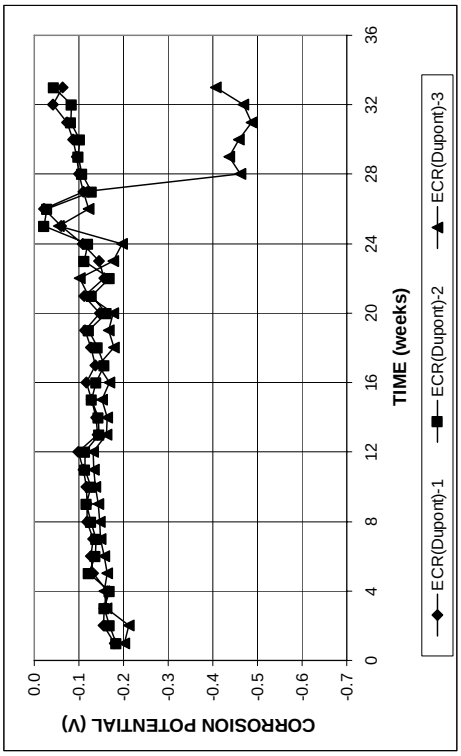

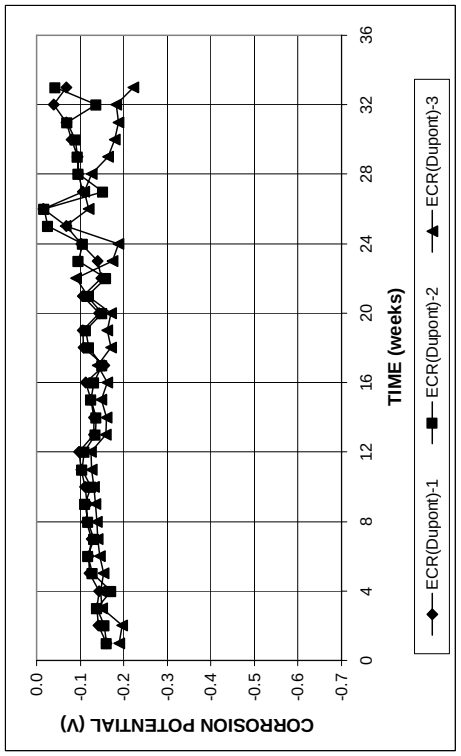

Figure A. 131 - (a) Top mat corrosion potentials and (b) bottom mat corrosion potentials as measured in the Southern Exposure test for specimens containing ECR(Dupont) bars

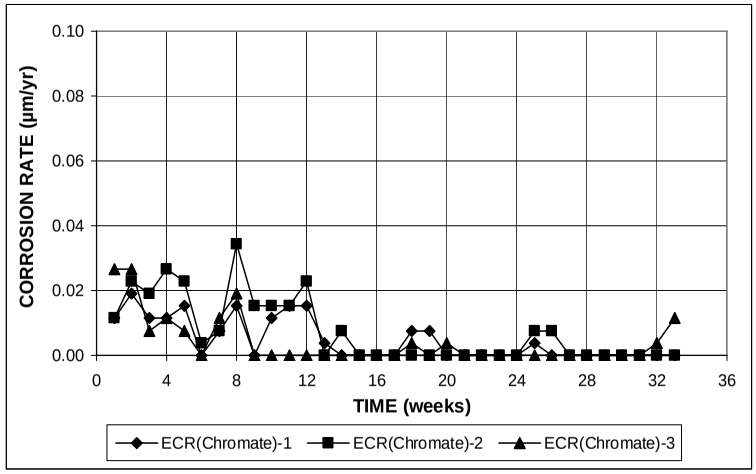

(a)

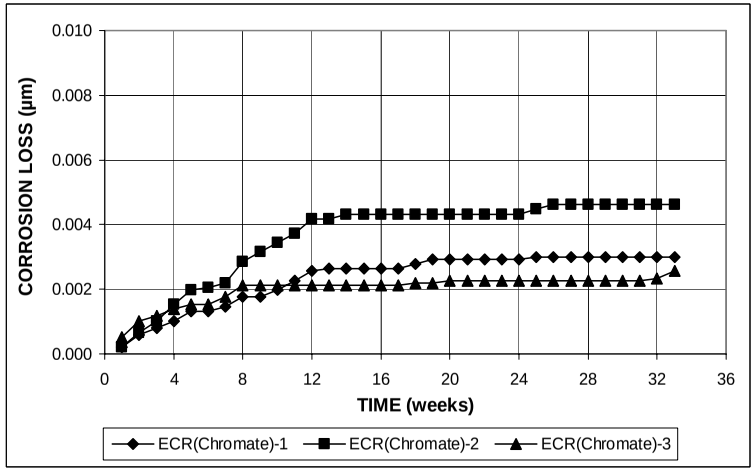

(b)

Figure A. 133 - (a) Corrosion rates and (b) total corrosion losses based on total bar area as measured in the Southern Exposure test for specimens containing ECR(Chromate) bars

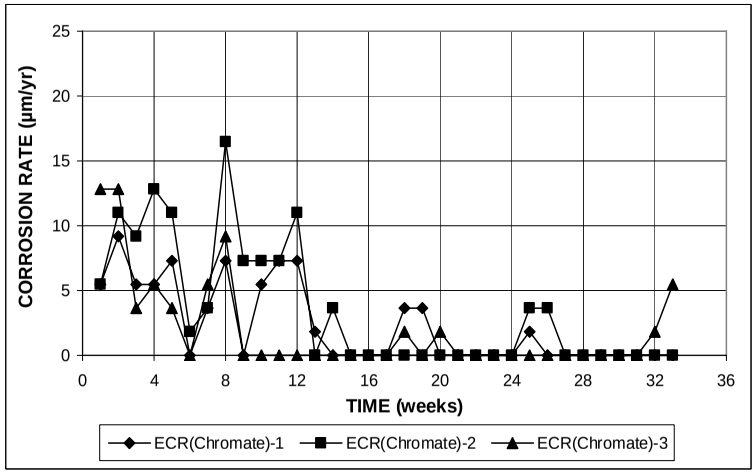

(a)

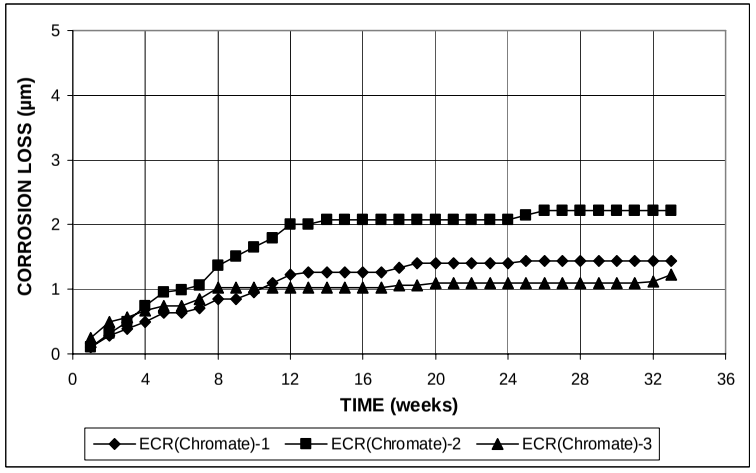

(b)

Figure A. 134 - (a) Corrosion rates and (b) total corrosion losses based on total bar area as measured in the Southern Exposure test for specimens containing ECR(Chromate) bars

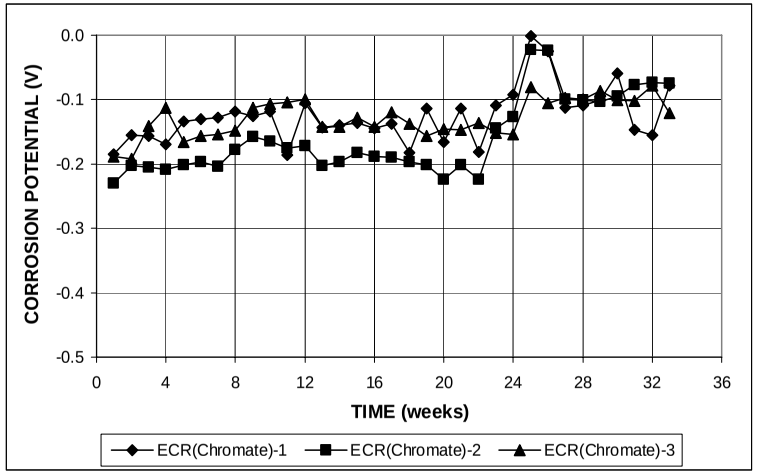

(a)

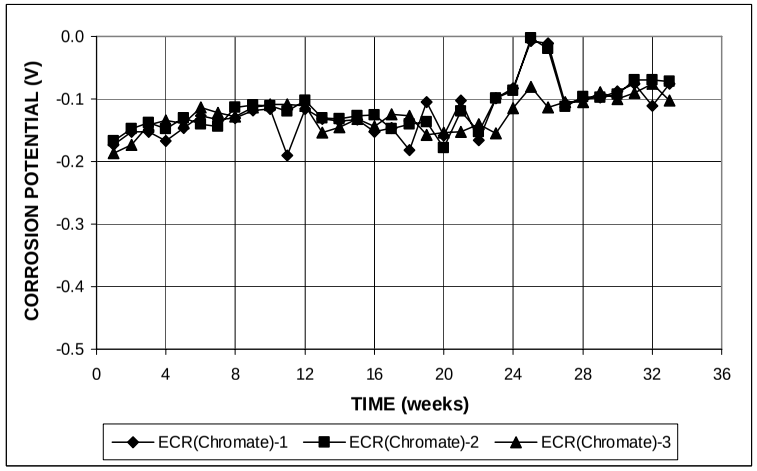

(b)

Figure A. 135 - (a) Top mat corrosion potentials and (b) bottom mat corrosion potentials as measured in the Southern Exposure test for specimens containing ECR(Chromate) bars

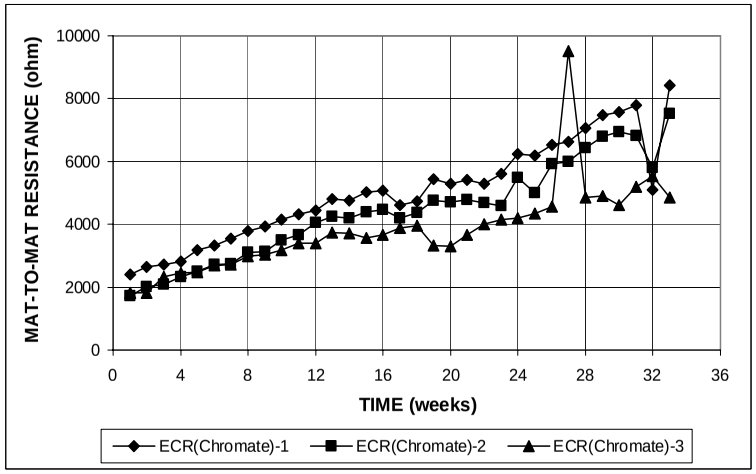

Figure A. 136 - Mat-to-mat resistances as measured in the Southern Exposure test for specimens containing ECR(Chromate) bars

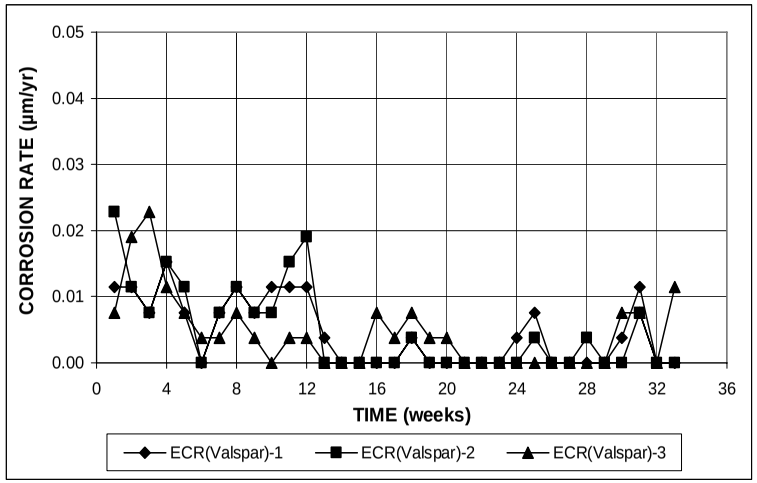

(a)

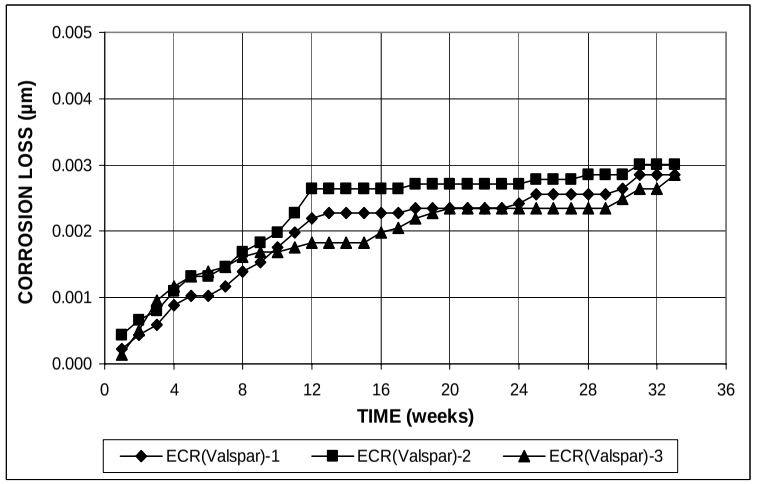

(b)

Figure A. 137 - (a) Corrosion rates and (b) total corrosion losses based on total bar area as measured in the Southern Exposure test for specimens containing ECR(Valspar) bars

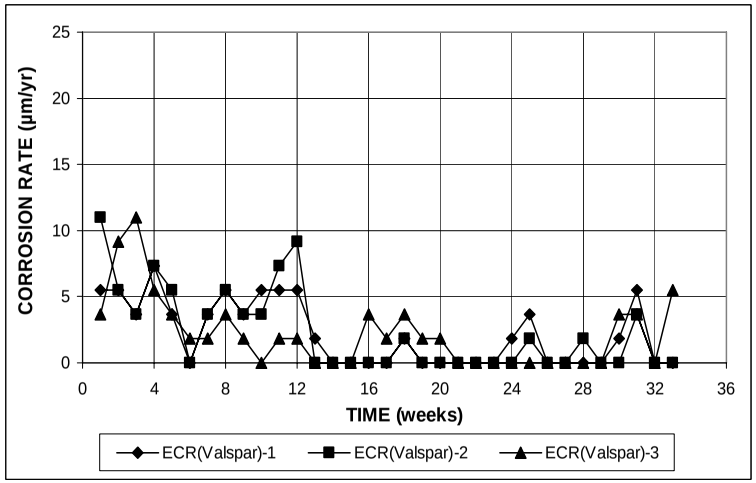

(a)

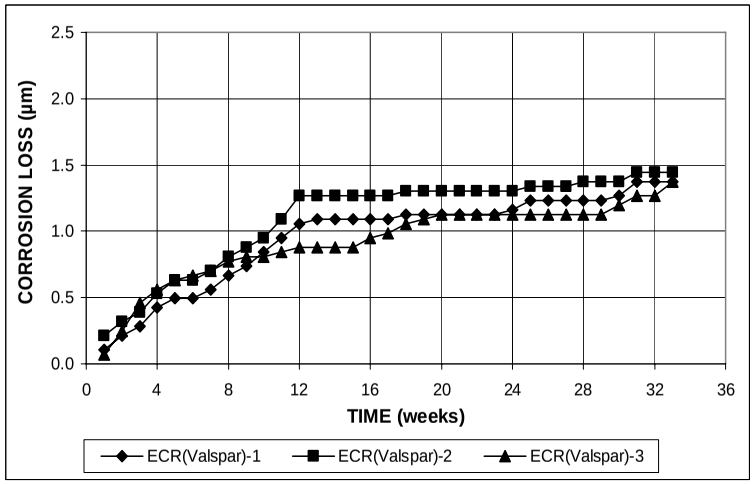

(b)

Figure A. 138 - (a) Corrosion rates and (b) total corrosion losses based on total bar area as measured in the Southern Exposure test for specimens containing ECR(Valspar) bars

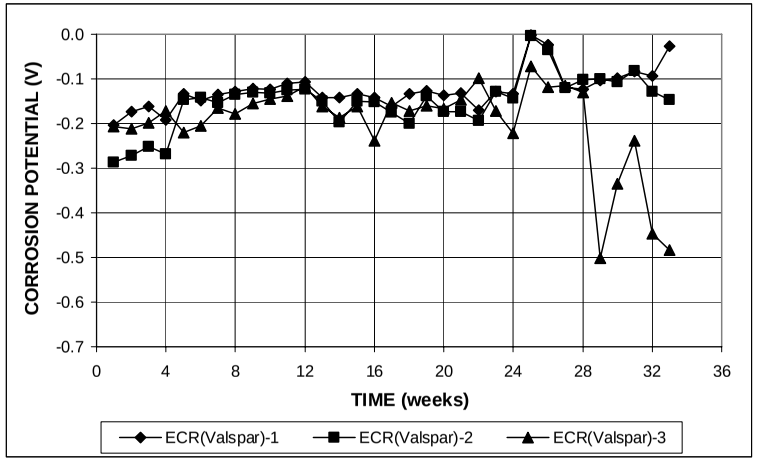

(a)

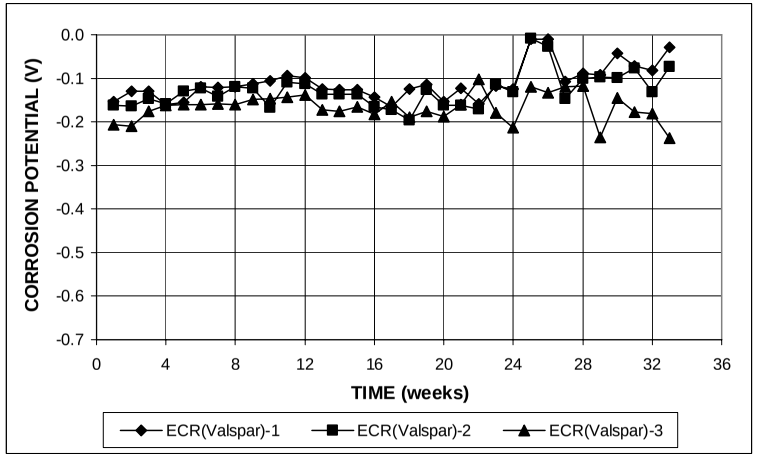

(b)

Figure A. 139 - (a) Top mat corrosion potentials and (b) bottom mat corrosion potentials as measured in the Southern Exposure test for specimens containing ECR(Valspar) bars

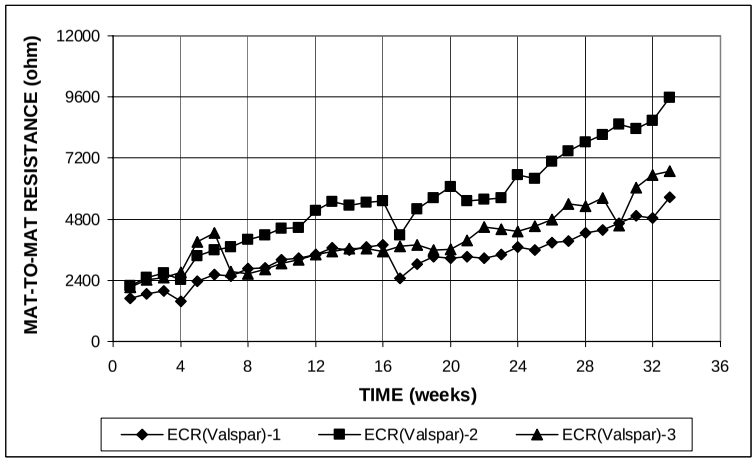

Figure A. 140 - Mat-to-mat resistances as measured in the Southern Exposure test for specimens containing ECR(Valspar) bars

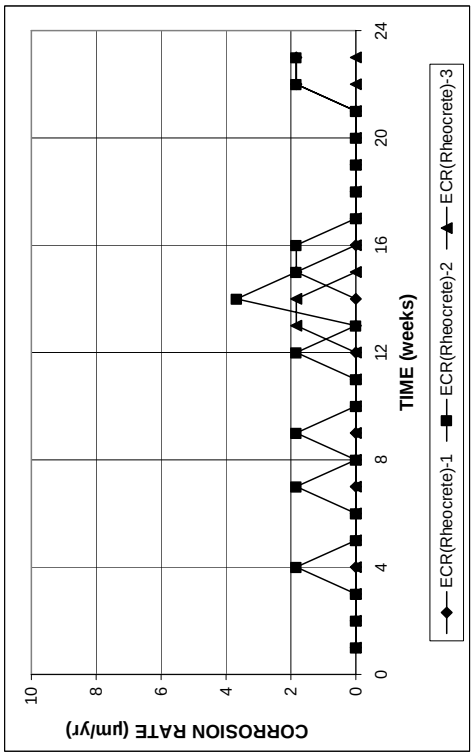

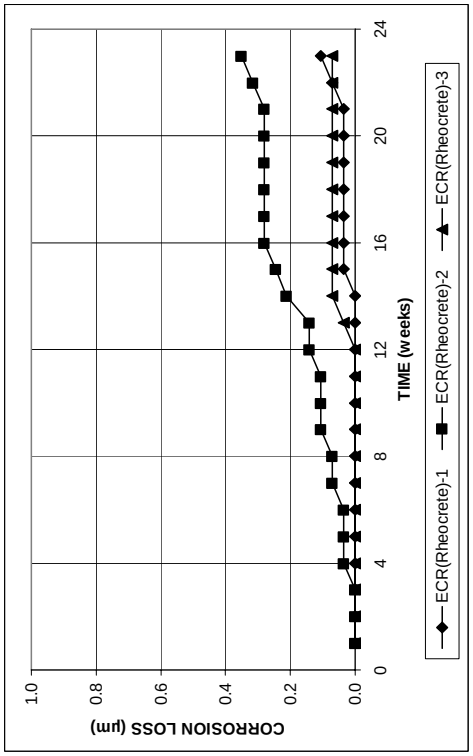

Figure A. 142 - (a) Corrosion rates and (b) total corrosion losses based on exposed area as measured in the Southern Exposure test for specimens containing epoxy-coated steel and corrosion inhibitor Rheocrete

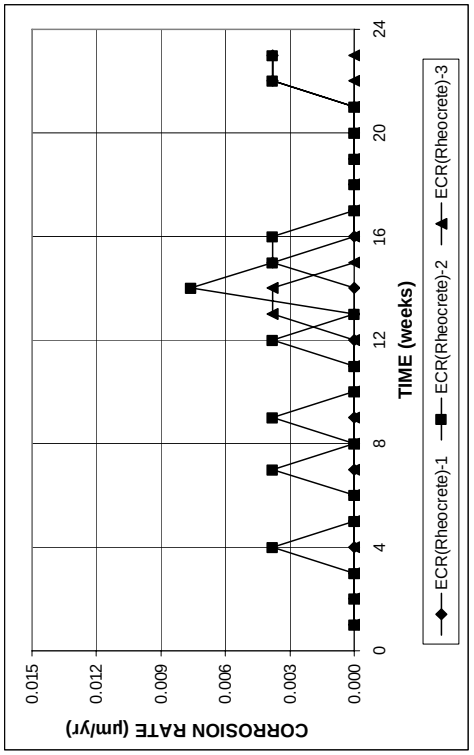

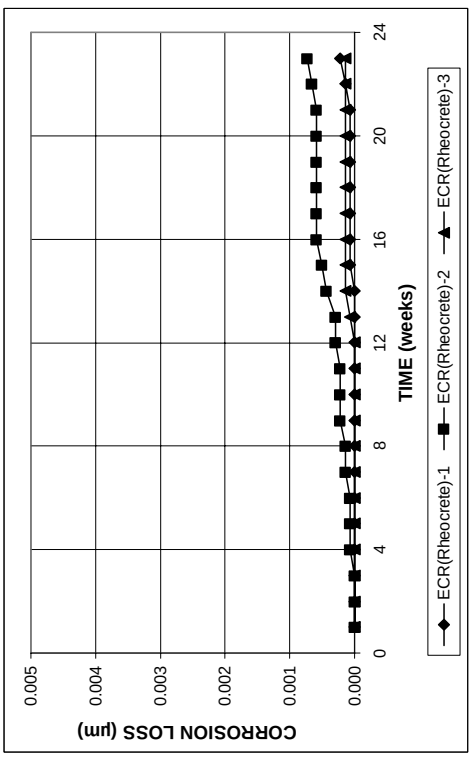

Figure A. 141 - (a) Corrosion rates and (b) total corrosion losses based on total bar area as measured in the Southern Exposure test for specimens containing epoxy-coated steel and corrosion inhibitor Rheocrete

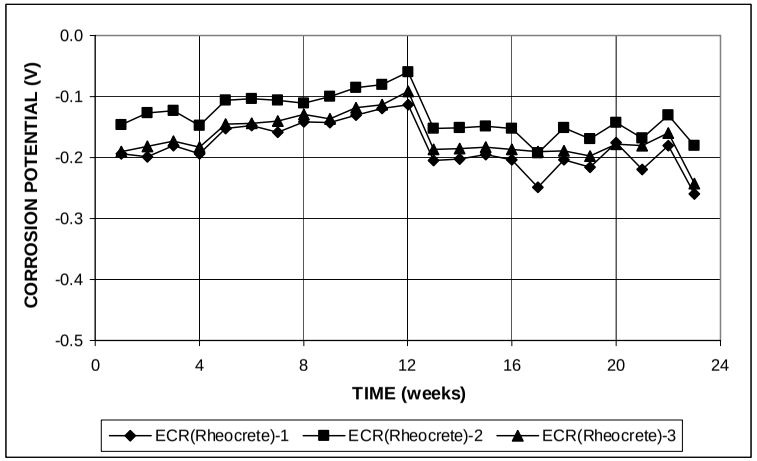

(a)

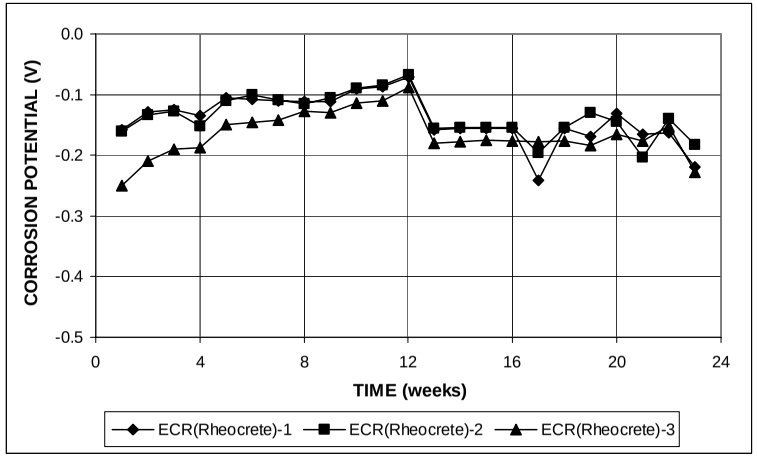

(b)

Figure A. 143 - (a) Top mat corrosion potentials and (b) bottom mat corrosion potentials as measured in the Southern Exposure test for specimens containing epoxy-coated steel and corrosion inhibitor Rheocrete

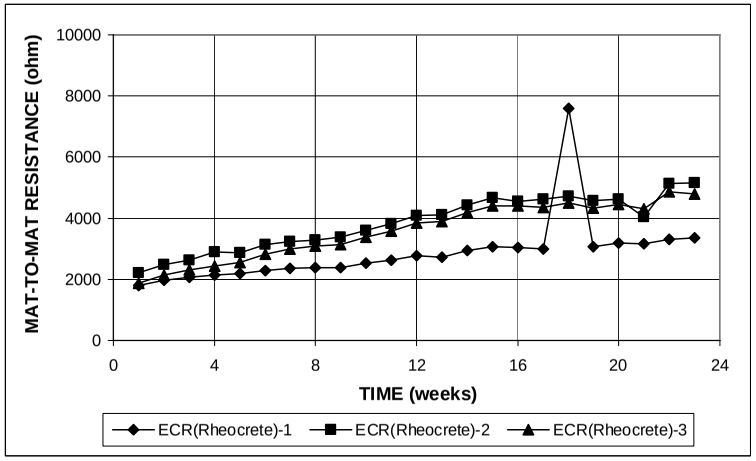

Figure A. 144 - Mat-to-mat resistances as measured in the Southern Exposure test for specimens containing epoxy-coated steel and corrosion inhibitor Rheocrete

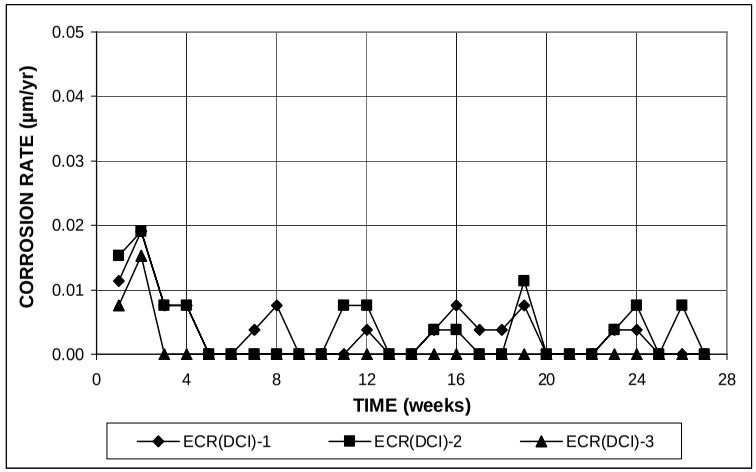

(a)

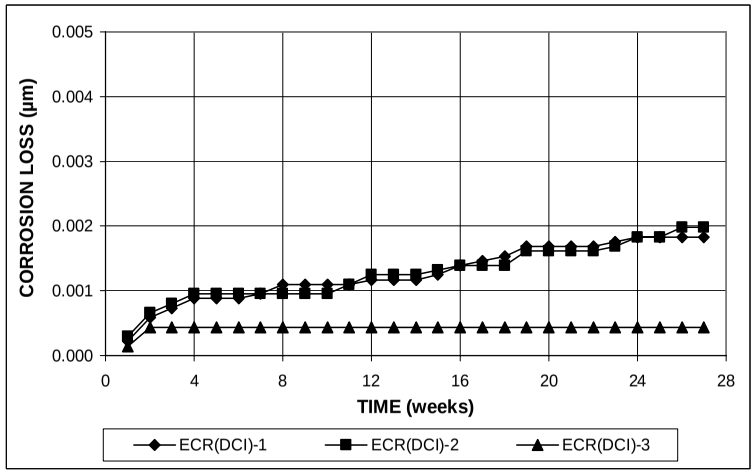

(b)

Figure A. 145 - (a) Corrosion rates and (b) total corrosion losses based on total bar area as measured in the Southern Exposure test for specimens containing epoxy-coated steel and corrosion inhibitor DCI

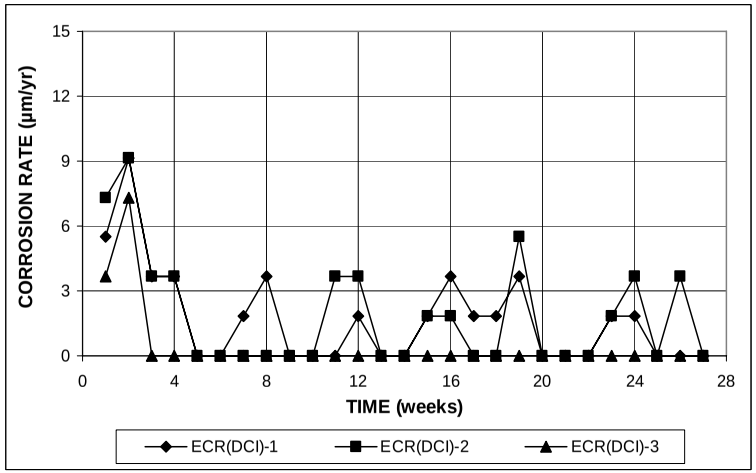

(a)

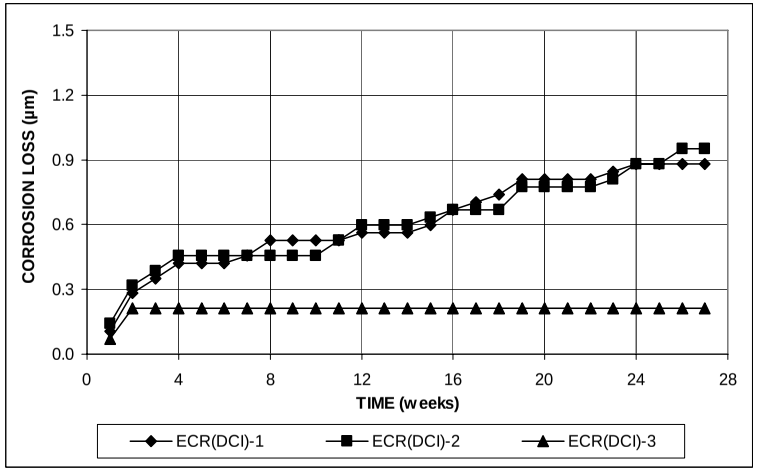

(b)

Figure A. 146 - (a) Corrosion rates and (b) total corrosion losses based on exposed area as measured in the Southern Exposure test for specimens containing epoxy-coated steel and corrosion inhibitor DCI

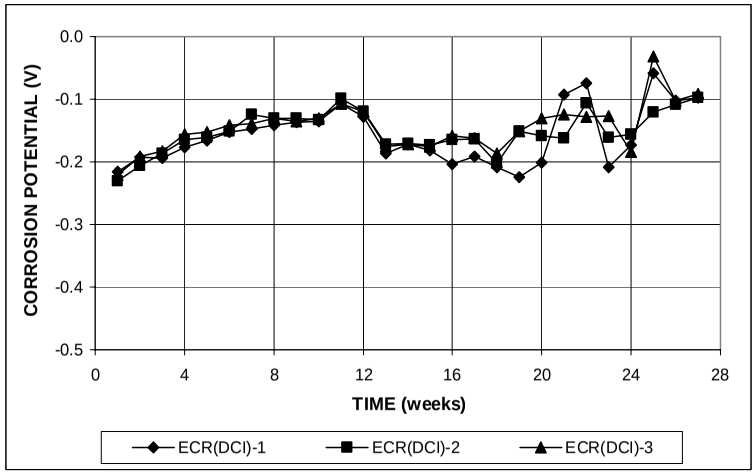

(a)

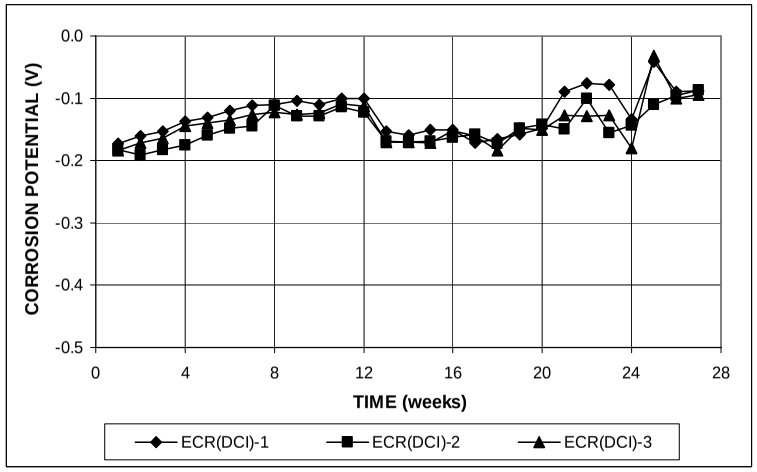

(b)

Figure A. 147 - (a) Top mat corrosion potentials and (b) bottom mat corrosion potentials as measured in the Southern Exposure test for specimens containing epoxy-coated steel and corrosion inhibitor DCI

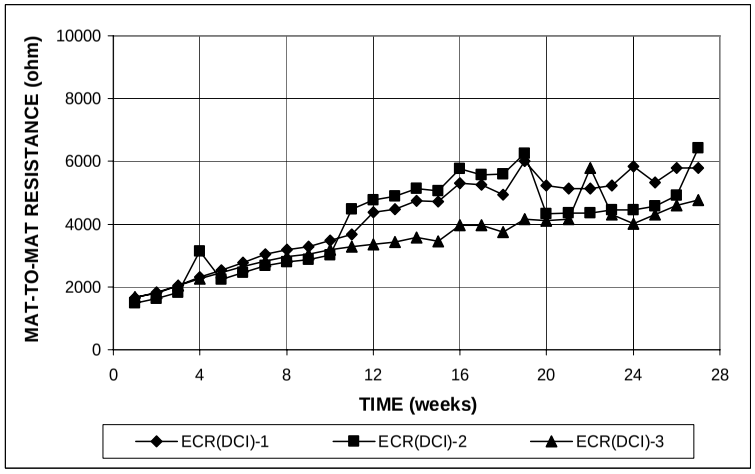

Figure A. 148 - Mat-to-mat resistances as measured in the Southern Exposure test for specimens containing epoxy-coated steel and corrosion inhibitor DCI

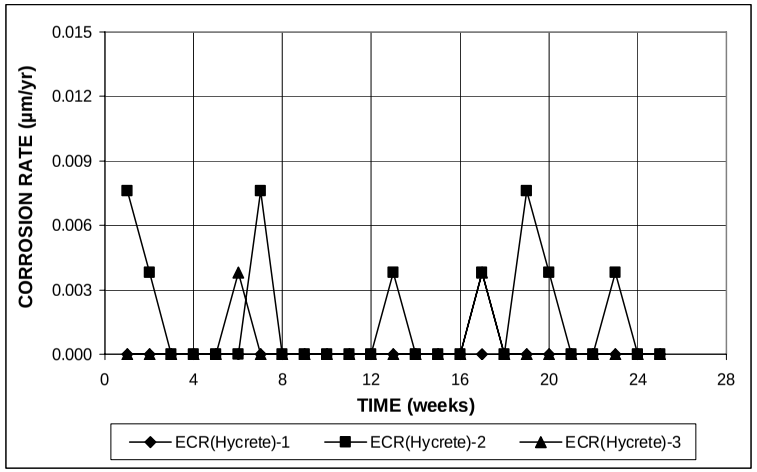

(a)

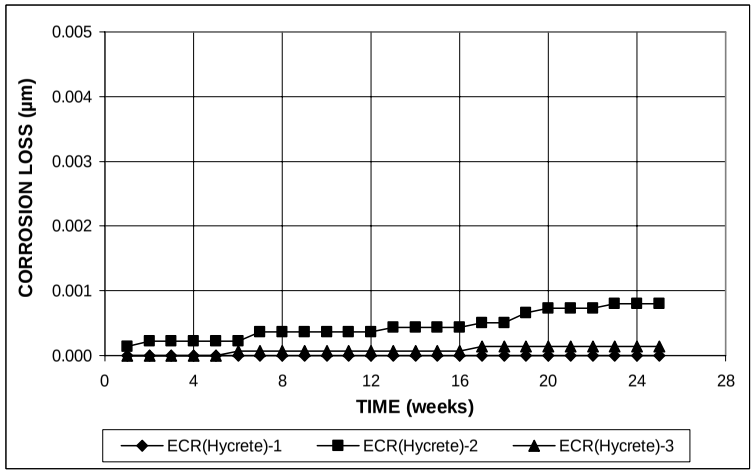

(b)

Figure A. 149 - (a) Corrosion rates and (b) total corrosion losses based on total bar area as measured in the Southern Exposure test for specimens containing epoxy-coated steel and corrosion inhibitor Hycrete

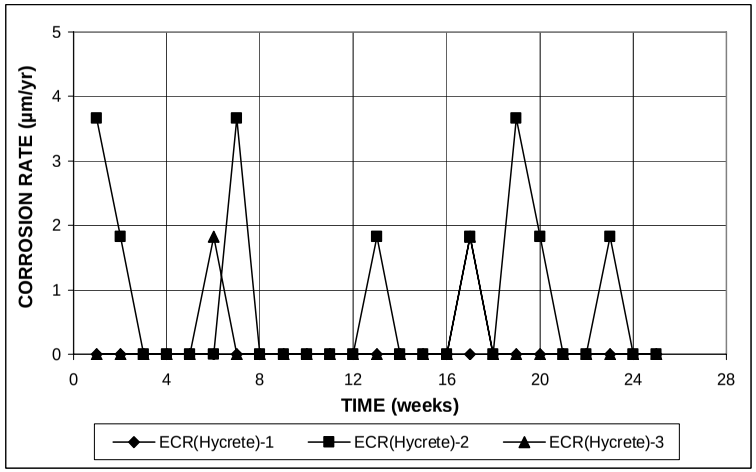

(a)

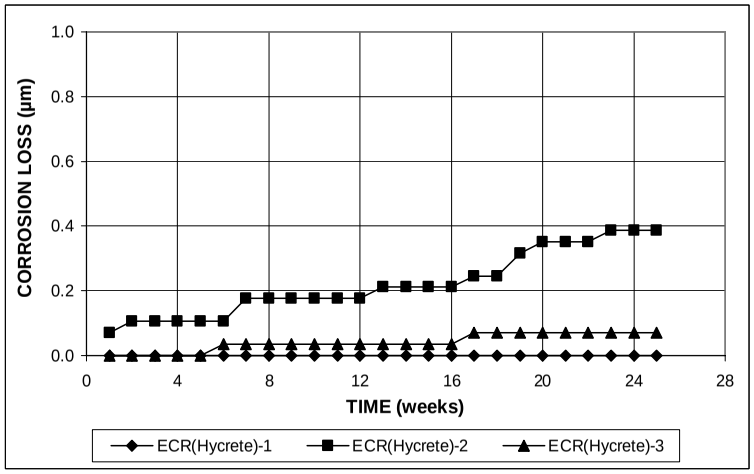

(b)

Figure A. 150 - (a) Corrosion rates and (b) total corrosion losses based on total bar area as measured in the Southern Exposure test for specimens containing epoxy-coated steel and corrosion inhibitor Hycrete

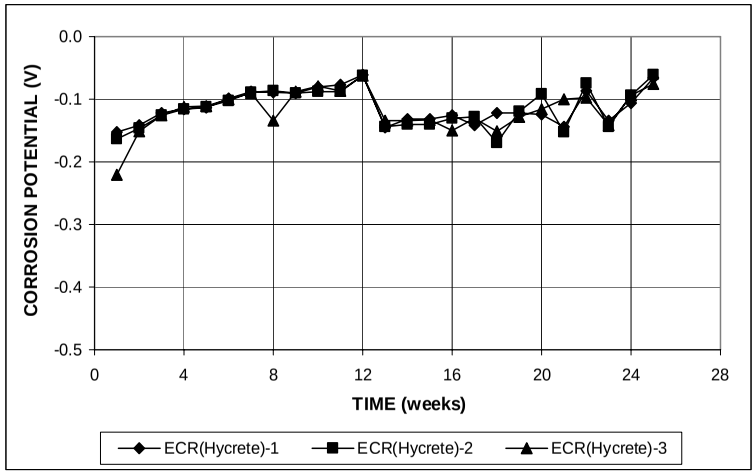

(a)

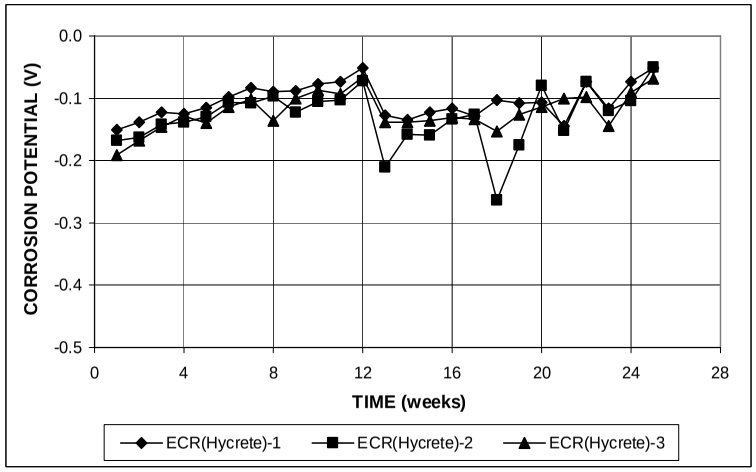

(b)

Figure A. 151 - (a) Top mat corrosion potentials and (b) bottom mat corrosion potentials as measured in the Southern Exposure test for specimens containing epoxy-coated steel and corrosion inhibitor Hycrete

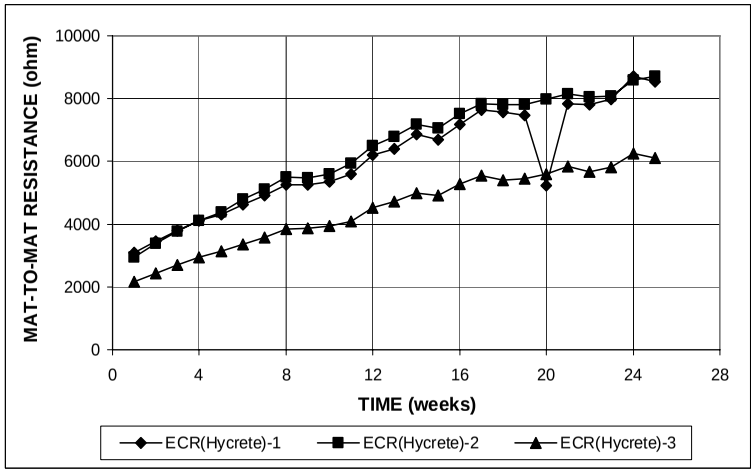

Figure A. 152 - Mat-to-mat resistances as measured in the Southern Exposure test for specimens containing epoxy-coated steel and corrosion inhibitor Hycrete

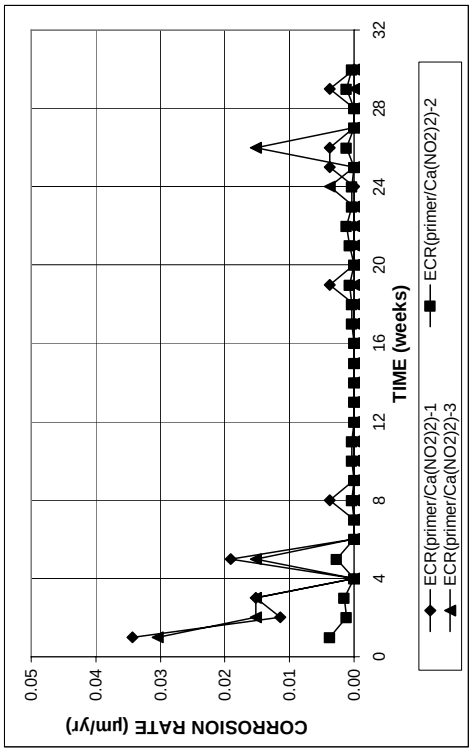

Figure A. 153 - (a) Corrosion rates and (b) total corrosion losses based on total bar area as measured in the Southern Exposure test for specimens containing ECR(primer/$Ca(NO_2)_2$) bars

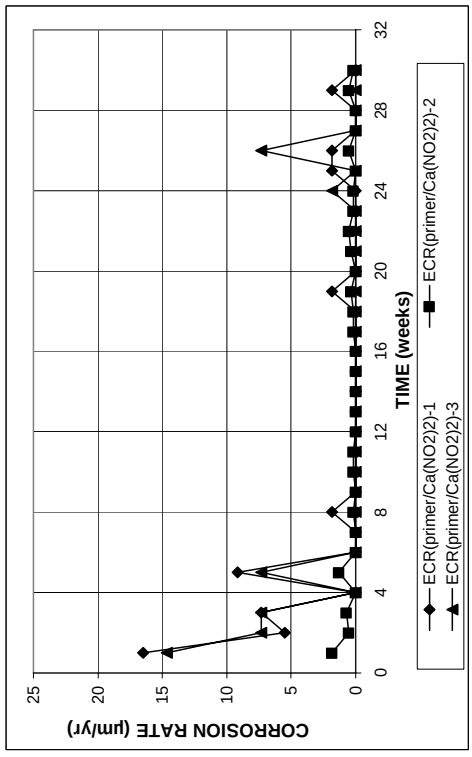

Figure A. 154 - (a) Corrosion rates and (b) total corrosion losses based on exposed area as measured in the Southern Exposure test for specimens containing ECR(primer/$Ca(NO_2)_2$) bars

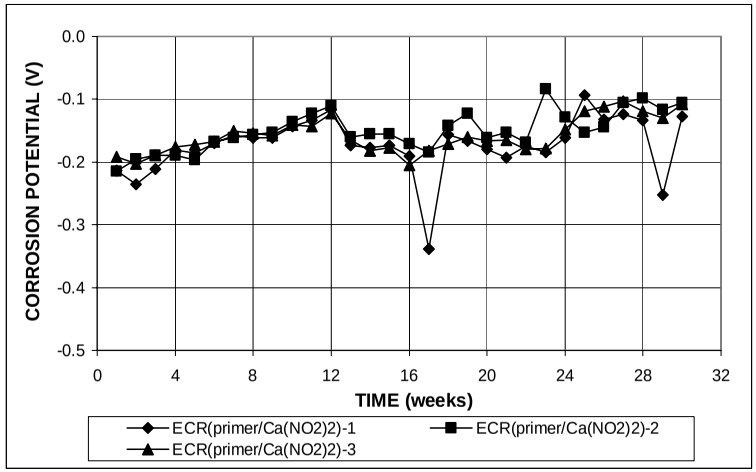

(a)

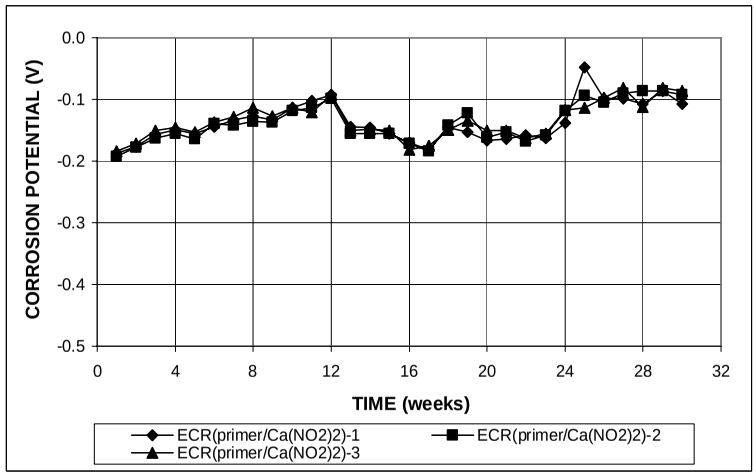

(b)

Figure A. 155 - (a) Top mat corrosion potentials and (b) bottom mat corrosion potentials as measured in the Southern Exposure test for specimens containing ECR(primer/$Ca(NO_2)_2$) bars

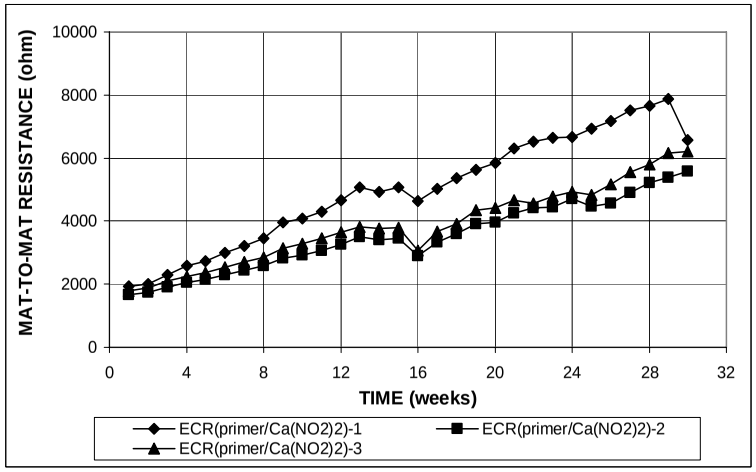

Figure A. 156 - Mat-to-mat resistances as measured in the Southern Exposure test for specimens containing ECR(primer/$Ca(NO_2)_2$) bars

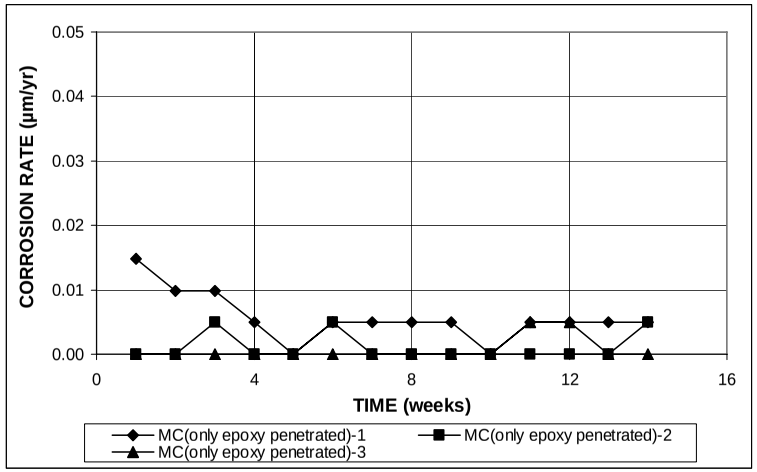

(a)

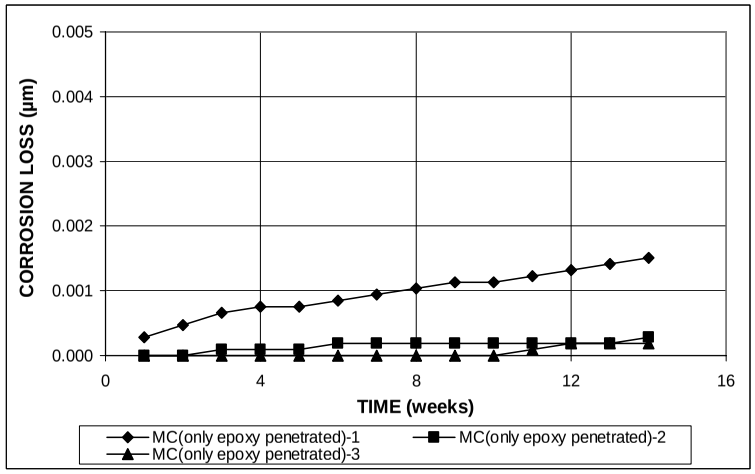

(b)

Figure A. 157 - (a) Corrosion rates and (b) total corrosion losses based on total bar area as measured in the Southern Exposure test for specimens containing multiple coated steel with only epoxy penetrated

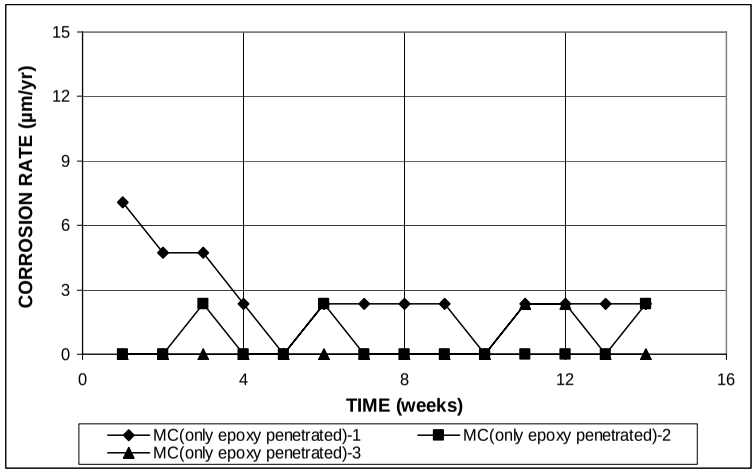

(a)

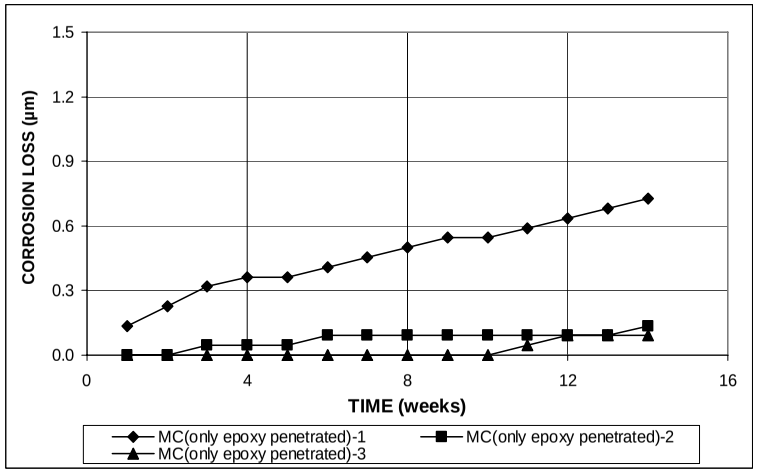

(b)

Figure A. 158 - (a) Corrosion rates and (b) total corrosion losses based on exposed area as measured in the Southern Exposure test for specimens containing multiple coated steel with only epoxy penetrated

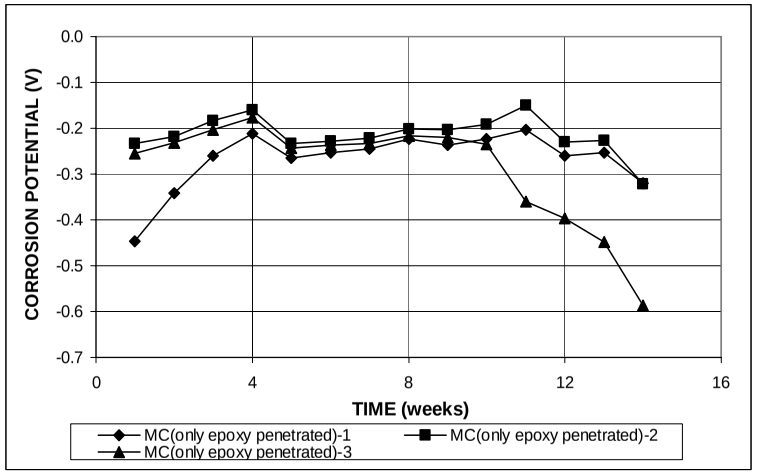

(a)

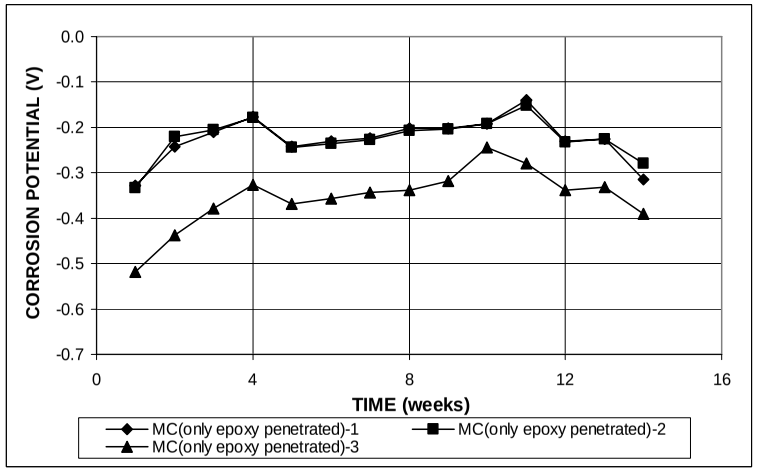

(b)

Figure A. 159 - (a) Top mat corrosion potentials and (b) bottom mat corrosion potentials as measured in the Southern Exposure test for specimens containing multiple coated steel with only epoxy penetrated

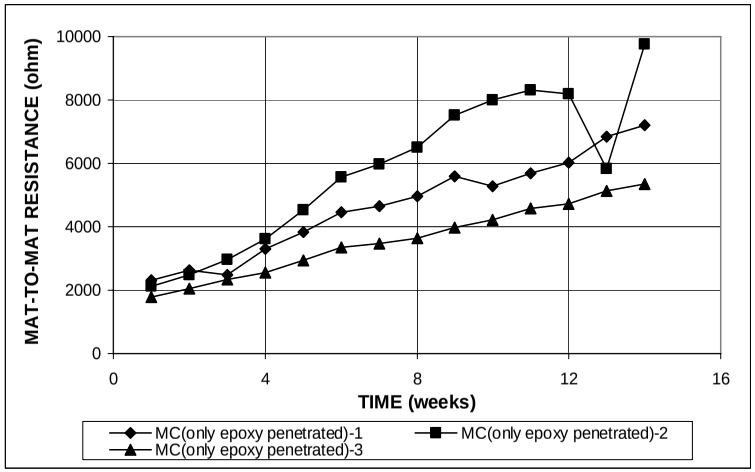

Figure A. 160 - Mat-to-mat resistances as measured in the Southern Exposure test for specimens containing multiple coated steel with only epoxy penetrated

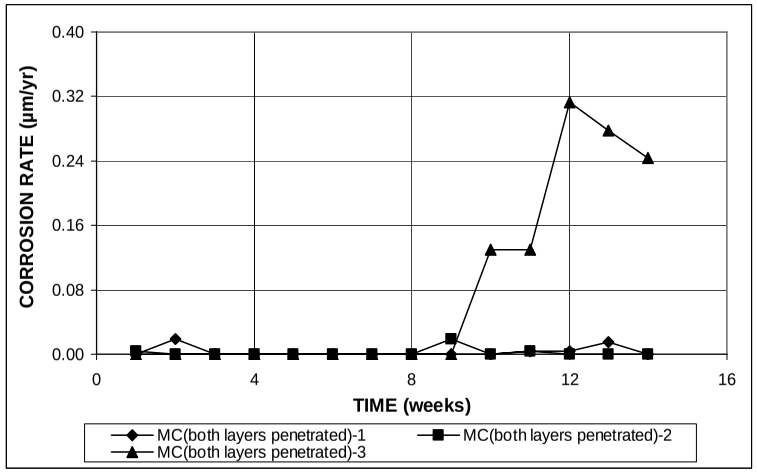

(a)

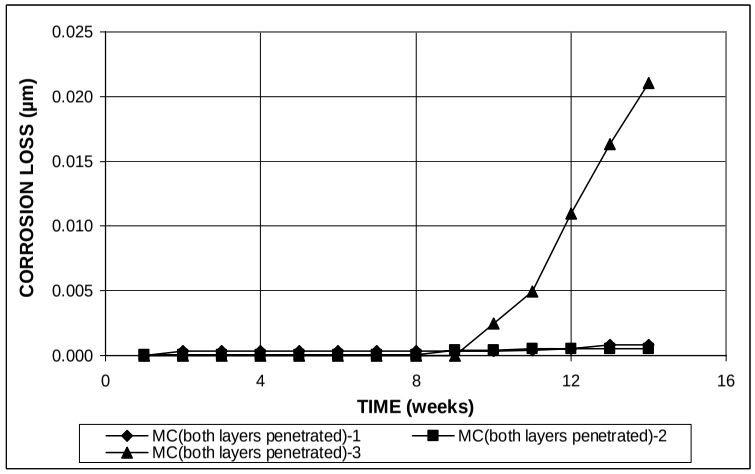

(b)

Figure A. 161 - (a) Corrosion rates and (b) total corrosion losses based on total bar area as measured in the Southern Exposure test for specimens containing multiple coated steel with both layers penetrated

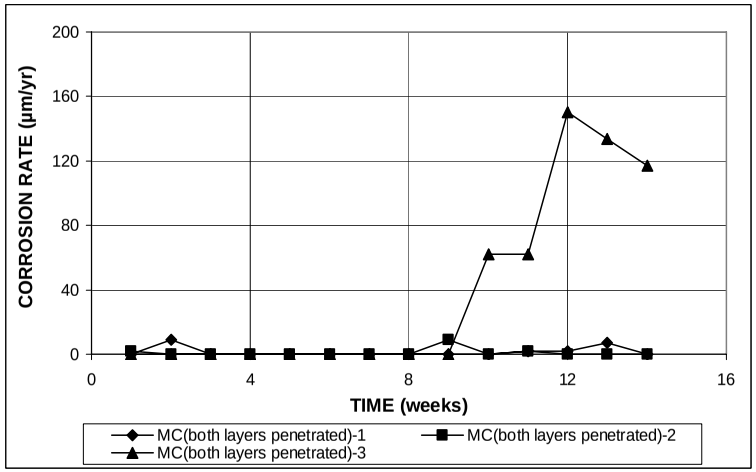

(a)

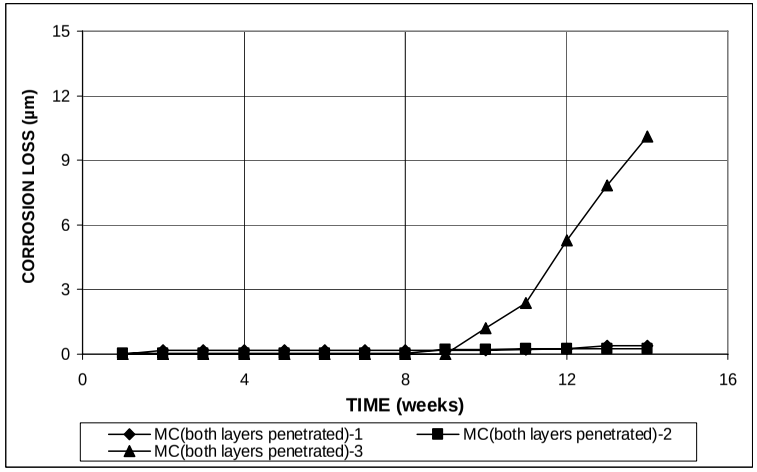

(b)

Figure A. 162 - (a) Corrosion rates and (b) total corrosion losses based on exposed area as measured in the Southern Exposure test for specimens containing multiple coated steel with both layers penetrated

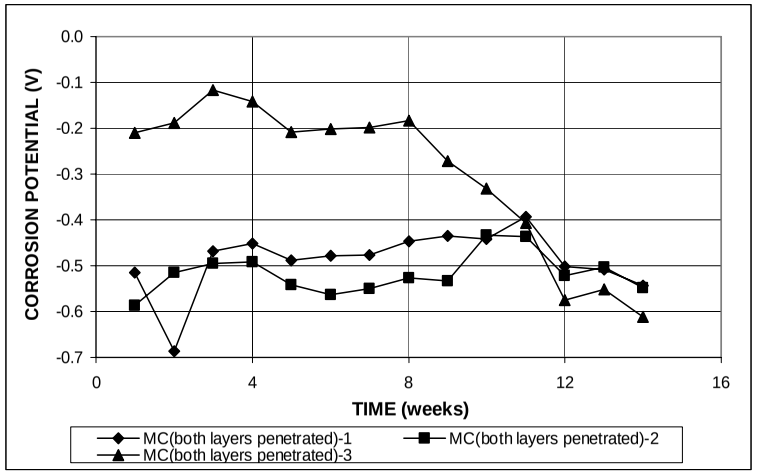

(a)

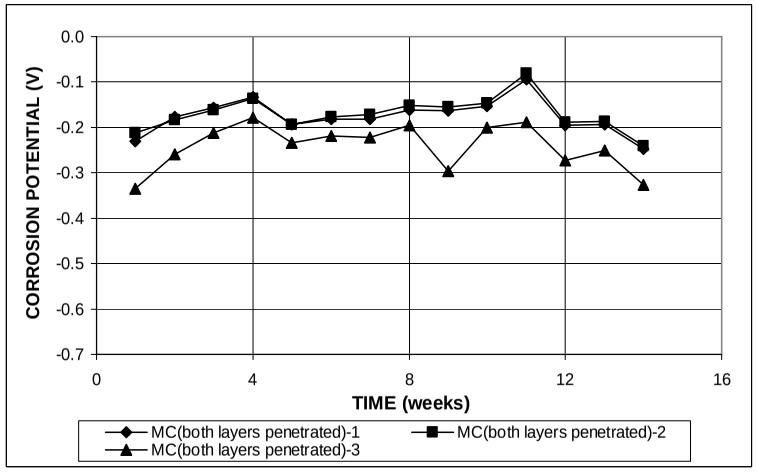

(b)

Figure A. 163 - (a) Top mat corrosion potentials and (b) bottom mat corrosion potentials as measured in the Southern Exposure test for specimens containing multiple coated steel with both layers penetrated

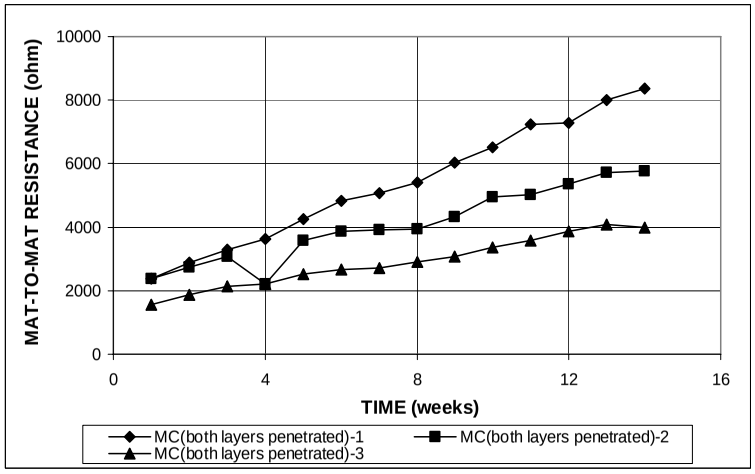

Figure A. 164 - Mat-to-mat resistances as measured in the Southern Exposure test for specimens containing multiple coated steel with both layers penetrated

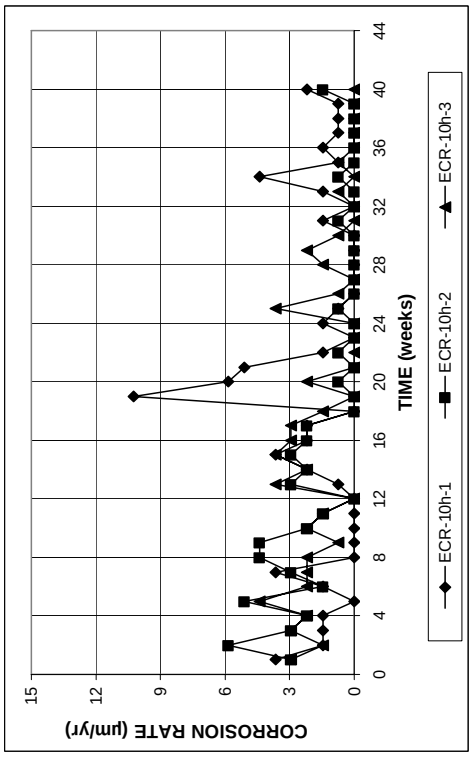

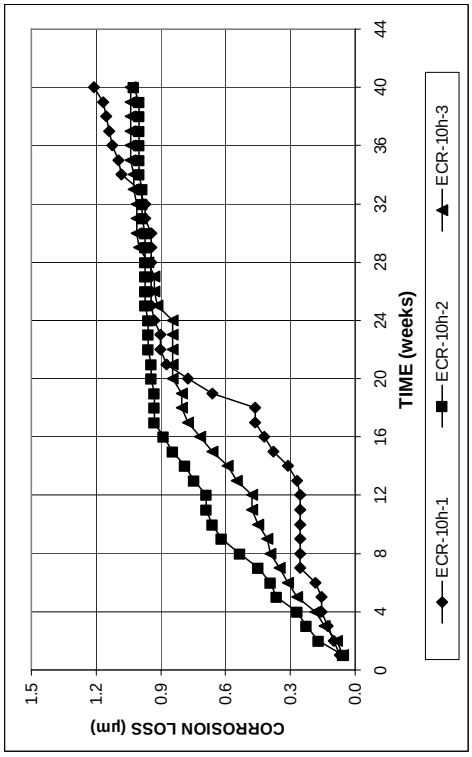

Figure A. 166 - (a) Corrosion rates and (b) total corrosion losses based on exposed area as measured in the Southern Exposure test for specimens containing epoxy-coated steel with 10 drilled holes

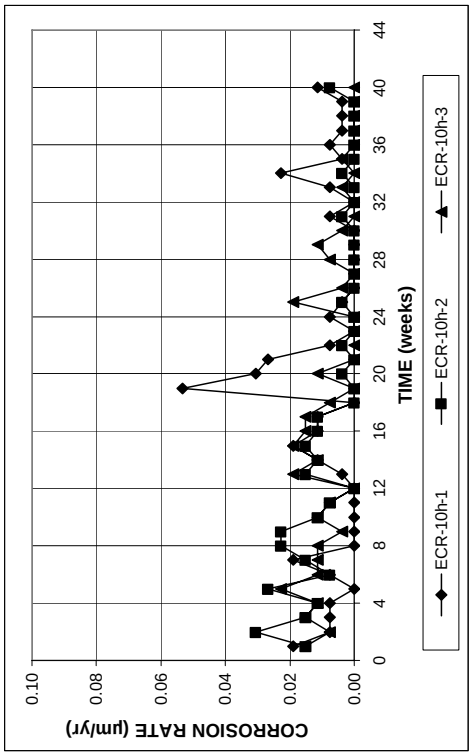

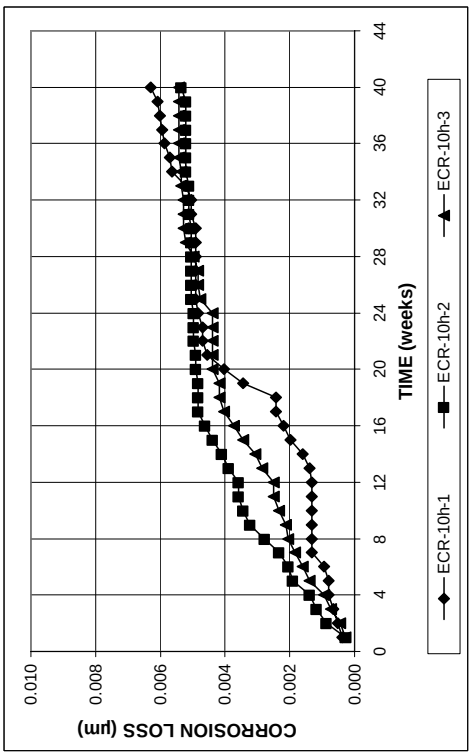

Figure A. 165 - (a) Corrosion rates and (b) total corrosion losses based on total bar area as measured in the Southern Exposure test for specimens containing epoxy-coated steel with 10 drilled holes

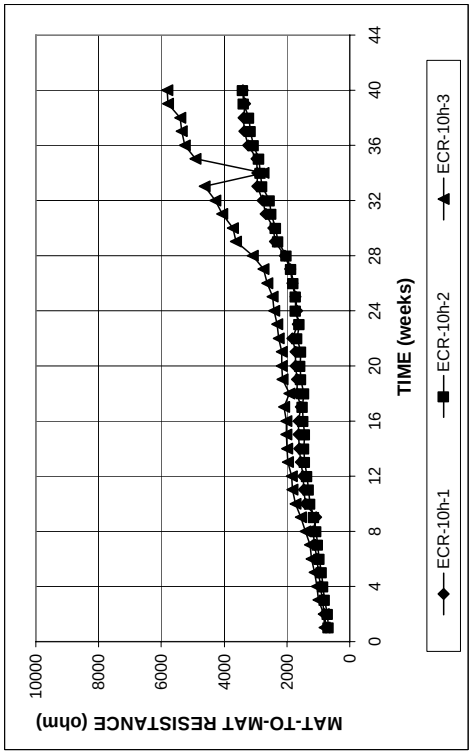

Figure A. 168 - Mat-to-mat resistances as measured in the Southern Exposure test for specimens containing epoxy-coated steel with 10 drilled holes

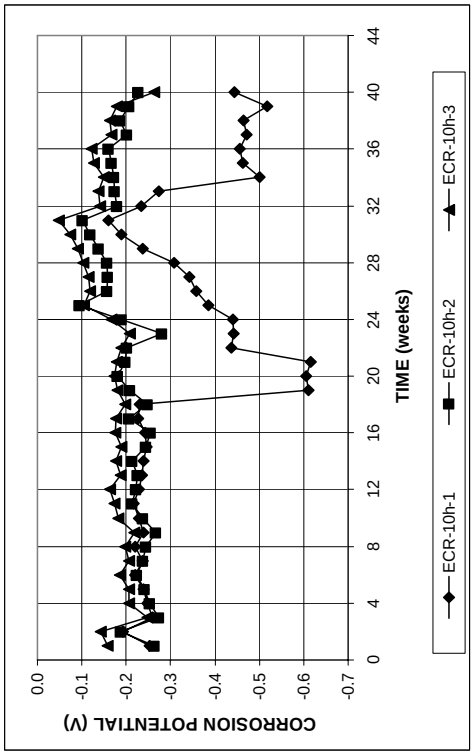

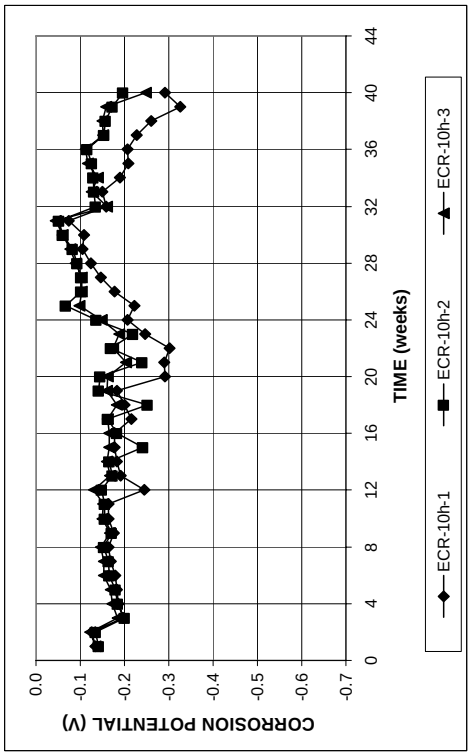

Figure A. 167 - (a) Top mat corrosion potentials and (b) bottom mat corrosion potentials as measured in the Southern Exposure test for specimens containing epoxy-coated steel with 10 drilled holes

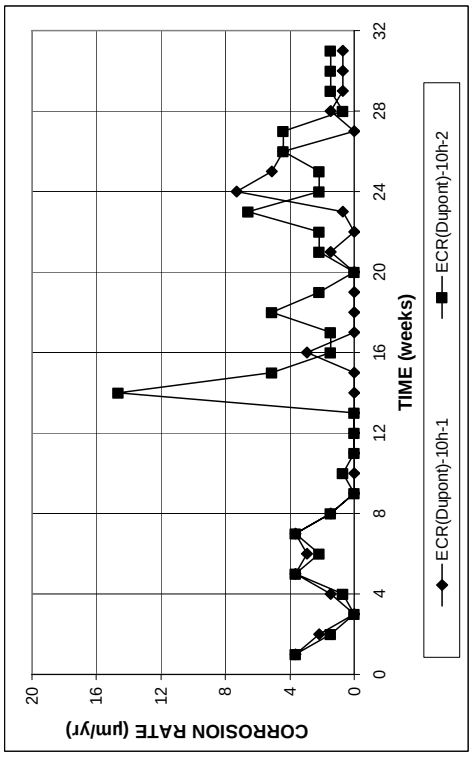

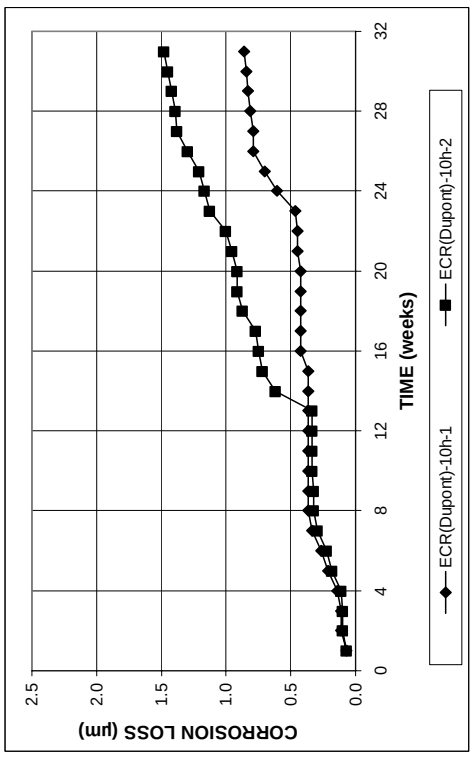

Figure A. 170 - (a) Corrosion rates and (b) total corrosion losses based on total bar area as measured in the Southern Exposure test for specimens containing ECR(Dupont) bars with 10 drilled holes

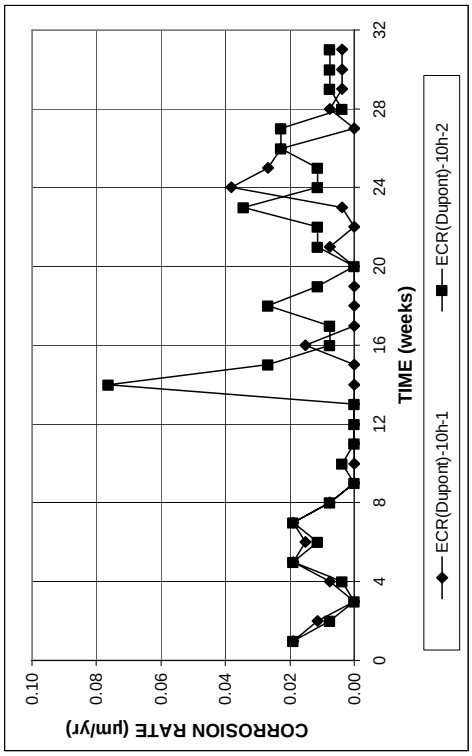

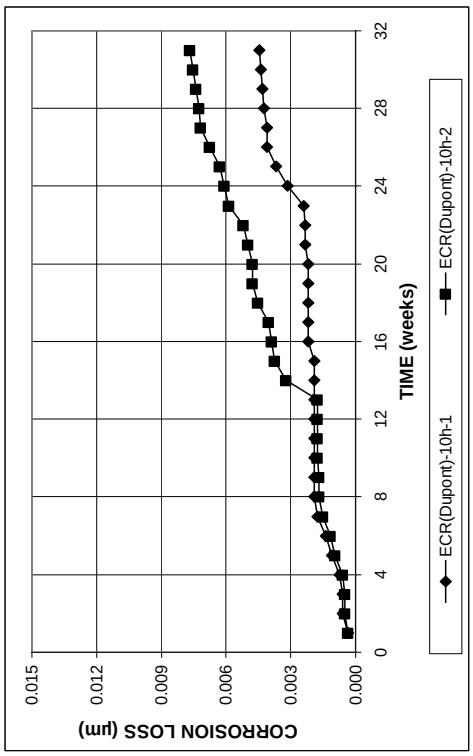

Figure A. 169 - (a) Corrosion rates and (b) total corrosion losses based on total bar area as measured in the Southern Exposure test for specimens containing ECR(Dupont) bars with 10 drilled holes

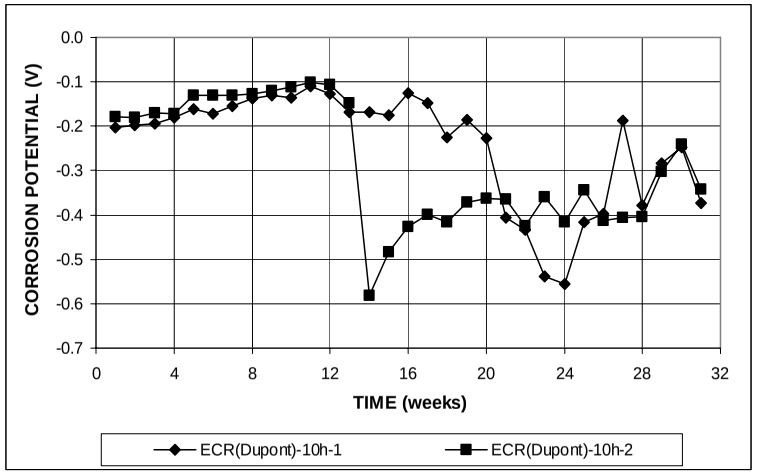

(a)

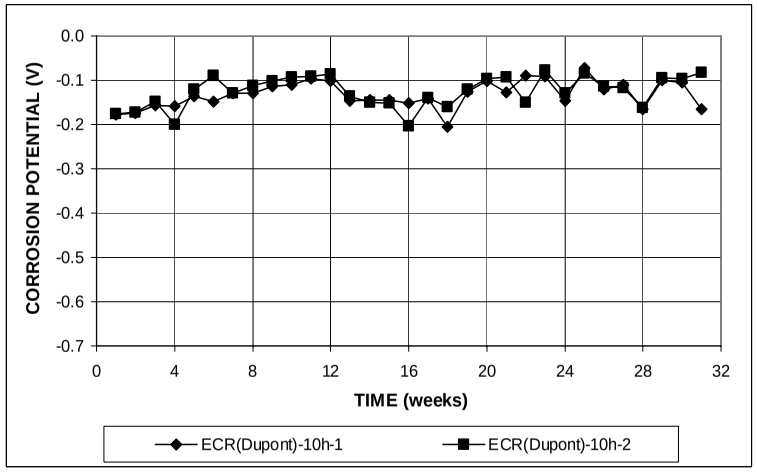

(b)

Figure A. 171 - (a) Top mat corrosion potentials and (b) bottom mat corrosion potentials as measured in the Southern Exposure test for specimens containing ECR(Dupont) bars with 10 drilled holes

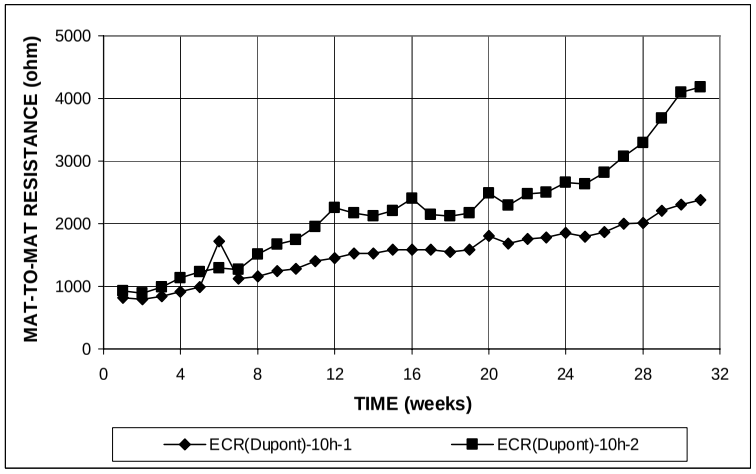

Figure A. 172 - Mat-to-mat resistances as measured in the Southern Exposure test for specimens containing ECR(Dupont) bars with 10 drilled holes

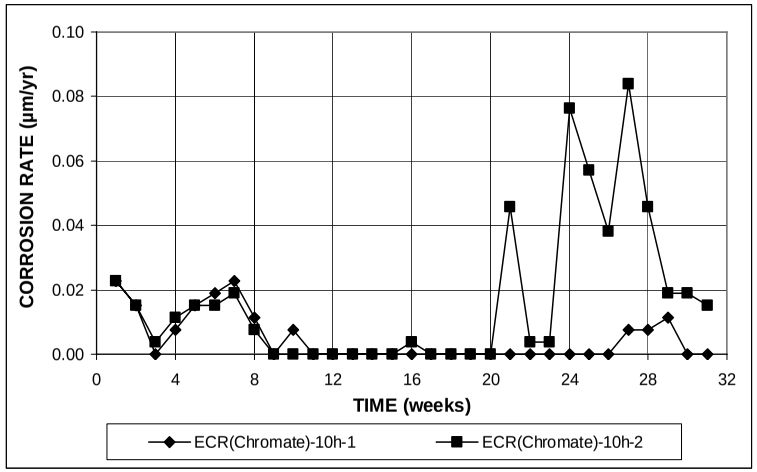

(a)

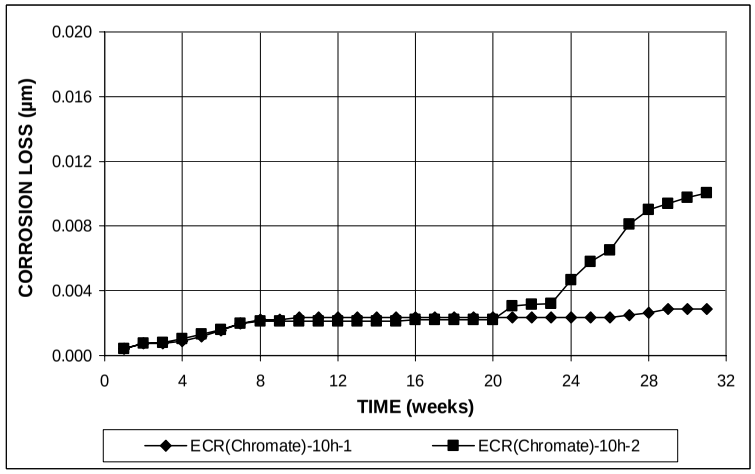

(b)

Figure A. 173 - (a) Corrosion rates and (b) total corrosion losses based on total bar area as measured in the Southern Exposure test for specimens containing ECR(Chromate) bars with 10 drilled holes

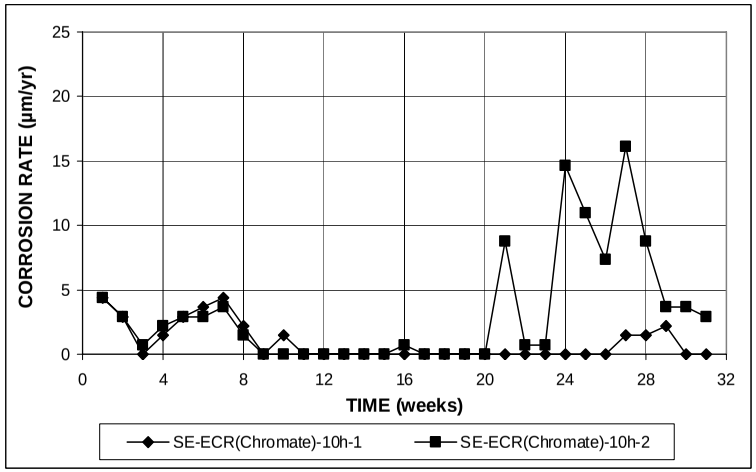

(a)

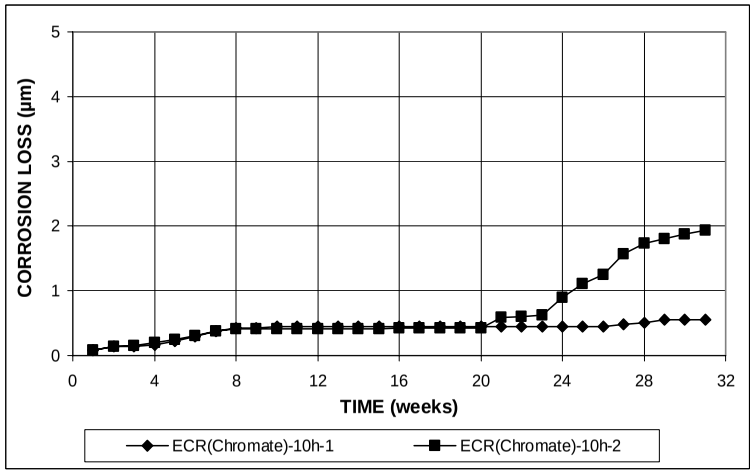

(b)

Figure A. 174 - (a) Corrosion rates and (b) total corrosion losses based on total bar area as measured in the Southern Exposure test for specimens containing ECR(Chromate) bars with 10 drilled holes

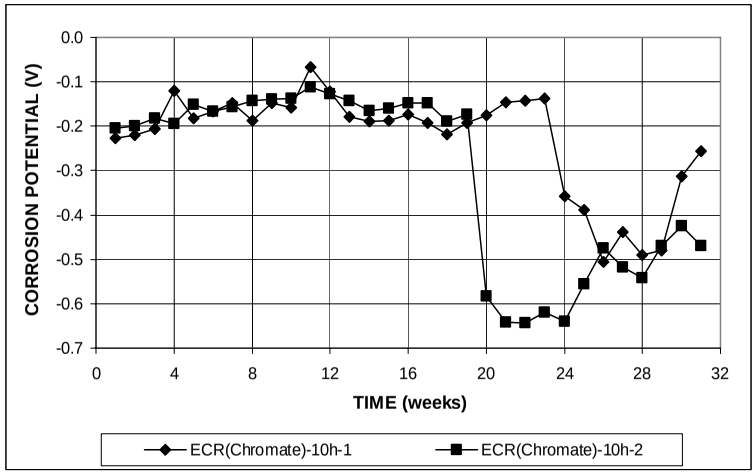

(a)

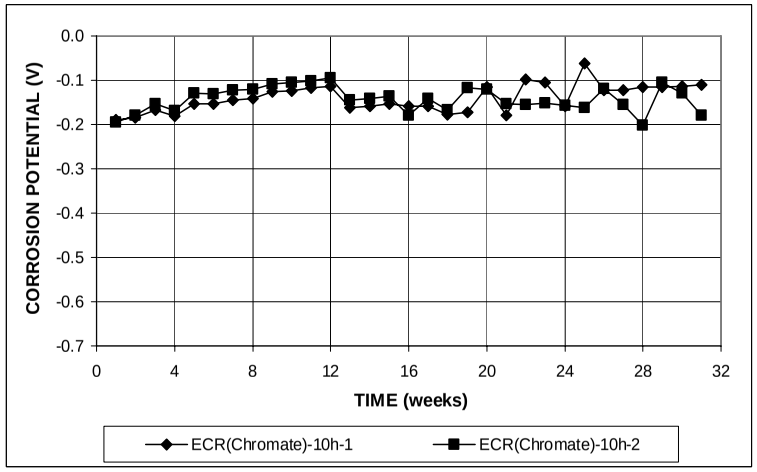

(b)

Figure A. 175 - (a) Top mat corrosion potentials and (b) bottom mat corrosion potentials as measured in the Southern Exposure test for specimens containing ECR(Chromate) bars with 10 drilled holes

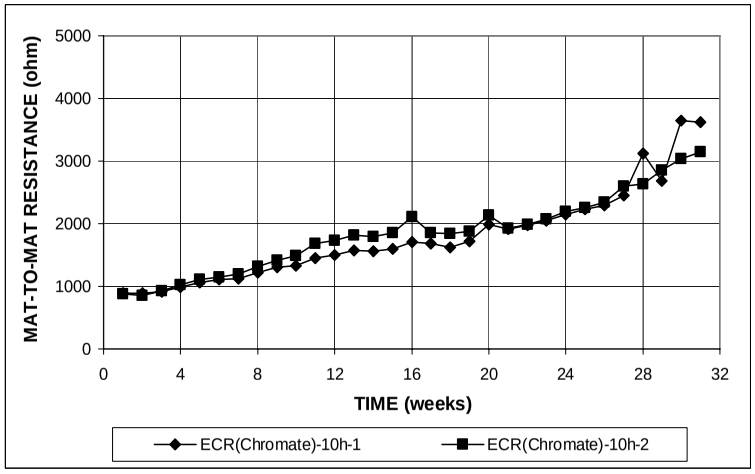

Figure A. 176 - Mat-to-mat resistances as measured in the Southern Exposure test for specimens containing ECR(Chromate) bars with 10 drilled holes

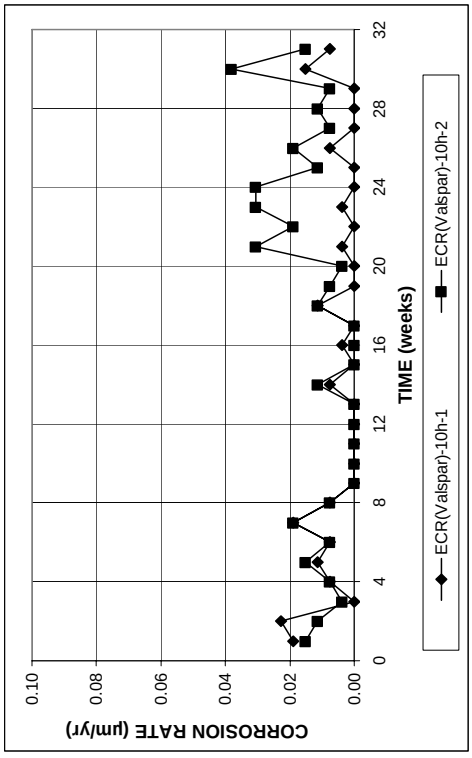

Figure A. 177 - (a) Corrosion rates and (b) total corrosion losses based on total bar area as measured in the Southern Exposure test for specimens containing ECR(Valspar) bars with 10 drilled holes

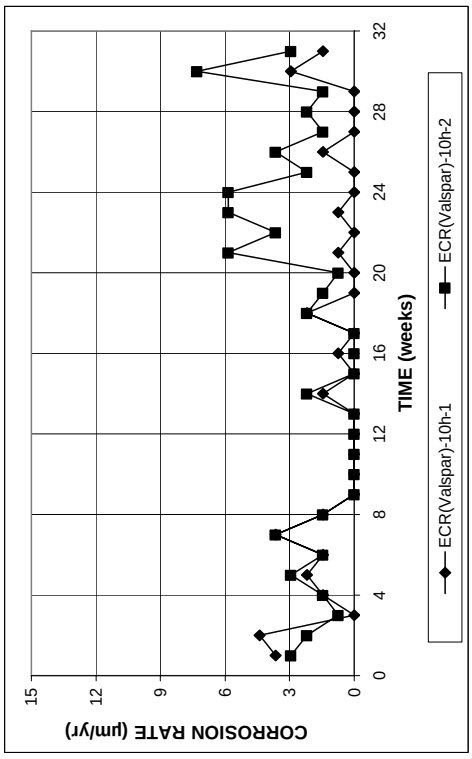

Figure A. 178 - (a) Corrosion rates and (b) total corrosion losses based on exposed area as measured in the Southern Exposure test for specimens containing ECR(Valspar) bars with 10 drilled holes

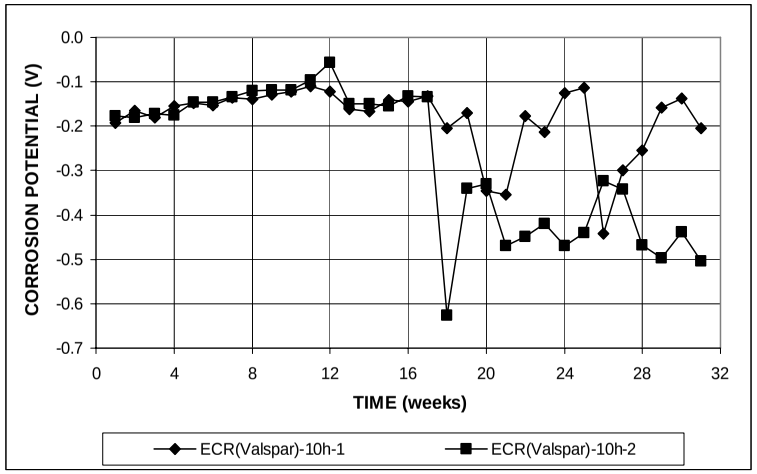

(a)

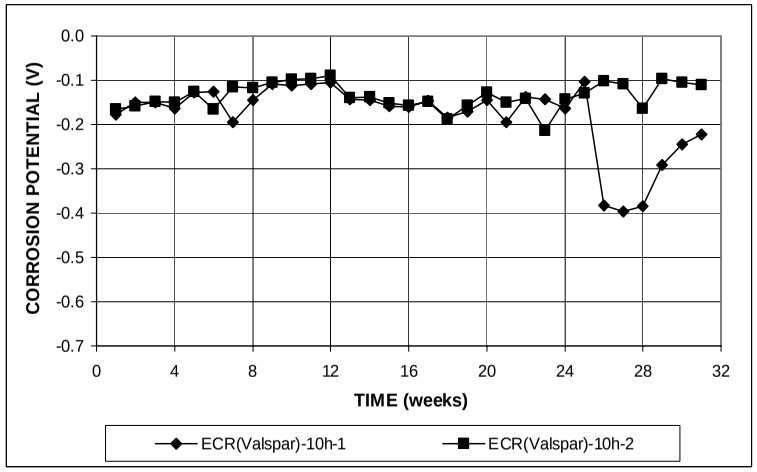

(b)

Figure A. 179 - (a) Top mat corrosion potentials and (b) bottom mat corrosion potentials as measured in the Southern Exposure test for specimens containing ECR(Valspar) bars with 10 drilled holes

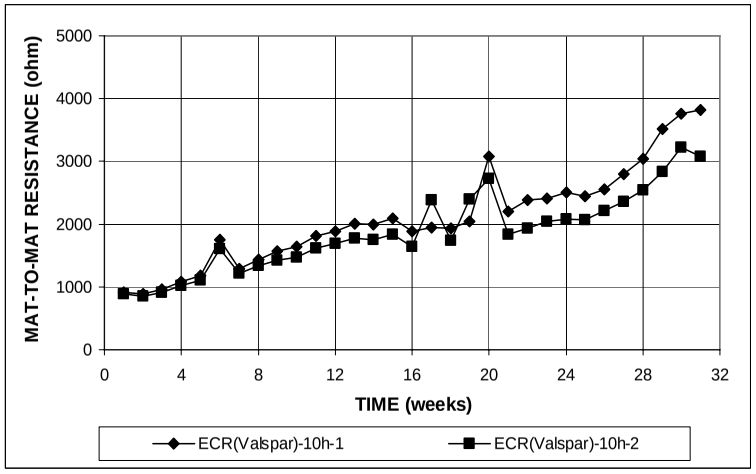

Figure A. 180 - Mat-to-mat resistances as measured in the Southern Exposure test for specimens containing ECR(Valspar) bars with 10 drilled holes

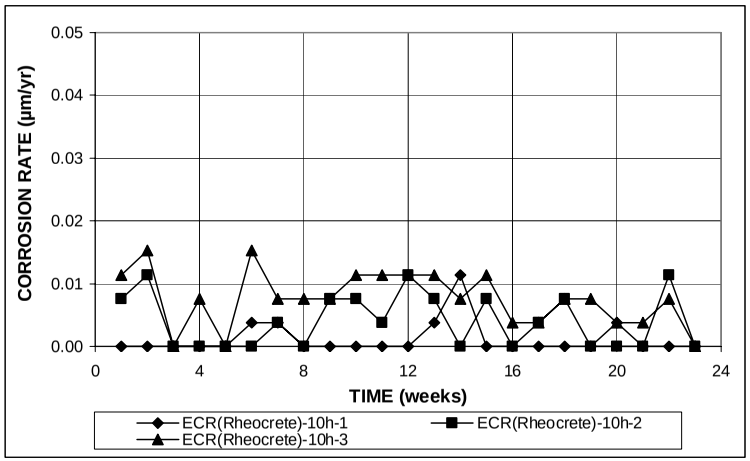

(a)

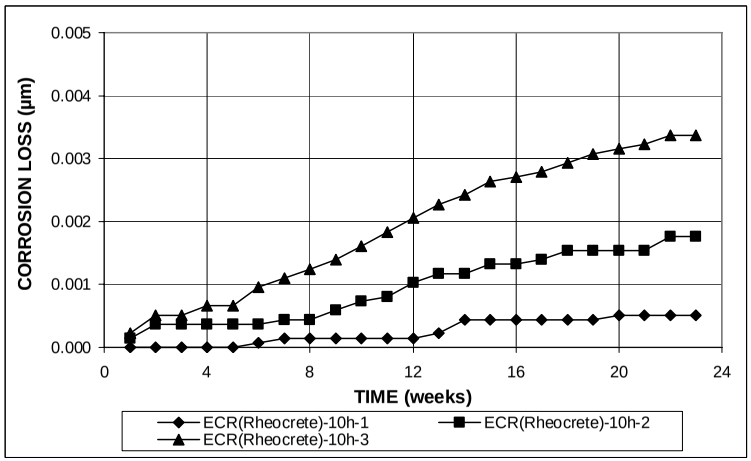

(b)

Figure A. 181 - (a) Corrosion rates and (b) total corrosion losses based on total bar area as measured in the Southern Exposure test for specimens containing epoxy-coated steel with 10 drilled holes and corrosion inhibitor Rheocrete

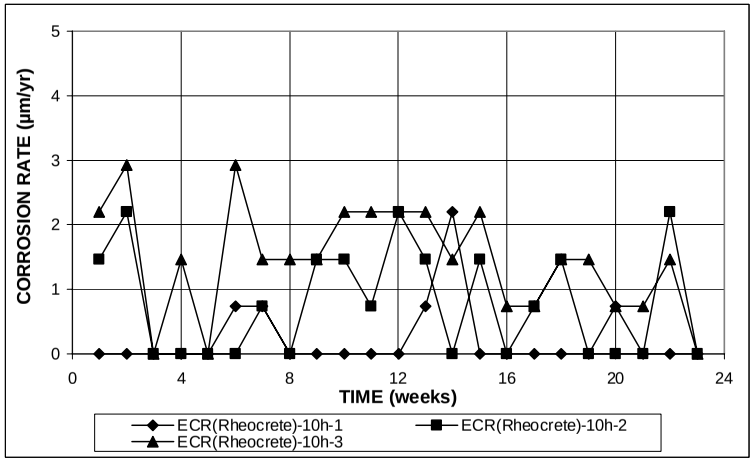

(a)

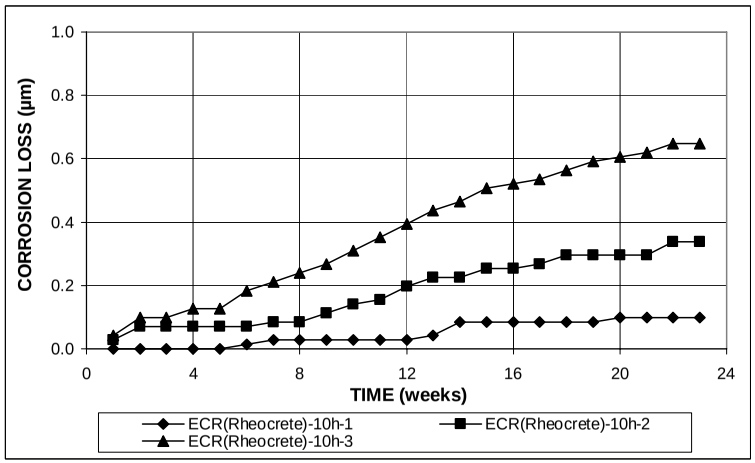

(b)

Figure A. 182 - (a) Corrosion rates and (b) total corrosion losses based on exposed area as measured in the Southern Exposure test for specimens containing epoxy-coated steel with 10 drilled holes and corrosion inhibitor Rheocrete

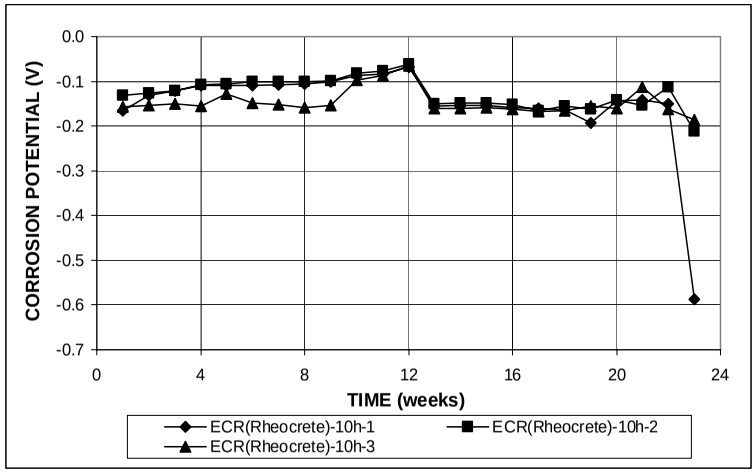

(a)

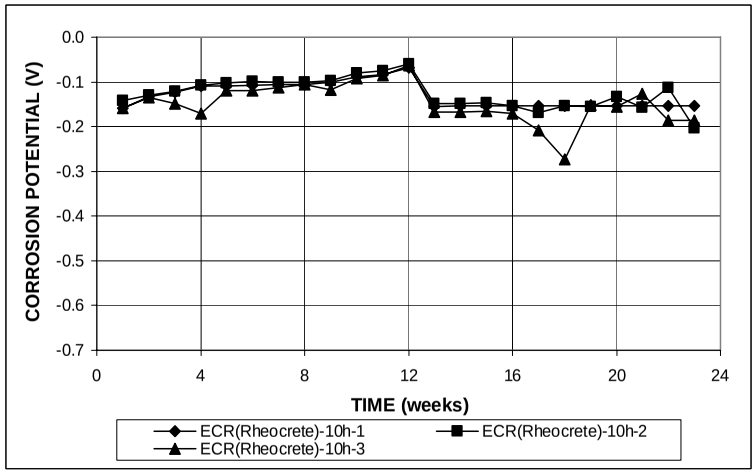

(b)

Figure A. 183 - (a) Top mat corrosion potentials and (b) bottom mat corrosion potentials as measured in the Southern Exposure test for specimens containing epoxy-coated steel with 10 drilled holes and corrosion inhibitor Rheocrete

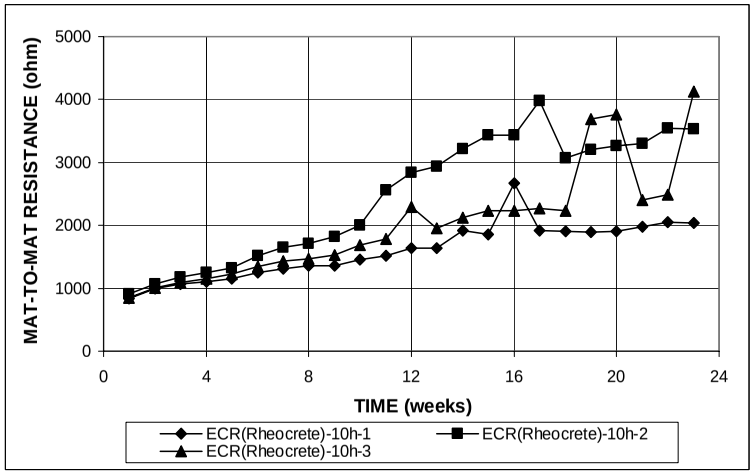

Figure A. 184 - Mat-to-mat resistances as measured in the Southern Exposure test for specimens containing epoxy-coated steel with 10 drilled holes and corrosion inhibitor Rheocrete

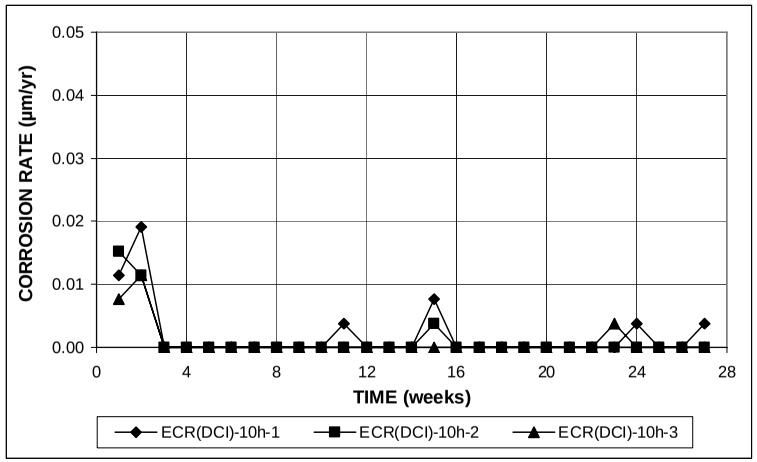

(a)

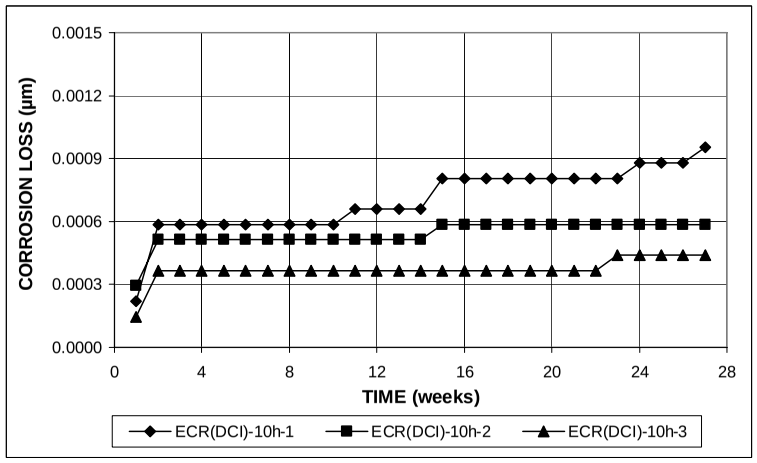

(b)

Figure A. 185 - (a) Corrosion rates and (b) total corrosion losses based on total bar area as measured in the Southern Exposure test for specimens containing epoxy-coated steel with 10 drilled holes and corrosion inhibitor DCI

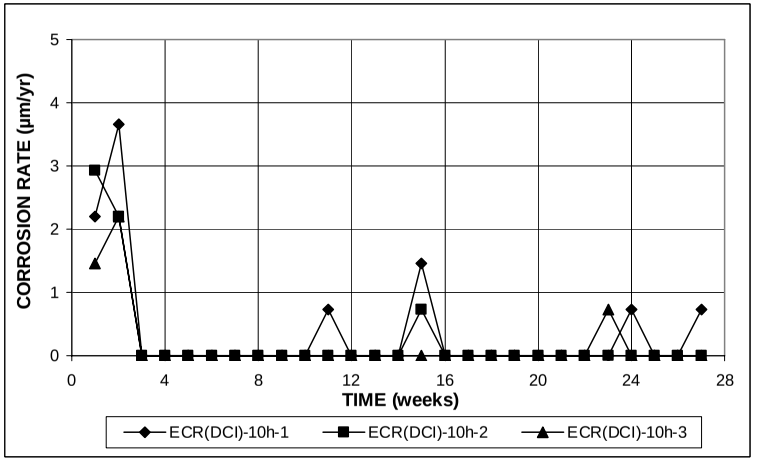

(a)

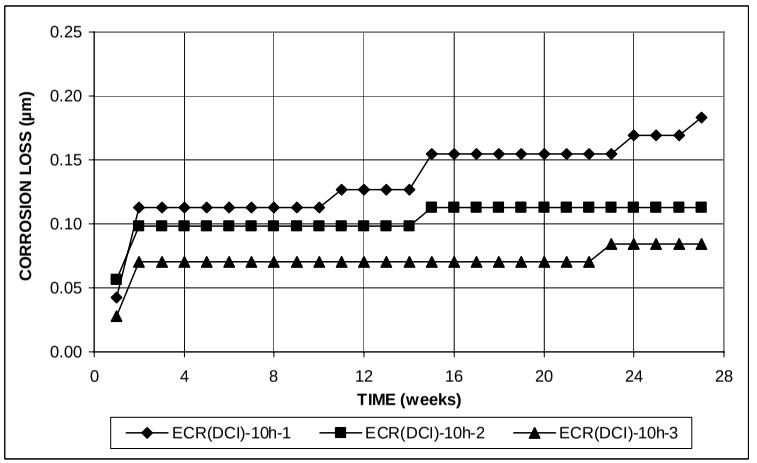

(b)

Figure A. 186 - (a) Corrosion rates and (b) total corrosion losses based on exposed area as measured in the Southern Exposure test for specimens containing epoxy-coated steel with 10 drilled holes and corrosion inhibitor DCI

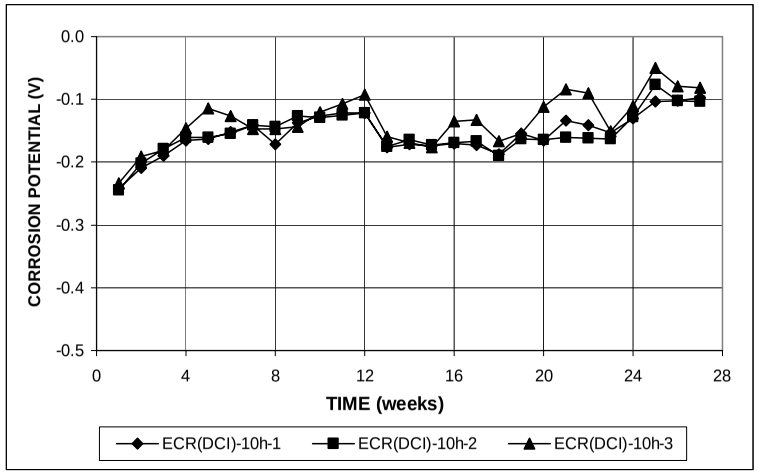

(a)

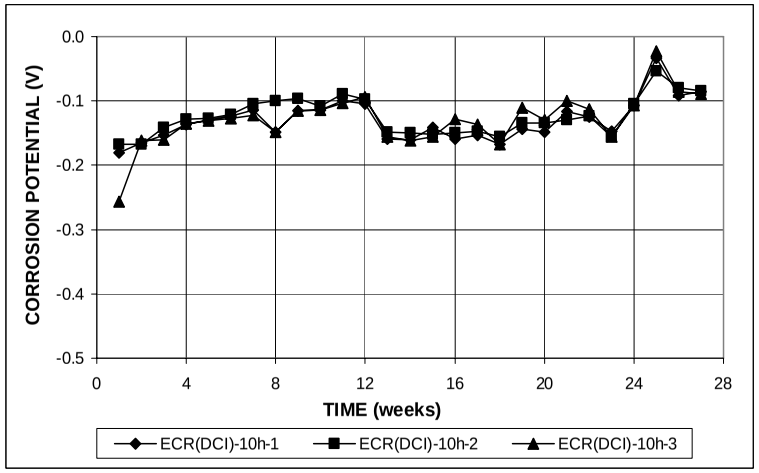

(b)

Figure A. 187 - (a) Top mat corrosion potentials and (b) bottom mat corrosion potentials as measured in the Southern Exposure test for specimens containing epoxy-coated steel with 10 drilled holes and corrosion inhibitor DCI

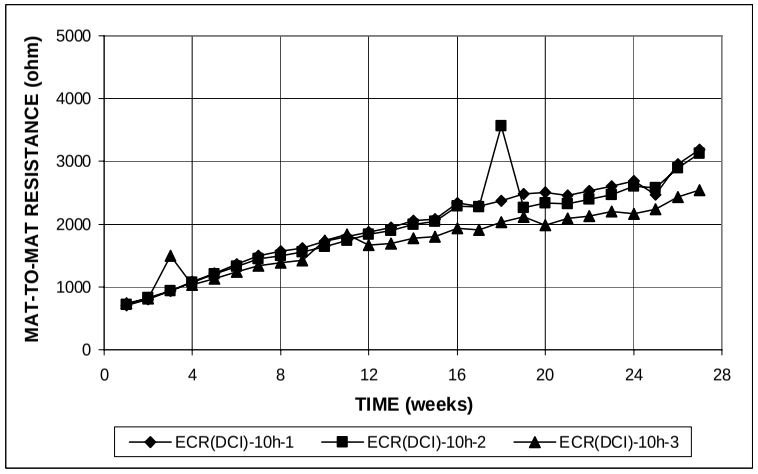

Figure A. 188 - Mat-to-mat resistances as measured in the Southern Exposure test for specimens containing epoxy-coated steel with 10 drilled holes and corrosion inhibitor DCI

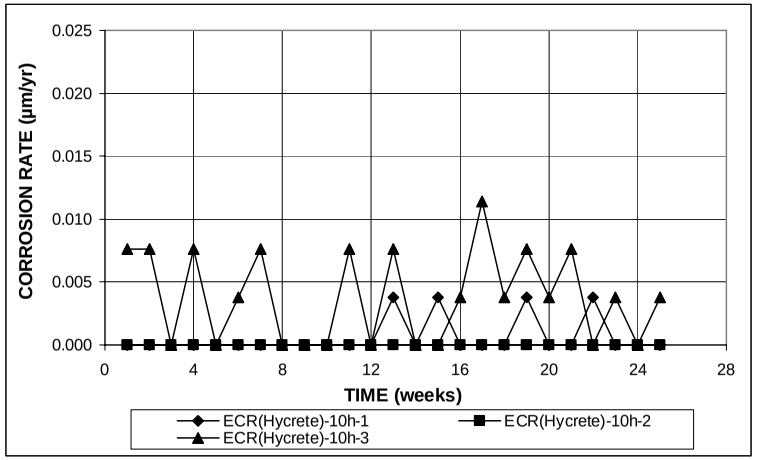

(a)

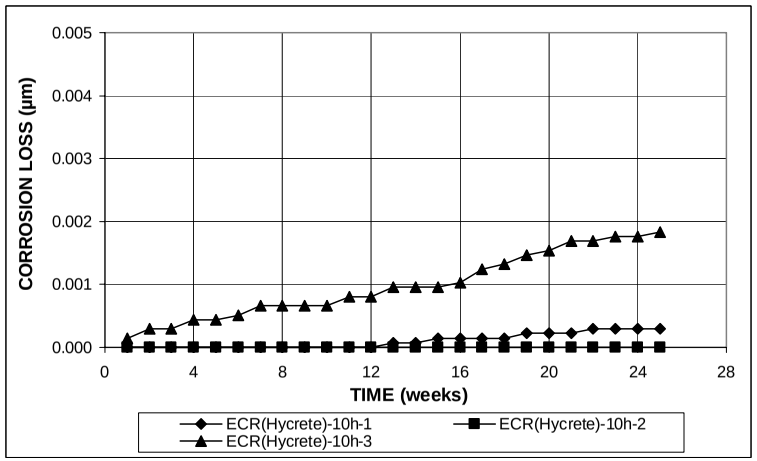

(b)

Figure A. 189 - (a) Corrosion rates and (b) total corrosion losses based on total bar area as measured in the Southern Exposure test for specimens containing epoxy-coated steel with 10 drilled holes and corrosion inhibitor Hycrete

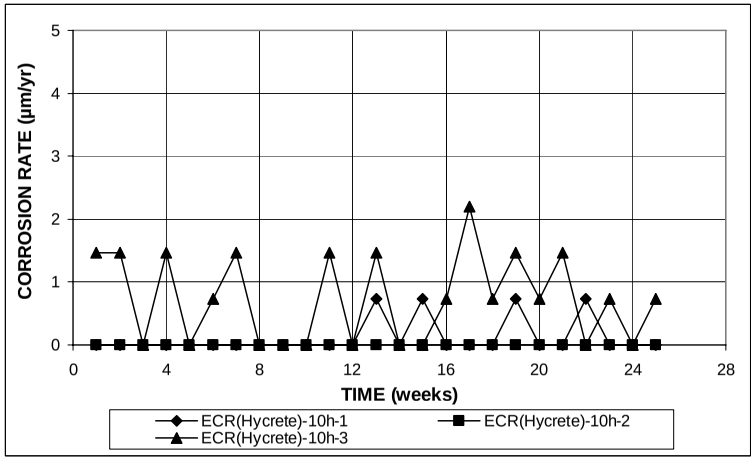

(a)

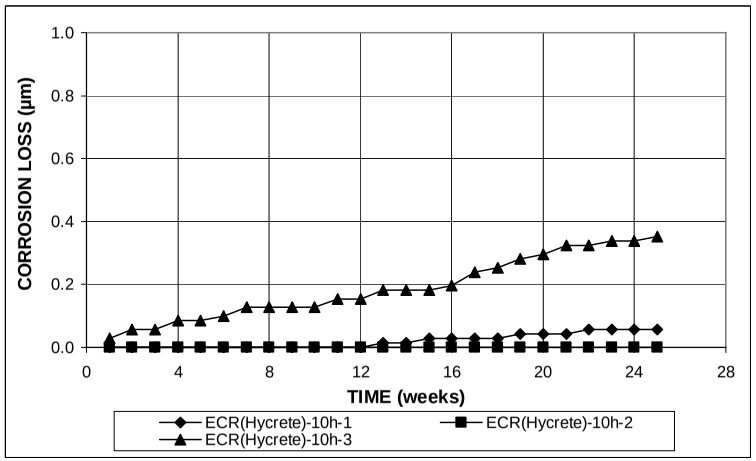

(b)

Figure A. 190 - (a) Corrosion rates and (b) total corrosion losses based on total bar area as measured in the Southern Exposure test for specimens containing epoxy-coated steel with 10 drilled holes and corrosion inhibitor Hycrete

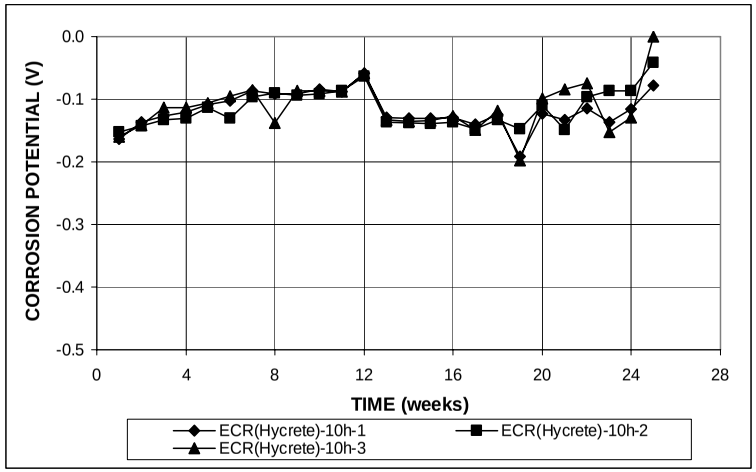

(a)

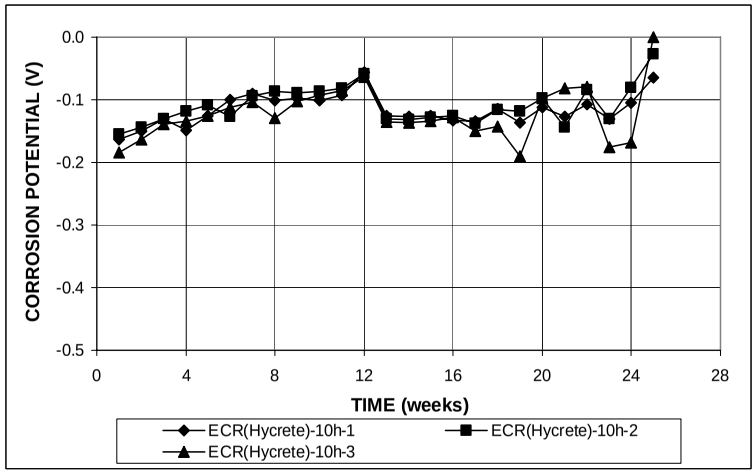

(b)

Figure A. 191 - (a) Top mat corrosion potentials and (b) bottom mat corrosion potentials as measured in the Southern Exposure test for specimens containing epoxy-coated steel with 10 drilled holes and corrosion inhibitor Hycrete

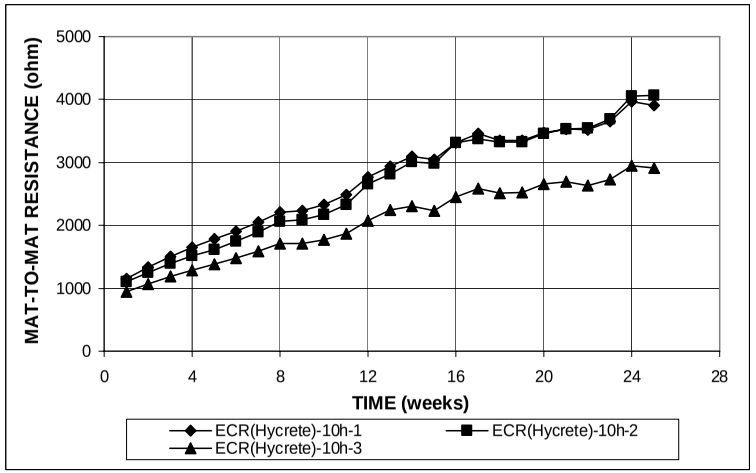

Figure A. 192 - Mat-to-mat resistances as measured in the Southern Exposure test for specimens containing epoxy-coated steel with 10 drilled holes and corrosion inhibitor Hycrete

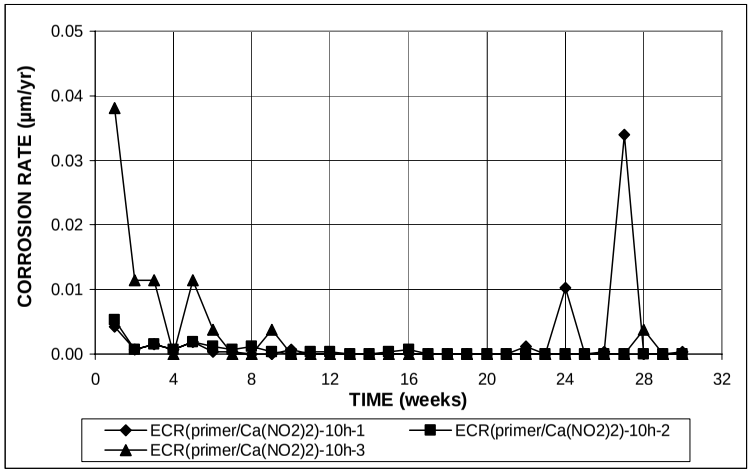

(a)

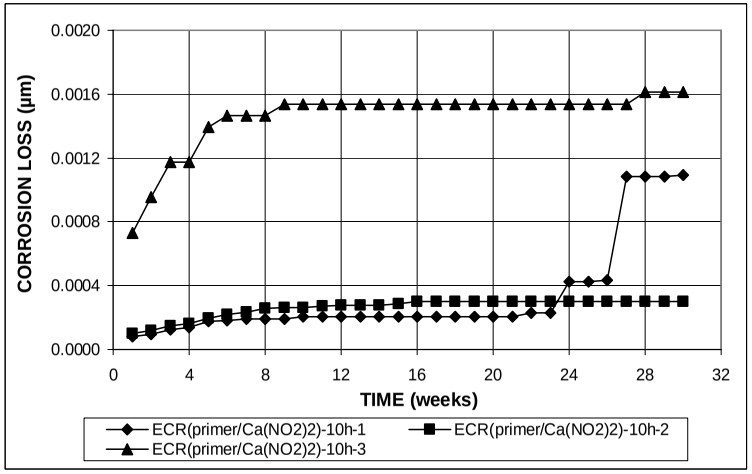

(b)

Figure A. 193 - (a) Corrosion rates and (b) total corrosion losses based on total bar area as measured in the Southern Exposure test for specimens containing ECR(primer/Ca$(NO_2)_2$) bars with 10 drilled holes

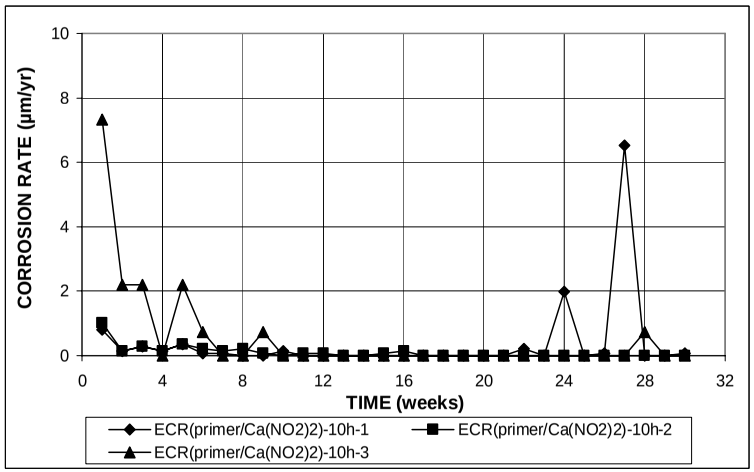

(a)

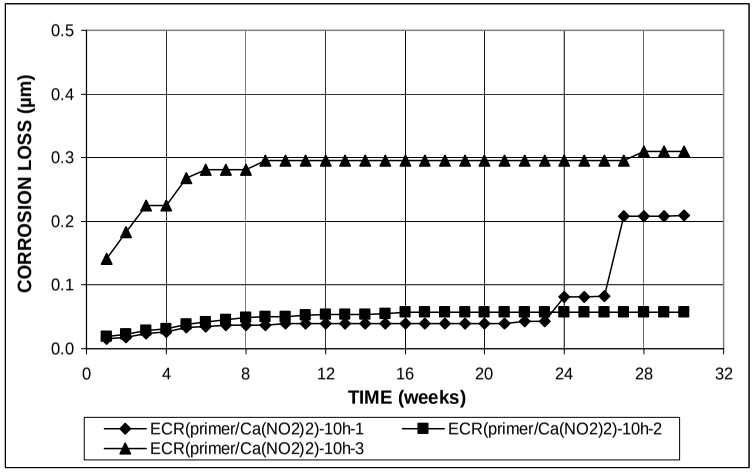

(b)

Figure A. 194 - (a) Corrosion rates and (b) total corrosion losses based on exposed area as measured in the Southern Exposure test for specimens containing ECR(primer/Ca$(NO_2)_2$) bars with 10 drilled holes

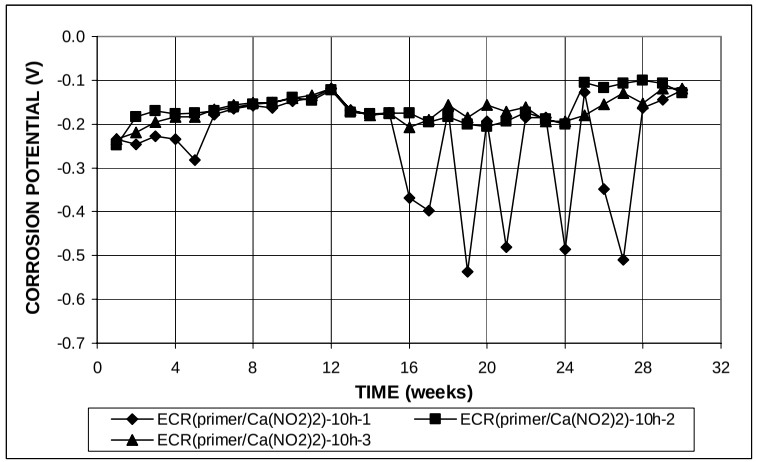

(a)

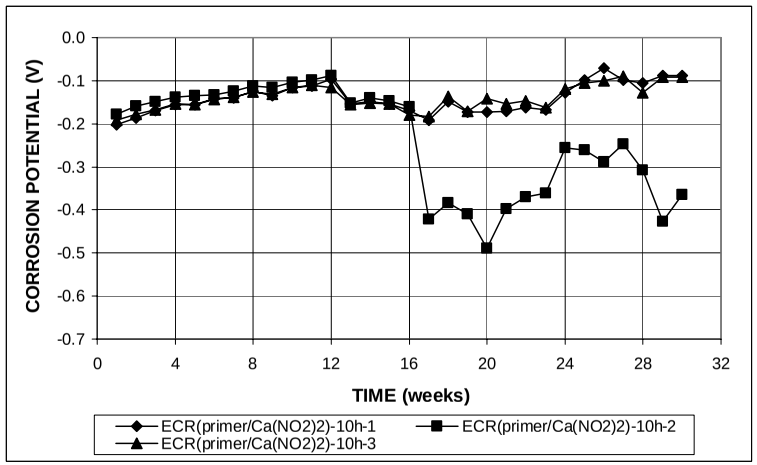

(b)

Figure A. 195 - (a) Top mat corrosion potentials and (b) bottom mat corrosion potentials as measured in the Southern Exposure test for specimens containing ECR(primer/$Ca(NO_2)_2$) bars with 10 drilled holes

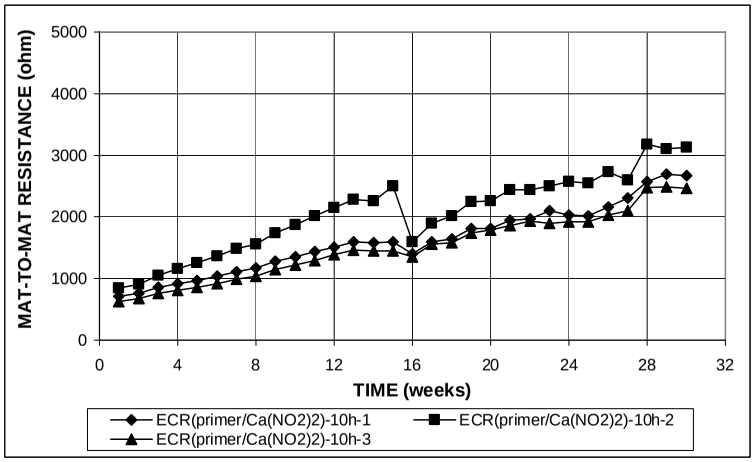

Figure A. 196 - Mat-to-mat resistances as measured in the Southern Exposure test for specimens containing ECR(primer/$Ca(NO_2)_2$) bars with 10 drilled holes

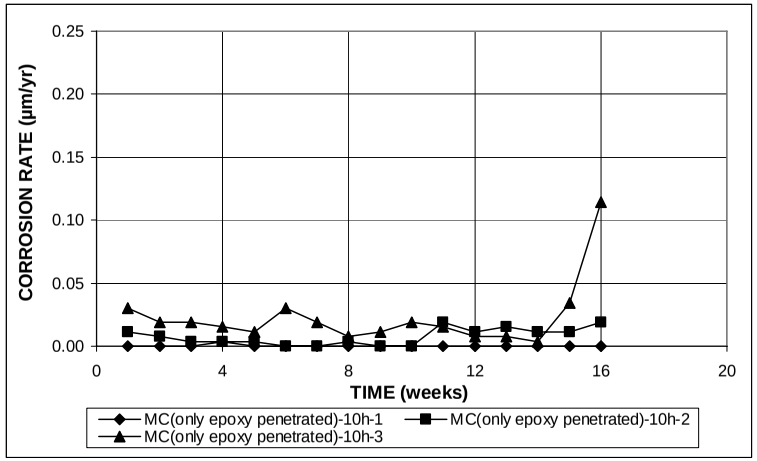

(a)

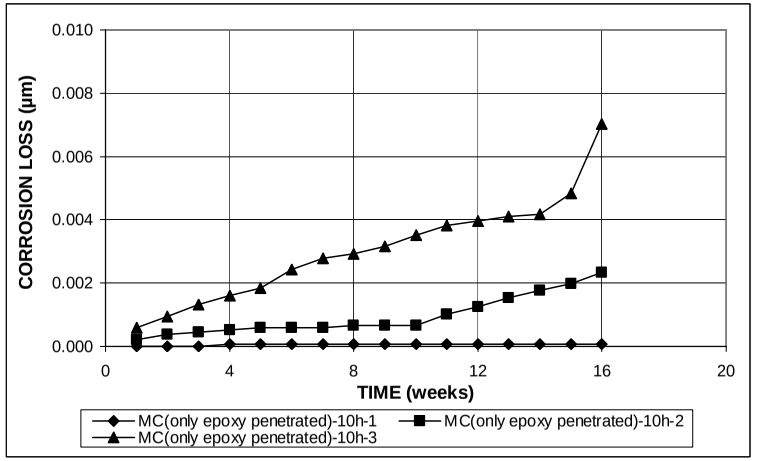

(b)

Figure A. 197 - (a) Corrosion rates and (b) total corrosion losses based on total bar area as measured in the Southern Exposure test for specimens containing multiple coated steel with only epoxy penetrated by 10 burned holes

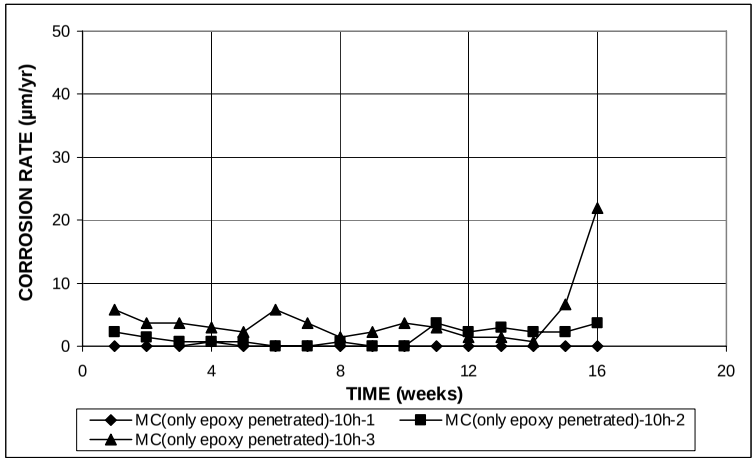

(a)

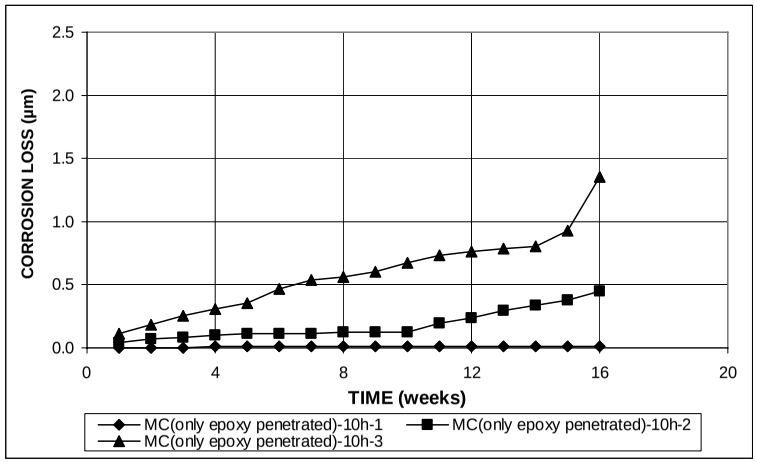

(b)

Figure A. 198 - (a) Corrosion rates and (b) total corrosion losses based on exposed area as measured in the Southern Exposure test for specimens containing multiple coated steel with only epoxy penetrated by 10 burned holes

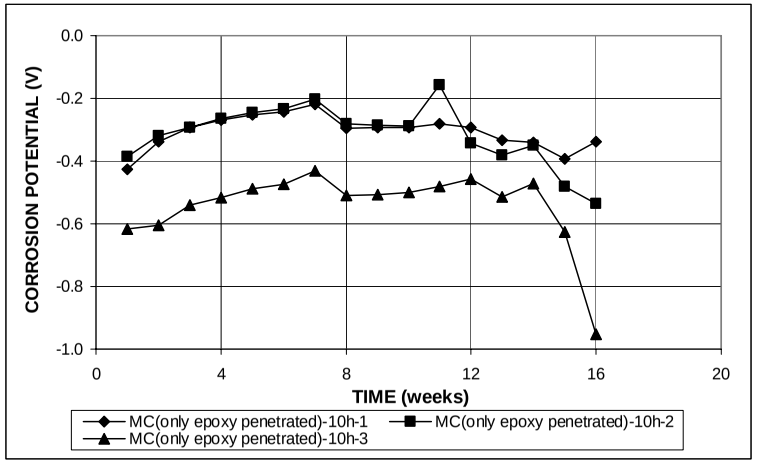

(a)

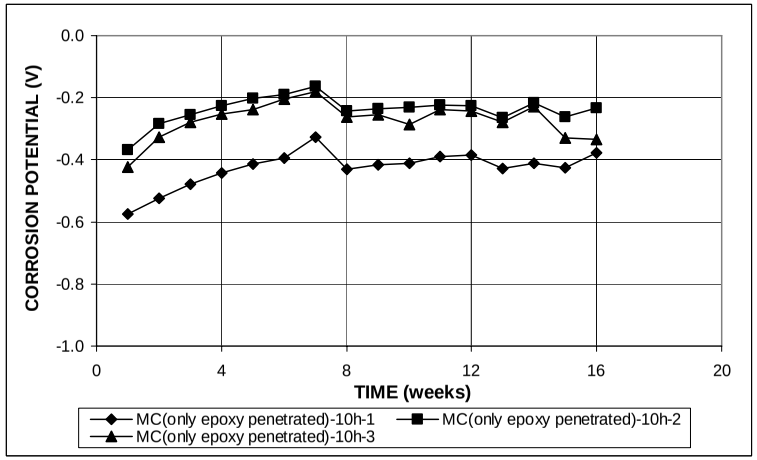

(b)

Figure A. 199 - (a) Top mat corrosion potentials and (b) bottom mat corrosion potentials as measured in the Southern Exposure test for specimens containing multiple coated steel with only epoxy penetrated by 10 burned holes

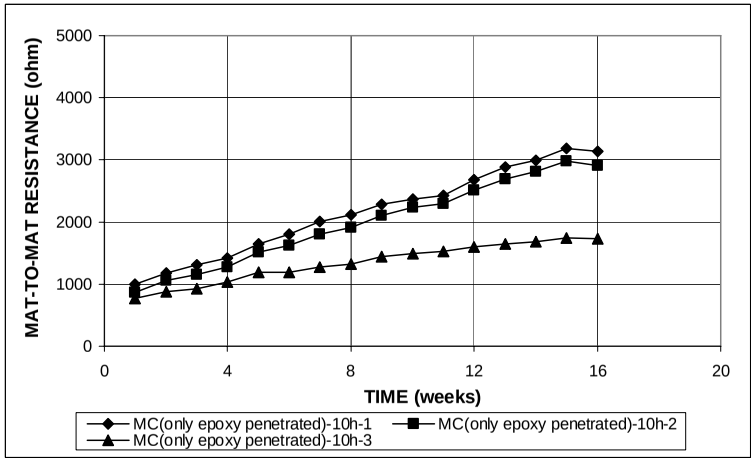

Figure A. 200 - Mat-to-mat resistances as measured in the Southern Exposure test for specimens containing multiple coated steel with only epoxy penetrated by 10 burned holes

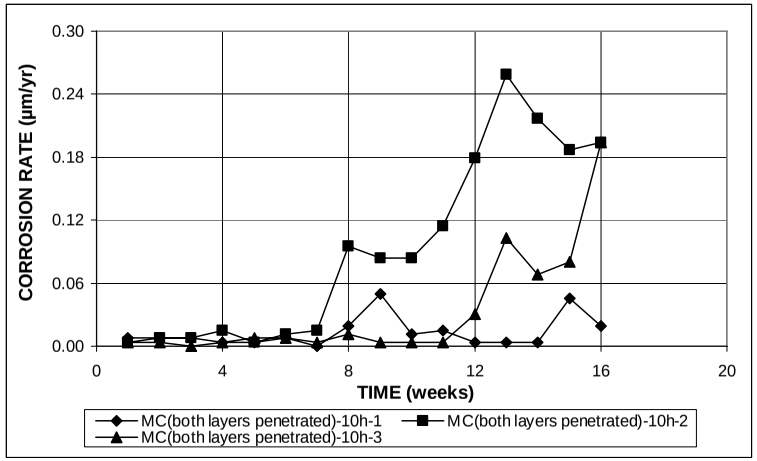

(a)

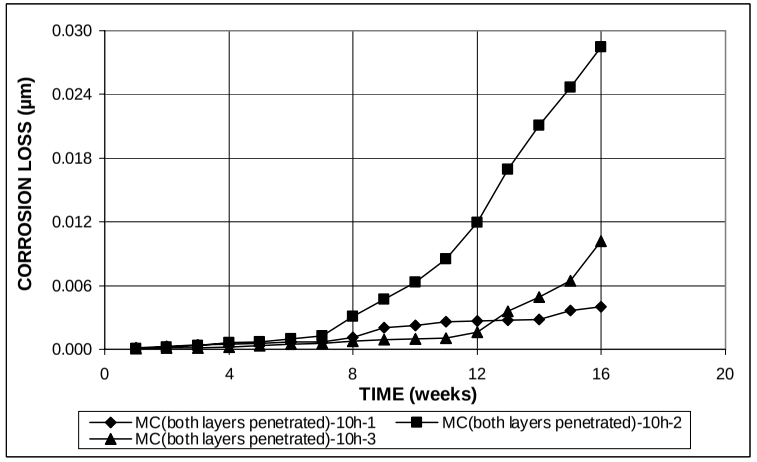

(b)

Figure A. 201 - (a) Corrosion rates and (b) total corrosion losses based on total bar area as measured in the Southern Exposure test for specimens containing multiple coated steel with both layers penetrated by 10 drilled holes

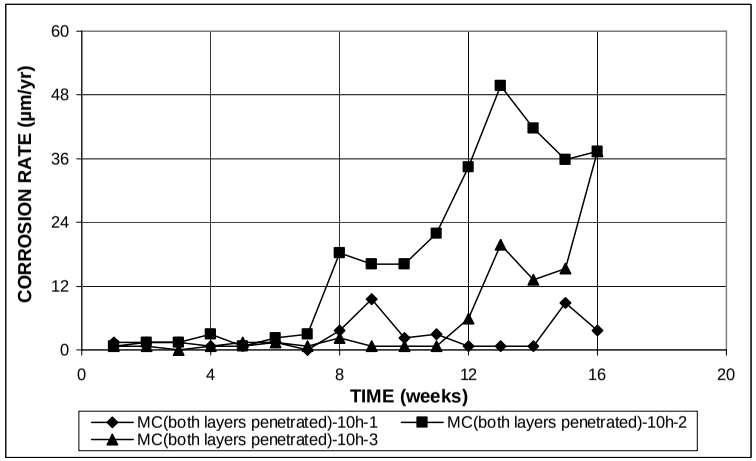

(a)

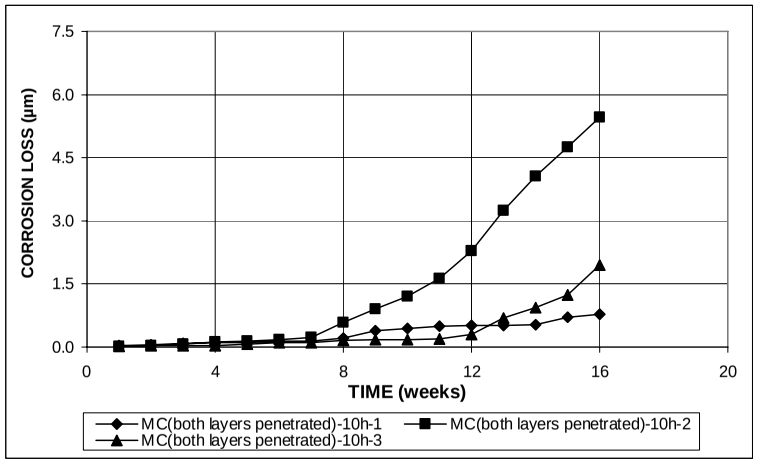

(b)

Figure A. 202 - (a) Corrosion rates and (b) total corrosion losses based on exposed area as measured in the Southern Exposure test for specimens containing multiple coated steel with both layers penetrated by 10 drilled holes

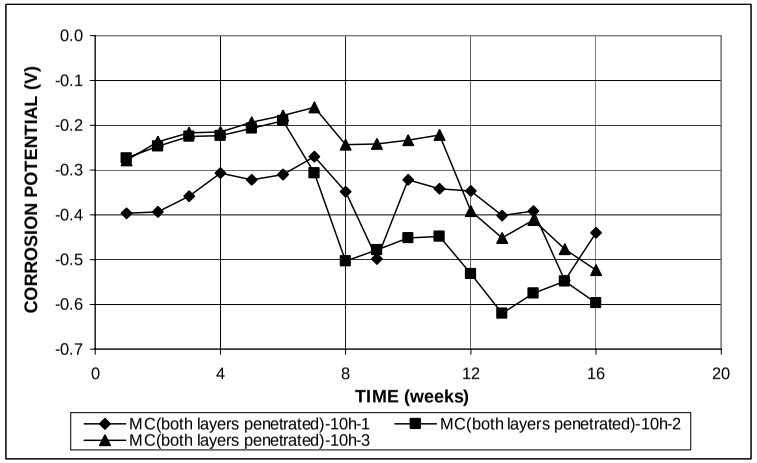

(a)

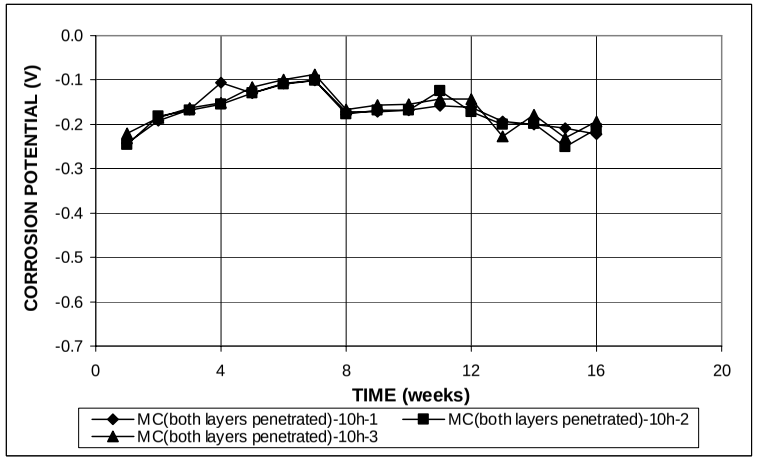

(b)

Figure A. 203 - (a) Top mat corrosion potentials and (b) bottom mat corrosion potentials as measured in the Southern Exposure test for specimens containing multiple coated steel with both layers penetrated by 10 drilled holes

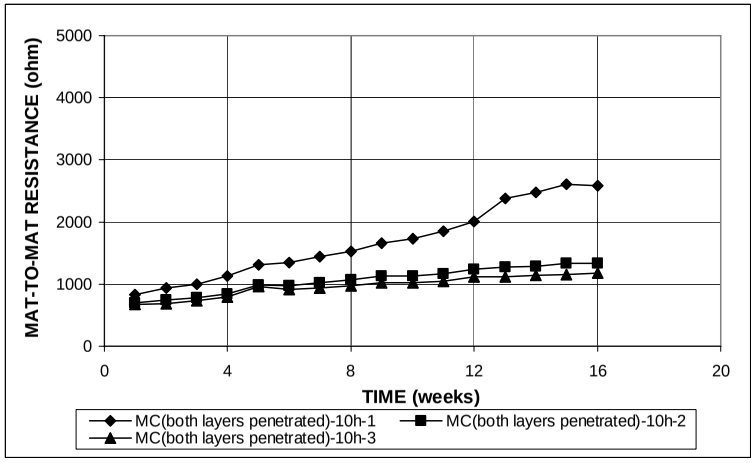

Figure A. 204 - Mat-to-mat resistances as measured in the Southern Exposure test for specimens containing multiple coated steel with both layers penetrated by 10 drilled holes

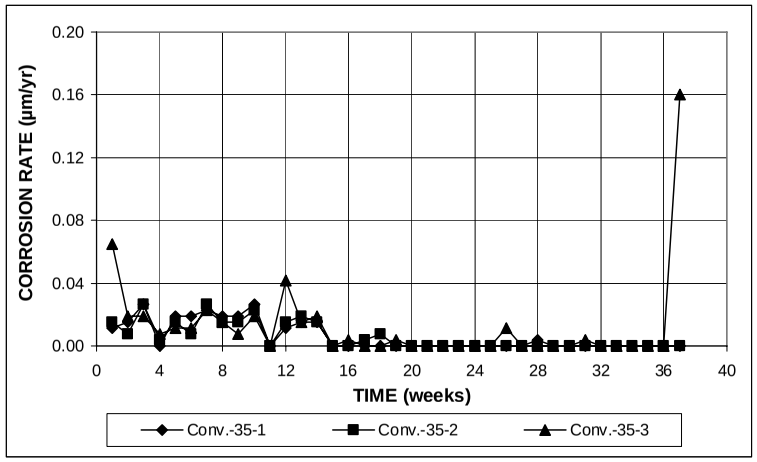

(a)

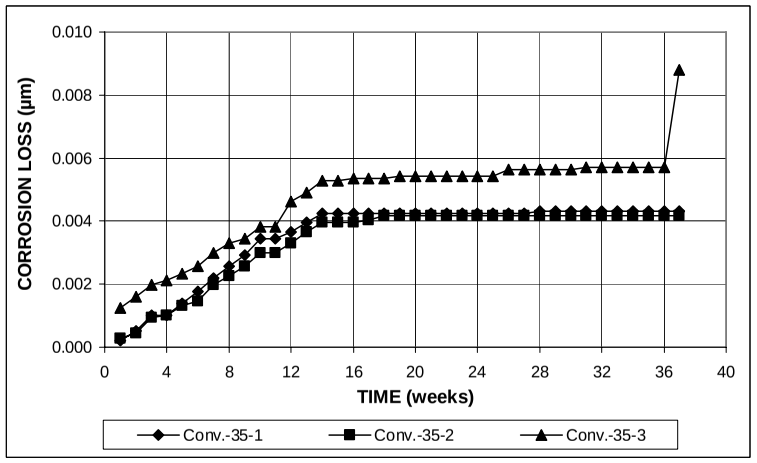

(b)

Figure A. 205 - (a) Corrosion rates and (b) total corrosion losses based on total bar area as measured in the Southern Exposure test for specimens containing conventional steel

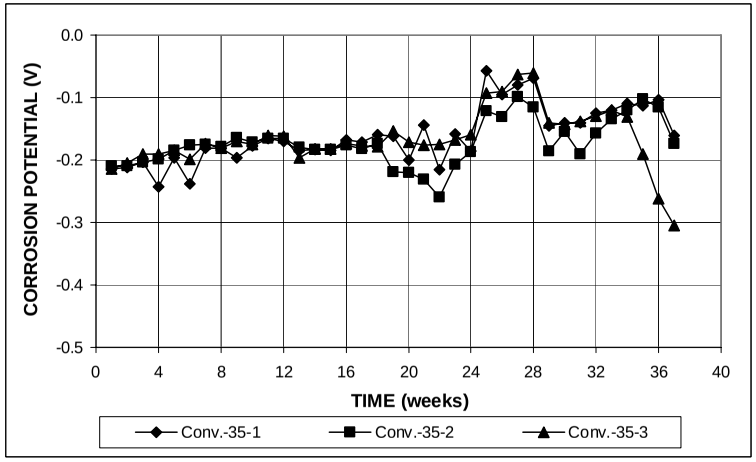

(a)

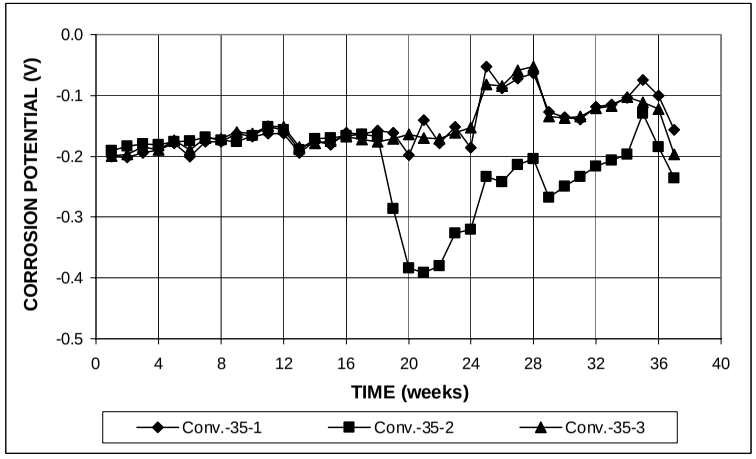

(b)

Figure A. 206 - (a) Top mat corrosion potentials and (b) bottom mat corrosion potentials as measured in the Southern Exposure test for specimens containing conventional steel

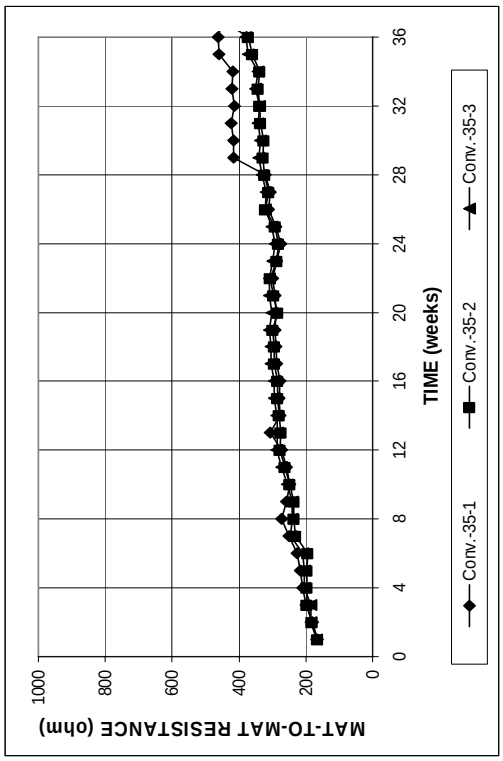

Figure A. 207 - Mat-to-mat resistances as measured in the Southern Exposure test for specimens containing conventional steel

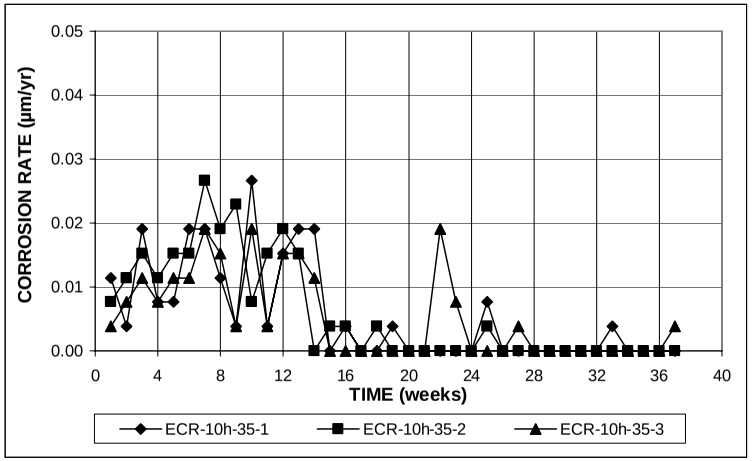

(a)

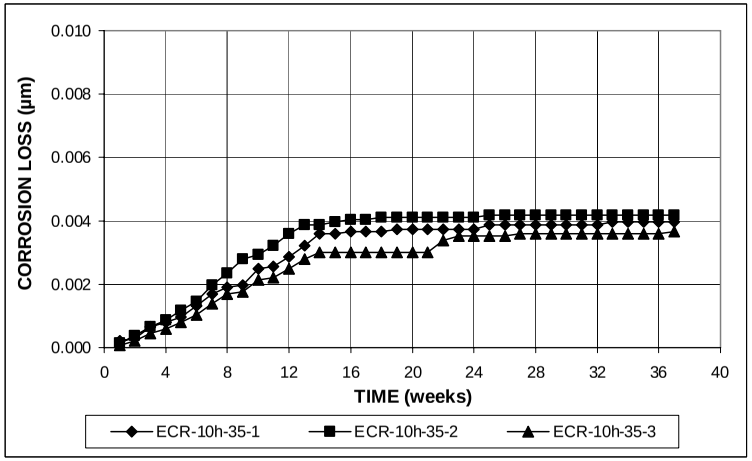

(b)

Figure A. 208 - (a) Corrosion rates and (b) total corrosion losses based on total bar area as measured in the Southern Exposure test for specimens containing epoxy-coated steel with 10 drilled holes in a w/c ratio of 0.35

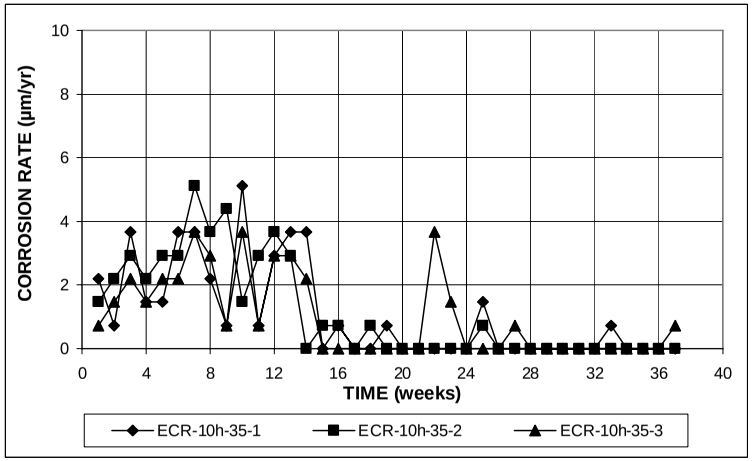

(a)

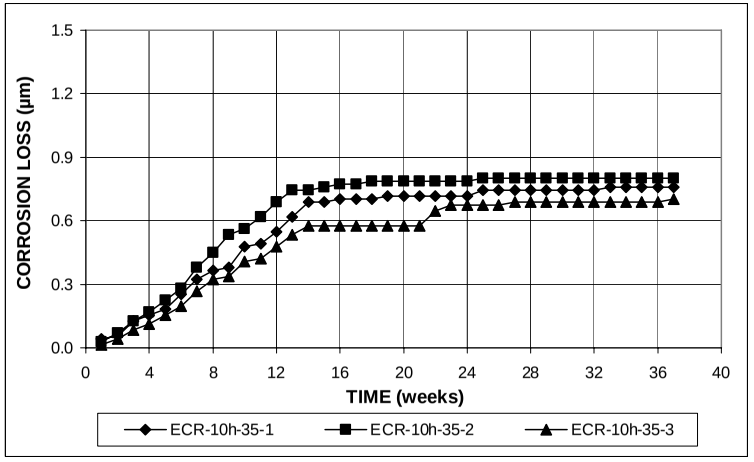

(b)

Figure A.209 - (a) Corrosion rates and (b) total corrosion losses based on total bar area as measured in the Southern Exposure test for specimens containing epoxy-coated steel with 10 drilled holes in a w/c ratio of 0.35

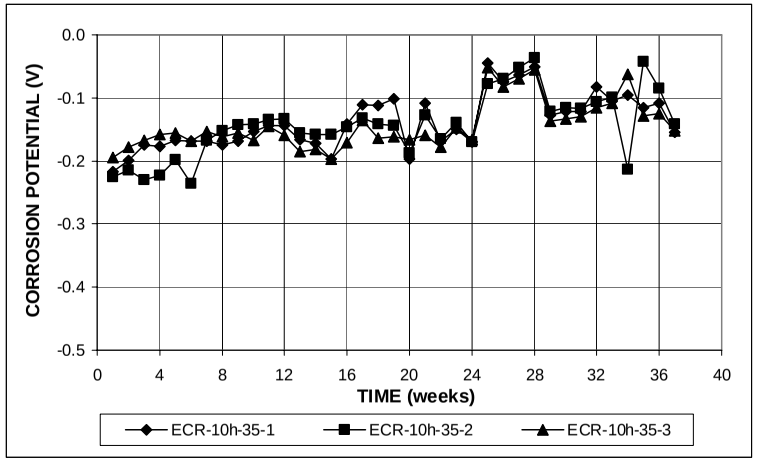

(a)

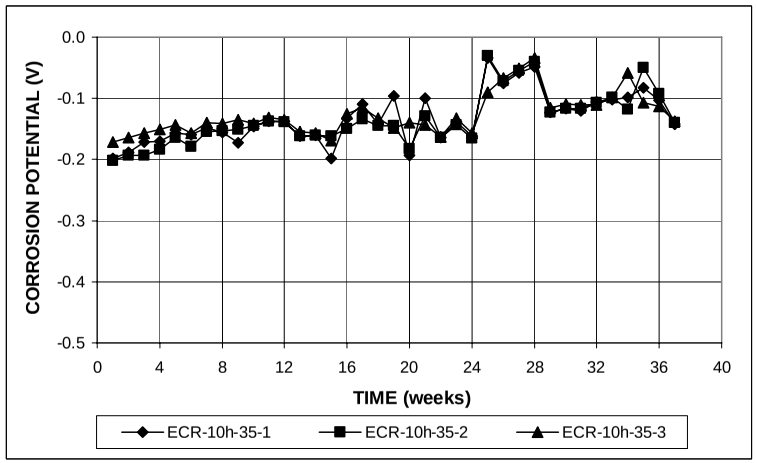

(b)

Figure A. 210 - (a) Top mat corrosion potentials and (b) bottom mat corrosion potentials as measured in the Southern Exposure test for specimens containing epoxy-coated steel with 10 drilled holes in a w/c ratio of 0.35

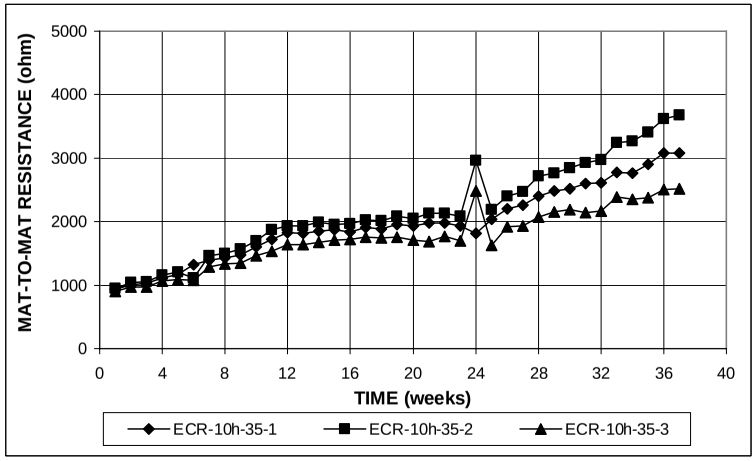

Figure A. 211 - Mat-to-mat resistances as measured in the Southern Exposure test for specimens containing epoxy-coated steel with 10 drilled holes in a w/c ratio of 0.35

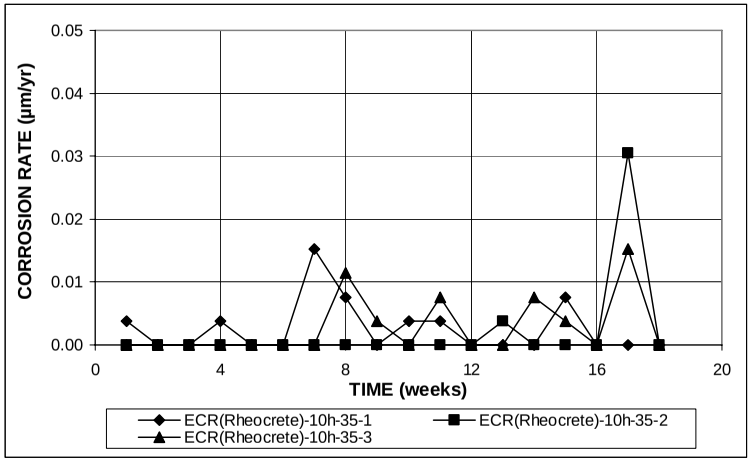

(a)

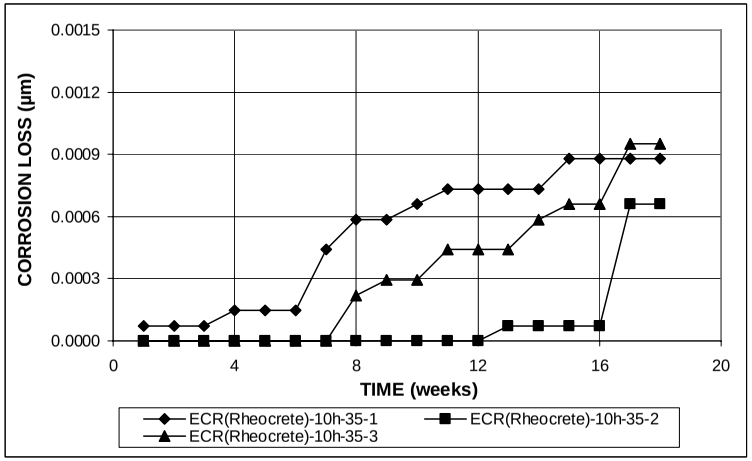

(b)

Figure A. 212 - (a) Corrosion rates and (b) total corrosion losses based on total bar area as measured in the Southern Exposure test for specimens containing epoxy-coated steel with 10 drilled holes and corrosion inhibitor Rheocrete in a w/c ratio of 0.35

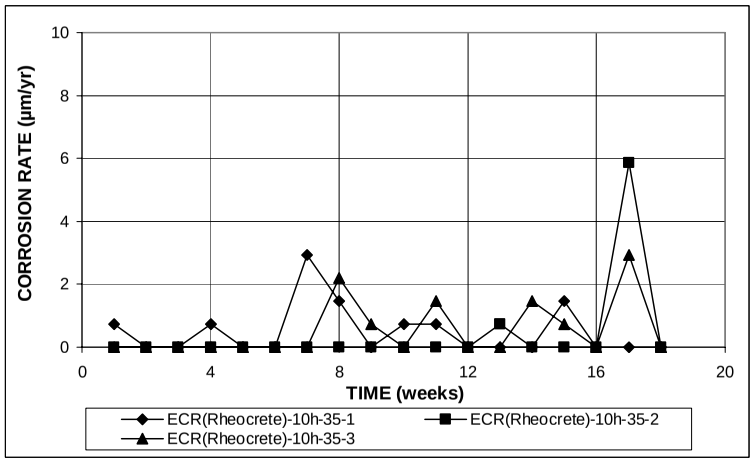

(a)

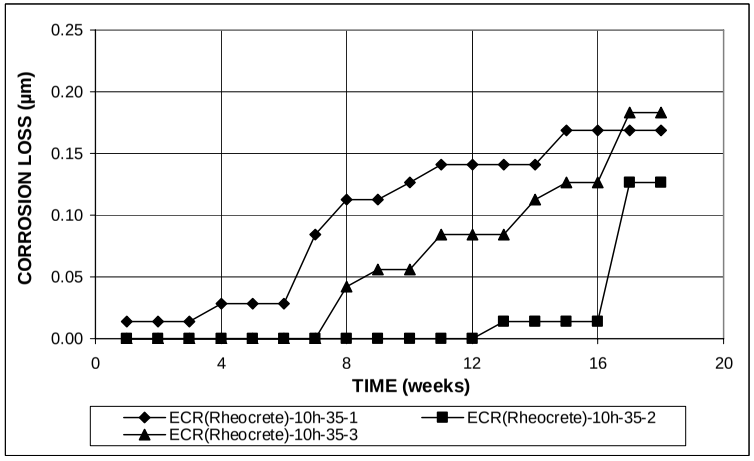

(b)

Figure A. 213 - (a) Corrosion rates and (b) total corrosion losses based on exposed area as measured in the Southern Exposure test for specimens containing epoxy-coated steel with 10 drilled holes and corrosion inhibitor Rheocrete in a w/c ratio of 0.35

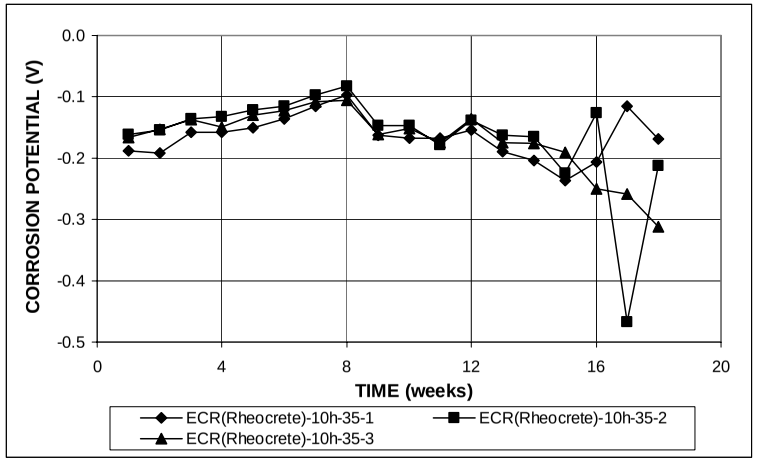

(a)

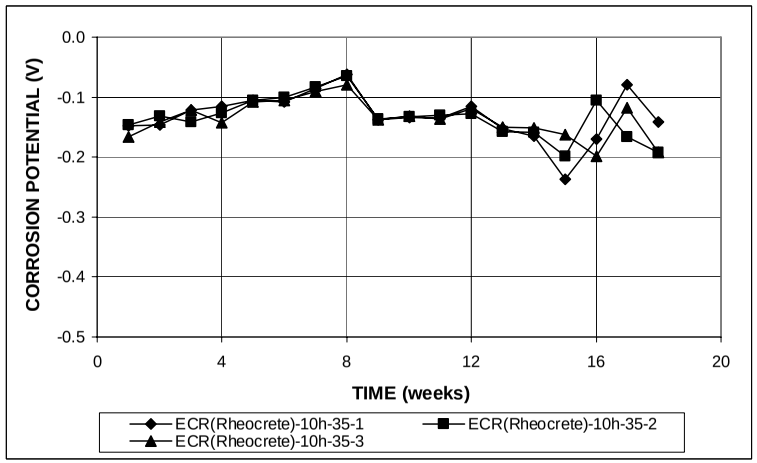

(b)

Figure A. 214 - (a) Top mat corrosion potentials and (b) bottom mat corrosion potentials as measured in the Southern Exposure test for specimens containing epoxy-coated steel with 10 drilled holes and corrosion inhibitor Rheocrete in a w/c ratio of 0.35

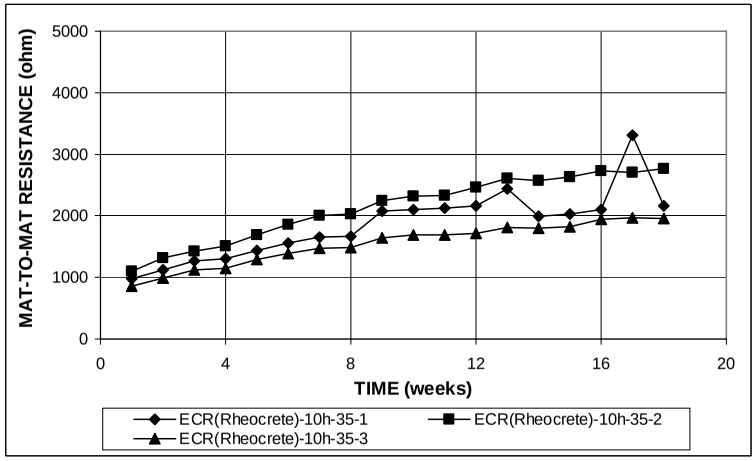

Figure A. 215 - Mat-to-mat resistances as measured in the Southern Exposure test for specimens containing epoxy-coated steel with 10 drilled holes and corrosion inhibitor Rheocrete in a w/c ratio of 0.35

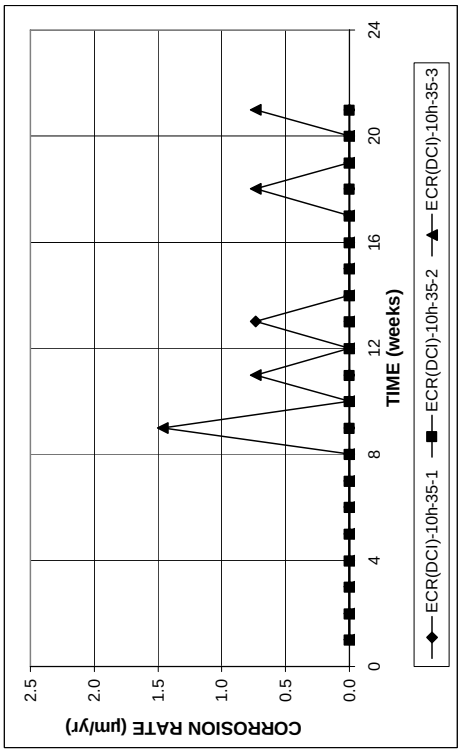

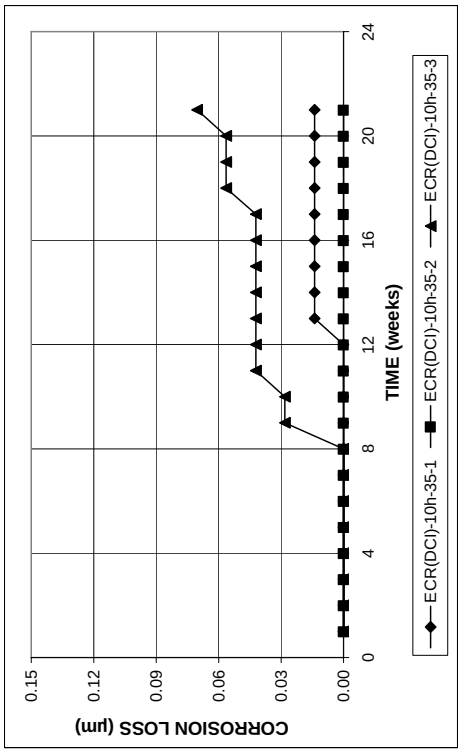

Figure A. 217 - (a) Corrosion rates and (b) total corrosion losses based on total bar area as measured in the Southern Exposure test for specimens containing epoxy-coated steel with 10 drilled holes and corrosion inhibitor DCI in a w/c ratio of 0.35

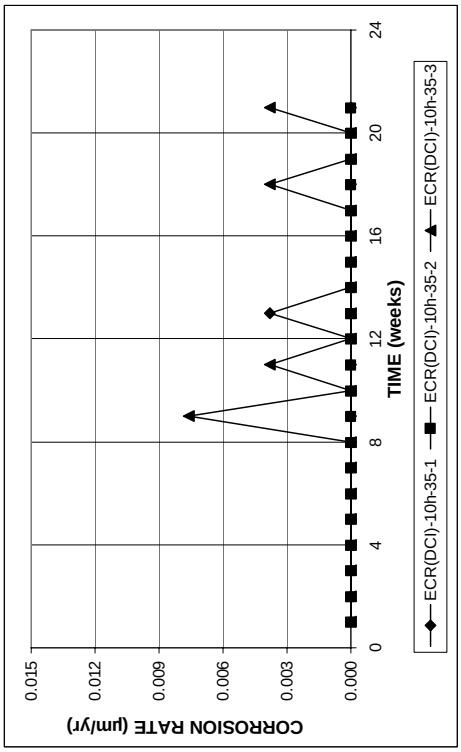

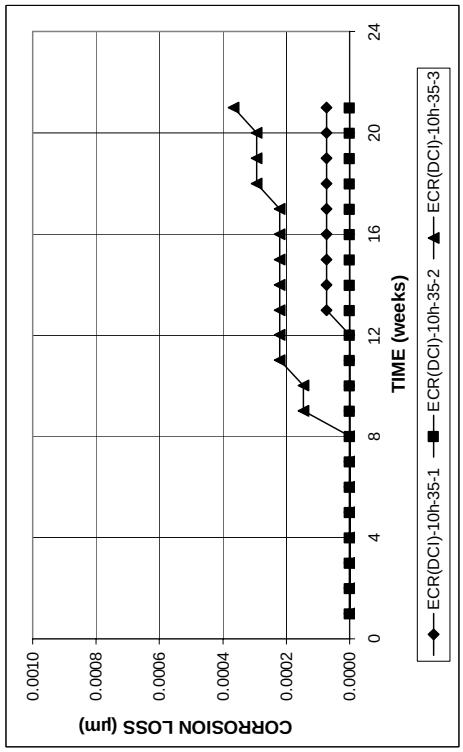

Figure A. 216 - (a) Corrosion rates and (b) total corrosion losses based on total bar area as measured in the Southern Exposure test for specimens containing epoxy-coated steel with 10 drilled holes and corrosion inhibitor DCI in a w/c ratio of 0.35

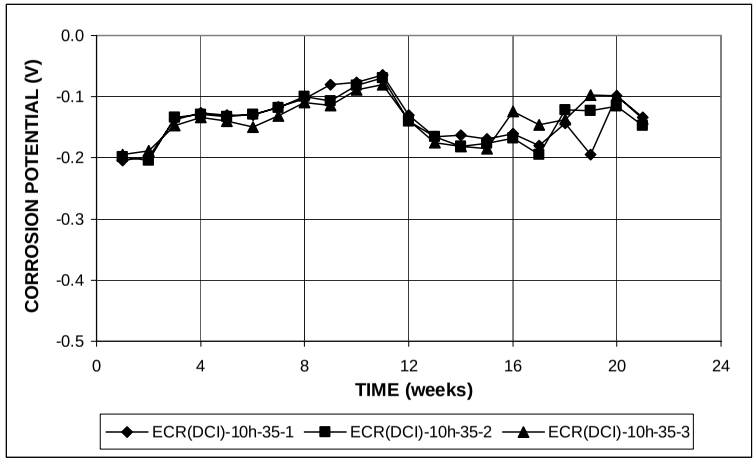

(a)

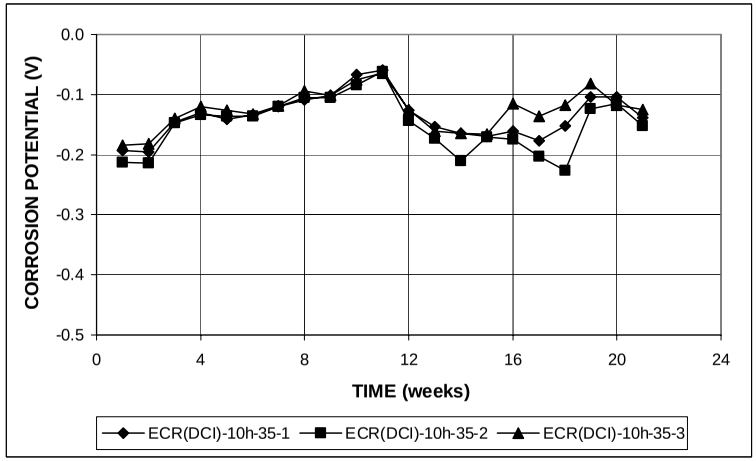

(b)

Figure A. 218 - (a) Top mat corrosion potentials and (b) bottom mat corrosion potentials as measured in the Southern Exposure test for specimens containing epoxy-coated steel with 10 drilled holes and corrosion inhibitor DCI in a w/c ratio of 0.35

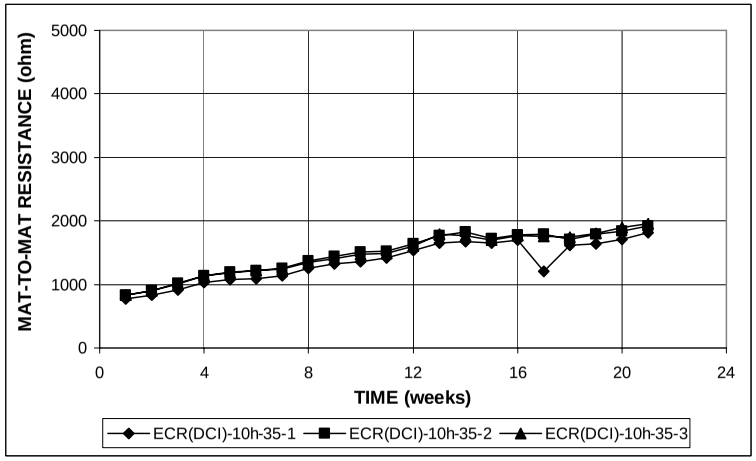

Figure A. 219 - Mat-to-mat resistances as measured in the Southern Exposure test for specimens containing epoxy-coated steel with 10 drilled holes and corrosion inhibitor DCI in a w/c ratio of 0.35

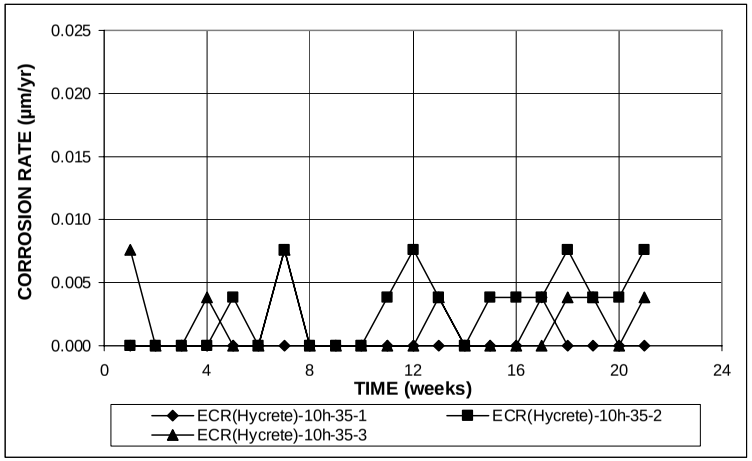

(a)

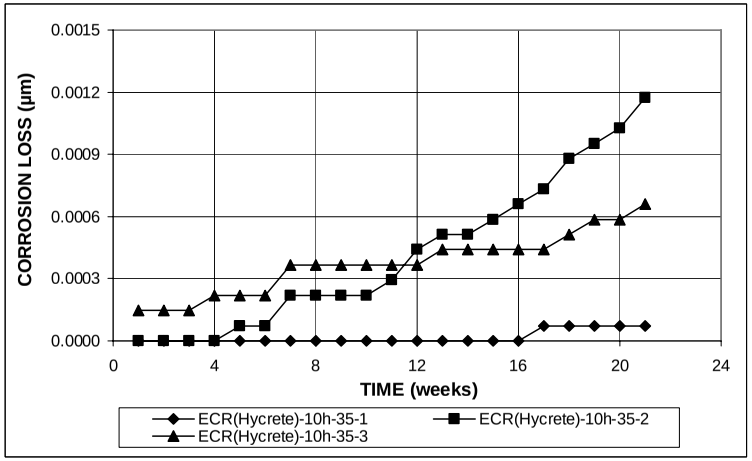

(b)

Figure A. 220 - (a) Corrosion rates and (b) total corrosion losses based on total bar area as measured in the Southern Exposure test for specimens containing epoxy-coated steel with 10 drilled holes and corrosion inhibitor Hycrete in a w/c ratio of 0.35

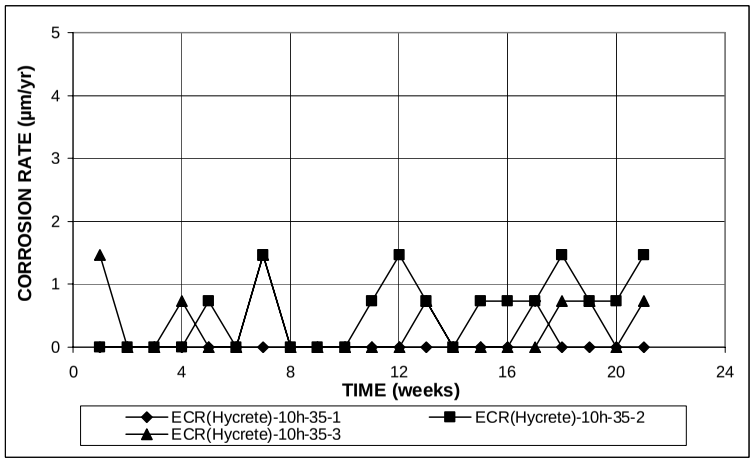

(a)

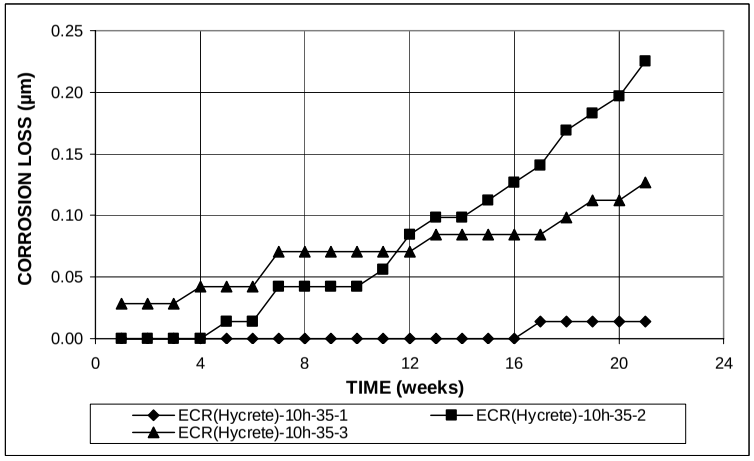

(b)

Figure A. 221 - (a) Corrosion rates and (b) total corrosion losses based on exposed area as measured in the Southern Exposure test for specimens containing epoxy-coated steel with 10 drilled holes and corrosion inhibitor Hycrete in a w/c ratio of 0.35

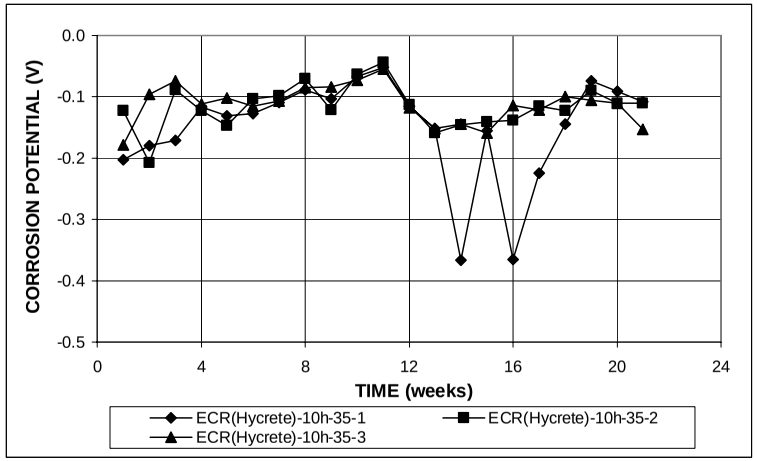

(a)

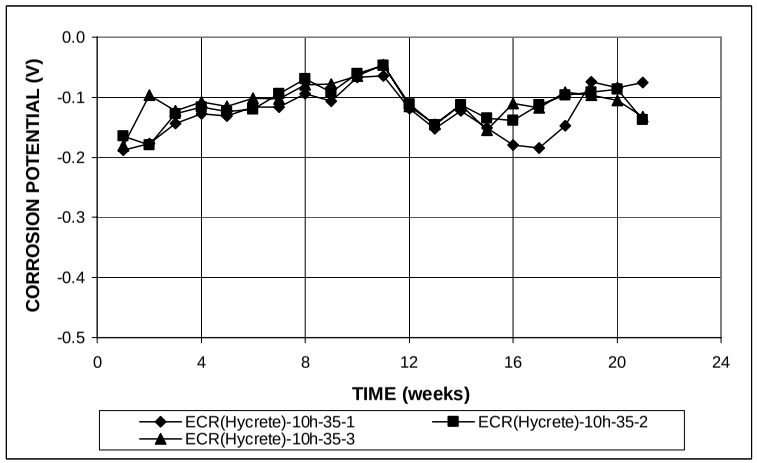

(b)

Figure A. 222 - (a) Top mat corrosion potentials and (b) bottom mat corrosion potentials as measured in the Southern Exposure test for specimens containing epoxy-coated steel with 10 drilled holes and corrosion inhibitor Hycrete in a w/c ratio of 0.35

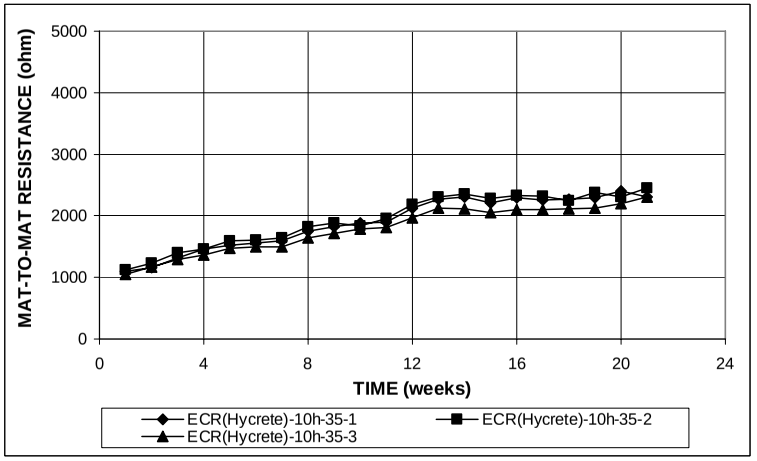

Figure A. 223 - Mat-to-mat resistances as measured in the Southern Exposure test for specimens containing epoxy-coated steel with 10 drilled holes and corrosion inhibitor Hycrete in a w/c ratio of 0.35

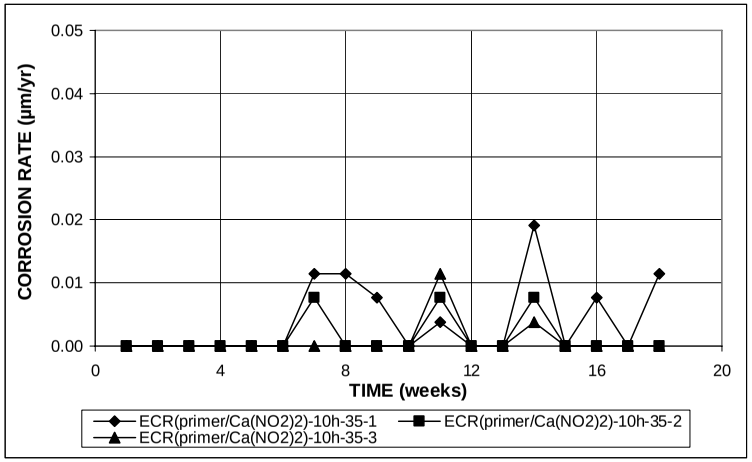

(a)

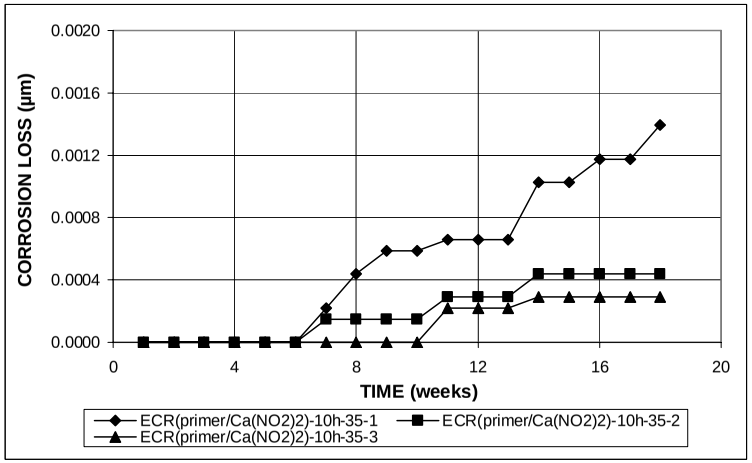

(b)

Figure A. 224 - (a) Corrosion rates and (b) total corrosion losses based on total bar area as measured in the Southern Exposure test for specimens containing ECR(primer/Ca(NO_2)$_2$) bars with 10 drilled holes in a w/c of 0.35

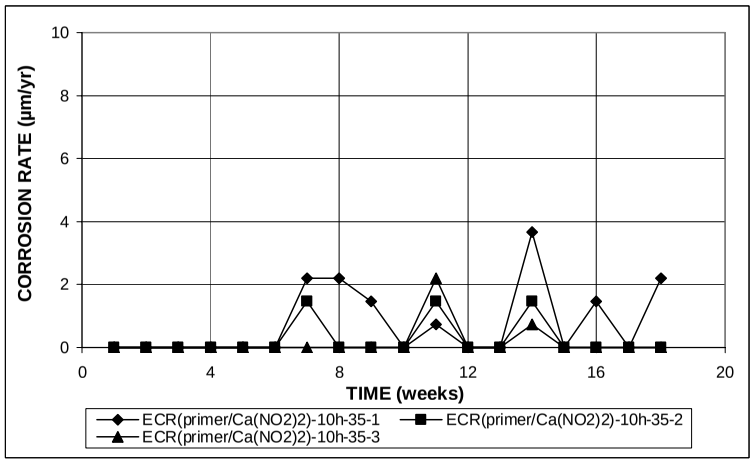

(a)

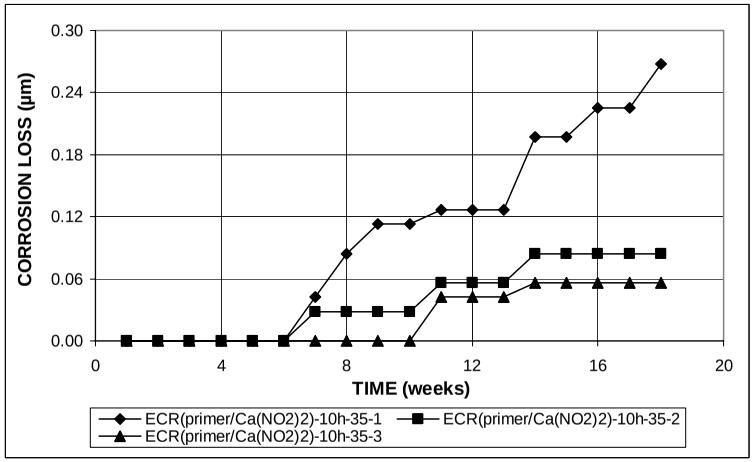

(b)

Figure A. 225 - (a) Corrosion rates and (b) total corrosion losses based on exposed area as measured in the Southern Exposure test for specimens containing ECR(primer/Ca(NO_2)$_2$) bars with 10 drilled holes in a w/c of 0.35

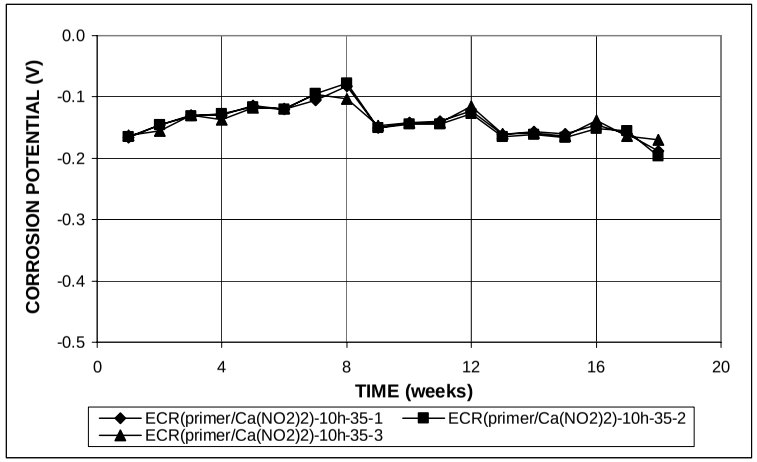

(a)

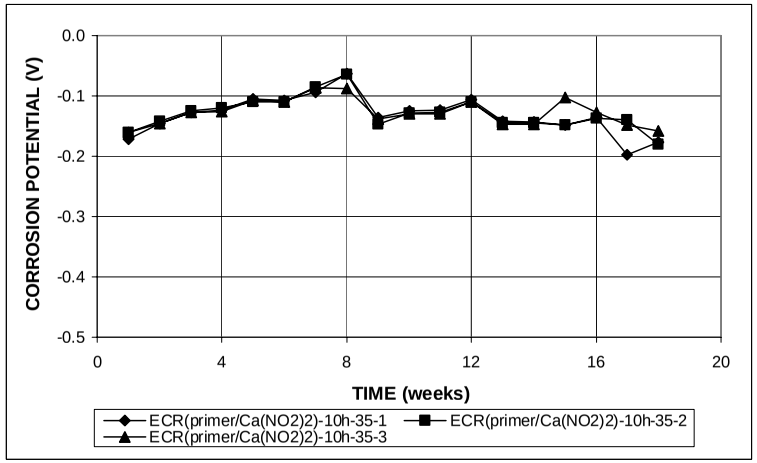

(b)

Figure A. 226 - (a) Top mat corrosion potentials and (b) bottom mat corrosion potentials as measured in the Southern Exposure test for specimens containing ECR(primer/Ca$(NO_2)_2$) bars with 10 drilled holes in a w/c of 0.35

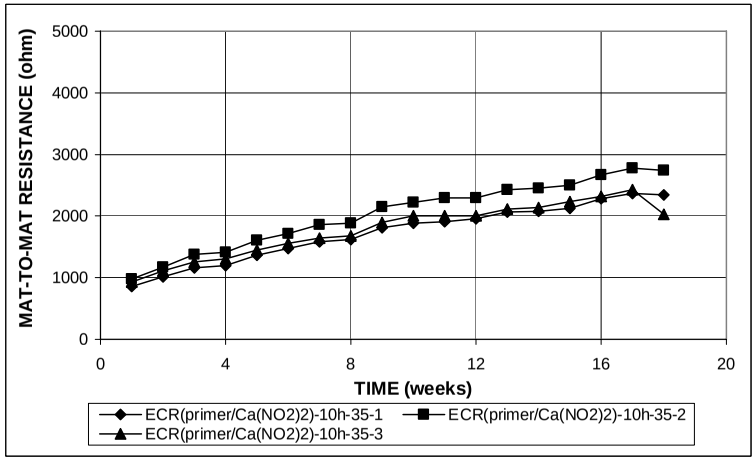

Figure A. 227 - Mat-to-mat resistances as measured in the Southern Exposure test for specimens containing ECR(primer/Ca$(NO_2)_2$) bars with 10 drilled holes in a w/c of 0.35

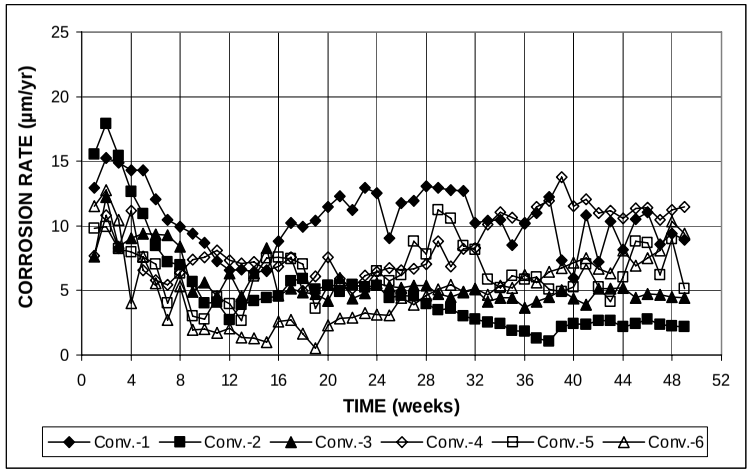

(a)

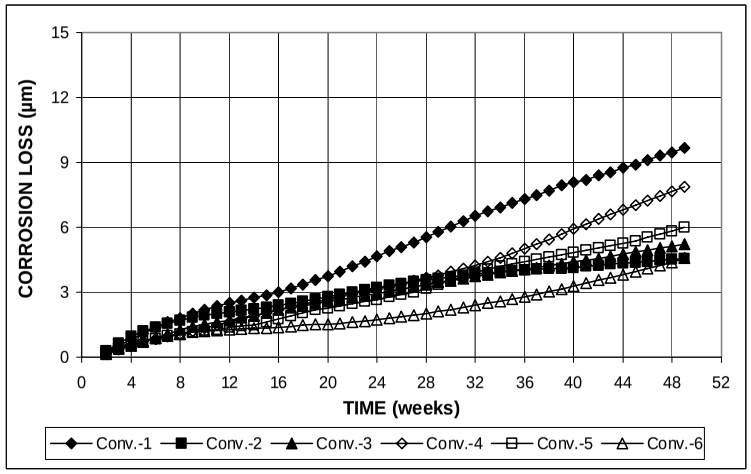

(b)

Figure A. 228 - (a) Corrosion rates and (b) total corrosion losses based on total bar area as measured in the cracked beam test for specimens containing conventional steel

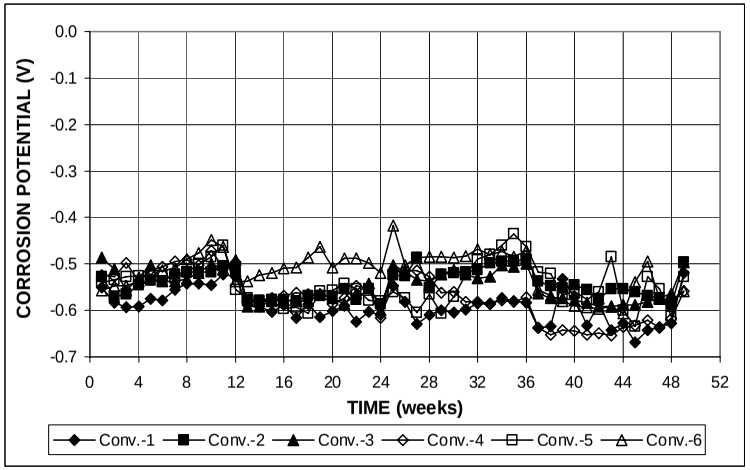

(a)

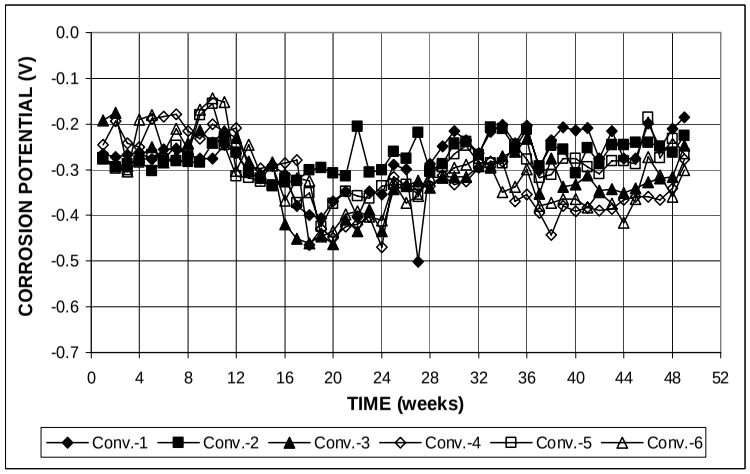

(b)

Figure A. 229 - (a) Top mat corrosion potentials and (b) bottom mat corrosion potentials as measured in the cracked beam test for specimens containing conventiional steel

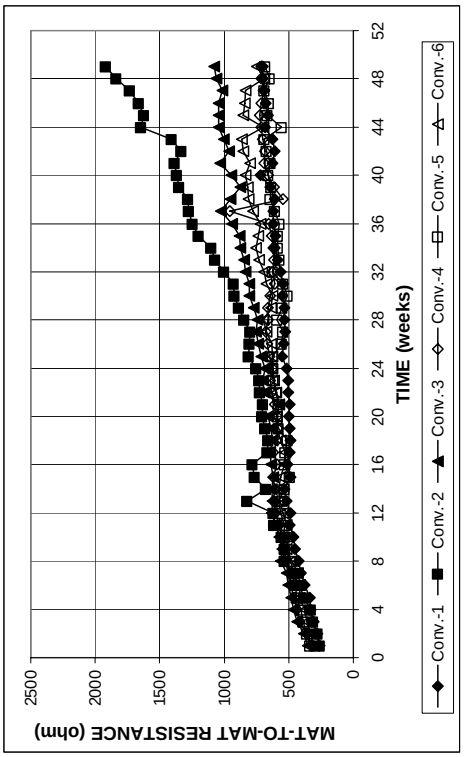

Figure A. 230 - Mat-to-mat resistances as measured in the cracked beam test for specimens containing conventional steel

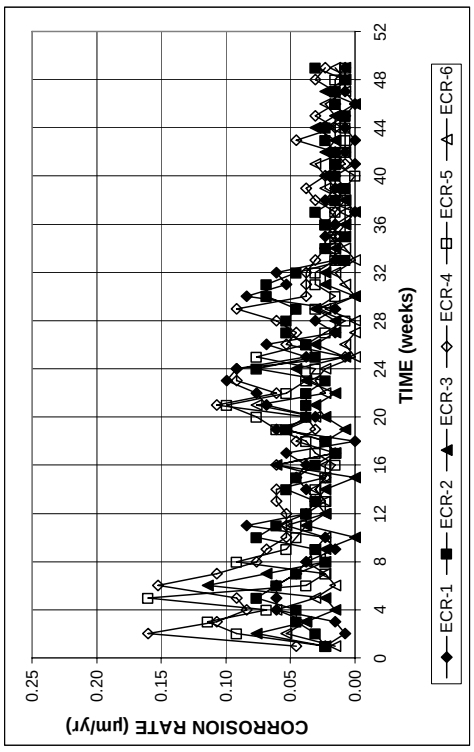

Figure A. 231 - (a) Corrosion rates and (b) total corrosion losses based on total bar area as measured in the cracked beam test for specimens containing epoxy-coated bars

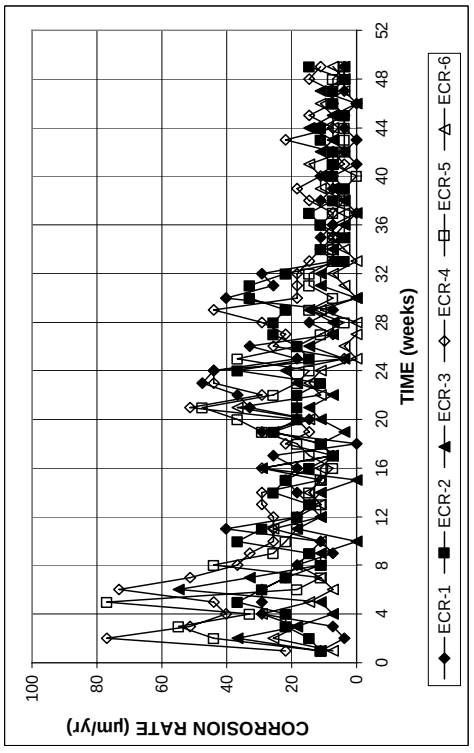

Figure A. 232 - (a) Corrosion rates and (b) total corrosion losses based on exposed area as measured in the cracked beam test for specimens containing epoxy-coated bars

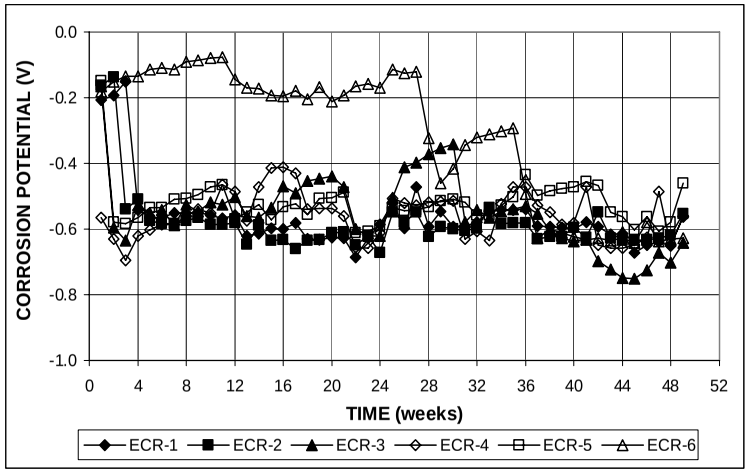

(a)

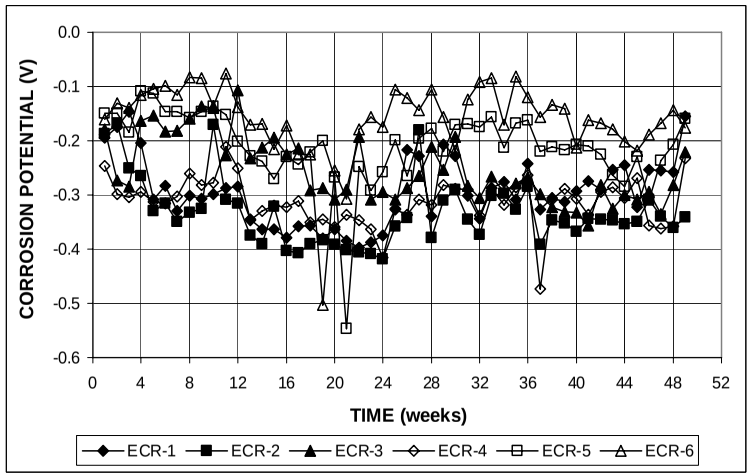

(b)

Figure A. 233 - (a) Top mat corrosion potentials and (b) bottom mat corrosion potentials as measured in the cracked beam test for specimens containing epoxy-coated bars

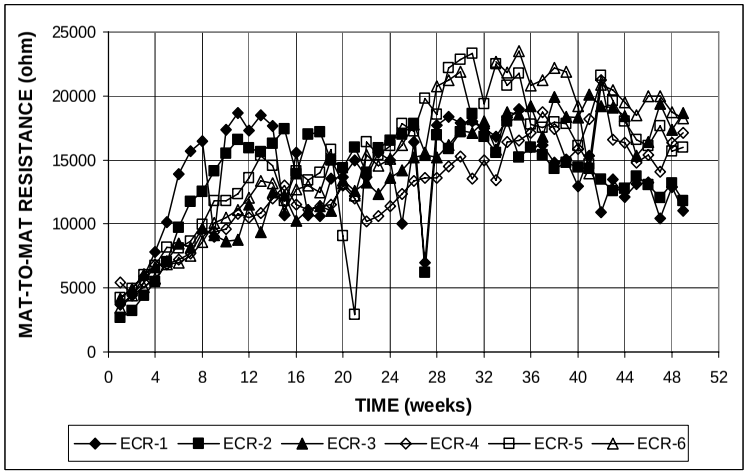

Figure A. 234 - Mat-to-mat resistances as measured in the cracked beam test for specimens containing epoxy-coated bars

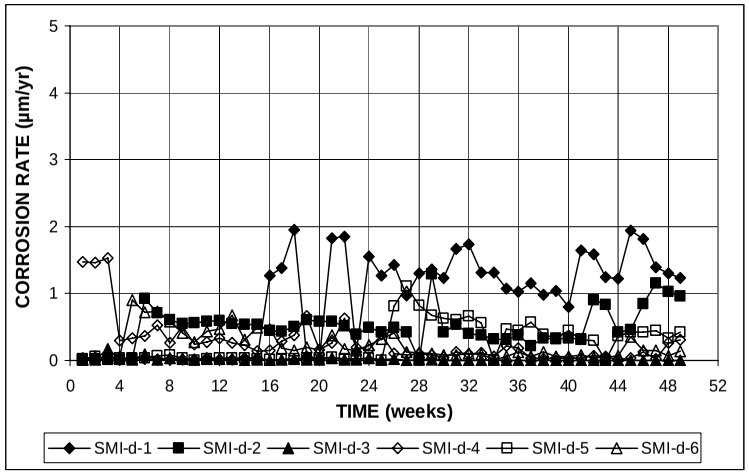

(a)

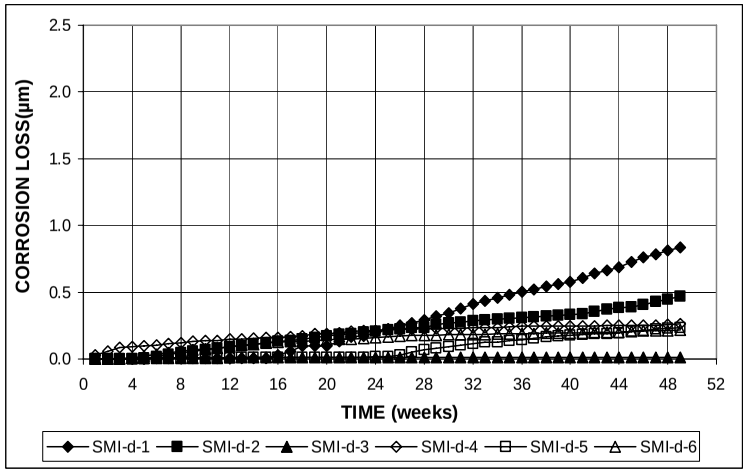

(b)

Figure A. 235 - (a) Corrosion rates and (b) total corrosion losses based on total bar area as measured in the cracked beam test for specimens containing stainless steel clad bars with drilled holes

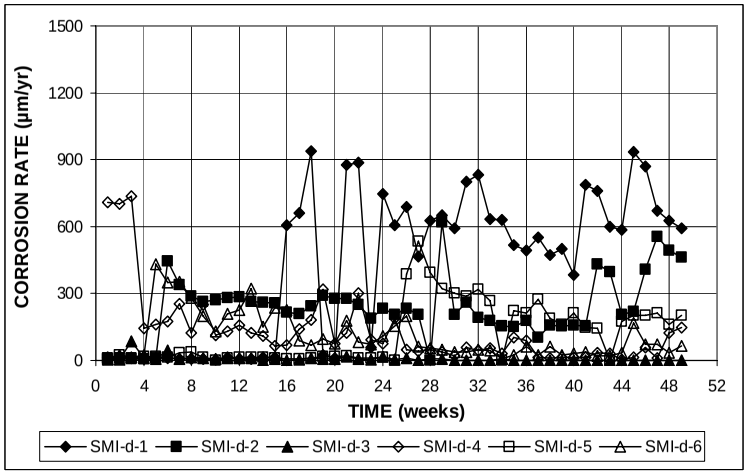

(a)

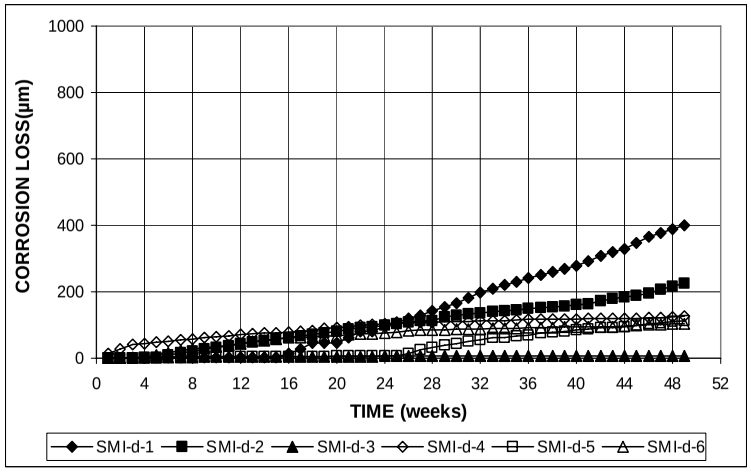

(b)

Figure A. 236 - (a) Corrosion rates and (b) total corrosion losses based on exposed area as measured in the cracked beam test for specimens containing stainless steel clad bars with drilled holes

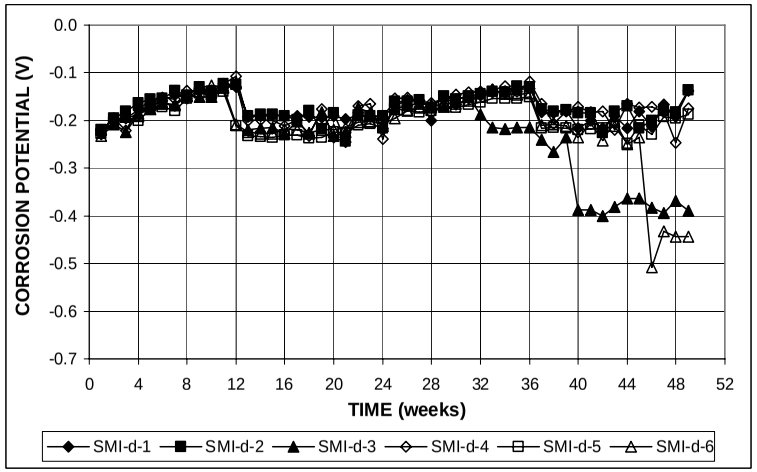

(a)

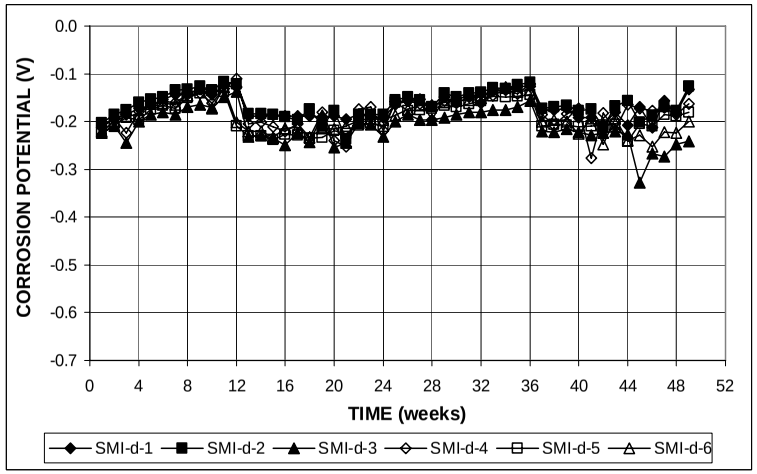

(b)

Figure A. 237 - (a) Top mat corrosion potentials and (b) bottom mat corrosion potentials as measured in the cracked beam test for specimens containing stainless steel clad bars with drilled holes

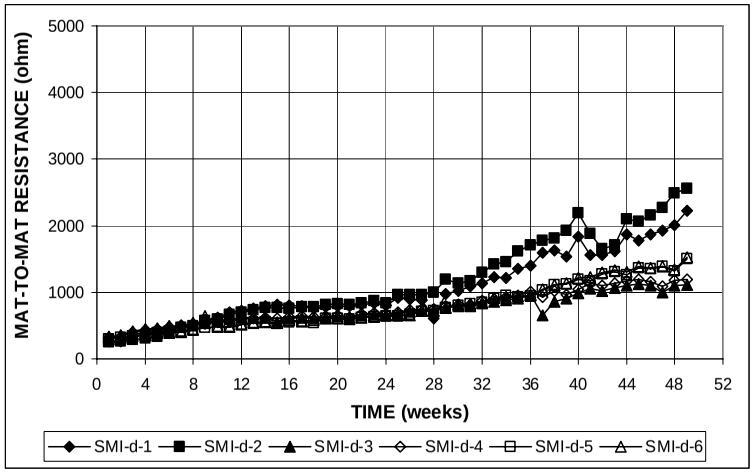

Figure A. 238 - Mat-to-mat resistances as measured in the cracked beam test for specimens containing stainless steel clad bars with drilled holes

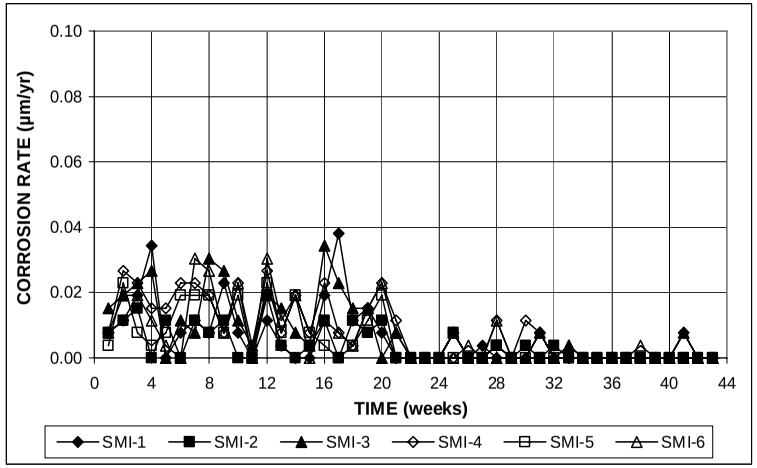

(a)

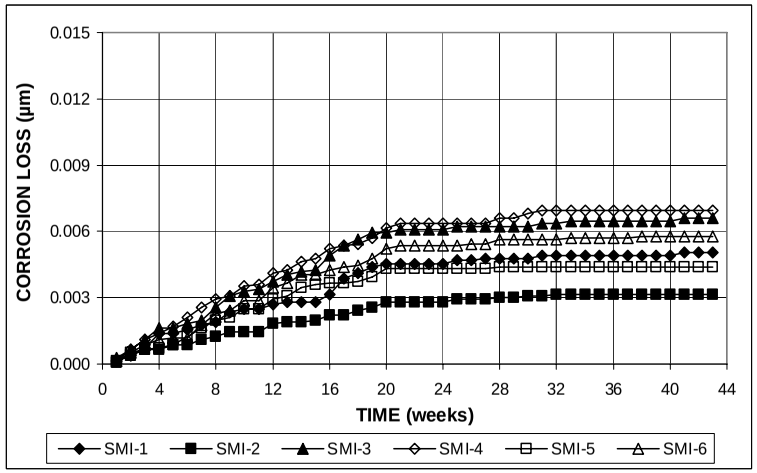

(b)

Figure A. 239 - (a) Corrosion rates and (b) total corrosion losses based on total bar area as measured in the cracked beam test for specimens containing stainless steel clad bars

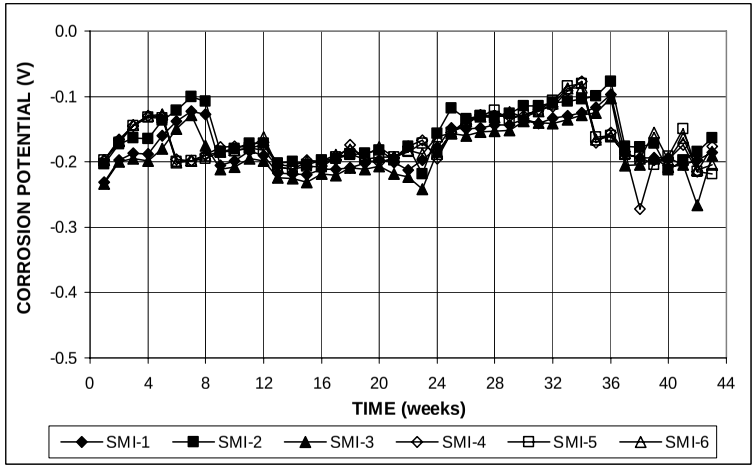

(a)

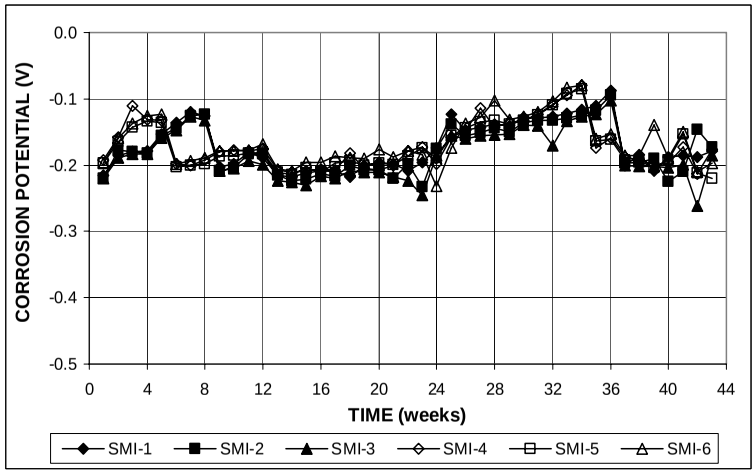

(b)

Figure A. 240 - (a) Top mat corrosion potentials and (b) bottom mat corrosion potentials as measured in the cracked beam test for specimens containing stainless steel clad bars

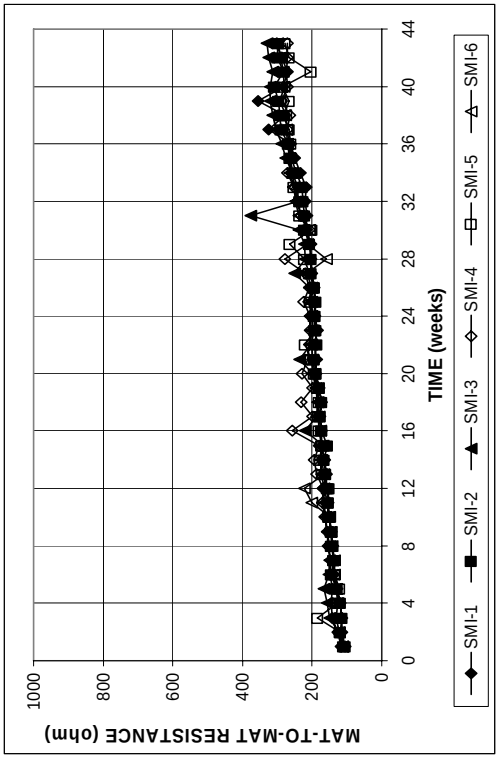

Figure A. 241 - Mat-to-mat resistances as measured in the cracked beam test for specimens containing stainless steel clad bars

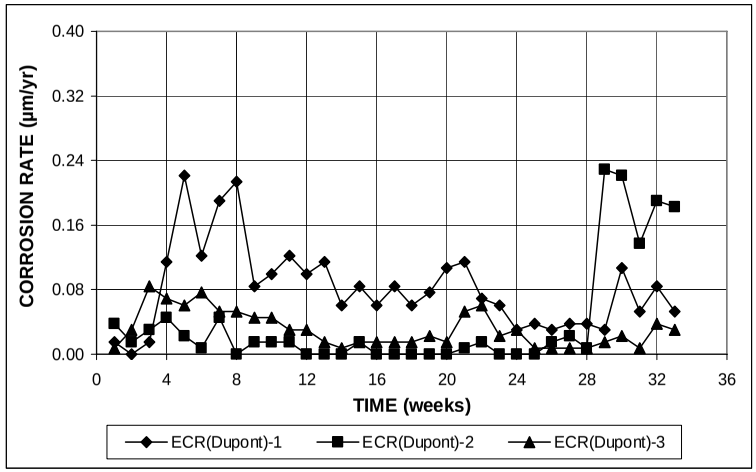

(a)

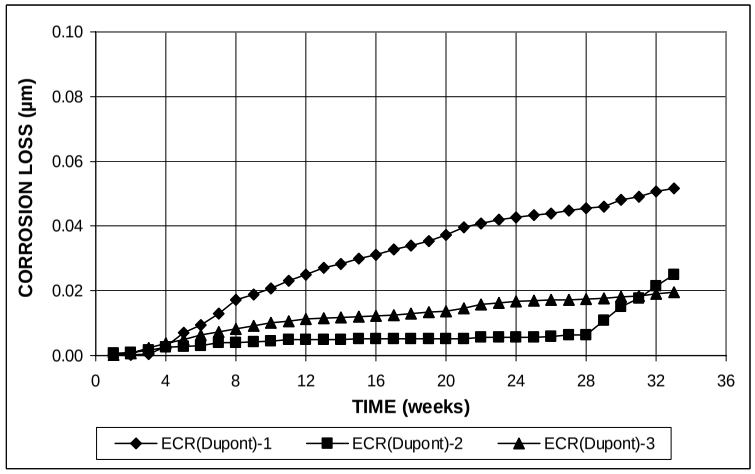

(b)

Figure A. 242 - (a) Corrosion rates and (b) total corrosion losses based on total bar area as measured in the cracked beam test for specimens containing ECR(Dupont) bars

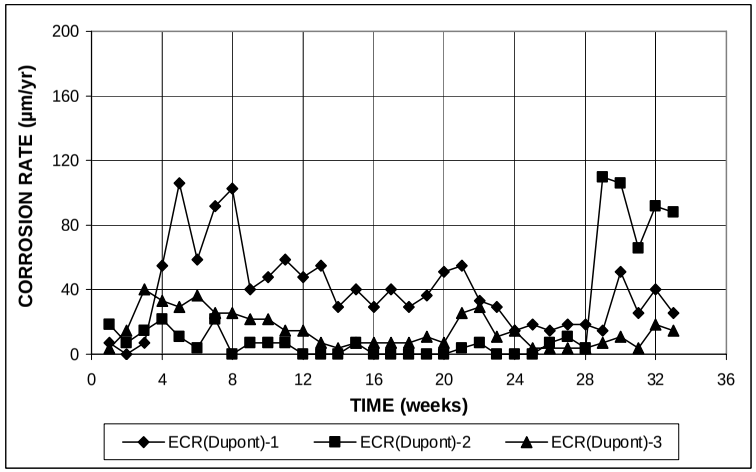

(a)

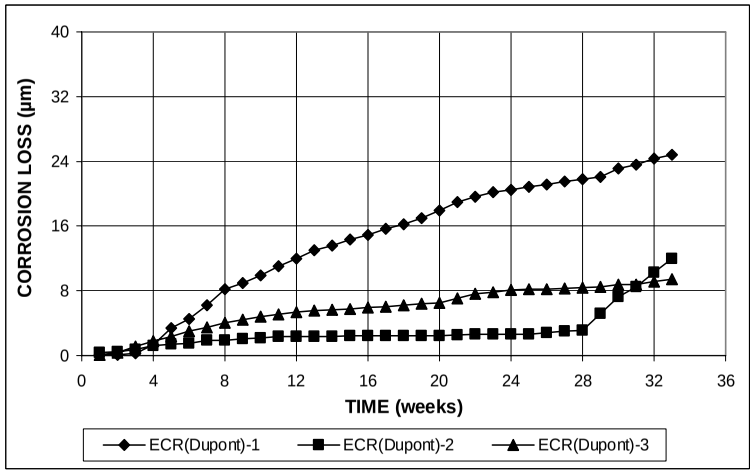

(b)

Figure A. 243 - (a) Corrosion rates and (b) total corrosion losses based on total bar area as measured in the cracked beam test for specimens containing ECR(Dupont) bars

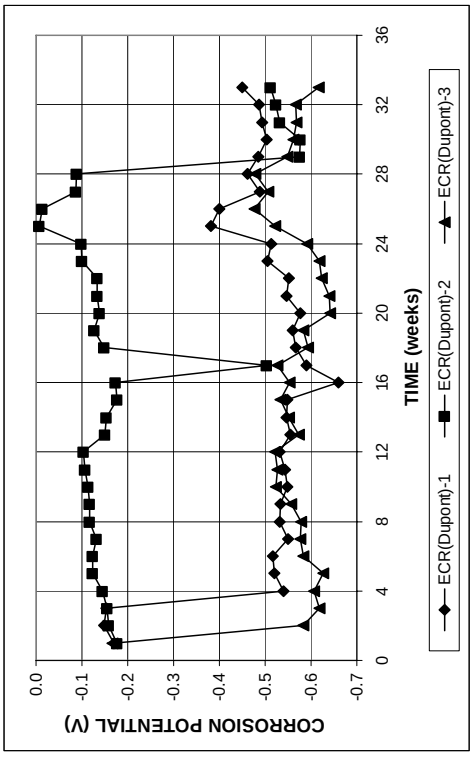

(a)

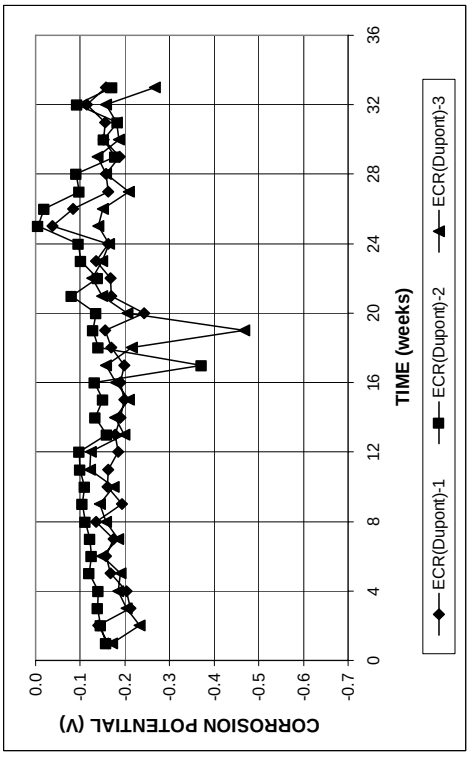

(b)

Figure A. 244 - (a) Top mat corrosion potentials and (b) bottom mat corrosion potentials as measured in the cracked beam test for specimens containing ECR(Dupont) bars

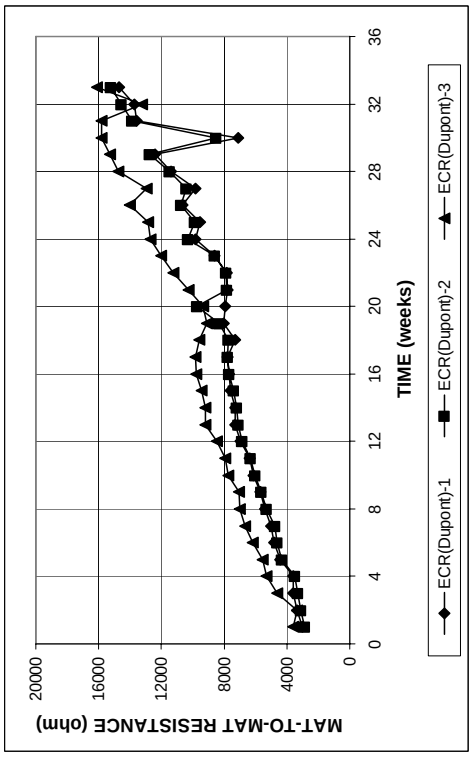

Figure A. 245 - Mat-to-mat resistances as measured in the cracked beam test for specimens containing ECR(Dupont) bars

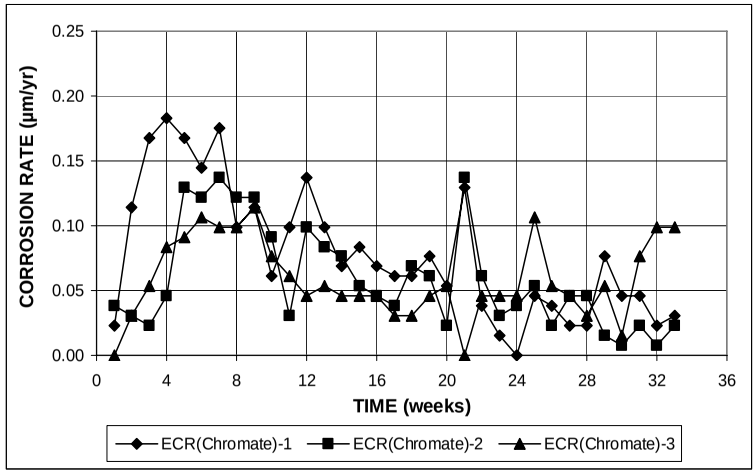

(a)

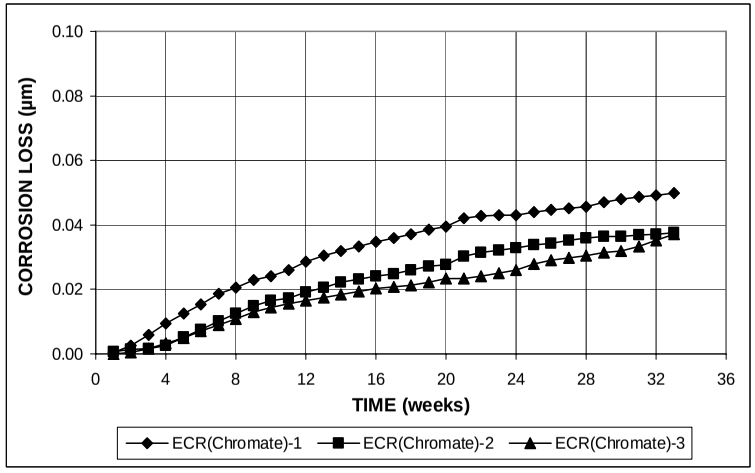

(b)

Figure A. 246 - (a) Corrosion rates and (b) total corrosion losses based on total bar area as measured in the cracked beam test for specimens containing ECR(Chromate) bars

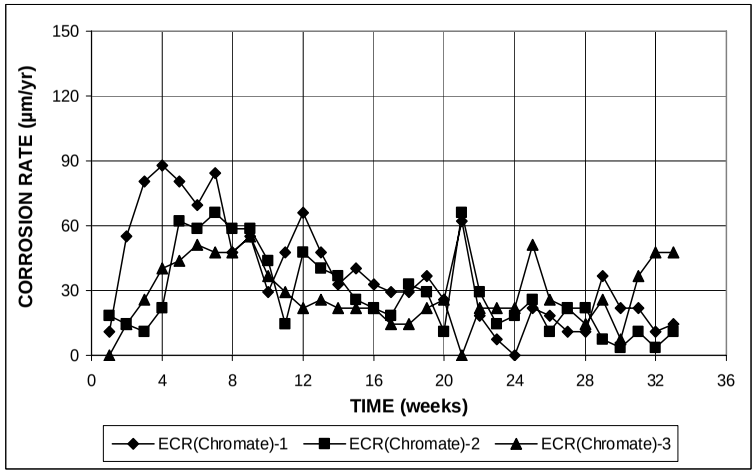

(a)

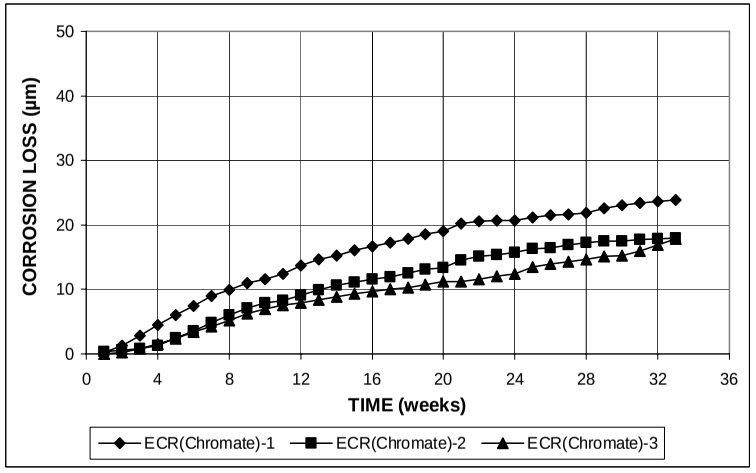

(b)

Figure A. 247 - (a) Corrosion rates and (b) total corrosion losses based on total bar area as measured in the cracked beam test for specimens containing ECR(Chromate) bars

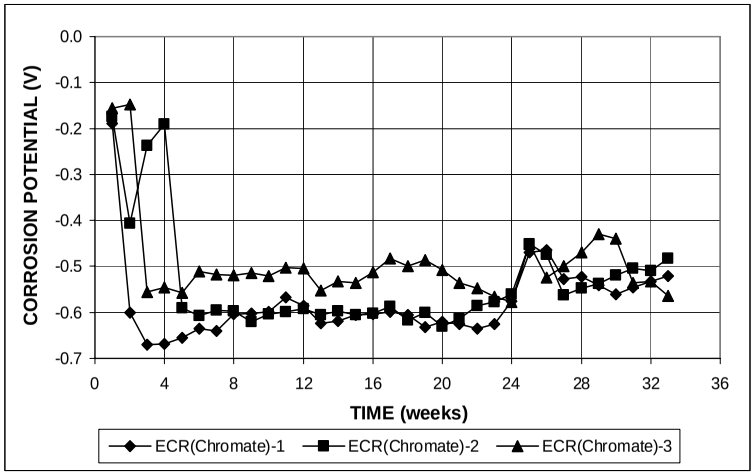

(a)

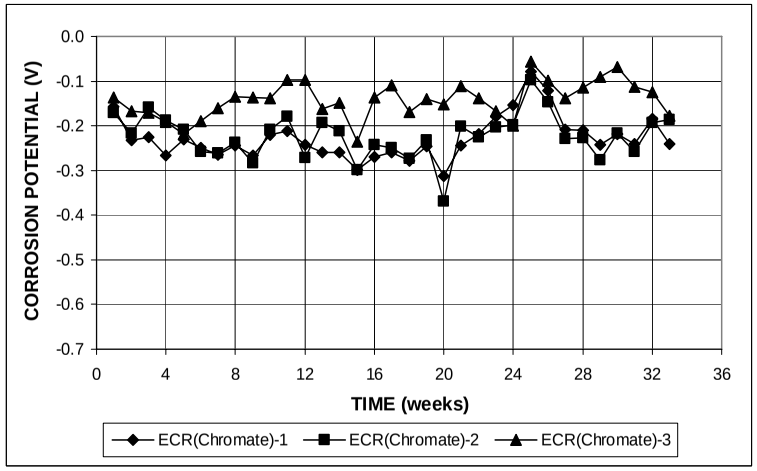

(b)

Figure A. 248 - (a) Top mat corrosion potentials and (b) bottom mat corrosion potentials as measured in the cracked beam test for specimens containing ECR(Chromate) bars

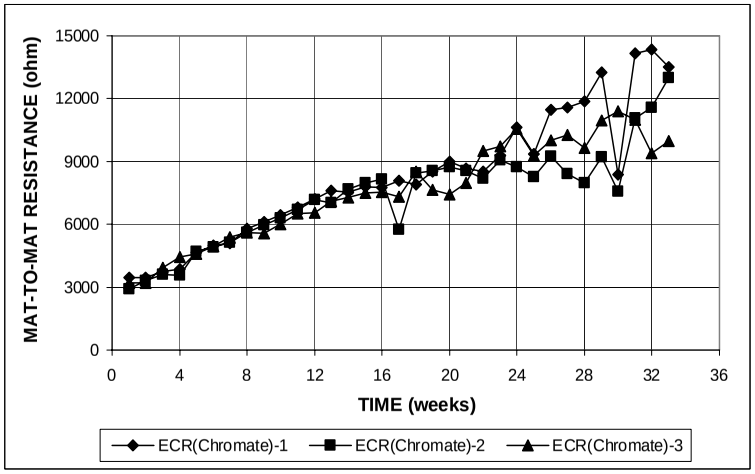

Figure A. 249 - Mat-to-mat resistances as measured in the cracked beam test for specimens containing ECR(Chromate) bars

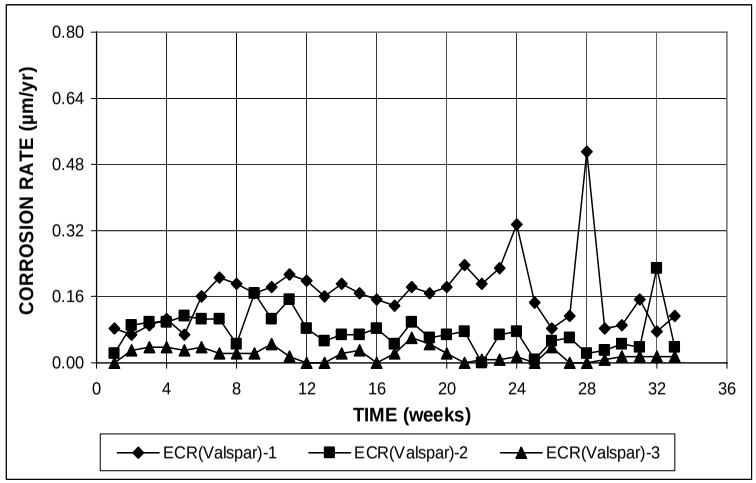

(a)

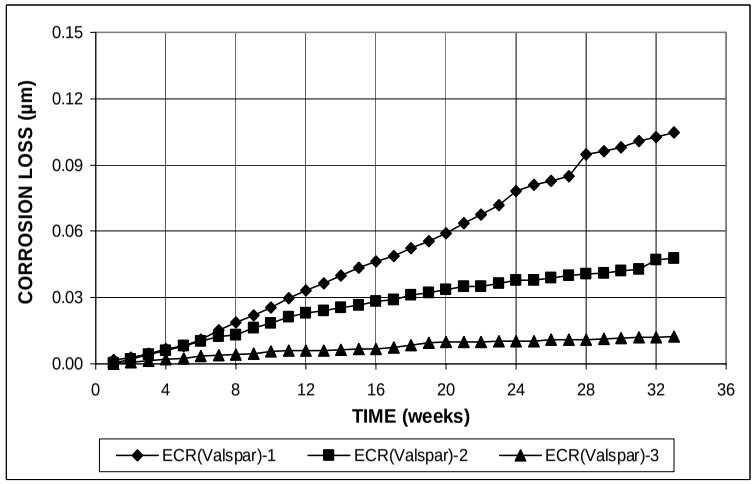

(b)

Figure A. 250 - (a) Corrosion rates and (b) total corrosion losses based on total bar area as measured in the cracked beam test for specimens containing ECR(Valspar) bars

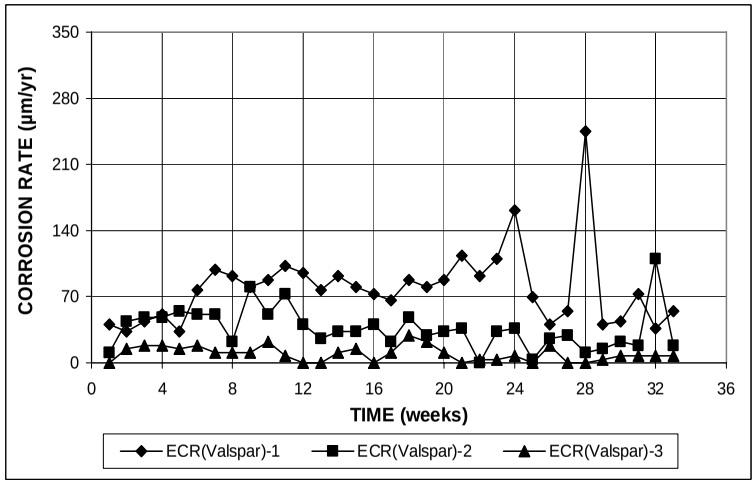

(a)

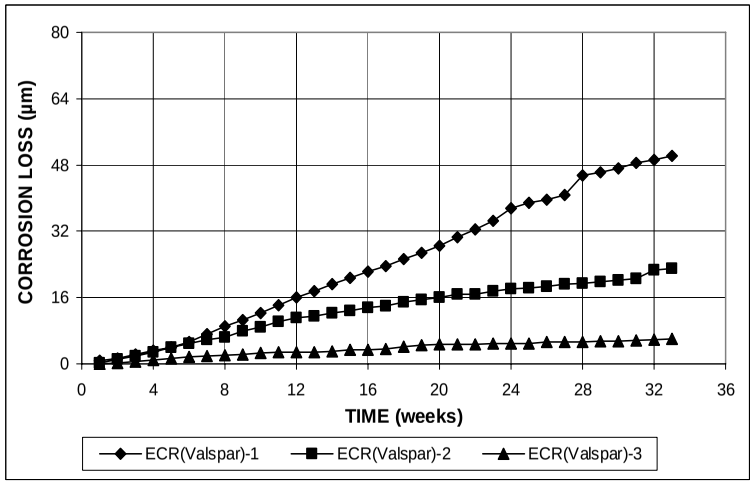

(b)

Figure A. 251 - (a) Corrosion rates and (b) total corrosion losses based on total bar area as measured in the cracked beam test for specimens containing ECR(Valspar) bars

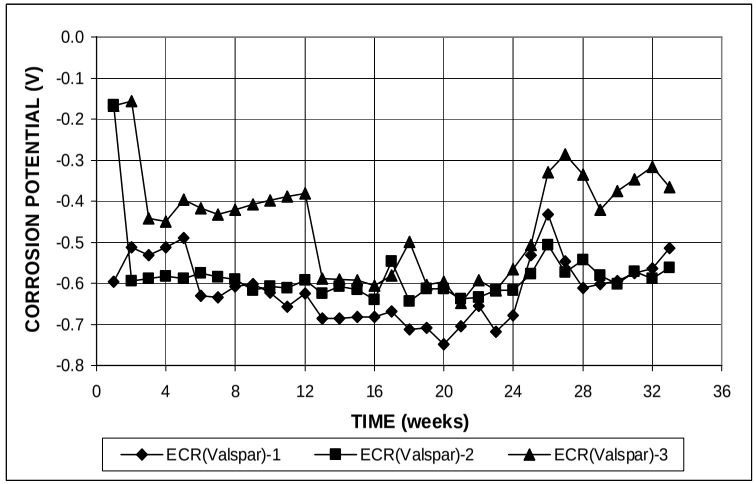

(a)

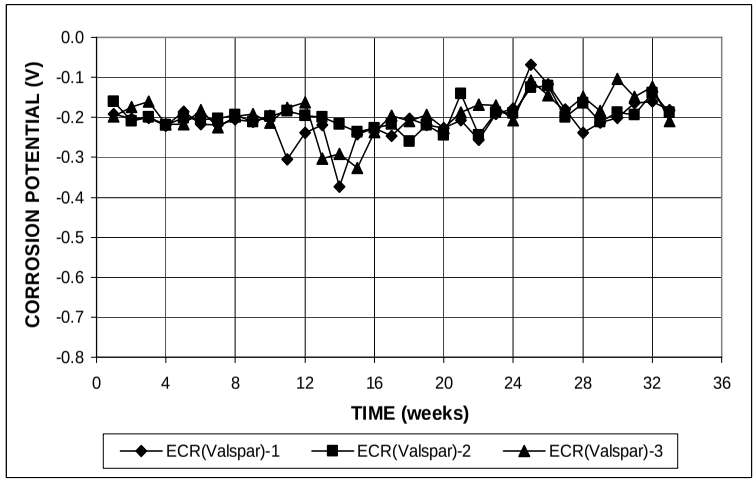

(b)

Figure A. 252 - (a) Top mat corrosion potentials and (b) bottom mat corrosion potentials as measured in the cracked beam test for specimens containing ECR(Valspar) bars

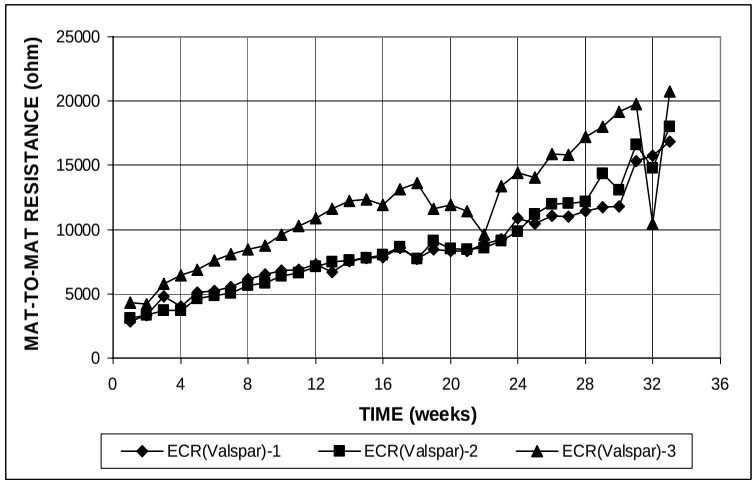

Figure A. 253 - Mat-to-mat resistances as measured in the cracked beam test for specimens containing ECR(Valspar) bars

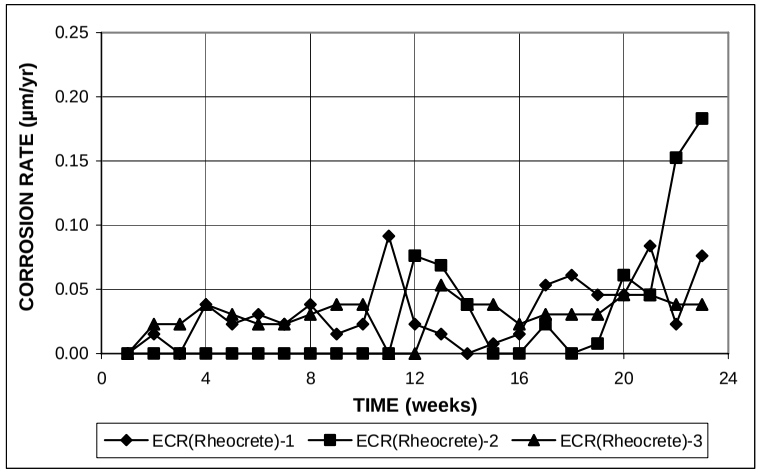

(a)

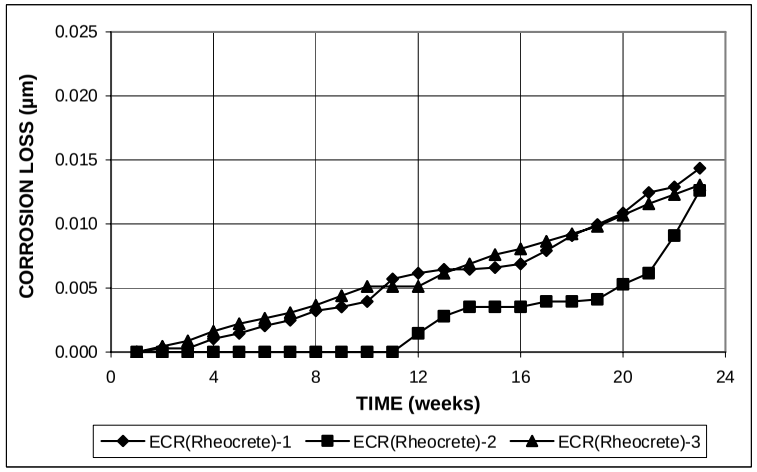

(b)

Figure A. 254 - (a) Corrosion rates and (b) total corrosion losses based on total bar area as measured in the cracked beam test for specimens containing epoxy-coated steel and corrosion inhibitor Rheocrete

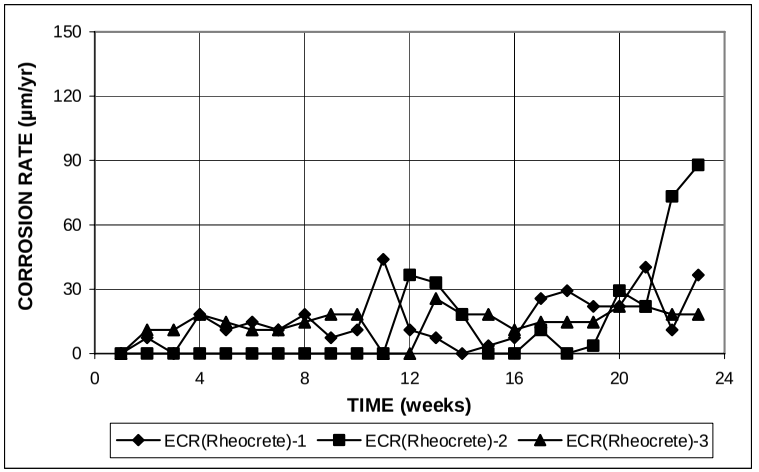

(a)

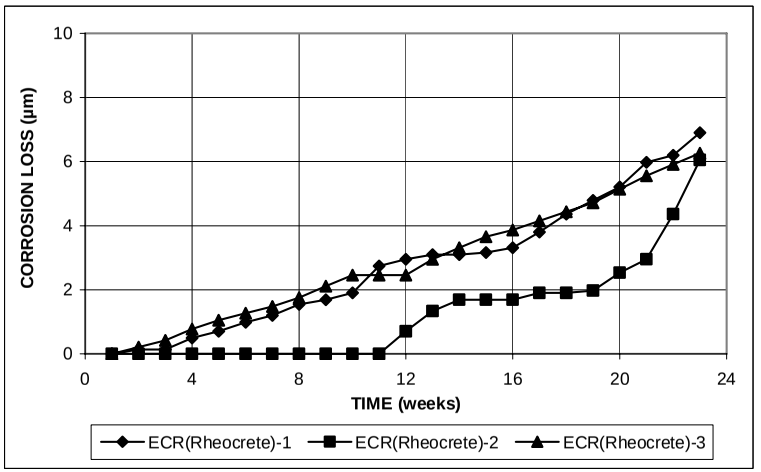

(b)

Figure A. 255 - (a) Corrosion rates and (b) total corrosion losses based on exposed area as measured in the cracked beam test for specimens containing epoxy-coated steel and corrosion inhibitor Rheocrete

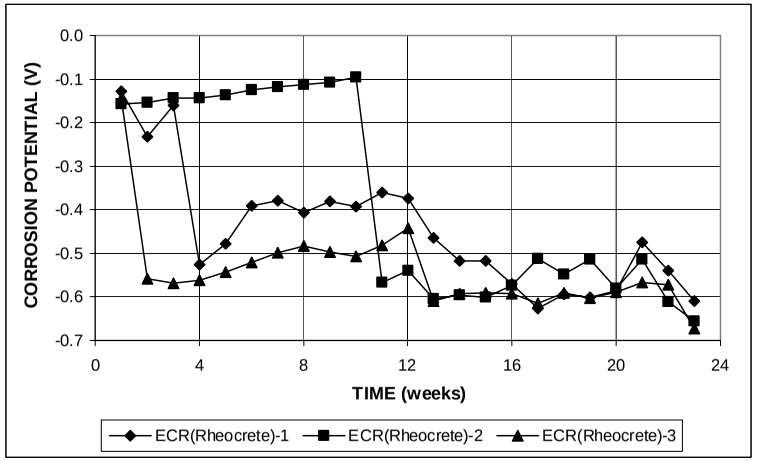

(a)

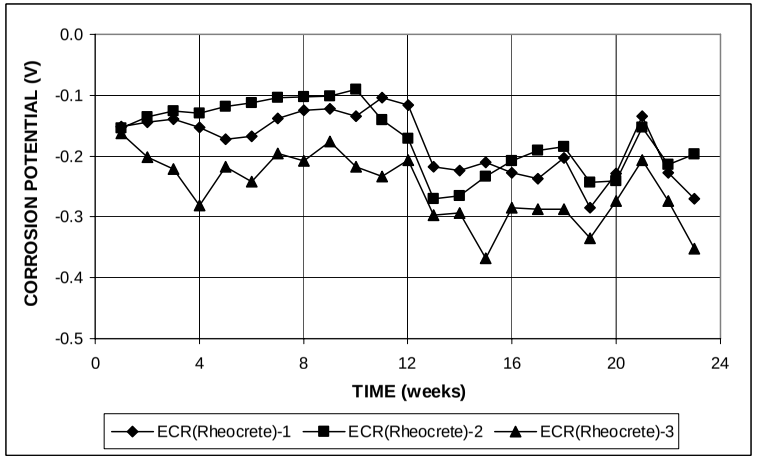

(b)

Figure A. 256 - (a) Top mat corrosion potentials and (b) bottom mat corrosion potentials as measured in the cracked beam test for specimens containing epoxy-coated steel and corrosion inhibitor Rheocrete

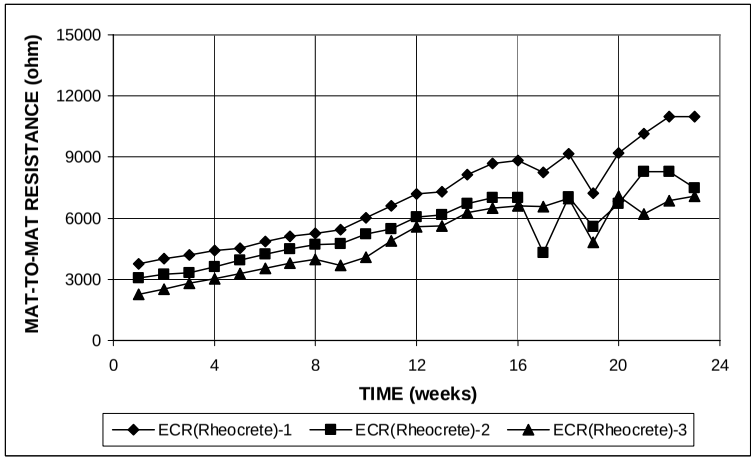

Figure A. 257 - Mat-to-mat resistances as measured in the cracked beam test for specimens containing epoxy-coated steel and corrosion inhibitor Rheocrete

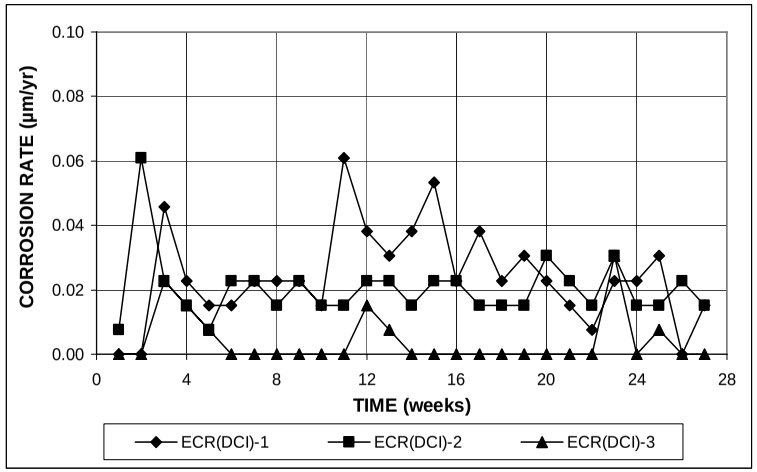

(a)

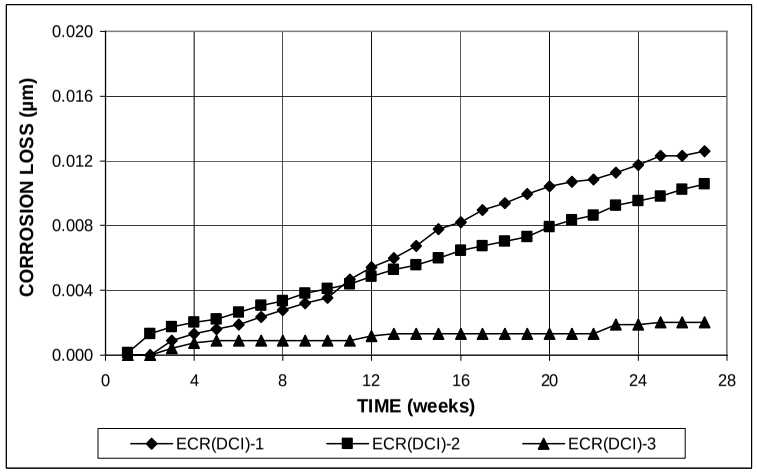

(b)

Figure A. 258 - (a) Corrosion rates and (b) total corrosion losses based on total bar area as measured in the cracked beam test for specimens containing epoxy-coated steel and corrosion inhibitor DCI

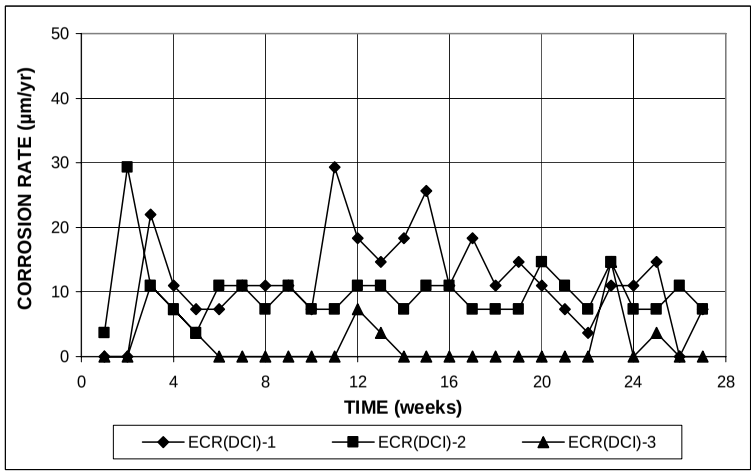

(a)

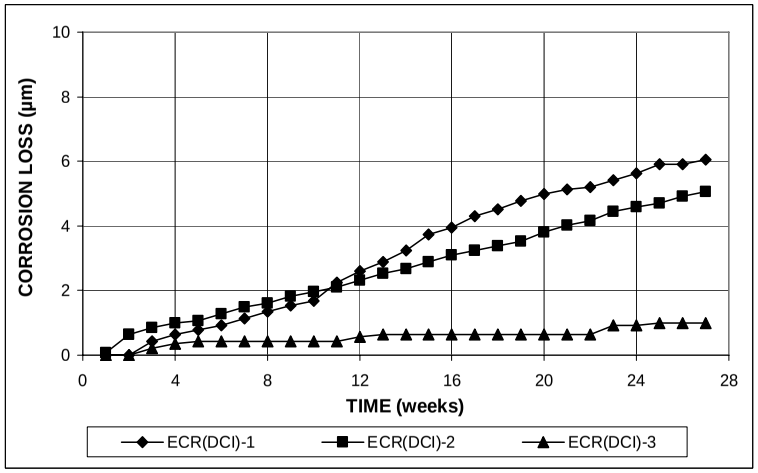

(b)

Figure A. 259 - (a) Corrosion rates and (b) total corrosion losses based on exposed area as measured in the cracked beam test for specimens containing epoxy-coated steel and corrosion inhibitor DCI

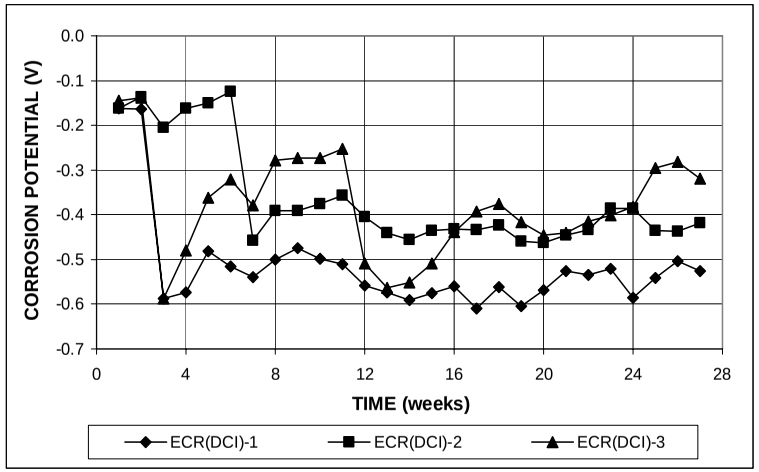

(a)

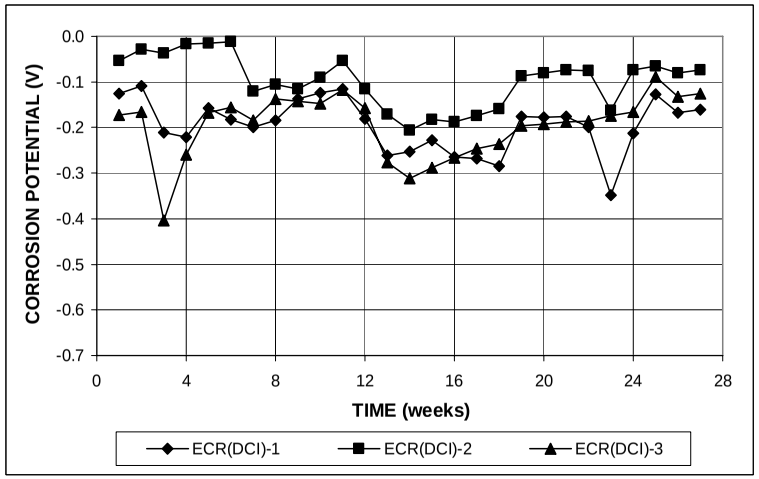

(b)

Figure A. 260 - (a) Top mat corrosion potentials and (b) bottom mat corrosion potentials as measured in the cracked beam test for specimens containing epoxy-coated steel and corrosion inhibitor DCI

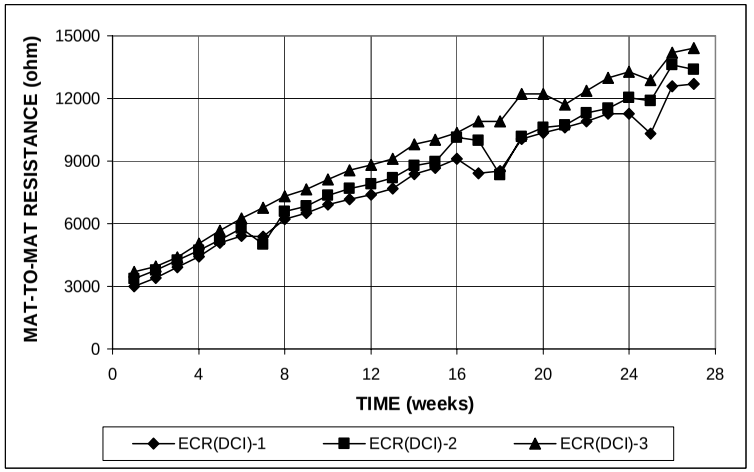

Figure A. 261 - Mat-to-mat resistances as measured in the cracked beam test for specimens containing epoxy-coated steel and corrosion inhibitor DCI

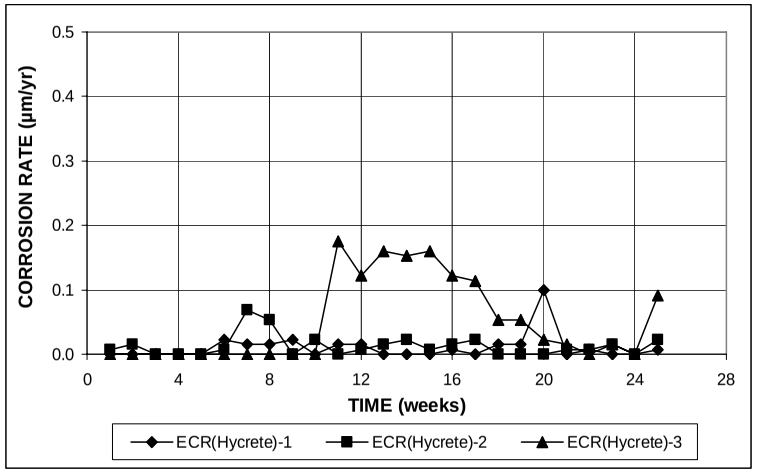

(a)

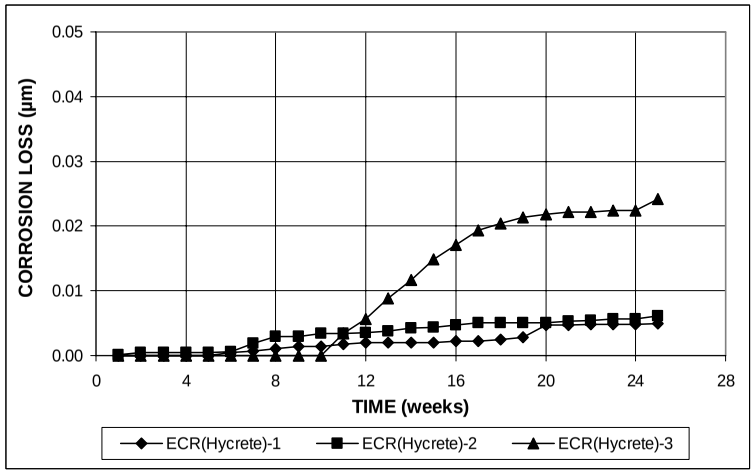

(b)

Figure A. 262 - (a) Corrosion rates and (b) total corrosion losses based on total bar area as measured in the cracked beam test for specimens containing epoxy-coated steel and corrosion inhibitor Hycrete

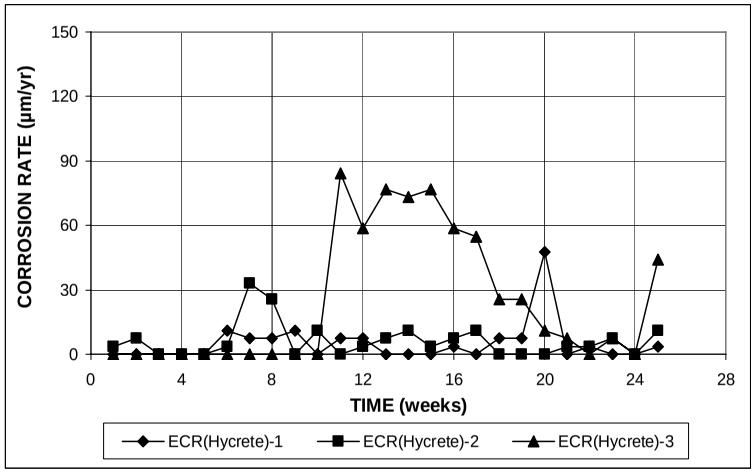

(a)

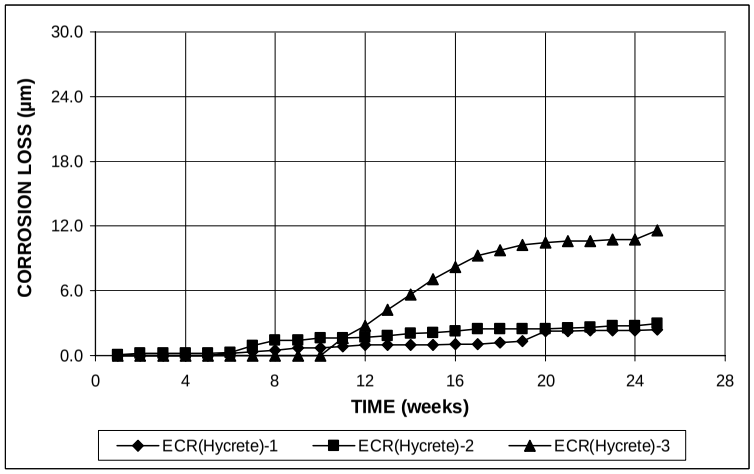

(b)

Figure A. 263 - (a) Corrosion rates and (b) total corrosion losses based on total bar area as measured in the cracked beam test for specimens containing epoxy-coated steel and corrosion inhibitor Hycrete

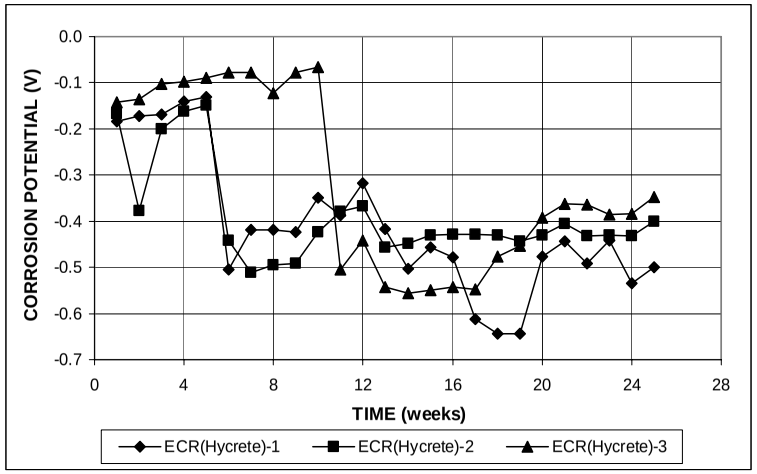

(a)

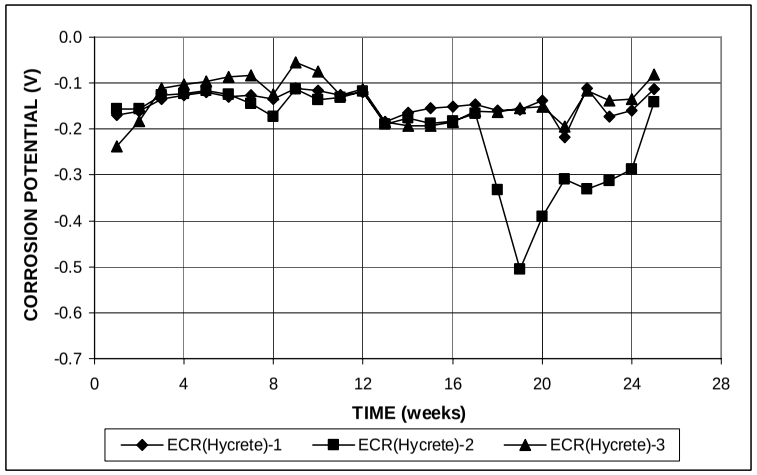

(b)

Figure A. 264 - (a) Top mat corrosion potentials and (b) bottom mat corrosion potentials as measured in the cracked beam test for specimens containing epoxy-coated steel and corrosion inhibitor Hycrete

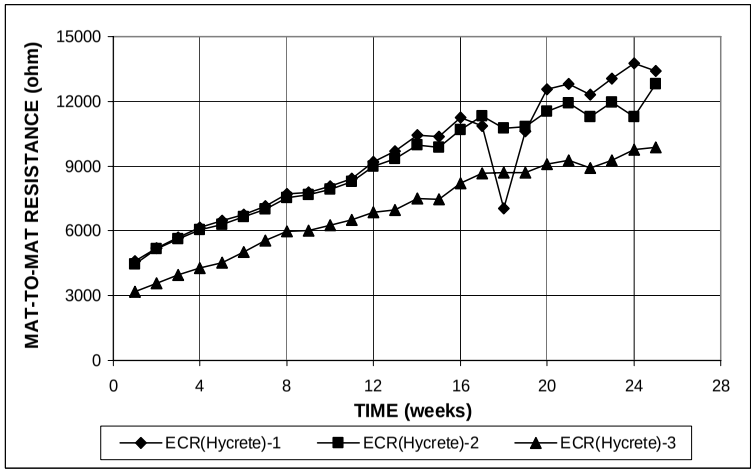

Figure A. 265 - Mat-to-mat resistances as measured in the cracked beam test for specimens containing epoxy-coated steel and corrosion inhibitor Hycrete

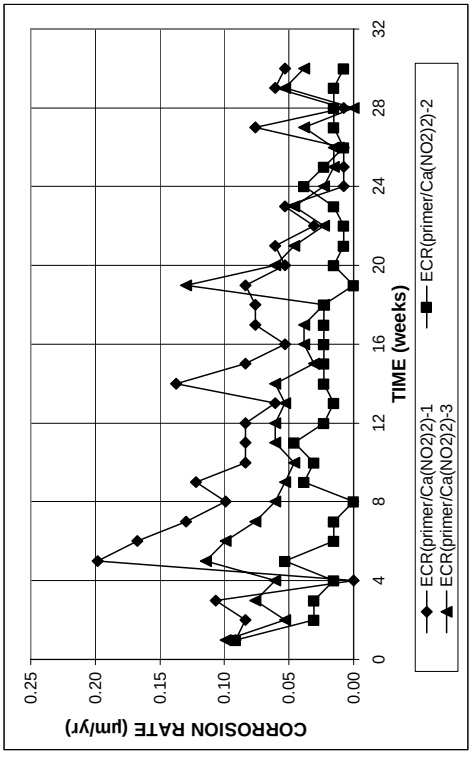

Figure A. 266 - (a) Corrosion rates and (b) total corrosion losses based on total bar area as measured in the cracked beam test for specimens containing ECR(primer/$Ca(NO_2)_2$) bars

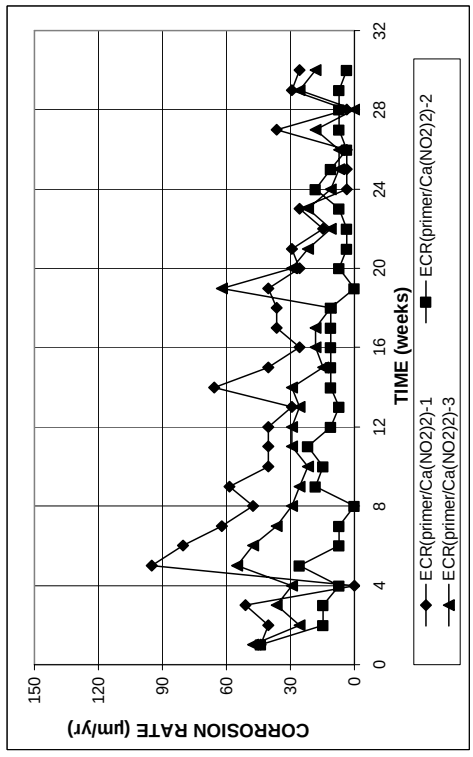

Figure A. 267 - (a) Corrosion rates and (b) total corrosion losses based on exposed area as measured in the cracked beam test for specimens containing ECR(primer/$Ca(NO_2)_2$) bars

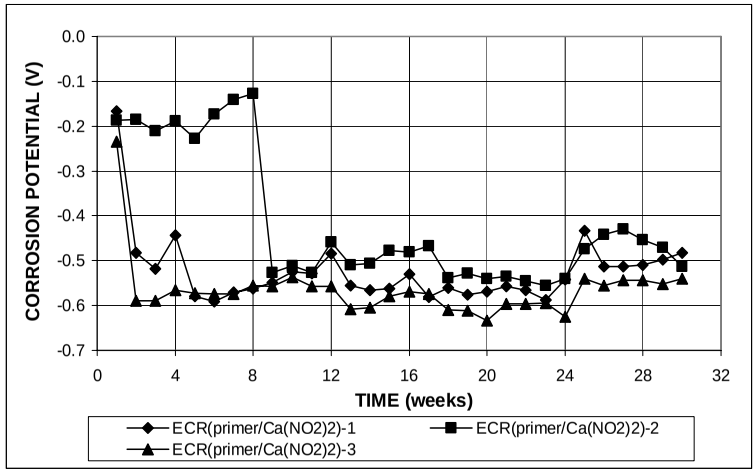

(a)

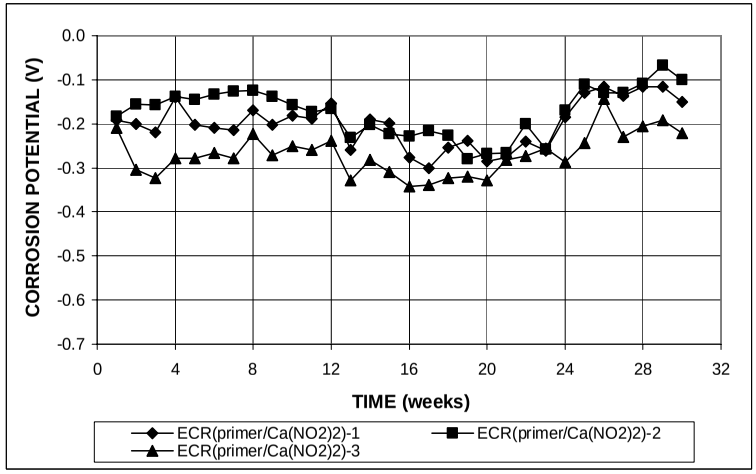

(b)

Figure A. 268 - (a) Top mat corrosion potentials and (b) bottom mat corrosion potentials as measured in the cracked beam test for specimens containing ECR(primer/$Ca(NO_2)_2$) bars

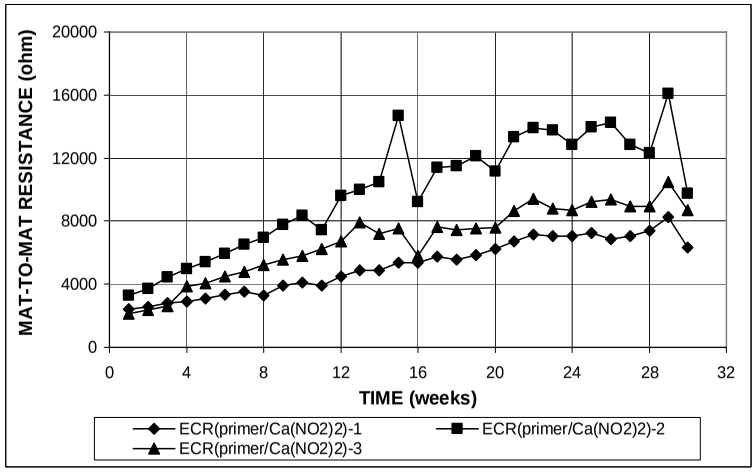

Figure A. 269 - Mat-to-mat resistances as measured in the cracked beam test for specimens containing ECR(primer/$Ca(NO_2)_2$) bars

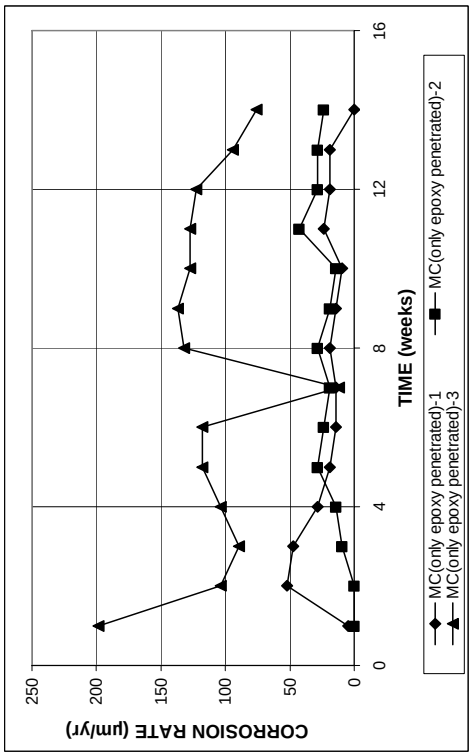

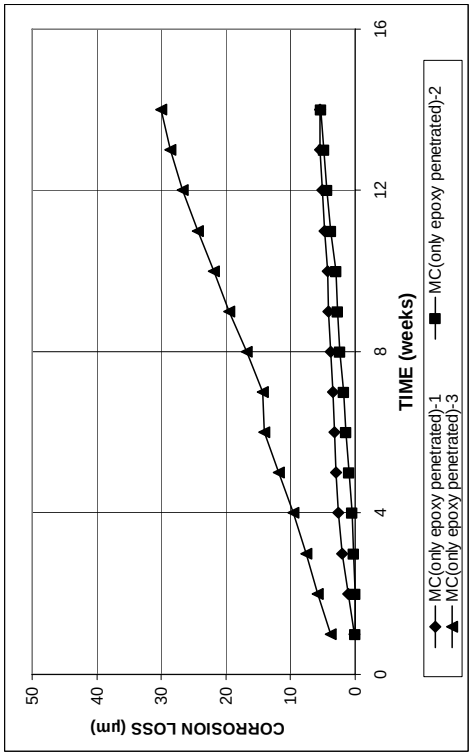

Figure A. 271 - (a) Corrosion rates and (b) total corrosion losses based on exposed area as measured in the cracked beam test for specimens containing multiple coated steel with only epoxy penetrated

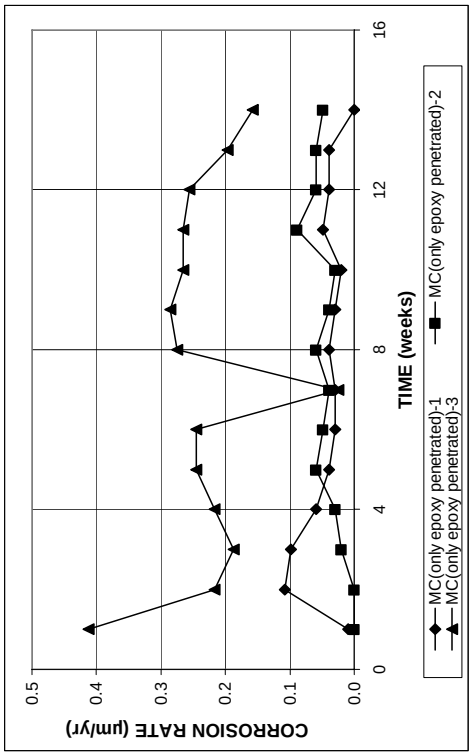

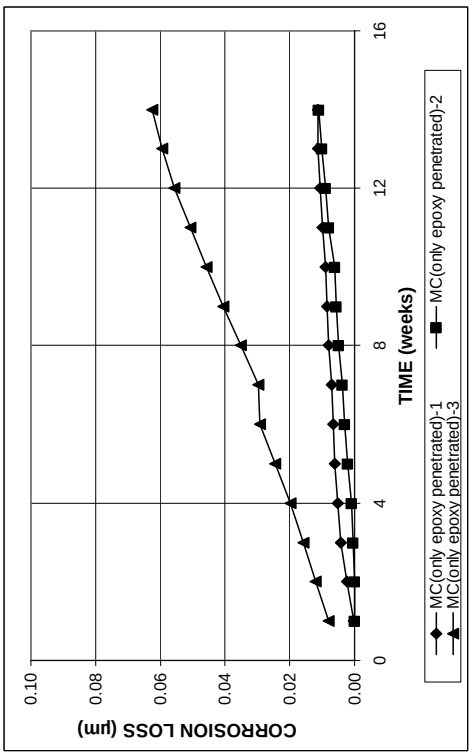

Figure A. 270 - (a) Corrosion rates and (b) total corrosion losses based on total bar area as measured in the cracked beam test for specimens containing multiple coated steel with only epoxy penetrated

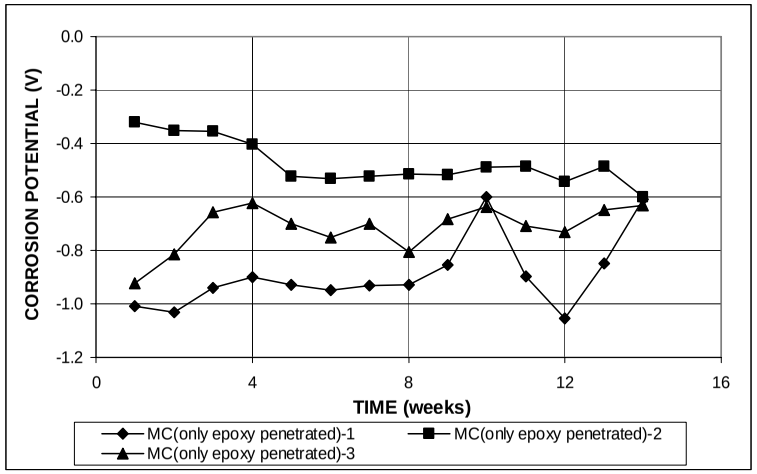

(a)

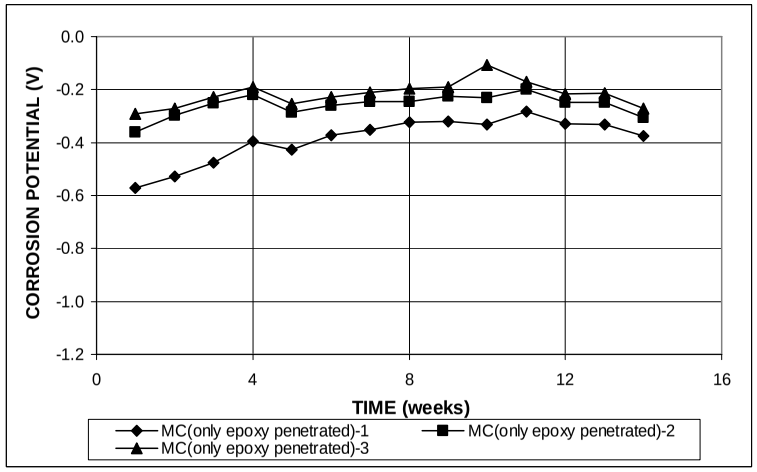

(b)

Figure A. 272 - (a) Top mat corrosion potentials and (b) bottom mat corrosion potentials as measured in the cracked beam test for specimens containing multiple coated steel with only epoxy penetrated

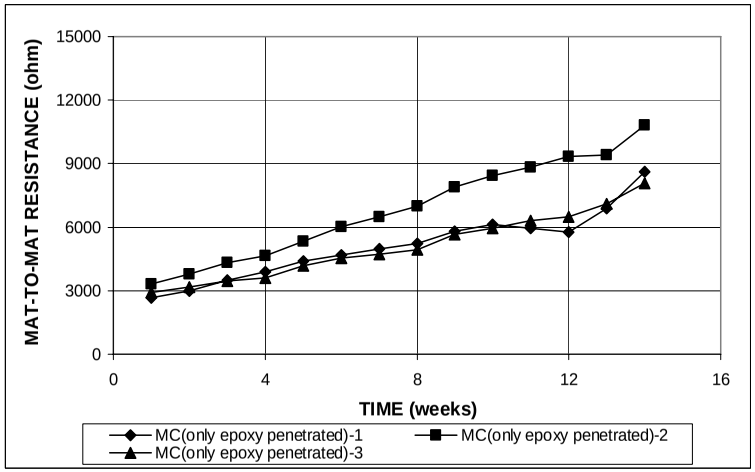

Figure A. 273 - Mat-to-mat resistances as measured in the cracked beam test for specimens containing multiple coated steel with only epoxy penetrated

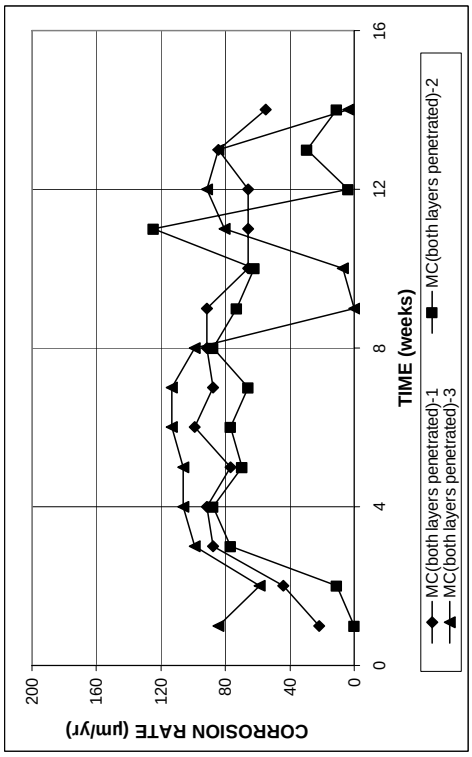

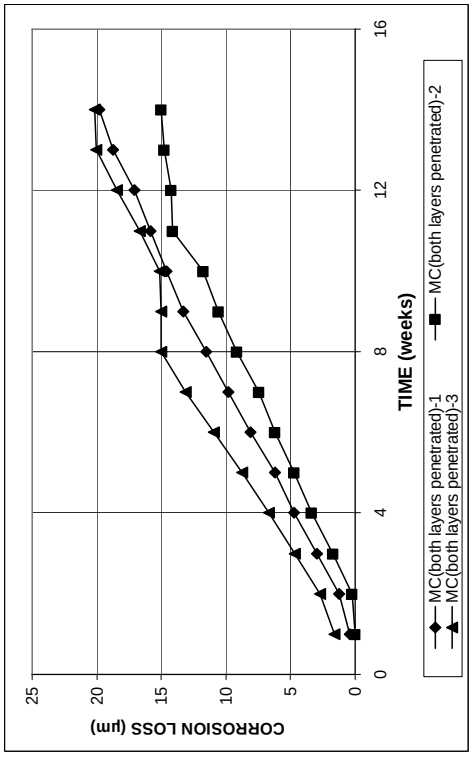

Figure A. 275 - (a) Corrosion rates and (b) total corrosion losses based on exposed area as measured in the cracked beam test for specimens containing multiple coated steel with both layers penetrated

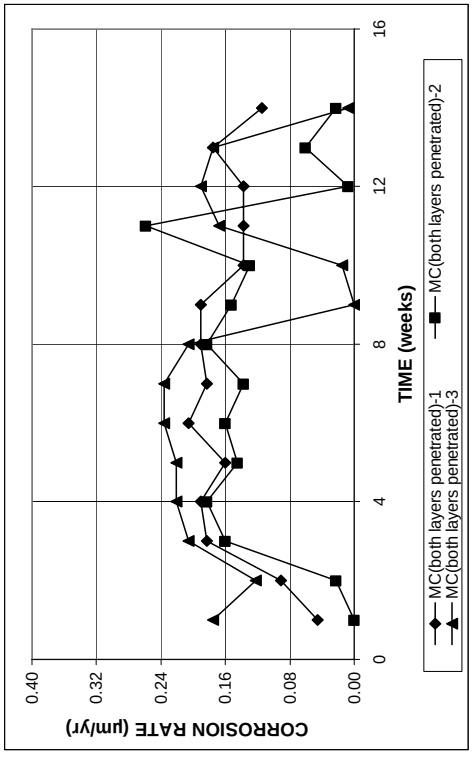

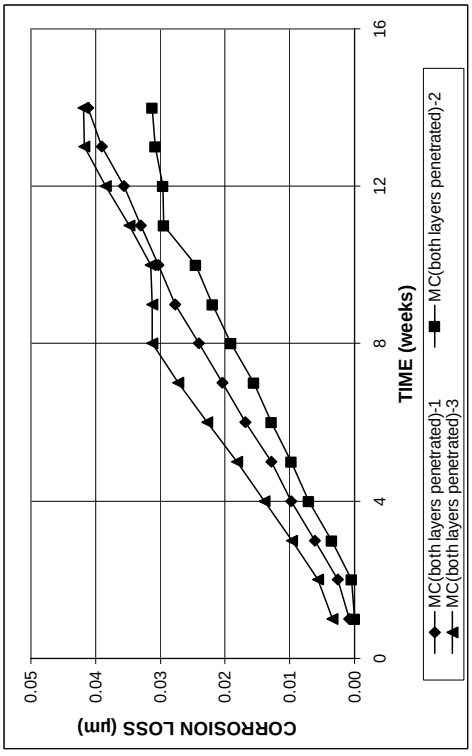

Figure A. 274 - (a) Corrosion rates and (b) total corrosion losses based on total bar area as measured in the cracked beam test for specimens containing multiple coated steel with both layers penetrated

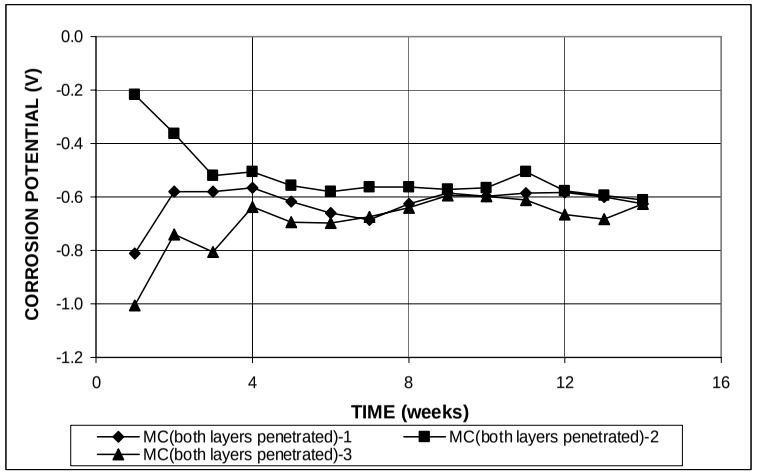

(a)

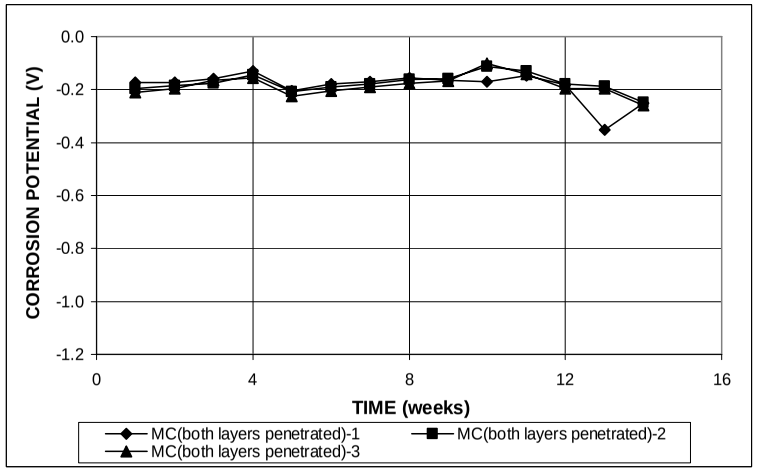

(b)

Figure A. 276 - (a) Top mat corrosion potentials and (b) bottom mat corrosion potentials as measured in the cracked beam test for specimens containing multiple coated steel with both layers penetrated

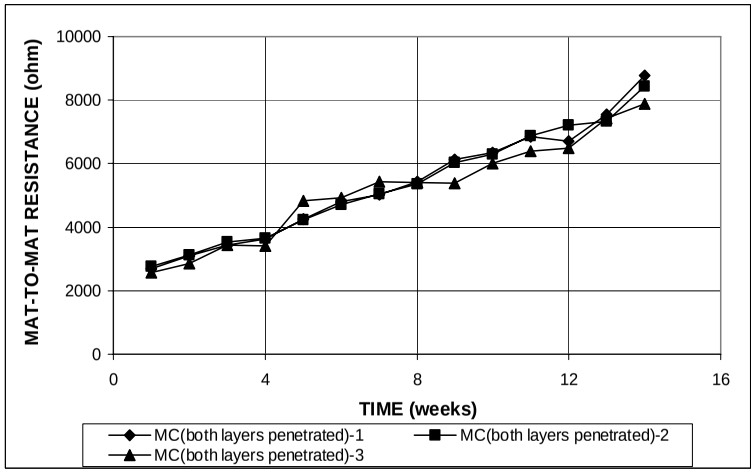

Figure A. 277 - Mat-to-mat resistances as measured in the cracked beam test for specimens containing multiple coated steel with both layers penetrated

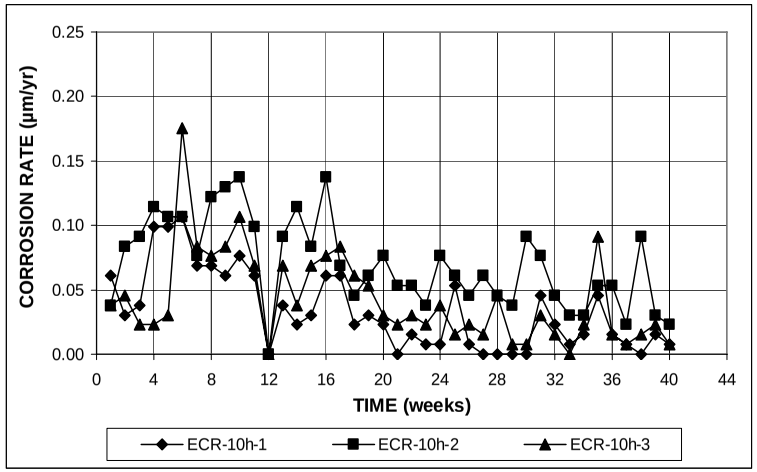

(a)

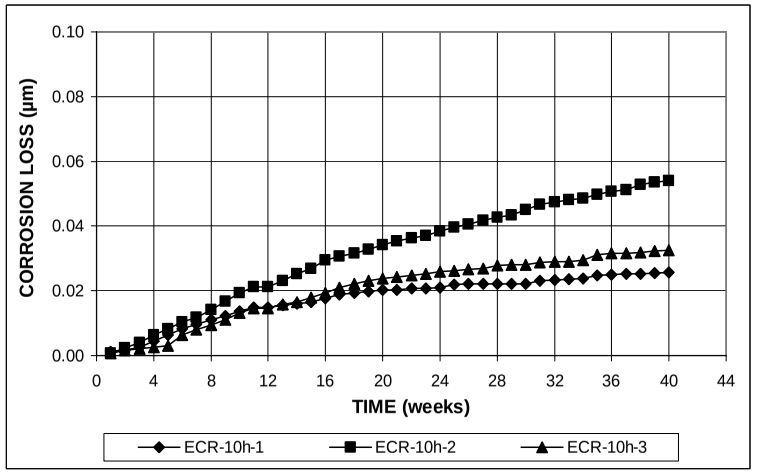

(b)

Figure A. 278 - (a) Corrosion rates and (b) total corrosion losses based on total bar area as measured in the Southern Exposure test for specimens containing epoxy-coated steel with 10 drilled holes

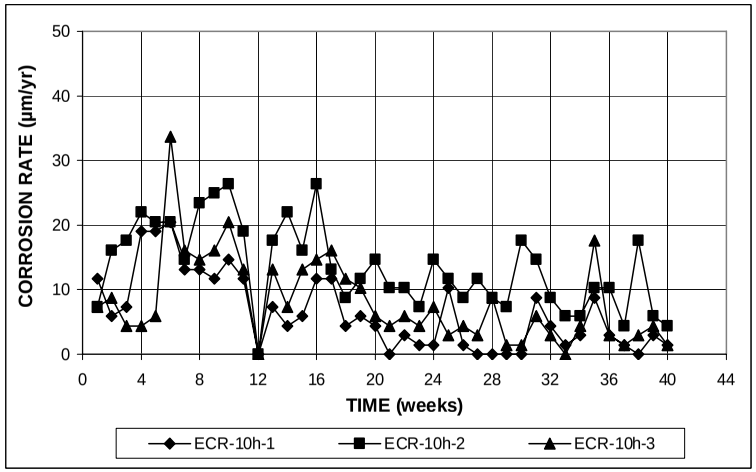

(a)

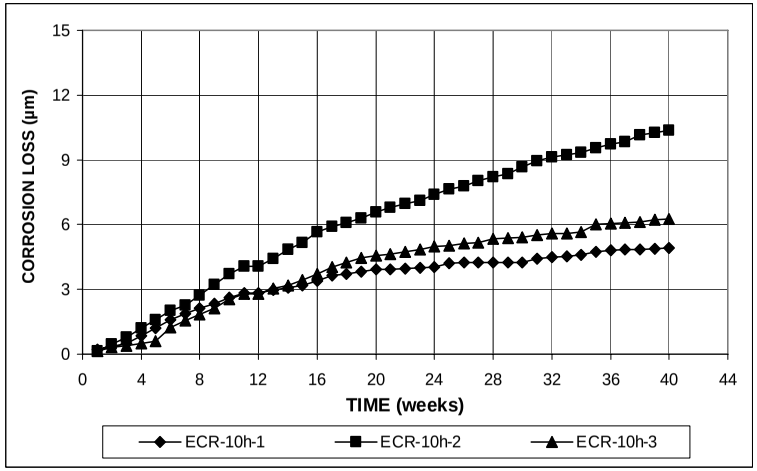

(b)

Figure A. 279 - (a) Corrosion rates and (b) total corrosion losses based on exposed area as measured in the Southern Exposure test for specimens containing epoxy-coated steel with 10 drilled holes

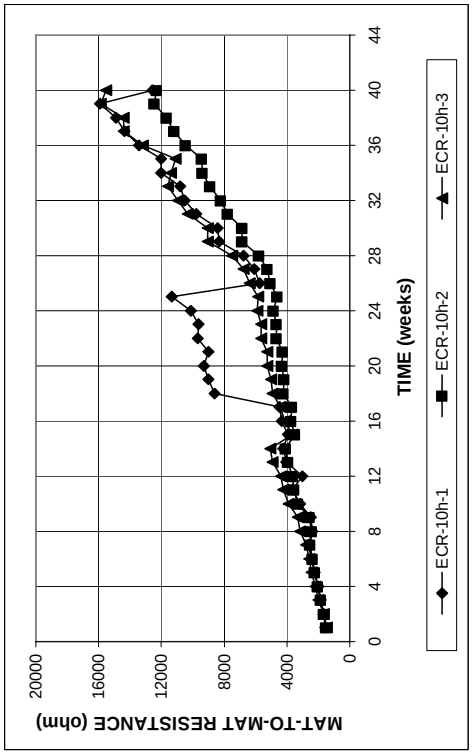

Figure A. 281 - Mat-to-mat resistances as measured in the Southern Exposure test for specimens containing epoxy-coated steel with 10 drilled holes

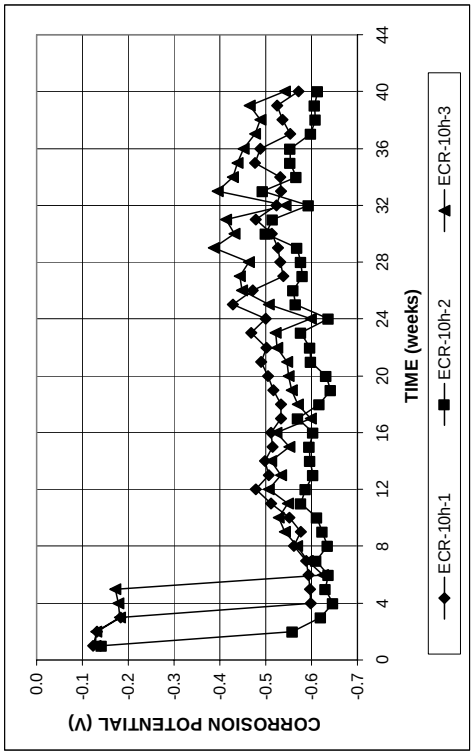

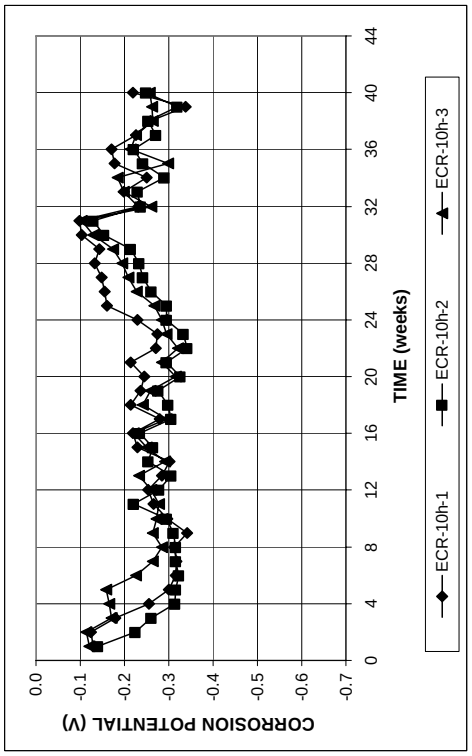

Figure A. 280 - (a) Top mat corrosion potentials and (b) bottom mat corrosion potentials as measured in the Southern Exposure test for specimens containing epoxy-coated steel with 10 drilled holes

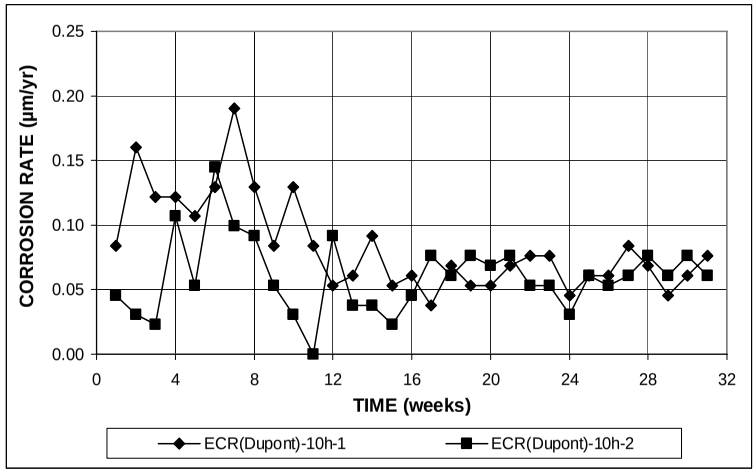

(a)

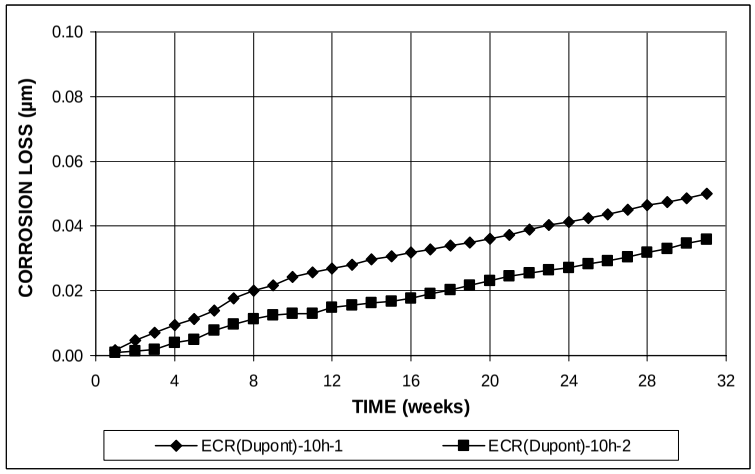

(b)

Figure A. 282 - (a) Corrosion rates and (b) total corrosion losses based on total bar area as measured in the cracked beam test for specimens containing ECR(Dupont) bars with 10 drilled holes

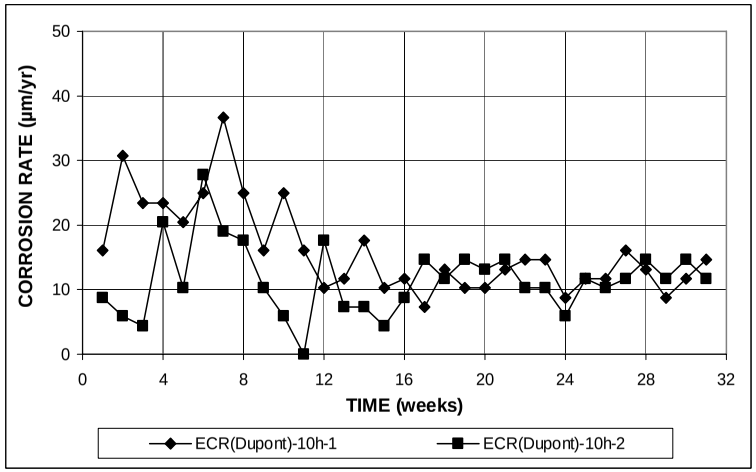

(a)

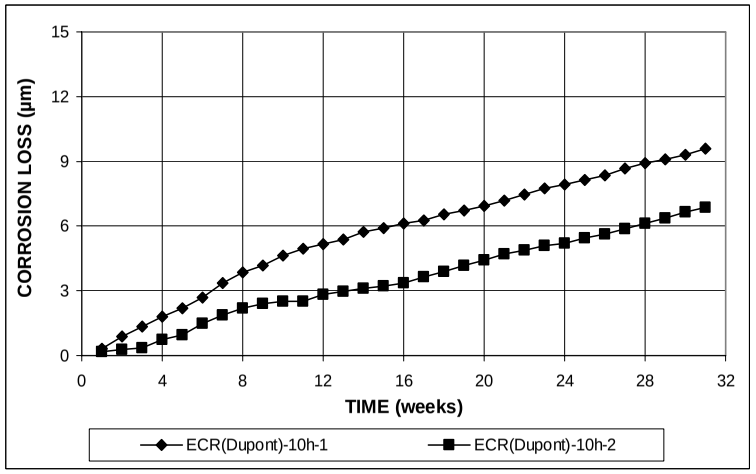

(b)

Figure A. 283 - (a) Corrosion rates and (b) total corrosion losses based on total bar area as measured in the cracked beam test for specimens containing ECR(Dupont) bars with 10 drilled holes

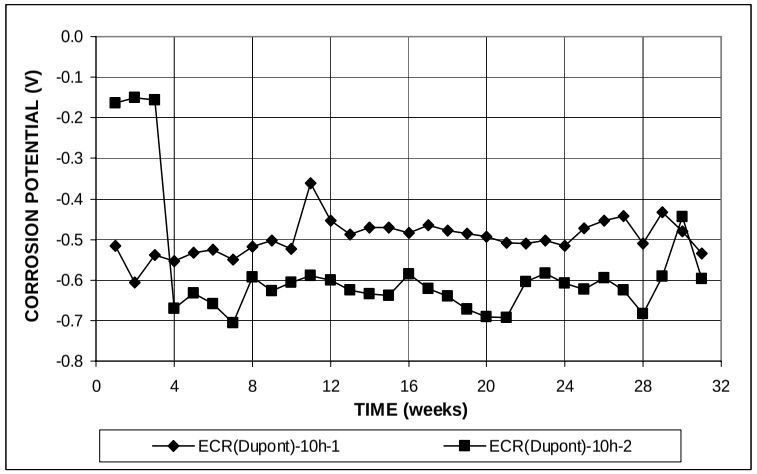

(a)

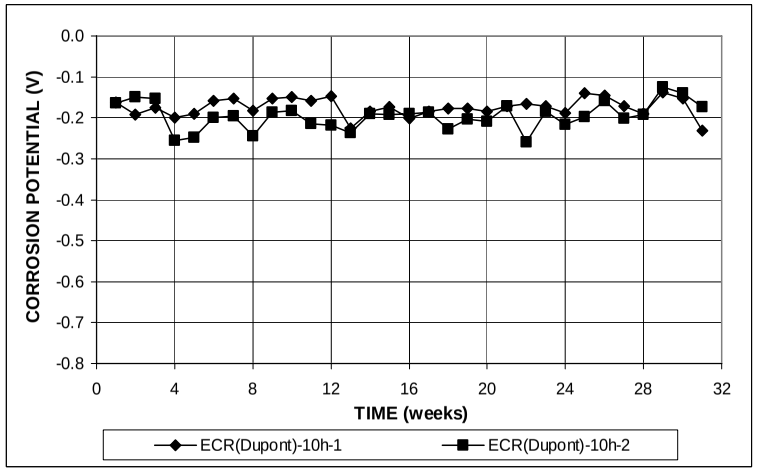

(b)

Figure A. 284 - (a) Top mat corrosion potentials and (b) bottom mat corrosion potentials as measured in the cracked beam test for specimens containing ECR(Dupont) bars with 10 drilled holes

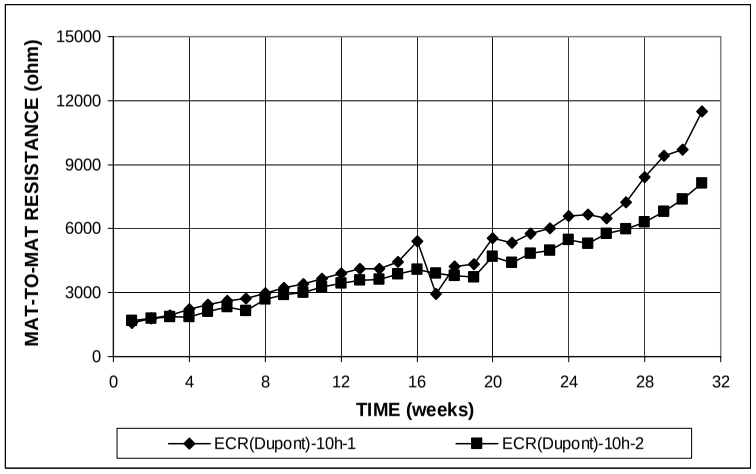

Figure A. 285 - Mat-to-mat resistances as measured in the cracked beam test for specimens containing ECR(Dupont) bars with 10 drilled holes

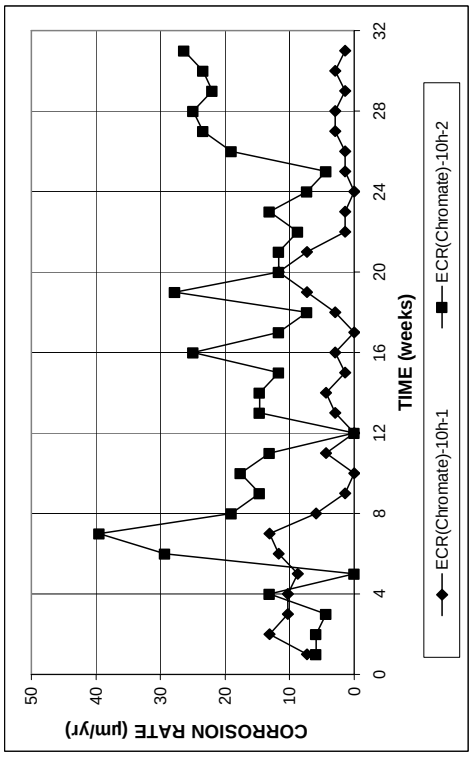

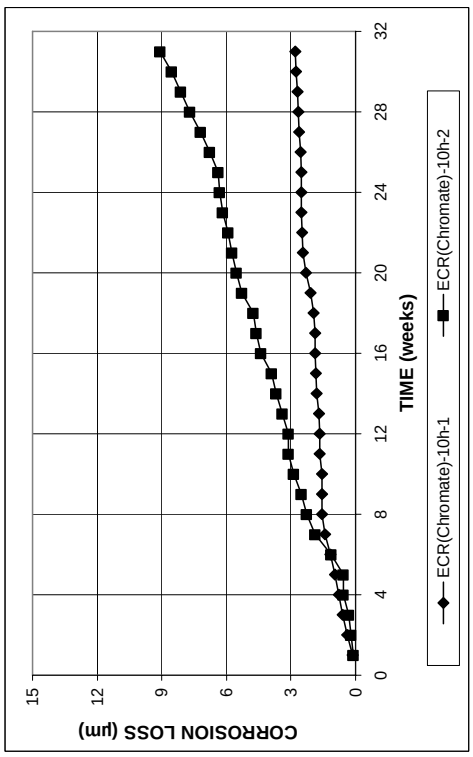

Figure A. 287 - (a) Corrosion rates and (b) total corrosion losses based on total bar area as measured in the Southern Exposure test for specimens containing ECR(Chromate) bars with 10 drilled holes

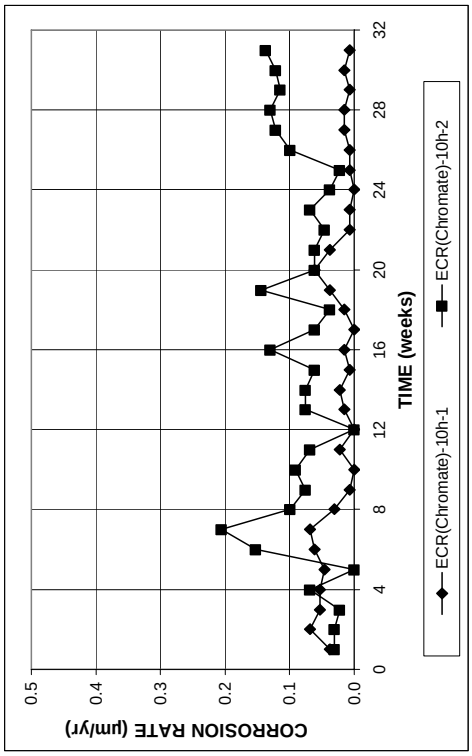

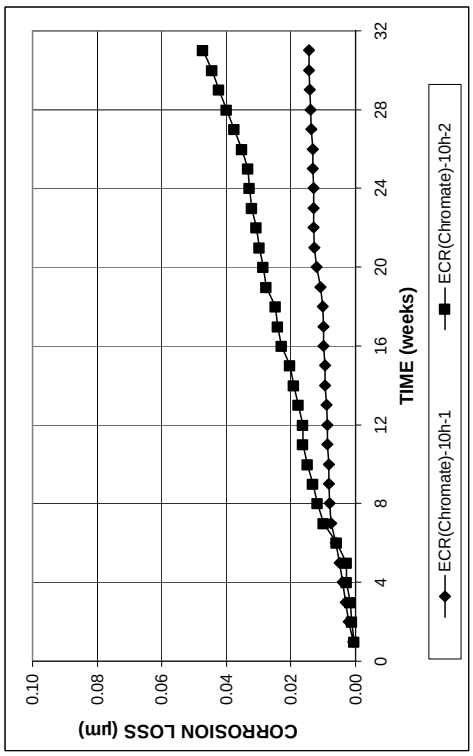

Figure A. 286 - (a) Corrosion rates and (b) total corrosion losses based on total bar area as measured in the Southern Exposure test for specimens containing ECR(Chromate) bars with 10 drilled holes

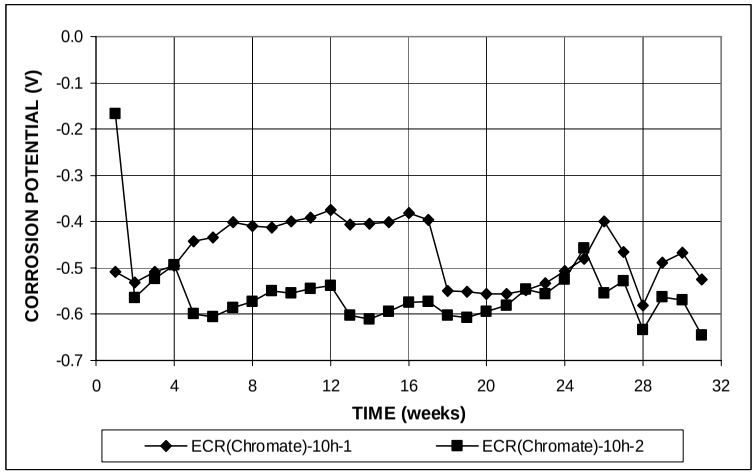

(a)

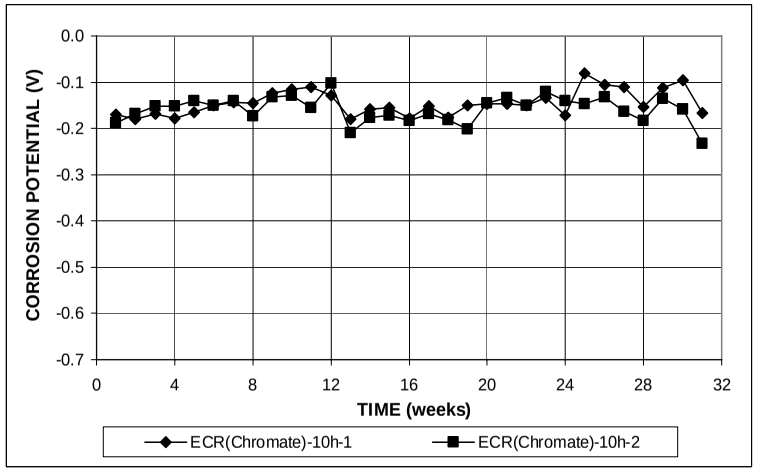

(b)

Figure A. 288 - (a) Top mat corrosion potentials and (b) bottom mat corrosion potentials as measured in the Southern Exposure test for specimens containing ECR(Chromate) bars with 10 drilled holes

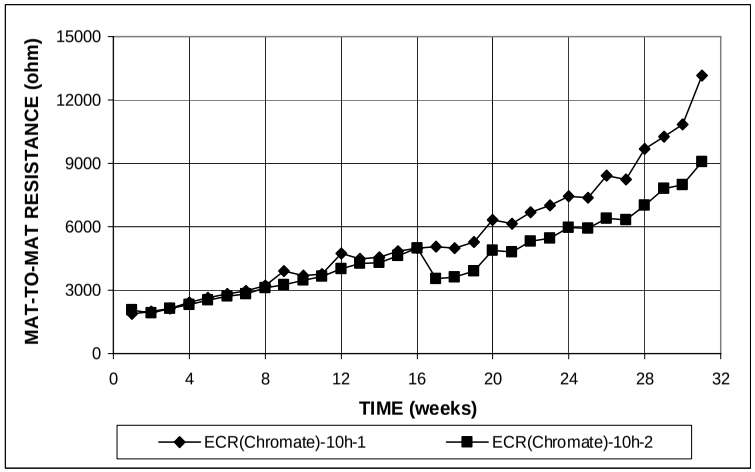

Figure A. 289 - Mat-to-mat resistances as measured in the Southern Exposure test for specimens containing ECR(Chromate) bars with 10 drilled holes

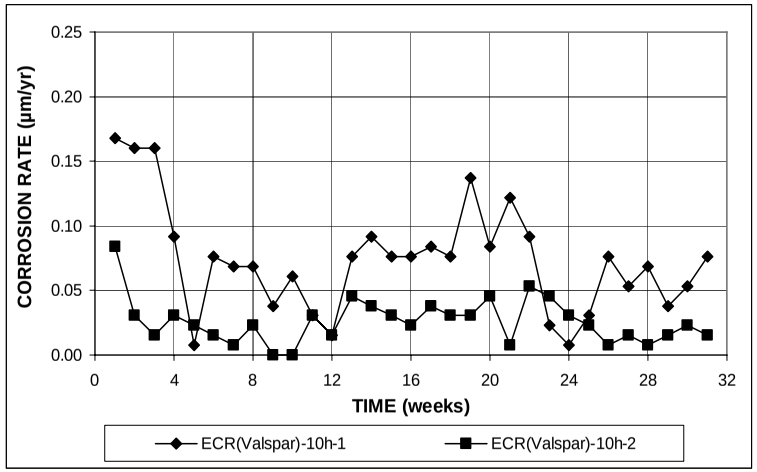

(a)

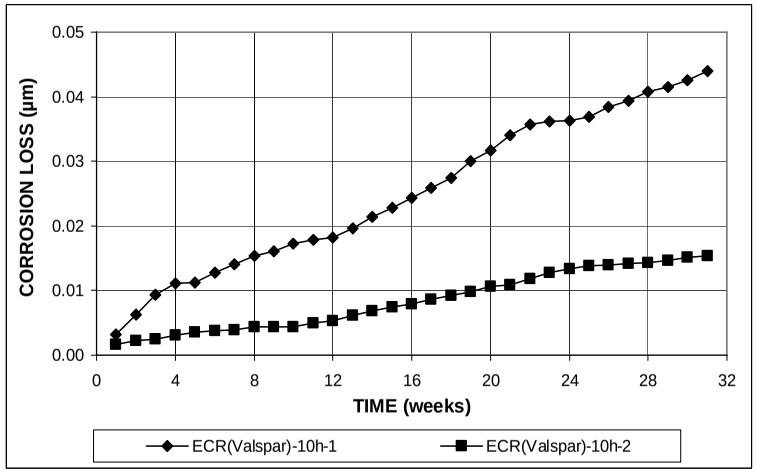

(b)

Figure A. 290 - (a) Corrosion rates and (b) total corrosion losses based on total bar area as measured in the cracked beam test for specimens containing ECR(Valspar) bars with 10 drilled holes

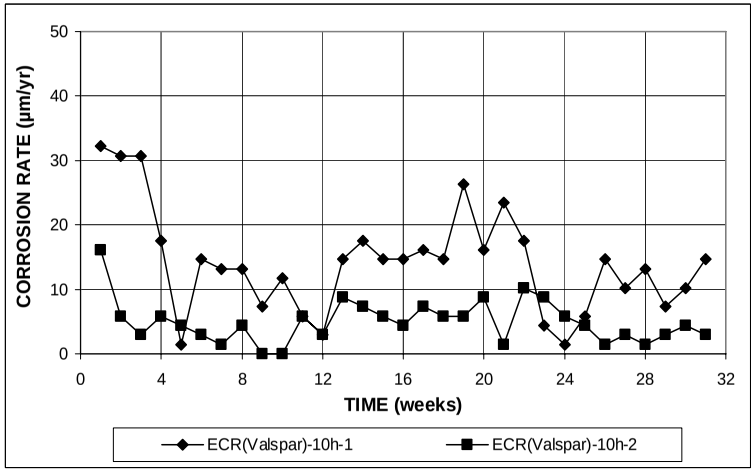

(a)

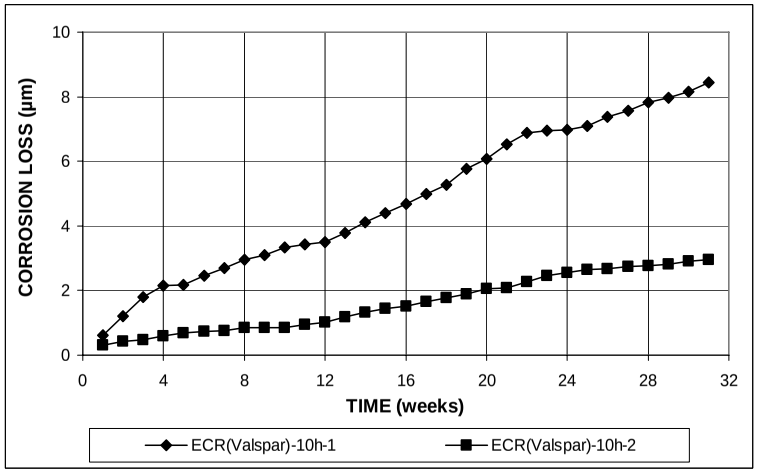

(b)

Figure A. 291 - (a) Corrosion rates and (b) total corrosion losses based on exposed area as measured in the cracked beam test for specimens containing ECR(Valspar) bars with 10 drilled holes

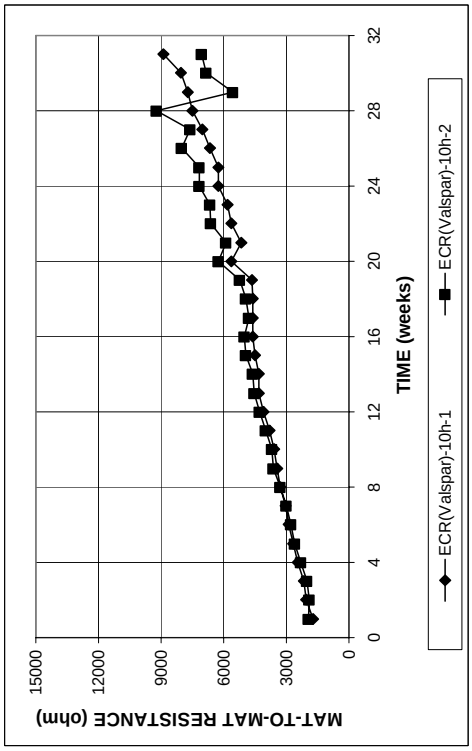

Figure A. 293 - Mat-to-mat resistances as measured in the cracked beam test for specimens containing ECR(Valspar) with 10 drilled holes

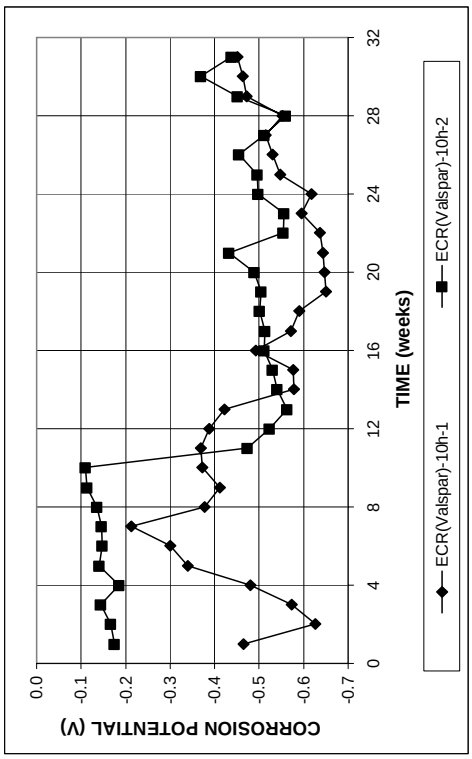

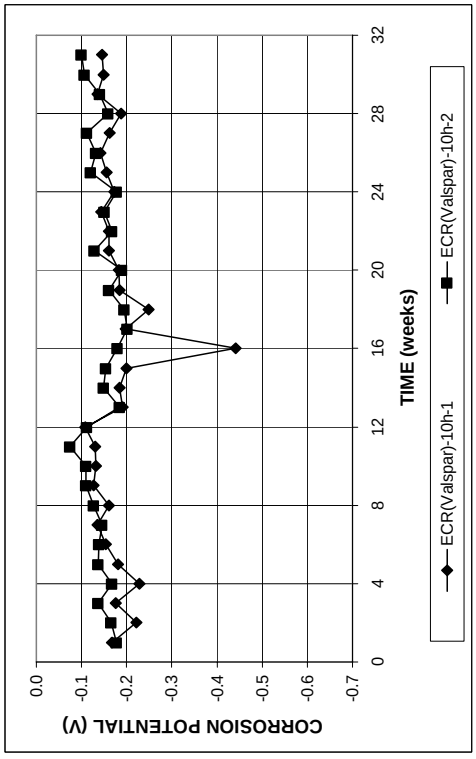

Figure A. 292 - (a) Top mat corrosion potentials and (b) bottom mat corrosion potentials as measured in the cracked beam test for specimens containing ECR(Valspar) bars with 10 drilled holes

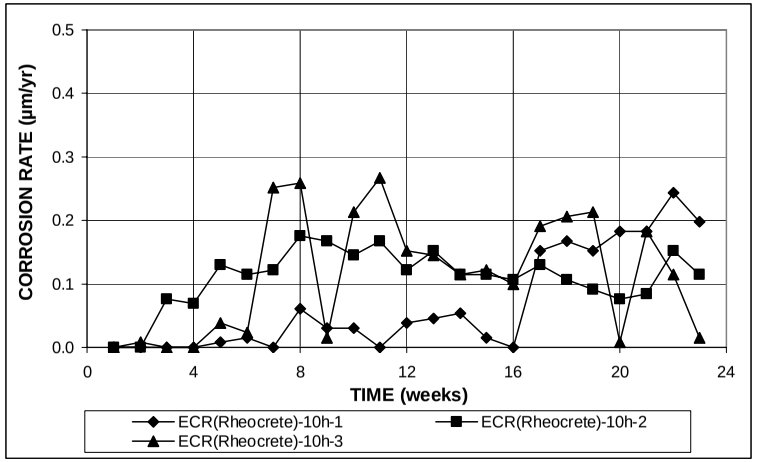

(a)

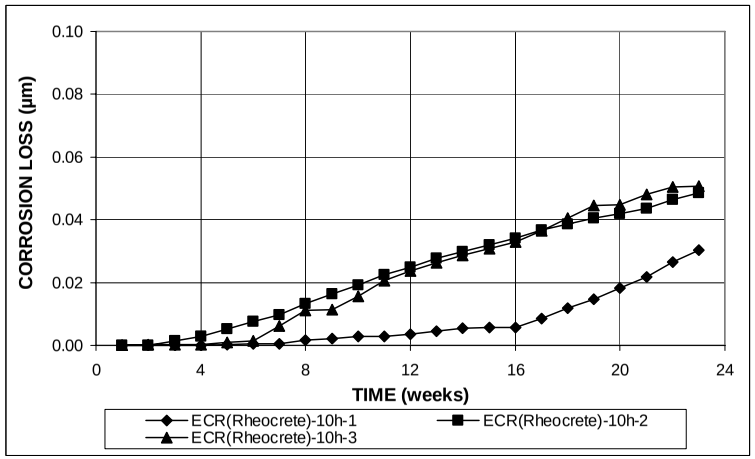

(b)

Figure A. 294 - (a) Corrosion rates and (b) total corrosion losses based on total bar area as measured in the cracked beam test for specimens containing epoxy-coated steel with 10 drilled holes and corrosion inhibitor Rheocrete

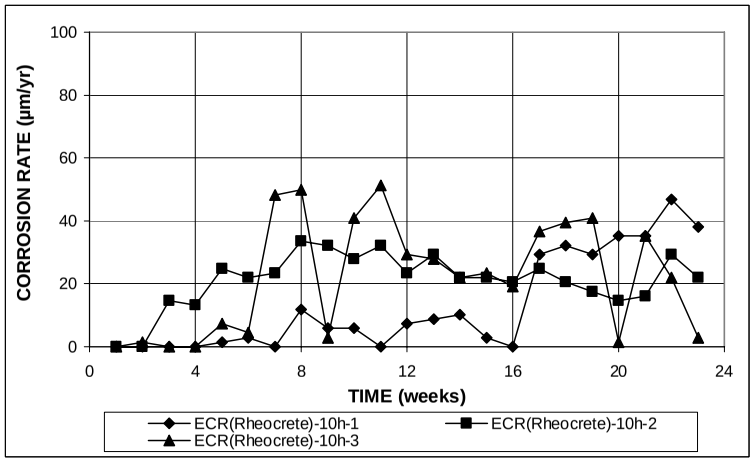

(a)

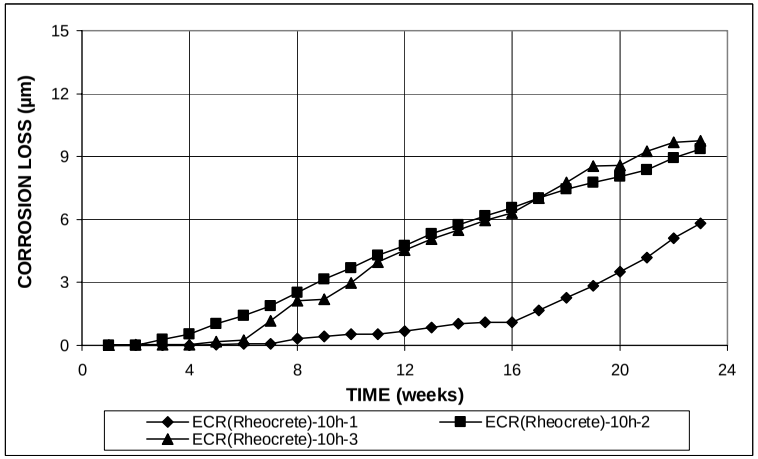

(b)

Figure A. 295 - (a) Corrosion rates and (b) total corrosion losses based on exposed area as measured in the cracked beam test for specimens containing epoxy-coated steel with 10 drilled holes and corrosion inhibitor Rheocrete

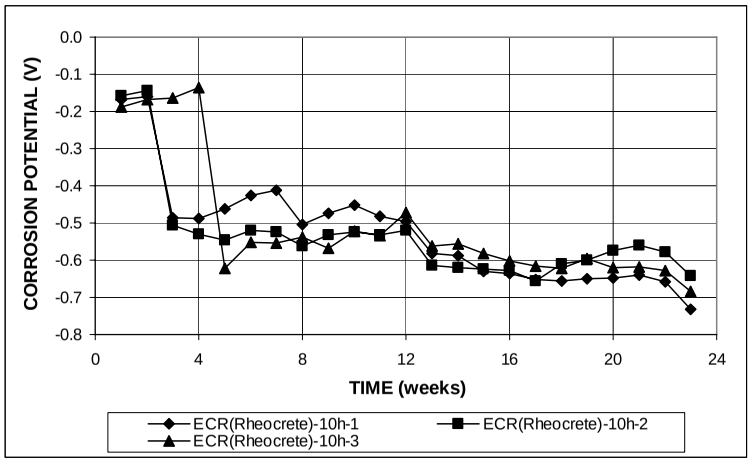

(a)

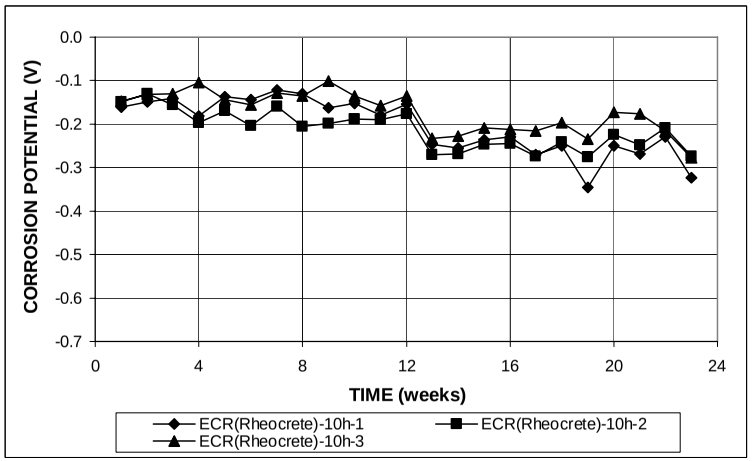

(b)

Figure A. 296 - (a) Top mat corrosion potentials and (b) bottom mat corrosion potentials as measured in the cracked beam test for specimens containing epoxy-coated steel with 10 drilled holes and corrosion inhibitor Rheocrete

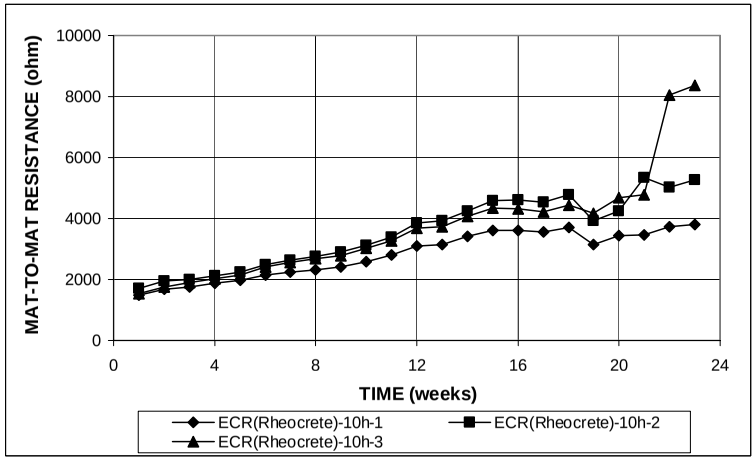

Figure A. 297 - Mat-to-mat resistances as measured in the cracked beam test for specimens containing epoxy-coated steel with 10 drilled holes and corrosion inhibitor Rheocrete

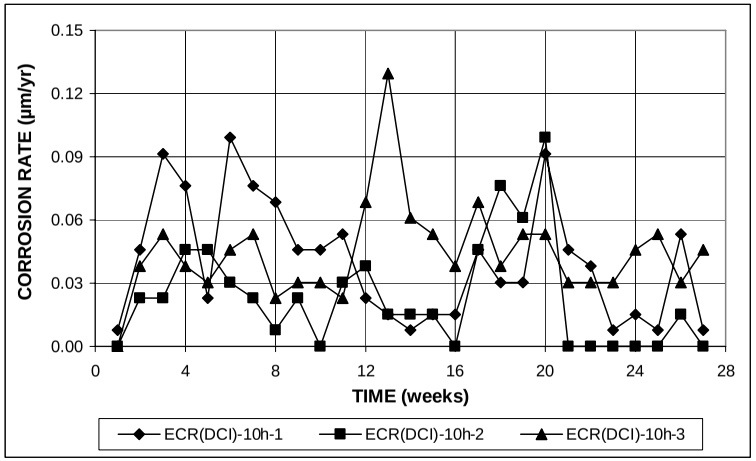

(a)

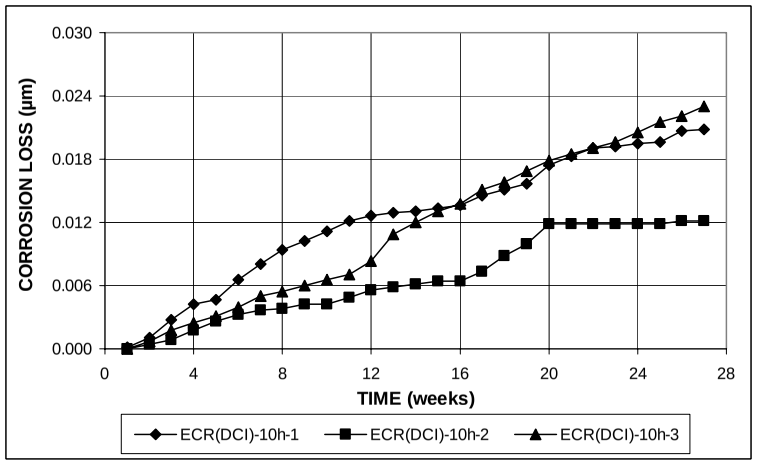

(b)

Figure A. 298 - (a) Corrosion rates and (b) total corrosion losses based on total bar area as measured in the cracked beam test for specimens containing epoxy-coated steel with 10 drilled holes and corrosion inhibitor DCI

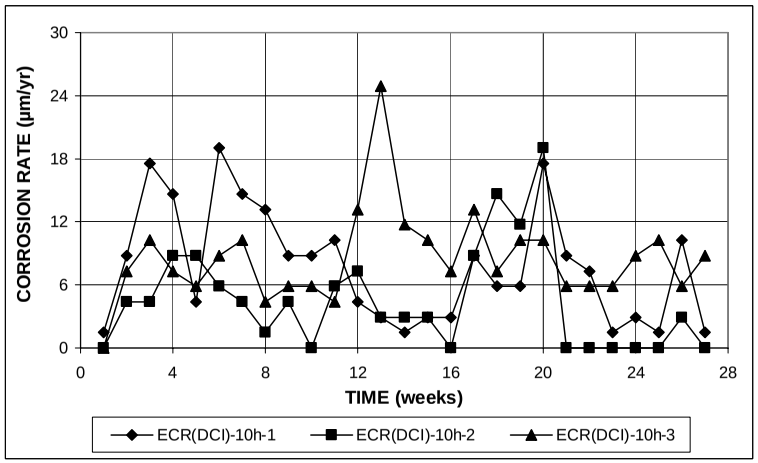

(a)

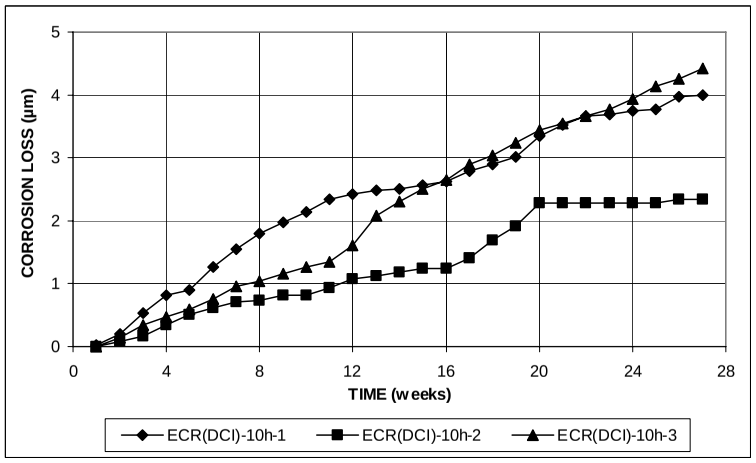

(b)

Figure A. 299 - (a) Corrosion rates and (b) total corrosion losses based on exposed area as measured in the cracked beam test for specimens containing epoxy-coated steel with 10 drilled holes and corrosion inhibitor DCI

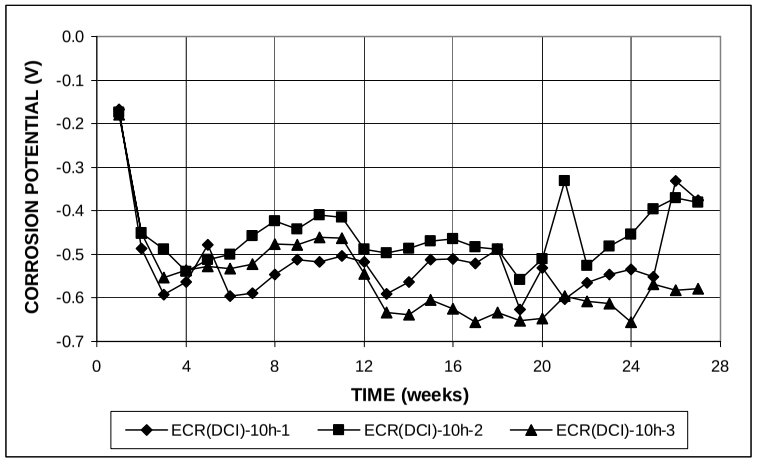

(a)

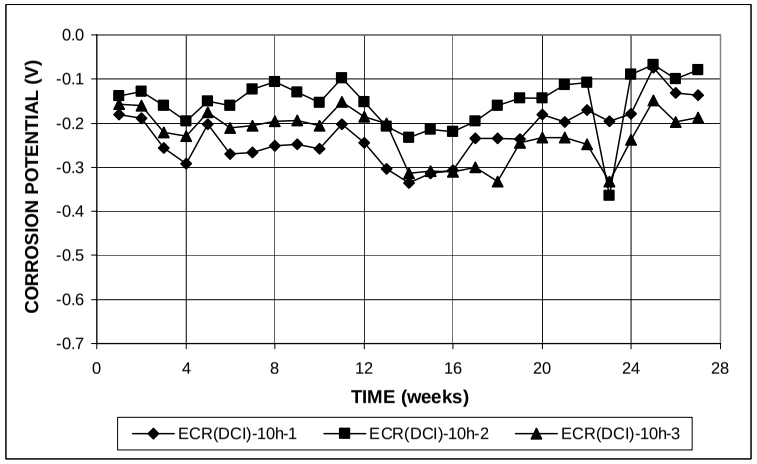

(b)

Figure A. 300 - (a) Top mat corrosion potentials and (b) bottom mat corrosion potentials as measured in the cracked beam test for specimens containing epoxy-coated steel with 10 drilled holes and corrosion inhibitor DCI

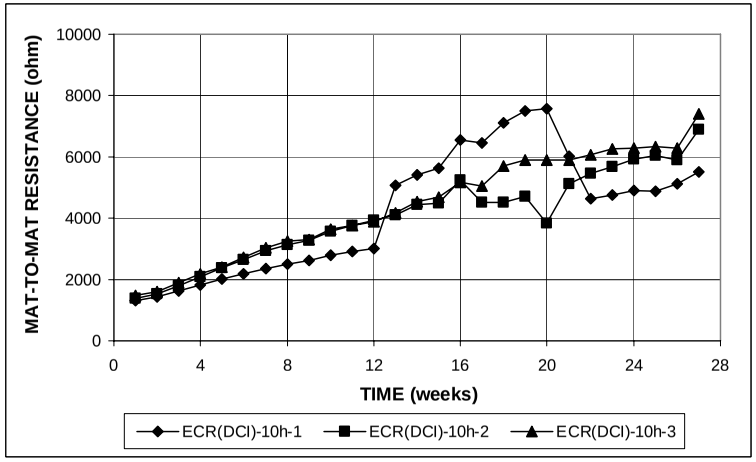

Figure A. 301 - Mat-to-mat resistances as measured in the cracked beam test for specimens containing epoxy-coated steel with 10 drilled holes and corrosion inhibitor DCI

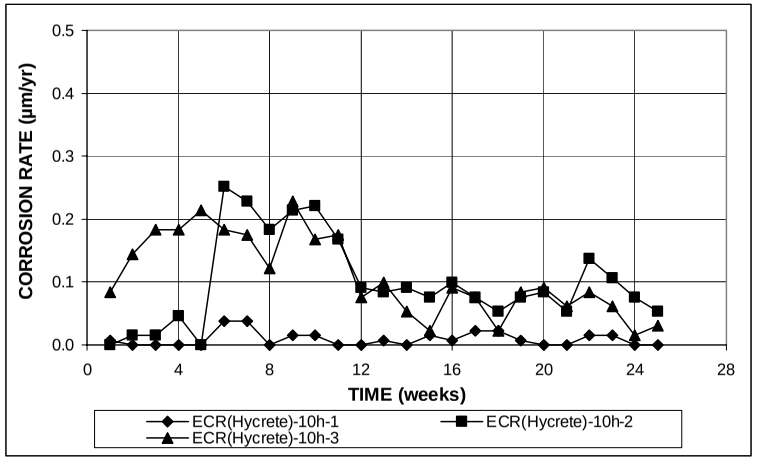

(a)

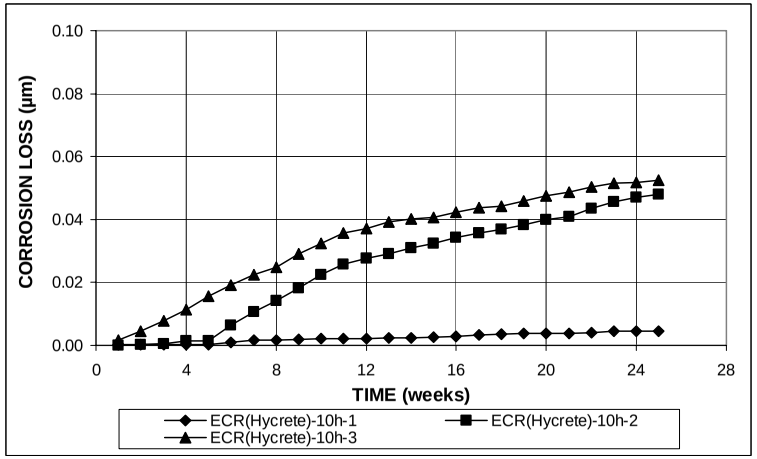

(b)

Figure A. 302 - (a) Corrosion rates and (b) total corrosion losses based on total bar area as measured in the cracked beam test for specimens containing epoxy-coated steel with 10 drilled holes and corrosion inhibitor Hycrete

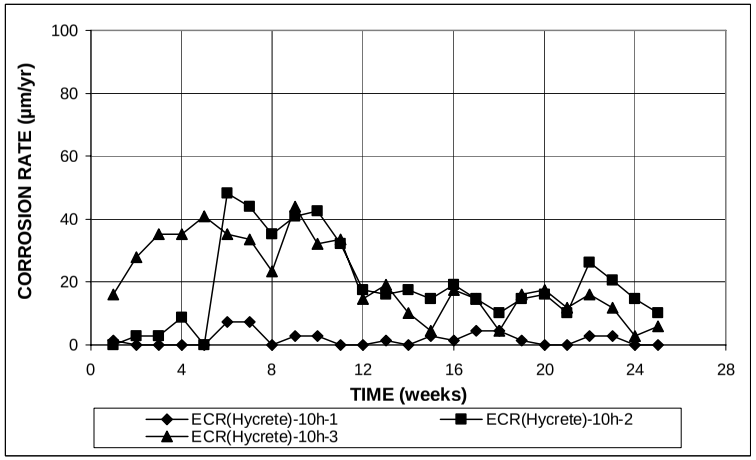

(a)

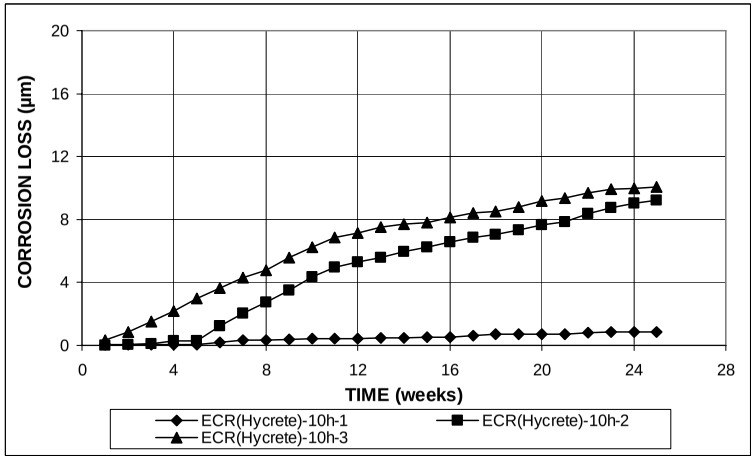

(b)

Figure A. 303 - (a) Corrosion rates and (b) total corrosion losses based on total bar area as measured in the Southern Exposure test for specimens containing epoxy-coated steel with 10 drilled holes and corrosion inhibitor Hycrete

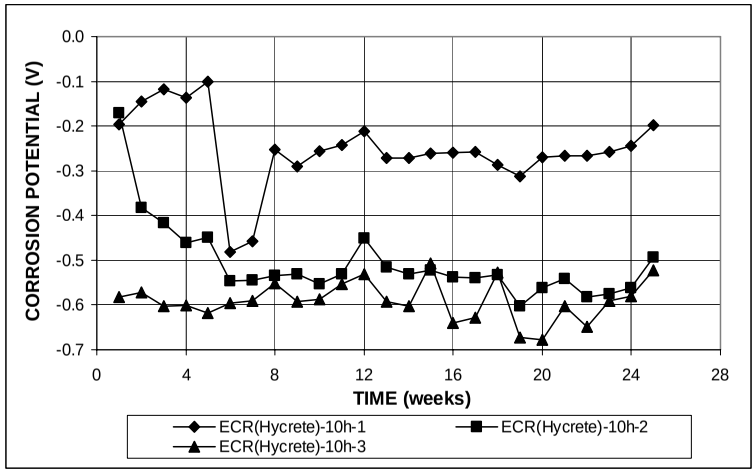

(a)

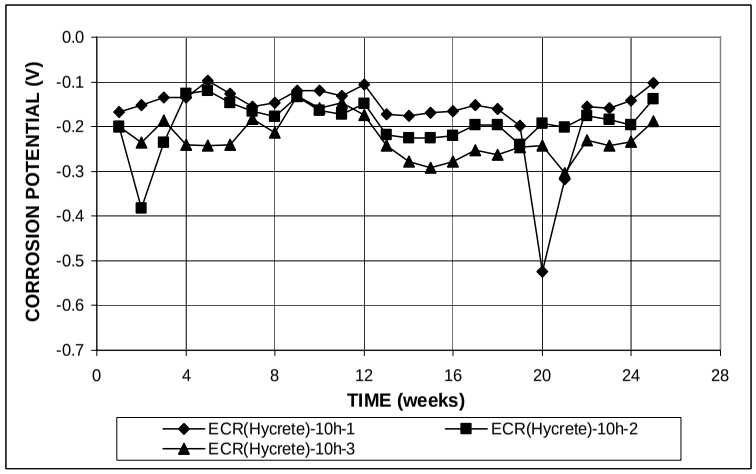

(b)

Figure A. 304 - (a) Top mat corrosion potentials and (b) bottom mat corrosion potentials as measured in the Southern Exposure test for specimens containing epoxy-coated steel with 10 drilled holes and corrosion inhibitor Hycrete

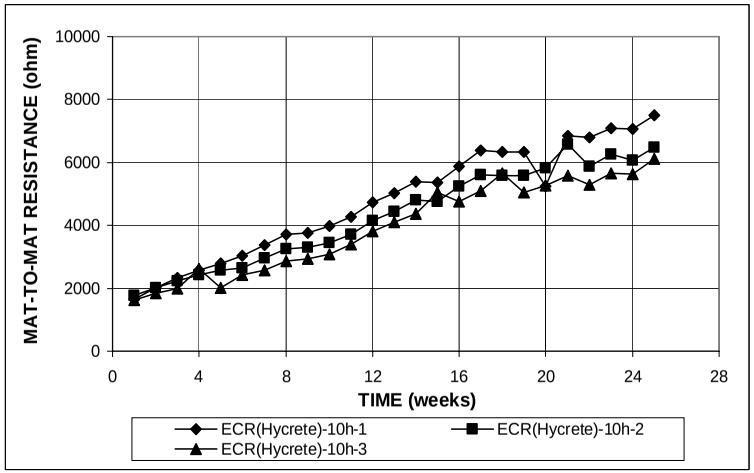

Figure A. 305 - Mat-to-mat resistances as measured in the Southern Exposure test for specimens containing epoxy-coated steel with 10 drilled holes and corrosion inhibitor Hycrete

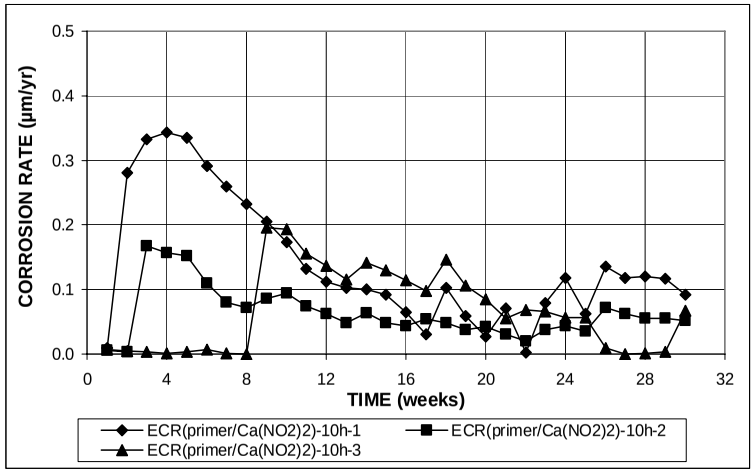

(a)

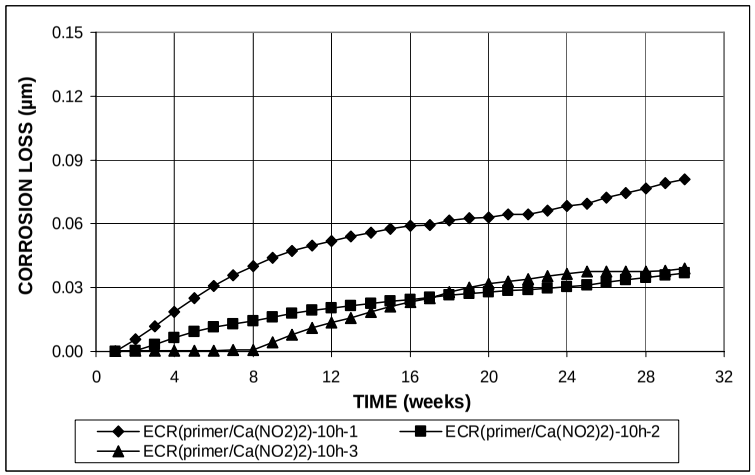

(b)

Figure A. 306 - (a) Corrosion rates and (b) total corrosion losses based on total bar area as measured in the cracked beam test for specimens containing ECR(primer/Ca$(NO_2)_2$) bars with 10 drilled holes

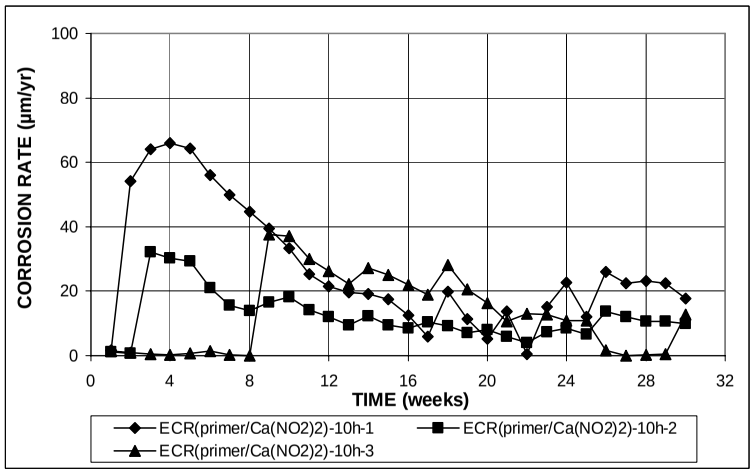

(a)

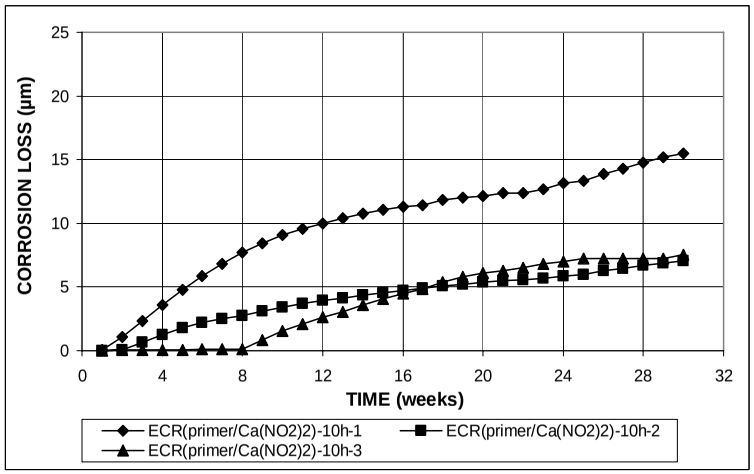

(b)

Figure A. 307 - (a) Corrosion rates and (b) total corrosion losses based on exposed bar area as measured in the cracked beam test for specimens containing ECR(primer/Ca$(NO_2)_2$) bars with 10 drilled holes

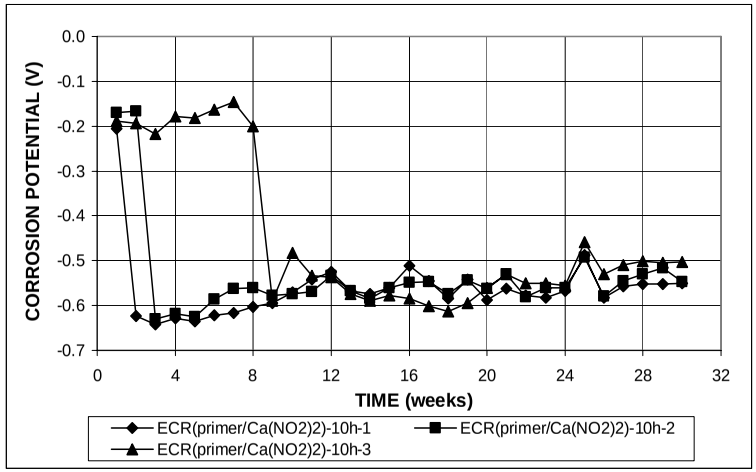

(a)

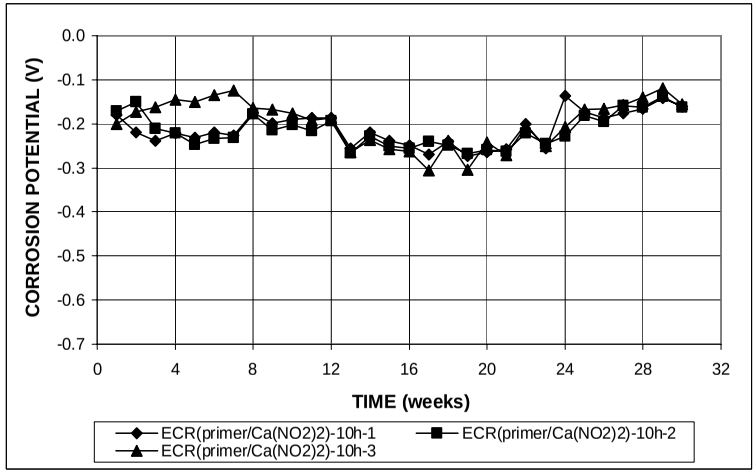

(b)

Figure A. 308 - (a) Top mat corrosion potentials and (b) bottom mat corrosion potentials as measured in the cracked beam test for specimens containing ECR(primer/$Ca(NO_2)_2$) bars with 10 drilled holes

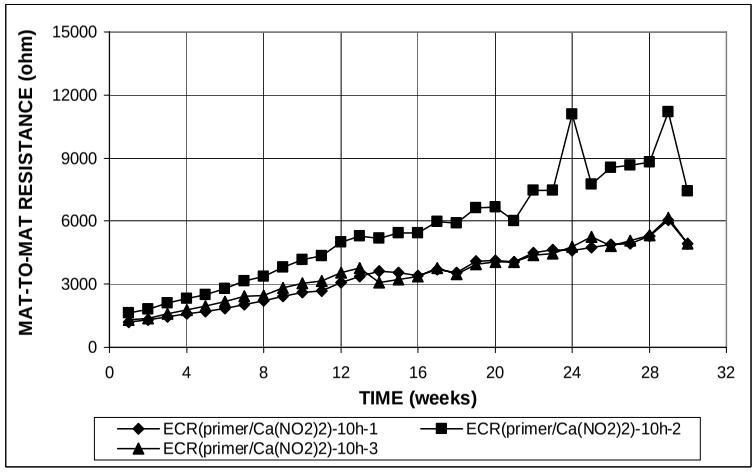

Figure A. 309 - Mat-to-mat resistances as measured in the cracked beam test for specimens containing ECR(primer/$Ca(NO_2)_2$) bars with 10 drilled holes

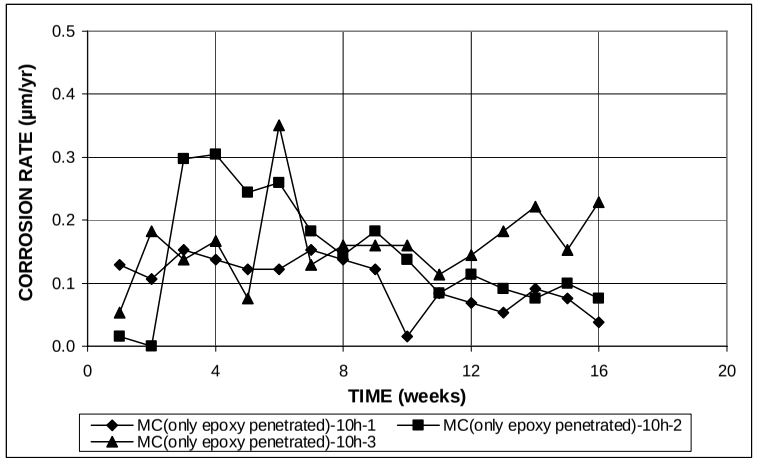

(a)

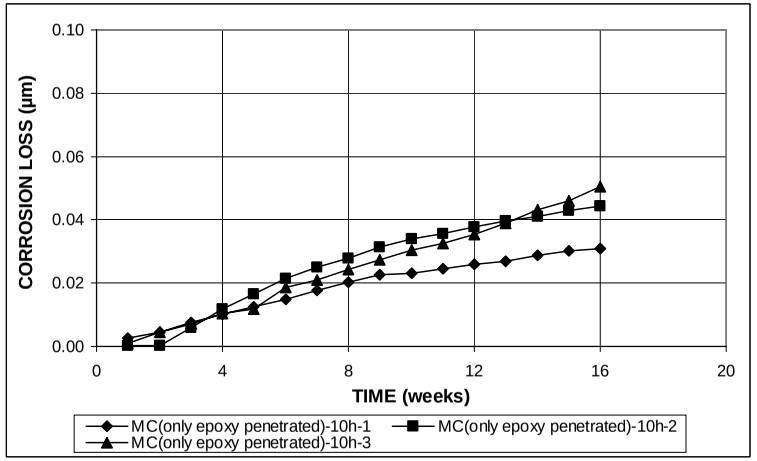

(b)

Figure A. 310 - (a) Corrosion rates and (b) total corrosion losses based on total bar area as measured in the cracked beam test for specimens containing multiple coated steel with only epoxy penetrated by 10 burned holes

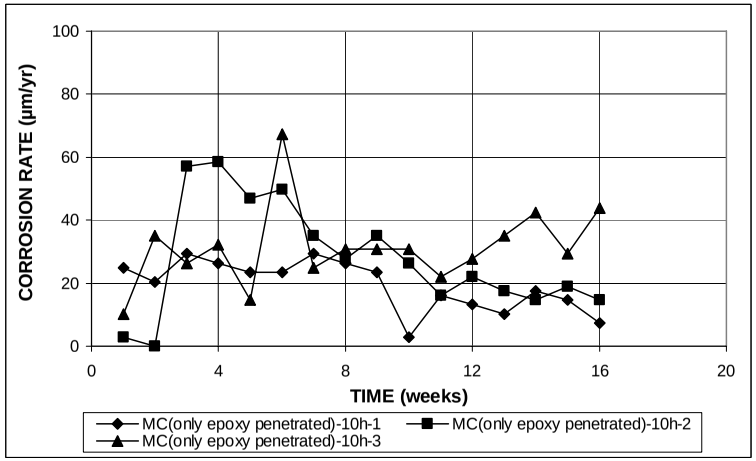

(a)

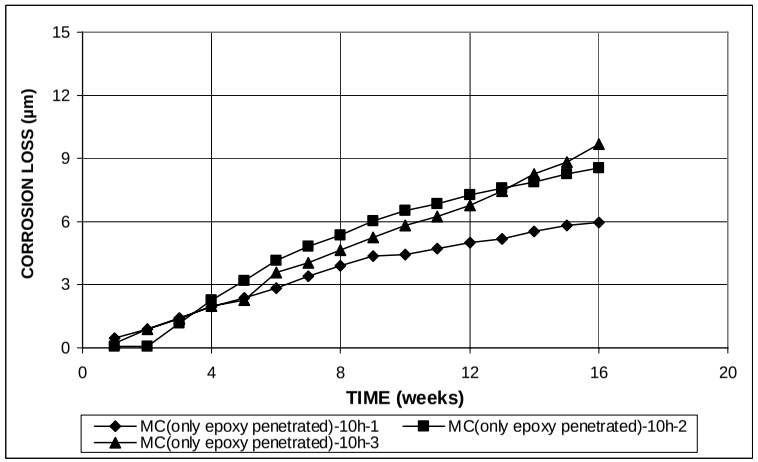

(b)

Figure A. 311 - (a) Corrosion rates and (b) total corrosion losses based on exposed area as measured in the cracked beam test for specimens containing multiple coated steel with only epoxy penetrated by 10 burned holes

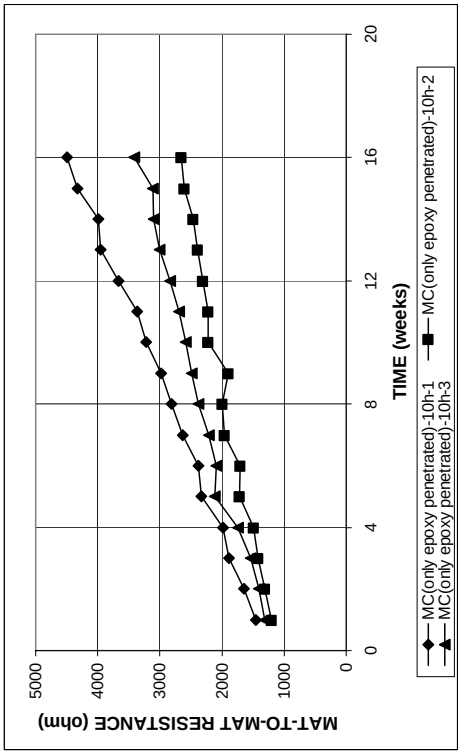

Figure A. 313 - Mat-to-mat resistances as measured in the cracked beam test for specimens containing multiple coated steel with only epoxy penetrated by 10 burned holes

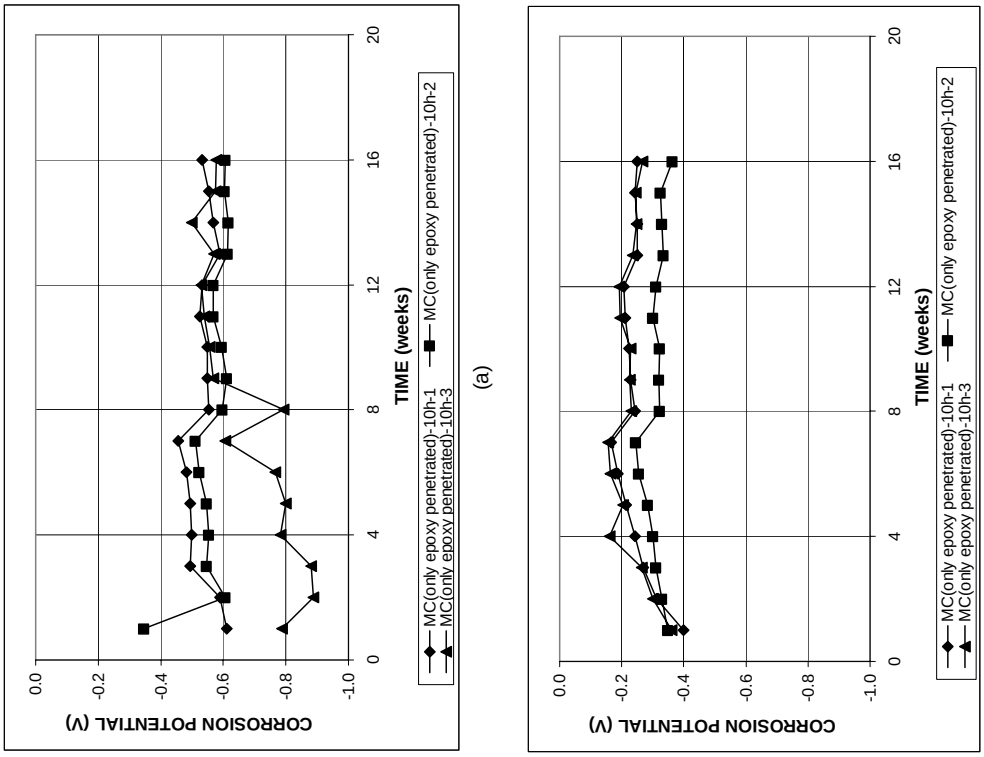

Figure A. 312 - (a) Top mat corrosion potentials and (b) bottom mat corrosion potentials as measured in the cracked beam test for specimens containing multiple coated steel with only epoxy penetrated by 10 burned holes

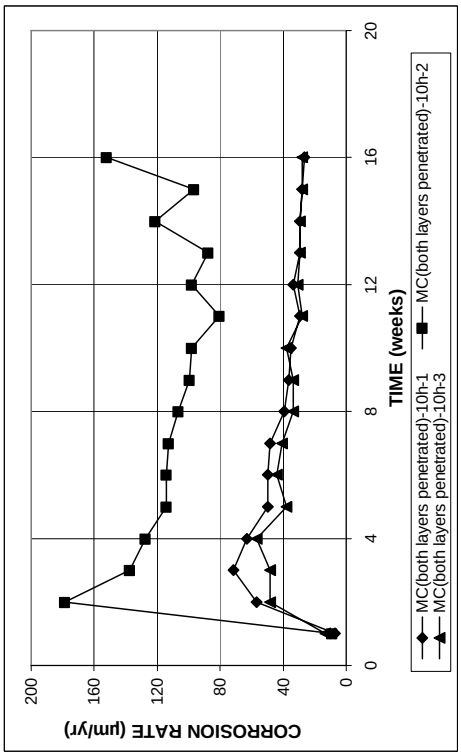

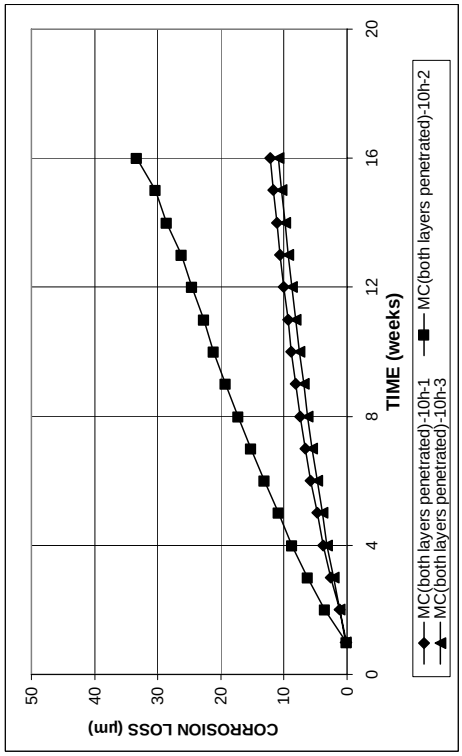

Figure A. 315 - (a) Corrosion rates and (b) total corrosion losses based on exposed area as measured in the crackd beam test for specimens containing multiple coated steel with both layers penetrated by 10 drilled holes

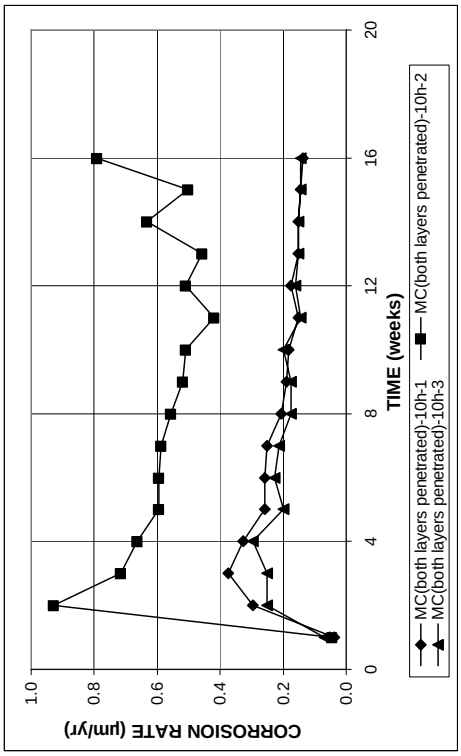

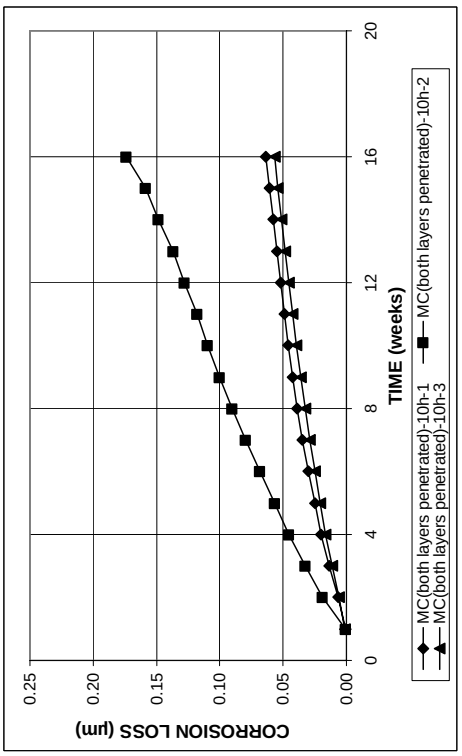

Figure A. 314 - (a) Corrosion rates and (b) total corrosion losses based on total bar area as measured in the cracked beam test for specimens containing multiple coated steel with both layers penetrated by 10 drilled holes

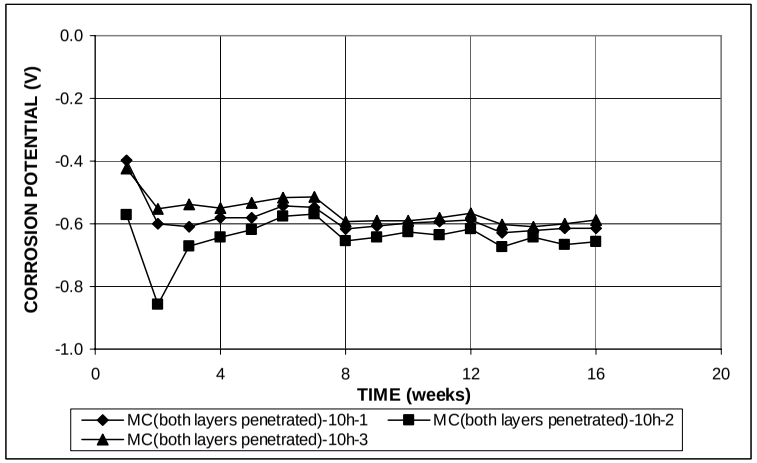

(a)

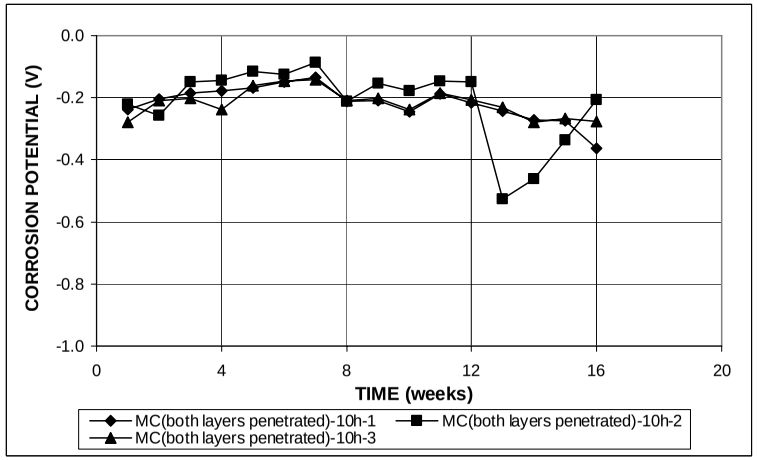

(b)

Figure A. 316 - (a) Top mat corrosion potentials and (b) bottom mat corrosion potentials as measured in the Southern Exposure test for specimens containing multiple coated steel with both layers penetrated by 10 drilled holes

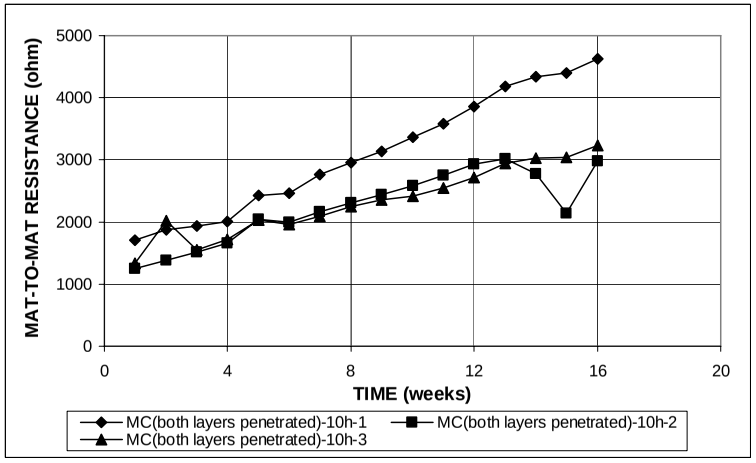

Figure A. 317 - Mat-to-mat resistances as measured in the Southern Exposure test for specimens containing multiple coated steel with both layers penetrated by 10 drilled holes

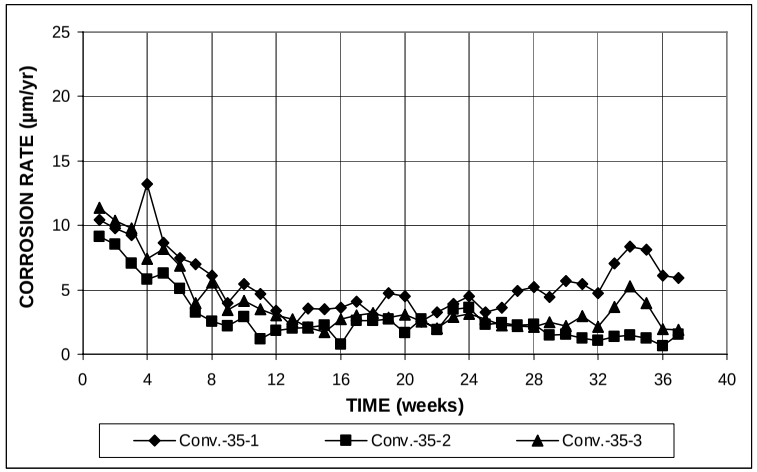

(a)

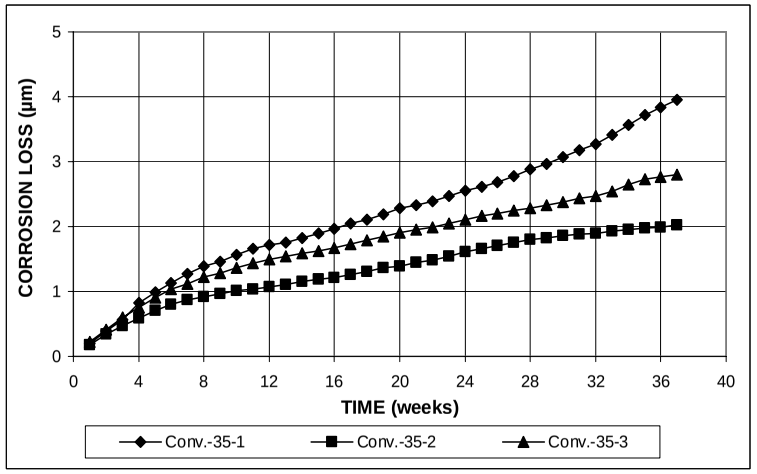

(b)

Figure A. 318 - (a) Corrosion rates and (b) total corrosion losses based on total bar area as measured in the cracked beam test for specimens containing conventional steel

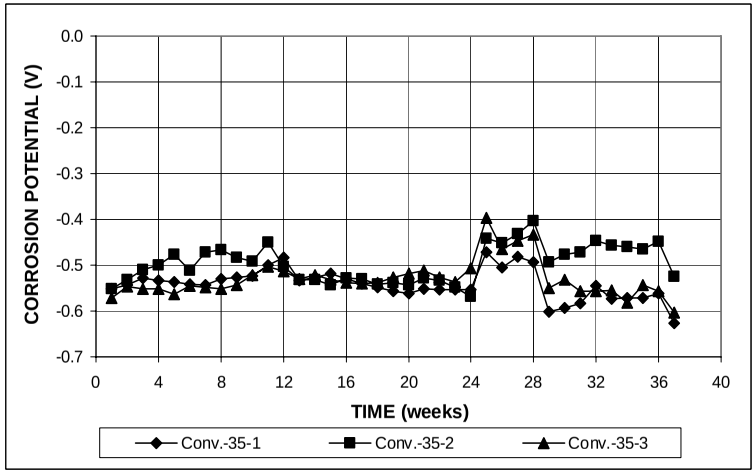

(a)

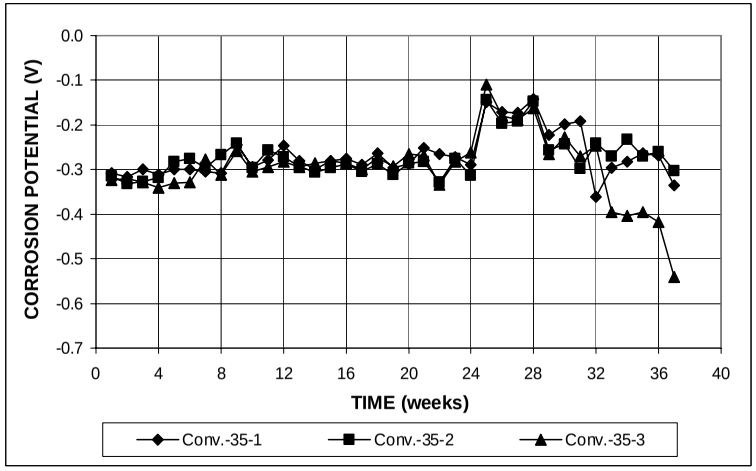

(b)

Figure A. 319 - (a) Top mat corrosion potentials and (b) bottom mat corrosion potentials as measured in the cracked beam test for specimens containing conventional steel

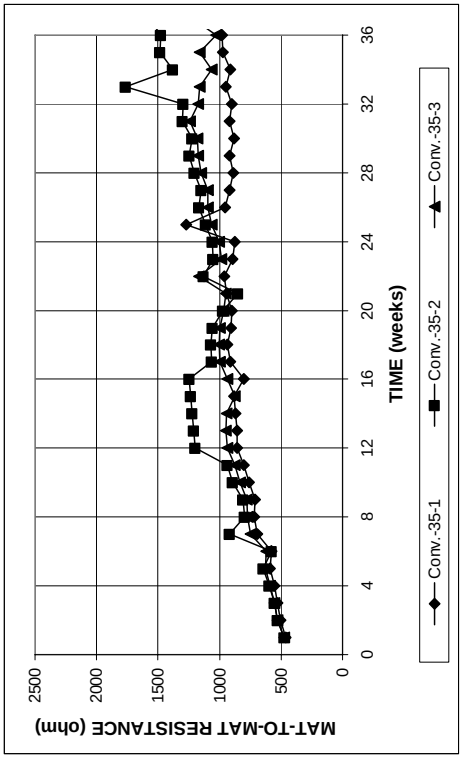

Figure A. 320 - Mat-to-mat resistances as measured in the cracked beam test for specimens containing conventional steel

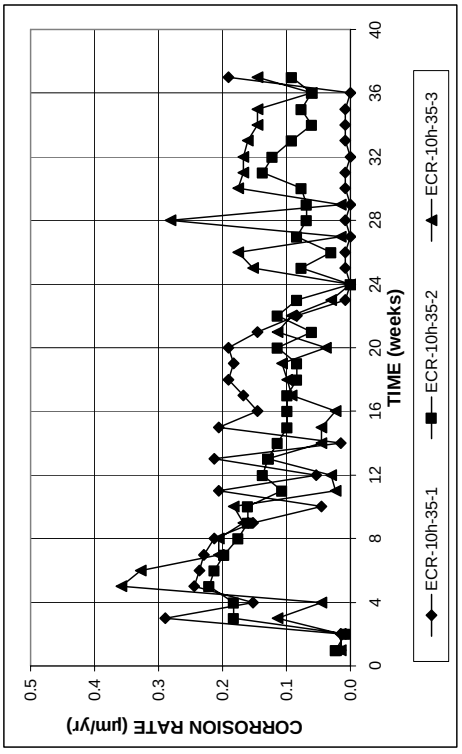

Figure A. 321 - (a) Corrosion rates and (b) total corrosion losses based on total bar area as measured in the cracked beam test for specimens containing epoxy-coated steel with 10 drilled holes in a w/c ratio of 0.35

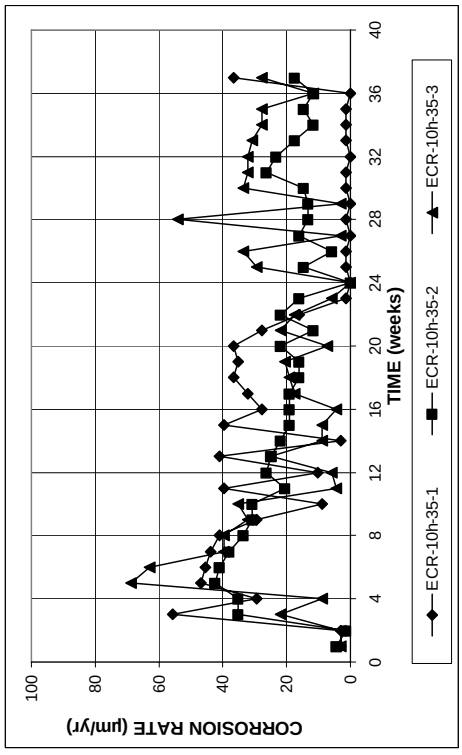

Figure A. 322 - (a) Corrosion rates and (b) total corrosion losses based on total bar area as measured in the cracked beam test for specimens containing epoxy-coated steel with 10 drilled holes in a w/c ratio of 0.35

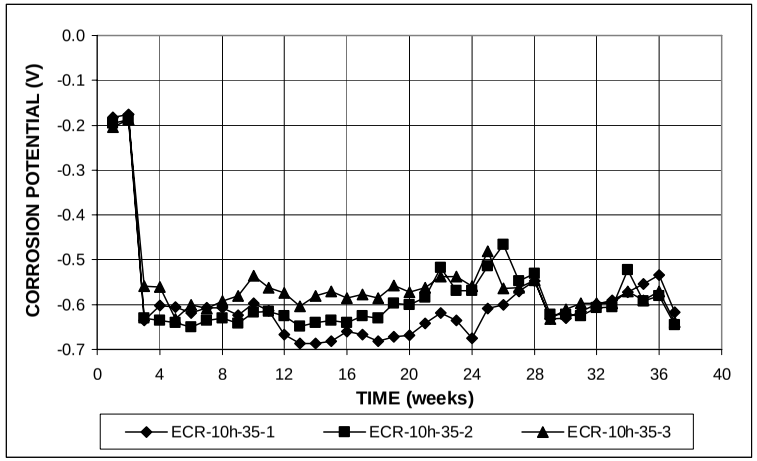

(a)

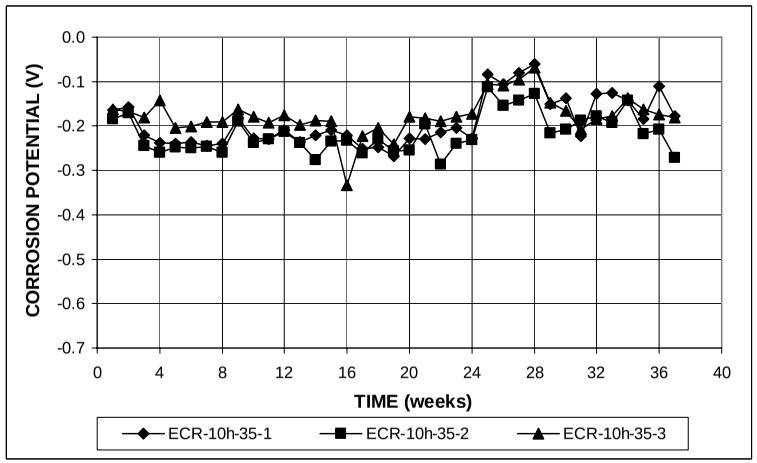

(b)

Figure A. 323 - (a) Top mat corrosion potentials and (b) bottom mat corrosion potentials as measured in the cracked beam test for specimens containing epoxy-coated steel with 10 drilled holes in a w/c ratio of 0.35

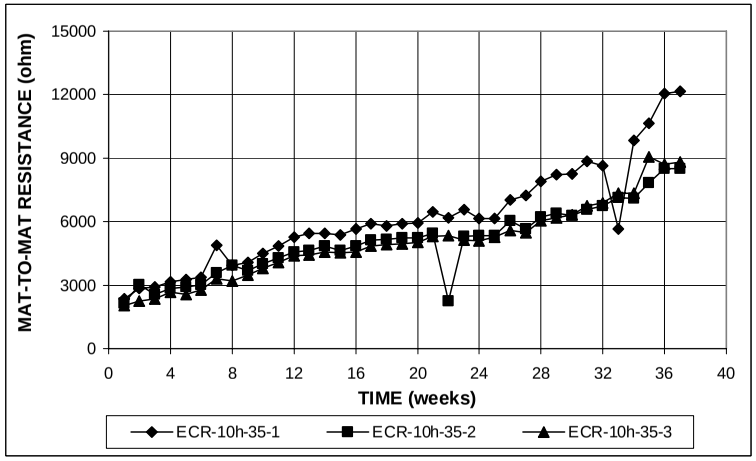

Figure A. 324 - Mat-to-mat resistances as measured in the cracked beam test for specimens containing epoxy-coated steel with 10 drilled holes in a w/c ratio of 0.35

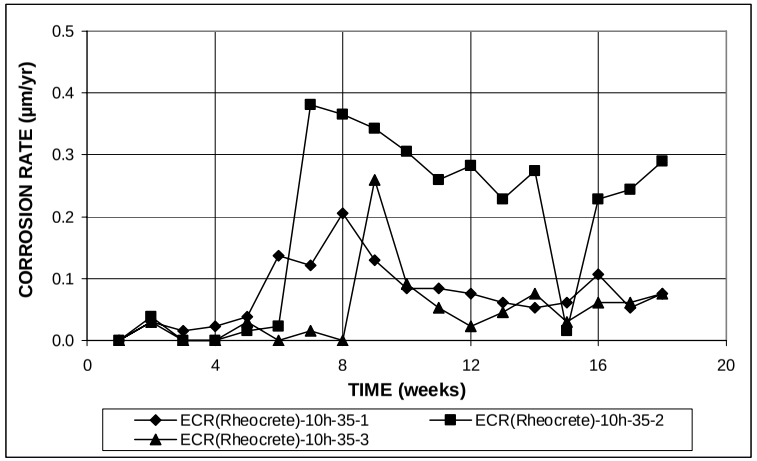

(a)

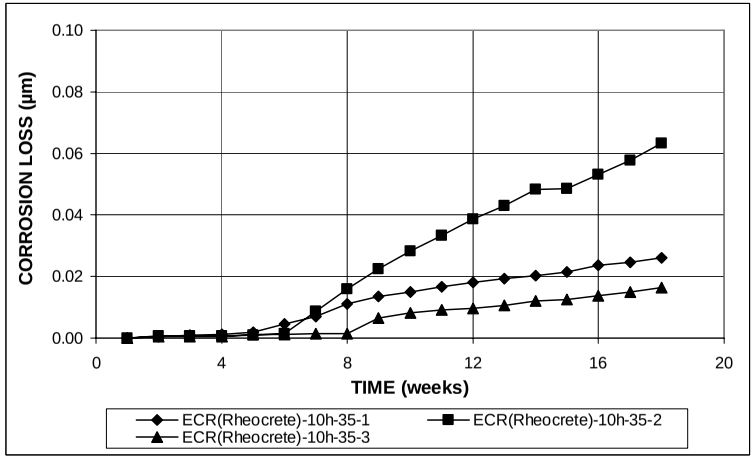

(b)

Figure A. 325 - (a) Corrosion rates and (b) total corrosion losses based on total bar area as measured in the cracked beam test for specimens containing epoxy-coated steel with 10 drilled holes and corrosion inhibitor Rheocrete in a w/c ratio of 0.35

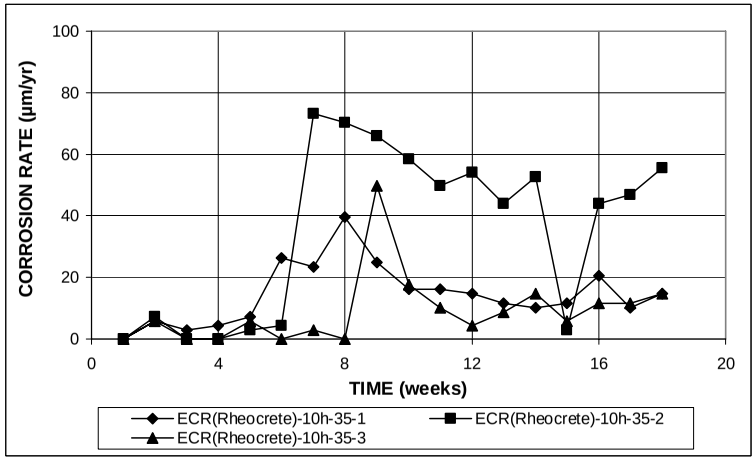

(a)

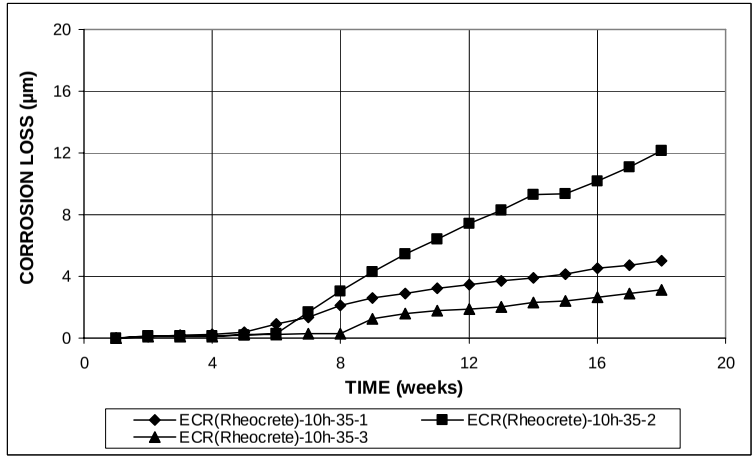

(b)

Figure A. 326 - (a) Corrosion rates and (b) total corrosion losses based on exposed area as measured in the cracked beam test for specimens containing epoxy-coated steel with 10 drilled holes and corrosion inhibitor Rheocrete in a w/c ratio of 0.35

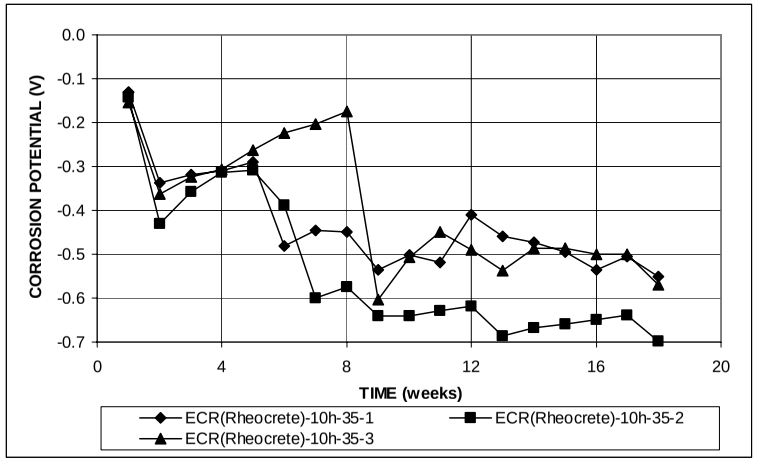

(a)

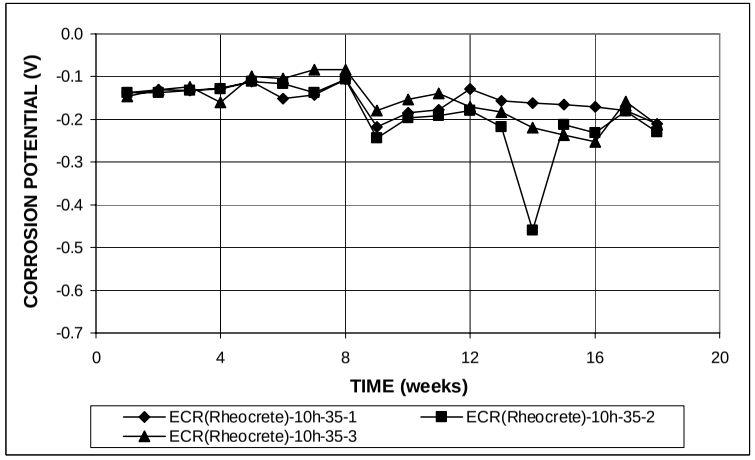

(b)

Figure A. 327 - (a) Top mat corrosion potentials and (b) bottom mat corrosion potentials as measured in the cracked beam test for specimens containing epoxy-coated steel with 10 drilled holes and corrosion inhibitor Rheocrete in a w/c ratio of 0.35

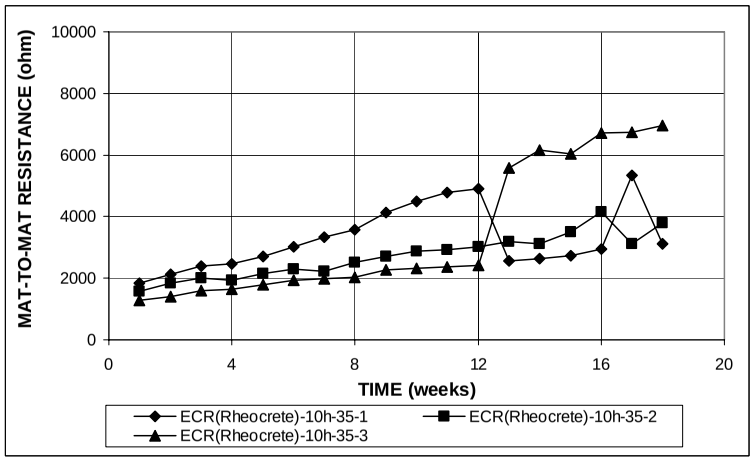

Figure A. 328 - Mat-to-mat resistances as measured in the cracked beam test for specimens containing epoxy-coated steel with 10 drilled holes and corrosion inhibitor Rheocrete in a w/c ratio of 0.35

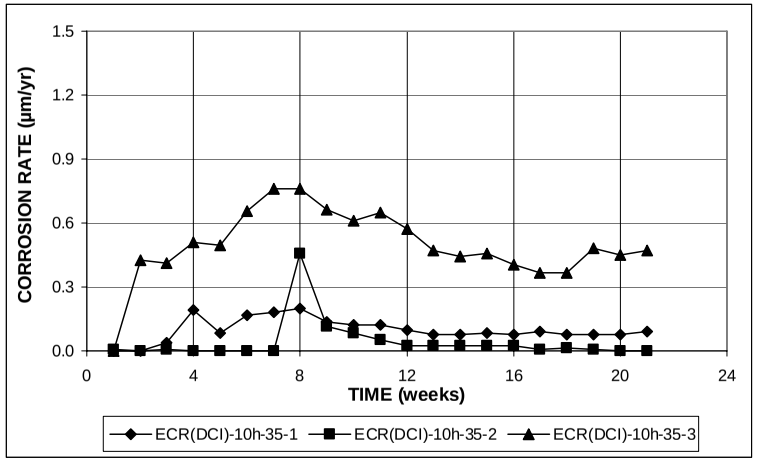

(a)

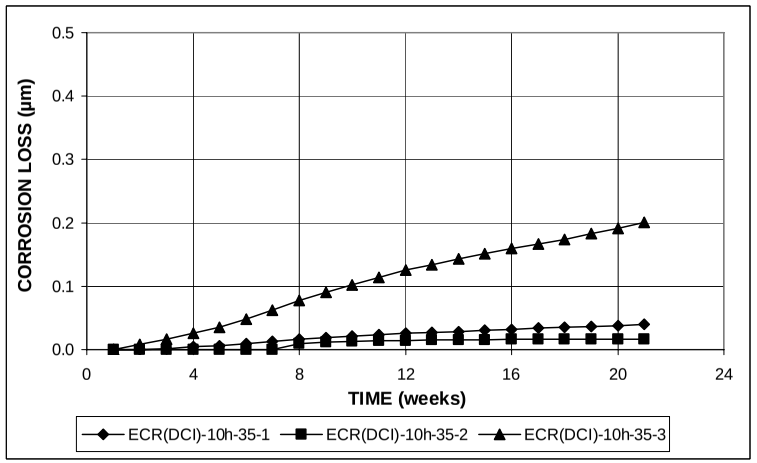

(b)

Figure A. 329 - (a) Corrosion rates and (b) total corrosion losses based on total bar area as measured in the cracked beam test for specimens containing epoxy-coated steel with 10 drilled holes and corrosion inhibitor DCI in a w/c ratio of 0.35

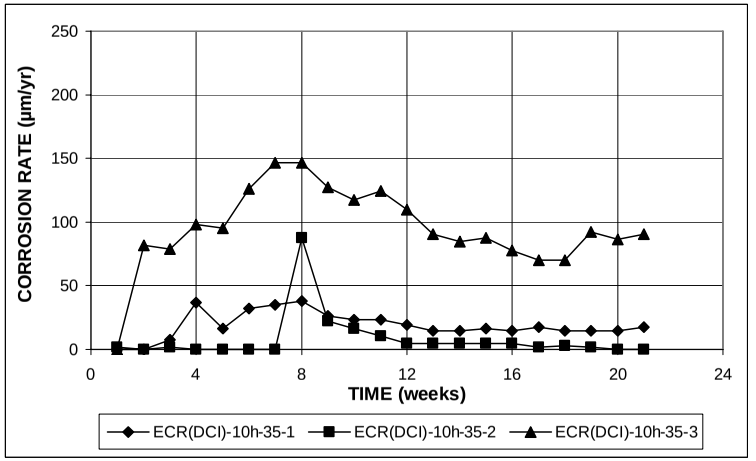

(a)

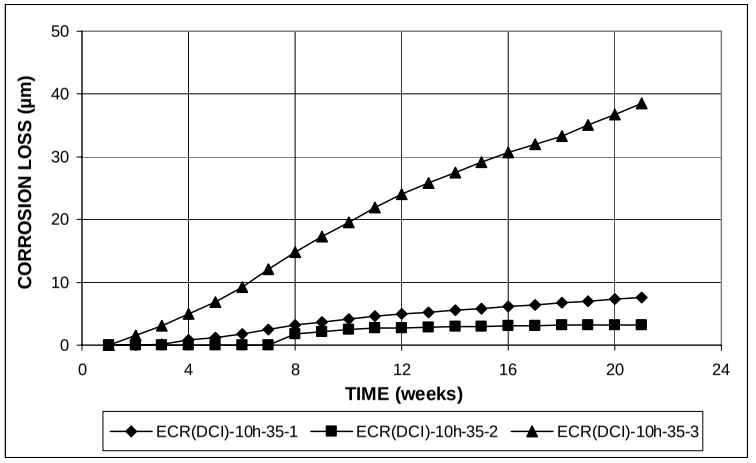

(b)

Figure A. 330 - (a) Corrosion rates and (b) total corrosion losses based on total bar area as measured in the cracked beam test for specimens containing epoxy-coated steel with 10 drilled holes and corrosion inhibitor DCI in a w/c ratio of 0.35

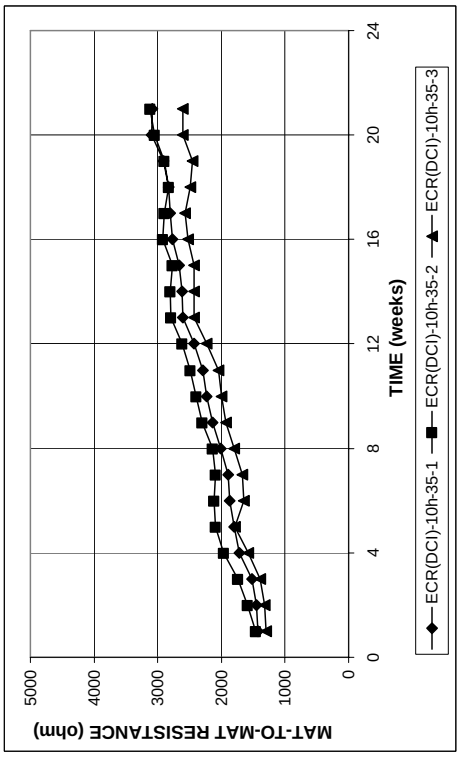

Figure A. 332 - Mat-to-mat resistances as measured in the cracked beam test for specimens containing epoxy-coated steel with 10 drilled holes and corrosion inhibitor DCI in a w/c ratio of 0.35

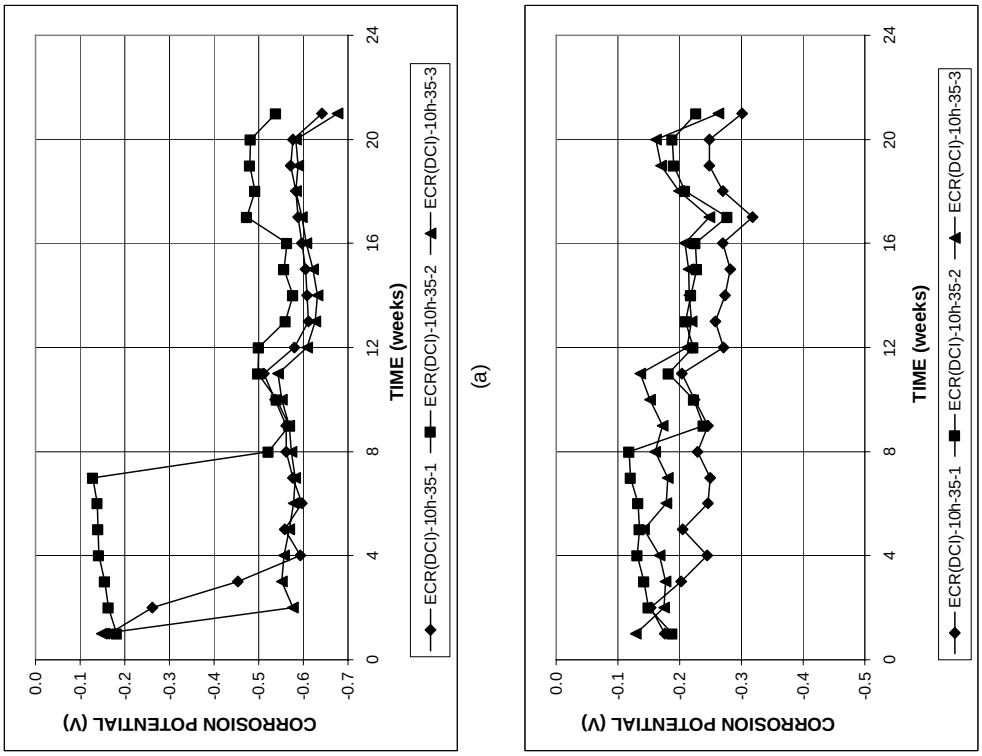

Figure A. 331 - (a) Top mat corrosion potentials and (b) bottom mat corrosion potentials as measured in the cracked beam test for specimens containing epoxy-coated steel with 10 drilled holes and corrosion inhibitor DCI in a w/c ratio of 0.35

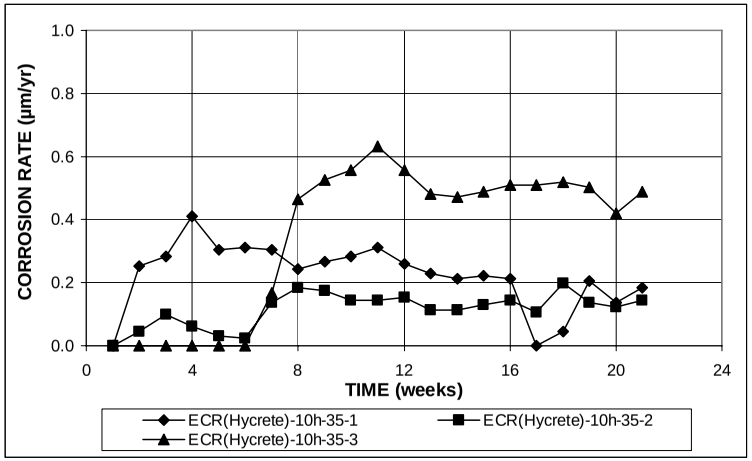

(a)

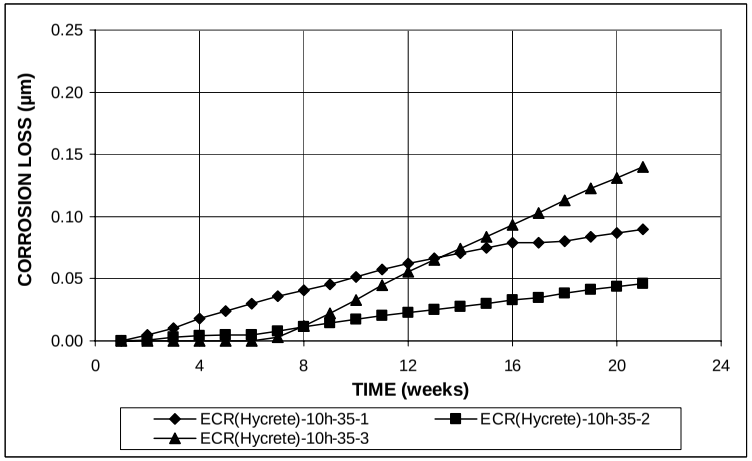

(b)

Figure A. 333 - (a) Corrosion rates and (b) total corrosion losses based on total bar area as measured in the cracked beam test for specimens containing epoxy-coated steel with 10 drilled holes and corrosion inhibitor Hycrete in a w/c ratio of 0.35

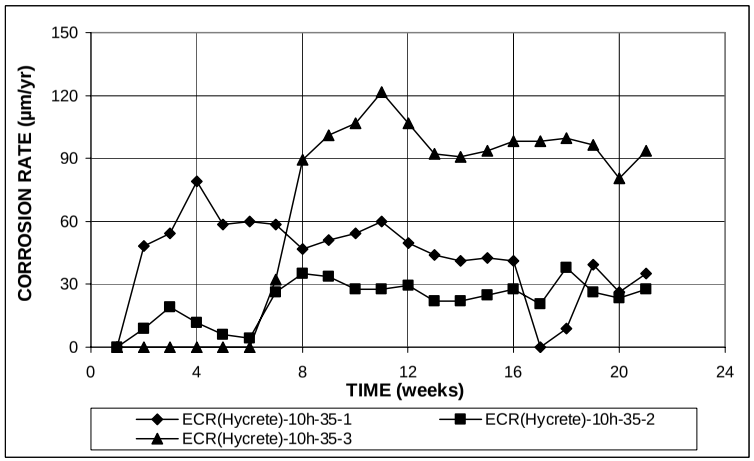

(a)

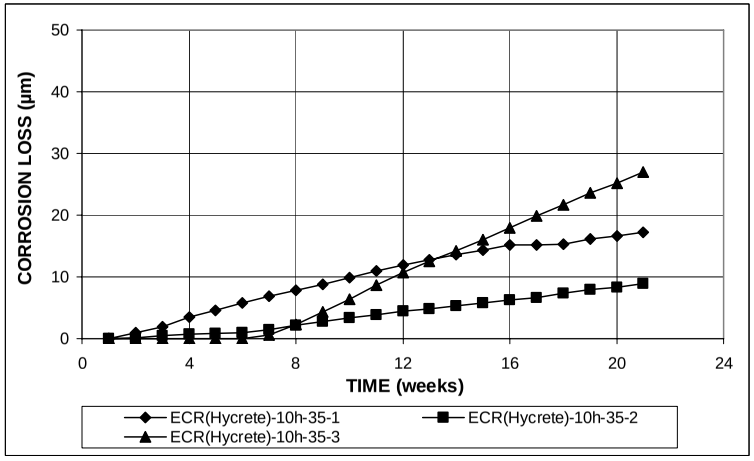

(b)

Figure A. 334 - (a) Corrosion rates and (b) total corrosion losses based on exposed area as measured in the cracked beam test for specimens containing epoxy-coated steel with 10 drilled holes and corrosion inhibitor Hycrete in a w/c ratio of 0.35

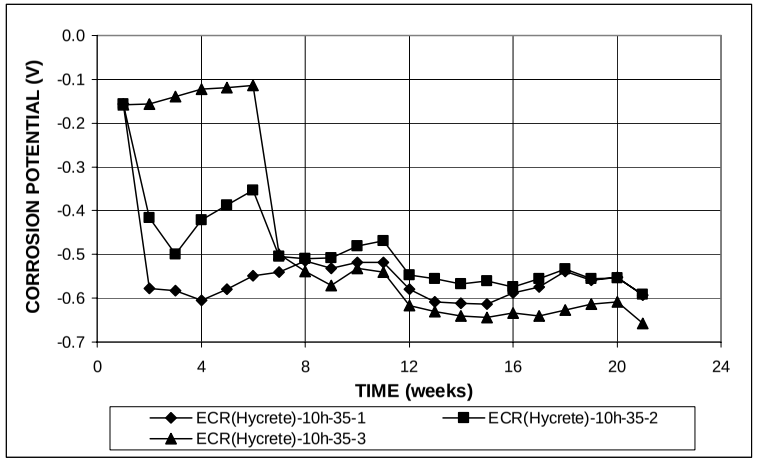

(a)

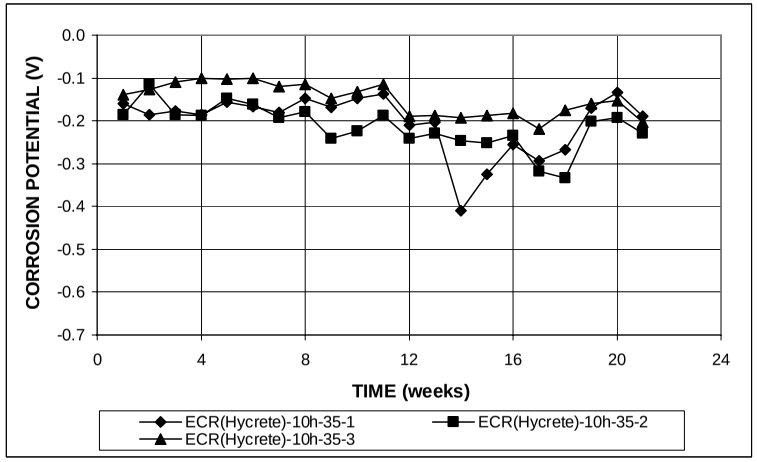

(b)

Figure A. 335 - (a) Top mat corrosion potentials and (b) bottom mat corrosion potentials as measured in the cracked beam test for specimens containing epoxy-coated steel with 10 drilled holes and corrosion inhibitor Hycrete in a w/c ratio of 0.35

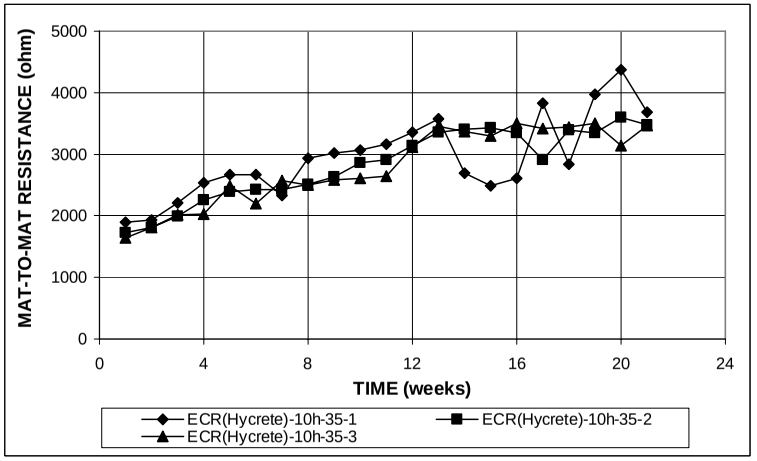

Figure A. 336 - Mat-to-mat resistances as measured in the cracked beam test for specimens containing epoxy-coated steel with 10 drilled holes and corrosion inhibitor Hycrete in a w/c ratio of 0.35

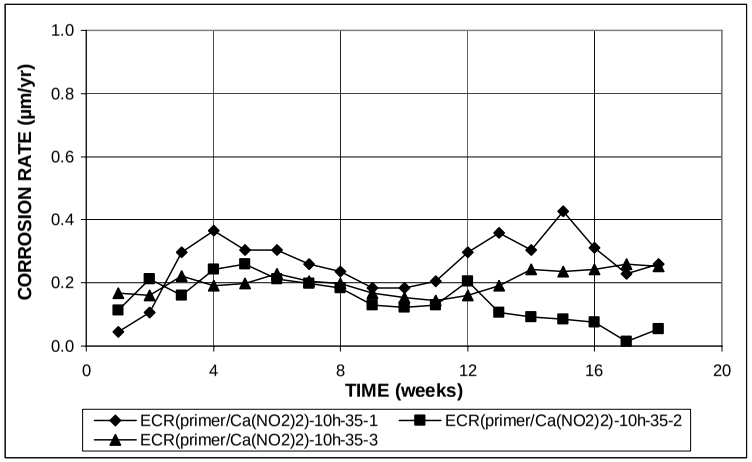

(a)

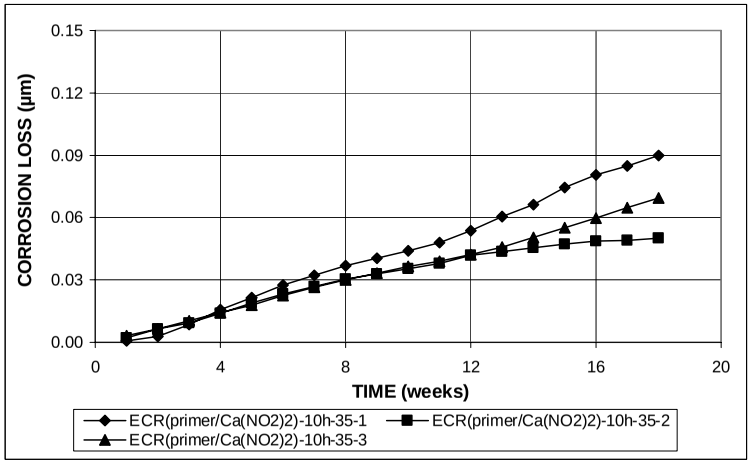

(b)

Figure A. 337 - (a) Corrosion rates and (b) total corrosion losses based on total bar area as measured in the cracked beam test for specimens containing ECR(primer/Ca(NO_2)$_2$) bars with 10 drilled holes in a w/c of 0.35

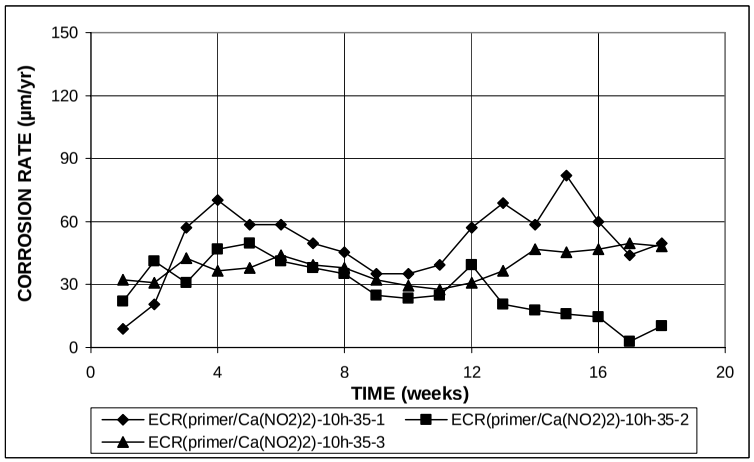

(a)

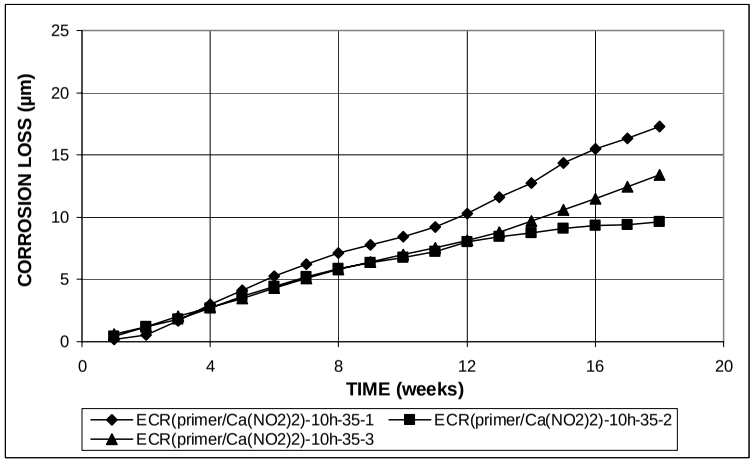

(b)

Figure A. 338 - (a) Corrosion rates and (b) total corrosion losses based on exposed area as measured in the cracked beam test for specimens containing ECR(primer/Ca(NO_2)$_2$) bars with 10 drilled holes in a w/c of 0.35

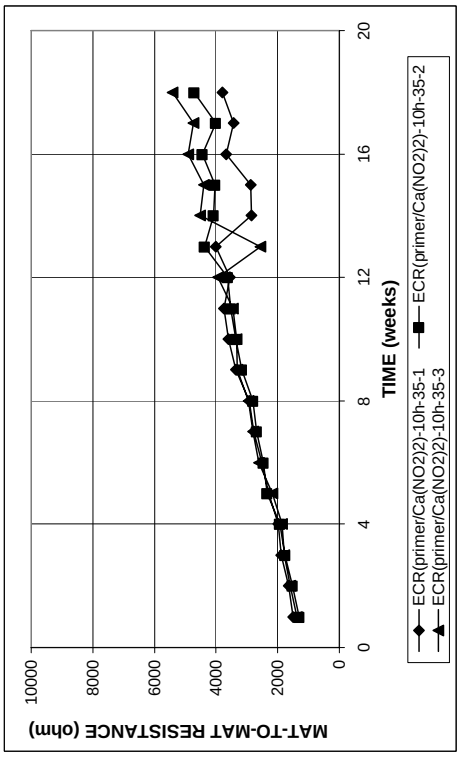

Figure A. 340 - Mat-to-mat resistances as measured in the cracked beam test for specimens containing ECR(primer/$Ca(NO_2)_2$) bars with 10 drilled holes in a w/c of 0.35

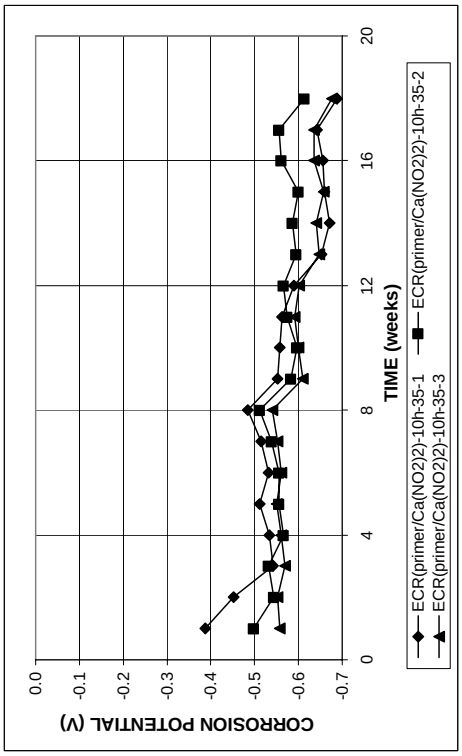

Figure A. 339 - (a) Top mat corrosion potentials and (b) bottom mat corrosion potentials as measured in the cracked beam test for specimens containing ECR(primer/$Ca(NO_2)_2$) bars with 10 drilled holes in a w/c of 0.35

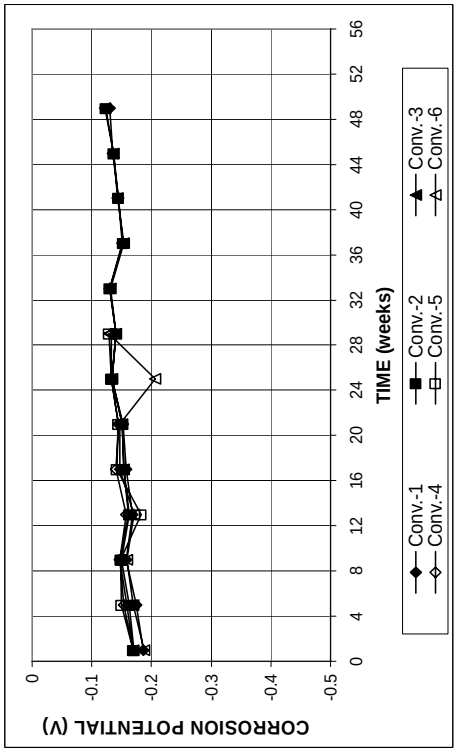

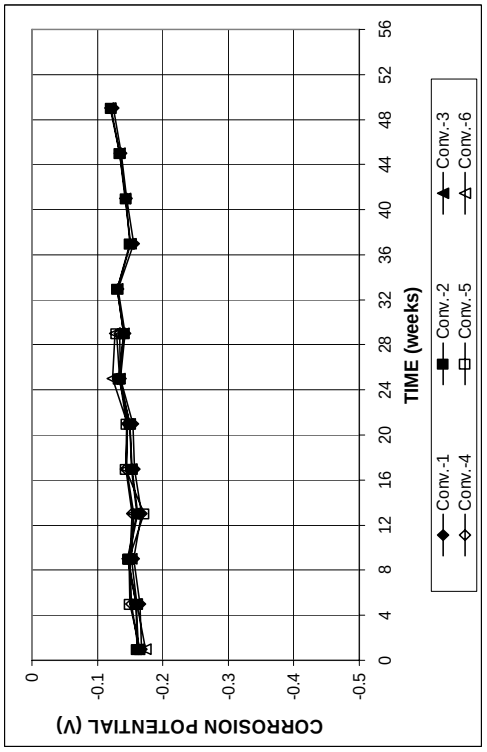

Figure A. 342 - (a) Top mat corrosion potentials and (b) bottom mat corrosion potentials as measured in the ASTM G 109 test for specimens containing conventional steel

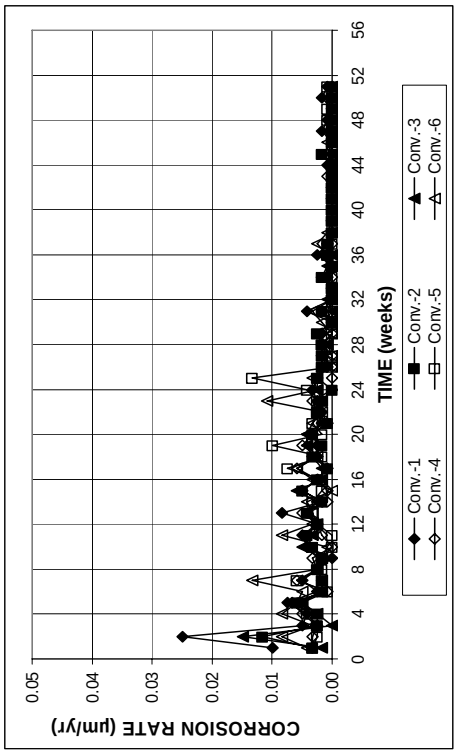

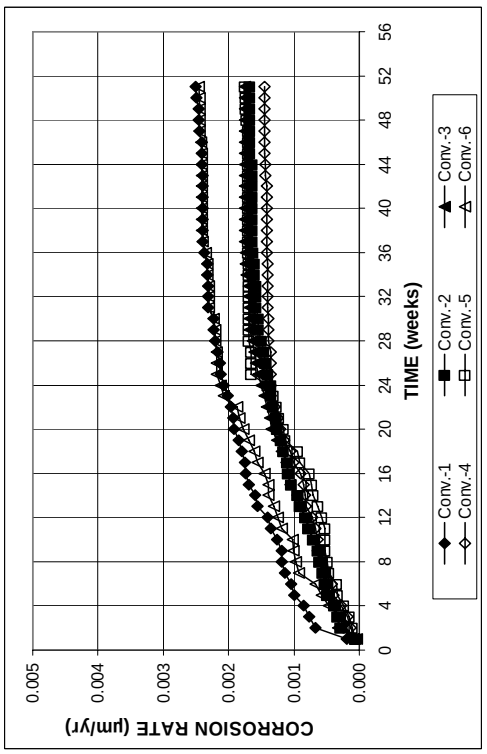

Figure A. 341 - (a) Corrosion rates and (b) total corrosion losses based on total bar area as measured in the ASTM G 109 test for specimens containing conventional steel

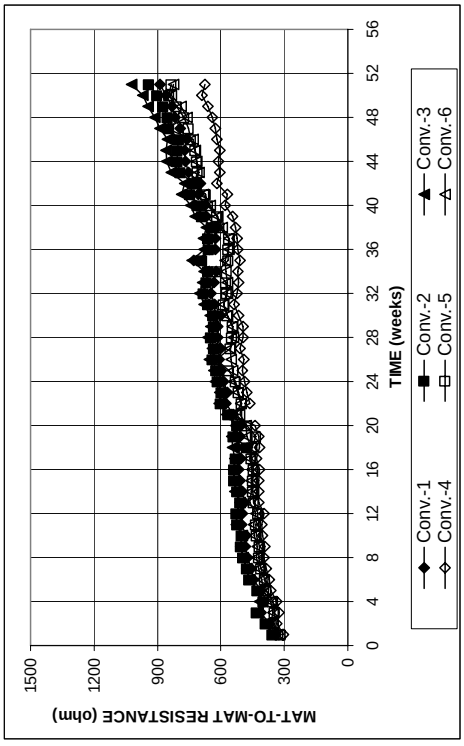

Figure A. 343 - Mat-to-mat resistances as measured in the ASTM G 109 test for specimens containing conventional steel

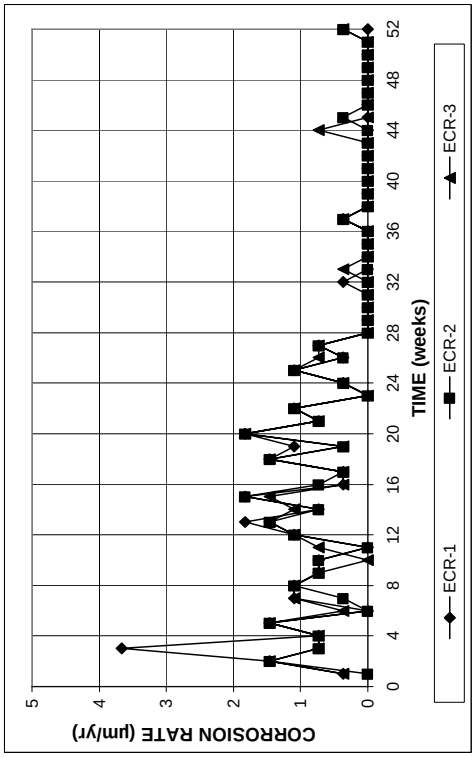

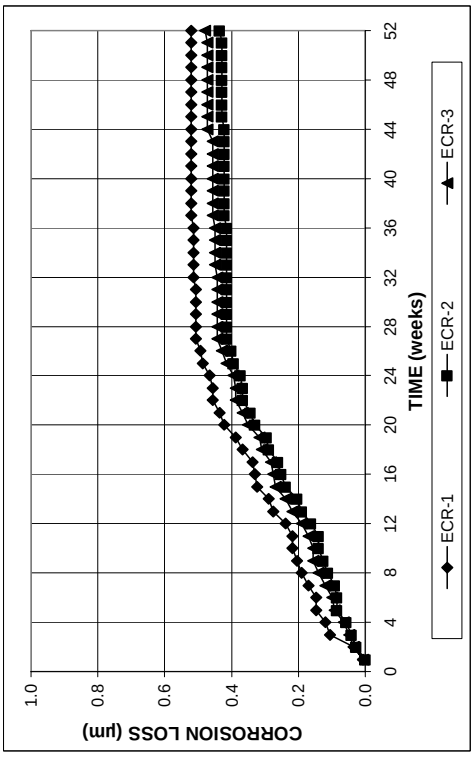

Figure A. 345 - (a) Corrosion rates and (b) total corrosion losses based on exposed area as measured in the ASTM G 109 test for specimens containing epoxy-coated bars

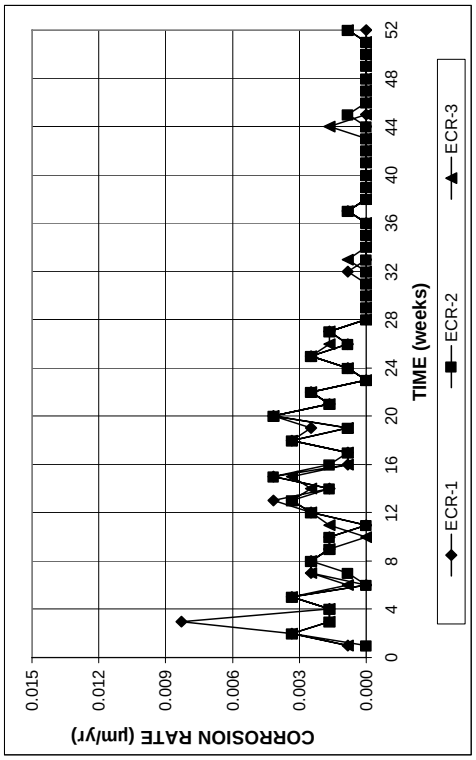

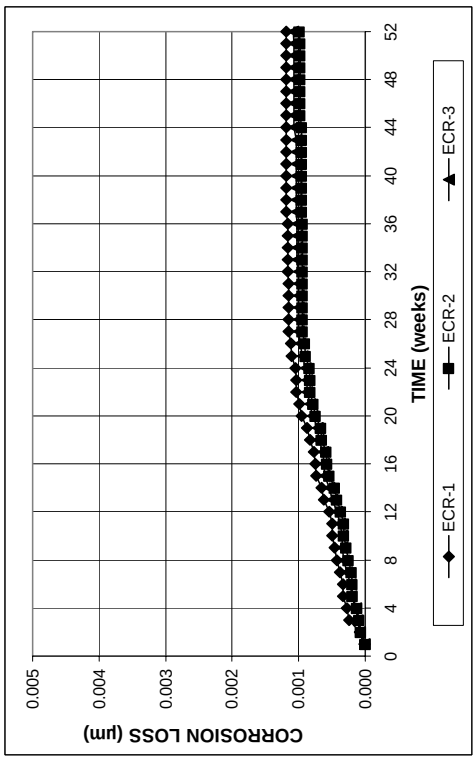

Figure A. 344 - (a) Corrosion rates and (b) total corrosion losses based on total bar area as measured in the ASTM G 109 test for specimens containing epoxy-coated bars

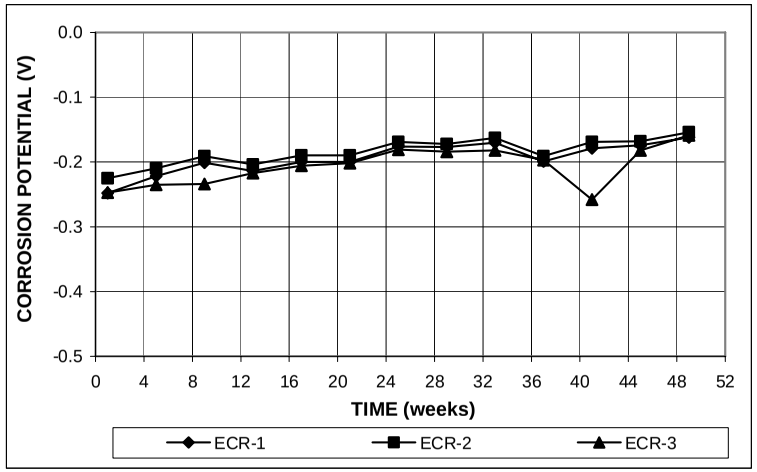

(a)

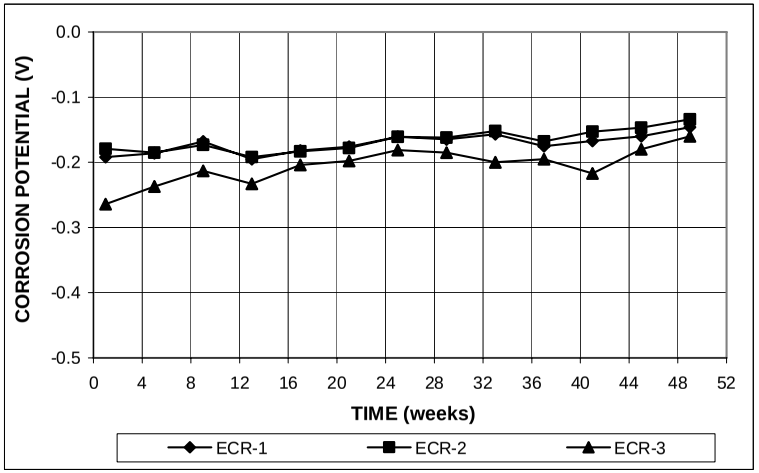

(b)

Figure A. 346 - (a) Top mat corrosion potentials and (b) bottom mat corrosion potentials as measured in the ASTM G 109 test for specimens containing epoxy-coated bars

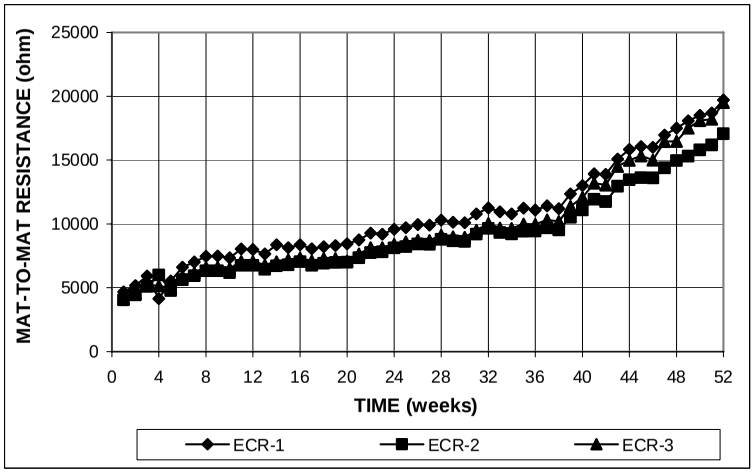

Figure A. 347 - Mat-to-mat resistances as measured in the ASTM G 109 test for specimens containing epoxy-coated bars

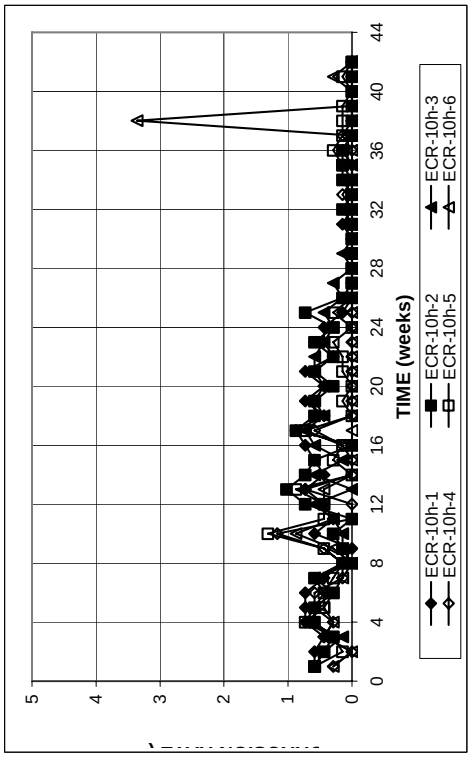

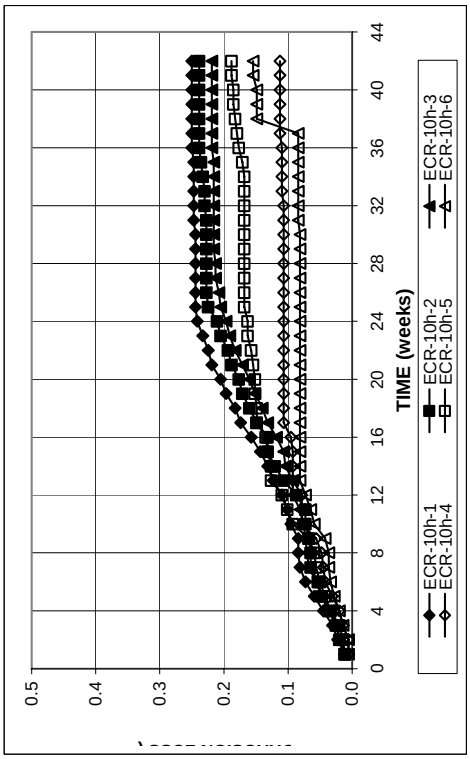

Figure A. 349 - (a) Corrosion rates and (b) total corrosion losses based on exposed area as measured in the ASTM G 109 test for specimens containing epoxy-coated steel with 10 drilled holes

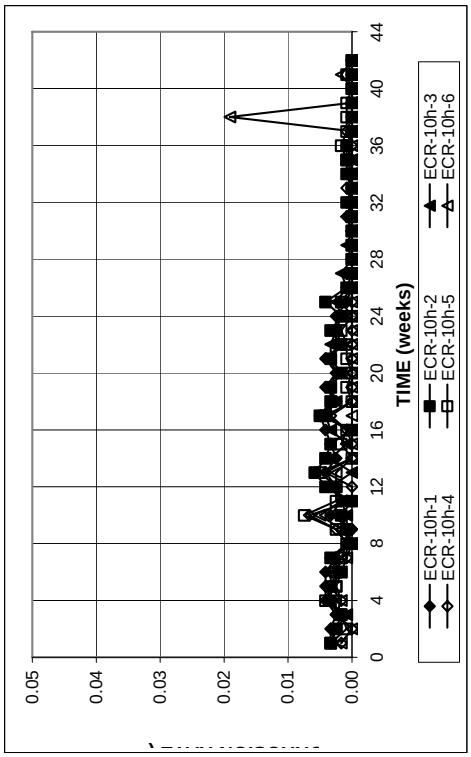

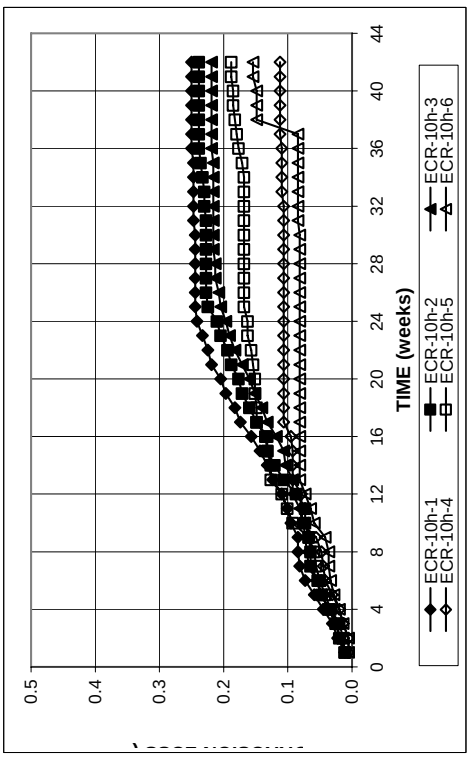

Figure A. 348 - (a) Corrosion rates and (b) total corrosion losses based on total bar area as measured in the ASTM G 109 test for specimens containing epoxy-coated steel with 10 drilled holes

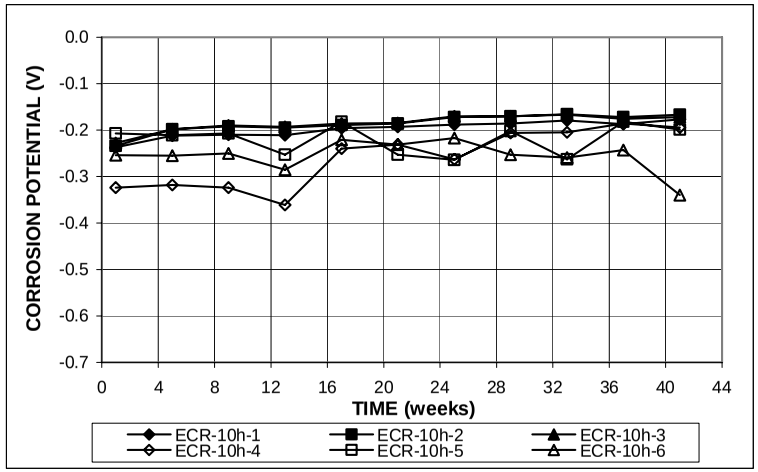

(a)

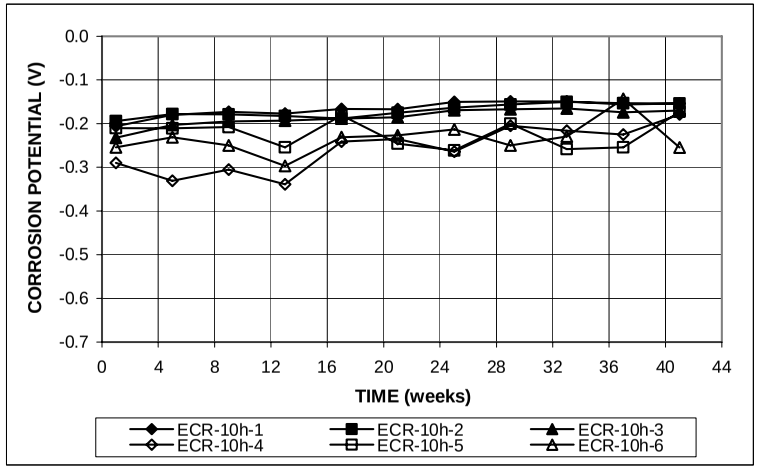

(b)

Figure A. 350 - (a) Top mat corrosion potentials and (b) bottom mat corrosion potentials as measured in the ASTM G 109 test for specimens containing epoxy-coated steel with 10 drilled holes

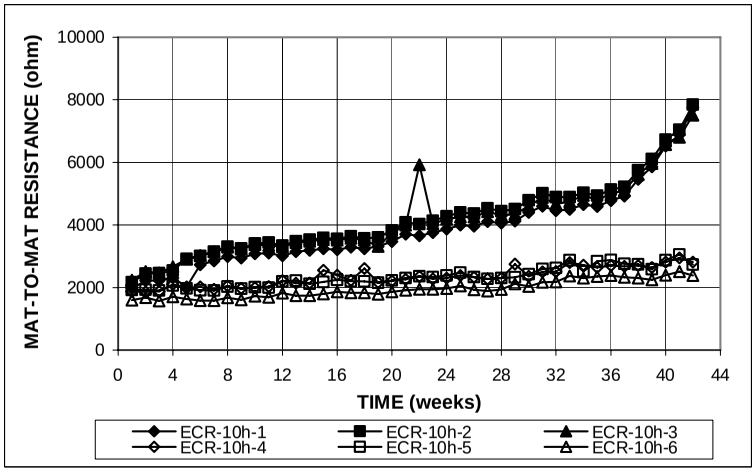

Figure A. 351 - Mat-to-mat resistances as measured in the ASTM G 109 test for specimens containing epoxy-coated steel with 10 drilled holes

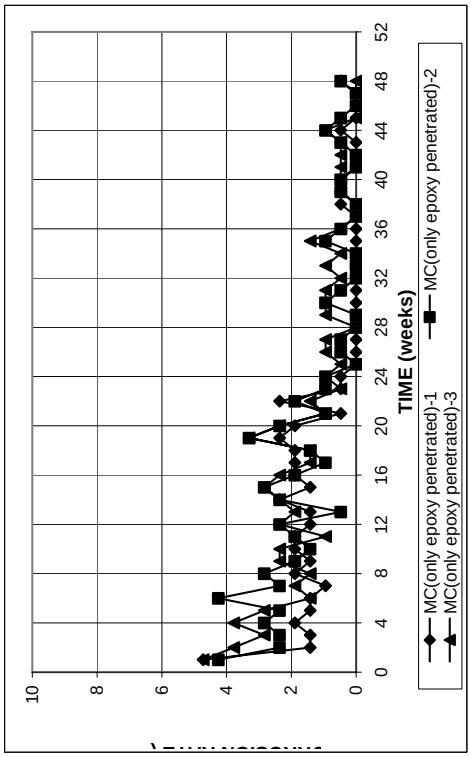

(a)

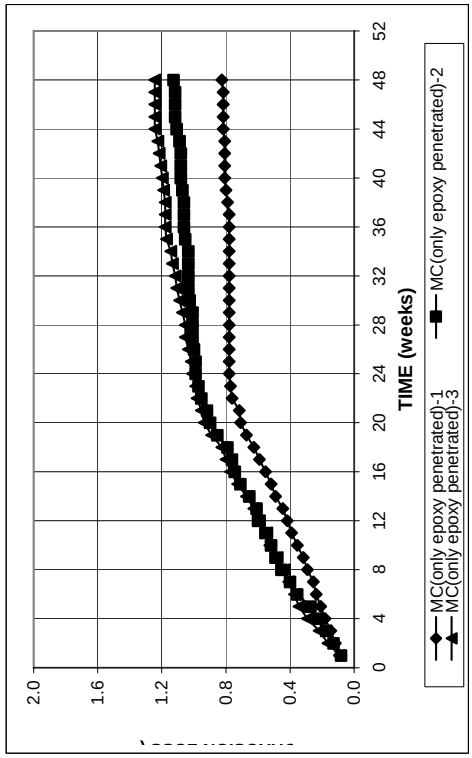

(b)

Figure A. 352 - (a) Corrosion rates and (b) total corrosion losses based on total bar area as measured in the ASTM G 109 test for specimens containing multiple coated steel with only epoxy penetrated

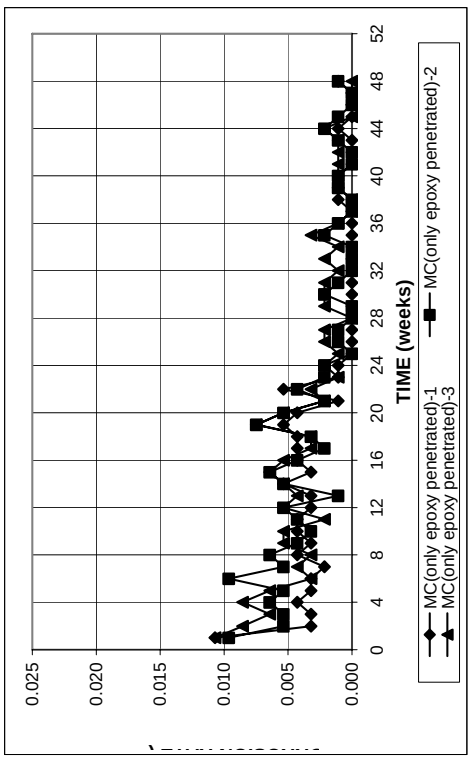

(a)

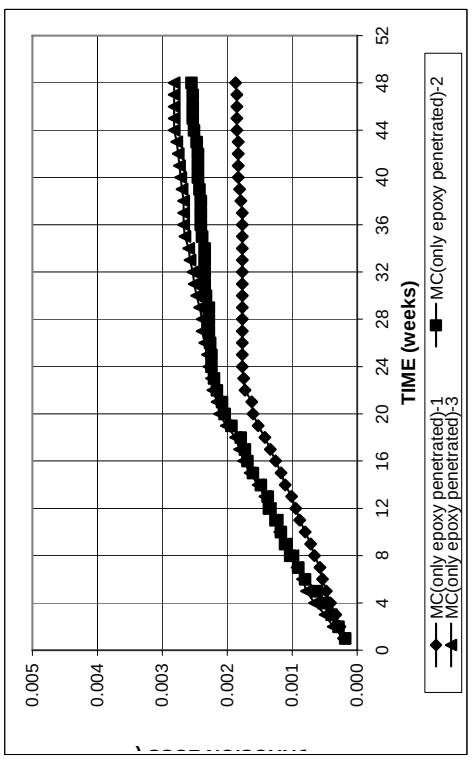

(b)

Figure A. 353 - (a) Corrosion rates and (b) total corrosion losses based on exposed area as measured in the ASTM G 109 test for specimens containing multiple coated steel with only epoxy penetrated

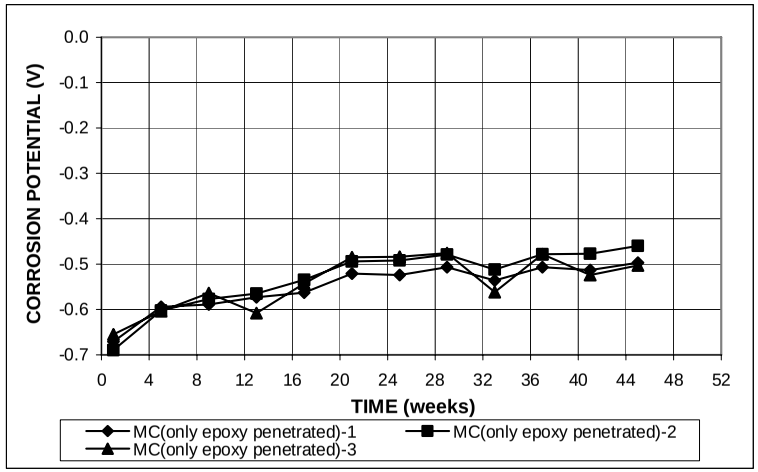

(a)

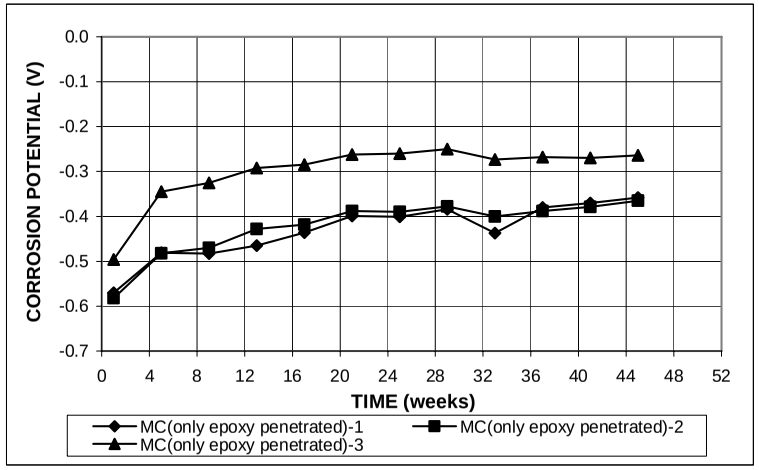

(b)

Figure A. 354 - (a) Top mat corrosion potentials and (b) bottom mat corrosion potentials as measured in the ASTM G 109 test for specimens containing multiple coated steel with only epoxy penetrated

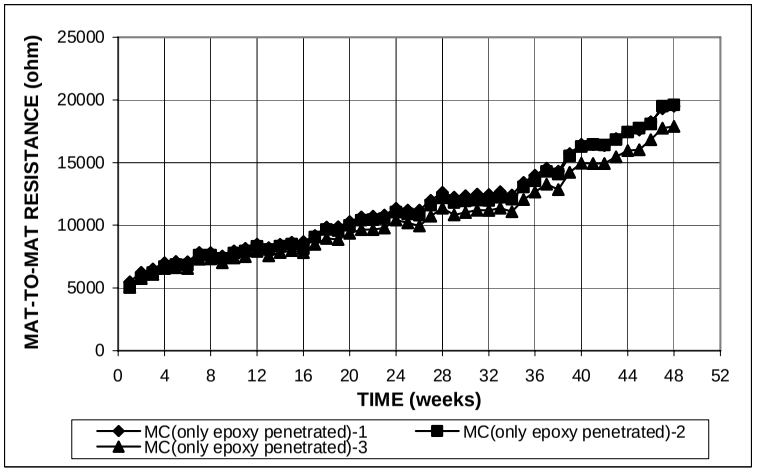

Figure A. 355 - Mat-to-mat resistances as measured in the ASTM G 109 test for specimens containing multiple coated steel with only epoxy penetrated

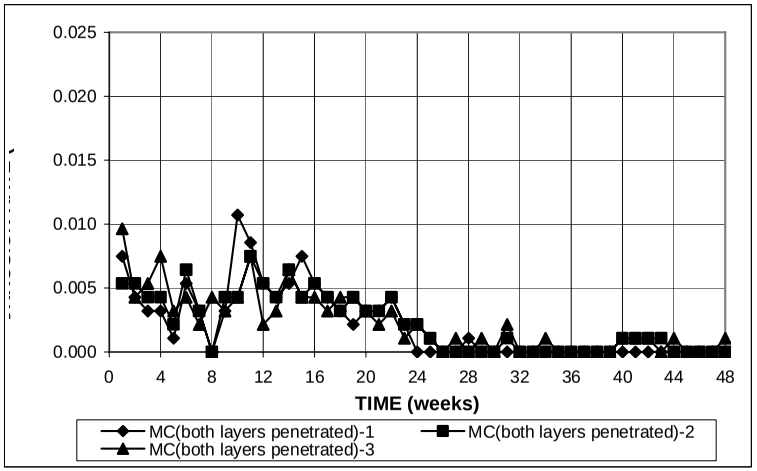

(a)

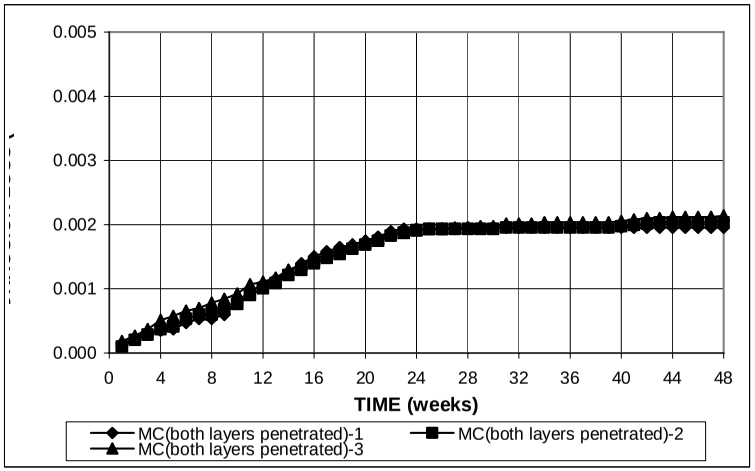

(b)

Figure A. 356 - (a) Corrosion rates and (b) total corrosion losses based on total bar area as measured in the ASTM G 109 test for specimens containing multiple coated steel with both layers penetrated

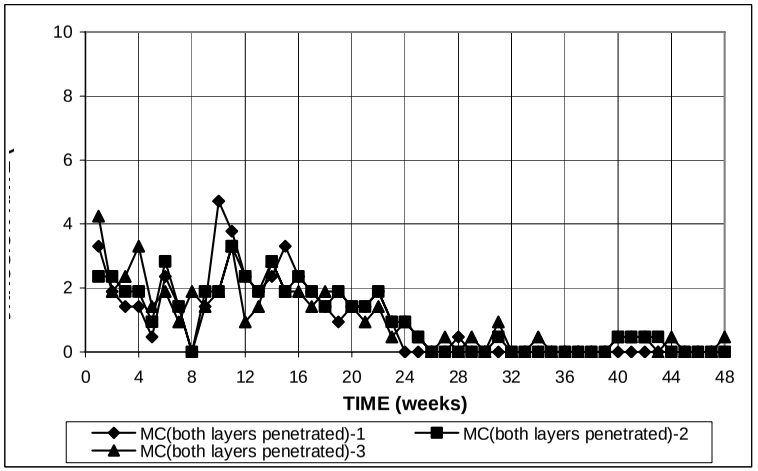

(a)

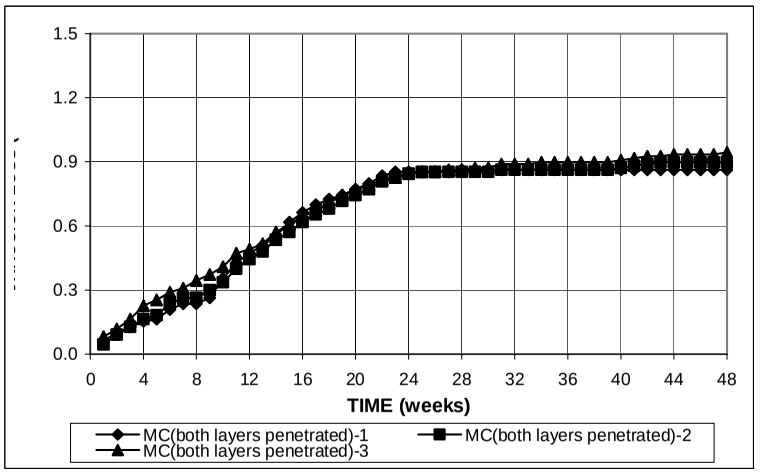

(b)

Figure A. 357 - (a) Corrosion rates and (b) total corrosion losses based on exposed area as measured in the ASTM G 109 test for specimens containing multiple coated steel with both layers penetrated

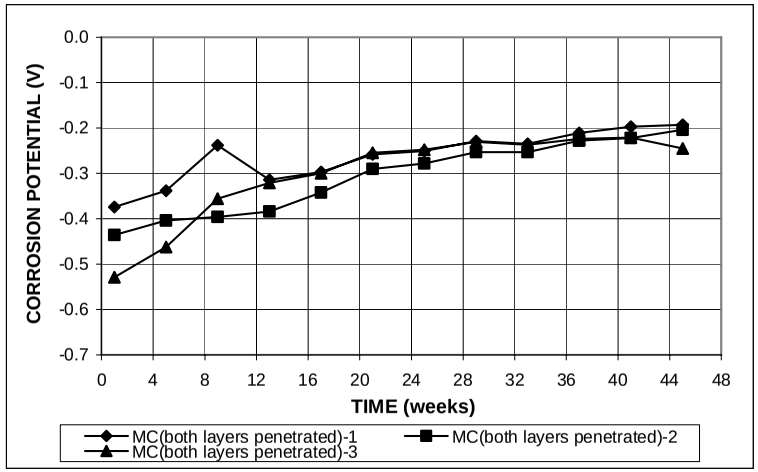

(a)

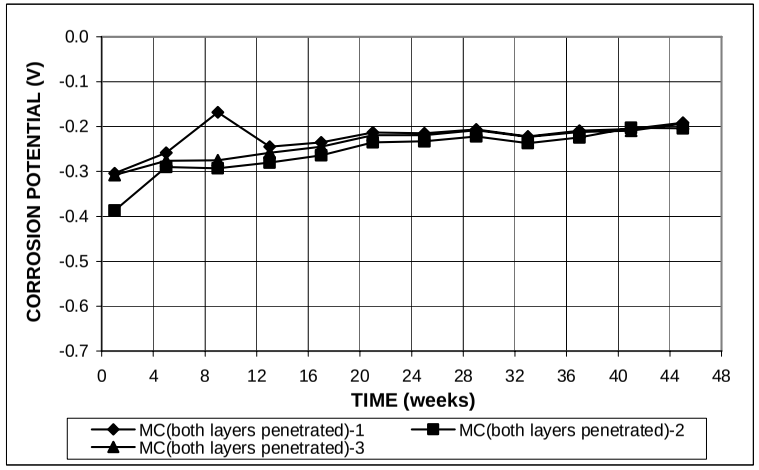

(b)

Figure A. 358 - (a) Top mat corrosion potentials and (b) bottom mat corrosion potentials as measured in the ASTM G 109 test for specimens containing multiple coated steel with both layers penetrated

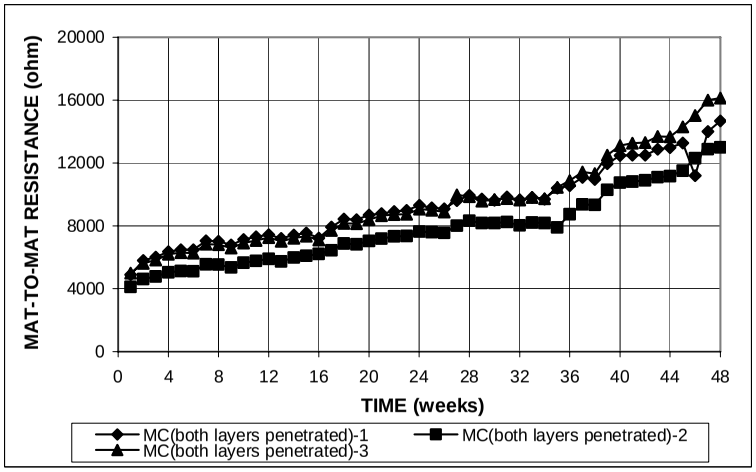

Figure A. 359 - Mat-to-mat resistances as measured in the ASTM G 109 test for specimens containing multiple coated steel with both layers penetrated

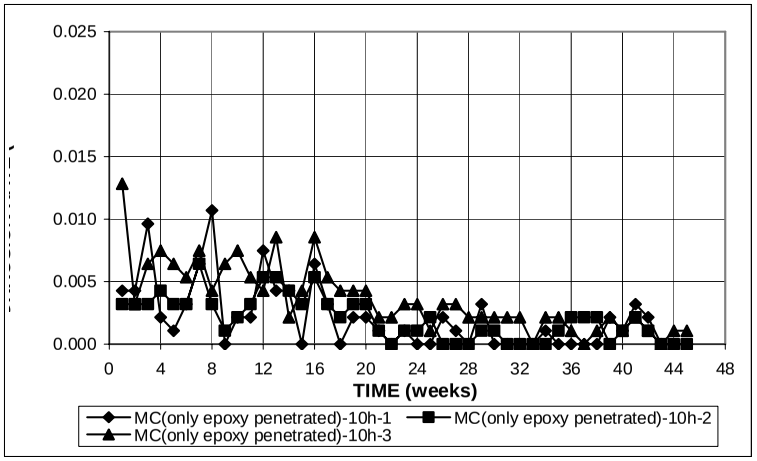

(a)

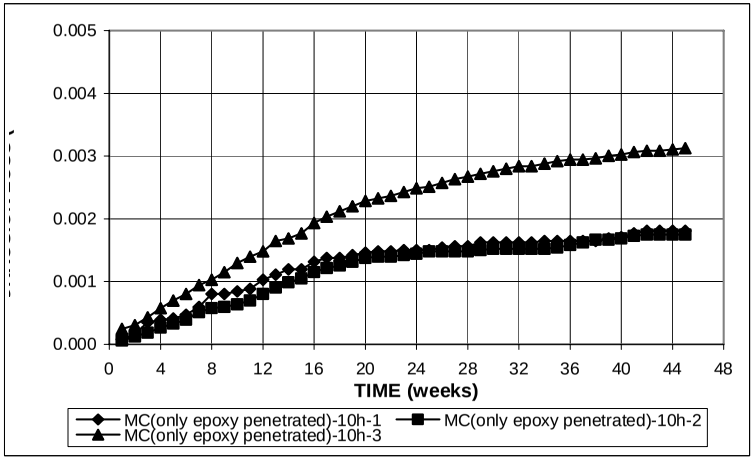

(b)

Figure A. 360 - (a) Corrosion rates and (b) total corrosion losses based on total bar area as measured in the ASTM G 109 test for specimens containing multiple coated steel with only epoxy penetrated by 10 burned holes

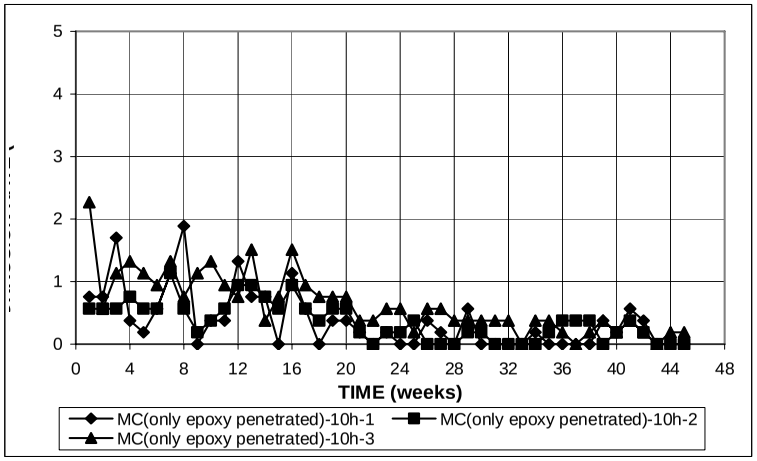

(a)

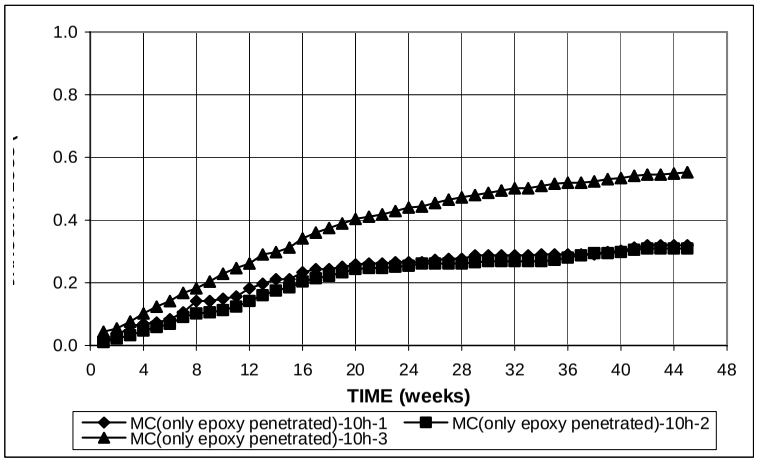

(b)

Figure A. 361 - (a) Corrosion rates and (b) total corrosion losses based on exposed area as measured in the ASTM G 109 test for specimens containing multiple coated steel with only epoxy penetrated by 10 burned holes

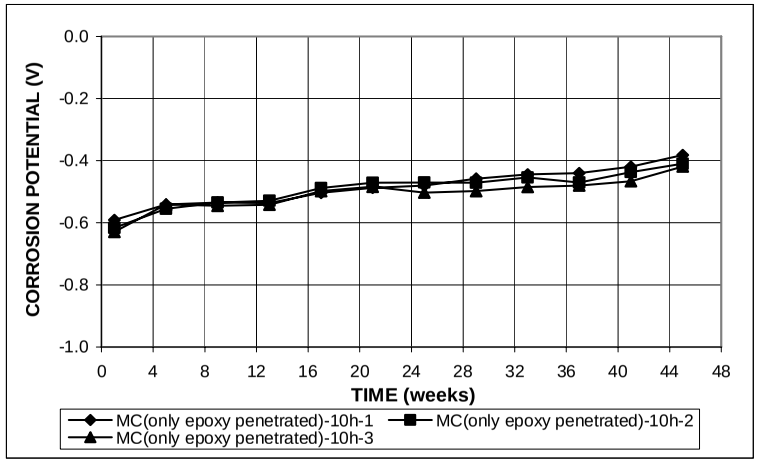

(a)

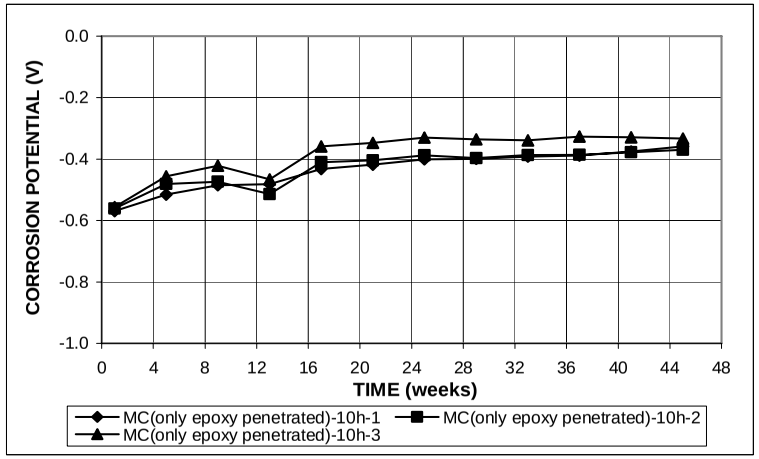

(b)

Figure A. 362 - (a) Top mat corrosion potentials and (b) bottom mat corrosion potentials as measured in the ASTM G 109 test for specimens containing multiple coated steel with only epoxy penetrated by 10 burned holes

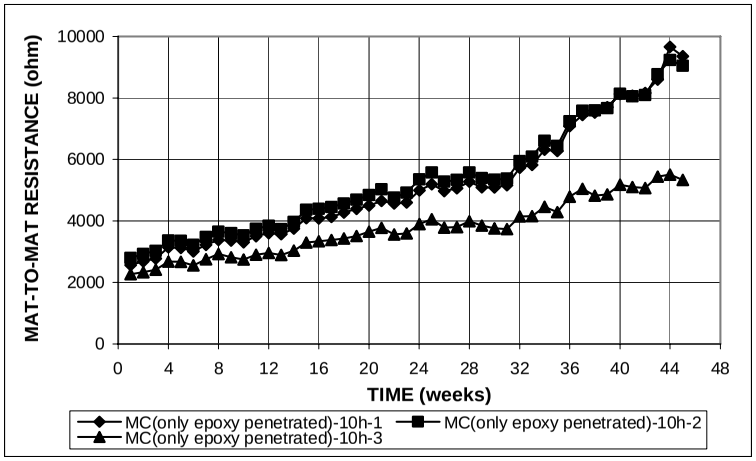

Figure A. 363 - Mat-to-mat resistances as measured in the ASTM G 109 test for specimens containing multiple coated steel with only epoxy penetrated by 10 burned holes

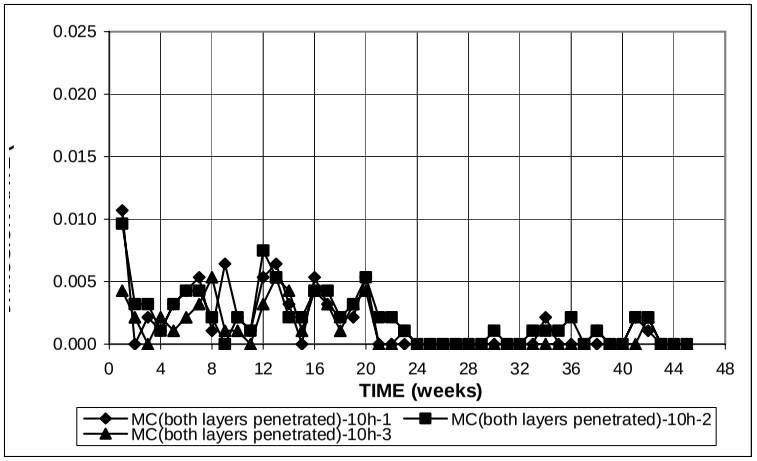

(a)

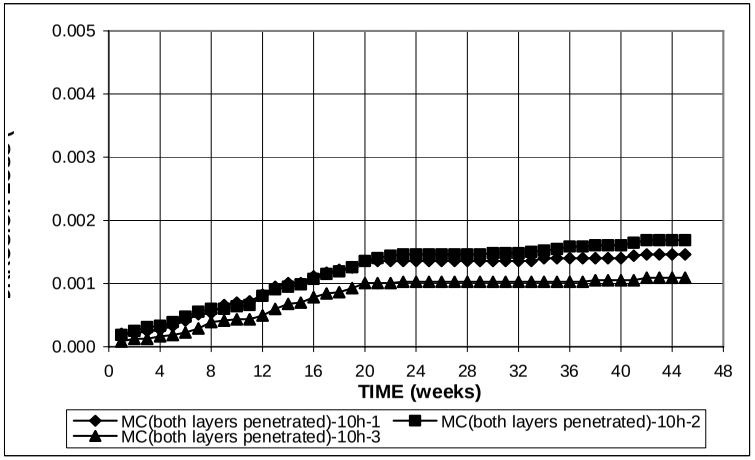

(b)

Figure A. 364 - (a) Corrosion rates and (b) total corrosion losses based on total bar area as measured in the ASTM G 109 test for specimens containing multiple coated steel with both layers penetrated by 10 drilled holes

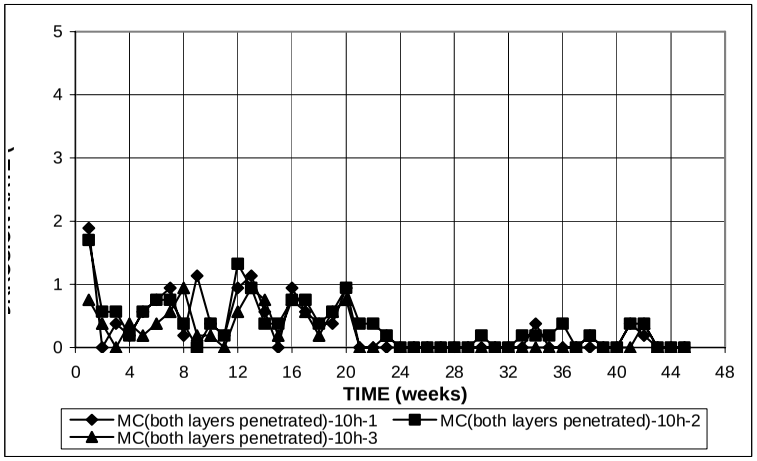

(a)

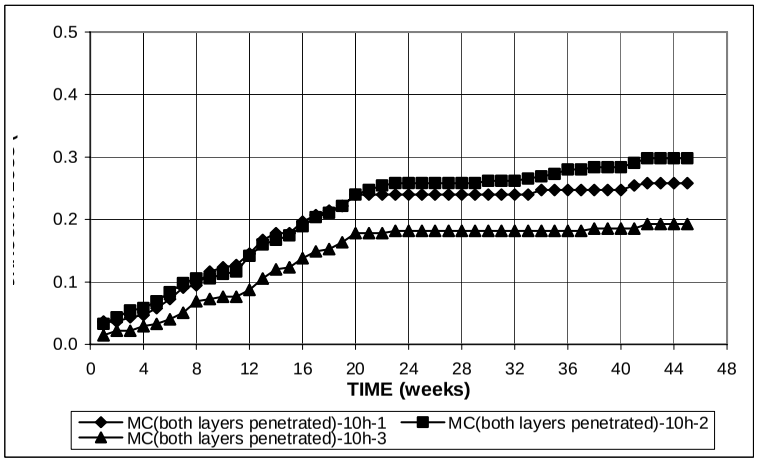

(b)

Figure A. 365 - (a) Corrosion rates and (b) total corrosion losses based on exposed area as measured in the ASTM G 109 test for specimens containing multiple coated steel with both layers penetrated by 10 drilled holes

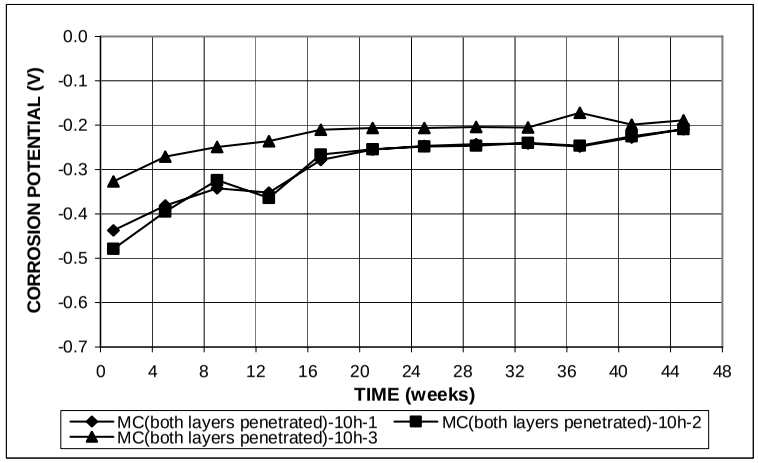

(a)

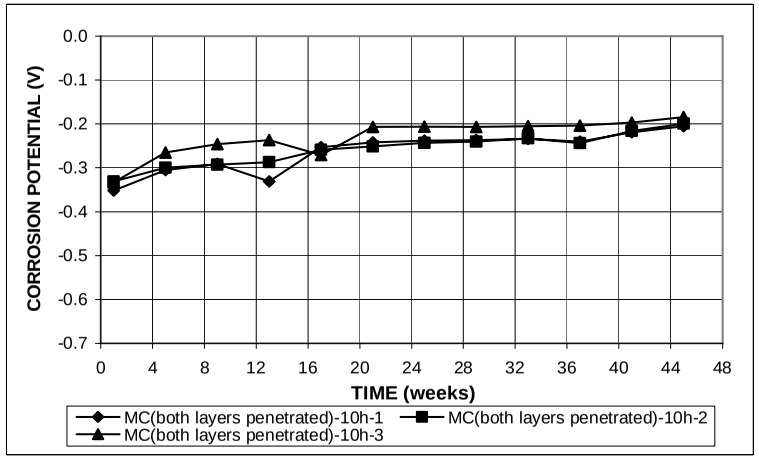

(b)

Figure A. 366 - (a) Top mat corrosion potentials and (b) bottom mat corrosion potentials as measured in the ASTM G 109 test for specimens containing multiple coated steel with both layers penetrated by 10 drilled holes

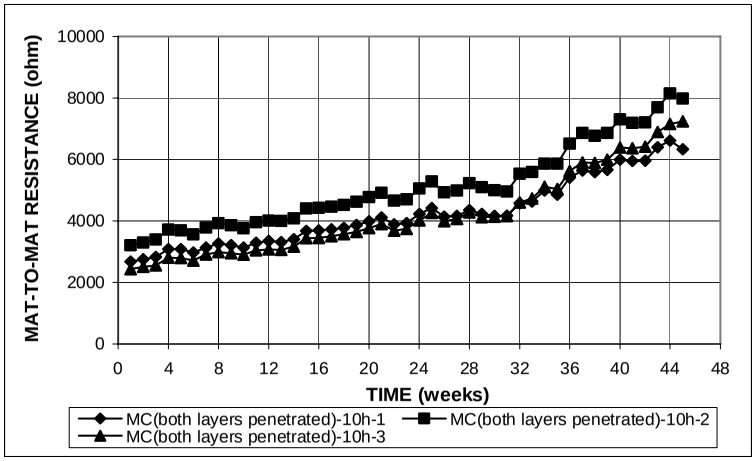

Figure A. 367 - Mat-to-mat resistances as measured in the ASTM G 109 test for specimens containing multiple coated steel with both layers penetrated by 10 drilled holes

APPENDIX B

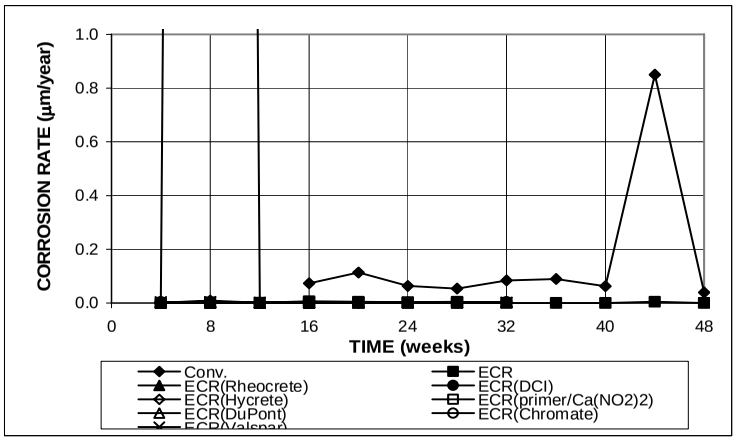

(a)

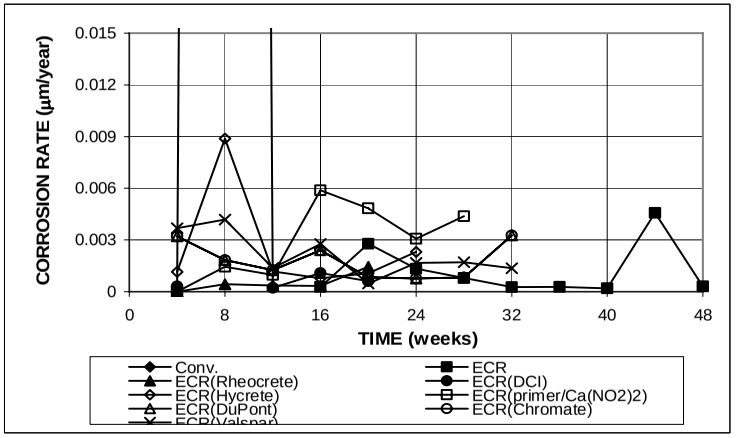

(b)

Figure B.1 - Microcell corrosion rates of bottom mats as measured in the Southern Exposure test for specimens containing conventional and epoxy-coated steel, epoxy-coated steel cast with corrosion inhibitors, epoxy-coated steel with a calcium nitrite primer, and high adhesion ECR steel. All epoxy-coated specimens penetrated with four holes.

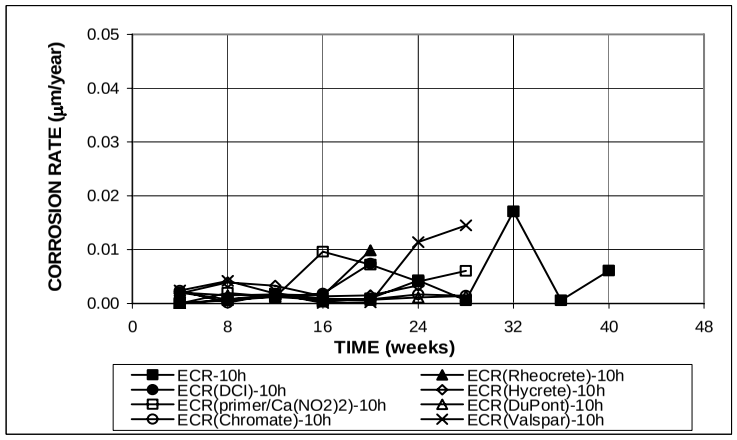

(a)

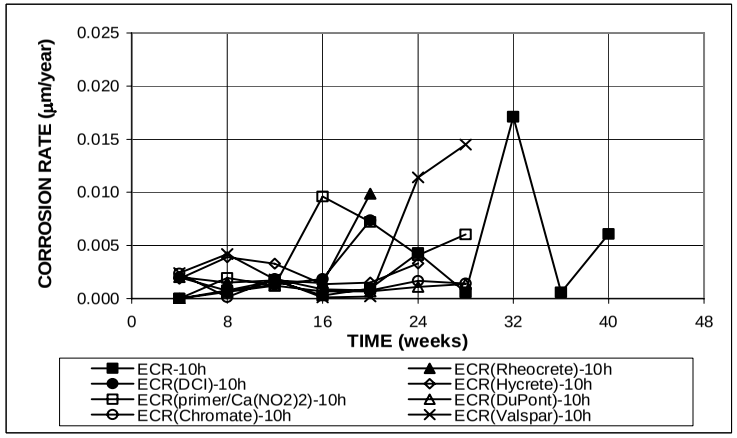

(b)

Figure B.2 - Microcell corrosion rates of bottom mats as measured in the Southern Exposure test for specimens containing conventional and epoxy-coated, steel, epoxy-coated steel cast with corrosion inhibitors, epoxy-coated steel with a calcium nitrite primer, and high adhesion ECR steel. All epoxy-coated specimens penetrated with 10 holes.

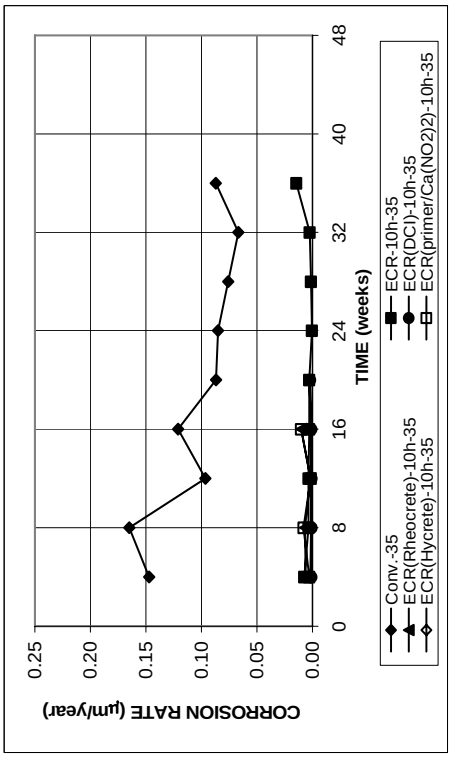

Figure B.3 - Microcell corrosion rates of bottom mats as measured in the Southern Exposure test for specimens containing conventional and epoxy-coated, steel, epoxy-coated steel cast with corrosion inhibitors, epoxy-coated steel with a calcium nitrite primer, and high adhesion ECR steel in a w/c ratio of 0.35. All epoxy-coated specimens penetrated with 10 holes.

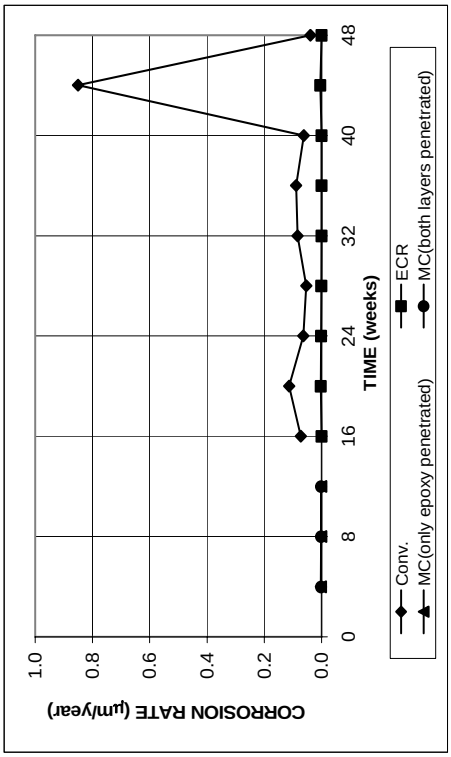

Figure B.4 - Microcell corrosion rates of bottom mats as measured in the Southern Exposure test for specimens containing conventional, epoxy-coated, and multiple coated steel. All epoxy-coated specimens penetrated with four holes

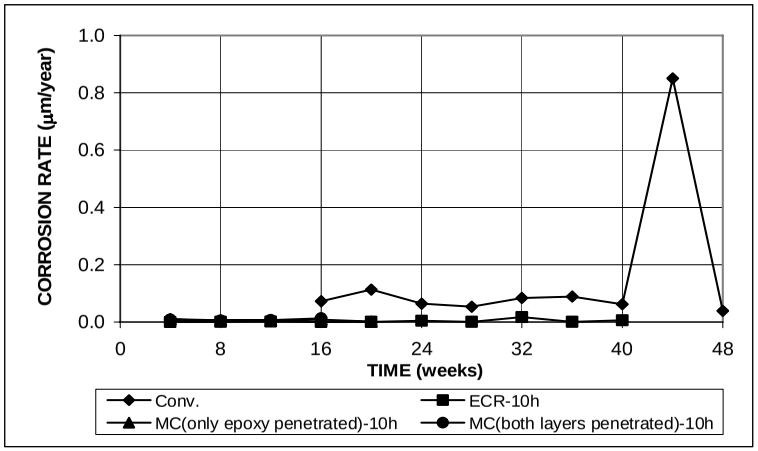

(a)

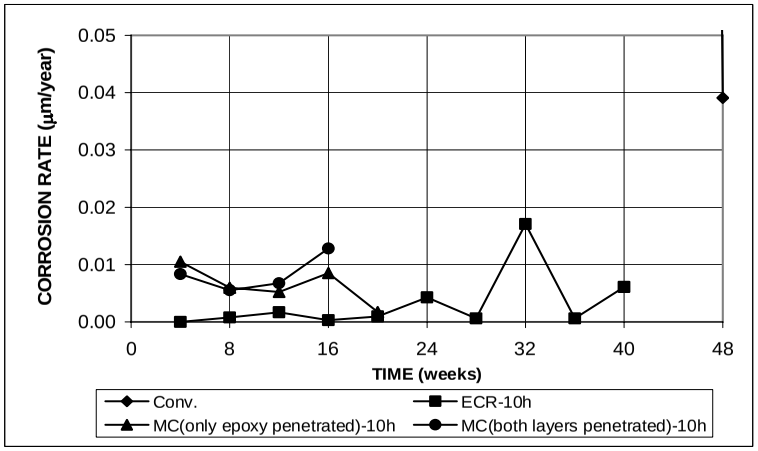

(b)

Figure B.5 - Microcell corrosion rates of bottom mats as measured in the Southern Exposure test for specimens containing conventional, epoxy-coated, and multiple coated steel. All epoxy-coated specimens penetrated with 10 holes

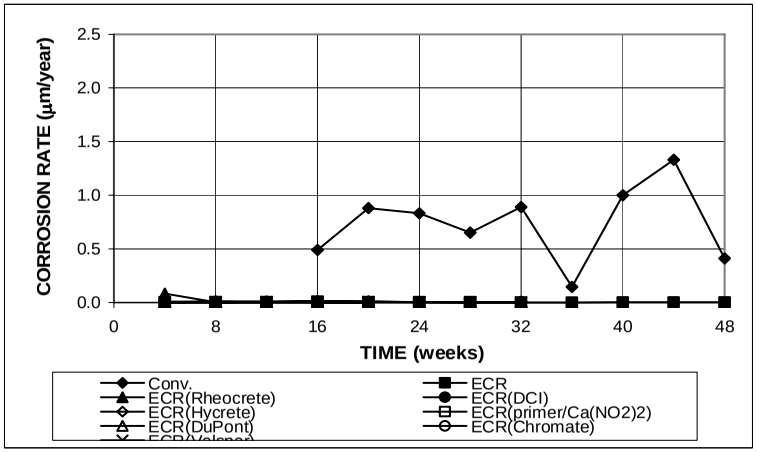

(a)

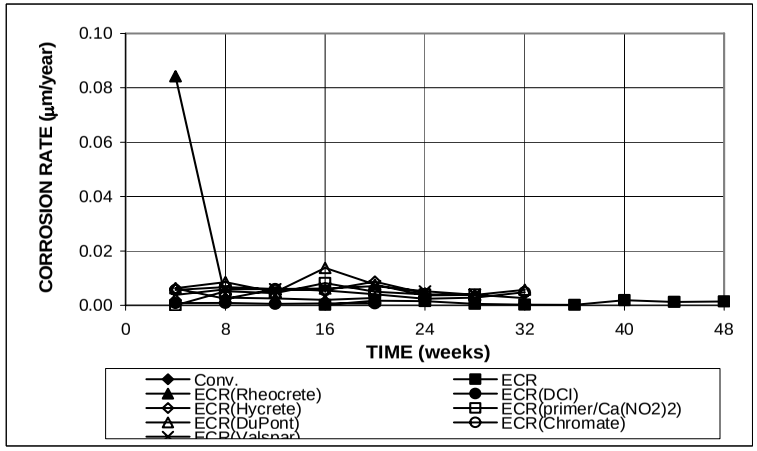

(b)

Figure B.6 - Microcell corrosion rates of bottom mats as measured in the cracked beam test for specimens containing conventional and epoxy-coated steel, epoxy-coated steel cast with corrosion inhibitors, epoxy-coated steel with a calcium nitrite primer, and high adhesion ECR steel. All epoxy-coated specimens penetrated with four holes.

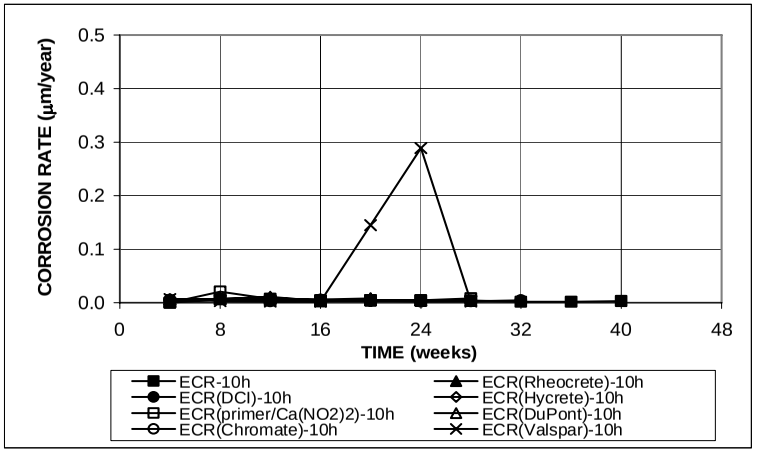

(a)

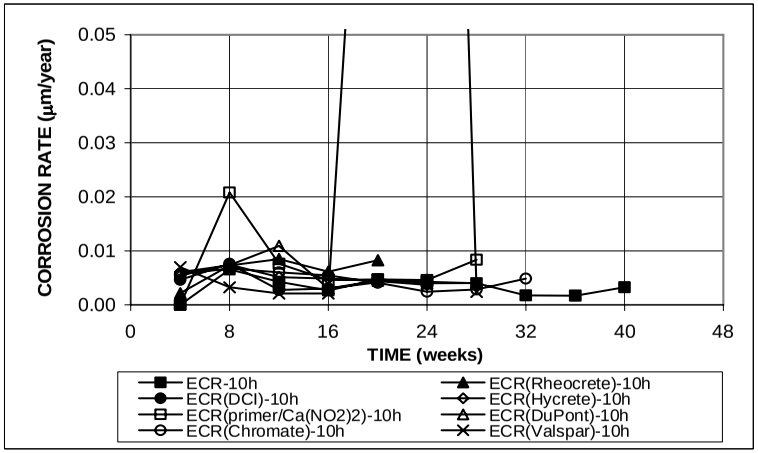

(b)

Figure B.7 - Microcell corrosion rates of bottom mats as measured in the cracked beam test for specimens containing conventional and epoxy-coated steel, epoxy-coated steel cast with corrosion inhibitors, epoxy-coated steel with a calcium nitrite primer, and high adhesion ECR steel. All epoxy-coated specimens penetrated with 10 holes.

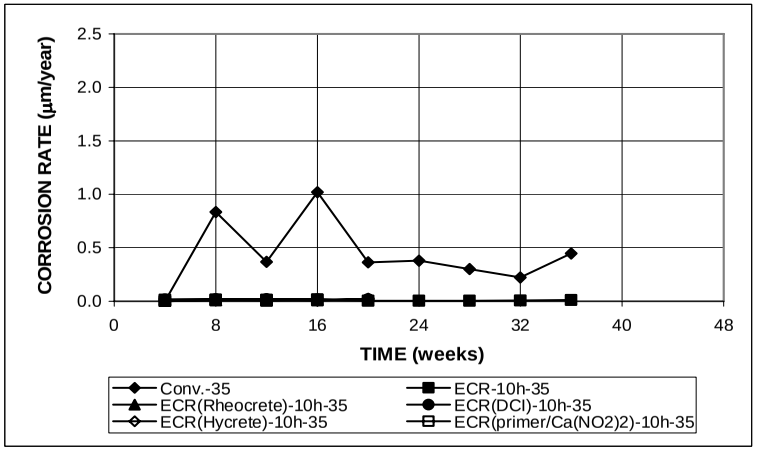

(a)

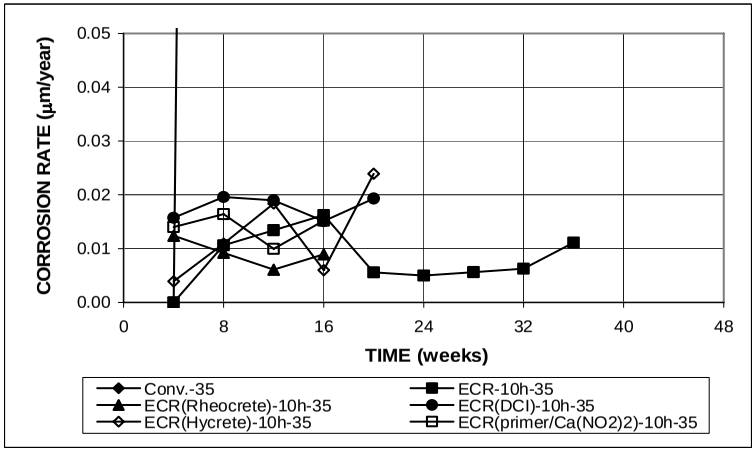

(b)

Figure B.8 - Microcell corrosion rates of bottom mats as measured in the cracked beam test for specimens containing conventional and epoxy-coated steel, epoxy-coated steel cast with corrosion inhibitors, epoxy-coated steel with a calcium nitrite primer, and high adhesion ECR steel in a w/c ratio of 0.35. All epoxy-coated specimens penetrated with 10 holes.

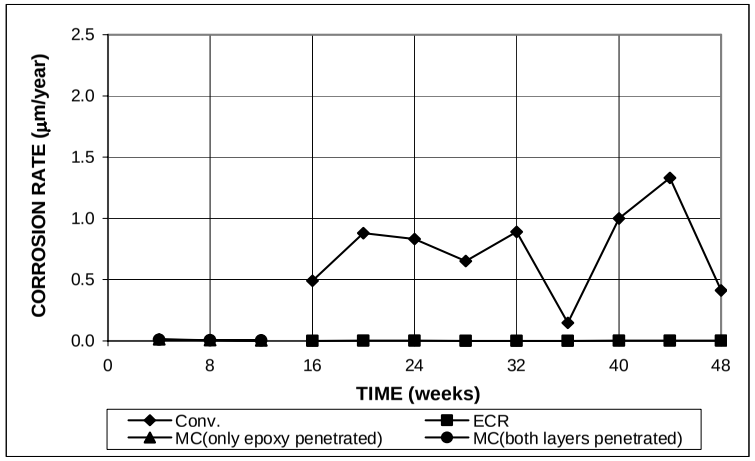

(a)

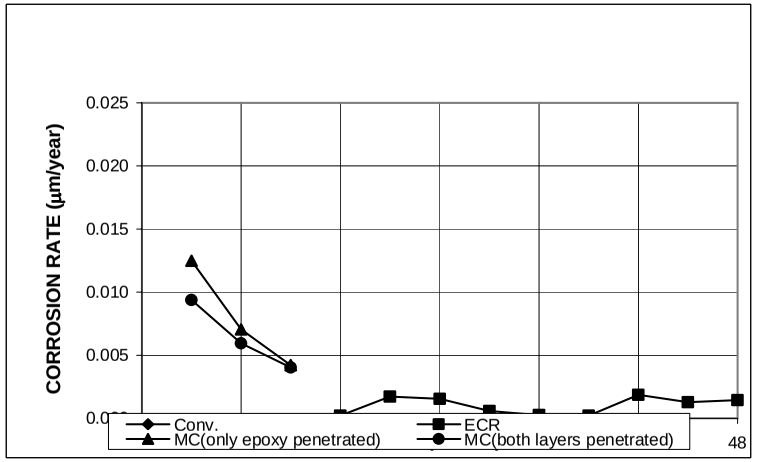

(b)

Figure B.9 - Microcell corrosion rates of bottom mats as measured in the cracked beam test for specimens containing conventional, epoxy-coated, and multiple coated steel. All epoxy-coated specimens penetrated with four holes

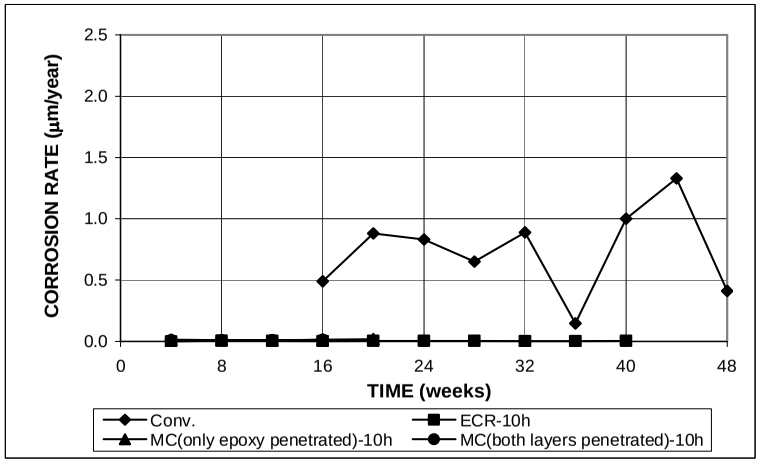

(a)

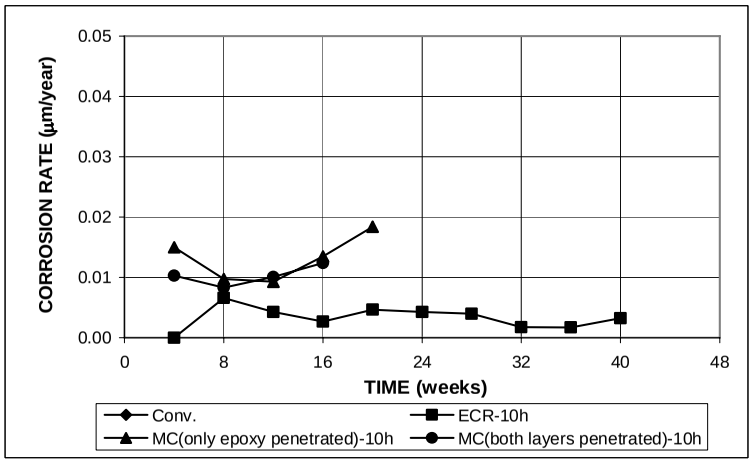

(b)

Figure B.10 - Microcell corrosion rates of bottom mats as measured in the cracked beam test for specimens containing conventional, epoxy-coated, and multiple coated steel. All epoxy-coated specimens penetrated with 10 holes

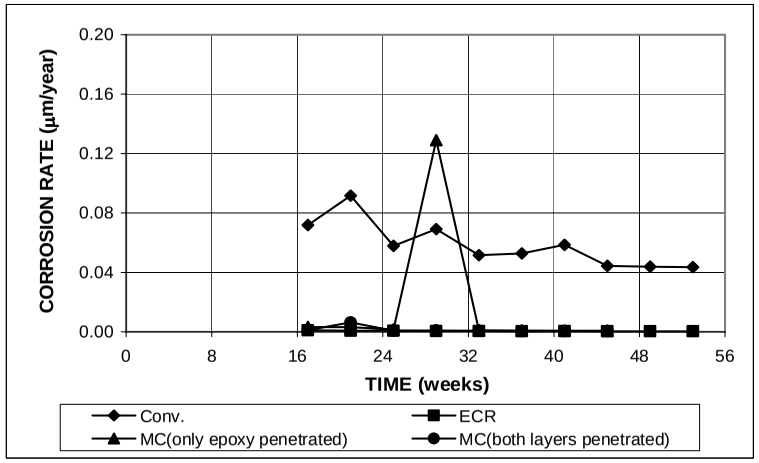

(a)

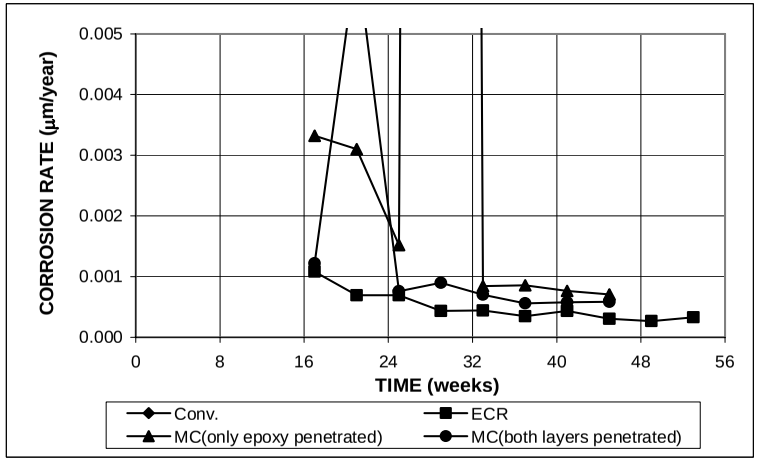

(b)

Figure B.11 - Microcell corrosion rates of bottom mats as measured in the ASTM G 109 test for specimens containing conventional, epoxy-coated, and multiple coated steel. All epoxy-coated specimens penetrated with four holes

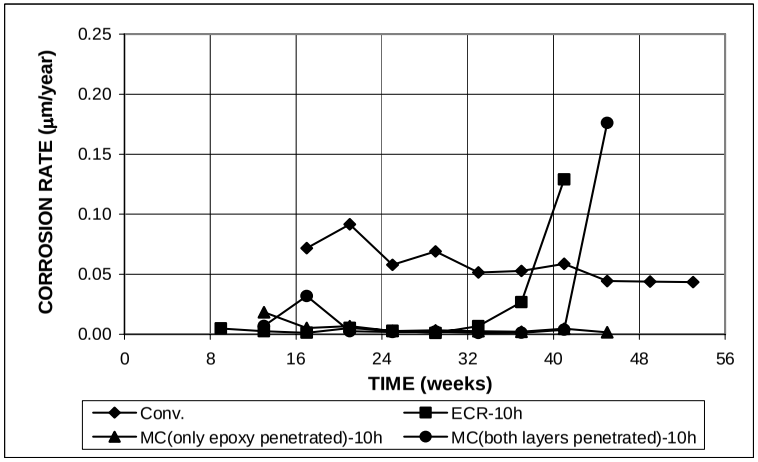

(a)

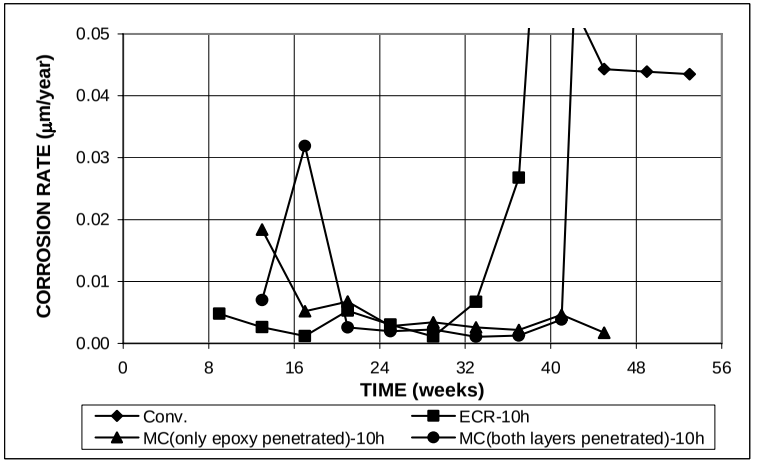

(b)

Figure B.12 - Microcell corrosion rates of bottom mats as measured in the ASTM beam test for specimens containing conventional, epoxy-coated, and multiple coated steel. All epoxy-coated specimens penetrated with10 holes

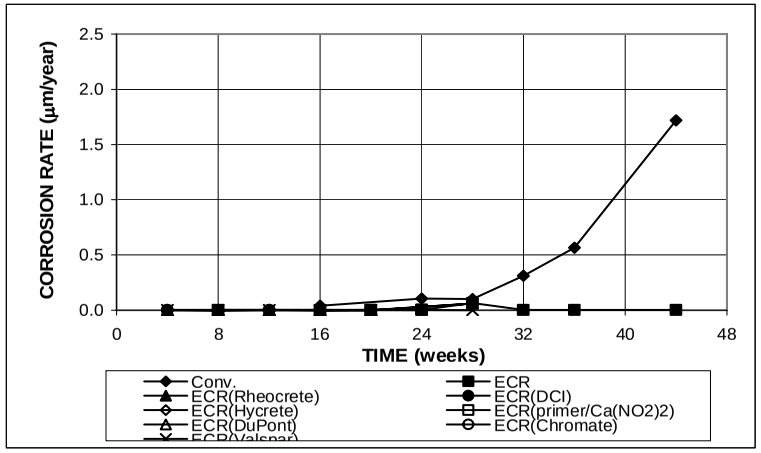

(a)

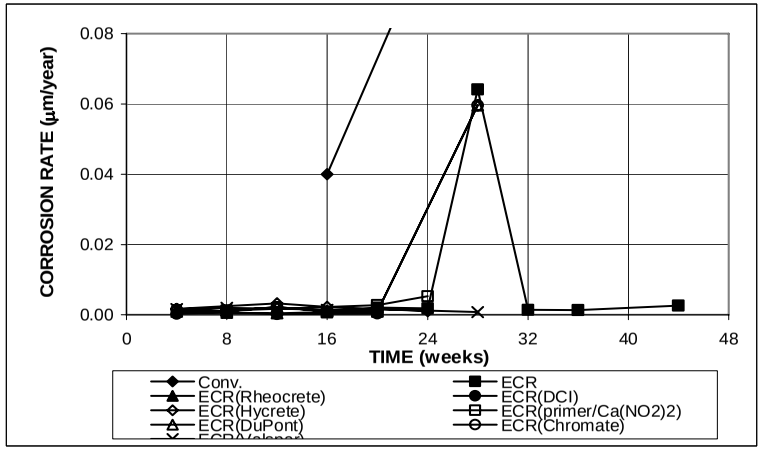

(b)

Figure B.13 - Microcell corrosion rates of connected circuits as measured in the Southern Exposure test for specimens containing conventional and and epoxy-coated steel, epoxy-coated steel cast with corrosion inhibitor, epoxy-coated steel with a calcium nitrite primer, and high adhesion ECR steel. All epoxy-coated specimens penetrated with four holes.

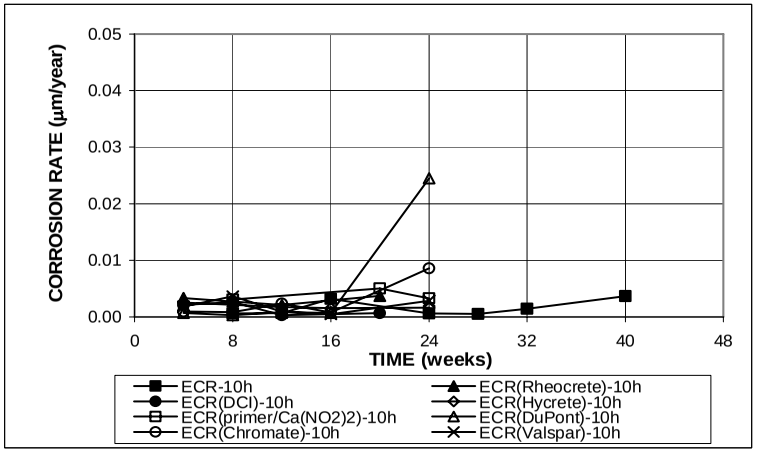

(a)

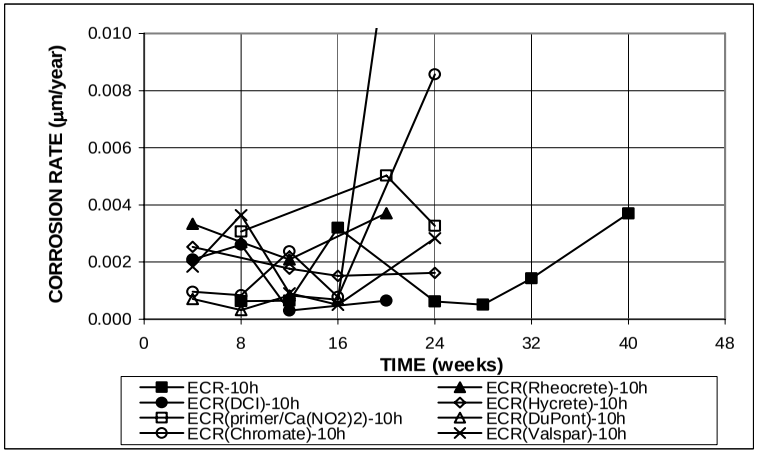

(b)

Figure B.14 - Microcell corrosion rates of connected circuits as measured in the Southern Exposure test for specimens containing conventional and and epoxy-coated steel, epoxy-coated steel cast with corrosion inhibitor, epoxy-coated steel with a calcium nitrite primer, and high adhesion ECR steel. All epoxy-coated specimens penetrated with10 holes.

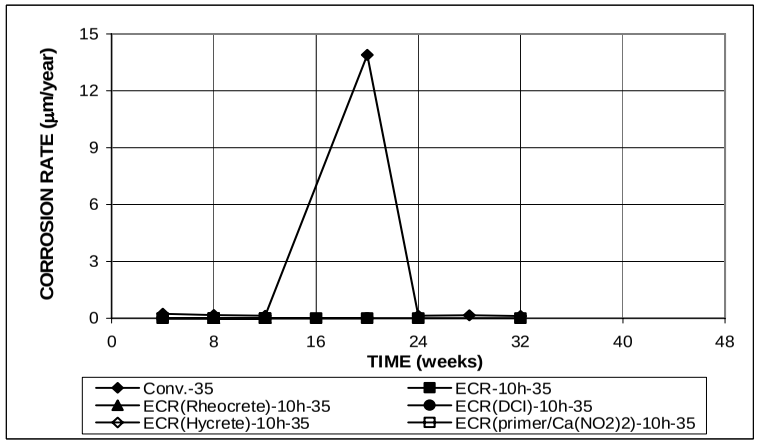

(a)

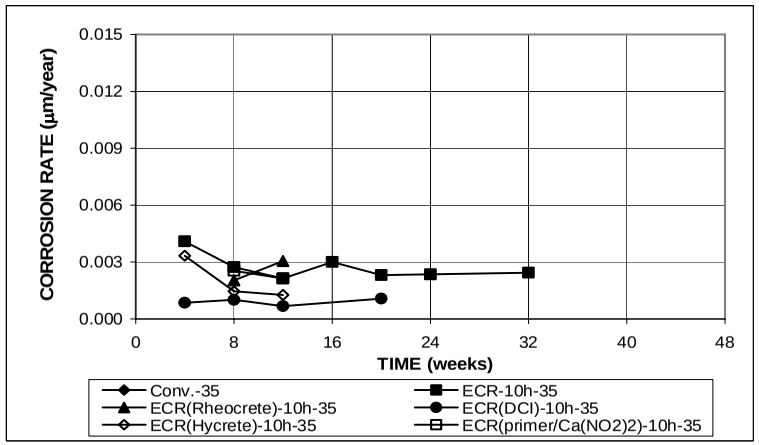

(b)

Figure B.15 - Microcell corrosion rates of connected circuits as measured in the Southern Exposure test for specimens containing conventional and and epoxy-coated steel, epoxy-coated steel cast with corrosion inhibitor, epoxy-coated steel with a calcium nitrite primer, and high adhesion ECR steel in a w/c ratio of 0.35. All epoxy-coated specimens penetrated with 10 holes.

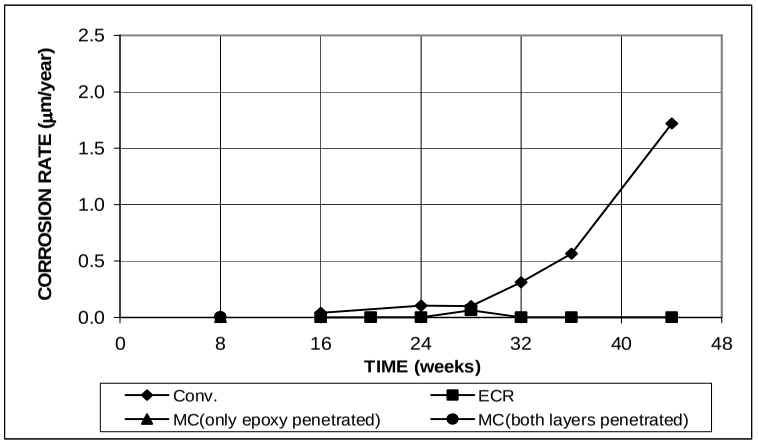

(a)

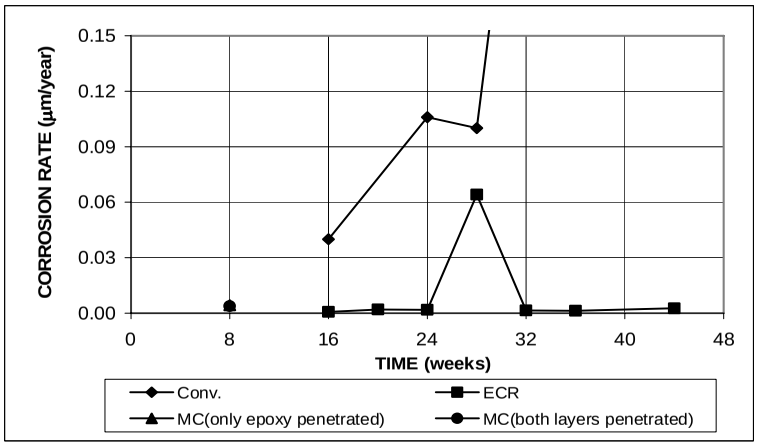

(b)

Figure B.16 - Microcell corrosion rates of connected circuits as measured in the Southern Exposure test for specimens containing conventional, epoxy-coated, and multiple coated steel. All epoxy-coated specimens penetrated with four holes

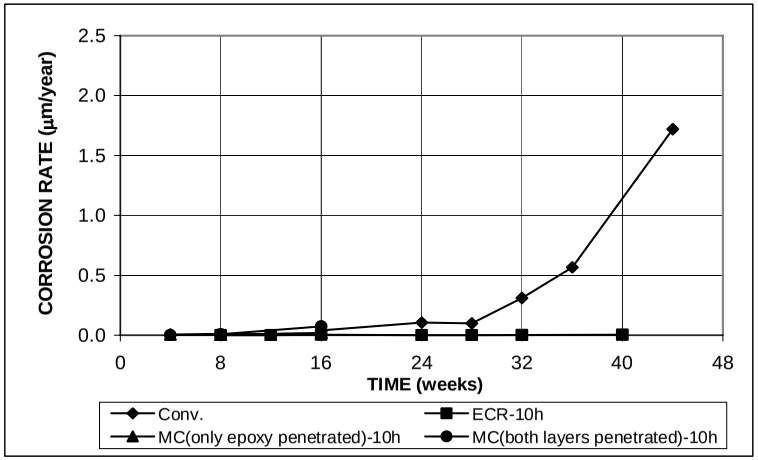

(a)

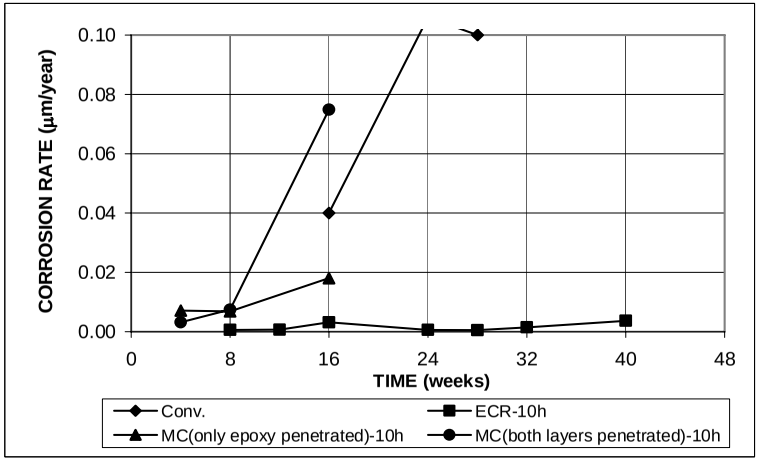

(b)

Figure B.17 - Microcell corrosion rates of connected circuits as measured in the Southern Exposure test for specimens containing conventional, epoxy-coated, and multiple coated steel. All epoxy-coated specimens penetrated with 10 holes

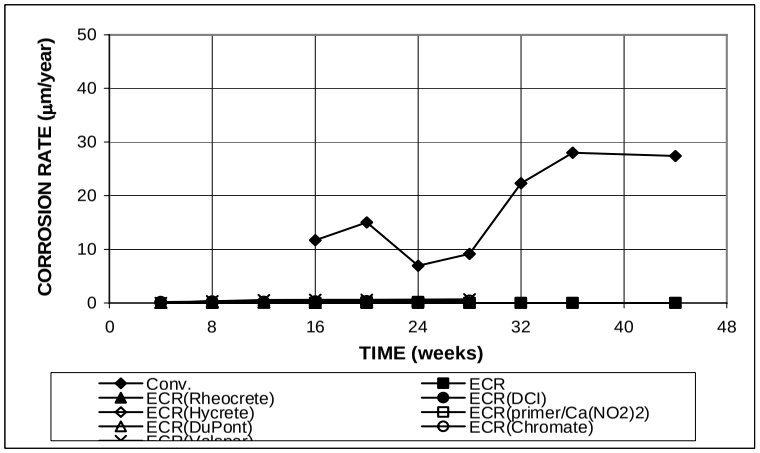

(a)

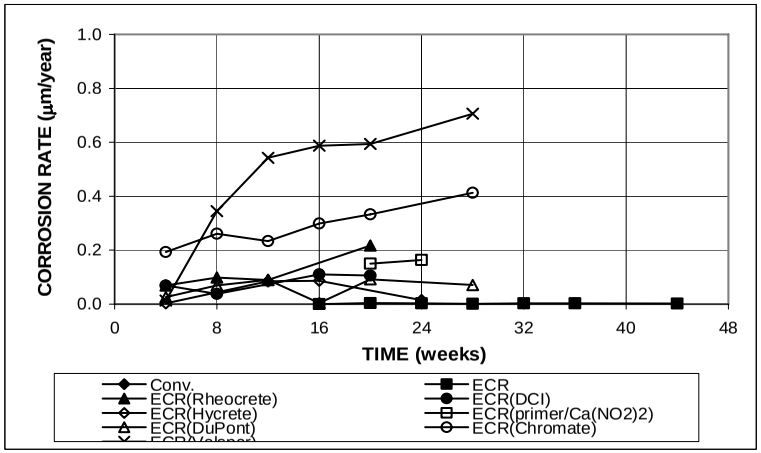

(b)

Figure B.18 - Microcell corrosion rates of connected circuits as measured in the cracked beam test for specimens containing conventional and epoxy-coated steel, epoxy-coated steel cast with corrosion inhibitors, epoxy-coated steel with a calcium nitrite primer, and high adhesion ECR steel. All epoxy-coated specimens penetrated with four holes.

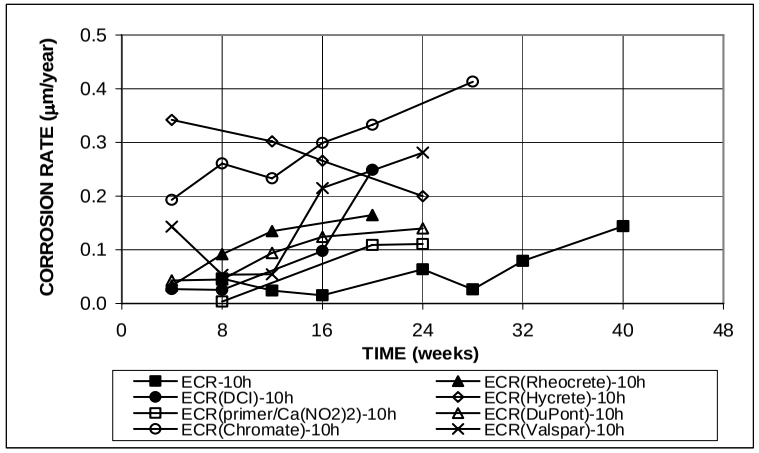

Figure B.19 - Microcell corrosion rates of connected circuits as measured in the cracked beam test for specimens containing conventional and epoxy-coated steel, epoxy-coated steel cast with corrosion inhibitors, epoxy-coated steel with a calcium nitrite primer, and high adhesion ECR steel. All epoxy-coated specimens penetrated with10 holes.

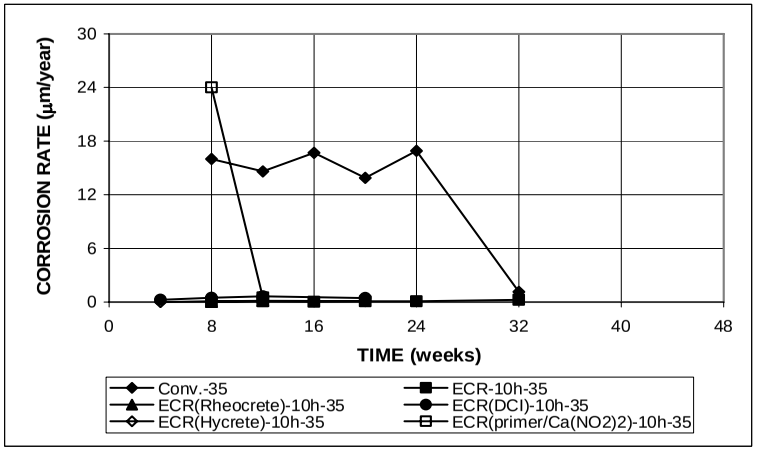

(a)

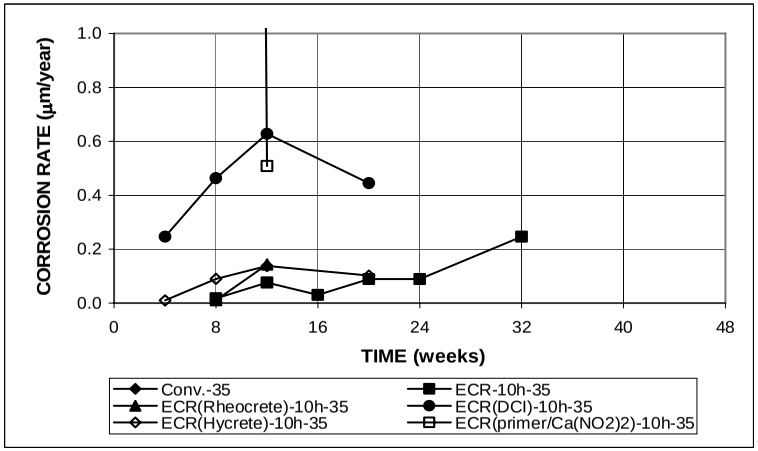

(b)

Figure B.20 - Microcell corrosion rates of connected circuits as measured in the cracked test for specimens containing conventional and epoxy-coated steel, epoxy-coated steel cast with corrosion inhibitors, epoxy-coated steel with a calcium nitrite primer, and high adhesion ECR steel in a w/c ratio of 0.35. All epoxy-coated specimens penetrated with 10 holes

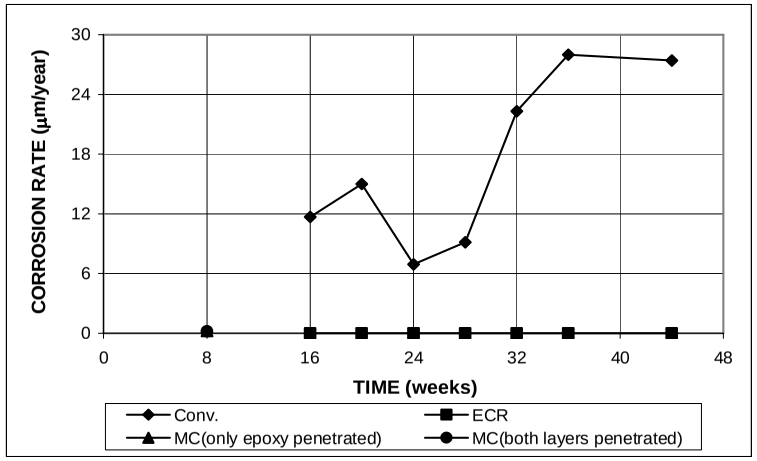

(a)

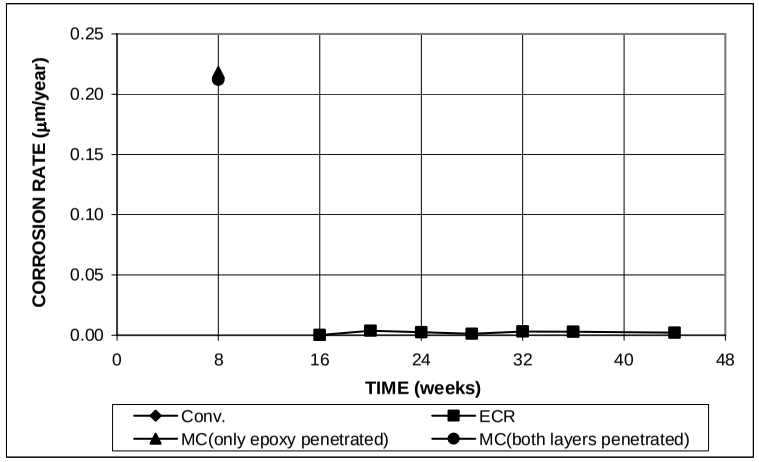

(b)

Figure B.21 - Microcell corrosion rates of connected circuits as measured in the cracked beam test for specimens containing conventional, epoxy-coated, and multiple coated steel. All epoxy-coated specimens penetrated with four holes

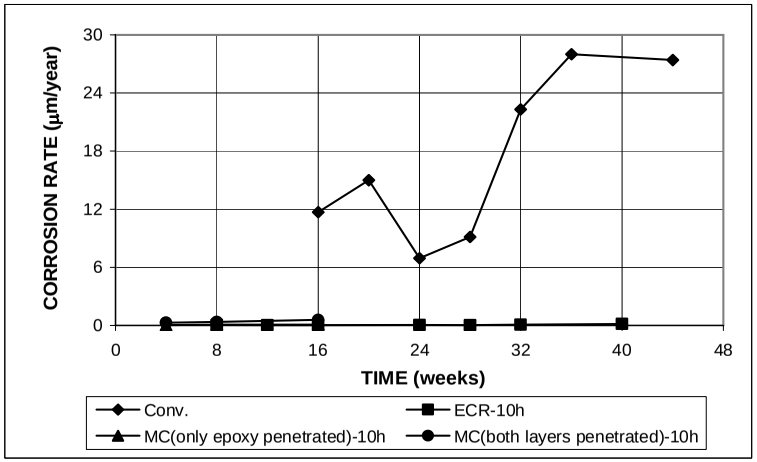

(a)

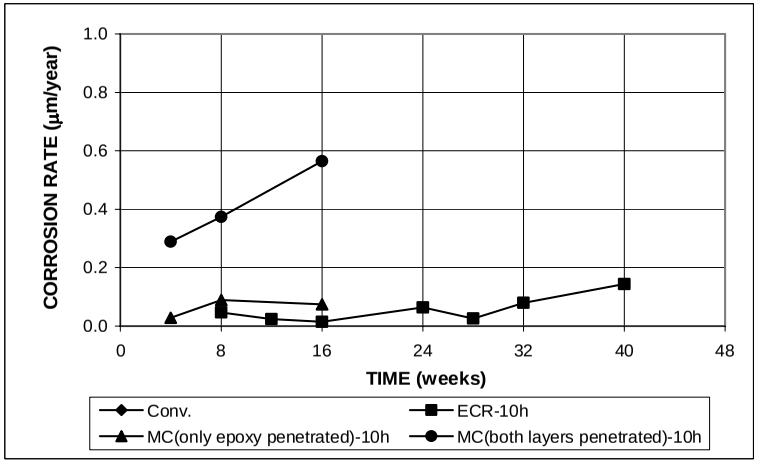

(b)

Figure B.22 - Microcell corrosion rates of connected circuits as measured in the cracked beam test for specimens containing conventional, epoxy-coated, and multiple coated steel. All epoxy-coated specimens penetrated with 10 holes

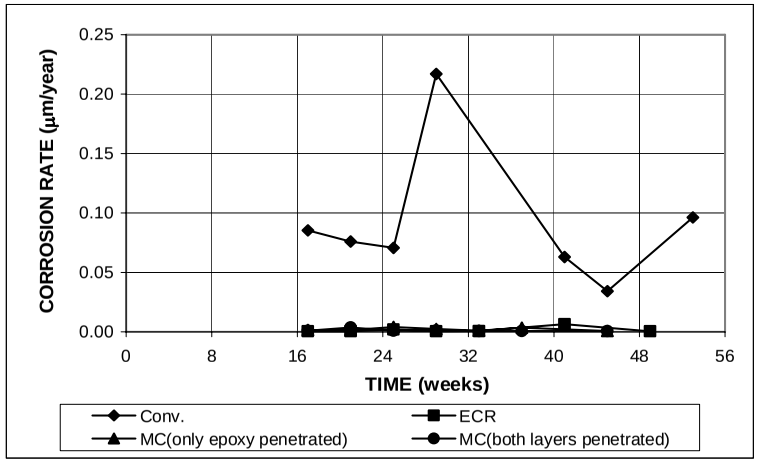

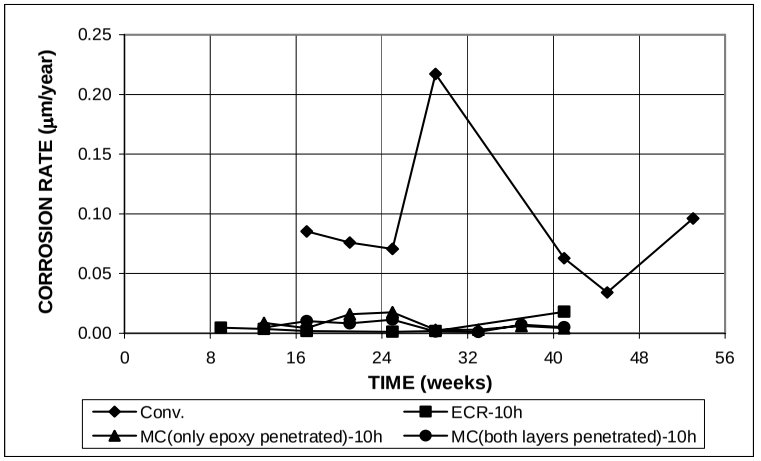

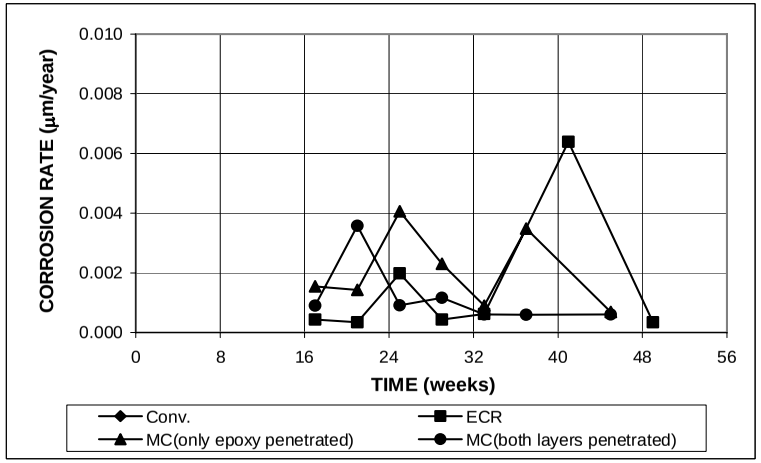

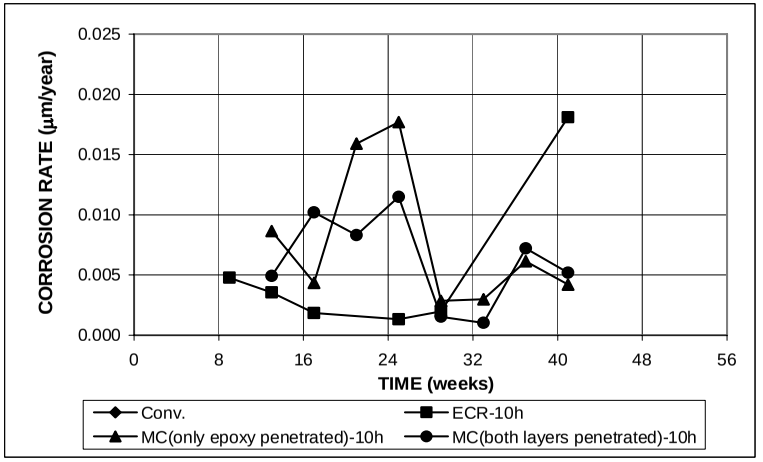

Figure B.23 - Microcell corrosion rates of connected circuits as measured in the ASTM G 109 test for specimens containing conventional, epoxy-coated, and multiple coated steel. All epoxy-coated specimens penetrated with four holes

Figure B.24 - Microcell corrosion rates of connected circuits as measured in the ASTM G 109 test for specimens containing conventional, epoxy-coated, and multiple coated steel. All epoxy-coated specimens penetrated with 10 holes